

VNIVERSIDAD DE SALAMANCA

FACULTAD DE CIENCIAS QUÍMICAS

DEPARTAMENTO DE QUÍMICA ORGÁNICA



VNIVERSIDAD
DE SALAMANCA

CAMPUS DE EXCELENCIA INTERNACIONAL

“Organocatalizadores en los que se simula un
agujero oxianiónico”

“Organocatalysts in which an oxyanion hole is simulated”

Memoria presentada por Ángel Luis Fuentes de Arriba para optar al grado de “Doctor Europeo” en Ciencias Químicas por la Universidad de Salamanca.

En Salamanca, junio de 2014.

Ángel Luis Fuentes de Arriba



D. Joaquín Rodríguez Morán, catedrático del Departamento de Química Orgánica de la Universidad de Salamanca, D. Luis Manuel Simón Rubio, profesor contratado doctor del Departamento de Ingeniería Química de la Universidad de Salamanca y Dña. Victoria Alcázar Montero, profesora titular del Departamento de Ingeniería Química Industrial y del Medio Ambiente de la Universidad Politécnica de Madrid, certifican:

Que la Tesis Doctoral, con el título “Organocatalizadores en los que se simula un agujero oxianiónico” presentada por D. Ángel Luis Fuentes de Arriba para optar al grado de Doctor en Ciencias Químicas, ha sido realizada en el Departamento de Química Orgánica de la Universidad de Salamanca.

Y para que conste a los efectos oportunos, firmamos la presente en Salamanca, con fecha junio de 2014.

Fdo.: Joaquín Rodríguez
Morán

Fdo.: Luis Manuel Simón
Rubio

Fdo.: Victoria Alcázar
Montero

Fdo.: Ángel Luis Fuentes de Arriba

A mi familia y amigos

*“Es más bonito el camino que te lleva hacia una meta
que el propio hecho de conseguir la meta en sí”*

Carlos Moyà

ACKNOWLEDGEMENTS

Todo esto comenzó gracias a una beca de colaboración que no sabía con quién pedir. El caso es que un buen día aparecí en el despacho de Quino para pedirle consejo y desde entonces el laboratorio se convirtió en mi segundo hogar. Creo que fue la ilusión con la que me explicó que soñaba con poder crear una enzima artificial la que me convenció para que me quedara allí. Desde entonces, no tengo palabras suficientes para agradecerte todo lo que has hecho por mí en este tiempo. Aunque hemos pasado temporadas buenas y malas, siempre nos hemos apoyado el uno en el otro, siempre has tenido un consejo para mí, una palabra de aliento o un chiste para hacerme sonreír. Gracias por todo lo que me has enseñado y por todo lo que has hecho por mí. Y no dudes de que, tarde o temprano, volveré y conseguiremos nuestra ansiada enzima artificial.

Fue durante dicha beca de colaboración, entre valoración y valoración en el Bruker, donde te vi por primera vez. Desde entonces, Victoria, te has convertido en una persona muy especial para mí, por todo lo que me has ayudado, animado, por la paciencia que has tenido conmigo,... por estar siempre pendiente de mí, tanto que hasta te convirtieron en mi madre adoptiva... El laboratorio fue mucho más frío y aburrido sin ti. Muchas gracias por ser como eres, esta tesis no hubiera sido tesis sin ti.

Durante esos primeros meses, había una persona que se pasaba el día en el despacho de Quino escribiendo publicaciones. Muñiz, aunque al poco tiempo dejaste el laboratorio, sin embargo, siempre estuviste cercano a mí. Ya fuera desde Tarragona, Madrid o Chile, por teléfono, Skype o mail encontrabas la ocasión para recordarme que no se debe trabajar solo en un laboratorio. Siempre dejaste en un lugar secundario tus obligaciones para corregir cualquier cosa que te mandara y encontrar la coma, punto o espacio que faltaba. Así que, una parte de esta tesis también es tuya.

Aún recuerdo cómo, durante los primeros años, siempre que nos atascábamos Quino y yo en el laboratorio bajábamos a contarle nuestras penas a César, quien enseguida sacaba un papel y se ponía a garabatearnos nuevas opciones. César, gracias por estar siempre ahí cuando te he necesitado, cuando no funcionaba el Bruker, cuando tenía una ecuación con tropecientos incógnitas que resolver o una gráfica que representar...y cuando tenía cualquier duda. Y siempre con una sonrisa en la boca. Y gracias por fichar a Angélica. Chica-masas: la verdad es que fue un placer bajar a Masas y charlar contigo, saludarte desde el Bruker, apostar cuál sería nuestro siguiente exceso enantiomérico, bajar centrifugadoras desde el ático o hacer excursiones suicidas por las Quilamas... Fue una pena que tu beca se acabara tan pronto, te eché de menos.

Y fue en el servicio de Espectrometría de Masas de César, una mañana de septiembre, donde conocí por primera vez a Simón, recién llegado de Cambridge. Me habían contado maravillas de él y, con toda la razón: es una persona excepcional, tanto, que se convirtió en mi modelo a seguir. Muchas gracias por confiar en mí y preocuparte por mí. Gracias por llevarme de congreso a París y porque sin tus ánimos no me hubiera ido de estancia. Muchas gracias por tener siempre la puerta de tu despacho abierta para mí y por lanzar unos cálculos tras otros...*If only everything in life was as reliable as Luis Simón...*

En estos primeros meses también me presentaron a Paqui, responsable del Servicio de Difracción de Rayos X, mujer trabajadora al 100 %, capaz de conseguir que cristales diminutos difractaran lo suficiente para devolvernos una estructura. Muchas gracias Paqui porque siempre lo intentaste por pequeños que fueran los cristales.

Todo novato que entra en el departamento tiene que realizar el curso de Resonancia Magnética Nuclear. Ahí fue donde te conocí por primera vez, Anna, y donde me intentaste convencer que había que echarle más cloroformo al tubo, que no se podían mezclar disolventes deuterados ni hacerle espectros a tubos con "pececillos". Muchas gracias por pelearte por mis estructuras "que no relajaban

bien” y por toda tu ayuda. Gracias también por sacrificar vacaciones por rellenar el nitrógeno del Bruker, gracias a ti conseguiremos que sea el más longevo del mundo. Gracias también a Sergio, “chico-RMN”, por ajustarme el cloroformo cada vez que necesité el Varian. Fue una pena que la beca no durara más.

Lo cierto es que durante los primeros meses me sentía un poco solo en el laboratorio y envidiaba el buen ambiente que había en el laboratorio de al lado. Sin embargo, siempre estaban ahí cada vez que necesitaba una cosa, para organizar *group meetings* o para compartir congresos. Gracias Soledad por estar siempre a mi lado. Gracias Pablo por ese congreso en Oviedo, por las cenas de becarios en la sala de ordenadores hasta las tantas y por ser como eres, ojalá pudieras heredar un día ese laboratorio que tanto te gusta. Gracias Andrés por tu optimismo, por los buenos momentos en el frontón y por tu alma reivindicativa. Gracias Raquel por todo tu cariño, ojalá encuentres tiempo para acabar la tesis. Gracias David Benito por tu química imaginativa.

Con el tiempo fue apareciendo más gente. Gracias David G. Seisdedos, Rebeca y Tere (adoptada temporalmente de química-física), porque por fin tuve compañeros de laboratorio con los que compartir penas y alegrías, muchas gracias por la compañía. También a Silvia, aunque tu paso fue fugaz y casi no coincidimos. Gracias a Isabel y Ramón, porque las tardes de los viernes fueron menos solitarias con vosotros. Gracias Belén por dejarme colaborar contigo y enseñarme a medir valoraciones, y a Marina, por tu paciencia con Belén y conmigo con el fluorímetro, por tu alegría y optimismo.

También en el laboratorio de al lado se incorporaba más gente. Gracias David Clemente por todas tus palabras de ánimo, por tu ayuda, y por esos momentos de guitarrero en la facultad hasta las tantas. Gracias Maribel, Alejandro, Elisabeth y Matthias. Aunque no compartí mucho tiempo con vosotros, hicisteis que los *San Alberto* y las cenas en la sala de ordenadores fueran más animadas.

Aunque oficialmente realizaba la Tesis en el Departamento de Química Orgánica, apenas pasaron unos meses fui “adoptado” por el departamento de Química Analítica. Muchas gracias a todos y todas, de corazón, por acogerme como un analítico más, por permitirme acompañaros en cafés, cenas, cañas y fiestas hasta las tantas. Gracias Sarita, por compartir el congreso de Granada conmigo. Gracias Josemi, por las tardes de fútbol 7 y las cañas de después. Gracias Gloria, por todos tus consejos y tu amistad, no se me ha olvidado que tengo pendiente una visita a La Coruña. Gracias Lara por tu alegría, por tus palabras de ánimo y por enseñarme que no todo en la vida es química. Gracias Sara por tu sinceridad, por decir las cosas como las piensas y por esos dos conciertos de despedida. Gracias Raquel, ojos negros, por estar cerca de mí aunque estuviéramos lejos, por las noches de *messenger* durante la estancia, por los cafés en la máquina de los sábados y por todo tu cariño, mua. Gracias María, guapa, lista y madridista, por tener siempre una sonrisa en la boca. Gracias Ana, aunque siempre serás Valentina, por entenderme, por tu compañía las tediosas tardes de Escuela de Idiomas y por ser como eres, ¡no cambies nunca! Gracias Maite, por tus palabras de ánimo, por “huesitos” y “RR”, espero que vuelvas a rematar la tesina. Gracias Rosa y Leticia, por vuestra alegría y buen humor. Gracias también a Casas (prometo no volver a contaminar tus muestras con tolueno) y a Miguel, Patricia, Marta, Pedro, CrisFer, CrisGil y CrisPe. Gracias Milton por todos tus ánimos y por tu amistad a pesar de mi carácter.

Cabe destacar también que en este tiempo la cafetería de la facultad se convirtió en una extensión más del laboratorio: lugar donde discutir la síntesis de la siguiente molécula sobre una servilleta delante de una coca-cola. Esto no hubiera sido posible sin Vicente, “*Zidane de la hostelería*” y “*catedrático del fútbol*”, por todo lo que me has enseñado, por tu amistad, por guardarme los pinchos de las 7 de la tarde y por esos desayunos geniales. Gracias también a Estrella, no solo por tus exquisitas comidas, bocatas y tortilla de patatas, sino por ser como eres, gran amiga y mejor persona, gracias por cuidarme, preocuparte y estar pendiente de mí, por querer que fuera tu ojito derecho y también por darme un toque de atención cuando me estresaba demasiado, como solo hacen las personas que te quieren. Sé que aunque me vaya, seguiremos juntos. Gracias también a Alberto Lamas, Pirri o Sergi Roberto para los

amigos, por estar siempre pendiente de nosotros en el bar y por aguantar por las tardes hasta que bajaba a rematar los pinchos.

Llegó el momento de irse de estancia...y elegí Oxford...I would like to thank Professor Darren J. Dixon for the opportunity he gave me to spend three fabulous months in his research group in Oxford. It was an unforgettable experience for me. I am enormously acknowledged to Marta G. Núñez, because if you had not been there, I would not have gone. Thank you very much because you trust on me and all your help, not only with accommodation but also in the lab and with the postdoc!, and also thank you Dave, maybe one day we will be lab mates again. Thank you so much to Filippo Sladojevich, who was not only an excellent supervisor for me whom I learnt a lot of chemistry, but also a great friend. I wish we could work together someday. Thank you all of you, who helped me a lot in the lab and you accepted me as one of your own: Pavol, Eddy, Ben, Dave, Meiling, Swarup, Andrew, Alison, Michael, Isabelle, Iacovos and also Alba (although you were not in the DJD lab).

Cuando volví al laboratorio me encontré que se estaba llenando de gente, ¡ya no cabíamos! Llegó Sofía desde Lisboa y nos hizo internacionales, muchas gracias por tu compañía. María, con la que compartí la recolección de gramos de compuestos por el rotavapor, la mesa, el suelo... Muchas gracias por permitirme formar parte de tu trabajo. También Omayra, muchas gracias por esa sonrisa permanente que alegra el laboratorio, por tu compañía en el congreso de San Sebastián y por todos los buenos ratos. Te dejo como sucesora... ¡mucho suerte!... y... ¡cuídame a Quino! Además, se incorporó Laura, muchas gracias por poner un poco de orden en el laboratorio y estar siempre pendiente de destilar disolventes. Llegaron los gemelos, Fran y Ángel, muchas gracias por toda vuestra ayuda, por trabajar codo con codo conmigo, por muchos de los receptores de esta tesis, por estar siempre dispuestos para pasarme esta y aquella receta y, sobre todo... por los partidos de frontenis. Nos hicisteis mejores. Muchas gracias, porque sé que puedo contar con vosotros para cualquier cosas. Sois grandes. Gracias también a Olga, porque colaboraste conmigo en la síntesis de muchos huéspedes. Siento que tu paso por aquí no fuera más agradable, ojalá pudiera haber hecho algo más por ayudarte. Lo siento. Pero seguro que el futuro te deparará cosas grandes, mucha suerte.

Víctor y Leire, vuestro paso por aquí fue más breve de lo que me hubiera gustado, pero bueno, cada uno sigue su camino y... ¿quién sabe si nos volveremos a encontrar? Gracias Víctor por ser como eres, porque contigo el laboratorio fue mucho más divertido y las horas se pasaban más rápido entre chistes, bromas y rimas. Gracias sobre todo por la compañía los sábados. Eres un tío grande y llegarás lejos... ¡mucho suerte! Gracias Leire por irradiar esa alegría en el laboratorio y por quedarte hasta las tantas, así me sentía menos solo cuando daban las 9 y pico de la noche... Ojalá hubieras podido quedarte más tiempo por aquí. Eso sí, si alguna vez tengo mi propio grupo de investigación te buscaré para ficharte. Gracias también a Álvaro (que también has colaborado en este trabajo) y a Pablo, aunque vuestro paso haya sido un poco fugaz por el laboratorio, dejasteis huella, espero que volváis a hacer la tesina. Gracias también a todos los que han pasado por el masas de César y han compartido café con nosotros: a Pili, por todos tus ánimos y por ese remedio a base de zanahoria y miel contra la tos, ya verás como a partir de ahora va todo mucho mejor; gracias también a Diego, Tamara, Alba y Borja.

Gracias también a todos los que aún seguís por aquí, Sara (¡¡¡bueeenoooo!!!) ¡por fin una guijuelense en el laboratorio!, mucha suerte con la tesina, ¡ya la tienes acabada!; Antonio (por aquellos viernes por la tarde de beca de colaboración) y Guillermo, por continuar experimentando con este receptor que le va a dar al grupo muchas alegrías.

Y gracias a todos los profesores del departamento. Gracias Josefa por confiar en mí, por tu sinceridad y por todos tus consejos para que disfrutara más de la vida, ¡cuánta razón tienes! Gracias Cruz por estar siempre pendiente de mí y permitirme formar parte de tu trabajo. Gracias Rosa, Paco, Manolo y Chema por vuestras palabras de ánimo. Gracias también Jorge Cuéllar, Patricia y Alexandra, por esa

colaboración fructífera en el tema del biodiésel, creo que fue muy positiva para ambos y que nos enriquecimos mutuamente.

Gracias también a todos los becarios de Villabajo, por vuestra paciencia esperando a que acabara de ajustar el cloroformo en el Varian y por la compañía en los congresos. Ojalá llegue el día en que no estemos separados y Villarriba y Villabajo sean todo uno.

Esta tesis no hubiera sido posible sin el trabajo de Marisol y Marisa. Muchas gracias por encargarnos de todo el papeleo, por estar siempre pendientes de qué formulario teníamos que firmar, facturas que pagar, etc. Sin vosotras todo esto hubiera sido un caos. Gracias también a M^a José, por estar siempre dispuesta a llenarme el bote del cloroformo deuterado, por controlar que siempre tuviéramos disolventes y todo el material a punto y porque tú también sacrificaste tu tiempo libre para llenar de nitrógeno el Bruker.

Lo cierto es que es difícil seguir un orden cronológico en los agradecimientos, porque muchas de las personas a las que les estoy agradecido han convivido conmigo durante todos estos años. Mención especial merecen todos los que, afortunadamente, me habéis mostrado que hay una vida fuera del laboratorio:

Gracias Tere y Jorge, porque la amistad adquirida durante la carrera se mantuvo en estos años de doctorado. Gracias por los momentos de café donde contarnos nuestras penas y donde desconectar del trabajo diario. Muchas gracias también a M^a Jesús, Luis y Raquel Louçao, porque aunque nos veamos con poca frecuencia, siempre habéis sido un apoyo desde la distancia.

Gracias Cristina González-Maza, por tu amistad de toda la vida, por estar siempre ahí para un café, un batido, una peli o un concierto de Loquillo. Gracias por el viaje a Oporto y por animarme siempre que lo he necesitado. Gracias Cristina Encinas por todas esas San Silvestres, excursiones y partidos de fútbolín, gracias por ser una persona encantadora y por los grandes momentos que hemos compartido. Gracias Pepe Cerveró, porque fuiste el culpable de que me apuntara a la moda del *running* y por tus sabios consejos en este tramo final de la tesis. ¡Ojalá pudieras estar aquí! Gracias Beatriz por todo tu apoyo y comprensión constante, por animarme y prestarme tu ayuda, por las conversaciones por Skype... Gracias por preocuparte por mí. Gracias Carmen Plaza, porque por culpa de la tesis Quino pasó menos tiempo contigo y Sara, sin embargo, no te importó. Gracias por organizar esas fantásticas excursiones, ideales para desconectar del laboratorio y por todo tu ánimo y frases de apoyo: *"En esta vida, si no se es persistente, no se consigue nada"*.

Aunque os haya dejado para el final, en realidad os conozco desde hace casi 11 años y prácticamente desde que llegué a Salamanca os convertisteis en mi segunda familia. Muchas gracias Diego, Soledad y Juan. Gracias por cuidar de mí, por estar pendientes, por la compañía, por no dejarme solo y por dejarme formar parte de vuestros grandes momentos. Gracias Diego por estar siempre pendiente del papeleo, las becas, los impresos... Sin ti a mi lado creo que se me hubieran pasado todos los plazos. Gracias por tu paciencia conmigo y sobre todo por darme un toque de atención cuando más lo necesitaba, como sólo los amigos de verdad saben hacer. Gracias Soledad, la mejor química orgánica que conozco. Al estar cerca de mí, en el laboratorio de al lado, siempre me diste tranquilidad. Gracias por todo tu cariño, tus palabras de ánimo, por tu confianza, por escucharme cuando estaba hecho un lío y no sabía qué decidir. Gracias por los paseos, excursiones, cenas, baños en el Puente Congosto... no sé cómo te lo podré agradecer. Gracias Juan, la persona más increíble que conozco, por estar siempre ahí, por todos tus consejos y ayuda, por cuidar de mí, por los correos, sms y *whatsapps* con un mensaje de ánimo. Todo el mundo sabe que eres una persona excepcional y, para mí, ha sido un lujo poder compartir alegrías, tristezas y confidencias... contigo, no cambies nunca por favor.

Gracias Oscar por estar siempre a mi lado en estos años, por poner un poco de sentido común en mi cabeza de cabra loca, por escucharme y porque siempre encontraste momentos para hacerme desconectar del trabajo, una pena que no pudiéramos compartir piso más tiempo. Gracias papá y mamá, por todo lo que habéis trabajado, luchado y sacrificado para que yo haya podido llegar hasta aquí. Nunca podré agradeceros todo lo que habéis hecho por mí. Muchas gracias por vuestra comprensión, por todos los fines de semana que esperabais que fuera a veros y me quedaba trabajando y siempre sin ningún reproche; sin vosotros a mi lado yo no sería nada.

Para ser políticamente correcto (o incorrecto), creo que también es necesario mencionar a los evaluadores del Ministerio y de la Junta de Castilla y León que financiasteis solo una parte de este trabajo y que considerasteis que parte de la tesis que aquí se presenta no debería haber existido. Gracias también porque, a pesar de ponérselo difícil, nos hicisteis más fuertes.

Gracias a todos aquellos que haya olvidado mencionar y que habéis compartido estos años conmigo y habéis hecho que este trabajo fuera posible.

INDEX

Abbreviations and Acronyms.....	XIX
INTRODUCTION.....	1
- Introduction.....	3
- Background of our research group.....	11
- Objectives.....	17
CHAPTER 1: L-proline-derived catalysts for aldol reactions.....	19
1.1 Introduction.....	21
1.1.1. Advantages of proline as catalyst.....	34
1.1.2. Disadvantages of proline as catalyst.....	35
1.1.3. Other catalysts used in the intramolecular aldol reaction.....	36
1.2. Methods and results.....	39
1.2.1. Synthesis of xanthene derived catalysts.....	39
1.2.2. Catalytic studies.....	43
1.2.3. Prolinamides synthesis.....	44
1.2.4. Catalytic studies in the preparation of the Hajos-Wiechert ketone.....	45
1.2.5. Study of the reaction intermedia in the preparation of the Hajos-Wiechert ketone.....	46
1.2.6. Catalytic studies in the preparation of the Wieland-Miescher ketone.....	48
1.2.7. Study of the reaction intermedia in the preparation of the Wieland-Miescher ketone.....	49
1.3. Conclusions.....	51
1.4. Experimental.....	53
CHAPTER 2: Study of the aldol reaction mechanism catalysed by prolinamides.....	61
2.1. Introduction.....	63
2.2. Methods and results.....	67
2.2.1. Mechanistic studies in CDCl ₃	67
2.2.1.1. Reaction between acetone and 4-nitrobenzaldehyde catalysed by prolinamide 20	67
2.2.1.2. Imidazolidinones isolation.....	70
2.2.1.3. Influence of acidity of the prolinamide NH in the imidazolidinone formation.....	74
2.2.1.4. Influence of various additives on the rate of formation of the imidazolidinones.....	75
2.2.2. Mechanistic studies in deuterioacetone.....	77
2.2.2.1. Reaction between acetone and 4-nitrobenzaldehyde catalysed by prolinamide 20	77
2.2.2.2. Deuteration and enamine formation studies.....	80
2.2.2.3. Reactivity studies of imidazolidinone 23	83
2.2.3. Mechanistic studies in deuteromethanol.....	87
2.2.3.1. Reaction between imidazolidinone 23 and 4-nitrobenzaldehyde.....	87
2.2.4. Reaction between imidazolidinone 30 and different aldehydes.....	88
2.2.5. Racemization studies of aldol 25 in CDCl ₃	89
2.2.6. Deuteration in CD ₃ OD: Ene Mechanism.....	92
2.2.7. Formation of the iminium salt.....	93
2.2.8. Measure of acidity through competitive titrations.....	94
2.2.9. Reaction between acetone and 4-nitrobenzaldehyde under catalytic conditions.....	96

2.2.10. Proposed reaction mechanism.....	99
2.3. Conclusions.....	103
2.4. Experimental.....	105
CHAPTER 3: Organocatalysts derived from <i>trans</i>-1,2-cyclohexanediamine.....	111
3.1. Introduction.....	113
3.2. Methods and results.....	121
3.2.1. Preparation of urea 39	121
3.2.2. Ureas synthesis.....	122
3.2.3. Carbamoyl derivatives preparation.....	123
3.2.4. Thiocarbamoyl derivatives preparation.....	124
3.2.5. Sulfonamides preparation.....	126
3.2.6. Direct preparation (" <i>one-pot</i> ") of carbamate 47 from urea 39	125
3.2.7. Preparation of other cyclohexanediamine derivatives from compound 47	125
3.2.8. Catalytic properties of the synthesized organocatalysts.....	127
3.3. Conclusions.....	133
3.4. Experimental.....	135
CHAPTER 4: Catalysts for transesterification reactions.....	143
4.1. Introduction.....	145
4.1.1. Catalysts used in biodiesel obtention.....	149
4.1.2. Twitchell reagents.....	153
4.2. Methods and results.....	155
4.2.1. Synthesis of Twitchell catalyst.....	155
4.2.2. Catalytic properties of Twitchell reagents.....	156
4.2.3. Lipophilic sulfonic acids.....	157
4.2.4. Influence of free fatty acids in the oil.....	161
4.2.5. Influence of water content.....	162
4.2.6. Influence of methanol/triglyceride ratio.....	163
4.2.7. Influence of the catalyst amount.....	164
4.2.8. Influence of temperature.....	165
4.2.9. Influence of the oil type.....	165
4.2.10. Catalyst recovery.....	166
4.2.11. Measure of the biodiesel acidity.....	169
4.2.12. Study of the reaction mechanism.....	170
4.2.13. Catalysts with two sulfonic acids.....	179
4.2.14. Other catalysts.....	192
4.2.14.1. Catalysts with two and three sulfonic groups.....	192
4.2.14.2. Catalysts based on phosphonic acids.....	194
4.2.14.3. Catalysts with a nucleophilic hydroxyl group.....	195
4.3. Conclusions.....	199
4.4. Experimental.....	201
CHAPTER 5: Benzofuran-based tripodal receptors.....	211
5.1. Introduction.....	213
5.1.1. The three-point model.....	214
5.1.2. Previous research in our group.....	217
5.2. Methods and results.....	221
5.2.1. Benzofuran skeleton preparation.....	221
5.2.2. Functionalization of the skeleton to create an oxyanion-hole analogue.....	229
5.2.3. Study of receptor 94 supramolecular properties.....	238

5.2.4. Study of receptor 94 enantioselective recognition.....	242
5.2.5. Search for the chiral guest.....	247
5.2.6. Resolution of receptor 94 racemic mixture.....	257
5.2.7. Complexes structure.....	262
5.3. Conclusions.....	273
5.4. Experimental.....	275
CHAPTER 6: New benzofuran-derived receptors.....	293
6.1. Introduction.....	295
6.2. Methods and results.....	297
6.2.1. Receptor with less steric hindrance.....	297
6.2.2. Receptor with more hydrogen bond donors.....	299
6.2.3. Enol receptor.....	303
6.2.3.1. Synthesis and properties.....	303
6.2.3.2. Racemic mixture resolution through enantioselective extraction.....	311
6.2.3.3. Racemic mixture resolution through fractional crystallization.....	323
6.2.3.4. Amino acids and its derivatives extraction.....	329
6.2.4. Other receptors.....	333
6.3. Conclusions.....	343
6.4. Experimental.....	345
CHAPTER 7: Bifunctional benzofuran-derived catalysts	363
7.1. Introduction.....	365
7.2. Methods and results.....	367
7.2.1. Receptor 149 synthesis.....	347
7.2.2. Receptor 149 racemic mixture resolution.....	371
7.2.3. Receptor 182 synthesis.....	374
7.2.4. Receptor 182 racemic mixture resolution.....	375
7.2.5. Study of receptor 182 properties.....	381
7.2.5.1. Amino acids extraction.....	383
7.2.5.2. Catalysis studies.....	388
7.2.5.2.1. Diels-Alder reaction.....	388
7.2.5.2.2. Michael additions.....	389
7.2.5.2.3. Aldol reaction.....	390
7.2.5.2.4. Morita-Baylis-Hillman.....	390
7.2.5.2.5. Addition of alcohols to epoxides and tetrahydropyrans.....	391
7.2.5.2.6. Transesterification.....	391
7.2.5.2.7. Anhydrides alcoholysis.....	392
7.2.5.2.8. Dynamic kinetic resolution of azlactones.....	393
7.2.5.2.8.1. Kinetic study.....	399
7.2.5.2.8.2. Catalysis study.....	403
7.2.6. Preparation of a catalyst soluble in non-polar solvents.....	407
7.3. Conclusions.....	411
7.4. Experimental.....	413
APPENDIX A.1.....	419
A.1.1. Instrumental and chromatographic techniques.....	421
A.1.2. Scientific articles.....	427
APPENDIX A.2. Spectroscopy and Spectrometry.....	473

CD-ROM content:

A CD-ROM is included at the end of the memory with a digitized version of the Thesis in Spanish and English. ^1H NMR, ^{13}C NMR, IR, MS and HRMS of all new synthesized compounds have also been attached. Bidimensional spectra such as COSY, HMQC, HMBC and ROESY have been included for receptors. Crystal and refinement data are also collected.

ABBREVIATIONS AND ACRONYMS

α : specific rotation

A: ampere

Å: Ångström

ac: acid

AcOH: acetic acid

Ala: alanine

Ar: aromatic ring

Arg: arginine

Asn: asparagine

Asp: aspartic acid

AZ: azlactone

B3LYP: 3-parameter hybrid Becke exchange/Lee-Yang-Parr correlation functional

Bn: benzyl

Boc: *tert*-butyloxycarbonyl

Bz: benzoyl

c: concentration (g/100 mL)

calcd: calculated

cat: catalyst

Cbz: carboxybenzyl

CCD: charge-coupled device

¹³C NMR: carbon nuclear magnetic resonance

CoA: coenzyme A

COSY: correlation spectroscopy

CPK: molecular models created by R. Corey, L. Pauling and W. Koltun.

δ : chemical shift in parts per million downfield from tetramethylsilane

d: doublet

DABCO: 1,4-diazabicyclo[2.2.2]octane

DBU: 1,8-diazabicyclo[5.4.0]undec-7-ene

DCC: *N,N'*-dicyclohexylcarbodiimide

dd: doublet of doublets

DFT: density functional theory

Diglyme: diethylene glycol dimethyl ether

DMAP: 4-(*N,N*-dimethylamino)pyridine

DMF: dimethylformamide

DMSO: dimethyl sulfoxide

DNA: deoxyribonucleic acid

dt: doublet of triplets

E: electrófilo

ee: exceso enantiomérico

EI: ionización por impacto electrónico

eq/equiv: equivalent

ESI: ionización por electrospray

ET: estado de transición

EtOAc: ethyl acetate

exp: experimental

Glu: ácido glutámico

Gly: glicina

h: horas

HFPA: hexafluorophosphoric acid

His: histidine

HMBC: heteronuclear multiple bond correlation

HMPA: hexamethylphosphoric triamide (hexamethylphosphoramide)

HMQC: heteronuclear multiple quantum correlation

¹H NMR: proton nuclear magnetic resonance

HOMO: highest occupied molecular orbital

HPLC: high performance liquid chromatography

HRMS: high-resolution mass spectrometry

Hz: hertz

***i*Pr:** isopropilo

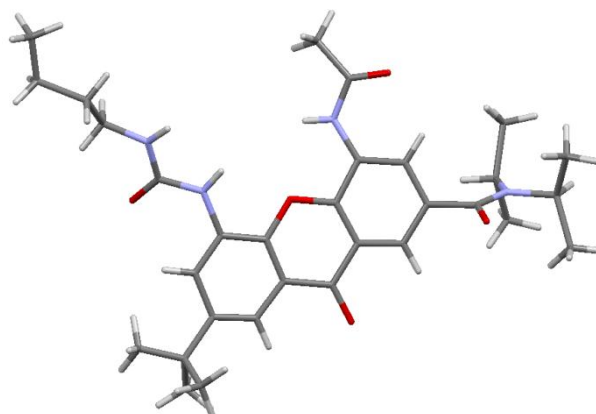
***i*-PrOH**: isopropyl alcohol
IR: infrared
J: coupling constant
***K*_{ass}**: association constant
kcal: kilocalories
 λ : wavelength
Leu: leucine
LUMO: lowest unoccupied molecular orbital
Lys: lysine
m: multiplet
min: minutes
Ms: mesyl (methylsulfonyl)
MS: mass spectrometry
n.d.: not determined
Nu: nucleophile
o: orto
ORTEP: oak ridge thermal-ellipsoid plot program
p: para
PCM: polarizable continuum model
Ph: phenyl
Phe: phenylalanine
PheGly: phenylglycine
ppm: part(s) per million
Pro: proline
***p*TsOH**: *p*-toluensulfonic acid
q: quartet
quant: quantitative
quint: quintet
ref: reference
refl: reflux



**VNIVERSIDAD
D SALAMANCA**

CAMPUS DE EXCELENCIA INTERNACIONAL

INTRODUCTION



Introduction

Since its beginnings, humans have always tried to mimic nature, not only in the idea of flying like birds or diving like fish. In 1941, the Swiss engineer George Mestral invented Velcro® after removing from his dog a species of thistle and watch carefully how had become entangled in its hair. Nowadays, intense research has led to the invention of new materials with incredible properties, thanks to a careful observation of nature: thus, shark skin has been used to create new materials that reduce friction with water or prevent growth of bacteria, termite mounds have been used as inspiration to build new ventilation systems, and the spider web to create new bulletproof vests.¹ However, this is not a simple copy of nature, humans are inspired by what they see in nature and then they modify or improve it: thus, a Boeing 747 is not just a bird on a larger scale, but man has taken the basic idea of using wings as birds and insects, finding other ways to generate the power needed to fly.²

¹ Benyus, J. M. *Biomimicry: Innovation Inspired by Nature*; William Morrow & Company: New York, 1997.

² Ball, P. *Stories of the Invisible: A Guided Tour of Molecules*; Oxford University Press: Oxford, 2001.



R. Breslow

Chemistry has not been left behind in this trend and in 1972, Ronald Breslow coined the term "Biomimetic Chemistry"³ to refer to the part of chemistry that is inspired by the way living systems work. The field of catalysis of chemical reactions has not remained immune to this idea and since its inception, organic chemists have tried to mimic the most efficient catalysts known: the enzymes. Enzymes are protein molecules selected over millions of years to catalyse chemical reactions in nature. They are composed of hundreds or thousands of amino acids, although only a few residues are directly involved in catalysis. The remaining amino acids are responsible for generating a defined three-dimensional structure capable of associating a specific substrate, in the so-called "hydrophobic pocket" with hydrophobic interactions, hydrogen bonds, electrostatic attractions, van der Waals forces, dipole interactions, etc.

So far, there is still no consensus on how enzymes catalyse chemical reactions, having been proposed many different hypotheses: enzyme-substrate complementarity, transition state theory, reduction of activation entropy, destabilization of the ground state, low barrier hydrogen bond formation, tunnelling proton effect, cooperative effect, etc. Probably several of these theories are complementary, and the mode of action of a certain enzyme depends on its nature.

In 2013, the Nobel Prize in Chemistry was awarded to Karplus, Levitt and Warshel by the development of "multiscale models for complex chemical systems". One of the most important and striking applications of these models is precisely the study of enzymatic reactions.⁴

The "mimics" of enzymes began in the 60s with the pioneering work of Curtis,⁵ Busch,⁶ Jäger⁷ and Pedersen,⁸ describing macrocycles able to associate metal cations. Conceptually, these systems can be considered a model of existing macrocycles in nature (ionophores, heme groups, porphyrins, etc.).

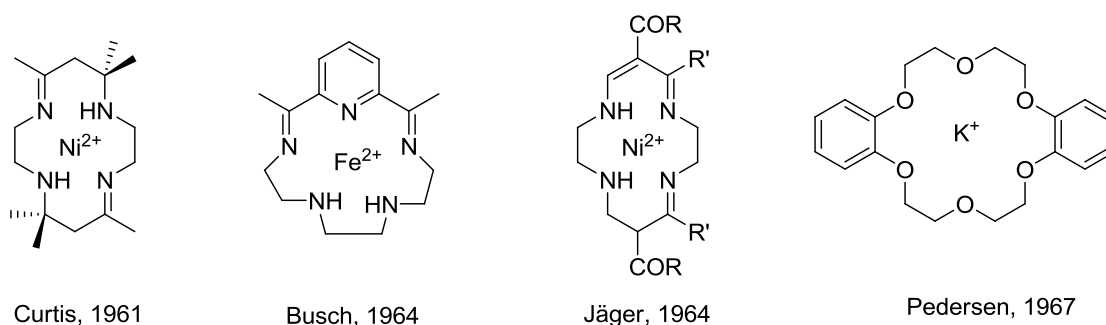


Figure 1. Macrocycles developed by Curtis, Busch, Jäger and Pedersen in the 60s.

³ Breslow, R. *Chem. Soc. Rev.* **1972**, *1*, 553-580.

⁴ <http://www.nobelprize.org>, consulted in march 2014.

⁵ Curtis, N. F.; House, D. A. *Chem. and Ind.* **1961**, *42*, 1708-1709.

⁶ Curry, J. D.; Busch, D. H. *J. Am. Chem. Soc.* **1964**, *86*, 592-594.

⁷ Jäger, E. G. *Z. Chem.* **1964**, *4*, 437-438.

⁸ (a) Pedersen, C. J. *J. Am. Chem. Soc.* **1967**, *89*, 2495-2496; (b) Pedersen, C. J. *J. Am. Chem. Soc.* **1967**, *89*, 7017-7036.

Here we must add the work done by Donald Cram⁹ on macrocyclic cyclophanes (in the 50s) and Jean-Marie Lehn¹⁰ on spherands and carcerands (in the 60s). These contributions showed that a molecule was capable of interacting with another molecule to produce a complex or supermolecule by noncovalent interactions as hydrogen bonds, ion-pair interactions, π - π interactions, van der Waals forces, etc.

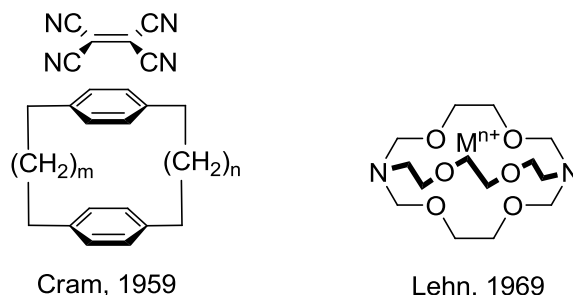


Figure 2. Macrocycles developed by Cram and Lehn.

This work laid the foundations for the "Host-Guest" or Supramolecular Chemistry,¹¹ which was established after the concession of the 1987 Nobel Prize in Chemistry to Donald J. Cram, Jean-Marie Lehn and Charles J. Pedersen "for the development and use of high-specific structural selectivity" molecules.



Donald J. Cram Jean-Marie Lehn Charles J. Pedersen

This new possibility, the interaction between molecules to generate supramolecular aggregates, is an approach to the form in which enzymes act on nature, forming an enzyme-substrate complex. Quickly, molecules capable of associating not only metal cations, but any other compound of interest were developed, in a similar way to an enzyme which associates its substrate.

Breslow, in 1969,¹² using cyclodextrins, made the first molecules capable of behaving as enzymes. Afterwards many other compounds were created: calixarenes, cyclophanes, carcerands, spherands, etc. They act as hosts that simulate the hydrophobic pocket of the enzymes at a molecular level. They associate the substrates in a similarly way enzymes do, yielding catalysis with reaction rate increases on the order of 10^{10} because they are capable of positioning the substrate close to the active site in a favourable orientation.

⁹ Cram, D. J.; Bauer, R. H. *J. Am. Chem. Soc.* **1959**, *81*, 5971-5977.

¹⁰ (a) Dietrich, B.; Lehn, J.-M.; Sauvage, J.-P. *Tetrahedron Lett.* **1969**, *10*, 2885-2888; (b) Dietrich, B.; Lehn, J.-M.; Sauvage, J.-P. *Tetrahedron Lett.* **1969**, *10*, 2889-2892.

¹¹ Steed, J. W.; Atwood, J. L. *Supramolecular Chemistry*, 2nd ed.; John Wiley & Sons: Chichester, 2009.

¹² Breslow, R.; Campbell, P. *J. Am. Chem. Soc.* **1969**, *91*, 3085-3085.

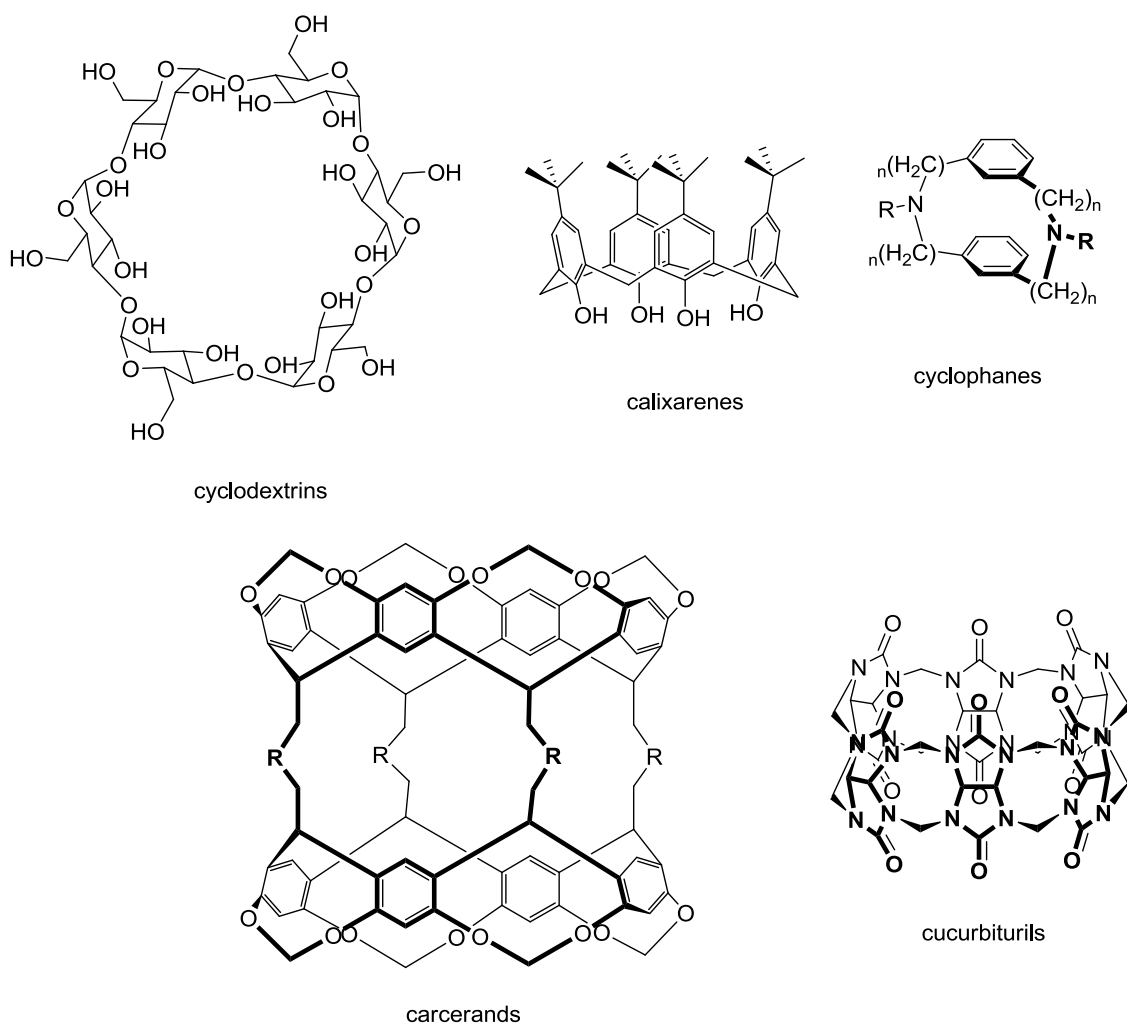


Figure 3. Molecules that mimic the hydrophobic pocket of the enzyme.

Furthermore, different groups could be attached on these compounds to provide catalytic activity, just as several residues in the active center of the enzymes confer catalytic activity to them. In addition, it was found that all these compounds followed Michaelis-Menten kinetics and, in fact, began to be called "artificial enzymes" (although this term is now used to refer to the compounds obtained by site-directed mutagenesis). Thus, men and women have succeeded in the preparation of molecules that mimic the mode of action of many enzymes, being able to carry out hydrolysis reactions (nucleases, proteases and artificial chymotrypsin), esterifications, transesterifications (artificial transacylases), benzoin condensations (thiamine artificial pyrophosphate), oxidations (methane monooxygenase, artificial cytochrome P450), etc.

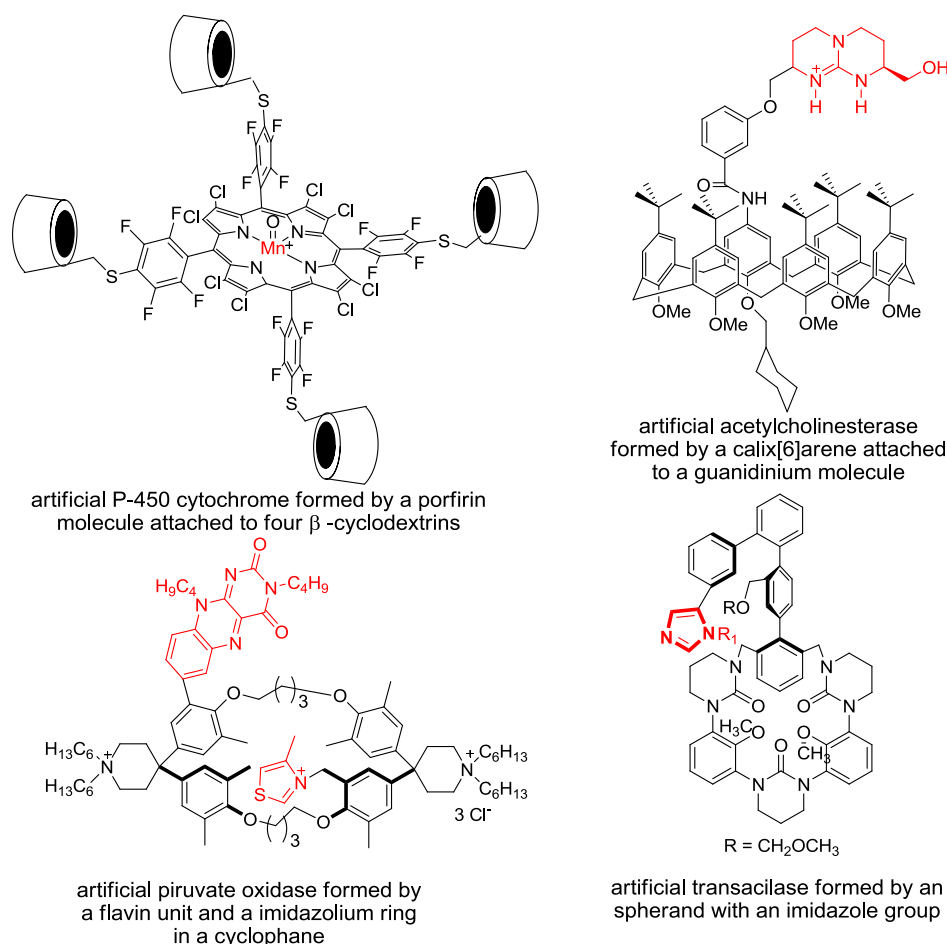


Figura 4. Examples of artificial enzymes.¹³ The catalytic group is shown in red.

Advances in this field have been enormous, as can be seen in several review articles.¹⁴ However, it has not been achieved reaction rates comparable to those of the enzymes yet, so this field continues in full development.

¹³ (a) Yang, J.; Gabriele, B.; Belvedere, S.; Huang, Y.; Breslow, R. *J. Org. Chem.* **2002**, *67*, 5057-5067; (b) Cuevas, F.; Di Stefano, S.; Magrans, J. O.; Prados, P.; Mandolini, L.; de Mendoza, J. *Chem. Eur. J.* **2000**, *6*, 3228-3234; (c) de Mendoza, J.; Alcázar, V.; Botana, E.; Galán, A.; Lu, G.; Magrans, J. O.; Martín-Portugués, M.; Prados, P.; Salmerón, A.; Sánchez-Quesada, J.; Seel, C.; Segura, M. *Pure Appl. Chem.* **1997**, *69*, 577-582; (d) Magrans, J. O.; Ortiz, A. R.; Molins, A.; Lebouille, P. H. P.; Sánchez-Quesada, J.; Prados, P.; Pons, M.; Gago, F.; de Mendoza, J. *Angew. Chem., Int. Ed. Engl.* **1996**, *35*, 1712-1715; (e) Cram, D. J.; Lam, P. Y.-S.; Ho, S. P. *J. Am. Chem. Soc.* **1986**, *108*, 839-841; (f) Mattei, P.; Diederich, F. *Helv. Chim. Acta* **1997**, *80*, 1555-1588.

¹⁴ (a) Breslow, R. *Artificial Enzymes*; Wiley-VCH: Weinheim, 2005; (b) Raynal, M.; Ballester, P.; Vidal-Ferran, A.; van Leeuwen, P. W. N. M. *Chem. Soc. Rev.* **2014**, *43*, 1660-1733; (c) Raynal, M.; Ballester, P.; Vidal-Ferran, A.; van Leeuwen, P. W. N. M. *Chem. Soc. Rev.* **2014**, *43*, 1734-1787; (d) Bjerre, J.; Rousseau, C.; Marinescu, L.; Bols, M. *Appl. Microbiol. Biotechnol.* **2008**, *81*, 1-11; (e) Marinescu, L.; Bols, M. *Trends Glycosci. Glycotechnol.* **2009**, *21*, 309-323; (f) Geibel, B.; Merschky, M.; Rether, C.; Schmuck, C. *Supramolecular Chemistry: From Molecules to Nanomaterials*; Steed, J. W.; Gale, P. A., Ed.; John Wiley & Sons: New York, 2012; (g) Dong, Z. Y.; Luo, Q.; Liu, J. Q. *Chem. Soc. Rev.* **2012**, *41*, 7890-7908; (h) Feiters, M. C.; Rowan, A. E.; Nolte, R. J. M. *Chem. Soc. Rev.* **2000**, *29*, 375-384; (i) Motherwell, W. B.; Bingham, M. J.; Six, Y. *Tetrahedron* **2001**, *57*, 4663-4686; (j) Karakhanov, E. E.; Maksimov, A. L.; Runova, E. A.; Kardasheva, Y. S.; Terenina, M. V.; Buchneva, T. S.; Guchkova, A. Y. *Macromol. Symp.* **2003**, *204*, 159-173; (k) Vriezema, D. M.; Aragones, M. C.; Elemans, J. A. A. W.; Cornelissen, J. J. L. M.; Rowan, A. E.;

In 2000, a new way to catalyse chemical reactions in addition to enzymatic (natural or artificial) and organometallic catalysis appears: "organocatalysis" or the catalysis of chemical reactions with small organic molecules.¹⁵ Actually, organocatalysts could also be considered artificial enzymes which lack the hydrophobic environment of cyclodextrins, calixarenes, cyclophanes, etc. but mimic the "active site", with two or three functional groups which are enough to carry out catalysis with good reaction rates and excellent enantiomeric excesses.

Although several authors had used alkaloids to catalyse different reactions in the early and mid-twentieth century,¹⁶ the key event in the history of organocatalysis was the discovery, in the early 1970s, of the asymmetric Robinson annulation of a triketone, by a molecule as simple as *L*-proline.¹⁷

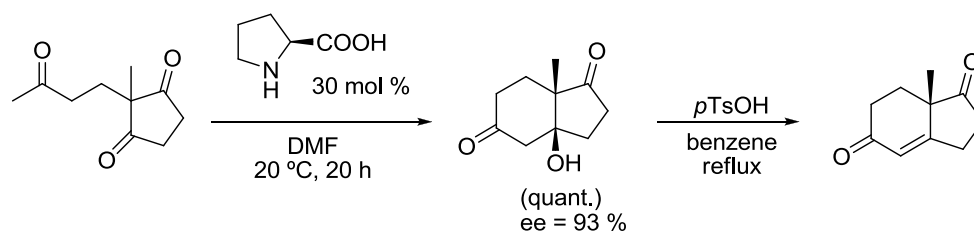


Figure 5. Intramolecular aldol condensation mediated by *L*-proline.

This ketone and other similar materials have proven to be very important chiral starting materials in the preparation of many compounds of biological and pharmaceutical interest.¹⁸

Nolte, R. J. M. *Chem. Rev.* **2005**, *105*, 1445-1489; (l) Bellia, F.; La Mendola, D.; Pedone, C.; Rizzarelli, E.; Saviano, M.; Vecchio, G. *Chem. Soc. Rev.* **2009**, *38*, 2756-2781; (m) Schuhle, D. T.; Peters, J. A.; Schatz, J. *Coord. Chem. Rev.* **2011**, *255*, 2727-2745.

¹⁵ Ahrendt, K. A.; Borths, C. J.; MacMillan, D. W. C. *J. Am. Chem. Soc.* **2000**, *122*, 4243-4244.

¹⁶ (a) Breiding, G.; Fajans, K. *Ber. Deutsch. Chem. Ger.* **1908**, *41*, 752-763; (b) Vavon, M. M.; Peignier, P. *Bull. Soc. Fr.* **1929**, *45*, 293; (c) Wegler, R. *Justus Liebigs Ann. Chem.* **1932**, *498*, 62-76; (d) Prelog, V.; Wilhelm, M. *Helv. Chim. Acta* **1954**, *37*, 1634-1660; (e) Pracejus, H. *Justus Liebigs Ann. Chem.* **1960**, *634*, 9-22; (f) Helder, R.; Arends, R.; Bolt, W.; Hiemstra, H.; Wynberg, H. *Tetrahedron Lett.* **1977**, *25*, 2181-2182; (g) Wynberg, H. *Top. Stereochem.* **1986**, *16*, 87-129.

¹⁷ (a) Hajos, Z. G.; Parrish, D. R. *J. Org. Chem.* **1974**, *39*, 1615-1621; (b) Eder, U.; Sauer, G.; Wiechert, R. *Angew. Chem. Int., Ed. Eng.* **1971**, *10*, 496-497.

¹⁸ Guillena, G.; Nájera, C.; Ramón, D. J. *Tetrahedron: Asymmetry* **2007**, *18*, 2249-2293.

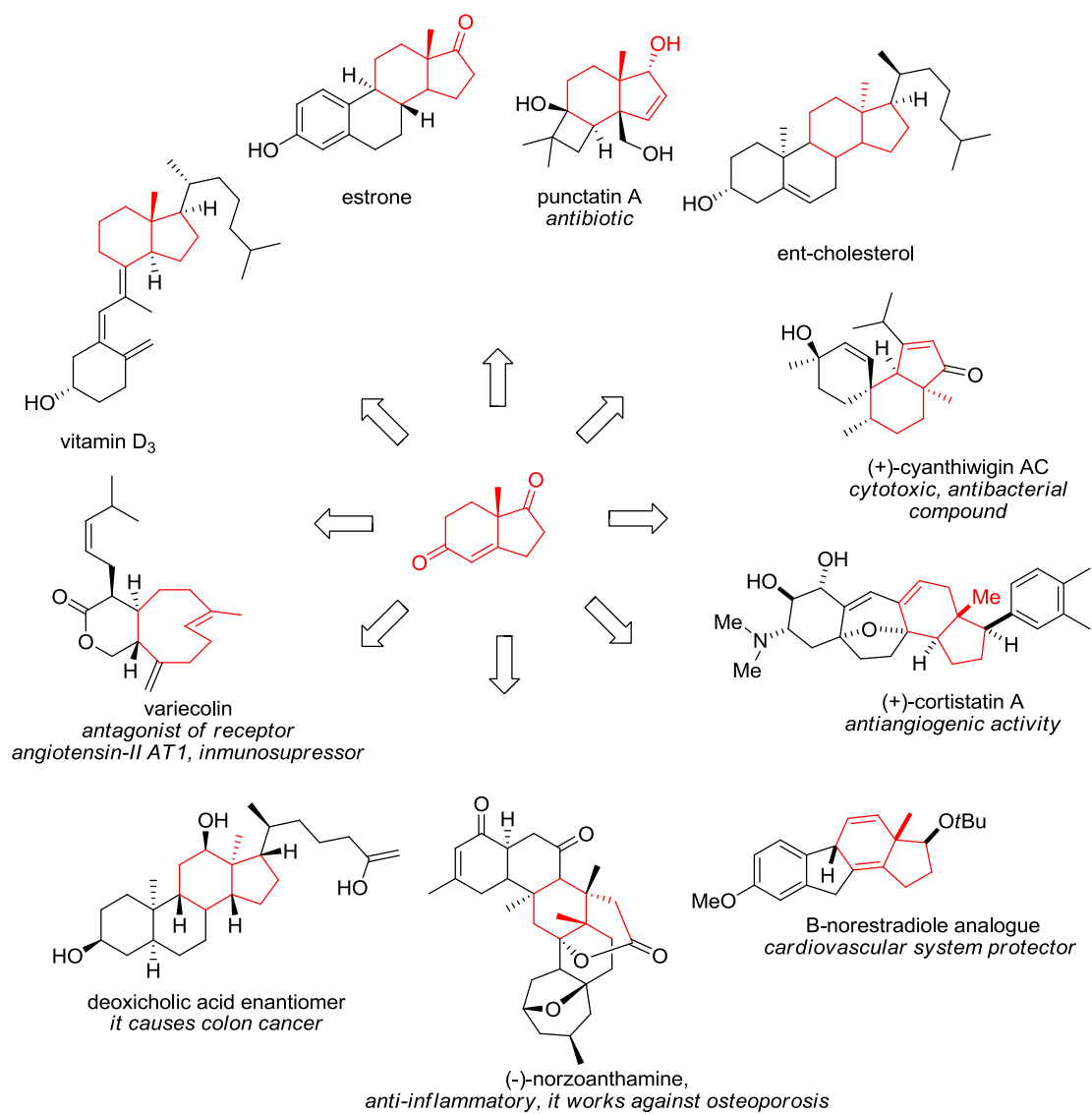


Figure 6. Compounds with biological activity obtained from the Hajos-Wiechert ketone.

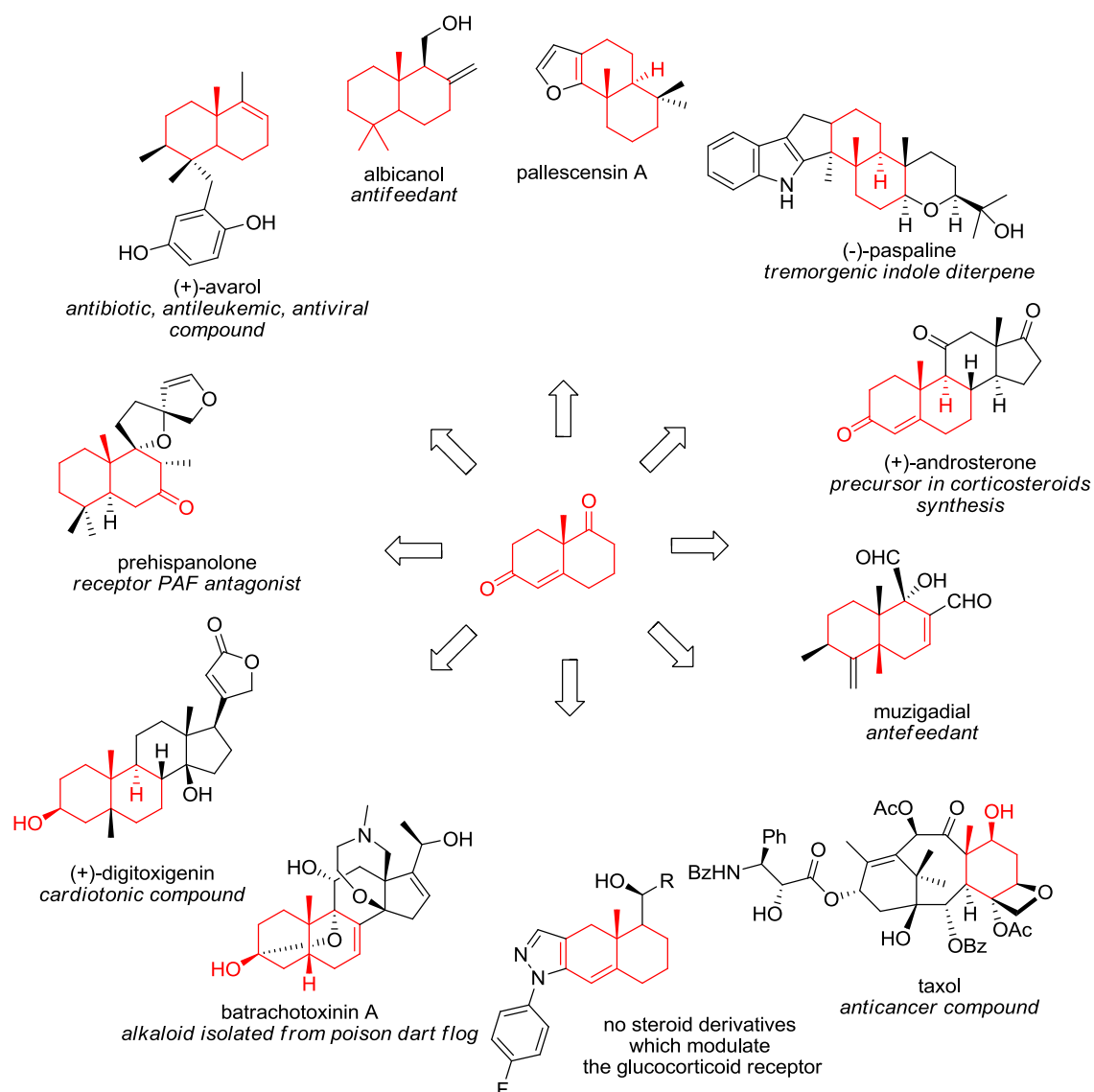


Figure 7. Compounds with biological activity obtained from the Wieland-Miescher ketone.

Few years later, proline showed great versatility in various reactions: intermolecular aldol reaction, Mannich, Michael, Diels-Alder, Baylis-Hillman, etc.¹⁹ in such a way that Jacobsen came to baptize proline as “the simplest enzyme”.²⁰

In fact, its mode of action in aldol reactions is similar to the mode action of type I aldolases, where a lysine residue forms an enamine which attacks a carbonyl group, activated by a carboxyl group of a glutamic acid residue. In the case of proline, the amino group and the carboxyl group are located in the same molecule.²¹

¹⁹ List, B. *Tetrahedron* **2002**, *58*, 5573-5590.

²⁰ Movassaghi, M.; Jacobsen, E. N. *Science* **2002**, *298*, 1904-1905.

²¹ Gröger, H.; Wilken, J. *Angew. Chem., Int. Ed.* **2001**, *40*, 529-532.

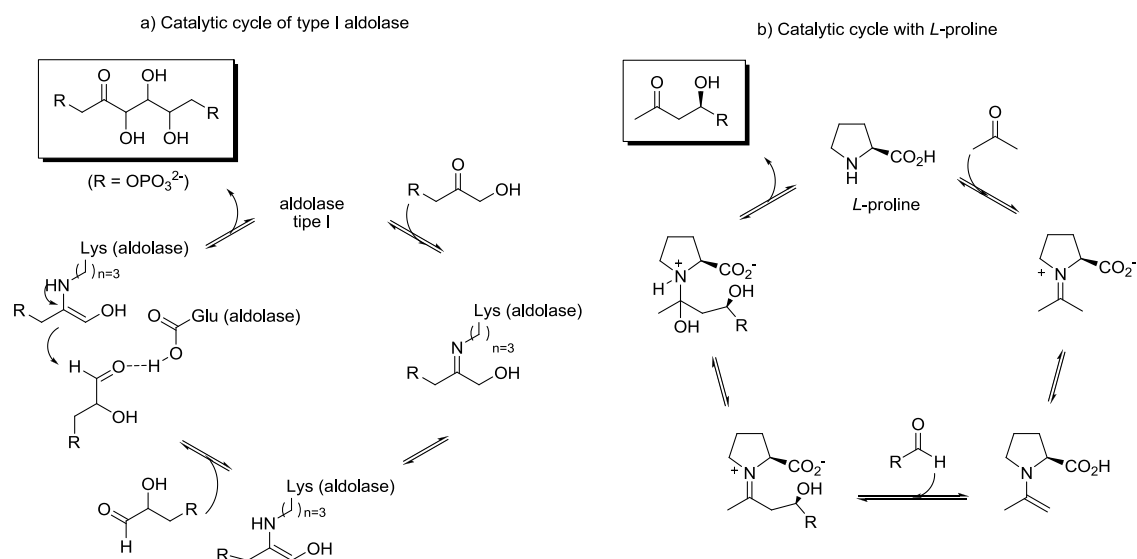


Figure 8. Catalytic cycle of the aldol reaction catalysed by a type I aldolase (a) and L-proline (b).

Background of our research group

Traditionally, our research group has developed catalysts for several chemical reactions, based on forming an associate between the substrate and a receptor so that the substrate is enabled to carry out the reaction in the asymmetric environment of the host, ensuring the enantioselectivity of the product. In addition, it is intended that in the transition state of the reaction the associate is stronger (Pauling hypothesis), with the intention of decreasing the activation barrier and achieve catalysis.

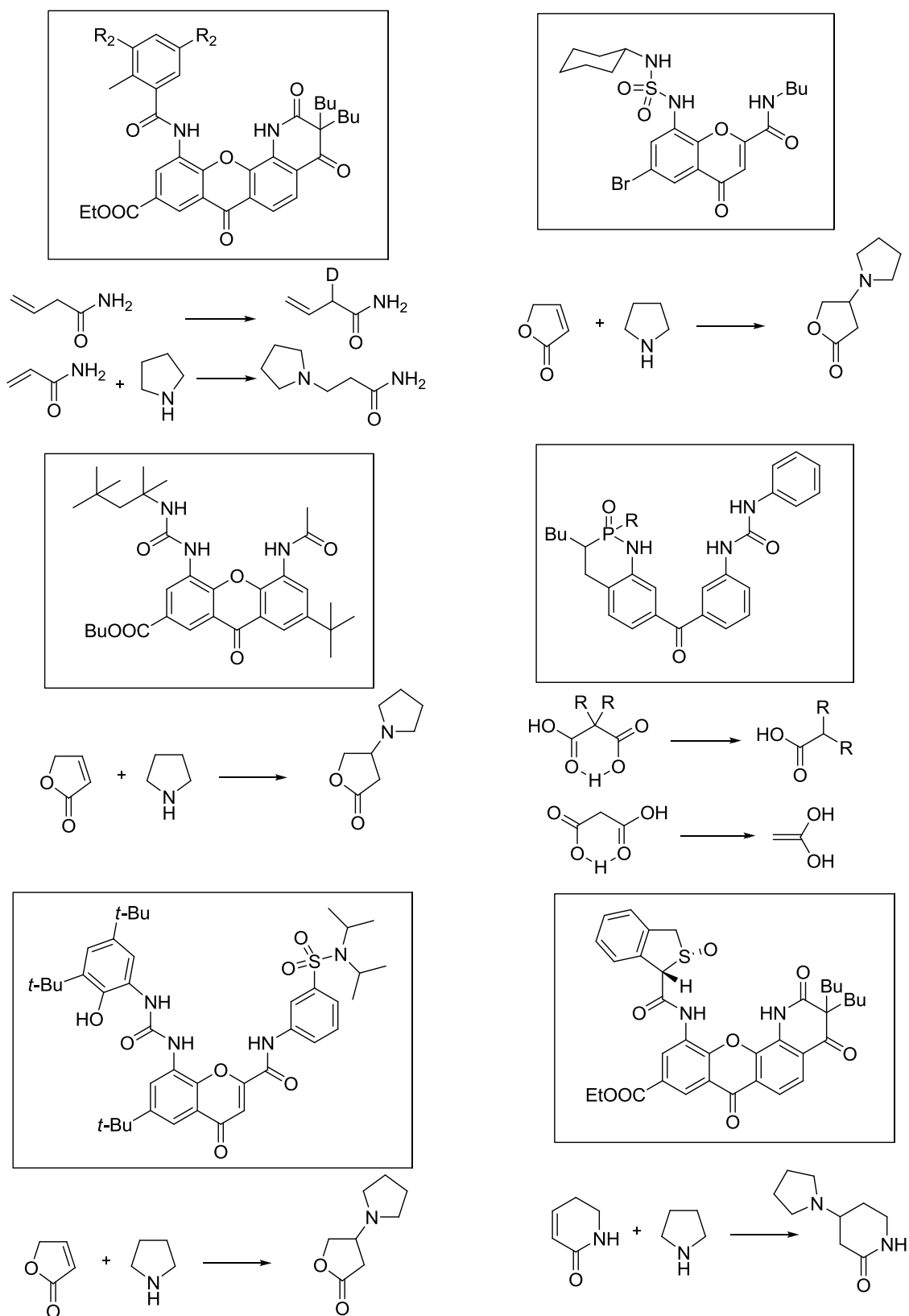


Figure 9. Some of the receptors prepared in the group and the reactions they catalyze.²²

²² (a) Simón, L.; Muñiz, F. M.; Sáez, S.; Raposo, C.; Morán, J. R. *ARKIVOC* **2007**, 47-64; (b) Simón, L.; Muñiz, F. M.; Sáez, S.; Raposo, C.; Morán, J. R. *Eur. J. Org. Chem.* **2008**, 2397-2403; (c) Simón, L.; Muñiz,

Most of the reactions that have been studied in our research group are based on unsaturated additions to carbonyl compounds. In these reactions a negatively charged oxygen is generated in the transition state. To catalyse these reactions, we studied the strategies used by enzymes to associate carbonyl compounds. In Figure 10 the active site of enzymes capable of associating various carbonyl compounds are shown.²³

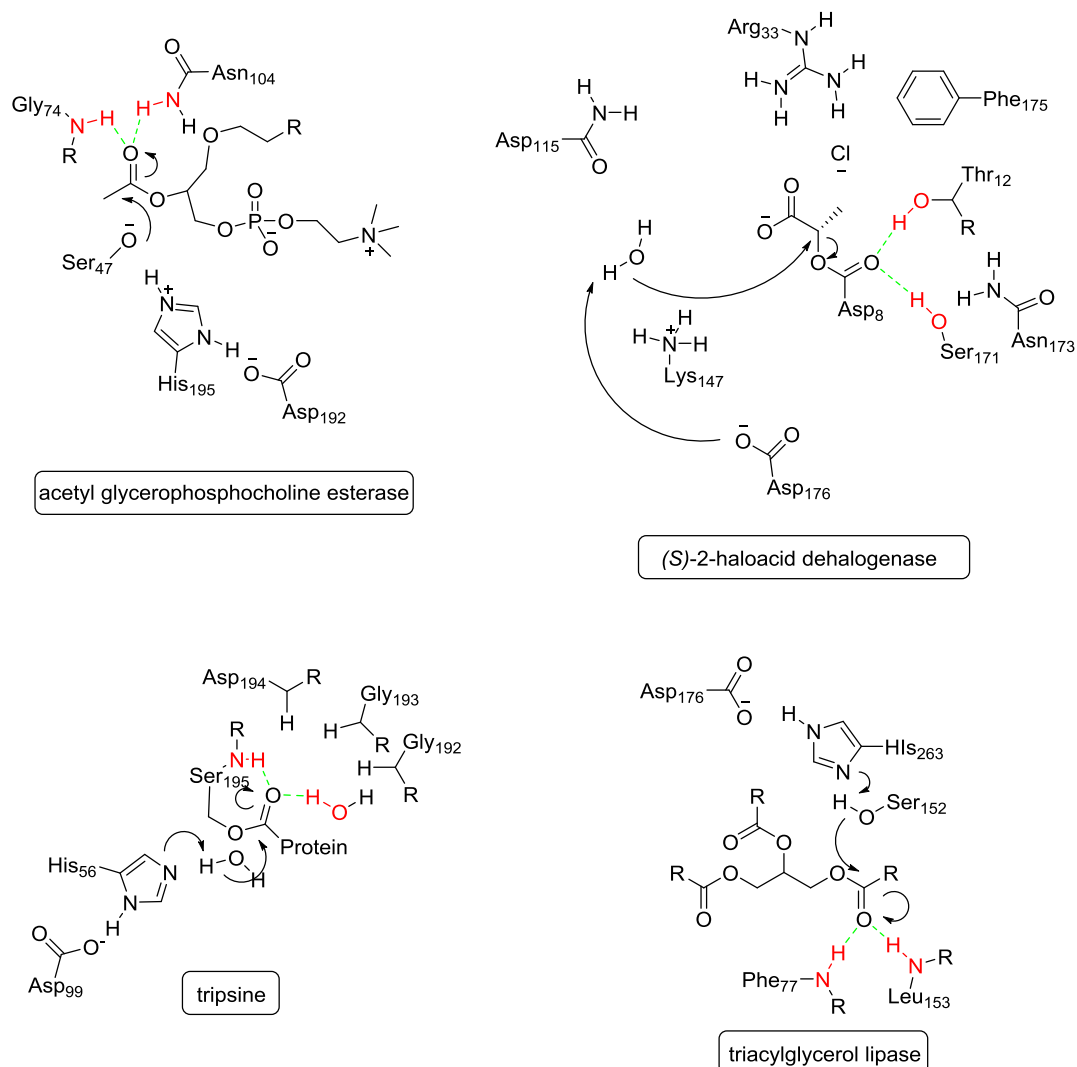


Figure 10. Active site of several enzymes capable of associating carbonyl compounds in which the oxyanion hole is shown in red.

F. M.; Sáez, S.; Raposo, C.; Sanz, F.; Morán, J. R. *Helv. Chim. Acta* **2005**, *88*, 1682-1701; (d) Crego, M.; Raposo, C.; Mussons, M^a L.; Berrocal, A.; Caballero, M^a C.; Morán, J. R. *Heterocycles* **1995**, *40*, 139-140; (e) Simón, L.; Muñiz, F. M.; Fuentes de Arriba, Á.; Alcázar, V.; Raposo, C.; Morán, J. R. *Org. Biomol. Chem.* **2010**, *8*, 1763-1768; (f) Raposo, C.; Almaraz, M.; Martín, M.; Caballero, M^a C.; Morán, J. R. *Tetrahedron Lett.* **1996**, *37*, 6947-6950; (g) Raposo, C.; Crego, M.; Partearroyo, A.; Mussons, M^a L.; Caballero, M^a C.; Morán, J. R. *Tetrahedron Lett.* **1993**, *34*, 1995-1998; (h) Raposo, C.; Luengo, A.; Almaraz, M.; Martín, M.; Mussons, M^a L.; Caballero, M^a C.; Morán, J. R. *Tetrahedron* **1996**, *52*, 12323-12332; (i) Raposo, C.; Almaraz, M.; Crego, M.; Mussons, M^a L.; Pérez, N.; Caballero, M^a C.; Morán, J. R. *Tetrahedron Lett.* **1994**, *35*, 7065-7068; (j) Crego, M.; Raposo, C.; Mussons, M^a L.; Caballero, M^a C.; Morán, J. R. *Tetrahedron Lett.* **1994**, *35*, 1929-1932.

²³ MACiE, Mechanism, Annotation and Classification in Enzymes, <https://www.ebi.ac.uk/thornton-srv/databases/MACiE/>, consulted in december 2013.

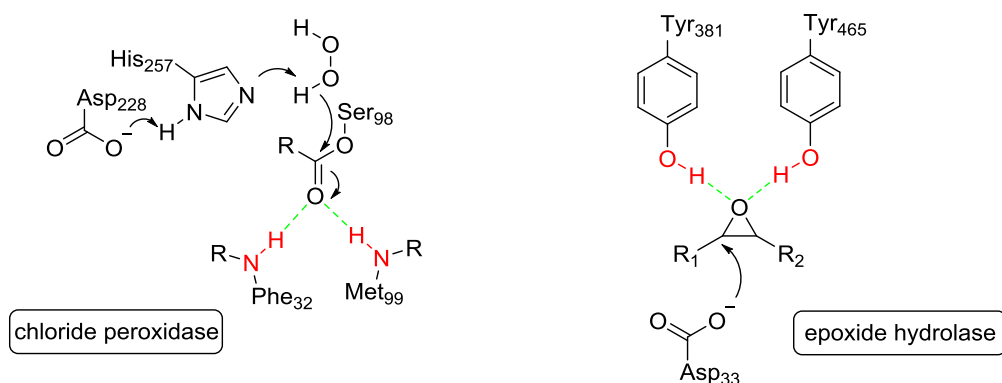


Figure 10 (continuation). Active site of several enzymes capable of associating carbonyl compounds in which the oxanion hole is shown in red.

As can be seen in figure 9, all of these molecules try to have the same structural feature as the enzymes in figure 10, and it is the presence, in the hydrophobic pocket, of two NH groups forming two strong hydrogen bonds with a carbonyl group (there are enzymes able to form three hydrogen bonds).²⁴ This is what it has been called the "oxanion hole". The study of the active site of the crystal structures of hundreds of enzymes has led to significant conclusions about the oxanion-hole geometry, for example, that the average distance between hydrogen donors is between 4.3 and 4.6 Å, that they belong to the backbone of the enzyme and are placed in a rigid environment, or that the carbonyl group is preferably perpendicular to the plane determined by the NHs.²⁵

Many organocatalysts that include ureas or thioureas have tried to reproduce the structure of two hydrogen bond donors.²⁶ However, the distance between the hydrogen bond donors on ureas and thioureas is not comparable to that presented by the NHs of enzymes in oxanion holes. Therefore it is interesting to develop organocatalysts with skeletons in which the two hydrogen bond donors are in a similar way to that of the NHs of natural ones. Xanthene derivatives developed in our group are a good example, and have shown excellent association constants with triphenylarsine or trioctylphosphine oxide, compounds that can be considered analogues of carbonyl transition states. In fact, they have shown better associations than the famous Schreiner thiourea and good catalytic activity in the Diels-Alder reaction between cyclopentadiene and methylvinylketone.²⁷

²⁴ (a) Lo, Y. C.; Lin, S. C.; Shaw, J. F.; Liaw, Y. C. *J. Mol. Biol.* **2003**, *330*, 539-551; (b) Zhu, X.; Larsen, N. A.; Basran, A.; Bruce, N. C.; Wilson, I. A. *J. Biol. Chem.* **2003**, *278*, 2008-2014; (c) Nachon, F.; Asojo, O. A.; Borgstahl, G. E. O.; Masson, P.; Lockridge, O. *Biochemistry* **2005**, *44*, 1154-1162; (d) Zhang, Y.; Kua, J.; McCammon, J. A. *J. Am. Chem. Soc.* **2002**, *124*, 10572-10577.

²⁵ (a) Simón, L.; Goodman, J. M. *J. Org. Chem.* **2010**, *75*, 1831-1840; (b) Simón, L.; Goodman, J. M. *Org. Biomol. Chem.* **2012**, *10*, 1905-1913.

²⁶ Taylor, M. S.; Jacobsen, E. N. *Angew. Chem., Int. Ed.* **2006**, *45*, 1520-1543.

²⁷ Muñiz, F. M.; Alcázar Montero, V.; Fuentes de Arriba, Á. L.; Simón, L.; Raposo, C.; Morán, J. R. *Tetrahedron Lett.* **2008**, *49*, 5050-5052.

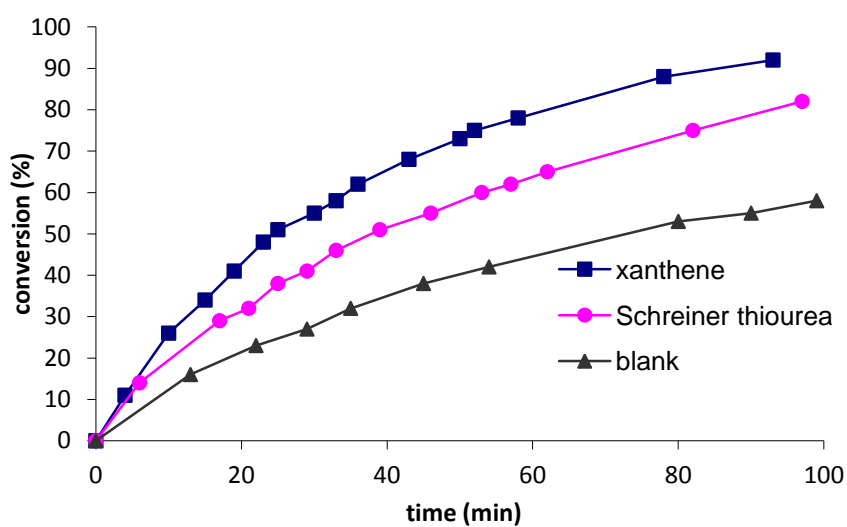
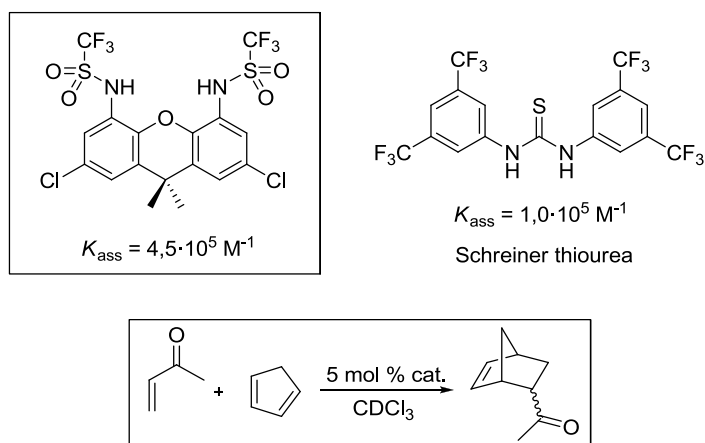
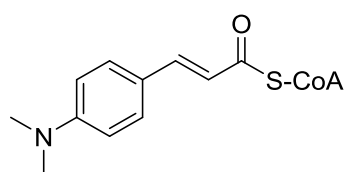


Figure 11. Receptor based on a xanthone skeleton. The value of the association constant with triphenylarsine oxide in CDCl₃ at 20 ° C and the conversion of the reaction between cyclopentadiene and methylvinylketone are shown.

The fact that its structure resembles the active site of some enzymes is illustrated in figure 12, where a xanthone is overlapped in the active center of an enoyl-CoA hydratase.

Complex with:



Superposition of the active site with:

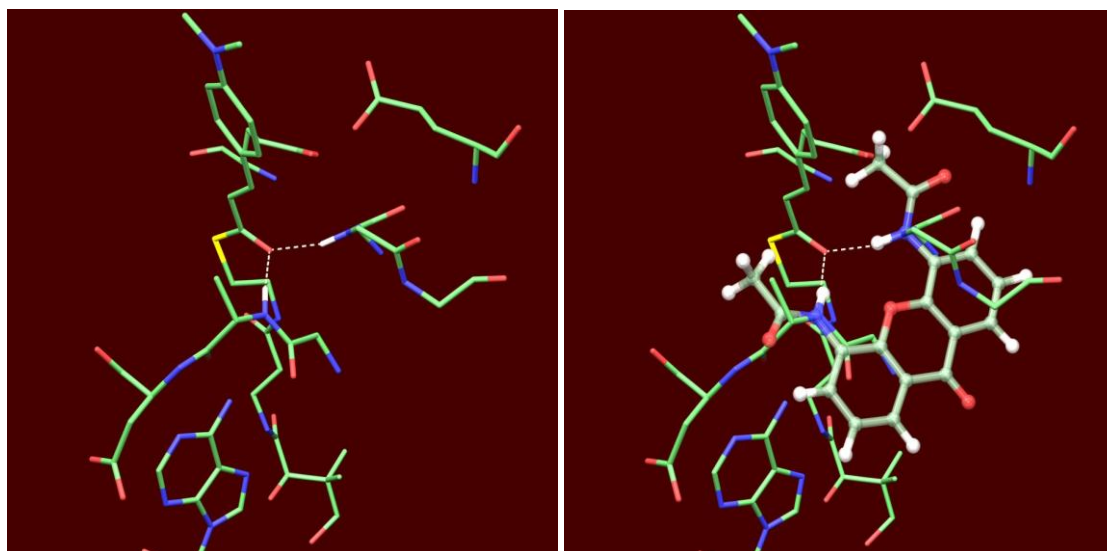
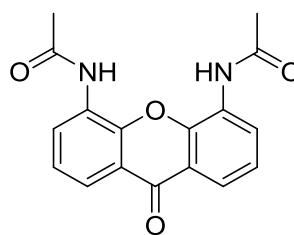


Figure 12 Representation where the active site of a enoyl-CoA hydratase linked to a guest is shown, and overlay with a xanthone skeleton (key of colors: green-carbon, red-oxygen, yellow-sulfur, blue-nitrogen, white-hydrogen).

Objectives

The work presented in this Thesis is a contribution to the further development of new catalysts and new artificial enzymes that, using an oxyanion hole, are capable of carrying out the enantioselective catalysis of several reactions with an applied interest.

Thus, in the first part of the work the xanthene skeleton functionalization will be studied in order to generate new catalysts for aldol reactions. The idea is to keep two NHs in the xanthene structure to create the ideal oxyanion hole for attaching a carbonyl group. In addition, we pretend to include a proline molecule to have a nitrogen group capable of generating an enamine with the donor carbonyl group. Also, the acidity of the oxyanion hole will be tuned by incorporating more or less acid groups in the structure.

These catalysts will be used in the synthesis of the Hajos-Wiechert ketone, which has been used as starting material in the preparation of biological interesting compounds.

We will subsequently develop new organocatalysts, more economically affordable, to catalyse the same reaction (Chapter 1). The simplicity of these catalysts will allow us to perform a mechanistic study of the reaction, which today is not fully understood and there are still some factors that remain in doubt (Chapter 2).

This mechanistic study will help us to understand the lack of activity of some catalysts and will allow us to develop a new generation of cyclohexane derivatives with interesting applications in the Hajos-Parrish-Eder-Sauer-Wiechert cyclization. In addition, a new synthetic procedure, faster and cheaper than the ones developed so far, will be presented for the preparation of *trans*-cyclohexanediamine derivatives (Chapter 3).

In a second phase of this work, a study of new structures that are capable of generating a suitable oxyanion hole will be carried out, analyzing thioxanthenes, differently substituted naphthalenes, carbazoles, etc. Furthermore, the catalytic potential of the new receptors will be applied to transesterification reactions, which also requires the association of a carbonyl group. Also they will be used in a transesterification reaction with industrial utility, as is the generation of biodiesel. This will involve carrying out a thorough study of the mechanism of this reaction in order to develop the most suitable catalysts (Chapter 4).

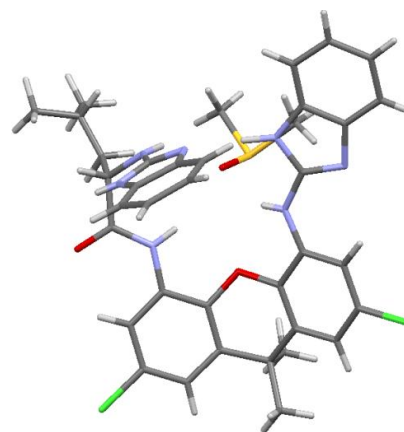
In the search for new oxyanion holes, in the last part of this work, a new chiral tripodal skeleton derived from benzofurane will be synthesized. Its functionalization will be studied as well as the possibility of supporting multiple functional groups in its structure. These new receptors will be applied to the enantioselective extraction of amino acids and derivatives (Chapters 5 and 6) and also in the catalysis of several reactions of industrial interest, such as the dynamic kinetic resolution of azlactones (Chapter 7).



**VNIVERSIDAD
D SALAMANCA**

CAMPUS DE EXCELENCIA INTERNACIONAL

***CHAPTER 1: L-proline-derived catalysts for aldol
reactions***



1.1 INTRODUCTION

As mentioned above, one of the reactions that laid the foundations for this new area of organocatalysis was the intramolecular asymmetric aldol reaction catalysed by *L*-proline.²⁸ The reaction was carried out independently in the early 70s by two research groups. Hajos and Parrish (Hoffmann La Roche)²⁹ published intramolecular aldol reactions catalysed by *L*-proline of triketones such as **1** and **4** to generate aldols **2** and **5** in good yields and enantiomeric excesses. Then the dehydration of these aldols catalysed by acid allowed the obtention of enones **3** and **6** without a significant enantioselectivity loss. Hajos and Parrish got better results for cyclopentanediones than cyclohexanediones, as shown in figure 1.1.

²⁸ List, B. *Tetrahedron* **2002**, *58*, 5573-5590.

²⁹ Hajos, Z. G.; Parrish, D. R. *J. Org. Chem.* **1974**, *39*, 1615-1621.

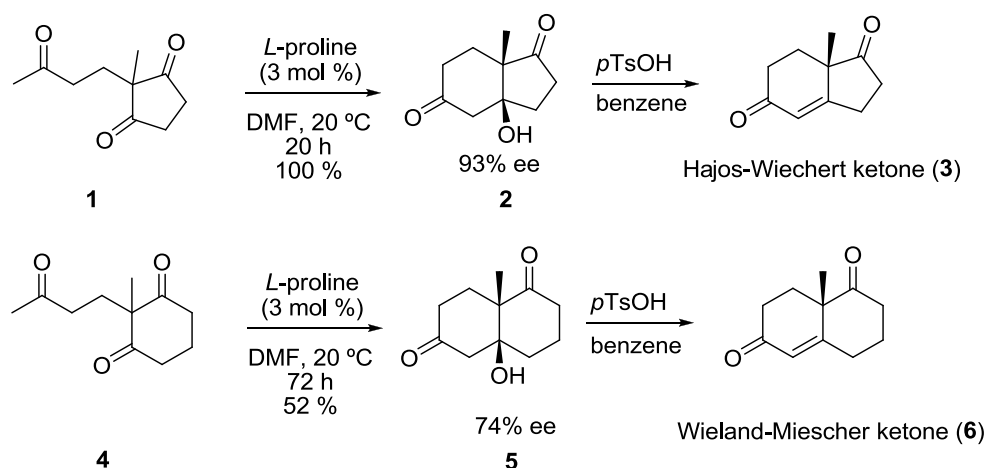


Figure 1.1. Hajos and Parrish intramolecular reactions with L-proline.

Furthermore, Eder, Sauer and Wiechert (Schering)³⁰ led directly to enone condensation, using L-proline as catalyst and HClO₄ as co-catalyst. They also obtained good yields and enantiomeric excesses.

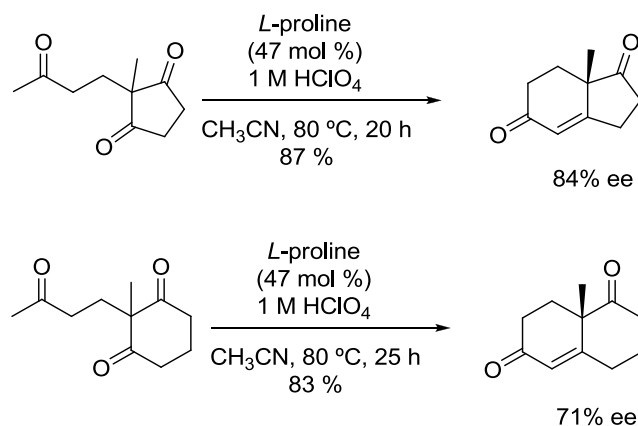


Figure 1.2. Intramolecular reactions performed by Eder, Sauer and Wiechert with L-proline

In regard to the reaction mechanism, it has been controversial almost since its discovery. Hajos and Parrish proposed initially two mechanisms. Its first proposal was based on a protonated enamine (figure 1.3), in which a hydrogen transfer occurred from nitrogen to oxygen. However, they discarded it, since experiments with labelled H₂O showed low isotope incorporation in the reaction product, which would be inconsistent with a similar mechanism in aldolase enzymes. Moreover, this mechanism was later criticized because a protonated enamine would reduce the nucleophilic character of the C=C.

³⁰ Eder, U.; Sauer, G.; Wiechert, R. *Angew. Chem., Int. Ed. Eng.* **1971**, *10*, 496-497.

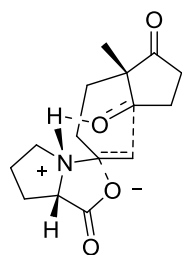


Figure 1.3. First mechanistic proposal from Hajos and Parrish, now rejected.

The final Hajos-Parrish alternative was to activate one of the enantiotopic ring carbonyl groups as carbinolamine which then undergoes a nucleophilic attack from the side chain enol (figure 1.4).

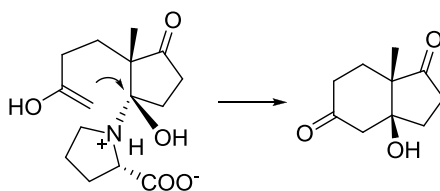


Figure 1.4. Hajos-Parrish second proposal.

However, it is striking to perform an S_N2 reaction on a tertiary carbon. In fact, this mechanism is subsequently rejected by Jung³¹ because it would involve configuration retention in an S_N2 type process, which is well known that inverts the configuration. Thus, Jung in 1976, and later Eschenmoser³² in 1978, proposed a model based on the formation of an *L*-proline enamine in the side chain, as shown in figure 1.5.

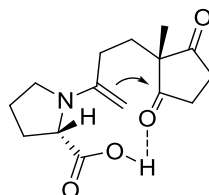


Figure 1.5. Mechanism proposed by Jung.

Some years later, in 1984, Agami³³ published a new model in which two molecules of *L*-proline were involved in the enantioselectivity determining step (figure 1.6). A molecule was responsible for carrying out the formation of the enamine with the acyclic carbonyl group, while the other molecule of *L*-proline transports the proton to the alkoxide. Agami reaches this conclusion on the basis of kinetic studies performed and a nonlinear effect observed in asymmetric catalysis.

³¹ Jung, M. E. *Tetrahedron* **1976**, *32*, 3-31.

³² Brown, K. L.; Damm, L.; Dunitz, J. D.; Eschenmoser, A.; Hobi, R.; Kratky, C. *Helv. Chim. Acta* **1978**, *61*, 3108-3135.

³³ (a) Agami, C.; Meynier, F.; Puchot, C.; Guilhem, J.; Pascard, C. *Tetrahedron* **1984**, *40*, 1031-1038; (b) Agami, C.; Puchot, C.; Sevestre, H. *Tetrahedron Lett.* **1986**, *27*, 1501-1504; (c) Puchot, C.; Samuel, O.; Dunach, E.; Zhao, S.; Agami, C.; Kagan, H. B. *J. Am. Chem. Soc.* **1986**, *108*, 2353-2357.

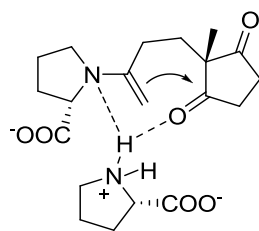


Figure 1.6. Agami mechanism.

Swaminathan³⁴ proposed in 1999 a new acid/base concerted mechanism based on heterogeneous catalysis, due to the low solubility of proline in DMSO and CH₃CN, and noting that in the absence of proline crystals the reaction does not take place (figure 1.7). Swaminathan proposes a model in which he positions the triketone in the plane of the paper and situates the proline in a perpendicular plane, in such a way that the carboxylate group abstracts a proton alpha to the carbonyl in the acyclic chain, and then this carbon attacks another carbonyl group which is being activated by an H-bond with the ammonium group.

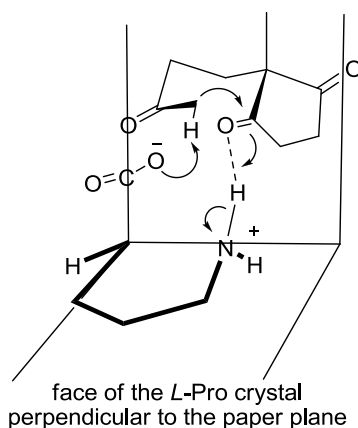


Figure 1.7. Proposed mechanism by Swaminathan.

Although in 1976 Jung had already proposed a mechanism involving a single molecule of proline in an intermediate enamine, with concerted C-C bond formation and proton transfer of the carboxyl group to the carbonyl group, this model remained forgotten until the year 2000, when List, Lerner and Barbas,³⁵ in a pioneering work on intermolecular aldol reactions catalysed by proline, proposed a similar mechanism (figure 1.8).

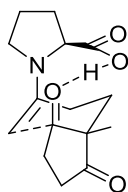


Figure 1.8. Houk and List model.

³⁴ Rajagopal, D.; Moni, M. S.; Subramanian, S.; Swaminathan, S. *Tetrahedron: Asymmetry* **1999**, *10*, 1631-1634.

³⁵ List, B.; Lerner, R. A.; Barbas, C. F. *J. Am. Chem. Soc.* **2000**, *122*, 2395-2396.

The latter mechanism was confirmed by Houk,³⁶ based on quantum mechanical calculations, showing that between all transition states proposed for the formation of the C-C bond, that of List, Lerner and Barbas (**D**) was the most stable, showing 10.0 kcal/mol less than the non catalysed reaction (**E**). The mechanism which involves the zwitterionic form of the enamine (**B**) is 30.0 kcal/mol more unfavourable than **D**, whereas the carbinolamine mechanism (**A**) is 12.0 kcal/mol more unstable (Figure 1.9).

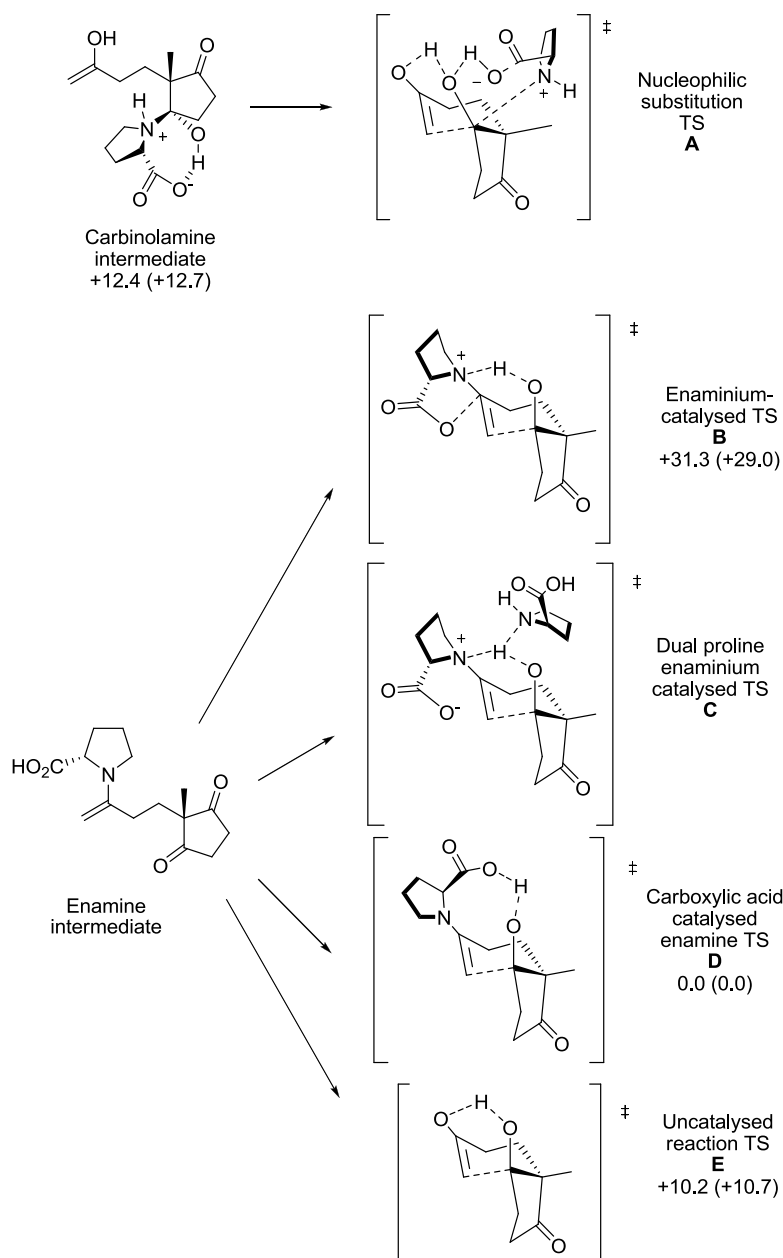


Figure 1.9. Relative energies of several transition states proposed for the reaction of Hajos-Parrish-Eder-Sauer-Wiechert. Values in parentheses include solvation energies in DMSO using the PCM / UAKS model. A) Carbinolamine model proposed by Hajos-Parrish ; B) Model of the intermediate type ion enaminium rejected at first by Hajos-Parrish ; C) Agami model in which two molecules of L-Pro are involved ; D) Jung Model via enamine type ; E) uncatalysed reaction.

³⁶ (a) Bahmanyar, S.; Houk, K. N. *J. Am. Chem. Soc.* **2001**, 123, 12911-12912; (b) Clemente, F. R.; Houk, K. N. *Angew. Chem., Int. Ed.* **2004**, 43, 5766-5768.

In the scheme below, the mechanism for the enantioselective triketone **1** aldol cyclization catalysed by L-proline together with the relative energies of the intermediates and transition states (in kcal/mol) is shown.

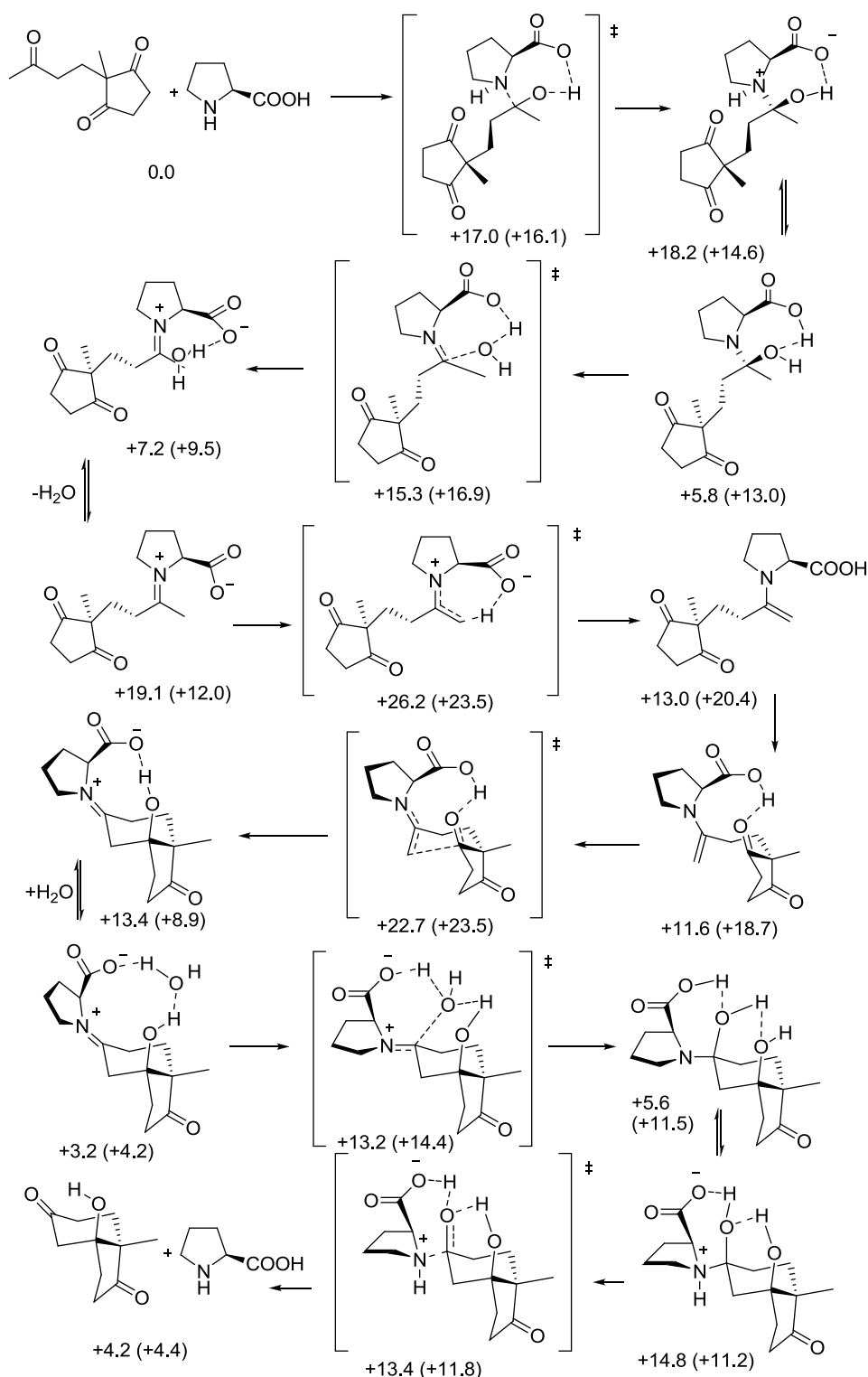


Figure 1.10. Mechanism proposed for the cyclisation of 2-methyl-2-(3-oxobutyl)cyclopentane-1,3-dione **1** catalysed by L-proline. Relative energy values in the gaseous state are in kcal/mol. Values in parentheses include solvation energy in DMSO using the PCM/UAKS model.

According to the mechanism proposed by Houk, one molecule of *L*-proline is capable of forming an enamine with the acyclic carbonyl group. Then, this enamine performs an enantioselective nucleophilic attack on a carbonyl group in the ring, which is being activated by a hydrogen bond with the carboxyl group of proline, thus increasing the electrophilicity of the carbonyl which is being approached. After C-C bond formation, hydrolysis takes place to generate the iminium aldol condensation product and the catalyst is regenerated.

Recently, careful repetition of the experiments from Hajos-Parrish and Agami has shown that the initial findings were wrong, since the incorporation of ^{18}O (> 90 %) was observed in the final product acyclic carbonyl group when the reaction was carried out in ^{18}O enriched water. Furthermore, it was also shown that the dilution and non-linear effects were not correct.³⁷

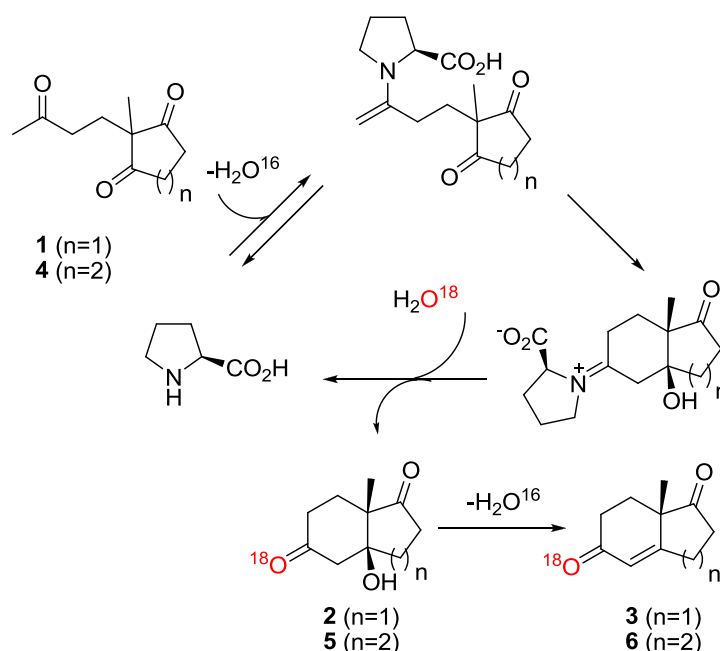


Figure 1.11. If Houk mechanism is true, the Hajos-Parrish-Eder-Sauer-Wiechert reaction requires incorporation of ^{18}O to the ketone product when the reaction is carried out in the presence of ^{18}O enriched water.

This latter proposed mechanism is similar to that performed by aldolase enzymes, in which a lysine residue is capable of forming an enamine with the carbonyl group donor and then attacks the carbonyl group acceptor (figure 8, introduction).

The main feature of enamine catalysis is that it is capable of activating the nucleophilicity of a ketone or aldehyde by forming an enamine, changing the characteristics of the keto/enol tautomerism and the energy of the highest occupied molecular orbital (HOMO). While the keto/enol tautomerism is shifted to the keto form, in the case of the iminium/enamine tautomerism is shifted to the enamine. Furthermore, as the electron pair of a nitrogen atom is

³⁷ (a) Hoang, L.; Bahmanyar, S.; Houk, K. N.; List, B. *J. Am. Chem. Soc.* **2002**, *125*, 16-17; (b) List, B.; Hoang, L.; Martin, H. J. *Proc. Natl. Acad. Sci.* **2004**, *101*, 5839-5842.

higher in energy than that of an oxygen atom, the HOMO energy of the enamine is increased respect to the enol, increasing its reactivity.³⁸

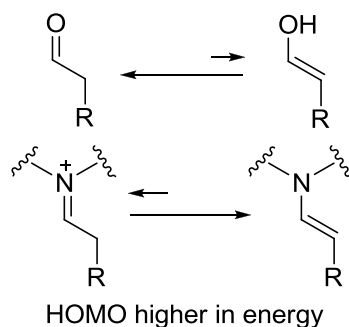


Figure 1.12. Aldehydes activation increasing the HOMO energy via enamine formation.

However, further studies are trying to explain the mechanism of the aldol reaction via enamine. Although the mechanism proposed by Houk looks quite convincing and is currently accepted, in the last decade several articles have questioned this mechanism.

In 2007, Patil³⁹ found that protic solvents, such as methanol, were able to reduce the enamine formation activation energy, suggesting for this process a "proton-relay" mechanism in which two molecules of methanol participate.

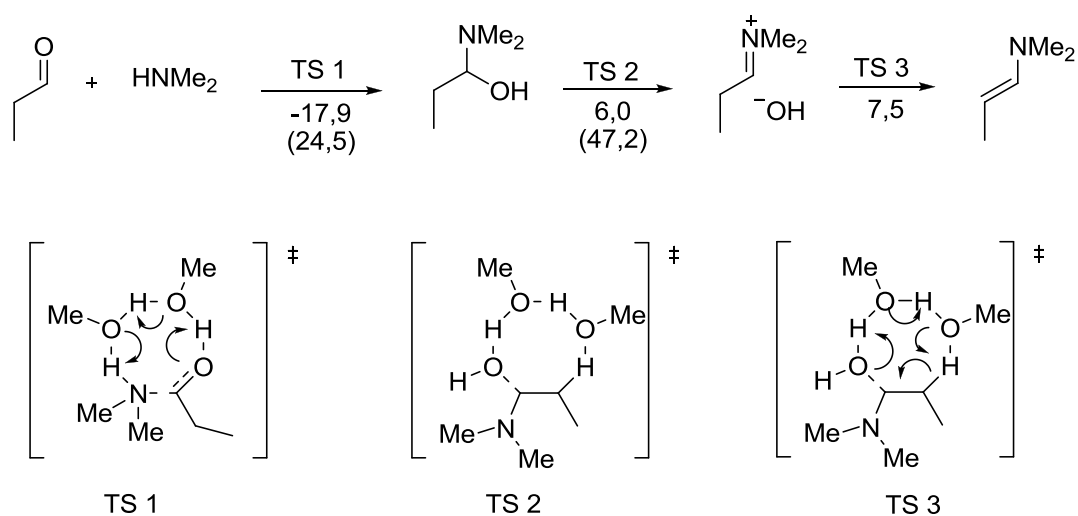


Figure 1.13. Activation energies (kcal/mol) for the formation of hemiacetal, iminium ion and enamine in the presence and absence (values in brackets) of two methanol molecules.

In fact, the discovery of oxazolidinones as reaction intermediates in the intermolecular proline-catalysed aldol condensation caused the appearance of new theories. Indeed, the formation of oxazolidinones of aldehydes was already known since the 80s,⁴⁰ and in 2004,

³⁸ Nielsen, M.; Worgull, D.; Zweifel, T.; Gschwend, B.; Bertelsen, S.; Jorgensen, K. A. *Chem. Commun.* **2011**, 47, 632-649.

³⁹ Patil, M. P.; Sunoj, R. B. *J. Org. Chem.* **2007**, 72, 8202-8215.

⁴⁰ (a) Orsini, F.; Pelizzoni, F.; Forte, M.; Sisti, M.; Bombieri, G.; Benetollo, F. *J. Heterocycl. Chem.* **1989**, 26, 837-841; (b) Seebach, D.; Boes, M.; Naef, R.; Schweizer, W. B. *J. Am. Chem. Soc.* **1983**, 105, 5390-5398; (c) Seebach, D.; Weber, T. *Tetrahedron Lett.* **1983**, 24, 3315-3318.

List^{37b} also observed the formation of ketone oxazolidinones, while the enamine proposed in the mechanism is not isolated, it is even difficult to detect if non-activated carbonyl groups are used (although some groups say they have characterized it by mass spectrometry).⁴¹ However, it has been possible to characterize the oxazolidinone of several ketones and calculate the equilibrium constant:^{37b}

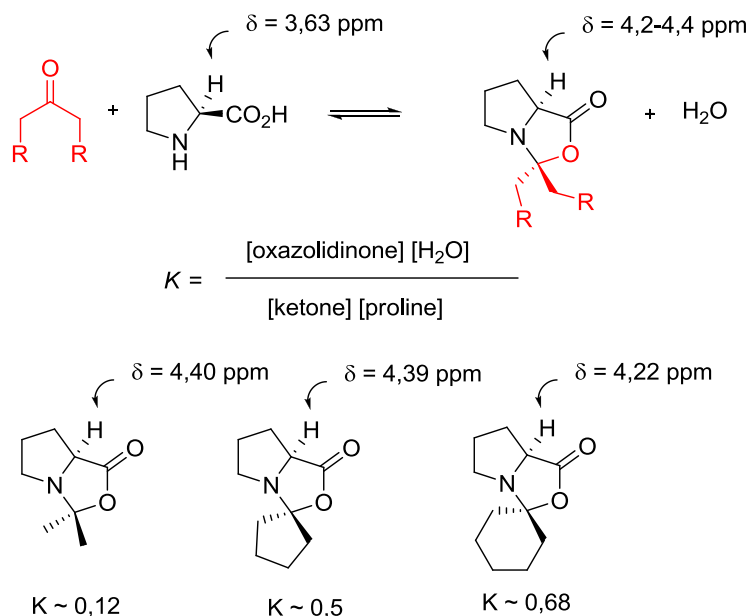


Figure 1.14. Oxazolidinones are formed from ketones and L-proline in a reversible reaction, being possible to calculate the equilibrium constant.

Although initially oxazolidinones were proposed as parasitic species, since they were not able to promote the aldol reaction,^{37b} other authors consider that these compounds could help to keep proline in solution,⁴² and they even assigned them a key role.⁴³ Thus, the initial work of Seebach⁴³ shows that the oxazolidinone of the cyclohexanone can be opened if lithium bromide is added to the reaction medium, and readily reacts with electrophiles (figure 1.15).

⁴¹ Marquez, C.; Metzger, J. O. *Chem. Commun.* **2006**, 1539-1541.

⁴² (a) Zotova, N.; Franzke, A.; Armstrong, A.; Blackmond, D. G. *J. Am. Chem. Soc.* **2007**, *129*, 15100-15101; (b) Iwamura, H.; Wells, D. H.; Mathew, S. P.; Klussmann, M.; Armstrong, A.; Blackmond, D. G. *J. Am. Chem. Soc.* **2004**, *126*, 16312-16313; (c) Sharma, A. K.; Sunoj, R. B. *Angew. Chem., Int. Ed.* **2010**, *49*, 6373-6377.

⁴³ Seebach, D.; Beck, A. K.; Badine, D. M.; Limbach, M.; Eschenmoser, A.; Treasurywala, A. M.; Hobi, R.; Prikoszovich, W.; Linder, B. *Helv. Chim. Acta* **2007**, *90*, 425-471.

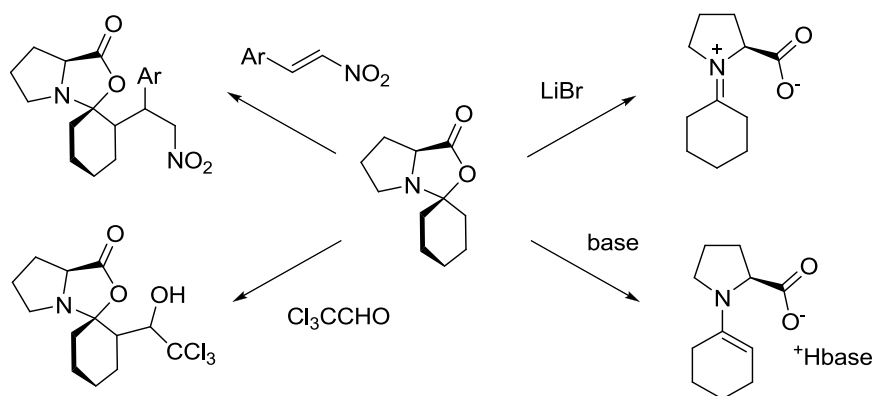


Figure 1.15. Reactions of the proline oxazolidinone and cyclohexanone described by Seebach.

Further, he suggests that during the cyclization the proline carboxylate acts as the nucleophile, attacking the double bond of the enamine at the same time that the aldol condensation is being produced. Thus, during this stage of the reaction the oxazolidinone ring is closed (figure 1.16), which represents an alternative to the proposed mechanism by Houk and List. Nevertheless, no experimental data support this last mechanism.

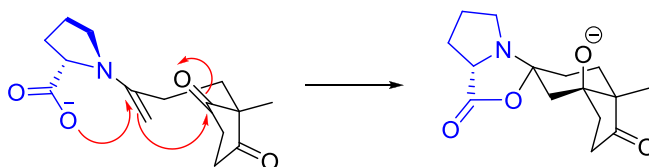


Figure 1.16. Mechanism wherein the oxazolidinone is a true intermediate in the reaction mechanism and not a parasitic species.

The stereochemistry of the product is due to the formation of the most stable oxazolidinone instead of the kinetic product, which is favoured by stereoelectronic reasons. Based in some observations in which a base is able to catalyse the reaction of oxazolidinones with electrophiles, Seebach thinks that after the COOH deprotonation, the *trans* addition of the carboxylate to the *s-cis* enamine double bond takes place. This reaction yields an oxazolidinone with the larger substituent in *exo* position. In this geometry, the electrophile approaches the substrate from the less hindered face, which corresponds to the opposite site of the carboxylate. Although the stereoelectronically favoured trajectory for the *trans* addition would correspond to the attack to the *s-trans* enamine carboxylate, this geometry would generate an enamine with the larger substituent in an hindered position.

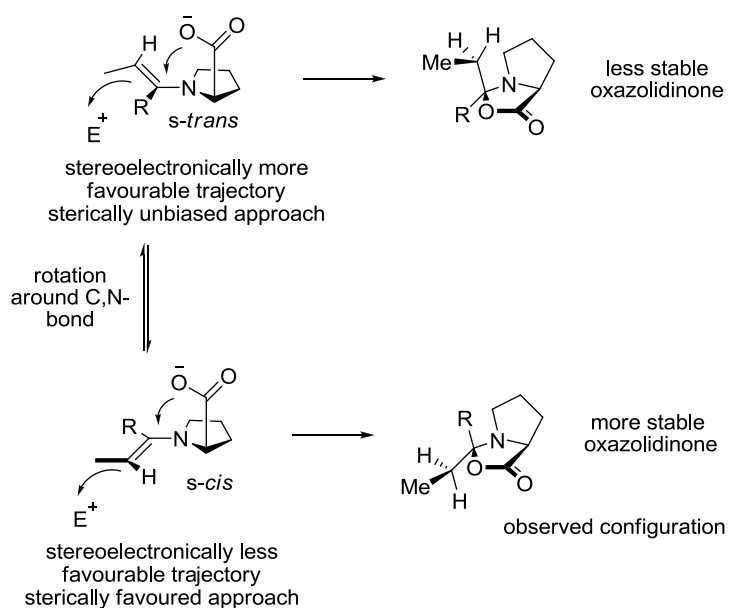


Figure 1.17. Seebach model for ketone additions to an electrophile (E^+) catalysed by proline.

Gschwind⁴⁴ has suggested that the formation of the enamine takes place via the oxazolidinone and not from the iminium ion. He bases his studies on the species observed by ^1H NMR in the propanal aldol condensation catalysed with proline.

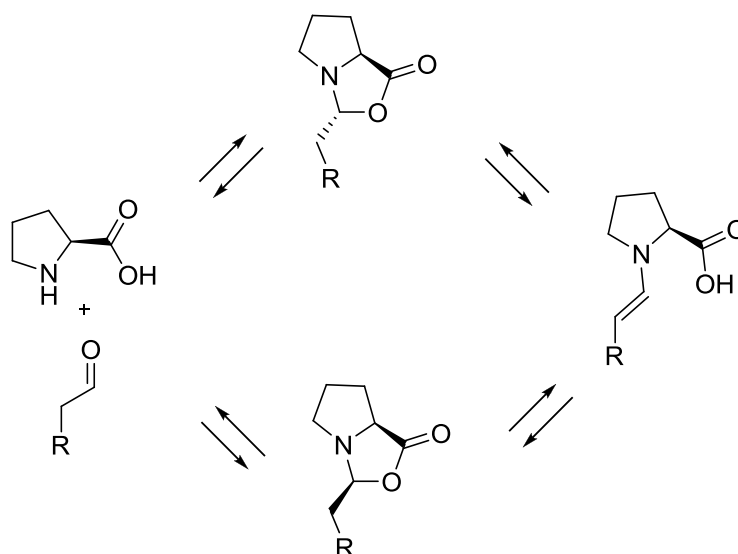


Figure 1.18. Mechanism proposed by Gschwind for enamine formation through oxazolidinone.

These oxazolidinones have been used by Vilarrasa⁴⁵ to perform aldol reactions with good enantiomeric excesses, thus increasing the uncertainty about the actual role of these compounds in the aldol reaction.

⁴⁴ Schmid, M. B.; Zeitler, K.; Gschwind, R. M. *Angew. Chem., Int. Ed.* **2010**, *49*, 4997-5003.

⁴⁵ Isart, C.; Burés, J.; Vilarrasa, J. *Tetrahedron Lett.* **2008**, *49*, 5414-5418.

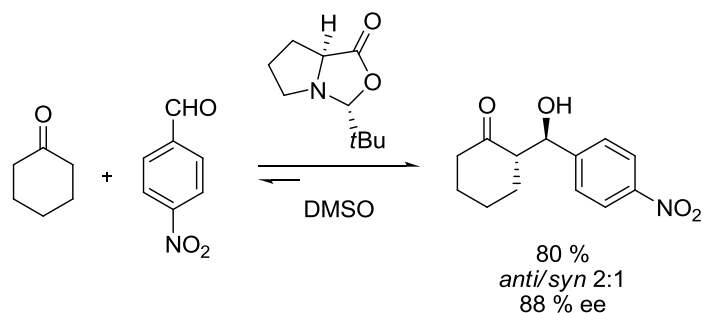


Figure 1.19. Aldol reaction catalysed by an oxazolidinone.

Another fact to consider is that the Houk and List mechanism proposes charged intermediates which should be strongly stabilized in polar solvents. Therefore, it would be expected that these reactions were slow in apolar solvents. However, this is not the case, since the reaction has similar rates in solvents of different polarities such as benzene, chloroform or methanol, showing a similar behaviour as electrocyclic reactions. In fact the choice of polar solvents such as DMF, DMSO or even water is justified by the low solubility of proline in apolar solvents, but not because these solvents favour the reaction rate.

The Houk-List mechanism always requires the participation of a proton donor to reduce the activation energy of the process, otherwise the alkoxide obtained in the aldol condensation generates a much higher energy barrier. However, prolinamides catalyse the reaction at a comparable rate to proline, despite lacking the acidic proton. Although it may be argued that, despite the large difference in pK_a between acids and amides, the amide proton plays a similar role to the carboxylic acid, it is known that the prolinol also acts as a catalyst for these processes⁴⁶ (it produces an enantiomeric excess of 17 %). In the latter case, it is difficult to understand what the advantage is in the proton transfer, since protonation of the alkoxide generated in the aldol condensation would, in turn, generate another alkoxide in the prolinol molecule of similar stability. The fact that the methyl ester of proline catalyses the reaction in an analogous manner, with the same enantiomeric excess as prolinol,⁴⁷ allows ruling out a strong low barrier hydrogen bond, responsible for accelerating the reaction. In our laboratory the results described in the literature have been confirmed,⁴⁸ using proline butyl ester: the chiral induction is poor, but the reaction rate in chloroform is at least ten times higher than in the case of prolinamides.

Another curious fact, which has not yet been explained, is that the reactions catalysed by proline or their esters generate mostly the same enantiomer, corresponding to the attack on the more hindered face of proline, whereas if bulkier groups as methylphenylprolinamides are used (figure 1.19), the selectivity is reversed and now the attack occurs on the least hindered face of proline. Consequently, both the ester and the alcohol group of prolinol seem to accelerate the reaction, but it is not obvious the mechanism by which they do it.

⁴⁶ Drauz, K.; Kleeman, A.; Martens, J. *Angew. Chem., Int. Ed. Eng.* **1982**, *21*, 584-608.

⁴⁷ Nagasawa, K.; Takahashi, H.; Hiroi, K.; Yamada, S. I. *J. Pharm. Soc. Japan* **1975**, *95*, 33-45.

⁴⁸ de Arriba, Á. L. F.; Simón, L.; Raposo, C.; Alcázar, V.; Morán, J. R. *Tetrahedron* **2009**, *65*, 4841-4845.

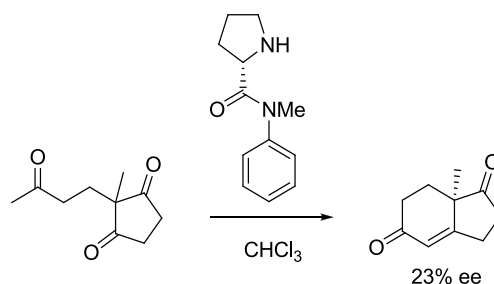


Figure 1.20. The prolinamide of the figure shows the opposite selectivity to that of proline or its methyl ester in the Hajos-Parrish-Eder-Sauer-Wiechert reaction.

Seebach⁴³ has also noted that in the intermolecular aldol reactions between aldehydes and unsymmetrical ketones, condensation occurs always at the more substituted carbon of the ketone, despite the presence of allylic tension when the enamine is generated in that position. So far there is no good explanation for this phenomenon. Furthermore, in the case of prolinamides, the opposite effect can be obtained.

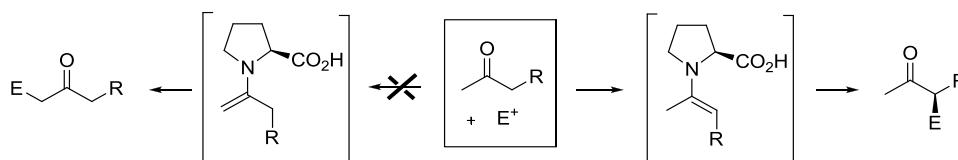


Figure 1.21. Reaction of an unsymmetrical ketone in which the reaction only occurs in the more substituted carbon.

Houk has recently published, along with Meyer,⁴⁹ a study of the isotope effects observed after preparing the Hajos-Wiechert ketone enriched with ¹³C in certain positions. The results show that C-C bond formation is not significant to the overall reaction rate, however the rate limiting step could be the formation of the initial carbinolamine or iminium salt.

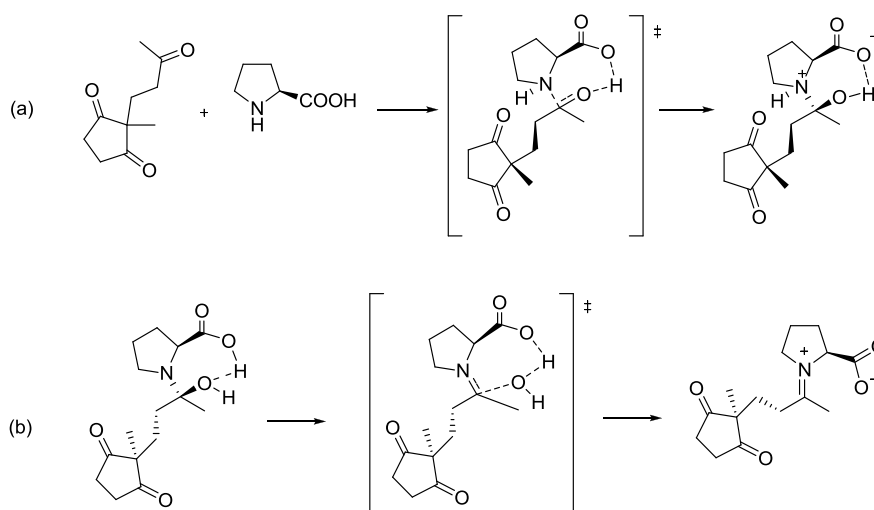


Figure 1.22. Possible reaction rate limiting steps of the aldol reaction of ketone **1** in the presence of L-proline, according to an isotope effect study.

⁴⁹ Zhu, H.; Clemente, F. R.; Houk, K. N.; Meyer, M. P. *J. Am. Chem. Soc.* **2009**, *131*, 1632-1633.

Consequently, although the Houk-List transition state which justifies the quiral assistance of the reaction is widely accepted (with the exception of any new proposal, like Seebach one) we are still far from clarifying the processes that, from reactants, lead to the transition states (or the processes that from the addition product lead to the recovery of the catalyst and the final aldol product). The overall reaction rate and, eventually, the applicability of this reaction depends on these processes. A correct model of this reaction must be able to accommodate the existence of intermediates as oxazolidinones and clarify its role in the reaction. It should also explain the mechanism of this reaction in less polar media which are unable to stabilize charges proposed in the Houk pathway.

1.1.1. Advantages of proline as catalyst²⁸

There are several reasons to explain why proline has become such an important molecule in asymmetric catalysis. Proline is a bifunctional catalyst because it has a carboxylic acid group and an amino group. These two functional groups can act either as acid or base to facilitate the chemical transformations in a concerted manner, similar to enzymatic catalysis. In addition, proline can act as a chiral bidentate ligand capable of forming catalytically active metallic complexes. Although all of these criteria can be applied to the remaining amino acids, proline is unusual because it possesses a secondary amine, which has a higher pK_a , compared with the primary amino acids. Another consequence of the pyrrolidine ring of proline is the bicyclo[3.3.0]octane ring ("open book structure") of its metal complexes. However, the most important difference of proline to other amino acids is its effectiveness in Lewis base aminocatalysis because it facilitates iminium and enamine type based transformations. In fact, the nucleophilicity of proline is also a consequence of the pyrrolidine ring, forming enamines and iminium ions with carbonyl compounds much faster than other amines, as has been shown by Mayr in its nucleophilicity scale.⁵⁰ Furthermore, the carboxylate contributes to proline catalysis acting as Brønsted co-catalyst, although some authors also propose anchimeric assistance in the enamine addition to the electrophilic group.⁵¹

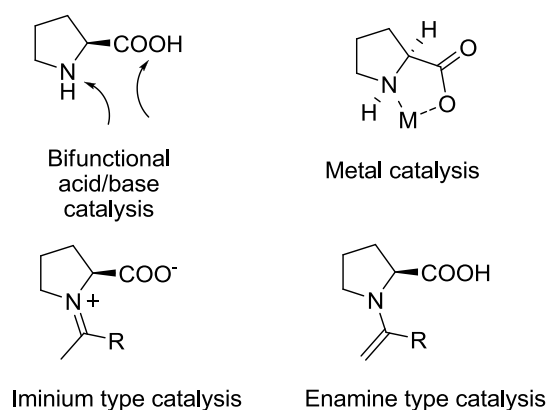


Figure 1.23. Activation modes in catalysis by proline.

⁵⁰ Mayr, H.; Ofial, A. R. *J. Phys. Org. Chem.* **2008**, *21*, 584-595.

⁵¹ Kanzian, R.; Lakhdar, S.; Mayr, H. *Angew. Chem., Int. Ed.* **2010**, *49*, 9526-9529.

The advantages of proline as organocatalyst are listed below:³⁵

- It is not a toxic catalyst, it is cheap, and also readily available in both enantiomeric forms.
- Reactions do not require moisture-free conditions and can take place at room temperature.
- Prior modification of carbonyl substrates such as silylation or deprotonation is not required.
- It is water soluble and can be recovered by aqueous extraction.
- Typically, the reactions can be carried out on an industrial scale.

1.2.1. Disadvantages of proline as catalyst

Although proline has been used in a variety of reactions with satisfactory results, it has a number of drawbacks that can be solved by introducing some changes in its structure. The problems presented are summarized below:

- According to Houk and List mechanism, the carboxyl group of proline participates activating the carbonyl group which acts as electrophile. If this mechanism is true, the protonation of the intermediate reactive always occurs from the carboxylic acid in a *syn* conformation, when it is proven that *anti* carboxylic acids are more stable due to stereoelectronic effects.⁵²

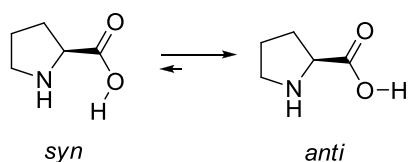


Figure 1.24. Possible conformations of proline carboxyl group.

- Proline has a zwitterionic structure very soluble in polar solvents, but with low solubility in apolar organic solvents, used in many chemical reactions in which proline may be useful.

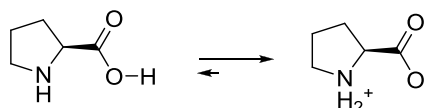


Figure 1.25. Equilibrium showing proline zwitterionic form.

⁵² (a) Dale, J. *Stereochemistry and Conformational Analysis*; Verlag Chemie: New York-Weinheim, 1978; (b) Fausto, R.; Batista de Carvalho, A. E.; Teixeira-Dias, J. J. C.; Ramos, M. N. *J. Chem. Soc., Faraday Trans. 2* **1989**, 85, 1945-1962.

- To generate the intermediate enamine the nucleophilic attack of the proline nitrogen is necessary; however, the free amine concentration is very low due to the high acidity of the carboxyl group of proline, which transfers the proton to the basic nitrogen of the pyrrolidine ring.

- Comparison of the action mechanism of proline with type I aldolase enzymes shows that the geometry of the active site is very different.

1.1.3. Other catalysts used in intramolecular aldol reactions

It seems judicious, therefore, to find derivatives of L-proline that do not present the above drawbacks. Several authors have tried to solve these problems using catalysts with very different structures, emphasizing the increased solubility in organic solvents and providing adequate control of acidity. The results have been very different, as shown in figure 1.26, for the reaction of Hajos-Parrish-Eder-Sauer-Wiechert:

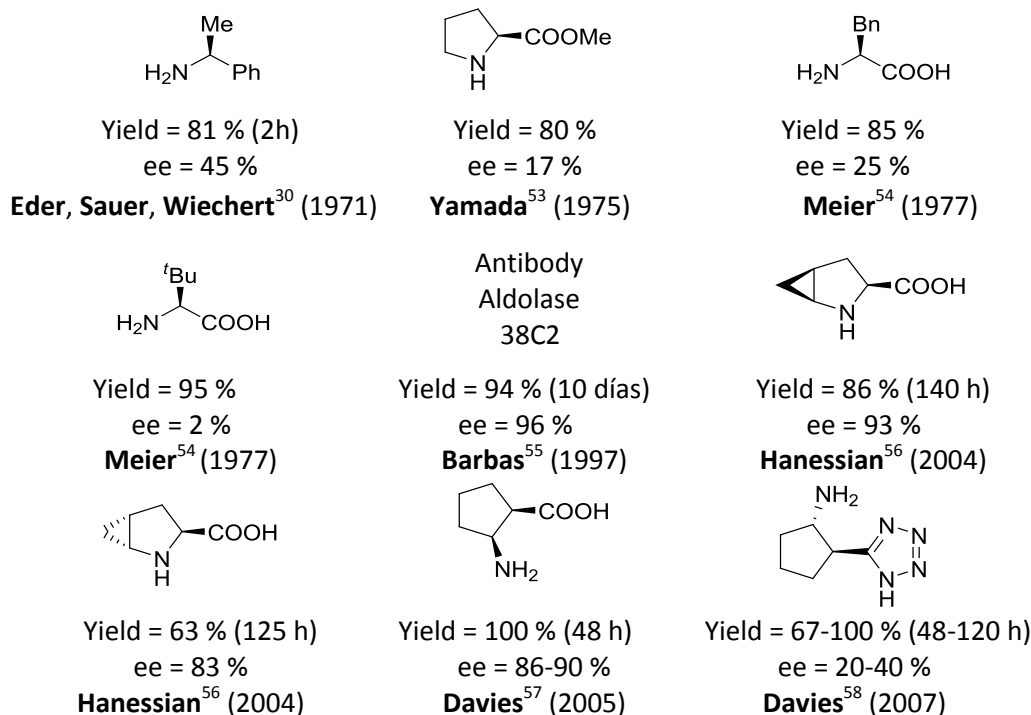


Figure 1.26. Different catalysts used in the Hajos-Parrish-Eder-Sauer-Wiechert reaction.

⁵³ Nagasawa, K.; Takahashi, H.; Hiroi, K.; Yamada, S. *Yakugaku Zasshi* **1975**, *95*, 33-45.

⁵⁴ Buchschacher, P.; Cassal, J.-M.; Fürst, A.; Meier, W. *Helv. Chim. Acta* **1977**, *60*, 2847-2755.

⁵⁵ Zhong, G.; Hoffmann, T.; Lerner, R. A.; Danishefsky, S.; Barbas III, C. F. *J. Am. Chem. Soc.* **1997**, *119*, 8131-8132.

⁵⁶ Cheong, P. H.-Y.; Houk, K. N.; Warriar, J. S.; Hanessian, S. *Adv. Synth. Catal.* **2004**, *346*, 1111-1115.

⁵⁷ Davies, S. G.; Sheppard, R. L.; Smith, A. D.; Thomson, J. E. *Chem. Commun.* **2005**, 3802-3804.

⁵⁸ Davies, S. G.; Russell, A. J.; Sheppard, R. L.; Smith, A. D.; Thomson, J. E. *Org. Biomol. Chem.* **2007**, *5*, 3190-3200.

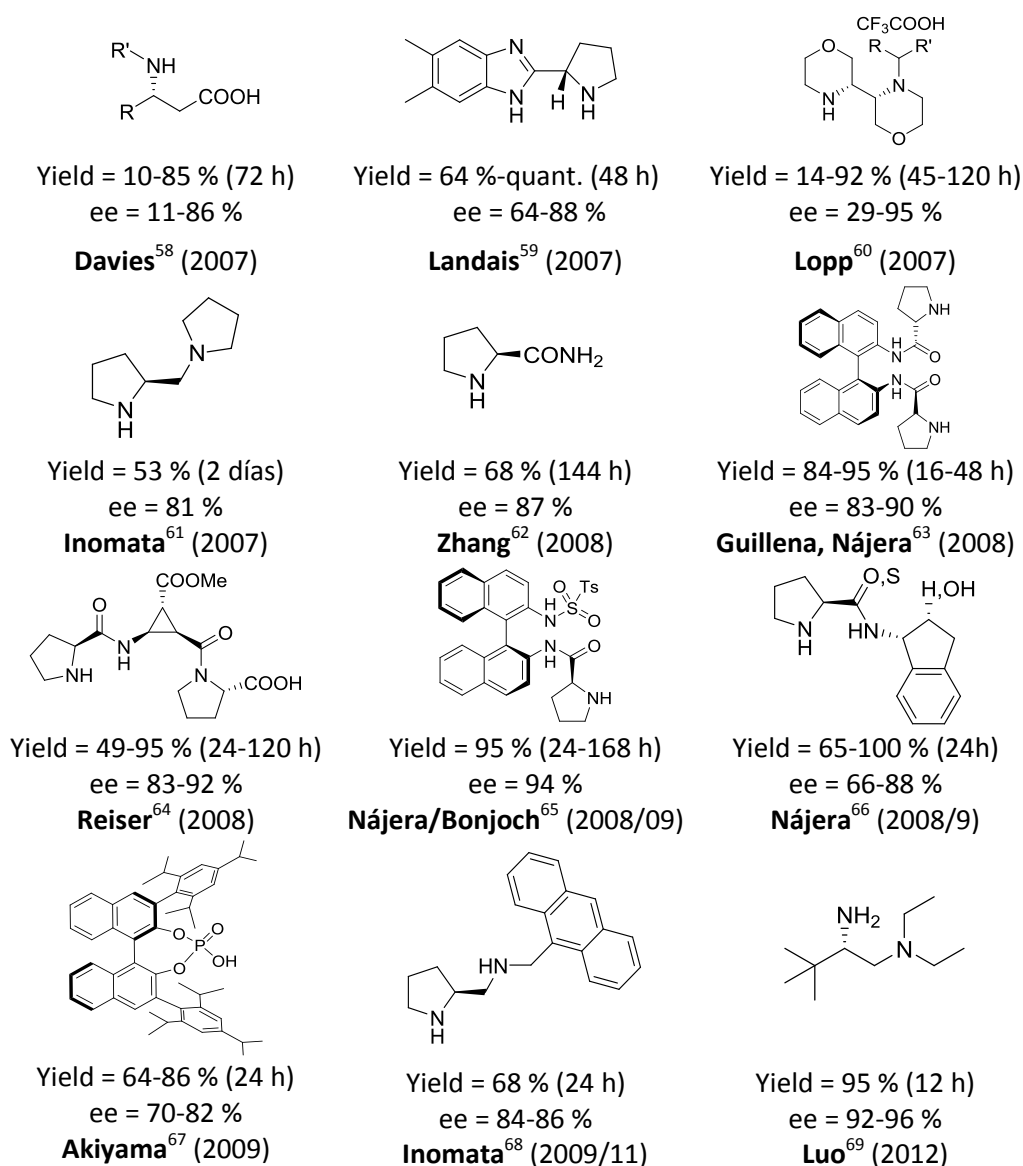


Figure 1.26 (continuation). Different catalysts used in the Hajos-Parrish-Eder-Sauer-Wiechert reaction.

⁵⁹ Lacoste, E.; Vaique, E.; Berlande, M.; Pianet, I.; Vincent, J.-M.; Landais, Y. *Eur. J. Org. Chem.* **2007**, 167-177.

⁶⁰ Kanger, T.; Kriis, K.; Laars, M.; Kailas, T.; Müürisepp, A.-M.; Pehk, T.; Lopp, M. *J. Org. Chem.* **2007**, *72*, 5168-5173.

⁶¹ Akahane, Y.; Inage, N.; Nagamine, T.; Inomata, K.; Endo, Y. *Heterocycles* **2007**, *74*, 637-648.

⁶² Zhang, X. M.; Wang, M.; Tu, Y. Q.; Fan, C. A.; Jiang, Y. J.; Zhang, S. Y.; Zhang, F. M. *Synlett* **2008**, 2831-2835.

⁶³ Guillena, G.; Nájera, C.; Vióquez, S. F. *Synlett* **2008**, 3031-3035.

⁶⁴ D'Elia, V.; Zwicknagl, H.; Reiser, O. *J. Org. Chem.* **2008**, *73*, 3262-3265.

⁶⁵ (a) Bradshaw, B.; Etxebarria-Jardi, G.; Bonjoch, J.; Vióquez, S. F.; Guillena, G.; Nájera, C. *Adv. Synth. Catal.* **2009**, *351*, 2482-2490; (b) Guillena, G.; Nájera, C.; Vióquez, S. F.; *Synlett* **2008**, 3031-3035.

⁶⁶ (a) Almaši, D.; Alonso, D. A.; Balaguer, A.-N.; Nájera, C. *Adv. Synth. Catal.* **2009**, *351*, 1123-1131; (b) Almaši, D.; Alonso, D. A.; Nájera, C. *Adv. Synth. Catal.* **2008**, *350*, 2467-2472.

⁶⁷ Mori, K.; Katoh, T.; Suzuki, T.; Noji, T.; Yamanaka, M.; Akiyama, T. *Angew. Chem., Int. Ed.* **2009**, *48*, 9652-9654.

⁶⁸ (a) Akahane, Y.; Inomata, K.; Endo, Y. *Heterocycles* **2009**, *77*, 1065-1078; (b) Akahane, Y.; Inomata, K.; Endo, Y. *Heterocycles* **2011**, *82*, 1727-1737.

⁶⁹ Zhou, P.; Zhang, L.; Luo, S.; Cheng, J.-P. *J. Org. Chem.* **2012**, *77*, 2526-2530.

1.2. METHODS AND RESULTS

1.2.1. Synthesis of xanthene derived catalysts

As mentioned in the introduction, proline has several solubility and geometry disadvantages that can be solved by performing a suitable design of the catalyst. Xanthenes may provide a suitable framework for generating an oxyanion hole. Specifically, in our research group several of these derivatives have already been used as receptors for carboxylic acids, anions and as sensors.⁷⁰ In figure 1.27 it is shown the X-ray structure of one of these xanthenes. On the left, it appears the oxyanion hole between the two NHs, with a distance of 4.3 Å, very similar to the average distance found in many enzymes using this strategy. In the right figure it can be corroborated the existence of the oxyanion hole since both NHs are forming respective hydrogen bonds with a DMSO molecule (used as solvent to obtain crystals suitable for X-ray analysis) which is perfectly housed in the cavity, with heteroatom-heteroatom hydrogen bonds N-H...O of 3.0 and 3.2 Å.

⁷⁰(a) Muñiz, F. M.; Alcázar, V.; Sanz, F.; Simón, L.; Fuentes de Arriba, Á. L.; Raposo, C.; Morán, J. R. *Eur. J. Org. Chem.* **2010**, 6179-6185; (b) Muñiz, F. M.; Simón, L.; Alcázar, V.; Raposo, C.; Fuentes de Arriba, Á. L.; Morán, J. R. *Eur. J. Org. Chem.* **2009**, 5350-5354; (c) Muñiz, F. M.; Alcázar, V.; Simón, L.; Raposo, C.; Calle, E.; Morán, J. R. *Eur. J. Org. Chem.* **2009**, 1009-1015; (d) Muñiz, F. M.; Simón, L.; Sáez, S.; Raposo, C.; Alcázar, V.; Morán, J. R. *Sensors* **2008**, *8*, 1637-1644.

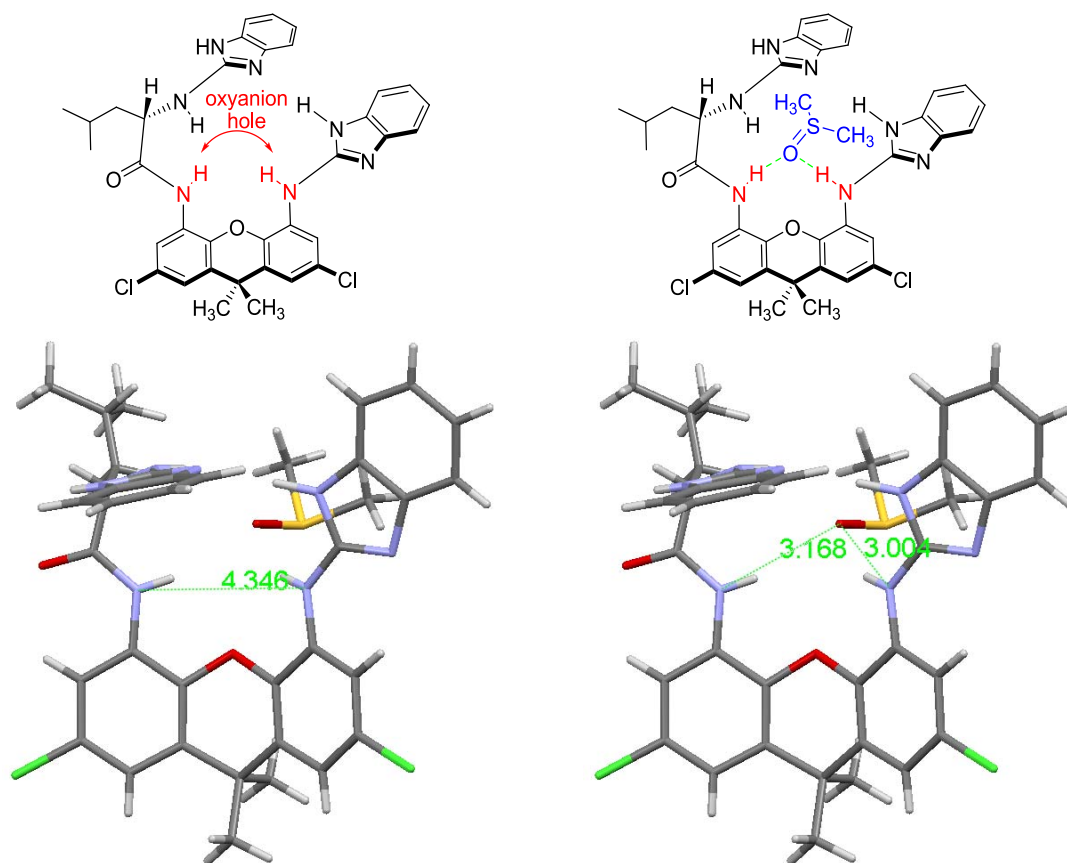


Figure 1.27. X-ray structure of a xanthene derivative.^{70a}

Once confirmed the ability of these receptors to associate carbonyl groups, we decided to functionalize them properly to catalyse aldol reactions. If the xanthene is able to associate carbonyl groups, the inclusion of a proline molecule in one of the substituents of this scaffold would be enough to generate the enamine with a carbonyl group. Then this enamine attacks the acceptor carbonyl group which will be found forming two H-bonds with the xanthene NHs.

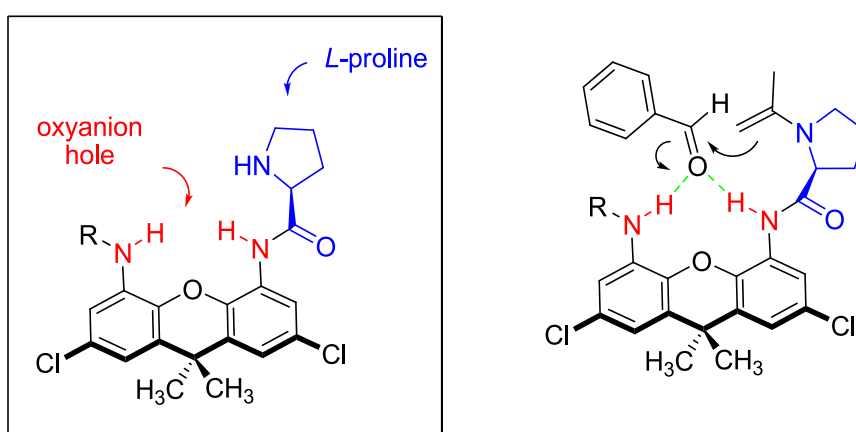


Figure 1.28. Possible catalyst based on a xanthene skeleton and a proline unit and the proposed reaction mechanism.

It would also be possible to tune the acidity of one of the NHs changing the nature of the R group. Thus, we carried out the synthesis of the following compounds:

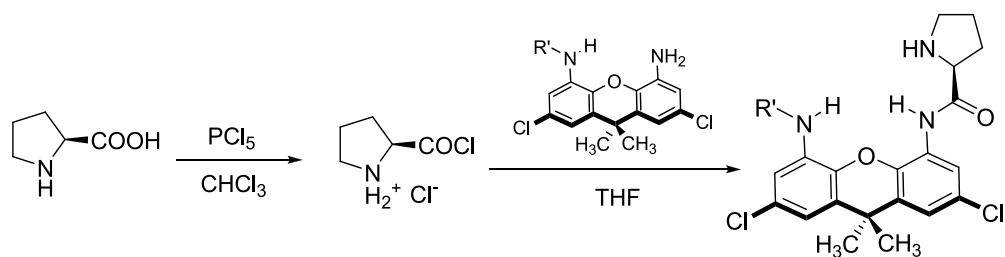


Figure 1.31. Prolinamide synthesis.

This reaction is an obvious advantage over the commonly used synthesis for the preparation of prolinamides (figure 1.32),⁷² which needs protected proline with the *tert*-butoxycarbonyl (Boc) group and the carboxyl group being activated with ethylchloroformate or dicyclohexylcarbodiimide (DCC). In our case, the hydrochloride of the acid chloride of proline has the amino group protonated and the carboxyl group is activated as an acid chloride. This new synthesis is simpler, uses less expensive reagents and is also faster.

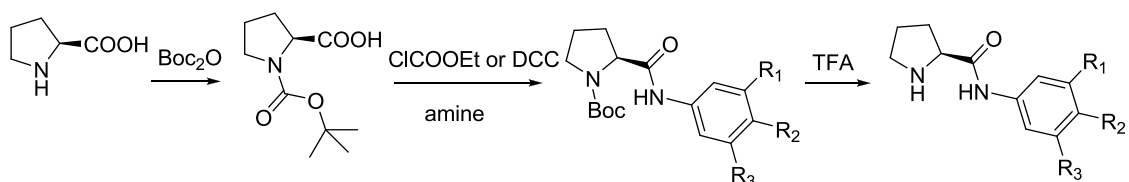


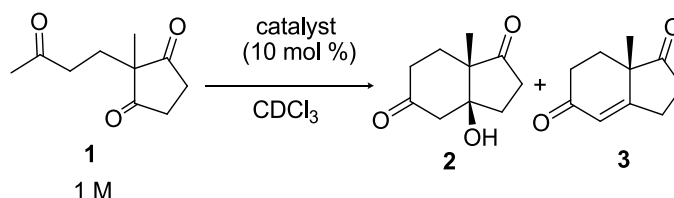
Figure 1.32. Synthesis traditionally used for preparing prolinamides.

⁷² (a) Tang, Z.; Jiang, F.; Cui, X.; Gong, L. Z.; Mi, A. Q.; Jiang, Y. Z.; Wu, Y. D. *Proc. Natl. Acad. Sci.* **2004**, *101*, 5755-5760; (b) Moorthy, J. N.; Saha, S. *Eur. J. Org. Chem.* **2009**, 739-748; (c) Sato, K.; Kuriyama, M.; Shimazawa, R.; Morimoto, T.; Kakiuchi, K.; Shirai, R. *Tetrahedron Lett.* **2008**, *49*, 2402-2406.

1.2.2. Catalytic studies

We tested the catalytic activity of compounds **7-9** in the cyclization reaction to obtain the Hajos-Wiechert ketone, which was prepared according to the existing methods in the literature.²⁹ Results in terms of conversion and enantioselectivity are summarized in table 1.1.

Table 1.1. Results obtained in the preparation of Hajos-Wiechert ketone in $CDCl_3$ at $20\text{ }^\circ\text{C}$ at 1.0 M concentration of ketone **1** in the presence of 10 mol % of catalyst.



entry	catalyst	conversion (%)			time (h)	ee (%)
		aldol 2	ketone 3	total		
1	7	56	14	70	332	98
2	8	58	33	91	97	80
3	9	16	82	98	66	97
4	9·HCl	15	76	91	318	99

The results obtained show very good enantiomeric excesses although the reaction rates were somewhat slow. In view of data obtained, a certain influence on the acidity of the second xanthene NH in the reaction rate and enantioselectivity can be observed. Thus, catalyst **9** having the triflate group (more acid NH) produces the best reaction rate, which diminishes when the acidity of the second NH is reduced. However, there is no relationship between the acidity of this NH and the enantiomeric excess, as catalyst **7** with the Boc group generates an ee of 98%, falling to 80% for the methanesulfonamide catalyst **8**, which has a more acidic NH. For triflamide **9**, which is characterized by the most acidic NH of the three catalysts, the enantiomeric excess only reaches 97%. It is remarkable entry 4, in which catalyst **9** is used as hydrochloride. In this case, an ee of 99% is achieved, but at the expense of reducing by a factor of 5 the reaction rate, relative to the neutral catalyst. Since the amine is protonated, it cannot produce the enamine easily, thereby decreasing the reaction rate. Therefore, the acidity of NH has not a direct influence on the enantioselectivity of the reaction, although it influences the reaction rate.

1.2.3. Prolinamide synthesis

To try to understand the real influence of xanthen second hydrogen bond in the reaction rate and enantiomeric excess, we synthesized several aromatic prolinamides lacking this NH. Some of them had already been used in the intermolecular aldol reaction, with different results.

In absence of the xanthen second acid NH, the idea was to study the influence of the acidity of the NH closer to the prolinamide both in the reaction rate and the enantiomeric excess of the obtained bicyclic ketones. NH acidity is easily adjustable through the use of aromatic rings with different donor and electron-withdrawing group substituents.

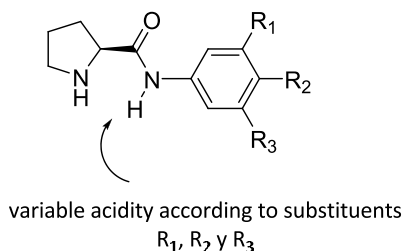


Figure 1.33. Prolinamides with different NH acidity depending on the substituents on the ring.

We used the synthetic procedure described above for preparing prolinamides **10-13**.

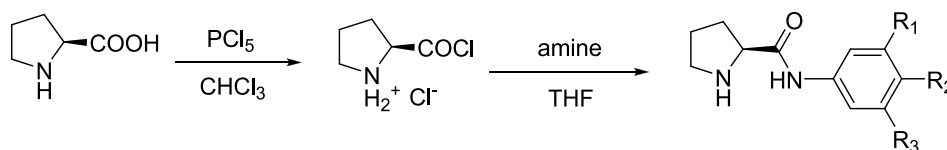


Figure 1.34. Synthesis used for the preparation of prolinamides.

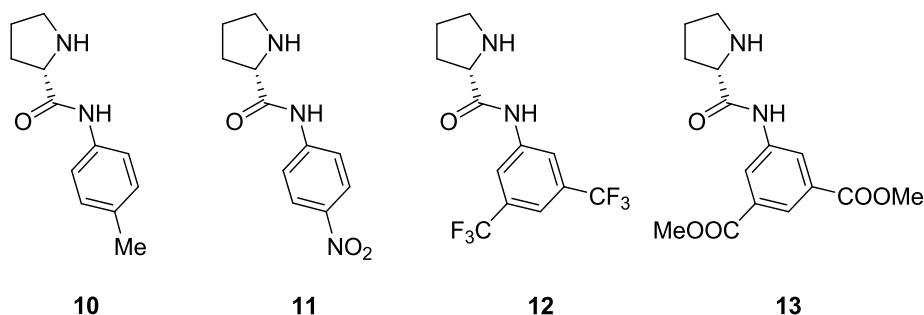


Figure 1.35. Prolinamides studied in the Hajos-Parrish-Eder-Sauer-Wiechert reaction.

To verify the true NH influence in the rate and enantioselectivity of the reaction, we prepared other catalysts lacking this NH, such as a prolinamide **14** with a secondary nitrogen and the butyl ester of proline **15**.

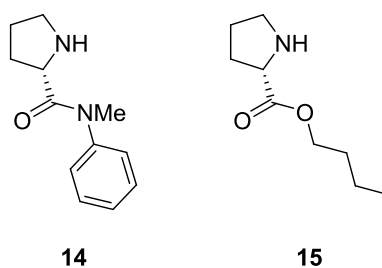
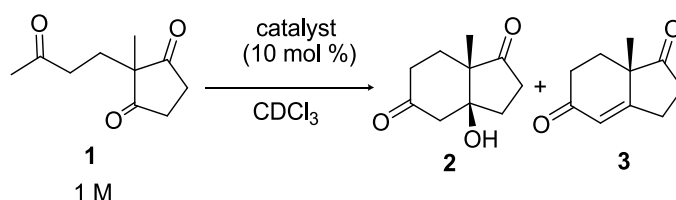


Figure 1.36. NH lacking catalysts.

1.2.4. Catalytic studies in the preparation of the Hajos-Wiechert ketone

Table 1.2 lists the results in terms of conversion, time and enantioselectivity for the intramolecular cyclization which generates the Hajos-Wiechert ketone.

Table 1.2. Results obtained in the preparation of the Hajos-Wiechert ketone in CDCl_3 at $20\text{ }^\circ\text{C}$ at 1.0 M concentration of ketone **1** in the presence of $10\text{ mol } \%$ catalyst.



entry	catalyst	conversion (%)			time (h)	ee (%)
		aldol 2	ketone 3	total		
1	10	58	14	72	330	91
2	11	57	35	92	95	92
3	12	72	20	92	101	95
4	13	44	40	84	167	98
5	14	72	23	95	24	-23
6	15	52	46	98	18	17
7	L-pro	49	42	91	316	63

These results highlight the need for the NH to achieve large enantiomeric excesses. In the case of the catalysts with the secondary amine **14** and ester **15**, which lack the NH, it can be seen that enantiomeric excesses are less than $24\text{ } \%$. Interestingly, in the case of **14**, the enantioselectivity achieved is opposite to that generated by *L*-proline. It is possible that the methyl group attached to the nitrogen atom hinders the approach of the catalyst to the ketone. Furthermore, it appears that the increase in the NH acidity thanks to electron withdrawing groups on the aromatic ring pushes up the enantiomeric excess value (with a

maximum of 98 % in the case of prolinamide **13** with two methoxycarbonyl substituents in the ring).

Interestingly, higher reaction rates are achieved with catalysts lacking NH **14** and **15**, although it is likely that they follow a different mechanism than prolinamides, since they do not have the NH group.

1.2.5. Study of the reaction intermedia in the preparation of the Hajos-Wiechert ketone

When the previous reactions were carried out in the NMR tube, we observed the presence of more signals than the corresponding to reagents, products and catalyst. As catalysis via enamine requires several pre-cyclization steps (addition of the amine to the carbonyl donor, the formation of an iminium salt which subsequently evolves into the enamine, etc.) we performed a study to try to understand the intermediates related to each signal and if they could affect the reaction rate.

We chose the Proton Nuclear Magnetic Resonance (^1H NMR) technique to monitor the reaction, because it allows analysing, in almost real time, what is happening in the bulk of the solution. It is possible to interpret the signals corresponding to each compound, calculate conversions and analyse intermediates. Moreover, the procedure is quite convenient if the reaction proceeds in an NMR tube with deuterated solvents.

Thus, we performed the reaction with 2-methyl-2-(3-oxo-butyl)-cyclopentane-1,3-dione (**1**) in 1.0 M concentration and catalyst **12** also in the same concentration, so that we could distinguish individual compounds without difficulty in the spectrum. We chose to work at 0 °C to isolate the reaction intermediates and avoid elimination. After two hours we could differentiate three different compounds. The percentages obtained by integration of the ^1H NMR signals were: 12% of the starting material **1**, 12 % of aldol **2** and 76 % of a new compound, probably imidazolidinone **16**. These results are similar to those reported by Seebach and List, working with proline, as they had characterized the oxazolidinones of proline with several aldehydes and ketones.

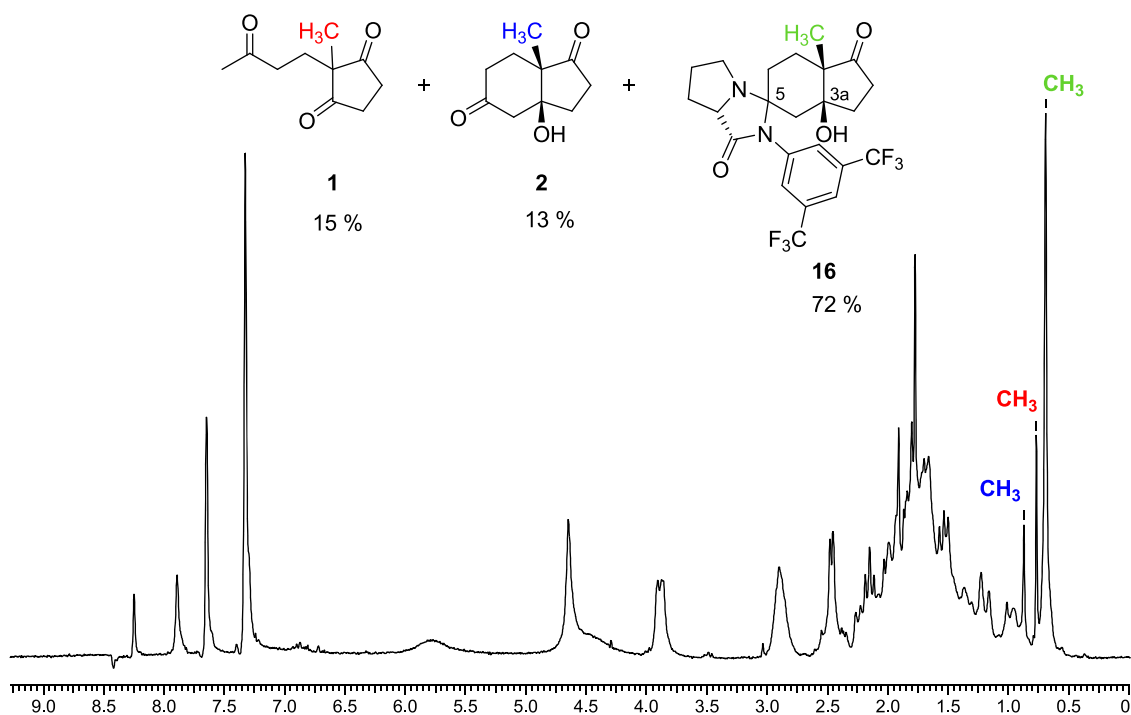


Figure 1.37. Compounds obtained after two hours in the reaction of 2-methyl-2-(3-oxo-butyl-cyclopentane-1,3-dione (**1**) with catalyst **12** in CDCl_3 , both at 1.0 M concentration and at 0 °C.

In a previous work, working with prolinamides, Gryko⁷³ obtained the corresponding thioimidazolidinones (figure 1.38) from acetone, but so far no author has observed them in the reaction product, only in the starting materials (ketones or aldehydes, and always in intermolecular reactions, as shown in figure 1.38).

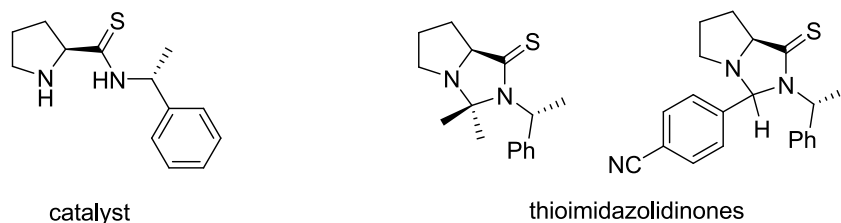


Figure 1.38. Catalyst used by Gryko and thioimidazolidinones detected in the intermolecular aldol reaction.

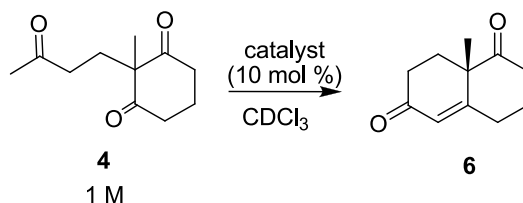
The imidazolidinone **16** structure was elucidated from the proton and carbon spectra obtained, as well as the mass spectrum, which generates a signal at 491 u. The two quaternary carbons characteristic of this structure appears at 77.9 (C-5) and 82.5 ppm (C-3a) (see figure 1.37). Although attempts to isolate it were unsuccessful, we could identify it properly (see experimental part).

⁷³ (a) Gryko, D.; Zimnicka, M.; Lipinski, R. *J. Org. Chem.* **2007**, *72*, 964-970; (b) Gryko, D.; Lipinski, R. *Adv. Synth. Catal.* **2005**, *347*, 1948-1952; (c) Gryko, D.; Lipinski, R. *Eur. J. Org. Chem.* **2006**, 3864-3876.

1.2.6. Catalytic studies in the preparation of the Wieland-Miescher ketone

We also studied the preparation of the Wieland-Miescher ketone,⁷⁴ catalysed with 10 mol % of prolinamides **10-15**. The results are summarized in table 1.3.

Table 1.3. Results obtained in the preparation of the Wieland-Miescher ketone in CDCl₃ at 20 °C at 1.0 M concentration of ketone **4** in the presence of 10 mol % catalyst.



entry	catalyst	conversion 6 (%)	time (h)	ee (%)
1	10	>99	7	94
2	11	94,4	7	87
3	12	>99	7	96
4	13	63,6	7	92
5	14	94,0	24	-0,2
6	15	82,6	17	11
7	L-Pro	19,4	118	60

First, it is noteworthy that only the elimination product and not the aldol compound is obtained. Furthermore, it can be seen that the reactions are faster than in the case of the Hajos-Wiechert ketone, in contrast with most of the results observed in the literature, where it seems that the reaction for the Wieland-Miescher ketone is slower than in the case of the Hajos-Wiechert ketone.

In this case, it appears to be a no clear correlation between the NH acidity and the reaction rate, even with prolinamide lacking the NH, as in compound **14** (the pyrrolidine nitrogen is methylated) the reaction rate is smaller. Regarding the enantiomeric excess, the catalyst that produces the best result is **12** (with two CF₃ groups), although there is no clear relationship with NH acidity: catalyst **10** (toluidine derivative) theoretically less acid than **12**, generates the Wieland-Miescher ketone with higher enantiomeric excess. In any case, results are better than those of L-proline, which yields a smaller enantiomeric excess and reaction rate. With respect to catalyst **14**, in which the amino group of proline is methylated, ketone **6** is essentially racemic.

⁷⁴ Triketone **4** was synthesized according to reference 30.

1.2.7. Study of the reaction intermedia in the preparation of the Wieland-Miescher ketone

Again, we observed several intermediate compounds in the previous catalytic study. To follow more closely the progress of the reaction, we decided to perform it with equimolar amounts of reactant and catalyst **12** (1.0 M) in CDCl_3 at 0°C , so that the progress of the reaction could be analyzed by ^1H and ^{13}C NMR. The first spectra showed the formation of imidazolidinone **17** (see figure 1.39), but nearly simultaneously a new compound started to accumulate, probably with structure **18**, as it can be seen by the presence of olefinic signals (singlet at 5.68 ppm (C-5) and a triplet ($J = 4$ Hz) at 5.17 ppm (C-4) in ^1H NMR and 99.5 ppm for the CH in ^{13}C NMR).

After 6 hours, imidazolidinone **17** had disappeared from the reaction medium, but enamine **18** was still present 24 hours later, in a 20 % respect to the elimination product **6**.

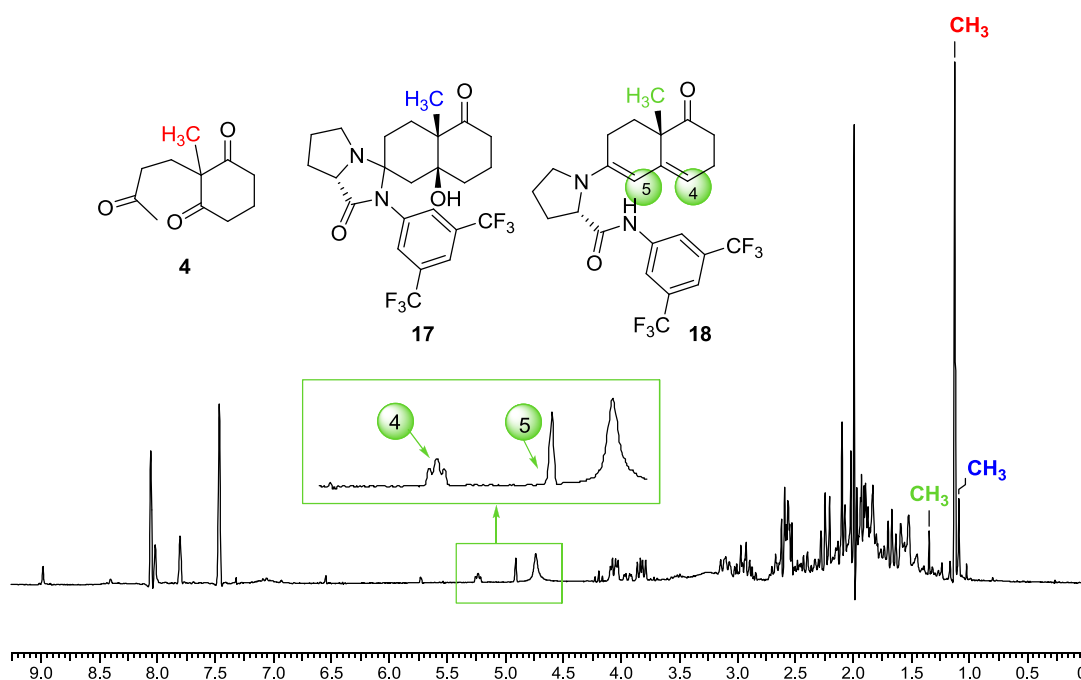


Figure 1.39. Compounds identified after 57 minutes in the reaction between 2-methyl-2-(3-oxobutyl)-cyclohexane-1,3-dione **4** and catalyst **12** in CDCl_3 , both in 1.0 M concentration at 0°C .

After 6 hours, imidazolidinone **17** had disappeared from the reaction medium, but enamine **18** was still present 24 hours later, with a 20 % conversion in comparison with elimination product **6**.

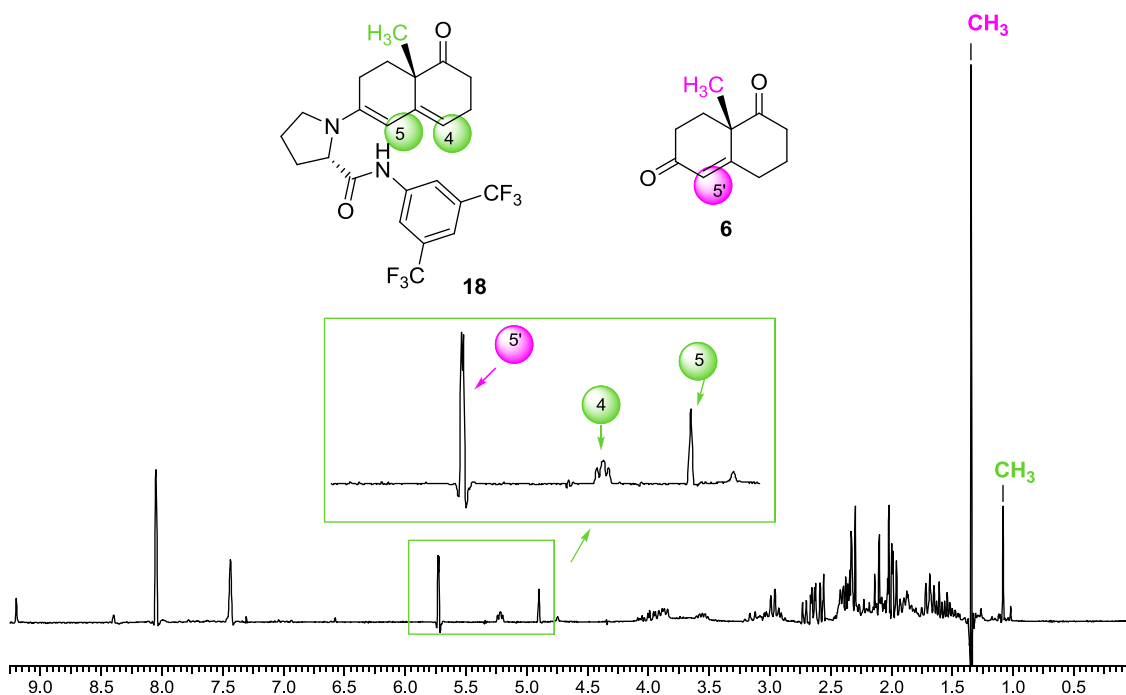


Figure 1.40. Compounds identified after 6 hours in the reaction between 2-methyl-2-(3-oxobutyl)-cyclohexane-1,3-dione **4** and catalyst **12** in CDCl_3 , both in 1.0 M concentration at 0 °C.

Working under conditions previously described by Stork,⁷⁵ we could isolate enamine **19** (for full characterization see experimental part). A similar compound had already been NMR detected by Swaminathan working with *L*-proline.³⁴ The importance of this compound is that it could be used for the synthesis of steroids and other natural products, because this enamine could allow the enantioselective incorporation of different compounds able to make new cycles. Similarly, it would be interesting to try to obtain these enamines with the Hajos-Wiechert ketone. This would be a valuable way for the preparation of steroids with high enantioselectivities. A proposal is shown in figure 1.41.

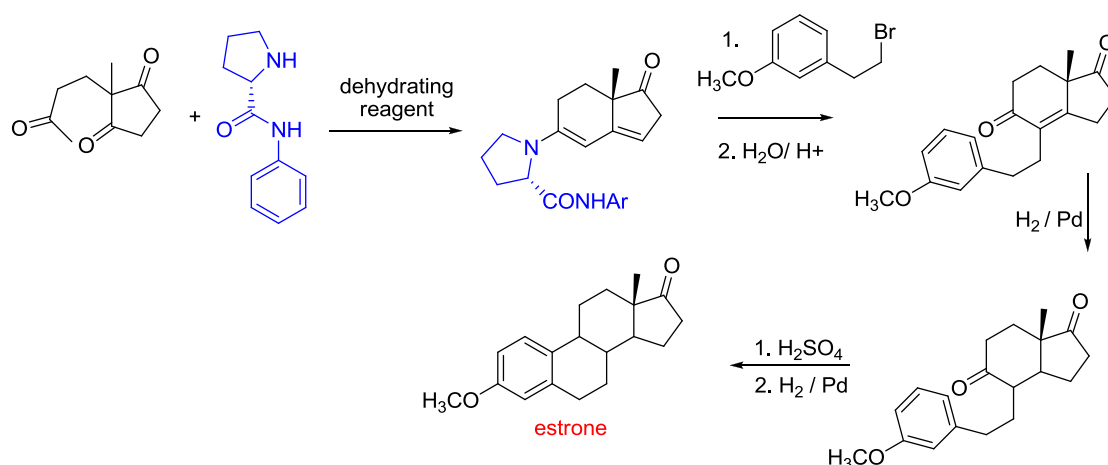


Figure 1.41. A possible way to obtain steroids enantioselectively using the enamine derived from the Hajos-Wiechert ketone.

⁷⁵ Stork, G.; Brizzolara, A.; Landesman, H.; Szmuszkovicz, J.; Terrell, R. *J. Am. Chem. Soc.* **1963**, *85*, 207-222.

1.3. CONCLUSIONS

As predicted in the introduction, the xanthene skeleton has proven to be an excellent scaffold for generating an oxyanion hole as well as to attach a proline molecule responsible of carrying out aldol reactions.

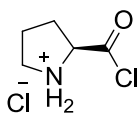
Thus, it has been possible to prepare the Hajos-Wiechert ketone with excellent enantioselectivity (up to 99 %). Trying to study the influence of one of the NHs of the oxyanion hole in the reaction rate and enantioselectivity, we synthesized several aromatic prolinamides with electron withdrawing and donor groups on the ring.

Generally, prolinamides with more acid NH show better enantiomeric excesses and reaction rates (up to 98 % ee for the Hajos-Wiechert ketone and 96 % ee for the Wieland-Miescher ketone). Furthermore, it has been shown the need for the NH to generate high enantiomeric excesses.

Carrying out these reactions, it was observed the formation of several reaction intermedia. A detailed study of the course of the reaction allowed us to characterize aldol imidazolidinone of the Hajos-Wiechert ketone and to isolate the enamine of the Wieland-Miescher ketone, which could show an interesting application in the preparation of steroids and derivatives.

1.4. EXPERIMENTAL

- L-proline hydrochloride acid chloride



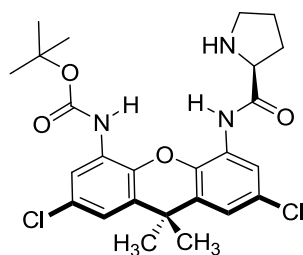
PCl_5 (38.0 g, 182 mmol) was suspended in chloroform (100 mL) under argon in an ice bath. *L*-proline (20.0 g, 173 mmol) was added to the reaction mixture in small portions, keeping the temperature below 10 °C. After 30 minutes, the crystalline solid was filtered under argon and vacuum dried. 25.3 g (149 mmol) were obtained as a white solid with a yield of 86 %.

This compound is stable under argon at -20 °C for several months, but it could not be characterized since it hydrolyses easily.

- General procedure for the preparation of 7-15 prolinamides

The appropriate amine (30 mmol) was dissolved in dry THF (30.0 mL) under argon. *L*-proline hydrochloride acid chloride (6.80 g, 40 mmol) was added and the mixture stirred a few minutes. The reaction can be followed by thin layer chromatography (TLC). When the reaction had ended, a small amount of H_2O (5.0 mL) was added to hydrolyze the excess of acid chloride. THF was evaporated and the residue dissolved in ethyl acetate and washed with saturated sodium carbonate. The organic fractions were dried over anhydrous Na_2SO_4 and the solvent evaporated. The obtained compound was purified by chromatography on silica gel (CH_2Cl_2).

- *Tert*-butyl-2,7-dichloro-9,9-dimethyl-5-(pyrrolidin-2-carboxamido)-9*H*-xanthene-4-ylcarbamate (7)



Colourless solid; yield: 75 %.

$[\alpha]_D^{20} = +72.5$ ($c = 1.30$, CHCl_3).

mp: 90-92 °C.

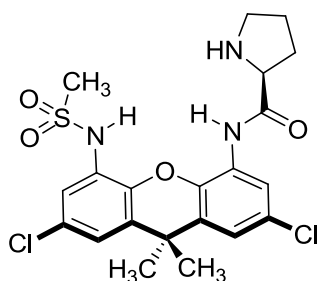
$^1\text{H RMN}$ (CDCl_3) δ (ppm): 1.53 (s, 3H), 1.57 (s, 9H), 1.59 (s, 3H), 1.66-1.92 (m, 2H), 2.10-2.26 (m, 2H), 2.97-3.26 (m, 2H), 3.97 (dd, $J = 5.9, 7.8$ Hz, 1H), 7.02 (d, $J = 2.3$ Hz, 1H), 7.05 (d, $J = 2.3$ Hz, 1H), 7.33 (s, NH), 8.14 (1H, s), 8.27 (d, $J = 2.3$ Hz, 1H), 10.84 (s, NH).

$^{13}\text{C RMN}$ (CDCl_3) δ (ppm): 26.5 (CH_2), 28.3 ($\text{CH}_3 \times 3$), 30.5 (CH_2), 31.0 (CH_3), 32.4 (CH_3), 34.9 (C), 47.7 (CH_2), 61.4 (CH), 81.5 (C), 117.4 (CH $\times 2$), 119.3 (CH), 120.0 (CH), 126.8 (C), 127.8 (C), 129.0 (C), 129.1 (C), 130.6 (C), 130.6 (C), 136.7 (C), 137.5 (C), 152.3 (C), 172.8 (C).

IR (film, cm^{-1}): 3416, 3371, 3253, 3111, 29745, 2929, 2865, 1736, 1703, 1638, 1541, 1405, 1223, 1158, 879, 756.

HRMS (ESI) 506.1613 ($\text{M} + \text{H}^+$), calcd for $\text{C}_{25}\text{H}_{30}\text{Cl}_2\text{N}_3\text{O}_4$ 506.1608.

- *N*-(2,7-dichloro-9,9-dimethyl-5-(methylsulfonamido)-9*H*-xanthen-4-yl)pyrrolidine-2-carboxamide (8)



Colourless solid; yield: 75 %.

$[\alpha]_D^{20} = +44.1$ ($c = 0.64$, CHCl_3).

mp: vitreous compound.

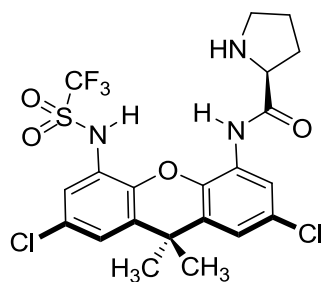
$^1\text{H RMN}$ (CDCl_3) δ (ppm): 1.57 (s, 3H), 1.64 (s, 3H), 1.70-1.89 (m, 2H), 2.00-2.37 (m, 2H), 2.91-3.12 (m, 1H), 3.19-3.34 (m, 1H), 3.10 (s, 3H), 3.97 (dd, $J = 5.1, 9.0$ Hz, 1H), 7.08 (d, $J = 2.3$ Hz, 1H), 7.18 (d, $J = 2.3$ Hz, 1H), 7.52 (d, $J = 2.3$ Hz, 1H), 8.24 (d, $J = 2.3$ Hz, 1H), 10.80 (s, NH).

$^{13}\text{C RMN}$ (CDCl_3) δ (ppm): 27.1 (CH_2), 30.7 (CH_2), 31.1 (CH_3), 32.8 (CH_3), 35.3 (C), 40.1 (CH_3), 47.9 (CH_2), 62.0 (CH), 118.0 (CH), 118.1 (CH), 120.4 (CH), 122.1 (CH), 126.3 (C), 127.0 (C), 129.6 (C), 129.8 (C), 130.6 (C), 132.1 (C), 137.6 (C), 138.1 (C), 173.1 (C).

IR (film, cm^{-1}): 3358, 3260, 2975, 2923, 2865, 1690, 1619, 1534, 1431, 1346, 1268, 1236, 1165, 1106, 1015, 970, 873, 834, 730.

HRMS (ESI) 484.0859 ($\text{M} + \text{H}^+$), calcd for $\text{C}_{21}\text{H}_{24}\text{Cl}_2\text{N}_3\text{O}_4\text{S}$ 484.0859.

- ***N*-(2,7-dichloro-9,9-dimethyl-5-(trifluoromethylsulfonamido)-9*H*-xanthen-4-yl)pyrrolidine-2-carboxamide (9)**



Colourless solid; yield: 77 %.

$[\alpha]_D^{20} = -61.2$ ($c = 1.20$, CHCl_3).

mp: 163-165 °C.

$^1\text{H RMN}$ (CDCl_3) δ (ppm): 1.59 (s, 3H), 1.66 (s, 3H), 1.80-2.15 (m, 3H), 2.70-2.95 (m, 1H), 3.43 (t, $J = 7.0$ Hz, 2H), 4.89 (dd, $J = 7.8, 8.2$ Hz, 1H), 6.98 (d, $J = 2.8$ Hz, 1H), 7.04 (d, $J = 2.8$ Hz, 1H), 7.11 (d, $J = 2.8$ Hz, 1H), 7.71 (d, $J = 2.4$ Hz, 1H), 9.46 (s, NH).

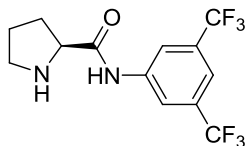
$^{13}\text{C RMN}$ (CDCl_3) δ (ppm): 24.6 (CH_2), 29.0 (CH_3), 30.0 (CH_2), 34.7 (CH_3), 35.2 (C), 45.6 (CH_2), 61.1 (CH), 117.7 (CH), 121.5 (CH x 2), 125.8 (CH), 126.0 (C), 127.8 (C), 128.1 (C), 131.2 (C), 131.3 (C), 131.8 (C), 137.9 (C), 144.0 (C), 166.4 (C), 174.6 (C).

IR (film, cm^{-1}): 3371, 3293, 3118, 2968, 2929, 1703, 1625, 1547, 1450, 1288, 1236, 1197, 1171, 1132, 1054.

HRMS (ESI) 538.0582 ($\text{M} + \text{H}^+$), calcd for $\text{C}_{21}\text{H}_{21}\text{Cl}_2\text{F}_3\text{N}_3\text{O}_4\text{S}$ 538.0576.

-Compounds **10**^{72a} and **11**^{72,76} were prepared according to the general procedure and their physical and spectroscopic properties are consistent with those described in the literature.

- (S)-N-(3,5-bis(trifluoromethyl)phenyl)pyrrolidin-2-carboxamide (**12**)



Pale yellow oil; yield: 68 %.

$[\alpha]_D^{25} = -37.2$ ($c = 1.33$, CHCl_3).

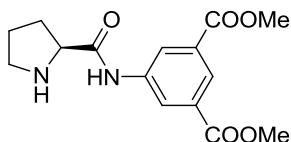
$^1\text{H NMR}$ (CDCl_3) δ (ppm): 1.74-1.81 (m, 2H), 2.01-2.14 (m, 1H), 2.15-2.30 (m, 1H), 2.95-3.20 (m, 2H), 3.90 (dd, $J = 9.0, 3.0$ Hz, 1H), 7.58 (s, 1H), 8.12 (s, 2H), 10.13 (s, NH).

$^{13}\text{C NMR}$ (CDCl_3) δ (ppm): 26.5 (CH_2), 30.9 (CH_2), 47.6 (CH_2), 61.2 (CH), 117.3 (CH), 119.1 (CH x 2), 126.1 (C x 2), 132.1 (C x 2), 139.4 (C), 174.3 (C).

IR (nujol, cm^{-1}): 3247, 2922, 1696, 1625.

HRMS (ESI): 327.0904 ($\text{M} + \text{H}$)⁺, calcd for $\text{C}_{13}\text{H}_{13}\text{N}_2\text{OF}_6$: 327.0927

- (S)-dimethyl-5-(pyrrolidin-2-carboxamido)isophthalate (**13**)



White solid; Yield: 69 %.

$[\alpha]_D^{25} = -30.2$ ($c = 1.12$, EtOH).

mp: 128-130 °C.

$^1\text{H NMR}$ (CDCl_3) δ (ppm): 1.73-1.80 (m, 2H), 1.90-2.30 (m, 2H), 2.90-3.10 (m, 2H), 3.85-3.96 (m, 1H), 3.94 (s, 6H), 8.40 (s, 1H), 8.46 (s, 2H).

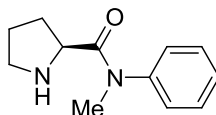
$^{13}\text{C NMR}$ (CDCl_3) δ (ppm): 26.0 (CH_2), 30.9 (CH_2), 47.0 (CH_2), 51.8 (CH_3 x 2), 61.0 (CH), 124.4 (CH x 2), 125.3 (CH), 131.2 (C x 2), 139.1 (C), 166.0 (C x 2), 174.8 (C).

⁷⁶ Tang, Z.; Yang, Z.-H.; Chen, X.-H.; Cun, L.-F.; Mi, A.-Q.; Jiang, Y.-Z.; Gong, L.-Z. *J. Am. Chem. Soc.* **2005**, *127*, 9285-9289.

IR (nujol, cm^{-1}): 2924, 2854, 1729, 1586, 1462.

HRMS (ESI): 307.1284 ($\text{M}+\text{H}^+$), calcd for $\text{C}_{15}\text{H}_{19}\text{N}_2\text{O}_5$: 307.1288.

- (S)-N-methyl-N-phenylpyrrolidine-2-carboxamide (14)



White solid; Yield: 83 %.

$[\alpha]_{\text{D}}^{25} = -37.8$ ($c = 1.29$, CHCl_3).

mp: 96-98 °C.

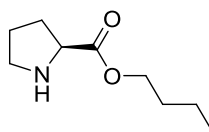
$^1\text{H NMR}$ (CDCl_3) δ (ppm): 1.52-1.68 (m, 2H), 2.67 (m, 2H), 2.80-3.15 (m, 2H), 3.20 (s, 3H), 3.46-3.60 (m, 1H), 7.19 (dd, $J = 6.0, 1.4$ Hz, 2H), 7.35-7.43 (m, 3H).

$^{13}\text{C NMR}$ (CDCl_3) δ (ppm): 26.9 (CH_2), 31.8 (CH_2), 38.0 (CH_3), 48.0 (CH_2), 58.8 (CH), 127.9 (CH x 2), 128.3 (CH), 129.9 (CH x 2), 143.3 (C), 174.6 (C).

IR (nujol, cm^{-1}): 2923, 2845, 1658, 1593, 1463, 1379, 1268, 1093, 730.

HRMS (ESI): 205.1323 ($\text{M} + \text{H}^+$), calcd for $\text{C}_{12}\text{H}_{17}\text{N}_2\text{O}$: 205.1335.

- (S)-butyl-pyrrolidin-2-carboxylate (15)



L-proline (5.0 g, 43.4 mmol), thionyl chloride (5.0 mL, 68 mmol) and *n*-butanol (50.0 mL) were mixed and heated to reflux for 2 hours. The solvent was evaporated and the residue extracted with ethyl acetate (50.0 mL). Then 100 mL of aqueous sodium carbonate (10 %) was added. The organic phase was dried over Na_2SO_4 and the solvent was evaporated to obtain an oily compound (85 % yield).

$[\alpha]_{\text{D}}^{25} = -37.9$ ($c = 1.38$, CHCl_3).

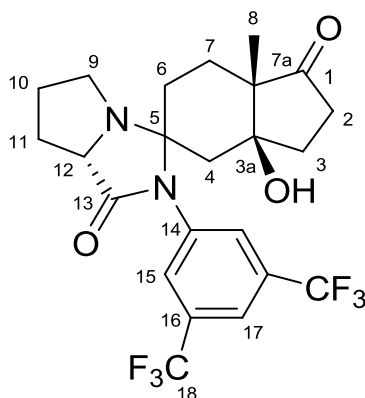
$^1\text{H NMR}$ (CDCl_3) δ (ppm): 0.90 (t, $J = 7.2$ Hz, 3H), 1.29-1.40 (m, 2H), 1.56-1.89 (m, 5H), 2.03-2.20 (m, 1H), 2.81-2.92 (m, 1H), 3.02-3.11 (m, 1H), 3.71 (dd, $J = 8.8, 5.8$ Hz, 1H), 4.09 (t, $J = 6.7$ Hz, 2H).

^{13}C NMR (CDCl_3) δ (ppm): 13.9 (CH_3), 19.3 (CH_2), 25.7 (CH_2), 30.5 (CH_2), 30.9 (CH_2), 47.3 (CH_2), 60.0 (CH), 64.9 (CH_2), 175.8 (C).

IR (nujol, cm^{-1}): 1469, 1677, 1742, 2858, 2917.

HRMS (ESI): 172.1326 ($\text{M} + \text{H}$) $^+$, calcd for $\text{C}_9\text{H}_{18}\text{NO}_2$: 172.1332.

- (3a*S*,7a*S*,7a'*S*)-2'-(3,5-bis(trifluoromethyl)phenyl)-3a-hydroxy-7a-methyldecahydrospiro[indene-5,3'-pyrrolo[1,2-*c*]imidazole]-1,1'(2'*H*,6*H*)-dione (**16**)



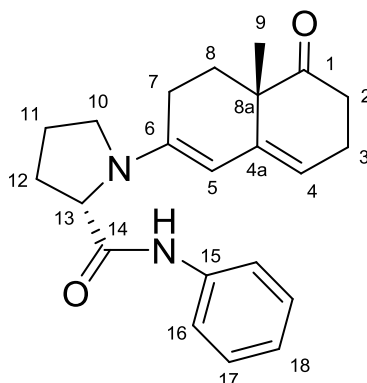
2-methyl-2-(3-oxobutyl)-cyclopentane-1,3-dione (**1**) (224 mg, 1.23 mmol) and prolinamide **12** (393 mg, 1.20 mmol) were mixed in 0.4 mL of CDCl_3 . The mixture, when dissolved, was transferred to an NMR tube and kept at 0 °C. After two hours, integration of the ^1H NMR signals reveals imidazolidinone **16** in 76 % conversion.

^1H NMR (CDCl_3) δ (ppm): 0.95 (s, 3H, H-8), 1.50-2.50 (m, 14H), 3.10 (m, 2H, H-9), 4.10 (dd, 1H, H-12), 7.43 (s, 2H, H-15), 8.06 (s, 1H, H-17).

^{13}C NMR (CDCl_3) δ (ppm): 19.0 (C-8), 24.9 (C-7), 25.4 (C-10), 28.9 (C-6), 29.2 (C-3), 30.6 (C-2), 33.4 (C-11), 42.8 (C-4), 47.1 (C-9), 52.3 (C-7a), 63.2 (C-12), 77.9 (C-3a), 82.5 (C-5), 122.0 (C-17), 122.7 (q, $J = 275.0$ Hz, C-18), 129.8 (C-15), 132.8 (q, $J = 35.0$ Hz, C-16), 137.2 (C-14), 176.3 (C-13), 217.8 (C-1).

MS (ESI): 491.3 ($\text{M} + \text{H}$) $^+$, calcd for $\text{C}_{23}\text{H}_{25}\text{F}_6\text{N}_2\text{O}_3$ 491.18.

- (S)-1-((S)-4a-methyl-5-oxo-3,4,4a,5,6,7-hexahydronaphthalen-2-yl)-N-phenylpyrrolidine-2-carboxamide (**19**)



2-methyl-2-(3-oxobutyl)-cyclohexane-1,3-dione (**4**) (530 mg, 2.70 mmol) and the aniline prolinamide (513 mg, 2.7 mmol)⁷⁷ were dissolved in toluene (5 mL) and maintained at 40 °C and 20 mmHg for 2 hours. As the reaction became more viscous additional portions of toluene under argon were added. Once elapsed the two hours, diethyl ether was added (20 mL) and the mixture was cooled to -80 °C. The product precipitated and was filtered under argon (the crystals melt before reaching room temperature and decomposes in the presence of oxygen) and were dried under vacuum (0.1 mmHg, 100 °C, 3h) to afford enamine **19** (600 mg, 65% yield).

$[\alpha]_D^{25} = -124.0$ ($c = 0.62$, CHCl_3).

¹H NMR (CDCl_3) δ (ppm): 1.20 (s, 3H, H-9), 2.74-1.58 (m, 12H), 3.20 (q, $J = 9.6$ Hz, 1H, H-10), 3.58 (t, $J = 9.0$ Hz, 1H, H-10), 4.07 (dd, $J = 3.0, 9.0$ Hz, 1H, H-13), 5.05 (s, 1H, H-5), 5.34 (t, $J = 4.8$ Hz, 1H, H-4), 7.10 (t, $J = 8.0$ Hz, 1H, H-18), 7.29 (t, $J = 8.0$ Hz, 2H, H-17), 7.48 (d, $J = 8.0$ Hz, 2H, H-16), 8.16 (s, NH).

¹³C NMR (CDCl_3) δ (ppm): 22.2 (C-9), 23.9 (C-3, C-7, C-11), 28.9 (C-12), 31.3 (C-8), 35.7 (C-2), 44.8 (C-8a), 49.1 (C-10), 63.6 (C-13), 99.9 (C-5), 115.6 (C-4), 119.8 (C-18), 124.4 (C-17 x 2), 128.9 (C-16 x 2), 137.3 (C-4a), 139.5 (C-15), 142.3 (C-6), 172.1 (C-14), 215.4 (C-1).

IR (nujol, cm^{-1}): 3285, 2923, 1716, 694.

HRMS (ESI): 351.2054 ($\text{M} + \text{H}$)⁺, calcd for $\text{C}_{22}\text{H}_{27}\text{N}_2\text{O}_2$ 351.2067.

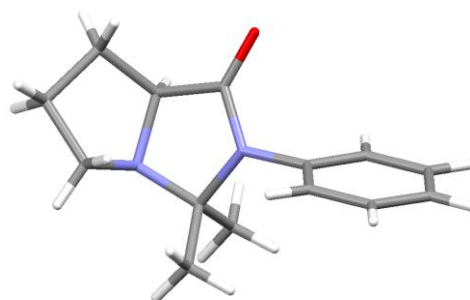
⁷⁷ This prolinamide was chosen by its simplicity. It was prepared according to the general procedure and its spectroscopic properties are the same as that published in reference 72.



VNIVERSIDAD
D SALAMANCA

CAMPUS DE EXCELENCIA INTERNACIONAL

***CHAPTER 2: Study of the aldol reaction mechanism
catalysed by prolinamides***

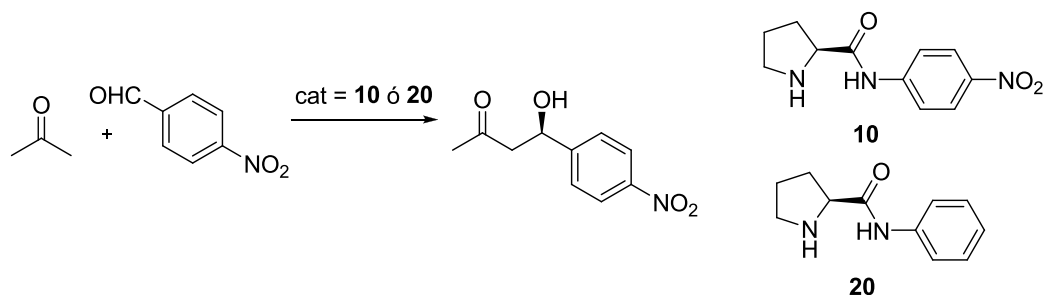


2.1. INTRODUCTION

The formation of imidazolidinones in the intramolecular aldol reaction was quite striking for us. Although initially it would be expected to be compounds with a short half-life, surprisingly, imidazolidinones were formed with high yields in the reaction media and even could be isolated. At this point, we thought that imidazolidinones could be the key to understand the mechanism of the reaction, so we decided to carry out further research on its properties, its formation and reactivity.

In order to try to understand the formation of the above intermedia and its degree of participation in the reaction mechanism, we performed several experiments working with simpler molecules. We chose the intermolecular aldol reaction between acetone and 4-nitrobenzaldehyde (working at concentration levels of 1.0 M) and in different deuterated solvents, in order to conduct a thorough study of the diverse intermedia formed over time by ^1H and ^{13}C NMR.

A first literature search revealed, however, the existence of contradictory results for this type of reactions. Even working with the same catalyst, yields and enantiomeric excesses were highly variable depending on the reaction conditions and the additives used.

Table 2.1. Different results obtained in the intermolecular aldol reaction between acetone and 4-nitrobenzaldehyde with prolinamides **10** and **20** (20 mol %).

entry	catalyst	yield (%)	ee (%)
1 ^a	10	80	39
2 ^b	10	80	54
3 ^c	10	76	72
4 ^b	20	88	8
5 ^d	20	87	15
6 ^a	20	88	37
7 ^c	20	68	71

^a 4-Nitrobenzaldehyde (0.5 mmol, 0.5 M) in neat acetone and catalyst (0.1 mmol, 0.1 M).⁷⁸

^b The reaction of aldehyde (0.3 mmol, 1 equiv) with acetone (6.0 mmol, 20 equiv) was run in HMPA/H₂O in the presence of catalyst (0.06 mmol, 0.2 equiv).⁷⁹

^c The reaction was run in DMF with 4-nitrobenzaldehyde (0.66 mmol, 1 equiv), catalyst (0.13 mmol, 0.2 equiv), acetone (13.2 mmol, 20 equiv) and TFA (0.066 mmol, 0.1 equiv).⁸⁰

^d 4-Nitrobenzaldehyde (2 mmol, 1 equiv), acetone (40 mmol, 20 equiv) in H₂O using **20**·HBr (0.4 mmol, 0.2 equiv).⁸¹

The reason for these variations is unclear. It appears that the solvent may have a key importance, and also the presence of acid or water, additives that may be critical to avoid the formation of reaction intermediates such as imidazolidinones. However, as discussed above, even Houk proposed mechanism is unable to resolve some issues that are still enigmatic. Therefore, it seems logic to begin with a detailed study of the mechanism of this reaction. With acetone and 4-nitrobenzaldehyde (the model compounds used in the literature) as starting

⁷⁸ Tang, Z.; Jiang, F.; Cui, X.; Gong, L. Z.; Mi, A. Q.; Jiang, Y. Z.; Wu, Y. D. *Proc. Natl. Acad. Sci.* **2004**, *101*, 5755-5760.

⁷⁹ Sato, K.; Kuriyama, M.; Shimazawa, R.; Morimoto, T.; Kakiuchi, K.; Shirai, R. *Tetrahedron Lett.* **2008**, *49*, 2402-2406.

⁸⁰ Moorthy, J. N.; Saha, S. *Eur. J. Org. Chem.* **2009**, 739-748.

⁸¹ Chimni, S. S.; Singh, S.; Kumar, A. *Tetrahedron: Asymmetry* **2009**, *20*, 1722-1724.

materials, we studied the reaction intermedia formed, the influence of the solvent and the presence of different additives.

2.2. METHODS AND RESULTS

2.2.1. Mechanistic studies in CDCl_3

2.2.1.1. Reaction between acetone and 4-nitrobenzaldehyde catalysed by prolinamide **20**

We began the study of this intermolecular reaction with the same conditions we had employed in the intramolecular reaction. The catalyst employed, prolinamide **20**, with no substituents on the aromatic ring, is very easily obtained in one step, treating aniline with the acid chloride of the proline hydrochloride.

The reaction studied was carried out by mixing reactants and catalyst in equimolar amounts at 1.0 M concentration in CDCl_3 . After 5 minutes, the ^1H NMR spectrum showed several compounds: signals of the aldehyde, acetone and the starting prolinamide **20** could be seen, but also other intermedia:

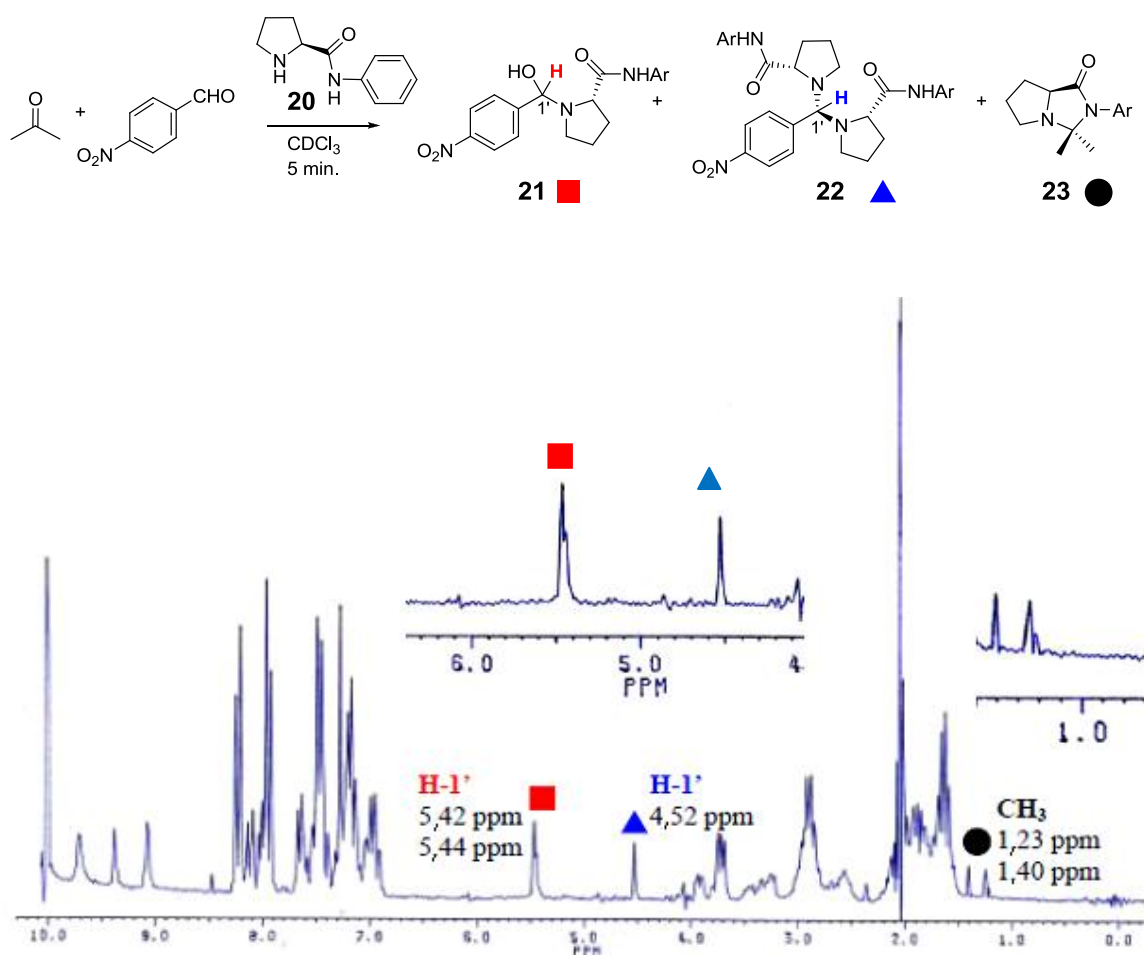


Figure 2.1. ^1H NMR spectrum corresponding to the reaction between acetone and 4-nitrobenzaldehyde in CDCl_3 catalysed by prolinamide **20** after 5 minutes.

The observed signals suggested the presence of the addition product of prolinamide to 4-nitrobenzaldehyde **21** (two singlets at 5.42 ppm and 5.44 ppm corresponding to the two possible stereoisomers), 4-nitrobenzaldehyde aminal **22**, formed by the introduction of two molecules of prolinamide (singlet at 4.52 ppm) and acetone imidazolidinone **23** (2 singlets at 1.23 ppm and 1.40 ppm for the methyl groups), a cyclic compound formed by the reaction between **20** and acetone prolinamide.

In the following 5 to 15 minutes it could be seen an increase in aminal **22** at the expense of hemiaminal **21**. The amount of imidazolidinone **23** continued increasing.

After 25 minutes new signals appeared. These signals were still too small to provide a reliable assignment, but subsequent spectra showed that they corresponded to aldehyde imidazolidinones (**24a** and **24b**), aldol **25** and imidazolidinones of this aldol (**26a** and **26b**). These new signals continued growing in the next few hours while the corresponding hemiaminal **21** and aminal **22** reduced their intensities.

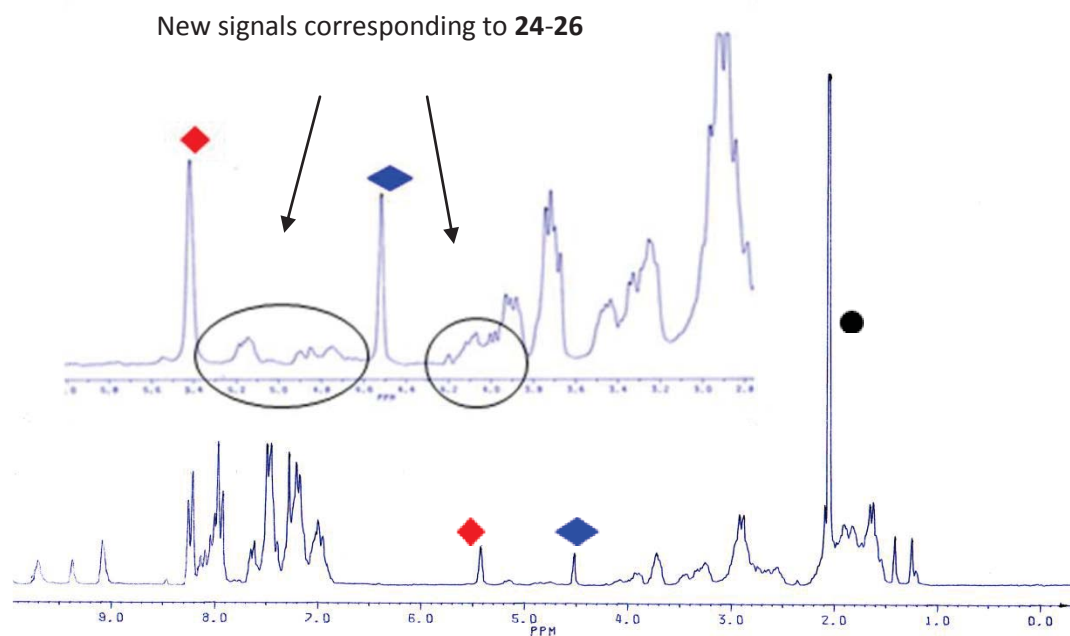
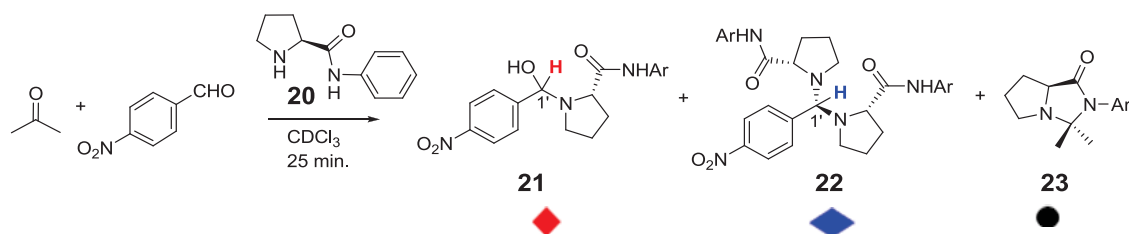


Figure 2.2. ^1H NMR spectrum corresponding to the reaction between acetone and 4-nitrobenzaldehyde in CDCl_3 catalysed by prolinamide **20** after 25 minutes.

After 16 hours the hemiaminal **21** was no longer observed in the reaction medium and the proportion of aminoral **22** was minimal.

After three days aminoral **22** signals were no longer seen in the spectrum, although the free aldehyde could still be observed.

After 9 days the NMR spectrum showed the existence of aldehyde imidazolidinones (56 % conversion) (**24a** and **24b**) (6.34 and 5.72 ppm, respectively), acetone imidazolidinone **23** (4.05 ppm, 30 % conversion), aldol **25** (5.1 ppm) and imidazolidinones of these aldols (**26a**, 4.87 ppm; **26b**, 5.13 ppm). Acetone and 4-nitrobenzaldehyde were only found in trace amounts.

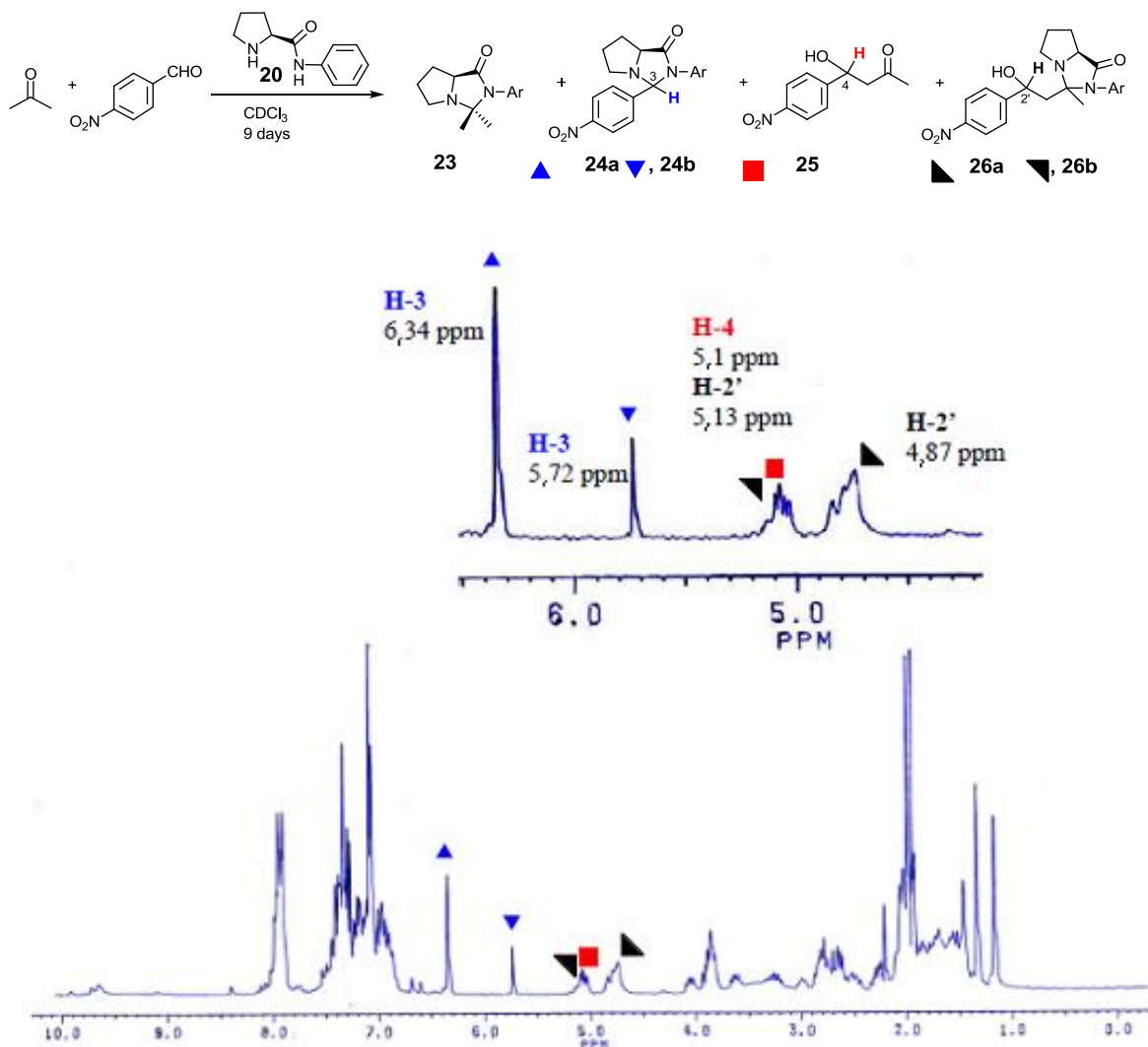


Figure 2.3. NMR spectrum corresponding to the reaction between acetone and 4-nitrobenzaldehyde in CDCl₃ catalysed by prolinamide **20** after 9 days.

2.2.1.2. Imidazolidinones isolation

The adducts of the aldehyde (**21** and **22**) are unstable reaction intermedia which are rapidly hydrolysed and therefore difficult to isolate. However, it was possible to obtain acetone imidazolidinone **23** dissolving prolinamide **20** in acetone in the presence of a dehydrating agent as Na_2SO_4 or K_2CO_3 (see experimental part). We were even able to obtain crystals suitable for X-ray analysis.

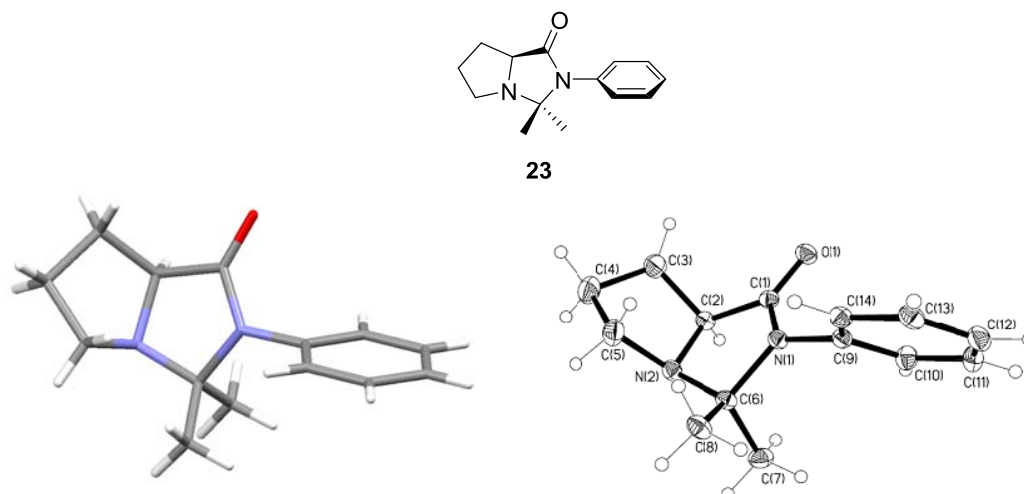


Figure 2.4. (Left) X-ray structure of imidazolidinone **23** and (right) ORTEP representation.

One interesting feature that can be seen in this structure is the great tension that exists due to the dihedral angle of nearly 90° between the aniline aromatic ring and the carbonyl group of proline, causing a great loss of conjugation energy. This same feature can be observed in solution, comparing the ^1H NMR spectra of prolinamide **20** and imidazolidinone **23**: in the latter, *ortho* protons are strongly shielded (7.12 ppm) compared to the same protons in prolinamide (7.69 ppm). These last protons undergo the anisotropic effect of the carbonyl group located in the plane of the ring, causing its deshielding in the NMR spectrum.

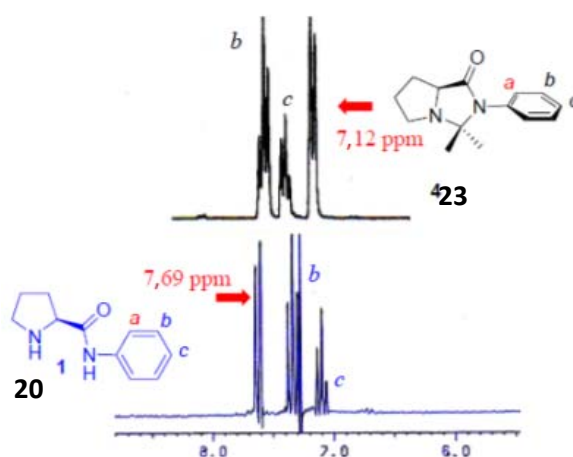


Figure 2.5. Region of the ^1H NMR spectrum between 6.0 ppm and 8.5 ppm showing the shielding of the protons ortho to the aromatic ring of the imidazolidinone **23** (7.12 ppm) in comparison with prolinamide **20** (7.69 ppm).

It was also possible to prepare imidazolidinones of 4-nitrobenzaldehyde and prolinamide **20**. This preparation was carried out by mixing both compounds in deuteriochloroform (to follow the progress of the reaction by NMR). The reaction was slow, but after 9 days a mixture (5:1) of both imidazolidinones (**24a**, **24b**) was obtained.

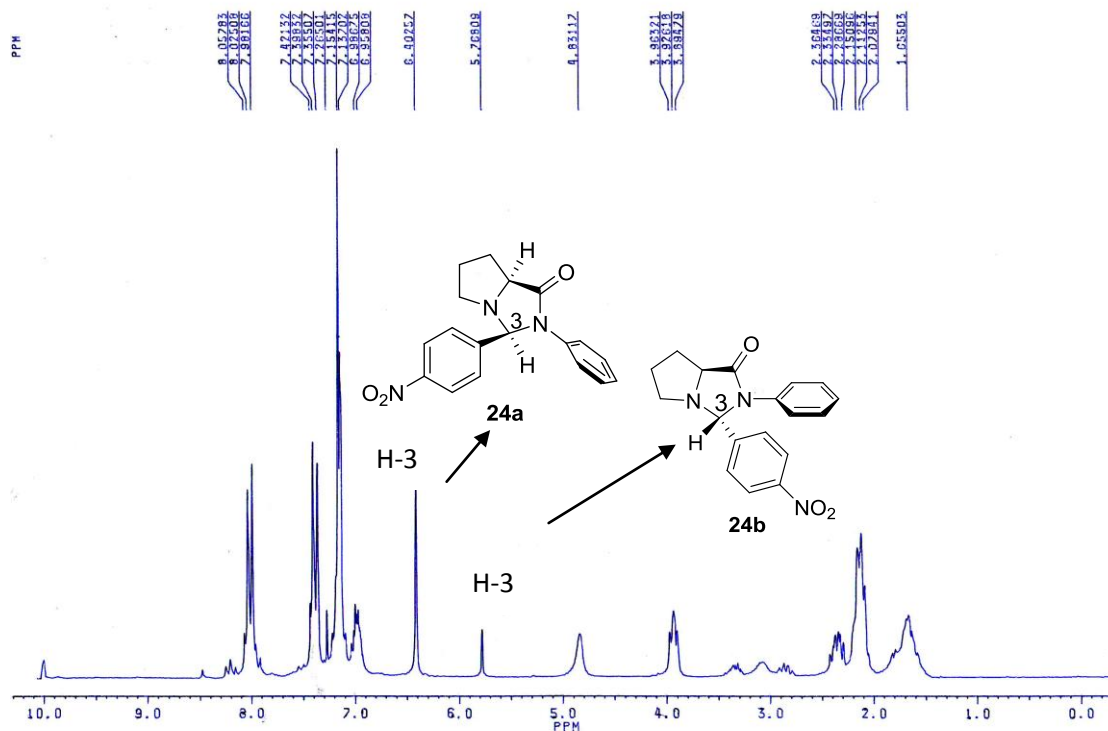


Figure 2.6. ^1H NMR spectrum of imidazolidinones **24a** and **24b** mixture formed in the reaction between 4-nitrobenzaldehyde and prolinamide **20** in CDCl_3 after 9 days.

The major compound was purified by crystallization from CH_2Cl_2 /hexane to afford suitable crystals for X-ray analysis, which revealed a structure with the 4-nitrophenyl ring in *endo*-position. The ^1H NMR spectrum confirms this structure, since a large shielding of the H-5 protons of proline is observed ($\Delta\delta = 0.6$ ppm). These protons undergo the anisotropic effect caused by the aromatic ring located just below the methylene group (figure 2.8).

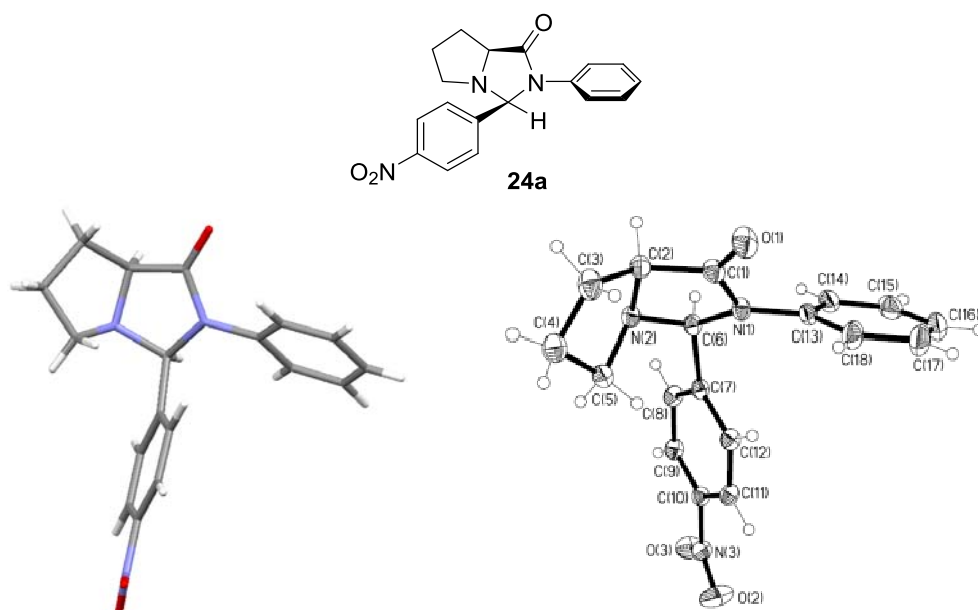


Figure 2.7. (Left) X-ray structure of imidazolidinone **24b** and (right) ORTEP representation.

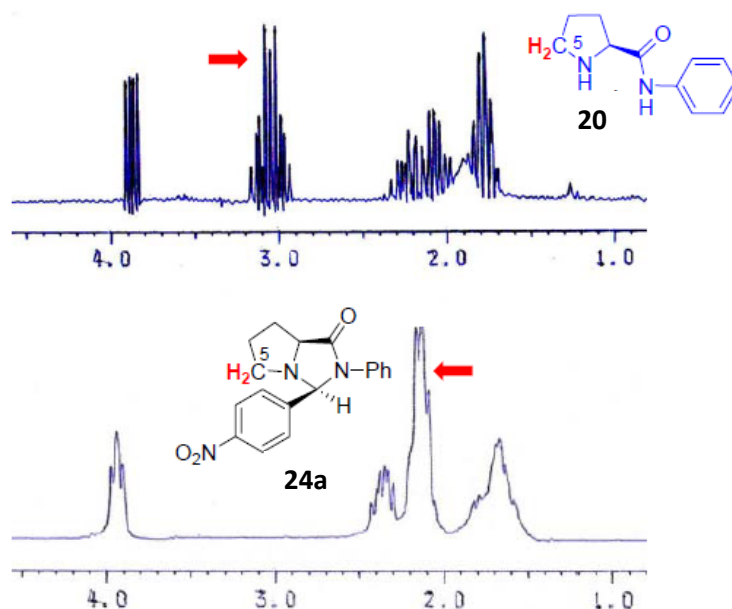


Figure 2.8. Region of the ^1H NMR spectrum between 1.0 ppm and 4.5 ppm showing the shielding of the H-5 protons of the imidazolidinone **24a** pyrrolidine ring and comparison with the free prolinamide **20**.

Moreover, the initially minority imidazolidinone could be isolated under thermodynamic conditions. The reaction between prolinamide **20** and 4-nitrobenzaldehyde in acetic acid at 60–70 °C led to the thermodynamic isomers mixture in the equilibrium, which mainly generated the imidazolidinone possessing the nitrophenyl ring in *exo* position, much more thermodynamically stable as result of the lower steric hindrance. This is evident in the X-ray structure obtained for this compound.

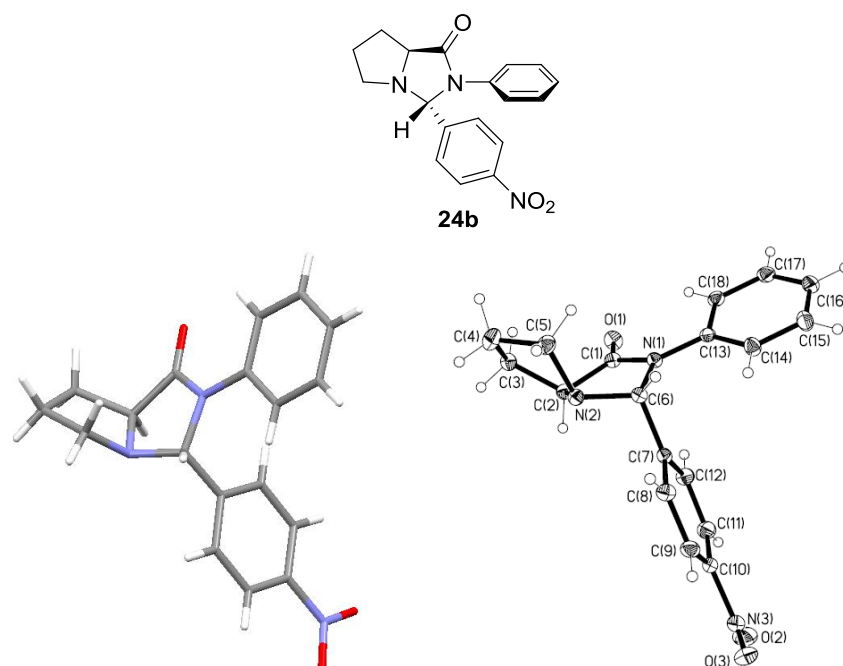


Figure 2.9. (Left) X-ray structure of imidazolidinone **24b** and (right) ORTEP representation.

It is possible that when the reaction is carried out in CDCl_3 , cyclization from the more stable iminium salt takes place: the one which undergoes no steric hindrance between the aromatic rings, although this leads to the more hindered imidazolidinone **24a** with the 4-nitrophenyl ring in *endo* position. However, using more extreme conditions the least hindered imidazolidinone can be formed from the less stable iminium salt **24b**.

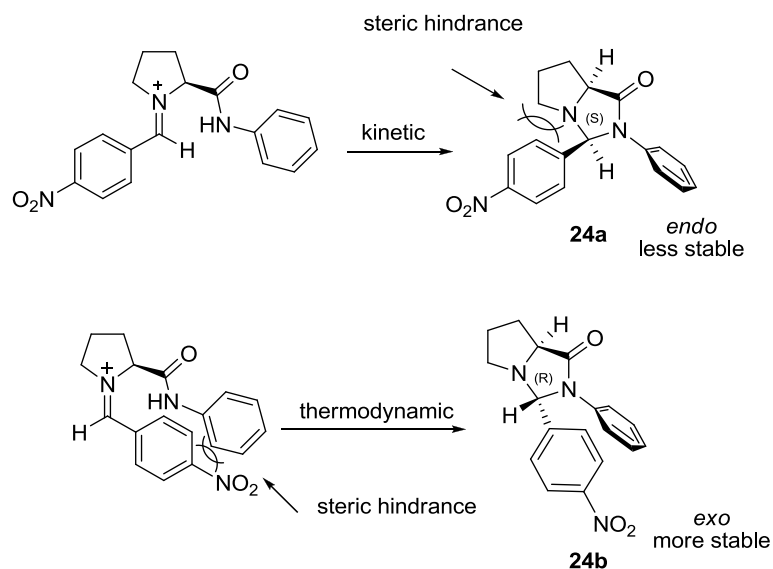


Figure 2.10. Formation of imidazolidinones of 4-nitrobenzaldehyde **24a** and **24b**.

2.2.1.3. Influence of acidity of the prolinamide NH in the imidazolidinone formation

Regardless of whether they are actual intermediates in the reaction medium or only parasitic equilibria, imidazolidinones are the first compounds which are detected by mixing acetone, 4-nitrobenzaldehyde and prolinamide **20**. It is interesting, therefore, to try to understand the reaction conditions which lead to its formation and if the characteristics of the prolinamide (such as NH acidity) have influence on the formation rate of acetone imidazolidinone **23**. For this purpose, we dissolved several prolinamides in 0.4 mL of deuterioacetone. The reaction was carried out in an NMR tube so that its progress could be monitored by ^1H NMR. The prolinamides studied were the following:

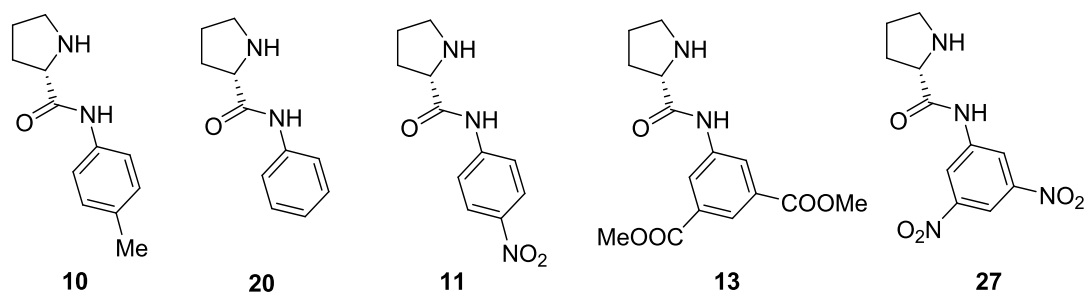


Figure 2.11. Prolinamides studied in the formation of acetone imidazolidinones.

The half-life time of each reaction was measured and is summarized in table 2.2.

Table 2.2. Half-life time (minutes) of the imidazolidinone formation with different prolinamides in deuterioacetone.

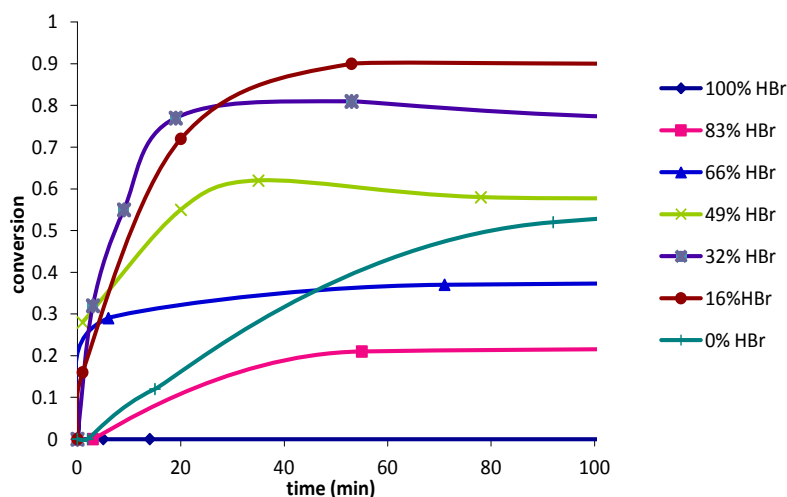
entry	prolinamide	concentration (M)	$t_{1/2}$ (min)
1	10	0.08	36.0
2	20	0.08	27.0
3	11	0.06	4.5
4	13	0.05	8.7
5	27	0.05	5.0

In view of the results obtained, it appears that the acidity of the NHs has some importance in the rate of formation of the imidazolidinones, since if the aromatic ring is substituted with a nitro group (catalysts **11** and **27**) reaction times are shorter, although there is no straightforward relationship, since dinitroaniline derivative **27** shows a half-life of 5 minutes, while the mononitroderivative reacts faster with a half-life of 4.5 minutes.

2.2.1.4. Influence of several additives on the imidazolidinones formation rate

The above experiment showed that the acidity of the NHs could affect imidazolidinone formation rate, since the more acidic prolinamides provided the faster reactions. The next step would be to study which is the influence of an external acid in the formation of the acetone imidazolidinone.

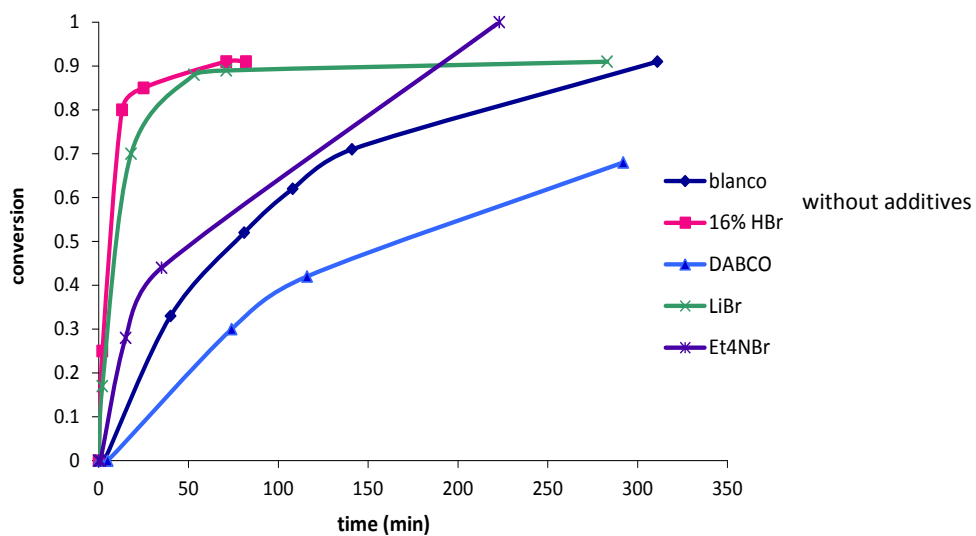
To further explore the influence of the external acid we decided to carry out a series of reactions between prolinamide **20** and deuterated acetone in chloroform, changing the acid concentration. In this case we use hydrobromic acid, which was included in the reaction medium as the prolinamide hydrobromide **20**. This salt is easily obtained by mixing the aniline prolinamide and hydrobromic acid, and subsequently evaporating the solvent. Maintaining prolinamide concentration fixed (4×10^{-2} M) and with a total volume of 0.4 mL of solvent (CDCl_3 with 25 % deuterated acetone), the relative concentrations of acid was varied respect to the prolinamide: 0, 16, 32, 49, 66, 83 and 100 %.



*Graph 2.1. Influence of the acid concentration on the imidazolidinone **23** formation rate.*

As seen in the above chart, 100% of the acid completely stops the reaction, but a certain amount accelerates the process, so that the best rate of imidazolidinone formation is obtained under an acid concentration of 16 %.

We also tested the influence of other additives in the reaction: DABCO (18 mol % relative to prolinamide), LiBr (20 mol % relative to prolinamide) and Et_4NBr (16 mol % relative to prolinamide) noting that LiBr provided a significant rate acceleration, in the same order of magnitude as the presence of 16 % HBr. In contrast, the presence of a base such as DABCO decreases the reaction rate below the blank experiment (figure 2.2). It is possible that traces of acid catalyse the reaction, and a base such as DABCO is capable of neutralizing them, making the reaction slower.



Graph 2.2. Graphical representation of the generation of imidazolidinone **23** against time (in minutes) under the influence of different additives.

2.2.2. Mechanistic studies in deuterioacetone

2.2.2.1. Reaction between acetone and 4-nitrobenzaldehyde catalysed by prolinamide **20**

Next step we decided to study the reaction in deuterated acetone, thinking that if one of the reactants was in excess, the reaction intermediates could change. Moreover, many of the catalysts described in literature are tested under these conditions, so it can be very interesting to study in detail the reaction in this solvent to try to explain the apparent contradictions that have been observed in the literature.

In this case, prolinamide **20** (1.0 M) and 4-nitrobenzaldehyde (1.0 M) were dissolved in 0.4 mL deuterated acetone and the reaction was monitored by NMR. A few minutes after mixing the reagents the formation of acetone imidazolidinone **23** could be detected. Under these conditions, no formation of adducts with the aldehyde (**21** and **22**) or imidazolidinones (**24a** and **24b**) were observed, probably due to the large excess of acetone. After 5 hours the reaction was virtually completed, it could be detected the aldol **25**, imidazolidinone **23** and aldol imidazolidinones **26a** and **26b**, (2:1 ratio, 30 % and 15 % conversion, respectively).

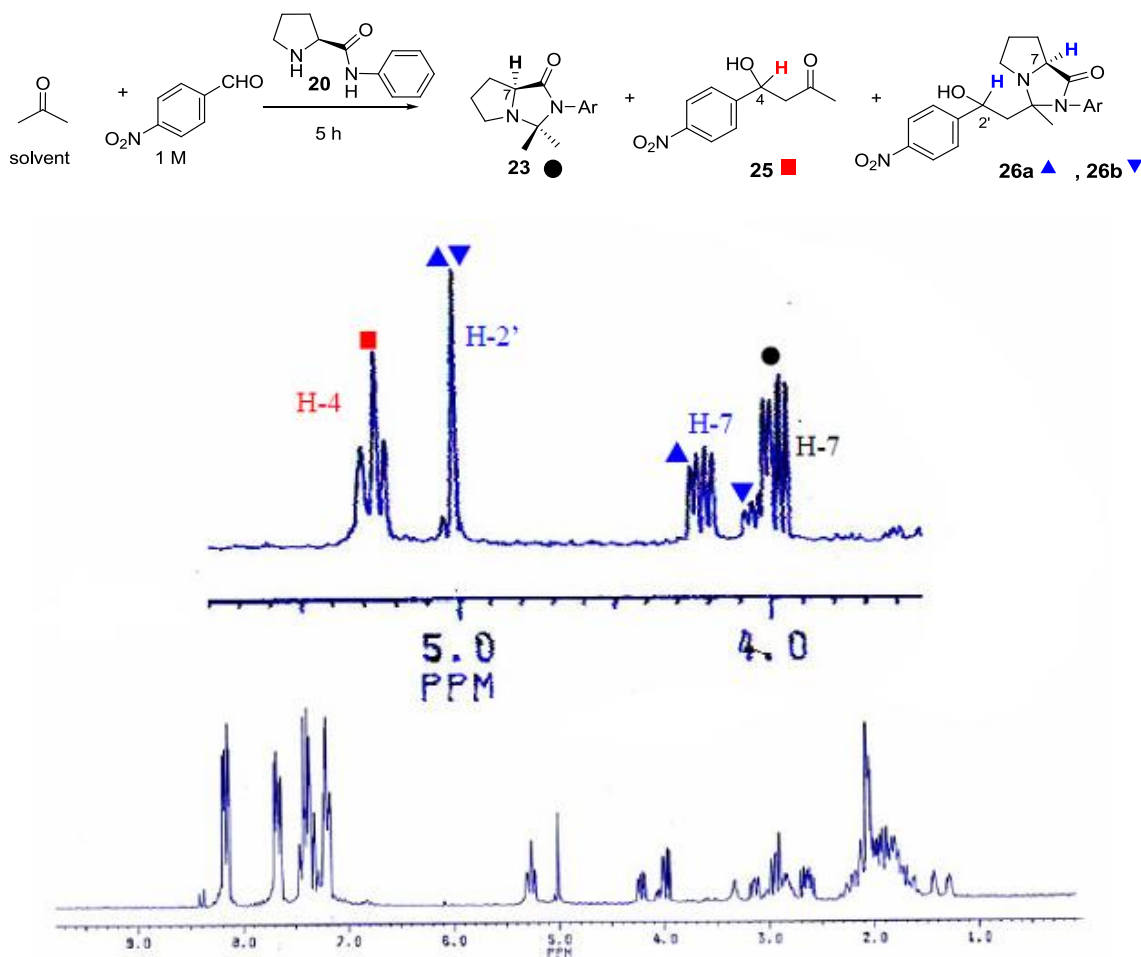


Figure 2.12. ^1H NMR spectrum corresponding to the reaction of acetone (solvent) and 4-nitrobenzaldehyde catalysed by prolinamide **20**, after 5 hours.

One of these two imidazolidinones, the minority one undergoes a more rapid transcarbonylation than the majority one, i.e., it transforms faster to generate the aldol product **25**. Thus, after 20 hours, aldol imidazolidinone **26b** was no longer observed in the reaction medium (figure 2.13).

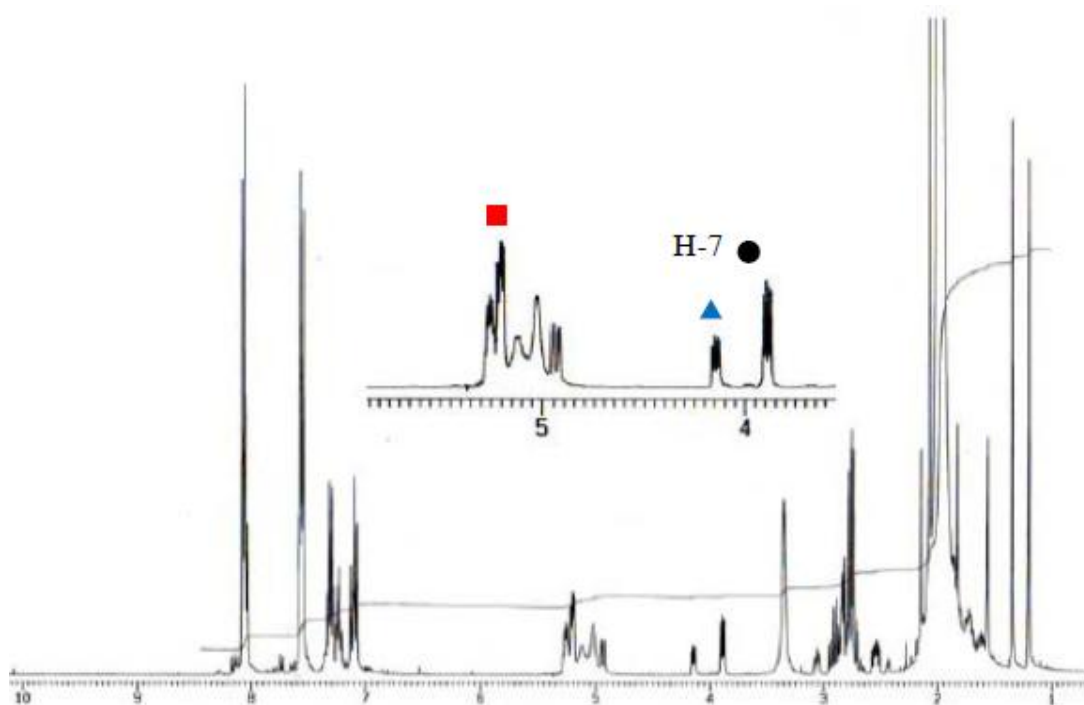


Figure 2.13. ^1H NMR spectrum corresponding to the reaction of acetone (solvent) and 4-nitrobenzaldehyde catalysed by prolinamide **20**, after 20 hours.

After two weeks, the major aldol imidazolidinone **26b** had also completely transcarbonylated since it only could be detected in the reaction medium a mixture of aldol imidazolidinone **25** and acetone imidazolidinone **23**.

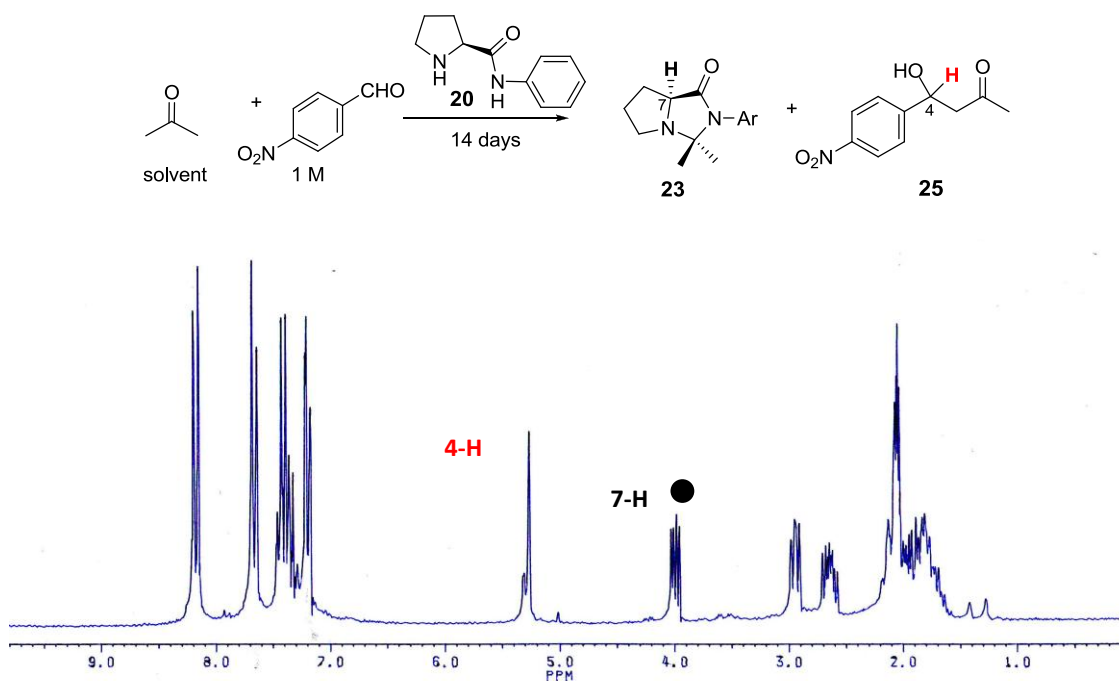


Figure 2.14. ^1H NMR spectrum corresponding to the reaction of acetone (solvent) and 4-nitrobenzaldehyde catalysed by prolinamide **20**, after 14 days.

Imidazolidinone structures **26a** and **26b** were determined by NMR spectra. It was possible to make an unambiguous assignment of all the signals. Both compounds show aminal carbons at 82.8 ppm and 82.1 ppm. The comparison of the ^{13}C chemical shifts of the methyl groups of **26a** (19.7 ppm) and **26b** (22.1 ppm) of acetone imidazolidinone **23** (23.7 ppm for the *endo* methyl group, 28.4 ppm for the *exo* methyl group) assigned using two-dimensional correlations, showed that only the *exo* methyl group is experiencing the aldol reaction, since in any of the aldol imidazolidinones the methyl group which remained unreacted was the one in *endo* position, the most shielded of the two methyl groups of imidazolidinone **23**.

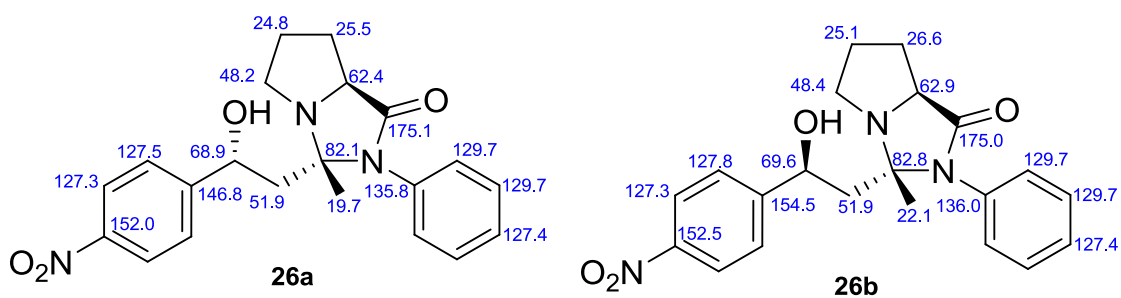


Figure 2.15. ^{13}C NMR assignments for aldol imidazolidinones **26a** and **26b**.

2.2.2.2. Deuteration and enamine formation studies

Since imidazolidinone **23** is the first product that is generated when the reaction is carried out in deuterioacetone, we studied this compound further. The imidazolidinone generated in deuterioacetone (deuteration degree: 99.8 %) should show deuterium atoms in the methyl groups. Even though these deuteriums could be easily exchanged (for example, due to a keto-enol equilibrium), the only source of labile ^1H is the prolinamide itself, which is located in a small proportion relative to the acetone used as solvent. However, at the beginning of the reaction it was observed that deuteriums atoms of both methyl groups of the imidazolidinone were replaced by ^1H atoms. After 45 minutes, the integration of the signals in the ^1H NMR spectrum corresponding to these atoms and comparison with other signals of the imidazolidinone allowed to estimate that, on average, each methyl imidazolidinone had incorporated 0.7 ^1H atoms. Statistically, from the two protons of the prolinamide (both NHs) one would expect an average of 0.75 ^1H atoms in each methyl group of the imidazolidinone, provided that the formation of this compound is not reversible in these first few minutes. If the formation of the imidazolidinone is reversible, most ^1H atoms should finish on the methyl groups of acetone. In fact, after two weeks, the integral of the ^1H atoms signal was reduced to 0.1.

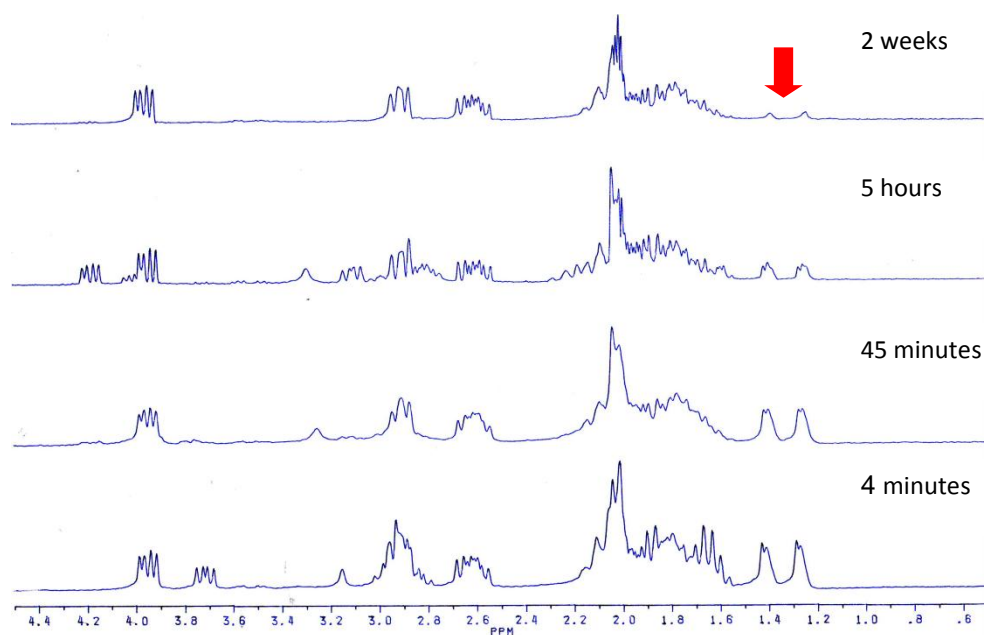


Figure 2.16. ^1H NMR spectral region between 0.6-4.4 ppm corresponding to the reaction between prolinamide **20** and 4-nitrobenzaldehyde in deuterioacetone at different times in which the deuteration process of imidazolidinone **23** methyl groups is shown.

This would be consistent with a mechanism in which enamines are generated and can exchange deuterium atoms to a greater speed at which the formation of the imidazolidinone occurs (figure 2.17). Once the enamine is formed, it undergoes rapid exchange between the protons of the water molecule produced in the reaction and the methyl groups.

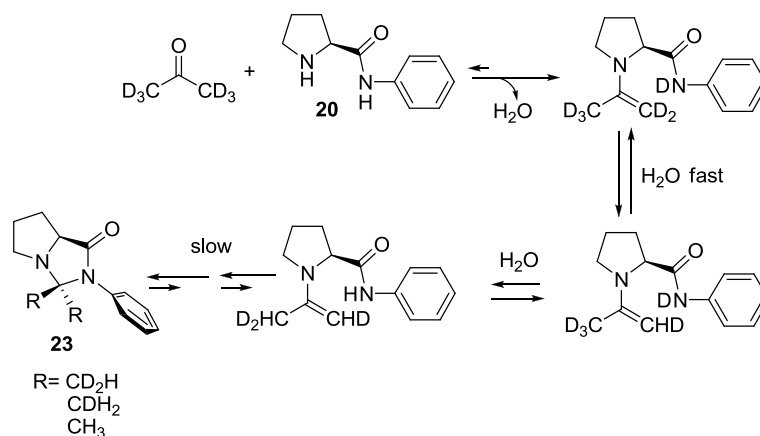


Figure 2.17. Formation of imidazolidinone **23** (with different deuteration degrees) in deuterioacetone

This hypothesis is supported by the results obtained in the reaction between butyraldehyde (0.1 M) and prolinamide **20** (0.1 M) in $CDCl_3$. The initial product observed in 1H NMR was enamine **28**. However, then a slow cyclization occurs to generate imidazolidinones **29a** and **29b**, which are stable products which accumulate in the reaction medium. In this case only the most stable imidazolidinone **29b** with a propyl group in *exo* position can be isolated through equilibration in acetic acid at 60-70 °C.

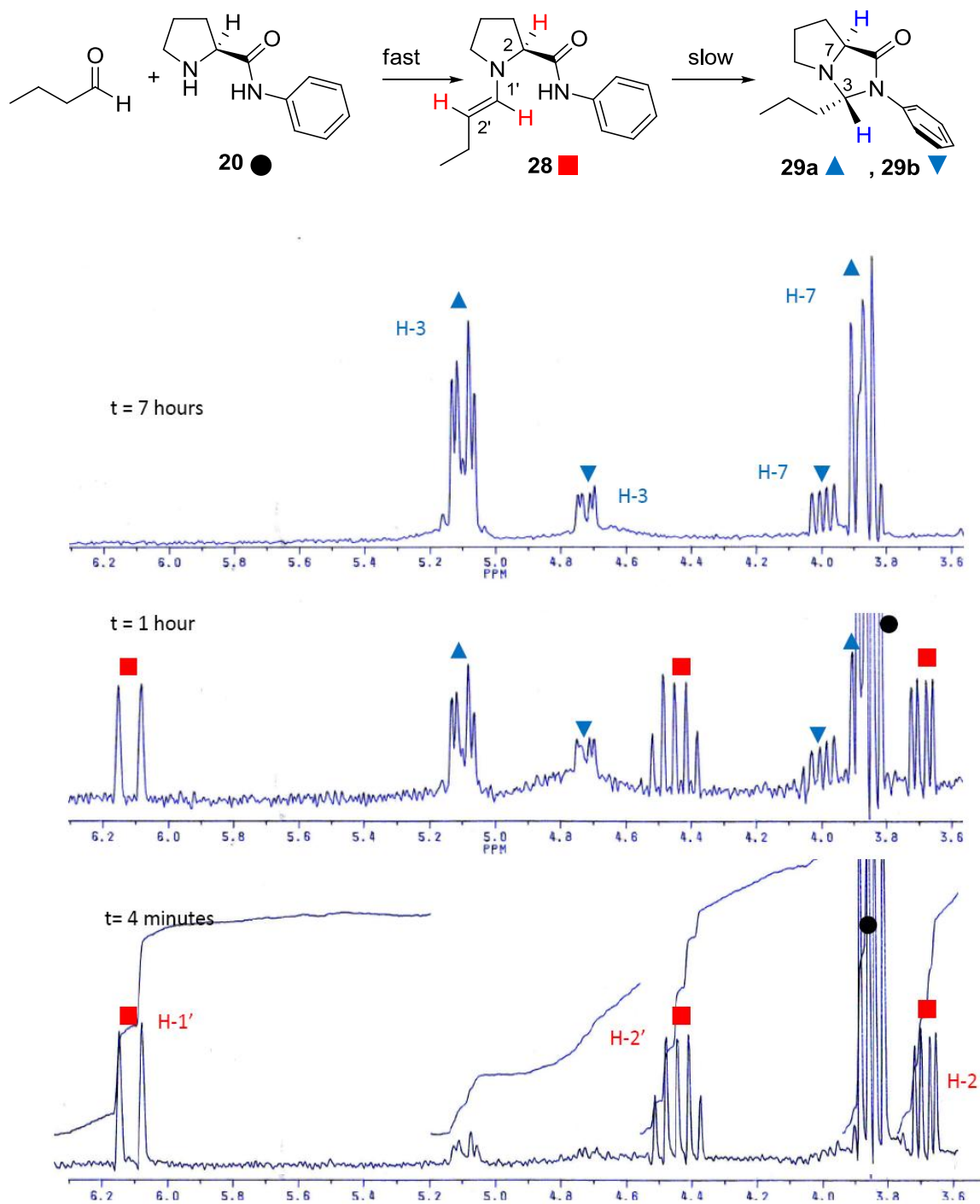


Figure 2.18. ^1H NMR spectra (region 3.6-6.2 ppm) at different times of the reaction between prolinamide **20** (0.1M) and n -butyraldehyde (0.1 M) in CDCl_3 .

2.2.2.3. Reactivity studies of imidazolidinone **23**

Gryko⁸² has already identified that the use of thioimidazolidinones produces slower reactions with lower enantioselectivities when thioimidazolidinone is used in equimolar amounts with the aldehyde (figure 2.19a). However, when this thioimidazolidinone is used in catalytic conditions, the results in terms of reaction rate and enantioselectivity are virtually identical to those obtained with the free thioprolineamide (Figure 2.19 b and c).

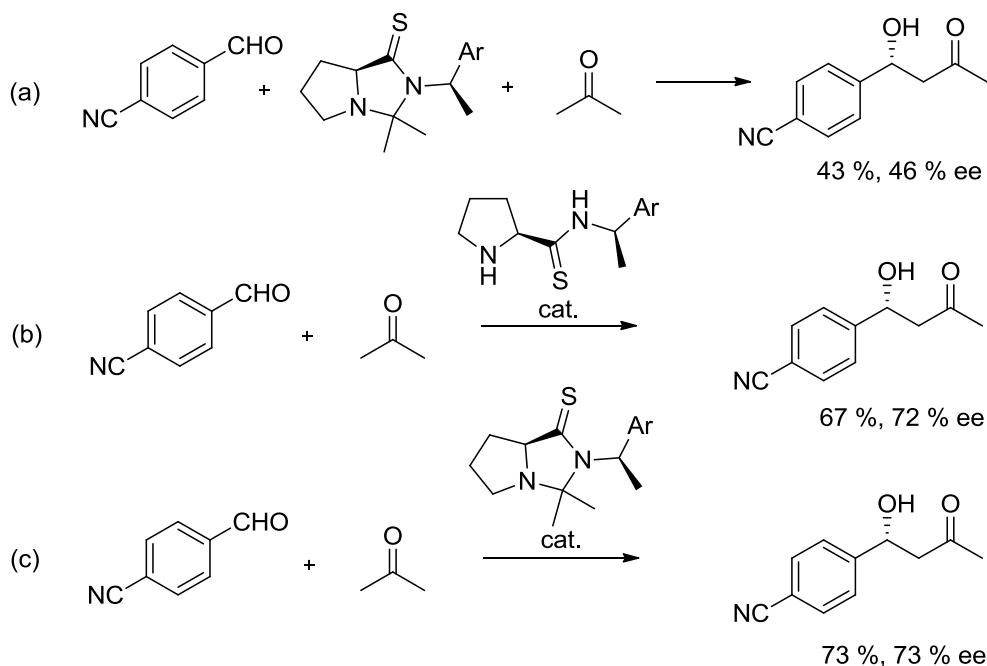


Figure 2.19. (a) Reaction between 4-cyanobenzaldehyde and acetone thioimidazolidinone in equimolar conditions in acetone. (b) Reaction between 4-cyanobenzaldehyde and acetone catalysed by a thioprolineamide. (c) Reaction between 4-cyanobenzaldehyde and acetone catalysed by the acetone thioimidazolidinone.

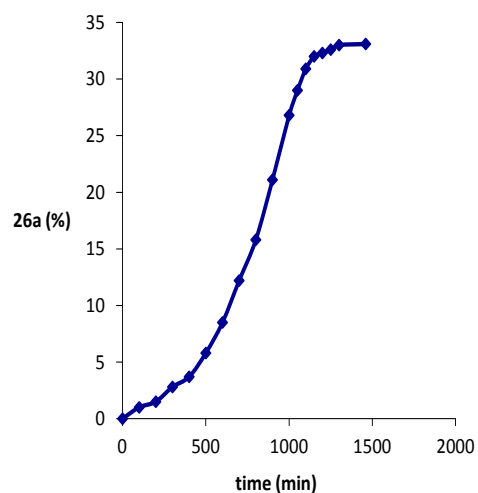
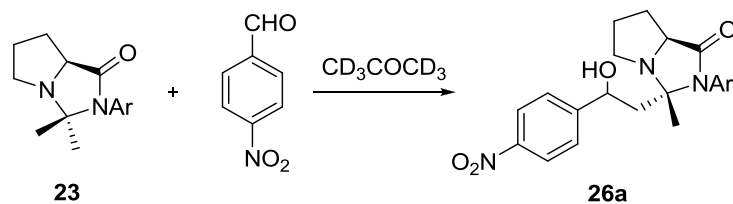
To try to better understand the results obtained by Gryko, we decided to study carefully the above reaction, but with the carbonyl derivatives (prolineamide and imidazolidinone) instead of the corresponding thiocarbonyl compounds (thioprolineamide and thioimidazolidinone). To do this, we conducted the reaction between imidazolidinone **23** (1.0 M) with 4-nitrobenzaldehyde (1.0 M) in deuterated acetone at 20 °C. The reaction mixture was placed in an NMR tube and the spectrometer was programmed to perform a spectrum every 20 minutes. This way we could observe the appearance of different species over time.

The study of the spectra showed that the generation of aldol **26a** needed an induction period, possibly its formation occurs autocatalytically, thanks to the presence of a hydroxyl group in the aldol product that accelerates the reaction (graph 2.3). In fact, some authors⁸³

⁸² (a) Gryko, D.; Lipinski, R. *Adv. Synth. Catal.* **2005**, *347*, 1948-1952; (b) Gryko, D.; Lipinski, R. *Eur. J. Org. Chem.* **2006**, 3864-3876.

⁸³ (a) Mauksch, M.; Wei, S. W.; Freund, M.; Zamfir, A.; Tsogoeva, S. B. *Orig. Life. Evol. Biosph.* **2010**, *40*, 79-91; (b) Mauksch, M.; Tsogoeva, S. B.; Wei, S. W.; Martynova, I. M. *Chirality* **2007**, *19*, 816-825; (c) Mauksch, M.; Tsogoeva, S. B.; Martynova, I. M.; Wei, S. W. *Angew. Chem., Int. Ed.* **2007**, *46*, 393-396.

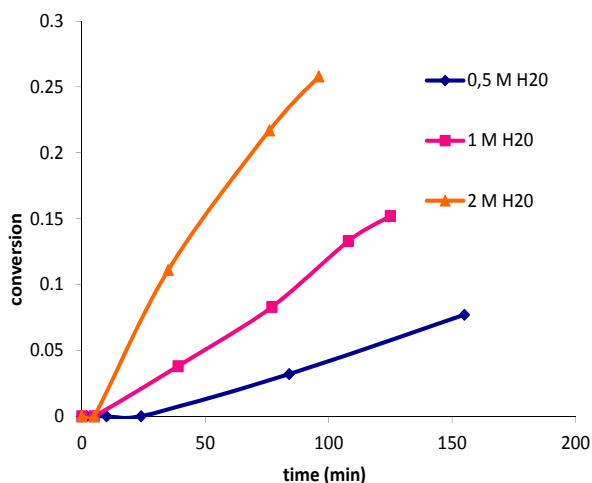
claim that the autocatalysis could have played a key role in the initial aldol reactions which introduced homochirality on Earth.



Graph 2.3. Generation of aldol **26a** in the reaction between imidazolidinone **23** (1.0 M) and 4-nitrobenzaldehyde (1.0 M) in deuterioacetone at 20 °C.

After observing that the presence of a hydroxyl group in the aldol products increased the reaction rate, we decided to check whether an external hydroxyl group had the same effect. Thus, it was found that the presence of water catalysed the aldol reaction between imidazolidinone **23** (0.5 M) and 4-nitrobenzaldehyde (0.8 M) in deuterated acetone.

This need for water in the reaction medium could explain the results obtained by Gryko, since the reaction of acetone with prolinamide generates this water molecule, which allows the reaction to be effective; on the contrary when thioimidazolidinone is used, the reaction medium is anhydrous, and a long induction period is required to achieve the necessary aldol concentration to accelerate the reaction.



Graph 2.4. Reaction between imidazolidinone **23** and 4-nitrobenzaldehyde in deuterated acetone in the presence of different amounts of H₂O.

Then the effect of other nucleophiles and acids were explored as catalysts (0.5-1.0 M) of the aldol reaction between imidazolidinone **23** (1.0 M) and 4-nitrobenzaldehyde (1.0 M). It is expected that both nucleophiles and acids are capable of promoting the opening of the imidazolidinone to generate the enamine, which is the reactive species which undergoes the aldol reaction. The results are summarized in table 2.3 and figure 2.5.

Table 2.3. Half-life times (in min) obtained with different catalysts in the reaction between imidazolidinone **23** and 4-nitrobenzaldehyde in deuterioacetone at 20 °C.

entry	catalyst	$t_{1/2}$ (min)
1	-	700
2	4-nitrophenol	2
3	decanoic acid	5
4	imidazole	28
5	dodecanthiol	31
6	phenol	46
7	H ₂ O	260

It can be seen that nucleophiles such as dodecanethiol or imidazole catalyse the reaction, but also acids such as phenol, 4-nitrophenol or decanoic acid. 4-nitrophenol showed a high efficiency, as it can be seen by the high degree of deuteration in the methylene group of the

aldol imidazolidinone. This suggests that the opening of the imidazolidinone to generate the enamine is very fast, which greatly accelerates the reaction rate.

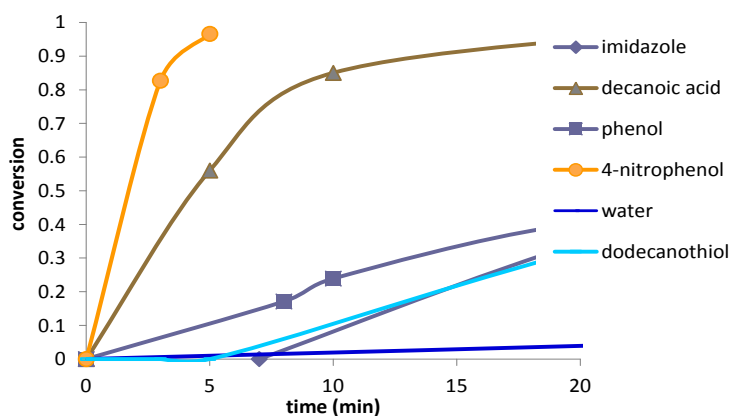


Figure 2.5. Reaction between imidazolidinone **23** and 4-nitrobenzaldehyde in deuterioacetone catalysed by several compounds.

We also studied the reaction between acetone imidazolidinone **23** (0.5 M) and 4-nitrobenzaldehyde (0.8 M) catalysed by 4-nitrophenol (0.5 M) and dodecanethiol (0.5 M), but this time in deuteriochloroform. Catalysis was also observed, but the reaction was slower compared with the reaction using only 4-nitrophenol as catalyst: more hydrolysis occurs, and the formation of the thioacetal and thiohemiacetal of 4-nitrobenzaldehyde is observed (figure 2.20). The formation of these compounds liberate water which hydrolyzes the acetone imidazolidinone appearing the characteristic signals of the free prolinamide and acetone in the ^1H NMR spectrum

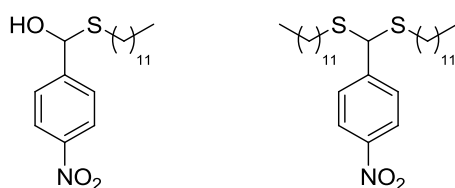


Figure 2.20. Intermediate species observed in the reaction between imidazolidinone **23** and 4-nitrobenzaldehyde in CDCl_3 catalysed by 4-nitrophenol and dodecanethiol.

2.2.3. Mechanistic studies in deuteromethanol

2.2.3.1. Reaction between imidazolidinone **23** and 4-nitrobenzaldehyde

The above results demonstrate the need to employ a nucleophile or an acid to accelerate the reaction when imidazolidinone is used as a reagent. Probably both additives are able to promote the opening of the imidazolidinone. Therefore, it would be interesting to study the reactivity of imidazolidinone in a solvent such as methanol, which already provides the required hydroxyl groups to speed up the process. To do this, we carried out the reaction between imidazolidinone **23** (0.5 M) and 4-nitrobenzaldehyde (0.5 M) at 20 °C in deuteromethanol, noting the rapid formation of an equilibrium. After 14 hours there were 50 % of the starting material and 50 % of the aldol imidazolidinone (figure 2.21).

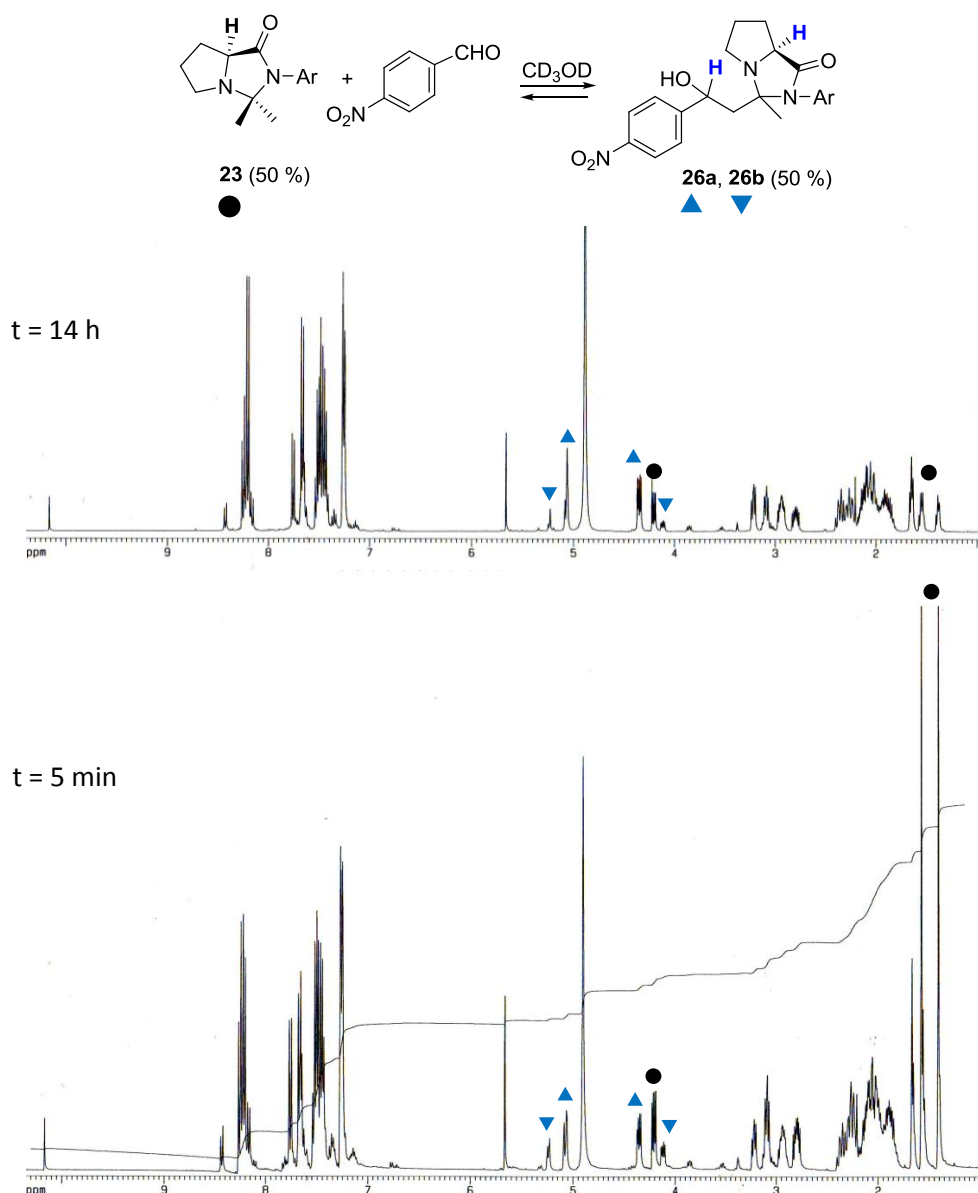


Figure 2.21. Reaction between imidazolidinone **23** (0.5 M) and 4-nitrobenzaldehyde (0.5 M) in deuteromethanol after 5 minutes and 14 hours.

2.2.4. Reaction between imidazolidinone **30** and different aldehydes

We could check that the nature of the aldehyde affects this equilibrium, and results changed working with aldehydes with different reactivities: 4-nitrobenzaldehyde, 4-chlorobenzaldehyde and *n*-butyraldehyde. We employed imidazolidinone **30**, derived from bis(trifluoromethyl)aniline, with the aim to check if its reactivity was higher than imidazolidinone **23**.

The reactions were carried out in deuteriomethanol, so that analysis of the reaction products was performed by ^1H NMR. We worked with a 0.25 M concentration for imidazolidinone **30** (figure 2.22) and 0.6 M for the aldehydes. The NMR spectra showed that aldol reactions occurred very fast after mixing the reagents, but after a while, aldehyde imidazolidinones appeared. 4-Nitrobenzaldehyde is the aldehyde which reached first the equilibrium. Working with butyraldehyde no aldol reaction was observed, only the formation of the aldehyde imidazolidinones: first the kinetic one and then the more thermodynamically stable. Interestingly, the prolinamide trifluoromethyl groups do not appear to have a significant effect on the reaction rate in comparison with the results obtained previously with imidazolidinone **23**.

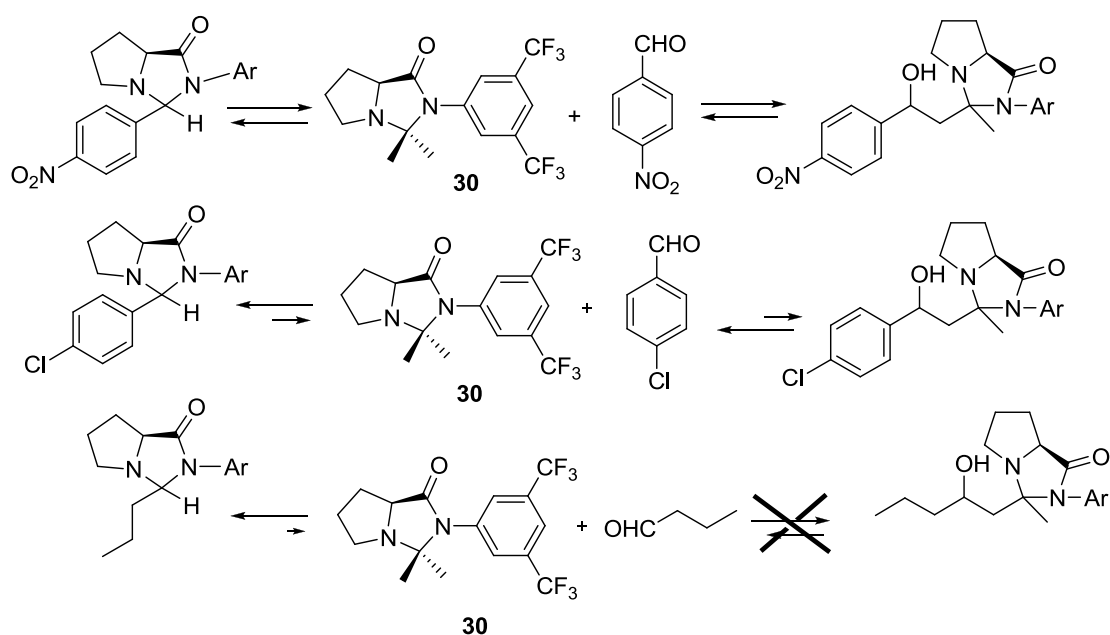


Figure 2.22. Reactions between imidazolidinone **30** and several aldehydes in CD_3OD with the aim to study the aldehydes reactivity in the equilibrium.

These experiments showed that the aldol reaction between imidazolidinone **30** and different aldehydes is an equilibrium process. The fact that the latter is shifted to one or the other sense depends strongly on the reactivity of the aldehyde and the solvent employed. Consequently, it is likely that all these factors decisively influence the enantiomeric excess of the aldol product. As explained below, the fact that the reaction of C-C bond formation is an equilibrium process will cause racemization of the aldol-imidazolidinone product unless this reaction is followed by an irreversible step that does not affect the chiral center formed. The

imidazolidinone transcarbonylation is this irreversible reaction, so to obtain a high enantiomeric excess this reaction must be a fast step.

2.2.5. Racemization studies of aldol **25** in CDCl_3

In order to check this hypothesis, we decided to mix the enantiomerically enriched aldol **25** (1.0 M) with aniline prolinamide **20** (1.0 M) in deuterated chloroform, and follow the evolution of the reaction with time. In this way, we were able to study the presence of new products in the reaction medium and the possible variation in the enantiomeric excess (determined by chiral HPLC analysis of a small sample of the crude reaction).

NMR spectra showed that a mixture of products was obtained, due to the retro-aldol reaction. We could observe imidazolidinones **23**, **24a**, **24b** and **26a**, and even acetone and 4-nitrobenzaldehyde (figure 2.23) besides the initial aldol racemization, as reflected in table 2.4.

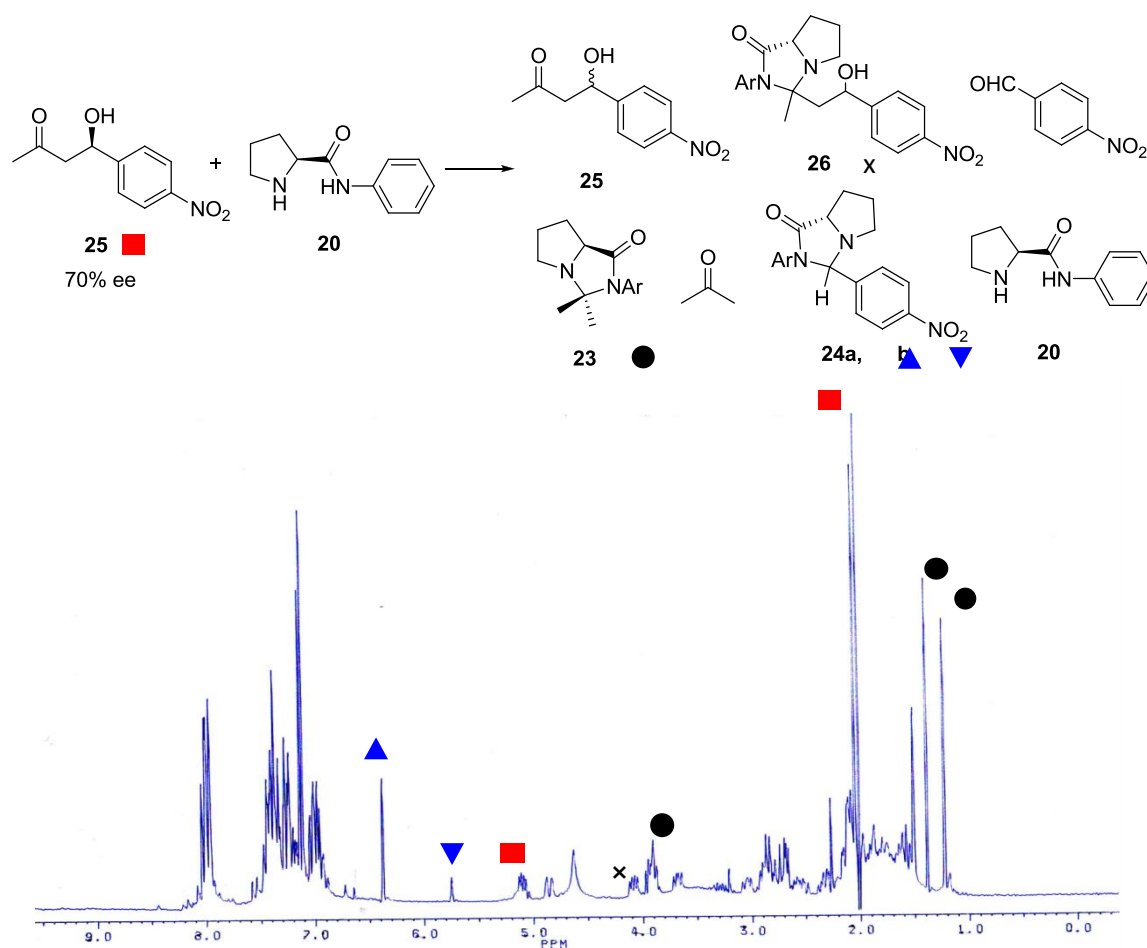


Figure 2.23. ^1H NMR spectrum corresponding to the retro-aldol reaction between the enantioenriched aldol **25** and prolinamide **20** after 68 hours.

Table 2.4. Variation in the enantioselectivity of the aldol reaction between **25** (70 % ee) (1.0 M) and prolinamide **20** (1.0 M) in CDCl₃.

entry	t (min)	ee (%)
1	0	70
2	170	60
3	237	43
4	1188	6

Furthermore, by carrying out the reaction between racemic aldol **25** and prolinamide **20** it could be observed the appearance of an enantiomeric excess up to 18% in a first stage of the reaction but, finally, after a long reaction period it returned to an almost racemic aldol. This experiment confirms that one of the aldols reacts faster with prolinamide to generate the corresponding imidazolidinone, which subsequently leads to the complex mixture of products shown in figure 2.23.

Table 2.5. Variation of enantioselectivity in the aldol reaction between racemic aldol **25** (1.0 M) and prolinamide **20** (1.0 M) in CDCl₃.

entry	t (min)	ee (%)
1	0	0
2	14	1
3	66	8
4	144	18
5	4060	2

Actually this result is not surprising when the low driving force of aldol reactions is considered. In fact, after mixing enamine **31** (0.16 M) and 4-nitrobenzaldehyde (0.16 M) in deuteriochloroform, the aldol formation in the initial instants is observed, but the final product is the compound generated by the Mannich reaction, in which the presence of the cyclohexanone strong carbonyl bond causes this reaction to have a significant driving force.

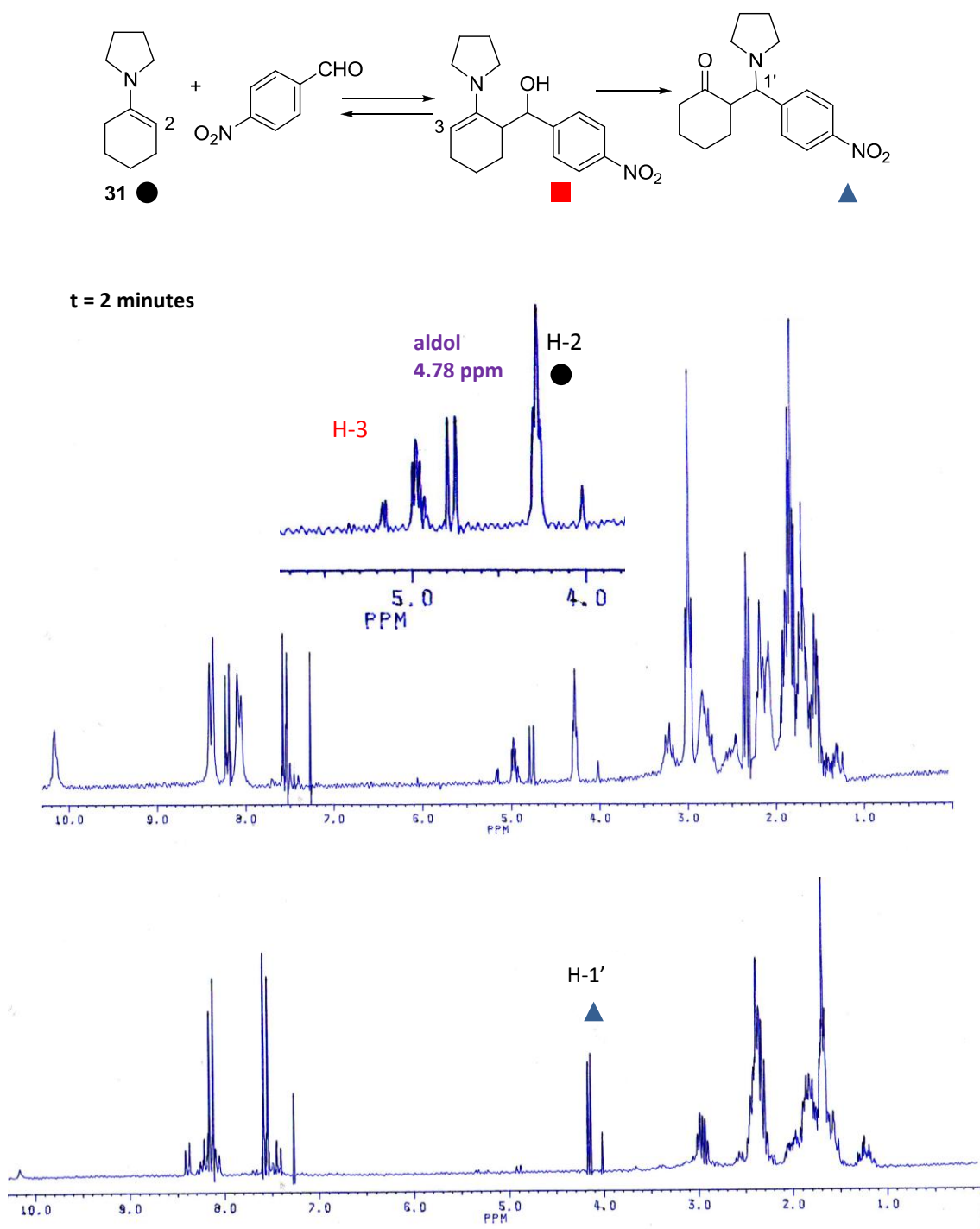


Figure 2.24. ^1H NMR spectrum corresponding to the reaction between enamine **31** (0.16 M) and 4-nitrobenzaldehyde (0.16 M) in CDCl_3 .

This could explain the absence of aldol reactions in review articles about enamines published until a few years ago.⁸⁴ The remarkable success in the current literature corresponds to reactions in which the enamine is formed in catalytic amounts and is always hydrolyzed or suffers transcarbonylation immediately after the C-C bond formation.

⁸⁴ (a) Hickmott, P. W. *Tetrahedron* **1982**, *38*, 1975-2050; (b) Hickmott, P. W. *Tetrahedron* **1982**, *38*, 3363-3446.

2.2.6. Deuteration in CD₃OD: Ene Mechanism

Another remarkable feature of the reaction between imidazolidinone **23** (0.5 M) and 4-nitrobenzaldehyde (0.5 M) in deuteromethanol was the deuterium exchange: it can be seen in the integral and form of the NMR signals a large incorporation of deuterium in the methyl group of the aldol imidazolidinone, while the degree of deuteration is lower in the methylene group. It thus appears that the methyl groups of the aldol imidazolidinones (**26a** and **26b**) are partially deuterated, while the methylene is not, because the H-2' of **26a** and **26b** is coupled with the CH₂, generating a doublet of doublets in the spectrum. If that methylene had been deuterated the signal of H-2' should have been a broad singlet, because the coupling constant with deuterium is much smaller than with proton.

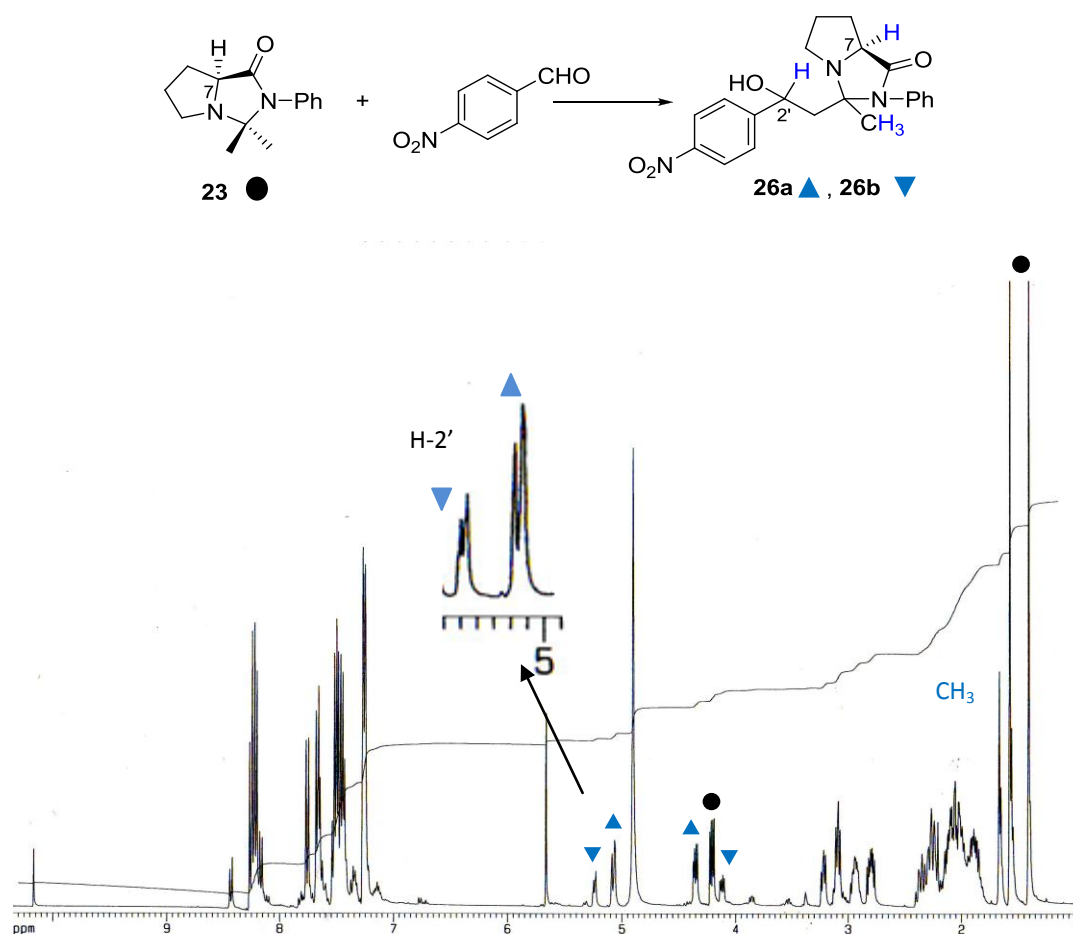


Figure 2.25. ¹H NMR spectrum of the reaction between imidazolidinone **23** (0.5 M) and 4-nitrobenzaldehyde (0.5 M) in deuteromethanol. The deuterium exchange is shown in the imidazolidinone methyl groups.

A possible explanation for the selective incorporation of deuterium in the ketone methyl group of the aldol product is that the enamine is formed in the α'-carbon through a concerted ene-type mechanism, in which the role of the prolinamide NH would be to establish an H-bond with the aldehyde carbonyl group, thereby stabilizing the transition state as shown in figure 2.26.

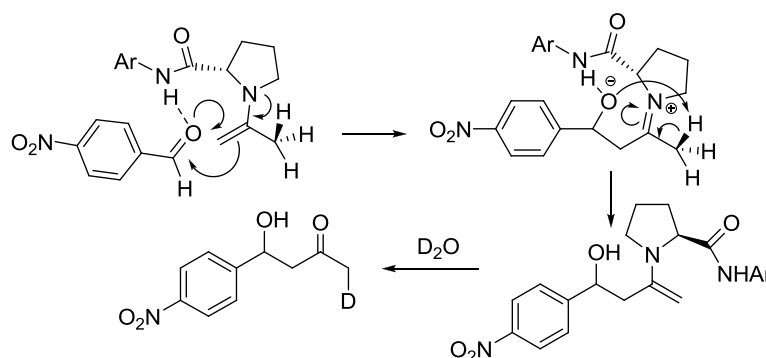


Figure 2.26. Possible ene-type mechanism for aldol reactions catalysed by prolinamides.

2.2.7. Formation of the iminium salt

As already shown in table 2.1, the reaction between acetone and 4-nitrobenzaldehyde catalysed by prolinamide **20** produces different enantiomeric excesses depending on the reaction conditions, solvents and additives used. It has also been shown that the presence of an acid influences enantioselectivity. Imidazolidinones **26a** and **26b** formation as reaction intermedia in the absence of acid may explain low enantiomeric excesses. If such imidazolidinones are in equilibrium with the starting materials and are controlling the reaction rate, according to the Curtin-Hammett principle, imidazolidinones will also control the enantiomeric excesses obtained. Thus, the initial aldol product that would be generated with good chiral excess at the beginning of the reaction reverts to the reagents, losing part of the enantioselectivity of the product, as can be seen in the schematic representation of the activation energies of the C-C bond formation and the transcarbonylation or hydrolysis of imidazolidinones in figure 2.27.

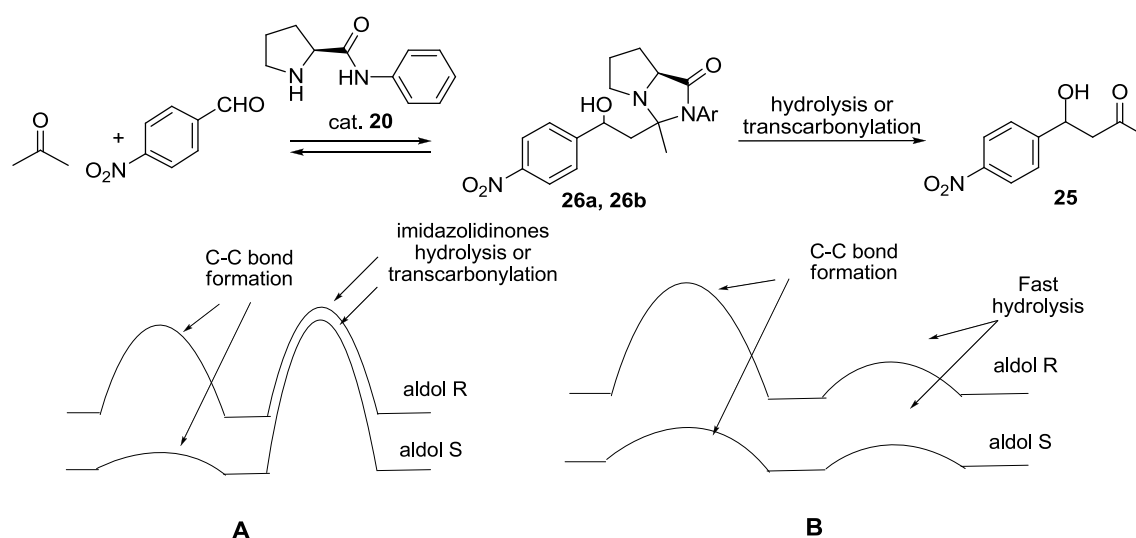


Figure 2.27. Aldol imidazolidinones could act as intermedia in the reaction between acetone and 4-nitrobenzaldehyde catalysed by prolinamide **20**. At the bottom a schematic profile of the activation energy of the C-C bond formation and imidazolidinone hydrolysis (or transcarbonylation) is depicted.

Since the catalyst is not designed to catalyse the hydrolysis (or transcarbonylation) of imidazolidinones, it is normal to obtain small enantiomeric excesses. For this reason it is important a fast hydrolysis (or transcarbonylation) of the imidazolidinones. The addition of an acid such as trifluoroacetic, *p*-toluenesulfonic or camphorsulfonic acid could solve this problem, because under these new conditions imidazolidinones do not accumulate in the reaction medium. In fact, by dissolving imidazolidinone **23** in CDCl_3 and adding one of these three acids, iminium salt generation was observed, in addition to the protonated prolinamide. These results have been described by other authors.⁸⁵

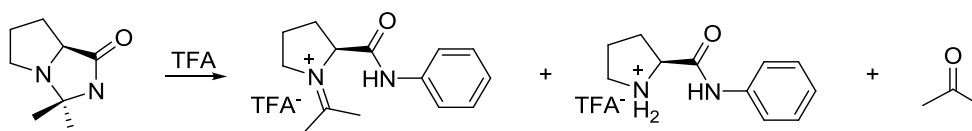


Figure 2.28. Iminium salt and protonated prolinamide generated from imidazolidinone **23** in CDCl_3 in the presence of TFA.

We suggest that the absence of imidazolidinones under acidic conditions is due to its low $\text{p}K_a$. This could be checked after adding *p*-toluenesulfonic acid to a mixture of prolinamide **20** and imidazolidinone **23** in deuteriochloroform, since the protonation is initially observed only at the nitrogen of the prolinamide and once this compound is fully protonated, imidazolidinone protonation begins.

2.2.8. Measure of acidity through competitive titrations

To try to get an idea of the $\text{p}K_a$ of the imidazolidinone we conducted several competitive titrations with different reference compounds. Thus, two compounds were dissolved in CDCl_3 in an NMR tube and increasing amounts of anhydrous *p*TsOH was added, recording a ^1H NMR spectrum after each addition. Protonation of the most basic compound will cause deshielding of its signals. Adding more acid, protonation of the second compound will start, now shifting their signals downfield in the spectrum. Then, the displacement suffered by one of the protons of the most basic compound was plotted against the displacement experienced by the less basic compound. Adjusting these points to a curve generated by a Monte Carlo method, allows to obtain a competitive constant, which will give us the relative basicity between both compounds.

⁸⁵ Gryko, D.; Zimnicka, M.; Lipinski, R. *J. Org. Chem.* **2007**, 72, 964-970.

Table 2.6. Competitive constants obtained between different compounds, using imidazole, pyridine and pyrrolidine as references.

entry	more basic compound	less basic compound	competitive constant
1			10000
2			1
3			1
4			1900
5			5.6
6			93
7			1.1

The results in the previous table demonstrate the large difference in basicity between imidazolidinone **23** and prolinamide **20**, being the latter more basic. Furthermore, pyrrolidine is, in turn, much more basic than prolinamide **20**, probably due to formation of an intramolecular H-bond between the amide NH and the nitrogen atom of the pyrrolidine ring. Another striking feature is that the basicity of the prolinamide practically does not change, despite the introduction of electron withdrawing groups on the aromatic ring (entries 2 and 3).

To determine the basicity of imidazolidinone **23** competitive titrations with compounds of known pK_a , such as pyridine and imidazole, were made, finding a relationship with pyridine: $pK_{a \text{ pyridine}}/pK_{a \text{ imidazolidinone } 23} = 1.34$, while the ratio with imidazole was almost 1. An approximate basicity scale is shown from the studied compounds in figure 2.29, placing the more basic compounds on the left.

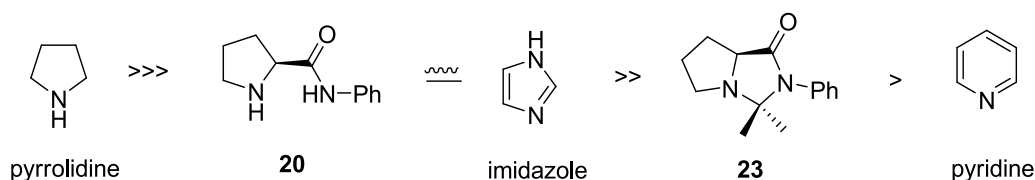


Figure 2.29. Basicity scale (in CDCl_3 at 20°C) of different compounds, from highest to lowest basicity from left to right.

We did not find any explanation to justify the small basicity of imidazolidinones as it does not seem to present anomeric effects, or some other type of stereoelectronic effects which could explain that these compounds are so much less basic than pyrrolidine.

2.2.9. Reaction between acetone and 4-nitrobenzaldehyde under catalytic conditions

Mechanistic studies conducted so far show the need to use an acid or a nucleophile in aldol reactions catalysed by prolinamides. To check the veracity of this claim under catalytic conditions we decided to conduct several trials mixing acetone and 4-nitrobenzaldehyde catalysed by prolinamide **20** using different additives. Deuteroacetone was used as solvent, with the aim of analyzing the progress of the reaction by NMR. The following table shows the variation of the enantiomeric excess for different reaction conditions:

Table 2.7. Enantiomeric excesses obtained by mixing deuterated acetone (0.5 mL, 13.6 M) with 4-nitrobenzaldehyde (0.68 M) using prolinamide **20** as catalyst (10 mol % with respect to aldehyde) with different additives (mol % relative to the catalyst) at 20°C .

entry	additive (mol %)	ee (%)
1	-	10
2	H_2O (1990)	3-5
3	4-nitrophenol (100)	30
4	TFA (100)	62
5	TFA (100)+ H_2O (1960)	46
6 ^a	TFA (100)	70
7	TFA (214)	22
8	TFA (86)	64
9	TFA (50)	62
10 ^b	TFA (10)	-

^a Reaction carried out at -19°C .

^b Without **20**, and only with TFA, there is no reaction

Results demonstrate that the presence of acid is important in obtaining high enantiomeric excesses, reaching values close to 65 % ee when a similar concentration of TFA and catalyst is

employed (entry 4). Reducing the reaction temperature causes an increase in enantioselectivity, but at the expense of reducing the reaction rate (entry 6). The presence of 4-nitrophenol only slightly increases the enantiomeric excess (entry 3), while water leads to a virtually racemic aldol (entry 2). An assay was also performed in the absence of catalyst and 10 mol % of TFA (entry 10), with the objective of verifying whether the presence of acid alone could cause the aldol reaction and therefore, the racemization of the product. However, the presence of trifluoroacetic acid as the sole catalyst did not yield reaction.

We also studied other prolinamides whose NH possesses different acidity, both aromatic (**12**, **20**, **32**, **33**) with different electron withdrawing substituents such as aliphatic (**34**, **35**) (figure 2.28).

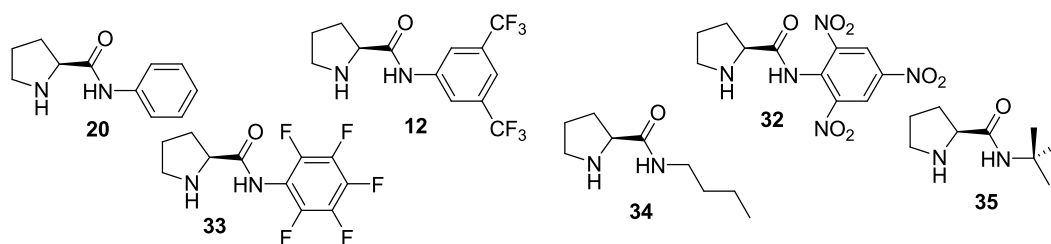


Figure 2.30. Prolinamides employed as catalysts (10 mol %) in the reaction between acetone and 4-nitrobenzaldehyde.

In addition, we performed each of the reactions with an equivalent of trifluoroacetic acid (respect to the catalyst), and also in the absence of acid, to study the effect in both enantioselectivity and reaction rate with the different catalysts. The reaction conditions were the same as above: deuterioacetone as solvent, 0.68 M aldehyde and 10 mol % catalyst.

Table 2.8. Conversions and enantiomeric excesses (determined by HPLC) obtained by conducting the aldol reaction between deuterated acetone (as solvent, 13.6 M) and 4-nitrobenzaldehyde 0.68 M) with 10 mol % catalyst.

entry	catalyst	time (h)	conversion (%)	ee (%)
1	20^a	70	21	10
2	20·TFA	5	21	61
3	12	12	31	2
4	12·TFA	11	35	65
5	32^b	2	>99	60
6	32·TFA	7	72	82
7	33^c	67	95	13
8	33·TFA	43	66	80
9	34^d	5	93	32
10	34·TFA	126	24	16
11	35^e	3	86	28
12	35·TFA	47	18	2

^a For results published with the same catalyst, see references 78 and 81.

^b For results published with the same catalyst, see reference 80.

^c For results published with the same catalyst, see reference 79.

^d For results published with the same catalyst, see reference 86.

^e For results published with the same catalyst, see reference 78.

The results show again the need for an acid to achieve high enantioselectivity, when aromatic prolinamides are used. The effect is quite remarkable with both prolinamide **12** with CF₃ groups, in which an increase from 2 to 65 % is produced and the catalyst derived from pentafluoroaniline **33**, with a change from 13 to 80 % enantiomeric excess. The effect of the prolinamide **20** is similar to that obtained with catalyst **12** with two CF₃ groups, in both cases an increase in the enantiomeric excess by using an equivalent of acid is produced, but the values are not very high.

The results obtained with non-aromatic prolinamides is striking. On one hand, the presence of trifluoroacetic acid reduces the reaction rate, as in the case of aromatic prolinamides but, unlike with aromatic prolinamides, the enantioselectivity of the reaction is greatly reduced in the presence of acid. In the case of prolinamide **34** with the butyl group, the enantiomeric excess is reduced from 32 to 16 %. For the prolinamide derivative of *t*-butylamine **35**, the effect is more dramatic, since it decreases the enantiomeric excess from 28 % to 2 %, in the presence of acid. This prolinamide also presented the feature of not forming imidazolidinones under neutral conditions, probably due to the *t*-butyl group steric hindrance.

⁸⁶ Chimni, S. S.; Mahajan, D. *Tetrahedron: Asymmetry* **2006**, *17*, 2108-2119.

Another fact to consider is that the presence of acid leads to the appearance of the elimination product from aldol **25**, while the absence of traces of acid generates the double aldol condensation product (figure 2.31).

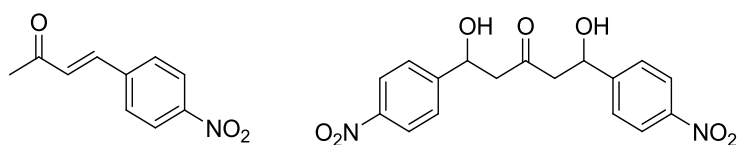
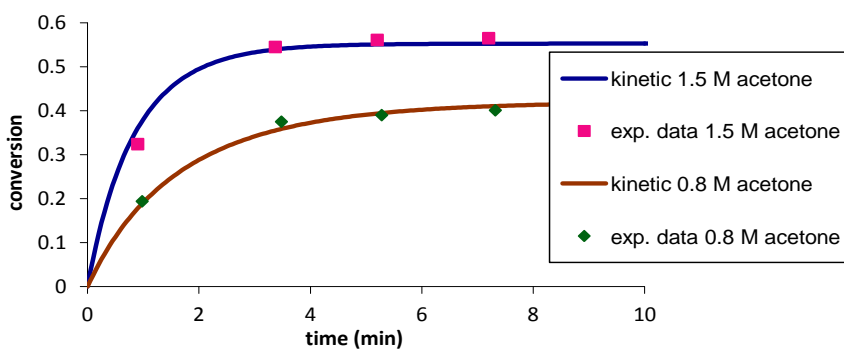


Figure 2.31. Other products which appears in the aldol reaction between acetone and 4-nitrobenzaldehyde.

2.2.10. Proposed reaction mechanism

Before proposing a possible reaction mechanism, we studied the reaction order of acetone in the imidazolidinone formation. We performed several experiments that changed the initial concentration of acetone (0.8 to 1.5 M), keeping fixed the concentration of prolinamide **12** (0.2 M). We measured the conversion of aldol product versus time and then performed a simulation from these concentration data (Euler method), adjusting the rate constant to the best possible approach to the experimental data.

a) Unimolecular reaction between acetone and prolinamide.



Graph 2.6. Unimolecular reaction for prolinamide and acetone, with a rate constant $k = 0.8 \text{ M}^{-1}\text{min}^{-1}$.

It can be seen that the predicted kinetic fits very well to the experimental data for both concentration values.

b) Bimolecular reaction in acetone and unimolecular reaction in prolinamide.

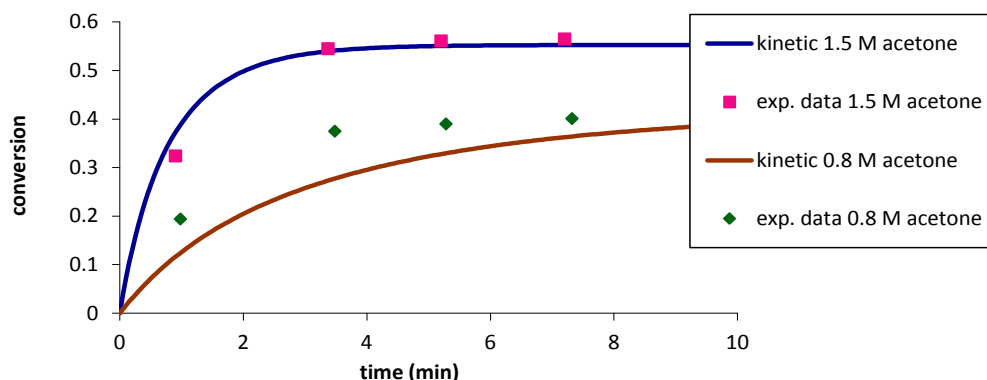


Figure 2.7. Bimolecular reaction in acetone and unimolecular in prolinamide, with a rate constant $k = 0.6 \text{ M}^{-2} \text{ min}^{-1}$.

In this case it is observed that the fit of the experimental data to the predicted kinetics agrees well to an acetone concentration of 1.5 M, but this adjustment is not working to 0.8 M with the same rate constant, so it could be concluded that the reaction is not bimolecular in acetone.

c) Unimolecular reaction in acetone and bimolecular in prolinamide.

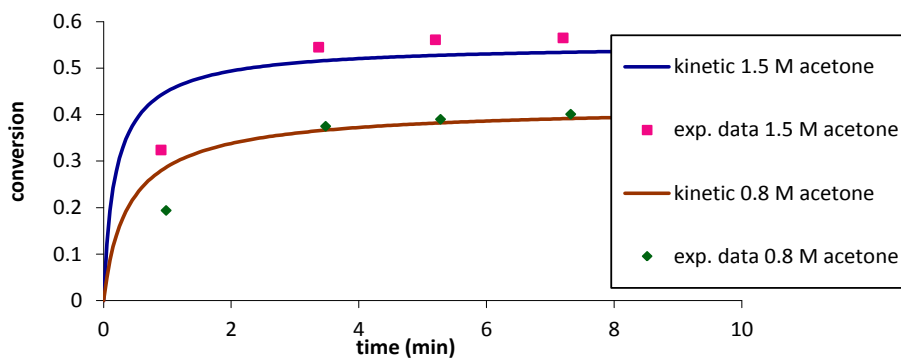


Figure 2.8. Unimolecular reaction in acetone and bimolecular in prolinamide, with a rate constant $k = 14 \text{ M}^{-2} \text{ min}^{-1}$.

In this case it is impossible to fit a curve approximating the experimental points for any of the two concentrations, so that we could summarize that in view of the results, the reaction is not bimolecular in prolinamide.

Therefore, the reaction is unimolecular in acetone and in prolinamide.

Then, we will try to justify the observed deuteration experiments. First, the reaction between prolinamide **20** and deuterated acetone generates the addition product **36** in a slow process. Compound **36** loses a water molecule to generate iminium salt **37**, which is in fast equilibrium with enamine **38** and slower equilibrium with imidazolidinone **23**, which is the compound that accumulates in the reaction medium (figure 2.32).

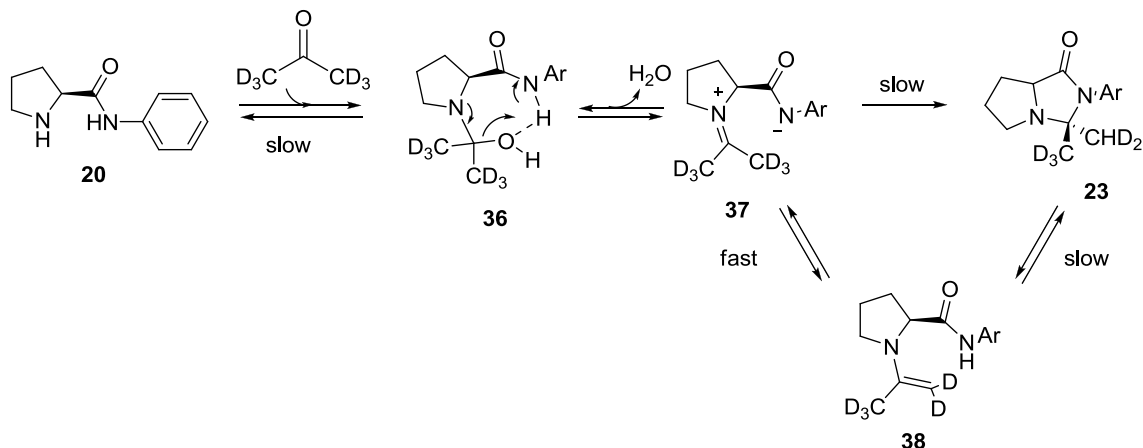


Figure 2.32. Equilibrium between prolinamide **20** and deuterioacetone.

The incorporation of protons in the deuterated methyl groups of deuterioacetone (see spectra in figure 2.16, page 82) could be explained if in the formation of the enamine intervenes the water molecule that is produced in the formation of iminium salt **37**, so that this molecule partially deuterated could transport a proton to the methyl groups of deuterioacetone as follows:

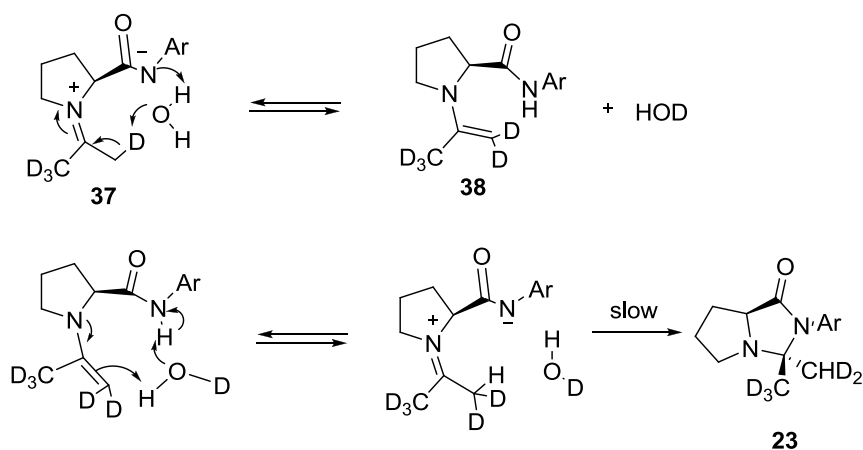


Figure 2.33. Enamine formation with participation of a water molecule and subsequent loss of deuterium in the methyl groups of the imidazolidinone.

The experiments have shown that the opening of imidazolidinone **23** occurs slowly, however, the presence of a nucleophile or an acid catalyses its opening, promoting the reaction with an electrophile such as an aldehyde. In the case of the reaction carried out in CD_3OD , we observed deuteration in the methyl group at the beginning of the reaction, but not in the methylene, which we explain via a concerted ene-type mechanism, after which the methyl group incorporates deuteriums with the involvement of a CD_3OD molecule.

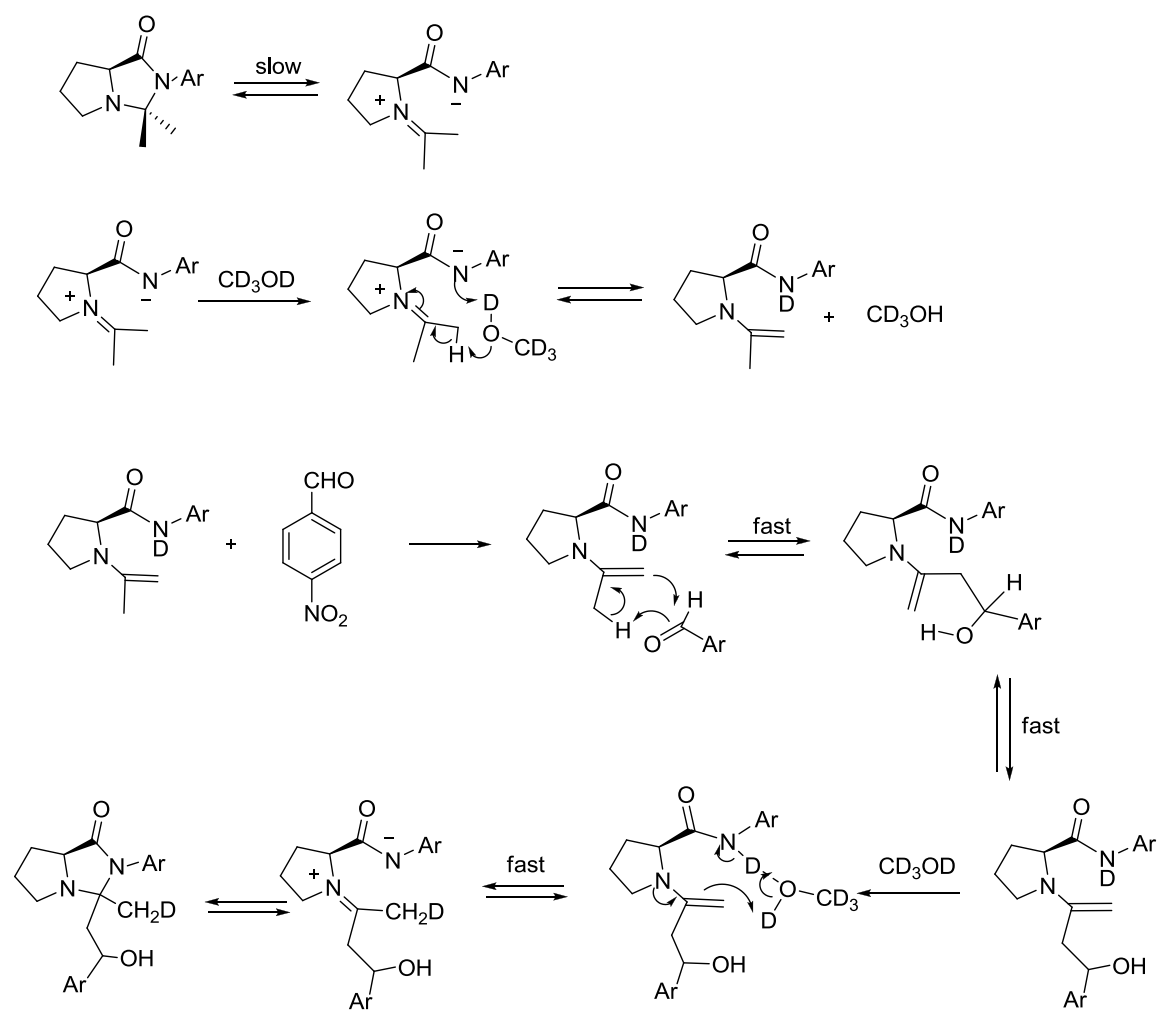


Figure 2.34. Imidazolidinones **23a**, **b** formation in the reaction catalysed by CD_3OD and justification of the deuteration in the methyl group but not in the methylene.

Although the above mechanism is not completely confirmed experimentally, we believe it is the most likely, and in any case, is very different from the one proposed nowadays for proline, in which the ene-type mechanism has not even been contemplated.

2.3. CONCLUSIONS

Throughout this chapter it has been highlighted the complexity of a seemingly simple reaction such as the aldol reaction. This explains the different results found in literature working with the same catalysts but varying the reaction conditions slightly.

A detailed study of the reaction mechanism in different solvents has shown that this is an equilibrium reaction in which the formation of many intermediate compounds occurs: hemiaminals, amins and imidazolidinones. These intermedia modify the equilibrium and the reaction rate.

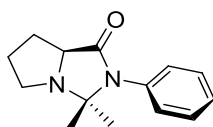
Although the participation of the enamine in the reaction has been demonstrated and we could register its NMR spectrum (something that had not been described in the literature), it appears that the formation of diastereomeric imidazolidinones in aldol products could influence the enantiomeric excess of the reaction. These imidazolidinones possess different stabilities and experiment hydrolysis (or transcarbonylation) at different rates, being these last reactions, the ones which can control the enantiomeric excess of the reaction.

To solve this problem it was found that the presence of nucleophiles or acids promotes imidazolidinone opening. Using the appropriate conditions, it has been achieved an enantiomeric excess of 82 % in the organocatalyzed reaction between acetone and 4-nitrobenzaldehyde.

2.4. EXPERIMENTAL

- Prolinamides **20**,^{78,80,87} **27**,⁸⁰ **32**^{79,88} and **33**⁸⁰ are known compounds which were prepared according to the experimental procedure described in Chapter 1. Physical and spectroscopic data are in good agreement with properties shown in the literature.

- (**S**)-3,3-Dimethyl-2-phenyl-hexahydropyrrolo[1,2-*e*]imidazol-1-one (**23**)



Prolinamide **20** (1.27 g, 6.68 mmol) was dissolved in acetone (10 mL) and either anhydrous Na₂SO₄ or K₂CO₃ (1 g) was added. The mixture was stirred for 12 h at room temperature and then filtered to remove salts. Then, acetone was evaporated to afford the crude product which was purified by recrystallization from acetone (1.13 g, 73.5 %).

$[\alpha]_D^{25} = +46.0$ ($c = 0.98$, CHCl₃).

mp: 89-92 °C.

¹H RMN (CD₃COCD₃): 1.72 (s, 3H), 1.86 (s, 3H), 2.13 (m, 1H), 2.24 (m, 1H), 2.33 (m, 1H), 2.48 (m, 1H), 3.05 (m, 1H), 3.35 (t, $J = 7.6$ Hz, 1H), 4.36 (dd, $J = 4.6, 9.6$ Hz, 1H), 7.60 (d, $J = 8.0$ Hz, 2H), 7.72 (t, $J = 8.0$ Hz, 1H), 7.82 (t, $J = 8.0$ Hz, 2H).

¹³C RMN (CD₃COCD₃) δ (ppm): 23.1 (CH₃), 25.3 (CH₂), 26.0 (CH₂), 27.8 (CH₃), 48.6 (CH₂), 63.4 (CH), 80.6 (C), 127.5 (CH x 2), 129.1 (CH x 3), 137.7 (C), 175.6 (C).

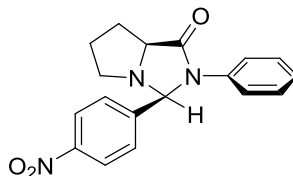
IR (nujol, cm⁻¹): 3059, 1690, 1378, 717.

HRMS (ESI): 253,1316 (M + Na)⁺, calcd for C₁₄H₁₈N₂ONa 253,1311.

⁸⁷ (a) Tang, Z.; Yang, Z.-H.; Chen, X.-H.; Cun, L.-F.; Mi, A.-Q.; Jiang, Y.-Z.; Gong, L.-Z. *J. Am. Chem. Soc.* **2005**, *127*, 9285-9289; (b) Rhyoo, H. Y.; Yoon, Y.-A.; Park, H.-J.; Chung, Y. K. *Tetrahedron Lett.* **2001**, *42*, 5045-5048.

⁸⁸ Sato, K.; Kuriyama, M.; Shimazawa, R.; Morimoto, T.; Kakiuchi, K.; Shirai, R. *Tetrahedron Lett.* **2008**, *49*, 2402-2406.

- (3*S*,7*aS*)-3-(4-Nitrophenyl)-2-phenylhexahydropyrrolo[1,2-*e*]imidazol-1-one (24a)



4-Nitrobenzaldehyde (72 mg, 0.48 mmol) and aniline prolinamide **20** (94.7 mg, 0.50 mmol) were dissolved in CDCl₃ (0.5 mL). The reaction was monitored by ¹H NMR. After nine days, the solvent was evaporated off under reduced pressure and the crude product was recrystallized from CH₂Cl₂/undecane.

[α]_D²⁵ = +16.9 (c = 0.95, CHCl₃).

P.f.: 71-72 °C.

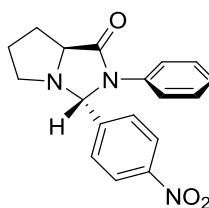
¹H RMN (CDCl₃) δ (ppm): 1.79 (m, 2H), 2.29 (m, 3H), 2.40 (m, 1H), 4.03 (dd, *J* = 3.4, 8.4 Hz, 1H), 6.45 (s, 1H), 7.09 (m, 1H), 7.28 (m, 4H), 7.45 (d, *J* = 8.8 Hz, 2H), 8.14 (d, *J* = 8.8 Hz, 2H).

¹³C RMN (CDCl₃) δ (ppm): 25.1 (CH₂), 27.2 (CH₂), 49.2 (CH₂), 65.9 (CH), 78.2 (CH), 122.2 (CH x 2), 124.0 (CH x 2), 125.7 (CH), 129.2 (CH x 2), 129.6 (CH x 2), 137.2 (C), 141.9 (C), 148.3 (C), 176.7 (C).

IR (nujol, cm⁻¹): 1703, 1599, 1346, 729.

HRMS (ESI): 346,1146 (M + Na)⁺, calcd for C₁₈H₁₇N₃O₃Na 346,1168.

- (3*R*,7*aS*)-3-(4-Nitrophenyl)-2-phenylhexahydropyrrolo[1,2-*e*]imidazol-1-one (24b)



4-Nitrobenzaldehyde (0.42 g, 2.78 mmol) and aniline prolinamide **20** (0.52 g, 2.74 mmol) were dissolved in glacial acetic acid (1 mL) and heated at 75-80 °C for three hours. The reaction mixture was then treated with an aqueous solution of sodium carbonate (4 %) and extracted with ethyl acetate. The combined organic layers were dried over Na₂SO₄ and the solvent was evaporated off to yield a crude compound that was purified by recrystallization (CH₂Cl₂/undecane) to afford compound **24b** as a white solid (0.84 g, 95 %).

[α]_D²⁵ = -19.2 (c = 1.20, CHCl₃).

mp: 159-161 °C.

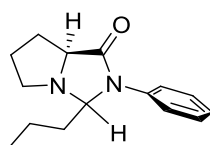
$^1\text{H RMN}$ (CDCl_3) δ (ppm): 1.92 (m, 2H), 2.22 (m, 2H), 2.92 (m, 1H), 3.44 (m, 1H), 3.99 (t, $J = 6.8$ Hz, 1H), 5.77 (s, 1H), 7.13 (t, $J = 6.6$ Hz, 1H), 7.29 (t, $J = 6.6$ Hz, 2H), 7.44 (t, $J = 6.6$ Hz, 2H), 7.47 (d, $J = 14.6$ Hz, 2H), 8.18 (d, $J = 14.6$ Hz, 2H).

$^{13}\text{C RMN}$ (CDCl_3) δ (ppm): 25.1 (CH_2), 27.9 (CH_2), 56.5 (CH_2), 64.7 (CH), 82.9 (CH), 121.5 ($\text{CH} \times 2$), 124.5 ($\text{CH} \times 2$), 125.9 (CH), 127.5 ($\text{CH} \times 2$), 129.5 ($\text{CH} \times 2$), 137.3 (C), 146.8 (C), 148.1 (C), 174.8 (C).

IR (nujol, cm^{-1}): 3072, 1696, 1339, 827, 762.

HRMS (ESI): 346,1146 ($\text{M} + \text{Na}$) $^+$, calcd for $\text{C}_{18}\text{H}_{17}\text{N}_3\text{O}_3\text{Na}$ 346,1168.

- (7a*S*)-2-Phenyl-3-propyl-hexahydropyrrolo[1,2-*e*]imidazol-1-one (**29b**)



Aniline prolinamide **20** (0.14 g, 0.74 mmol) and butyraldehyde (0.28 mL, 3.10 mmol) were dissolved in glacial acetic acid (0.14 mL) and heated at 70-80 °C for ten minutes. Then, the solution was quenched with a saturated solution of sodium carbonate and extracted with ethyl acetate. The combined organic layers were dried (Na_2SO_4) and the solvent was evaporated off under reduced pressure. Purification by column chromatography on silica gel (eluent, CH_2Cl_2 -ethyl acetate) afforded imidazolidinone **29b** as a pale yellow oil (0.14 g, 80 %).

$[\alpha]_D^{25} = -31.4$ ($c = 2.50$, CHCl_3).

$^1\text{H RMN}$ (CDCl_3) δ (ppm): 0.87 (t, $J = 7.4$ Hz, 3H), 1.51 (m, 3H), 1.83 (m, 2H), 2.10 (m, 3H), 2.70 (m, 1H), 3.25 (m, 1H), 3.98 (dd, $J = 4.7, 8.8$ Hz, 1H), 4.71 (dd, $J = 3.4, 7.3$ Hz, 1H), 7.17 (t, $J = 8.0$ Hz, 1H), 7.37 (t, $J = 8.0$ Hz, 2H), 7.48 (d, $J = 8.0$ Hz, 2H).

$^{13}\text{C RMN}$ (CDCl_3) δ (ppm): 14.0 (CH_3), 18.4 (CH_2), 25.2 (CH_2), 27.9 (CH_2), 36.8 (CH_2), 56.7 (CH_2), 65.3 (CH), 82.7 (CH), 122.7 ($\text{CH} \times 2$), 125.8 (CH), 129.4 ($\text{CH} \times 2$), 137.3 (C), 174.3 (C).

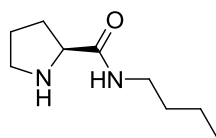
IR (nujol, cm^{-1}): 3059, 1696, 1488, 786.

HRMS (ESI): 245,1651 ($\text{M} + \text{H}$) $^+$, calcd for $\text{C}_{15}\text{H}_{22}\text{N}_2\text{O}$ 245,1648.

- Compounds **31**⁸⁹ and **35**⁷⁸ were prepared according to the experimental procedure described in literature, showing the same physical and spectroscopic properties.

⁸⁹ Stork, G.; Brizzolara, A.; Landesman, H.; Szmuszkovicz, J.; Terrell, R. *J. Am. Chem. Soc.* **1963**, *85*, 207-222.

- (S)-N-butylpyrrolidine-2-carboxamide (**34**)



The butyl ester of *L*-proline **15**⁹⁰ (0.5 g, 2.92 mmol) was dissolved in butylamine (1.0 mL, 10.1 mmol) and after 14 hours butylamine was evaporated under reduced pressure obtaining 450 mg of a yellowish oil, with 91 % yield.

Physical and spectroscopic data agree with those described in literature.⁸⁹

General Procedures

- Reaction between acetone and 4-nitrobenzaldehyde

Aldol reaction in deuteriochloroform: 4-nitrobenzaldehyde (75.3 mg, 0.5 mmol), aniline prolinamide **20** (94.2 mg, 0.5 mmol) and acetone (0.037 mL, 0.5 mmol) were dissolved in 0.46 mL of CDCl₃ at room temperature. The reaction was monitored by ¹H NMR.

Aldol reaction in deuterioacetone: 4-nitrobenzaldehyde (60.7 mg, 0.4 mmol) and aniline prolinamide **20** (76.6 mg, 0.4 mmol) were dissolved in CD₃COCD₃ (0.4 mL, 5.4 mmol) at room temperature. The reaction was monitored by ¹H NMR.

- Reaction between acetone imidazolidinone 23 and 4-nitrobenzaldehyde.

Aldol reaction between acetone imidazolidinone 23 and 4-nitrobenzaldehyde in deuteromethanol: 4-nitrobenzaldehyde (37.8 mg, 0.25 mmol) and acetone imidazolidinone **23** (57.5 mg, 0.25 mmol) were dissolved in 0.5 mL of deuteromethanol at room temperature. The reaction was monitored by ¹H NMR.

Aldol reaction between acetone imidazolidinone 23 and 4-nitrobenzaldehyde in deuterioacetone: 4-nitrobenzaldehyde (76.5 mg, 0.5 mmol) and acetone imidazolidinone **23** (116.8 mg, 0.5 mmol) were dissolved in 0.5 mL of deuterioacetone at room temperature. The reaction was monitored by ¹H NMR.

⁹⁰ Compound **15** was already prepared in Chapter 1.

- Reaction between acetone and 4-nitrobenzaldehyde in presence of trifluoroacetic acid catalysed by compounds 12, 20, 32-35

4-nitrobenzaldehyde (51.3 mg, 0.34 mmol), catalyst (0.034 mmol) and trifluoroacetic acid (2.6 mL, 0.034 mmol) were dissolved in deuterioacetone (0.5 mL) at room temperature. The reaction was monitored by ^1H NMR and the enantiomeric excesses were determined by HPLC analysis from the reaction mixture.

- Reaction between butyraldehyde and prolinamide 20

Aniline prolinamide **20** (9.6 mg, 0.05 mmol) and butyraldehyde (4.5 mL, 0.05 mmol) were dissolved in CDCl_3 (0.5 mL) at room temperature. The reaction was monitored by ^1H NMR.

- Reaction between pyrrolidine cyclohexanone enamine 31 and 4-nitrobenzaldehyde

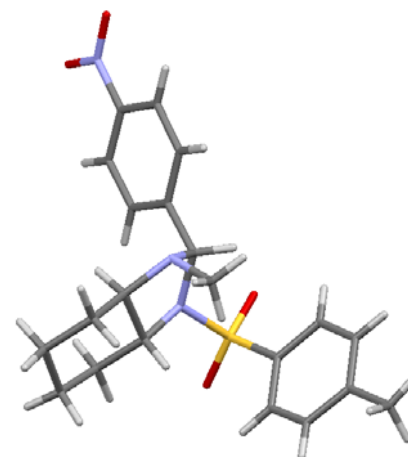
Pyrrolidine cyclohexanone enamine **31** (11.3 mg, 0.075 mmol) and 4-nitrobenzaldehyde (11.3 mg, 0.075 mmol) were dissolved in CDCl_3 (0.45 mL) at room temperature. The reaction was monitored by ^1H NMR.



**UNIVERSIDAD
DE SALAMANCA**

CAMPUS DE EXCELENCIA INTERNACIONAL

***CHAPTER 3: Organocatalysts derived from trans-1,2-
cyclohexanediamine***



3.1. INTRODUCTION

Despite the good results obtained with prolinamides described in the previous chapter, we thought that it would be possible to improve them. X-ray structures of several prolinamides described in literature⁹¹ have shown that there exist an intramolecular hydrogen bond between the nitrogen atom of the pyrrolidine ring and the amide NH of around 2.6 Å (heteroatom-heteroatom distance, figure 3.1).

According to the classification of hydrogen bonds conducted by Jeffrey,⁹² it would be between moderate and strong hydrogen bonds.

Table 3.1. Classification of hydrogen bonds by Jeffrey.

	Strong	Moderate	Weak
Donor-acceptor distance (Å)	2.2-2.5	2.5-3.2	3.2-4.0
Energy (kcal/mol)	40-14	15-4	<4
Bond type	Preferently covalent	Preferently electrostatic	Electrostatic

⁹¹ (a) Pieczonka, A. M.; Mloston, G.; Linden, A.; Heimgartner, H. *Helv. Chim. Acta* **2012**, *95*, 1521-1530;

(b) Moorthy, J. N.; Saha, S. *Eur. J. Org. Chem.* **2009**, 739-748.

⁹² Jeffrey, G. A. *An introduction to hydrogen bonding*; Oxford University Press: New York, 1997.

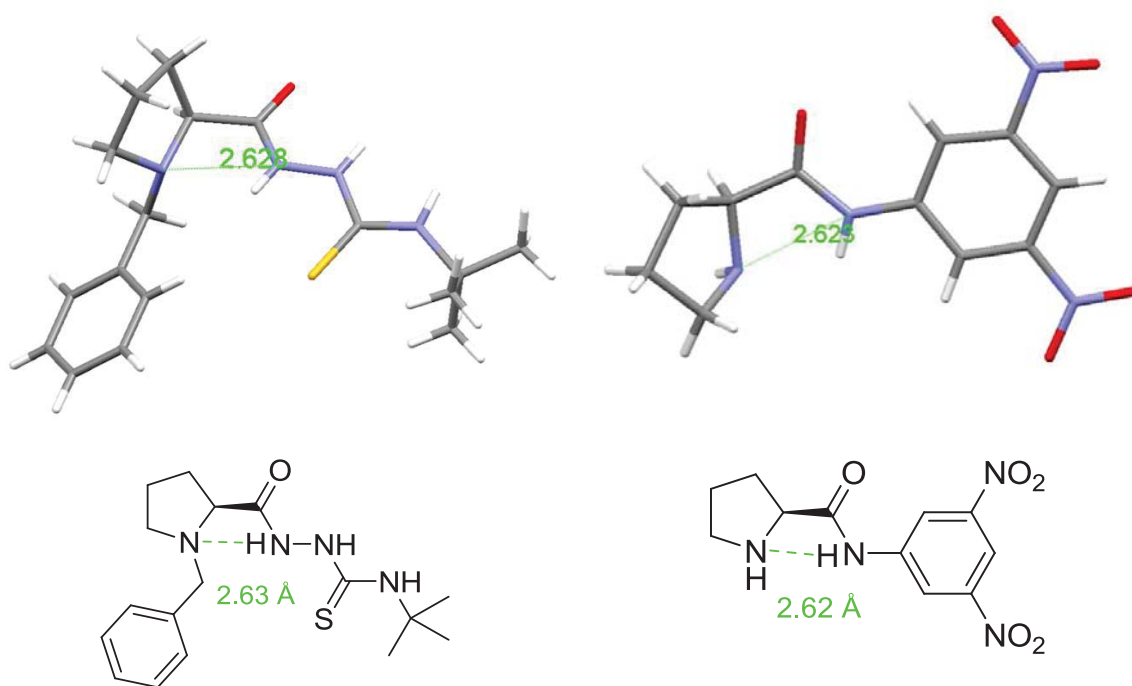


Figure 3.1. X-ray structure of several prolinamides described in literature, in which the formation of a moderate hydrogen bond between the amide NH and the N of the pyrrolidine ring can be observed.

Our experimental results also show that prolinamides are much less basic than pyrrolidine (chapter 2, table 2.6). The intramolecular hydrogen bond may well explain this effect, since pyrrolidine nitrogen protonation in the prolinamide implies the loss of the intramolecular H-bond. Since the prolinamide loses basicity due to the hydrogen bond, it is also expected a large loss in its nucleophilicity, and hence the prolinamide is probably a much poorer catalyst than an amine which lacks this H-bond. Therefore it should be possible to improve the catalytic results with new catalysts in which there were no such intramolecular hydrogen bond. An initial literature search led us to *trans*-1,2-cyclohexanediamine derivatives. In these, the two amino groups occupy equatorial positions in the cyclohexane ring that make them to be positioned above and below the plane of the cyclohexane; in these conditions, the distance between amine groups makes difficult the formation of a strong intramolecular H-bond.

This distance between the two amino groups depends heavily on the cyclohexane derivative chosen, but it is always superior to the same distance in prolinamides. Figure 3.2 shows the X-ray structure of the Takemoto catalyst,⁹³ a bifunctional catalyst for Michael additions, based on a chiral *trans*-1,2-cyclohexanediamine acting as a base, and a thiourea activating the electrophile.

⁹³ Okino, T.; Hoashi, Y.; Furukawa, T.; Xu, X.; Takemoto, Y. *J. Am. Chem. Soc.* **2005**, *127*, 119-125.

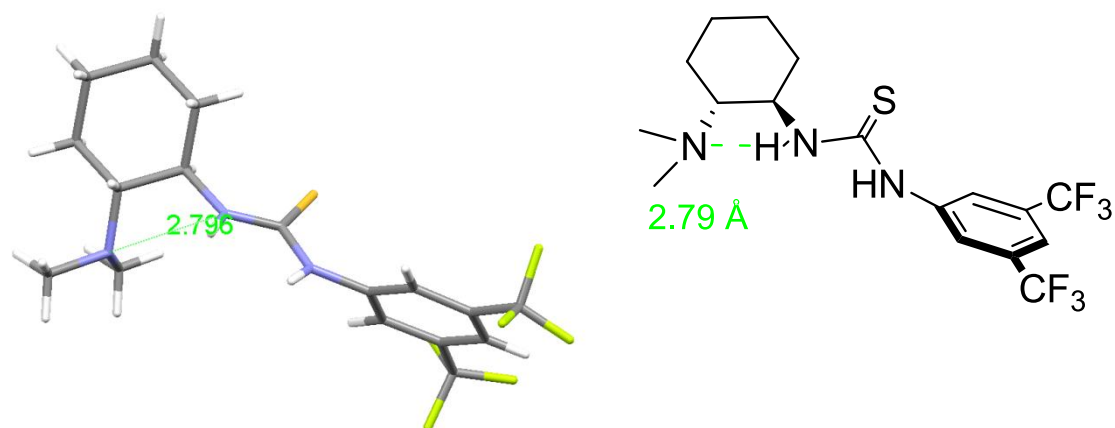


Figure 3.2. X-ray structure of Takemoto catalyst, in which the intramolecular hydrogen bond between one of the thiourea NHs and the dimethylated N of the cyclohexane ring is shown.

Other derivatives of *trans*-1,2-cyclohexanediamine have still shown weaker hydrogen bonds, with heteroatom-heteroatom distances close to 3 Å, as can be seen in figure 3.3.⁹⁴

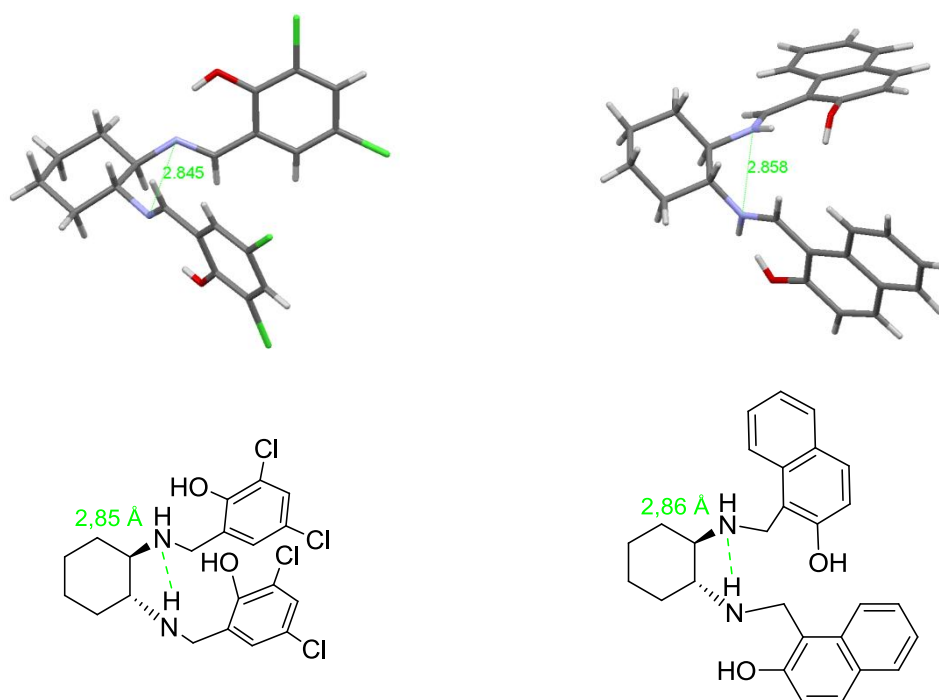


Figure 3.3. X-ray structures of *trans*-1,2-cyclohexanediamine derivatives with intramolecular hydrogen bonding near 3 Å.

⁹⁴ (a) Hadjoudis, E.; Rontoyianni, A.; Ambroziak, K.; Dziembowska, T.; Mavridis, I. M. *J. Photochem. Photobiol., A* **2004**, *162*, 521-530; (b) Galland, A.; Dupray, V.; Lafontaine, A.; Berton, B.; Sanselme, M.; Atmani, H.; Coquerel, G. *Tetrahedron: Asymmetry* **2010**, *21*, 2212-2217; (c) Kwit, M.; Plutecka, A.; Rychlewska, U.; Gawronski, J.; Khlebnikov, A. F.; Kozhushkov, S. I.; Rauch, K.; de Meijere, A. *Chem. Eur. J.* **2007**, *13*, 8688-8695.

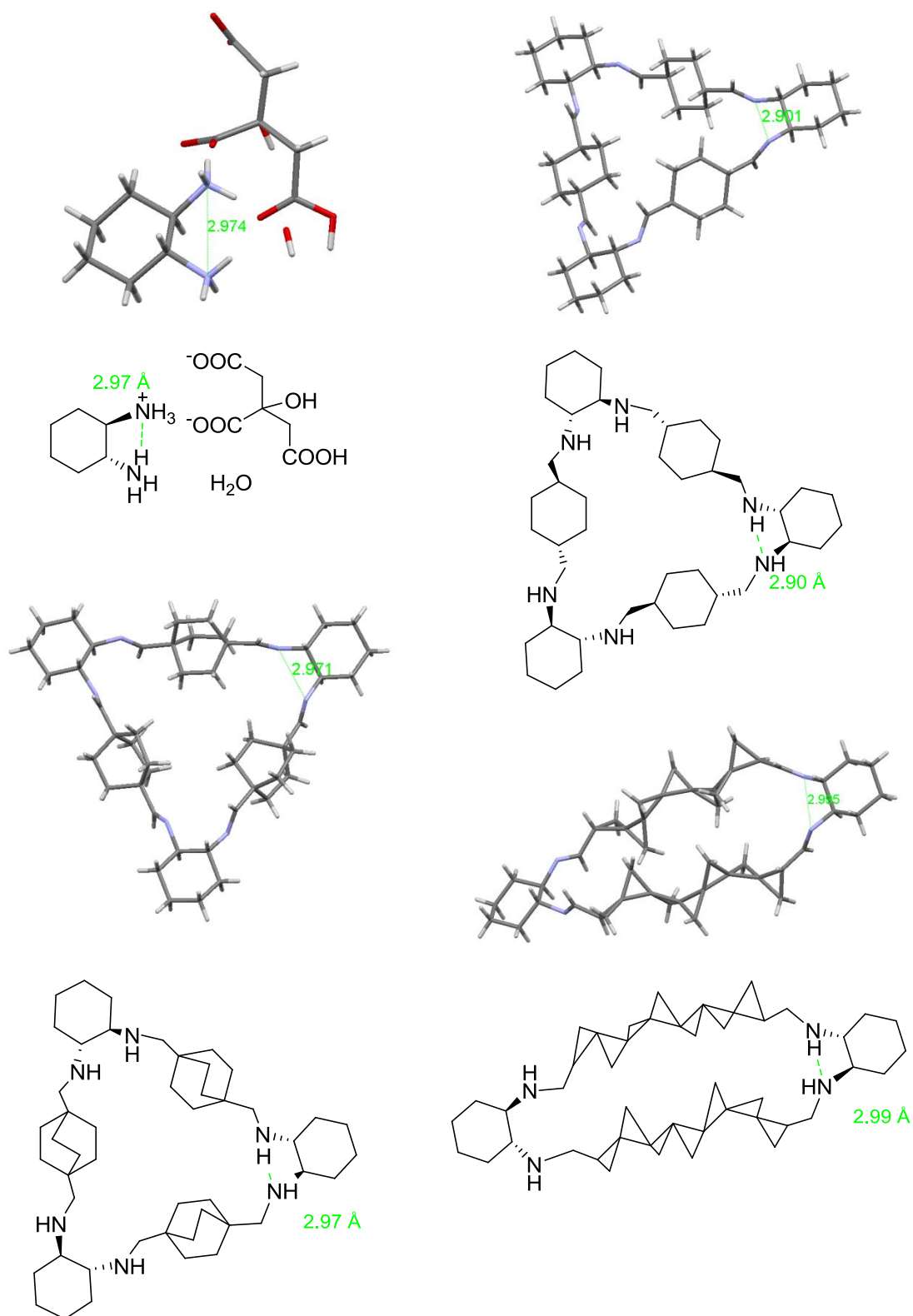


Figure 3.3 (continuation). X-ray structures of *trans*-1,2-cyclohexanediamine derivatives with intramolecular hydrogen bonding close to 3 Å.

The above structures show that the fragment of *trans*-1,2-cyclohexane can be a good starting point for the design of new organocatalysts for aldol reactions.

However, Takemoto catalyst is not useful for aldol condensations via enamine, since the amine group is doubly methylated and cannot form an enamine with the carbonyl group. However, it would be attractive to leave unmethylated an amine group of the *trans*-1,2-cyclohexane, while the other could be acylated with different groups, with the aim of studying the influence of the NH acidity, or even to include this part of the molecule into an oxyanion hole. Indeed, the *trans*-1,2-cyclohexanediamine has been widely exploited as a source of chirality in many organic reactions,⁹⁵ and numerous bifunctional catalysts have been prepared (figure 3.4).

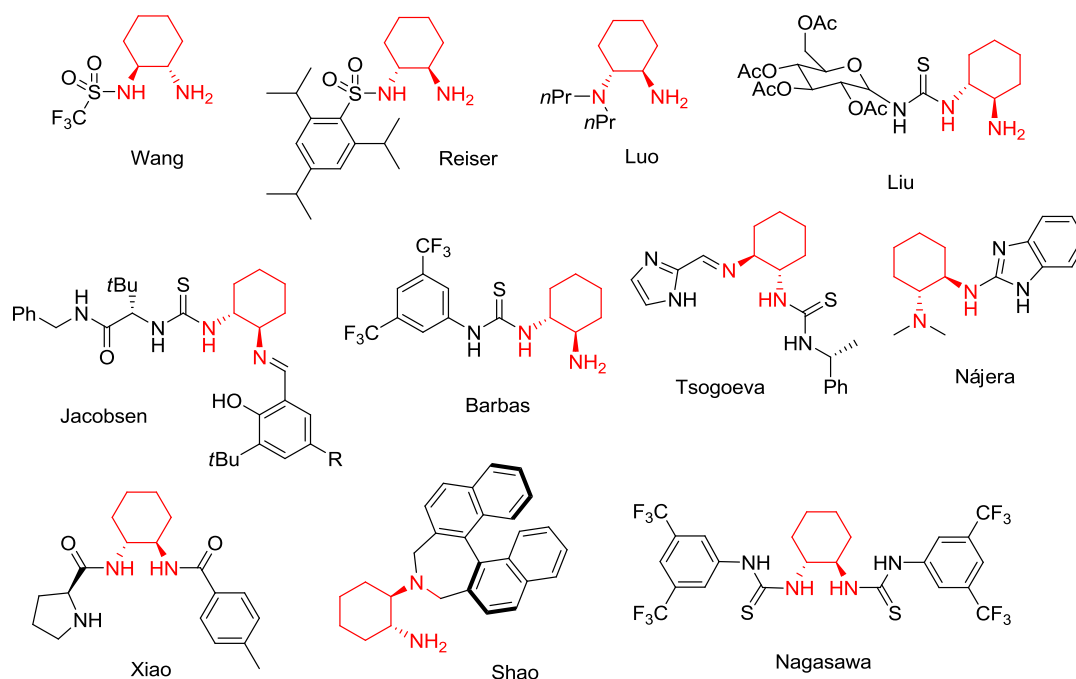


Figure 3.4. Some *trans*-1,2-cyclohexanediamine derived organocatalysts.

Although amide bond formation by reaction of amines with acid chlorides is a well established procedure in organic synthesis, monoacylation of symmetric diamines with high performance can be a difficult process in some cases. The reason is that it requires a strategy

⁹⁵ (a) Xue, F.; Zhang, S.; Duan, W.; Wang, W. *Adv. Synth. Catal.* **2008**, *350*, 2194-2198; (b) Lalonde, M. P.; Chen, Y.; Jacobsen, E. N. *Angew. Chem., Int. Ed.* **2006**, *45*, 6366-6370; (c) Uehara, H.; Barbas III, C. F. *Angew. Chem., Int. Ed.* **2009**, *48*, 9848-9852; (d) Tsogoeva, S. B.; Wei, S. *Chem. Commun.* **2006**, 1451-1453; (e) Sohtome, Y.; Tanatani, A.; Hashimoto, Y.; Nagasawa, K. *Chem. Pharm. Bull.* **2004**, *52*, 477-480; (f) Rasappan, R.; Reiser, O. *Eur. J. Org. Chem.* **2009**, 1305-1308; (g) Peng, F.; Shao, Z. *J. Mol. Catal. A: Chem.* **2008**, *285*, 1-13; (h) Luo, S.; Xu, H.; Li, J.; Zhang, L.; Cheng, J.-P. *J. Am. Chem. Soc.* **2007**, *129*, 3074-3075; (i) Mei, K.; Jin, M.; Zhang, S.; Li, P.; Liu, W.; Chen, X.; Xue, F.; Duan, W.; Wang, W. *Org. Lett.* **2009**, *11*, 2864-2867; (j) Wang, J.; Wang, X.; Ge, Z.; Cheng, T.; Li, R. *Chem. Commun.* **2010**, 1751-1753; (k) Ma, H.; Liu, K.; Zhang, F.-G.; Zhu, C.-L.; Nie, J.; Ma, J.-A. *J. Org. Chem.* **2010**, *75*, 1402-1409; (l) Huang, H.; Jacobsen, E. N. *J. Am. Chem. Soc.* **2006**, *128*, 7170-7171; (m) Liu, K.; Cui, H.-F.; Nie, J.; Dong, K.-Y.; Li, X.-J.; Ma, J.-A. *Org. Lett.* **2007**, *9*, 923-925; (n) Tsogoeva, S. B.; Yalalov, D. A.; Hateley, M. J.; Weckbecker, C.; Huthmacher, K. *Eur. J. Org. Chem.* **2005**, 4995-5000; (o) Almasi, D.; Alonso, D. A.; Gomez-Bengoa, E.; Najera, C. *J. Org. Chem.* **2009**, *74*, 6163-6168; (p) Chen, J.-R.; Lu, H.-H.; Li, X.-Y.; Cheng, L.; Wan, J.; Xiao, W.-J. *Org. Lett.* **2005**, *7*, 4543-4545; (q) Peng, F.-Z.; Shao, Z.-H.; Pu, X.-W.; Zhang, H.-B. *Adv. Synth. Catal.* **2008**, *350*, 2199-2204; (r) Sohtome, Y.; Tanatani, A.; Hashimoto, Y.; Nagasawa, K. *Tetrahedron Lett.* **2004**, *45*, 5589-5592; (s) Sohtome, Y.; Takemura, N.; Takagi, R.; Hashimoto, Y.; Nagasawa, K. *Tetrahedron* **2008**, *64*, 9423-9429.

which depends on the selective monoacylation of one of the amine groups.⁹⁶ A 1:1 stoichiometry of the diamine and the acylating agent produces statistically 50 % of the desired mono-amide, 25 % of the diamide and 25 % of the starting diamine (if the nucleophycity of the second NH₂ is not affected by the acylation of the first NH₂), which is synthetically acceptable if the three compounds are easy to separate and the acylating agent is cheap. Moreover, in cases where the diamine is a cheap and easily removable volatile compound, the use of a great excess of diamine should increase the yield of the monoamide. However, due to the fact that the second acylation reaction may be faster than the first one, the use of an excess of the diamine (sometimes even as solvent) can produce mainly the diacylated product.⁹⁷ Several hypotheses have been proposed to explain the preference for diacylation, as an inefficient mixing of the reactants (the mono-acylated product is more soluble than the diamine and it is more easily acylated) or intramolecular catalysis by the first amide group (figure 3.5).

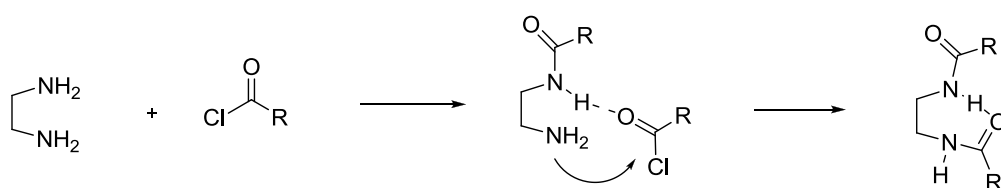


Figure 3.5. Intramolecular catalysis of the first amide group would favour the second acylation.

However, it has been possible to effect monoacylation working with compounds of lower reactivity as esters or carbonates,⁹⁸ using aggregation effects⁹⁹ or steric hindrance,¹⁰⁰ although sometimes, as in the latter case, additional steps are required for the synthesis (figure 3.6).

⁹⁶ Jacobson, A. R.; Makris, A. N.; Sayre, L. M. *J. Org. Chem.* **1987**, *52*, 2592-2594.

⁹⁷ (a) Bergeron, R. J.; Garlich, J. R.; Stolowich, N. J. *J. Org. Chem.* **1984**, *49*, 2997-3001; (b) Stoutland, O.; Helgen, L.; Agre, C. L. *J. Org. Chem.* **1959**, *24*, 818-820; (c) Moore, T. S.; Boyle, M.; Thorn, V. M. *J. Chem. Soc.* **1929**, 39-51; (d) Lawson, W. B.; Leafer, M. D., Jr.; Tewes, A.; Rao, G. J. S. *Hoppe-Seyler's Z. Physiol. Chem.* **1968**, *349*, 251-262; (e) Stahl, G. L.; Walter, R.; Smith, C. W. *J. Org. Chem.* **1978**, *43*, 2285-2286.

⁹⁸ Tang, W.; Fang, S. *Tetrahedron Lett.* **2008**, *49*, 6003-6006.

⁹⁹ Muñiz, F. M.; Simón, L.; Sáez, S.; Raposo, C.; Morán, J. R. *Tetrahedron Lett.* **2008**, *49*, 790-793.

¹⁰⁰ Kim, Y. K.; Lee, S. J.; Ahn, K. H. *J. Org. Chem.* **2000**, *65*, 7807-7813.

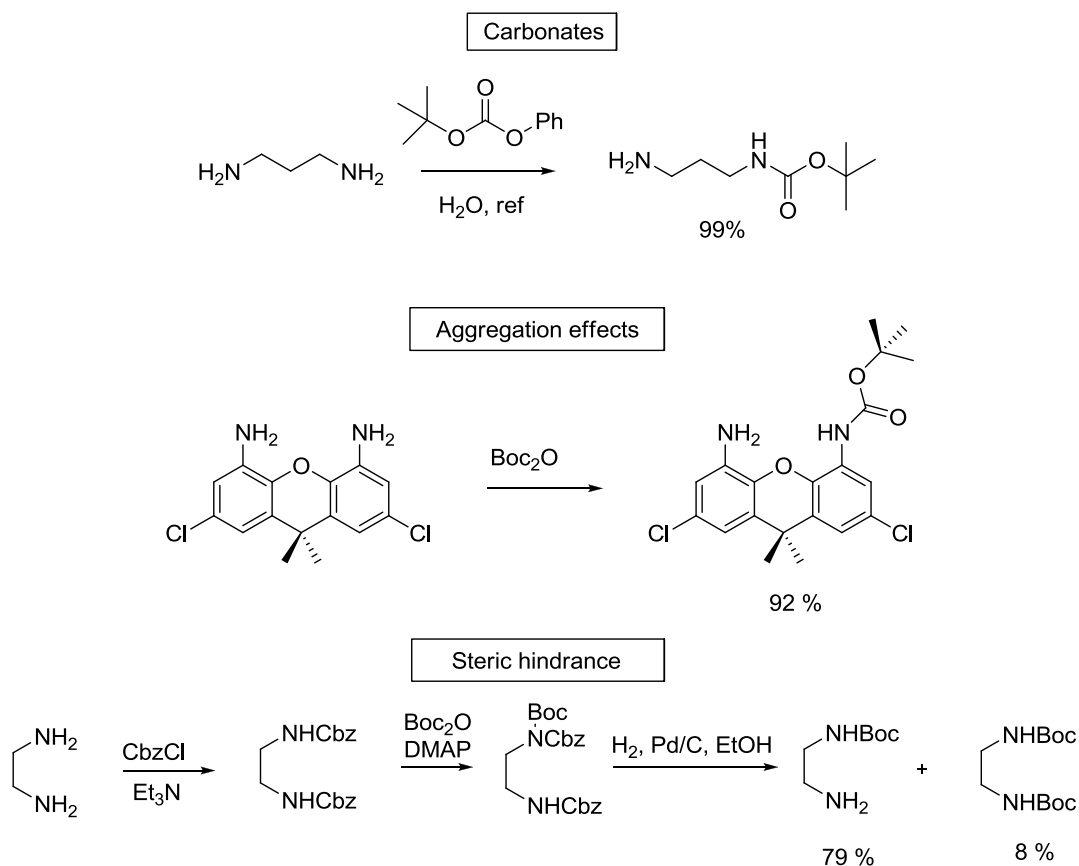


Figure 3.6. Different strategies used in diamine monoacylation.

The monoacylation of cyclohexanediamine can be achieved in several ways. Most of them are quite laborious and involve several steps of synthesis, so yields are usually not very good. For example, the proposed method by Kim¹⁰⁰ involves first protecting both amines with the benzyloxycarbonyl group, thereafter introducing a Boc group with Boc₂O in one of the amines and finally deprotection of the Cbz group by hydrogenolysis.

In this chapter we develop a faster and cheaper method to carry out the monofunctionalization of *trans*-1,2-cyclohexanediamines.

The procedure we have used is based on the reactivity exhibited by urea **39**, whose formation we discovered incidentally attempting to monofunctionalize *trans*-1,2-cyclohexanediamine with diphenylcarbonate, using the procedure described by Fang.⁹⁸

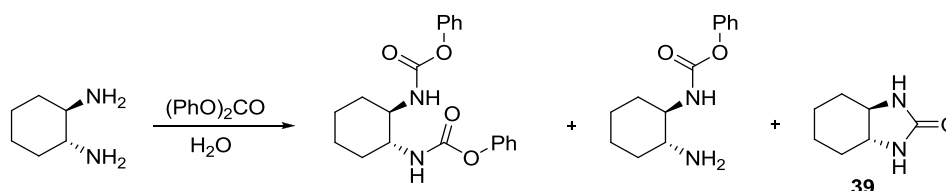


Figure 3.7. Urea **39** formation.

This cyclohexane urea has *trans* fused rings, and it is strained. We believe that, under appropriate conditions, it should be reactive towards nucleophiles,¹⁰¹ since there will be a release in the tension of the ring fusion. Thus, we found that we could open this urea in the presence of amines, alcohols and thiols, resulting ureas, carbamates and thiocarbamates, respectively.

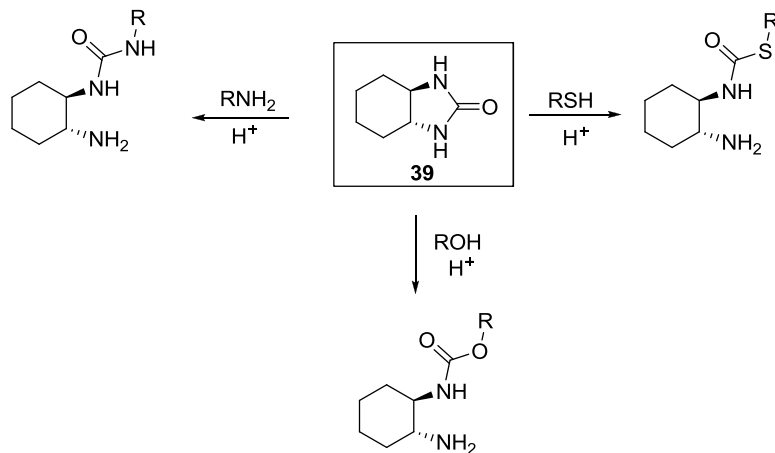


Figure 3.8. Reactivity against nucleophiles shown by urea **39**.

¹⁰¹ Hutchby, M.; Houlden, C. E.; Ford, J. G.; Tyler, S. N. G.; Gagné, M. R.; Lloyd-Jones, G. C.; Booker-Milburn, K. I. *Angew. Chem., Int. Ed.* **2009**, *48*, 8721-8724.

3.2. METHODS AND RESULTS

3.2.1. Preparation of urea **39**

In the literature there are several methods for the synthesis of cyclic urea **39** as shown in the following figure.

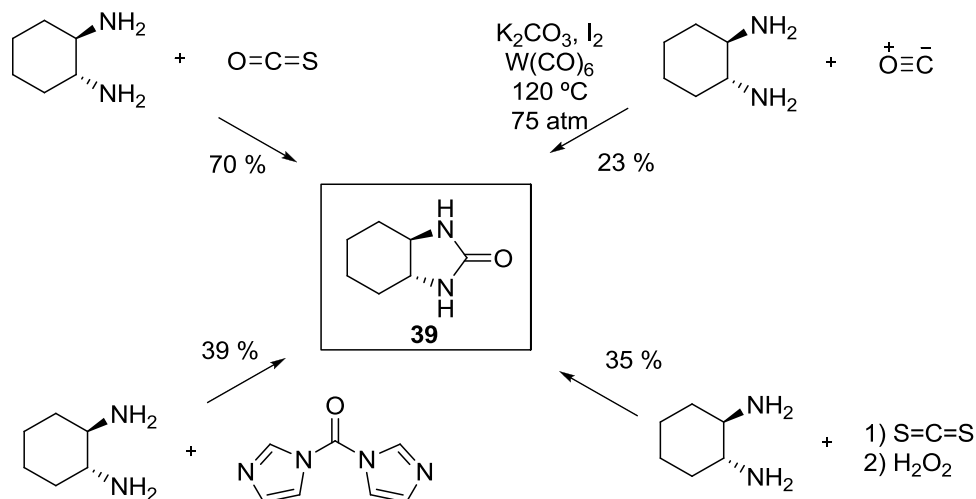


Figure 3.9. Existing methods in literature for the synthesis of urea **39**.

Although it would be expected that the most direct method would be the treatment of *trans*-1,2-cyclohexanediamine with phosgene or diethylcarbonate, these reagents result in the formation of polymers in organic solvents and the lack of reactivity in water. For urea **39** formation, it is necessary to resort to carbonyl sulphide,¹⁰² however, this gas is a toxic and expensive compound. Other attempts with carbon disulfide,¹⁰³ carbon monoxide¹⁰⁴ or carbonyldiimidazole¹⁰⁴ have generated lower yields.

In our case, we have developed a simpler alternative synthesis, with milder reaction conditions and higher yields using diphenylcarbonate, a cheap compound. The starting material is (*R,R*)-cyclohexanediamine-*L*-tartrate, which is the crystalline compound obtained in the chiral resolution of cyclohexanediamine racemic mixture with *L*-tartaric acid.¹⁰⁵

¹⁰² Davies, S. G.; Mortlock, A. A. *Tetrahedron* **1993**, *49*, 4419-4438.

¹⁰³ Apps, J. F. S.-L. *Synthesis and application of thiourea-S,S-dioxide derivatives*, Doctoral Thesis, University of Warwick, 2008.

¹⁰⁴ Zhang, Y.; Forinash, K.; Phillips, C. R.; McElwee-White, L. *Green Chem.* **2005**, *7*, 451-455.

¹⁰⁵ Schanz, H.-J.; Linseis, M. A.; Gilheany, D. G. *Tetrahedron: Asymmetry* **2003**, *14*, 2763-2769.

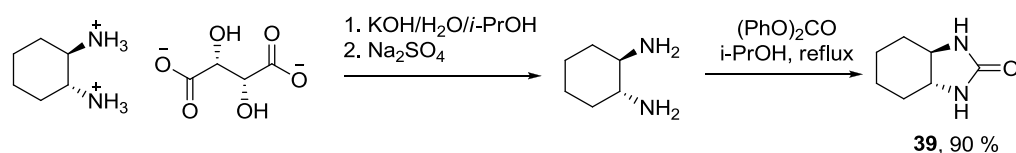


Figure 3.10. Preparation of urea **39** from (R,R)-1,2-cyclohexanediamine-L-tartrate and diphenylcarbonate.

Then we studied the opening reaction of this urea with amines, alcohols and thiols.

3.2.2. Ureas synthesis

As previously mentioned, amines are able to promote the opening of urea **39** in acid media. The acid is necessary to increase the electrophilicity of the urea carbonyl and make the ring opening easy. However, under these conditions only aromatic amines are able to produce the urea opening. Aliphatic amines, which are more basic, are almost fully protonated in the acid medium, and the concentration of free amine necessary to attack the urea is too small. In contrast, aromatic amines, being less basic, have a greater concentration of free amine in the equilibrium, so they are able to carry out the reaction. Thus, we studied the opening of urea **39** with several aromatic amines in the presence of methanesulfonic acid, generating the corresponding aminoureas (**40-44**).

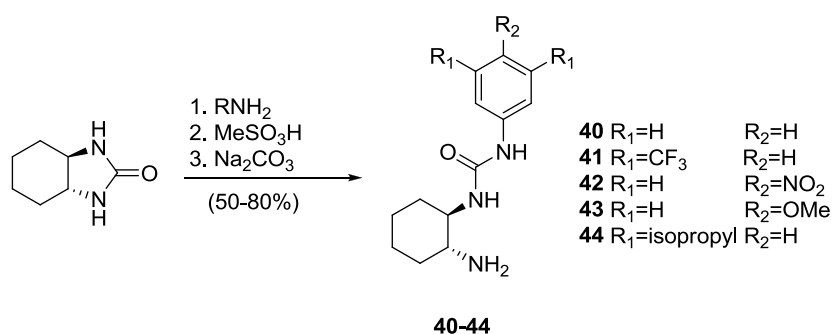


Figure 3.11. Preparation of ureas from (R,R)-1,2-cyclohexanediamine.

As can be seen in figure 3.11, the reaction is quite general for all types of anilines, including those with electron-withdrawing substituents (**41**, **42**), electron donors (**43**) and steric hindrance (**44**). We verified that the opening of the ring can also take place without methanesulfonic acid, using the appropriate aniline hydrochloride.

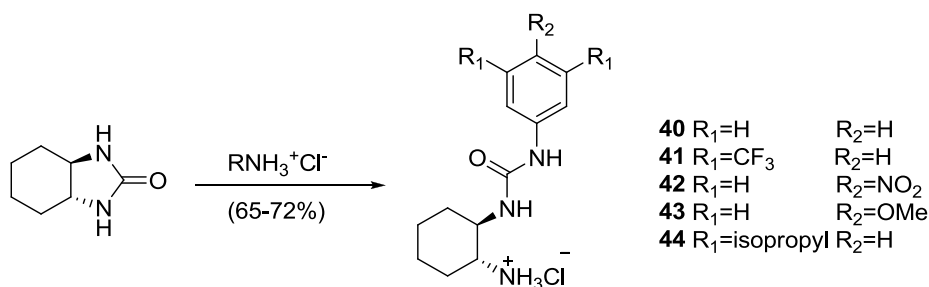


Figure 3.12. Preparation of ureas hydrochlorides from aniline hydrochlorides.

In this case, the reaction proceeds with acceptable yields and isolation of the corresponding ureas can be readily accomplished by precipitation of the urea hydrochloride adding ether or hexane.

3.2.3. Carbamoyl derivatives preparation

The opening of urea **39** with alcohols produces monocarbamates (figure 3.13). Compound **45** was obtained in the reaction between urea **39** and MeOH/HCl.

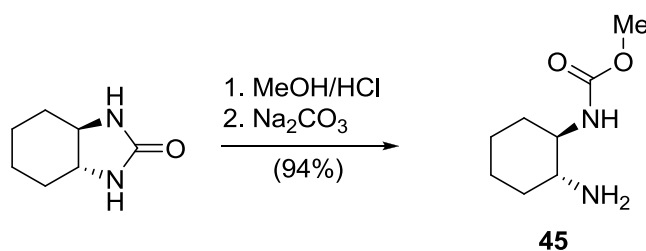


Figure 3.13. Preparation of monocarbamoyl derivatives by reaction with methanol and hydrogen chloride.

Methanesulfonic acid can also be used. Thus we performed the synthesis of carbamoylated derivatives **46** and **47** by mixing urea **39** with the corresponding alcohols.

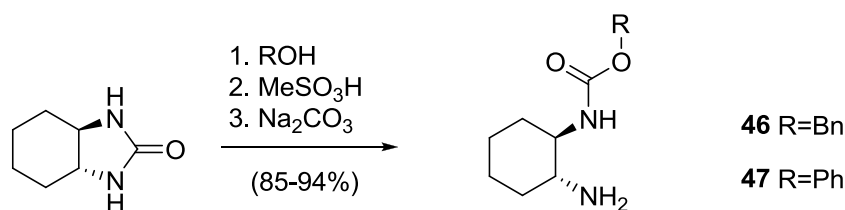


Figure 3.14. Preparation of other monocarbamoyl derivatives.

These carbamoylated derivatives can be used as precursors of monoamides and sulfonamide-based catalysts, acting the carbamoyl as a protecting group.

3.2.4. Thiocarbamoyl derivatives preparation

Under the same conditions, dodecanethiol is also able to promote the opening of urea **39** to generate the corresponding thiocarbamoyl derivative **48**.

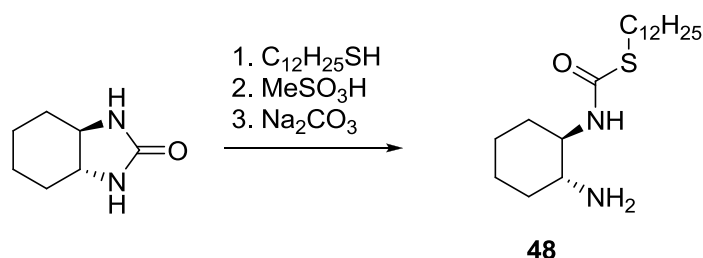


Figure 3.15. Monoprotection as the thiocarbamoyl derivative.

3.2.5. Sulfonamides preparation

As discussed above, the monocarbamoylated derivatives of (*R,R*)-1,2-cyclohexanediamine **45-47** can be used as precursors to synthesize other derivatives by incorporating other functional groups in the free amine group, then, hydrolysis of the carbamoyl group releases a free amine.

Thus, starting with compounds **45** or **46**, reaction with tosyl chloride yields compounds **49** and **50**, which then can be deprotected. Deprotection of both compounds under basic conditions generates sulfonamide **51**. This is a known organocatalyst used in literature.¹⁰⁶ In the case of compound **49**, deprotection can also be carried out by nucleophilic displacement.¹⁰⁷ Additionally, this derivative **49** provides the ability to generate the methylated organocatalyst **51**, by reduction of the carbamoyl group with LiAlH_4 . Compound **50** can also be deprotected under mild conditions by hydrogenolysis.

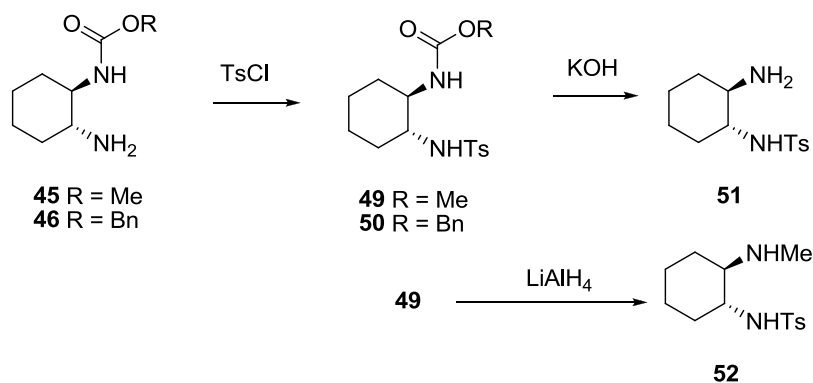


Figure 3.16. Carbamoylated derivatives transformed in sulfonamides.

¹⁰⁶ (a) Jiang, Z.-Y.; Yang, H.-M.; Ju, Y.-D.; Li, L.; Luo, M.-X.; Lai, G.-Q. Jiang, J.-X.; Xu, L.-W. *Molecules* **2010**, *15*, 2551-2563; (b) Lao, J.-H.; Zhang, X.-J.; Wang, J.-J.; Li, X.-M.; Yan, M.; Luo, H.-B. *Tetrahedron: Asymmetry* **2009**, *20*, 2818-2822; (c) Rasappan, R.; Reiser, O. *Eur. J. Org. Chem.* **2009**, 1305-1308.

¹⁰⁷ Elsinger, F.; Schreiber, J.; Eschenmoser, A. *Helv. Chim. Acta* **1960**, *43*, 113-118.

3.2.6. Direct preparation ("one-pot") of carbamate **47** from urea **39**

Once reactivity of urea **39** against different nucleophiles is known, we improved the synthesis of monocarbamoylated derivatives. Since in the preparation of urea **39** from (*R,R*)-1,2-cyclohexanediamine and diphenylcarbonate two equivalents of phenol are generated, we thought this phenol could be used *in situ* to produce the corresponding monocarbamoylated derivative. Indeed, after the urea **39** is formed, the addition of methanesulfonic acid to the reaction mixture promotes the ring opening of the urea and generates the carbamoylated derivative **47**. This compound is highly water soluble as methanesulphonic salt but crystallizes in good yield as the corresponding hydroiodide, after addition of potassium iodide. It is therefore possible to obtain the monocarbamoylated derivative directly from cyclohexanediamine in a practical, quickly and easy way, and with very good yield in a direct process ("one-pot") from the cyclohexanediamine tartrate (figure 3.17).

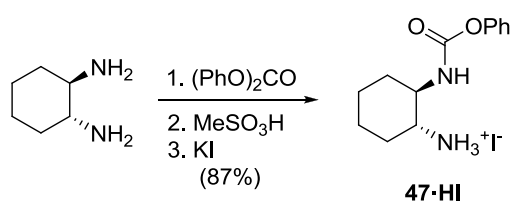


Figure 3.17. Direct synthesis ("one-pot") of carbamate **47**.

3.2.7. Preparation of other cyclohexanediamine derivatives from compound **47**

Starting now from carbamate **47**, it is possible to prepare the tosyl derivative **51**. By treatment with tosyl chloride and triethylamine in chloroform, tosylate **53** is originated. The phenylcarbamoyl group can be hydrolyzed under mild basic conditions resulting in the sulfonamide **51**.

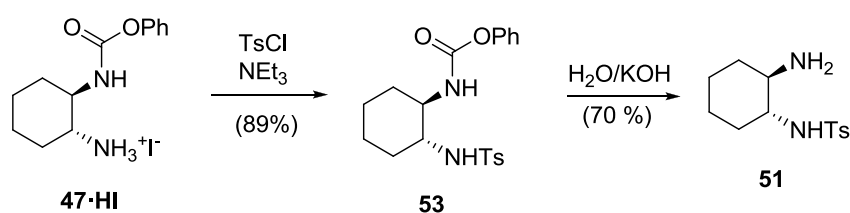


Figure 3.18. Preparation of sulfonamide **51** from carbamate **47**.

Similarly, intermediate **47** can also be benzoylated under the same conditions, generating compound **54**, which is hydrolyzed under basic conditions to yield amide **55**.

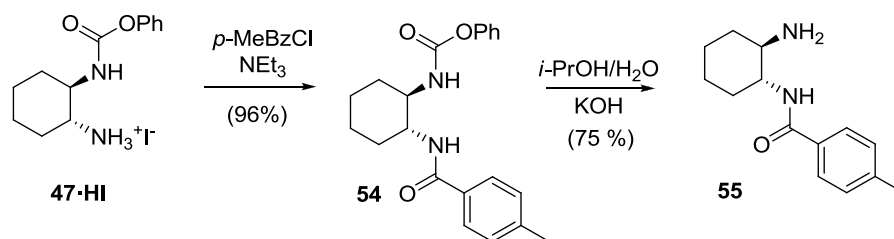


Figure 3.19. Preparation of amide **55** from carbamate **47**.

Many of the compounds synthesized so far from (*R,R*)-1,2-cyclohexanediamine, as compounds **40**, **41** and **51**, have been used directly as organocatalysts^{95c,f,106,108} or as fragments of these^{95p,109}.

In our case, to improve the properties of the (*R,R*)-1,2-cyclohexanediamine derivatives as organocatalysts, we synthesized a compound in which we incorporated a oxyanion-hole motif. Knowing the properties of isophthalic acid derivatives in the association of carbonyl groups,¹¹⁰ we decided to include the fragment **56** in compound **47**. Fragment **56** was prepared according to literature¹¹¹ as shown in figure 3.20. The acid chloride of isophthalic acid monoamide was synthesized and mixed with carbamate **47** prepared directly ("one-pot"). Deprotection of the carbamoyl group under basic conditions yielded directly the chiral amine **57**.

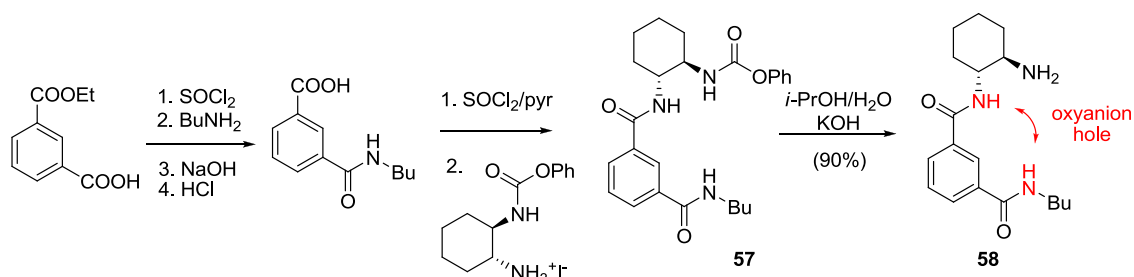


Figure 3.20. Synthesis of an organocatalyst with an oxyanion hole **57**.

¹⁰⁸ Lao, J.-H.; Zhang, X.-J.; Wang, J.-J.; Li, X.-M.; Yan, M.; Luo, H.-B. *Tetrahedron: Asymmetry* **2009**, *20*, 2818-2822.

¹⁰⁹ (a) Sarkar, D.; Harman, K.; Ghosh, S.; Headley, A. D. *Tetrahedron: Asymmetry* **2011**, *22*, 1051-1054; (b) Jiang, Z.-Y.; Yang, H.-M.; Ju, Y.-D.; Li, L.; Luo, M.-X.; Lai, G.-Q.; Jiang, J.-X.; Xu, L.-W. *Molecules* **2010**, *15*, 2551-2563.

¹¹⁰ (a) Dixon, R. P.; Geib, S. J.; Hamilton, A. D. *J. Am. Chem. Soc.* **1992**, *114*, 365-366; (b) Gale, P. A. *Coord. Chem. Rev.* **2003**, *240*, 191-221; (c) Muñiz, F. M.; Montero, V. A.; Fuentes de Arriba, Á. L.; Simón, L.; Raposo, C.; Morán, J. R. *Tetrahedron Lett.* **2008**, *49*, 5050-5052.

¹¹¹ Oliva, A. I.; Simón, L.; Muñiz, F. M.; Sanz, F.; Morán, J. R. *Tetrahedron* **2004**, *60*, 3755-3762.

3.2.8. Catalytic properties of the synthesized organocatalysts

In the literature there are many chiral amines derived from cyclohexanodiamine which have shown to be efficient catalysts for the aldol reaction.¹¹² However, in almost all of these articles the donor substrates used in the intermolecular aldol reaction are cyclic ketones, hydroxyketones or derivatives of pyruvic acid. There are only a few papers in which acetone is used as donor group.

So, we decided to try some of our catalysts in the intermolecular aldol reaction between acetone and 4-nitrobenzaldehyde. However, the reactions were very slow (even using the same molar amounts of catalyst and aldehyde) and generated very small enantiomeric excesses, as shown in table 3.2.

Table 3.2. Enantiomeric excesses (determined by HPLC) obtained with amines **51**, **52** and **55** (1 eq respect to the aldehyde) for the reaction between CD_3COCD_3 (as solvent, 13.6 M) and 4-nitrobenzaldehyde (0.5 M) at 20 °C.

entry	catalyst	ee (%)
1	51	1
2	52	11
3	52	3 ^a
4	52	17 ^b
5	55	4

^a In DMSO- d_6 as solvent.

^b In DMSO- d_6 as solvent and 0,2 M benzoic acid.

We observed that under these reaction conditions, nitrobenzaldehyde reacts rapidly with the primary amine of the catalyst generating an imine which is fairly stable under the reaction conditions (figure 3.21). This intermediate may explain the low yields and poor enantiomeric excesses (entries 1 and 5).

¹¹² (a) Raj, M.; Parashari, G. S.; Singh, V. K. *Adv. Synth. Catal.* **2009**, *351*, 1284-1288; (b) Nakayama, K.; Maruoka, K. *J. Am. Chem. Soc.* **2008**, *130*, 17666-17667; (c) Luo, S.; Xu, H.; Chen, L.; Cheng, J.-P. *Org. Lett.* **2008**, *10*, 1775-1778; (d) Luo, S. Z.; Xu, H.; Li, J. Y.; Zhang, L.; Cheng, J. P. *J. Am. Chem. Soc.* **2007**, *129*, 3074-3075; (e) Mei, K.; Zhang, S.; He, S.; Li, P.; Jin, M.; Xue, F.; Luo, G.; Zhang, H.; Song, L.; Duan, W.; Wang, W. *Tetrahedron Lett.* **2008**, *49*, 2681-2684; (f) Liu, J.; Yang, Z.; Wang, Z.; Wang, F.; Chen, X.; Liu, X.; Feng, X.; Su, Z.; Hu, C. *J. Am. Chem. Soc.* **2008**, *130*, 5654-5655.

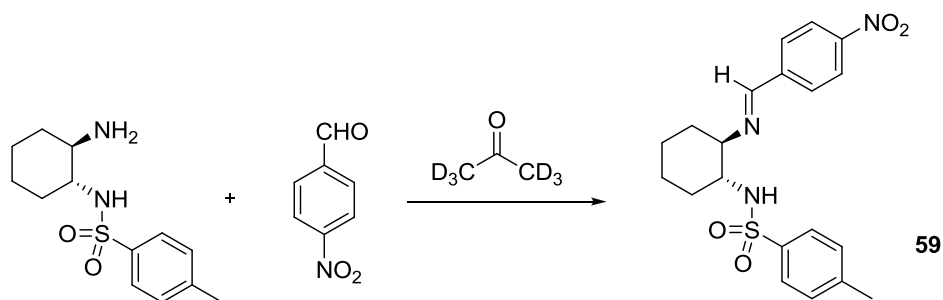


Figure 3.21. Formation of an imine between catalyst **51** and 4-nitrobenzaldehyde.

The use of a secondary amine in the catalyst would prevent the unwanted formation of imines. The use of catalyst **52**, which presents a methylated amine group, actually improves the enantiomeric excess (entry 2). This catalyst has a low solubility in the reaction medium, so DMSO- d_6 was used as the solvent. However, in this medium a reduction of the enantiomeric excess was produced, probably because DMSO is a better H-bond acceptor than acetone (entry 3). The addition of benzoic acid slightly improves the enantiomeric excess (entry 4).

The use of the catalyst with the secondary amine **52** solves the problem of imine formation but generates, in turn, imidazolidinones, in a similar manner as prolinamides did. The intermediate imidazolidinones hinder the progress of the reaction, rendering a poor catalytic process. We were able to obtain crystals of the imidazolidinone between catalyst **52** and nitrobenzaldehyde. These crystals allowed us to confirm the structure by X-ray diffraction (figure 3.22).

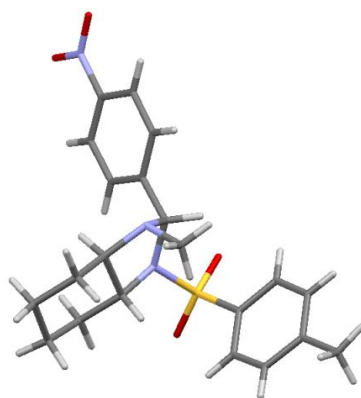
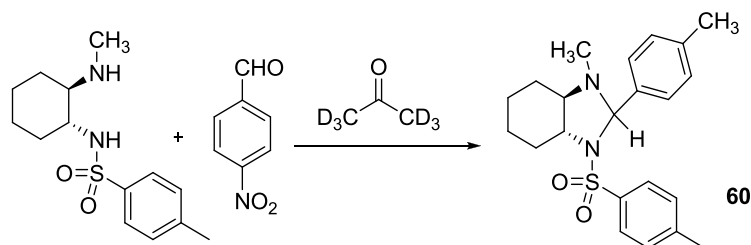


Figure 3.22. (Top) Formation of the imidazolidinone **60** from catalyst **52** and (bottom) X-ray structure of **60**.

Since the previous problems arise due to aldehyde reactivity, we seek a reaction that lacked this functional group. We studied the catalytic effect of amine **52** (21 mol %) in the addition of acetone (13.6 M) to nitrostyrene (0.6 M). Under these conditions, the reaction is completed in 3-4 days and an enantiomeric excess of 31 % is generated.

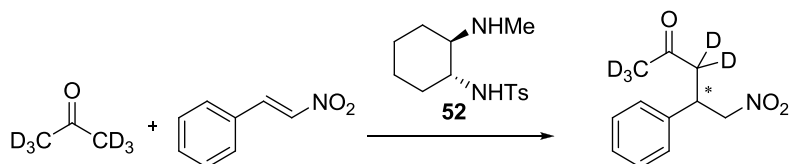
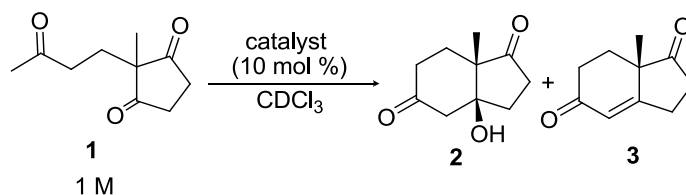


Figure 3.23: Reaction of acetone with nitrostyrene catalyzed by **52**.

Another alternative that we found attractive was to test the previous catalysts in the preparation of the Hajos-Wiechert and Wieland-Miescher ketones.¹¹³ We pretended to improve the results obtained in Chapter 1.

¹¹³ (a) Almasi, D.; Alonso, D. A.; Balaguer, A.-N.; Najera, C. *Adv. Synth. Catal.* **2009**, *351*, 1123-1131; (b) Almasi, D.; Alonso, D. A.; Najera, C. *Adv. Synth. Catal.* **2008**, *350*, 2467-2472; (c) Bradshaw, B.; Etxebarria-Jardi, G.; Bonjoch, J.; Viozquez, S. F.; Guillena, G.; Najera, C. *Adv. Synth. Catal.* **2009**, *351*, 2482-2490; (d) Davies, S. G.; Sheppard, R. L.; Smith, A. D.; Thomson, J. E. *Chem. Commun.* **2005**, 3802-3804; (e) Lacoste, E.; Vaique, E.; Berlande, M.; Pianet, I.; Vincent, J.-M.; Landais, Y. *Eur. J. Org. Chem.* **2007**, 167-177; (f) He, L. *Hecheng Huaxue (Chin. J. Synth. Chem.)* **2007**, *15*, 231-232; (g) Akahane, Y.; Inage, N.; Nagamine, T.; Inomata, K.; Endo, Y. *Heterocycles* **2007**, *74*, 637-648; (h) Akahane, Y.; Inomata, K.; Endo, Y. *Heterocycles* **2009**, *77*, 1065-1078; (i) D'Elia, V.; Zwicknagl, H.; Reiser, O. *J. Org. Chem.* **2008**, *73*, 3262-3265; (j) Guillena, G.; Hita, M. d. C.; Najera, C.; Viozquez, S. F. *J. Org. Chem.* **2008**, *73*, 5933-5943; (k) Kanger, T.; Kriis, K.; Laars, M.; Kailas, T.; Muurisepp, A.-M.; Pehk, T.; Lopp, M. *J. Org. Chem.* **2007**, *72*, 5168-5173; (l) Davies, S. G.; Russell, A. J.; Sheppard, R. L.; Smith, A. D.; Thomson, J. E. *Org. Biomol. Chem.* **2007**, *5*, 3190-3200; (m) Guillena, G.; Najera, C.; Viozquez, S. F. *Synlett* **2008**, *19*, 3031-3035; (n) Kriis, K.; Kanger, T.; Laars, M.; Kailas, T.; Muurisepp, A.-M.; Pehk, T.; Lopp, M. *Synlett* **2006**, *11*, 1699-1702; (o) Nozawa, M.; Akita, T.; Hoshi, T.; Suzuki, T.; Hagiwara, H. *Synlett* **2007**, *4*, 661-663; (p) Zhang, X.-M.; Wang, M.; Tu, Y.-Q.; Fan, C.-A.; Jiang, Y.-J.; Zhang, S.-Y.; Zhang, F.-M. *Synlett* **2008**, *18*, 2831-2835; (q) Agami, C.; Meynier, F.; Puchot, C.; Guilhem, J.; Pascard, C. *Tetrahedron* **1984**, *40*, 1031-1038; (r) Bui, T.; Barbas, C. F. *Tetrahedron Lett.* **2000**, *41*, 6951-6954.

Table 3.3. Results obtained in the preparation of the Hajos-Wiechert ketone in CDCl_3 at 20 °C, 1.0 M concentration of ketone **1** and 10 mol % catalyst.



entry	catalyst	conversion (%)			time (h)	ee (%)
		aldol 2	ketone 3	total		
1	41	47	49	96	46	96
2	42	49	46	95	123	96
3	46	69	12	81	123	82
4	51	9	3	12	284	82
5	52	22	3	25	120	70
6	55	23	73	96	123	84
7	58	73	20	93	94	91

As seen in table 3.3, ureas **41** and **42** substituted with electron withdrawing groups, showed very good results in the preparation of the Hajos-Wiechert ketone (entries 1 and 2), generating 96 % enantiomeric excess. Carbamate **46** is less enantioselective, probably due to the lack of the second NH (entry 3). Regarding tosylamide **51**, it produced a similar enantiomeric excess than catalyst **46**, although the reaction rate was considerably reduced (entry 4). Tosylamide **52**, which has a secondary amine, rendered an even smaller enantiomeric excess, although the reaction rate was doubled with respect to the primary tosylamide (entry 5). The results improved with amide **55** (entry 6), reaching values similar to carbamate **46** (entry 7). With catalyst **56**, which simulates the oxyanion hole of enzymes, the enantiomeric excess exceeded 90 % (entry 7), although the results were not as good as in the case of urea **41**.

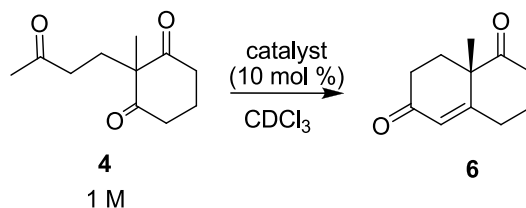
These results suggest that the second NH of ureas is important to improve the enantiomeric excess, since the catalysts **46**, **51**, **52** and **55**, which only have one NH, do not exceed 84 % ee. Also, the place of the second NH in the molecule seems to be important, since catalyst **56** derived from isophthalic acid only improves enantiomeric excess from 84 to 91 % in comparison with the catalyst without the oxyanion hole, while ureas **41** and **42** achieves a 96 % enantiomeric excess.

Regarding the reaction rate, it seems that it is also convenient the presence of the urea in the catalyst, although some simple catalysts such as **46** and **55** generate reaction rates similar

to those of the urea derivative **42** or isophthalic acid derivative **58**. Anyway, the catalyst that provides the best results in terms of reaction rate and enantioselectivity is urea **41**.

We also tested the above catalysts in the cyclization reaction leading to the Wieland-Miescher ketone. In this case, ketone **6** was isolated with a silica gel column. Results are summarized in table 3.4.

Table 3.4. Results obtained in the reaction for obtaining the Wieland-Miescher ketone in CDCl_3 at 20°C , 1.0 M concentration of ketone **4** and 10 mol % catalyst.



entry	catalyst	conversion (%)	yield (%)	time (h)	ee (%)
1	40^d	95	76	22	85
2	41	94	82	30	89
3	42	81	63	117	75
4	46	76	59	117	65
5	51	3	n.d.	161	61
6	52	24	n.d.	161	-11
7	55	94	77	44	91
8	58^d	100	85	16	95

^d2,0 M concentration of ketone **4** and 10 mol % catalyst.

In the case of the Wieland-Miescher ketone, ureas **40-42** were found to be good organocatalysts for this reaction, showing enantiomeric excesses between 75 and 89 % and short reaction times (entries 1-3). It can be observed a slight increase in the enantiomeric excess when the acidity of the second urea NH increases, thanks to two CF_3 groups in the catalyst. In the case of carbamoylated derivative **46**, enantioselectivity and yield were reduced compared with previous ureas (entry 4), showing the importance of the second NH to achieve good results. Sulfonamide **51**, which also lacks the second NH, produced an enantiomeric excess similar to the carbamoylated derivative **46**, but reaction rate decreased sharply (entry 5). To study the influence of a secondary amine in conversion and enantioselectivity we conducted a reaction with sulfonamide **52**, which has a methyl group in the amine. Surprisingly, this catalyst showed lower enantioselectivity and yielded the opposite enantiomer (entry 6). Fortunately, amide **55** produced an enantiomeric excess of 91 % (entry 7) despite the lack of the second NH as ureas **40-42**. In this case the best results in terms of

enantiomeric excess (95 %) was obtained with the isophthalic acid derivative **58**, which has a geometry that simulates the oxyanion hole of enzymes. In addition, a complete conversion in only 16 hours working at 2.0 M concentration of ketone **4** (entry 8) was achieved.

The good results obtained with catalyst **58** in the obtention of the Wieland-Miescher ketone is encouraging, since this process often shows worse enantioselectivities than the Hajos-Wiechert ketone, for which it has been easier to find suitable organocatalysts. Moreover, these results show the great importance of the exact geometry of the hydrogen bond donor in the catalyst.

3.3. CONCLUSIONS

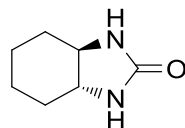
This chapter has presented a new synthetic procedure for monofunctionalization of *trans*-1,2-cyclohexanediamine derivatives, which have been widely used as organocatalysts in the literature.

This method is based on the high reactivity of the cyclic urea of *trans*-1,2-cyclohexanediamine against several nucleophiles, such as amines, alcohols or thiols. This has led to ureas as well as carbamoylated and thiocarbamoylated derivatives.

Some of these compounds have been used as organocatalysts for different reactions, showing the best results in the intramolecular aldol reaction for the preparation of the Hajos-Wiechert ketone (with enantiomeric excesses up to 96 %) and Wieland-Miescher ketone (95 % ee). Specifically, a catalyst that combines the skeleton of *trans*-1,2-cyclohexanediamine with the presence of an oxyanion hole has been quite promising. In this structure the possible existence of an intramolecular hydrogen bond between the amide NH and the basic nitrogen is avoided. This H-bond exists in the prolinamides summarized in Chapter 1, yielding slower reactions.

3.4. EXPERIMENTAL

- (3*aR*,7*aR*)-hexahydro-1*H*-benzo[*d*]imidazol-2(3*H*)-one (39)



Enantiopure (*R,R*)-cyclohexanediamine tartrate salt was readily obtained starting from the racemic *trans*-cyclohexane-1,2-diamine and *L*-tartaric acid.¹¹⁴ This tartrate salt (40.0 g, 150.8 mmol) and KOH (17.0 g, 303.6 mmol) were dissolved in H₂O (30 mL) to generate the free diamine. The reaction mixture was heated until all solid had been dissolved. Then, 2-propanol (100 mL) was added, and the solution was stirred and cooled (ice bath) to yield a potassium tartrate precipitate. To complete the precipitation and remove water, powdered sodium sulfate (40.0 g) was added and the precipitate was filtered off. The solid was washed with more 2-propanol (2 x 20 mL), diphenylcarbonate (35.0 g, 163 mmol) was added to the filtrate, and the mixture was refluxed for 30 min. Steam distillation and water evaporation allowed us to obtain a crude urea which could be further purified by recrystallization from EtOH/H₂O (1:1) to yield 18.8 g (90% yield) of a compound with the same physical properties as those described in literature.¹¹⁵

- General procedure for the preparation of monoureas (40-44) with methanesulfonic acid (Procedure A).

To a mixture of urea **39** (2.2 mmol) and the aromatic amine (2.2 mmol) in diglyme (2 mL) methanesulfonic acid (0.15 mL) was added, and the reaction mixture was heated at 120 °C for 1 h with stirring under argon atmosphere. Then the mixture was cooled to room temperature, H₂O (10 mL) and Na₂CO₃ (2.0 g, 19 mmol) were added and the crystalline solid which precipitated was filtered to afford the desired compound. If the urea did not crystallize spontaneously, diethyl ether (2 mL) was added to assist the precipitation. This procedure can be scale up to 15 mmol.

- General procedure for the preparation of monoureas (40-44) starting from the hydrochloride salts of these amines (Procedure B).

Urea **39** (3.5 mmol) and the amine hydrochloride (3.5 mmol) were heated in diglyme (2 mL) at 120 °C. Then, the mixture was heated for 1 h, and a solid precipitated from the reaction medium. ¹H NMR analysis of an aliquot confirmed the reaction had finished. The mixture was

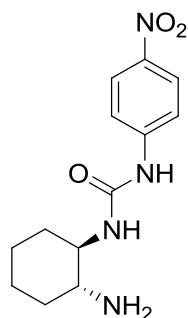
¹¹⁴ Schanz, H.-J.; Linseis, M. A.; Gilheany, D. G. *Tetrahedron: Asymmetry* **2003**, *14*, 2763-2369.

¹¹⁵ Davies, S. G.; Mortlock, A. A. *Tetrahedron* **1993**, *49*, 4419-4438.

cooled to room temperature, and diethyl ether (10 mL) was added. The solid was filtered and dried under vacuum (0.1 mmHg) heating at 90 °C to remove completely the traces of diglyme, affording the monoureas as their hydrochloride salts. This procedure has been carried out on a 1-5 mmol scale.

- The physical and spectroscopic properties of ureas **40**,¹¹⁶ **41**¹¹⁷ and **43**¹¹⁴ are in agreement with the properties described in the literature.

- **(1R,2R)-1,2-diaminocyclohexane 4-nitrophenylurea (42)**



Yellow solid; yield: 80 % (procedure A).

$[\alpha]_D^{20} = -13.3$ ($c = 0.4$, MeOH).

mp: 203-205 °C.

¹H NMR (CDCl₃-CD₃OD) δ (ppm): 1.23-1.05 (m, 4H), 1.67-1.63 (m, 2H), 1.91-1.87 (m, 2H), 2.30 (m, 1H), 3.28 (m, 1H), 7.45 (d, $J = 10$ Hz, 2H), 8.03 (d, $J = 10$ Hz, 2H).

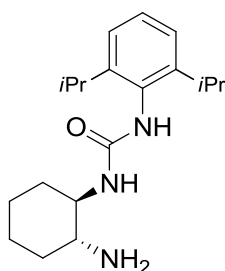
¹³C NMR (CDCl₃-CD₃OD) δ (ppm): 24.6 (CH₂), 24.8 (CH₂), 32.6 (CH₂), 34.4 (CH₂), 54.9 (CH), 55.5 (CH), 117.1 (CH x 2), 124.9 (CH x 2), 141.4 (C), 146.2 (C), 155.3 (C).

IR (nujol, cm⁻¹): 3325, 1670, 1592, 1456, 1333.

HRMS (ESI): 279,1446 (M + H)⁺, calcd for C₁₃H₁₉N₄O₃ 279,1452.

¹¹⁶ Bied, C.; Moreau, J. J. E.; Wong Chi Man, M. *Tetrahedron: Asymmetry* **2001**, *12*, 329-336.

¹¹⁷ Sohtome, Y.; Tanatani, A.; Hashimoto, Y.; Nagasawa, K. *Chem. Pharm. Bull.* **2004**, *52*, 477-480.

- (1*R*,2*R*)-1,2-diaminocyclohexane 2,6-diisopropylphenylurea (**44**)

White solid; yield: 64 % (procedure B).

$[\alpha]_D^{20} = -23.9$ ($c = 14.2$, CHCl_3).

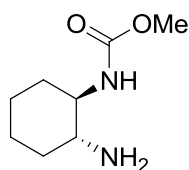
mp: the substance sublimes without melting.

$^1\text{H NMR}$ (CDCl_3) δ (ppm): 0.83-1.06 (m, 3H), 1.06-1.31 (m, 12H), 1.57-1.73 (m, 2H), 1.81-1.98 (m, 2H), 2.07-2.24 (m, 1H), 3.17-3.49 (m, 3H), 3.98 (d, $J = 9.8$ Hz, 1H), 7.18-7.40 (m, 3H).

$^{13}\text{C NMR}$ (CDCl_3) δ (ppm): 23.5 ($\text{CH}_3 \times 2$), 24.6 ($\text{CH}_3 \times 2$), 25.3 (CH_2), 25.5 (CH_2), 28.6 ($\text{CH} \times 2$), 33.3 (CH_2), 35.0 (CH_2), 56.1 (CH), 57.4 (CH), 124.4 ($\text{CH} \times 2$), 129.3 (CH), 130.9 (C), 148.2 ($\text{C} \times 2$), 158.1 (C).

IR (nujol, cm^{-1}): 3338, 3247, 2936, 1638, 1560, 1456.

HRMS (ESI): 318,2179 ($\text{M} + \text{H}^+$), calcd for $\text{C}_{19}\text{H}_{32}\text{N}_3\text{O}$ 318,2540.

- Methyl (1*R*,2*R*)-2-aminocyclohexylcarbamate (**45**)

Urea **39** (4 g, 28 mmol) and SOCl_2 (1 mL) were dissolved in 50 mL of methanol and the reaction mixture was heated at 60-70 °C for an hour and allowed to stand overnight at room temperature. Then the solution was concentrated under reduced pressure to afford 5.6 g (94 % yield) of the hydrochloride salt of compound **45**, from which the free amine was liberated by treatment with saturated aqueous Na_2CO_3 and extraction with ethyl acetate.

$[\alpha]_D^{20} = -30.8$ ($c = 0.5$, CHCl_3).

mp: 87-89 °C.

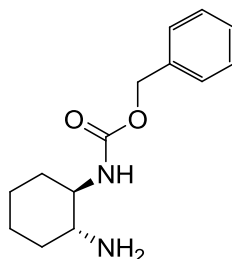
$^1\text{H NMR}$ (CDCl_3) δ (ppm): 1.02-1.27 (m, 4H), 1.45-1.65 (m, 2H), 1.87-1.91 (m, 2H), 2.24-2.36 (m, 1H), 3.07-3.12 (m, 1H), 3.59 (s, 3H), 5.10 (d, $J = 8.2$ Hz, 1H).

$^{13}\text{C NMR}$ (CDCl_3) δ (ppm): 25.2 (CH_2), 25.3 (CH_2), 33.0 (CH_2), 35.4 (CH_2), 52.2 (CH_3), 55.4 (CH), 58.3 (CH), 157.5 (C).

IR (nujol, cm^{-1}): 3370, 1703, 1599, 1462.

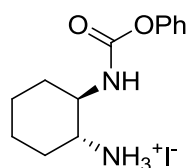
HRMS (ESI): 173.1292 ($\text{M} + \text{H}^+$), calcd for $\text{C}_8\text{H}_{17}\text{N}_2\text{O}_2$ 173.1285.

- **Benzyl (1*R*,2*R*)-2-aminocyclohexylcarbamate (46)**



To a mixture of urea **39** (1.0 g, 7.1 mmol) and benzyl alcohol (1.0 g, 9.2 mmol), methanesulfonic acid (0.7 g, 7.2 mmol) was added and the reaction was heated at 80 °C for ten minutes. After cooling to room temperature, water (50 mL) and diethyl ether (50 mL) were added and the layers were separated. The aqueous layer was treated with Na_2CO_3 (2.0 g, 18 mmol) and the precipitate obtained was filtered to afford 1.5 g (85 % yield) of the desired compound **46**, whose physical properties are in agreement with those published.¹¹⁸

- **Phenyl (1*R*,2*R*)-2-aminocyclohexylcarbamate (47)**



Initially, (*R,R*)-cyclohexane-1,2-diamine tartrate salt (10.0 g, 37.9 mmol) was reacted under the same conditions described for the preparation of urea **39**. Then the mixture was refluxed with diphenylcarbonate (8.1 g, 37.9 mmol) in 2-propanol, the solvent was evaporated under reduced pressure and the crude residue was dried through azeotropic distillation with benzene (100 mL). To this mixture of phenol and the urea **39** was added 1 equiv. of methanesulfonic acid (2.5 mL), and the reaction was heated at 110 °C with stirring for 1 h under Argon atmosphere. Then the solution was cooled, water (30 mL) was added and phenol was extracted with ethyl acetate (2-30 mL). To the aqueous layer, cooled to 0 °C, was added KI

¹¹⁸ Minarini, A.; Marucci, G.; Bellucci, C.; Giorgi, G.; Tumiatti, V.; Bolognesi, M. L.; Matera, R.; Rosini, M.; Melchiorre, C. *Bioorg. Med. Chem.* **2008**, *16*, 7311.

(7.0 g, 42 mmol) and a precipitate of the hydroiodide salt of compound **47** (12 g, 87 % yield) was obtained.

$[\alpha]_D^{20} = -6.3$ ($c = 0.6$, MeOH).

mp: 187-189 °C.

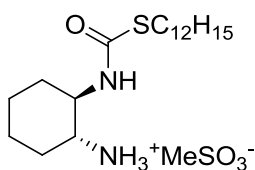
$^1\text{H NMR}$ ($\text{CDCl}_3\text{-CD}_3\text{OD}$) δ (ppm): 1.16-1.30 (m, 4H), 1.55-1.65 (m, 2H), 1.84-1.94 (m, 2H), 3.03 (m, 1H), 3.38 (m, 1H), 6.97-7.06 (m, 3H), 7.15-7.22 (m, 2H).

$^{13}\text{C NMR}$ ($\text{CDCl}_3\text{-CD}_3\text{OD}$) δ (ppm): 23.7 (CH_2), 24.4 (CH_2), 29.9 (CH_2), 31.7 (CH_2), 53.1 (CH), 54.6 (CH), 121.8 ($\text{CH} \times 2$), 125.6 (CH), 129.3 ($\text{CH} \times 2$), 150.9 (C), 155.9 (C).

IR (nujol, cm^{-1}): 3565, 3318, 1729, 1599, 1462.

HRMS (ESI): 235.1441 ($\text{M} + \text{H}^+$), calcd for $\text{C}_{13}\text{H}_{19}\text{N}_2\text{O}_2$ 235.1441.

- S-dodecyl (1R,2R)-2-aminocyclohexylcarbamothioate (48)



Urea **39** (200 mg, 1.4 mmol), dodecanthiol (1 mL, 4.2 mmol) and methanesulfonic acid (0.1 mL) were heated at 110 °C. After heating at about one hour, $^1\text{H NMR}$ analysis of an aliquot confirmed that the reaction had finished. The crude residue was purified by column chromatography with mixtures $\text{CH}_2\text{Cl}_2/\text{MeOH}$ of increasing polarity to afford 550 mg (68 %) of the compound **48** as its methanesulfonate salt.

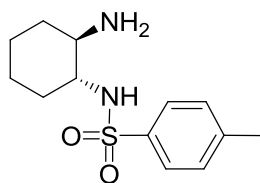
$[\alpha]_D^{20} = -6.1$ ($c = 0.7$, MeOH).

$^1\text{H NMR}$ (CD_3OD) δ (ppm): 0.88 (t, $J = 6.2$ Hz, 3H), 1.28 (m, 24H), 1.56-1.70 (m, 2H), 1.80 (m, 2H), 2.73 (s, 3H), 2.86 (m, 2H), 3.05 (m, 1H), 3.31 (m, 1H).

$^{13}\text{C NMR}$ (CD_3OD) δ (ppm): 13.4 (CH_3), 22.6 (CH_2), 23.7 (CH_2), 24.4 (CH_2), 28.7 (CH_2), 29.1 (CH_2), 29.3 (CH_2), 29.4 (CH_2), 29.5 (CH_2), 29.6 (CH_2), 29.9 ($\text{CH}_2 \times 3$), 30.4 (CH_2), 31.6 (CH_2), 31.9 (CH_2), 38.5 (CH_3), 52.9 (CH), 54.4 (CH), 169.6 (C).

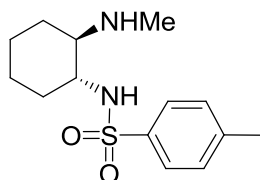
IR (nujol, cm^{-1}): 3353, 1664, 1458, 1367, 1207, 1035.

HRMS (ESI): 343.2781 ($\text{M} + \text{H}^+$), calcd for $\text{C}_{19}\text{H}_{39}\text{N}_2\text{OS}$ 343.2778.

- N-((1R,2R)-2-aminocyclohexyl)-4-methylbenzenesulfonamide (51)

To a solution of **47**·HI (1.1 g, 3.0 mmol) in CHCl₃ (30 mL), tosyl chloride (0.7 g, 3.8 mmol) and triethylamine (0.8 mL) were added. The mixture was stirred at room temperature for 4 hours and the progress of the reaction could be monitored by TLC. Pyridine (1 mL) and water (10 mL) were then added to destroy the TsCl excess. Washing with 2 M HCl, and evaporation of the organic solvent yielded sulfonamide **15** (1.04 g, 89 %) which was used without further purification in the next step.

To a solution of KOH (0.4 g, 7.1 mmol) in 10 mL H₂O compound **53** (0.1 g, 0.30 mmol) was added. The reaction mixture was heated under reflux for 20 minutes, cooled down to room temperature and acidified with 12 M HCl. Then, phenol was removed by steam distillation and the remaining solution was washed with CHCl₃. The two phases were separated and to the aqueous layer Na₂CO₃ was added until basic pH. The basic solution was extracted with EtOAc (2 × 10 mL) and the solvent evaporated under reduced pressure to yield 0.06 g (70 % yield) of the desired compound **51**, whose physical and spectroscopic properties are in agreement with those published.¹¹⁹

- 4-Methyl-N-((1R,2R)-2-(methylamino)cyclohexyl)benzenesulfonamide (52)

To a solution of the hydrochloride salt of compound **45** (1.0 g, 4.8 mmol) in a mixture 1:1 EtOAc/saturated aqueous Na₂CO₃ (4 mL each), tosyl chloride (0.95 g, 5 mmol) was added. The mixture was stirred at room temperature for 30 minutes and the progress of the reaction was monitored by TLC. Once the reaction had finished more EtOAc (10 mL) and water (10 mL) were added and the organic layer was dried over sodium sulphate and evaporated to give **49** (1.5 g, 89 % yield), which was used in the next step without further purification.

To a suspension of LiAlH₄ (0.2 g, 5.3 mmol) in dry THF (5 mL) in a two-necked flask equipped with a reflux condenser and under atmosphere of argon, sulfonamide **49** (0.4 g, 1.2 mmol) was added. The reaction mixture was heated under reflux to complete the reaction. After cooling to room temperature, the excess of LiAlH₄ was destroyed by careful addition of wet THF and then aqueous Na₂CO₃ (5 mL) was added. The solvent was removed under vacuum and the

¹¹⁹ Balsells, J.; Mejorado, L.; Phillips, M.; Ortega, F.; Aguirre, G.; Somanathan, R.; Walsh, P. J. *Tetrahedron: Asymmetry* **1998**, *9*, 4135-4142.

remaining salts were extracted twice with EtOAc (2 × 15 mL) to afford finally 260 mg (80 % yield) of the target compound **52** as a yellow solid.

$[\alpha]_D^{20} = -58.7$ ($c = 3.5$, CHCl_3).

mp: 99-101 °C.

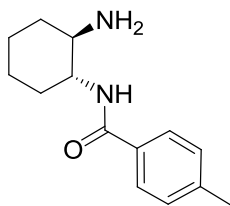
$^1\text{H NMR}$ (CDCl_3) δ (ppm): 0.80-1.28 (m, 4H), 1.46-1.74 (m, 2H), 1.84-2.20 (m, 3H), 2.24 (s, 3H), 2.39 (s, 3H), 2.55-2.75 (m, 1H), 3.44 (s ancho, 1H), 7.26 (d, $J = 8.1$ Hz, 2H), 7.74 (d, $J = 8.4$ Hz, 2H).

$^{13}\text{C NMR}$ (CDCl_3) δ (ppm): 21.4 (CH_3), 24.4 (CH_2), 24.4 (CH_2), 30.1 (CH_2), 32.3 (CH_2), 32.4 (CH_3), 56.9 (CH), 61.7 (CH), 127.1 (CH x 2), 129.5 (CH x 2), 137.4 (C); 143.1 (C).

IR (nujol, cm^{-1}): 3286, 2929, 2858, 1599, 1450, 1327, 1165, 1106.

HRMS (ESI): 283.1478 ($\text{M} + \text{H}$)⁺, calcd for $\text{C}_{14}\text{H}_{23}\text{N}_2\text{O}_2\text{S}$ 283.1475.

- *N*-((1*R*,2*R*)-2-aminocyclohexyl)-4-methylbenzamide (**55**)

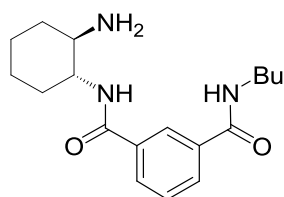


To a solution of **47**·HI (1.2 g, 3.2 mmol) in CHCl_3 (30 mL), toluoyl chloride (0.5 g, 3.5 mmol) and triethylamine (0.8 mL) were added. The mixture was stirred at room temperature and the progress of the reaction could be monitored by TLC. Pyridine (1 mL) and water (10 mL) were then added to destroy the toluoyl chloride excess. Washing with 2 M HCl and evaporation of the organic solvent yielded amide **16** (1.1 g, 96 %) which was used without further purification in the next step.

To a solution of KOH (1.0 g, 17.8 mmol) in 10 mL H_2O /100 mL of isopropanol, compound **54** (1.0 g, 2.7 mmol) was added. The reaction mixture was stirred at room temperature and TLC monitoring showed that the hydrolysis took place in a few minutes (about 10 minutes). Then, the reaction mixture was acidified with 2 M HCl and the phenol was removed by steam distillation.

The remaining solution was treated with aqueous Na_2CO_3 until basic pH and extracted with EtOAc to yield 0.47 g (75 %) of the desired compound **55**, whose physical and spectroscopic properties are in agreement with those published.¹²⁰

¹²⁰ Wenjing, X.; Jiarong, C.; Haihua, L.; Xinyong, L., CN 1740152 A20060301, 2006.

- N^1 -((1*R*,2*R*)-2-aminocyclohexyl)- N^3 -butylisophthalamide (58)

The isophthalic acid monobutyl amide¹²¹ (0.87 g, 3.9 mmol) was dissolved in thionyl chloride (5 mL) and refluxed until no more hydrogen chloride was evolved. Then, the solvent was evaporated under reduced pressure. The crude acid chloride was dissolved in EtOAc (5 mL) and then was poured into a saturated Na₂CO₃ solution (10 mL) containing crushed ice with stirring. Next, compound **47**·HI (1.1 g, 3.9 mmol) in ethyl acetate (10 mL) was added. The progress of the reaction could be monitored by TLC. After separation of the layers and evaporation of the organic solvent, the crude residue was purified by chromatography (CH₂Cl₂/EtOAc, 8:2) to afford 1.2 g (72 %) of the intermediate carbamoyl derivative which was used in the next step without further purification.

To a solution of KOH (1.0 g, 17.8 mmol) in 10 mL H₂O/100 mL of isopropanol, the intermediate carbamoyl derivative (1.0 g, 2.2 mmol) was added. The reaction mixture was stirred at room temperature and TLC monitoring showed that the hydrolysis took place in a few minutes (about 10 minutes). Then, the reaction mixture was acidified with 2 M HCl and phenol was removed by steam distillation. The remaining solution was treated with aqueous Na₂CO₃ until basic pH and extracted with EtOAc. The crude product was purified by chromatography (methanol as eluent) to afford 0.6 g (90 % yield) of the desired compound **58**.

$[\alpha]_D^{20} = -28.0$ ($c = 0.5$, CHCl₃).

mp: 65 °C.

¹H NMR (CDCl₃) δ (ppm): 0.93 (t, 3H), 1.23-1.56 (m, 6H), 1.60-1.74 (m, 4H), 1.94-2.20 (m, 2H), 2.56 (m, 1H), 3.39-3.48 (m, 2H), 3.69 (m, 1H), 6.70 (t ancho, NH), 6.88 (d, $J = 7.8$ Hz, NH), 7.45 (t, $J = 7.7$ Hz, 1H), 7.88-7.93 (m, 2H), 8.23 (s, 1H).

¹³C NMR (CDCl₃) δ (ppm): 13.7 (CH₃), 20.1 (CH₂), 24.9 (CH₂ x 2), 31.5 (CH₂), 32.2 (CH₂), 35.0 (CH₂), 39.9 (CH₂), 54.6 (CH), 56.1 (CH), 125.3 (CH), 128.6 (CH), 130.1 (CH x 2), 134.6 (C), 134.8 (C), 167.0 (C), 167.1 (C).

IR (nujol, cm⁻¹): 3286, 1631, 1540, 1365.

HRMS (ESI): 318.2176 (M + H)⁺, calcd for C₁₈H₂₈N₃O₂ 318.2176.

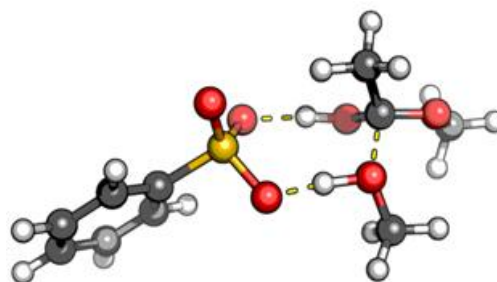
¹²¹ Oliva, A. I.; Simón, L.; Muñiz, F. M.; Sanz, F.; Morán, J. R. *Tetrahedron* **2004**, *60*, 3755-3762.



**VNIVERSIDAD
D SALAMANCA**

CAMPUS DE EXCELENCIA INTERNACIONAL

CHAPTER 4: Catalysts for transesterification reactions



4.1. INTRODUCTION

Once studied the aldol reaction for the preparation of Hajos-Wiechert and Wieland-Miescher ketones, we applied our catalysts with oxyanion-hole structure in other interesting reactions. Again, a look at the way nature uses the oxyanion hole led us to lipase enzymes, which are able to catalyse ester hydrolysis by a combination of three amino acids known as "*catalytic triad*". In this strategy, the ester to be hydrolyzed reacts first with the hydroxyl of a serine residue, which is activated as a nucleophile by a hydrogen bond with a histidine imidazole. This group has an increased basicity due to an H-bond which establishes with the carboxylate of an aspartic acid residue.

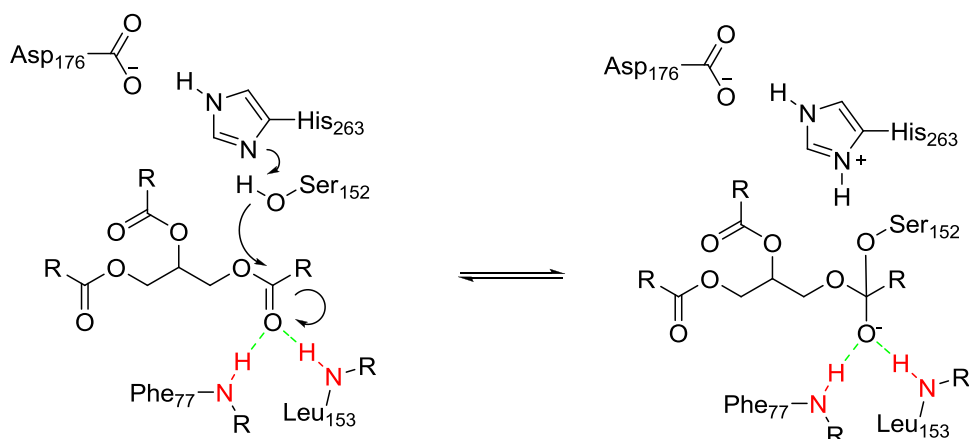


Figure 4.1. Hydrolysis mechanism of the 1hpl triacylglycerine lipase wherein the catalytic triad and the oxyanion hole are shown.

The idea is to transform a trimolecular reaction (in which the ester, water and the enzyme should interact) in two bimolecular reactions. The result is a large increase in the reaction rate. In addition, in the active site of the enzyme there are two NHs forming an oxyanion hole. These NHs stabilize the negative charge generated in the tetrahedral intermediate, after the addition of a water molecule to the ester group.

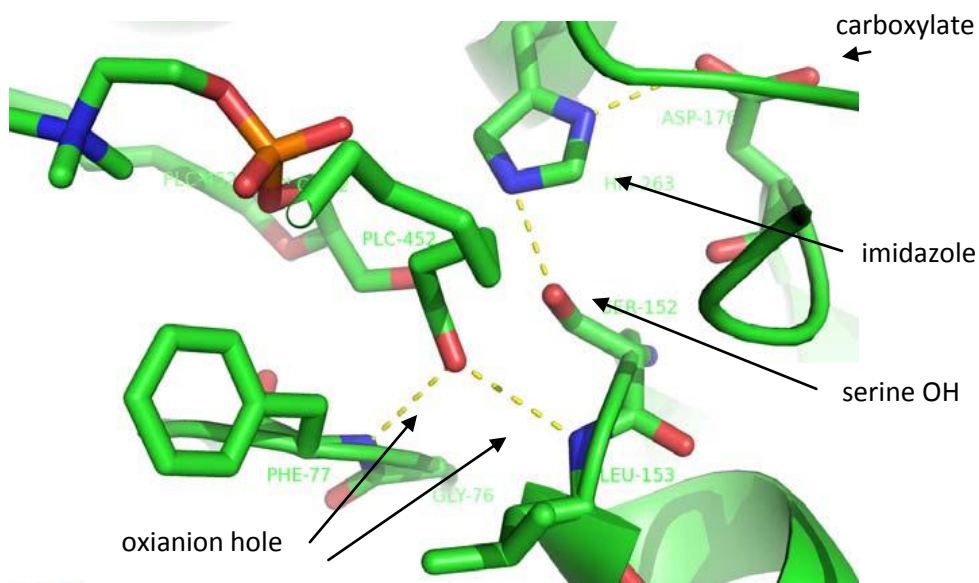


Figure 4.2. Active site of a lipase (1lpa) in which the oxyanion hole is associating the carbonyl of the guest via two linear hydrogen bonds, formed by the NHs of phenylalanine-77 and leucine-153.

Some enzymes, instead of carrying out the ester hydrolysis, are capable of performing the transesterification with an alcohol. Thus, triglycerides (esters of glycerine and fatty acids) can be transformed into the corresponding esters of fatty acids. Some cells, such as adipocytes, use triglycerides as "energy storage".¹²² Thus, similarly, esters of short-chain alcohols have

¹²² Darnell, J.; Lodish, H.; Baltimore, D. *Molecular Cell Biology*, 2nd ed.; W. H. Freeman and Company: New York, 1990.

been used by men and women as a reservoir of energy as fuel, is what it has been called biodiesel.

The use of biodiesel as fuel arises from the concern for environmental problems generated as a result of the emission of gases that cause the greenhouse effect. This fact has generated further studies to find alternative energy sources to solve this problem.¹²³ Thus, biofuels such as biomass, bioethanol and biodiesel have recently become very important. Specifically, biodiesel has a number of advantages that justify its development:¹²⁴

- Biodiesel is renewable and does not contribute to global warming. A life cycle analysis of biodiesel has shown that CO₂ emissions would be reduced by 78 % when compared to conventional diesel emissions.¹²⁵
- Emissions of CO, unburned hydrocarbons and biodiesel particulates are lower than diesel emissions (although NOx emissions are slightly higher).
- When added to conventional diesel in amounts of 1.0-2.0 % improves its lubricating properties.
- It decreases (but not eliminates) the dependence on imported oil.
- It provides a market for excess production of vegetable oils and animal fats.



Rudolf Diesel

By 1900,¹²⁶ Rudolf Diesel showed in a world exhibition in Paris an engine with worked with peanut oil. However, the direct use of vegetable oils as fuel had the problem of soot formation, high viscosity and poor ignition.¹²⁷ To solve these problems, the best procedure is the transesterification of vegetable or animal oils with short-chain alcohols, such as methanol or ethanol, to obtain the corresponding esters of fatty acids. Glycerine is an interesting byproduct in this process.¹²⁸ In fact, most of the processes developed in the early 40's for biodiesel production¹²⁹ were aimed to simplify the method for

¹²³ (a) European Parliament and the Council. Directive 2003/30/EC of the European Parliament and of the Council of 8 May 2003 on the promotion of the use of biofuels or other renewable fuels for transport. Official Journal of the European Union, 2003; (b) Demirbas, M. F.; Balat, M.; Balat, H. *Energy Convers. Manage.* **2011**, *52*, 1815-1828; (c) Lin, L.; Cunshan, Z.; Vittayapadung, S.; Xiangqian, S.; Mingdong, D. *Appl. Energy* **2011**, *88*, 1020-1031; (d) Janaun, J.; Ellis, N. *Renewable Sustainable Energy Rev.* **2010**, *14*, 1312-1320.

¹²⁴ Van Gerpen, J. *Fuel Process. Technol.* **2005**, *86*, 1097-1107.

¹²⁵ Sheehan, J.; Camobreco, V.; Duffield, J.; Graboski, M.; Shapouri, H. Life cycle inventory of biodiesel and petroleum diesel for use in an urban bus, final report for U.S. Dept. of Energy's Office of Fuel Development and the U.S. Dept. of Agriculture's Office of Energy, by the National Renewable Energy Laboratory, NREL/ SR-580-24089 (Mayo 1998).

¹²⁶ Kohse-Höinghaus, K.; Oßwald, P.; Cool, T. A.; Kasper, T.; Hansen, N.; Qi, F.; Westbrook, C. K.; Westmoreland, P. R. *Angew. Chem., Int. Ed.* **2010**, *49*, 3572-3597.

¹²⁷ Agarwal, A. K. *Prog. Energy Combust. Sci.* **2007**, *33*, 233-271.

¹²⁸ (a) Ma, F.; Hanna, M. A. *Bioresour. Technol.* **1999**, *70*, 1-15; (b) Leung, D. Y. C.; Wu, X.; Leung, M. K. H. *Appl. Energy*, **2010**, *87*, 1083-1095.

¹²⁹ (a) Bradshaw, G. B. *Soap* **1942**, *18*, 23-24, 69-70; (b) Bradshaw, G. B.; Meuly, W.C., U. S. Patent 2271619, 1942; (c) Bradshaw, G.B.; Meuly, W.C., U. S. Patent 2360844, 1944; (d) Arrowsmith, C. J.; Ross,

glycerine production in the manufacture of soaps, ie, the biodiesel was a byproduct generated in the separation of glycerine. In World War II, the efficient production of glycerine was highly prized for the manufacture of explosives. Converting oils and fats into methyl esters, glycerine could be separated much better than the simple hydrolysis of these triglycerides, being much denser than the methyl esters. Then, triglycerides were later hydrolyzed to soap production.¹²⁴

In 1942,^{129a-c} Bradshaw patented a method in which 1,6 equivalents of alcohol were mixed with 0.1-0.5 % of NaOH or KOH. At 80 °C the process reached 98 % conversion to obtain high quality glycerine. However, there were a number of disadvantages in this process:¹³⁰

- A molar excess of alcohol is required to complete the reaction. Although the amount of alcohol can be decreased by carrying out the reaction in several steps, this process is expensive.
- The presence of water in the alcohol increases soaps generation, reducing the process efficiency.
- The existence of free fatty acids in oils makes the procedure more expensive, since direct transesterification with NaOH generates soaps which lead to emulsions, preventing phase separation. In this case it is necessary to perform a first esterification step of the fatty acids, usually by treatment with H₂SO₄. These additional steps increase the cost of the production process.
- An acid is required to neutralize NaOH, which makes the process more expensive and causes the glycerine to be obtained in the presence of salts. This fact increases the cost of purifying the glycerine, which is an important product for the process to be cost effective.

However, it was not until the late 70s and early 80s when high oil prices led to a growing interest in biodiesel. New studies to try to improve the process and new catalysts were developed.¹³¹

Before studying our oxyanion-hole based catalysts in this reaction, we will do a literature study on the compounds that have been used so far to catalyse this reaction.

J., U. S. Patent 2383580, 1945; (e) Allen, H. D.; Kline, W. A., U. S. Patent 2383579, 1945; (f) Percy, J. H., U. S. Patent 2383614, 1945; (g) Keim, G. I., U. S. Patent 2383601, 1945; (h) Trent, W. R., U. S. Patent 2383632, 1945; (i) Trent, W. R., U. S. Patent 2383633, 1945; (j) Dreger, E. E., U. S. Patent 2383596, 1945.

¹³⁰ Vicente, G.; Martínez, M.; Aracil, J. *Bioresour. Technol.* **2004**, *92*, 297-305.

¹³¹ (a) Macrae, A. R. *J. Am. Oil Chem. Soc.* **1983**, *60*, 291-294; (b) Sonntag, N. O. V. *J. Am. Oil Chem. Soc.* **1982**, *59*, 795-802; (c) Sonntag, N. O. V. *Bailey's Ind. Oil Fat Prod.*; Swern, D., Ed.; 4th ed.; Interscience: New York, 1982; Vol. 2, pp 97-173; (d) Zardoya, J. M. *Química e Industria* **1980**, *26*, 173-175; (e) Sonntag, N. O. V. *J. Am. Oil Chem. Soc.* **1979**, *56*, 751-754; (f) Bhagade, S. S.; Nageshwar, G. D. *Chemicals & Petrochemicals Journal* **1978**, *9*, 3-12; (g) Joly, F.; Lang, J. P. *Revue Francaise des Corps Gras* **1978**, *25*, 423-429; Sreenivasan, B. *J. Am. Oil Chem. Soc.* **1978**, *55*, 796-805.

4.1.1. Catalysts used in biodiesel obtention

In general, the catalysts used for biodiesel production are summarized into three categories: bases, acids and enzymes. Enzymes^{128b} avoid soap formation, the purification process is simple and have shown good tolerance for free fatty acids present in the oil. However, its price is too high (although many groups have attempted to prevent this problem by immobilizing enzymes on different media), the reaction times are longer and it is difficult to drive the reaction to complete conversion.¹³²

The acidic and basic catalysts can be classified as homogeneous or heterogeneous, and their advantages and disadvantages are summarized in the following table.^{128b}

¹³² (a) Nelson, L. A.; Foglia, T. A.; Marmer, W. N. *J. Am. Oil Chem. Soc.* **1996**, *73*, 1191-1195; (b) Shimada, Y.; Watanabe, Y.; Samukawa, T.; Sugihara, A.; Noda, H.; Fukuda, H. *J. Am. Oil Chem. Soc.* **1999**, *76*, 789-793; (c) Watanabe, Y.; Shimada, Y.; Sugihara, A.; Noda, H.; Fukuda, H.; Tominga, Y. *J. Am. Oil Chem. Soc.* **2000**, *77*, 355-360; (d) Wu, W. H.; Foglia, T. A.; Marmer, W. N.; Phillips, J. G. *J. Am. Oil Chem. Soc.* **1999**, *76*, 517-521.

Table 4.1. Advantages and disadvantages of different types of catalysts used in biodiesel production.

Type	Example	Advantages	Disadvantages
Base			
Homogeneous	NaOH, KOH.	High catalytic activity, low cost, favorable kinetics, modest operation conditions.	Low free fatty acids requirement, anhydrous conditions, saponification, emulsion formation, more waste water from purification, disposable.
Heterogeneous	CaO, CaTiO ₃ , CaZrO ₃ , CaO-CeO ₂ , CaMnO ₃ , Ca ₂ Fe ₂ O ₅ , KOH/Al ₂ O ₃ , KOH/NaY, Al ₂ O ₃ /KI, ETS-10 zeolite, alumina/silica supported K ₂ CO ₃ .	Non corrosive, environmentally benign, recyclable, fewer disposal problems, easily separation, higher selectivity, longer catalyst lifetimes.	Low free fatty acids requirement, anhydrous conditions, more wastewater from purification, high molar ratio of alcohol to oil requirement, high reaction temperature and pressure, diffusion limitations, high cost.
Acid			
Homogeneous	Concentrated sulfuric acid.	Catalyse esterification and transesterification simultaneously, avoid soap formation.	Equipment corrosion, more waste from neutralization, difficult to recycle, higher reaction temperature, long reaction times, weak catalytic activity.
Heterogeneous	ZnO/I ₂ , ZrO ₂ /SO ₄ ²⁻ , TiO ₂ /SO ₄ ²⁻ , carbon-based solid acid catalysts, carbohydrate-derived catalysts, vanadyl phosphate, niobic acid, sulphated zirconia, Amberlyst-15, Nafion-NR50.	Catalyse esterification and transesterification simultaneously, recyclable, eco-friendly.	Low acid site concentrations, low microporosity, diffusion limitations, high cost.
Enzymes	<i>Candida antarctica</i> fraction B lipase, <i>Rhizomucor mieher</i> lipase.	Avoid soap formation, nonpolluting, easier purification.	Expensive, denaturation.

Recently new methods have emerged to carry out the transesterification reaction:^{128b}

- The "Biox co-solvent" process¹³³ developed by Boocock in 1996, which uses an inert cosolvent to transform the process in a single-phase.
- Reaction in supercritical conditions, conducting the reaction at high pressure and temperature it does not need a catalyst.¹³⁴

¹³³ Boocock, D. G. B.; Konar, S. K.; Mao, V.; Sidi, H. *Biomass Bioenergy* **1996**, *11*, 43-50.

- *In situ* process, developed by Harrington and D'Arcy-Evans in 1985,¹³⁵ in which the seeds are directly treated at high temperature and pressure with a solution of methanol in which the catalyst has been previously dissolved.

For the production of biodiesel from oils to be meaningful and profitable, the triglycerides should consist of non-edible low cost oils. It would be illogical and unethical to use as fuel biodiesel made from oils used for food. Moreover, the non-edible low cost oils possess high contents of free fatty acids, making them unsuitable as raw materials especially when it is intended to use a basic catalyst. Also, as a general rule, plants that usually produce this low cost oils do not need soils rich in nutrients for cultivation, so wastelands which are not currently cultivated can be employed. Another option is the use of used cooking oils, which also tend to have high levels of free fatty acids as well as large amounts of impurities such as proteins, carbohydrates, etc. coming from the meals that were prepared.

Recently, algae have emerged as an alternative feedstock for oils. In some varieties up to 80 % of its dry weight is composed of triglycerides, so that they can become a very attractive possibility in the future.¹³⁶

All these raw materials with high contents of free fatty acids need acid type catalysts to prevent the previous esterification steps, which increase production costs. However, it has been shown that acidic catalysts produce slower transesterification reactions than the basic ones (up to 4000 times slower).¹³⁷ Trying to find an explanation for this fact, we found some surprising results in the hydrolysis of triglycerides, which had been studied up to the 50s, due to its importance in the manufacture of soap and glycerine. Prominent among others are the contributions of Spanish Lucio Lascaray. The findings obtained in these studies are:¹³⁸



Ignacio y
Lucio Lascaray

- Hydrolysis of triglycerides is a biphasic reaction due to the low solubility of oil and water.
- Esters that have partial solubility in water are hydrolyzed in the aqueous phase following the classical Ingold mechanism.¹³⁹ Kinetics are zero-order in the esters, since its concentration remains constant, due to the continued solubilisation from the apolar phase as they are reacting.

¹³⁴ (a) Demirbas, A. *Energy Convers. Manage.* **2002**, *43*, 2349-2356; (b) Saka, S.; Kusdiana, D. *Fuel* **2001**, *80*, 225-231; (c) Han, H. W. Cao, W. L.; Zhang, J. C. *Process Biochem.* **2005**, *40*, 3148-3151; (d) Bunyakiat, K.; Makmee, S.; Sawangkeaw, R.; Ngamprasertsith, S. *Energy Fuels* **2006**, *20*, 812-817.

¹³⁵ Harrington, K. J.; D'Arcy-Evans, C. *Ind. Eng. Chem. Prod. Res. Dev.* **1985**, *24*, 314-318.

¹³⁶ (a) Chisti, Y. *Biotechnol. Adv.* **2007**, *25*, 294-306; (b) Banerjee, A.; Sharma, R.; Chisti, Y.; Banerjee, U. C. *Crit. Rev. Biotechnol.* **2002**, *22*, 245-279.

¹³⁷ (a) Srivastava, A.; Prasad, R. *Renewable Sustainable Energy Rev.* **2000**, *4*, 111-133; (b) Formo, M. W. *J. Am. Oil Chem. Soc.* **1954**, *31*, 548-559.

¹³⁸ (a) Suen, T. J.; Chien, T. P. *Ind. Eng. Chem.* **1941**, *33*, 1043-1045; (b) Lascaray, L. *Ind. Eng. Chem.* **1949**, *41*, 786-790.

¹³⁹ Ingold, C. K. *J. Chem. Soc.* **1930**, 1032-1039.

- Esters which are sparingly soluble in water, such as triglycerides, prefer to react quickly in the apolar phase, with only a small contribution from the aqueous phase. In this case, complex kinetics are obtained, which have an induction period, followed by the fast reaction in the triglyceride and finally a slow reaction due to consumption of the reagents.

- Hydrophilic acids, such as hydrochloric acid or sulphuric acid, prefer to carry out the reaction in the aqueous phase and therefore are ineffective catalysts for the hydrolysis of triglycerides. Moreover, sulfonic acids with a long hydrocarbon chain (Twitchell reagents)¹⁴⁰ are good catalysts for this reaction because they prefer to dissolve in the triglyceride phase.

In fact, the transesterification of triglycerides with methanol in the presence of an acid catalyst shows a great similarity with the previously described hydrolysis reaction. In this case, the water molecule is replaced by methanol, more lipophilic, but the mutual solubility with the triglyceride is still small and the reaction remains biphasic. As in the case of hydrolysis, the triglyceride can react with methanol in both the polar and the apolar phase. Hydrophilic catalysts, such as sulphuric acid, produce the fastest reaction in the methanol phase. This can be shown because the reaction rate is proportional to the methanol volume.¹⁴¹

To study why the reaction is so slow in an acidic medium, we decided to conduct an experiment to measure the concentration of triglyceride in the methanol phase. To this end, 0.5 mL of deuterated methanol and 0.5 mL of sunflower seed oil were introduced in an NMR tube. The tube was shaken and then centrifuged to separate the phases. Deuterated methanol, less dense than the oil floats over the fatty phase, it is extracted with a pipette and placed in another NMR tube. Integrating the signals of the triglyceride in the deuterated methanol it could be seen that the triglyceride-methanol relationship was 1:300 mol/mol, which means that the amount of oil dissolved in the methanol phase was really small. This may explain the slow reaction rate of the processes catalysed by hydrophilic acids, as the reaction rate is proportional to the concentration of triglyceride times the methanol concentration. In this case, the first concentration is small and makes the reaction rate very slow.

The fact that the lack of solubility of the triglyceride is the main problem, can easily be demonstrated by comparing the transesterification rate with the esterification of fatty acids. Since fatty acids are soluble in methanol, they undergo the esterification reaction at a reasonable rate. This reaction can be used in industrial processes for the preparation of biodiesel. In fact, oil transesterification reactions with high contents of free fatty acids, catalysed with sulphuric acid, yield as the first process the esterification of the free fatty acids. This reaction generates water, which further decreases the solubility of the triglycerides in methanol, making transesterification even harder.

As in the fat hydrolysis, a good alternative is to catalyse the reaction in the apolar phase of the triglyceride, as the molar concentration of methanol in this phase (measured as in the previous experiment, 1,0:0,4 mol/mol) is much greater than the concentration of the triglyceride in the polar phase. In this case, the reaction rate is proportional to the

¹⁴⁰ (a) Twitchell, E. *J. Am. Chem. Soc.* **1900**, 22, 22-26; (b) Twitchell, E. *J. Am. Chem. Soc.* **1906**, 28, 196-200; (c) Twitchell, E. *J. Am. Chem. Soc.* **1907**, 29, 566-571.

¹⁴¹ Zheng, S.; Kates, M.; Dub, M. A.; McLean, D. D. *Biomass Bioenergy* **2006**, 30, 267-272.

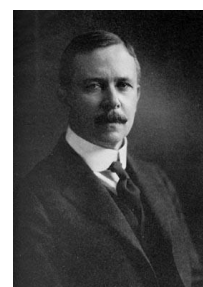
concentration of methanol and triglyceride, and is greater than within the methanol phase, where the triglyceride acts as the limiting reagent, slowing down the reaction.

To use this feature, the acid catalyst should dissolve in the triglyceride phase. It is possible to dissolve a sulfonic acid in the triglyceride phase (instead of the methanol phase where it experiments ionization) if it possesses a long aliphatic chain. This type of catalyst is called "Twitchell reagent"¹⁴⁰ and it can offer some interesting advantages in biodiesel preparation:

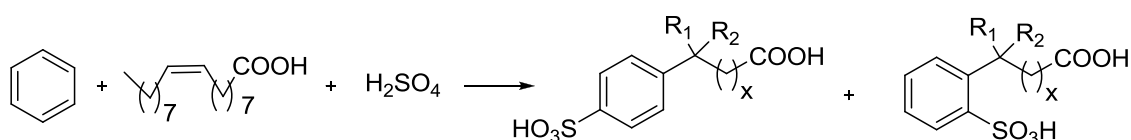
- As an acid catalyst, the presence of large amounts of free fatty acids (characteristic of non-edible low cost oils) would have little effect on the transesterification reaction.
- Small amounts of water (from the esterification of fatty acids, or from low quality methanol or wet fat) remain in the methanol phase and hardly influence the kinetics of the reaction which takes place mostly in the apolar phase.
- Because methanol is saturating the triglyceride phase, the total amount does not affect the reaction rate and, therefore, the amount of methanol can be minimized.
- Glycerine is obtained in the absence of salts, this makes purification easier.

4.1.2. Twitchell reagents

As noted previously, the Twitchell reagents used in the 50s for fat hydrolysis consist on sulfonic acids with a long hydrocarbon chain. For its synthesis, in the first articles, Twitchell used oleic acid, an aromatic hydrocarbon (benzene or naphthalene) and sulphuric acid.¹⁴⁰



Ernst Twitchell



R₁ and R₂ = alkyl chains of variable length
x = methylene number to determine

Figure 4.3. Twitchell reagents synthesis.

Shortly after, new procedures with new raw materials arose, either by changing the aromatic ring (xylenes, phenol)¹⁴² or by substituting oleic acid with a triglyceride, petroleum derivatives¹⁴³ or butanol.¹⁴⁴ These reagents which were marketed under different names as Pfeilring, Neokontakt, Idrapid or Divuslon, are currently out of market and can no longer be purchased commercially.

¹⁴² Sonntag, N. O. V. *J. Am. Oil Chem. Soc.* **1979**, *56*, 729-732.

¹⁴³ Petrov, G. S.; Dimakov, S. I.; Taksa, F. T. *Seifensieder-Ztg.* **1927**, *54*, 168-166, 182-184, 204-205, 221-222, 241-242, 261-262, 284-285.

¹⁴⁴ Fukuzumi, K.; Ozaki, S. *J. Chem. Soc. Jpn. Ind. Chem. Sect.* **1951**, *54*, 727.

4.2. METHODS AND RESULTS

4.2.1. Synthesis of Twitchell catalyst

After a literature review about Twitchell reagents, we found no articles in which such compounds had been used for the transesterification of triglycerides with methanol. Therefore, we decided to carry out its synthesis using the conditions described by Twitchell.¹⁴⁰ Twitchell reagents are usually synthesized from the corresponding unsaturated fatty acids, but the triglyceride can also be used directly, as sulphuric acid leads to the hydrolysis of the esters. For this reason we synthesized two Twitchell reagents, **61** and **62** (figure 4.4) based on olive oil (due to its high content in oleic acid), benzene/phenol and sulphuric acid. Under these conditions, the double bonds undergo protonation, being alkylated by the aromatic rings. The aromatic compounds were used in excess over its stoichiometric amount to prevent dialkylation as much as possible. Despite this, we found that the Twitchell reagents consist on complex mixtures of compounds, due to the different substitution patterns in the aromatic ring, and transposition of the alkyl chains from oleic acid.

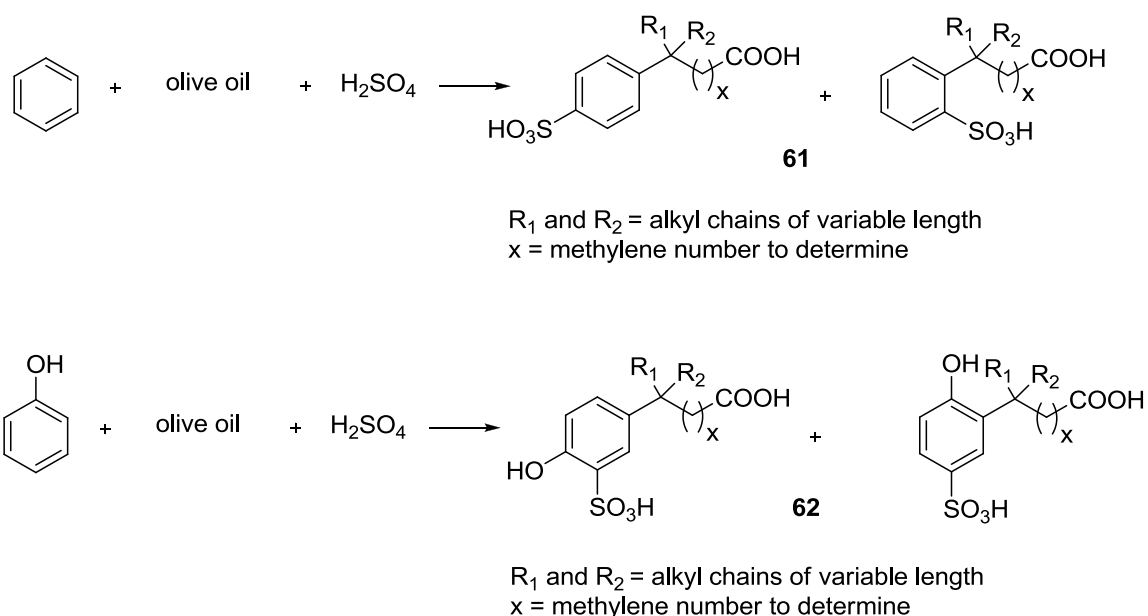
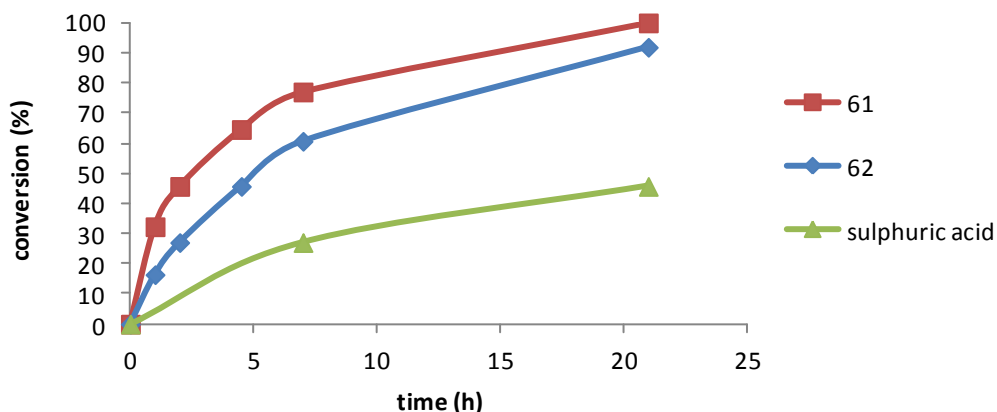


Figure 4.4. Twitchell reagents synthesis

However, the aromatic fragments of both Twitchell reagents **61** and **62** can be easily recognized in the ¹H NMR spectrum (see experimental part) and are consistent with the structures shown in figure 4.3.

4.2.2. Catalytic properties of Twitchell reagents

The catalytic properties of catalysts **61** and **62** were tested for the transesterification of commercial sunflower seed oil and compared with sulphuric acid. Experimentally, methanol (6 mmol) and oil (1 mmol) were mixed at 60 °C in the presence of 1 % weight sulphuric acid (96 %) and the same molar amount of Twitchell reagents **61** and **62**. The conversion of the starting material in the biodiesel was followed by ^1H NMR. Results are shown in graph 4.1.

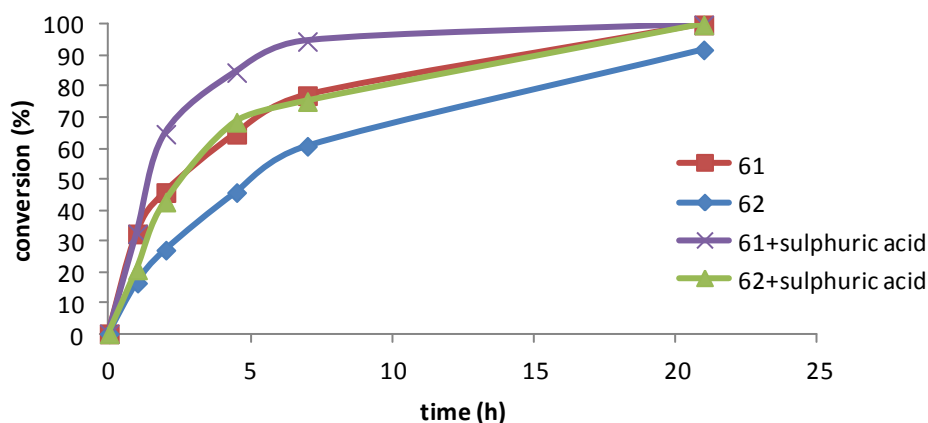


Graph 4.1. Sunflower seed oil transesterification with 1 wt % sulphuric acid and the same molar amounts of Twitchell reagents **61** and **62**. The molar ratio of methanol to triglyceride was kept 6:1 and the temperature 60 °C.

As can be seen, the sulphuric acid (with hydrophilic character) showed little catalytic activity (as predicted above) while the benzene derivative catalyst **61** provided the best results. The phenolic group of the catalyst **62**, while increasing the hydrophilicity of the molecule, generated smaller reaction rates due to partitioning into the aqueous phase which is shown below.

It is described that one of the reasons for the loss of catalytic activity of Twitchell reagents in fat hydrolysis is its distribution between the aqueous phase and the oil phase, in such a way that up to 45 % of the catalyst may remain in the aqueous phase.¹⁴² Thus, if the reaction rate is reduced by an unfavourable partition constant between the two phases, a simple way to improve the catalytic properties of the Twitchell reagents is to add a small amount of sulphuric acid to the aqueous phase. The presence of a strong acid decreases the dissociation of the sulfonic acid, increasing the concentration of the Twitchell reagent in the apolar phase.^{143,145} The partition constant between methanol and triglyceride may be even less favourable than in the case of water, so we checked the effect of adding sulphuric acid to the reaction catalysed with Twitchell reagents. As can be seen in figure 4.2, the catalytic properties of both Twitchell reagents **61** and **62** improved in the presence of 1 wt % of sulphuric acid, compared to the previous conditions.

¹⁴⁵ Lascaray, L. *J. Am. Oil Chem. Soc.* **1952**, *29*, 362-366.



Graph 4.2. Sunflower seed oil transesterification with Twitchell reagents **61** and **62**, in the presence and absence of 1 wt % sulphuric acid. The molar ratio methanol to triglyceride was kept at 6:1 and the temperature at 60 °C.

However, the use of sulphuric acid as an additive has some drawbacks:

- Sulphuric acid is a sulfonating and dehydrating compound which can transform glycerine into acrolein.¹⁴⁶
- The need to separate the sulphuric acid from the polar phase increases the cost of the transesterification process.
- Sulphuric acid is a corrosive reagent, and therefore requires appropriate equipment, more expensive than the conventional one.

Since the main role of sulphuric acid is only increasing the catalyst partition constant towards the apolar phase, this may not be necessary if a highly lipophilic catalyst is obtained with a partition constant favouring the triglyceride.

4.2.3. Lipophilic sulfonic acids

To confirm this hypothesis we prepared catalyst **63**, whose synthesis is described in literature.¹⁴⁷ Although the Friedel-Crafts acylation procedure involves a longer synthesis, we considered it would be preferable to conventional alkylation, which would have led to a complex mixture of products derived from the carbocation rearrangement.

¹⁴⁶ (a) Adkins, H.; Hartung, W. H. *Organic Syntheses Coll.* **1941**, *1*, 15; (b) Adkins, H.; Hartung, W. H. *Organic Syntheses Coll.* **1926**, *6*, 1.

¹⁴⁷ Hu, C.; Wang, J.; Zhou, J.; Chen, H.; Shi, X.; Yang, H.; Xu, X.; Wang, Y.; Zhang, J.; Xiang, W., CN 101716475A20100602, 2010.

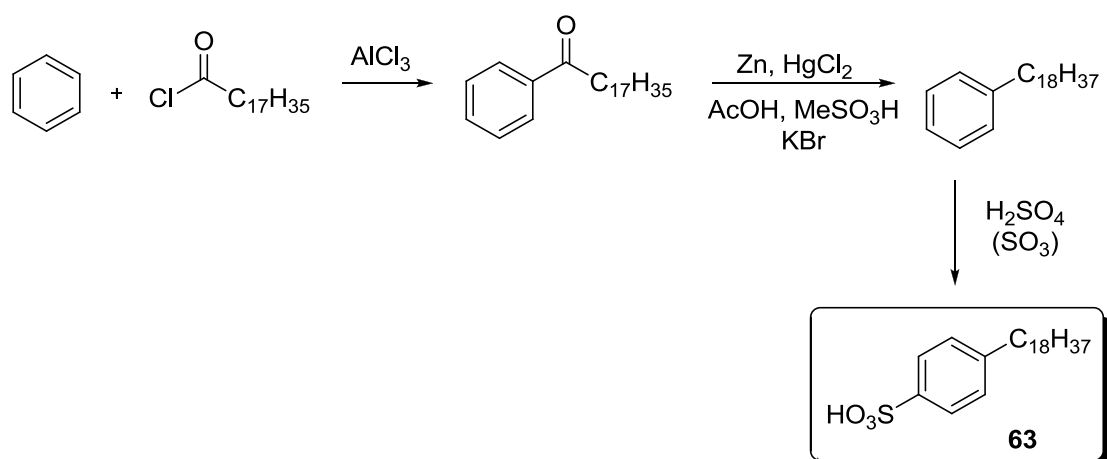
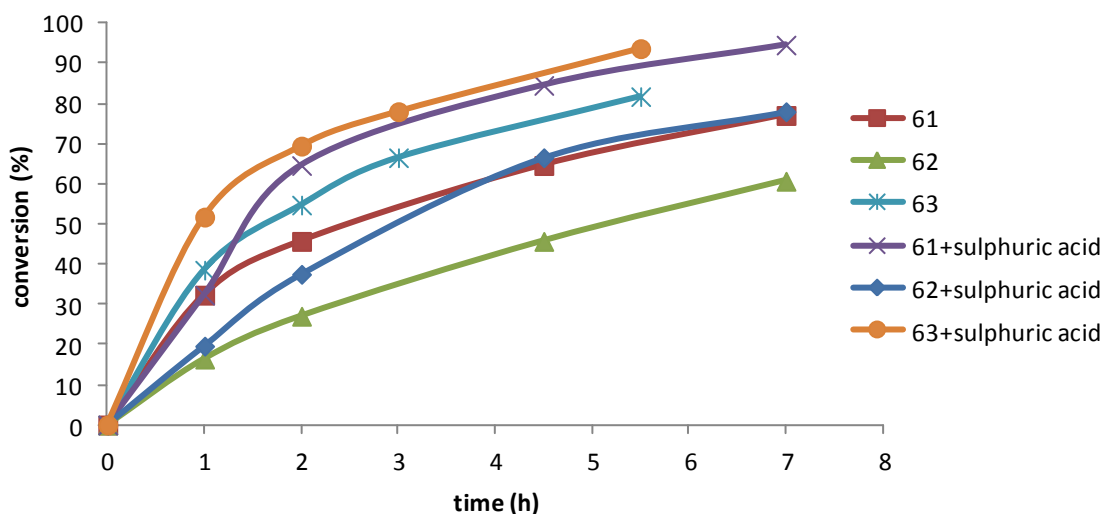


Figure 4.5. Synthesis and structure of catalyst **63**.

Compound **63** should be more lipophilic than Twitchell reagents since its structure lacks the carboxyl group. Its catalytic activity was tested in the same conditions as Twitchell reagents **61** and **62**, in the presence and absence of sulphuric acid.



Graph 4.3. Sunflower seed oil transesterification with Twitchell reagents **61** and **62** and the catalyst **63**, in the presence and absence of 1 wt % sulphuric acid. The molar ratio methanol to triglyceride was kept at 6:1 and the temperature at 60 °C.

To confirm the relevance of the lipophilicity of the catalyst, the partition constant of this compound between sunflower seed oil and methanol was measured by ^1H NMR. In an NMR tube, the catalyst **63** (20.0 mg, 48.7 μmol) was dissolved in deuteromethanol (0.5 mL), the spectrum was recorded and the catalyst signals were integrated and compared to the methyl protons of the solvent. Then 1.0 mL of sunflower oil was added. The NMR tube was stirred and centrifuged to favour the phase separation. The methanol phase was removed, placed in

another tube and the NMR spectrum was recorded, the catalyst signals were integrated and the new catalyst concentration was calculated in the deuterated methanol phase, providing the partition constant.

Table 4.2. Partition constants between methanol and sunflower seed oil calculated by integration of ^1H NMR signals.

entry	catalyst	partition constant CD ₃ OD/oil
1	63	9/1
2	64	1/1
3	64	6/4 ^a
4	65	2/98 ^b

^a CD₃OD with 10 % v/v of D₂O. ^b Estimated.

As shown in table 4.2, catalyst **63** still prefers the methanol phase and, therefore, a more lipophilic catalyst is required to improve the results.

For this purpose, we proceeded to the synthesis of a new catalyst **64**, characterized by two long aliphatic chains of 16 and 17 carbons atoms (figure 4.6).

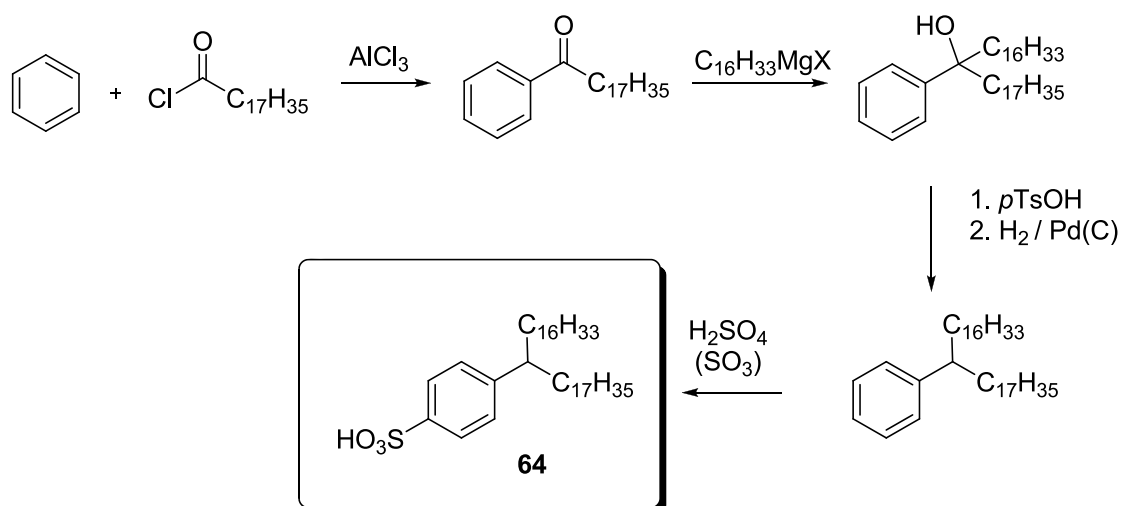
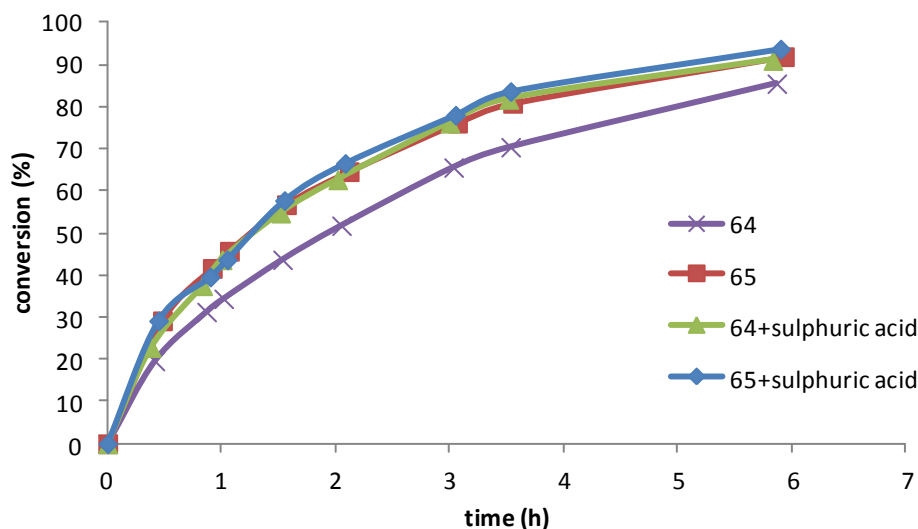


Figure 4.6. Synthesis of catalyst **64**.

This catalyst showed a partition constant with similar affinity for both phases: methanol and oil (table 4.2, entry 2). However, if it is considered the small volume of methanol used in the conditions of the transesterification reaction (0.67 mL of methanol to 2.5 g of oil), most of the catalyst should be in the oily phase. The catalytic properties of the catalyst **64** are shown in graph 4.4. According to the major partition constant, compound **64** has a higher catalytic activity and the addition of sulphuric acid leads to a less pronounced effect on catalysis.



Graph 4.4. Sunflower seed oil transesterification with catalysts **64** and **65**, in the presence and absence of sulphuric acid (1 wt %). The molar ratio methanol/triglyceride was kept 6:1 and the temperature at 60 °C.

However, we did not know if an increase in the lipophilicity of the catalyst could cause a better partition constant in favour of the oily phase or if it had been already reached a maximum. For this, a more lipophilic catalyst was synthesized from isophthalic acid methyl ester, with four 16-carbon hydrocarbon chains, as shown in figure 4.7.

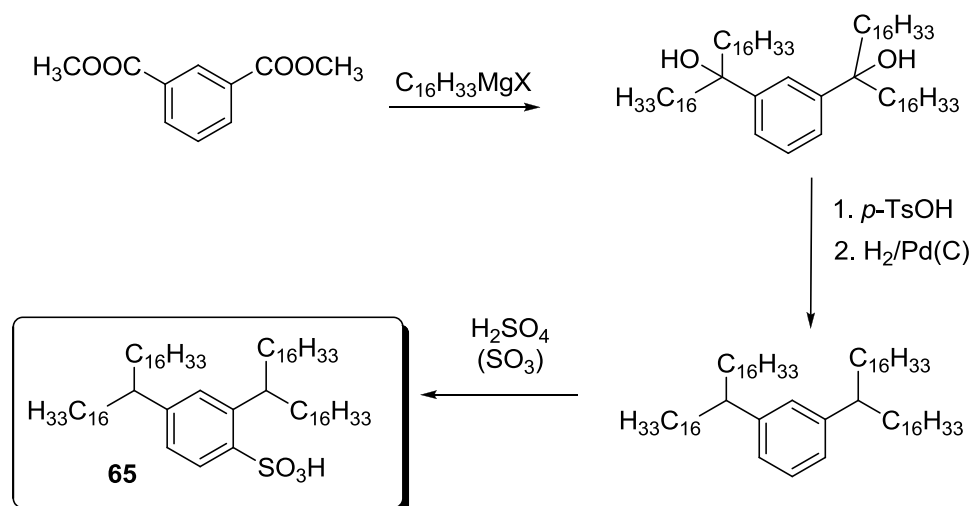


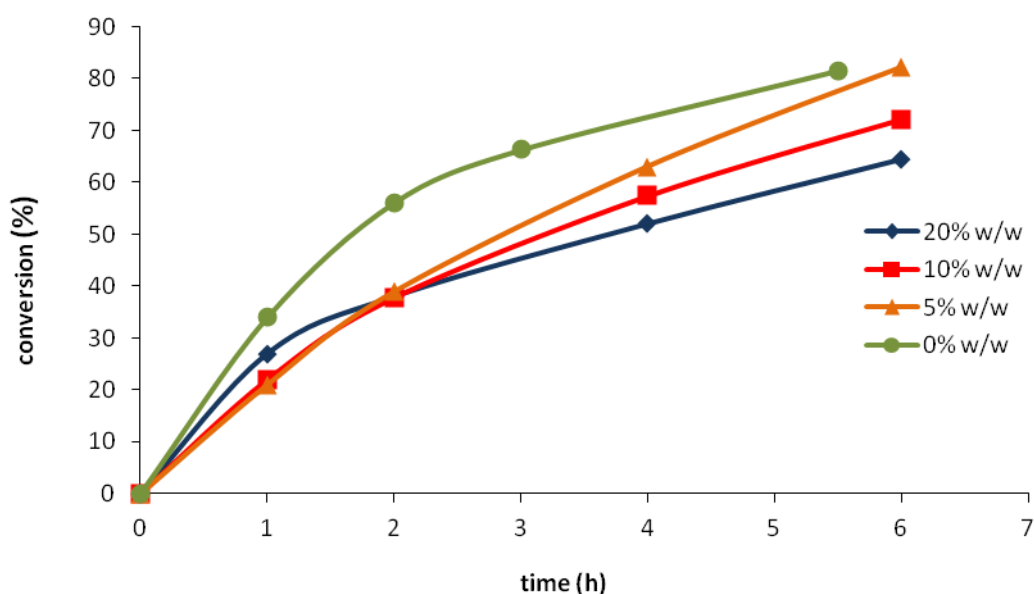
Figure 4.7. Synthesis of catalyst **65**.

Catalyst **65** proved to be a crystalline compound with low solubility in methanol, and with a partition constant very favourable to the triglyceride phase (table 4.2, entry 4). Accordingly, a greater reaction rate than with catalyst **64** could be observed. The reaction rate was similar to those of the catalysts combined with 1 % sulphuric acid. In fact, the addition of sulphuric acid to catalyst **65** produced no improvement in its catalytic activity, which indicates it is no longer necessary to increase the lipophilicity of the catalyst because this would not imply an increase in the reaction rate.

Since catalysts **64** and **65** showed the best results, both were selected to study the influence of different factors in the transesterification reaction.

4.2.4. Influence of free fatty acids in the oil

As noted above, the presence of free fatty acids in the oil makes the conventional alkaline transesterification inadequate.¹⁴⁸ However, this drawback does not exist using acid catalysts such as **61-65**. To substantiate this claim, we conducted a study in which we performed the transesterification reaction of the previous oil, but with different amounts of stearic acid: 5, 10 and 20 % by weight relative to sunflower oil.



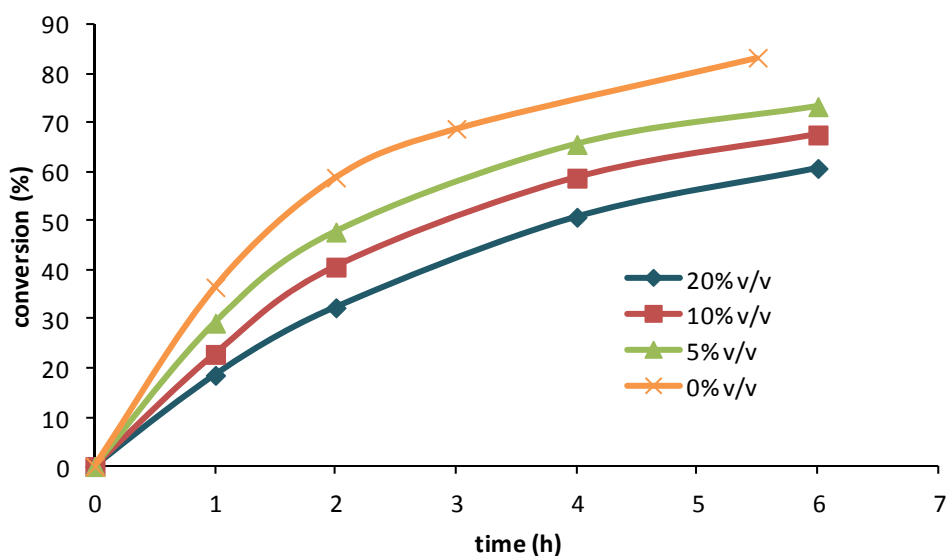
*Graph 4.5. Sunflower seed oil transesterification with catalyst **64**, in the presence of oil containing 5, 10 and 20 % (weight) of stearic acid. The molar ratio of methanol to triglyceride was kept at 6:1 and the temperature at 60 °C.*

In the above graph it can be seen that the presence of high levels of free fatty acids exerts a small influence on the reaction rate, in spite of the generation of a certain amount of water, due to the esterification of free fatty acids. In fact, the esterification of those acids is prior to the transesterification reaction, and this is the reason why during the first two reaction hours, the reaction rate is greater for those reactions which have a higher content of free fatty acids.

¹⁴⁸ (a) Markley, K. S. *Fatty acids*, 1st ed.; Interscience: New York, 1960; (b) Canakci, M.; Van Gerpen, J. *Trans. Am. Soc. Agric. Eng.* **2001**, *44*, 1429-1436.

4.2.5. Influence of water content

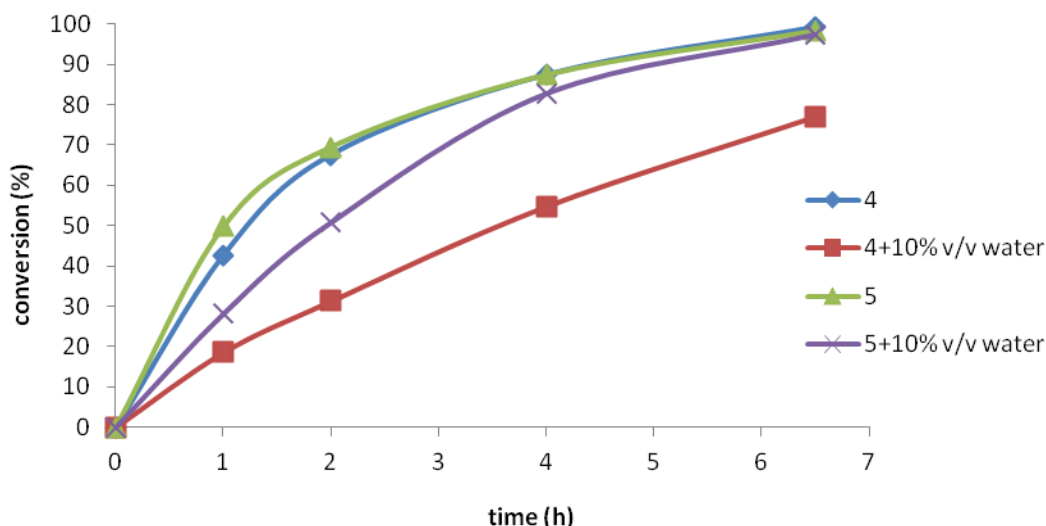
The presence of water in the reaction medium was also studied. For this objective we conducted the transesterification reaction catalysed with compound **64** in the absence and presence of 5, 10 and 20 % water (volume percent to methanol).



Graph 4.6. Sunflower seed oil transesterification with catalyst **64** in the presence of methanol with 5, 10 and 20 % (v/v) water. The molar ratio methanol/triglyceride was kept at 6:1 and the temperature at 60 °C.

In view of the above graph, the presence of water in the reaction medium decreases slightly the yield and reaction rate.

However, the effect of water is less pronounced with catalyst **65** than with catalyst **64**, since the former has two more hydrocarbon chains, thereby increasing its lipophilicity and its solubility in the triglyceride phase (graph 4.7).

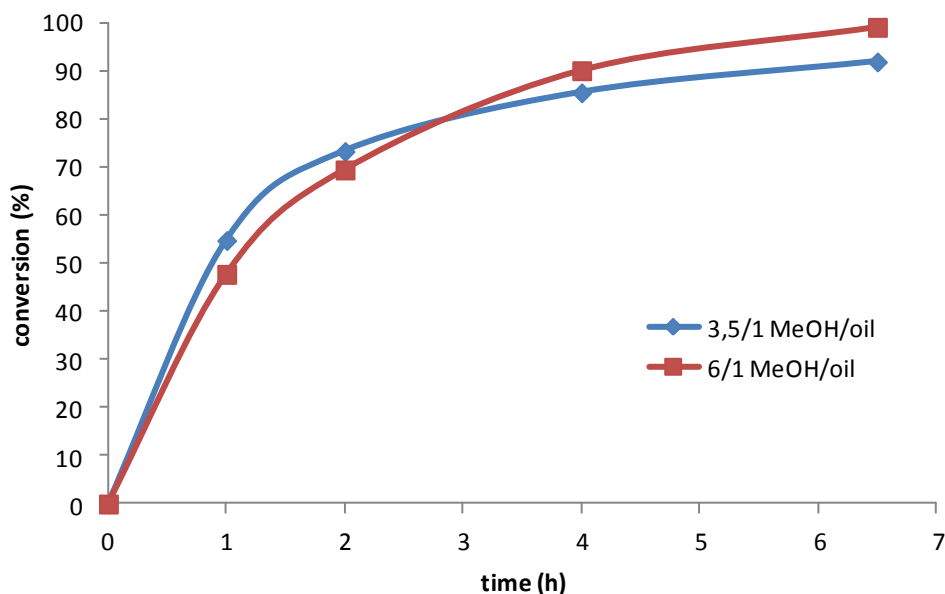


Graph 4.7. Sunflower seed oil transesterification with catalysts **64** and **65**, in the presence of methanol containing 0, 10% (v/v) of water. The molar ratio methanol/triglyceride was kept at 6:1 and the temperature at 60 °C.

These results can be explained by a change in the partition constant between methanol and triglyceride phases. In the presence of water, the partition constant for catalyst **64** increases from 1/1 to 6/4 (table 4.2, entries 2 and 3) in favour of the methanol phase. Since the amount of catalyst present in the oil phase is now lower, a slower reaction rate is expected. Moreover, this effect is less pronounced in the case of the more lipophilic catalyst **65**, which prefers the oily phase and therefore is reasonable to expect a smaller water effect (graph 4.7). Since these catalysts are insoluble in water, the effect of water is somewhat surprising, but it may be explained considering the basicity of the water molecule which probably promotes ionization of the sulfonic acid in the methanol phase, at least when a relatively small amount of water is used. In any case, the effect of water in this reaction is relatively small.

4.2.6. Influence of methanol/triglyceride ratio

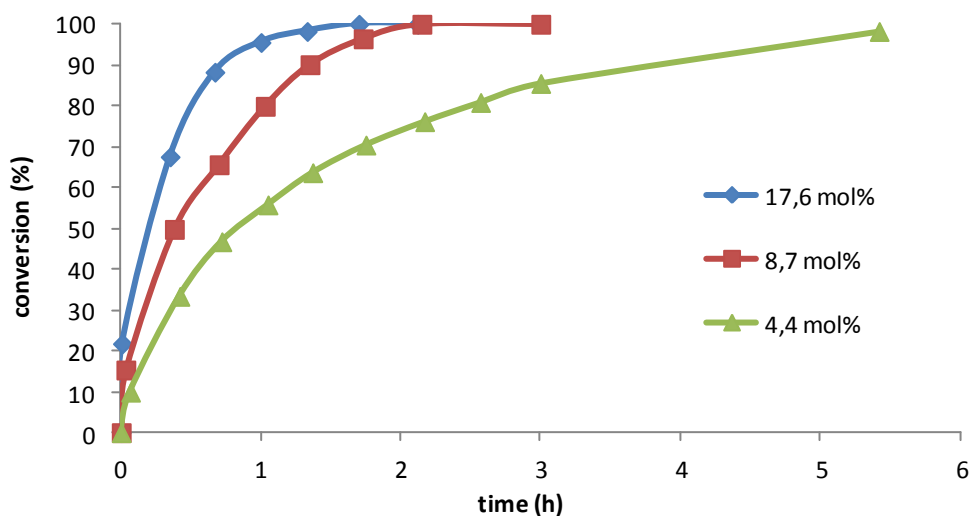
One advantage of using catalysts active in the apolar phase of the triglyceride, is that they do not require large excesses of methanol to obtain a good reaction rate. To check this effect, we analysed the influence of only a small excess of methanol in the reaction catalysed with compound **64**. Working with a methanol/triglyceride ratio 3.5:1, the reaction is slightly faster in the beginning. This fact agrees with an increased catalyst concentration in the apolar phase. However, as the reaction proceeds and the bulk of the methanol is consumed, the reaction rate is reduced, so that after three hours the reaction with methanol/triglyceride ratio 6:1 has a slightly higher rate.



Graph 4.8. Sunflower seed oil transesterification with catalyst **64** and molar ratios methanol to triglyceride of 3.5:1 and 6:1. The temperature was kept at 60 °C.

4.2.7. Influence of the catalyst amount

In view of graph 4.9, within the range of concentrations studied, the reaction rate increases linearly with the concentration of catalyst. This is interesting, since it is well known that in the hydrolysis reactions with Twitchell reagents there is a saturation effect when the amount of catalyst is around 1 % (by weight).¹⁴⁵



Graph 4.9. *Jatropha* seed oil transesterification with 4.4, 8.7 and 17.6 mol % of catalyst **65**. The molar ratio methanol to triglyceride was kept 6:1 and the temperature at 80 °C.

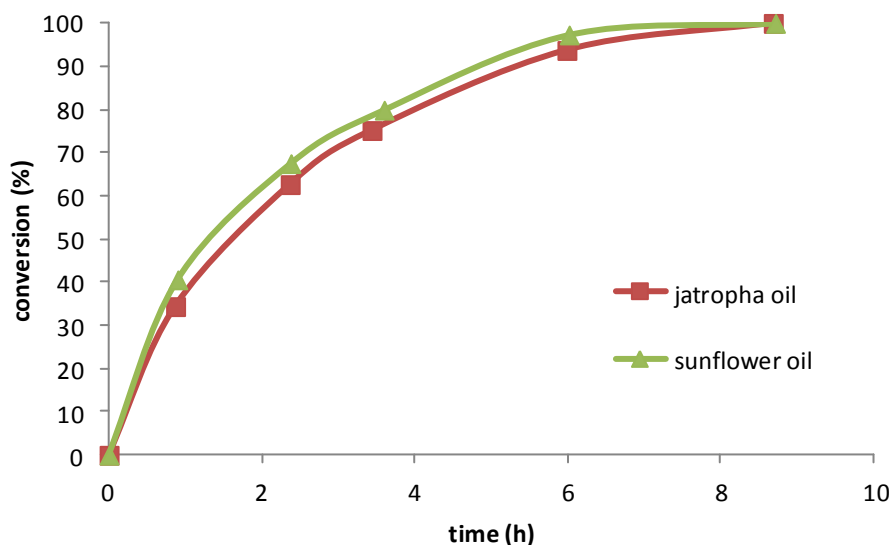
4.2.8. Influence of temperature

Regarding the effect of temperature, it was observed that, as expected, higher temperatures yield higher reaction rates and, therefore, shorter reaction times. Working at 80 °C with catalyst **65**, the reaction is substantially complete after 90 minutes (graph 4.9).

It is also possible to work at room temperature, although in this case the reaction times are greatly increased. Under these conditions, catalyst **65** was unsuccessful due to its low solubility; however, good conversions were obtained after three days with catalysts **63** (78 %) and **64** (97 %).

4.2.9. Influence of the oil type

To verify that these lipophilic catalysts can be used in the preparation of biodiesel from low cost oils, we performed the transesterification reaction with *jatropha* oil and we compared the kinetics with that of the sunflower seeds oil. As can be seen in graph 4.10, results are very similar in both cases, indicating that the synthesized catalysts are perfect for carrying out the transesterification reaction of low cost oils with high free fatty acid contents.



Graph 4.10. *Jatropha* oil and sunflower seed oil transesterification catalysed by compound **65**. The molar ratio methanol to triglyceride was kept 6:1 and the temperature at 60 °C.

4.2.10. Catalyst recovery

In this biodiesel production technology, catalyst recovery is a very important factor for the following reasons:

- The sulfonic acids are corrosive and can damage the fuel tank and the engine.
- The maximum sulphur content in fuels is limited.¹⁴⁹
- The acidity of biodiesel is provided for a maximum of 0.50 mg of KOH per gram of biodiesel.¹⁵⁰
- The cost of the catalyst synthesis makes its recovery important for the overall process to be economically profitable.

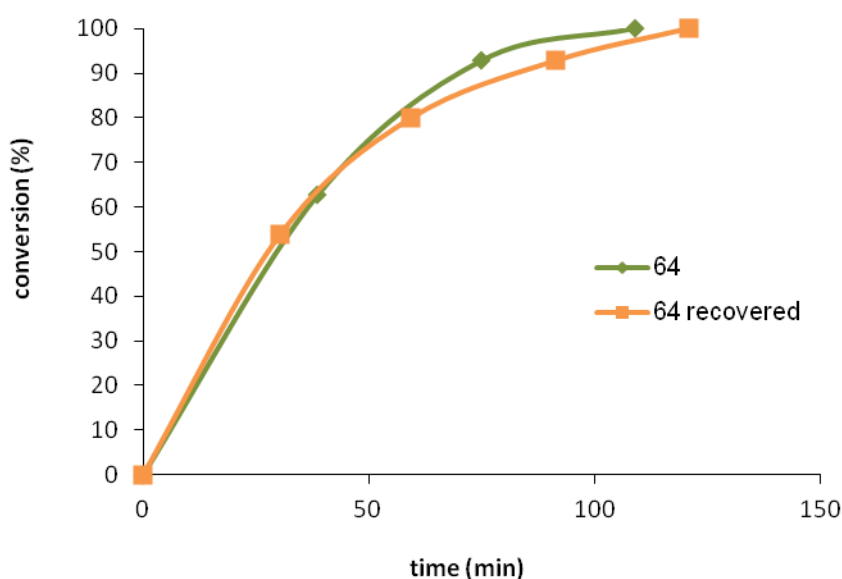
The separation of catalyst **64** from biodiesel was performed by adsorption of the catalyst on a silica gel column. For a reaction in which 16.0 g of triglyceride and 1.0 g of catalyst are mixed, once the reaction is completed, the glycerine is separated from the crude biodiesel by decantation. Being a denser compound, the glycerine decants below biodiesel. To purify it is only necessary to work under reduced pressure to remove a small amount of methanol.

Then, methanol from the biodiesel phase is evaporated and the remaining liquid (17.0 g) is dissolved in hexane or commercial diesel (32 mL) and passed through a small silica gel column. The catalyst, possessing highly polar sulfonic groups, protonates the basic groups of the

¹⁴⁹ EN 590:2009.

¹⁵⁰ ASTM D 6751 and EN 14214.

stationary phase and remains adsorbed, while biodiesel (fatty acid methyl esters) is eluted from the column. In principle, 10.0 g of silica per gram of catalyst are enough to provide a clean separation of the catalyst. Biodiesel can be eluted from the column with hexane (32 mL), but in this case the solvent must be evaporated before biodiesel commercialization. Alternatively, since biodiesel is sold as a mixture with conventional diesel fuel, the latter (32 mL) may be used to elute the biodiesel directly generating the commercial fuel. In either case, the final amount of biodiesel would be 14.0 g. Finally, elution with methanol (32 mL) allowed the recovery of the catalyst (0.9 g) together with methyl esters (1.4 g), diglycerides and monoglycerides (0.7 g), a mixture which, after evaporation of methanol, was used directly in a further reaction, showing no loss of catalytic activity compared to the original catalyst (graph 4.11).



*Graph 4.11 Sunflower seed oil transesterification catalysed by 18.5 mol % of fresh compound **64** and after catalyst **64** recovery. The molar ratio methanol to triglyceride was kept and the temperature at 80 °C.*

In Figure 4.8 the reaction process and catalyst recovery is schematized.

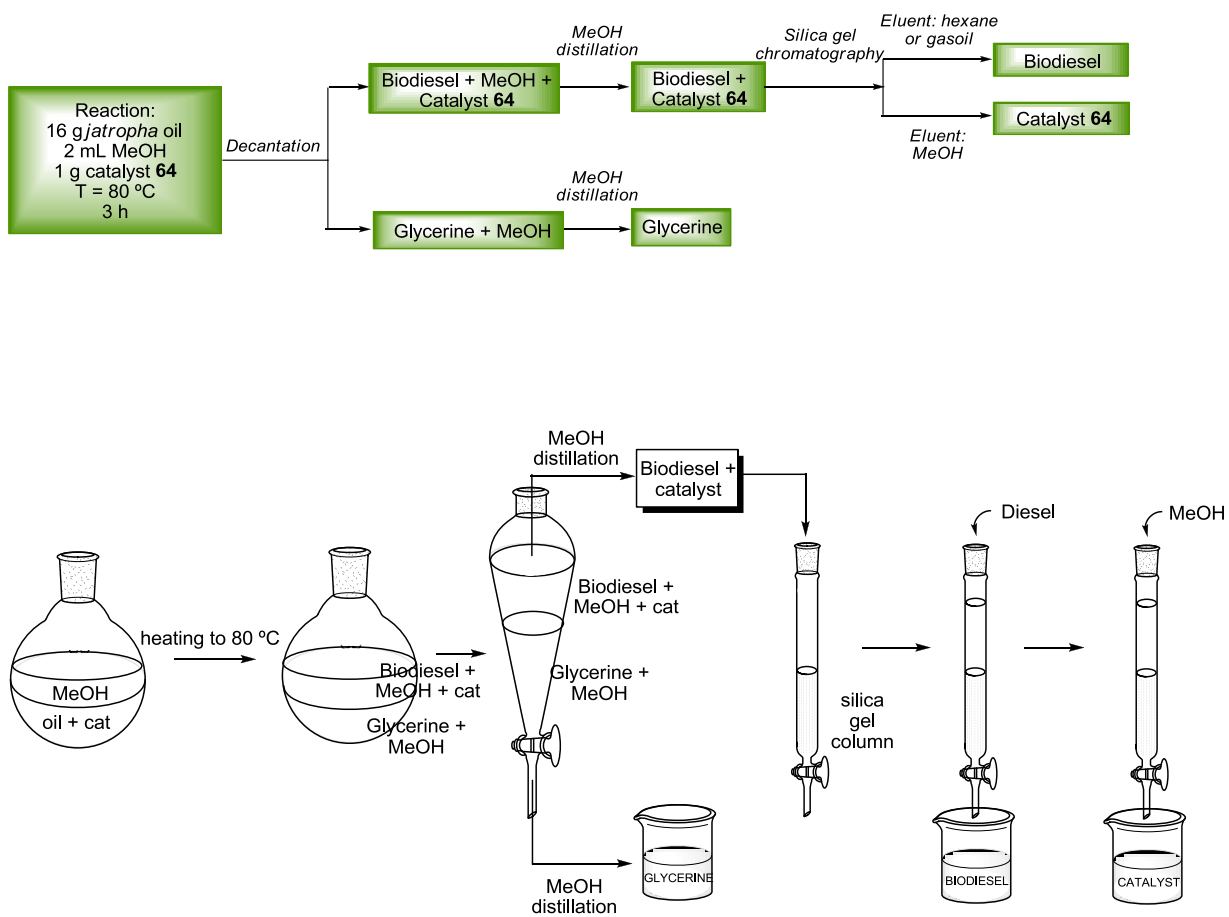


Figure 4.8. Scheme of catalyst 64 recovery.

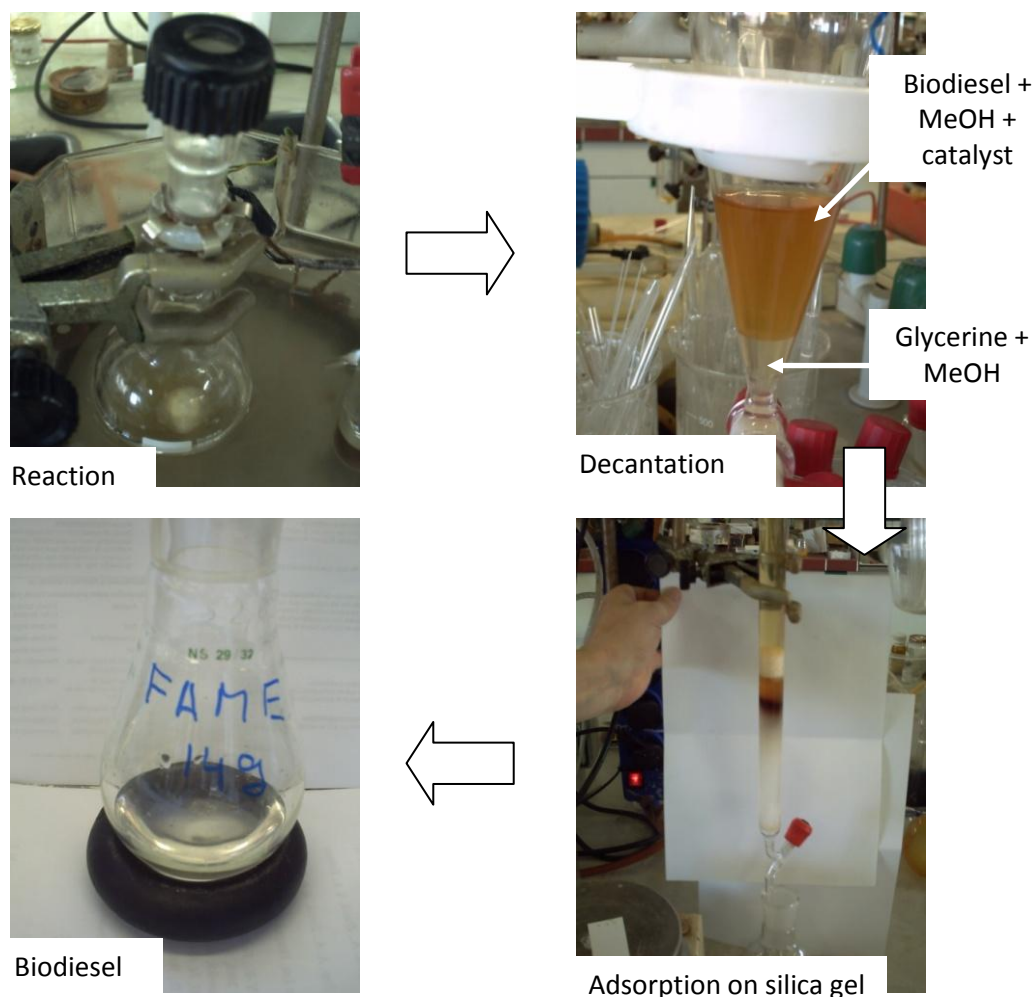


Figure 4.9. Pictures of the transesterification process and catalyst recovery.

4.2.11. Measure of the biodiesel acidity

For biodiesel to be marketed it must meet certain quality standards, and one of them is its acidity which must be below a minimum value.

Using methyl orange as indicator (pH 3.1-4.4) it could be observed that the crude biodiesel obtained upon completion of the reaction owned strong sulfonic acids, because it produced a colour change in the indicator. However, this colour change disappeared after performing the adsorption on silica gel to recover the catalyst.

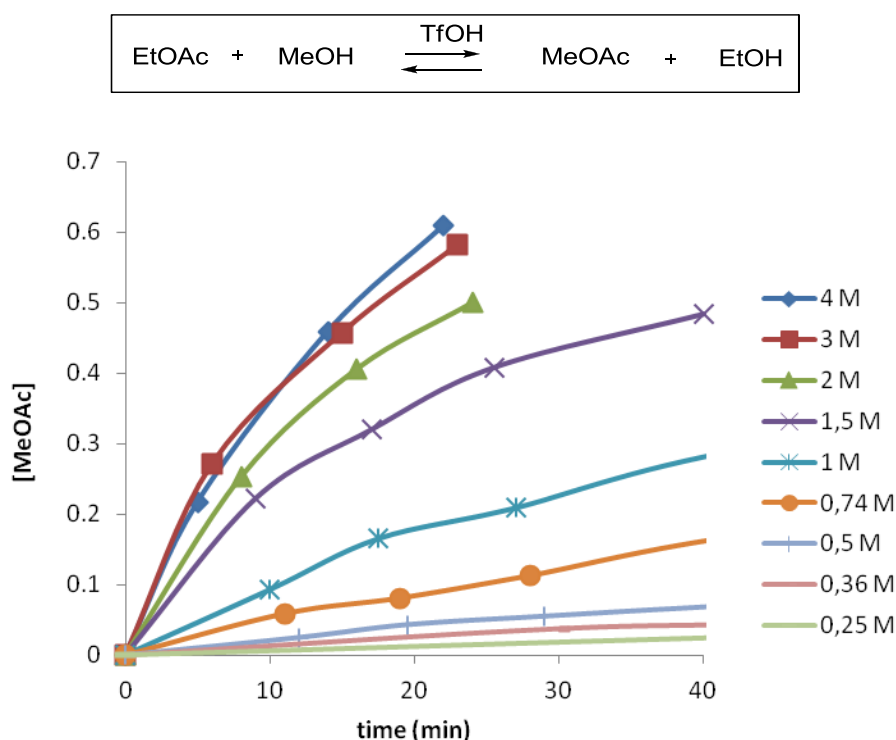
The determination of acid content in biodiesel was carried out following the procedure described in the UNE-EN 14104,¹⁵¹ providing an acidity of 0.16 mg KOH/g, a value that perfectly meets the requirements of ASTM D 6751 and EN 14214 standards, according to which the acidity of biodiesel must be below 0.5 mg KOH/g. Moreover, it was found that the acidity of *jatropha* oil used in the reaction was of 5.33 to 5.86 mg KOH/g.

¹⁵¹ UNE-EN 14104.

4.2.12. Study of the reaction mechanism

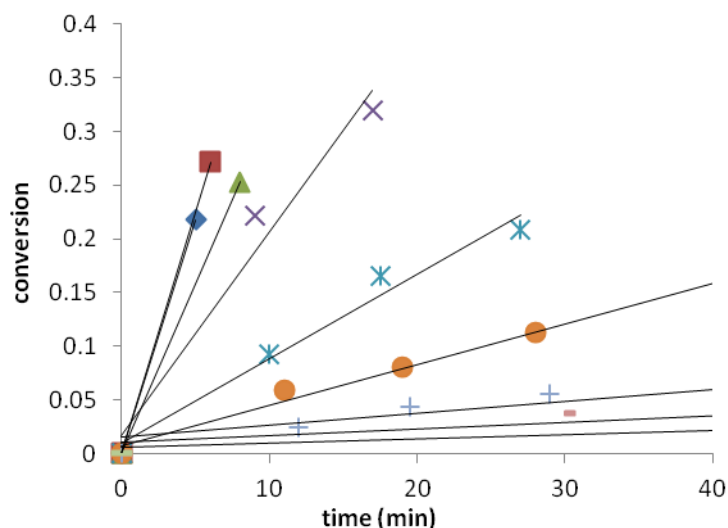
As the transesterification reaction catalysed by our sulfonic acids is performed in a non-polar medium, we thought that there could be some differences with the classical mechanism, so we decided to further study the mode in which sulfonic acid catalyse the reaction in an apolar solvent. To do this, we conducted several kinetics substituting triglyceride with a simpler ester. EtOAc was selected to facilitate the interpretation of the NMR spectra. So, we dissolved EtOAc and MeOH at different concentrations in CDCl_3 , in order to analyse the reaction with ^1H NMR. We employed triflic acid (TfOH) as acid catalyst, which is chloroform soluble.

Thus we prepared several NMR tubes in which we kept constant EtOAc and catalyst concentrations and changed MeOH amounts. The following graph shows how MeOAc concentration varies as function of time according to MeOH concentration.



Graph 4.12. Variation of the concentration of MeOAc versus time in function of MeOH concentration (legend). Triflic acid concentration was kept constant in all NMR tubes (1.13 M).

Then, we determined the initial rates of each of the kinetics. In the initial stages, the variation of the MeOAc concentration versus time can be approximated to a straight line whose slope corresponds to the rate constant.



Graph 4.13. Determination of the rate constants in the initial stages.

Carrying out the reactions in CDCl_3 , it is easy to know the concentration of each species by integration. Furthermore, we can estimate the rate of protonation of EtOAc and MeOH as a function of its chemical shift. Thus, it can be determined the concentration of protonated EtOAc, MeOAc and MeOH and the same for the unprotonated species.

According to the classic transesterification mechanism,¹³⁹ in the rate limiting step of the reaction a methanol molecule attacks a protonated molecule of EtOAc.

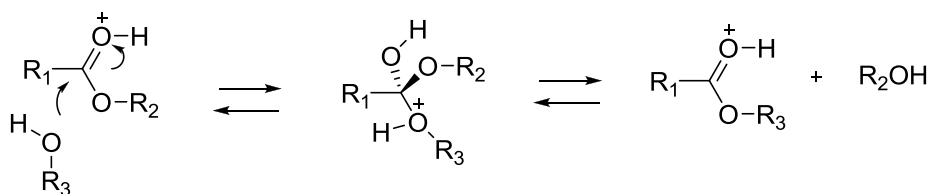
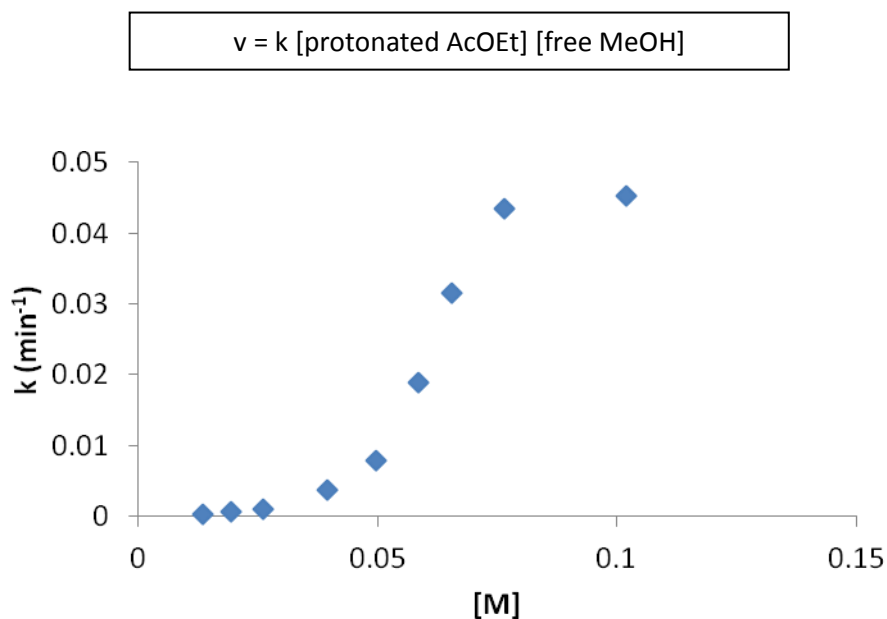


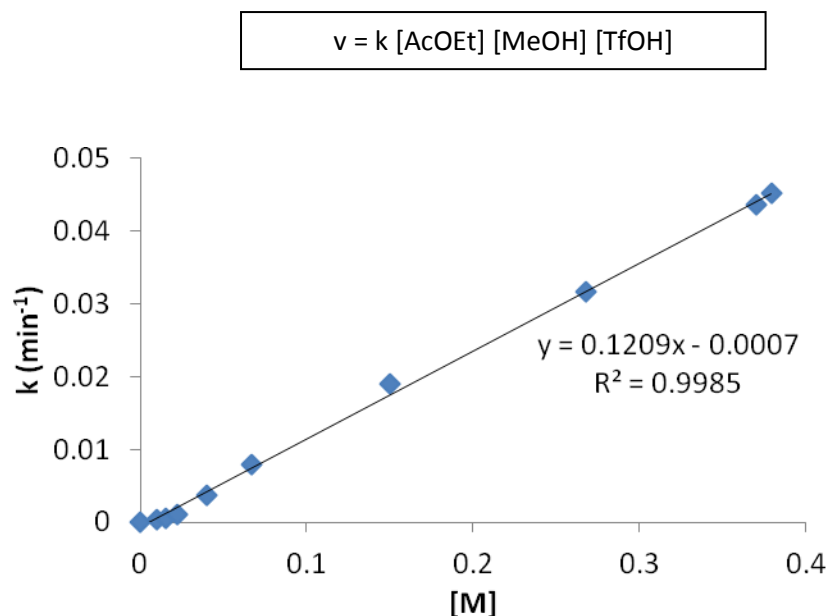
Figure 4.10. Classic transesterification mechanism.

If this mechanism is operational, the representation of the reaction rate against the concentration of protonated EtOAc and unprotonated MeOH should result in a straight line. However, a sigmoid curve was obtained, as can be seen in graph 4.14.



Graph 4.14 Graphic representation of the reaction rate of the transesterification between EtOAc and MeOH versus concentration of protonated EtOAc and neutral MeOH ($[M] = [\text{protonated EtOAc}] [\text{unprotonated MeOH}]$).

In no case we observed reaction rates proportional to the concentration of protonated EtOAc and free MeOH as the conventional mechanism indicates. Surprisingly, the best fit is obtained when the reaction rate against the concentration of neutral species is represented.



Graph 4.15. Graphic representation of the reaction rate of the transesterification between EtOAc and MeOH respect to the concentration of EtOAc, MeOH and neutral TfOH ($[M] = [\text{EtOAc}] [\text{MeOH}] [\text{TfOH}]$).

Therefore, we think that, perhaps, in a nonpolar medium such as the triglyceride, the classical carbonyl protonation mechanism may not be operative. In these less polar solvents

charged species may undergo complex aggregation states, which hinder their reactivity. This is, for example, the case of alkyl lithium compounds, which should be very nucleophilic, and they are not, but in the presence of HMPA recover their nucleophilicity because in this solvent the aggregates break down (figure 4.11).

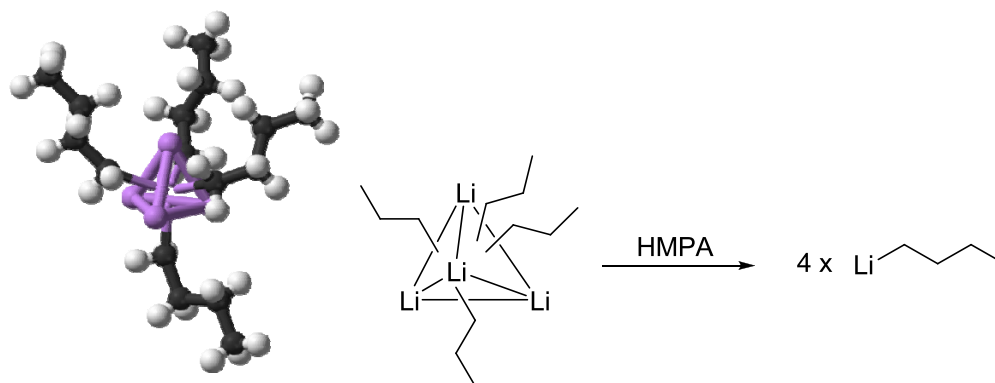


Figure 4.11. Aggregate of BuLi forming a tetrahedron and breaking of it in the presence of HMPA.

For these reasons we believe that an electrocyclic mechanism could be operative. In it, the acidic proton of the sulfonic acid is forming a hydrogen bond with the ester carbonyl while the alcohol hydroxyl establishes another hydrogen bond with one of the sulfonyl groups of the sulfonic acid. Thus, the electrophilicity of the ester is enhanced, while the nucleophilicity of methanol is increased, activating simultaneously the nucleophile and electrophile to the attack. Thus, the proton of the alcohol goes to the sulfonic acid while the sulfonic acid proton jumps to the tetrahedral intermediate. Finally, the tetrahedral intermediate evolves to the carbonyl compound (figure 4.12).

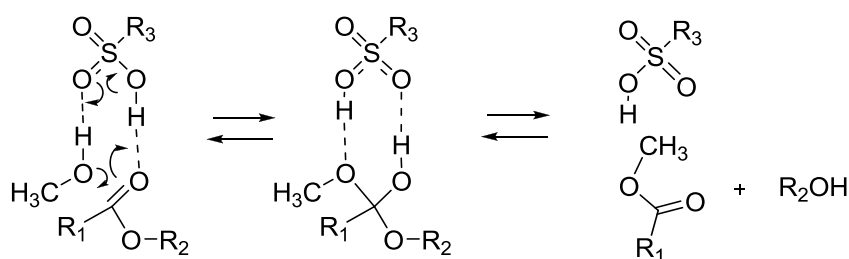
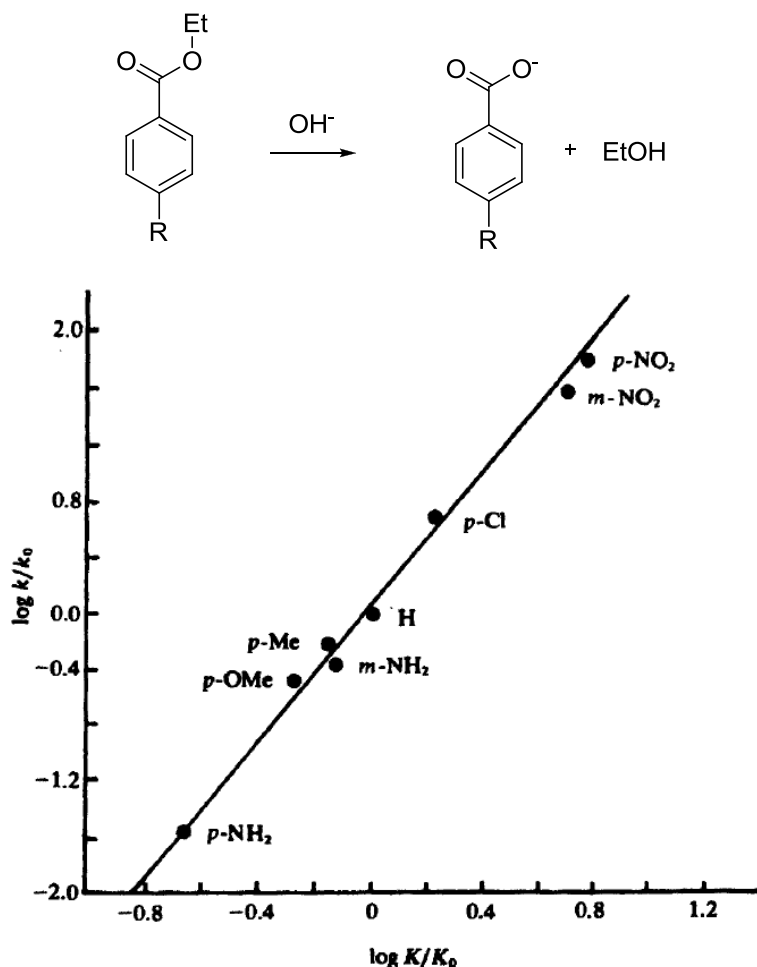


Figure 4.12. Proposed mechanism for transesterification in an apolar medium.

We have done other experiments that support the electrocyclic mechanism. In them we have used aromatic esters with different substituents on the ring. When the hydrolysis reactions occur via a conventional nucleophilic addition mechanism to the carbonyl, the literature shows that the nature of the substituent has a great importance in the reaction rate.¹⁵² This is the case of the benzoate hydrolysis in basic medium. Thus, for example, the relationship between the rates of hydrolysis of nitrobenzoate and methoxybenzoate is 150 (graph 4.16).

¹⁵² Hammett, L. P. *J. Am. Chem. Soc.* **1937**, *59*, 96-103.



Graph 4.16. Correlation between acid dissociation constants of different benzoic acids and alkali hydrolysis rate of the corresponding ethyl benzoates.

To perform a comparison under acidic conditions, we chose an ester with electron withdrawing substituents and one with a donor substituent, and we worked with an excess of *p*-toluenesulfonic acid, so that the carbonyls of both esters were protonated (figure 4.13). Under these conditions, the nitrobenzoate again becomes more reactive, as corresponds to a substrate which should have a low energy LUMO, but the difference in hydrolysis rates is very small, only a factor of 1.8, which indicates that the mechanism may not be the conventional nucleophilic addition to the carbonyl. An electrocyclic mechanism, which depends on the association of the three fragments, can better explain the small difference in reactivity.

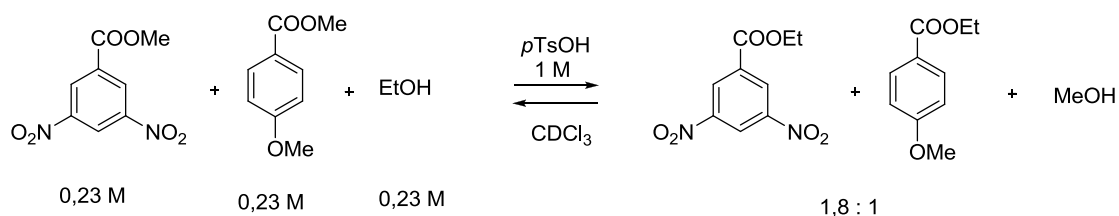
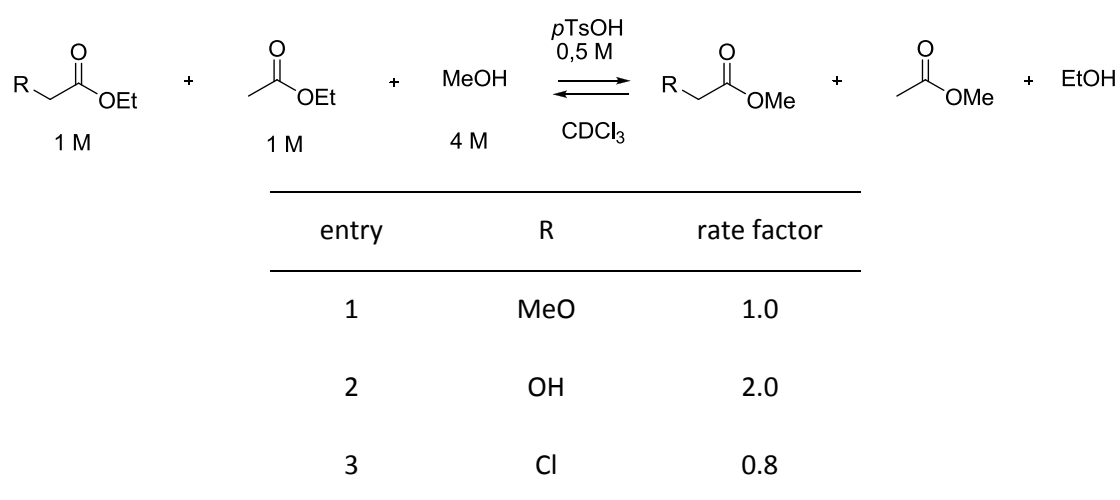


Figure 4.13. Competitive transesterification reactions of esters with withdrawing and electron donor substituents.

We have also studied the difference in the transesterification rate of aliphatic esters. The presence of a chlorine atom on the alpha carbon of the ester is expected to reduce the energy of the LUMO and consequently favour conventional nucleophilic addition to the carbonyl group. The experimental results show the opposite effect, the ethyl chloroacetate reacts more slowly than the ethyl acetate, while ethyl hydroxyacetate shows an increased reaction rate. Although the difference in reaction rates is very small, the explanation for the observed reactivity fits better with the electrocyclic mechanism, which depends on the hydrogen bond formation between the carbonyl and the sulfonic acid. Accordingly, the chloroacetate carbonyl is the worst hydrogen bond acceptor, due to the electron withdrawing effect of the chlorine atom.

Table 4.3. Relative transesterification rate of several esters with different alpha substitution versus ethyl acetate.



We also carried out kinetics to study the isotope effect. If the proton from methanol would be involved in the reaction rate limiting step, the reaction rate could be affected if the proton is exchanged for deuterium. However, carrying out the transesterification of EtOAc (1.0 M) in CDCl_3 with MeOH and MeOD (3.0 M) with *p*-toluenesulfonic acid as catalyst (10 mol %) no significant change in the reaction rate was detected. This result does not support neither discard the proposed electrocyclic mechanism, since early or late proton transfers can yield small isotopic effects.

To study the hypothesis of an electrocyclic mechanism we carried out quantum mechanical calculations,¹⁵³ which showed that it is entirely possible a transition state for concerted transesterification of esters in the gas phase. The activation barrier found was 24 kcal/mol for benzenesulfonic acid. It should be mentioned that attempts to obtain ionic transition states, in which the carbonyl group was protonated, were unsuccessful, despite including in the model low polarity solvents, using conventional solvation models. Only when explicitly molecules of methanol or ether were included in the calculations, transition states were obtained, but higher in energy. In any case, it is unlikely the presence of these additional molecules in the apolar medium.

¹⁵³ Quantum mechanical calculations (B3LYP/6-31G**) carry out by Dr. Luis Manuel Simón.

higher in energy. In any case, it is unlikely the presence of these additional molecules in the apolar medium.

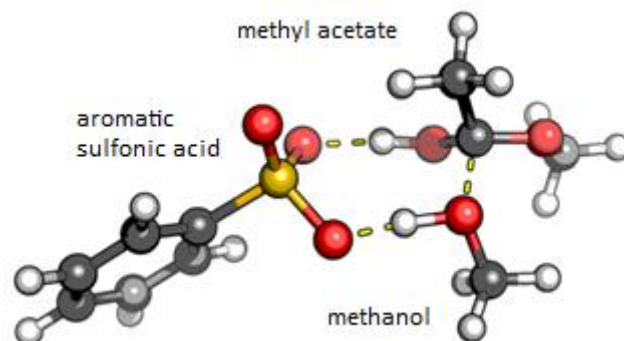


Figure 4.14. Transition state obtained by molecular calculations for the transesterification reaction between methanol and methyl acetate (model compounds) catalysed by benzenesulfonic acid (B3LYP/6-31G **).

Although an electrocyclic mechanism for esters hydrolysis may seem an unusual proposal, such mechanisms have already been described in the literature for similar cases. In 2007, Simon and Goodman¹⁵⁴ proposed an electrocyclic mechanism for the polymerization of lactones catalysed by guanidines, such as TBD (triazabicyclo[4.4.0]dec-5-ene) in an apolar medium. The reaction is similar to a transesterification, and the guanidine acts as a bifunctional catalyst, on one hand increasing the electrophilicity of the carbonyl by formation of a hydrogen bond and, secondly, as a base abstracting the proton of the methanol molecule which acts as the nucleophile.

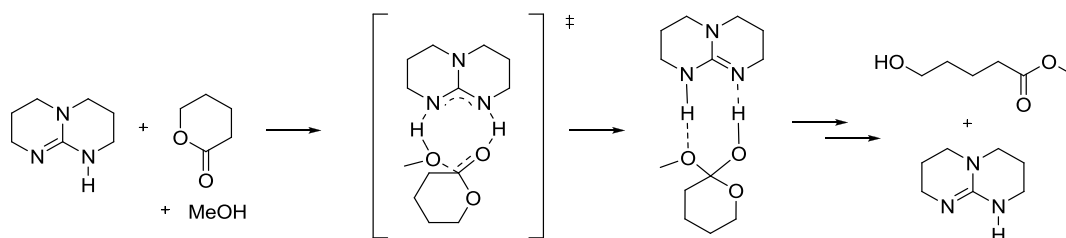


Figure 4.15. Lactone polymerization reaction catalysed by TBD following an electrocyclic mechanism.

In 2010, Bourissou and Maron¹⁵⁵ hold a computationally calculation for the ϵ -caprolactone polymerization catalysed by sulfonic acids and propose a similar mechanism to that of TBD. In their mechanism the sulfonic acid also acts as a bifunctional catalyst, transferring a hydrogen and accepting an H-bond from methanol. Quantum mechanical calculations performed show that the activation of the molecule of MeOH forming a hydrogen bond with the sulfonic basic oxygen reduces the activation energy of the nucleophilic addition in 21.5 kcal/mol.

¹⁵⁴ Simón, L.; Goodman, J. J. *Org. Chem.* **2007**, 72, 9656-9662.

¹⁵⁵ Susperregui, N.; Delcroix, D.; Martin-Vaca, B.; Bourissou, D.; Maron, L. *J. Org. Chem.* **2010**, 75, 6581-6587.

This would agree with the fact that two acids with different acidities (more than 10 pK_a units of difference)¹⁵⁶ such as methanesulfonic acid ($pK_a = 1.6$ in DMSO) and trifluoromethanesulfonic acid ($pK_a = 0.3$ in DMSO) carried out polymerization of ϵ -caprolactone at similar rates.¹⁵⁷

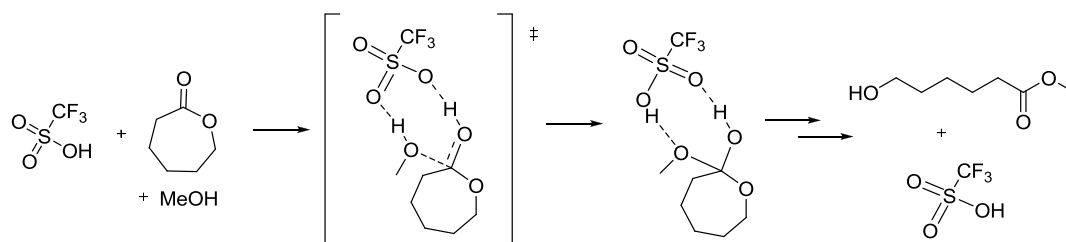


Figure 4.16. Polymerization reaction of ϵ -caprolactone catalysed by triflic acid following an electrocyclic mechanism.

In the literature there are many more reactions in which a sulfonic acid may act according to an electrocyclic mechanism, releasing on the one hand an acidic proton and capturing another proton in one of its sulfonyl groups. In 2008, Norrby and Ellervik¹⁵⁸ performed an experimental and theoretical study of the nucleophilic aromatic substitution of β -naphthol with propylthiol catalysed by *p*-toluenesulfonic acid. The mechanism in polar solvents is assumed to be similar to the Bucherer reaction,¹⁵⁹ in which charged species are formed. However, when the reaction is carried out in nonpolar solvents, this mechanism is not operative (energies of more than 200 kJ/mol are estimated). In the proposal of these authors, the sulfonic acid has a dual role: first protonating the carbonyl group and also accepting a hydrogen atom from the thiol (figure 4.17).

¹⁵⁶ (a) Bordwell, F. G. *Acc. Chem. Res.* **1988**, *21*, 456-463; (b) Patai, S.; Rappoport, Z. *The Chemistry of Sulphonic Acids, Esters and their Derivatives*; John Wiley and Sons: New York, 1991; p 251.

¹⁵⁷ Gazeau-Bureau, S.; Delcroix, D.; Martín-Vaca, B.; Bourissou, D.; Navarro, C.; Magnet, S. *Macromolecules* **2008**, *41*, 3782-3784.

¹⁵⁸ Jacobson, M.; Oxgaard, J.; Abrahamsson, C.-O.; Norrby, P.-O.; Goddard III, W. A.; Ellervik, U. *Chem. Eur. J.* **2008**, *14*, 3954-3960.

¹⁵⁹ Bucherer, H. T. *J. Prakt. Chem.* **1904**, *69*, 49-91.

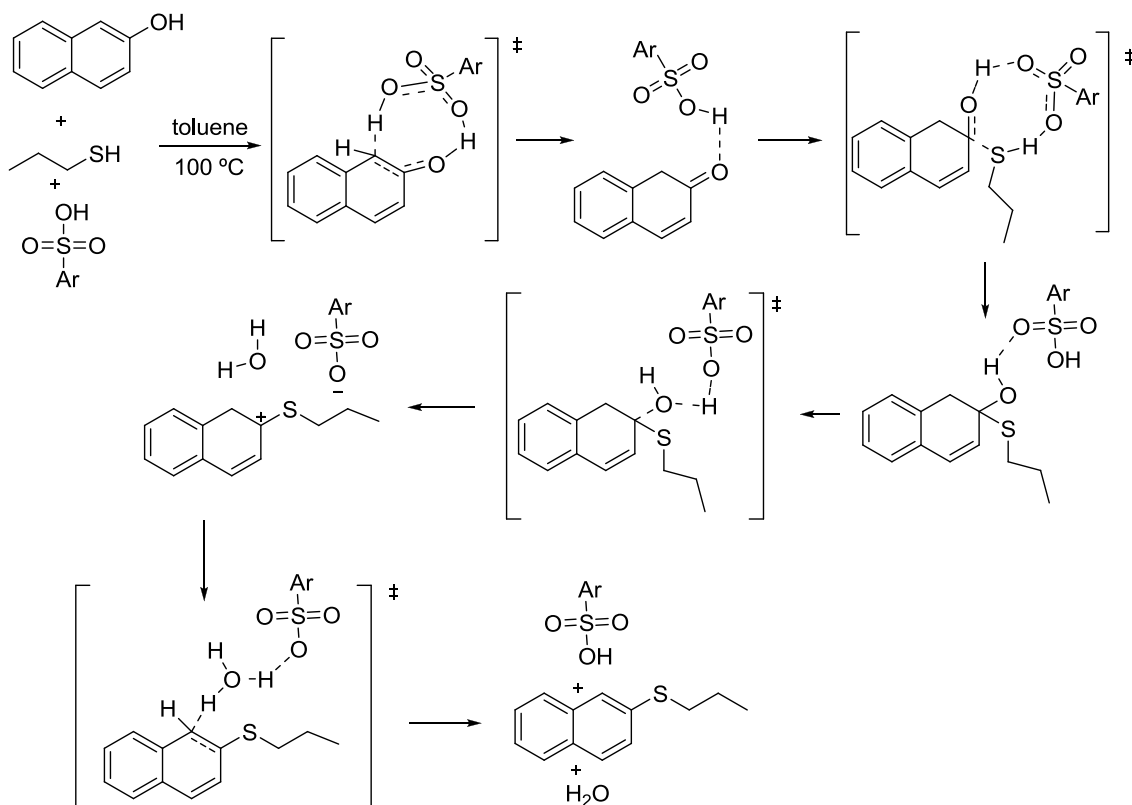


Figure 4.17. Aromatic nucleophilic substitution reaction catalysed by *p*-toluenesulfonic acid.

In 2008, Yu¹⁶⁰ performed a similar study to the addition of phenols and protected amines to olefins catalysed by Brønsted acids. The proposed mechanism involves an eight member ring transition state for the addition of phenol or amine to the double bond.

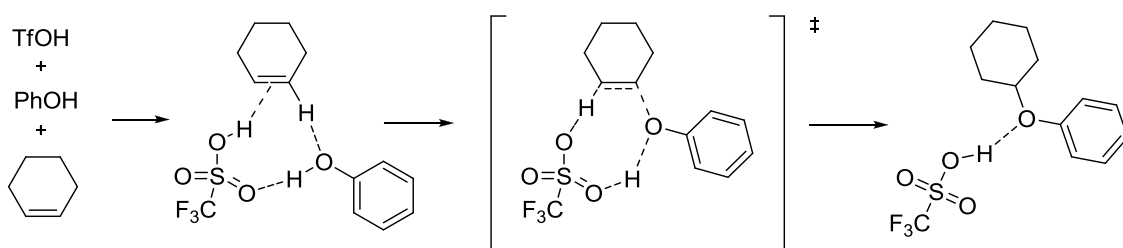


Figure 4.18. Addition reaction of phenols to double bonds catalysed with triflic acid.

This electrocyclic mechanism has also been proposed to explain the enantioselective polymerisation of *rac*-lactide in the presence of binolphosphoric acids. Thus, according to Terada and Satoh,¹⁶¹ phosphoric acid activates the carbonyl group of the monomer, and also the hydroxyl group of the propagating chain. These interactions are demonstrated by NMR and IR spectra (figure 4.19).

¹⁶⁰ Li, X.; Ye, S.; He, C.; Yu, Z.-X. *Eur. J. Org. Chem.* **2008**, 4296-4303.

¹⁶¹ Makiguchi, K.; Yamanaka, T.; Kakuchi, T.; Terada, M.; Satoh, T. *Chem. Commun.* **2014**, 50, 2883-2885.

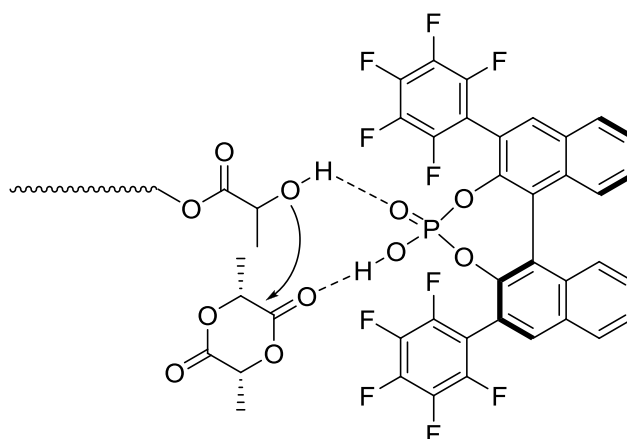


Figure 4.19. Proposed reaction mechanism for the polymerization of rac-lactide catalyzed by a binolphosphoric acid.

A similar mechanism might explain the kinetic resolution of hydroxy esters and the desymmetrization of γ -hydroxyl diesters reported by Petersen.¹⁶²

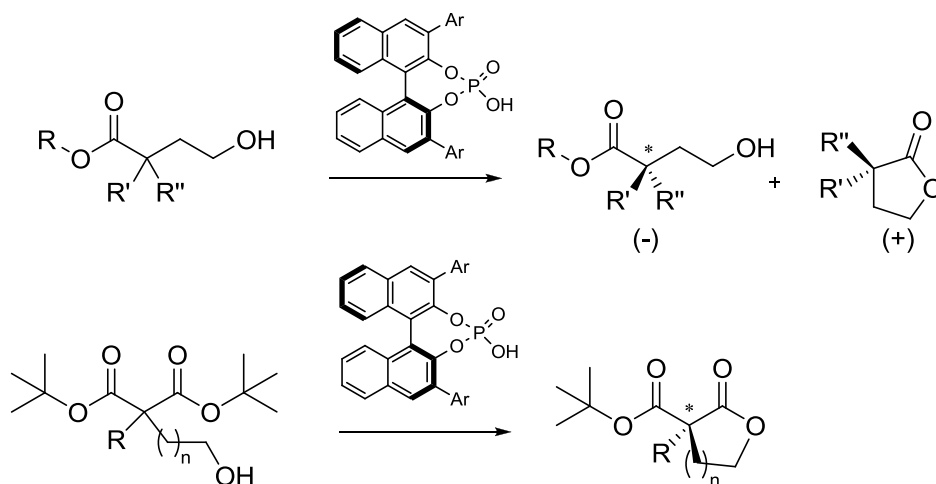


Figure 4.20. Other reactions catalyzed by binolphosphoric acids according to an electrocyclic mechanism.

4.2.13. Catalysts with two sulfonic acids

Despite the good results obtained in the transesterification reaction with catalysts **63-65**, we believe that the associate concentration between the catalyst and the ester is small, because the sulfonic acids have a greater tendency to protonate methanol than the ester carbonyl group, according to its pK_a values.¹⁶³ To verify this fact we conducted a competitive titration with ^1H NMR in CDCl_3 between methanol and ethyl acetate by adding increasing amounts of

¹⁶² (a) Qabaja, G.; Wilent, J. E.; Benavides, A. R.; Bullard, G. E.; Petersen, K. S. *Org. Lett.* **2013**, *15*, 1266-1269; (b) Wilent, J.; Petersen, K. S. *J. Org. Chem.* **2014**, *79*, 2303-2307.

¹⁶³ (a) Olmstead, W. N.; Margolin, Z.; Bordwell, F. G. *J. Org. Chem.* **1980**, *45*, 3295-3299; (b) Zhang, X. M.; Bordwell, F. G.; Van Der Puy, M.; Fried, H. E. *J. Org. Chem.* **1993**, *58*, 3060-3066.

triflic acid. Under these conditions, a constant ratio of 14 is observed for methanol protonation, so the natural tendency of hydrogen bonds formation is the opposite of the one needed in the electrocyclic mechanism.

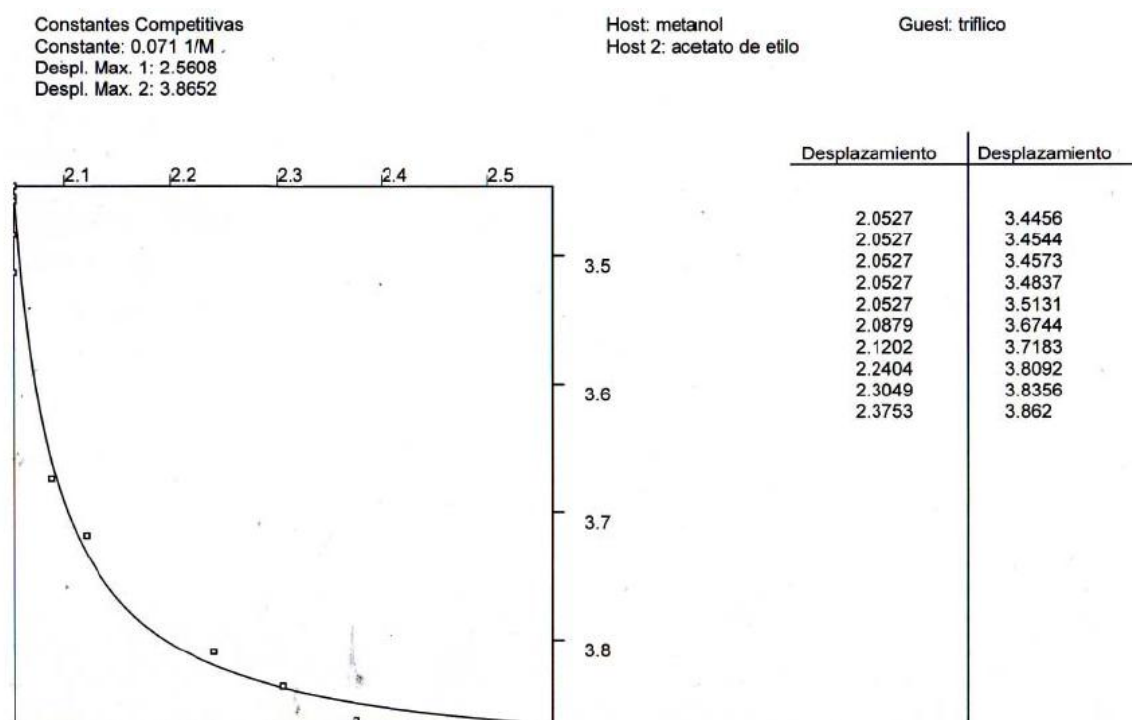


Figure 4.21. Competitive titration between methanol and ethyl acetate versus triflic acid (CDCl_3 , 20 °C).

This is disadvantageous because in the proposed mechanism, the sulfonic acid must form a hydrogen bond with the carbonyl of the ester as well as methanol must form another hydrogen bond with one of the S=O groups of the sulfonic acid.

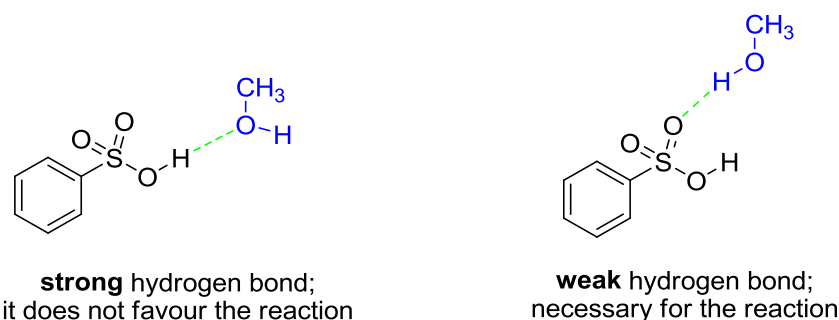


Figure 4.22. (Left) Strong hydrogen bond formed spontaneously in a nonpolar medium and (right) weak bond required for transesterification.

According to the electrocyclic mechanism, it is necessary to form an associate between one carbonyl in the triglyceride and the sulfonic acid catalyst. To get an idea of the strength of this associate we measured an absolute titration between catalyst **63** and ethyl acetate in CDCl_3 . Ethylacetate was chosen to facilitate interpretation of the NMR signals. Therefore, ethyl acetate was added on a catalyst solution in CDCl_3 , observing the deshielding of the catalyst

signals. Representing the increase of these displacements versus the equivalents of ethyl acetate, an association constant of 34 M^{-1} was obtained.

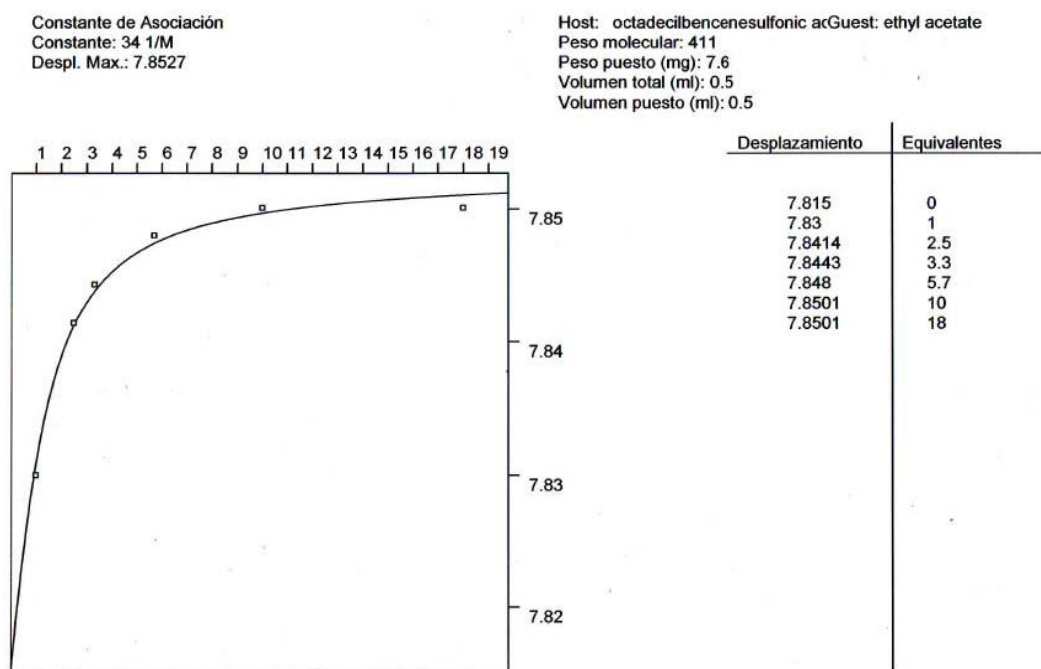


Figure 4.23. Absolute titration of catalyst **63** with ethyl acetate in CDCl_3 at $20 \text{ }^\circ\text{C}$.

The value of the constant is high enough to form the associate in the pure triglyceride; however, the presence of methanol necessary to carry out the reaction will reduce the stability of the associate, competing for the H-bonds. So, we thought that sulfonic acids with additional functional groups to form more hydrogen bonds with the carbonyl of the ester should exhibit a higher association constant and thus could improve the catalytic activity.

It is here where the oxyanion hole of our receptors comes into play. However, almost all receptors designed in our research group have amides or ureas in its structure to generate acids NHs capable of giving rise to hydrogen bonds. Amides and ureas have basic carbonyl groups and they accept the proton of the sulfonic acid catalyst, so acidity is lost and the reaction rate becomes slow.

A possible solution to this problem would be the use of sulfonamides as hydrogen bond donors, since they do not undergo protonation by sulfonic acids.

So, the first idea was to carry out the sulfonation of a xanthene, which had offered good results in our research group. However, in this case, the xanthene functionalization with sulfonic acids or sulfonamides generates intramolecular hydrogen bonds, collapsing the oxyanion-hole structure, as seen in figure 4.24. Using molecular modelling, we have found that, indeed, the cavity is closed, being the activation barrier of the transesterification catalysed with this compound of 40 kcal/mol , while the barrier presented by benzenesulfonic acid is only 24 kcal/mol . The formation of intramolecular hydrogen bonds justifies this phenomenon as they are lost in the transition state.

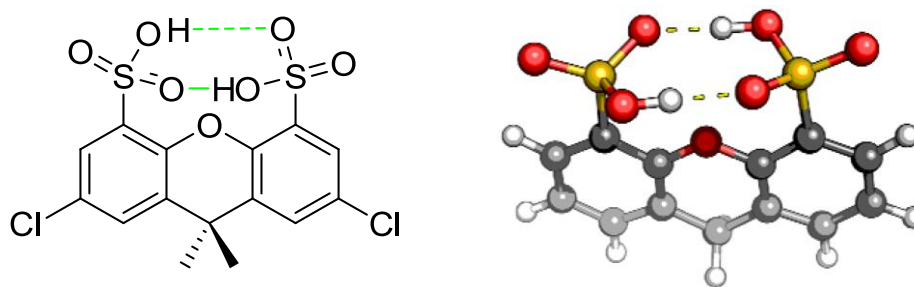


Figure 4.24. (Left) Disulfonated xanthene skeleton and (right) molecular modelling of the compound in which intramolecular hydrogen bonds are shown (B3LYP/6-31G **).

To avoid formation of intramolecular hydrogen bonds in the catalyst we considered several skeletons, which are shown in figure 4.25.

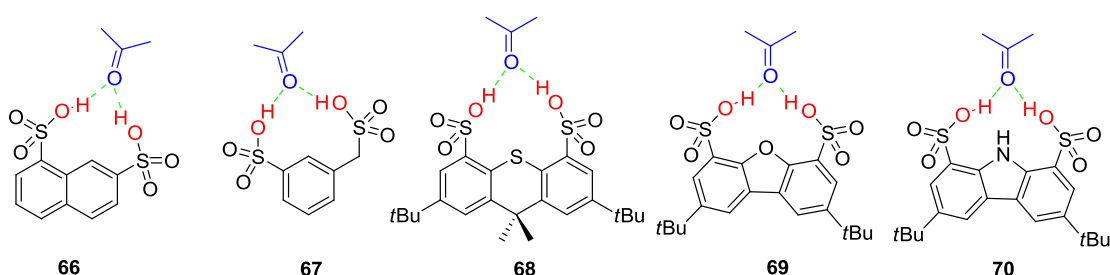


Figure 4.25. Other skeletons with two sulphonic groups and similar geometry to that of the oxyanion holes of enzymes.

Compounds **66**, **68** and **69** were difficult to synthesize, so preparation was postponed. Regarding receptor **67**, it has many degrees of freedom, so it may be, a priori, less suitable than the other catalysts, which have a more rigid structure. Therefore, we focus on the carbazole, which is a cheap commercial compound and easy to functionalize. Most functionalized carbazoles employed in molecular recognition have two amino groups at positions 1 and 8, however, they are too far apart to produce an oxyanion hole (figure 4.26). To solve this problem we decided to sulfonate the carbazole. This allows the creation of a smaller cavity, making the distances more similar to that of the oxyanion holes of enzymes.

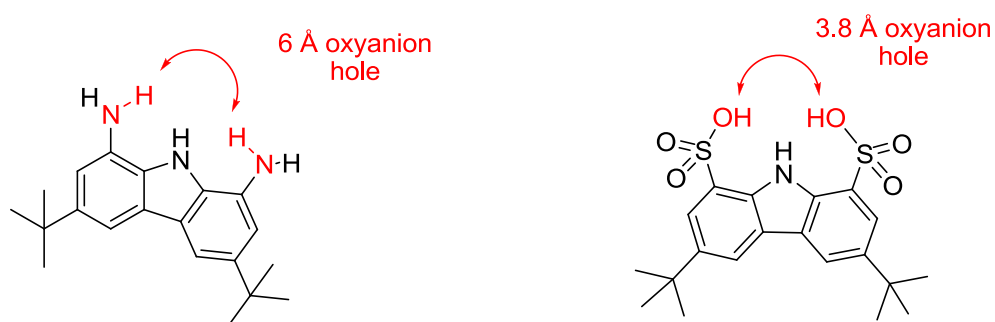


Figure 4.26. Possible oxyanion holes from functionalized carbazoles.

Since the exact geometry and the distance between the carbazolesulfonic OHs were the key to get a suitable catalyst, we tried to obtain the crystal structure of carbazolesulfonic acid. We achieved suitable crystals slowly evaporating a methanol/water solution, and the

study of X-ray diffraction showed that the compound was promising. Its structure is shown in figure 4.27 and it can be seen that the sulfonic acids protonate water molecules, so that this compound is obtained as the corresponding disulfonate. As the sulfonic acid groups are negatively charged, they become good hydrogen bond acceptors, so that the oxygen atoms from the sulfonyl appear very close to the carbazole NH (2.7 and 2.8 Å), forming strong hydrogen bonds. The distance between the sulfonyl oxygens which form the oxyanion hole is short, only 3.8 Å, but a small rotation of the sulfur-carbon bonds should leave the right size.

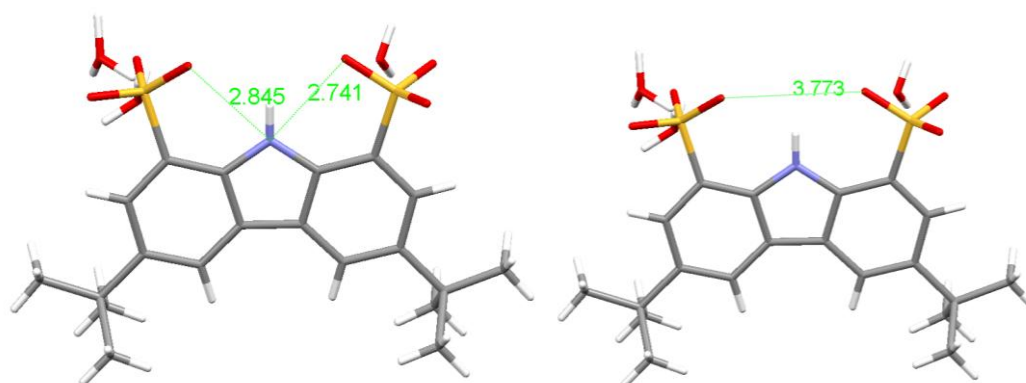


Figure 4.27. Structure of carbazolesulfonic acid **70** obtained by X-ray diffraction.

Since the aim was to get the associate with a carbonyl group, we tried to carry out the crystallization of carbazolesulfonic acid with several guests, in the absence of water. The possibility to obtain suitable crystals with ethyl acetate, acetone, dimethylformamide, acrylamide and cinnamamide was studied.

Both acrylamide and cinnamamide were suitable to obtain crystals for X-ray analysis, however, the structure obtained showed no carbonyl in the position we hoped. Figure 4.28 shows the X-ray representations of the complexes formed with cinnamamide.

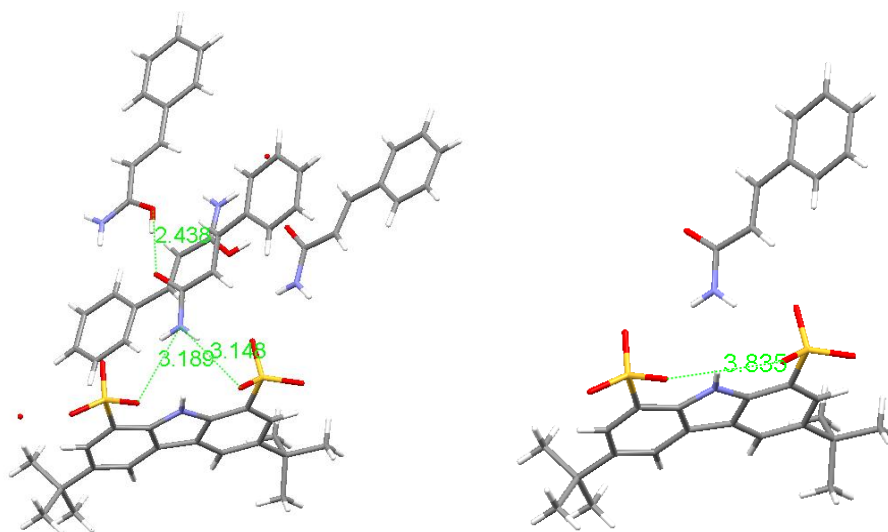


Figure 4.28. X-ray structure of the complex formed between cinnamamide and the disulfonated receptor **70**.

In the crystalline state there is transfer of a proton from one of the sulfonic acid groups to the carbonyl of the cinnamamide, which makes a hydrogen bond with another cinnamamide carbonyl group. The amino group of the protonated cinnamamide, which is an excellent hydrogen bond donor, occupies the corresponding position in the oxyanion hole, with distances of 3.1 and 3.2 Å to the sulfonyl group oxygens. The distance between the oxygens of the sulphonyl is again small, 3.8 Å, because they close the intramolecular hydrogen bond with the carbazole NH, but it seems appropriate for an oxyanion hole, as it forms hydrogen bonds with the cinnamamide NHs.

Although in the crystalline state the carbazolesulfonic acid did not associate the carbonyl group as we had hoped, we conducted a preliminary study in an NMR tube to study the catalytic activity of receptor **70** in the transesterification between ethyl acetate and methanol.

The kinetic study showed that compound **70** had a catalytic activity similar to that of *p*-toluenesulfonic acid, which was initially surprising to us, because we thought that it should associate the ester carbonyl with two hydrogen bonds.

We believe the reason why carbazolesulfonic **70** is a poor catalyst for the transesterification reaction is because it preferably associates methanol molecule, as shown in figure 4.29.

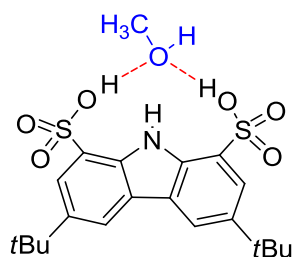
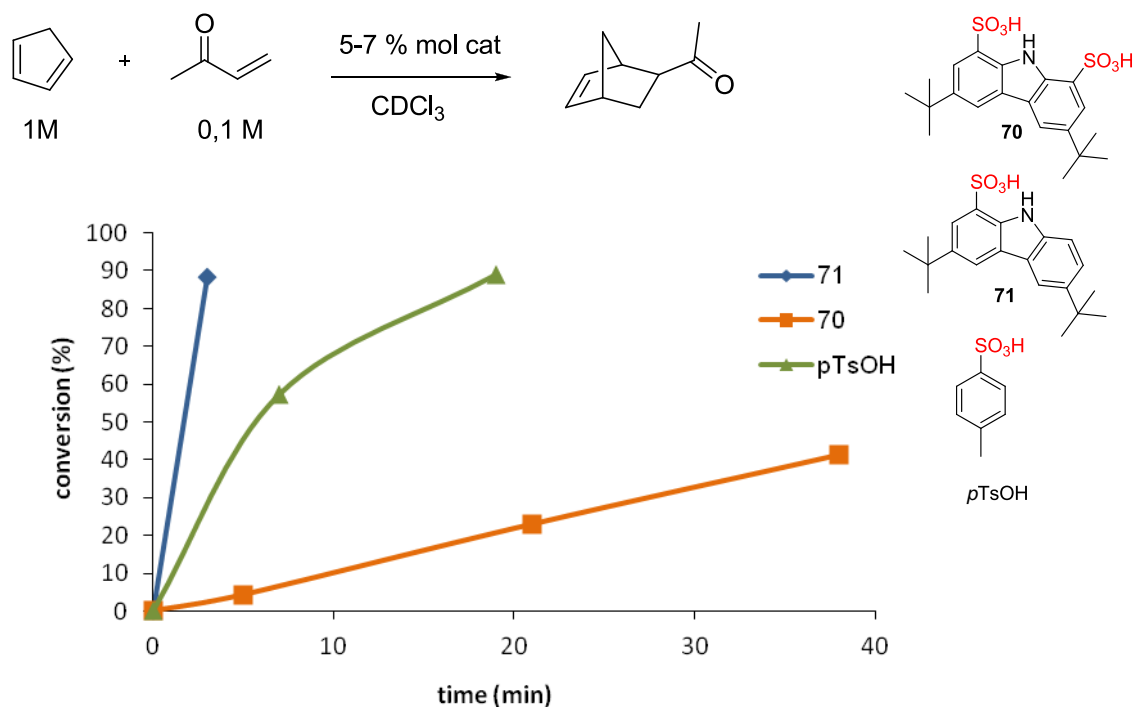


Figure 4.29. Complex formed between carbazolesulfonic acid **70** and methanol.

We have attempted to measure the association constant between methanol and carbazolesulfonic acid **70**, however, it has not been possible because this receptor is highly insoluble in chloroform. However, the high affinity that this compound has for methanol has been confirmed because the presence of methanol in chloroform allows dissolving just one equivalent of carbazolesulfonic acid **70**.

In the absence of a reagent with the structure of methanol, the catalyst itself has shown very good results. For example, it catalyses the Diels-Alder reaction between cyclopentadiene and methylvinylketone.¹⁶⁴ In this reaction, the oxyanion hole only can choose the associate with the carbonyl group, which is activated due to the formation of two H-bonds.

¹⁶⁴ H. Rubio, O. *Organocatalysts for Diels-Alder reactions with oxyanion-hole structure*; Final Master Project: University of Salamanca, 2011.



Graph 4.17. Diels-Alder reaction catalysed by **70**, **71** and *p*TsOH.

In the above figure it can be seen that the presence of two sulfonic acids on carbazole is very important to have a good catalytic activity, because the carbazolemonosulfonic acid is a worse catalyst than *p*-toluenesulfonic acid, which is logical because carbazole nitrogen must act as electron donating group, reducing the acidity of the sulfonic acid.

Another piece of evidence supporting the carbazole as a suitable oxyanion hole is that when the sulfonic acids are replaced by sulfonamides, it becomes an excellent anion receptor, with association constants of up to $7.9 \times 10^6 \text{ M}^{-1}$.¹⁶⁵

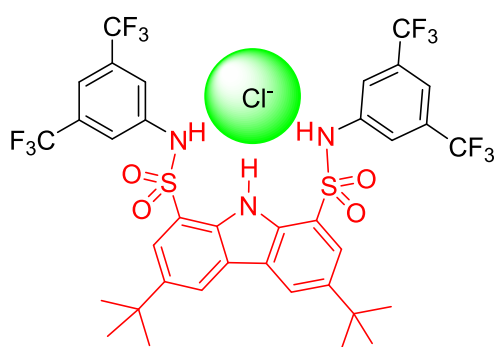


Figure 4.30. Anion receptor based on a carbazole skeleton developed in our research group.

¹⁶⁵ Fuentes de Arriba, Á. L.; Turiel, M. G.; Simón, L.; Sanz, F.; Boyero, J. F.; Muñiz, F. M.; Morán, J. R.; Alcázar, V. *Org. Biomol. Chem.* **2011**, *9*, 8321-8327.

The carbazoledisulfonic acid has also been used as a structural fragment in a macrocycle for enantioselective amino acid extraction.¹⁶⁶

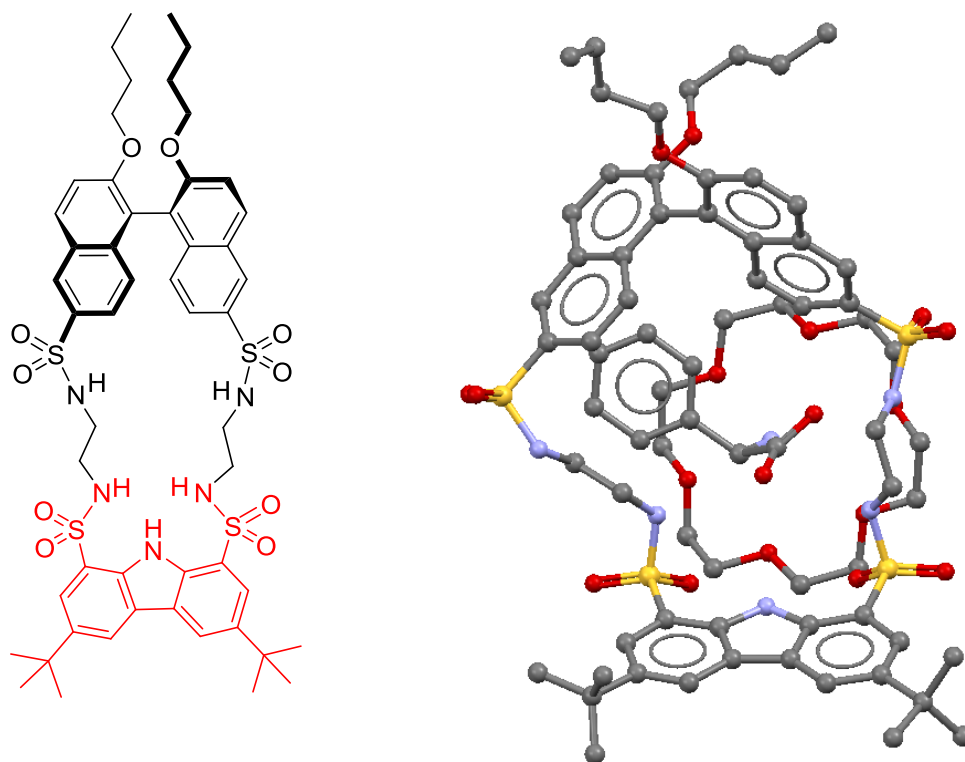


Figure 4.31. (Left) Macrocycle formed with a carbazole unit and (right) X-ray structure of the complex formed with D-phenylglycine and 18-crown-6-ether.

According to the above results, methanol competes with the carbonyl of the ester for receptor **70**. Methanol oxygen has a relatively similar geometry to the ester carbonyl, and also fits well into the oxyanion hole. Without formation of hydrogen bonds between the catalyst and the carbonyl of the ester, which is displaced by methanol, the effect of the sulfonic acid catalyst is inhibited.

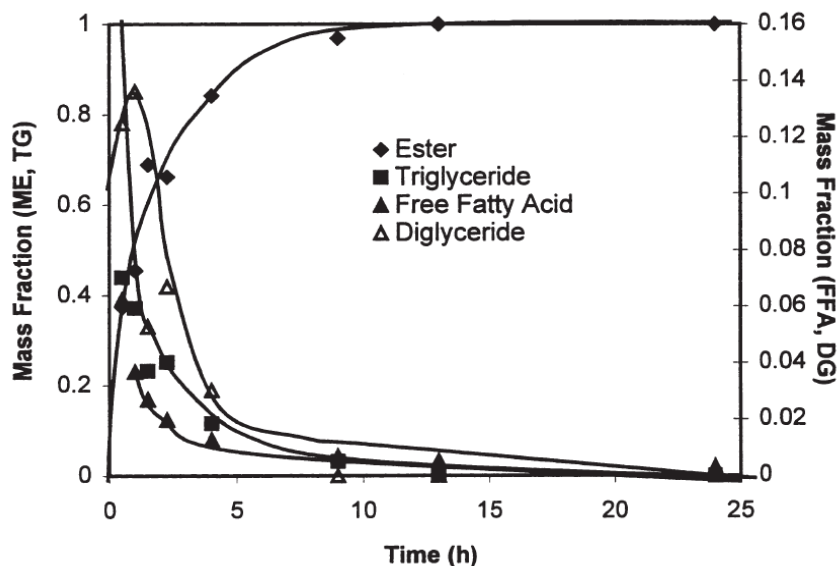
At this point, we thought that one way to solve this problem would be to propose catalysts able to form additional hydrogen bonds with the carbonyls of the triglyceride, so that the cooperative effect of multiple hydrogen bonds could increase the affinity of the catalyst compared to the triglyceride respect to methanol, avoiding competition for the latter.

Although one might expect that a very active catalyst in the transesterification of triglycerides should be inactive in the transesterification of monoglycerides, this is not the case, because according to literature,¹⁶⁷ the rate limiting step of triglycerides transesterification is the first attack of the alcohol; that is, the reaction of triglyceride to diglyceride is slower than the reactions of di- and monoglycerides. Thus, it has been found activation barriers of 15.5 kcal/mol for converting triglycerides to diglycerides and 11.2 and

¹⁶⁶ Turiel, M. G. *Carbazole based receptors with sulfonamide functions for anion association*; Final Degree Project: University of Salamanca, 2013.

¹⁶⁷ Freedman, B.; Butterfield, R. O.; Pryde, E. H. *J. Am. Oil Chem. Soc.* **1986**, *63*, 1375-1380.

11.6 kcal/mol for the transformations of diglycerides to monoglycerides and then to glycerine, respectively. In graph 4.18 it is showed how the concentrations of these species change in a transesterification reaction catalysed by sulphuric acid.¹⁶⁸ It can be seen how methyl esters are more easily obtained than diglycerides, while monoglycerides do not even show up.



Graph 4.18. Graphic representation of triglyceride, diglyceride and free fatty acid methyl esters concentrations versus time in a transesterification reaction catalysed by sulphuric acid.

To design these new catalysts it is necessary to know the exact geometry that adopts the triglyceride in solution. We have conducted several modelling studies to analyse the possible conformations of the triglyceride, which approximate fairly well to the proposals in the literature.¹⁶⁹

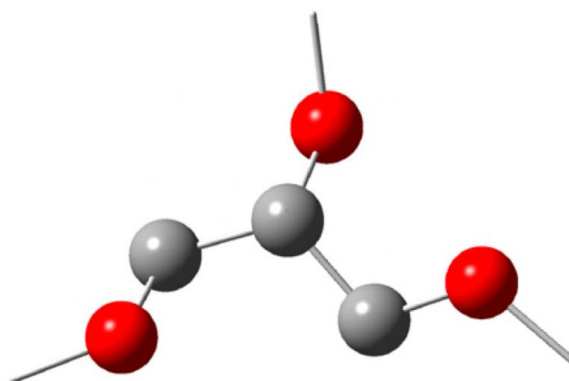


Figure 4.32. More stable conformation of triglycerides in solution (DFT).

Based on these modelling studies, the preparation of several disulfonic acids were proposed, which are shown in figure 4.33.

¹⁶⁸ Goff, M. J.; Bauer, N. S.; Lopes, S.; Sutterlin, W. R.; Suppes, G. J. *J. Am. Oil Chem. Soc.* **2004**, *81*, 415-420.

¹⁶⁹ Limpanuparb, T.; Punyain, K.; Tantirungrotechai, Y. *J. Mol. Struct. (THEOCHEM)* **2010**, *955*, 23-32.

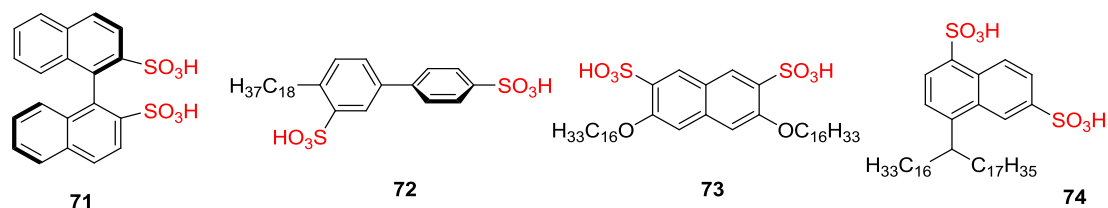


Figure 4.33. Disulfonic acid studied in the transesterification of triglycerides.

Compound **71** can be easily obtained from 1,1'-binaphthyl by the method described in the literature.¹⁷⁰ The preparation of compounds **72-74** is summarized in figure 4.34.

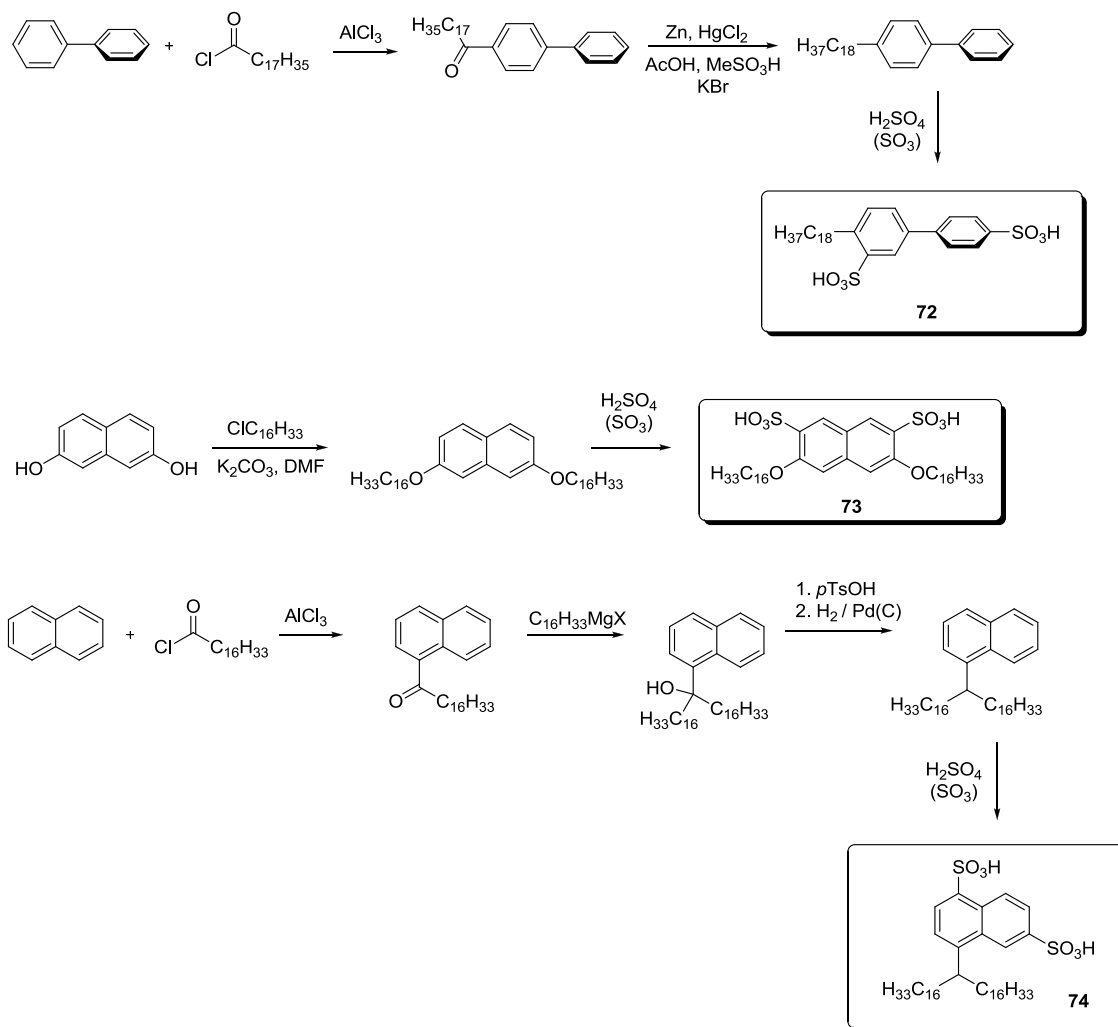
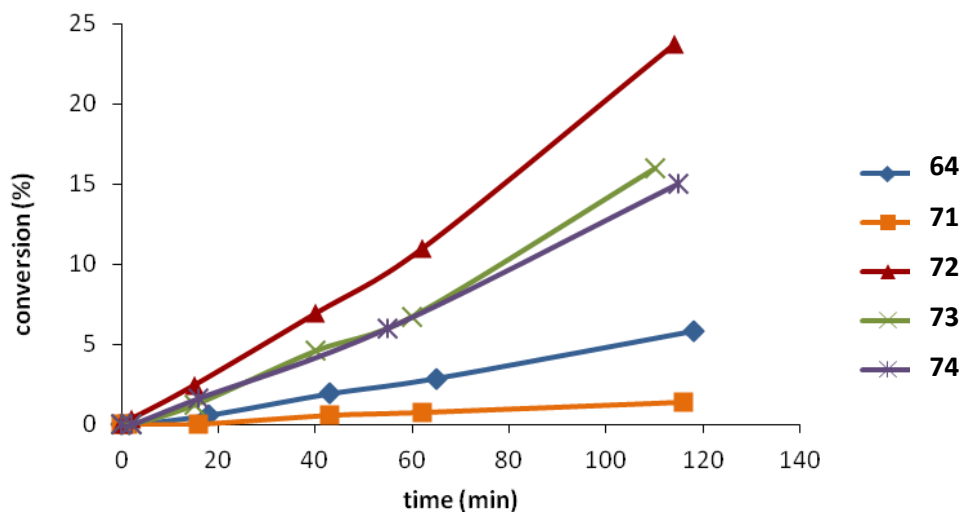


Figure 4.34. Synthesis of several disulfonic acids studied in the transesterification of triglycerides.

To facilitate interpretation of the NMR spectra, we substituted triglycerides by triacetin (glycerine triacetate), and we carried out the study of the catalytic activity of the above catalysts **71-74** in the transesterification of triacetin (1.6 M) with MeOH (4.9 M) with 5 mol%

¹⁷⁰ García-García, P.; Lay, F.; García-García, P.; Rabalakos, C.; List, B. *Angew. Chem., Int. Ed.* **2009**, *48*, 4363-4366.

catalyst at 20 °C in CDCl_3 . In this way we could follow the reaction almost in real time with just one spectrum. Catalyst **64**, which only has a sulfonic acid group, was used as a reference.



Graph 4.19. Triacetin transesterification with methanol catalysed by disulfonic acids.

In view of the results obtained, it is surprising that the catalytic activity of catalyst **71** is even lower than sulfonic acid **64**, but is likely the formation of an intramolecular hydrogen bond between the two sulfonic acid groups that reduces its activity.

It can be seen that catalyst **72** has a greatly improved catalytic activity in comparison to the reference **64**, although perhaps less than expected if the association takes place with two carbonyl groups of the triacetin.

Catalysts **73** and **74** have a similar activity, tripling compound **64** catalytic activity. However, it is considered that the effect of association is small, because with two sulfonic groups it would be expected double catalytic activity. Therefore, although it has been achieved an improvement in the reaction rate, we believe that it could be further increased.

Due to the fact that catalyst **72** is not sufficiently soluble in the triglyceride, another chain was introduced into its structure (figure 4.35).

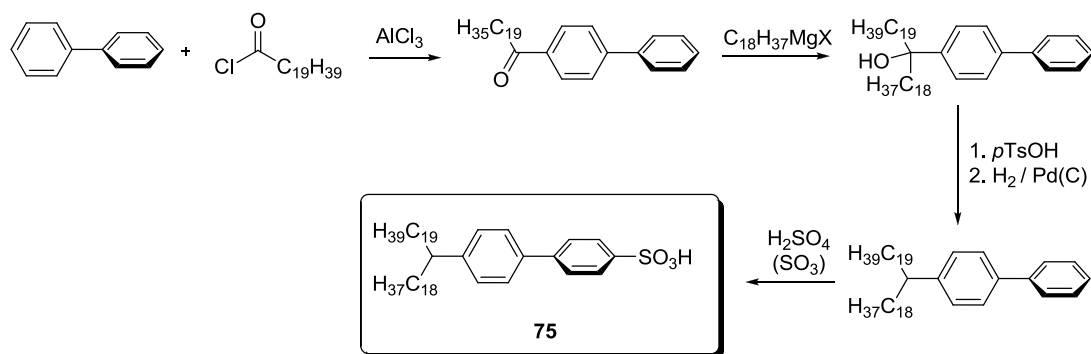


Figure 4.35. More lipophilic catalyst **75** through the introduction of an alkyl chain of 18 carbons.

This new catalyst **75**, already soluble in the triglyceride, was studied in the sunflower seed oil transesterification with methanol, observing, under these conditions, an improvement in the reaction rate by only a factor of 2. Therefore, it seems that the increase in the association of the triglyceride by the catalyst is poor, and that the catalytic activity is doubled only because it has two sulfonic groups.

One possible explanation is the formation of aggregates. So, when an NMR spectrum of **72** in chloroform was recorded, the catalyst generated broad signals. Deuterated methanol addition to the tube caused rupture of the associates yielding sharper signals (figure 4.36).

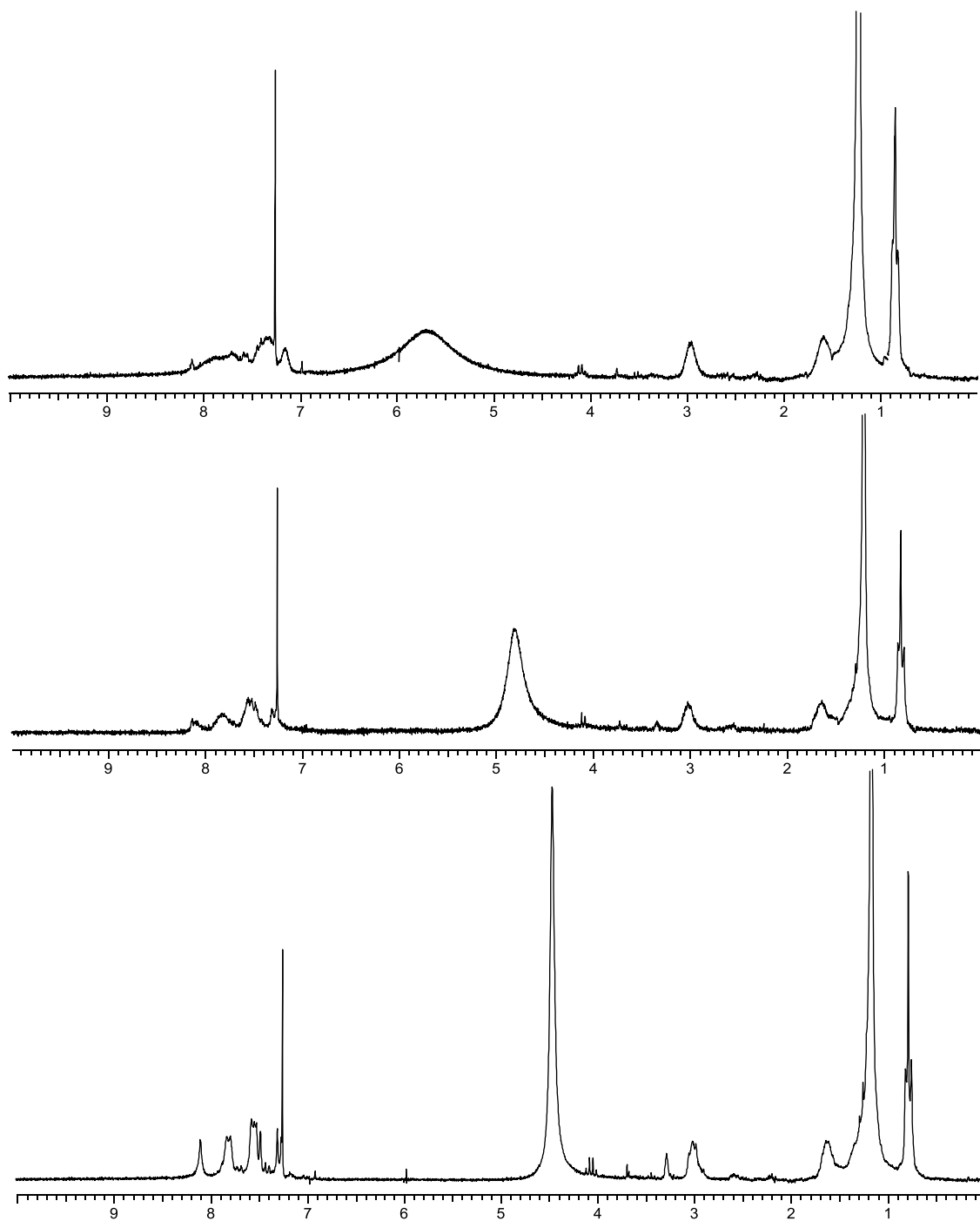


Figure 4.36. ^1H NMR spectra of receptor **72** in CDCl_3 in presence of growing amounts of CD_3OD , where it can be seen an improvement in signals resolution.

4.2.14. Other catalysts

4.2.14.1. Catalysts with two and three sulfonic groups

According to CPK molecular models, the binaphthyl skeleton could be a good template to place two sulfonic groups able of associating the triglyceride. Thus, we performed the synthesis of the following catalysts:

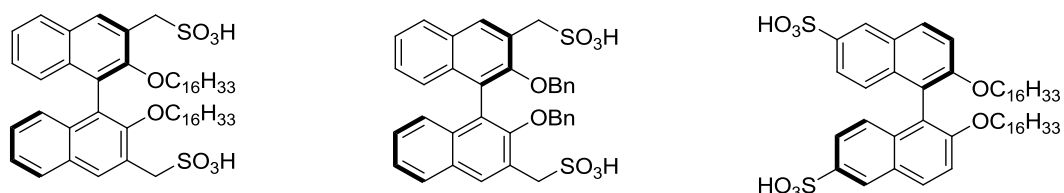


Figure 4.37. Synthesis of several binaphthyl disulfonic acids.

However, the results obtained did not improve those obtained with the previous catalysts.

Since the presence of two sulfonic groups had not shown the expected effectiveness, we designed a catalyst with a third sulfonic group where the association with triglyceride should be enhanced.

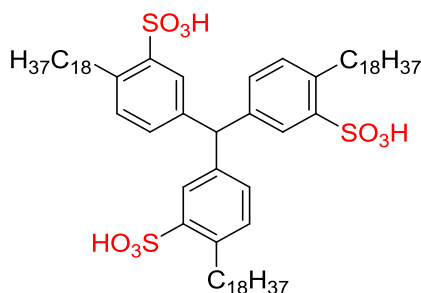


Figure 4.38. Structure of a catalyst which includes three sulfonic groups.

The effect of the third hydrogen bond could be very important in the stability of the associate, since the first two hydrogen bonds have to compensate the loss of entropy associated to the three degrees of translational freedom which disappear in the associate and the rotations frozen in the complex. Therefore, the third hydrogen bond should significantly increase the association constant, as already shown in our research group with other receptors.¹⁷¹ Quantum mechanical calculations show that the geometry could be appropriate to fit the low-energy conformations of triacetin, forming three hydrogen bonds between the sulfonic groups and the triacetin carbonyls.

¹⁷¹ (a) Crego, M.; Partearroyo, A.; Raposo, C.; Mussons, M. L.; López, J. L.; Alcázar, V.; Morán, J. R. *Tetrahedron Lett.* **1994**, 35, 1435-1438; (b) Raposo, C.; Almaraz, M.; Pérez, N.; Martín, M.; Weinrich, V.; Grande, M.; Caballero, C.; Morán, J. R. *Tetrahedron Lett.* **1996**, 37, 1485-1488.

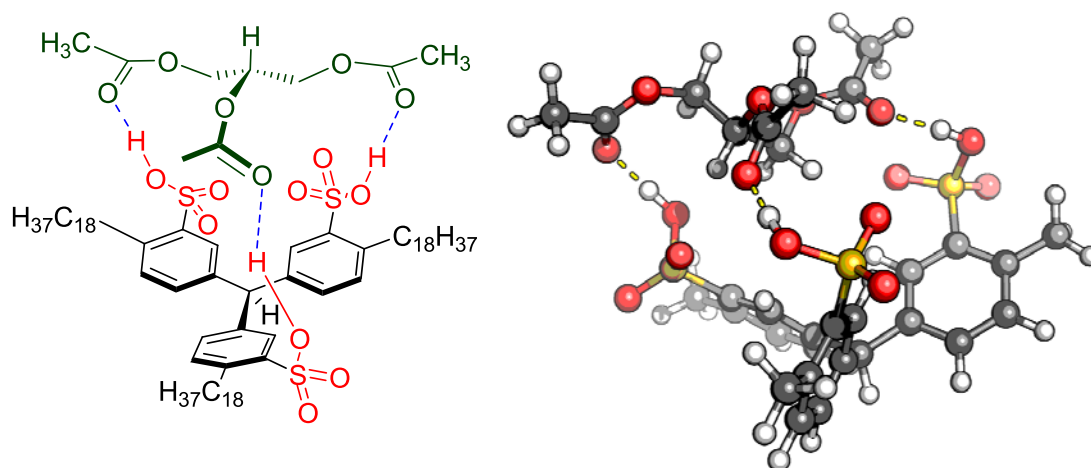


Figure 4.39. (Left) Proposed structure for the complex formed between triacetin and catalyst and (right) complex modelling study (B3LYP/6-31G **).

However, by adding increasing amounts of this catalyst to a solution of triacetin in CDCl_3 we were unable to observe displacement of the signals. Probably the catalyst forms dimers, in such a way that the sulfonic acid groups of a molecule of catalyst prefer to form a hydrogen bond with another sulfonic group of other molecule instead of triacetin. This type of structure is shown in figure 4.40.

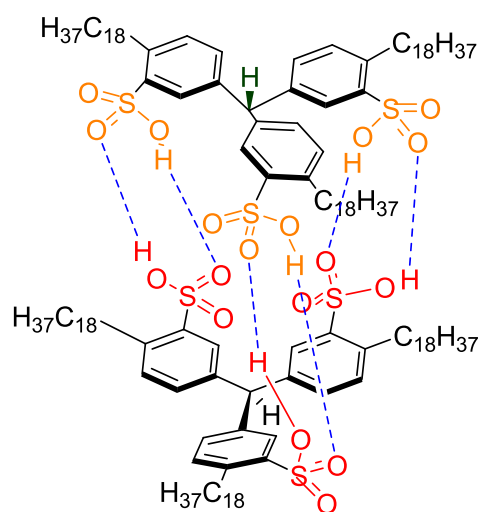


Figure 4.40. Aggregate of the trisulfonic acid which reduces its catalytic activity.

4.2.14.2. Catalysts based on phosphonic acids

Until now, almost all catalysts synthesized have shown the problem of preferential protonation of methanol relative to the activation of the ester carbonyl group. Although we have tried to solve this problem with catalysts which establish more hydrogen bonds with the triglyceride, we have not come up with a geometry in which this stabilization energy is greater than the energy of methanol protonation.

We believe that a way that could solve this problem could be to use a weaker acid. According to the electrocyclic mechanism by which these reactions may proceed in an apolar medium, a phosphoric acid may catalyse the reaction as well as a sulfonic acid. As it is a weaker acid than a sulfonic acid, the hydrogen bond with the carbonyl group will be weaker, but on the contrary, the hydrogen bond between methanol and one of the phosphoryl groups will be stronger, so that both factors could be compensated.

So, we first developed phosphonic acids which in its structure had another hydrogen bond donor group, so that the association of the carbonyl group could be stronger.

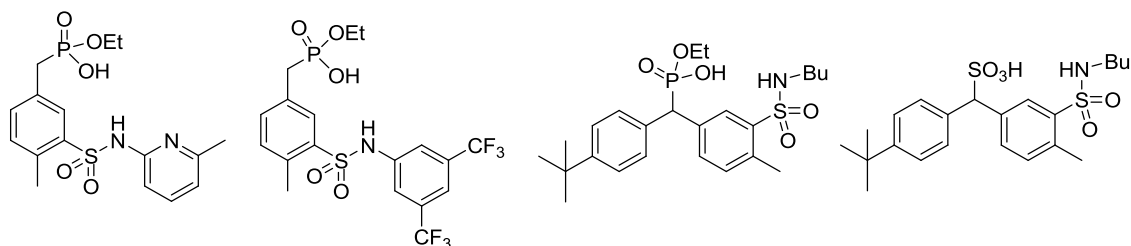


Figure 4.41. Catalysts based on a phosphonic acid compared with a sulfonic acid.

However, the results were not as expected because in spite of the fact that catalysis was observed, the reaction rate acceleration was inferior to the previous values.

We decided then to combine in a single structure two phosphonic groups, as previously tested with sulfonic groups. However, results did not improved the previous values. The synthesized catalysts are shown in figure 4.42.

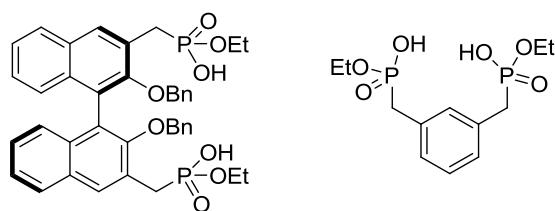


Figure 4.42. Acid catalysts with two phosphonic groups.

4.2.14.3. Catalysts with a nucleophilic hydroxyl group

According to the proposed mechanism, the transesterification process requires that in the transition state the triglyceride, the alcohol and the acid catalyst meet simultaneously. As trimolecular collisions are considered virtually impossible,¹⁷² this is only achieved through the formation of aggregates. The drawback of these aggregates is that in the case of the transesterification, they are rather ineffective, since the sulfonic acid prefers to establish a hydrogen bond with methanol instead of the ester.

Enzymes¹⁷³ have solved this problem by transforming a trimolecular reaction in two bimolecular reactions incorporating in the active centre a hydroxyl group (figures 4.1 and 4.2) close to the group forming the oxyanion hole with the ester, so that the initial triglyceride reacts first with the hydroxyl of the enzyme to form an intermediate which then reacts with a molecule of alcohol. The idea we will try to develop would be to place in a single frame a sulfonic acid and a hydroxyl group in order to transform a trimolecular reaction in two bimolecular ones and reduce the translational entropy (which should be less unfavourable in the transition state).

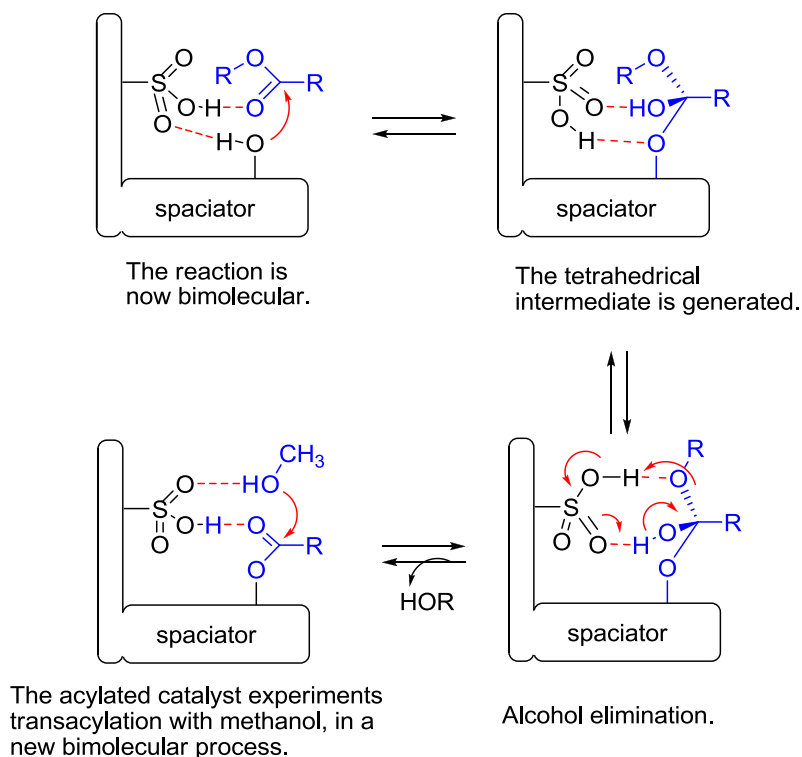


Figure 4.43. Graphical representation of how an acid catalyst with a hydroxyl group in the molecule transforms a trimolecular reaction in two bimolecular reactions.

We studied several molecules using molecular modelling (B3LYP/6-31G**). In figure 4.44 the transition states for the intramolecular attack of the hydroxyl group are shown as well as the calculated energies (in kcal/mol).

¹⁷² House, J. E. *Principles of chemical kinetics*; 2nd ed.; Academic Press Elsevier: San Diego, 2007.

¹⁷³ Carter, P.; Wells, J. A. *Nature* **1988**, 332, 564-568.

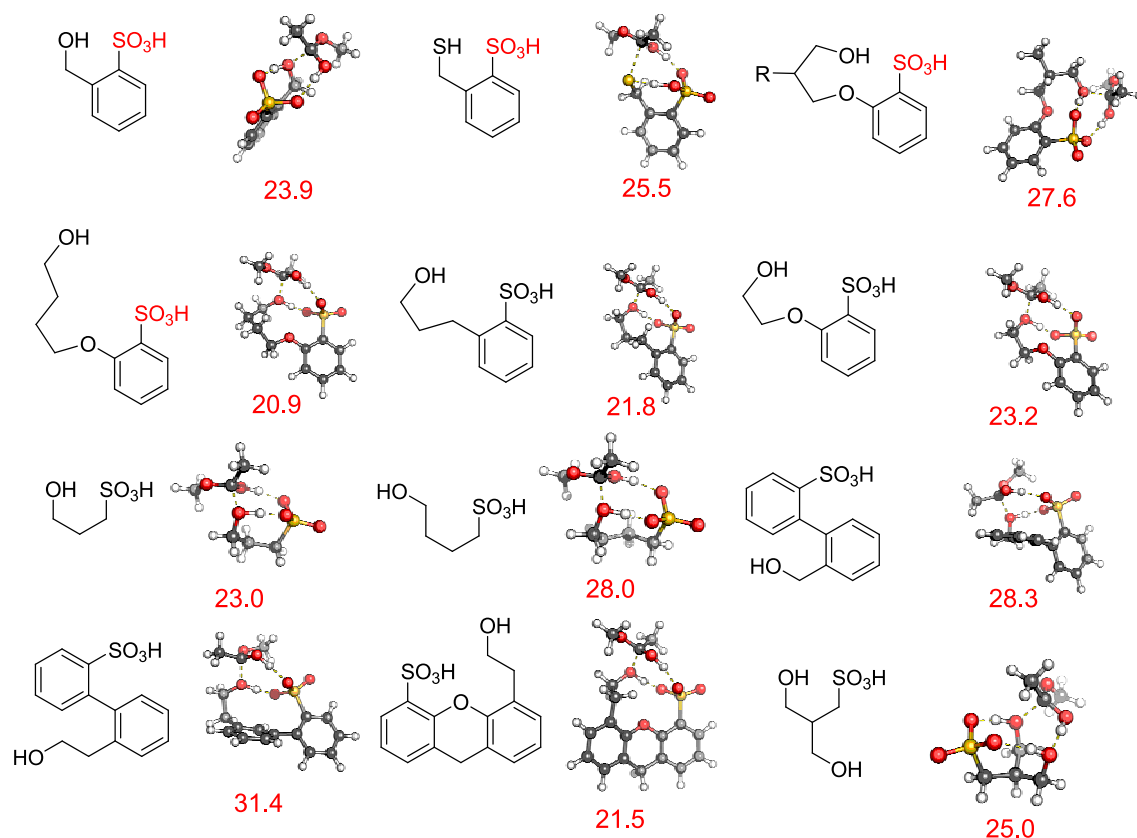


Figure 4.44. Evaluation of catalysts consisting of a sulfonic acid and an intramolecular hydroxyl group, with transition states and energies (in kcal/mol).

In view of these results, we synthesized several catalysts, which are shown in figure 4.45.

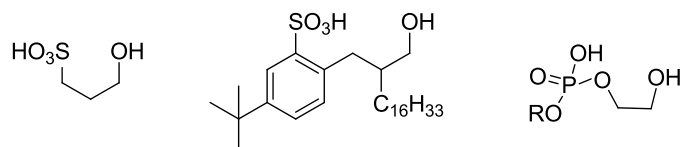


Figure 4.45. Catalysts studied

The results, however, were not as expected and we found no significant improvements in the reaction rate. Probably the hydroxyl group is forming a hydrogen bond with the sulfonic group decreasing its reactivity. This hydrogen bond, although it may be considered weaker in the phosphonic acid derivative, also deactivates the catalyst.

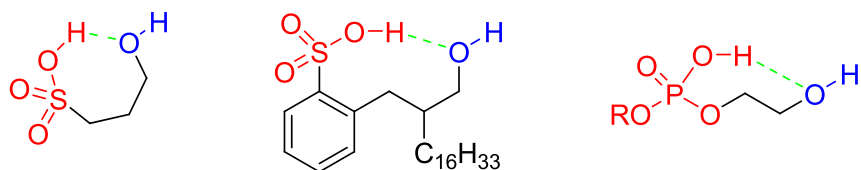


Figure 4.46. Possible explanation why these catalysts would be deactivated.

Indeed, when acids of figure 4.46 were acetylated and treated with methanol, it was observed that the transesterification was very fast. It is likely that the intramolecular hydrogen bond is fixed on the ester carbonyl (figure 4.47).

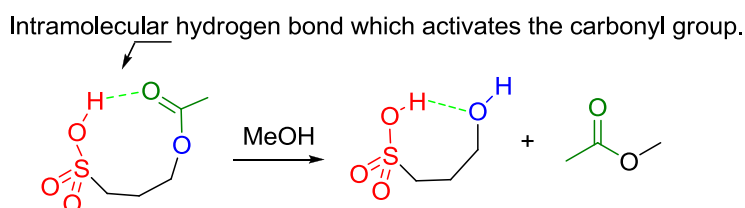


Figure 4.47. Methanolysis of an acetylated hydroxysulfonic acid.

Furthermore, it can be many degrees of freedom in the rotation of the carbons separating the hydroxyl group from the sulfonic acid, which would need to be frozen in the transition state. Thus, it can occur that the energetic advantage obtained by the intramolecular attack is lost due to entropy, needed to freeze those rotational degrees.

It is necessary to consider that it is likely that the activation energies shown by the calculations are not fully reliable because of the difficulty to establish the energy in the ground state, in which it must already exist some interactions between the reactants through hydrogen bonds, which makes them to form aggregates and makes difficult to estimate its energy.

As has been noted throughout this chapter, the design of catalysts that preferentially associate triglycerides versus methanol is not a trivial issue due to the formation of associates. Nor it is easy to include in the sulfonic acid structure suitable nucleophiles that promote transesterification. The design of more efficient catalysts requires a new and more throughout theoretical work, which we hope to carry out in the future.

4.3. CONCLUSIONS

In this chapter we have attempted to use organocatalysts with an oxyanion hole in its structure to catalyse a reaction with industrially important applications such as the transesterification of triglycerides. This has required a deep study of the reaction, in order to use acid catalysts, which are the only catalysts which would allow to carry out the transesterification of low cost oils with high free fatty acid content. However, acid catalysts may seem, at first glance, less attractive because they generate slower reactions when compared with basic catalysts. Through a careful literature review and different experiments, we have found the reason for this lower reactivity, which is the lack of solubility of the acid catalysts in the triglyceride phase. Once known this drawback, we have synthesized a series of sulfonic acids of increasing lipophilicity, so that we have established a relationship between the lipophilicity of the catalyst and the reaction rate, in such a way that the catalysts with a large number of alkyl chains are the compounds with the best activities.

Furthermore, these organocatalysts have shown to be practically insensitive to the presence of free fatty acids or water, so they are ideal for performing transesterification of low cost oils, with high free fatty acids content. Furthermore, these catalysts can work at temperatures below the boiling point of methanol and the reaction times are short.

The catalyst recovery process, based on adsorption onto silica gel, has proved to be completely effective, so that the recovered catalyst has virtually shown the same catalytic activity as the original catalyst. In these conditions, the biodiesel obtained possesses a much lower acidity than the regulated limit value, showing therefore good properties for marketing.

The study of the mechanism of the reaction has shown us many surprises, since we have found that probably, in a nonpolar medium such as triglyceride, the most likely mechanism by which the reaction proceeds is electrocyclic.

In the last part of the chapter we have tried to improve the catalytic results with the synthesis of different compounds, in which the oxyanion hole of enzymes is simulated. However, although some have shown good reaction rates, catalytic activity has not greatly improved in comparison with the lipophilic sulfonic acids synthesized in the first part of the chapter. We believe that the formation of strong aggregates between two or more molecules of the catalyst is primarily responsible for this effect, so that a possible solution could be the incorporation of different groups in the catalysts which hinder the formation of self-associates.

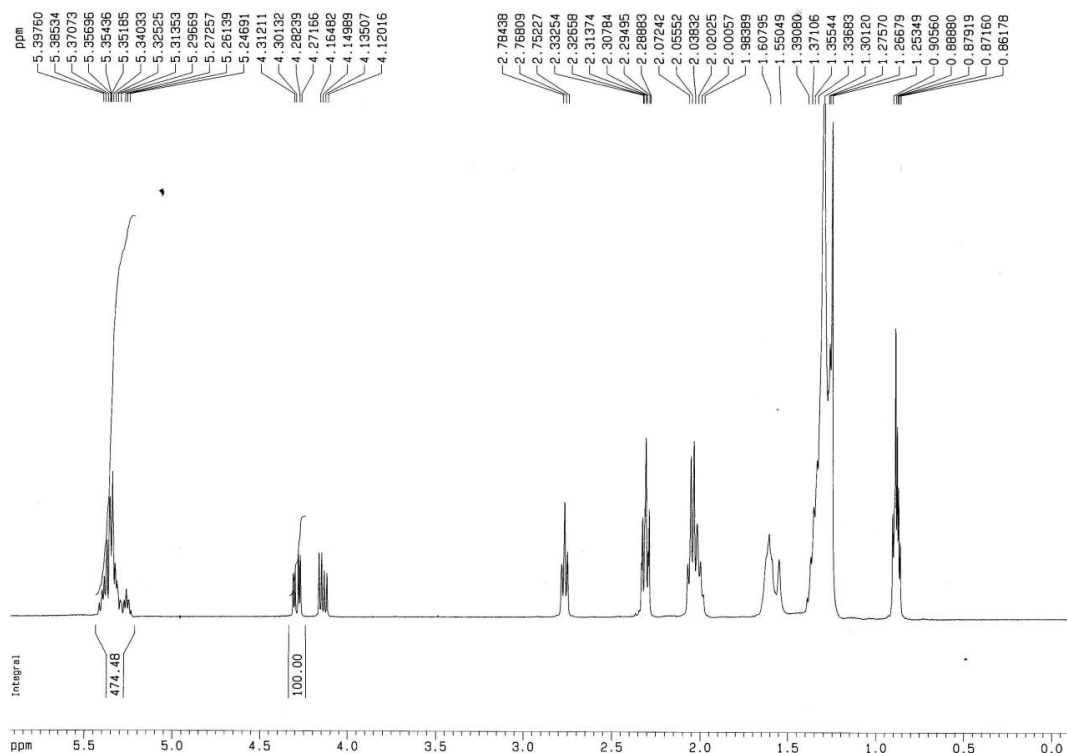
4.4. EXPERIMENTAL

- General procedure for the transesterification reaction

Methanol (0.67 mL, 16.7 mmol) and triglyceride (2.5 g, 2.8 mmol) were reacted in the presence of catalyst in a glass tube equipped with a screw cap with septum and magnetic stirring. The temperature of the sample was kept constant with a thermostat bath. The progress of the reaction was monitored by ^1H NMR analysis of aliquots. The initial biphasic reaction may turn homogeneous (15 min at 80 °C). Close to the end of the reaction, glycerine decantation provides a biphasic reaction mixture again (45 min at 80 °C). The conversion was measured by integration of the glycerine protons of the triglyceride or from the methyl ester signal of the fatty acids methyl esters by comparison with the multiplet at 5.35 ppm from the double bonds which can be considered as a constant reference (see Supporting Information).

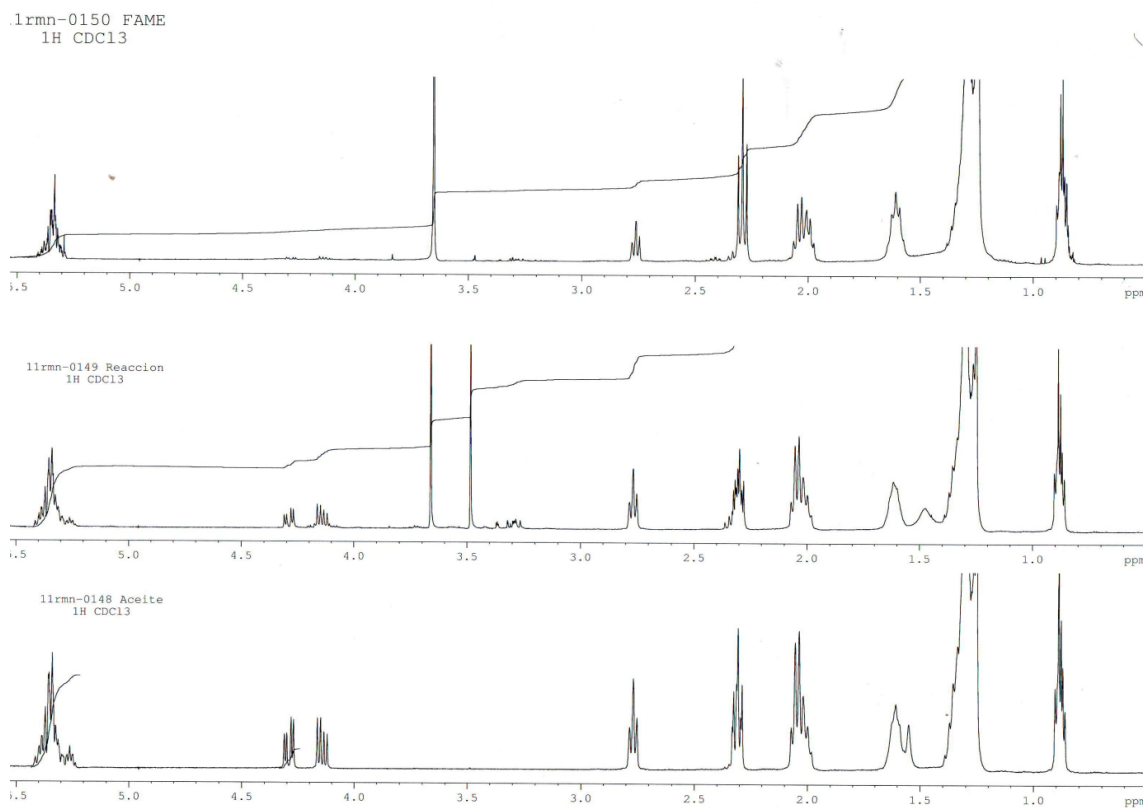
- ^1H NMR spectrum of triglyceride displaying the integral of the region of interest

^1H RMN (CDCl_3 , 400 MHz)

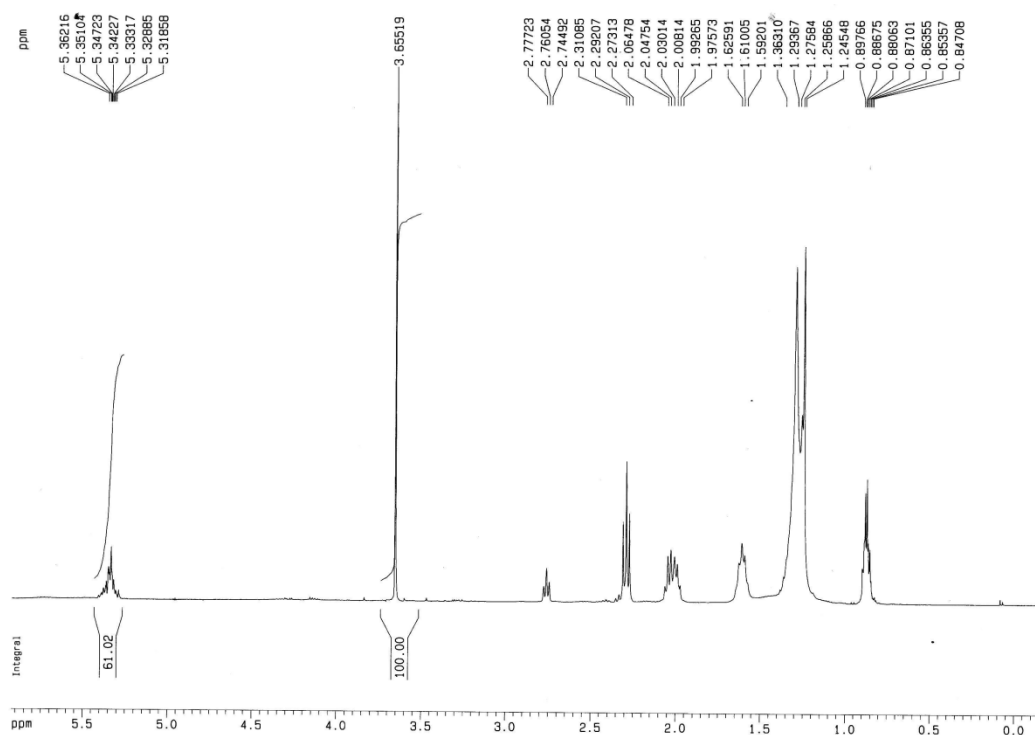


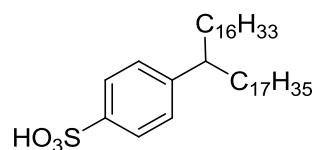
- ^1H NMR spectrum of the progress of the transesterification reaction catalysed by 64

^1H RMN (CDCl_3 , 400 MHz)



^1H NMR spectrum of fatty acids methyl esters (FAMES)



- 4-(Tetratriacontan-17-yl)benzenesulfonic acid (64)

A solution of 1-phenyloctadecan-1-one¹⁴⁷ (26.5 g, 77 mmol) in diethyl ether (100 mL) was added dropwise to a Grignard reagent prepared from a mixture of 1-iodohexadecane (2.0 g, 5.7 mmol) and 1-chlorohexadecane (27.6 g, 106 mmol) with magnesium turnings (7.5 g) and a small crystal of iodine in ether (80 mL). After the addition, the reaction was stirred at room temperature for 12 h. Then the mixture was poured onto ice and acidified with 2 M hydrochloric acid. The aqueous phase was discarded, the organic layer dried over Na₂SO₄ and the solvent evaporated to dryness. The residue was purified by column chromatography on silica gel with dichloromethane as eluent, yielding the corresponding alcohol, 17-phenyltetratriacontan-17-ol, as a white solid; yield: 37.4 g (85 %).

The above alcohol (13.7 g, 24 mmol) and a catalytic amount of *p*-toluenesulfonic acid (162 mg, 0.94 mmol) were refluxed in toluene (280 mL) until no further water appeared. The mixture was washed with aqueous NaHCO₃ and the toluene was evaporated under reduced pressure. The crude residue was purified by column chromatography with hexane as eluent to afford the dehydrated compound; yield: 11.0 g (83 %).

This unsaturated compound (11.0 g, 19.9 mmol) was dissolved in ethanol (40 mL) and hydrogenated (4 bar) in the presence of Pd/C (5 %) (450 mg) at room temperature. After 12 h the catalyst was filtered and the solvent was removed. Silica gel percolation with hexane furnished the expected saturated hydrocarbon, tetratriacontan-17-ylbenzene; yield: 9.40 g (85 %).

Finally, fuming sulfuric acid (20 % SO₃, 6.8 g) was added to a solution of tetratriacontan-17-ylbenzene (9.40 g, 17 mmol) in dry CH₂Cl₂ (100 mL). After stirring for 5 min, ¹H NMR analysis of an aliquota revealed that the reaction had finished. Ice was then added to the reaction mixture and the layers were separated. The organic layer was dried over cellulose and the solvent removed under reduced pressure to afford the desired compound **64**, as a white solid; yield: 10.5 g (98 %).

mp: 33-35 °C.

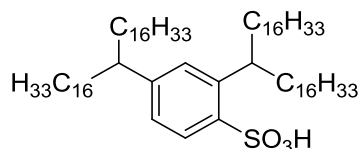
¹H NMR (CDCl₃) δ (ppm): 0,88 (t, *J* = 6.6 Hz, 6H), 1,25 (br s, 58H), 1,50 (m, 4H), 2,50 (m, 1H), 7,16 (d, *J* = 8.0 Hz, 2H), 7,74 (d, *J* = 8.0 Hz, 2H).

¹³C NMR (CDCl₃) δ (ppm): 14.3 (CH₃ x 2), 22.9 (CH₂ x 2), 27.8 (CH₂ x 2), 29.6 (CH₂ x 2), 29.8 (CH₂ x 19), 30.0 (CH₂ x 2), 32.2 (CH₂ x 2), 36.9 (CH₂ x 2), 46.3 (CH), 126.3 (CH x 2), 128.2 (CH x 2), 138.7 (C), 151.1 (C).

IR (nujol, cm⁻¹): 3409, 2916, 2851, 1735, 1469, 1378, 1150, 1041, 1002.

HRMS (ESI): 679.5065 (M - H + Na) + Na⁺, calcd for C₄₀H₇₃Na₂O₃S 679.5070.

- 2,4-Di(tritriacontan-17-yl)benzenesulfonic acid (65)



A solution of dimethyl isophthalate (3.9 g, 20.2 mmol) in diethyl ether (30 mL) was added dropwise to a Grignard reagent prepared from a mixture of 1-iodohexadecane (2.1 g, 6.0 mmol) and 1-chlorohexadecane (28.4 g, 109.0 mmol) with magnesium turnings (8.0 g) and a small crystal of iodine in ether (80 mL). After the addition, the resulting mixture was allowed to react at room temperature for 12 h. The reaction mixture was worked up in the same way as for the preparation of catalyst **64**, yielding the corresponding diol, 17,17'-(1,3-phenylene)dinitritriacontan-17-ol, yield: 19.0 g (89 %).

The diol (17.0 g, 16.5 mmol) was dehydrated with *p*-toluenesulfonic acid in refluxing toluene following the same procedure as described previously, affording the unsaturated hydrocarbon; yield: 16.0 g (96 %).

Hydrogenation of this compound (7.0 g, 7.0 mmol) was carried out in THF (40 mL) under 4 bar of hydrogen pressure at 40 °C with Pd/C (5 %) (500 mg) in 12 h. The catalyst was removed by filtration, the solvent evaporated and the residue purified by percolation through silica gel (hexane as eluent) to yield the saturated hydrocarbon, 1,3-di(tritriacontan-17-yl)benzene; yield: 6.1 g (86 %).

The sulfonation of this compound (6.1 g, 6.0 mmol) was carried out under the same conditions previously described for catalyst **64**, to afford the expected compound as a white solid; yield: 6.2 g (96 %).

mp: 79-80 °C.

¹H NMR (CDCl₃) δ (ppm): 0.88 (t, *J* = 6.4 Hz, 12H), 1.25 (br s, 112 H), 1.60 (m, 8H), 2.51 (m, 2H), 7.00 (d, *J* = 8.4 Hz, 2H), 7.14 (s, 1 H), 7.85 (d, *J* = 8.4 Hz, 2H).

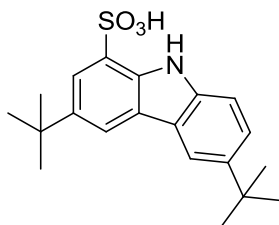
¹³C NMR (CDCl₃) δ (ppm): 14.3 (CH₃ x 4), 22.9 (CH₂ x 4), 27.6 (CH₂ x 4), 27.8 (CH₂ x 4), 29.6 (CH₂ x 4), 29.9 (CH₂ x 24), 30.0 (CH₂ x 4), 30.4 (CH₂ x 4), 32.2 (CH₂ x 4), 36.9 (CH₂ x 4), 37.1 (CH₂ x 4), 40.6 (CH), 46.2 (CH), 124.9 (CH), 127.7 (CH), 128.2 (CH), 135.7 (C), 146.5 (C), 151.8 (C).

IR (nujol, cm⁻¹): 3403, 2916, 2365, 1599, 1456, 1378, 1314, 1164, 1074, 1002, 892, 710.

HRMS (ESI): 1128.0108 (M - H + Na) + Na⁺, calcd for C₇₂H₁₃₇Na₂O₃S 1128.0078.

- Compound **70** was synthesized according to the experimental procedure described in the literature.¹⁶⁵

- **3,6-di-tert-butyl-9H-carbazole-1-sulfonic acid (71)**



3,6-Di-*tert*-butyl-9H-carbazole¹⁷⁴ (10.0 g, 35.8 mmol) was dissolved in CH₂Cl₂ (200 mL). While stirring, 60 mL of a 0.6 M solution of chlorosulfonic acid in CH₂Cl₂ was added dropwise at 0 °C. Then, the solvent was evaporated and the compound was purified by chromatography on silica gel with CH₂Cl₂ and EtOAc to give the desired monosulfonic acid **71** (10.7 g, 83 %).

mp: 103-105 °C.

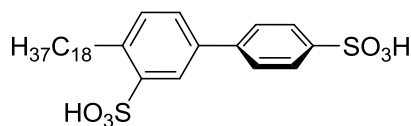
¹H NMR (CDCl₃) δ (ppm): 1.19 (s, 9H), 1.31 (s, 9H), 6.81 (d, *J* = 8.6 Hz, 1H), 6.90 (d, *J* = 8.6 Hz, 1H), 7.84 (s, 2H), 8.04 (s, 1H).

¹³C NMR (CDCl₃) δ (ppm): 31.9 (CH₃ x 3), 32.1 (CH₃ x 3), 111.0 (CH), 115.8 (CH), 120.6 (CH), 121.1 (CH), 122.2 (C), 122.6 (C), 124.5 (CH), 125.7 (C), 133.9 (C), 138.5 (C), 141.8 (C), 142.4 (C).

IR (film, cm⁻¹): 3444, 3224, 2961, 2906, 1713, 1487, 1248, 1041.

HRMS (ESI): 360.1637 (M + H)⁺, calcd for C₂₀H₂₆NO₃S 360.1628.

- **4-octadecylbiphenyl-3,4'-disulfonic acid (72)**



The introduction of the 18 carbon atoms chain in the biphenyl was carried out following the experimental procedure described for the synthesis of compound **63**.¹⁵⁸ Sulfonation of this compound (1.0 g, 2.5 mmol) was made by dissolving it in 10 mL of CH₂Cl₂ at 0 °C and adding fuming sulphuric acid (20 % SO₃, 1.0 mL). Under these conditions the anhydride is generated. Then the reaction mixture was added onto ice (5 g), the layers were separated, CH₂Cl₂ was decanted and evaporated. The filtrate was added to a solution of 10 mL dioxane with 10 % water and refluxed for two hours to hydrolyze the anhydride. The solution was evaporated

¹⁷⁴ Yang, X.; Lu, R.; Gai, F.; Xue, P.; Zhan, Y. *Chem. Commun.* **2010**, 46, 1088-1090.

under reduced pressure leaving a precipitate which was filtered to obtain the desired compound (300 mg, 21 % yield).

mp: 69-70 °C.

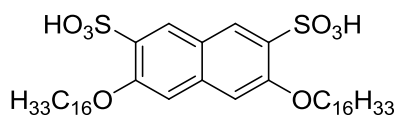
¹H NMR (CDCl₃-CD₃OD) δ (ppm): 0.79 (t, *J* = 6.3 Hz, 3H), 1.17 (br s, 30H), 1.54-1.73 (2H, m), 2.96-3.10 (2H, m), 7.29 (d, *J* = 7.8 Hz, 1H), 7.46-7.64 (m, 3H), 7.82 (d, *J* = 7.8 Hz, 2H), 8.11 (s, 1H).

¹³C NMR (CDCl₃-CD₃OD) δ (ppm): 14.0 (CH₃), 22.7 (CH₂), 29.4 (CH₂), 29.7 (CH₂), 29.7-29.8 (CH₂ x 10), 30.0 (CH₂), 31.1 (CH₂), 31.9 (CH₂), 32.6 (CH₂), 125.9 (CH), 126.2 (CH x 2), 126.8 (CH x 2), 129.0 (CH), 131.1 (CH), 136.7 (C), 141.1 (C), 141.6 (C x 2), 142.3 (C).

IR (nujol, cm⁻¹): 3423, 2936, 2955, 2852, 1456, 1385, 1152.

MS (ESI): 282.2 (M - 2H)²⁻, calcd for C₃₀H₄₄O₆S₂/2 282.13.

- 3,6-bis(hexadecyloxy)naphthalene-2,7-disulfonic acid (**73**)



The alkylation of 2,7-dihydroxynaphthalene was carried out following the conditions described in the literature.¹⁷⁵ The sulfonation of this compound (0.5 g, 0.82 mmol) was achieved dissolving it in 50 mL CH₂Cl₂ and adding fuming sulphuric acid (20 % SO₃, 0.5 mL) at 0 °C. The reaction workup was made according to the conditions used in compound **64** preparation.

mp: 54-55 °C.

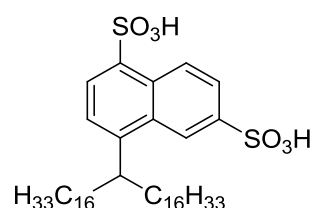
¹H NMR (CDCl₃-CD₃OD) δ (ppm): 0.79 (t, *J* = 6.3 Hz, 6H), 1.18 (br s, 48H), 1.33-1.50 (m, 4H), 1.73-1.94 (m, 4H), 4.07 (t, *J* = 6.8 Hz, 4H), 6.98 (s, 2H), 8.23 (s, 2H).

¹³C NMR (CDCl₃-CD₃OD) δ (ppm): 13,9 (CH₃ x 2); 22,6 (CH₂ x 2); 25,8 (CH₂ x 2); 28,6 (CH₂ x 2); 29,3 (CH₂ x 2); 29,3 (CH₂ x 2); 29,6 (CH₂ x 2); 29,6 (CH₂ x 14); 31,8 (CH₂ x 2); 69,0 (CH₂ x 2); 106,1 (CH x 2); 120,5 (C x 2); 130,2 (CH x 2); 130,7 (C); 138,7 (C); 155,4 (C x 2).

IR (nujol, cm⁻¹): 3410, 2916, 2845, 1658, 1132, 1061.

MS (ESI): 383.6 (M - 2H)²⁻, calcd for C₄₂H₇₀O₈S₂/2 383.23.

¹⁷⁵ Lohr, A.; Grüne, M.; Würthner, F. *Chem. Eur. J.* **2009**, *15*, 3691-3705.

- 4-(tritriacontan-17-yl)naphthalene-1,6-disulfonic acid (74)

Acylation of naphthalene and subsequent Grignard reaction was carried out following the same experimental procedure used in the preparation of compound **64**. The sulfonation of this compound (1.17 g, 1.93 mmol) was performed in 50 mL CH₂Cl₂ with fuming sulphuric acid (20 % SO₃, 3.5 mL) following the conditions described in compound **72** sulfonation.

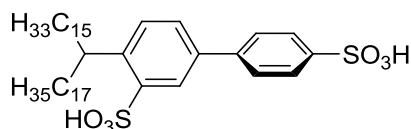
mp: 23-25 °C.

¹H NMR (CDCl₃-CD₃OD) δ (ppm): 0.82 (t, *J* = 6.4 Hz, 6H), 1.14 (br s, 17H), 1.20 (br s, 41H), 1.53-1.82 (m, 4H), 3.33-3.61 (m, 1H), 7.37 (d, *J* = 7.8 Hz, 1H), 7.92 (d, *J* = 9.0 Hz, 1H), 8.17 (d, *J* = 7.8 Hz, 1H), 8.70 (s, 1H), 8.81 (d, *J* = 9.0 Hz, 1H).

¹³C NMR (CDCl₃-CD₃OD) δ (ppm): 14.0 (CH₃ x 2), 22.6 (CH₂ x 2), 27.2 (CH₂ x 2), 29.3 (CH₂ x 2), 29.5 (CH₂ x 2), 29.6 (CH₂ x 2), 29.7 (CH₂ x 14), 29.9 (CH₂ x 2), 31.9 (CH₂ x 2), 36.1 (CH₂ x 2), 39.2 (CH), 121.4 (CH), 122.6 (CH), 122.9 (CH), 127.3 (CH), 127.5 (CH), 129.9 (C), 132.1 (C), 136.7 (C), 140.4 (C), 148.4 (C).

IR (nujol, cm⁻¹): 3474, 2923, 2839, 1690, 1456, 1139, 1048.

MS (ESI): 374.4 (M - 2H)²⁺, calcd for C₄₃H₇₂O₆S₂/2 374.24.

- 4-(octatriacontan-19-yl)biphenyl-3,4'-disulfonic acid (75)

Acylation of binaphthyl and subsequent Grignard reaction was carried out following the conditions described in compound **64** preparation. Then sulfonation was performed according to the conditions employed in the synthesis of compound **72**. The final product was purified by silica gel chromatography with CH₂Cl₂/MeOH 10:1 (22 % yield).

mp: 52-54 °C.

¹H NMR (CDCl₃-CD₃OD) δ (ppm): 0.84 (t, *J* = 6.1 Hz, 6H), 1.22 (br s, 62H), 2.98 (m, 1H), 7.23 (d, *J* = 7.5 Hz, 1H), 7.43 (d, *J* = 7.5 Hz, 1H), 7.49 (d, *J* = 8.2 Hz, 2H), 7.77 (d, *J* = 8.2 Hz, 2H), 8.06 (s, 1H).

¹³C NMR (CDCl₃-CD₃OD) δ (ppm): 14.3 (CH₃ x 2), 22.9 (CH₂ x 2), 26.7 (CH₂ x 2), 29.6 (CH₂ x 2), 29.9 (CH₂ x 23), 30.4 (CH₂ x 2), 32.1 (CH₂ x 2), 33.4 (CH₂ x 2), 38.4 (CH), 126.5 (CH x 2), 127.1 (CH x 2), 128.9 (CH), 131.7 (CH), 131.8 (CH), 136.9 (C), 140.4 (C), 140.5 (C), 141.9 (C), 142.6 (C).

IR (film, cm⁻¹): 3436, 2929, 2845, 1645, 1463, 1165, 1041.

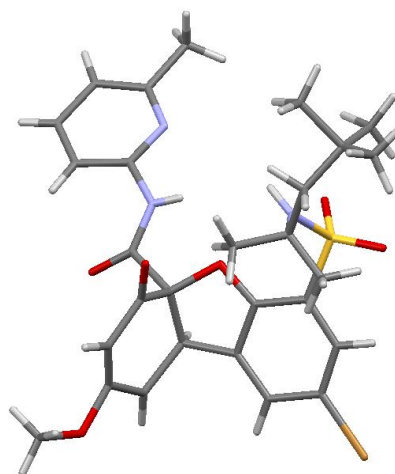
MS (ESI): 422.5 (M - 2H)²⁻, calcd for C₅₀H₈₄O₆S₂/2 422.29.



**VNiVERSiDAD
D SALAMANCA**

CAMPUS DE EXCELENCIA INTERNACIONAL

CHAPTER 5: Benzofuran-based tripodal receptors



5.1. INTRODUCTION

As we have seen in the previous chapters, in many cases the proposed catalysts for a certain reaction are not as efficient as it should be because the association with the substrate is not efficient enough.

In order to improve the results by increasing the association with the substrate, we decided to carry out the synthesis of a new tripodal asymmetric skeleton in which it would be possible to place several functional groups that generate an oxyanion hole and other functionalities which can favour substrate association or catalysis. The idea is to try to understand the mode of interaction of different guests with several receptors derived from this framework in order to predict, in a logical way, what kind of molecules the receptor can associate and what reactions could be catalyzed.

The objective is, therefore, to synthesize a three-dimensional structure capable of setting at least three interactions with the substrate, and which would ensure the union of a single enantiomer, in the case of chiral substrates. This model can be used in organocatalysis, since it

would allow performing enantioselective reactions, and also in molecular recognition, to distinguish between enantiomers in a racemic mixture.

5.1.1. The three-point model

Indeed, already in 1948, Ogston¹⁷⁶ proposed a three-point model to explain the stereospecific enzymatic formation of α -ketoglutarate from citrate. These compounds appear in the citric acid cycle, the process employed by aerobic organisms to oxidize acetyl CoA and generate energy.¹⁷⁷ As proposed in 1937 by Johnson and Krebs (figure 5.1), if acetic acid is isotopically marked with ^{14}C , it will condense with oxaloacetate so that one of the carboxyl groups of citric acid will be marked and the other not. These two carboxyl groups are those that give rise to the two carboxyl groups of α -ketoglutarate. Since both carboxyl groups are considered indistinguishable, it was expected that both α -ketoglutarate carbonyl groups were marked with ^{14}C . However, in 1940, Evans and Slotin¹⁷⁸ showed that, under these conditions, ^{14}C only appeared on one of the γ -carboxyl of α -ketoglutarate. This caused a big surprise; it seemed that the new ^{14}C marking tool was questioning not only the citric acid cycle, but also the methodology used to study the enzymatic metabolism.¹⁷⁹ Fortunately, in 1948, Ogston interpreted Evans and Slotin data obtained by isotopic labelling within the cycle proposed by Krebs and Johnson.



Alexander George Ogston

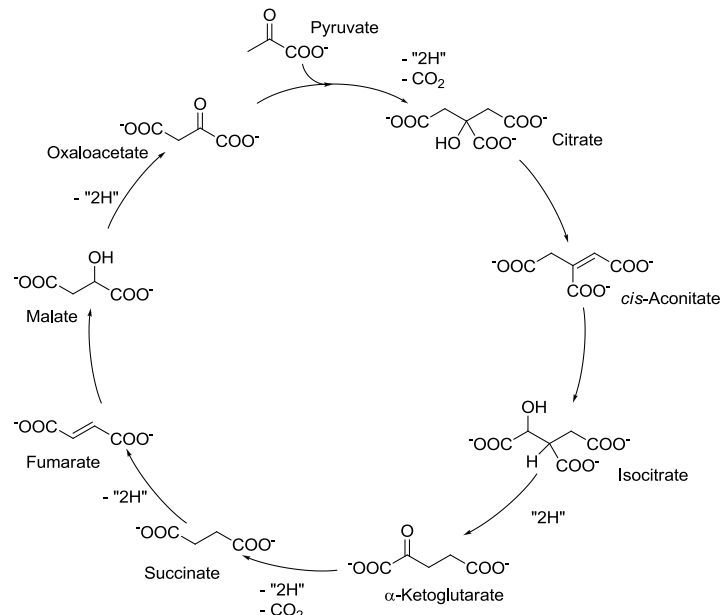


Figure 5.1. Citric acid cycle proposed by Krebs and Johnson in 1937.

¹⁷⁶ Ogston, A.G. *Nature* **1948**, 162, 963.

¹⁷⁷ Lehninger, A. L.; Nelson, D. L.; Cox, M. M. *Principles of Biochemistry*, 4th ed.; W. H. Freeman: New York, 2004.

¹⁷⁸ Evans Jr., E. A.; Slotin, L. J. *Biol. Chem.* **1940**, 136, 301.

¹⁷⁹ Koshland Jr., D. E. *Biochemistry and Molecular Biology Education* **2002**, 30, 27-29.

Ogston proposes that for a chiral receptor to be able to discriminate between two enantiomeric species, at least three points of the receptor must interact with three complementary points of the compound which has to be accommodated.¹⁸⁰ Thus, if three additional positions of an enzyme, A', B' and C' are placed in such a way that they can specifically bind only three groups (A, B and C) of the four substituents of a tetrahedral carbon, the enzyme will associate only one of the enantiomers and binding will be impossible with the other isomer in the same positions. However the enzyme is also able to differentiate one of the two A groups in a C_{AABC} tetrahedron. Thus, a molecule with two A groups also fit into the enzyme at the locations A', B' and C', but only one of the A groups is always staying at the top of the tetrahedron, and the other would always be in the surface A'. By similarity to the tetrahedron with a molecule of citric acid, if only one of the groups A is isotopically labelled, all the ¹⁴C from the isotopically labelled acetate go to one of the carboxyl groups of α -ketoglutarate and not to both of them. Thus, the Evans and Slotin data could be explained accepting the citric acid as a key intermediate in the citric acid cycle, and hence, respecting the proposed Krebs cycle.

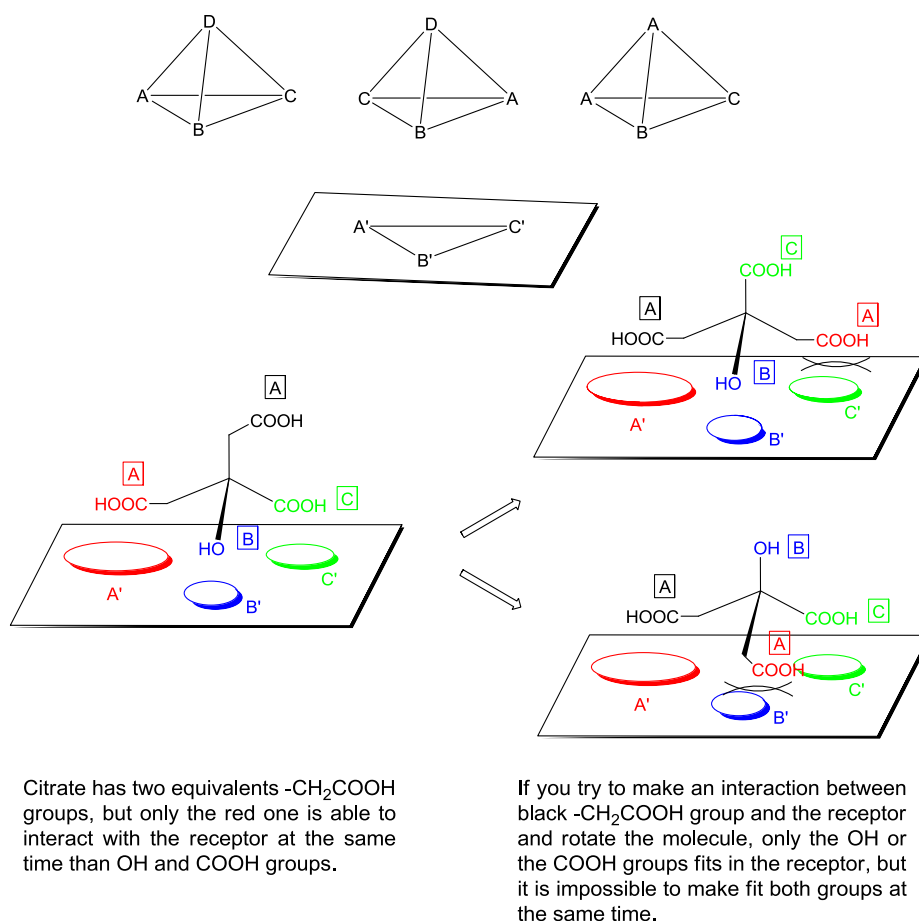


Figure 5.2. (Top) Ogston three points model; (below) example with citrate, only the enzyme-substrate complex on the left is effective.

¹⁸⁰ Davankov, V. A. *Chirality* **1997**, 9, 99-102.

In fact, the concept that two identical groups on the same carbon could be distinguished from each other in space was a provocative new concept quickly accepted, and laid the foundation of "prochirality" notion. Actually, this same model had been proposed 15 years before by Easson and Stedman¹⁸¹ to explain the resolution of *D* and *L* isomers in drug receptors, though probably was unknown to Ogston due to the lack of interdisciplinary communication.¹⁸² However, it was the Ogston model which has been accepted for the explanation of how enzymes distinguish *D* enantiomers from *L* enantiomers. Anyway, in 2000, Mesecar and Koshland,¹⁸³ studying the mechanism of enzyme isocitric dehydrogenase, found that the Ogston model could not be entirely correct (figure 5.3). They found that three groups of a tetrahedral carbon, for example, A, B and C of the *D*-enantiomer of the substrate (isocitrate) joined to the same amino acids in the surface of the isocitrate dehydrogenase enzyme (A', B' and C'). Therefore, a model of three points was not enough to distinguish between the two enantiomers. In this case, the major difference was the orientation of the fourth group D in the tetrahedron C_{ABCD} that corresponds to the OH on the C₂ carbon of isocitric acid. In the case of the *L*-isomer, the OH is linked to the Arg-119 while in the case of the *D*-isomer, the OH is linked to Mg²⁺, which in turn forms a complex with Asp-311, Asp-283 and Asp-307 in a completely different direction. Mesecar and Koshland proposed a new four points model.

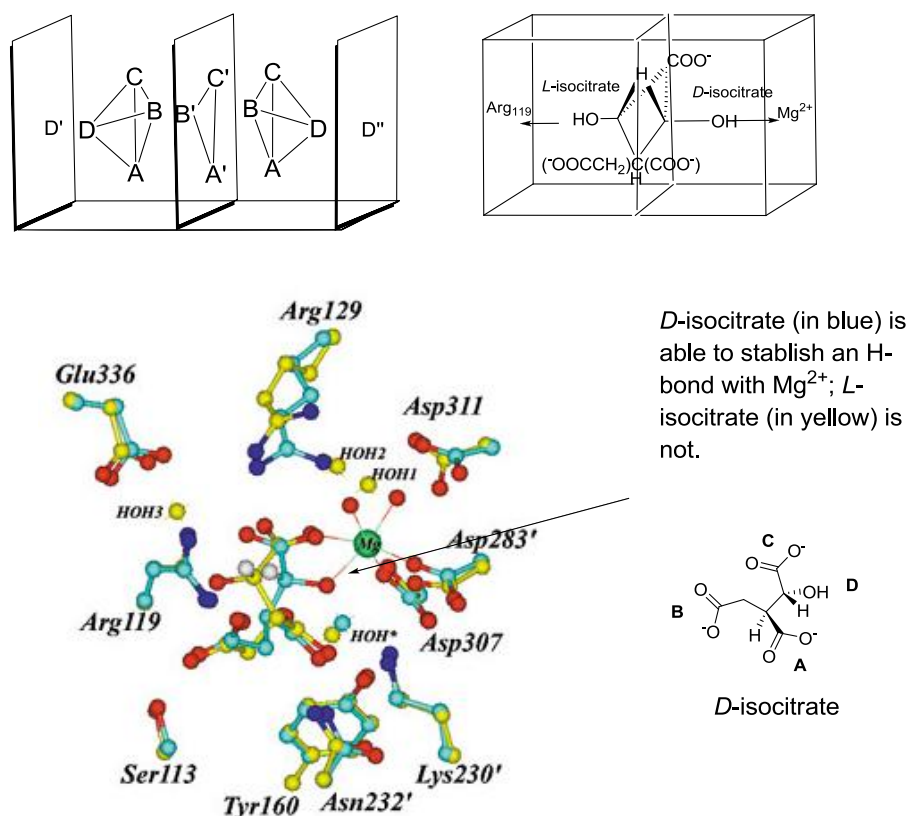


Figure 5.3. Mesecar and Koshland four points model.

¹⁸¹ Easson, I. H.; Stedman, E. *Biochem. J.* **1933**, *27*, 1257-1266.

¹⁸² Koshland Jr., D. E. *Biochemistry and Molecular Biology Education* **2002**, *30*, 27-29.

¹⁸³ Mesecar, A. D.; Koshland Jr., D. E. *Nature* **2000**, *403*, 614-615.

5.1.2. Previous research in our group

Traditionally, our research group has been working with a tripodal benzoxanthene skeleton derivative.¹⁸⁴ Good results have been achieved in the molecular recognition of amino acid derivatives, being able to achieve enantioselective extractions with preferences up to 10:1.

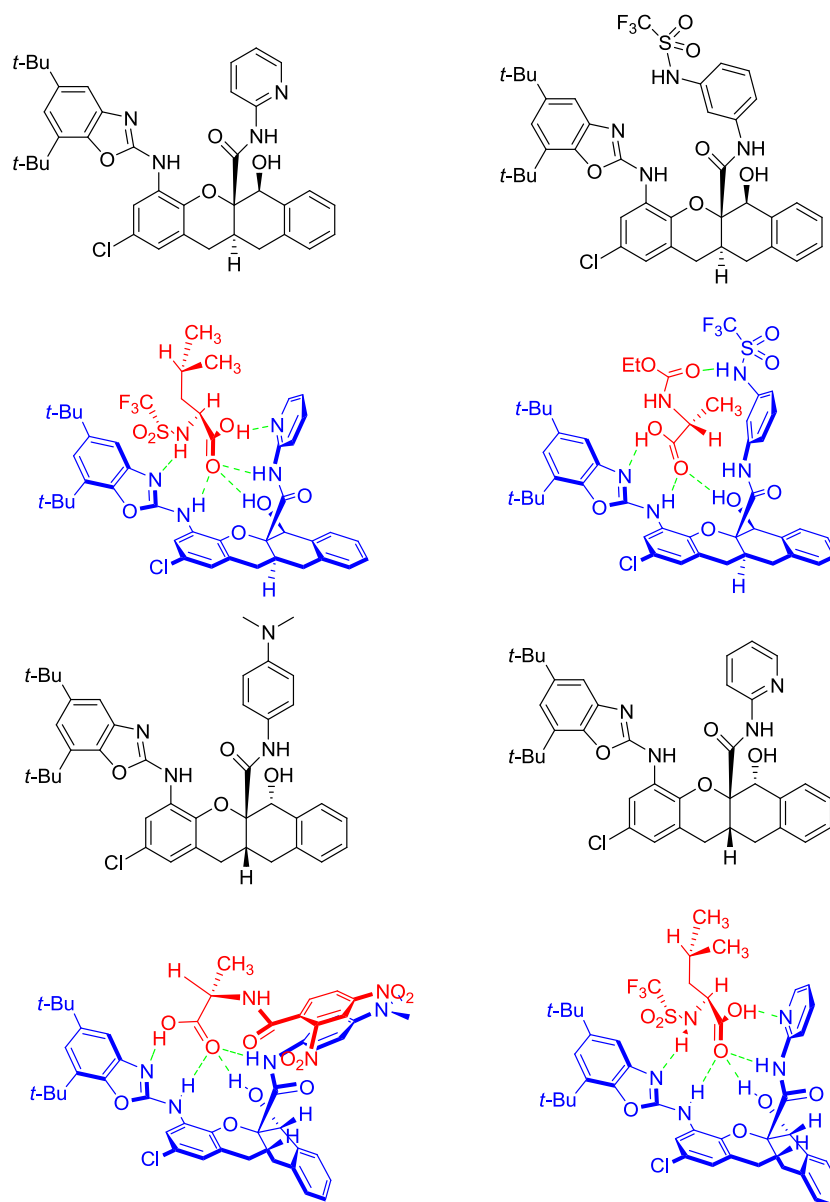


Figure 5.4. Several cis and trans benzoxanthene derivated receptors and their complexes with amino acid derivatives.

¹⁸⁴ (a) Oliva, A. I.; Simón, L.; Muñiz, F. M.; Sanz, F.; Morán, J. R. *Chem. Commun.* **2004**, 426-427; (b) Oliva, A. I.; Simón, L.; Muñiz, F. M.; Sanz, F.; Morán, J. R. *Eur. J. Org. Chem.* **2004**, 1698-1702; (c) Oliva, A. I.; Simón, L.; Muñiz, F. M.; Sanz, F.; Ruiz-Valero, C.; Morán, J. R. *J. Org. Chem.* **2004**, *69*, 6883-6885; (d) Oliva, A. I.; Simón, L.; Muñiz, F. M.; Sanz, F.; Morán, J. R. *Org. Lett.* **2004**, *6*, 1155-1157; (e) Oliva, A. I.; Simón, L.; Muñiz, F. M.; Sanz, F.; Morán, J. R. *Tetrahedron* **2004**, *60*, 3755-3762; (f) Oliva, A. I.; Simón, L.; Hernández, J. V.; Muñiz, F. M.; Lithgow, A.; Jiménez, A.; Morán, J. R. *J. Chem. Soc., Perkin Trans. 2* **2002**, *2*, 1050-1052; (g) Pérez, E. M.; Oliva, A. I.; Hernández, J. V.; Simón, L.; Morán, J. R.; Sanz, F. *Tetrahedron Lett.* **2001**, *42*, 5853-5856; (h) Raposo, C.; Almaraz, M.; Crego, M.; Mussons, M^a L.; Pérez, N.; Caballero, M^a C.; Morán, J. R. *Tetrahedron Lett.* **1994**, *35*, 7065-7068.

However, the synthesis of this skeleton is laborious, and it results in a mixture of *cis* and *trans* isomers.

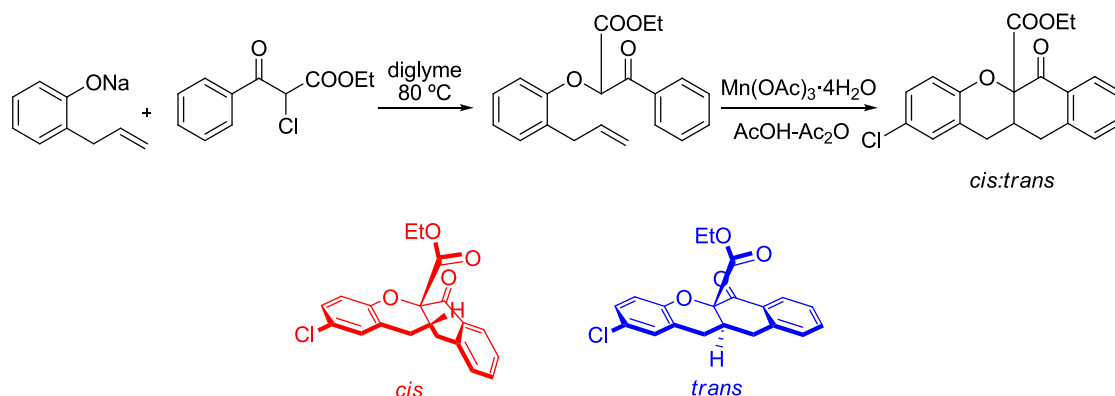


Figure 5.5. Benzoxanthene synthesis that produces a mixture of *cis* and *trans* isomers.

Therefore, we decided to undertake the preparation of a new molecular receptor whose synthesis was easier, but which allows the incorporation of three convergent functional groups in its structure.

In a previous laboratory work in our group¹⁸⁵ it had been carried out the synthesis of a benzofuran skeleton that had been useful as a receptor for sodium salts of carboxylic acids and lipophilic amino acids. This skeleton combined a binding pocket responsible for carrying out the association of the carboxylate group and other part, consisting of two polyethers, responsible for the association of Na^+ .

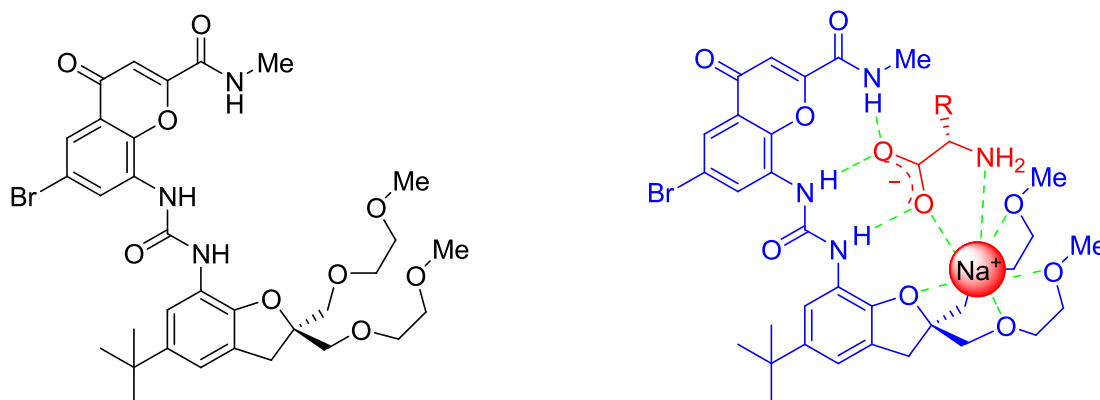


Figure 5.6. Receptor synthesized in our group and the associate formed with a sodium salt of an amino acid.

However, the presence of the two ether groups with free rotation in the guest is disadvantageous due to the existence of degrees of freedom that have to be frozen in the associate. This contributes to an increase in the entropic cost of the association process;¹⁸⁶ moreover it can enhance receptor adaptation to associate both enantiomers. Furthermore, the association of natural amino acids in their *zwitterionic* state was not achieved. On the other

¹⁸⁵ Pérez Payán, M^a N. *Synthesis of receptors for Na^+ and K^+ carboxylate salts*; Final Degree Project: University of Salamanca, 1994.

¹⁸⁶ Steed, J. W.; Atwood, J. L. *Supramolecular Chemistry*, 2^a ed.; John Wiley & Sons: Chichester, 2009.

hand, since both ether groups are equivalent, it would be necessary to introduce a distinguishing feature between the two groups to create an enantioselective receptor.

5.2. METHODS AND RESULTS

5.2.1. Benzofuran skeleton preparation

Although the receptor of figure 5.6 did not seem to be very attractive, it was a good starting point, so that, with minor modifications in the structure, it should be possible to get a more interesting receptor. Consequently with the intention of minimizing the problems of free rotation of the two ether groups on the furan ring, it was decided to incorporate a ring structure which also solves the problem of equivalence between the two groups. The ring introduces asymmetry in the molecule.

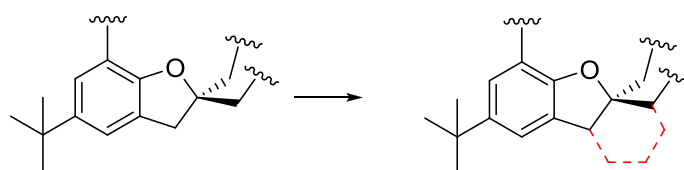


Figure 5.7. Scheme of the strategy to follow.

The preparation of the starting benzofuran **76** of figure 5.7 is described in the literature.¹⁸⁷ The treatment with bromine of the previous benzofuran halogenates the aromatic ring at position 4. At the same time, the hydrogen bromide which is generated in the reaction allows the conversion of the hydroxyl group to the corresponding bromide, as shown in figure 5.8.

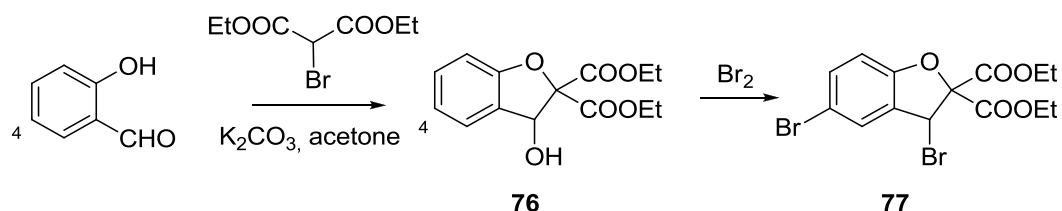


Figure 5.8. Synthesis of intermediate **77**.

To generate a new ring on the benzofuran skeleton we studied the replacement of the bromine atom by a suitable fragment. Since the bromide in the benzylic position must generate carbocations easily, we initially chose a Friedel-Crafts alkylation. The reaction did not proceed readily with benzene, but the presence of activating groups such as -OH or -OMe in phenol or anisole, respectively, makes the reaction to proceed cleanly to the substitution products, as shown in figure 5.9.

¹⁸⁷ Sargent, M. V.; Stransky, P. O. *J. Chem. Soc., Perkin Trans. 1*, **1982**, 1605-1610.

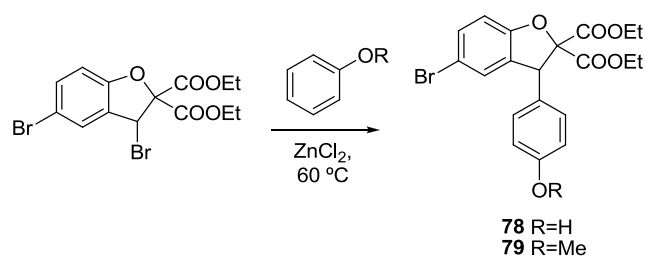


Figure 5.9. Friedel-Crafts alkylation.

We expected that an intramolecular Friedel-Crafts acylation of the aromatic ring with one of the molecule esters would generate only the stereoisomer with *cis* fusion between the pentagonal rings, since the *trans* compound would have rendered a stressed ring. This cyclization was studied in several possible ways, as shown in figure 5.10, but in no case the desired cyclization was achieved, being the major product of the reaction, in most cases, the aromatization compound of the furan ring, generated by loss of one of the molecule carboxyl groups (figure 5.10 (e)).

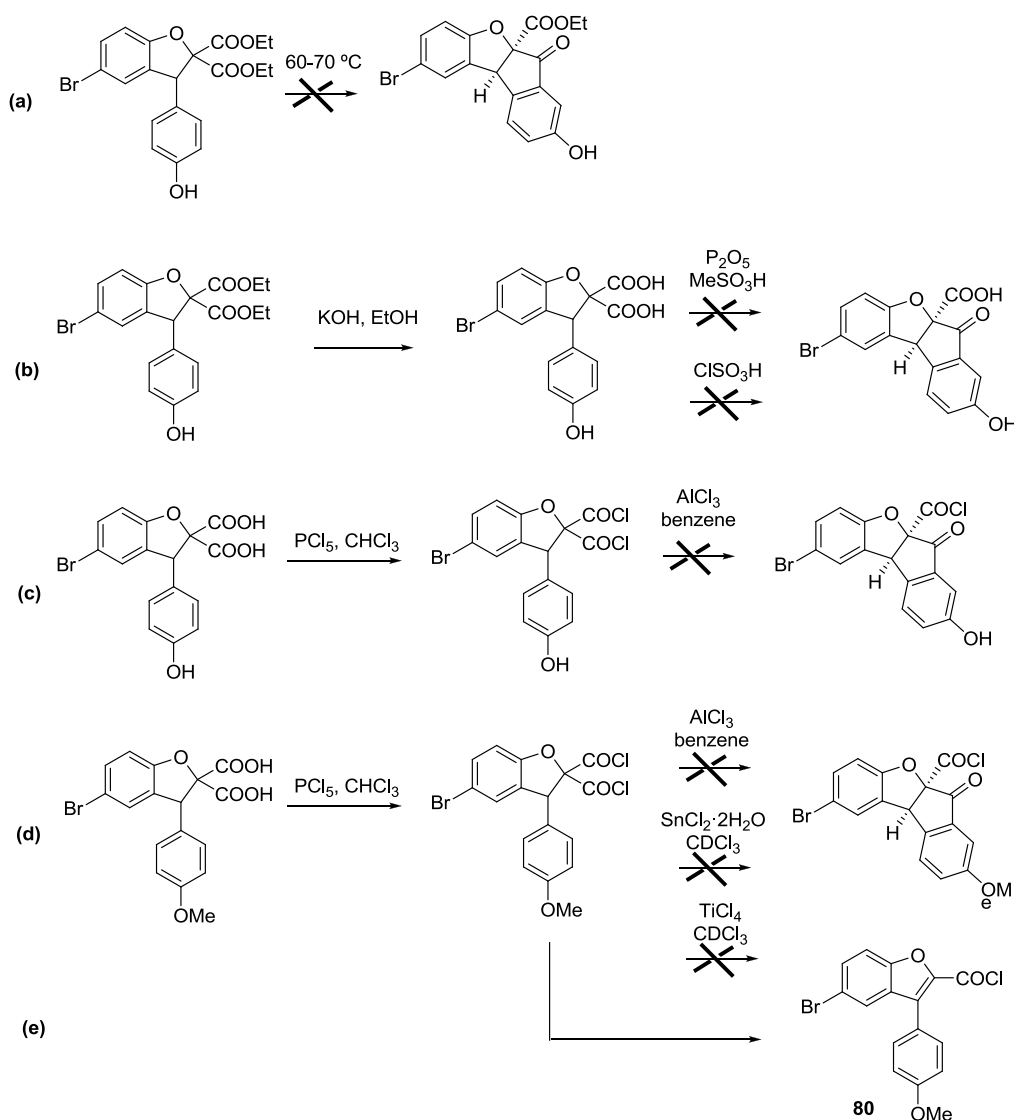
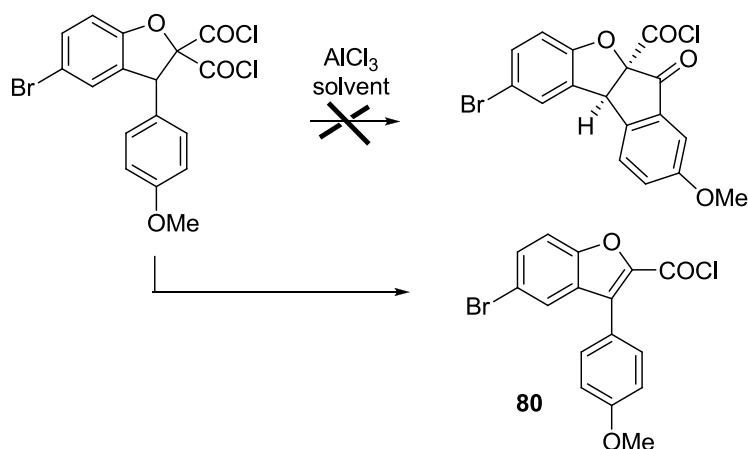


Figure 5.10. Unsuccessful attempts to cyclise compounds 78-79.

The use of different solvents, as shown in table 5.1 did not lead to the desired cyclization compound:

Table 5.1. Study with different solvents.



Solvent	
Benzene	Mixture of several compounds
CS ₂	80
Hexane	No reaction

The fact that the above compounds did not cyclise to generate the corresponding pentagonal ketone was surprising to us, because according to the Baldwin rules, it should correspond to a *5-exo-trig* allowed process, as shown in figure 5.11. Indeed, it is easy to find in the literature similar cyclizations.¹⁸⁸

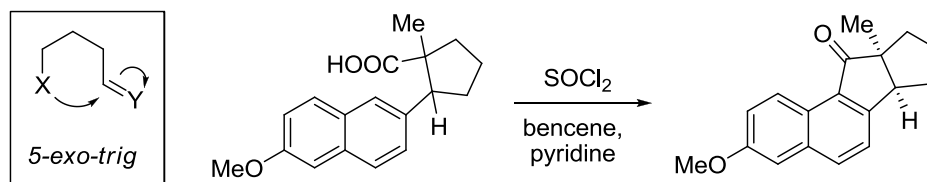


Figure 5.11. Cyclization which according to Baldwin rules should correspond to a *5-exo-trig* process.

A factor that clearly hinders the cyclization of the above compounds is the position of the oxygen used as an activating group, since the cyclization must occur in the *meta* position, while the *ortho* and *para* positions are activated by this oxygen atom.

To prepare an aromatic ring in which the activating group was in the right position to facilitate the cyclization, the reaction of derivative **77** was studied with other aromatic rings. We found that the reaction with toluidine was promising because while the phenol replaced the bromine atom with C-alkylation, toluidine prefers to react in the nitrogen atom, generating compound **81**. In this compound, the intramolecular Friedel-Crafts acylation could generate

¹⁸⁸ Eglinton, G.; Nevenzel, J. C.; Scott, A. I.; Newman, M. S. *J. Am. Chem. Soc.* **1956**, *78*, 2331-2335.

the corresponding hexagonal ring, since the electrophilic attack takes place on the carbon in the *ortho* position to the nitrogen atom.

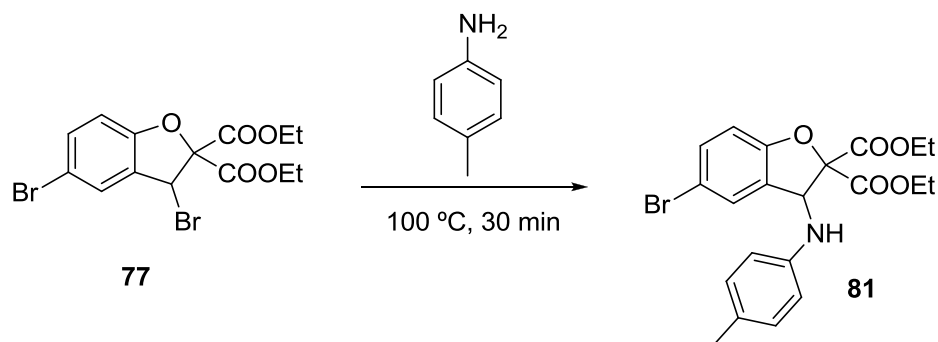


Figure 5.12. Introduction of a toluidine molecule in derivative **77**.

The previous cyclization may be classified as a 6-*exo-trig* process according to Baldwin rules and, in fact, such cyclizations have been found in literature,¹⁸⁹ although none of them involving a furan ring.

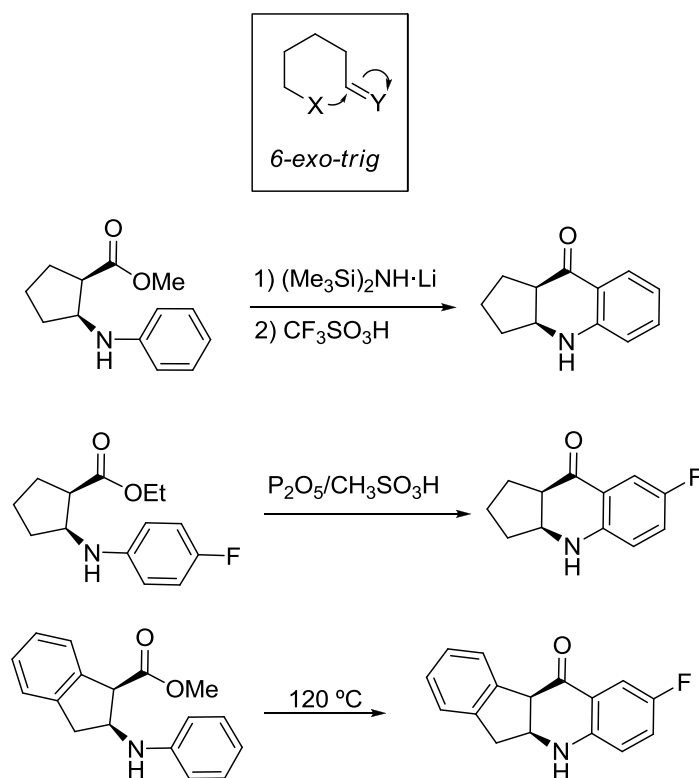


Figure 5.13. 6-Exo-trig cyclization and examples found in literature.

However, it was not possible for us to carry out this reaction with compound **81**. Figure 5.14 summarizes the conditions tested for this purpose.

¹⁸⁹ (a) Huang, X.; Brubaker, J.; Peterson, S. L.; Butcher, J. W.; Close, J. T.; Martinez, M.; MacCoss, R. N.; Jung, J. O.; Siliphaivanh, P.; Zhang, H.; Aslanian, R. G.; Biju, P. J.; Dong, L.; Huang, Y.; McCormick, K. D.; Palani, A.; Shao, N.; Zhou, W., U. S. Patent 0329743, 2012; (b) Lee, C. G.; Lee, K. Y.; GowriSankar, S.; Kim, J. N. *Tetrahedron Lett.* **2004**, 45, 7409-7413.

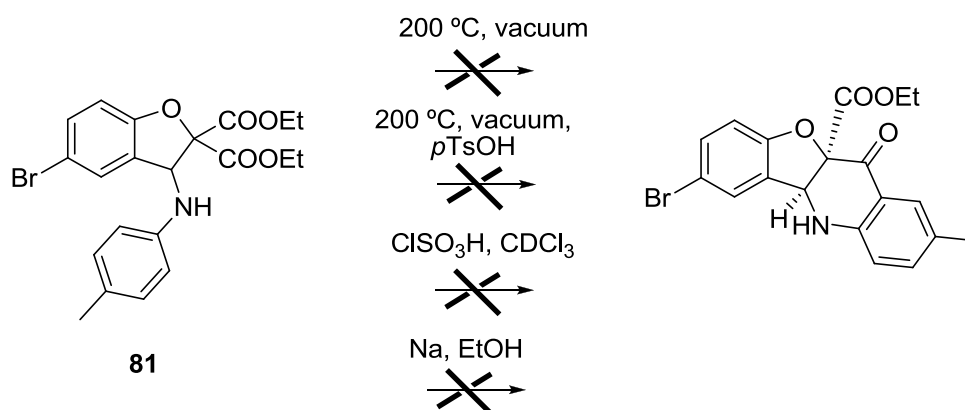


Figure 5.14. Unsuccessful attempts to cyclise compound **81**.

Probably under the reaction acidic conditions, protonation of the amine takes place, yielding a loss of activation in the aromatic ring. To solve this problem, acetylation of the aniline nitrogen was carried out, but the results in regard to the cyclization were equally negative.

The major problem with these aniline derivatives is that in the presence of a nucleophile (NuH), the nitrogen can act as a leaving group and consequently decarboxylative elimination products are favoured. The aromatic furan is generated, as shown in figure 5.15.

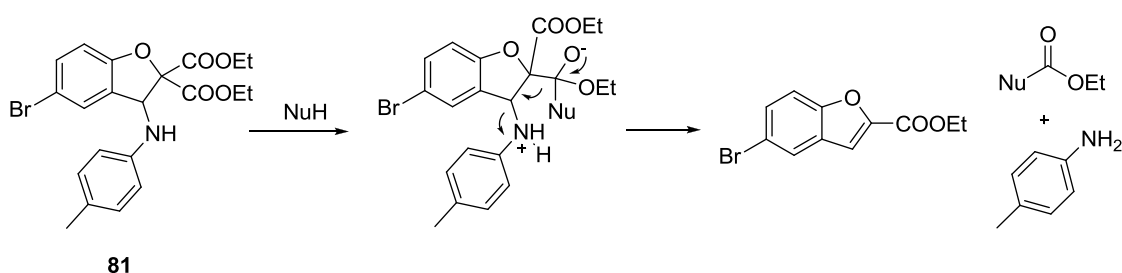


Figure 5.15. Decarboxylative elimination leading to furans.

Due to the difficulties found in the cyclization reactions, we searched in the literature to find an alternative synthesis. This study led us to a work by Xie¹⁹⁰ in which he carries out the synthesis of several benzofuran derivatives. Domino reactions promoted by K_2CO_3 were used for the synthesis of *clofibrate* derivatives. *Clofibrate* is a compound used to control high levels of cholesterol and triglycerides in blood.

¹⁹⁰ Li, Q.-B.; Zhou, F.-T.; Liu, Z.-G.; Li, X.-F.; Zhu, W.-D.; Xie, J.-W. *J. Org. Chem.* **2011**, *76*, 7222-7228.

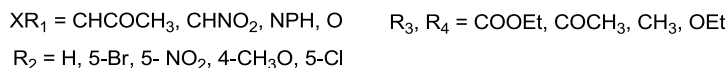
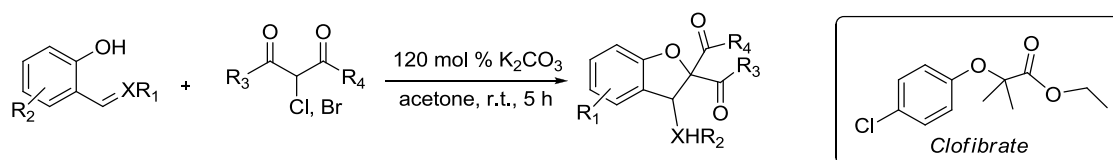


Figure 5.16. K_2CO_3 mediated cyclization conducted by Xie.

The possibility to directly achieve compound **82** by reaction of commercial compounds such as salicylaldehyde and diethyl chloromalonate was very attractive because it allows obtaining large amounts of this compound in a cheap way, so we carried out its preparation.

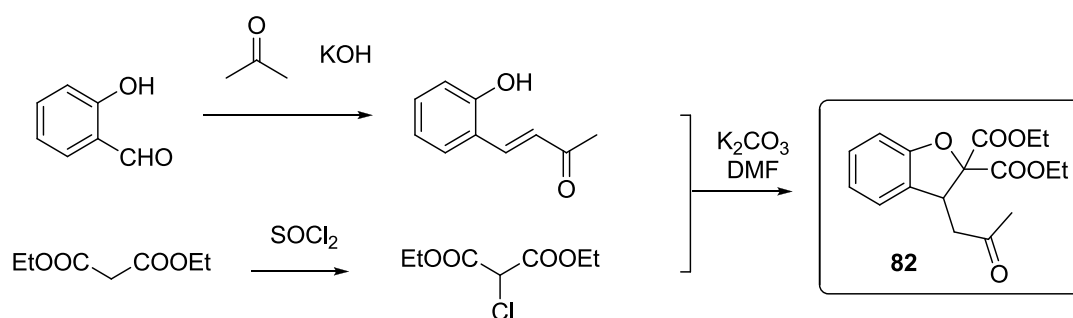
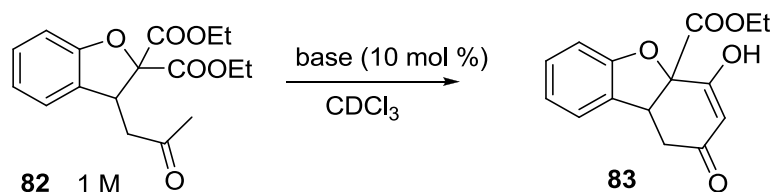


Figure 5.17. Synthesis of intermediate **82**.

Although compound **82** cyclization seems an obvious process in basic medium, Xie did not describe this process, and neither have we found it in the literature, so we decided to explore the best conditions for the cyclization of compound **82**. We studied different bases, as is indicated in figure 5.18.



base = pyrrolidine, DBU, DABCO

Figure 5.18. Cyclization attempts with compound **82**.

We could observe that weak bases such as triethylamine or DABCO were not able to promote the reaction, but it was possible to carry out the cyclization with DBU. However, the yield obtained with the latter base was not satisfactory, so we preferred to cyclize under standard conditions using sodium ethoxide. With this base, the reaction proceeds rapidly at room temperature. During the cyclization low temperatures are required, because high temperatures lead to decarboxylation. Moreover, it is essential to avoid the presence of water, which generates carboxylates.

Optimal conditions were achieved drying EtOH with ethyl orthoacetate and a trace of MeSO₃H and using a Na molar excess (about 5 eq, 3.6 M approx). Once sodium ethoxide is generated it is necessary to cool the solution to 0 °C before adding the ketoester. The mixture is stirred and the enolate sodium salt precipitates in the reaction medium.

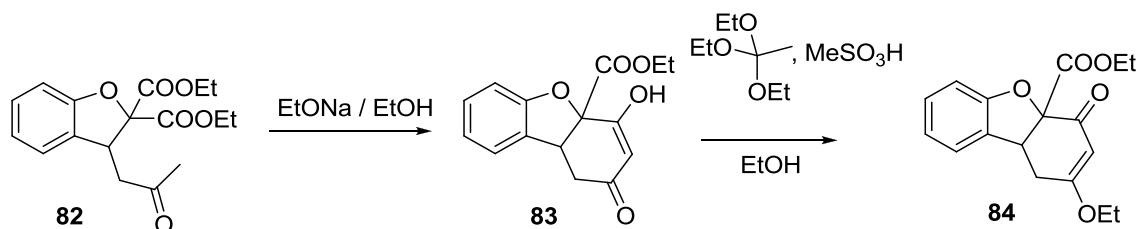


Figure 5.19. Cyclization with EtONa/EtOH.

The way to neutralize the basic reaction medium was not trivial. The problem is that the enol, after acidification with hydrochloric acid, is partly soluble in water, due to the high proportion of oxygen versus carbon atoms in this molecule, and in the aqueous medium, the ester of the molecule is hydrolyzed very fast, leading to an acid that is even more water soluble and which undergoes decarboxylation. To solve this drawback, we decided to transform the enol into the corresponding enol ether, in order to increase the lipophilicity of the compound. To achieve this goal, a solution of ethyl orthoacetate and MeSO₃H in dry ethanol was added to the above mixture. MeSO₃Na precipitated, so that it could be filtered off, and the filtrate was evaporated to obtain the corresponding enol ether. Under these conditions the *cis* compound (figure 5.20) was always obtained as we could confirm by X-ray diffraction.

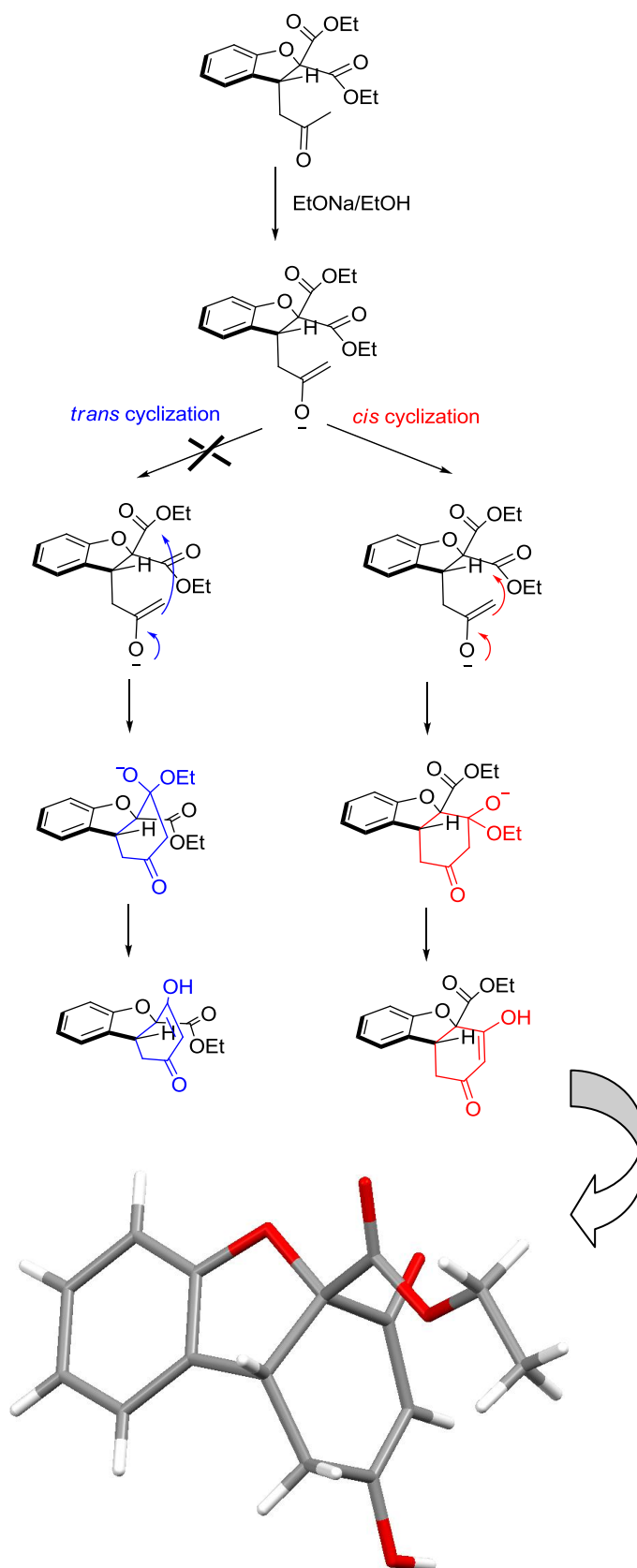


Figure 5.20. Cyclization with EtONa/EtOH in which only the product from the cis cyclization is obtained and X-ray structure of the cyclization product.

After the preparation of the asymmetric tricyclic skeleton, in which one of the carbonyl groups of the starting esters is transformed into a ketone, we considered the introduction of suitable functional groups for simulating the oxyanion hole.

5.2.2. Functionalization of the skeleton to create an oxyanion-hole analogue

Although they are similar compounds, the geometry of the benzofuran skeleton in compound **84** is different from the benzoxanthene we have been working with in recent years (figures 5.5 and 5.6). This implies that the formation of the oxyanion hole cannot be performed with the same functional groups. A modelling study revealed us that in the case of substituting the benzofuran with an amino group, in analogy to benzoxanthene, the distance between the NHs, 5.06 Å, would be greater than the average distance in the oxyanion holes of enzymes (4.3 Å), as shown in figure 5.21 (a).

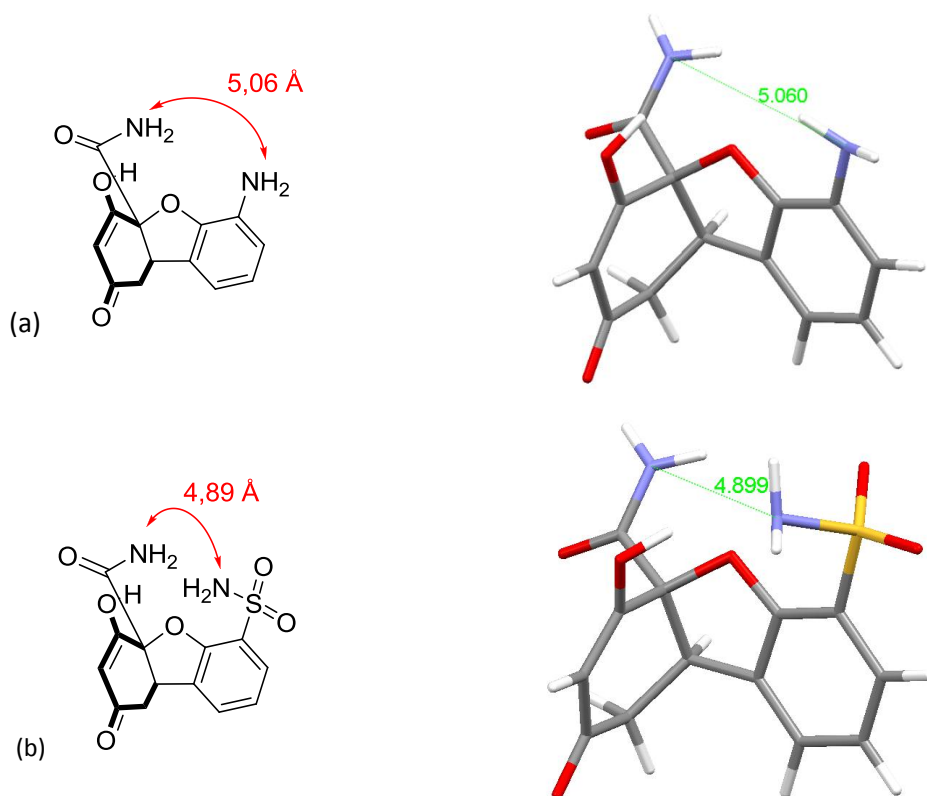


Figure 5.21. Distance between NHs groups in two potential receptors derived from benzofuran.

In these circumstances, the association of the carbonyl will be weak, since both hydrogen bonds will present a weak cooperative effect due to the large distance between them.

CPK molecular models showed us that a good solution to reduce the distance between the NHs that should form the oxyanion hole in the benzofuran skeleton was to place a sulfonamide on the benzene ring (figure 5.21 (b)). Assuming that the NHs of the sulfonamide and the amide are forming intramolecular hydrogen bonds with the oxygen of the furan, the distance between NHs would reduce to 5.89 Å, a little bit wide in comparison with the average distance

in enzymes. However, the molecule could adopt the two conformations shown in figure 5.22, with the distances between the NHs indicated.

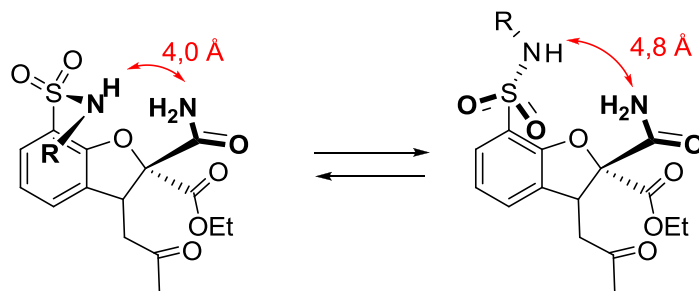


Figure 5.22. Two possible geometries for the oxyanion hole of a receptor with a benzofuran skeleton substituted with a sulfonamide, and the distance between the NHs obtained by molecular modelling.

Consequently, we proceeded to functionalize the position 6 of the benzene ring by sulfonation. However, the most reactive position on the aromatic ring of compound **84** against electrophilic substitution is carbon 8, so that it is necessary to block this position. With this objective we made several tests with bromine and *t*-butyl chloride. However, they lead to the breakdown of the molecule, presumably by attack to the sensitive vinyl ether, as indicated by the fact that the analysis by ^1H NMR spectroscopy revealed the disappearance of the double bond proton signal.

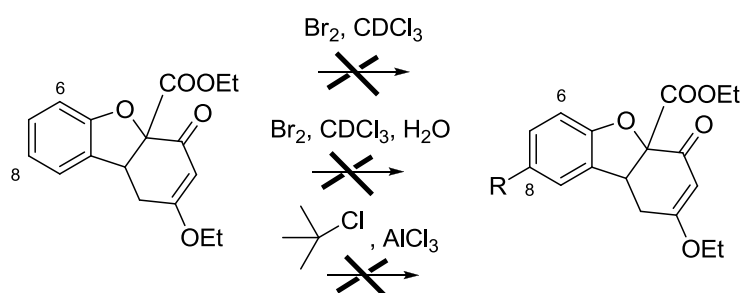


Figure 5.23. Protection of position 8.

This drawback made us propose a new synthesis, so we decided to introduce the blocking group at the 4 position of salicylaldehyde before synthesizing the chalcone with acetone and KOH. Furthermore, we changed diethyl malonate by methyl malonate, to facilitate the crystallization of the intermedia, making easy the workup of the reaction. In addition, it would allow obtaining crystals for X-ray diffraction analysis, which is highly recommended to know the exact geometry of the receptor: distances, bond angles, etc. Then, to create the oxyanion hole, we proposed the introduction of a sulfonyl group *ortho* to the oxygen atom of the furan ring. This sulfonyl group will become a sulfonamide with an acid NH. *t*-Octylamine was chosen as amine, which thanks to the bulky *t*-octyl group reduces the solubility in water of the compounds, facilitating its extraction in organic solvents.

The synthesis was carried out by the procedure described in figure 5.24.

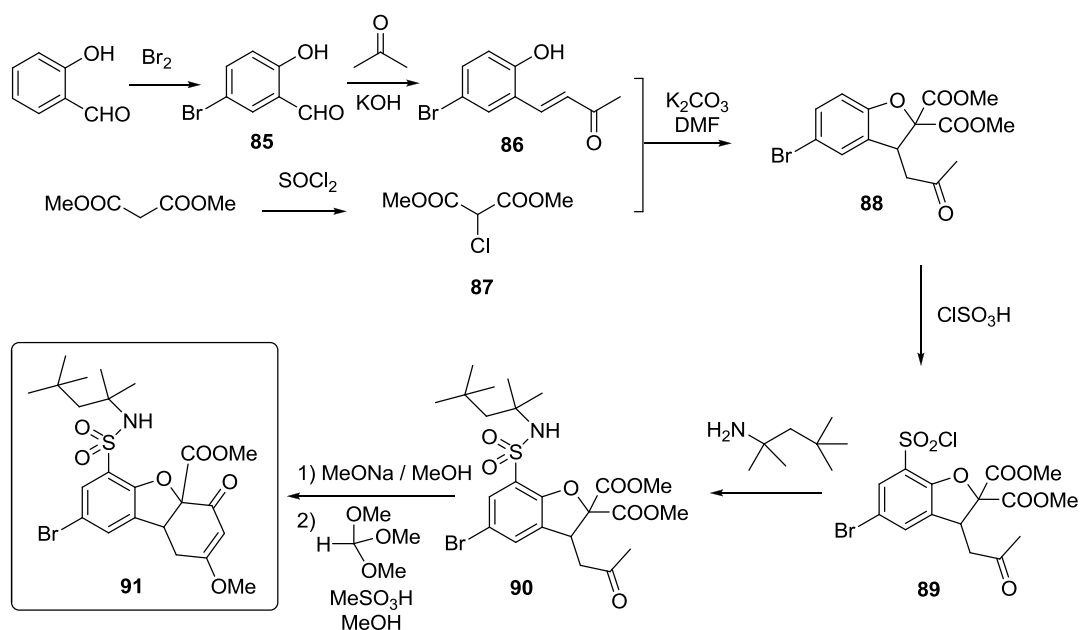


Figure 5.24. Synthesis of skeleton **91**.

Following the previous scheme the preparation of the basic skeleton was achieved.

The above compound **91** only has a single hydrogen bond donor, so that it does not allow the direct simulation of the oxyanion hole. To obtain more hydrogen bond donors we thought to reduce compound **91** ketone with NaBH_4 in MeOH. Interestingly, the methyl ester was also reduced to give compound **92**, which was purified by crystallization obtaining crystals of enough quality for X-ray diffraction analysis.

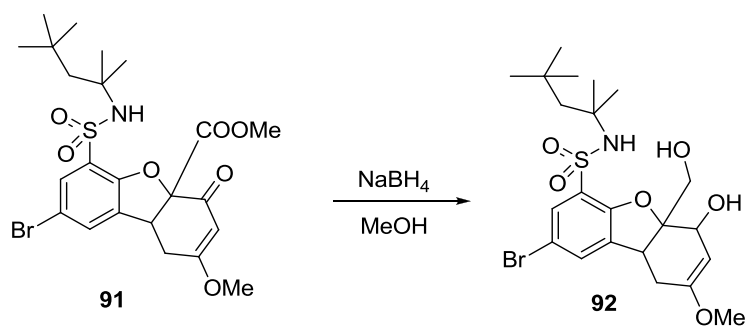


Figure 5.25. Reduction of intermediate **91**.

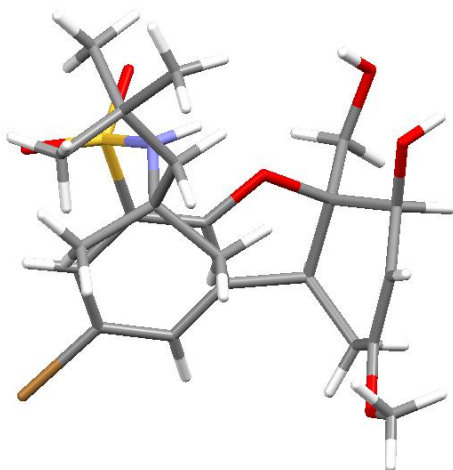


Figure 5.26. X-ray structure of receptor **92**.

The X-ray diffraction study has allowed us to confirm the proposed structure and the configuration of the hydroxyl on the ring. This configuration was generated by *exo* hydride attack to the ketone by the least hindered face. It is curious that the cyclohexenyl ring adopts a *pseudo-boat* conformation, probably because in this way the hydroxyl group is in the equatorial position.

Although receptor sulfonamide could have chosen any of the hydroxyl groups in the molecule to form the oxyanion hole, the X-ray study reveals that in this case the oxyanion hole is formed between the NH of the sulfonamide and the hydroxyl group from the ketone reduction.

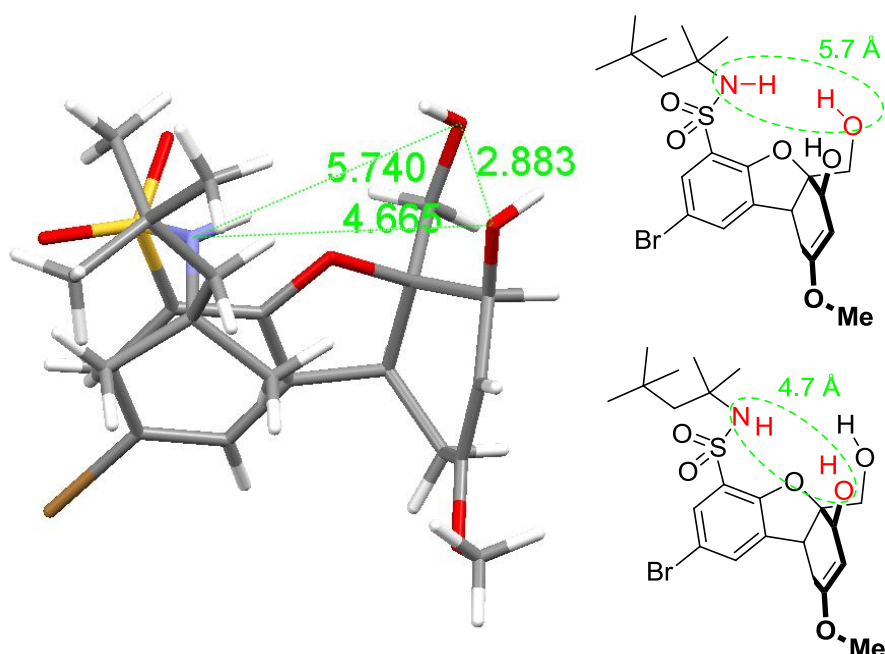


Figure 5.27. (Left) X-ray structure of receptor **92** and heteroatom-heteroatom distances (Å) between the sulfonamide-NH and the hydroxyl groups, and between primary and secondary OH; (right) the two possible oxyanion holes.

As can be seen in figure 5.27, the distance between the sulfonamide NH and the secondary OH on the cyclohexenyl ring is about 4.7 Å, very close to the existing values of the oxyanion holes in enzymes which range from 4.3 Å to 4.6, according to literature.¹⁹¹ So apparently, the oxyanion hole formed between these two groups is very good. The distance between the sulfonamide NH and primary OH, 5.7 Å, is too large to generate an oxyanion hole, and the distance between the two hydroxyls is very short (2.9 Å), probably existing some kind of intramolecular hydrogen bond between them. The choice of the secondary hydroxyl for oxyanion-hole formation is favoured in this case, because it lies on a *pseudo-axial* substituent, allowing to approach the sulfonamide. Accordingly, the hydroxymethyl occupies a *pseudo-equatorial* position, which moves away from the sulfonamide, thus justifying the large distance of 5.7 Å between this group and the sulfonamide NH.

By extending the unit cell of the X-ray structure, dimer formation was observed, what justifies the existence of the oxyanion hole between the sulfonamide NH and the secondary OH. In this case the primary OH of another receptor molecule is included in the oxyanion hole, forming H-bonds with the NH and the secondary OH. In turn, the primary OH of the first molecule is acting as the guest of the second receptor molecule. In addition, the secondary OH of the first molecule establishes an H-bond of 2.8 Å with one of the sulfonyl oxygen atoms of the second molecule of the dimer.

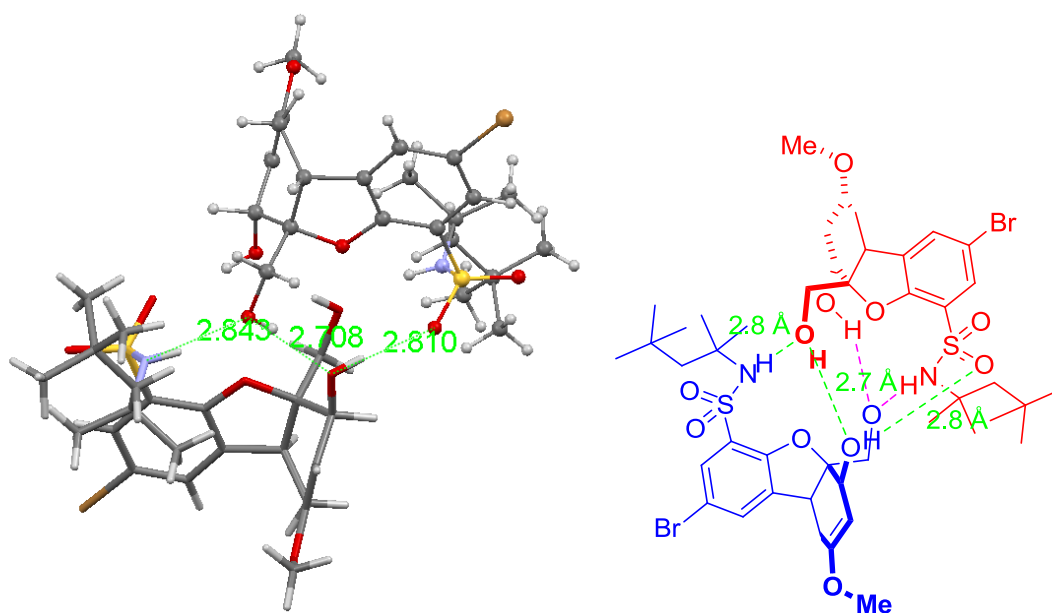


Figure 5.28. Dimer formed between two molecules of receptor **92** in which the oxyanion hole is observed.

In addition, the hydrogen bonds formed, 2.7 and 2.8 Å, are quite good as rated by Jeffrey (Chapter 3, page 113). Therefore, the skeleton formed is promising as a tripodal oxyanion hole, leaving a cavity in which, potentially, three hydrogen bond donors may act together to associate a carbonyl, an anion or any similar guest.

¹⁹¹ Simón, L.; Goodman, J. M. *J. Org. Chem.*, **2010**, *75*, 1831-1840.

To improve the properties of these compounds as molecular receptors we considered to replace the ester by a more attractive functional group to enable greater number of interactions. For this objective, a molecule of methylaminopyridine was introduced into the ester group, following the methodology already described.¹⁸⁴ The introduction of a basic group can create a bifunctional receptor, so that one part of the skeleton would act as hydrogen bond donor and other part as an H-bond acceptor. Thus the chances of interaction with a larger number of guests would be increased.

In our case, it was not possible to introduce the aminopyridine by hydrolysis of the ester and formation of the compound **91** acid chloride, since under these conditions the decarboxylation product is obtained. To avoid the problematic hydrolysis step we turn to generate the lithium anion of the aminopyridine by treating it with BuLi in THF. Reaction of the ester with this amide proceeds rapidly at -30 °C, and generates the amidopyridine with acceptable yield. In this case we did not use the intermediate **91** since under these conditions the amidopyridine anion will probably add to the double bond of the conjugated ketone, substituting the methyl ether. In fact, it was observed that by treating intermediate **91** with butylamine, the aminolysis of the ester and methyl ether substitution by butylamine occurred.

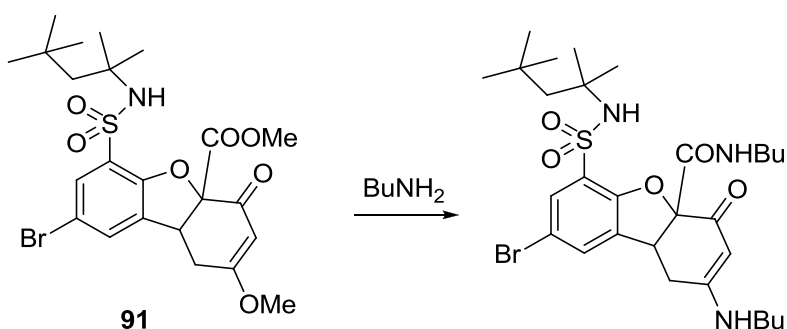


Figure 5.29. Aminolysis of the ester and methyl ether substitution by treating intermediate **91** with butylamine.

For this reason, after compound **91** cyclization, the reaction was worked up over an aqueous solution of methanesulfonic acid. The *t*-octyl group of the sulfonamide confers lipophilic properties to the molecule preventing hydrolysis and decarboxylation problems, which we had found with the non-functionalized intermediate **83** (figure 5.19). This enol can be treated with methylaminopyridine lithium anion for ester aminolysis. Under these conditions, the excess of BuLi deprotonates the enol producing an enolate, which can no longer add aminopyridine. After neutralizing the reaction medium, addition of methyl orthoformate in MeOH allows to obtain the methyl ether **94**.

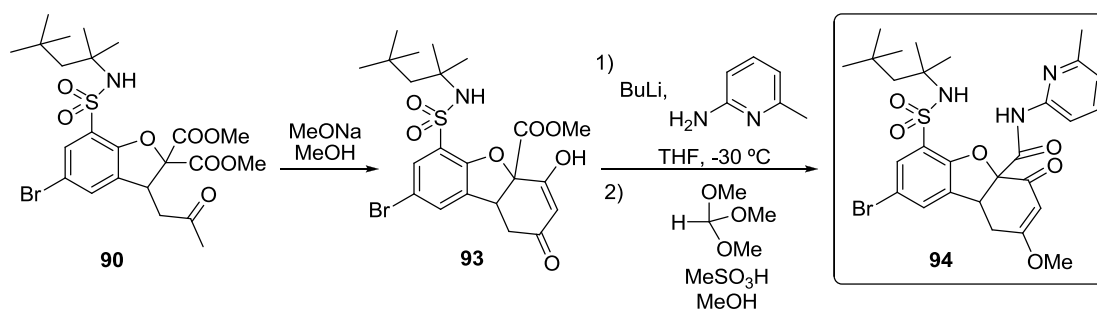


Figure 5.30. Receptor **94** obtention.

Thus it has been achieved a first tripodal receptor with an oxyanion hole created between two NHs and also with several functional groups (a basic N of the pyridine ring and a ketone group) which could be used for anchoring different molecules.

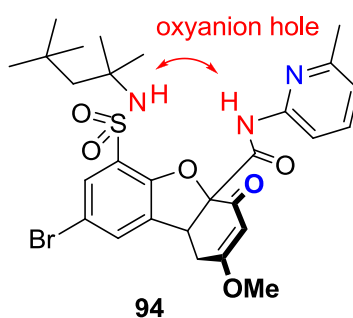


Figure 5.31. Receptor **94** in which the oxyanion hole and other functional groups are shown.

Crystallization of compound **94** in MeOH gave good results. Crystals of enough size to carry out the X-ray diffraction study were obtained.

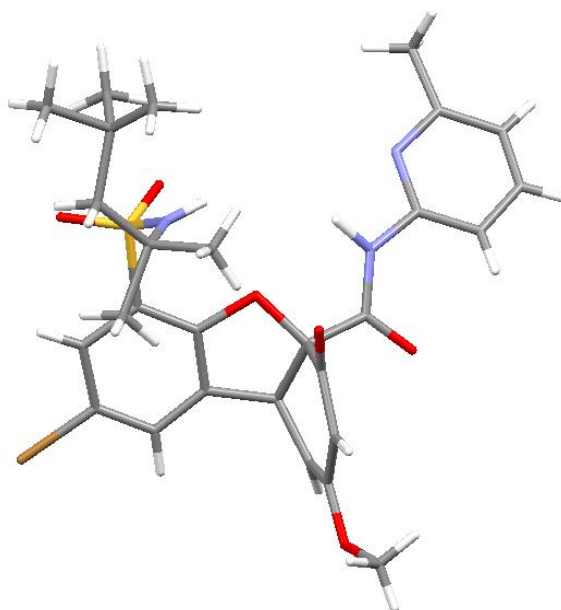


Figure 5.32. Receptor **94** X-ray structure.

The projection of receptor **94** from its top presents a three-pointed star model, in which the NHs generating the oxyanion-hole are located between two of the points, whereas the ketone group is placed on the third tip.

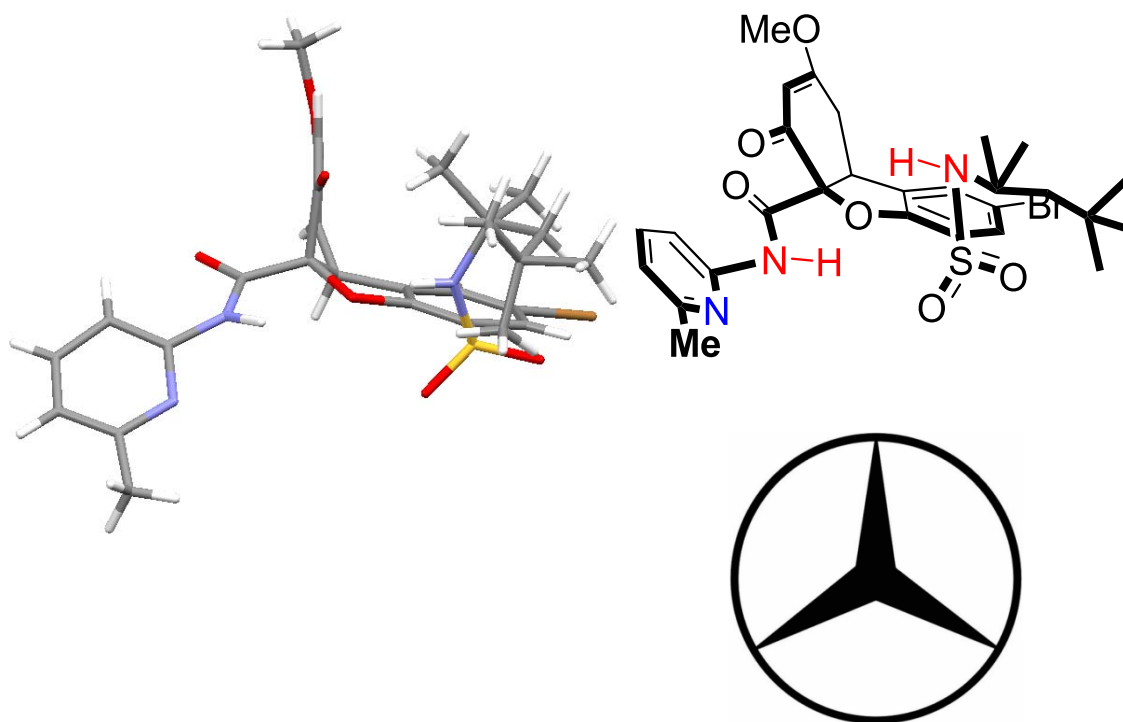


Figure 5.33. Receptor **94** top view.

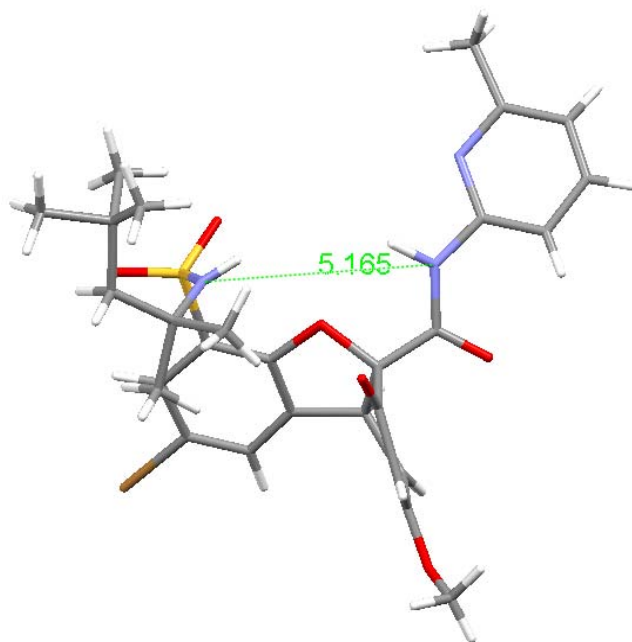


Figure 5.34. X-ray structure in which the distance (heteroatom-heteroatom, Å) between NHs responsible for generating the oxyanion hole is shown.

The analysis of the X-ray structure showed a distance of 5.12 Å between the NHs of the sulfonamide and the amidopyridine, distance which is larger than the typical distance in oxyanion holes of enzymes. However, if more molecules are incorporated in the X-ray unit cell, it can be observed that indeed, an oxygen atom (corresponding to the methyl ether of another receptor molecule) is forming two hydrogen bonds with the sulfonamide NH and the amidopyridine NH with distances N...O of 3.5 Å and 3.3 Å, respectively. Figure 5.35 shows this structural feature.

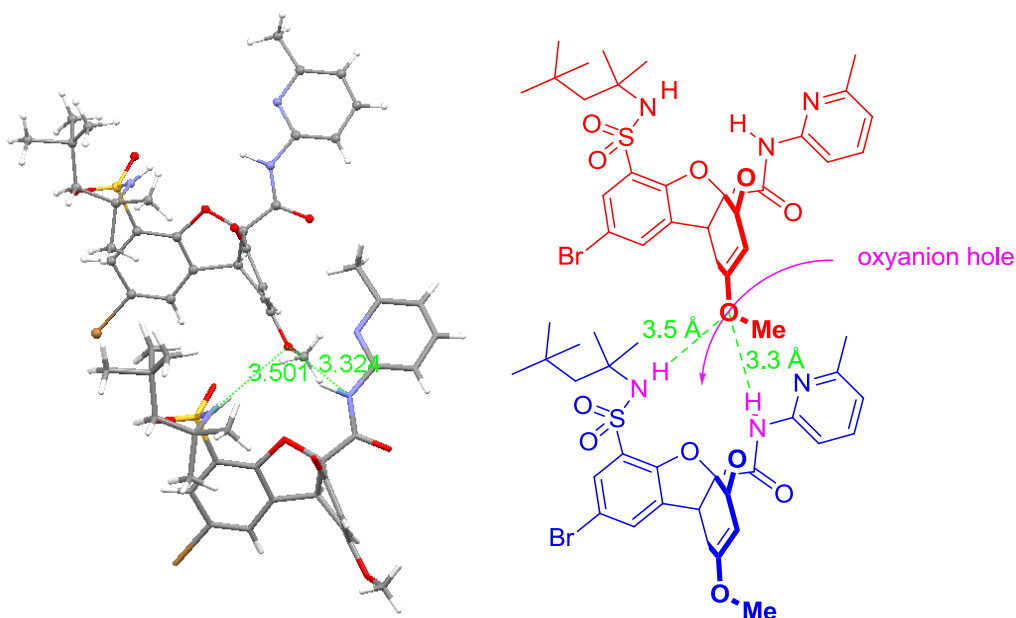


Figure 5.35. X-ray structure in which the receptor oxyanion hole and the hydrogen bonds with the methyl ether of another receptor molecule are shown.

Although these hydrogen bonds can be classified as moderate-weak, in the existing X-ray studies of proteins, it is considered that there may be an energetic significant hydrogen bond when the distance donor-acceptor is about 3.5 Å. Moreover, the strength of a hydrogen bond depends not only of its length but also of its linearity, the nature of the microenvironment and the difference in pK_a between conjugate acids of the electronegative atoms which share the proton.¹⁹²

This kind of structure, in which the oxygen of the enol ether acts as an H-bond acceptor was surprising for us, as other oxygen atoms in the molecule, such as the carbonyl of the carboxamide are, theoretically, much better hydrogen bond acceptors. Since in the crystalline state there are many other forces in addition to hydrogen bonds, they must compensate for the absence of stronger H-bonds.

Moreover, the large size of the oxyanion hole in this structure is probably caused because the oxygen of the vinyl ether is a poor hydrogen bond acceptor and forms long H-bonds. If the oxyanion hole finds a guest which is a better H-bond acceptor, it can easily adapt the size of the cavity to form stronger H-bonds turning the sulphur-carbon bond of the sulfonamide.

¹⁹² Cleland, W. W.; Frey, P. A.; Gerlt, J. A. *J. Biol. Chem.* **1998**, 273, 25529-25532.

Molecular models show that it is possible to reduce the size of the cavity to a distance of only 4.0 Å between the NH of the sulfonamide and the primary alcohol.

5.2.3. Study of receptor **94** supramolecular properties

The study of the supramolecular properties of receptor **94** was started with an absolute titration between this receptor and acetic acid, in order to know the stability of the associate between the receptor and a simple acid, which only have interactions with the oxyanion hole and the pyridine.

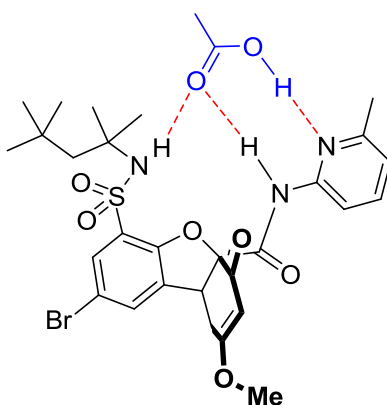


Figure 5.36. Proposed structure for the associate between receptor **94** and acetic acid.

In this case, 3.5 mg of receptor **94** were dissolved in 0.5 mL CDCl_3 and the spectrum was recorded. A known volume of a solution of acetic acid in CDCl_3 (2.9×10^{-2} M) was added and the NMR spectrum was recorded. This operation was repeated and the spectra recorded until saturation. As can be seen, when acetic acid is added, the signals corresponding to the amidopyridine are deshielded. If the variation of the chemical shift of these signals is plotted versus the equivalents of acetic acid added, a graphical representation is obtained, from which, by applying a nonlinear fitting method based on a Monte Carlo algorithm, it can be obtained a value for the association constant, as shown in figure 5.37. In this case the value is 360 M^{-1} , a relatively small number, because the simple associate between amidopyridines and carboxylic acids already show constants around hundreds.¹⁹³ The value obtained, albeit small, is within the order of magnitude expected for an associate stabilized by three H-bonds.

¹⁹³ Lindoy, L. F.; Atkinson, I. M. *Self-Assembly in Supramolecular Systems*; Royal Society of Chemistry: Cambridge, 2000.

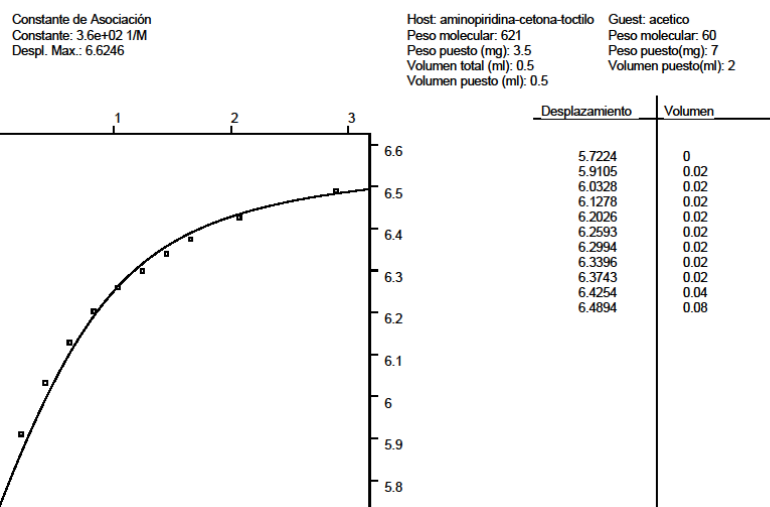


Figure 5.37. Absolute titration between receptor **94** and AcOH.

There are several reasons that could justify the small value obtained for receptor **94** association constant with acetic acid. One is the formation of receptor dimers that the guest has to break before it can form the associate. If this is the case, the energy required to break the dimer has to be obtained from the association energy with the guest, so a small association constants is expected. Figure 5.38 shows a plausible geometry for the formation of a receptor **94** dimer which would be stabilized with four H-bonds.

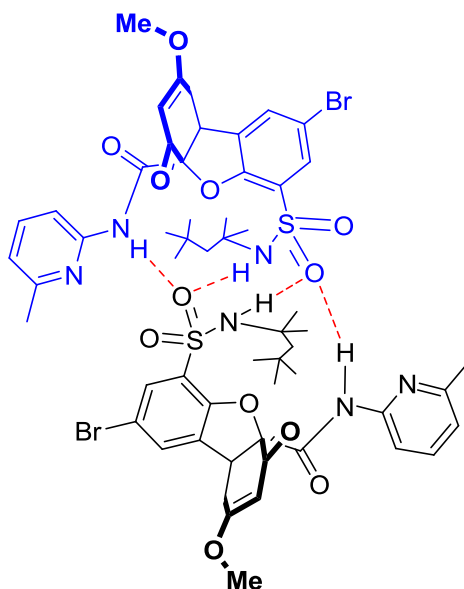


Figure 5.38. Receptor **94** dimer stabilized by four hydrogen bonds.

To measure the receptor **94** dimerization constant, a 0.027 M solution of receptor **94** was progressively diluted in CDCl_3 and spectra were recorded. If the receptor has a tendency to self-associate, dimers formation would take place to a greater extent at high concentrations while as the solution is diluted, such dimers would break down and therefore it would be observed that the signals from the receptor are slowly shifted upon dilution. The graphical

representation of the values for the chemical shifts of receptor **94** versus its concentration allows the calculation of the dimerization constant and, as seen in figure 5.39, this number ($K_{ass} = 13$) is small and we do not expect it can strongly affect the association constant with conventional carboxylic acids.

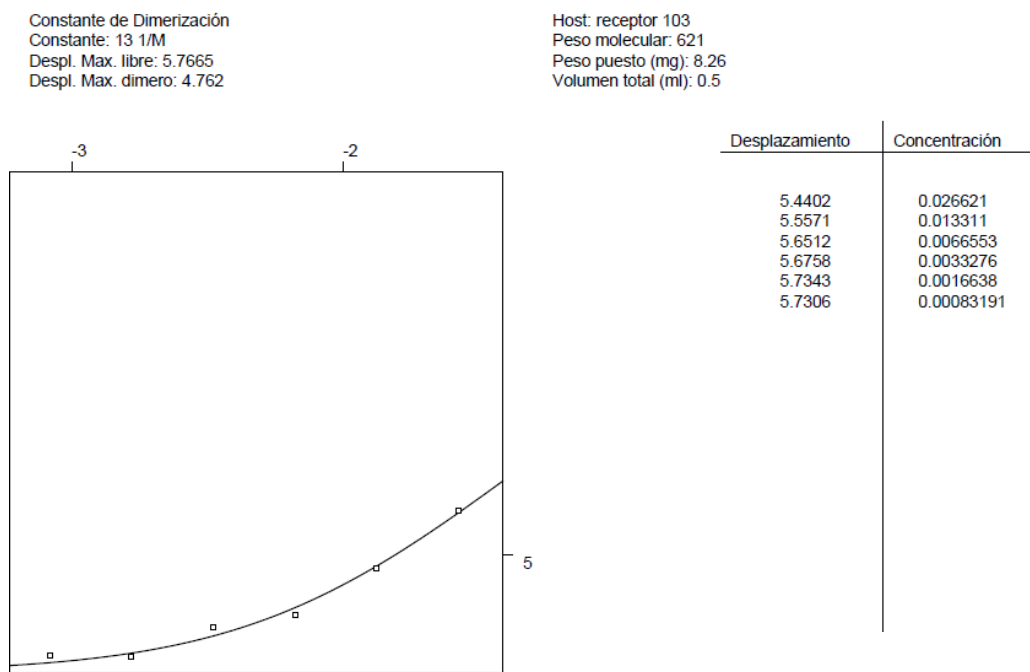


Figure 5.39. Dimerization constant of receptor **94**.

Another possibility which may justify a small association constant with a simple carboxylic acid is the existence of intramolecular hydrogen bonds in receptor **94**. Reviewing the X-ray structure of receptor **94** it can be observed the presence of two intramolecular hydrogen bonds with the furan oxygen atom. The amidopyridine NH is forming a strong intramolecular H-bond of 2.7 Å with the furan oxygen atom, although the angle between the heteroatoms and the hydrogen atom (116°) is not very suitable for hydrogen bond formation. In any case it is possible that this NH generates weak hydrogen bonds with the guest due to the presence of the furan oxygen. Instead the sulfonamide NH is 3.2 Å far from the furan O atom. If we consider that, in addition, the angle between the two heteroatoms with the nitrogen is again unsuitable for the formation of the hydrogen bond, this interaction should not greatly affect the stability of the associate with the carboxylic acid. A third possible hydrogen bond between the amidopyridine NH and the cyclohexanone oxygen can be ruled out, since its distance measures 3.5 Å.

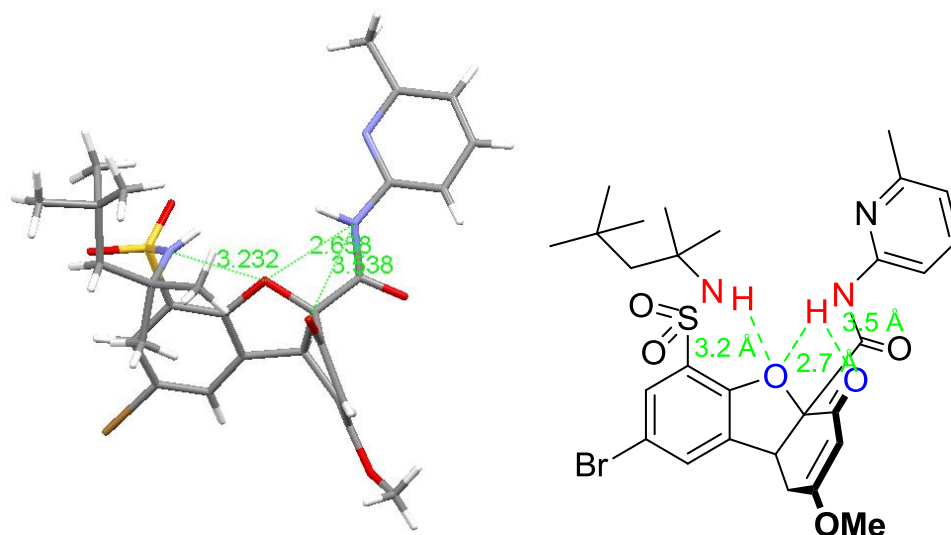


Figure 5.40. X-ray structure in which the intramolecular hydrogen bonds of receptor **94** are shown.

In order to quantify how the presence of such intramolecular hydrogen bonds affects the stability of receptor **94** associates with simple carboxylic acids, the following competitive titrations were carried out using trichloroacetic acid as guest:

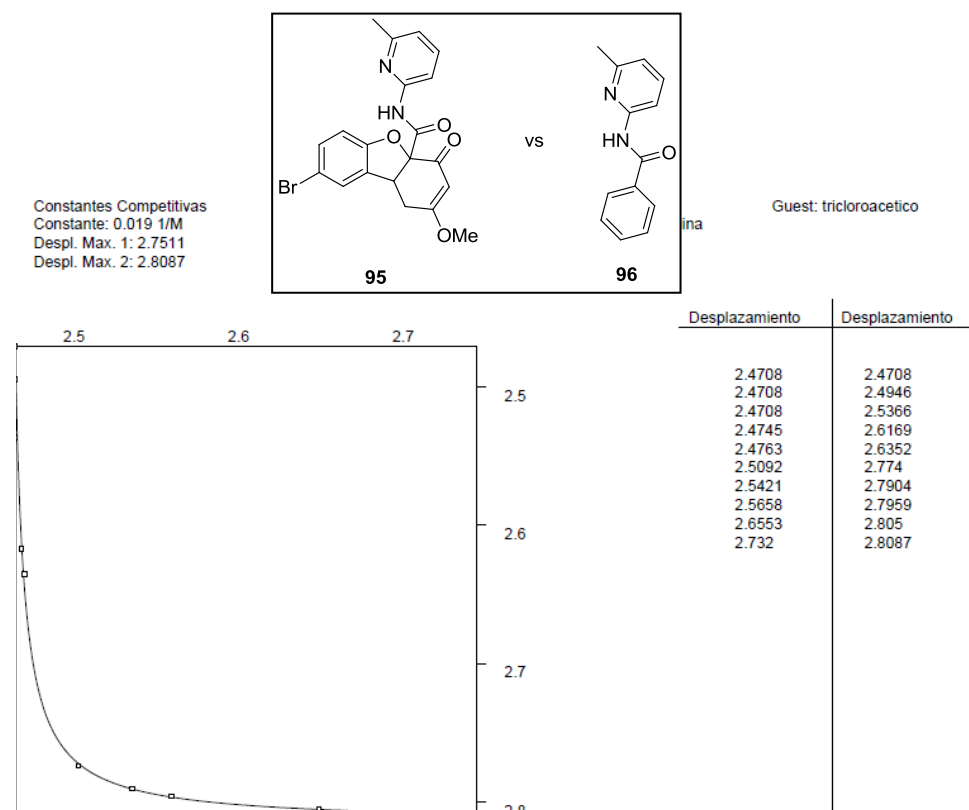


Figura 5.41. Competitive titration between compounds **95** and **96** which justifies the importance of the intramolecular H-bond.

The competitive titration between furan derivative **95** and benzoyl derivative **96** generates a relative constant of $K = 53$ in favour of compound **96**. It can be considered that the hydrogen bond between the amidopyridine NH and the furan oxygen is making the acid association more difficult.

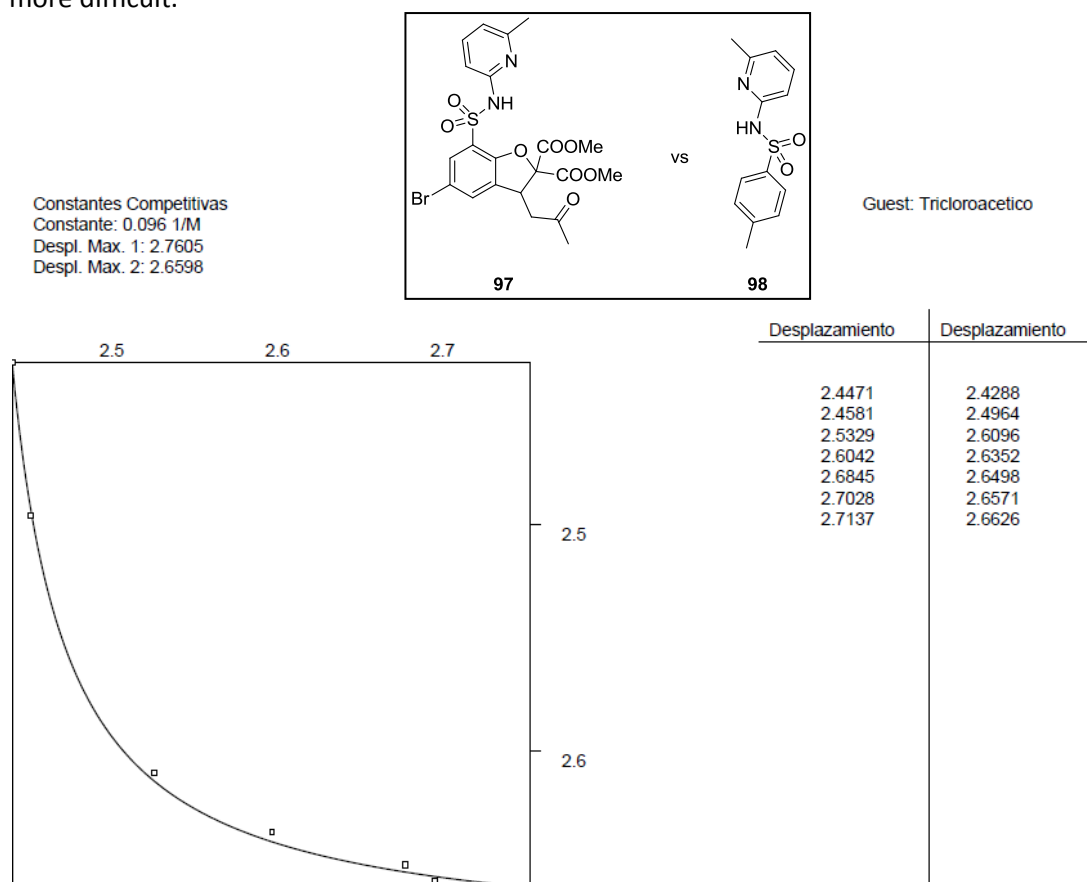


Figure 5.42. Competitive titration between compounds **97** and **98**.

Instead, the competitive titration between compounds **97** and **98** generates a relative constant of $K = 10$ in favour of the furan derivative. Then, it seems that the existence of an intramolecular hydrogen bond between the sulfonamide NH and the furan oxygen can be disregarded.

5.2.4. Study of receptor **94** enantioselective recognition

The molecular receptor **94** has two chiral centres, however, as the cyclization is only *cis*, instead of obtaining a mixture of four diastereoisomers, the racemic mixture of compound **94** is achieved because we did not use any asymmetric auxiliary in the synthesis.

In the literature there are many methods to resolve a racemic mixture, as summarized in figure 5.43.¹⁹⁴

¹⁹⁴ Schuur, B.; Verkuijl, B. J. V.; Minnaard, A. J.; de Vries, J. G.; Feringa, B. L. *Org. Biomol. Chem.* **2011**, *9*, 36-51.

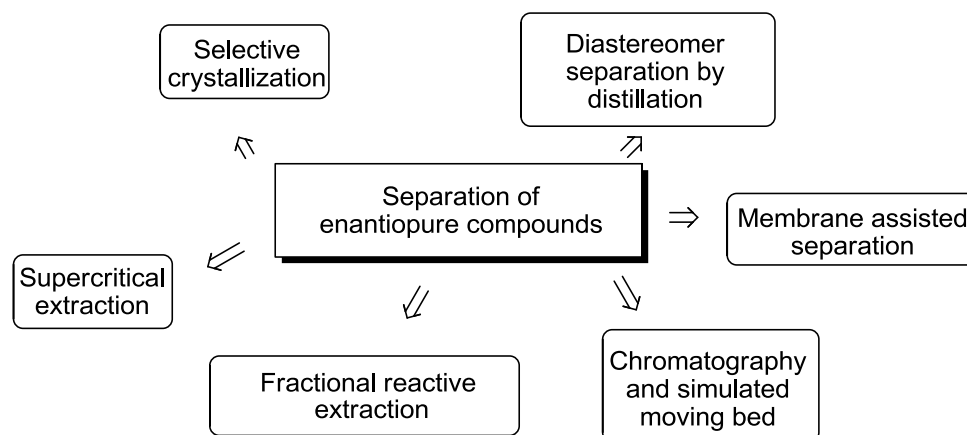


Figure 5.43. Available methods for acquiring enantiopure compounds.

On an industrial scale, the method most used for obtaining enantiomerically pure compounds from racemic mixtures is crystallization,¹⁹⁵ but it has a number of drawbacks, including low flexibility, maximum yields of 50 %, etc. (with the exception of Viedma deracemization). This has led to the development of other techniques such as chromatography or capillary electrophoresis, which, however, are still complicated and expensive to implement on a large scale (also they all have maximum yields of 50 %).¹⁹⁶ Centrifugal partition chromatography¹⁹⁷ and simulated moving bed chromatography¹⁹⁸ have also been used in several preparative scale chiral separations. Similarly, membranes have been used to carry out chiral separations; however, transport speeds are relatively low, which requires large membrane surfaces and a careful pressure control.¹⁹⁹

In the liquid-liquid extraction, transport mechanisms are diffusion and convection, allowing high transport speeds²⁰⁰ and the easy scaling up for industrial processes. These features make liquid-liquid extraction a very interesting technique for enantiomers separation.

We decided to study the supramolecular properties of receptor **94** to decide which technique would be suitable for the racemic mixture resolution. Our group has extensive

¹⁹⁵ (a) Bruggink, A. *Rational Design in Resolutions*, en *Chirality in Industry II*; Collins, A. N.; Sheldrake, G. N.; Crosby, J., Eds.; John Wiley & Sons: Chichester, 1997; pp. 81-98; (b) Faigl, F.; Fogassy, E.; Nogradi, M.; Palovics, E.; Schindler, J. *Tetrahedron: Asymmetry* **2008**, *19*, 519-536; (c) Fogassy, E.; Nogradi, M.; Kozma, D.; Egri, G.; Palovics, E.; Kiss, V. *Org. Biomol. Chem.* **2006**, *4*, 3011-3030; (d) Kozma, D. *CRC Handbook of Optical Resolutions Via Diastereomeric Salt Formation*; CRC Press LLC: Boca Raton, 2002; (e) Leeman, M.; Brasile, G.; Gelens, E.; Vries, T.; Kaptein, B.; Kellogg, R. *Angew. Chem., Int. Ed.* **2008**, *47*, 1287-1290; (f) Viedma, C. *Phys. Rev. Lett.* **2005**, *94*, 065504.

¹⁹⁶ (a) Davankov, V. A. *J. Chromatogr., A* **1994**, *666*, 55-76; (b) Jira, T.; Bunke, A.; Schmid, M. G.; Gubitz, G.; *J. Chromatogr., A* **1997**, *761*, 269-275; (c) Steensma, M.; Kuipers, N. J. M.; de Haan, A. B.; Kwant, G. *Chirality* **2006**, *18*, 314-328.

¹⁹⁷ Gavioli, E.; Maier, N. M.; Minguillon, C.; Lindner, W. *Anal. Chem.* **2004**, *76*, 5837-5848.

¹⁹⁸ (a) Francotte, E.; Leutert, T.; La Vecchia, L.; Ossola, F.; Richert, P.; Schmidt, A. *Chirality* **2002**, *14*, 313-317; (b) Zenoni, G.; Quattrini, F.; Mazzotti, M.; Fuganti, C.; Morbidelli, M. *Flavour Fragrance J.* **2002**, *17*, 195-202.

¹⁹⁹ (a) Maier, N. M.; Franco, P.; Lindner, W. *J. Chromatogr., A* **2001**, *906*, 3-33; (b) Afonso, C. A. M.; Crespo, J. G.; *Angew. Chem., Int. Ed.* **2004**, *43*, 5293-5295; (c) Keurentjes, J. T. F.; Nabuurs, L. J. W. M.; Vegter, E. A. J. *Membr. Sci.* **1996**, *113*, 351-360; (d) Maximini, A.; Chmiel, H.; Holdik, H.; Maier, N. W. *J. Membr. Sci.* **2006**, *276*, 221-231; (e) Xie, R.; Chu, L. Y.; Deng, J. G. *Chem. Soc. Rev.* **2008**, *37*, 1243-1263.

²⁰⁰ Viegas, R. M. C.; Afonso, C. A. M.; Crespo, J. G.; Coelho, I. M. *Sep. Purif. Technol.* **2007**, *53*, 224-234.

experience in the resolution of racemic receptors using preparative chromatography on silica plates, impregnated with a guest who has a different affinity for each of the two receptor enantiomers.¹⁸⁴

In this technique, the basic idea is to find a chiral guest which fits better in one of the receptor enantiomers.

To study which guests are suitable for the receptor **94** racemic mixture resolution, we have chosen ¹H NMR competitive titrations. These titrations have been carried out with around 2.0 mg of the racemic receptor dissolved in 0.5 mL of CDCl₃. Then, a small amount of chiral guest is added and the proton spectrum is recorded again. The guest will interact with the receptor forming hydrogen bonds, causing the splitting of the receptor signals (since the magnetic environment is different for both enantiomers). Afterwards, more chiral guest is added and the spectrum is recorded again. At this point several situations can take place:

- If the preference for one of the enantiomers of the receptor is very large, most of the guest will prefer to form the complex with a single enantiomer, producing a very tight complex, causing a large variation in the NMR signals of this enantiomer, compared to the free receptor. In contrast, the other receptor enantiomer will be unable to associate the guest, remaining its signals essentially at the same chemical shift than the signals of the free receptor. As more chiral guest is added to the NMR tube, the enantiomer forming the stronger complex will undergo saturation, so its NMR signals will stop moving. Then, the excess of the chiral guest begins to associate the other enantiomer, causing a shift of its signals, while the strong complex remains in the same place.

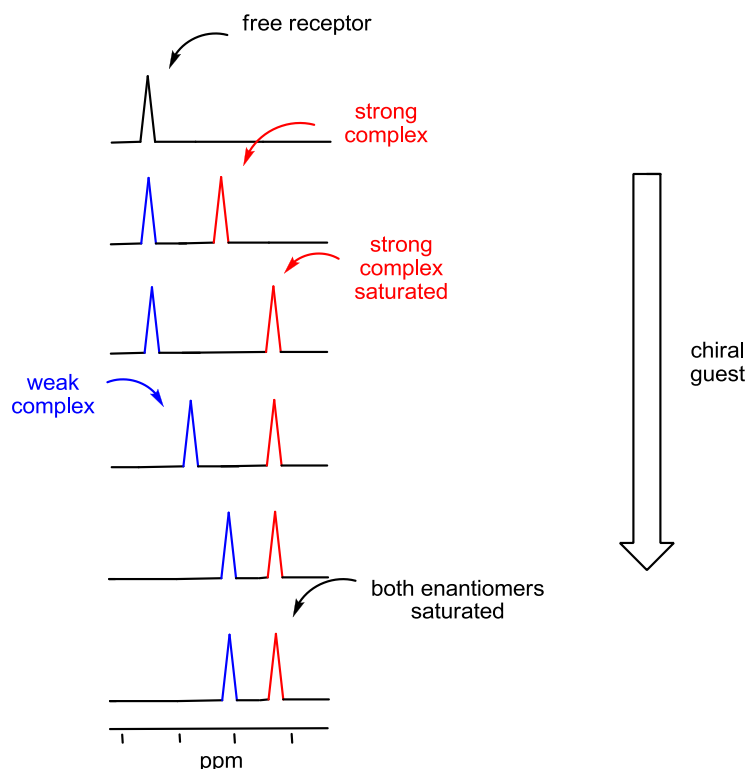


Figure 5.44. Schematic representation of a competitive titration in which one of the receptor enantiomers has a greater preference for a chiral guest than the other enantiomer.

- If the preference for both enantiomers is similar, the chiral guest will form complexes of the same strength with both enantiomers, causing similar movements of both enantiomer signals.

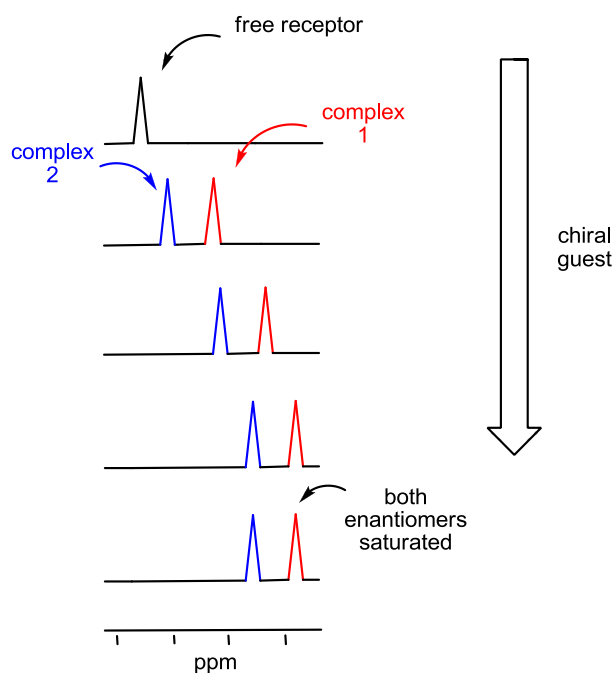


Figure 5.45. Schematic representation of a competitive titration where both receptor enantiomers have similar preferences for a chiral guest.

- It may also happen that the signals from the racemic receptor does not undergo splitting in the presence of the chiral guest. In this case, it is usual that there is no enantioselective recognition. Finally, if the addition of the guest does not lead to any movement of the receptor signals, it is likely that there is no complex formation under these conditions.

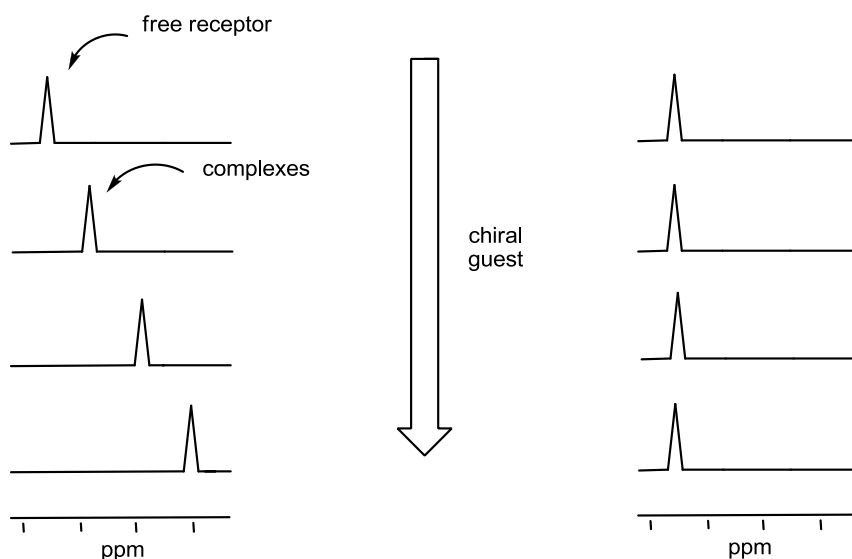


Figure 5.46. Schematic representation of a competitive titration where there is no chiral recognition (left) and the complex is not formed (right).

To quantify the preference of the chiral guest for one of the receptor enantiomers, the variation of the chemical shift of the proton signals corresponding to the receptor in one of the diastereomeric complexes is represented against the movement in the other complex. Thus by applying a nonlinear fitting method based on a Monte Carlo algorithm, we can determine the value for the competitive association constant.²⁰¹

Once a suitable chiral guest which has a preference for one receptor enantiomer is found, the racemic mixture resolution can be tried. Among the options discussed above (crystallization, extraction, chiral chromatography, etc.) silica gel chiral preparative chromatography is characterized by the simplicity with which it can be carried out.

In this method, first, a TLC plate is impregnated with a solution of the chiral guest and then dried (to eliminate the solvent). Then, using a pipette or a capillary, the racemic receptor is deposited in the TLC plate and eluted with a suitable solvent. As the receptor moves in the silica plate, it will form two different spots, corresponding to the two diastereomeric complexes formed in the silica. Typically, the stronger complex will elute before the weak complex, since the polar groups that could interact with the silica are forming H-bonds with the guest, so that this complex is easily eluted. The other receptor enantiomer, which has low affinity for the chiral guest, maintains its NHs and other polar groups interacting with silica, so that it is retained on its surface. Thus, two different spots, whose separation depends on the relative association constant between both enantiomers, are obtained. The solvent polarity also plays an important role, because if the solvent is very polar it competes for the hydrogen bonds between the host and the guest and prevents separation.

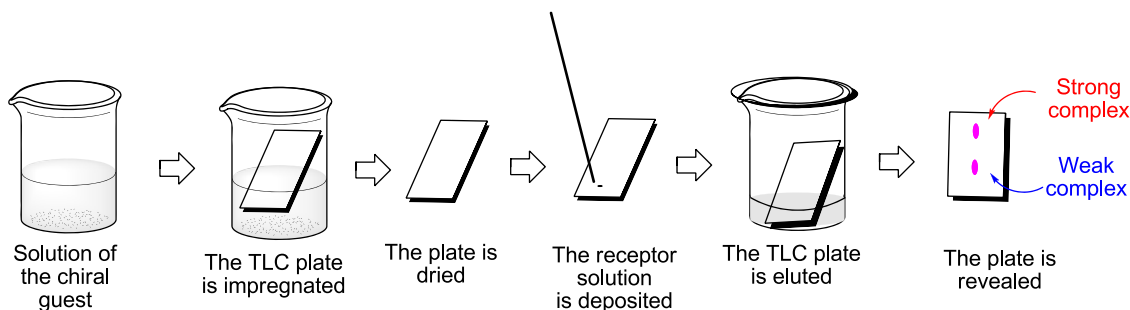


Figure 5.47. Scheme of the separation by chiral chromatography.

Once both enantiomers have been separated by TLC, the procedure will be repeated but with a larger receptor amount. For this aim it is necessary to prepare silica gel plates (preparatory) impregnated in the chiral guest and elute them in a larger cuvette. Then the silica with each complex is isolated and passed through a column of silica gel to obtain, finally, only one of the enantiomers of the receptor already free from the guest.

²⁰¹ Fielding, L. *Tetrahedron* **2000**, *56*, 6151-6170.

5.2.5. Search for the chiral guest

With the help of CPK models²⁰² we screened a chiral guest able to separate both enantiomers of receptor **94**. Following the idea of the Ogston three-point model shown at the beginning of the chapter, the strategy is to find a molecule that is able to establish three different interactions with receptor **94**. As can be seen in figure 5.48, this receptor has an amidopyridine which is ideal for forming a complex with a carboxylic acid group. The oxyanion hole that generates the two acidic NHs can also contribute to the association of the carboxyl group. Simultaneously, the O atoms of the sulfonyl groups or the ketone may provide an additional point for attachment. The third interaction may be determined by a bulky group present in the guest and which generates stereo hindrance with one enantiomer of the receptor but not with the other.

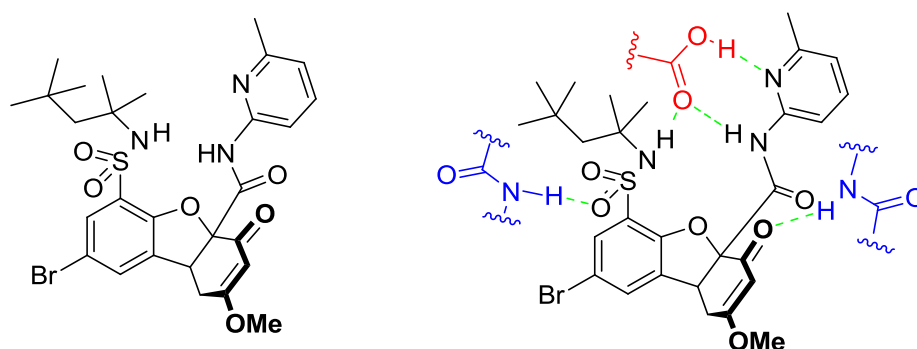


Figure 5.48. Synthesized receptors and possible points of interaction with a chiral guest.

Natural α -amino acids, except for glycine, are chiral molecules with a carboxylate group and an ammonium group. Protonation of the carboxylate group generates a suitable carboxylic acid to associate the amidopyridine. The ammonium group can be suitably functionalized to generate amides, sulfonamides, ureas or thioureas which leave active NHs. These NHs can form hydrogen bonds with the oxygen atoms of the sulfonyl groups or with the ketone. Moreover, depending on the amino acid used, we can study the effect of the side chains, and it is also possible to use amino acids with functional groups in its side chain to establish a greater number of interactions with the receptor, which can improve the separation, if it is necessary.

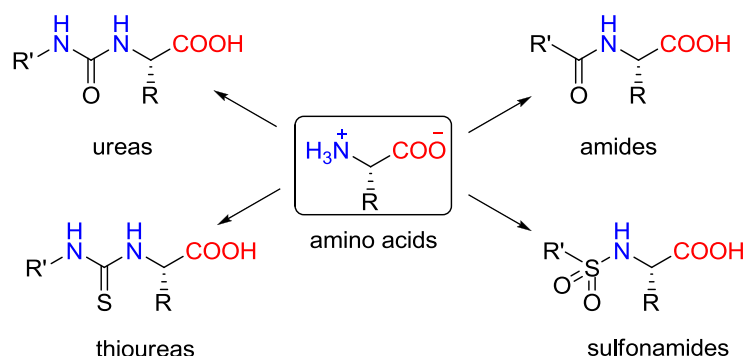


Figure 5.49. Chiral guests derived from α -amino acids.

²⁰² (a) Corey, R. B.; Pauling, L. *Review of Scientific Instruments* **1953**, *24*, 621-627; (b) Koltun, W. L., U. S. Patent 3170246, 1965.

The generic guests proposed in the above figure can form with the amidopyridine of receptor **94** Watson-Crick type hydrogen bonds as shown in figure 5.50, while the sulfonamide can establish a Hoogsteen type model of hydrogen bonds, also common in DNA. In Watson-Crick hydrogen bonds the donor-acceptor relation is 1.3 to 1.3 while in the Hoogsteen model the hydrogen bond pattern is 1.3-1.4.²⁰³

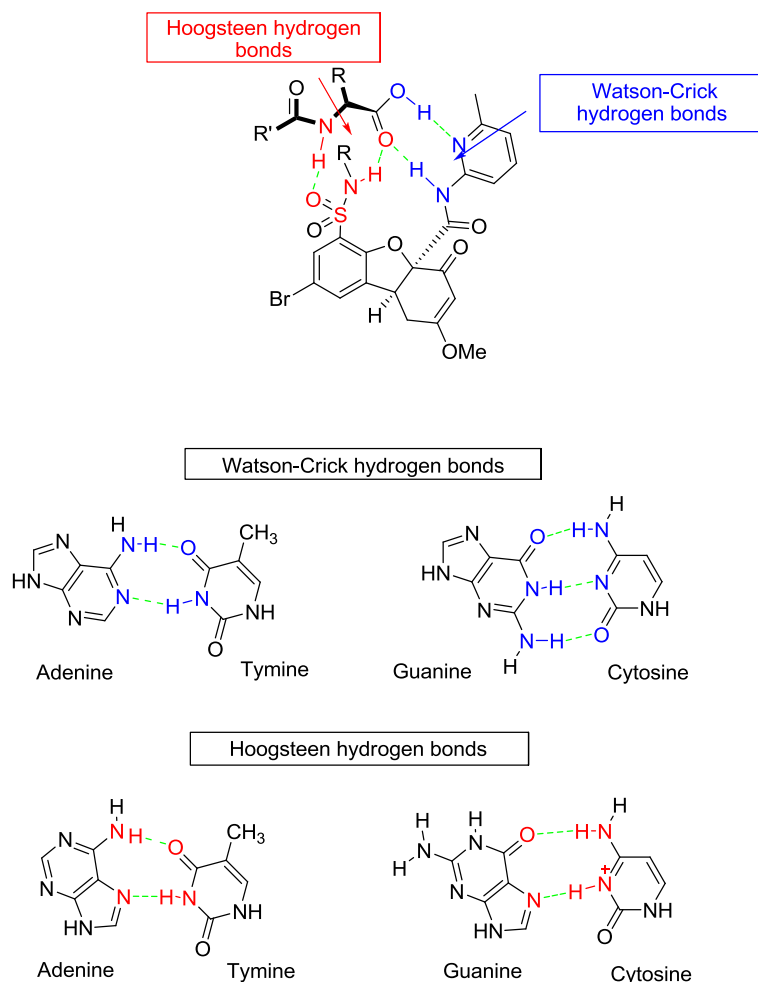


Figure 5.50. Hydrogen bonding patterns for receptor **94**. Watson-Crick and Hoogsteen type hydrogen bonding common in DNA.

To confirm that the NH of the alpha position of the amino acid derivative forms a hydrogen bond with the receptor, we studied the relative stability constant of the associates between a normal carboxylic acid and a derivative of an alpha amino acid. As a simple carboxylic acid we chose phenylacetic acid, because it is a trouble-free to handle solid and has a singlet at 3.66 ppm easily recognizable in the NMR spectrum. The amino acid derivative used was glycine trifluoroacetate, because this compound is not chiral and therefore presents no splitting of the NMR receptor **94** signals. Moreover, the presence of the CF₃ group should enhance the strength of the NH hydrogen bond. Competitive titration conducted under standard conditions resulted in a relative constant of 14, forming the amino acid derivative the strongest associate.

²⁰³ (a) Watson, J. D.; Crick, F. H. C. *Nature* **1953**, *171*, 737-738; (b) Hoogsteen, K. *Acta Crystallographica* **1963**, *16*, 907-916.

Constantes Competitivas
 Constante: 14 1/M
 Despl. Max. 1: 4.3331
 Despl. Max. 2: 3.699

Host: ácido fenilacético
 Host 2: trifluoroacetato glicina

Guest: receptor 94

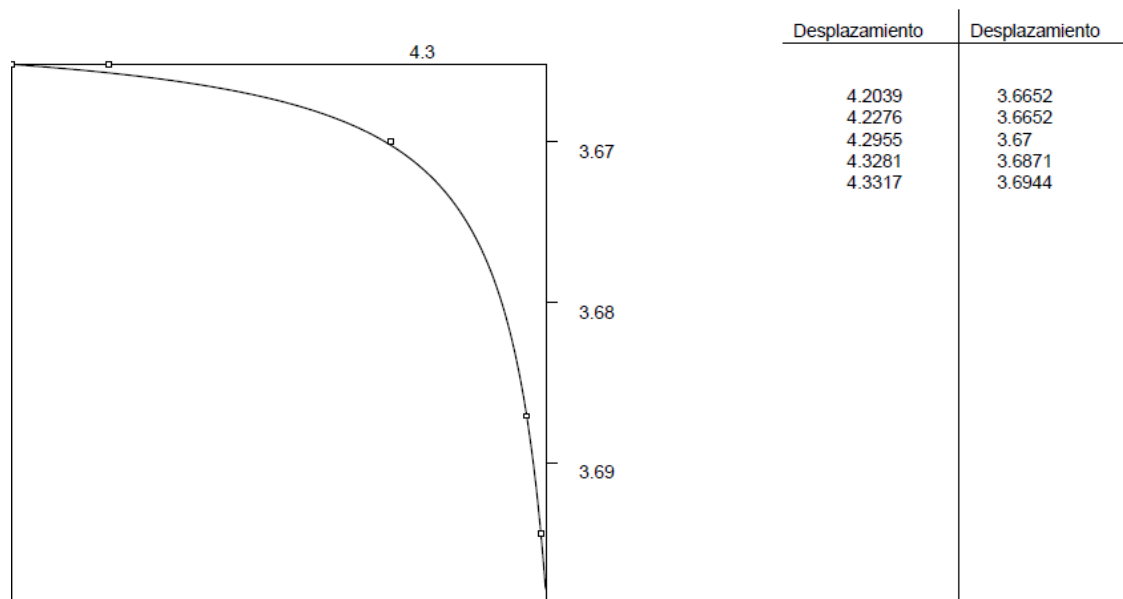


Figure 5.51. Competitive titration between phenylacetic acid and glycine trifluoroacetate.

In our opinion this experiment demonstrates that the amino acid derivative establishes a fourth hydrogen bond in the associate, probably between the NH of the alpha position of the guest and the receptor sulfonyl oxygen.

For this reason we studied the following guests for which we expected enantioselective recognition with receptor **94**.

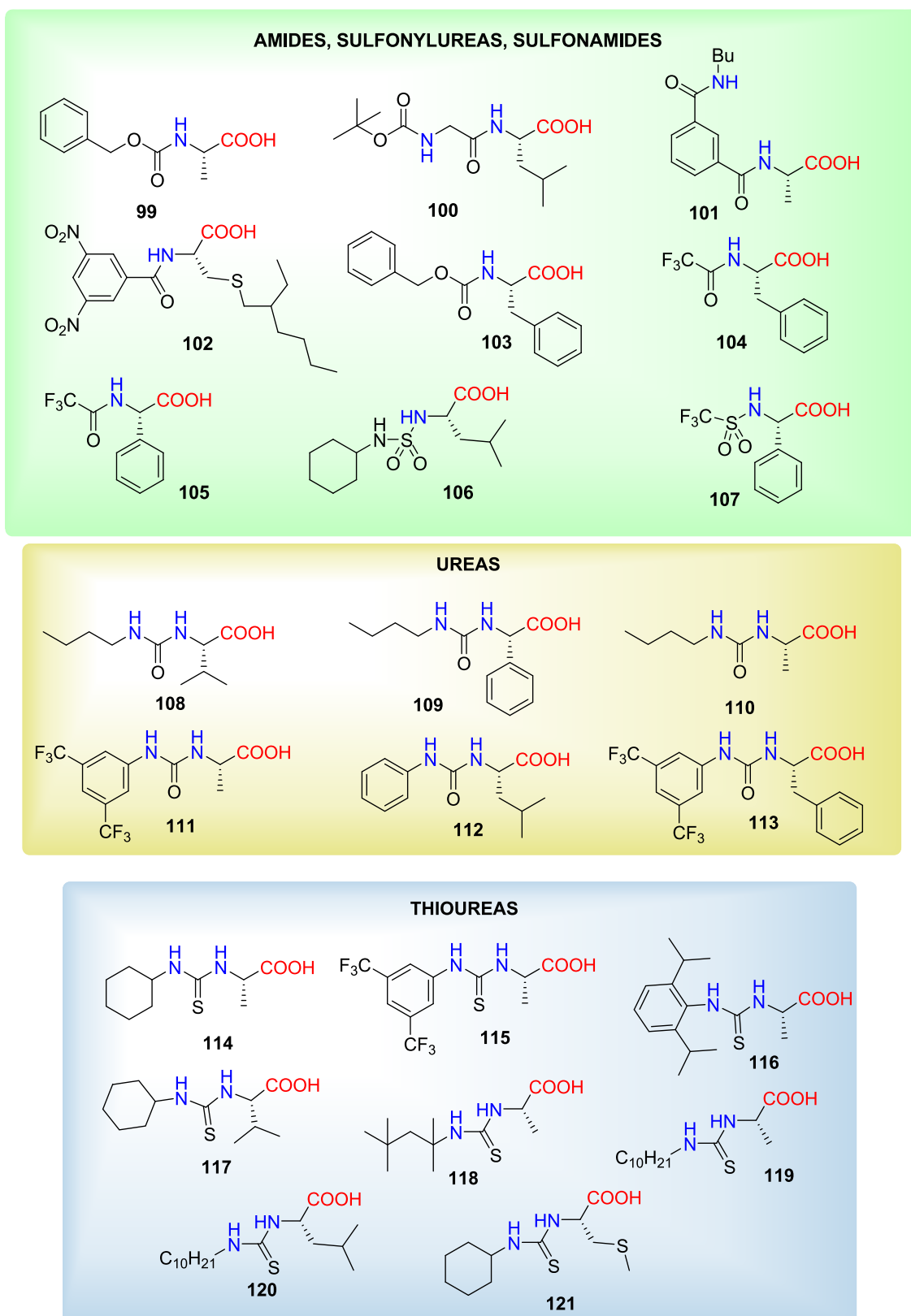


Figure 5.52. Chiral guests studied.

Once obtained the guests of the above figure, the enantioselective recognition was measured with receptor **94**, performing competitive titrations. The ratio between the association constants of each of the enantiomers of the receptor and each of the enantiomerically pure guests was obtained. The values are shown in table 5.2.

Table 5.2. Competitive association constants between the enantiomers of receptor **94**.

entry	guest	<i>K</i>	entry	guest	<i>K</i>
1	99	1.3	13	111	1.6
2	100	2.1	14	112	1.3
3	101	1.9	15	113	1.5
4	102	1.0	16	114	6.6
5	103	1.7	17	115	3.5
6	104	2.2	18	116	2.5
7	105	1.4	19	117	2.3
8	106	(a)	20	118	2.0
9	107	1.1	21	119	6.0
10	108	1.5	22	120	4.2
11	109	1.0	23	121	2.5
12	110	4.2			

(a) The receptor is not associated.

As seen in the above table, the values obtained with the amino acid amides are small, fluctuating between 1.0 and 2.2.

The effect of an increase in the NHs acidity was studied with sulfonylurea **106** and sulfonamide **107**. With these guests results were worse than those with carbonyl groups. It is likely that the spatial shape adopted by these compounds is not suitable, since sulfonamides present very different geometries than amides and the sulfonamide NH from the guest is unable to reach the oxygen atom of the sulfonyl group or the receptor ketone.

Molecular models show that amino acid-derived ureas may form an additional hydrogen bond with the receptor sulfonyl group. The associates thus obtained should be more stable and more rigid, so higher enantioselective recognition was expected.

The results show that the nature of the side chain has a great importance, because in the case of guests **108** and **109** derived from valine and phenylglycine, the values of the relative constants are small. However, the constant increases to a value of 4.2 for alanine derivative **110**, which has a methyl group in the side chain. To improve the relative association constant we tried to increase the acidity of the NH urea. We used a bistrifluoromethylaniline unit in guest **111**. Practically no splitting of the receptor signals was observed, probably due to the presence of some sort of strong intramolecular hydrogen bond in the guest.

The next step was to use thioureas as guests, since thiourea NHs are more acidic than those of urea (pK_a thiourea = 21.1, pK_a urea = 26.9 in DMSO).²⁰⁴ Stronger H-bonds are expected

²⁰⁴ Bordwell, F. G. *Acc. Chem. Res.* **1988**, *21*, 456-463.

and hence more stable complexes.²⁰⁵ In fact, thiourea **114** provided a relative constant of 6.6, higher than all the previous ones.

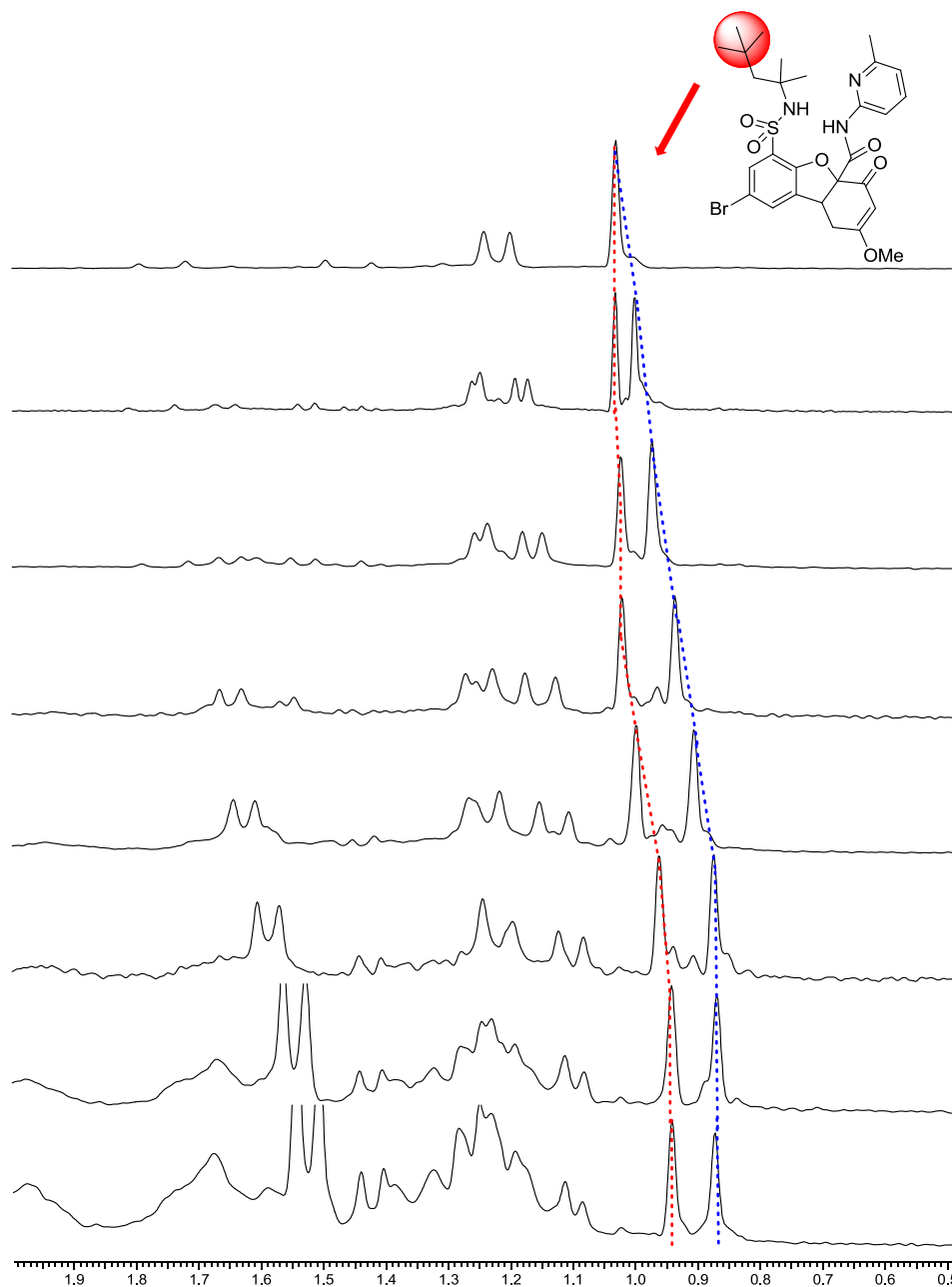


Figure 5.53. Spectra (region between 0.5–2.0 ppm) corresponding to the competitive titration using thiourea **114** as a guest.

²⁰⁵ Gómez, D. A.; Fabbrizzi, L.; Licchelli, M.; Monzani, E. *Org. Biomol. Chem.* **2005**, *3*, 1495–1500.

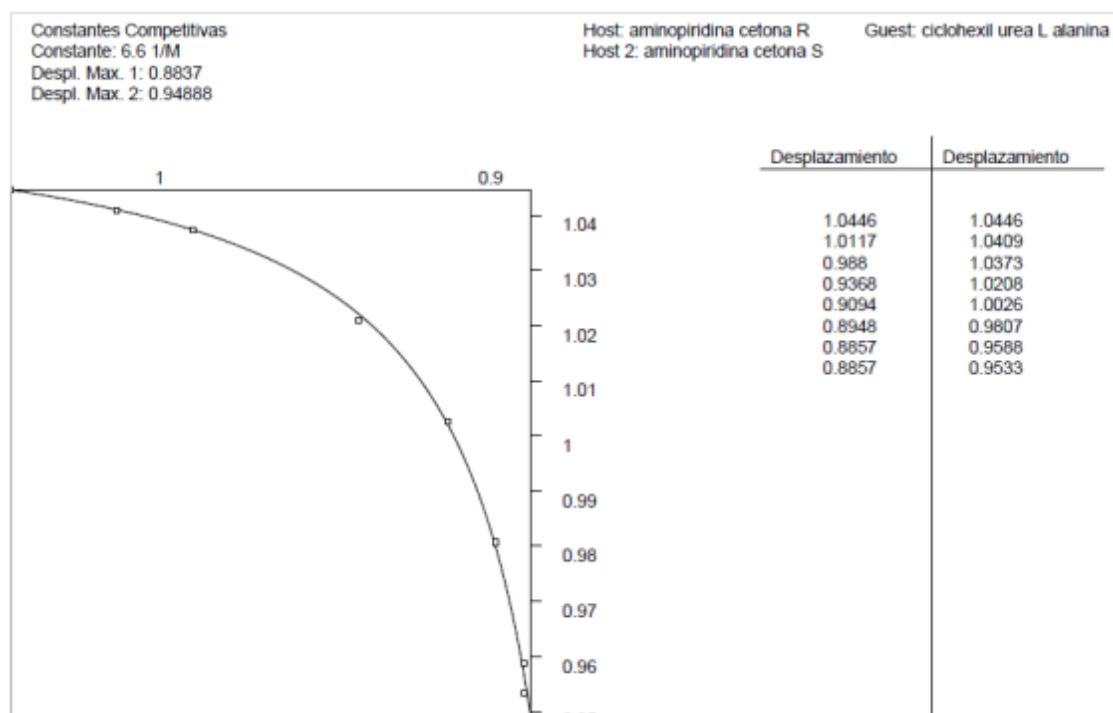


Figure 5.54. Graphical representation of the displacements variation of the t-butyl groups in the competitive titration between enantiomers of receptor **94** and guest **114**.

However, any attempt to improve this value by increasing the acidity of the NH (**115**), or increasing the steric hindrance in positions close to the NH (**116**, **118**) or in the side chain (**117**, **121**) was unsuccessful. Since the receptors are soluble in chloroform, the first points of the titration are obtained from a homogeneous solution; however, since many guests are poorly soluble in chloroform, at the end of the titration the guest remains as a suspension, therefore, the last points of the titration were not achieved. In this case the graph curvature necessary to obtain a reliable value of the constant would not be obtained, and the relative constant generated may be lower than the actual value. To solve this problem long alkyl chains were introduced, in order to increase the solubility of the guests (**119**, **120**), however, the results did not improve.

We also studied other chiral carboxyl acids, such as phenyl-lactic acid or mandelic acid, or with two carboxyl groups, such as dibenzoyltartaric acid. Also other guests as sulfonic acids, sulfoxides or imides, which should be able to set other types of interactions with the receptor. Although some of them are commercial, others were synthesized.

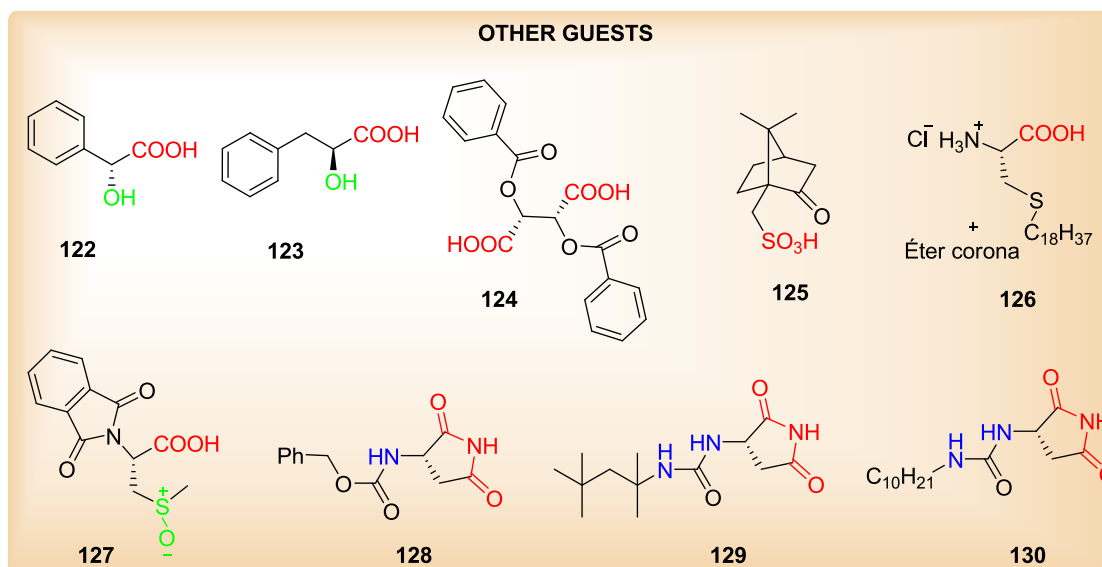


Figure 5.55. Other chiral guests.

The following table shows the values of the relative association constants obtained with the previous guests.

Table 5.3. Competitive association constants between both enantiomers of receptor **94** and different guests.

entry	guest	K
1	122	1.3
2	123	1.1
3	124	1.5
4	125	1.0
5	126	(a)
6	127	(b)
7	128	(b)
8	129	(a)
9	130	1.0

(a) No association. (b) No splitting.

The competitive constants values did not improve the previous results of amides, ureas and thioureas. Moreover, in many cases, it was impossible to carry out the titration due to the insolubility of the guests. In any case, we found strange to get constants close to one, while the receptor signals splitting were large, so we suspected that some of the relative constants obtained could be below the real value. In fact, the above competitive titrations conducted by NMR are the fastest way to obtain preliminary data on enantioselective recognition, but the values obtained are accurate only if the complex formation equilibrium is the only one in the solution. In the case where both the receptor and the guest can form self-associates, the equations used to calculate the competitive constants are incorrect and its use may generate errors, distorting the data.

A case that we found striking was that of dibenzoyltartaric acid **124**, which produced large splitting in the receptor signals, but the representation of the chemical shifts lead to a relative association constant of only 1.5.

Since dibenzoyltartaric acid is likely to form self-associates in the chloroform solution, it seemed logical to measure this guest chiral recognition using another method. An alternative method can be used if the splitting of the receptor signals is large, as is the case of dibenzoyltartaric acid.

To avoid interference from other equilibria in solution, we carried out the measurement of enantioselective recognition forming complexes at saturation. The standard titration of the mixture of receptor **94** enantiomers with *L*-dibenzoyltartaric acid yields the chemical shifts of both receptors corresponding to the strong and weak complexes. Then, an additional experiment is performed, in which racemic dibenzoyltartaric acid is added to the mixture of enantiomeric receptors. The mixture of the two diastereomeric complexes is again obtained, but in this case, each of the receptor enantiomers can associate both enantiomers of the guest, leading to an average between the signals of each associate, and no longer splitting of the receptor signals takes place. Since the strongest complex is generated at a higher concentration, the average signal obtained in the experiment with the racemic guest is closest to the chemical shift of the stronger complex.

The relative concentration of strong to weak complex can be found using the following equation:

$$K = \frac{[\text{strong complex}]}{[\text{weak complex}]} = \frac{\delta_x - \delta_{\text{weak complex}}}{\delta_{\text{strong complex}} - \delta_x}$$

Where δ_x is the chemical shift of the mixture of the racemic guest and the racemic receptor, $\delta_{\text{strong complex}}$ is the chemical shift corresponding to the strong complex and $\delta_{\text{weak complex}}$ the corresponding to the weak complex.

The values of the displacement of the *t*-butyl group obtained in the two previous titrations were 0.9131 ppm for the strong complex, 0.9441 ppm for the weak complex and 0.9204 ppm for the average obtained with racemic dibenzoyltartaric acid.

Applying the above equation, we obtained a constant of 3.2, higher than the value of 1.5 obtained with the standard method.

$$K = \frac{0.9204 - 0.9441}{0.9131 - 0.9204} = \frac{-0.0237}{-0.0073} = 3.2$$

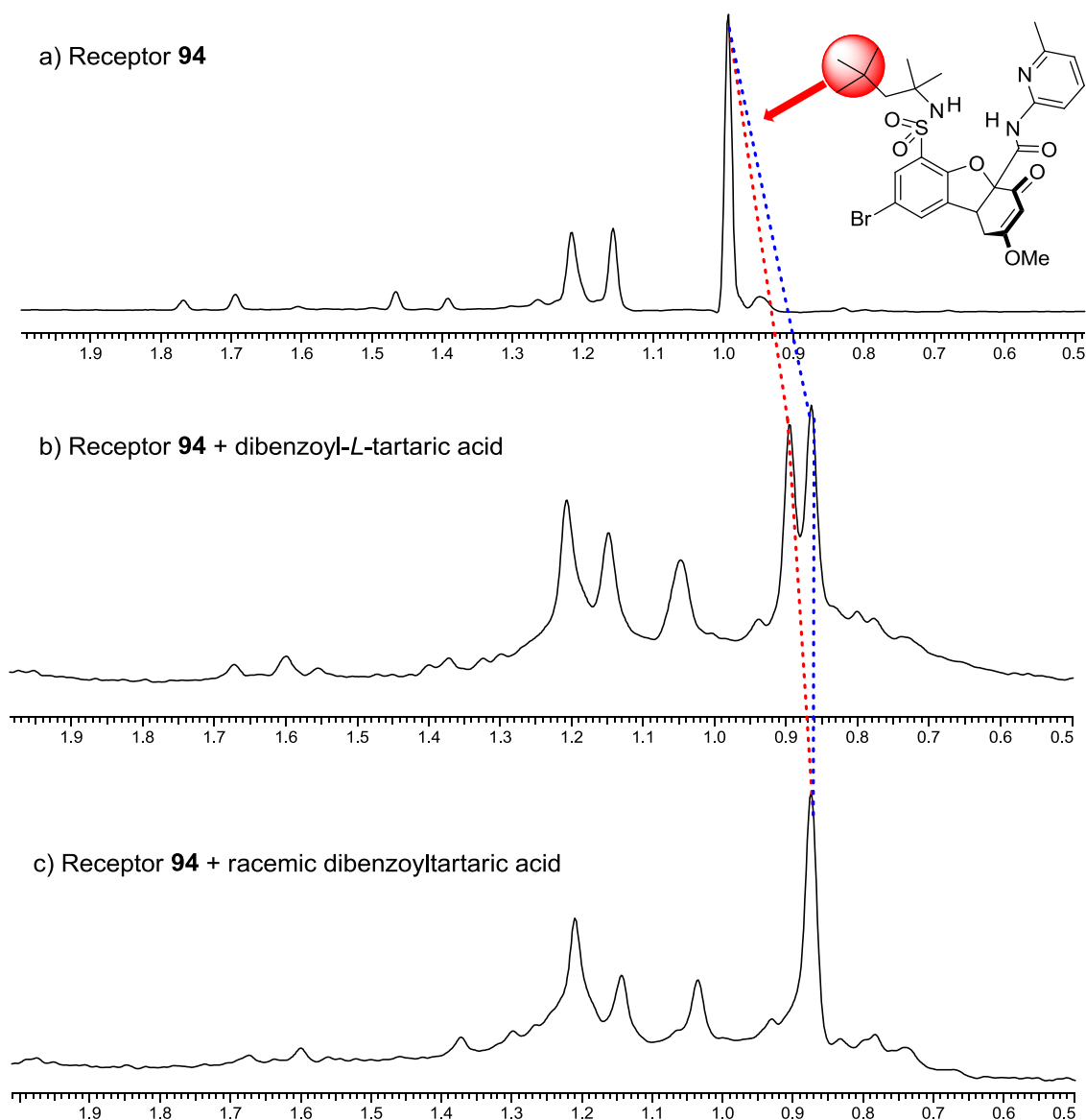


Figure 5.56. ¹H NMR spectra of receptor **94** between 0.5–2.0 ppm with splitting of the t-butyl group signal due to the presence of *L*-dibenzoyl tartaric acid and how these signals are averaged in the presence of racemic dibenzoyltartaric acid.

Finally, and before carrying out receptor **94** racemic resolution, we decided to check the cooperative effect of the sulfonamide NH and the amide NH. To do this, we used receptor **95**, which lacks the sulfonamide group and, hence, the oxyanion hole. Competitive titration of receptor **95** with dibenzoyl-*L*-tartaric acid yielded a value for the relative association constant of only 0.8, a small number compared to the 3.2 value obtained for receptor **94**. Similarly, titration of receptor **95** with amide **102** and thiourea **114** did not even produce splitting of the receptor signals. Therefore, it seems that the presence of the sulfonamide NH is necessary in the receptor to achieve reasonable enantioselective recognition.

5.2.6. Resolution of receptor **94** racemic mixture

After receptor **94** chiral recognition study using ^1H NMR titrations, we made a selection of the most promising guests to carry out the racemic mixture resolution, using preparative silica gel chromatography.

It is necessary to keep in mind that the guest, in addition to presenting enantioselective recognition with the receptor, must be soluble in the solvent in which the chromatography will take place. The choice of this solvent is limited by its polarity, so that highly polar solvents, which strongly compete for H-bonds, break down the associates, thus precluding the resolution of the receptor enantiomers. In practice, we prefer to use chloroform or methylene chloride as solvents, because we have the assurance that associates (as we know from the CDCl_3 NMR studies) are formed. For receptors that cannot be eluted with the solvents mentioned, a small amount of ether or ethyl acetate can be added, but we have tried to avoid these solvents, even if chromatography plates have to be eluted several times.

We started the study impregnating TLC plates as indicated in figure 5.47. Initially we began using a solution of 1 % guest in CH_2Cl_2 , to which the required amount of methanol to achieve complete dissolution of the guest was added (the eluent being impregnated in the plate is irrelevant because it is evaporated before performing the chromatography). Guests selected for this first study are described in figure 5.57.

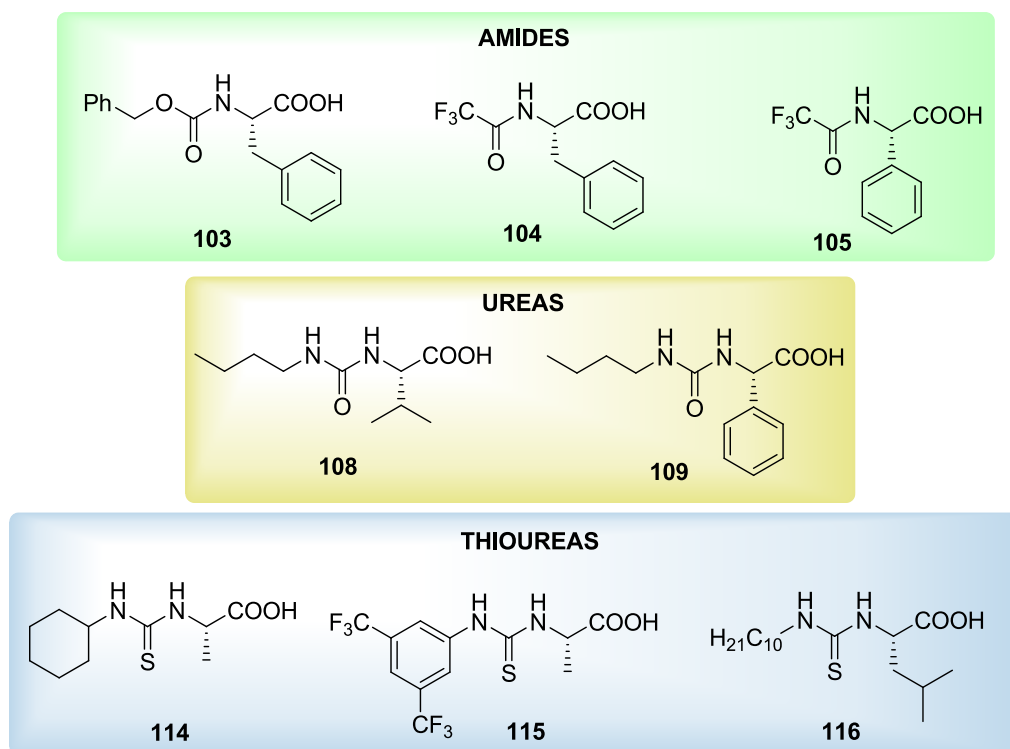


Figure 5.57. Guests studied in the resolution of receptor **94** racemic mixture.

None of the guests shown in figure 5.57 leads, under these conditions, to a satisfactory separation of the receptor enantiomers. The receptor may not present enough affinity for these guests, respect to the stationary phase. For this reason, we increased the concentration of the guests in the solution in which the plate was impregnated, between 2.5-10 %, according

to the guest used. Under these conditions we studied a new selection of guests shown in Figure 5.58.

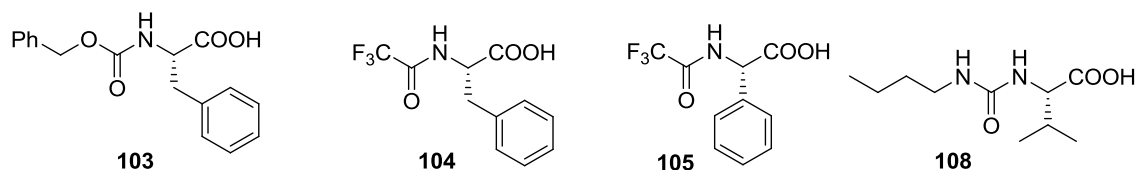


Figure 5.58. Selection of guests studied in 2.5-10 % concentration.

The only guests which allowed a satisfactory separation of the two enantiomers of receptor **94** were the benzyloxycarbonyl derivative of *L*-phenylalanine **103** and the *L*-phenylalanine trifluoroacetate **104**. Figure 5.59 shows photographs of the thin layer chromatographies corresponding to the separation of receptor **94** with both guests.

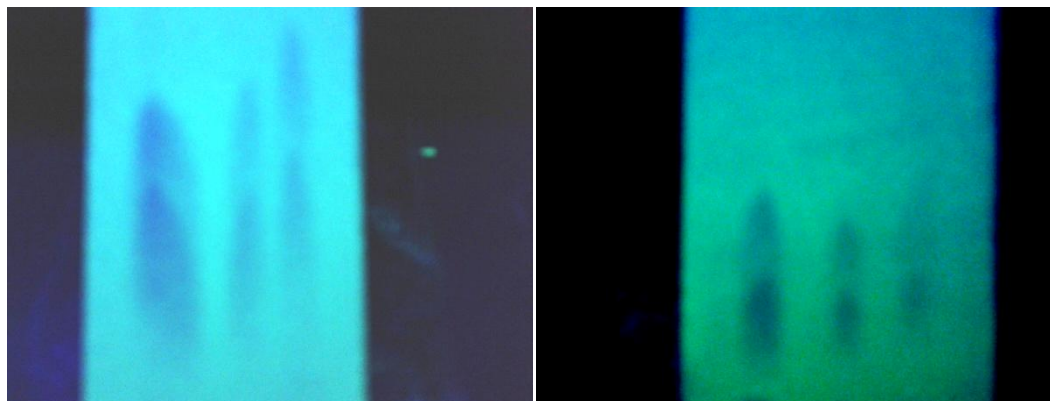


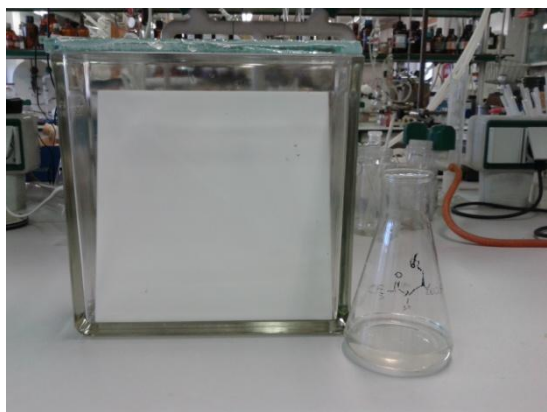
Figure 5.59. Thin layer chromatographies of receptor **94** racemic mixture, impregnated with Cbz-Phe-L (left) and the trifluoroacetate of L-Phe (right).

It may be surprising that the two previous guests, which do not have the best enantioselective recognition (constant of 1.7 for **103** and 2.2 for **104**) have been those which gave the best results in the separation. There are several reasons for this behaviour. The first is that guests that absorb strongly in the ultraviolet prevent the developing of plates by fluorescence, which is the ideal method when the plates have a high guest concentration. This is the case of cyclohexylthiourea *L*-alanine **114**, which exhibited the best competitive constant ($K = 6.6$). Chromatography plates did not produce any fluorescence under ultraviolet light, and other forms of developing, such as sulphuric acid/vanillin/sulphuric acid, anisaldehyde, potassium permanganate, phosphomolybdic acid or iodine, cannot allow to distinguish the receptor site from the coloured background of the guest. Other guests which have more hydrogen bonds as ureas, should therefore have a higher affinity for receptor **94**, but they also are associated more strongly to silica and this effect makes elution by the guest difficult, which is responsible for causing separation of the receptor spots.

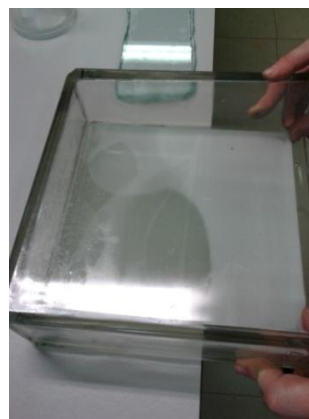
Accordingly, to carry out the separation of the receptor enantiomers by preparative scale, it was necessary to choose between benzyloxycarbonyl **103** and *L*-phenylalanine trifluoroacetate **104**. Between these two guests trifluoroacetate **104** was selected because with a much smaller

amount we could get an equivalent resolution (1.5 % trifluoroacetate vs 5 % of Cbz *L*-Phe). Furthermore, trifluoroacetate *L*-phenylalanine **104** has a smaller absorption in ultraviolet, which facilitates the plates developing.

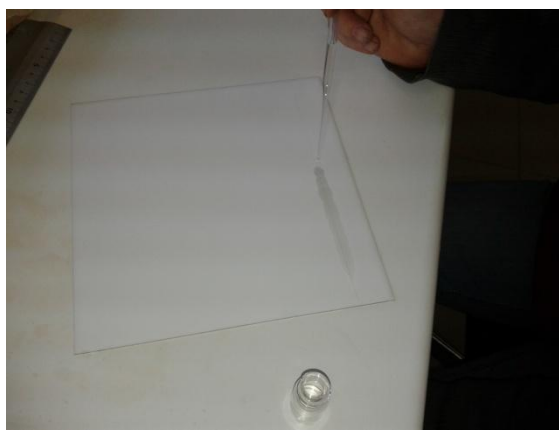
To carry out the preparative resolution of receptor **103** racemic mixture, a preparative plate was eluted with a 1.5 % solution of *L*-Phe trifluoroacetate in CH₂Cl₂. In the first place a guest solution was prepared (figure 5.60.a) and the plate was impregnated (figure 5.60.b). After evaporation of CH₂Cl₂, the plate was charged with a solution of 20 mg of receptor **94** in 2 mL of CH₂Cl₂ (figure 5.60.c). Then the plate was eluted in methylene chloride (figure 5.60.d). Developing by ultraviolet lamp allows following the course of the elution (figure 5.60.e-h). Then, under the UV lamp, each of the spots was delimited with a pencil (figure 5.60.i) and scraped with a spatula (figure 5.60.j-k). The scraped silica was introduced into a silica gel column (figure 5.60.l) and EtOAc was used for eluting the complex. The ethyl acetate phase was washed then with aqueous NaHCO₃ to break the associate, decanted, dried and evaporated to obtain the free receptor **94** enantiomers. Figure 5.60 shows several pictures of this process and the evolution of the two bands corresponding to the two receptor **94** enantiomers.



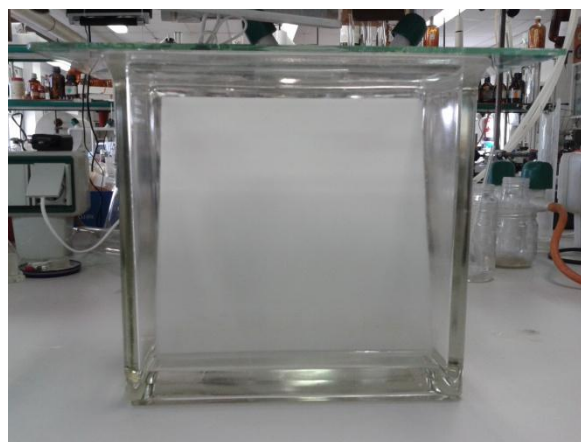
(a)



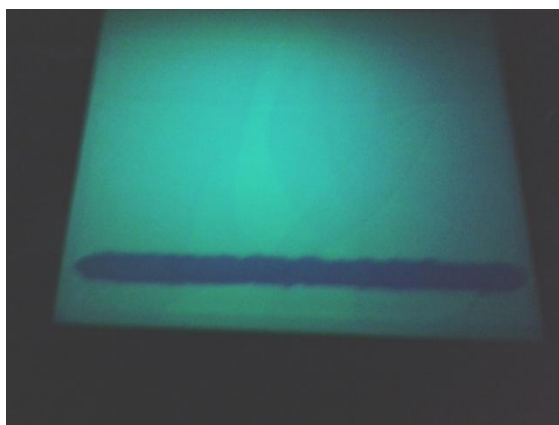
(b)



(c)



(d)



(e)

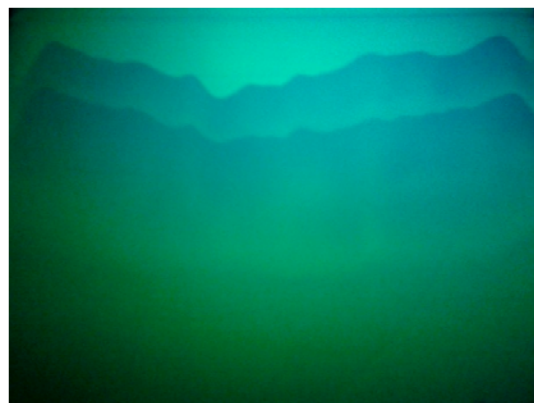


(f)

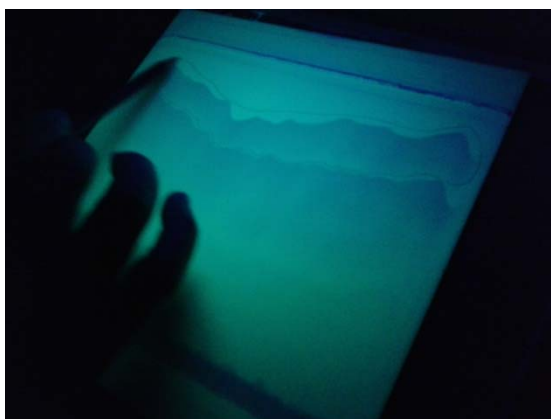
Figure 5.60. Separation of receptor **94** enantiomers by silica gel impregnated with L-Phe trifluoroacetate **104** in a preparative plate.



(g)



(h)



(i)



(j)



(k)



(l)

Figure 5.60. Separation of receptor **94** enantiomers by silica gel impregnated with L-Phe trifluoroacetate **104** in a preparative plate.

In this way the two enantiomers were separated to yield 8.2 mg of receptor **94** which forms the strong complex ($[\alpha]_D^{20} = -61.1$ ($c = 0.82$, CHCl_3)) and 7.3 mg of the enantiomer of receptor **94** which generates the weak complex ($[\alpha]_D^{20} = +58.8$ ($c = 0.73$, CHCl_3)).

Once the receptor racemic mixture was resolved, we measured the absolute association constant of the optically pure receptor that forms the more stable complex with *L*-phenylalanine trifluoroacetate **104**. This association constant was measured with the usual procedure, using a known concentration of receptor **94** in deuteriochloroform and adding increasing amounts of the guest. Once the NMR spectra were recorded, the *t*-butyl signals of the receptor were used to calculate the association constant. The graphical representation of the variation of the chemical shift of the *t*-butyl group versus the equivalents of added guest, allowed us to obtain, using a program which takes into account the dilution effect, the value of 6700 M^{-1} . With this number, and knowing the relative association constant between the two enantiomers of receptor **94** ($K = 2.2$), we obtain a value of 3350 M^{-1} for the weak associate.

These values fit quite well within the range of values we expected for the association constant, if we consider that the association constant for acetic acid is 360 M^{-1} , and hydrogen bonding of the trifluoroacetyl amino acid NH increases the association constant by a factor of 14.

5.2.7. Complexes structure

We have a great deal of NMR data to discuss the possible geometry of these complexes. Movements experienced by signals of the enantiomeric receptors change greatly depending on the guests used, making the interpretation difficult, but it is possible to make several generalizations.

1.- Associates formation with acid guests causes deshieldings in the aromatic signals of the amidopyridine; the triplet is generally the signal which undergoes the largest movement.

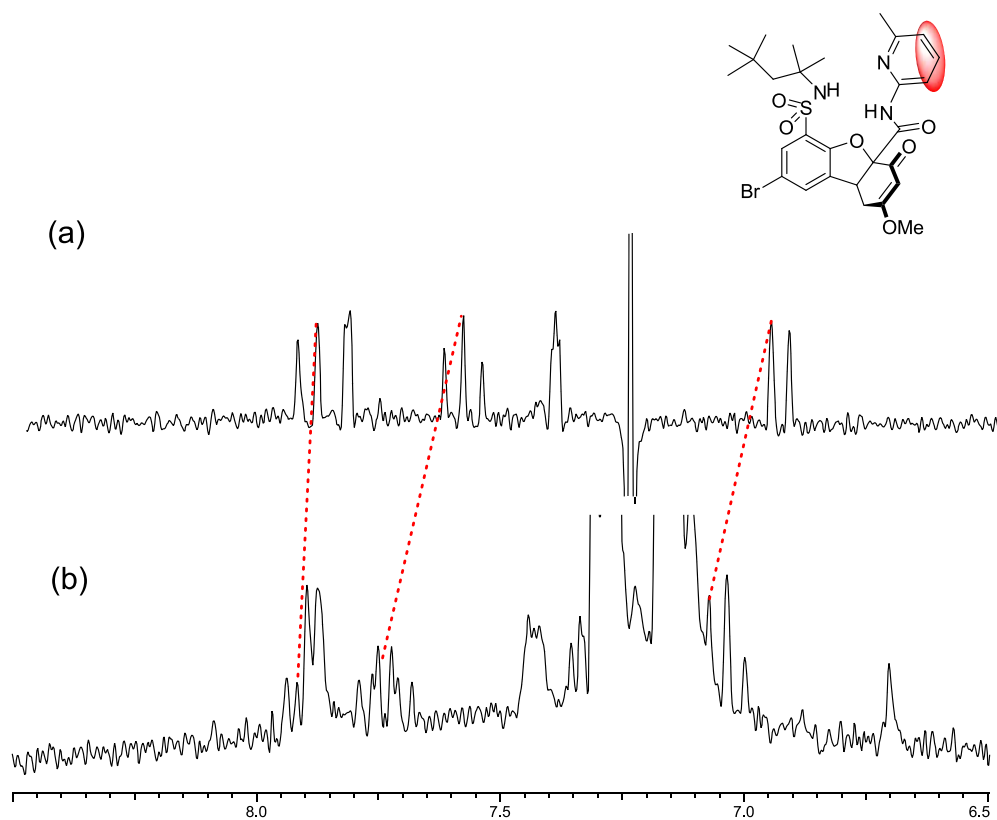


Figure 5.61. Aromatic amidopyridine signals before (a) and after (b) addition of L-Phe trifluoroacetate **104**.

It is particularly easy to visualize the movement of the amidopyridine methyl group. In the strong complex this signal moved downfield from 2.48 ppm to 2.54 ppm, while in the weak complex it finished at 2.44 ppm.

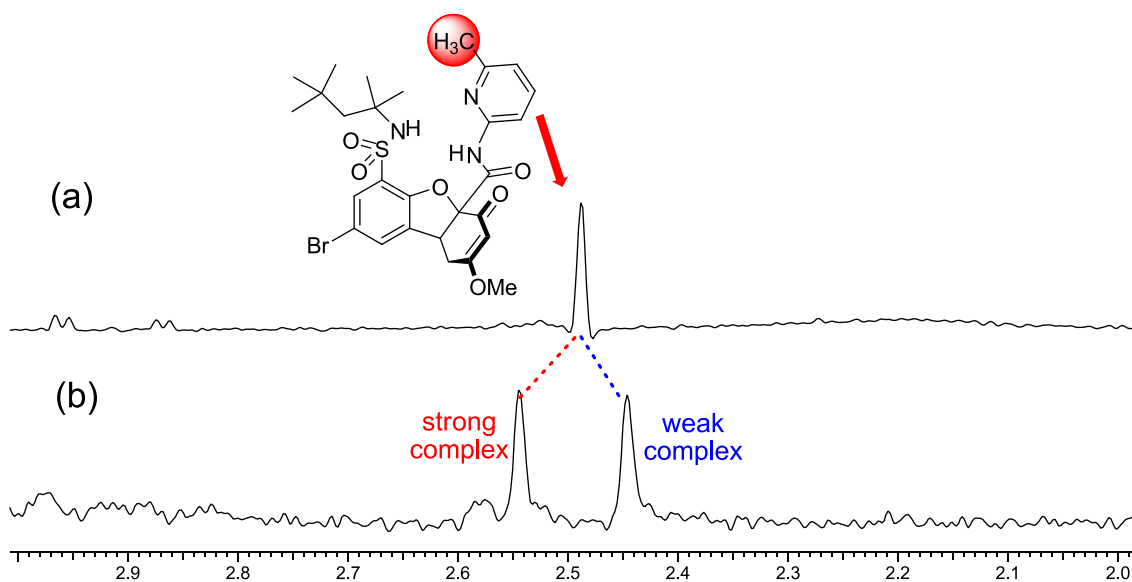


Figure 5.62. Methyl signals of amidopyridine before (a) and after (b) addition of L-Phe trifluoroacetate **104**.

2.- Guest addition results in a strong deshielding of receptor NHs. For example, in the case of titration with *L*-Phe trifluoroacetate **104**, the sulfonamide NH begins at 5.87 ppm; the addition of this guest splits this signal, ending one enantiomer at 6.77 ppm and the other at 7.21 ppm. This confirms the participation of the NHs in the oxyanion hole, which due to the proximity of the non-bonding electron pairs of the acid carbonyl, experiences a strong deshielding.

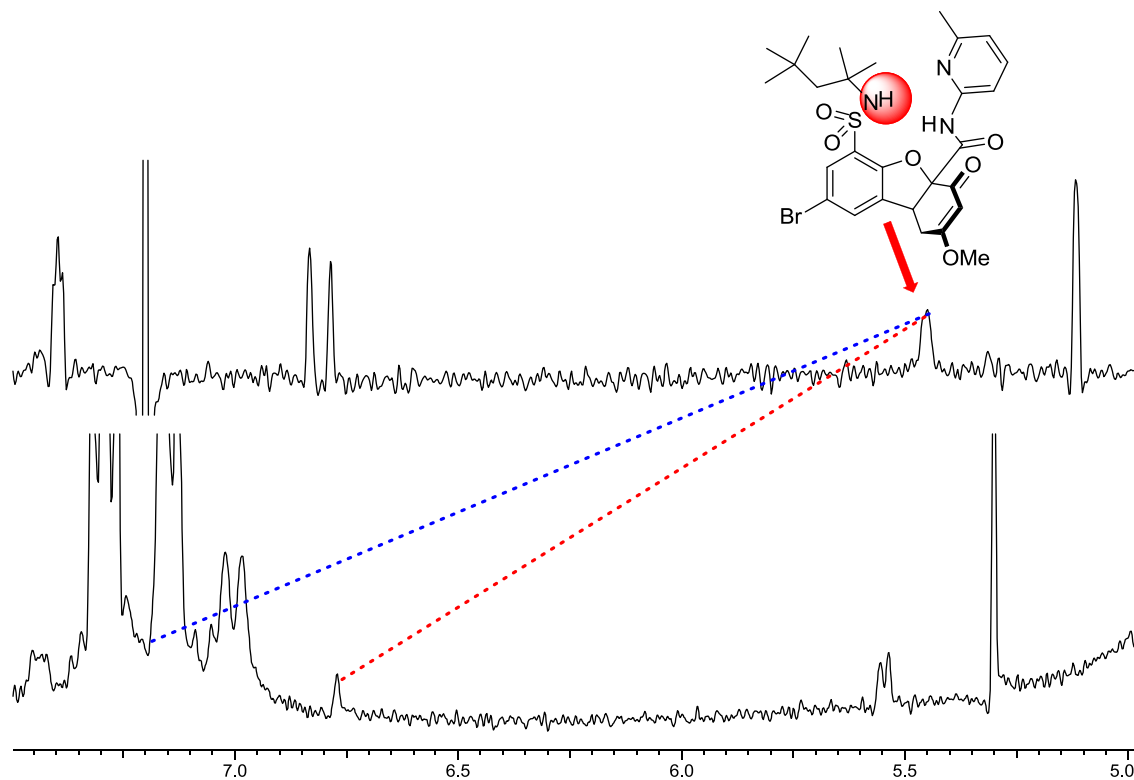


Figure 5.63. NHs of receptor **94** before and after the addition of *L*-Phe trifluoroacetate **104**.

3.- Addition of a simple guest, such as acetic acid, produces a small shielding of the *t*-butyl group. This shielding can be explained because the *t*-butyl group is partially situated within the shielding cone of the carbonyl guest. Other signals are also shielded, but the shielding is less significant.

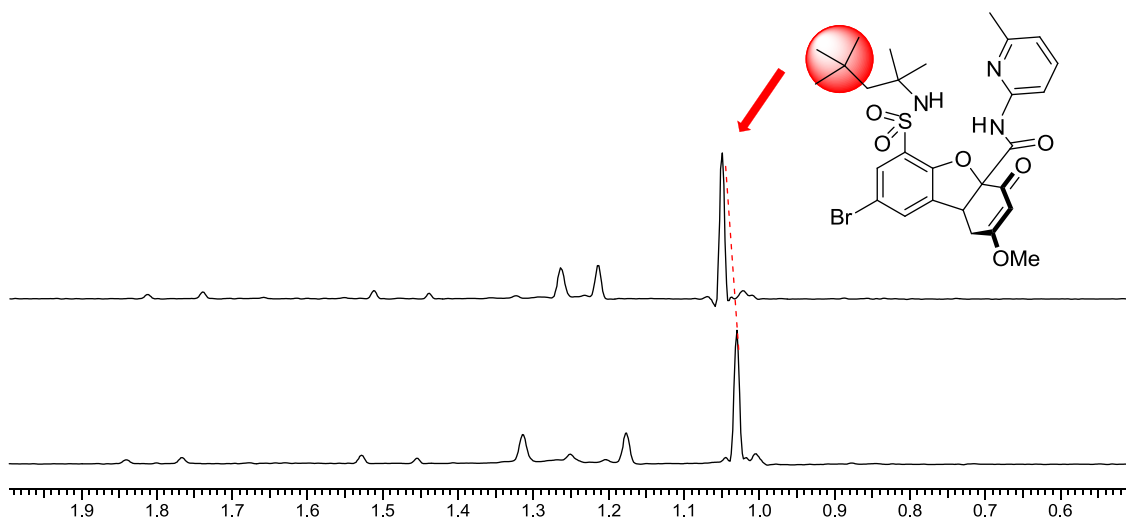


Figure 5.64. Slight shielding experienced by the *t*-butyl group of the receptor **94** after addition of acetic acid.

4.- Guest as lactic acid, which only have one carboxyl group in its structure, slightly shielded the *t*-butyl group (from 1.04 to 0.97 ppm) causing a small splitting (0.01 ppm).

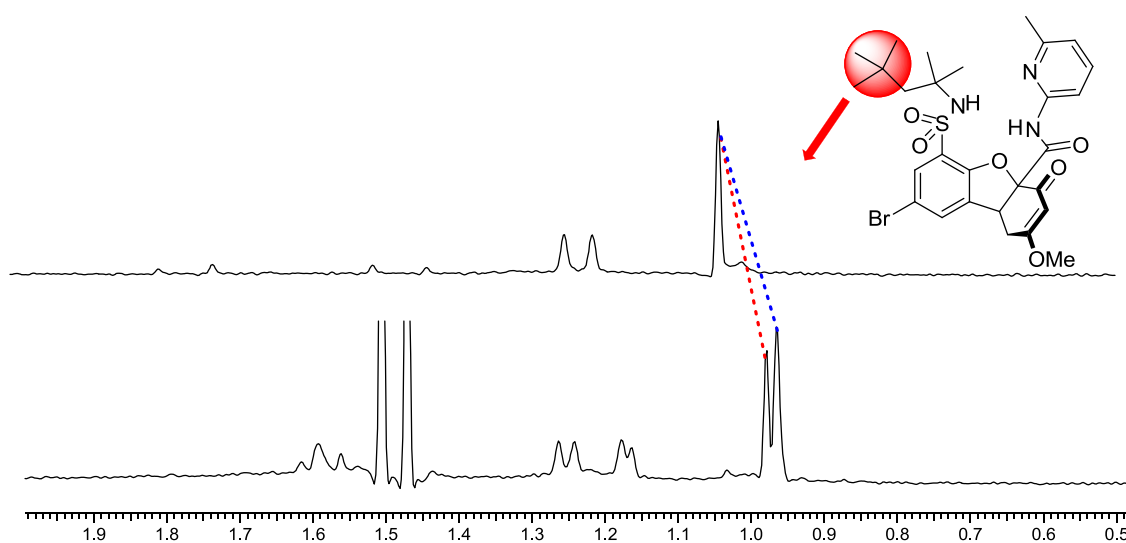


Figure 5.65. Shielding experienced by the *t*-butyl group of receptor **94** after L-lactic acid addition.

5.- Amino acids derivatives which have the amino group acylated (amide, carbamoyl, ureas and thioureas) generate strong signals splits in the receptor *t*-butyl signals. The shield which suffers in the weak complex corresponds essentially to the contribution of the carboxylic acid; in the strong complex, however, the shielding is much stronger, and in the case of bis(trifluoromethyl)phenylurea of *L*-phenylalanine **113**, this signal finished the titration below 0.75 ppm. This shielding in the strong complexes does not depend on the amino acid side chain, and we believe that is due to the urea acyl group. Other examples can be seen in an amide as *L*-phenylalanine trifluoroacetate **104** (the *t*-butyl of the receptor is shielded 0.18 ppm) or in the case of a carbamoyl such as Cbz-*L*-Phe, which is shielded 0.15 ppm.

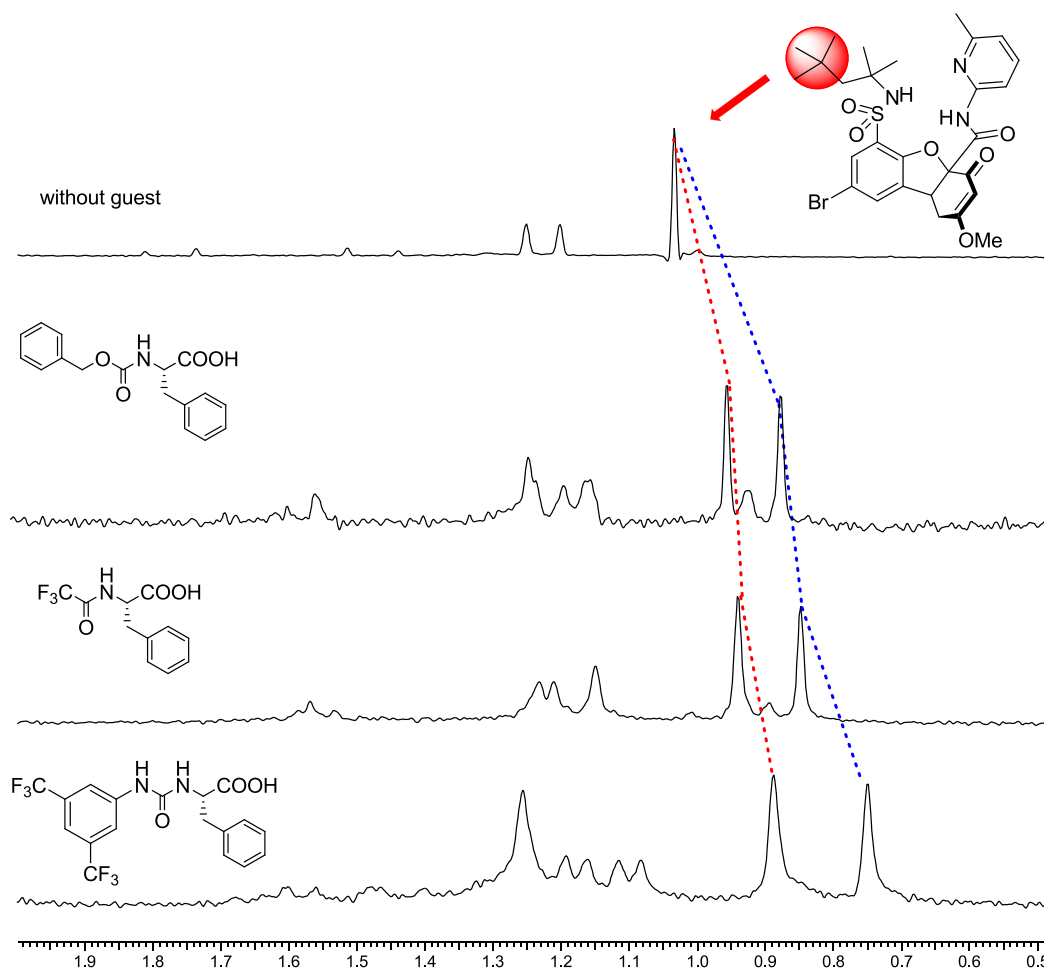


Figure 5.66. Splitting experienced by receptor **94** *t*-butyl group after addition of Cbz-L-Phe **103**, L-phenylalanine trifluoroacetate **104** and bis(trifluoromethyl)phenylurea of L-phenylalanine **113**.

The above generalizations allowed us to propose the structures shown in figure 5.67 for receptor **94** major and minor associates with acyl amino acid derivatives.

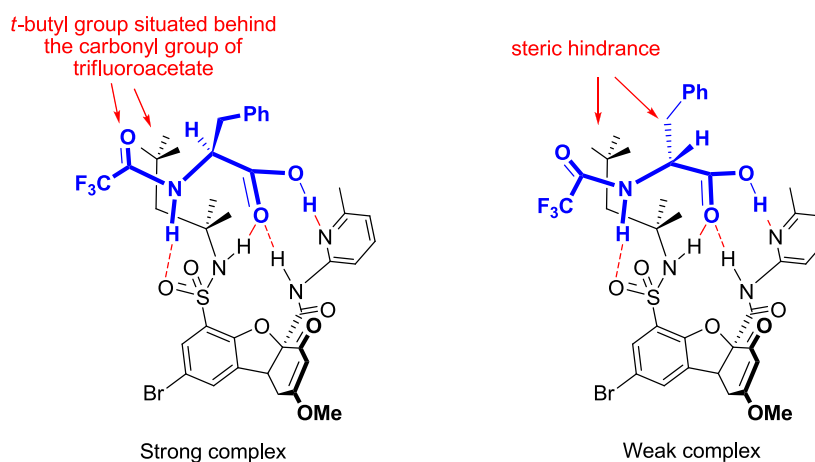


Figure 5.67. Structures proposed for receptor **94** strong and weak associates with L-phenylalanine trifluoroacetate **104**.

Regarding the geometry of the guest, we assume it adopts a conformation compatible with the Ramachandran plots.²⁰⁶ An intramolecular hydrogen bond between the NH of the alpha amino acid and the acid carbonyl group probably exists, stabilising this conformation.

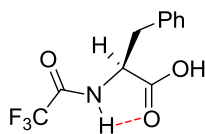


Figure 5.68. A possible geometry for L-phenylalanine trifluoroacetate **104**, according to Ramachandran plots.

The structures we have proposed are consistent with the generalizations we have seen before. Thus, the carboxyl group of the guest forms a strong hydrogen bond with the nitrogen of the amidopyridine. This binding effect produces an electron withdrawing effect, which makes the pyridine to lose charge showing deshielded signals.

The carboxylic acid is placed in the oxyanion hole, justifying the NHs deshielding experienced by the receptor. This is shown in the second generalization.

The position of the guest carboxyl justifies the small shielding experienced by the *t*-butyl group of the receptor, quoted from the third generalization.

The fourth and fifth generalizations are the key to understand the different structures which led to the strong and weak complexes. In the strong complex, the amide carbonyl is placed parallel to the *t*-butyl group in the receptor, so that the latter group is positioned in the shielding cone, explaining the effect shown in the fifth generalization. The proton in the alpha position remains next to the *t*-butyl group, while the amino acid side chain would point in the opposite direction.

If in the strong complex the hydrogen in the amino acid alpha position is exchanged with the side chain, steric tension between the latter and the *t*-octyl group will develop, for this reason, in the weak complex, the amide carbonyl group of the guest moves away from the *t*-octyl group, so that space can be generated for accommodating the side chain. In this new geometry the guest adopts a conformation in which the NH of the alpha position of the carbonyl of the amino acid moves away, thus losing a certain amount of energy which explains the enantioselectivity of this receptor.

To confirm that the proposed geometry for receptor **94** associates with amino acid derivatives is correct, we conducted Overhauser experiments with the complexes. *L*-Phe trifluoroacetate **104** was chosen as guest, since it had produced the best results.

In the proposed structure for the strong complex the proton of the alpha position of the amino acid and the *t*-butyl group are close, so we can expect Overhauser effect between these two groups. Moreover, in the weak complex the situation is reversed, and the Overhauser effect should appear between the side chain and the *t*-butyl group. We carried out a two-

²⁰⁶ Ramachandran, G. N.; Ramakrishnan, C.; Sasisekharan, V. *J. Mol. Biol.* **1963**, *7*, 95-99.

dimensional ROESY correlation with the strong complex, in which we were able to observe the presence of the expected Overhauser effect between the alpha proton and the *t*-butyl group.

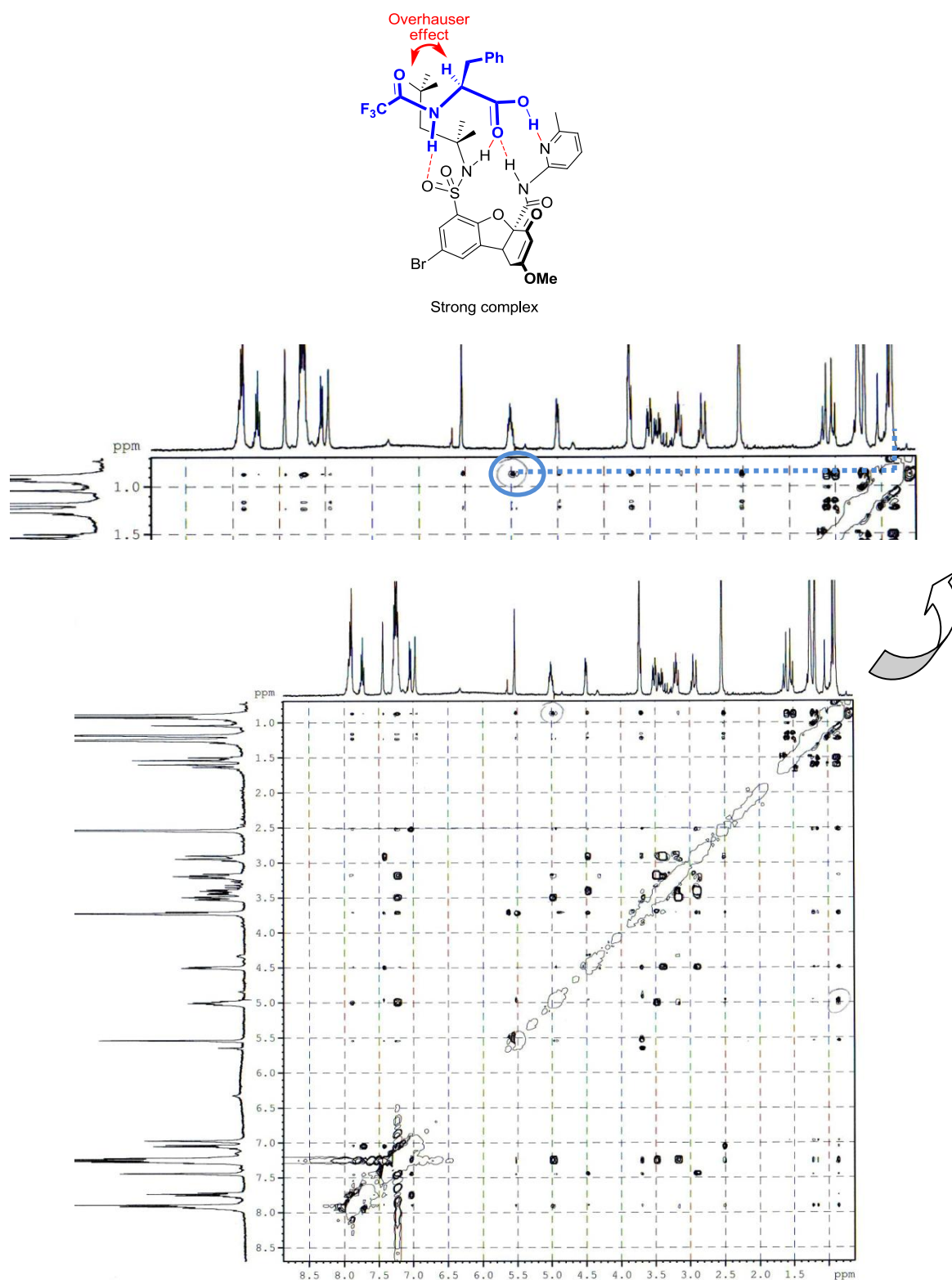


Figure 5.69. ROESY spectrum of the strong complex formed between (-)-receptor **94** and L-Phe trifluoroacetate **104**.

Once known the correlations in the more stable associate, the weak complex was studied in the racemic mixture so that it could be carried out a direct comparison between the intensities of the Overhauser effects in both complexes.

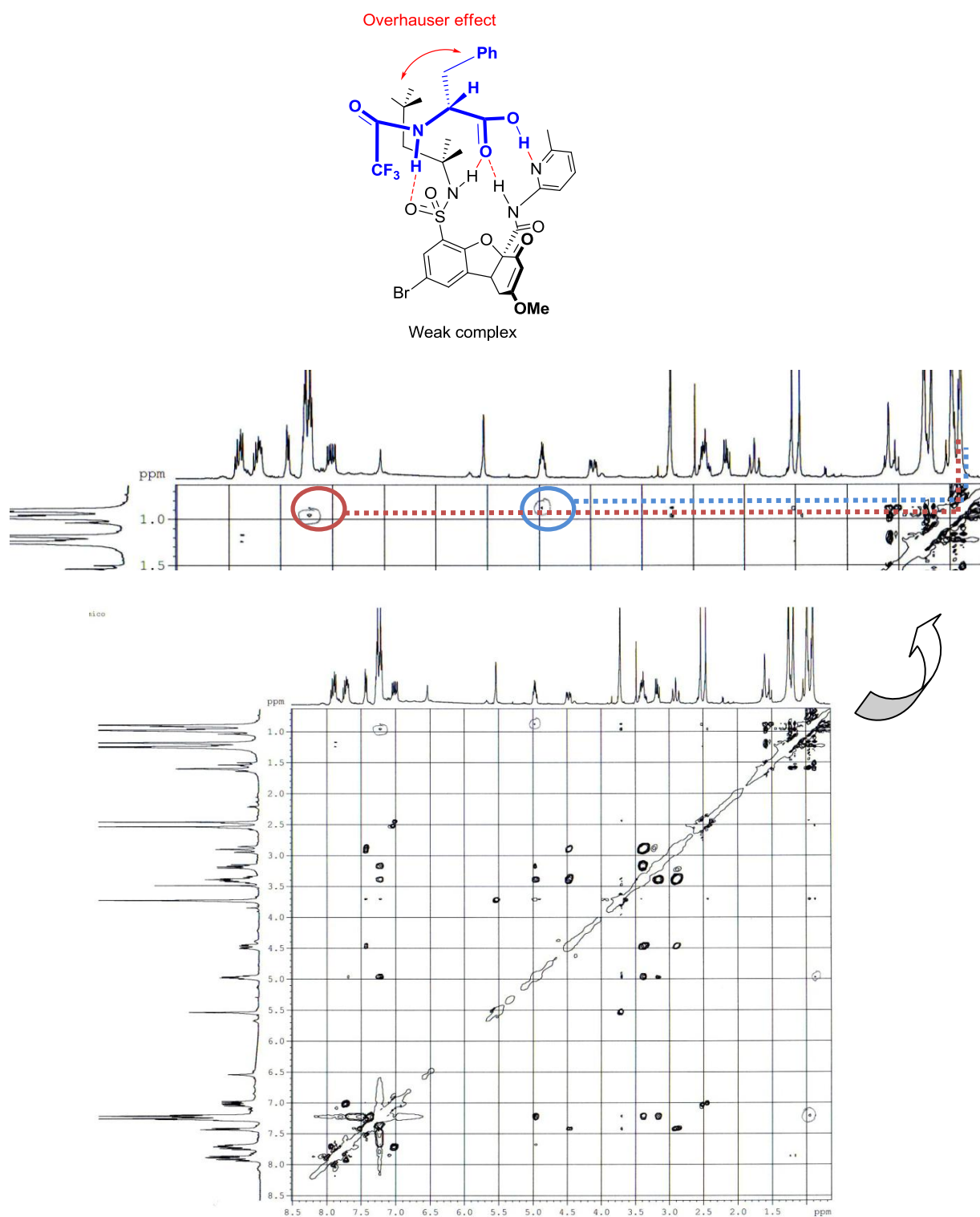


Figure 5.70. ROESY spectrum of the mixture of strong and weak complexes obtained between racemic receptor **94** and L-Phe trifluoroacetate **104**.

In figure 5.70 it can be seen that in the weak complex the aromatic ring of the phenylalanine side chain is close to the *t*-octyl group, since it shows the corresponding correlation, which is absent in the strong associate. However, this weak associate does not show the correlation between the *t*-octyl group and the alpha proton which is present in the more stable associate. This way we can unambiguously establish the configuration of the receptor which forms the most stable associate with *L*-phenylalanine trifluoroacetate **104** as **4aR** and **9bS**.

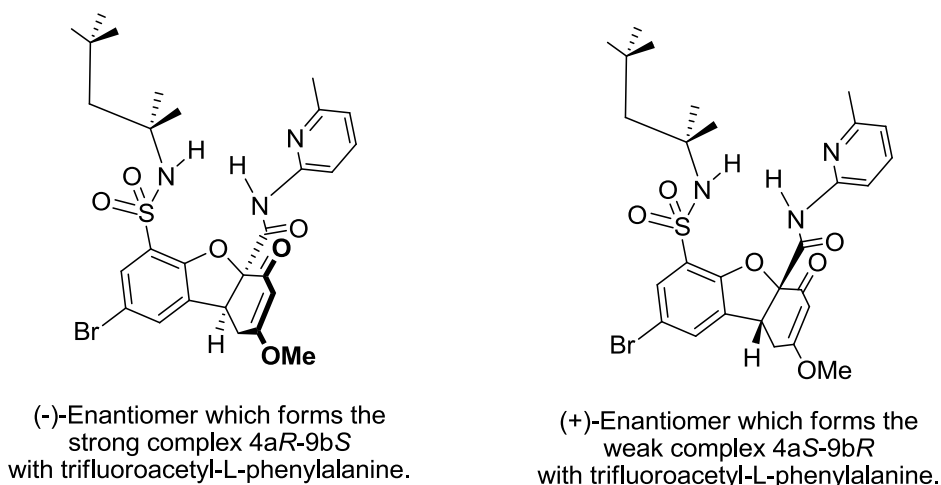


Figure 5.71. Absolute configuration of receptor **94** enantiomers.

To theoretically support the structures proposed above we performed a molecular modelling study.²⁰⁷ In figure 5.72 it can be seen the geometry of the complexes of receptor **94** with *L* and *D*-Phe trifluoroacetate, respectively.

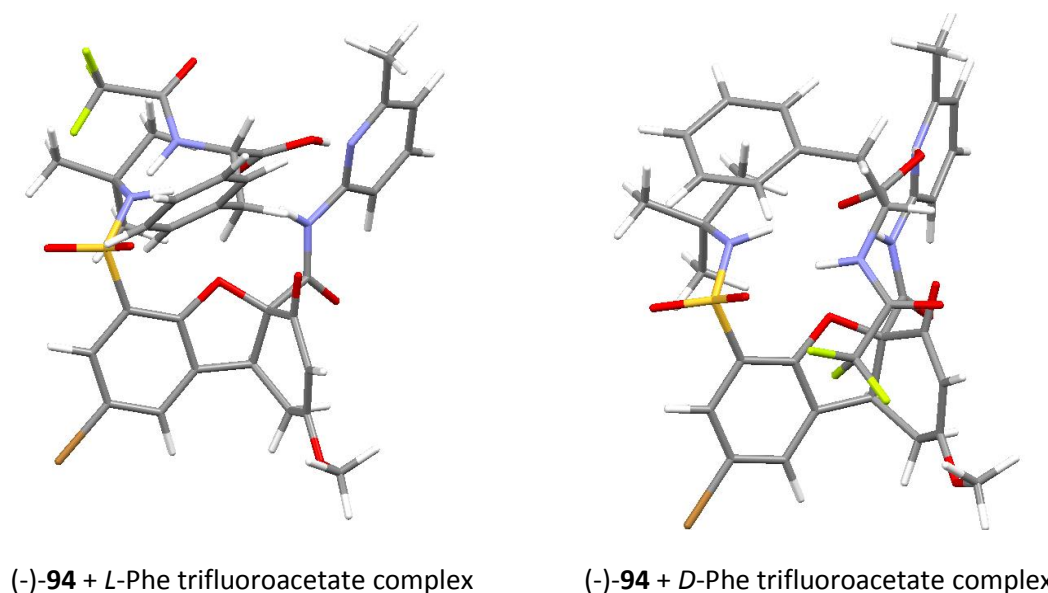


Figure 5.72. Molecular modelling study of receptor **94** and *L*-Phe trifluoroacetate (B3LYP/6-31G**).

²⁰⁷ Study carried out by Dr. Luis Simón Rubio.

The method described above allows to obtain small quantities of enantiomerically pure receptor **94**, but it does not allow obtaining it in a large scale, so we prefer to continue the work seeking a similar receptor, but which could be separated more easily.

5.3. CONCLUSIONS

In this chapter we have successfully synthesized a tripodal receptor with an oxyanion hole in its structure. Moreover, we have performed the resolution of the racemic mixture using its supramolecular properties.

As base skeleton we used a benzofuran derivative. For its preparation it was necessary to optimize the different steps of the synthesis with the objective of creating a three-dimensional scaffold. This structure has been suitably functionalized with a sulfonamide and an amidopyridine which allow carrying out the association of amino acid derivatives by a three-point model, which should be enough to resolve racemic mixtures of amino acid derivatives.

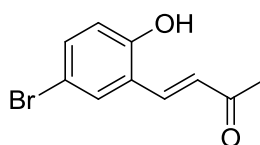
Receptor synthesis produces a racemic mixture which must be separated in order to use this compound in molecular recognition of racemic mixtures. To do this, we have synthesized several amino acids derivatives in order to select the one that offered the best features for separation. *L*-phenylalanine trifluoroacetate was chosen for impregnating a preparative silica gel plate and carrying out the separation of the receptor racemic mixture.

At the end of the chapter, the geometry of the complexes with the guest has been justified.

5.4. EXPERIMENTAL

Receptors synthesis

- (E)-4-(5-bromo-2-hydroxyphenyl)but-3-en-2-one (**86**)



To a solution of 5-bromo-2-hydroxybenzaldehyde (290 g, 1.44 mol) in 1.4 L of acetone an aqueous solution of NaOH 1.2 M was added from a dropping funnel. After addition, stirring was kept for 1 hour. Then the reaction mixture was added over ice and concentrated HCl, observing the appearance of a solid. The solid obtained was filtered and allowed to dry at room temperature, yielding 350 g of the desired product **86** with a 84 % yield

mp: 148-149 °C.

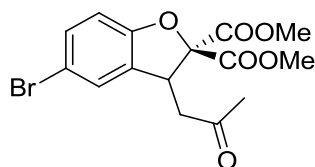
$^1\text{H NMR}$ (DMSO- d_6) δ (ppm): 2.29 (s, 3H), 6.88 (d, $J = 8.7$ Hz, 1H), 6.90 (d, $J = 16.4$ Hz, 1H), 7.37 (dd, $J = 2.5, 8.7$ Hz, 1H), 7.68 (d, $J = 16.4$ Hz, 1H), 7.77 (d, $J = 2.5$ Hz, 1H).

$^{13}\text{C NMR}$ (DMSO- d_6) δ (ppm): 27.6 (CH₃), 110.7 (C), 118.3 (CH), 123.3 (C), 127.8 (CH), 130.6 (CH), 133.8 (CH), 136.7 (CH), 156.1 (C), 198.0 (C).

IR (film, cm^{-1}): 3054, 2373, 2347, 1628, 1593, 1259, 748.

HRMS (ESI): 240.9865 (M + H)⁺, calcd for C₁₀H₁₀O₂Br 240.9859.

- 5-bromo-3-(2-oxopropyl)benzofuran-2, 2(3H)dicarboxylate (**88**)



Chalcone **86** (160 g, 0.66 mol), dimethyl chloromalonate (200 mL, 1.16 mol),²⁰⁸ K₂CO₃ (170 g, 1.23 mol) and DMF (590 mL) were added into a round bottom flask. The reaction mixture was kept under stirring for 2 hours at room temperature, monitoring the reaction progress by $^1\text{H NMR}$. After completion of the reaction, it was poured onto a mixture of water, ice, hexane,

²⁰⁸ Babu, G. R.; Rajesh, T.; Nagarjuna, R.; Krishna, A. V. G.; Madhusudhan, G. *Der Pharma Chemica* **2011**, *3*, 437-442.

ether and concentrated HCl, stirred and a precipitate was obtained. The obtained solid was vacuum filtered, washed with water and dried. The product was purified by crystallization in MeOH at 0 °C, obtaining 250 g of pure product **88** with 66 % yield.

mp: 90-93 °C.

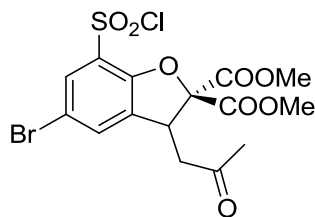
¹H NMR (CDCl₃) δ (ppm): 2.16 (s, 3H), 2.71 (dd, *J* = 8.9, 18.0 Hz, 1H), 2.87 (dd, *J* = 4.9, 18.0 Hz, 1H), 3.78 (s, 3H), 3.80 (s, 3H), 4.68 (dd, *J* = 4.9, 8.9 Hz, 1H), 6.76 (d, *J* = 8.5 Hz, 1H), 7.17 (d, *J* = 2.0 Hz, 1H), 7.23 (dd, *J* = 2.0, 8.5 Hz, 1H).

¹³C NMR (CDCl₃) δ (ppm): 30.1 (CH₃), 43.0 (CH), 44.9 (CH₂), 53.2 (CH₃), 53.7 (CH₃), 91.9 (C), 111.6 (CH), 114.1 (C), 127.7 (CH), 130.5 (C), 131.8 (CH), 156.3 (C), 166.9 (C), 167.4 (C), 204.7 (C).

IR (film, cm⁻¹): 3049, 1747, 1474, 1274, 1055, 743.

HRMS (ESI): 371.0131 (M + H)⁺, calcd for C₁₅H₁₆O₆Br 371.0125.

- 5-Bromo -7-(chlorosulfonyl)-3-(2-oxopropyl)benzofuran-2,2(3H)dicarboxylate (89)



In a two-necked flask equipped with a magnetic stirrer, a low-temperature thermometer and an addition funnel under argon atmosphere, thionyl chloride (60 mL, 0.83 mol) was added and cooled in an ice-salt bath. Once the temperature was below 0 °C, intermediate **88** was added (30.3 g, 0.082 mol). Chlorosulfonic acid (60 mL, 0.90 mol) was slowly poured from the addition funnel, controlling the temperature did not exceed 5 °C. Once the addition was completed, the mixture was maintained at 5 °C for 62 hours, monitoring the reaction progress by ¹H NMR. Once the reaction was finished, it was diluted with CH₂Cl₂ (200 mL) and slowly poured over a mixture of CH₂Cl₂ and ice with stirring. Then the phases were separated, the organic phase was dried over anhydrous Na₂SO₄ and the solvent was removed by evaporation under vacuum to yield 37.0 g of the title product with 96 % yield.

mp: 124-126 °C.

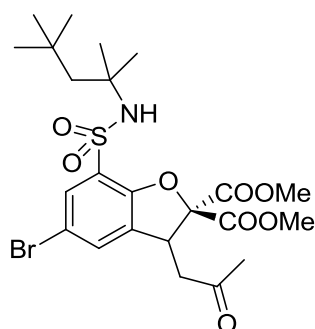
¹H NMR (CDCl₃) δ (ppm): 2.23 (s, 3H), 2.78 (dd, *J* = 9.4, 18.3 Hz, 1H), 3.04 (dd, *J* = 4.1, 18.3 Hz, 1H), 3.84 (s, 3H), 3.88 (s, 3H), 4.75 (dd, *J* = 4.1, 9.4 Hz, 1H), 7.54 (d, *J* = 1.9 Hz, 1H), 7.85 (d, *J* = 1.9 Hz, 1H).

^{13}C NMR (CDCl_3) δ (ppm): 30.1 (CH_3), 42.7 (CH), 44.2 (CH_2), 53.7 (CH_3), 54.1 (CH_3), 93.2 (C), 113.9 (C), 127.2 (C), 129.5 (CH), 134.5 (C), 135.2 (CH), 153.8 (C), 165.5 (C), 166.2 (C), 204.6 (C).

IR (nujol, cm^{-1}): 2916, 2949, 2852, 1768, 1748, 1723, 1599, 1456, 1372, 1301, 1242, 1184, 1165, 1061.

HRMS (ESI): 485.9629 ($\text{M} + \text{NH}_4$) $^+$, calcd for $\text{C}_{15}\text{H}_{18}\text{NO}_8\text{SClBr}$ 485.9620.

- 5-bromo-3-(2-oxopropyl)-7-(*N*-(2,4,4-trimethylpentan-2-yl)sulfamoyl)benzofuran-2,2(3*H*)dicarboxylate (90)



To a solution of *t*-octylamine (6.13 g, 47.4 mmol) and triethylamine (5.5 mL, 39.7 mmol) in 30 mL of EtOAc, a solution of the previous chlorosulfonyl compound **89** (11.8 g, 1 mmol) in 80 mL of EtOAc was added and stirred at room temperature for 5 hours. When the reaction was completed it was added over 2 M HCl (200 mL) with ice. The organic phase was separated, dried and evaporated. The solid obtained can be purified by crystallization from EtOAc yielding 5.3 g of the title compound (38 % yield).

mp: 138-140 °C.

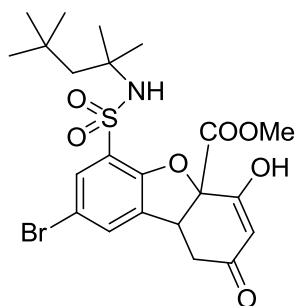
^1H NMR (CDCl_3) δ (ppm): 1.01 (s, 9H), 1.23 (s, 3H), 1.25 (s, 3H), 1.58 (d, $J = 14.9$ Hz, 1H), 1.63 (d, $J = 14.9$ Hz, 1H), 2.19 (s, 3H), 2.75 (dd, $J = 8.7, 18.2$ Hz, 1H), 2.96 (dd, $J = 4.4, 18.2$ Hz, 1H), 3.80 (s, 3H), 3.83 (s, 3H), 4.69 (dd, $J = 4.4, 8.7$ Hz, 1H), 4.94 (s, NH), 7.33 (s, 1H), 7.76 (s, 1H).

^{13}C NMR (CDCl_3) δ (ppm): 29.1 (CH_3), 29.2 (CH_3), 30.0 (CH_3), 31.6 (CH_3), 32.9 (C), 42.8 (CH), 44.5 (CH_2), 53.4 (CH_3), 53.9 (CH_3), 54.7 (CH_2), 58.9 (C), 92.3 (C), 113.9 (C), 128.1 (C), 129.6 (CH), 131.4 (CH), 132.3 (C), 152.4 (C), 165.9 (C), 166.6 (C), 204.5 (C).

IR (film, cm^{-1}): 3390, 3306, 2916, 2839, 1710, 1606, 1521, 1256, 1366, 1249, 1203, 1152 (check).

HRMS (ESI): 579.1365 ($\text{M} + \text{NH}_4$) $^+$, calcd for $\text{C}_{23}\text{H}_{36}\text{BrN}_2\text{O}_8\text{S}$ 579.1373.

- Methyl 8-bromo-2-hydroxy-2-oxo-6-(*N*-(2,4,4-trimethylpentan-2-yl)sulfamoyl)-1,4,4a,9b-tetrahydrodibenzo[*b,d*]furan-4a-carboxylate (**93**)



Under argon atmosphere, Na (1.0 g, 43.5 mmol) was added to 10 mL of MeOH (50 mL of MeOH were previously dried with 3.0 mL of methyl orthoformate and one drop of methanesulfonic acid). When the sodium was completely dissolved it was cooled with an ice bath and compound **90** (3.8 g, 6.8 mmol) was added. The ice bath was removed and within minutes a solid begins to crystallize. After 30 minutes, the reaction mixture was added over a 10 % v/v aqueous solution of HCl, yielding 3.3 g of compound **93** (91 % yield).

mp: 124-126 °C.

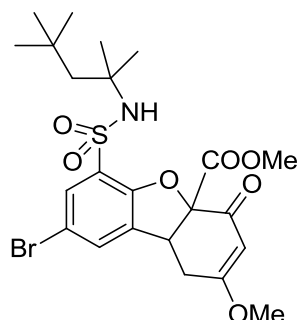
¹H RMN (CDCl₃-CD₃OD) δ (ppm): 0.90 (s, 9H), 1.02 (s, 3H), 1.07 (s, 3H), 1.38 (d, *J* = 14.8 Hz, 1H), 1.50 (d, *J* = 13.7, 1H), 2.77 (d, *J* = 17.6 Hz, 1H), 3.03 (d, *J* = 7.0, 17.6 Hz, 1H), 3.76 (s, 3H), 4.12 (m, 1H), 5.39 (s, 1H), 6.73 (s, NH), 7.58 (s, 1H), 7.62 (s, 1H).

¹³C RMN (CDCl₃-CD₃OD) δ (ppm): 28.5 (CH₃), 29.5 (CH₃), 31.4 (CH₃ x 3), 32.4 (CH₂), 41.6 (CH), 53.6 (CH₃), 54.5 (CH₂), 58.3 (C), 90.3 (C), 105.2 (CH), 113.9 (C), 127.8 (C), 130.0 (CH), 130.2 (CH), 132.9 (C), 151.9 (C), 168.9 (C), 171.3 (C), 179.2 (C), 188.7 (C).

IR (film, cm⁻¹): 3410, 2949, 2929, 2845, 1768, 1625, 1450, 1379, 1327, 1255, 1203, 1158, 1087, 1035, 736.

HRMS (ESI): 547.1111 (M + NH₄)⁺, calcd for C₂₂H₃₂BrN₂O₇S 547.1108.

- Methyl 8-bromo-2-methoxy-4-oxo-6-(*N*-(2,4,4-trimethylpentan-2-yl)sulfamoyl)-1,4,4a,9b-tetrahydrodibenzo[*b,d*]furan-4a-carboxylate (**91**)



The cyclization was carried out following the same experimental procedure for compound **93**, but the work up of the reaction was different. For 2.7 g (4.8 mmol) of compound **90**, a solution of methyl orthoformate (3.5 ml, 32.0 mmol) and methanesulfonic acid (3.5 mL, 53.9 mmol) in dry MeOH (20 mL) was prepared and cooled to -10 °C. The reaction mixture was added over this solution and then temperature was allowed to rise to room temperature and Na₂CO₃ (6 g, 56.6 mmol) in water (50 mL) was added. Then MeOH and THF were evaporated and the aqueous solution was extracted with EtOAc, yielding 2.2 g of the desired compound with 84 % yield. This compound was purified by silica gel column with CH₂Cl₂-EtOAc as eluents, yielding 0.9 g with a final yield of 34 %.

mp: 175-177 °C.

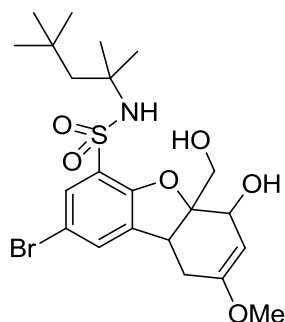
¹H NMR (CDCl₃) δ (ppm): 0.99 (s, 9H), 1.17 (s, 3H), 1.19 (s, 3H), 1.52 (d, *J* = 14.8 Hz, 1H), 1.64 (d, *J* = 14.8 Hz, 1H), 2.80 (dd, *J* = 3.2, 18.2 Hz, 1H), 3.19 (dd, *J* = 7.4, 18.2 Hz, 1H), 3.71 (s, 3H), 3.80 (s, 3H), 4.19 (dd, *J* = 3.2, 7.4 Hz, 1H), 5.27 (s, 1H), 5.52 (s, 1H), 7.36 (s, 1H), 7.73 (s, 1H).

¹³C NMR (CDCl₃) δ (ppm): 28.9 (CH₂), 29.1 (CH₃), 29.4 (CH₃), 31.6 (CH₃ x 3), 31.6 (C), 42.1 (CH), 53.5 (CH₃), 54.4 (CH₂), 56.5 (CH₃), 59.1 (C), 89.6 (C), 102.3 (CH), 113.9 (C), 128.6 (C), 129.8 (CH), 129.9 (CH), 131.8 (C), 152.8 (C), 167.5 (C), 176.0 (C), 187.4 (C).

IR (nujol, cm⁻¹): 3520, 3332, 3079, 2949, 2929, 2852, 1768, 1651, 1606, 1456, 1411, 1353, 1307, 1255, 1210, 1165, 1139, 1093, 1041, 983.

HRMS (ESI): 561.1264 (M + H)⁺, calcd for C₂₃H₃₄BrN₂O₇S 561.1265.

- **2-Bromo-6-hydroxy-5a-(hydroxymethyl)-8-methoxy-N-(2,4,4-trimethylpentan-2-yl)-5a,6,9,9a-tetrahydrodibenzo[*b,d*]furan-4-sulfonamide (92)**



Compound **91** (250 mg, 0.46 mmol) was dissolved in MeOH (6 mL) and NaBH₄ (34 mg, 0.90 mmol) was added. The reaction could be monitored by TLC, using CH₂Cl₂-AcOEt as eluent. When it was finished it was diluted with EtOAc and 18 mL of 0.6 M aqueous NH₄Cl was added. Then the organic phase was separated, dried and evaporated to give 210 mg of compound **92** which was purified by crystallization from CH₂Cl₂, obtaining 68 mg (29 % yield).

mp: 128-130 °C.

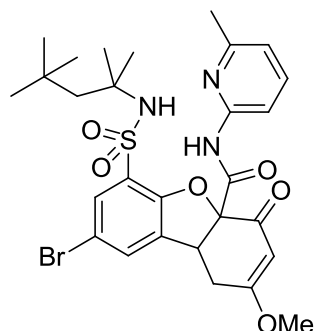
¹H NMR (CD₃OD) δ (ppm): 1.05 (s, 9H), 1.14 (s, 3H), 1.18 (s, 3H), 1.50 (d, *J* = 14.7 Hz, 1H), 1.70 (d, *J* = 14.7 Hz, 1H), 2.36 (dd, *J* = 2.5, 15.5 Hz, 1H), 2.53 (dd, *J* = 6.8, 15.5 Hz, 1H), 3.39 (s, 3H), 3.78 (dd, *J* = 2.5, 6.8 Hz, 1H), 3.85 (s, 2H), 4.46 (s, 1H), 4.58 (s, 1H), 7.51 (d, *J* = 2.0 Hz, 1H), 7.58 (d, *J* = 2.0 Hz, 1H).

¹³C NMR (CD₃OD) δ (ppm): 29.4 (CH₃), 30.8 (CH₃), 32.2 (CH₃ x 3), 32.6 (C), 33.3 (CH₂), 42.7 (CH), 55.1 (CH₃), 55.6 (CH₂), 58.8 (C), 64.9 (CH₂), 68.5 (CH), 96.7 (C), 98.7 (CH), 112.4 (C), 127.9 (C), 130.1 (CH), 132.4 (CH), 138.3 (C), 156.6 (C), 156.9 (C).

IR (film, cm⁻¹): 3455, 3221, 3105, 3179, 2923, 2832, 2728, 2670, 1677, 1586, 1463, 1379, 1314, 1262, 1236, 1216, 1139, 1041, 892, 814, 736.

HRMS (ESI): 535.1471 (M + NH₄)⁺, calcd for C₂₂H₃₆BrN₂O₆S 535.1472.

- **8-Bromo-2-methoxy-*N*-(6-methylpyridin-2-yl)-4-oxo-6-(*N*-(2,4,4-trimethylpentan-2-yl)sulfamoyl)-1,4,4a,9b-tetrahydrodibenzo[*b,d*]furan-4a-carboxamide (94)**



In a flask equipped with septum and argon 2-amino-6-methylpyridine (5.0 g, 46.2 mmol) was dissolved in dry THF (50 mL), and a trace of 2,2'-bipyridyl was added. The flask was cooled to -70 °C and added over 35 mL of a solution of BuLi in hexane (1.6 M, 0.87 mol) with stirring. At the beginning of the addition the solution takes on a yellow colour, as all the BuLi is used to abstract the proton of the aminopyridine. At the end of the addition the solution takes on a slightly reddish colour (due to 2,2'-bipyridyl presence), indicating that all aminopyridine had been deprotonated. Then the ester **93** was added (9.4 g, 17.7 mmol) and stirred until the entire solid had been dissolved. The reaction can be followed by TLC. After an hour a precipitate began to appear. The reaction was added to 2 M HCl solution and extracted with ethyl acetate. The phases were separated, Na₂SO₄ was added to the organic phase, filtered and evaporated to give 5.9 g of the desired compound (55 % yield).

Then, to a solution of methyl orthoformate (3.0 mL, 27 mmol) and acetyl chloride (350 μL, 4.92 mmol) in 18 mL of MeOH and cooled in an ice bath the enol prepared in the previous step was added (2.38 g, 3.92 mmol) and the solution was stirred. The reaction was monitored by TLC (DCM-EtOAc 1:1). The ice bath was removed and within minutes a precipitate corresponding to the hydrochloride of compound **94** showed up. The solid thus obtained was filtered, obtaining 1.0 g of compound **94** as the hydrochloride. To the filtrate solid Na₂CO₃ was added, the carbonate was filtered and washed with more EtOAc. This solution was left to stand for 12 h and a precipitate, which corresponds to the neutral compound **94** (700 mg) appeared. Receptor **94** hydrochloride was suspended in CHCl₃ and washed with aqueous saturated Na₂CO₃, yielding 0.5 g of compound **94**. Total yield is 49 %.

mp > 230 °C.

¹H NMR (CDCl₃) δ (ppm): 1.03 (s, 9H), 1.23 (s, 6H), 1.48 (d, *J* = 14.9 Hz, 1H), 1.74 (d, *J* = 14.9 Hz, 1H), 2.46 (s, 3H), 2.89 (d, *J* = 18.1 Hz, 1H), 3.40 (dd, *J* = 7.2, 18.1 Hz, 1H), 3.76 (s, 3H), 4.39 (d, *J* = 7.2 Hz, 1H), 5.45 (s, NH), 5.60 (s, 1H), 6.93 (d, *J* = 7.6 Hz, 1H), 7.42 (s, 1H), 7.57 (t, *J* = 7.9 Hz), 7.84 (s, 1H), 7.89 (d, *J* = 8.2 Hz, 1H), 9.23 (s, NH).

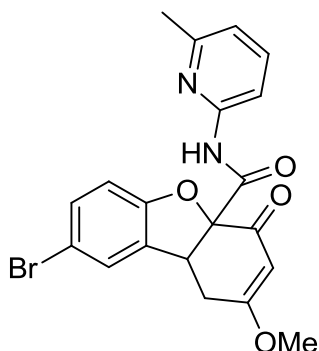
¹³C NMR (CDCl₃) δ (ppm): 23.9 (CH₃), 29.0 (CH₂), 29.2 (CH₃), 29.5 (CH₃), 31.6 (CH₃ x 3), 31.6 (C), 41.9 (CH), 54.5 (CH₂), 56.4 (CH₃), 59.1 (C), 90.2 (C), 102.6 (CH), 111.0 (CH), 114.4 (C), 120.2

(CH), 129.0 (C), 129.7 (CH), 130.3 (CH), 132.2 (C), 138.4 (CH), 149.2 (C), 152.2 (C), 157.4 (C), 165.6 (C), 176.2 (C), 188.7 (C).

IR (nujol, cm^{-1}): 3377, 3338, 2929, 2955, 2852, 1697, 1664, 1612, 1463, 1379, 1346, 1203, 1145, 1048, 976, 918.

HRMS (ESI): 620.1432 ($\text{M} + \text{H}^+$), calcd for $\text{C}_{28}\text{H}_{35}\text{BrN}_3\text{O}_6\text{S}$ 620.1424.

- **8-Bromo-2-methoxy-*N*-(6-methylpyridine-2-yl)-4-oxo-1,4,4a,9b-tetrahydrodibenzo[*b*,*d*]furan-4a-carboxamide (95)**



The cyclization was carried out following the experimental procedure described in the formation of compound **91** but taking compound **88** as starting material. The introduction of the aminopyridine fragment was carried out following the same steps as in the formation of compound **94** (62 % yield).

mp: 195-197 °C.

$^1\text{H NMR}$ (CDCl_3) δ (ppm): 2.32 (s, 3H), 2.75 (dd, $J = 18.0, 2.3$ Hz, 1H), 3.18 (dd, $J = 18.0, 7.6$ Hz, 1H), 3.62 (s, 3H), 4.19 (d, $J = 5.5$ Hz, 1H), 5.48 (s, 1H), 6.71 (d, $J = 8.6$ Hz, 1H), 6.82 (d, $J = 7.4$ Hz, 1H), 7.15 (s, 1H), 7.17 (d, $J = 7.8$ Hz, 1H), 7.47 (t, $J = 7.8$ Hz, 1H), 7.80 (d, $J = 8.2$ Hz, 1H).

$^{13}\text{C NMR}$ (CDCl_3) δ (ppm): 23.6 (CH_3), 29.1 (CH_2), 42.4 (CH), 56.3 (CH_3), 88.8 (C), 102.5 (CH), 111.0 (CH), 112.1 (CH), 114.5 (C), 120.1 (CH), 126.2 (CH), 130.0 (C), 132.2 (CH), 138.8 (CH), 149.1 (C), 156.0 (C), 157.0 (C), 167.1 (C), 177.0 (C), 190.3 (C).

IR (nujol, cm^{-1}): 3416, 2929, 2852, 1690, 1651, 1612, 1528, 1463, 1385, 1229, 1203, 1171, 1022, 983.

HRMS (ESI): 429.0452 ($\text{M} + \text{H}^+$), 429.0444 calcd for $\text{C}_{20}\text{H}_{18}\text{BrN}_2\text{O}_4$ 429.0444.

- Compounds **96**,²⁰⁹ **97**²¹⁰ and **98**²¹¹ were synthesized according to the experimental procedure described in the literature, matching its physical and spectroscopic properties.

Guest synthesis

- Guests **99**, **100**, **122-124** and **125** are commercially available.

- Guest **116**²¹² has been previously used in our research group.

- Guests **102**,²¹³ **103**,²¹⁴ **104**,²¹⁵ **105**,²¹⁶ **107**,²¹⁷ **108**,²¹⁸ **110**,²¹⁹ **112**,²²⁰ **113**²²¹ **126**,²²² **127**²²³ and **128**²²⁴ are described in the literature and were synthesized according to the experimental procedure described, matching its physical and spectroscopic properties.

²⁰⁹ del Amo, V.; Slawin, A. M. Z.; Philp, D. *Org. Lett.* **2008**, *10*, 4589-4592.

²¹⁰ Gómez Herrero, F., Final Degree Project (in redaction), University of Salamanca, 2014.

²¹¹ Beloso, I.; Castro, J.; García-Vázquez, J. A.; Pérez-Lourido, P.; Romero, J.; Sousa, A. *Polyhedron* **2006**, *25*, 2673-2682.

²¹² Oliva, A. I. *Enantioselective receptors with tetrahydrobenzoxanthene skeleton for amino acids Derivatives*; Doctoral Thesis: University of Salamanca, 2003.

²¹³ Oliva, A. I.; Simón, L.; Muñiz, F. M.; Sanz, F.; Ruiz-Valero, C.; Morán, J. R. *J. Org. Chem.* **2004**, *69*, 6883-6885.

²¹⁴ Hang, J.; Tian, S.-K.; Tang, L.; Deng, L. *J. Am. Chem. Soc.* **2001**, *123*, 12696-12697.

²¹⁵ Shimohigashi, Y.; Kato, T.; Kang, S.; Minematsu, Y.; Waki, M.; Izumiya, N. *Tetrahedron Lett.* **1979**, *15*, 1327-1328.

²¹⁶ Di Santo, R.; Costi, R.; Roux, A.; Artico, M.; Befani, O.; Meninno, T.; Agostinelli, E.; Palmegiani, P.; Turini, P.; Cirilli, R.; Ferretti, R.; Gallinella, B.; La Torre, F. *J. Med. Chem.* **2005**, *48*, 4220-4223.

²¹⁷ (a) Oliva, A. I.; Simón, L.; Muñiz, F. M.; Sanz, F.; Morán, J. R. *Org. Lett.* **2004**, *6*, 1155-1157; (b) Oliva, A. I.; Simón, L.; Muñiz, F. M.; Sanz, F.; Morán, J. R. *Chem. Commun.* **2004**, 426-427.

²¹⁸ Dydio, P.; Rubay, C.; Gadzikwa, T.; Lutz, M.; Reek, J. N. H. *J. Am. Chem. Soc.* **2011**, *133*, 17176-17179.

²¹⁹ Endo, T.; Sakai, K.; Chou, K.; Inamoto, Y.; Teshigawara, H. *Fr. Demande* 1981, FR 2470774 A1 19810612.

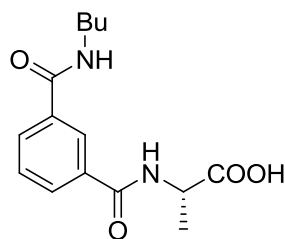
²²⁰ Thunberg, L.; Allenmark, S.; Friberg, A.; Ek, F.; Frejd, T. *Chirality* **2004**, *16*, 614-624.

²²¹ Xu, D.-Q.; Yue, H.-D.; Luo, S.-P.; Xia, A.-B.; Zhang, S.; Xu, Z.-Y. *Org. Biomol. Chem.* **2008**, *6*, 2054-2057.

²²² Georges, C.; Lewis, T. J.; Llewellyn, J. P.; Salvagno, S.; Taylor, D. M.; Stirling, C. J. M.; Vogel, V. *J. Chem. Soc. Faraday Transactions 1: Physical Chemistry in Condensed Phases* **1988**, *84*, 1531-1542.

²²³ (a) Ruano, J. L. G.; Cid, M. B.; Martín-Castro, A. M.; Aleman, J. *Science of Synthesis* **2007**, *39*, 245-390; (b) Holland, H. L.; Brown, F. M.; Johnson, D. V.; Kerridge, A.; Mayne, B.; Turner, C. D.; Van Vliet, A. J. *J. Mol. Catal. B: Enzym.* **2002**, *17*, 249-256.

²²⁴ Briere, J.-F.; Charpentier, P.; Dupas, G.; Queguiner, G.; Bourguignon, J. *Tetrahedron* **1997**, *53*, 2075-2086.

- (S)-2-(3-(butylcarbamoyl)benzamido)propanoic acid (101)

Isophthalic acid monobutylamide²²⁵ (0.4 g, 1.4 mmol) was dissolved in thionyl chloride (4 mL) and refluxed for 90 minutes. Then the excess of thionyl chloride was evaporated at reduced pressure.

KOH (255 mg, 4.55 mmol) was dissolved in 1 mL of H₂O, then *L*-alanine (500 mg 5.61 mmol) was added and the monobutylamide chloride of isophthalic acid (270 mg, 1.13 mmol) was added dropwise. The reaction was stirred until the reaction was homogeneous and was cooled to room temperature. 2 M HCl was then added and extracted with EtOAc. The organic phase was separated and dried with Na₂SO₄, filtered and evaporated to give the desired compound 231 mg (70 % yield).

$[\alpha]_D^{20} = -4.0$ ($c = 1.14$, MeOH).

mp: 68-70 °C.

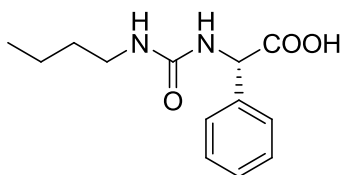
¹H NMR (CDCl₃) δ (ppm): 0.88 (t, $J = 7$ Hz, 3H), 1.17-1.42 (m, 2H), 1.46 (d, $J = 7.2$ Hz, 3H), 1.49-1.67 (m, 2H), 3.35 (t, $J = 7.2$ Hz, 2H), 4.64 (q, $J = 7.2$ Hz, 1H), 7.41 (t, $J = 7.8$ Hz, 1H), 7.82-7.94 (m, 2H), 8.14 (s, 1H).

¹³C NMR (CDCl₃) δ (ppm): 13.6 (CH₃), 17.8 (CH₃), 20.1 (CH₂), 31.4 (CH₂), 39.9 (CH₂), 48.7 (CH), 125.3 (CH), 128.8 (CH), 130.1 (CH), 130.6 (CH), 133.8 (C), 134.8 (C), 166.9 (C), 167.4 (C), 175.2 (C).

IR (film, cm⁻¹): 3319, 3079, 2962, 2929, 2858, 1716, 1638, 1528, 1463, 1301, 1223, 1184, 1158.

HRMS (ESI): 315.1316 (M + Na)⁺, calcd for C₁₅H₂₀N₂NaO₄ 315.1315.

²²⁵ Oliva, A. I.; Simón, L.; Muñiz, F. M.; Sanz, F.; Morán, J. R. *Tetrahedron* **2004**, *60*, 3755-3762.

- (S)-2-(3-butylureido)-2-phenylacetic acid (109)

KOH (328 mg, 5.85 mmol) was dissolved in 1 mL of H₂O, L-phenylglycine (978 mg, 6.47 mmol) was added and then butyl isocyanate (0.6 mL, 5.32 mmol). The solution was stirred and warmed spontaneously. Once it had been cooled it was diluted with H₂O, 2 M HCl was added until acidic pH and it was extracted with EtOAc, obtaining the desired compound 958 mg (72 % yield).

$[\alpha]_D^{20} = -6.7$ ($c = 1.04$, MeOH).

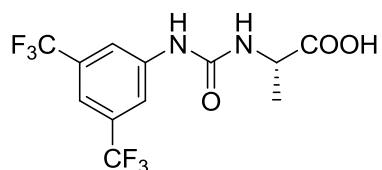
mp: 69-71 °C.

¹H NMR (CDCl₃) δ (ppm): 0.87 (t, $J = 7.2$ Hz, 3H), 1.26 (hexaplet, $J = 7.2$ Hz, 2H), 1.57 (q, $J = 7.2$ Hz, 2H), 3.43 (t, $J = 7.2$ Hz, 2H), 4.94 (s, 1H), 7.20-7.40 (m, 5H).

¹³C NMR (CDCl₃) δ (ppm): 13.6 (CH₃), 19.9 (CH₂), 30.0 (CH₂), 38.6 (CH₂), 60.6 (CH), 126.4 (CH x 2), 128.9 (CH), 129.0 (CH x 2), 134.5 (C), 158.3 (C), 172.5 (C).

IR (nujol, cm⁻¹): 3332, 3182, 2942, 1787, 1703, 1554, 1456, 1372, 1353, 1190, 1100, 918.

HRMS (ESI): 273.1213 (M + Na)⁺, calcd for C₁₃H₁₈N₂NaO₃ 273.1210.

- (S)-2-(3-(3,5-bis(trifluoromethyl)phenyl)ureido)propanoic acid (123)

KOH (20 mg, 0.365 mmol) was dissolved in 0.1 mL of H₂O, then L-alanine (50 mg, 0.56 mmol) and 3,5-bistrifluoromethylphenyl isocyanate (100 mg, 0.39 mmol) were added and a few drops of THF. The solution was stirred for one hour and then it was diluted with H₂O, 2mM HCl was added until acidic pH and extracted with EtOAc, obtaining the desired compound 87 mg (65 % yield).

$[\alpha]_D^{20} = -1.4$ ($c = 0.80$, MeOH).

mp: 132-134 °C.

$^1\text{H NMR}$ ($\text{CDCl}_3\text{-CD}_3\text{OD}$) δ (ppm): 1.39 (d, $J = 7.0$ Hz, 3H), 4.35 (m, 1H), 7.33 (s, 1H), 7.77 (s, 2H).

$^{13}\text{C NMR}$ ($\text{CDCl}_3\text{-CD}_3\text{OD}$) δ (ppm): 18.0 (CH_3), 48.6 (CH), 115.0 (CH), 117.9 (CH x 2), 123.2 (q, $J = 270.7$ Hz, CF_3 x 2), 131.8 (q, $J = 32.8$ Hz, C- CF_3 x 2), 140.8 (C), 155.1 (C), 176.3 (C).

IR (nujol, cm^{-1}): 3500, 3358, 3319, 1723, 1658, 1573, 1463, 1392, 1288, 1177, 1080, 1028, 886.

HRMS (ESI): 345.0667 ($\text{M} + \text{H}$) $^+$, calcd for $\text{C}_{12}\text{H}_{11}\text{F}_6\text{N}_2\text{O}_3$ 345.0668.

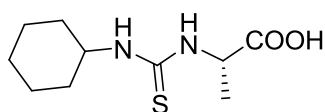
Preparation of thioureas 114-133

To a 1.6 M solution of KOH in water 1.2 equivalents of the corresponding amino acid and then 0.8 equivalent of the isothiocyanate were added. The reaction mixture was heated until it was homogeneous. It was cooled and diluted with water, acidified with 2 M HCl until slightly acidic pH, appearing a precipitate which was filtered. If no precipitate was obtained, it was extracted with EtOAc, the organic phase was decanted, dried with Na_2SO_4 , filtered and evaporated under reduced pressure. Yields between 60-70 % were obtained.

Preparation of amine isocyanates

36.7 mmol of Na_2CO_3 were added to a round bottom flask with 15 mL of a saturated aqueous solution of Na_2CO_3 and 20 mL of EtOAc. This flask was cooled with an ice bath and thiophosgene (1.4 mL, 18.4 mmol) and 17.5 mmol of the corresponding amine were added. The flask was stirred until the red colour of thiophosgene discoloured to yellow. Both phases were separated, the organic phase was dried and evaporated under reduced pressure to give yields of 80-90 %.

- (S)-2-(3-ciclohexylthioureido)propanoic acid (114)



$[\alpha]_{\text{D}}^{20} = +0.9$ ($c = 1.00$, MeOH).

mp: 133-135 °C.

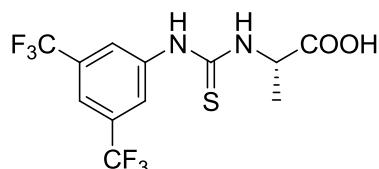
$^1\text{H NMR}$ (CDCl_3) δ (ppm): 0.98-1.35 (m, 5H), 1.39 (d, $J = 7.0$ Hz, 3H), 1.45-1.73 (m, 3H), 1.81-1.99 (m, 2H), 3.8 (m, 1H), 4.90 (q, $J = 7.0$ Hz, 1H).

$^{13}\text{C NMR}$ (CDCl_3) δ (ppm): 18.2 (CH_3), 24.6 (CH_2 x 2), 25.3 (CH_2), 32.5 (CH_2 x 2), 52.6 (CH), 52.4 (CH), 175.9 (C), 179.9 (C).

IR (nujol, cm^{-1}): 3377, 2929, 2852, 1703, 1651, 1547, 1463, 1379, 1255, 1106.

HRMS (ESI): 231.1165 ($\text{M} + \text{H}^+$), calcd for $\text{C}_{10}\text{H}_{19}\text{N}_2\text{O}_2\text{S}$ 231.1162.

- (S)-2-(3-(3,5-bis(trifluoromethyl)phenyl)thioureido) propanoic acid (115)



$[\alpha]_{\text{D}}^{20} = -2.4$ ($c = 0.96$, MeOH).

mp: 195-197 °C.

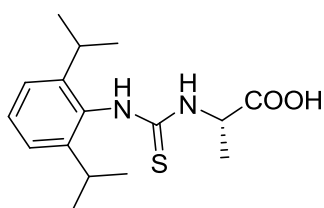
$^1\text{H NMR}$ (CDCl_3) δ (ppm): 1.60 (d, $J = 7.2$ Hz, 3H), 4.42 (q, $J = 7.2$ Hz, 1H), 7.89 (s, 2H), 7.96 (s, 1H), 8.48 (s, NH).

$^{13}\text{C NMR}$ (CDCl_3) δ (ppm): 16.8 (CH_3), 55.7 (CH), 122.7 (q, $J = 271.5$ Hz, $\text{CF}_3 \times 2$), 122.9 (CH), 128.8 (CH $\times 2$), 132.5 (q, $J = 34.0$ Hz, C- $\text{CF}_3 \times 2$), 133.8 (C), 173.4 (C), 181.9 (C).

IR (nujol, cm^{-1}): 3182, 2916, 2852, 1781, 1703, 1534, 1469, 1411, 1385, 1281, 1190, 1126.

HRMS (ESI): 341.0179 ($\text{M} - \text{H} - \text{H}_2\text{O}^-$), calcd for $\text{C}_{12}\text{H}_7\text{F}_6\text{N}_2\text{OS}$ 341.0188.

- (S)-2-(3-(2,6-diisopropylphenyl)thioureido)propanoic acid (116)



$[\alpha]_{\text{D}}^{20} = +.0$ ($c = 1.71$, CHCl_3).

mp: 68-70 °C.

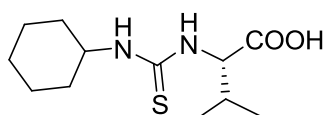
$^1\text{H NMR}$ (CDCl_3) δ (ppm): 1.10 (d, $J = 7.0$ Hz, 6H), 1.14 (d, $J = 7.0$ Hz, 6H), 1.40 (d, $J = 7.0$ Hz, 3H), 3.06 (hexaplet, $J = 6.8$ Hz, 2H), 5.15 (q, $J = 7.4$ Hz, 1H), 5.70 (s, NH), 7.20 (d, $J = 7.8$ Hz, 2H), 7.37 (t, $J = 7.8$ Hz, 1H), 7.96 (s, NH).

^{13}C NMR (CDCl_3) δ (ppm): 18.3 (CH_3), 22.6 (CH_3), 23.3 (CH_3), 24.3 (CH_3), 24.6 (CH_3), 28.5 ($\text{CH} \times 2$), 52.9 (CH), 124.5 (CH), 124.6 (CH), 129.4 (CH), 130.1 (C), 147.5 (C), 147.9 (C), 176.8 (C), 180.6 (C).

IR (nujol, cm^{-1}): 3364, 3241, 2968, 2910, 2858, 1722, 1651, 1541, 1469, 1255, 1171, 1067.

HRMS (ESI): 309.1633 ($\text{M} + \text{H}$) $^+$, calcd for $\text{C}_{16}\text{H}_{25}\text{N}_2\text{O}_2\text{S}$ 309.1631.

- (S)-2-(3-cyclohexylthioureido)-3-methylbutanoic acid (117)



$[\alpha]_{\text{D}}^{20} = +3.1$ ($c = 1.01$, MeOH).

mp: 159-161 $^{\circ}\text{C}$.

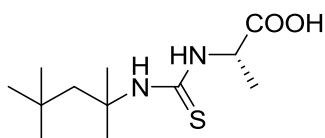
^1H NMR (CDCl_3) δ (ppm): 0.89 (d, $J = 6.2$ Hz, 6H), 0.95-1.40 (m, 5H), 1.41-1.72 (m, 3H), 1.79-1.98 (m, 2H), 2.04-2.26 (m, 1H), 3.70-4.00 (m, 1H), 4.79-4.95 (m, 1H).

^{13}C NMR (CDCl_3) δ (ppm): 18.0 (CH_3), 18.6 (CH_3), 24.6 ($\text{CH}_2 \times 2$), 25.4 (CH_2), 31.0 (CH), 32.5 ($\text{CH}_2 \times 2$), 52.6 (CH), 61.9 (CH), 174.9 (C), 181.0 (C).

IR (nujol, cm^{-1}): 3319, 3234, 2936, 1697, 1651, 1534, 1463, 1372, 1171, 1080, 892.

HRMS (ESI): 259.1481 ($\text{M} + \text{H}$) $^+$, calcd for $\text{C}_{12}\text{H}_{23}\text{N}_2\text{O}_2\text{S}$ 259.1475.

- (S)-2-(3-(2,4,4-trimethylpentan-2-yl)thioureido)propanoic acid (118)



$[\alpha]_{\text{D}}^{20} = -+0.8$ ($c = 2.09$, DMSO).

mp: 106-108 $^{\circ}\text{C}$.

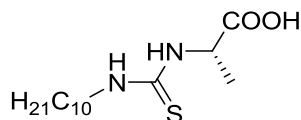
^1H NMR (CDCl_3) δ (ppm): 0.98 (s, 9H), 1.43 (s, 6H), 1.55 (d, $J = 7.0$ Hz, 3H), 1.71 (s, 2H), 5.05 (quin, $J = 6.3$ Hz, 1H), 6.38 (d, $J = 5.9$ Hz, NH), 6.67 (s, NH).

^{13}C NMR (CDCl_3) δ (ppm): 19.0 (CH_3), 30.6 ($\text{CH}_3 \times 2$), 31.5 ($\text{CH}_3 \times 3$), 31.9 (C), 51.9 (CH_2), 53.7 (CH), 57.2 (C), 177.5 (C), 179.5 (C).

IR (nujol, cm^{-1}): 3306, 2949, 2871, 1736, 1645, 1547, 1456, 1404, 1366, 1288, 1223, 1164, 1126, 1080, 918, 736.

HRMS (ESI): 261.1641 ($\text{M} + \text{H}^+$), calcd for $\text{C}_{12}\text{H}_{25}\text{N}_2\text{O}_2\text{S}$ 261.1631.

- (S) -2-(3-decylthioureido)propanoic acid (119)



$[\alpha]_{\text{D}}^{20} = -2.7$ ($c = 0.96$, CHCl_3).

mp: 43-46 °C.

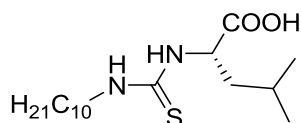
$^1\text{H NMR}$ (CDCl_3) δ (ppm): 0.85 (t, $J = 6.0$ Hz, 3H), 1.23 (s, 14H), 1.45 (d, $J = 7.0$ Hz, 3H), 1.63 (m, 2H), 3.75 (dd, $J = 6.6, 8.2$ Hz, 2H), 4.14 (q, $J = 7.0$ Hz, 1H), 8.33 (s, NH).

$^{13}\text{C NMR}$ (CDCl_3) δ (ppm): 14.1 (CH_3), 16.8 (CH_3), 22.6 (CH_2), 26.7 (CH_2), 27.7 (CH_2), 29.2 (CH_2), 29.3 (CH_2), 29.5 (CH_2), 29.5 (CH_2), 31.8 (CH_2), 41.3 (CH_2), 55.0 (CH), 175.0 (C), 183.7 (C).

IR (nujol, cm^{-1}): 3280, 2929, 2852, 1748, 1729, 1651, 1508, 1450, 1346, 1236, 1158, 1138, 1100.

HRMS (ESI): 269.1687 ($\text{M} - \text{H} - \text{H}_2\text{O}^-$), calcd for $\text{C}_{14}\text{H}_{25}\text{N}_2\text{O}_2\text{S}$ 269.1693.

- (S) -2-(3-decylthioureido)-4-methylpentanoic acid (120)



$[\alpha]_{\text{D}}^{20} = -6.8$ ($c = 0.93$, CHCl_3).

mp: 76-78 °C.

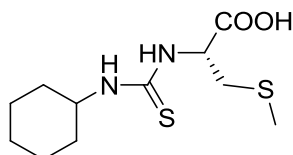
$^1\text{H NMR}$ (CDCl_3) δ (ppm): 0.85 (t, $J = 6.0$ Hz, 3H), 0.96 (d, $J = 6.2$ Hz, 6H), 1.23 (s, 14H), 1.47-1.94 (m, 5H), 3.75 (t, $J = 7.5$ Hz, 2H), 4.10 (dd, $J = 3.8, 9.8$ Hz, 1H), 8.64 (s, NH).

$^{13}\text{C NMR}$ (CDCl_3) δ (ppm): 14.1 (CH_3), 21.4 (CH_3), 22.6 (CH_2), 23.1 (CH_3), 25.1 (CH), 26.7 (CH_2), 27.6 (CH_2), 29.2 (CH_2), 29.3 (CH_2), 29.4 (CH_2), 29.5 (CH_2), 31.8 (CH_2), 40.4 (CH_2), 41.2 (CH_2), 58.0 (CH), 174.8 (C), 183.8 (C).

IR (nujol, cm^{-1}): 3189, 2955, 2929, 2838, 1748, 1696, 1528, 1469, 1444, 1346, 1262, 1249, 1132, 1087.

HRMS (ESI): 311.2160 ($\text{M} - \text{H} - \text{H}_2\text{O}$)⁻, calcd for $\text{C}_{17}\text{H}_{31}\text{N}_2\text{O}_2\text{S}$ 311.2162.

- (S)-2-(3-cyclohexylthioureido)-3-(methylthio)propanoic acid (121)



$[\alpha]_{\text{D}}^{20} = +0.96$ ($c = 0.96$, MeOH).

mp: 99-101 °C.

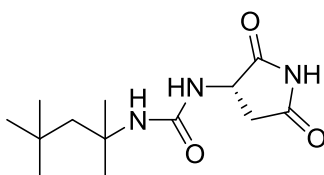
¹H NMR (CDCl_3) δ (ppm): 1.00-2.00 (m, 10H), 2.09 (s, 3H), 2.98 (dd, $J = 5.0, 14.0$ Hz, 1H), 3.15 (dd, $J = 5.0, 14.0$ Hz, 1H), 3.8 (m, 1H), 5.24 (t, $J = 5.0$ Hz, 1H).

¹³C NMR (CDCl_3) δ (ppm): 16.3 (CH_3), 25.0 ($\text{CH}_2 \times 2$), 25.8 (CH_2), 32.5 ($\text{CH}_2 \times 2$), 36.4 (CH_2), 52.6 (CH), 56.4 (CH), 173.8 (C), 180.2 (C).

IR (film, cm^{-1}): 3345, 2923, 2858, 2112, 1710, 1645, 1528, 1177.

HRMS (ESI): 277.1044 ($\text{M} + \text{H}$)⁺, calcd for $\text{C}_{11}\text{H}_{21}\text{N}_2\text{O}_2\text{S}_2$ 277.1039.

- (S)-1-(2,5-dioxopyrrolidin-3-yl)-3-(2,4,4-trimethylpentan-2-yl)urea (129)



Preparation of tert-octylamine isocyanate

In a round bottom phosgene 20 % solution in toluene (18.2 mL, 34.6 mmol) was dissolved in 60 mL of CH_2Cl_2 and placed in an ice bath. On this flask a solution of *t*-octylamine (2.0 g, 15.4 mmol) and triethylamine (4.85 mL, 34.8 mmol) in 60 mL of CH_2Cl_2 was added dropwise from a dropping funnel. After the addition was complete, 2 M HCl was added and phases were decanted. The organic phase was dried over anhydrous Na_2SO_4 , filtered and evaporated to give 1.36 g of the corresponding isocyanate (57 % yield).

Urea obtention

NaOH (0.56 g, 14.0 mmol) was dissolved in 0.7 mL of water and *L*-asparagine (2.6 g, 17.3 mmol) was added. Then *t*-octylamine isocyanate (1.0 g, 6.4 mmol) was incorporated and the mixture was heated until the reaction became homogeneous. When the reaction had finished it was diluted with water, 2 M HCl was added until acidic pH and it was cooled in an ice bath, appearing a precipitate which was filtered, obtaining 1.8 g (98 % yield).

Cyclization

It was carried out according to the conditions described in literature.²²⁶

$[\alpha]_D^{20} = -4.6$ ($c = 1.02$, MeOH).

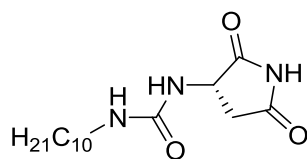
mp: 174-176 °C.

¹H NMR (CDCl₃) δ (ppm): 0.87 (s, 9H), 1.21 (s, 6H), 1.50 (dd, $J = 4.4, 14.8$ Hz, 1H), 1.67 (dd, $J = 5.2, 14.8$ Hz, 1H), 2.66 (dd, $J = 5.8, 18.0$ Hz, 1H), 2.86 (dd, $J = 9.0, 18.0$ Hz, 1H), 4.13 (dd, $J = 5.8, 9.0$ Hz, 1H), 5.52 (s, NH), 6.01 (s, NH), 10.40 (d, $J = 14.1$ Hz, NH).

¹³C NMR (CDCl₃) δ (ppm): 29.8 (CH₃), 29.9 (CH₃), 30.0 (CH₃), 31.2 (CH₃), 31.4 (CH₃), 37.3 (CH₂ x 2), 50.6 (CH), 51.1 (C), 53.8 (C), 157.1 (C), 176.3 (C), 180.0 (C).

IR (nujol, cm⁻¹): 3591, 3436, 3390, 3338, 3189, 2728, 1768, 1703, 1638, 1560, 1456, 1392, 1275, 1171, 1054, 736.

HRMS (ESI): 270.1818 (M + H)⁺, calcd for C₁₃H₂₄N₃O₃ 270.1812.

- (S) -1 -decyl-3-(2,5-dioxopyrrolidin-3-yl)urea (130)

The preparation was carried out similarly to the previous guest.

$[\alpha]_D^{20} = -3.0$ ($c = 1.17$, DMSO).

mp: 118-120 °C.

²²⁶ Maddaluno, J.; Corruble, A.; Leroux, V.; Ple, G.; Duhamel, P. *Tetrahedron: Asymmetry* **1992**, 3, 1239-1244.

¹H NMR (CDCl₃) δ (ppm): 0.81 (t, *J* = 6.3 Hz, 3H), 1.19 (s, 14H), 1.38 (m, 2H), 2.70 (dd, *J* = 6.0, 18.0 Hz, 1H), 2.94 (dd, *J* = 9.0, 18.0 Hz, 1H), 3.02 (t, *J* = 6.4 Hz, 2H), 4.26 (dd, *J* = 6.0, 9.0 Hz, 1H), 5.60 (s, NH), 6.13 (d, *J* = 7.0 Hz, NH), 10.26 (s, NH).

¹³C NMR (CDCl₃) δ (ppm): 14.0 (CH₃), 22.6 (CH₂), 26.8 (CH₂), 29.2 (CH₂), 29.3 (CH₂), 29.5 (CH₂ × 2), 30.0 (CH₂), 31.8 (CH₂), 37.3 (CH₂), 40.1 (CH₂), 50.8 (CH), 158.2 (C), 176.4 (C), 179.1 (C).

IR (film, cm⁻¹): 3332, 3299, 2916, 2852, 1716, 1619, 1547, 1463, 1177.

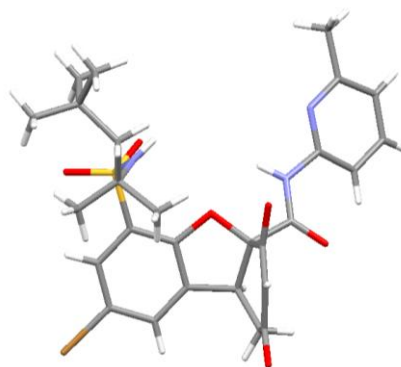
HRMS (ESI): 298.2127 (M + H)⁺, calcd for C₁₅H₂₈N₃O₃ 298.2125.



**VNIVERSIDAD
D SALAMANCA**

CAMPUS DE EXCELENCIA INTERNACIONAL

CHAPTER 6: New benzofuran-derived receptors



6.1. INTRODUCTION

Although receptor **94** racemic mixture resolution has been possible in the previous chapter, we thought it could be possible to achieve a better separation introducing changes in its structure. These changes could also lead to further improvements in the capacity of the receptor to associate different guests, and in better enantioselective recognition of racemic amino acid mixtures.

6.2. METHODS AND RESULTS

6.2.1. Receptor with less steric hindrance

To improve the results obtained with receptor **94** we started changing the large *t*-octyl group. This substituent may be too bulky and can hinder the formation of the complexes. To avoid this potential steric effect on the complex we substituted the *t*-octyl group of the sulfonamide with an *n*-butyl group, leading to receptor **131**. The synthesis was carried out in a similar way as receptor **94**, the only difference was the replacement of *t*-octylamine with *n*-butylamine in one of the synthetic steps.

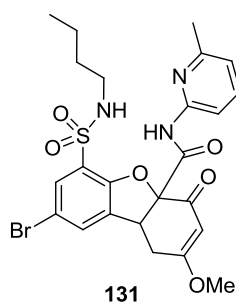


Figure 6.1. Receptor **131** whose *t*-octyl group on the sulfonamide was substituted by the less bulky *n*-butyl group.

Competitive titrations were carried out with receptor **131** and different guests. All the guests tested are shown in figure 6.2.

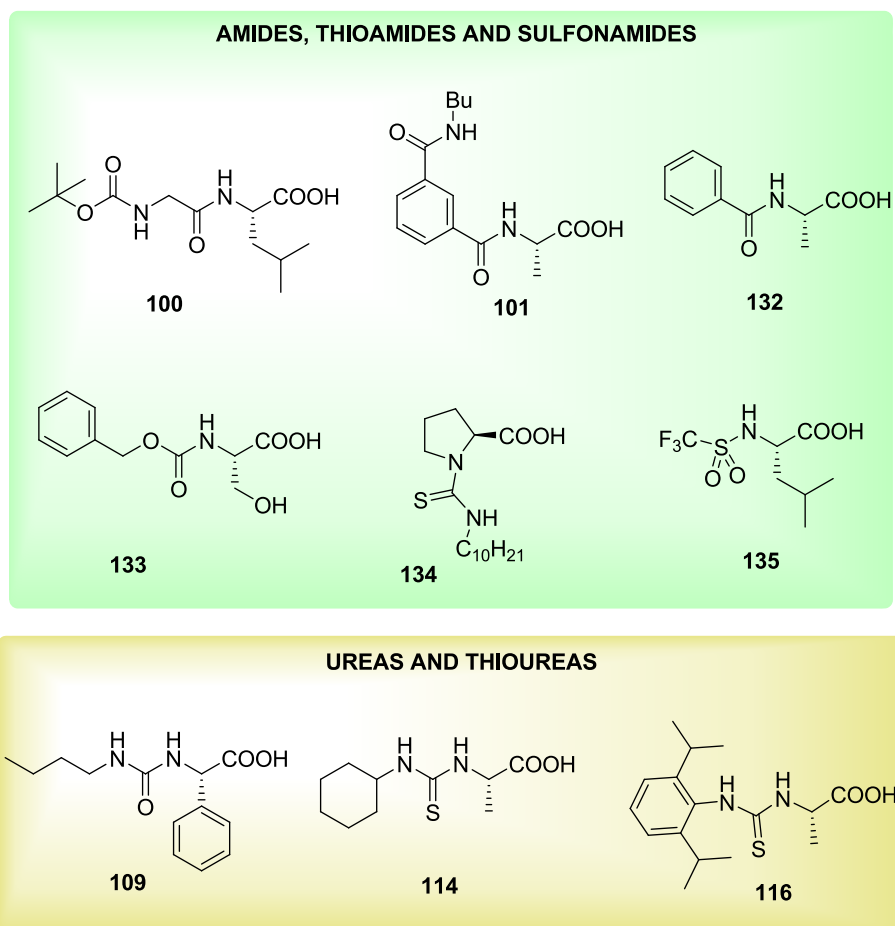


Figure 6.2. Guests studied in the resolution of receptor **131** enantiomers.

The results obtained are summarized in table 6.1.

Table 6.1. Relative association constants between the two receptor **131** enantiomers.

entry	guest	K
1	100	1.4
2	101	1.5
3	132	1.9
4	135	1.1
5	109	(a)
6	114	3.3
7	116	1.2
8	134	1.0
9	133	1.6

The results did not significantly improve the values of the association constants obtained for receptor **94**. Although thiourea **114** had generated the best constant ($K = 6.6$) with receptor **94**, the chiral discrimination with receptor **131** was reduced to 3.3. It seems that the structural change had achieved the opposite effect, and that the steric effect, postulated as a source of enantioselective discrimination, is more efficient with the bulky *t*-octyl group.

6.2.2. Receptor with more hydrogen bond donors

A new modification led us to seek a receptor that showed more interactions with the guest, so that the complex was more rigid and therefore more enantioselective. To do this, we performed the reduction of the carbonyl group to the alcohol.

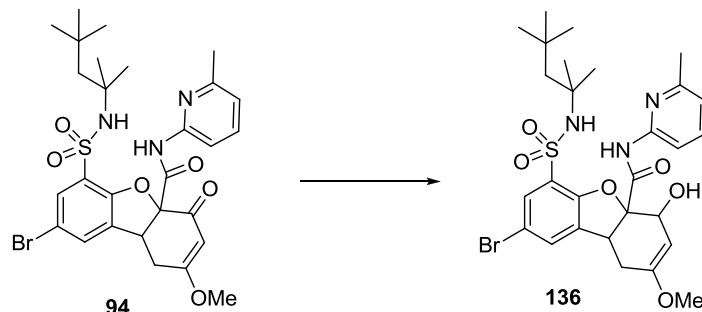


Figure 6.3. Receptor **131** prepared through reduction of compound **94**.

The hydroxyl group is a new hydrogen bond donor that can interact with the carbonyl of the guest, improving the association constant, as shown in figure 6.4.

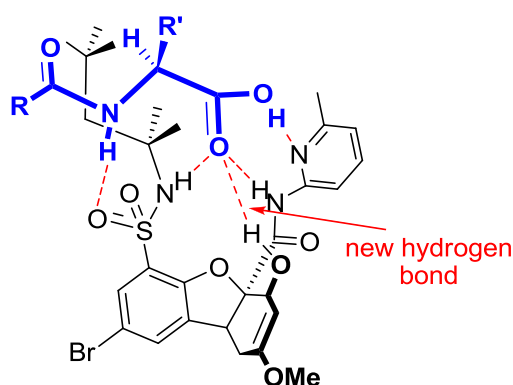


Figure 6.4. Geometry of an associate of receptor **131** in which an additional hydrogen bond is formed.

In contrast to the reduction of ester **91**, which generated a single isomer with NaBH_4 , the carbonyl reduction of receptor **94** was not trivial, because the two possible epimeric alcohols were generated. Major alcohol is produced by hydride attack by the *Re* face (which occupies the amidopyridine), corresponding the attack by the *Si* face (which occupies the furan) to the minor epimer. Reducing agents as NaBH_4 , $\text{BH}_3\text{-SMe}_2$, K-selectride, $\text{NaB(OMe)}_3\text{H}$ or $\text{H}_2/\text{Pd/C}$ generated mixtures of compounds and, interestingly, LiAlH_4 was the reducing agent that produced the best results, providing virtually a single stereoisomer. Actually, it is reported that the enol ethers of β -dicarbonyl compounds are reduced to allyl alcohols with LiAlH_4 , which can be later transformed into the α,β -unsaturated ketone.²²⁷

²²⁷ (a) Zimmerman, H. E.; Schuster, D. I. *J. Am. Chem. Soc.* **1962**, *84*, 4527-4540; (b) Gannon, W. F.; House, H. O. *Org. Synth.* **1960**, *40*, 14-16.

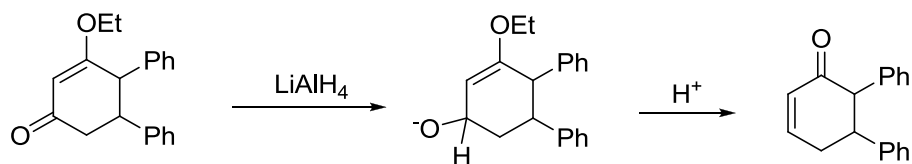


Figure 6.5. Reduction of the enol ether of α,β -dicarbonyl compound with LiAlH_4 .

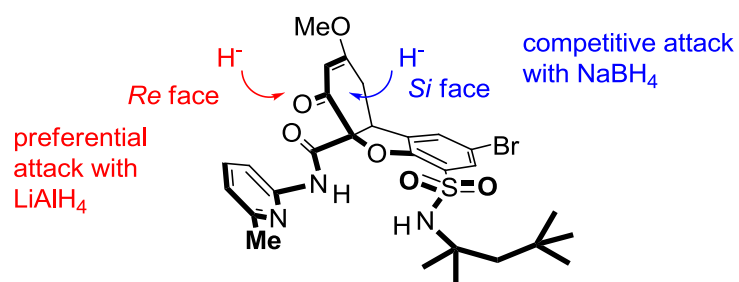
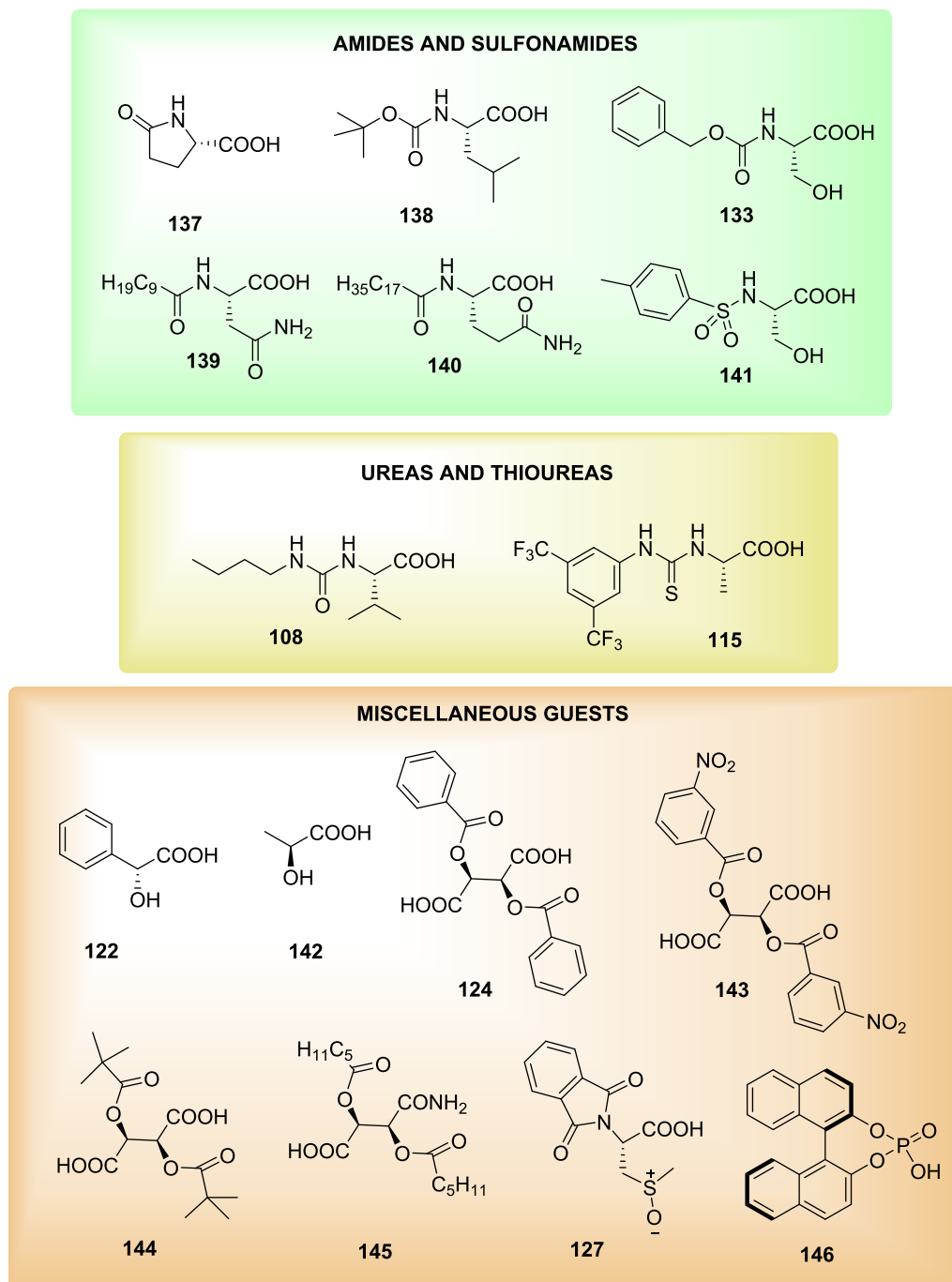
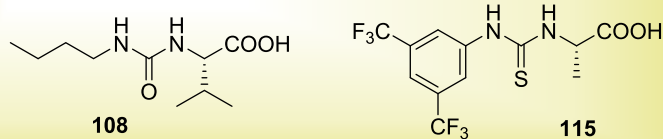


Figure 6.6. Receptor **94** reduction.

Then we performed several competitive titrations with some of the guests prepared previously and other new compounds shown in figure 6.7.



UREAS AND THIOUREAS



MISCELLANEOUS GUESTS

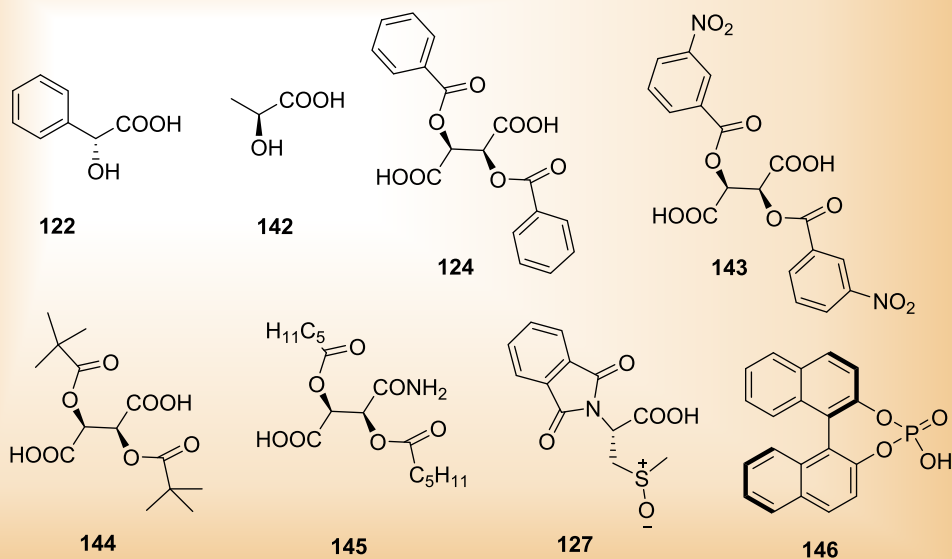


Figure 6.7. Guests studied in the racemic mixture resolution of receptor **136**.

The results are summarized in table 6.2.

Table 6.2. Competitive association constants between the enantiomers of receptor **136**.

entry	guest	<i>K</i>	entry	guest	<i>K</i>
1	137	1.3	9	122	4.2
2	138	5.6	10	142	1.2
3	133	3.4	11	124	4.8
4	139	(a)	12	143	2.6
5	140	1.0	13	144	0.6
6	141	(a)	14	145	(a)
7	108	5.5	15	127	1.0
8	115	2.5	16	146	2.4

(a) There is no splitting

It can be seen that with the exception of *L*-bis(trifluoromethyl)phenylthiourea **115** and sulfoxide **127**, the relative constants obtained are larger than in the case of receptor **94**. Thus, with *L*-valine butylurea **108** the constant improved from 1.5 to 5.5; for *D*-mandelic acid **122** from 1.3 to 4.2 and with dibenzoyl-*L*-tartaric acid **124** from 3.2 to 4.8. However, we failed to obtain constants larger than 5.6.

Furthermore, it is likely that in the case of some guests, such as dibenzoyl-*L*-tartaric acid **124**, the complex formed is different from the complexes formed with the rest of the compounds studied, because the signals showed splitting patterns different from those described in the previous section. Instead of the signals splitting corresponding to the *t*-butyl group or the amidopyridine methyl group, in this case, the signal which shows the largest splitting corresponds to the methyl ether singlet. There is probably some type of charge transfer or π -stacking between the benzoyl aromatic ring and the methyl ether group.

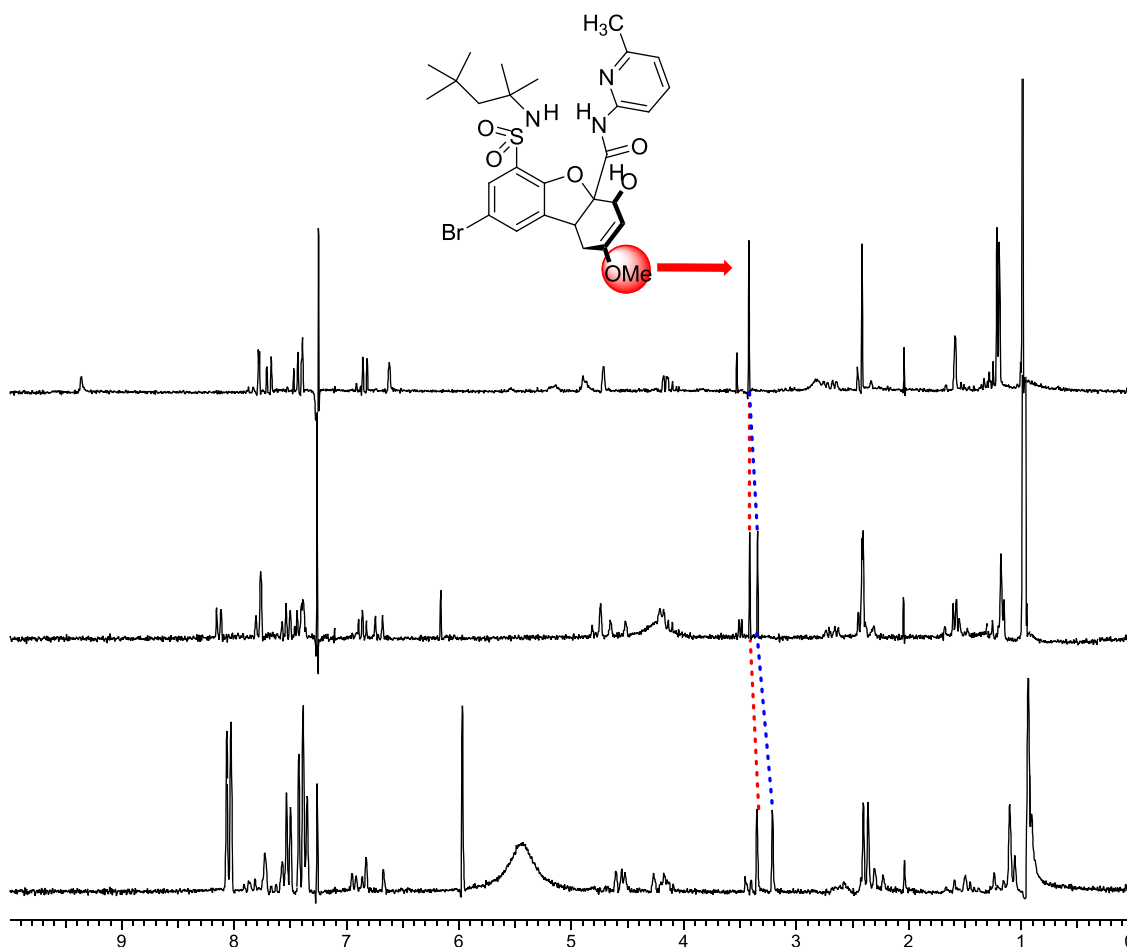


Figure 6.8. Splitting experienced by the singlet corresponding to the methyl ether in receptor **136** after addition of dibenzoyl-L-tartaric acid.

6.2.3. Enol receptor

6.2.3.1. Synthesis and properties

As receptor **136** had not produced the expected results, we thought that a better hydrogen bond donor could lead to higher competitive constants with the synthesized guests. This hydrogen bond donor could be obtained from the enol, as shown in figure 6.9.

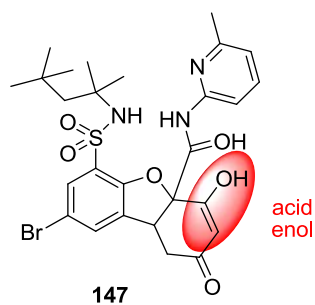


Figure 6.9. Receptor **147** with an acid enol.

The preparation of the new receptor **147** was carried out in a similar way to receptor **94**, but, in this case, the synthesis proceeded to the formation of the enol instead of the enol ether. If the enol proton points toward the cavity which defines the oxyanion hole, it may form an additional hydrogen bond with the carbonyl of the guest, and as the enol is an especially good hydrogen bond donor, the complex should be more stable.

In addition, we could simplify the synthesis to a large extent, as it was found that in these conditions the aminopyridine molecule can be introduced without the need of the expensive BuLi. In the presence of MeONa, the aminopyridine has enough nucleophilic character to carry out the aminolysis of the ester, while the enol system remains protected as the corresponding sodium enolate and does not react. In 0.5 hours in refluxing methanol, complete aminolysis of the ester is obtained.

Due to the presence of the pyridine in the receptor **147**, it is not desirable to work up the reaction by addition over hydrochloric acid, because the corresponding hydrochloride would be at least partially soluble in water. To neutralize the basic medium, we decided to add the reaction over an aqueous solution with one equivalent of a strong acid. We did an experiment with camphorsulfonic acid because it is solid and not hygroscopic, and it seemed ideal to us. This would greatly facilitate the isolation of the reaction product.

The proposed synthesis is shown in the following scheme:

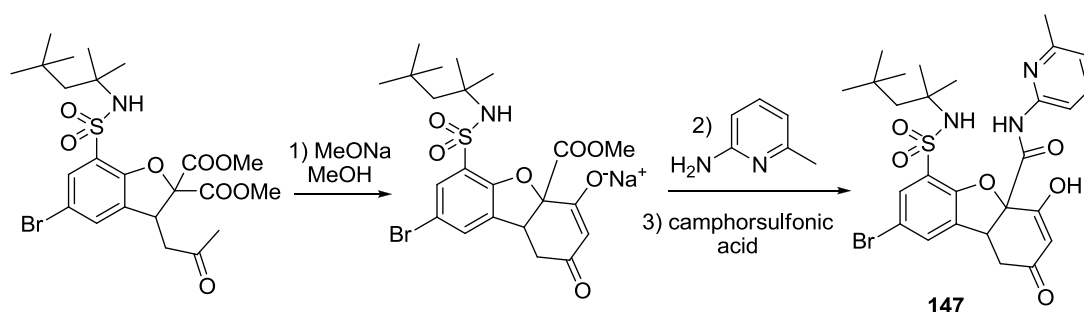


Figure 6.10. Receptor **147** synthesis.

The use of an aqueous solution of camphorsulfonic acid allowed us to obtain a precipitate in the reaction medium, which after filtration, showed the neutral receptor **147**, but in the presence of excess of unreacted aminopyridine. If an excess of camphorsulfonic acid is used, aminopyridine is eliminated, but a precipitate of receptor **147** and the camphorsulfonic acid is obtained.

Since the camphorsulfonic acid is a chiral compound, the obtained precipitate should be a mixture of two diastereomeric salts, which could facilitate the resolution of the racemic mixture of receptor **147**. The NMR spectrum of this solid confirmed the presence of both salts, as the receptor signals are split, as shown in figure 6.11.

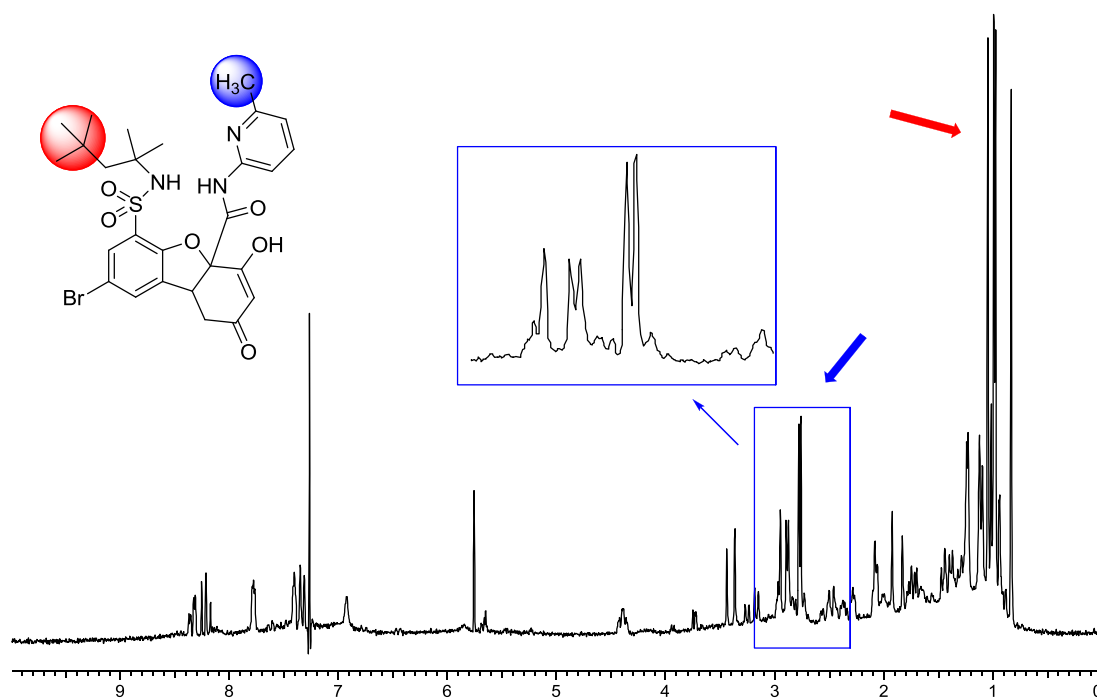


Figure 6.11. NMR spectrum in which it can be observed the signals splitting of receptor **147** in the presence of camphorsulfonic acid.

We tried to carry out a fractional crystallization of the mixture of the diastereomeric salts in several solvents, but the crystals always corresponded to mixtures.

A chromatographic resolution was also attempted. For this objective, TLC plates were impregnated with camphorsulfonic acid and then receptor **147** was eluted. Unfortunately, we did not succeed in resolving the two enantiomers of this receptor, because a single spot was always obtained in the silica plates. Silica probably competes for the receptor hydrogen bonds and breaks down the associate.

Although camphorsulfonic acid was well suited for directly obtaining the camphorsulfonates mixture of receptor **147**, it did not allowed us to obtain easily the neutral receptor **147**. If the mixture of diastereomeric salts was treated with a base such as Na_2CO_3 or NaHCO_3 , both camphorsulfonic acid and the receptor ended in the aqueous phase, because the receptor under these conditions also produces the sodium salt, which is water soluble. Because of this drawback, we preferred to look for a suitable acid with the appropriate pK_a to generate the neutral receptor without protonation of the amidopyridine.

In a first experiment, the reaction mixture was added over an aqueous solution of acetic acid, because this acid was not expected to protonate the amidopyridine, but it should neutralize all the sodium methoxide in the reaction mixture. The result was that a large amount of receptor **147** was lost in the water phase. We found that the reason for the high water solubility was that the receptor remained as the sodium salt, because acetic acid was not strong enough to protonate the enol. This fact, which we found surprising, was confirmed by NMR, since the enol proton of receptor **147** resonates at 5.79 ppm when the receptor is neutral whereas addition of tetrabutylammonium acetate leads to a strong shielding of this

proton, which resonates in the associate at 5.15 ppm. The best way to explain this strong shielding of the vinyl proton is the proton transference from the enol to the acetate.

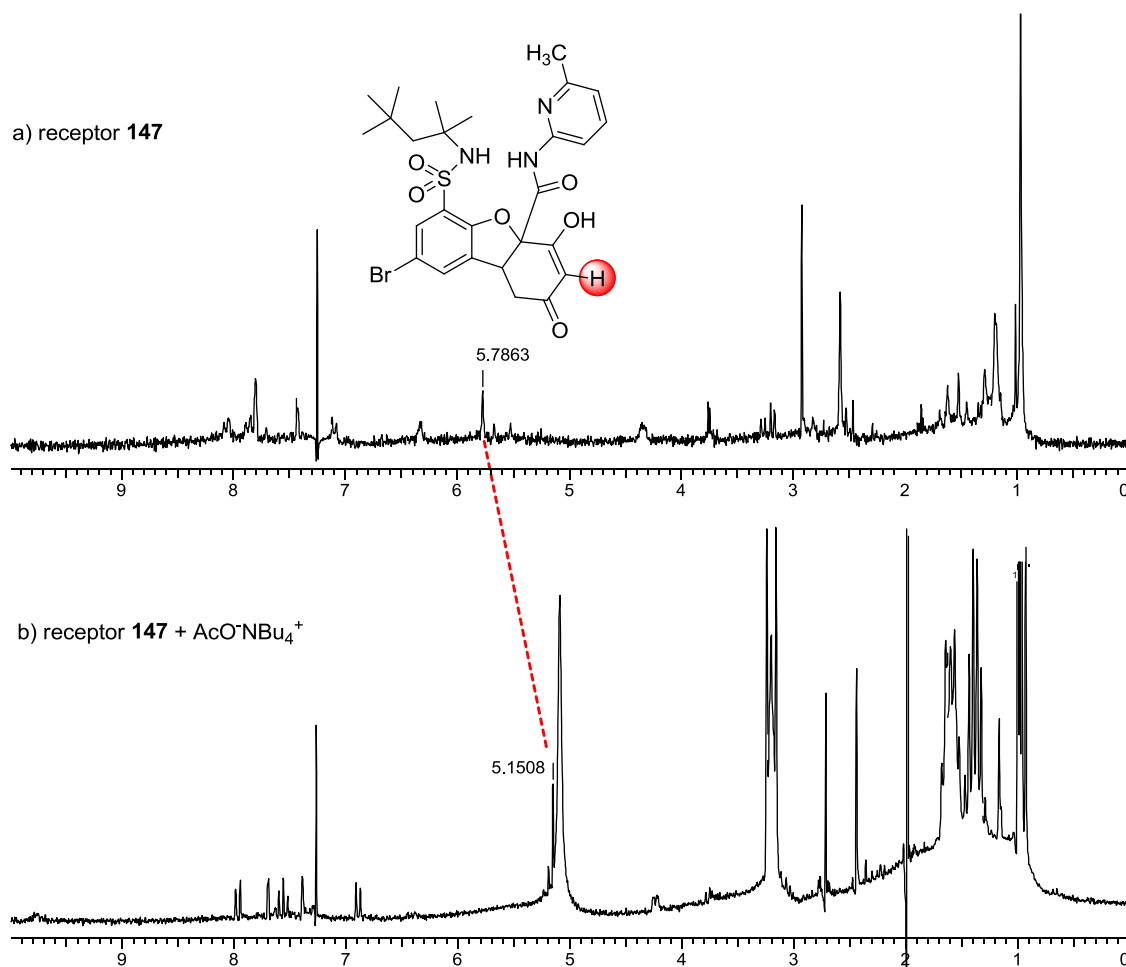


Figure 6.12. NMR spectra in which the shielding of the enol proton of receptor **147** in presence of tetrabutylammonium acetate can be observed

Fortunately, the use of a slightly stronger acid than acetic acid solved this problem. Formic acid is sufficiently acidic to protonate the enol, but does not transfer the proton to the amidopyridine, thus enabling us to obtain the neutral receptor by adding the reaction mixture over water with a molar excess of formic acid. Therefore, we estimated that the acidity of the enol group of receptor **147** must be between 3.77 and 4.76, which are the pK_a s (in water) of formic acid and acetic acid, respectively.

After obtaining the neutral receptor **147**, we studied the geometry presented by the keto-enol system.

In principle, it would be expected a mixture of several enols due to keto-enol tautomerism, as can be seen in figure 6.13.

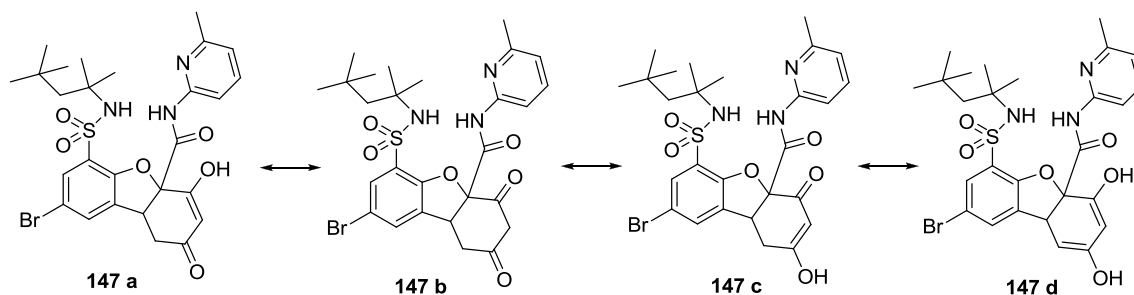


Figure 6.13. Possible tautomers of receptor **147**.

To set the position of the enol in the keto-enol system we conducted a long range carbon-proton HMBC-CIGAR correlation²²⁸ with $J = 10$ and 20 Hz. With these constants, one bond C-H correlations are eliminated. In this spectrum it can be seen a two bonds correlation between a proton in the methylene group and the ketone carbon. This correlation shows that **147a** is the predominant tautomer in solution.

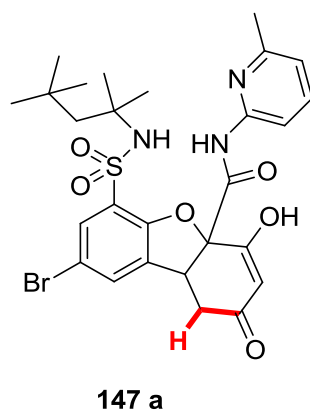


Figure 6.14. C-H correlation observed in the HMBC-CIGAR spectrum, which justifies the structure of the major tautomer

²²⁸ Hadden, C. E.; Martin, G. E.; Krishnamurthy, V. V. *Magn. Reson. Chem.* **2000**, *38*, 143-147.

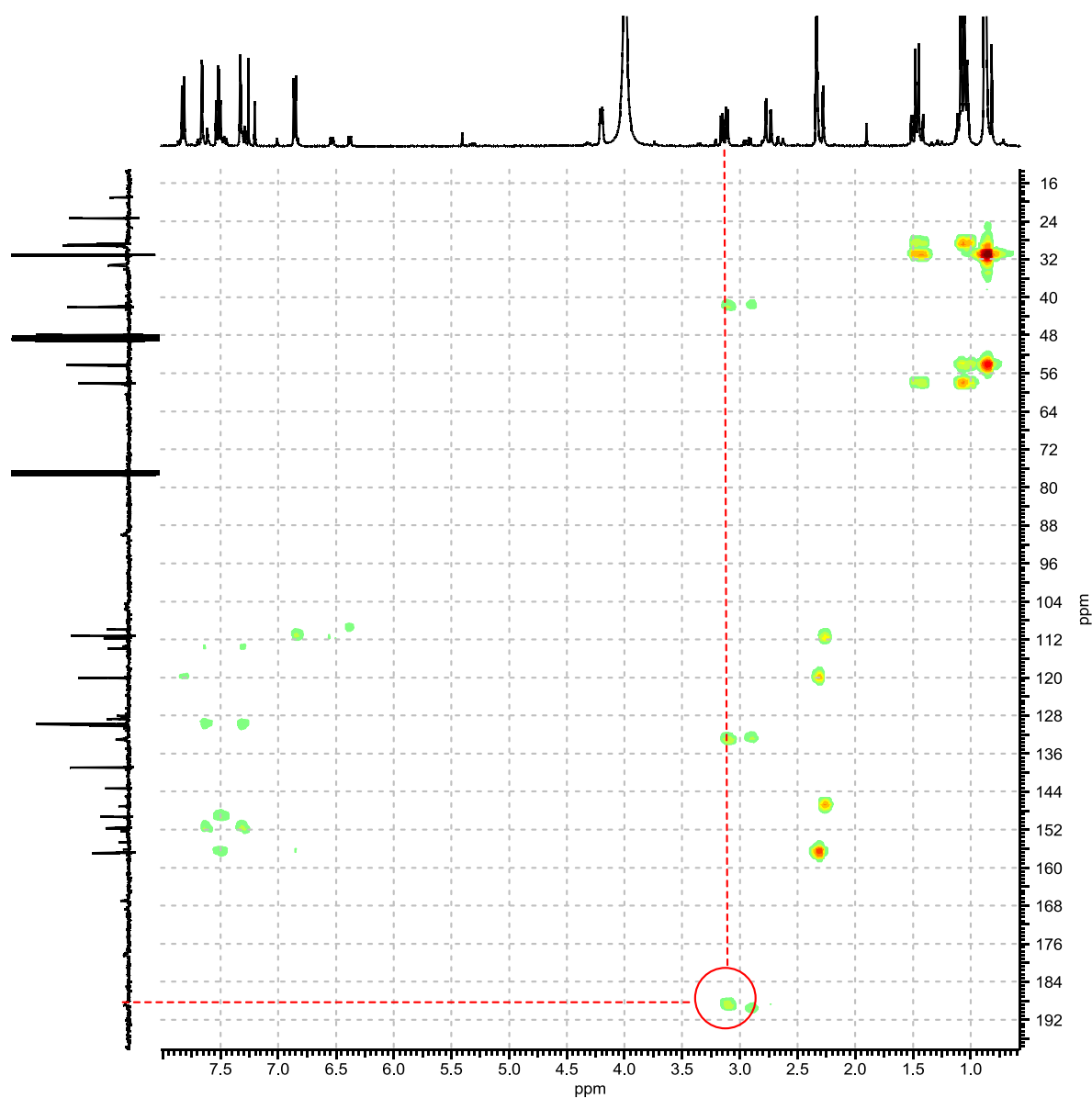


Figure 6.15. HMBC spectrum where correlations indicate that the major tautomer observed is **147 a**.

Moreover, crystallization of receptor **147** has been possible in THF and the X-ray study is consistent with the same structure **147 a** in the crystalline state.

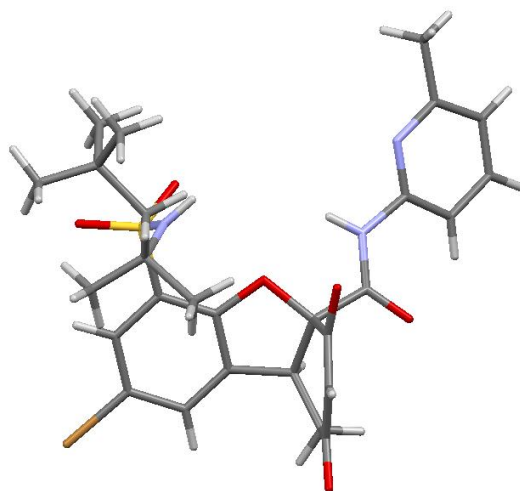


Figure 6.16. X-ray diffraction study of receptor **147**.

The bond distance of the ketone carbonyl of **147** is the shortest of all, with only 1.25 Å; however the carbon-oxygen distance in the enol is 1.32 Å, showing a lower bond order. The same conclusion can be reached from the carbon-carbon bonds distances. While the double bond shows 1.35 Å, the formally single carbon-carbon bond elongates to 1.42 Å, as shown in figure 6.17.

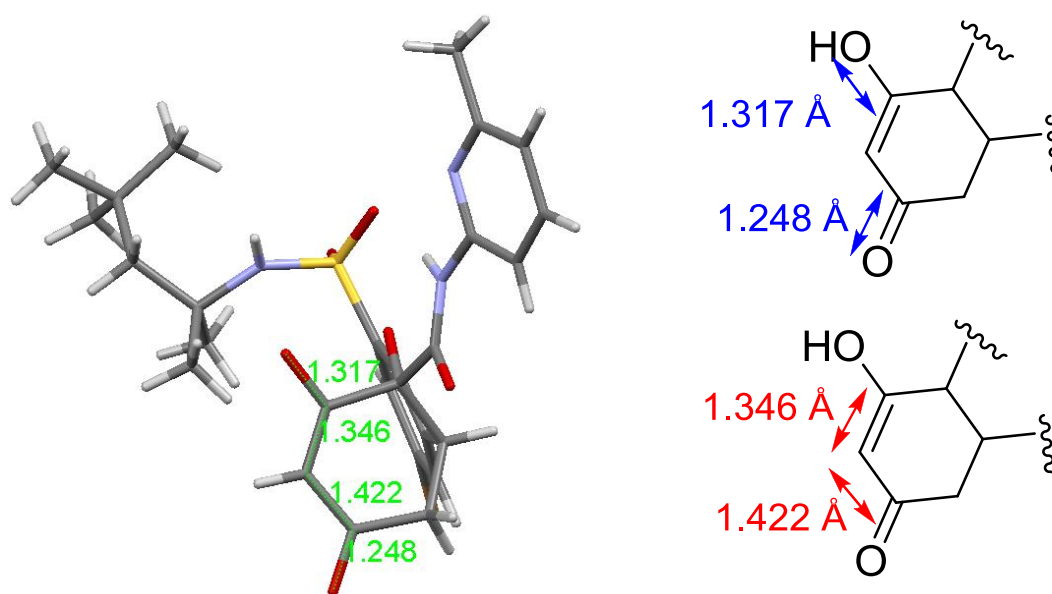


Figure 6.17. Distances of the keto-enol system of receptor **147**.

In the receptor **147** structure, the existence of an oxyanion hole is also observed. This structure is formed between the sulfonamide NH and the enol hydroxyl group. The distance between these heteroatoms is 4.25 Å, which is coincident with the ideal average distance of the oxyanion holes in natural enzymes. The distance between the sulfonamide and carboxamide NHs is much greater, 5.5 Å, as a result of the position of the amide, which is located in the equatorial substituent and therefore far away from the sulfonamide NH.

Another factor which justifies the long distance from the carboxamide is that the sulfonamide NH is positioned on the opposite face of the cyclohexenone ring, as seen in figure 6.18.

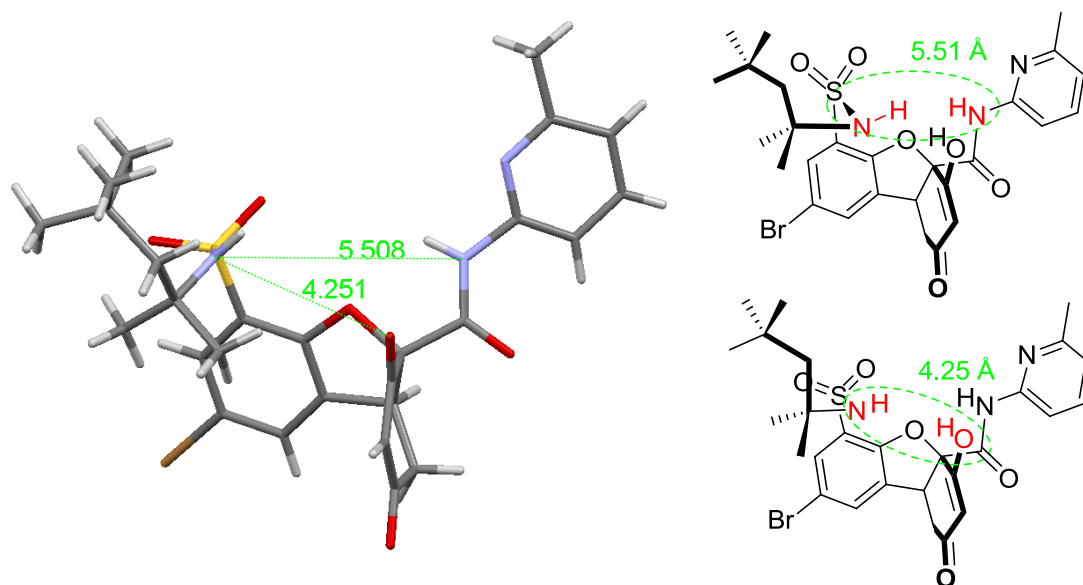


Figure 6.18. Oxyanion hole distances in the receptor **147**.

The packing of the crystalline compound showed that the carbonyl of the cyclohexenone is located near the oxyanion hole of another receptor molecule, but the bonding distances are surprisingly long: 3.22 Å with the sulfonamide NH and 4.11 Å with the enol. This last distance clearly indicates that there is no hydrogen bond between these heteroatoms.

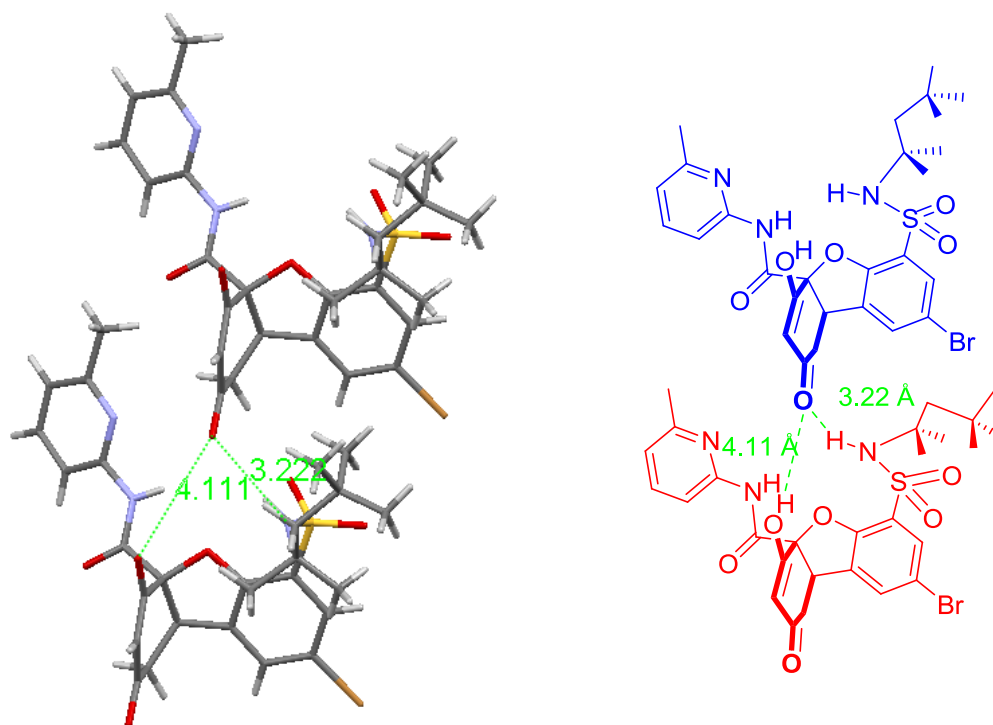


Figure 6.19. Packing of receptor **147** in which it is shown that the distances corresponding to the oxyanion hole are too long for hydrogen bonding.

A further analysis of the packing allowed us to observe that the enol is forming a short hydrogen bond of 2.6 Å with the carbonyl of another receptor molecule. This hydrogen bond positions the enol proton in the opposite direction to the furan oxygen, so the oxyanion-hole structure and the intramolecular hydrogen bond between the enol and the furan is lost (figure 6.20).

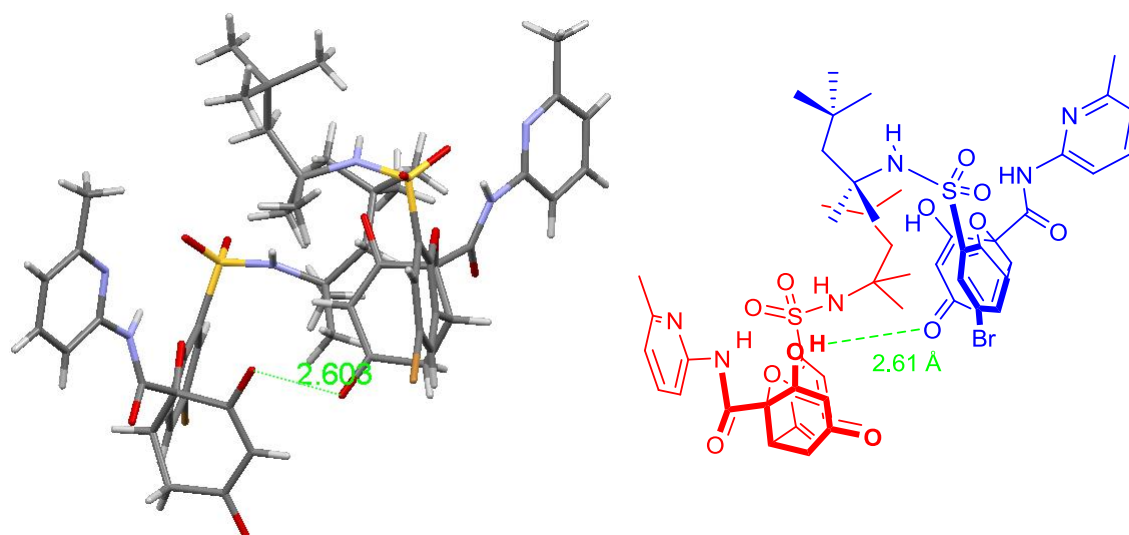


Figure 6.20. Packing of receptor **147** in which the hydrogen bond between the enol and the ketone is shown.

This severe loss of energy must be compensated by the lattice energy generated in the crystal packing; however, it is logical to think that the structure in solution favours the intramolecular hydrogen bond and the conventional oxyanion-hole structure.

6.2.3.2. Racemic mixture resolution through enantioselective extraction

The high acidity of receptor **147** suggests that it could form salts with amines. The difference in pK_a about 6 units should enable the transfer of the enol proton to an aliphatic amine nitrogen. This should be the case, since receptor **147** is easily transferred from chloroform to water by adding an ammonia solution.

This feature in receptor **147** opens a new way for resolution: since the enol group is an acid, the use of chiral amines could generate diastereomeric salts with different physical properties and therefore easily separable.

Competitive titrations with this receptor have been difficult to assess because it is poorly soluble in $CDCl_3$. However, the addition of a chiral amine to a suspension of receptor **147** in $CDCl_3$ facilitates the fast solution and the NMR spectrum shows the formation of two diastereomeric complexes with all signals fully split. Thus, several chiral amines (figure 6.21) which also had different groups in its structure: OH, amide NH, etc. were studied. More interactions between the guest and the receptor can be established with these groups and thus they can facilitate the resolution of receptor **147**.

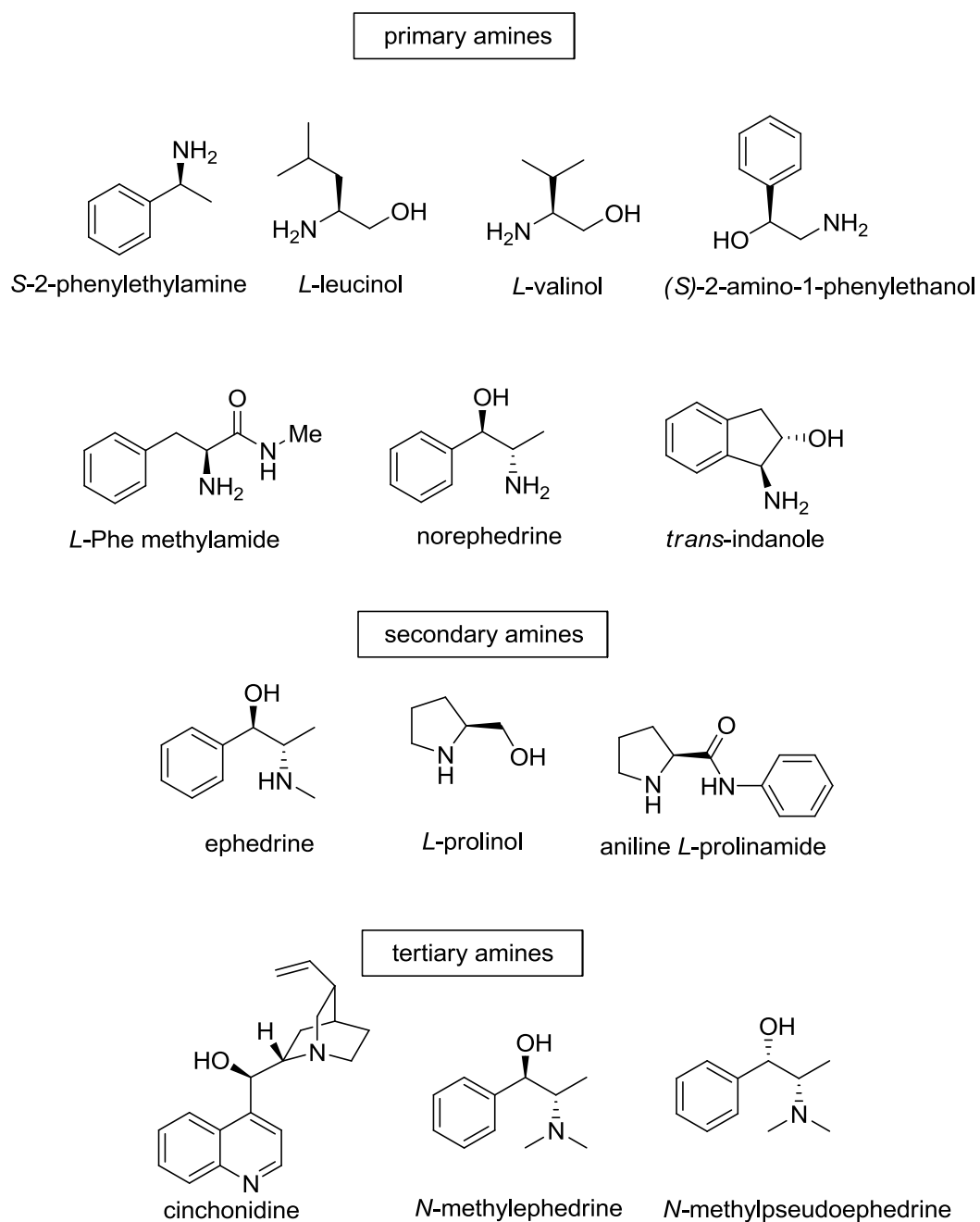


Figure 6.21. Several chiral amines used as guests for the resolution of receptor **147**.

All guests in figure 6.21 caused the splitting of the receptor **147** signals, although this effect was more pronounced in the case of ephedrine and norephedrine.

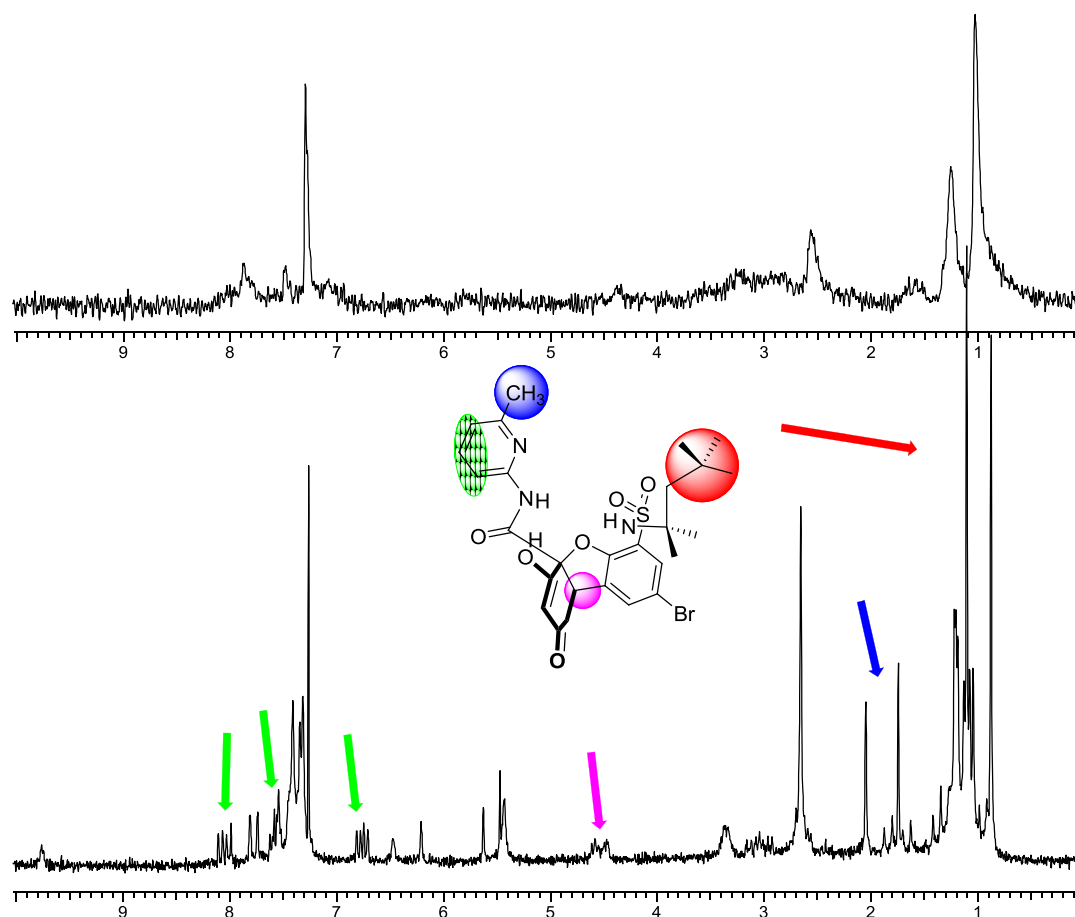


Figure 6.22. NMR spectrum of receptor **147** before (above, the signals are very broad due to the low solubility of the receptor in deuteriochloroform) and after addition of ephedrine (below). It can be seen that the signal/noise ratio is better than in the above spectrum, because the associate formation allows the solubilisation of receptor **147**. Most signals in the lower spectrum are split.

Since amines which offer the best results contain hydroxyl groups in its structure, we believe that there must be a hydrogen bond between the hydroxyl group and the receptor pyridine, which helps to establish a greater differentiation between the two diastereomeric complexes. At the same time, one of the NH groups of the ammonium may be forming a hydrogen bond with one of the sulfonyl groups of the receptor, saturating all NHs, in the case of ephedrine (figure 6.23).

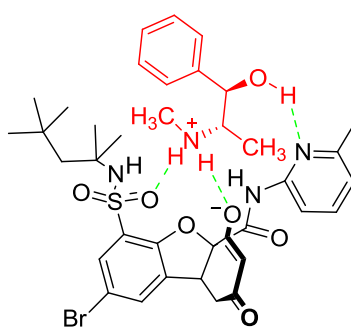


Figure 6.23. Proposed associate between receptor **147** and ephedrine.

Then we impregnated TLC plates with solutions of ephedrine, norephedrine and *L*-prolinol, which are the most promising guests. However, we failed to resolve the receptor racemic mixture. We noted that, under these conditions (these compounds are very polar and need methanol as eluent), the amine impregnated in the plate was eluted, so we changed our strategy by dissolving the guest in the eluent. However, it was not possible to get the resolution of the receptor. Probably, although they are diastereomeric salts, their structures are very similar and have similar R_f s.

Another procedure is to use liquid-liquid extraction to carry out the resolution of receptor **147**. The idea is to perform an enantioselective extraction using a chiral aminoalcohol as guest. Taking advantage of the dual solubility of receptor **147** in chloroform and water (when the receptor is in ionic form) we considered to obtain a balance in which one enantiomer had a preference for one of the two phases.

The strategy is as follows: an aqueous solution of the lithium salt of the racemic receptor **147** was prepared. Lithium salt was chosen because it exhibited the best solubility in aqueous phase, but the sodium or ammonium salts are also suitable. This aqueous solution was contacted with a chloroform solution of receptor **147** and 1 equivalent of the corresponding chiral aminoalcohol and stirred for the equilibrium to be established. If the amino alcohol has a preference for one of the enantiomers of receptor **147**, this enantiomer would increase its proportion in chloroform, because the formation of the more stable associate is favoured, while the enantiomer that forms the least stable associate will be transferred to the aqueous solution to maintain electrostatic neutrality. In the aqueous solution, the receptor anions are solvated and therefore they have the same stability, independent of their chirality.

In an ideal separation, one of the enantiomers of the receptor would form the strong complex with the chiral amine in chloroform and would remain in the chloroform phase, while the other enantiomer, which forms the weak complex, stays in the aqueous phase as the lithium salt.

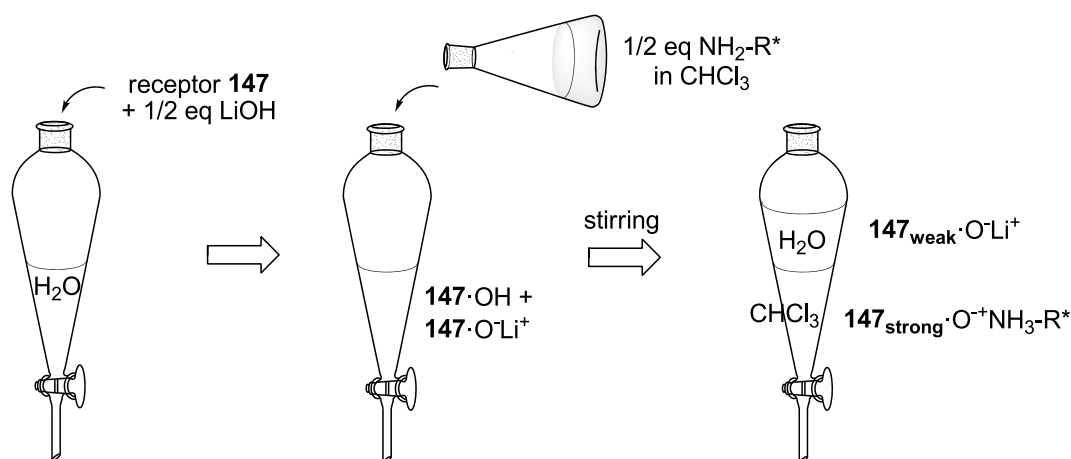


Figure 6.24. Scheme of receptor **147** enantiomers separation by liquid-liquid extraction.

To test this strategy, we weighted about 10 mg of racemic receptor **147** in an NMR tube. Half equivalent of an aqueous solution of LiOH of known concentration was added as well as one half equivalent of the corresponding chiral amine dissolved in CDCl_3 . The NMR tube was stirred and then centrifuged to promote phase separation. In this manner the ^1H NMR spectrum can be directly registered so that if the separation is enantioselective the split signals will have different sizes. The integration of the split signals allows calculating the preference of the chiral amine for the receptor enantiomers.

In figure 6.25 the spectrum obtained after carrying out the extraction experiment with ephedrine is shown. To obtain the ratio between the diastereomeric complexes in the chloroform phase, the signals corresponding to the more shielded doublet of amidopyridine were integrated. It is also noteworthy the large splitting experimented by the amidopyridine methyl group.

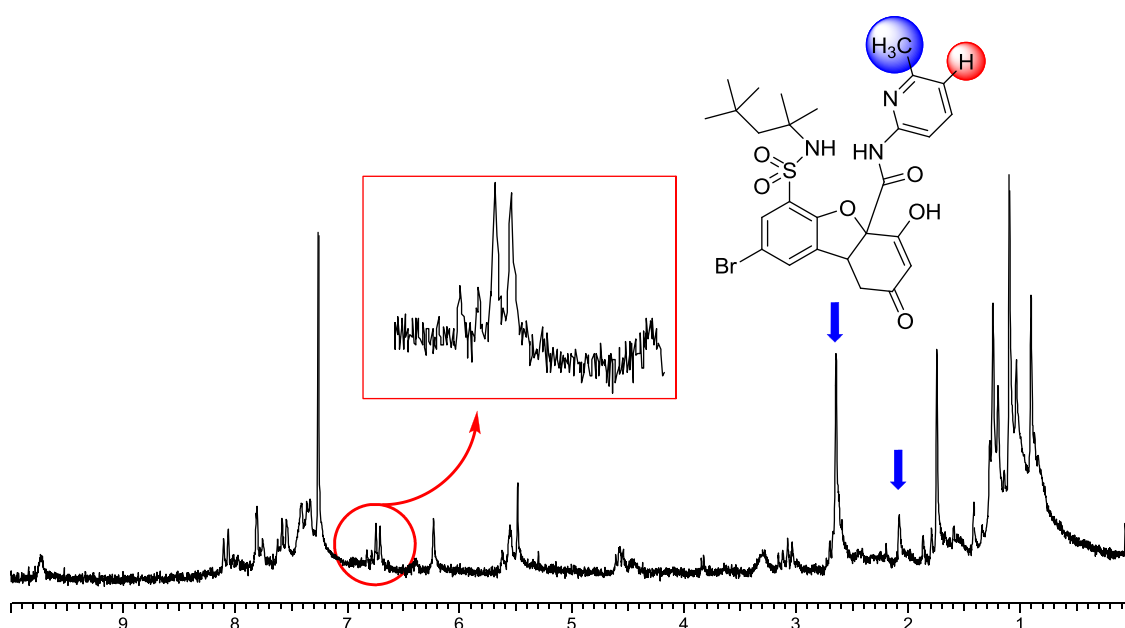


Figure 6.25. ^1H NMR spectrum obtained after the extraction experiment with ephedrine, in which an enantiomeric ratio of 4:1 is shown.

In table 6.3 the enantiomer ratio of receptor **147** in the chloroform phase upon addition of a chiral amine is shown.

Table 6.3. Enantiomeric ratio in the separation of receptor **147** by liquid-liquid extraction with 0.5 equivalents of each amine.

entry	amine	enantiomers ratio
1	<i>L</i> -leucinol	1.0 / 1.1
2	<i>L</i> -valinol	1.0 / 1.0
3	(<i>S</i>)-2-amino-1-phenylethanol	1.0 / 1.4
4	norephedrine	1.0 / 2.0
5	1 <i>S</i> , 2 <i>S</i> - <i>trans</i> indanole	1.2 / 1.0
6	ephedrine	1.0 / 4.0
7	<i>L</i> -prolinol	1.0 / 1.0
8	cinchonidine	1.3 / 1.0
9	<i>N</i> -methyl-ephedrine	1.0 / 1.0
10	<i>N</i> -methyl-pseudoephedrine	1.4 / 1.0

It can be observed that ephedrine provides the best enantioselective extraction (entry 6), in which a relationship between the concentrations of the enantiomers of 1/4 is obtained. It has to be considered that to obtain this enrichment, enantioselectivity produced by ephedrine must be very good: as the aqueous solution is depleted in the enantiomer which is transferred to the chloroform phase, making the extraction more difficult.

Thus, from the extraction experiment it is possible to calculate the relative association constant between both enantiomers. Assuming that the concentration of free guest in the organic phase and the aqueous phase is related through a distribution constant, it can be applied the following equation supposing that the distribution constant is the same for both free enantiomers:

$$K_{\text{rel}} = \frac{\text{Integral } R}{\text{Integral } S} \times \frac{\text{mmoles aqueous phase } S}{\text{mmoles aqueous phase } R}$$

To confirm that the extraction carried out with ephedrine was enantioselective, the aqueous phase was separated, acidified with formic acid and extracted with ethyl acetate. The NMR spectrum of the compound obtained corresponds to the free receptor **147**, and no splitting of the signals is shown, being unable to know its enantioselectivity. Fortunately, it is enough to add a small amount of ephedrine to the solution to check that the solution obtained corresponds to the complementary mixture to chloroform, with an enantiomer ratio of 4/1.

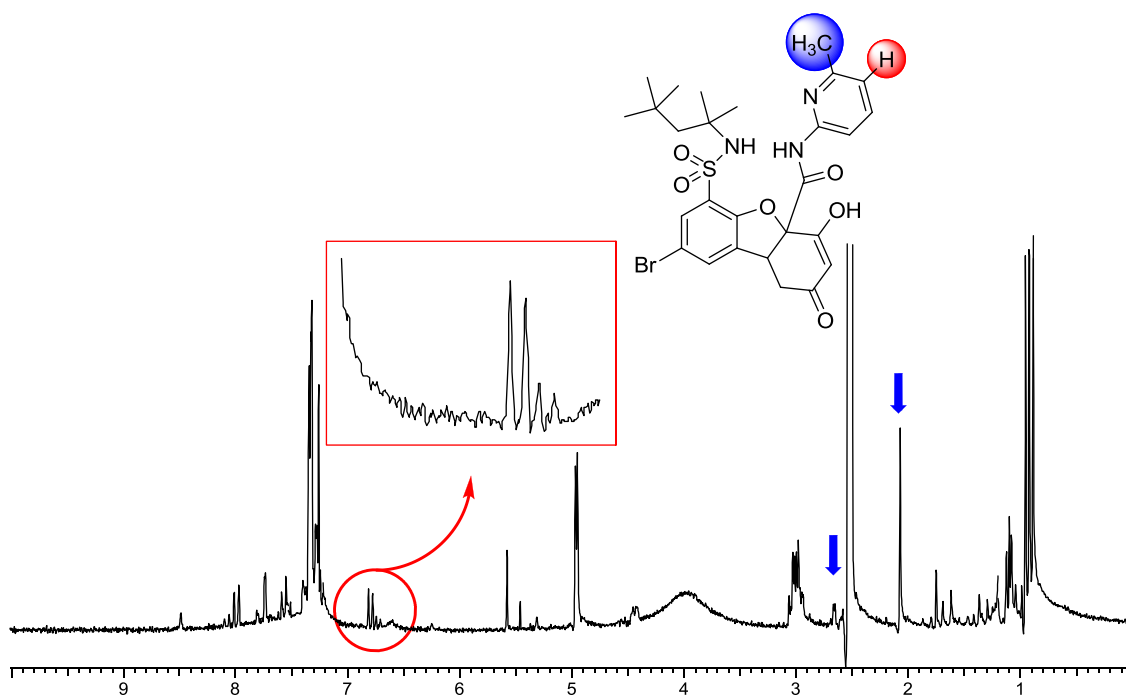


Figure 6.26. ^1H NMR spectrum of the receptor **147** enantiomer extracted with ephedrine from the aqueous phase.

The mmol ratio of each enantiomer of the receptor in the aqueous phase is proportional to the integral ratio. As the enantiomers ratio in the aqueous phase is 4/1 for ephedrine (figure 6.26), applying the above equation, it can be concluded that the enantioselective recognition is 16.

$$K_{\text{rel}} = \frac{4}{1} \times \frac{4}{1} = 16$$

From table 6.3 it can be seen that the extraction enantioselectivity decreases for both primary amines and tertiary amines. Norephedrine only generates a constant ratio of 1/2 (entry 4), the remaining amines leads to 1/1 mixtures.

To assess the importance of the amidopyridine and the sulfonamide fragments in the enantioselective extraction of receptor **147**, we conducted a similar experiment with receptors that do not possess either the amidopyridine, as in the case of the receptor **148**, or the sulfonamide, as in the case of receptor **149**. Both are shown in figure 6.27.

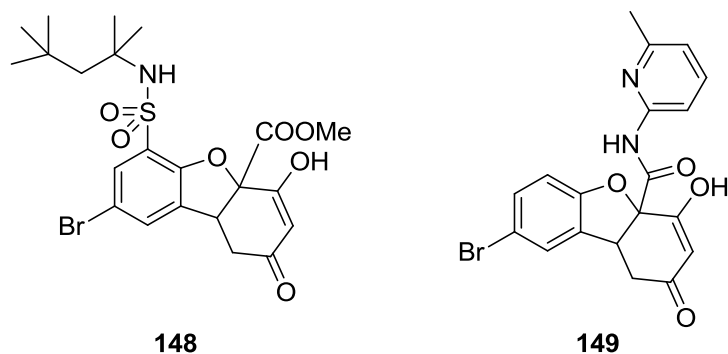


Figure 6.27. Receptors with partial structures related to receptor **147** studied in liquid-liquid extraction with ephedrine.

With both compounds a certain amount of the receptor was extracted, though much less than in the case of receptor **147**, showing large amounts of the amine. Furthermore, in no case the extraction was enantioselective, obtaining the same proportion of both enantiomers. It seems, therefore, that both the pyridine, as well as the *t*-octylsulfonamide, is necessary to achieve an enantioselective extraction.

Since there is a remarkable enantioselectivity in the formation of complexes between ephedrine and enantiomers of receptor **147**, it is possible to perform the resolution of the racemic mixture through liquid/liquid extraction. For this purpose it is necessary to perform more than one extraction, since the former only produces an enrichment of 1/4. If this solution is treated again with an aqueous solution which presents the lithium salt of the racemic mixture of receptor **147** a further enrichment is reached, this time beyond a 1/10 ratio. To obtain the enantiomerically pure receptor, the complex has to be broken with formic acid, and the crude compound has to be crystalized from ethyl acetate.

Since both enantiomers of ephedrine are commercially available, the other enantiomer of the receptor **147** can be obtained following a similar procedure. The aqueous phase is neutralized with formic acid, crystallizing a solid which is further subjected to extraction with the lithium salt of racemic receptor, but in the presence of the opposite enantiomer of ephedrine.

6.2.3.3. Racemic mixture resolution through fractional crystallization

Although the above procedure allows resolution of the racemic mixture of receptor **147**, it is not ideal because the lithium salt of the receptor exhibits properties as a surfactant, and this leads to the formation of emulsions. These emulsions can be broken, but require a long centrifugation. Therefore, we searched for a method that was simpler and easier to scale up.

The classical system for the separation of enantiomers is the crystallization of the diastereoisomeric salts formed with a chiral auxiliary. Ephedrine salts of receptor **147**, which have a high enantioselectivity, seemed ideal for this purpose, but so far we have only managed to obtain these salts as oil, so we studied the formation of salts with other chiral amino alcohols. Cinchonidine and cinchonine were initially selected. Both amines generated

crystalline salts in a solution of chloroform, methanol and ether. Filtration of the salts afforded, in the case of cinchonidine, a 1/1 mixture of both enantiomers, as receptor signals appeared split in NMR showing the same intensity. The same experiment with cinchonine yielded a salt, in which the NMR spectrum only showed one set of signals, so it could be a single receptor **147** enantiomer. The optical purity of this compound was confirmed by acidification with formic acid and extraction with ethyl acetate. The compound thus obtained was dissolved in deuterated chloroform and its NMR spectrum was recorded in the presence of ephedrine, which we knew split very well the receptor signals. The result was again a single set of signals for receptor **147**, which confirmed its enantiomeric purity.

In order to carry out the resolution in a preparative manner, so that we could separate the two enantiomers of receptor **147**, it was crucial a slow addition of ether to the solution of cinchonine and receptor **147** in a chloroform-methanol mixture. It is enough to maintain the solution in a closed container with ether, so that the high vapour pressure of this solvent makes it to slowly dissolve into the solution of the salts. Figure 6.28 shows the material used.

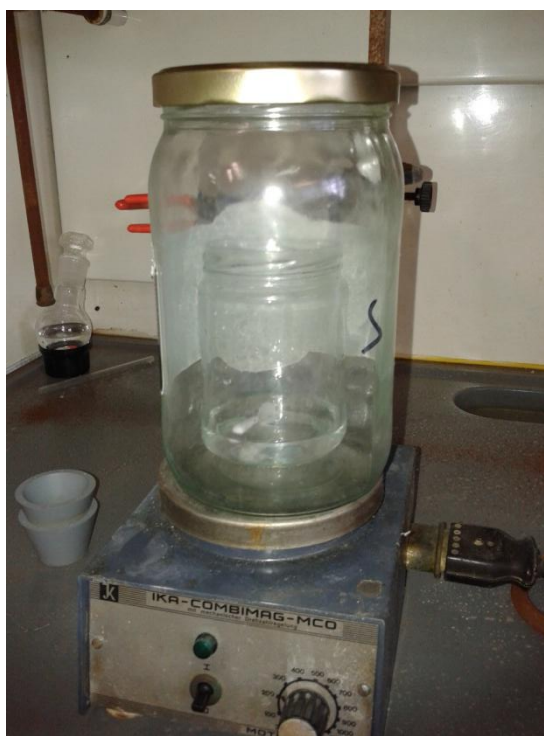


Figure 6.28. Equipment used in the resolution of receptor **147** racemic mixture by fractional crystallization.

Since the introduction of ether in the salts solution is a slow process, it is possible to analyze the progress of the crystallization easily by NMR spectroscopy. The filtration of a small aliquot allows separating the crystals from the mother liquor. Performing an NMR spectrum of the mother liquor allows us to know how much of each enantiomer is in this phase, since cinchonine produces a clear signals splitting. When the amount of the enantiomer that crystallizes in the first place is less than 5 % in the mother liquor, the crystallization is finished, since then, crystals with the other enantiomer are already obtained.

We have found that the best way to obtain the optically pure free receptor is dissolving the complex with cinchonine in methanol and add it to an aqueous solution of formic acid. Direct filtration of the solution leads to a receptor which typically has small amounts of cinchonine, but the extraction with ethyl acetate and subsequent evaporation allows isolation of the free receptor with a high purity ($[\alpha]_D^{20} = +212.3$ ($c = 0.99$, CHCl_3)).

From the mother liquor it is possible to obtain the other receptor **147** enantiomer, just by continuing the fractional crystallization and subsequent breakdown of the salt with an aqueous solution of formic acid and extraction with ethyl acetate ($[\alpha]_D^{20} = -203.9$ ($c = 1.09$, CHCl_3)).

A slower recrystallization of the more insoluble salt of receptor **147** in MeOH-chlorobenzene allowed us to obtain suitable size crystals for its analysis by X-ray diffraction. The structure of this salt can be seen in figure 6.29.

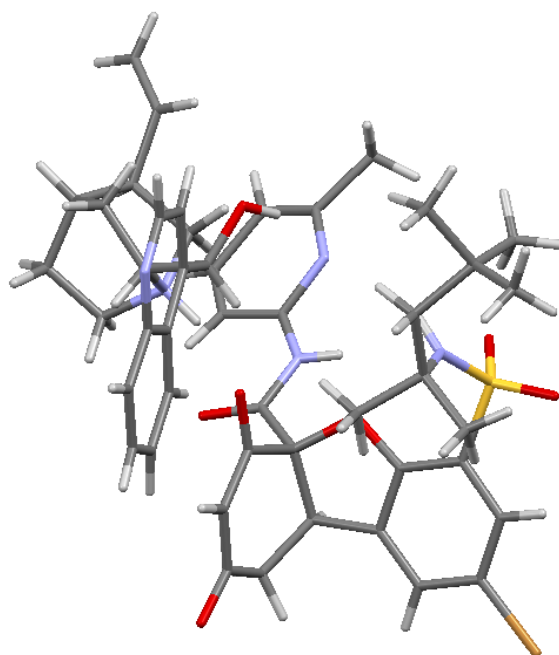


Figure 6.29. X-ray structure of receptor **147** and cinchonine more insoluble salt.

It can be seen that the enol releases the proton to the cinchonine, in such a way that the protonated nitrogen atom establishes a 2.62 Å hydrogen bond with the enolate (figure 6.30).

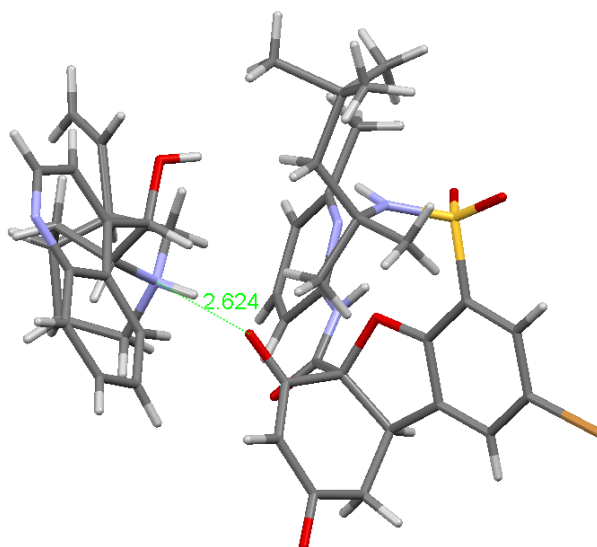


Figure 6.30. Hydrogen bond between the enolate and the protonated cinchonine.

However, it is surprising that the OH group of the cinchonine does not form a hydrogen bond with the nitrogen atom of the pyridine or the oxygen atoms of the sulfonyl groups. It is far away from these atoms (more than 6 Å), as it can be seen in figure 6.31.

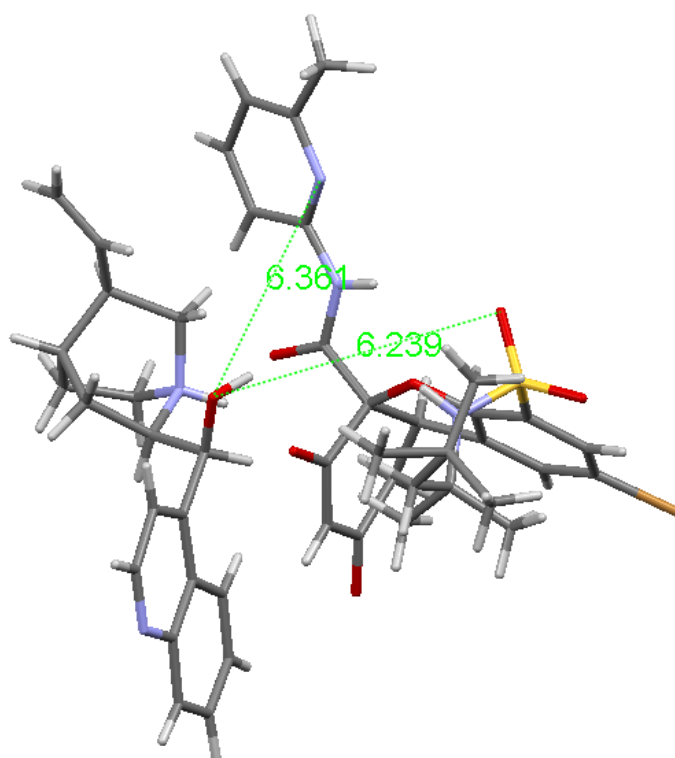


Figure 6.31. X-ray structure where it is shown the distance between the cinchonine OH group and the pyridine nitrogen atom and a sulfonyl oxygen atom.

When the unit cell was increased to observe interactions of the salt with the rest of molecules of the crystal structure we could observe that the cinchonine OH group established

a hydrogen bond of 2.66 Å with the enolate of other receptor molecule, as it can be seen in figure 6.32.

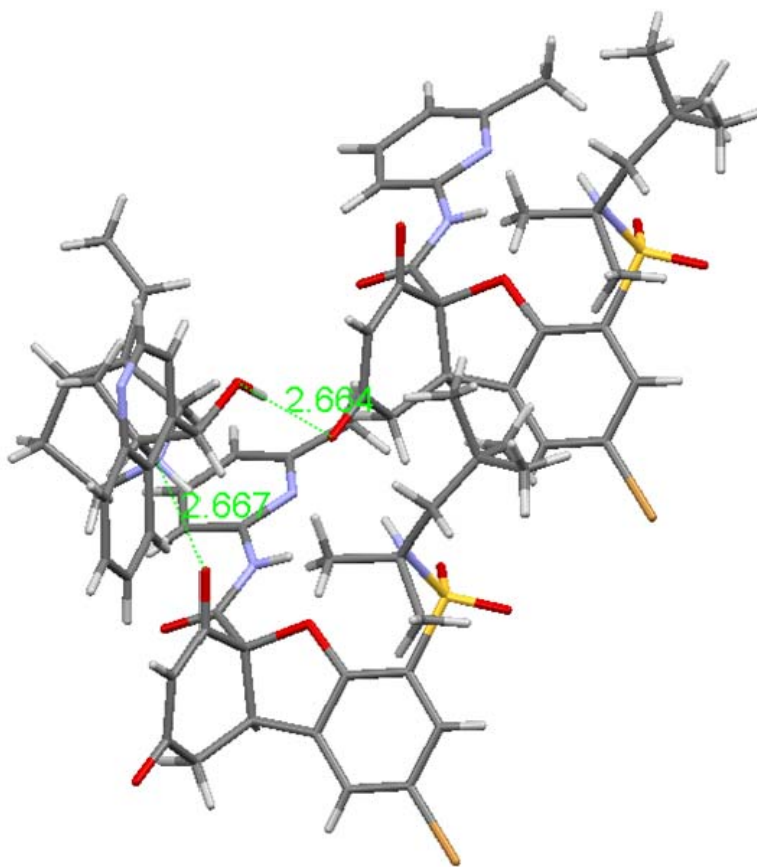


Figure 6.32. X-ray structure where it is shown the hydrogen bond between cinchonine OH and the enolate of another receptor molecule, as well as between the protonated N of cinchonine and other enolate.

Therefore, in the crystalline structure it can be observed the formation of chains of receptor molecules joined together by cinchonine molecules, as can be seen in figure 6.33.

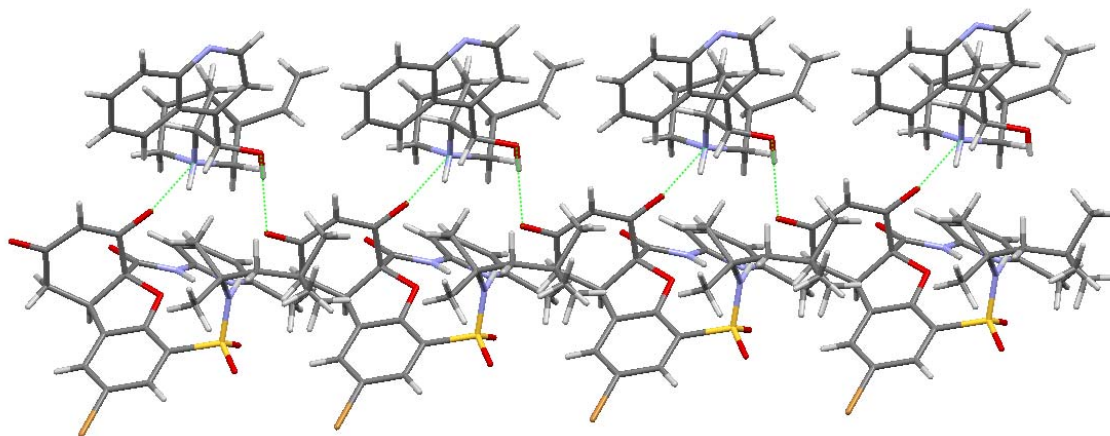


Figure 6.33. Crystal packing of receptor **147** salt with cinchonine.

6.2.3.4. Amino acids and its derivatives extraction

Due to the bifunctional nature of receptor **147**, the possibilities to carry out the resolution of racemic mixtures of different compounds are promising. Thus, the pyridine possesses a basic group which can form hydrogen bonds with acid groups such as carboxyls, or NHs from dinitrobenzoyl derivatives, triflates, etc. Moreover, the enol provides an acid group which may form a hydrogen bond with a carboxylate, or an ionic bond with an amine. Furthermore, sulfonamide and amidopyridine NHs can participate in hydrogen bond formation with the carbonyl group of the guest. It is also probable that the oxygen atoms of the sulfonyl groups act as hydrogen bond acceptors of acid NHs in the guest.

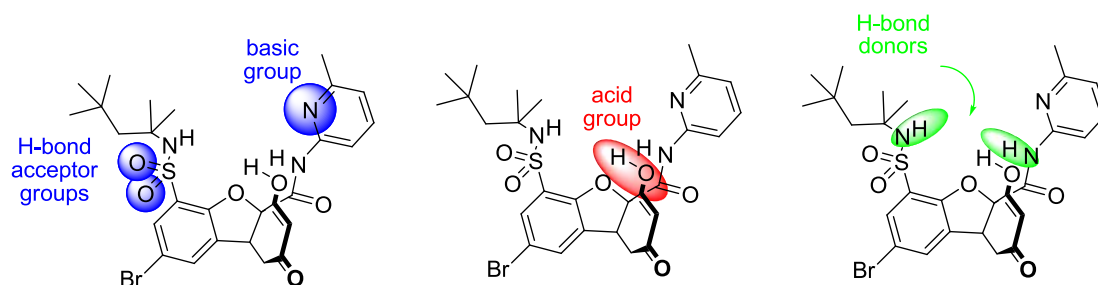


Figure 6.34. Functional groups from receptor **147**.

Furthermore, the enol can be deprotonated to generate an enolate. This negatively charged oxygen would be ideal for a guest with an acid proton.

All these functional groups make receptor **147** potentially useful in the association of amino acids and its derivatives, as shown in figure 6.35, where it is shown the predicted complexes between receptor **147** and *L*-Phe hydrobromide, dinitrobenzoyl-*L*-PheGly and the formyl derivative of *L*-Phe, respectively.

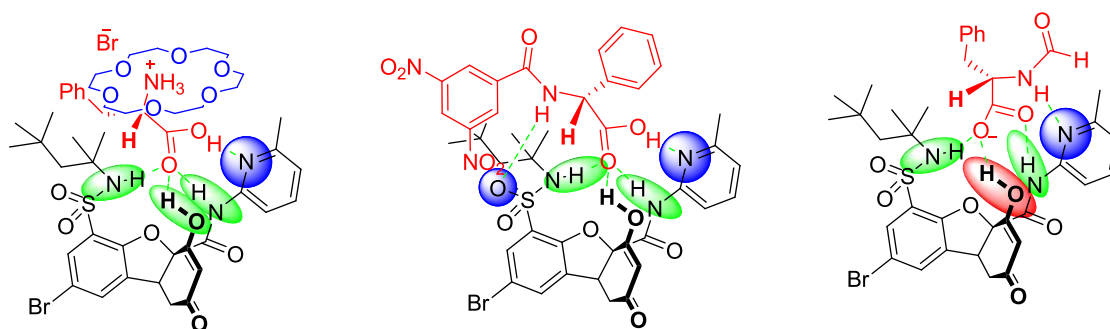


Figure 6.35. Complexes predicted between receptor **147** and different guests.

We started the study using natural amino acids as guests. These compounds have a high technical interest, and it is very important to find new ways to get them, either from natural sources or from enantioselective industrial synthesis. It has to be noted that both *L*-amino acids, of natural origin, and *D*-amino acids have utility.²²⁹

²²⁹ Martínez-Rodríguez, S.; Martínez-Gómez, A. I.; Rodríguez-Vico, F.; Clemente-Jiménez, J. M.; Las Heras-Vázquez, F. J. *Chem. Biodivers.* **2010**, *7*, 1531-1548.

Amino acids in their natural state have ionic structures, making them water soluble and generally very insoluble in organic solvents. Therefore they are guests difficult to associate in chloroform. Our objective is to obtain, thanks to the presence of the receptor, an amino acid complex which prefers to dissolve in chloroform, and thus can be extracted from the aqueous phase. Selective extraction of amino acids to an organic phase would allow the resolution of complex mixtures obtained by hydrolysis of proteins, and which at present are resolved by ion exchange chromatography.²³⁰ However, it is an expensive method because it requires large amounts of deionized water.

In the initial experiments we added natural amino acids as *zwitterions* directly to a deuteriochloroform solution of receptor **147** and we recorded the NMR spectra. However there was no extraction of the amino acids, since its signals did not show up in the spectrum, and the receptor **147** signals did not undergo any displacements. Due to this reason, we believe that this receptor is not sufficiently acidic to protonate the amino acid carboxylate. This result is logical, because amino acids are stronger acids than the corresponding carboxylic acids due to the field effect generated by the ammonium group.

Since our receptor itself does not carry out the extraction of zwitterionic amino acids, we proposed the extraction of amino acids as its bromhydrates. These compounds are very water soluble, because the ammonium group presents a positive charge.

Phenylalanine hydrobromide was chosen for the extraction experiment, because this is one of the more lipophilic amino acids. However, the addition of a saturated solution of *L*-phenylalanine hydrobromide to a receptor **147** chloroform solution generated no significant changes in the NMR spectrum, from which we conclude that no extraction took place.

Since the distribution of a salt between two solvents depends on both ions, we replaced the bromide counterion by another one in order to increase the amino acid solubility in the organic phase.

Tetraphenylborate seemed a good idea to us. Tetraphenylborates of amino acids are described in the literature and can be readily obtained by ion exchange from sodium tetraphenylborate.²³¹

The complex we hoped to be formed appears in figure 6.36.

²³⁰ (a) Moore, S.; Stein, W. H. *J. Biol. Chem.* **1951**, *192*, 663-681; (b) Moore, S.; Stein, W. H. *Methods Enzymol.* **1958**, *6*, 819-831.

²³¹ Buschmann, H.-J.; Mutihac, L. *J. Incl. Phenom.* **2002**, *42*, 193-195.

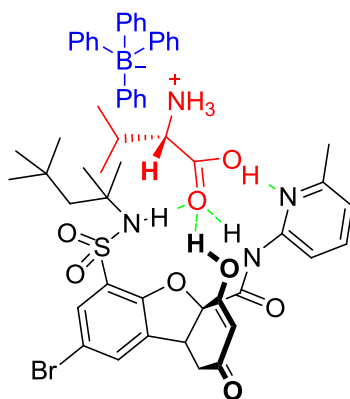


Figure 6.36. Expected complex between receptor **147** and L-valine tetraphenylborate.

Thus, we dissolved receptor **147** in $\text{CDCl}_3\text{-H}_2\text{O}$, *DL*-valine hydrobromide (5 eq) was added as well as one equivalent of sodium tetraphenylborate. After stirring the mixture vigorously we expected an equilibrium between the two phases, so that both enantiomers of valine were distributed between the aqueous phase and chloroform. However, under these conditions we did not observe the formation of complexes, it is likely that the decomposition of sodium tetraphenylborate occurs, which in an acid medium may evolve generating benzene. Indeed, we observed a signal at 7.26 ppm in the ^1H NMR spectrum, which corresponds to the benzene absorption.

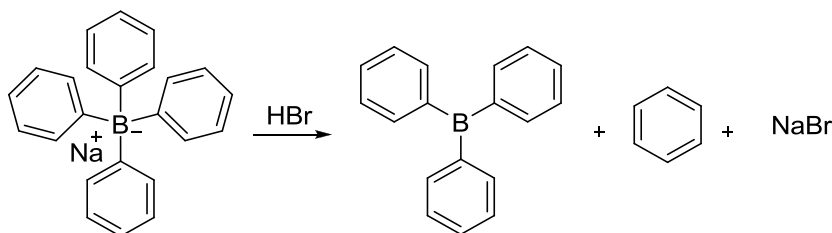


Figure 6.37. Decomposition of sodium tetraphenylborate in an acid medium.

These experiments were repeated with *DL*-phenylalanine hydrobromide under the same conditions, but again no extraction was observed.

Another way to increase the lipophilicity of the amino acids is the utilization of 18-crown-6 ether. This ether has the ideal geometry to associate the ammonium group. In the associate, protons of the ammonium group form hydrogen bonds with the oxygens of the crown ether, decreasing its interaction with water molecules. Since the ammonium group has already its hydrogen bonds saturated, hopefully the carboxylic acid in the oxyanion hole of receptor **147** will also form strong hydrogen bonds with the pyridine nitrogen as well as the enol group. These hydrogen bonds must be particularly efficient because both donor and acceptor groups have similar $\text{p}K_{\text{a}}$ s. The structure is shown in figure 6.38. We expected an enantioselective extraction under these conditions because the benzyl group of phenylalanine should be placed in the opposite face of the *t*-octyl group of the receptor.

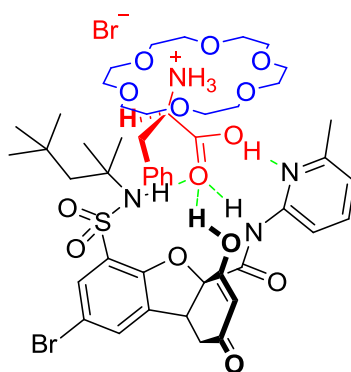


Figure 6.38. Proposed model for the association of *L*-phenylalanine hydrobromide in the presence of 18-crown-6-ether.

Initially, we worked with the racemic mixture of receptor **147** and *L*-amino acids. If the amino acid addition causes the splitting of the racemic receptor signals, then we would perform the inverse operation, that is, the use of the enantiomerically pure receptor **147** with the intention of removing a single phenylalanine enantiomer from the amino acid racemic mixture.

A first experiment was conducted by adding *L*-phenylalanine to a solution of racemic receptor **147** and 18-crown-6-ether in H₂O-CDCl₃. After stirring and phase separation, it was observed the presence of *L*-phenylalanine in the chloroform phase; however it did not cause the splitting of the receptor signals.

When we repeated the same experiment with *L*-phenylglycine hydrobromide we observed the splitting of the receptor signals. Encouraged by this result, we decided to study whether it was possible to carry out an enantioselective extraction of phenylglycine. For this, we dissolved in an NMR tube 5.85 mg of optically pure receptor **147** and we added one equivalent of racemic phenylglycine hydrobromide and crown ether. Then an aqueous solution with 10 equivalents of *DL*-PheGly was added. After stirring and phase separation, we observed the presence of 57 % of amino acid in relation to the receptor in chloroform. The aqueous phase was removed, the chloroform phase was dried and the enantiomeric excess was measured by chiral HPLC, but the enantiomeric ratio obtained was 52/48.

Another option to make the amino acid more soluble in chloroform without crown ether or a bulky counterion is to use functionalized amino acids. These compounds have acid NHs to establish more interactions with the receptor and thus the complex formed can be stronger. To study this possibility we conducted an experiment with Cbz-*L*-Phe. Again, first we used racemic receptor **147** to test if signal splitting takes place in the presence of the pure amino acid. Surprisingly, it was not. Then we added tetrabutylammonium hydroxide to generate Cbz-*L*-Phe carboxylate. We expected that the geometry of the complex between receptor **147** and the carboxylate of the guest was very different from the associate with the free acid, since the carboxylate, having no acidic proton, cannot form the strong H-bond with the pyridine, while the carbamoyl NH probably prefers the pyridine, which is a good hydrogen bond acceptor, respect to the sulfonyl group of the sulfonamide, as shown in figure 6.39. This change in

geometry offered a new possibility for enantioselective recognition. However, these new experiments yielded no splitting in the receptor signals.

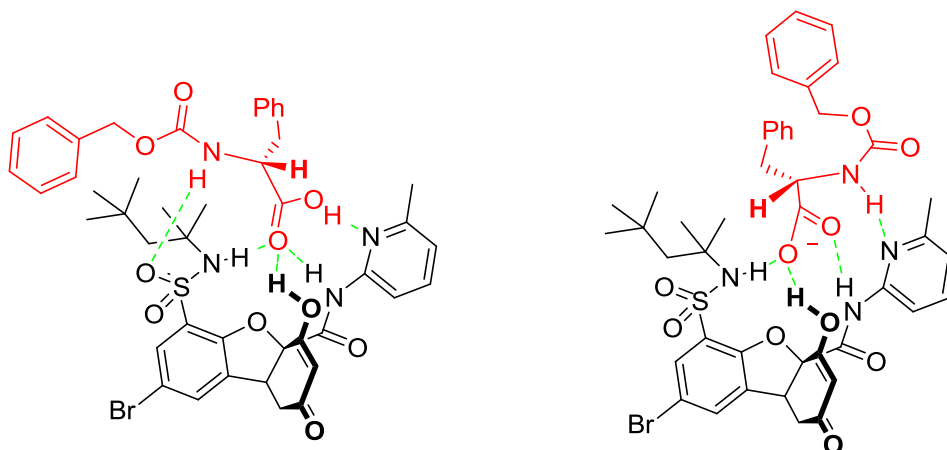


Figure 6.39. Models proposed for the formation of complexes with Cbz-L-Phe and Cbz-L-Phe carboxylate, which, however, did not cause the splitting of the racemic receptor signals.

Another attractive guest for enantioselective recognition is the dinitrobenzoyl derivative of phenylglycine. This compound has a more acidic NH due to the electron withdrawing character of nitro groups, so that the formation of stronger hydrogen bonds is expected. Furthermore, the dinitrobenzoyl ring is very suitable for generating charge-transfer interactions.

Here, we tried an extraction experiment in which we hoped to enrich the racemic mixture of a guest in one of the enantiomers due to the presence of the optically pure receptor. As phenylglycine has a bulky substituent in alpha, we hoped that this could favour the recognition of one enantiomer through steric hindrance. The experiment was carried out dissolving the guest in CDCl_3 . After adding a slight excess of the optically pure receptor **147**, we observed the splitting of the guest signals, which showed the formation of two diastereomeric complexes.

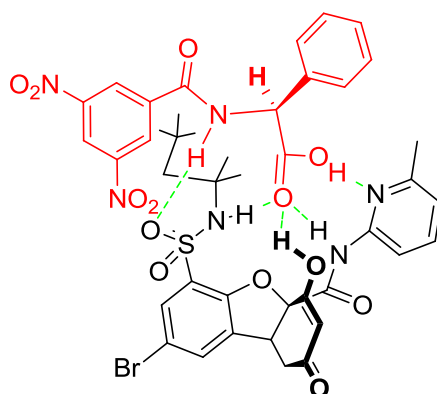


Figure 6.40. Model proposed for the complex formation between dinitrobenzoyl-L-phenylglycine and enantiomerically pure receptor **147**.

Then we prepared the potassium salt of the racemic guest and we added an aqueous solution of 10 equivalents of this salt to the NMR tube. The receptor will associate the carboxylic acid, which is usually soluble in organic solvents and is not well suited for

carboxylate association. In a two-phase equilibrium system with carboxylic acid/carboxylate mixtures, in the aqueous phase the two enantiomers of carboxylate will have similar stabilities, while in the organic phase one of the enantiomers will present a greater stability due to the formation of an enantioselective complex with the receptor. Thus, the system evolves by increasing the concentration of the guest which forms the most stable complex in the organic phase, decreasing this guest enantiomer in the aqueous phase until it reaches a new equilibrium (figure 6.41).

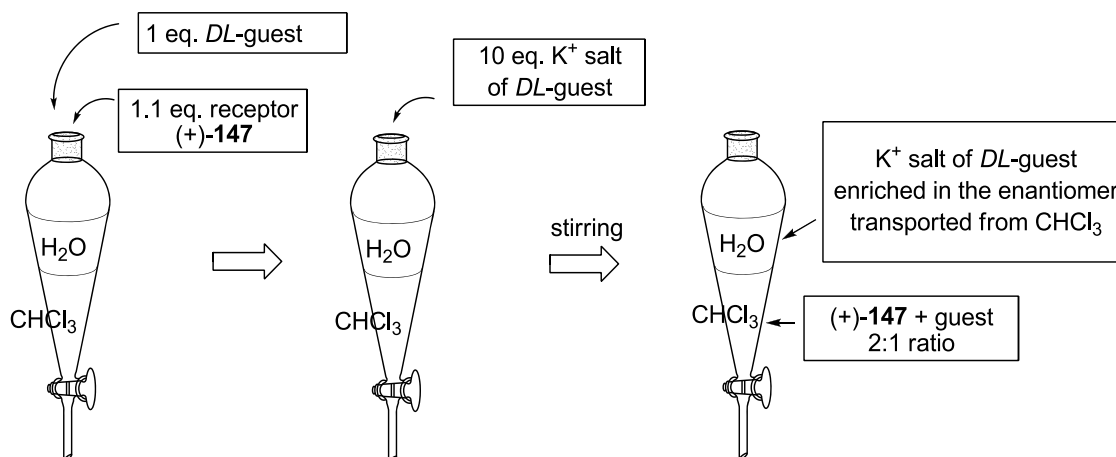


Figure 6.41. Resolution of a racemic mixture of guests by extraction in a biphasic system chloroform-water with receptor (+)-147. If instead of CHCl₃, CDCl₃ is used, the extraction can be performed directly in an NMR tube.

In this case, after adding the solution of the guest potassium, we obtained a 2/1 preference for one enantiomer, which shows that the extraction is enantioselective.

Since receptor **94**, which has the methyl enol ether instead of the enol, showed a competitive constant of 6.6 with *L*-alanine cyclohexylthiourea **114**, we decided to test if this guest was also able to cause the splitting of the racemic signals of receptor **147**. Indeed, it was, and we obtained an affinity five times greater for one of the enantiomers than for the other.

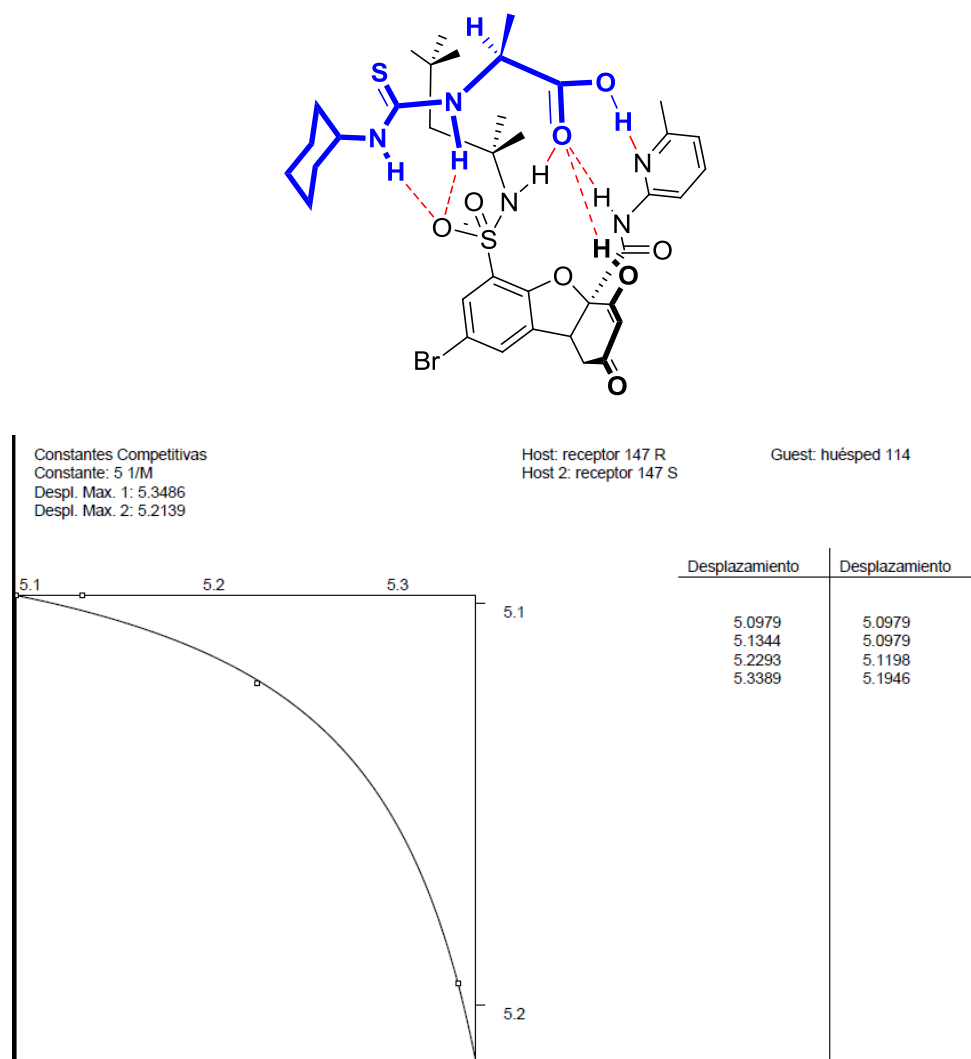


Figure 6.42. Proposed complex and titration between racemic receptor **147** and L-alanine cyclohexylthiourea **114**.

Since the titration with receptor **114** was clearly enantioselective with L-alanine cyclohexylthiourea **114**, we checked if this receptor could be useful in resolving the racemic mixture of the thiourea.

To this end, we designed an extraction experiment with DL-alanine cyclohexylthiourea **114** and chiral receptor **147**.

Similarly to the way in the previous experiments, we mixed receptor (+)-**147** and racemic guest **114** (less than one equivalent) in deuterated chloroform, observing the splitting of all signals. Next, we added 10 equivalents of the potassium salt (it can also be used the lithium or ammonium salt), noting that the signals corresponding to one enantiomer were maintained while the corresponding to the other enantiomer decreased significantly, as can be seen in figure 6.43.

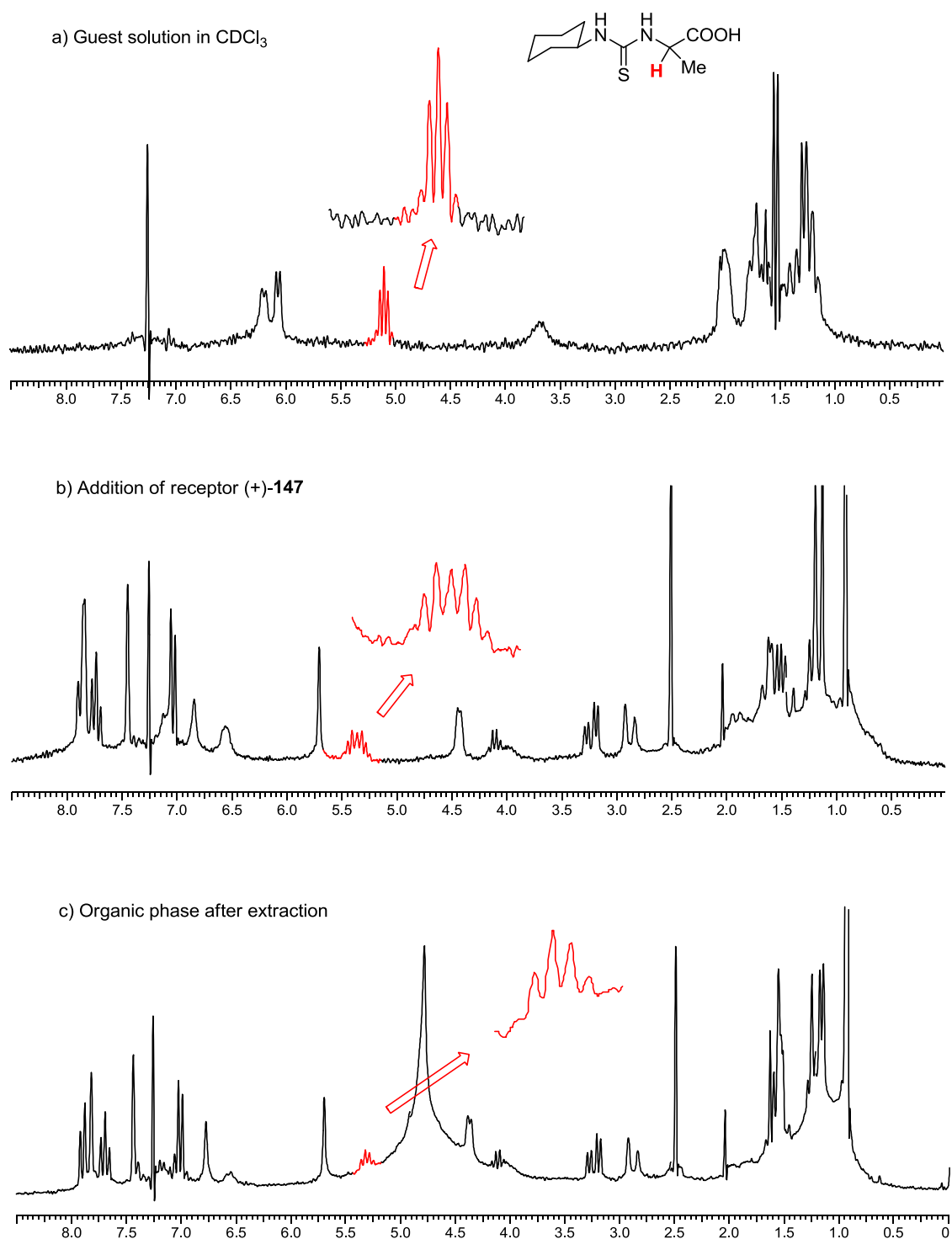


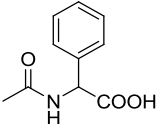
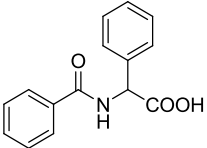
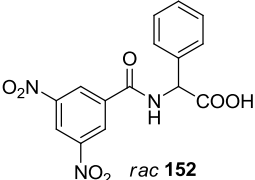
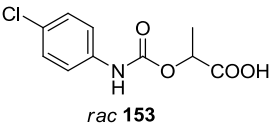
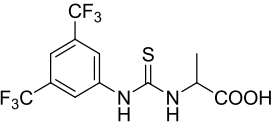
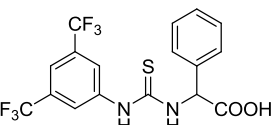
Figure 6.43. ¹H NMR spectra of the extraction experiment of DL-alanine cyclohexylthiourea with receptor (+)-147.

As shown in the above figure, the extraction creates a great change in the signals form of the diastereomeric protons in alpha to the alanine thiourea **114**. Quantification using NMR integrals was difficult because the signal is complex and is mounted on the side of the water protons. To get a more accurate assessment of the enantioselectivity in the extraction experiment, the measure was carried out by chiral HPLC, obtaining a 4/1 ratio, somewhat lower than the value measured in the competitive titration. This ratio is lower than expected

but it is necessary to consider that the aqueous phase loses concentration in the enantiomer which is extracted to the chloroform, and any small amount of water that has not been effectively separated from the chloroform phase negatively influences the enantiomeric excess, since the concentration of the guest in this phase is ten times greater.

Encouraged by these results we conducted a study with other guests. Results are summarized in table 6.4.

Table 6.4. Enantioselective extraction of different guests in the presence of receptor **147**.

entry	guest	enantiomers ratio
1	 <i>rac 150</i>	1.0 / 1.3
2	 <i>rac 151</i>	1.0 / 1.0
3	 <i>rac 152</i>	2.0 / 1.0
4	 <i>rac 153</i>	1.0 / 1.0
5	 <i>rac 115</i>	1.0 / 1.0
6	 <i>rac 154</i>	1.0 / 1.5

However, the enantiomers ratio obtained with guest **114** was not improved.

We also studied the extraction of trialkyl and tetraalkylammonium salts, since, as discussed above, the associates with carboxylates must have totally different geometries, and therefore the enantioselectivities may be different too.

The preparation of tetraalkylammonium guests can be performed from the acids by treatment with the corresponding tetraalkylammonium hydroxide, but these salts are expensive and are only available commercially in solution. This is an inconvenience, because the solutions are not stable to air, suffering carbonation or loss of solvent by evaporation, which makes difficult to know the real concentration of tetraalkylammonium hydroxide. An alternative is the preparation of triethylammonium salts, just dissolving the receptor in triethylamine and then eliminating the excess of triethylamine under vacuum. This would allow us to carry out extraction experiments with the triethylammonium salt of the receptor **147** and the corresponding amino acid derivative as a carboxylic acid.

Once prepared the triethylammonium salt of receptor **147** we performed the extraction of a *DL*-phenylalanine derivative (because Phe is a lipophilic amino acid). An analysis of the CPK models of the complex showed us that there might be some stereo repulsion between the methyl group of the amidopyridine and the substituent on the nitrogen of the guest, repulsion that could be minimized if this substituent is a hydrogen atom. For this reason we used the formyl derivative of phenylalanine **155**.

Under these conditions we believe that the carboxylic group of the amino acid will transfer the proton to the receptor enolate, resulting in a strong interaction between both groups, because the pK_a of both are similar. At the same time the guest NH can form a hydrogen bond with the pyridine of the receptor (figure 6.44).

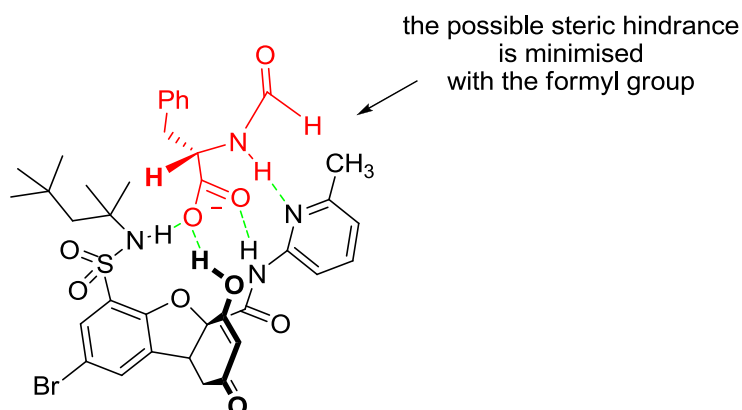


Figure 6.44. Proposed model for the complex between the triethylammonium salt of receptor **147** and the formyl derivative of phenylalanine **155** (the triethylammonium group has been omitted for clarity).

The experiment was carried out adding optically pure receptor **147** as its triethylammonium salt to an NMR tube containing the formyl derivative of *DL*-phenylalanine **155**. However, there was no splitting of the guest signals. Adding water to the previous tube makes the guest and triethylammonium signals vanish. The most plausible explanation is that the triethylammonium salt of the formyl derivative prefers to dissolve in the aqueous phase and the complex is not stable enough to produce the extraction to chloroform.

Having confirmed that the triethylammonium salt of the formyl derivative of phenylalanine was not extracted to the chloroform phase, we added an equivalent of the neutral guest to the biphasic mixture, and we observed, once established the equilibrium, the splitting of the

amino acid derivative signals. Integration of the guest signals showed an enantiomer ratio of 1/1.5, confirming that the receptor exhibits enantioselectivity for formyl-Phe **155**; however, the associate which is formed has the geometry of the neutral complex.

Although anionic complexes formed by the receptor and amino acid triethylammonium salts do not appear to be particularly stable, because of the rupture in the presence of water, the absence of water allow the obtention of complexes of well-defined geometry. Thus, the addition of formyl-*L*-leucine **156**, PheGly-*L*-triflate **107** or *D*-mandelic acid **142** to the racemic mixture of the receptor tetrabutylammonium salt, generates a clear splitting of the receptor signals, confirming the formation of diastereomeric complexes of well-defined geometry.

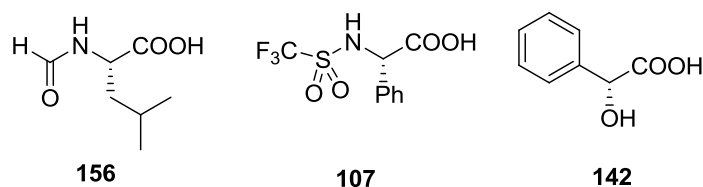


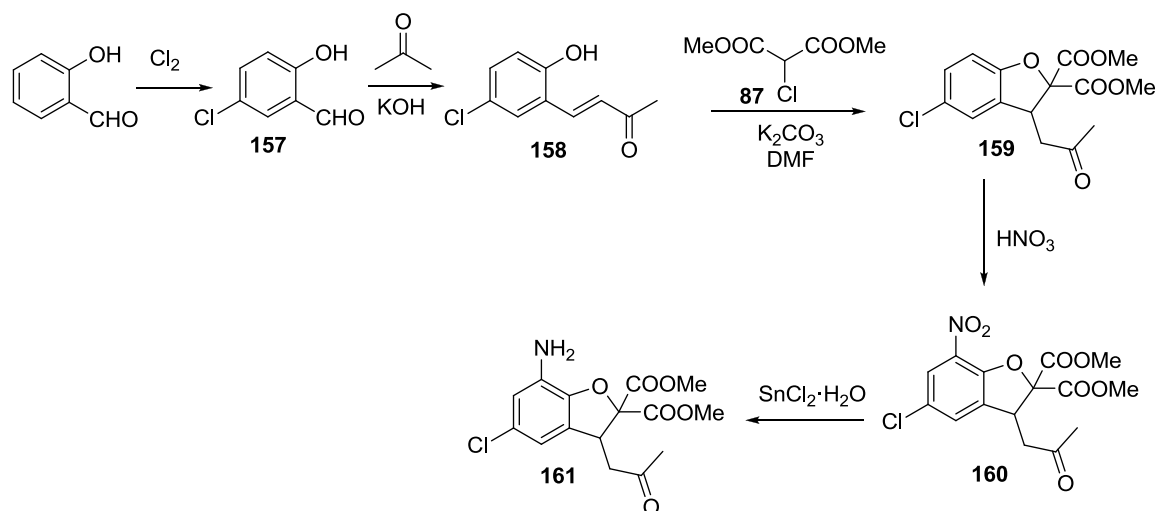
Figure 6.45. Other guest tested with receptor **147**.

The preparation of the receptor **147** tetrabutylammonium salt is very easy, because it does not require the use of tetrabutylammonium hydroxide, the reason is that the receptor is a lipophilic compound and the tetrabutylammonium salt prefers to dissolve in the organic phase instead of water and, therefore, it is sufficient to work with aqueous sodium carbonate and tetrabutylammonium chloride which, in general, is an economical and stable compound that can be easily weighed. During the extraction, the tetrabutylammonium salt of the receptor **147** dissolves in the ethyl acetate, while sodium chloride prefers the aqueous phase.

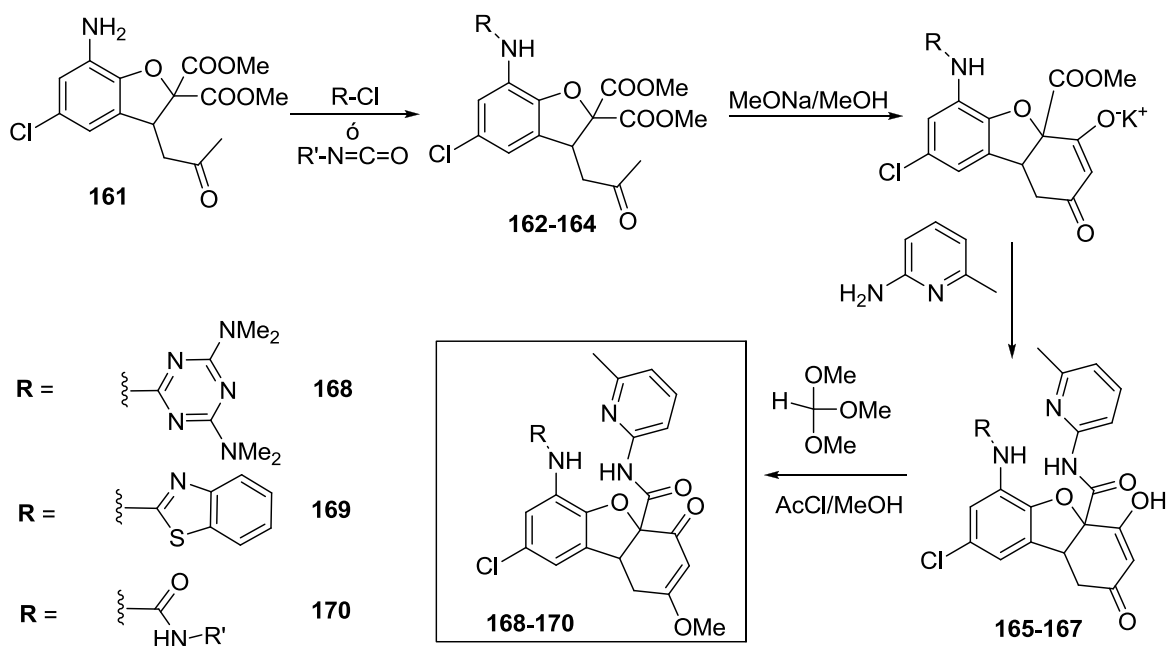
6.2.4. Other receptors

Trying to improve the above values in the recognition of racemic mixtures of amino acids and its derivatives, we decided to change the receptor geometry. Firstly, we introduced some changes in the structure of the receptor oxanion hole. Thus, we decided to eliminate the sulfonamide attached to the aromatic ring and place the NH directly on it. In this way we could quantify the influence of the sulfonamide in the existence of intramolecular hydrogen bonds in the receptor **94**, or the possible free rotation of this group. Although in first instance calculations had not been promising for such oxanion hole (chapter 5, page 231), we had not really considered the possibility that the ketone could be reduced or even work with the enol. The distance between the NH and this position should be shorter than with amidopyridine NH, as revealed by the X-ray structures obtained in this chapter and in the previous one.

The synthesis was carried out similarly to receptor **94**. However, in this case we used 4-chlorosalicylaldehyde instead of 4-bromosalicylaldehyde because the nitration of the aromatic bromoderivative proceeds with *ipso* substitution. To place the NH directly on the aromatic ring the desired position must be first nitrated with fuming nitric acid and then reduced to the amino group with tin chloride, thereby obtaining intermediate **161**.

Figure 6.46. Synthesis of intermediate **169**.

This compound is a versatile intermediate that can be functionalized in different ways through the amine. Thus, we performed the synthesis of several compounds and then proceeded to the cyclization under standard conditions with MeONa/MeOH, obtaining a family of receptors, as can be seen in figure 6.47.

Figure 6.47. **168-170** receptors synthesis.

Fortunately, we were able to obtain crystals from receptor **169** with the right size to solve its structure by X-ray diffraction, as can be seen in figure 6.48.

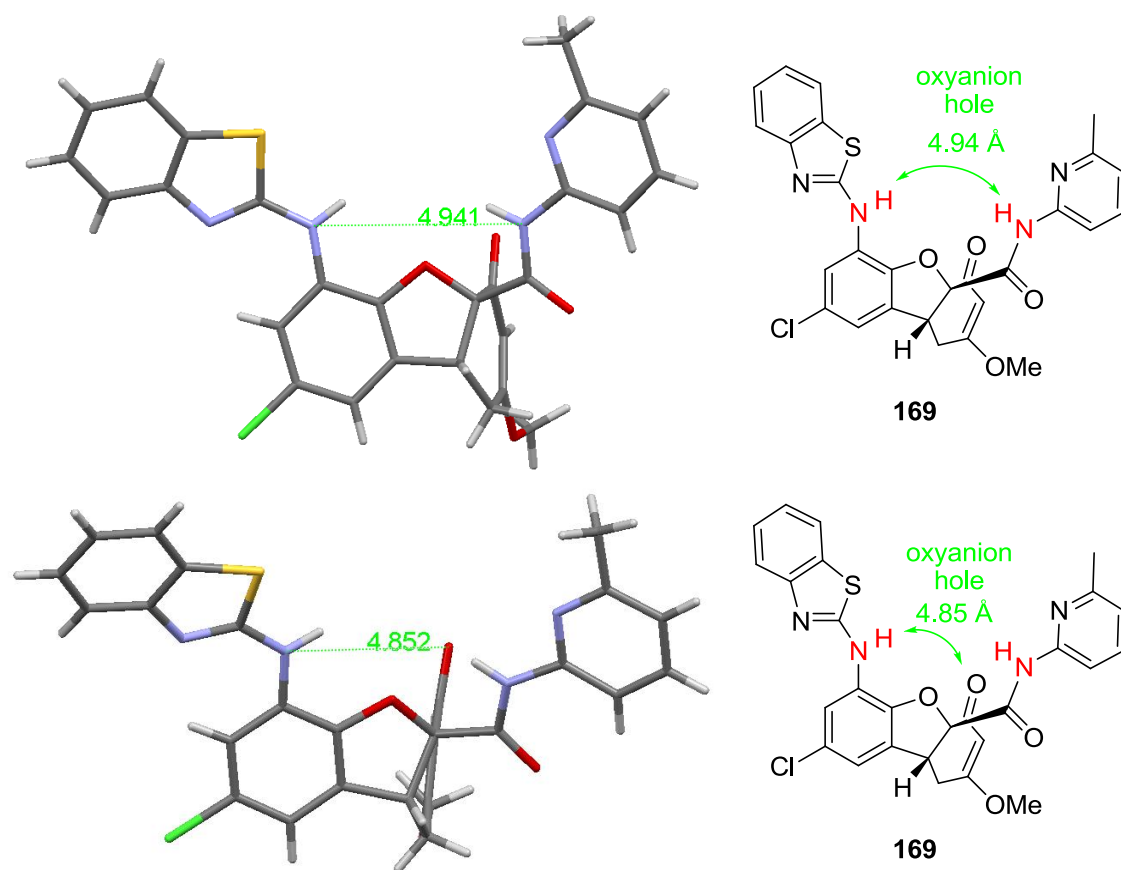


Figure 6.48. X-ray structure of receptor **169**.

As seen in the previous figure, the distance between the two NHs is 4.9 Å, slightly larger than the oxyanion hole in enzymes which is about 4.3-4.6 Å. However, by extending the unit cell it could be observed that this receptor was forming a dimer with another receptor molecule: the ketone carbonyl group of receptor **169** was perfectly placed on the oxyanion hole of another receptor molecule, forming two separate hydrogen bonds, of a moderate strength, with heteroatom-heteroatom distances of 3.0 and 3.3 Å. Meanwhile, the carbonyl of the first receptor molecule is forming hydrogen bonds with the oxyanion hole NHs of the second receptor molecule, as seen in figure 6.49.

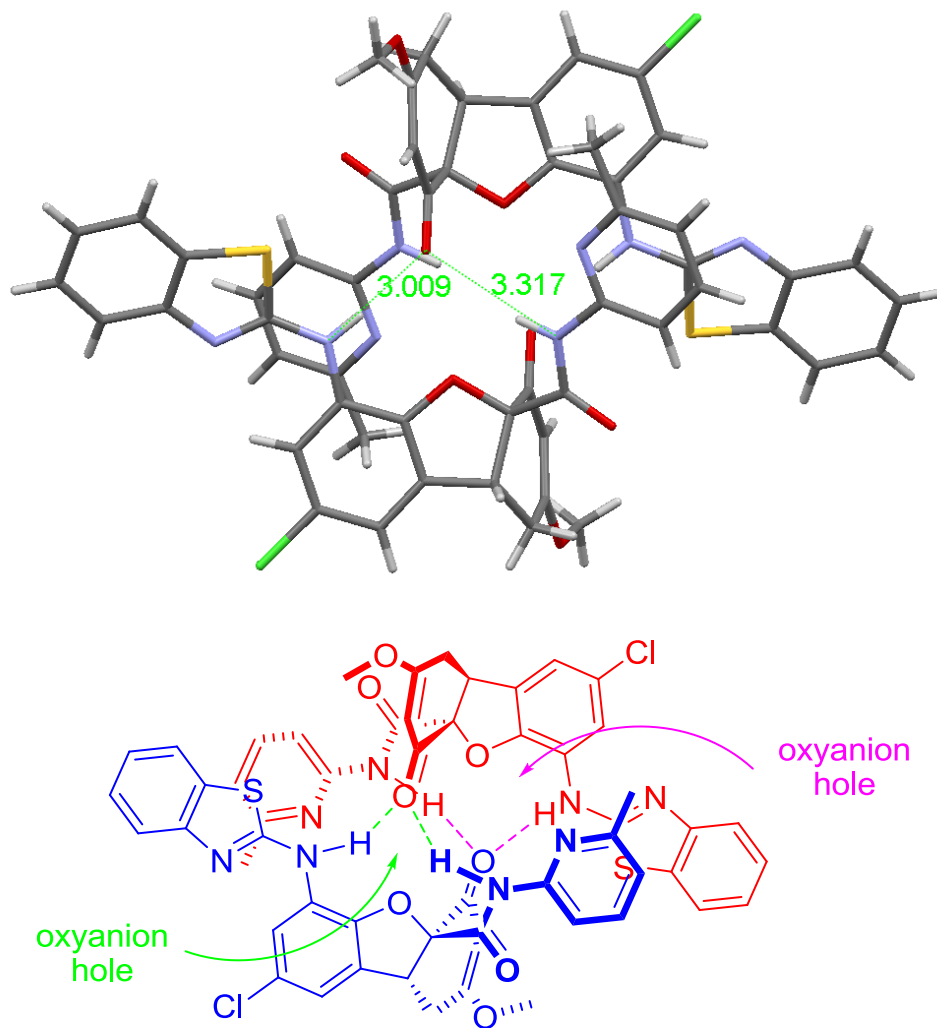


Figure 6.49. (Top) X-ray structure of receptor **169** dimer and (bottom) model of the associate formed in the dimer.

We conducted several preliminary experiments with racemic receptor **169**, so that if we got a high relative constant while carrying out titrations with a chiral guest, it would be worthwhile to study the resolution of the receptor. Then, it would be possible to perform enantioselective extraction of racemic mixtures of the guest. First, we worked with receptor **166** in its enol form.

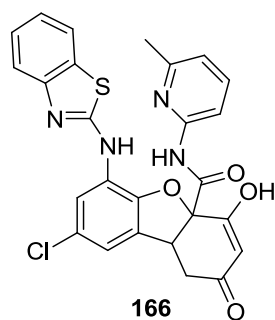
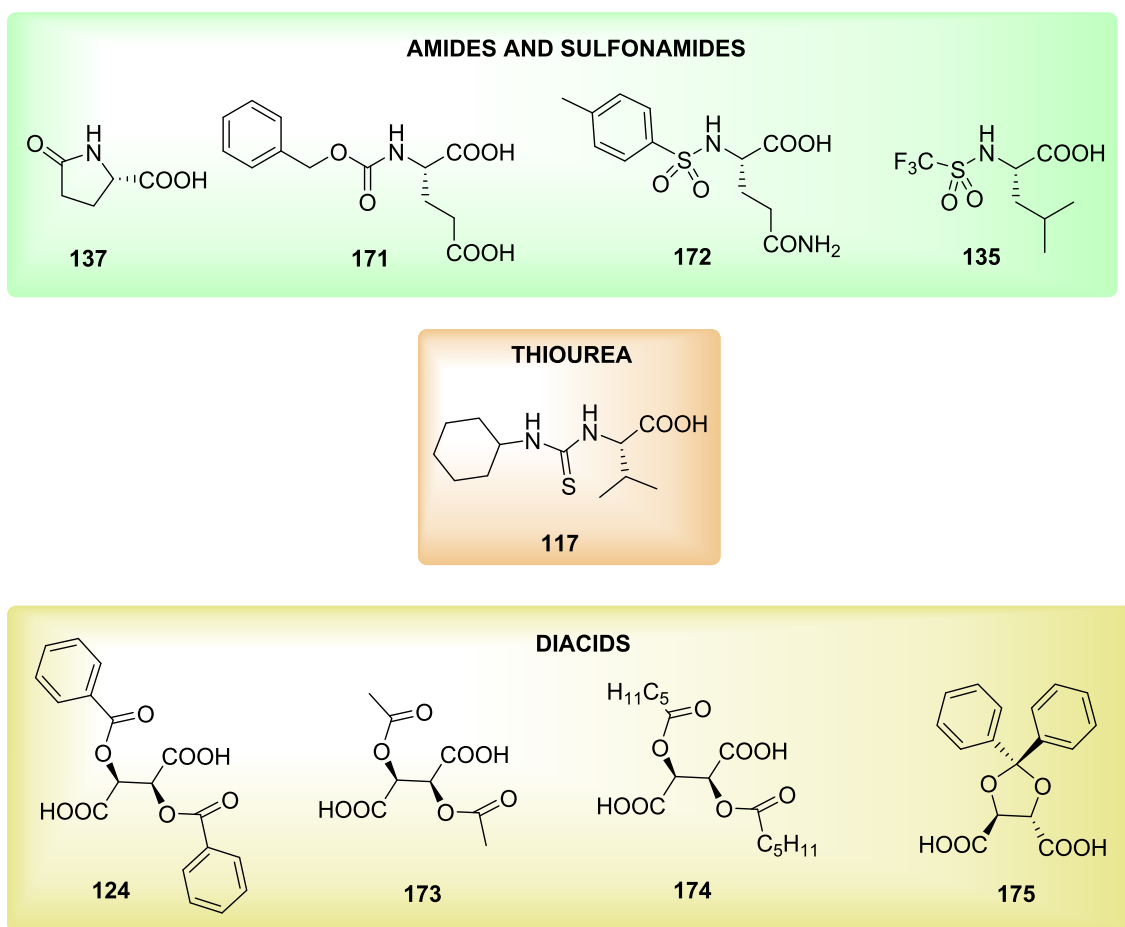


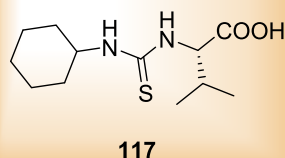
Figure 6.50. Receptor **174**.

We tried to see by NMR if the receptor experienced signal splitting by adding proline to the reaction medium or its hydriodide, but this effect was not observed. Neither using the camphorsulfonate of the receptor nor proline in its *zwitterionic* form yielded a positive result. Similarly, no signals splits of the receptor by using an aqueous solution of *L*-Phenylalanine were observed. Again, extraction experiments with *L*-aspartic acid and *L*-glutamic acid hydrochlorides in the presence of crown ether caused no splitting of the receptor signals, or the extraction of the amino acid to the chloroform phase.

Then, we decided to make some titrations with the receptor in its methyl ether form **169**, taking advantage of any of the guests prepared in the previous chapter and some new compounds.



THIOUREA



DIACIDS

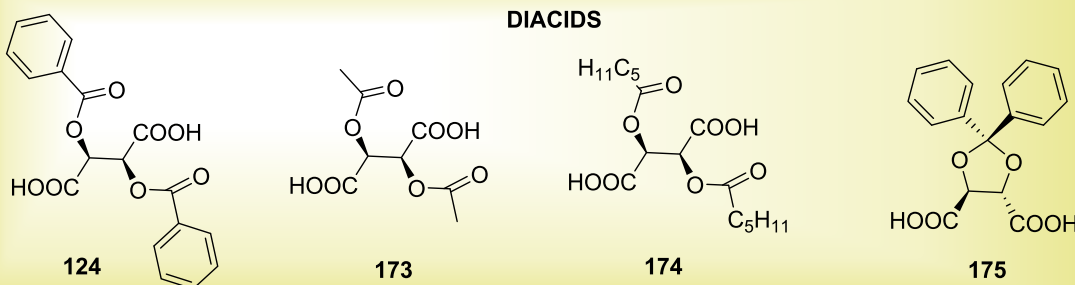


Figure 6.44. Guests tested in the resolution of receptor **169** enantiomers.

The results obtained are summarized in table 6.5.

Table 6.5. Competitive association constants between both enantiomers of receptor **169**.

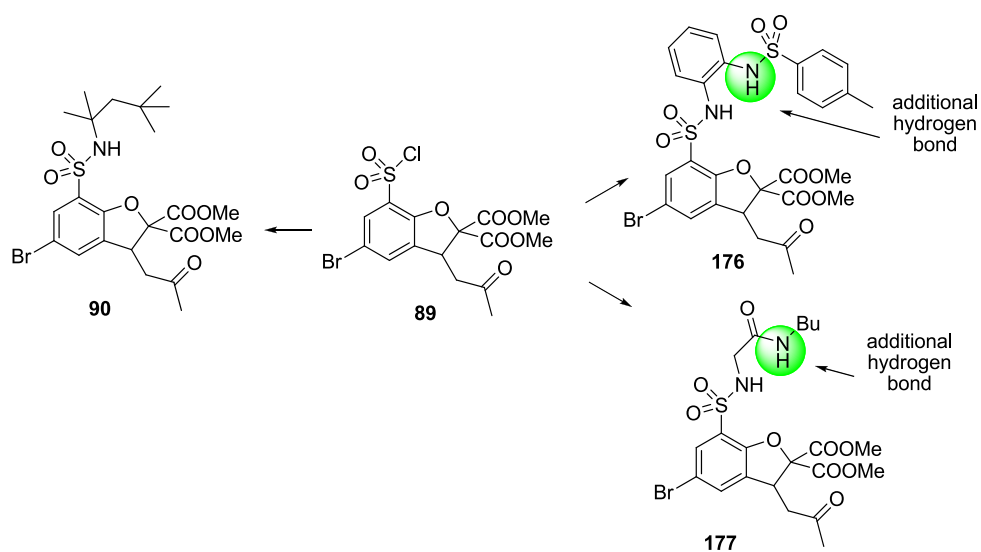
entry	guest	<i>K</i>
1	137	1.2
2	171	1.1
3	172	(a)
4	135	1.0
5	117	2.4
6	124	1.5
7	173	1.1
8	174	1.3
9	175	(b)

(a) The guest is not dissolved.

(b) There is no splitting.

The constants obtained were not very large, so we decided to try crystallization experiments with chiral amino alcohols such as cinchonidine, ephedrine, norephedrine, etc., but this work is still underway.²³²

In parallel with the preparation of receptor **169**, we have carried out the synthesis of new receptors in which it has been changed the place in which the acid of the guest fits in the receptor. Trying to find an optimal geometry which permits obtaining large enantioselective recognition of amino acids and its derivatives, we substituted the *t*-octylamine group of intermediate **90** for tosyl-*o*-phenylenediamine and the butyl amide of glycine, in such a way that now there was an additional hydrogen bond in the amine attached to the sulfonyl group, as can be seen in figure 6.52. This additional hydrogen bond could be enough to form a complex with a carboxylate, because thanks to the cooperative effect of the sulfonamide NH, amidopyridine would not be necessary.

Figure 6.52. New intermedia **176** and **177** in the preparation of enantioselective receptors.²³² Currently this work is being carried out by Álvaro Gacho for his Final Degree Project.

The idea was to carry out a preliminary study of these receptors with carboxylates and amino acids. To prepare a simple receptor with less synthesis steps as possible, we aminolyzed the ester with butylamine. The synthesis is shown in figure 6.53.

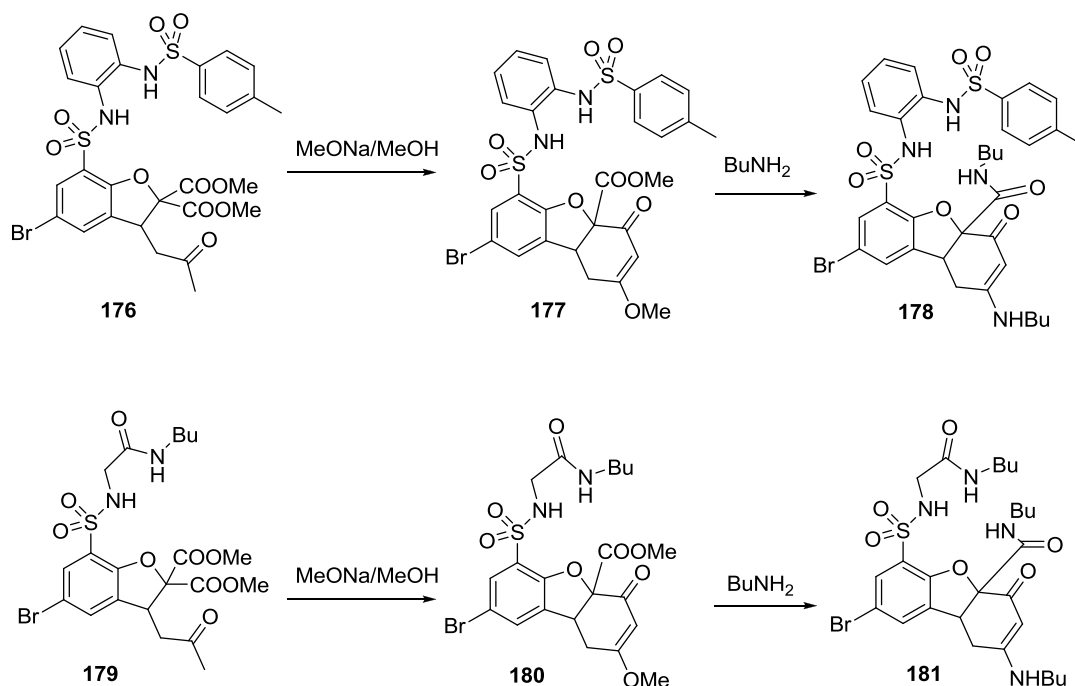


Figure 6.53. Synthesis of receptors **178** and **181**.

Both receptors **178** and **181** provide an ideal cavity for carboxylate association, with the formation of three hydrogen bonds, as shown in figure 6.54.

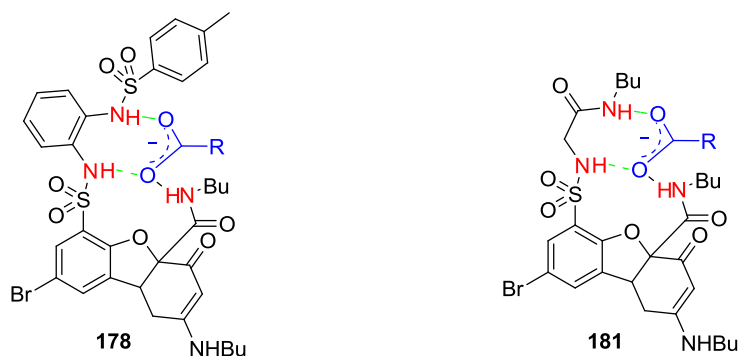
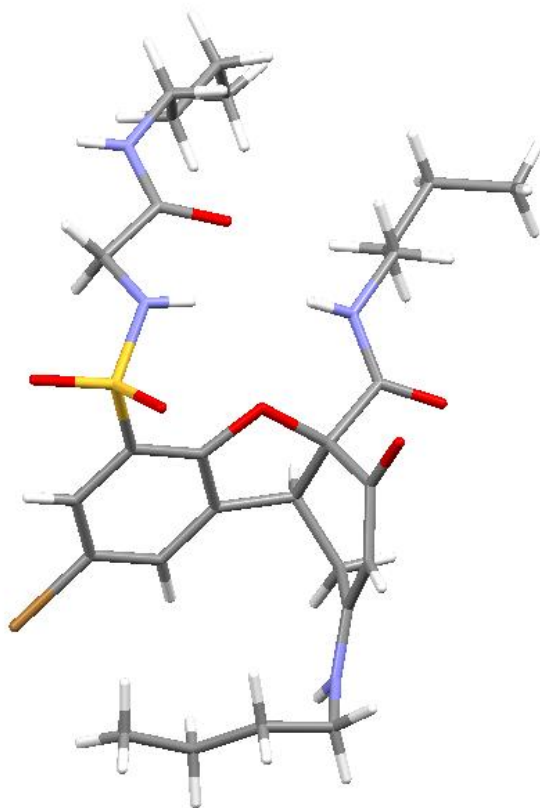


Figure 6.54. Complexes formed between receptors **178** and **181** and a carboxylate.

Early experiments with receptor **178** in the extraction of *L*-Leucine and *L*-phenylglycine in mixtures $\text{H}_2\text{O}-\text{CDCl}_3$ with crown ether have shown promising results in terms of extraction capacity to the chloroform phase, but the splitting of the receptor signals has not been achieved. Currently, further experiments with these receptors are underway, since it is possible to introduce structural modifications in both the nature of the amide substituent, as well as in the group attached to the second NH, which could improve the results obtained so far.

Regarding receptor **181**, we have succeeded in obtaining crystals with a suitable size for analysis by X-ray diffraction, as can be seen in figure 6.55.



*Figure 6.55. X-ray structure of receptor **181**.*

In view of the observed X-ray structure of the previous figure, it can be seen that receptor **181** presents a good oxyanion hole, since both the sulfonamide NH and the butylamide NH are oriented towards the cavity. The value of this distance is 4.5 Å, as shown in the following figure.

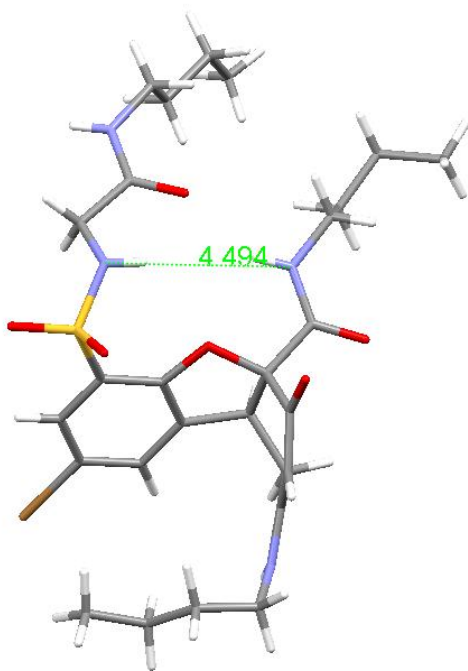


Figure 6.56. X-ray structure of compound **181** in which the distance between the sulfonamide NH and the butylamide NH are shown.

However, it is likely that the butyl amide NH is not available to form the oxyanion hole as it is forming intramolecular hydrogen bonds (between moderate and strong) with the carbonyl fragment of glycine (2.9 Å) and the oxygen atom of furan (2.7 Å).

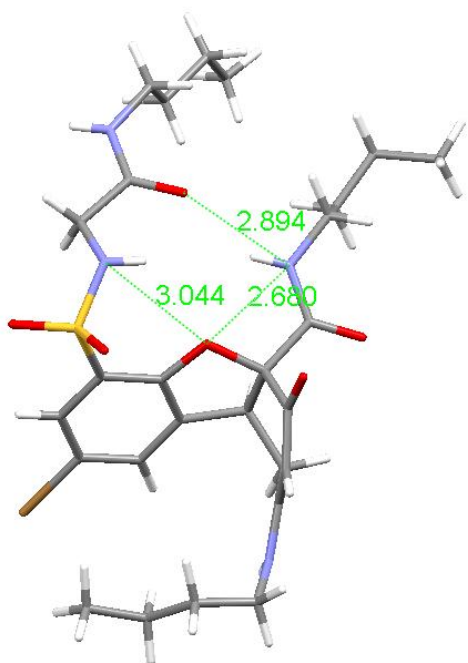


Figure 6.57. X-ray structure of compound **181** in which formation of intramolecular hydrogen bonds from the butylamide and sulfonamide NHs are shown.

The intramolecular hydrogen bond between the butyl amide NH and the oxygen atom of the fragment of glycine carbonyl makes this fragment to be directed outwards the oxyanion hole, so that it would no form part of it. However, it is possible than in solution, in the presence of a guest which produces a successful association, this conformation is not the most stable and rotations of the groups that maximize interactions with the guest in question occurs.

Currently extraction of amino acids and derivatives experiments have been conducting to confirm this fact and to analyze the potential of this receptor.

6.3. CONCLUSIONS

Throughout this chapter different receptors have been designed with the intention of improving the results obtained in chapter 5.

The replacement of the *t*-butyl group by a *t*-octyl group did not improve relative association constants; it seems that the stereo hindrance of the *t*-octyl group is necessary to have a good enantioselective recognition.

The reduction of the ketone can generate a hydroxyl group able to establish an additional hydrogen bond with the guest; however, although as a general rule the relative association constants improved, values were not very high.

It was much more interesting to obtain the enol receptor, since this group has a similar acidity of a carboxylic acid and allows forming stronger interactions. It also offers us the possibility to carry out their enantioselective separation by liquid-liquid extraction with chiral amino alcohols or crystallization with cinchonine.

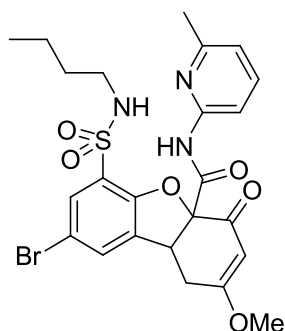
Once separated, the receptor has shown interesting properties in the enantioselective extraction of amino acid derivatives, with preferences close to 4/1.

In the last part of the chapter it has been presented the synthesis and structure of different receptors whose properties in the association of amino acids and derivatives are currently being studied in our research group.

6.4. EXPERIMENTAL

Receptors

- 8-Bromo-6-(*N*-butylsulfamoyl)-2-methoxy-*N*-(6-methylpyridin-2-yl)-4-oxo-1,4,4a,9b-tetrahydrobenzo[*b,d*]furan-4a-carboxamide (**131**)



Compound **131** was prepared following the experimental procedure described for receptor **94** with 12 % yield after cyclization.

mp: 94-96 °C.

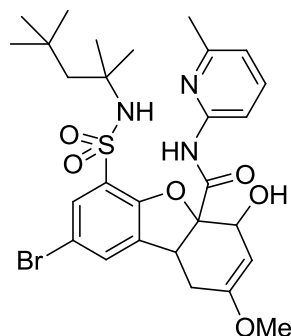
$^1\text{H NMR}$ (CDCl_3) δ (ppm): 0.81 (t, $J = 7.3$ Hz, 3H), 1.28 (hexaplet, $J = 7.3$, 2H), 1.39-1.53 (m, 2H), 2.40 (s, 3H), 2.63-2.73 (m, 1H), 2.82-3.00 (m, 2H), 3.39 (dd, $J = 7.0, 18.0$ Hz, 1H), 3.73 (s, 3H), 4.39 (d, $J = 6.7$ Hz, 1H), 5.55 (s, 1H), 6.01 (dd, $J = 4.8, 7.0$ Hz, NH), 6.89 (d, $J = 7.6$ Hz, 1H), 7.44 (s, 1H), 7.54 (dd, $J = 7.6, 8.2$ Hz, 1H), 7.77 (s, 1H), 7.85 (d, $J = 8.2$ Hz, 1H), 9.29 (s, NH).

$^{13}\text{C NMR}$ (CDCl_3) δ (ppm): 13.5 (CH_3), 19.6 (CH_2), 23.8 (CH_3), 28.8 (CH_2), 31.5 (CH_2), 41.8 (CH), 43.1 (CH_2), 56.5 (CH_3), 90.7 (C), 102.5 (CH), 111.1 (CH), 114.6 (C), 120.2 (CH), 125.0 (C), 130.2 (CH), 131.1 (CH), 132.4 (C), 138.6 (CH), 149.2 (C), 152.2 (C), 157.2 (C), 165.1 (C), 176.6 (C), 189.2 (C).

IR (nujol, cm^{-1}): 3571, 3377, 3286, 3072, 2955, 2923, 2852, 1690, 1664, 1606, 1541, 1450, 1398, 1346, 1249, 1203, 1152, 1093, 1041, 983.

HRMS (ESI): 564.0792 ($\text{M} + \text{H}$) $^+$, calcd for $\text{C}_{24}\text{H}_{27}\text{BrN}_3\text{O}_6\text{S}$ 564.0798.

- **8-Bromo-4-hydroxy-2-methoxy-*N*-(6-methylpyridin-2-yl)-6-(*N*-(2,4,4-trimethylpentan-2-yl)sulfamoyl)-1,4,4a,9b-tetrahydrodibenzo[*b,d*]furan-4a-carboxamide (136)**



Compound **94** (1.2 g, 1.9 mmol) was suspended in 33 mL of distilled THF, the suspension was cooled to 0 °C and LiAlH₄ (125 mg, 3.3 mmol) was added. The reaction could be followed by TLC with CH₂Cl₂-AcOEt 3:1 as eluent. Once the reaction had finished it was added over 50 mL of an aqueous solution of NH₄Cl with ice and stirring. It was extracted with EtOAc, washed with a solution of NaCl, decanted, dried over Na₂SO₄ and evaporated obtaining compound **136** (1.17 g, 97 % yield).

mp: vitreous compound.

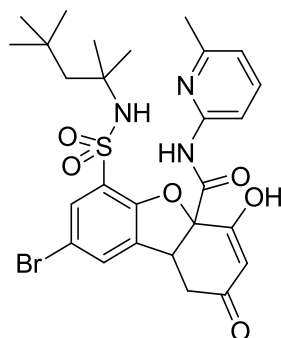
¹H NMR (CDCl₃) δ (ppm): 0.98 (s, 9H), 1.19 (s, 3H), 1.21 (s, 3H), 1.56 (d, *J* = 14.8 Hz, 1H), 1.61 (d, *J* = 14.8 Hz, 1H), 2.37 (d, *J* = 15.5 Hz, 1H), 2.40 (s, 3H), 2.69 (dd, *J* = 7.0, 15.5 Hz, 1H), 3.41 (s, 3H), 4.17 (d, *J* = 7.0 Hz, 1H), 4.71 (s, 1H), 4.86 (s, 1H), 6.82 (d, *J* = 7.6 Hz, 1H), 6.85 (s, NH), 7.38 (dd, *J* = 0.9, 2.1 Hz, 1H), 7.41 (t, *J* = 7.9 Hz, 1H), 7.69 (d, *J* = 8.2 Hz, 1H), 7.76 (dd, *J* = 0.6, 2.1 Hz, 1H), 0.93 (s, NH).

¹³C NMR (CDCl₃) δ (ppm): 23.9 (CH₃), 29.0 (CH₃), 30.1 (CH₃), 31.5 (CH₃ × 3), 31.5 (CH), 32.9 (CH₂), 44.1 (CH), 54.7 (CH₂), 54.8 (CH₃), 58.4 (C), 70.6 (CH), 94.9 (CH), 96.7 (C), 111.0 (CH), 113.5 (C), 119.8 (CH), 127.6 (C), 130.2 (CH), 131.0 (CH), 134.2 (C), 138.4 (CH), 149.4 (C), 153.5 (C), 154.9 (C), 156.8 (C), 170.6 (C).

IR (film, cm⁻¹): 3377, 2968, 1697, 1658, 1619, 1580, 1534, 1456, 1385, 1340, 1320, 1229, 1197, 1145, 1048, 1047, 996, 873.

HRMS (ESI): 622.1581 (M + H)⁺, calcd for C₂₈H₃₇BrN₃O₆S 622.1581.

- 8-Bromo-4-hydroxy-N-(6-methylpyridin-2-yl)-2-oxo-6-(N-(2,4,4-trimethylpentan-2-yl)sulfamoyl)-1,2,4a,9b-tetrahydrodibenzo[b,d]furan-4a-carboxamide (147)



In 75 mL of MeOH (previously dried using 3.0 mL of methyl orthoformate and two drops of methanesulfonic acid), a solution of Na (6.0 g, 0.26 mol) was prepared. When sodium was completely dissolved it was cooled with an ice-salt bath and compound **90** (25.0 g, 0.044 mol) was added. The temperature was raised to 10 °C. Initially compound **90** slowly dissolved in the reaction medium but then, it was observed the appearance of a precipitate. To check the progress of the reaction, an aliquot was added over water acidulated with MeSO₃H, appearing a white precipitated whose ¹H NMR analysis indicated that its structure corresponded to the cyclization product. At this time, 2-amino-6-methylpyridine (15.8 g, 0.15 mol) was added to the reaction flask. It was refluxed for two hours until all solid had been dissolved. Then the reaction mixture was cooled and added to excess of methanesulfonic acid (50 mL) in water and ice, and the obtained solid was filtered. The mother liquor was extracted with EtOAc, the layers were separated, and after evaporation of the organic solvent, the product obtained could be coupled with the above solid to afford 25.0 g of compound **147** (94 % yield).

This product could be purified according to the following procedure: the solid obtained (10.0 g, 0.016 mol) was dissolved in 20 mL of THF and 100 mL of ether. Then NH₃ was bubbled appearing a precipitate. The solution was stirred a few more minutes until no more precipitate appeared and was filtered, obtaining 7.5 g of pure compound as a white solid corresponding to the ammonium salt of receptor **147** with a yield of 75 %.

mp: 228-230 °C.

¹H NMR (DMSO-*d*₆) δ (ppm): 0.94 (s, 9H), 1.09 (s, 3 H), 1.19 (s, 3H), 1.42 (d, *J* = 14.6 Hz, 1H), 1.63 (d, *J* = 14.6 Hz, 1H), 2.41 (s, 3H), 3.00 (br s, 2H), 4.44 (t, *J* = 5.1 Hz, 1H), 5.47 (s, 1H), 7.06 (d, *J* = 7.3 Hz, 1H), 7.63 (d, *J* = 2.6 Hz, 1H), 7.72 (dd, *J* = 7.3, 8.0 Hz, 1H), 7.80 (d, *J* = 8.0 Hz, 1H), 7.83 (s, 1H), 9.99 (s, NH).

¹³C NMR (DMSO-*d*₆) δ (ppm): 23.5 (CH₃), 28,7 (CH₃), 29,1 (CH₃), 31.0 (CH₂), 31.2 (C), 31.4 (CH₃ x 3), 41.8 (CH), 53.6 (CH₂), 57.5 (C), 109.1 (C), 111.6 (CH), 112.9 (C), 120.0 (CH), 121.6 (C), 128.7 (CH), 129.1 (C), 130.3 (CH), 134.5 (CH), 138.6 (CH), 149.4 (C), 151.8 (C), 156.9 (C), 166.9 (C), 175.7 (C), 196.9 (C).

IR (nujol, cm⁻¹): 3390, 3306, 2916, 2839, 1710, 1606, 1521, 1456, 1366, 1249, 1203, 1152.

HRMS (ESI): 606.1284 (M + H)⁺, calcd for C₂₇H₃₃BrN₃O₆S 606.1268.

Receptor 147 resolution

Receptor **147** (6.4 g, 10.5 mmol) and cinchonine (3.1 g, 10.5 mmol) were dissolved in 56 mL of a CHCl₃-CH₃OH (8:1) solution. This solution was transferred into a container with magnetic stirring which at the same time was introduced within a receptacle with ether. The outer vessel was closed and allowed to stir overnight. After 13 hours, the solid obtained was filtered, yielding the crystals of the salt of one of the receptor enantiomers with cinchonine whereas the other enantiomer remains in the filtrate.

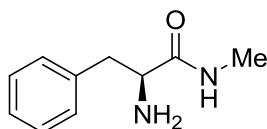
Then the complex with cinchonine was dissolved in methanol and was added to an aqueous solution of formic acid, crystallising the enantiomerically pure receptor. Direct filtration of the solution led to a receptor which typically has small amounts of cinchonine, but the extraction with ethyl acetate and subsequent concentration allowed isolation of the free receptor with a high purity and a yield of 70 %.

$$[\alpha]_{\text{D}}^{20} = +212.3 \text{ (} c = 0.99, \text{CHCl}_3\text{)}.$$

From the mother liquor it was possible to obtain the other enantiomer of receptor **147**, continuing fractional crystallization and after the subsequent breakdown of the salt with an aqueous solution of formic acid and extraction with ethyl acetate (72 % yield).

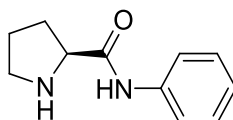
$$[\alpha]_{\text{D}}^{20} = -203.9 \text{ (} c = 1.09, \text{CHCl}_3\text{)}.$$

- (S)-2-amino-N-methyl-3-phenylpropanamide



Compound described in the literature.²³³

- (S)-N-phenylpyrrolidine-2-carboxamide



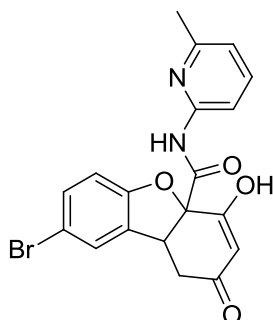
Compound described in chapter 2.

²³³ Samulis, L.; Tomkinson, N. C. O. *Tetrahedron* **2011**, *67*, 4263-4267.

- All amines described in figure 6.21, except for the two above compounds, are commercially available.

-Compound **148** was described in the previous chapter.

- **8-Bromo-4-hydroxy-N-(6-methylpyridine-2-yl)-2-oxo-1,2,4a,9b-tetrahydrodibenzo[*b,d*]furan-4a-carboxamide (149)**



The synthesis was carried out similarly to compound **147** but using compound **88** as starting material. In this case the purification was performed by silica gel chromatography with CH₂Cl₂-EtOAc mixtures (59 % yield).

mp: 112-114 °C.

¹H NMR (CDCl₃) δ (ppm): 2.42 (s, 3 H), 2.79 (dd, *J* = 2.7, 17.6 Hz, 1H), 2.96 (dd, *J* = 7.0, 17.6 Hz, 1H), 4.21 (m, 1H), 5.64 (s, 1H), 6.70 (d, *J* = 9.0 Hz, 1H), 6.93 (d, *J* = 7.4 Hz, 1H), 7.10-7.38 (m, 2H), 7.61 (t, *J* = 8.0 Hz, 1H), 7.93 (d, *J* = 8.2 Hz, 1H), 8.85 (br s, 1H).

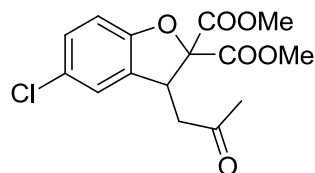
¹³C NMR (CDCl₃) δ (ppm): 23.4 (CH₃), 33.7 (CH₂), 42.9 (CH), 88.4 (C), 107.2 (CH), 111.7 (CH), 112.3 (CH), 114.8 (C), 120.5 (CH), 126.5 (CH), 130.5 (C), 132.3 (CH), 139.7 (CH), 148.9 (C), 155.5 (C), 156.6 (C), 167.7 (C), 177.8 (C), 189.5 (C).

IR (film, cm⁻¹): 3390, 3059, 2923, 2358, 1703, 1612, 1573, 1534, 1456, 1418, 1301, 1236, 1190, 1139, 1028.

HRMS (ESI): 415.0293 (M + H)⁺, 415.0288 calcd for C₁₉H₁₆BrN₂O₄ 415.0288.

- Compounds **157**²³⁴ and **158**²³⁵ were synthesized according to the experimental procedure described in literature, showing the same physical and spectroscopic properties.

- **5-Chloro-3-(2-oxopropyl)-benzofuran-2,2(3H)-dicarboxylate (159)**



To a suspension of compound **158** (54.0 g, 0.28 mol) and K_2CO_3 (76.0 g, 0.55 mol) in 194 mL of DMF, dimethyl chloromalonate (91.6 g, 0.55 mol) was added from an addition funnel over 45 min. After stirring for 30 min, it was added over HCl 35 % v/v diluted in water and ice. Hexane was added, crystallizing the desired compound. Then the compound was filtered and recrystallized from MeOH-H₂O, yielding 52.0 g (58 % yield).

mp: 71-73 °C.

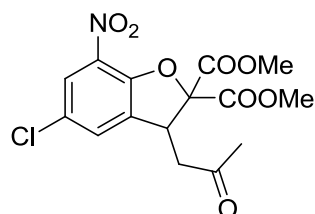
¹H NMR (CDCl₃) δ (ppm): 2.18 (s, 3H), 2.72 (dd, *J* = 8.6, 18.0, 1H), 2.90 (dd, *J* = 5.1, 18.0 Hz, 1H), 3.80 (s, 3H), 3.83 (s, 3H), 4.69 (dd, *J* = 5.1, 8.6, 1H), 6.83 (d, *J* = 8.2 Hz, 1H), 7.00 (dd, *J* = 2.0, 8.2 Hz, 1H), 7.05 (d, *J* = 2.0 Hz, 1H).

¹³C NMR (CDCl₃) δ (ppm): 30.4 (CH₃), 43.4 (CH), 45.1 (CH₂), 53.5 (CH₃), 54.0 (CH₃), 91.8 (C), 111.3 (CH), 125.2 (CH), 127.3 (C), 129.2 (CH), 130.1 (C), 156.1 (C), 167.0 (C), 167.7 (C), 205.1 (C).

IR (film, cm⁻¹): 3474, 3007, 2955, 1748, 1463, 1444, 1366, 1288, 1236, 1184, 1106, 1054, 827.

HRMS (ESI): 327.0628 (M + H)⁺, calcd for C₁₅H₁₆ClO₆ 327.0630.

- **5-Chloro-7-nitro-3-(2-oxopropyl) benzofuran-2,2(3H)-dicarboxylate (160)**



In a round bottom flask equipped with a solid addition funnel, fuming nitric acid (30 mL, 0.65 mol) was poured and cooled at -30 °C. Then compound **159** (10.0 g, 0.03 mol) was added

²³⁴ Aitken, R. A.; Bouquet, J.; Frank, J.; Gidlow, A. L. G.; Powder, Y. L.; Ramsewak, R. S.; Reynolds, W. F. *RSC Adv.* **2013**, *3*, 7230-7232.

²³⁵ Huang, X.; Zhang, T. *J. Org. Chem.* **2010**, *75*, 506-509.

gradually so that the temperature did not rise above -30 °C. After 35 min the addition was complete. Once all solid was dissolved (5 minutes later) a spectrum of an aliquot was directly made to verify that no starting material was left. The crude reaction was poured onto water with ice and filtered. To purify it, it was suspended in MeOH, crushed slightly to dissolve the impurities and was allowed to stir for two hours. It was filtered and dried, obtaining 6.6 g (58 % yield) of a light yellow solid.

mp: 148-150 °C.

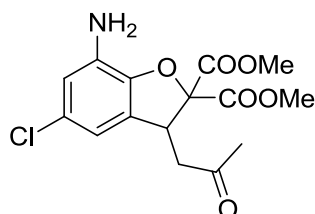
¹H NMR (CDCl₃) δ (ppm): 2.20 (s, 3H), 2.78 (dd, *J* = 9.0, 18.0 Hz, 1H), 3.01 (dd, *J* = 4.4, 18.0 Hz, 1H), 3.81 (s, 3H), 3.85 (s, 3H), 4.71 (dd, *J* = 4.4, 9.0 Hz, 1H), 7.33 (dd, *J* = 1.2, 2.0 Hz, 1H), 7.91 (dd, *J* = 0.8, 2.0 Hz, 1H).

¹³C NMR (CDCl₃) δ (ppm): 30.3 (CH₃), 42.8 (CH), 44.5 (CH₂), 53.9 (CH₃), 54.3 (CH₃), 93.1 (C), 124.5 (CH), 127.4 (C), 131.2 (CH), 133.0 (C), 135.0 (C), 151.2 (C), 166.0 (C), 166.6 (C), 204.8 (C).

IR (nujol, cm⁻¹): 2936, 2858, 2735, 2663, 1736, 1619, 1547, 1469, 1385, 1327, 1268, 1203, 1100, 1048, 736.

HRMS (ESI): 389.0731 (M + NH₄)⁺, calcd for C₁₅H₁₈ClN₂O₈ 389.0746.

- 7-Amino-5-chloro-3-(2-oxopropyl)-benzofuran-2,2(3H)-dicarboxylate (161)



SnCl₂·2H₂O (12.0 g, 0.05 mol) was dissolved in 20 mL of MeOH using few drops of concentrated HCl and heated to reflux. Once dissolved, compound **160** (6.6 g, 0.02 mol) was slowly added. In the first additions the reaction first became hot, facilitating its progress, but after the following additions refluxing was needed for dissolving the solid added. After refluxing 15 min, it was stopped and 5 min later the addition was completed. The solution was stirred 10 min more, following the progress of the reaction by TLC using CH₂Cl₂-EtOAc 9:1 as eluent. According to the TLC it was stirred 15 min more.

To work out the reaction it was transferred to a 500 mL Erlenmeyer flask, 30 mL of MeOH was added and then sodium carbonate (14.1 g, 0.13 mol) and EtOAc (approx 250 mL). It was heated a little and left stirring 5 minutes to allow the growing of the tin salts crystals and facilitate the subsequent filtration. It was settled for 5 min and then filtered. EtOAc was evaporated obtaining 5.3 g (80 % yield) of a viscous oil.

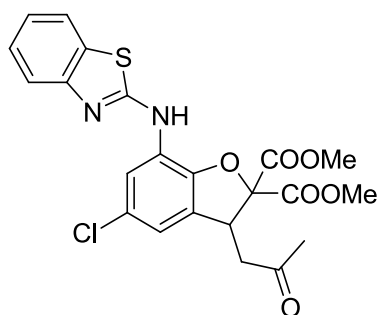
$^1\text{H NMR}$ (CDCl_3) δ (ppm): 2.18 (s, 3H), 2.71 (dd, $J = 8.2, 18.0$ Hz, 1H), 2.87 (dd, $J = 5.5, 18.0$ Hz, 1H), 3.81 (s, 3H), 3.84 (s, 3H), 4.70 (dd, $J = 5.5, 8.2$ Hz, 1H), 6.46 (dd, $J = 0.8, 2.0$ Hz, 1H), 6.56 (d, $J = 2.0$ Hz, 1H).

$^{13}\text{C NMR}$ (CDCl_3) δ (ppm): 30.5 (CH_3), 44.2 (CH), 45.2 (CH_2), 53.4 (CH_3), 53.9 (CH_3), 91.7 (C), 114.1 (CH), 115.6 (CH), 127.8 (C), 129.3 (C), 131.9 (C), 143.4 (C), 167.1 (C), 167.9 (C), 205.1 (C).

IR (film, cm^{-1}): 3740, 3468, 3371, 2955, 2929, 2845, 1755, 1638, 1482, 1437, 1288, 1229, 1113, 1067.

HRMS (ESI): 342.0739 ($\text{M} + \text{H}$) $^+$, 342.0739 calcd for $\text{C}_{15}\text{H}_{17}\text{ClNO}_6$ 342.0739.

- **7-(Benzo[d]thiazol-2-ylamino)-5-chloro-3-(2-oxopropyl)-benzofuran-2,2(3H)-dicarboxylate (163)**



The amine **161** (3.5 g, 10.2 mmol) and 2-chlorobenzothiazole (10.5 g, 61.9 mmol) were melted at 80 °C for 40 minutes. The reaction was worked out over aqueous Na_2CO_3 and extracted with EtOAc. It was purified by silica gel column, yielding 3.3 g (68 % yield).

mp: 124-126 °C.

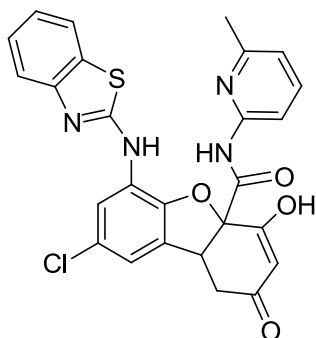
$^1\text{H NMR}$ (CDCl_3) δ (ppm): 2.18 (s, 3H), 2.76 (dd, $J = 8.6, 18.0$ Hz, 1H), 2.92 (dd, $J = 5.5, 18.0$ Hz, 1H), 3.83 (s, 3H), 3.85 (s, 3H), 4.78 (dd, $J = 5.5, 8.6$ Hz, 1H), 6.78 (dd, $J = 0.8, 1.9$ Hz, 1H), 7.20 (td, $J = 1.2, 7.6$ Hz, 1H), 7.37 (td, $J = 1.2, 7.6$ Hz, 1H), 7.66 (d, $J = 7.8$ Hz, 1H), 7.74 (d, $J = 8.2$ Hz, 1H), 8.37 (d, $J = 2.0$ Hz, 1H).

$^{13}\text{C NMR}$ (CDCl_3) δ (ppm): 30.5 (CH_3), 44.2 (CH), 45.1 (CH_2), 53.6 (CH_3), 54.1 (CH_3), 92.2 (C), 118.4 (CH), 118.5 (CH), 120.7 (CH), 121.0 (CH), 123.3 (CH), 125.3 (C), 126.4 (CH), 128.2 (C), 129.1 (C), 130.8 (C), 144.2 (C), 152.0 (C), 160.9 (C), 166.7 (C), 167.5 (C), 204.9 (C).

IR (nujol, cm^{-1}): 3384, 3195, 2942, 2916, 2858, 2728, 2669, 1755, 1710, 1638, 1521, 1463, 1366, 1281, 1190, 1080, 1022, 950, 860, 756, 717.

HRMS (ESI): 475.0729 ($\text{M} + \text{H}$) $^+$, calcd for $\text{C}_{22}\text{H}_{20}\text{ClN}_2\text{O}_6\text{S}$ 475.0725.

- 6-(Benzo[d]thiazol-2-ylamino)-8-chloro-4-hydroxy-N-(6-methylpyridin-2-yl)-2-oxo-1,2,4a,9b-tetrahydrodibenzo[b,d]furan-4a-carboxamide (166)



The cyclization was carried out following the experimental procedure described for compound **147** (50 % yield) but in this case the reaction was worked up into an aqueous solution of camphorsulfonic acid, washing the precipitate obtained with an aqueous solution of glycine to remove acid residues.

mp: 172-174 °C.

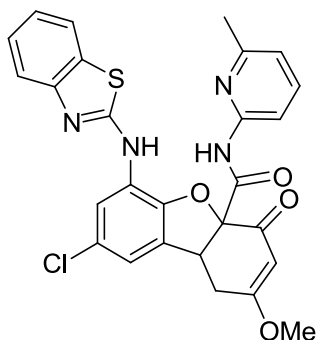
¹H NMR (CDCl₃-CD₃OD) δ(ppm): 2.46 (s, 3H), 2.81 (dd, *J* = 3.5, 17.6 Hz, 1H), 3.19 (dd, *J* = 7.4, 17.6 Hz, 1H), 4.32 (dd, *J* = 3.5, 7.4 Hz, 1H), 5.58 (s, 1H), 6.81 (s, 1H), 6.95 (d, *J* = 7.4 Hz, 1H), 7.16 (t, *J* = 7.4 Hz, 1H), 7.34 (t, *J* = 7.6 Hz, 1H), 7.59-7.73 (m, 3H), 7.99 (d, *J* = 8.2 Hz, 1H), 8.47 (s, 1H).

¹³C NMR (CDCl₃-CD₃OD) δ (ppm): 23.6 (CH₃), 32.7 (CH₂), 43.2 (CH), 88.7 (C), 106.2 (CH), 111.2 (CH), 116.7 (CH), 119.1 (CH), 120.0 (CH), 120.2 (CH), 120.6 (CH), 122.7 (CH), 125.9 (CH), 128.1 (C), 129.1 (C), 130.5 (C), 139.1 (CH), 143.5 (C), 149.3 (C), 151.7 (C), 156.9 (C), 161.5 (C), 167.4 (C), 180.2 (C), 180.3 (C), 187.0 (C).

IR (nujol, cm⁻¹): 3273, 2929, 2722, 2663, 1645, 1606, 1581, 1469, 1366, 1307, 1236, 1190, 1113, 1035, 840, 749.

HRMS (ESI): 519.0892 (M + H)⁺, calcd for C₂₆H₂₀ClN₄O₄S 519.0888.

- 6-(Benzo[d]thiazol-2-ylamino)-8-chloro-2-methoxy-N-(6-methylpyridin-2-yl)-4-oxo-1,4,4a,9b-tetrahydrodibenzo[b,d]furan-4a-carboxamide (169)



The formation of the methyl ether from compound **166** was carried out following the same experimental procedure described in the formation of receptor **91** (chapter 5).

mp: > 230 °C.

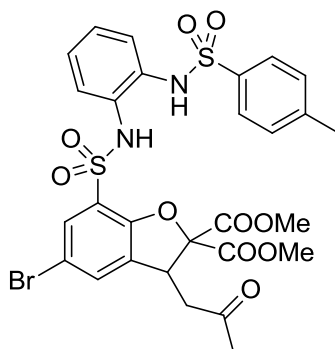
¹H NMR (CDCl₃-CH₃OH) δ (ppm): 2.45 (s, 3H), 2.85 (dd, *J* = 3.2, 18.0 Hz, 1H), 3.32 (dd, *J* = 7.3, 18.0 Hz, 1H), 3.76 (s, 3H), 4.40 (dd, *J* = 3.2, 7.3 Hz, 1H), 5.62 (s, 1H), 6.80 (dd, *J* = 1.1, 2.0 Hz, 1H), 6.93 (d, *J* = 7.5 Hz, 1H), 7.18 (dt, *J* = 0.9, 7.5 Hz, 1H), 7.35 (dt, *J* = 1.2, 7.6 Hz, 1H), 7.59 (dd, *J* = 7.7, 8.0 Hz, 1H), 7.66 (d, *J* = 7.9 Hz, 1H), 7.74 (d, *J* = 7.9 Hz, 1H), 7.95 (d, *J* = 8.2 Hz, 1H), 8.55 (dd, *J* = 0.5, 1.4 Hz, 1H), 9.48 (s, NH).

¹³C NMR (CDCl₃-CH₃OH) δ (ppm): 23.9 (CH₃), 29.5 (CH₂), 42.8 (CH), 56.4 (CH₃), 89.4 (C), 102.6 (CH), 111.0 (CH), 116.3 (CH), 119.1 (CH), 120.4 (CH), 120.5 (CH), 120.6 (CH), 122.8 (CH), 125.9 (CH), 126.0 (C), 128.3 (C), 128.5 (C), 130.8 (C), 138.9 (CH), 143.6 (C), 149.5 (C), 152.0 (C), 157.0 (C), 161.1 (C), 166.8 (C), 177.0 (C), 190.3 (C).

IR (nujol, cm⁻¹): 3455, 3286, 2955, 2923, 2852, 1690, 1645, 1534, 1469, 1379, 1301, 1236, 1190, 1100, 1054, 860.

HRMS (ESI): 533.1042 (M + H)⁺, calcd for C₂₇H₂₂ClN₄O₄S 533.1045.

- Dimethyl-5-bromo-7-(*N*-(2-(4-methylphenylsulfonamido)phenyl)sulfamoyl)-3-(2-oxopropyl)benzofuran-2,2(3*H*)-dicarboxylate (176)



The acid chloride **88** (2.69 g, 5.7 mmol) and tosylated orthophenylenediamine²³⁶ (1.5 g, 5.7 mmol) were dissolved in 3 mL of anhydrous pyridine and stirred for one hour. The product was purified by silica gel chromatography with CH₂Cl₂, yielding 1.4 g (36 % yield).

mp: vitreous compound.

¹H RMN (CDCl₃) δ (ppm): 2.21 (s, 3H), 2.40 (s, 3H), 2.80 (dd, *J* = 9.0, 18.4 Hz, 1H), 3.03 (dd, *J* = 4.3, 18.4 Hz, 1H), 3.84 (s, 3H), 3.88 (s, 3H), 4.70 (dd, *J* = 4.3, 9.0 Hz, 1H), 5.30 (s, NH), 7.00-7.07 (m, 2H), 7.14-7.19 (m, 2H), 7.25 (d, *J* = 7.8 Hz, 2H), 7.36 (dd, *J* = 0.8, 2.0 Hz, 1H), 7.56 (dd, *J* = 0.8, 2.0 Hz, 1H), 7.66 (d, *J* = 8.6 Hz, 2H).

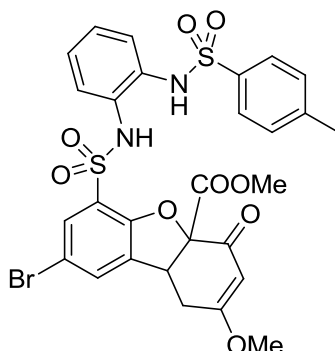
¹³C RMN (CDCl₃) δ (ppm): 21.8 (CH₃), 30.3 (CH₃), 43.2 (CH), 44.5 (CH₂), 54.0 (CH₃), 54.5 (CH₃), 92.9 (C), 114.3 (C), 123.0 (C), 125.2 (CH), 125.5 (CH), 127.0 (CH), 127.7 (CH x 2), 127.8 (CH), 129.4 (C), 129.9 (CH x 2), 131.4 (CH), 131.4 (C), 133.0 (C), 133.1 (CH), 136.4 (C), 144.3 (C), 153.3 (C), 166.4 (C), 166.9 (C), 204.9 (C).

IR (film, cm⁻¹): 3273, 3072, 2955, 1755, 1599, 1495, 1437, 1340, 1288, 1236, 1197, 1165, 1080, 1074, 931.

HRMS (ESI): 712.0637 (M + NH₄)⁺, calcd for C₂₈H₃₁BrN₃O₁₀S₂ 712.0629.

²³⁶ Saha, S.; Moorthy, J. N. *Tetrahedron Lett.* **2010**, *51*, 912-916.

- Methyl 8-bromo-2-methoxy-6-(*N*-(2-(4-methylphenylsulfonamido)phenyl)sulfamoyl)-4-oxo-1,4,4a,9b-tetrahydrodibenzo[*b,d*]furan-4a-carboxylate (177)



The cyclization was carried out following the same experimental procedure described for compound **81** in chapter 5.

mp: vitreous compound.

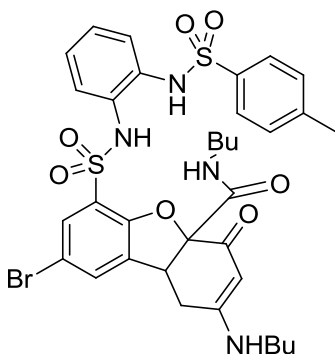
¹H RMN (CDCl₃) δ (ppm): 2.38 (s, 3H), 2.83 (dd, *J* = 1.3, 18.6 Hz, 1H), 3.24 (dd, *J* = 7.2, 18.6 Hz, 1H), 3.74 (s, 3H), 3.86 (s, 3H), 4.31 (d, *J* = 4.7 Hz, 1H), 5.56 (s, 1H), 6.86-7.08 (m, 3H), 7.23 (d, *J* = 7.8 Hz, 2H), 7.17-7.30 (m, 1H), 7.41 (s, 1H), 7.58 (s, 1H), 7.65 (d, *J* = 8.2 Hz, 2H), 8.06 (s, NH).

¹³C RMN (CDCl₃) δ (ppm): 21.8 (CH₃), 29.1 (CH₂), 42.1 (CH), 54.1 (CH₃), 56.9 (CH₃), 90.4 (C), 102.6 (CH), 114.4 (C), 123.7 (C), 124.6 (CH), 125.3 (CH), 126.9 (CH), 127.3 (CH), 127.5 (CH x 2), 129.3 (C), 130.0 (CH x 2), 131.1 (C), 131.5 (CH), 131.8 (CH), 132.5 (C), 136.8 (C), 144.2 (C), 153.2 (C), 167.8 (C), 177.0 (C), 187.9 (C).

IR (film, cm⁻¹): 3468, 3306, 3072, 2955, 1768, 1658, 1606, 1508, 1437, 1392, 1353, 1249, 1203, 1158, 1087, 924.

HRMS (ESI): 694.0515 (M + NH₄)⁺, calcd for C₂₈H₂₉BrN₃O₉S₂ 694.0523.

- 8-Bromo-*N*-butyl-2-(butylamino)-6-(*N*-(2-(4-methylphenylsulfonamido)phenyl)sulfamoyl)-4-oxo-1,4,4a,9b-tetrahydrodibenzo[*b,d*]furan-4a-carboxamide (178)



Compound **177** was dissolved in butylamine. Then the excess of butylamine was evaporated, obtaining compound **178** which can be purified by silica gel chromatography.

mp: 110-112 °C.

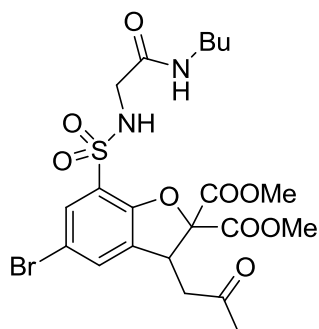
¹H NMR (CDCl₃) δ (ppm) : 0.86 (t, *J* = 7.3 Hz, 6H), 1.30 (q, *J* = 7.3 Hz, 4H), 1.40-1.60 (m, 4H), 2.39 (s, 3H), 2.78 (d, *J* = 16.9 Hz, 1H), 3.20-3.45 (m, 5H), 4.28 (s, 1H), 5.21 (s, 1H), 6.95-7.00 (m, 2H), 7.20-7.25 (m, 3H), 7.37 (s, 1H), 7.55 (s, 1H), 7.63 (d, *J* = 8.2 Hz, 1H), 7.71 (d, *J* = 8.2 Hz, 2H).

¹³C NMR (CDCl₃) δ (ppm): It was not possible to perform this spectrum due to relaxation problems of the molecule.

IR (nujol, cm⁻¹): 3552, 3390, 3293, 3202, 2949, 2936, 2852, 1664, 1567, 1502, 1469, 1379, 1346, 1262, 1210, 1152, 1087, 937.

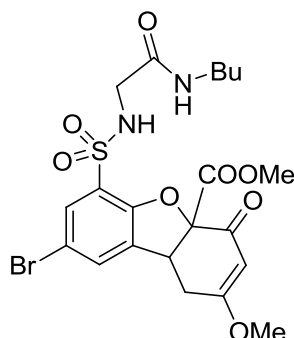
HRMS (ESI): 759.1522 (M + H)⁺, calcd for C₃₄H₄₀BrN₄O₇S₂ 759.1516.

- 5-Bromo-7-(*N*-(2-(butylamino)-2-oxoethyl)sulfamoyl)-3-(2-oxopropyl)-benzofuran-2,2(3*H*)-dicarboxylate (**179**)



Glycine butyl amide²³⁷ (0.7 g, 5.4 mmol) and triethylamine (0.8 mL, 5.7 mmol) were dissolved in 7 mL of CH₂Cl₂. To this solution, with stirring, a solution of compound **88** (2.5 g, 5.3 mmol) dissolved in 10 mL of CH₂Cl₂ was added dropwise. Water was then added and the organic phase was extracted twice. It was then dried and the solvent was removed by evaporation under reduced pressure. The solid obtained was purified by silica gel column with CH₂Cl₂ and CH₂Cl₂/EtOAc, obtaining 1.6 g of the desired compound (55 % yield).

- Methyl-8-bromo-6-(*N*-(2-(butylamino)-2-oxoethyl)sulfamoyl)-2-methoxy-4-oxo-1,4,4a,9b-tetrahydrobenzo[*b,d*]furan-4a-carboxylate (**180**)



The cyclization was carried out following the same experimental procedure described for compound **177**.

mp: vitreous compound.

¹H RMN (CDCl₃) δ (ppm): 0.90 (t, *J* = 7.0 Hz, 3H), 1.20-1.41 (m, 2H), 1.41-1.59 (m, 2H), 2.79 (dd, *J* = 3.7, 18.2 Hz, 1H), 3.18 (dd, *J* = 7.4, 18.2 Hz, 1H), 3.18-3.33 (m, 2H), 3.49 (d, *J* = 5.9 Hz, 2H), 3.76 (s, 3H), 3.81 (s, 3H), 4.23 (dd, *J* = 3.7, 6.4 Hz, 1H), 5.57 (s, 1H), 6.32 (t, *J* = 6.1 Hz, 1H), 6.78 (t, *J* = 5.1 Hz, 1H), 7.45 (s, 1H), 7.75 (s, 1H).

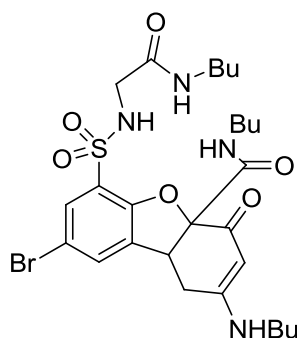
²³⁷ Kondo, S.-I.; Hiraoka, Y.; Kurumatani, N.; Yano, Y. *Chem. Commun.* **2005**, 1720-1722.

^{13}C RMN (CDCl_3) δ (ppm): 13.9 (CH_3), 20.1 (CH_2), 29.2 (CH_2), 31.5 (CH_2), 39.4 (CH_2), 42.2 (CH), 46.0 (CH_2), 53.8 (CH_3), 56.9 (CH_3), 90.3 (C), 102.5 (CH), 114.4 (C), 123.8 (C), 131.1 (CH), 131.4 (CH), 132.8 (C), 153.3 (C), 167.6 (C), 168.4 (C), 176.9 (C), 187.8 (C).

IR (nujol, cm^{-1}): 3539, 3390, 3306, 3085, 2955, 2865, 1781, 1677, 1612, 1541, 1456, 1398, 1359, 1249, 1210, 1080.

HRMS (ESI): 545.0591 ($\text{M} + \text{H}$) $^+$, calcd for $\text{C}_{21}\text{H}_{26}\text{BrN}_2\text{O}_8\text{S}$ 545.0588.

- 8-Bromo-*N*-butyl-2-(butylamino)-6-(*N*-(2-(butylamino)-2-oxoethyl)sulfamoyl)-4-oxo-1,4,4a,9b-tetrahydrodibenzo[*b,d*]furan-4a-carboxamide (181)



The experimental procedure was the same as described in the preparation of compound **178**.

mp: 188-190 °C.

^1H NMR (CDCl_3) δ (ppm): 0.85-0.96 (m, 9H), 1.28-1.40 (m, 6H), 1.44-1.63 (m, 6H), 2.72 (d, J = 16.8 Hz, 1H), 3.05-3.13 (m, 2H), 3.19-3.33 (m, 4H), 3.39 (dd, J = 7.0, 16.8 Hz, 1H), 3.47 (s, 2H), 4.21 (s, 1H), 5.27 (s, 1H), 7.41 (s, 1H), 7.75 (s, 1H).

^{13}C NMR (CDCl_3) δ (ppm): It was not possible to perform this spectrum due to relaxation problems of the molecule.

IR (film, cm^{-1}): 3299, 3079, 2955, 2916, 2852, 1645, 1534, 1437, 1346, 1190, 1158, 1054, 970.

HRMS (ESI): 627.1854 ($\text{M} + \text{H}$) $^+$, calcd for $\text{C}_{27}\text{H}_{40}\text{BrN}_4\text{O}_6\text{S}$ 627.1846.

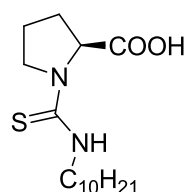
Guests

- Guests **132**, **133**, **137**, **138**, **142**, **144**, **146**, **152** and **171** are commercial.

- Guests **135** and **145** have been previously used in our group.²³⁸

- Guests **140**,²³⁹ **141**,²⁴⁰ **150**,²⁴¹ **151**,²⁴² **153**,²⁴³ **154**,²⁴⁴ **155**,²⁴⁵ **156**,²⁴⁶ **172**,²⁴⁷ **173**,²⁴⁸ **174**²⁴⁹ and **175**²⁵⁰ were prepared according to the experimental procedure described in literature, showing the same physical and spectroscopical properties.

- (**S**)-1-(decylcarbamotioyl) pyrrolidine-2-carboxylic acid (**134**)



The experimental procedure followed was the same described in chapter 5 for thioureas synthesis. 75 % yield.

$[\alpha]_D^{20} = -7.7$ ($c=1.07$, CHCl_3).

¹H RMN (CDCl_3) δ (ppm): 0.81 (t, $J = 6.5$ Hz, 3H), 1.19 (br s, 14H), 1.47-1.68 (m, 3H), 1.98-1.32 (m, 3H), 3.40-3.57 (m, 1H), 3.68 (dt, $J = 2.7, 7.4$ Hz, 2H), 3.80-3.98 (m, 1H), 4.05-4.19 (m, 1H).

¹³C RMN (CDCl_3) δ (ppm): 14.1 (CH_3), 22.6 (CH_2), 26.7 (CH_2), 26.8 ($\text{CH}_2 \times 2$), 27.5 (CH_2), 29.1 (CH_2), 29.2 (CH_2), 29.4 (CH_2), 29.5 (CH_2), 31.8 (CH_2), 41.8 (CH_2), 48.4 (CH_2), 65.0 (CH), 173.7 (C), 187.1 (C).

IR (nujol, cm^{-1}): 3461, 2923, 2865, 1755, 1431, 1353, 1268, 1229, 1190, 1145, 1048.

HRMS (ESI): 297.2002 ($\text{M} - \text{H}_2\text{O} + \text{H}^+$), calcd for $\text{C}_{16}\text{H}_{29}\text{N}_2\text{OS}$ 297.1995.

²³⁸ Oliva, A. I. *Enantioselective receptors with tetrahydrobenzoxanthene skeleton for amino acids Derivatives*; Doctoral Thesis: University of Salamanca, 2003.

²³⁹ Brotherton, C. A.; Balskus, E. P. *J. Am. Chem. Soc.* **2013**, *135*, 3359-3362.

²⁴⁰ Zhang, J.; Ma, L.; Lu, H.; Wang, Y.; Li, S.; Wang, S.; Zhou, G. *Eur. J. Med. Chem.* **2012**, *58*, 281-286.

²⁴¹ Bressi, J. C.; de Jong, R.; Wu, Y.; Jennings, A. J.; Brown, J. W.; O'Connell, S.; Tari, L. W.; Skene, R. J.; Vu, P.; Navre, M.; Cao, X.; Gangloff, A. R. *Bioorg. Med. Chem. Lett.* **2010**, *20*, 3138-3141.

²⁴² Liang, J.; Ruble, J. C.; Fu, G. C. *J. Org. Chem.* **1998**, *63*, 3154-3155.

²⁴³ Muñiz, F. M.; Alcázar, V.; Sanz, F.; Simón, L.; Fuentes de Arriba, Á. L.; Raposo, C.; Morán, J. R. *Eur. J. Org. Chem.* **2010**, 6179-6185.

²⁴⁴ Xu, D.-Q.; Yue, H.-D.; Luo, S.-P.; Xia, A.-B.; Zhang, S.; Xu, Z.-Y. *Org. Biomol. Chem.* **2008**, *6*, 2054-2057.

²⁴⁵ Palovics, E.; Schindler, J.; Faigl, F.; Fogassy, E. *Tetrahedron: Asymmetry* **2010**, *21*, 2429-2434.

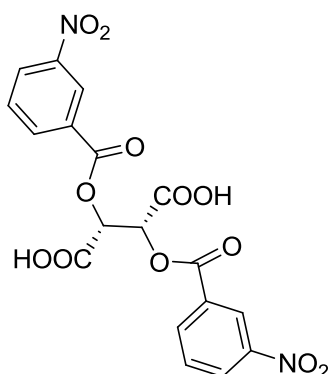
²⁴⁶ Muramatsu, I.; Murakami, M.; Yoneda, T.; Hagitani, A. *Bull. Chem. Soc. Japan* **1965**, *38*, 244-246.

²⁴⁷ Hartner, F. W.; Cvetovich, R. J.; Tsay, F.-R.; Amato, J. S.; Pipik, B.; Grabowski, E. J. J.; Reider, P. J. *J. Org. Chem.* **1999**, *64*, 7751-7755.

²⁴⁸ MacFarland, D. K.; Landis, C. R. *Organometallics* **1996**, *15*, 483-485.

²⁴⁹ Kawase, T.; Saito, I.; Oida, T. *Journal of Oleo Science* **2011**, *60*, 61-69.

²⁵⁰ Shim, Y.-J.; Choi, K. *Org. Lett.* **2010**, *12*, 880-882.

- Di(3-nitrobenzoyl)-L-tartaric acid (143)

A two necked round bottomed flask equipped with thermometer was placed in an ice bath. 90 % fuming nitric acid (3.0 mL, 65.4 mmol) was added and then dibenzoyl-*L*-tartaric acid (1.0 g, 2.8 mmol) in small portions so that temperature did not rise over 10 °C. The solution was stirred until added solid had completely dissolved. Then it was added over ice and extracted with ether. The organic phase was separated, dried over Na₂SO₄ and evaporated under reduced pressure. The compound was purified by recrystallization in CH₂Cl₂, obtaining 0.5 g (40 % yield).

$[\alpha]_D^{20} = -8.3$ ($c = 1.96$, MeOH).

mp: 186-187 °C.

¹H RMN (CDCl₃-CD₃OD) δ (ppm): 6.02 (s, 2H), 7.68 (t, $J = 8.0$ Hz, 2H), 8.41 (dd, $J = 1.8, 8.0$ Hz, 4H), 8.87 (t, $J = 2.0$ Hz, 2 H).

¹³C RMN (CDCl₃-CD₃OD) δ (ppm): 72.3 (CH x 2), 125.2 (CH x 2), 128.3 (CH x 2), 130.3 (CH x 2), 130.8 (C x 2), 135.8 (CH x 2), 148.5 (C x 2), 163.6 (C x 2), 167.6 (C x 2).

IR (film, cm⁻¹): 1742, 1619, 1541, 1469, 1379, 1353, 1249, 1126, 1061, 911, 723.

HRMS (ESI): 471.0285 (M + Na)⁺, calcd for C₁₈H₁₂N₂ONaO₁₂ 471.0282.

Chiral compounds

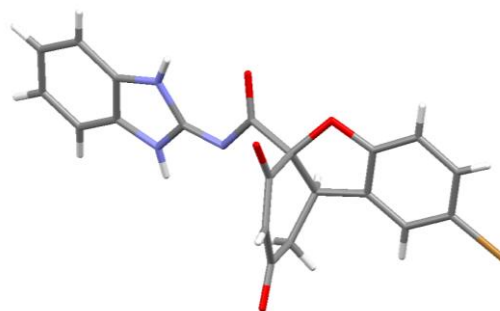
Enantiomeric ratio of racemic guest **114** extraction shown in figure 6.43 was determined by chiral HPLC using a IA-3 column (0.2 mL/min) with hexane/isopropyl alcohol 9/1 and 0.1 % HCOOH as eluent. Retention times were 5.9 and 11.1 minutes.



**VNIVERSIDAD
D SALAMANCA**

CAMPUS DE EXCELENCIA INTERNACIONAL

CHAPTER 7: Bifunctional benzofuran-derived catalysts



7.1. INTRODUCTION

As it was seen in the previous chapter, it was possible to isolate receptor **147** in the enol form. Although this enol should be found in a keto-enol equilibrium with the isomeric diketone **147 b** and the isomers **147 c** and **147 d**, according to ^1H NMR and HMBC spectra, we believe that, essentially, the predominant enol tautomer is **147 a**, which is forming an intramolecular hydrogen bond with the furan oxygen atom (figure 7.1).

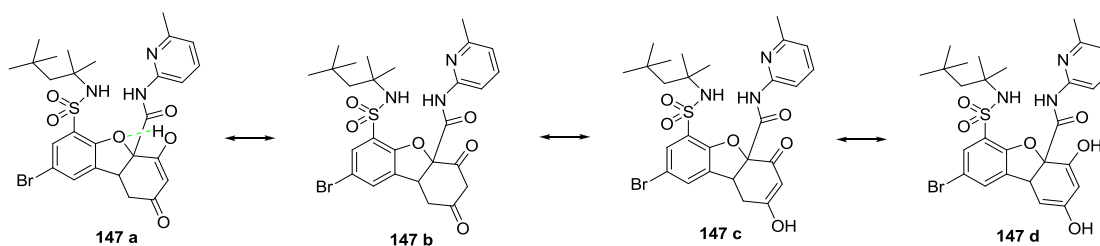


Figure 7.1. Keto-enol tautomerism of receptor **147**.

This characteristic offers us the possibility to use enol **147** as a Brønsted acid; in fact, in the previous chapter it has been made an estimation of the approximate pK_a of this enol, which is between 3.77 and 4.76. This feature would allow using this enol as a catalyst for several reactions. In addition, it is located near the receptor asymmetry centre, so it could offer an ideal geometry to use it as a chiral catalyst.

In general, carboxylic acids tend to show very low asymmetric induction in the reactions they catalyse. The problem is that the proton is far from the centre of asymmetry, even if it is in the carboxyl alpha carbon. This effect is shown in figure 7.2. The problem of obtaining asymmetric induction in acid catalysed reactions has been resolved in the literature using binaphthylphosphoric acids, or similar compounds, where large aromatic substituents are located close to the proton, as shown in figure 7.2.²⁵¹

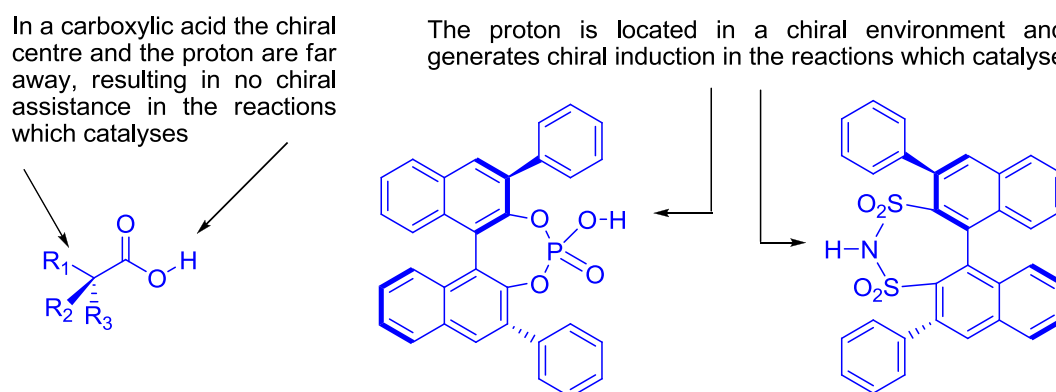


Figure 7.2. Carboxylic acid having a low asymmetric induction and the solutions offered in the literature.

The use of catalyst **147** can be an ingenious solution, since the enol would leave the acid proton in a chiral environment. Since we plan to study the catalytic activity of the enol, and the sulfonamide represented a further complication in the synthesis, we decided to prepare a catalyst without the latter group.

²⁵¹ (a) Brunel, J. M. *Chem. Rev.* **2005**, *105*, 857-898; (b) Zamfir, A.; Schenker, S.; Freund, M.; Tsogoeva, S. B. *Org. Biomol Chem.* **2010**, *8*, 5262-5276; (c) Phipps, R. J.; Hamilton G. L; Toste, F. D. *Nature Chem.* **2012**, *4*, 603-614; (d) Terada, M. *Synthesis* **2010**, 1929-1982.

7.2. METHODS AND RESULTS

7.2.1. Receptor **149** synthesis

Compound **149** was used in the previous chapter as a reference to observe the influence of the *t*-octylsulfonamide group in the extraction experiments. The preparation is similar to the receptor with sulfonamide **94**, but it is easier, because it is not necessary to include the sulfonamide group in the synthesis.

In figure 7.3 a scheme with the preparation of this compound is shown.

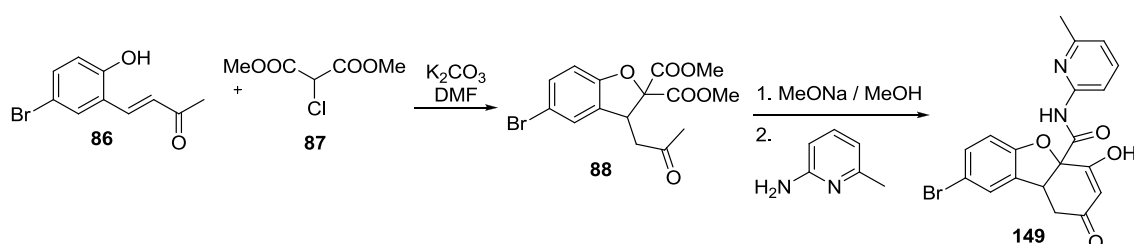


Figure 7.3. Receptor **149** synthesis.

The synthesis of receptor **149** proceeds with acceptable yields, so we undertook the resolution of the racemic mixture.

The NMR spectrum of receptor **149** clearly shows that an equilibrium mixture of tautomers exists in solution. The signal at 6.03 ppm corresponds to the olefinic proton of the enol tautomer, while the AB system centered at 3.76 ppm corresponds to the diketone isomer. The relative proportions of both tautomers depends on the concentration of the solution so that concentrated solutions favour the enol tautomer.

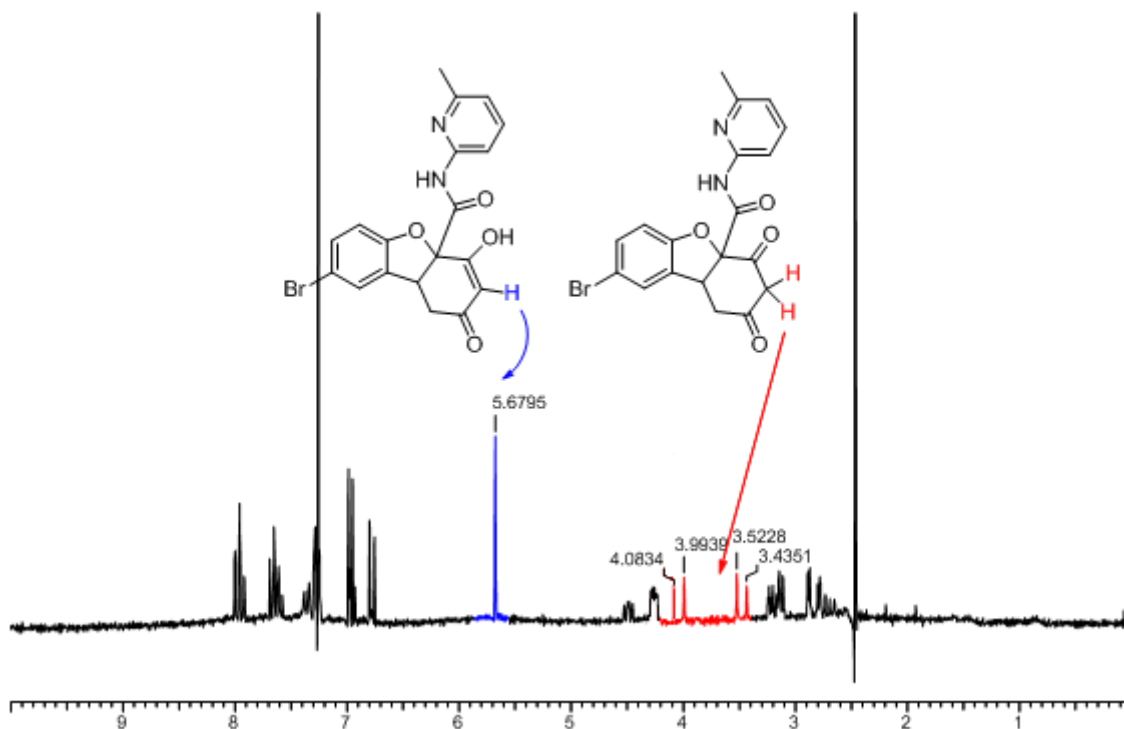


Figure 7.4. ^1H NMR spectrum in which the signals corresponding to enol and diketone tautomers are shown.

In the previous chapter we had proposed that the enol structure was favoured by the presence of an intramolecular hydrogen bond between the enol and furan oxygen, however, this effect does not explain why the equilibrium depends on the concentration.

To justify the change in the tautomeric equilibrium with concentration it is necessary to propose the presence of an aggregate in the solution. It is probable that the enol forms a dimer which is favoured when concentration is high. The presence of an acidic hydrogen bond donor in the enol collaborates in the generation of this dimer. The combination of the acidic hydrogen bond of the enol and the pyridine which is basic justifies this dimer formation.

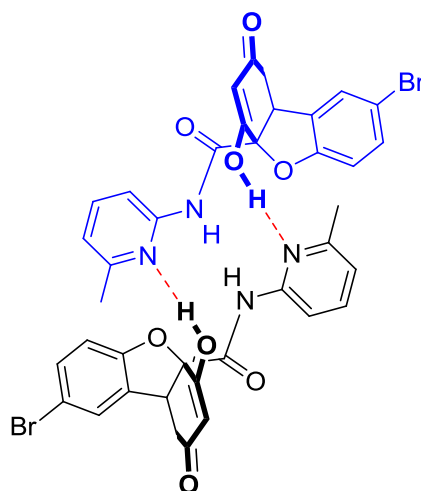
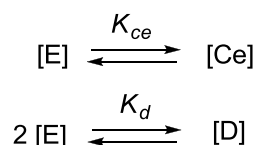


Figure 7.5. Structure of the proposed receptor **149** dimer.

Assuming the formation of a dimer with the enol tautomer, it is easy to calculate the dimerization constant performing NMR spectra at several concentrations.

Thus, receptor **149** (13.5 mg) was dissolved in 0.4 mL of CDCl_3 and the spectrum was recorded. Then, the solution was diluted several times, registering each spectrum. After each dilution it was observed a decrease in the signals of the enol and an increase of the diketone signals. The concentrations of both tautomers were calculated from their NMR integrals. As we start with a solution of known concentration, it is possible to calculate the dimerization constant as well as the keto-enolic equilibrium constant, according to the following equilibria:



where [E] corresponds to the enol concentration, [Ce] to the ketone concentration, [D] to the dimer concentration, K_d is the dimerization constant and K_{ce} the keto-enolic equilibrium constant.

Thus,

$$K_{ce} = \frac{[\text{Ce}]}{[\text{E}]} \quad K_d = \frac{[\text{D}]}{[\text{E}]^2} \quad \alpha = \frac{[\text{Ce}]}{2[\text{D}] + [\text{E}]}$$

where α is defined as the quotient between ketone concentration and dimer plus enol concentration. This ratio can be obtained by integration of the ketone and enol ^1H NMR signals. Combining these equations it is possible to obtain another equation as a function of the ketone concentration [Ce] and the NMR integral of the species in solution α :

$$\alpha = \frac{[\text{Ce}]}{2[\text{D}] + [\text{E}]} \quad ; \quad [\text{Ce}] = \alpha (2[\text{D}] + [\text{E}]) \quad ; \quad [\text{Ce}] = \alpha (2 K_d [\text{E}]^2 + [\text{E}]) \quad ;$$

$$[\text{Ce}] = \alpha \left[2 K_d \left(\frac{[\text{Ce}]}{K_{ce}} \right)^2 + \left(\frac{[\text{Ce}]}{K_{ce}} \right) \right] \quad ; \quad \frac{1}{\alpha} = \frac{2 K_d}{K_{ce}^2} [\text{Ce}] + \frac{1}{K_{ce}}$$

As the ketone concentration in solution is related with the initial concentration of receptor **149** in the tube [C], the later equation can be modified in this way:

$$[C] = [Ce] + [E] + 2[D] \quad ; \quad [C] = [Ce] \left(1 + \frac{[E] + 2[D]}{[Ce]} \right) \quad ;$$

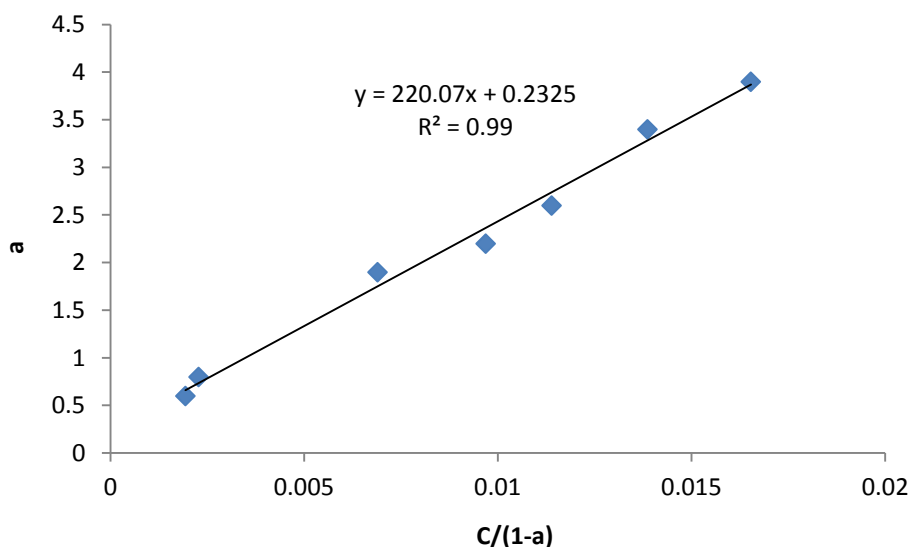
$$[C] = [Ce] \left(1 + \frac{1}{\alpha} \right) \quad ; \quad [Ce] = \frac{[C]}{\left(1 + \frac{1}{\alpha} \right)} \quad ;$$

$$\frac{1}{\alpha} = \frac{2K_d}{K_{ce}^2} \frac{[C]}{\left(1 + \frac{1}{\alpha} \right)} + \frac{1}{K_{ce}}$$

We have defined α such as the relation between ketone concentration and enol plus dimer concentration, which is directly obtained by integration. In addition, it is possible to simplify the last equation because we have referenced with a value of 1 the signal corresponding to the ketone. So, we have obtained an equation as a function of the NMR integral corresponding to dimer plus enol (a):

$$a = \frac{2K_d}{K_{ce}^2} \frac{[C]}{(1+a)} + \frac{1}{K_{ce}}$$

In this way, representing the integral values corresponding to dimer plus enol (giving the value of 1 to the ketone) versus receptor **149** concentration, it is possible to obtain a straight line whose y-intercept corresponds to K_{ce} inverse and whose slope is the quotient $2K_d/K_{ce}^2$, so it is possible to achieve the value of the dimerization constant, K_d .



$$\frac{1}{K_{ce}} = 0,2325; \quad K_{ce} = \frac{1}{0,2325}; \quad \boxed{K_{ce} = 4,3}$$

$$\frac{2K_d}{K_{ce}^2} = 220,07; \quad K_d = 220,07 \frac{K_{ce}^2}{2}; \quad K_d = 220,07 \frac{4,3^2}{2}; \quad \boxed{K_d = 2035}$$

Figure 7.6. Dimerization constant calculation.

The keto-enol equilibrium constant obtained is 4.3 and the dimerization constant 2035. This value is relatively high, so it should be seriously considered the possibility that the guest association not be good due to dimer formation. However, guest showing larger association constants should break dimers, so we proposed the racemic mixture resolution.

7.2.2. Receptor 149 racemic mixture resolution

The presence of the enol facilitates this process because compound **149** forms salts easily with amines. Given the success obtained in the previous chapter with chiral amino alcohols, we considered, first, a study by Nuclear Magnetic Resonance to allow us to select a promising chiral amine to perform the separation. The criterion we used to carry out this selection was to find a chiral agent which leads to a strong splitting of the receptor signals. We understand that a strong signal splitting corresponds to associates with well-defined geometries. Since large splitting also suggests different structures, they should be easily separable.

Work started with several chiral amines but, as it was the case with the previous receptor, the best results were obtained working with amino alcohols. In addition to the formation of an ionic bond between the nitrogen of the amine and the enol, the presence of the hydroxyl group can generate a new binding point which makes this complex a rigid structure. In this complex, there should be no free rotation of the receptor respect to the guest molecule, and the substituents cannot average their chemical shifts, so different signals for the two diastereomeric complexes show up.

In general, the receptor signals undergo splitting with all the guests tested (except with *L*-valinol and brucine). As our criterion was to choose the amine which produced the largest splitting, cinchonidine was found the most suitable compound, so we carried out the crystallization of receptor **149** with this amine. The good results obtained in the crystallization of receptor **94** dissolving the cinchonidine salt in chloroform-methanol and adding ether slowly, suggested us to use the same strategy for the resolution of receptor **149**. This procedure yielded a first crop of crystals, whose NMR spectrum showed a single set of signals for receptor **149**. From the mother liquor it was possible to obtain the optical image of the receptor, again by fractional crystallization.

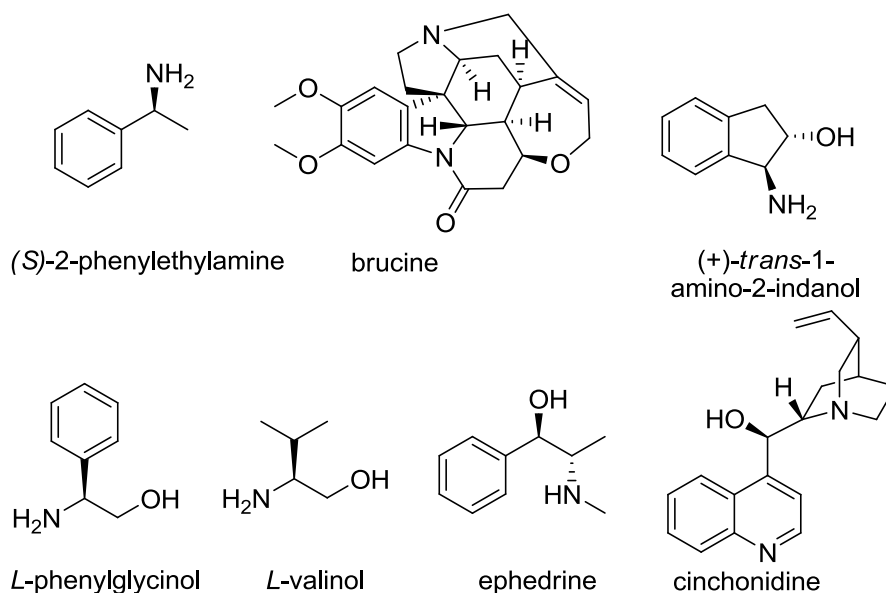


Figure 7.7. Amines studied in the receptor **149** racemic mixture resolution.

Slow evaporation of a methanol solution of the more insoluble salt allowed us to obtain crystals of sufficient quality for X-ray diffraction analysis. The obtained structure is shown in figure 7.8.

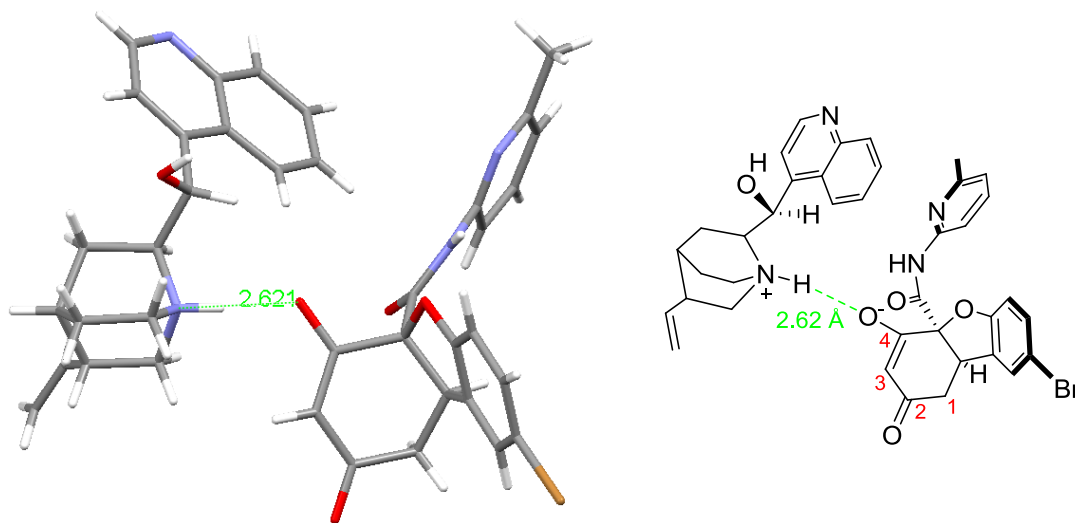


Figure 7.8. X-ray structure of receptor **149** salt with cinchonidine.

As occurred in the previous chapter with receptor (+)-**147** salt, the crystal structure of the above salt exhibits a very asymmetric keto-enol system, wherein the C2-O2 bond substantially corresponds to a double bond with a distance of 1.24 Å (1.21 Å is the distance of a conventional carbonyl group), while the C4-O4 bond measures 1.29 Å, slightly more than the 1.28 Å reported for dibenzoylacetone.²⁵² We believe this difference in bond distance is due to the quinuclidine, which forms a hydrogen bond with O4. Quinuclidine proximity with the oxygen makes most of the charge to be on this oxygen atom, so that the resonance form that best represents the structure is shown in figure 7.9.

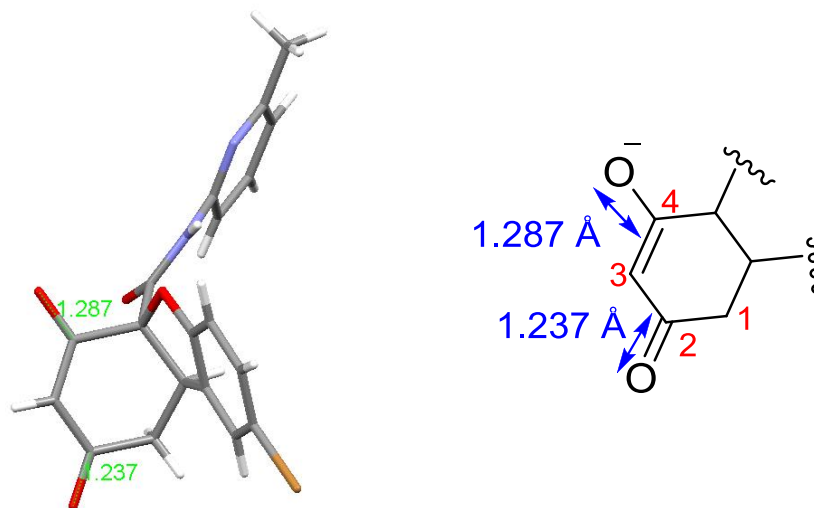


Figure 7.9. Resonance isomer which best represents the structure of receptor **149** salt with cinchonidine.

When more molecules around the quinuclidine are visualized in the crystalline structure, it can be seen that the hydroxyl group forms a strong hydrogen bond of 2.86 Å with the amide carbonyl group of another receptor molecule (figure 7.10).

²⁵² Herbstein, F. H.; Iversen, B. B.; Kapon, M.; Larsen, F. K.; Madsen, G. K. H.; Reisner, G. M. *Acta Cryst. B* **1999**, *55*, 767-787.

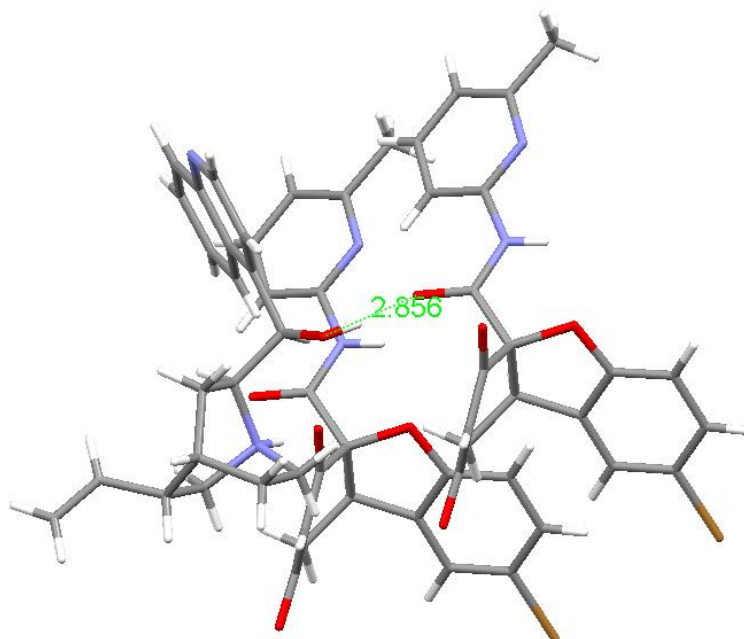


Figure 7.10. Observed hydrogen bond between the cinchonidine hydroxyl group and the amide carbonyl of a second receptor **149** molecule.

This X-ray structure, also allowed us to establish the absolute stereochemistry of the more insoluble salt of receptor **149** as 4a*S*, 9b*R*.

The free receptor **149** can be obtained by addition of the methanol solution of the complex to a 10 % aqueous solution of formic acid from which it is extracted with EtOAc. Evaporation of the EtOAc solution produced the free receptor crystallization.

The enantiomer that forms the more soluble salt is obtained by a similar procedure.

7.2.3. Receptor 182 synthesis

In parallel with the preparation of the above receptor, it was carried out the synthesis of receptor **182**. This compound has the advantage that the benzimidazole group is more basic than the aminopyridine, so that it can yield better results. The synthesis is similar to that of receptor **147**, but proceeds more smoothly because the benzimidazole is more nucleophilic than the aminopyridine and aminolyzes the ester at a lower temperature. The reaction conditions are milder and the product is obtained with a better yield.

The synthesis is summarized in figure 7.11.

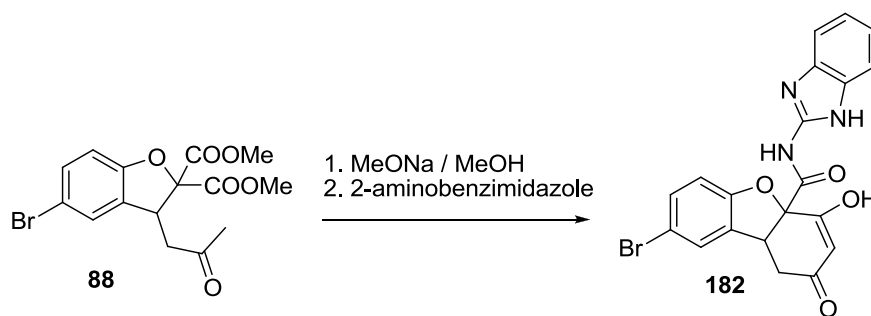


Figure 7.11. Receptor **182** synthesis.

Thus compound **182** is obtained in good yield. Purification is very simple, because this compound crystallizes in THF.

7.2.4. Receptor **182** racemic mixture resolution

To use compound **182** as an enantioselective receptor for chiral substrates or apply it in asymmetric organocatalysis, it is necessary to resolve its racemic mixture.

Following the success in resolving the above receptors with chiral amines, we decided to apply the same methodology in the resolution of this receptor. In order to select an appropriate amine, NMR experiments were carried out. To a solution of receptor **182** in deuteriochloroform, several chiral amines were added and the splitting of the receptor signals was studied.

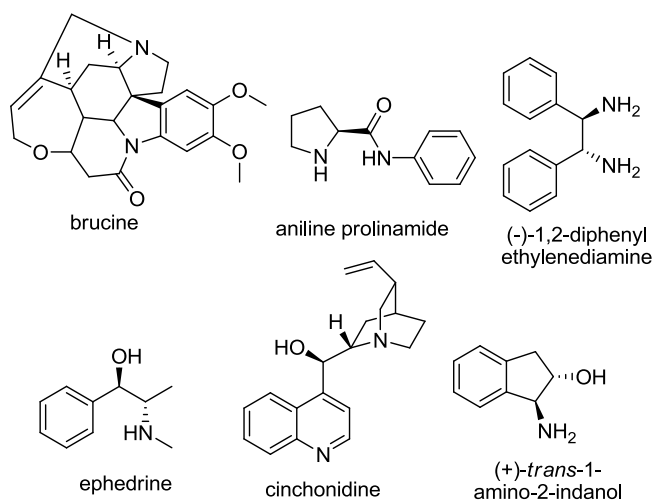


Figure 7.12. Chiral amines tested in the enantioselective crystallization of receptor **182** enantiomers.

All amines in figure 7.12 showed splitting of the receptor signals, but again, these splittings were higher with amino alcohols, so we believe that they are good candidates to carry out the resolution of receptor **182** racemic mixture.

Because of the speed with which the separation can be made, enantioselective liquid-liquid extraction using ephedrine was tested, as in the case of the previous sulfonamide receptor **94** which had been very successful. However, the new receptor is more hydrophilic than the previous one, and the result was not satisfactory. When the aqueous ammonia, chloroform and ephedrine system was used, the result is that the ammonium salt of the receptor prefers to dissolve in the aqueous phase, while ephedrine tends to remain in chloroform. If 0.5 equivalents of lithium hydroxide are used a small amount of associate between ephedrine and receptor can be extracted to the chloroform phase, but the NMR spectrum showed that this extraction was not enantioselective. Proton doublets in the position 6 of the receptor-ephedrine complexes appear at 6.56 and 6.60 ppm, as signals displaying the same intensity (figure 7.13).

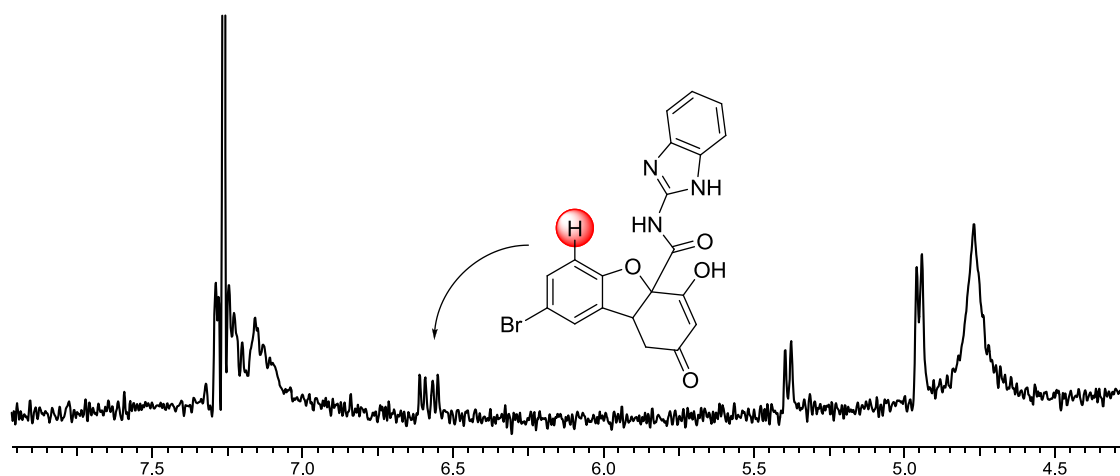


Figure 7.13. ^1H NMR spectrum (4.3-8.0 ppm) showing the characteristic doublets of receptor **182** after enantioselective extraction with ephedrine.

The use of other amines confirmed us that in the absence of the sulfonamide group the salts of these enols do not exhibit enough enantioselectivity to allow the racemic resolution by extraction.

Although the complexes formed between receptor **182** and amines present very similar energies in solution, this need not to be the case in the crystalline state. Since the NMR spectra showed structures with very different geometries, it seems logical a differentiation of the lattice energies, and therefore in melting points and solubilities.

So we decided to start studying crystallization with guests of figure 7.12. The experiments (50-100 mg of receptor in 2.0 mL of solvent) were prepared by mixing receptor and guest in equimolar amounts, in such a way that, if the diastereomeric complexes have different melting points, one will crystallize before the other.

Despite being ionic compounds in which it is expected a high electrostatic energy, most of the salts obtained with receptor **182** were oily compounds which do not have utility for the resolution of the receptor mixture by crystallization. Fortunately, the salt obtained with cinchonidine was a crystalline compound with a high melting point.

In the first crystallization, under conditions discussed above, it was observed preference for one of the receptor enantiomers. The slow evaporation of the chloroform led to a first crop of crystals which after filtration showed a single doublet corresponding to the proton of carbon 6. The spectrum of the mother liquor showed, however, the presence of two signals for this proton, in proportions 1/2, indicating us the need to continue concentrating the mother liquor. Since this guest was promising, we conducted a study with several solvents to optimize the crystallization process.

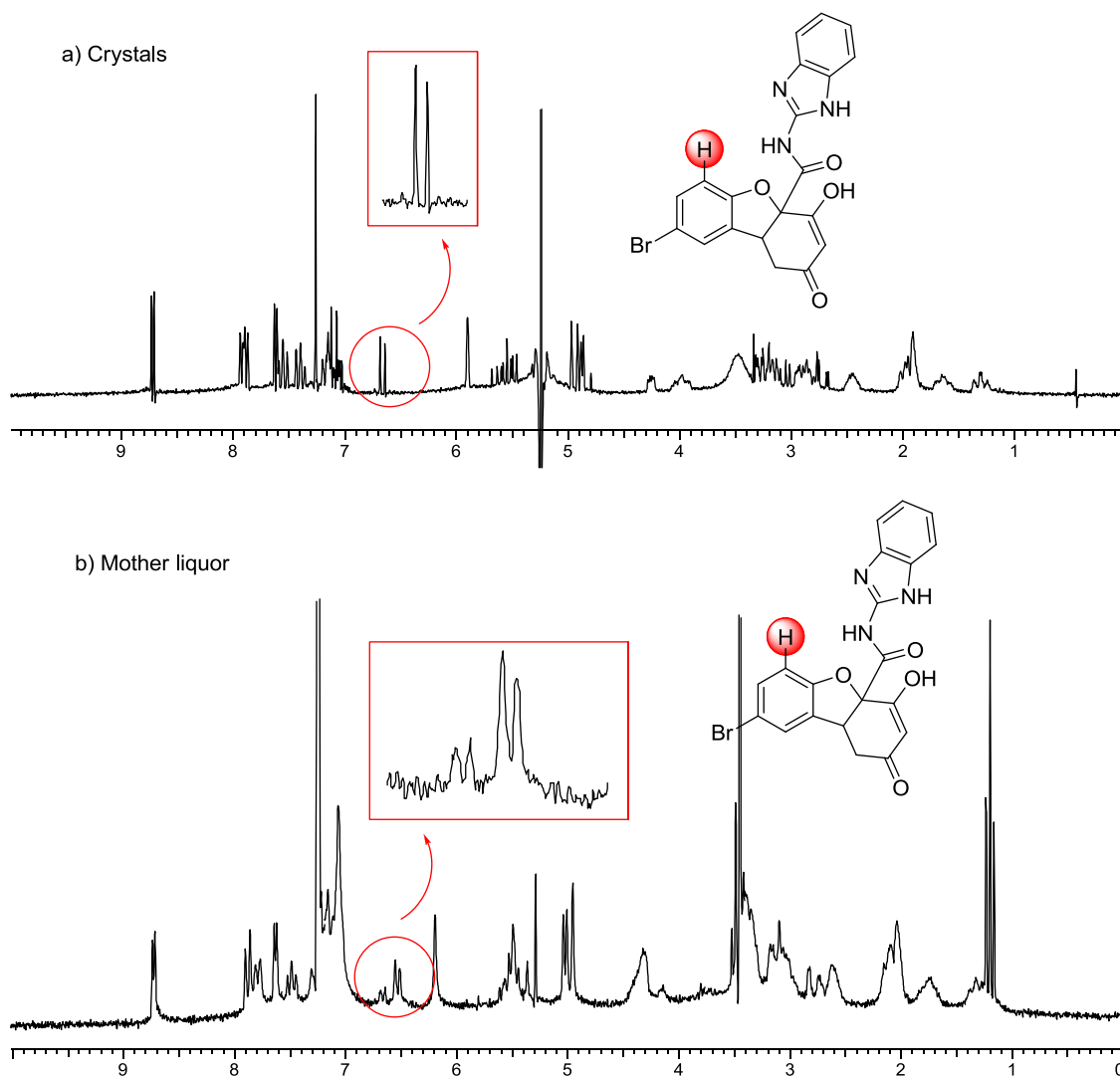


Figure 7.14. ^1H NMR spectra of receptor **182** in the presence of cinchonidine: (a) crystals and (b) mother liquor.

The best conditions were found using an equimolar mixture of receptor and cinchonidine in $\text{MeOH}/\text{CHCl}_3$ 1/5, in which ether is slowly added through diffusion from a container with this solvent. The equipment used is the same as that shown in figure 6.28 for the resolution of receptor **147**.

Under these conditions it was possible to obtain a 95 % yield of the more insoluble salt, leaving a solution enriched in the more highly soluble salt. If ether is added, the second salt crystallizes, from which the optical antipode of receptor **182** can be obtained, also in a high degree of enantiomeric purity.

Free receptor was obtained by addition of the methanolic solution of the salt over a formic acid aqueous solution. Under these conditions the receptor crystallizes and it is enough filtration, washing with water and drying, to obtain a receptor with enough purity to carry out its study.

Crystallization of the more insoluble salt in MeOH/H₂O allowed us to obtain a suitable solid for analysis by X-ray diffraction. The structure obtained is shown in figure 7.15.

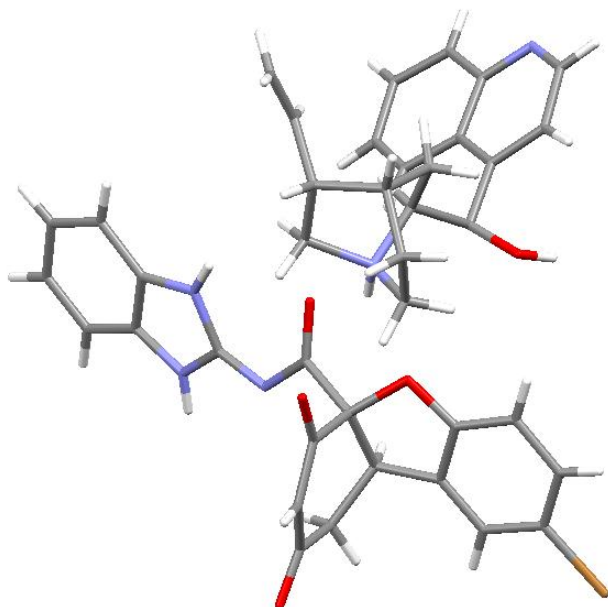


Figure 7.15. Structure obtained by X-ray diffraction of the more insoluble salt of compound **182** and cinchonidine.

Since the absolute configuration of cinchonidine is known, from figure 7.15 we can deduce that compound **182**, which first crystallizes with cinchonidine, possesses the absolute configuration 4*aS*,9*bR*.

The structure shown in figure 7.15 for compound **182** is, however, very different from the structure obtained with the previous receptors. The first feature that stands out is the conformation of the carboxamide. In all the preceding derivatives a geometry in which the NH established an intramolecular hydrogen bond with the furan oxygen was obtained. In this case, the carboxamide shows a conformation which is rotated 180°, and the carbonyl is located next to the furan oxygen. The loss of the intramolecular H-bond between carboxamide and furan oxygen, which we had considered strong, surprised us, so we included more molecules in the visualization of the crystal structure to study the packing. When more molecules were added, it could be seen that the quinuclidine nitrogen was protonated by the enol of compound **182**. In addition, C-O (1.24-1.25 Å) and C-C (1.37-1.38 Å) bond distances showed the structure of the enolate, unlike what happened with receptor **149** in which one C-O distance was different from the other. Protonated quinuclidine nitrogen was surrounded by three oxygen atoms (figure 7.16): one corresponds to the amide carbonyl, other to the furan oxygen and the last one to the negative enolate oxygen. The bond distances are similar for all three H-bonds, and surprisingly long for strong hydrogen bonds between charged heteroatoms. The three distances range around 3 Å.

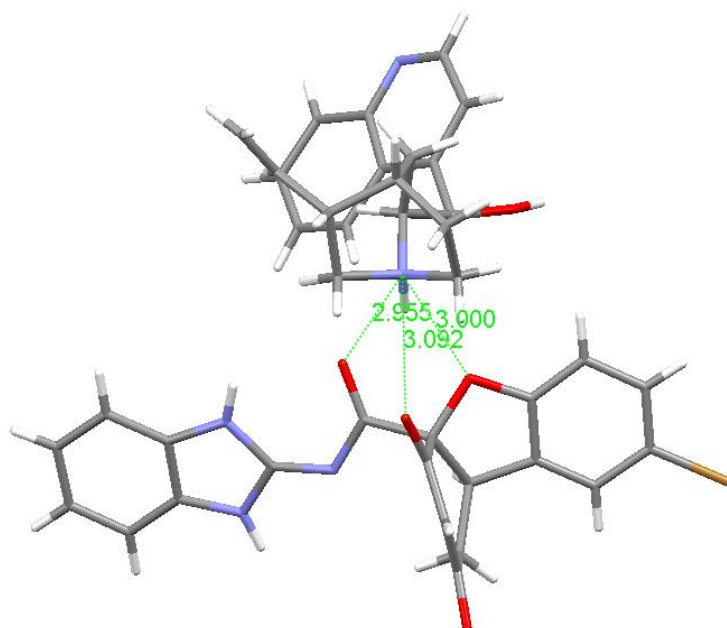


Figure 7.16. View of the X-ray structure of receptor **182** complex. It can be observed the nitrogen atom of the quinuclidine surrounded by three oxygen atoms.

When more molecules were visualized we could see that both negative enolate oxygens were located near (distance of 2.7-2.8 Å) the nitrogen atoms of the benzimidazole, with which these atoms must be establishing hydrogen bonds. This feature was again surprising since it was expected that only one of these nitrogens possessed a proton, while the other, should be forming the double bond.

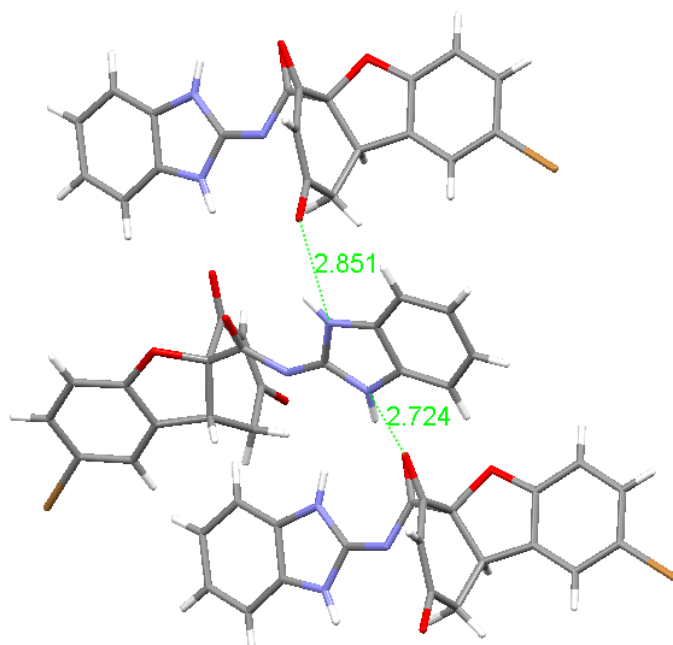


Figure 7.17. Packing view of the X-ray structure of compound **182**. It can be observed the hydrogen bonds established by the benzimidazole NHs with the enolates of two neighboring receptor **182** molecules.

The imidazole C-N distances showed that they were similar for both imidazole nitrogens, consequently, both should be protonated, while shortest C-N distance in receptor **182** corresponded to the bond between the exocyclic nitrogen and the imidazole (2.32 Å), which fitted well within the range of distances that present N=C double bonds, so we believe that our compound **182** has a fulvene type structure, as proposed in figure 7.18.

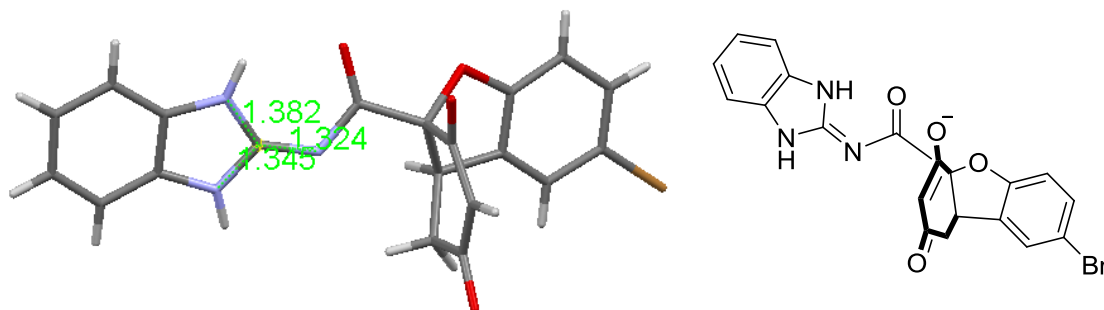


Figure 7.18. Proposed structure for the salt of compound **182** and cinchonidine.

Fulvene structure justifies well the change in conformation of the carboxamide, as in this tautomer the NH necessary to form the H-bond with the furan oxygen does not exist; however, it is unclear why this compound prefers a non-aromatic fulvene structure, instead of the aromatic structure of imidazole. We assume that is the own energy of the crystalline state that favours the less stable tautomer, apparently, because the molecule finds a geometry in which it can set a maximum number of hydrogen bonds between the NHs of the pentagonal ring and the magnificent hydrogen bond acceptors which are the enolate oxygens. It is possible that the carboxamide NH and the NH of benzimidazole can not make the same hydrogen bonds due to geometric reasons, which would have resulted in a less stable crystal structure.

A molecular modelling study of the different receptor **182** tautomers has revealed that the fulvene structure is perfectly possible.²⁵³ However, since the energy differences are small, it is probably that the presence of any guest shifts the equilibrium to the tautomer able to form the more stable associate.

²⁵³ Calculations were carried out by Dr. Luis Simón Rubio.

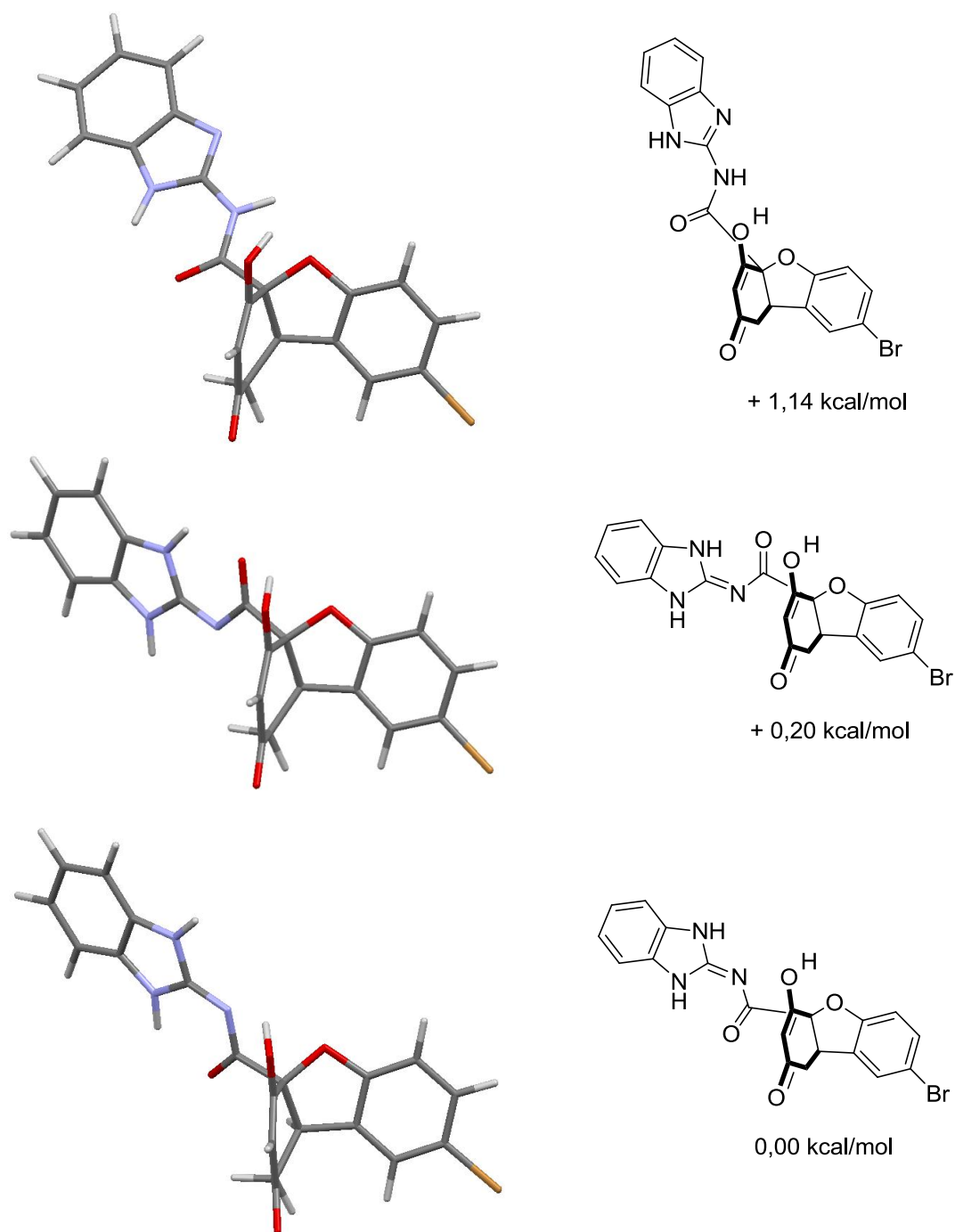


Figure 7.19. Different geometries obtained for receptor **182** with modelling studies (B3LYP/6-31G**).

7.2.5. Study of receptor **182** properties

Due to the geometry and functional groups of receptor **182**, it offers many possibilities in molecular recognition and organocatalysis.

First, it possesses the basic group of the aminobenzimidazole fragment. According to the literature,²⁵⁴ the pK_a of benzimidazole (in water) is 12.78. However, it is possible that the basicity of the benzimidazole joined to the benzofuran skeleton is lower, because the

²⁵⁴ Walba, H.; Isensee, R. W. *J. Org. Chem.* **1961**, *26*, 2789-2791.

carboxamide carbonyl group withdraws electron density from the imidazole ring, decreasing its basic character.

Receptor **182** also includes an enol group pointing to the benzofuran receptor cavity. As discussed in the introduction, although keto-enol tautomerism may rise to a complex mixture of diketone and enol pointing in different directions, it is likely that the intramolecular hydrogen bond between the enol and the oxygen atom of the benzofuran displaces the equilibrium towards the desired enol tautomer (figure 7.20). In this case, and unlike receptor **149**, it was not observed the characteristics signals of the diketone tautomer upon dilution of this compound in the NMR tube. This fact tells us that the formation of dimers is probable.

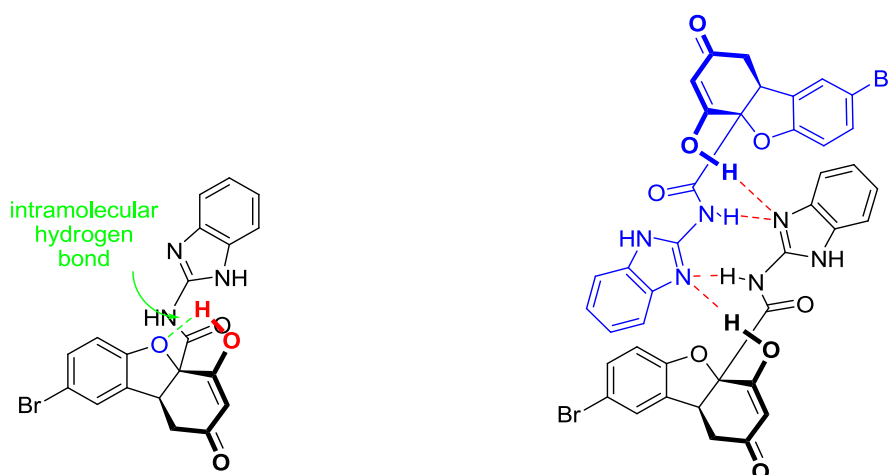


Figure 7.20. Intramolecular hydrogen bond between the enol and the oxygen atom of the benzofuran and a possible dimer.

As previously mentioned, the acidity of this enol lies between acetic and formic acid. Therefore, this enol group may interact with a basic group of a guest, and also offers the possibility to use the receptor to catalyse reactions promoted by weak Brønsted acids.

Additionally, the receptor has an amide NH able to establish hydrogen bonds with the guest.

Therefore, it is a bifunctional catalyst, similar to proline, which combines a basic group with a well tuned acidic group (since no proton transfer from one group to another is observed in chloroform solution), unlike proline, where the amino group is preferably protonated at the expense of the carboxyl group.

Additionally, both the acidic (enol) and the basic (benzimidazole) group can be combined in several ways to generate different types of bifunctional receptors:

- Neutral receptor: wherein the enol would act as an acid group and the benzimidazole as a basic one.
- Acid receptor: in this case the benzimidazole could be protonated ($pK_a(\text{water}) = 5.55$) and act as acid group, together with the enol.

- Basic receptor: wherein the enol would be deprotonated and could be used as a potassium or tetraalkylammonium salt, arranging two basic groups: the enolate and benzimidazole.

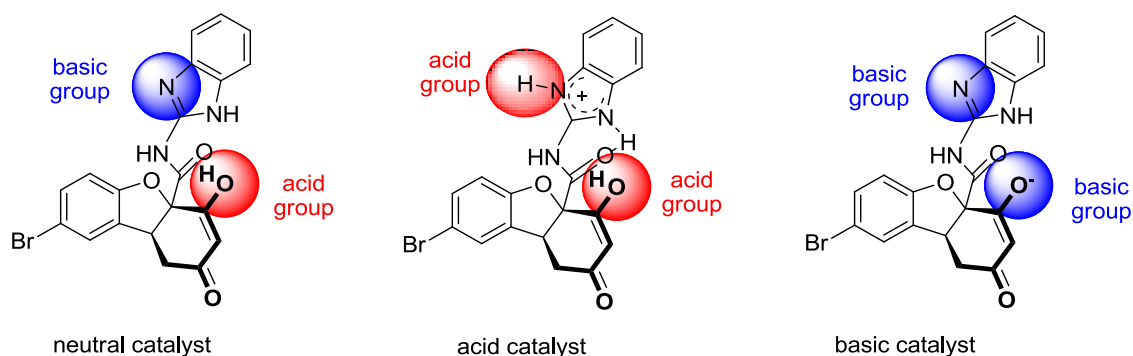


Figure 7.21. Different possibilities for receptor **182**.

7.2.5.1. Amino acids extraction

First, we studied the possibilities offered by the above compound as receptors for molecules with industrial interest. Thus, potentially, receptor **182** could be used to extract neutral amino acids in its *zwitterionic* form from aqueous solutions. Although this receptor is insoluble in deuterated chloroform as well as amino acids themselves, it is likely that if a sufficiently strong complex is formed with an amino acid or an amino acid derivative, the complex would be chloroform soluble.

We started conducting several experiments with racemic receptor **182** and enantiomerically pure amino acids (*L*-phenylalanine and *L*-valine, amino acids that are the best candidates for enantioselective extraction because they are more lipophilic than the others). Under these conditions no amino acid was observed in the chloroform phase. Addition of 18-crown-6 ether, which produces a complex with the ammonium group of the amino acid, transformed them into a more lipophilic species, so that if a compound capable of associating the carboxylate by hydrogen bonds is in the solution, extraction is more likely to occur. Adding to the suspension of *L*-phenylalanine, receptor **182** and 18-crown-6 ether, the receptor signals appeared in the chloroform phase. Furthermore, these signals were clearly split (in the case of the doublets in position 6 at 6.82 and 6.86 ppm), indicating the formation of diastereomeric complexes. The same experiment was carried out with *L*-valine, showing again the splitting of receptor **182** signals, and confirming the presence of diastereomeric complexes.

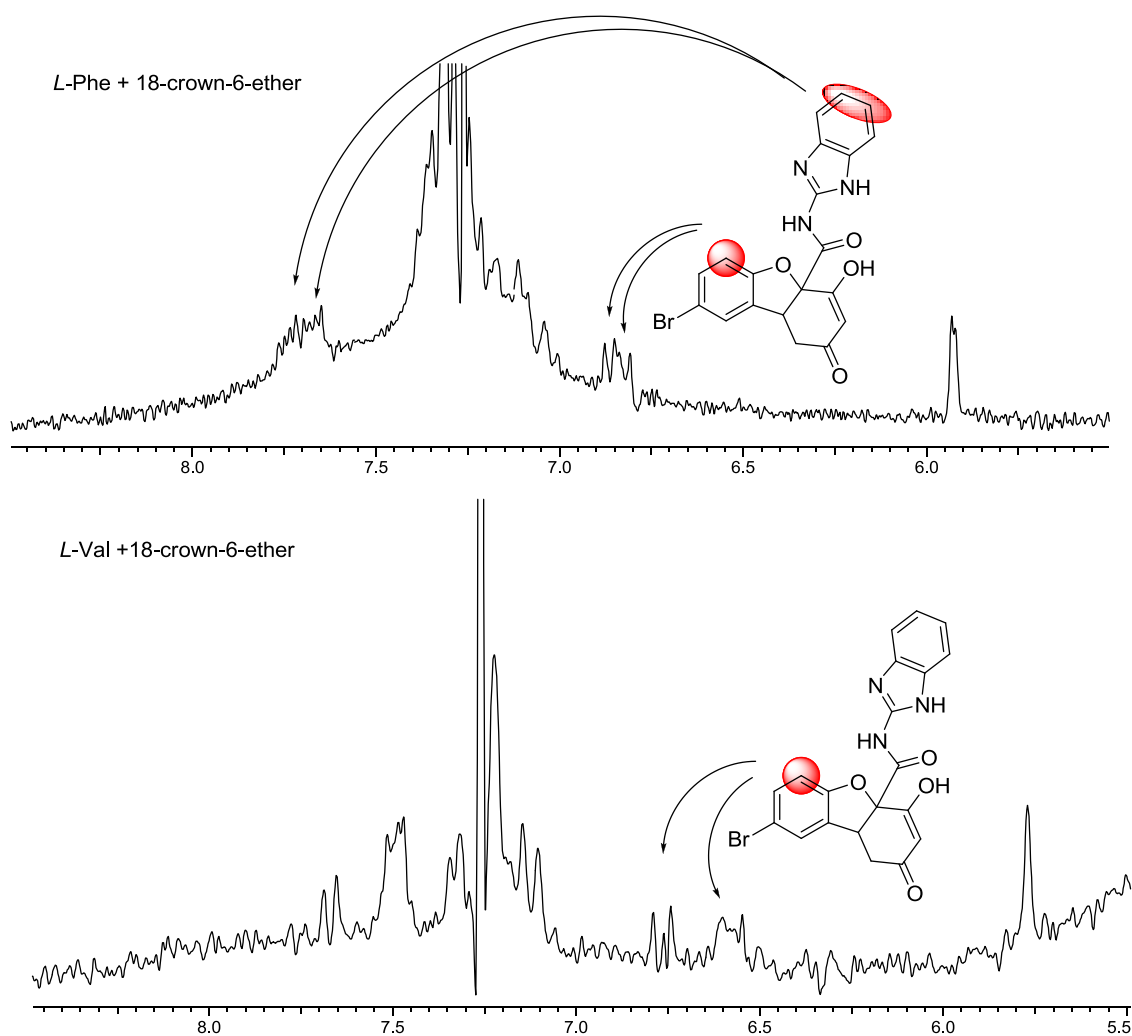


Figure 7.22. ¹H NMR spectrum region (5,5-8,5 ppm) in which the splitting of the racemic receptor **182** signals are shown upon addition of an aqueous solution of L-Phe and L-Val with 18-crown-6-ether.

Because of these good results, we conducted a study of the possible geometries of receptor **182** associates with amino acids. Molecular models revealed that two different geometries were possible for these complexes. In the free receptor, the NH of the benzimidazole ring is probably forming an intramolecular hydrogen bond with the amide carbonyl. If this intramolecular hydrogen bond remains in the complex, the more likely geometry for the carboxylate association is one in which it forms hydrogen bonds with the NH of the amide and the enol OH (figure 7.23, left). The latter should be especially strong because the pK_a of enol and amino acid are similar.

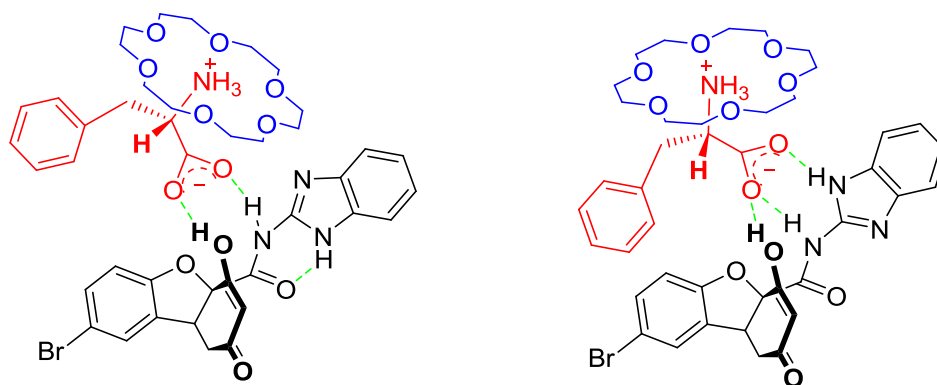


Figure 7.23. Possible complexes formed between receptor **182** (black), amino acid (red) and 18-crown-6-ether (blue).

There is a second possibility, because hydrogen bonds in which the acceptor is negatively charged are much more efficient than with a neutral acceptor. Thus, if the benzimidazole breaks its intramolecular hydrogen bond, a new strong hydrogen bond between the NH and the carboxylate could be established, as shown in figure 7.23 (right). Although the overall number of hydrogen bonds in the complex is the same, the strength of the hydrogen bond with the negatively charged carboxylate could stabilize the latter geometry.

As these two possible geometries are so similar, we found no spectroscopic arguments that allow us to rule out one of them, so we conducted a modelling study to suggest us which structure was the most likely. The modelling of both complexes, and the energy difference between them, is shown in figure 7.24.²⁵⁵ Glycine was used as guest in order to minimise the calculation time.

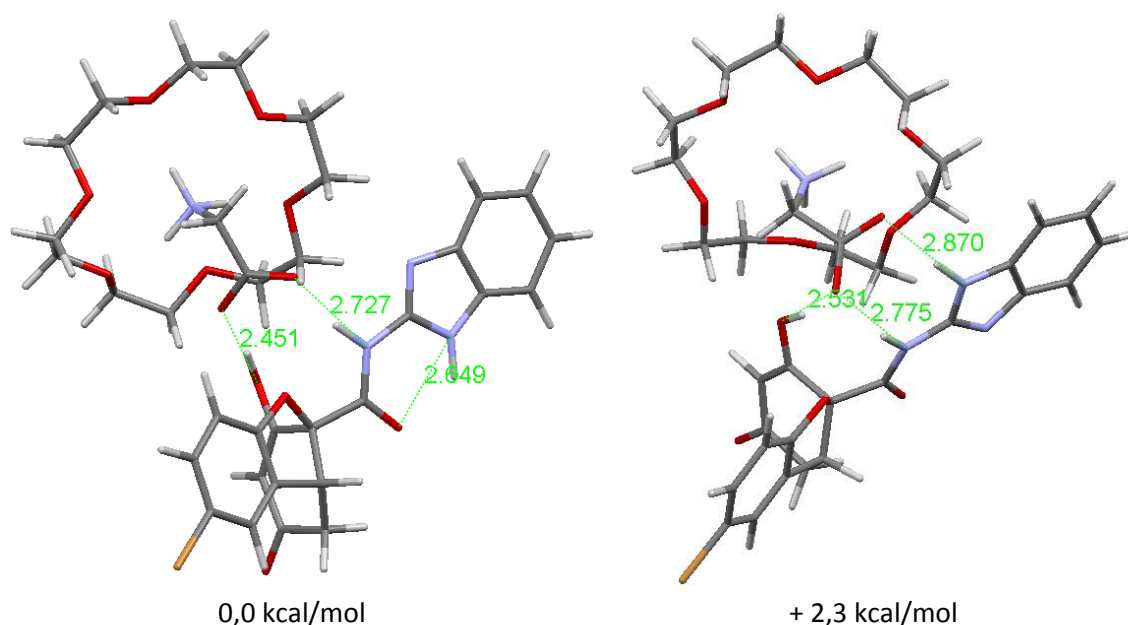


Figure 7.24. Molecular modelling of potential associates between receptor **182** and glycine (B3LYP/6-31G**).

²⁵⁵ Calculations were carried out by Dr. Luis Simón Rubio.

This molecular modelling study has allowed us to observe that receptor **182** prefers to establish an intramolecular hydrogen bond between benzimidazole NH and the amide carbonyl group (figure 7.23 left) instead to form a third intermolecular hydrogen bond with amino acid (figure 7.23 right).

Once known the more probable geometry of the complex between receptor **182**, 18-crown-6-ether and an amino acid, we made several extraction experiments.

The enantiomerically pure receptor and a racemic mixture of phenylalanine in a biphasic system chloroform/water in the presence of 18-crown-6 ether were used. The NMR spectrum showed the signals corresponding to phenylalanine, although integration of them was not easy, so that the analysis of enantiomeric purity was carried out by HPLC. The integration of the two signals obtained in the chiral HPLC chromatogram for phenylalanine enantiomers showed that the extraction was slightly enantioselective (ee = 8 %). Probably both *L*- and *D*-Phe fit well in the complex due to the free rotation of the side chain group.

A similar study was conducted with other amino acids, using the same methodology.

Table 7.1. Extraction experiments of racemic mixtures of amino acids with receptor **182**.

entry	amino acid	ee (%)
1	phenylalanine	8
2	valine	22
3	leucine	13
4	phenylglycine	0.2
5 ^a	serine	-

^aNo extraction

Lipophilic amino acids such as valine, which has a bulkier alpha chain, generated more enantioselective extractions (ee = 22 %). The result with leucine was only slightly better than with phenylalanine (ee = 13 %). Phenylglycine, which has a bulky aromatic ring in its side chain, led to disappointing results, with practically no enantioselectivity in the extraction (ee = 0.2 %). Hydrophilic amino acids such as serine are not extracted under these conditions, and it is not possible to measure the enantioselective recognition which they present with this methodology.

Another option which we tested was the extraction of amino acid hydrobromides. As the amino acid possesses a carboxylic acid in its structure, the formation of three hydrogen bonds in the cavity of the receptor is assured, thereby obtaining a more stable complex. The geometry we expected for this type of associate is shown in figure 7.25.

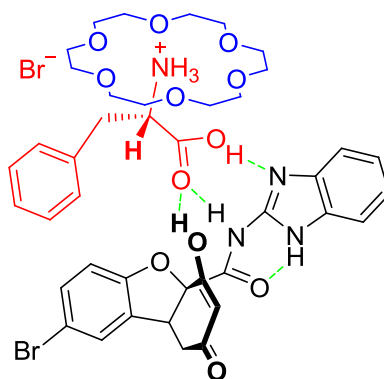


Figure 7.25. Proposed complex between receptor **182** and L-phenylalanine hydrobromide.

When extraction experiments were conducted with the racemic receptor and enantiomerically pure hydrobromides, we observed the amino acid extraction to the chloroform phase and the splitting of receptor **182** signals.

However, performing the reverse operation, that is, to try to extract from water only one of the enantiomers of a racemic mixture of amino acids with the enantiomerically pure receptor, enantioselectivity was not observed, nor with phenylalanine, phenylglycine or valine, which are the more lipophilic amino acids.

We changed the strategy slightly, employing the tetrabutylammonium salt of the receptor, so that the enol acts as a hydrogen bond acceptor instead of hydrogen bond donor.

The tetrabutylammonium salt of the receptor can be obtained in a similar way to the sulfonamide receptor, by extraction in a chloroform/water biphasic system. The use of a sodium carbonate solution generates the sodium salt of the receptor, which is water soluble, but in the presence of tetrabutylammonium chloride an ion exchange is produced, so that the tetrabutylammonium salt of the receptor keeps in the organic phase, while the sodium chloride generated prefers the aqueous phase.

In this manner, guests such as triflates or dinitrobenzoyl derivatives of amino acids may form stable complexes, since they have an acidic NH which should form a strong hydrogen bond with the receptor enolate, as seen in figure 7.26.

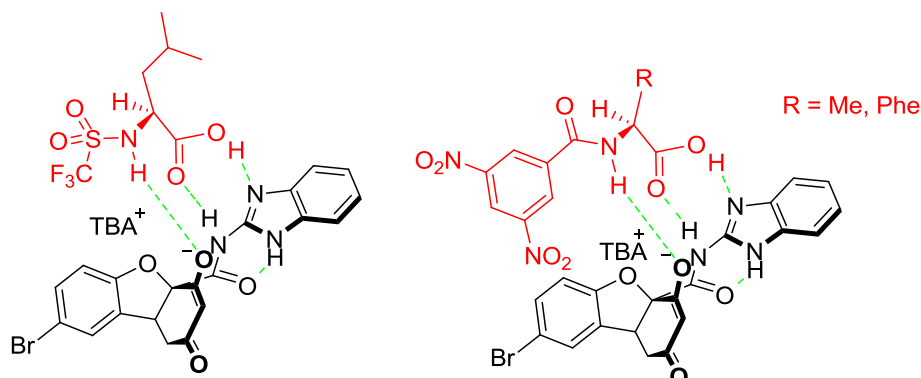


Figure 7.26. Proposed complexes between receptor **182** and L-leucine triflate (left) and dinitrobenzoyl-L-alanine or phenylglycine (right).

Again, when the racemic receptor is used, the splitting of the signals due to the formation of diastereomeric complexes occurs. However, when the enantiomerically pure receptor was used to carry out the extraction of a racemic mixture of guests, enantioselective extraction was not observed. According to CPK models, the acid NH is likely too far from the enolate, so that the hydrogen bond is too long and does not stabilize the complex.

7.2.5.2. Catalysis studies

We also decided to use receptor **182** as a catalyst, for which a set of reactions were studied. These processes are detailed below.

First, we prepared the hexafluorophosphoric acid salt of receptor **182**. To get an idea of the strength of the complex formed between this receptor and a carbonyl group, we conducted a titration in deuterioacetone with DMSO. The deuterioacetone is capable of dissolving the receptor; it presumably forms a complex with the catalyst which in turn is later displaced by DMSO.

Under these conditions an association constant of $K_{as} = 18 \text{ M}^{-1}$ was obtained, which can be considered quite good considering it is performed in a solvent that is competing for the guest hydrogen bonds.

7.2.5.2.1. Diels-Alder reaction

Thanks to the acidic character of the enol, we tested whether receptor **182** could catalyse the Diels-Alder reaction between cyclopentadiene and several dienophiles.

Under normal conditions, the Diels-Alder reaction between cyclopentadiene and acrylate does not take place, the carboxylic acid is necessary for the reaction to proceed at a reasonable rate. We expected that in the associate between receptor **182** and acrylate, proton transfers from the enol to the acrylate, and therefore the reaction could take place.

Thus, by successively adding small amounts of receptor **182** to a solution of potassium acrylate and 18-crown-6-ether in deuteriochloroform it was observed the partial dissolution of the receptor and the deshielding of the carboxylate signals. However, adding an equivalent of receptor **182**, we saw that the deshielding was not large enough to reach the chemical shift of the signals corresponding to acrylic acid. Adding an excess of cyclopentadiene, the Diels-Alder reaction product was not detected, but instead the cyclopentadiene dimer was generated. It is therefore possible that the enol is not acid enough to completely protonate the carboxylate, and for this reason, the reaction does not take place.

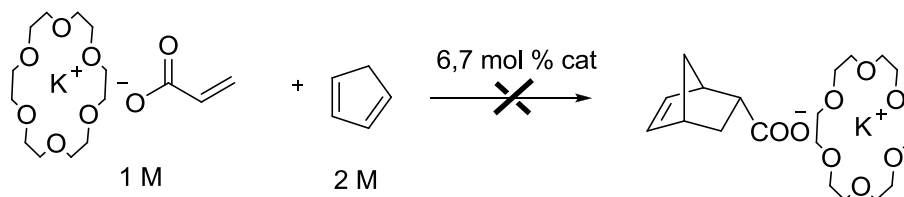


Figure 7.27. Diels-Alder reaction between cyclopentadiene, potassium acrylate and receptor **182**.

Since neutral receptor was unable to protonate the acrylate carboxylate, we decided to use the receptor as its hexafluorophosphoric acid salt. We also substituted potassium acrylate for acrylamide, since with potassium acrylate, proton transfer would occur from the protonated benzimidazole to the carboxylate, taking place the Diels-Alder reaction outside the asymmetric environment of the catalyst.

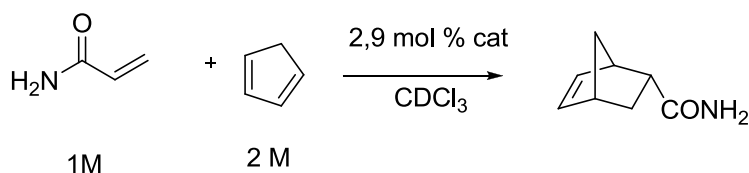


Figure 7.28. Diels-Alder reaction between acrylamide and cyclopentadiene catalysed by receptor **182**·HPF₆.

Although it can be observed a catalytic activity which doubles the reaction rate, the reaction is heterogeneous, being necessary to ultrasonicate and heat it slightly (about 50 °C) to get a partial dissolution of acrylamide and catalyst.

Therefore, we decided to change acrylamide for methyl vinyl ketone, which is soluble in chloroform. However, under these conditions the reaction becomes faster and as the catalyst hardly dissolves, the result is that the reaction without catalyst proceeds essentially at the same rate as the catalysed reaction.

Trying to increase the solubility of the dienophile without increasing too much its reactivity, we conducted a study with cinnamamide. However, solubility problems and the lack of substrate reactivity made impossible to achieve catalysis.

7.2.5.2.2. Michael additions

Another reaction that could catalyse compound **182** is the Michael addition, since it has an acidic group that might associate the acceptor compound and a basic group to deprotonate the nucleophile. To solve the receptor **182** solubility problems, we used its tetrabutylammonium salt. In this case, the enolate could also act as a base, abstracting the proton of the nucleophilic compound in a chiral environment.

Although **182**·TBA was able to catalyse the addition of acetylacetone to nitrostyrene, the addition product was racemic. With diethyl malonate or diethyl phosphite as nucleophiles catalysis was not even observed. Oximes also failed as electrophiles.

Recently, Carmen Nájera has described aminobenzimidazole-based catalysts with very good results in the addition of dicarbonyl compounds to maleimides.²⁵⁶

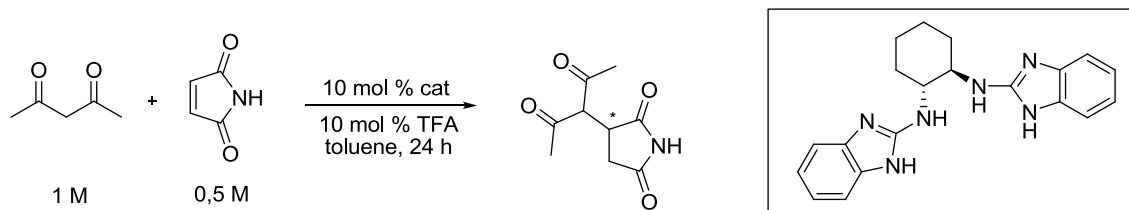


Figure 7.29. Addition of acetylacetone to maleimide catalysed by an aminobenzimidazole derivative.

Due to the similarity between Nájera catalyst and the ones developed in our group, we conducted an experiment to accelerate the same reaction with catalysts **182** and **182**·TBA in CDCl_3 . However, under these conditions, **182** did not dissolve in the reaction medium and **182**·TBA, although catalysed the reaction, it was much slower than the reaction described by Nájera (only 7 % conversion in 17 h working with 5 mol % catalyst) and the enantiomeric excess was low (ee = 17 %).

7.2.5.2.3. Aldol reaction

Theoretically, receptor **182** could catalyse aldol reactions in the same manner than proline. On one hand, it has a basic group able to form enamines and a carboxyl group which can activate the electrophilic carbonyl group with hydrogen bonds. In the case of proline, the carboxyl group is largely deprotonated as carboxylate and the amino group is protonated as ammonium. However, in receptor **182** the acid and the basic group are fine-tuned, so that most of the benzimidazole is free and the enol is in its protonated form.

Thus, an experiment was done to study the cyclization to synthesise the Wieland-Miescher ketone. Compound **182** was dissolved in the ketone without solvent. The reaction was stirred at room temperature without observing any progress. 140 °C were necessary to detect several reaction products by NMR, although none of them coincided with the Wieland-Miescher ketone. It is therefore likely that working with this catalyst, the reaction mechanism is completely different from that catalysed by proline.

7.2.5.2.4. Morita-Baylis-Hillman

Since this reaction, in which an aldehyde is coupled with an unsaturated compound to produce an allylic alcohol can be catalysed by nucleophilic amines such as DABCO, DMAP, DBU or

²⁵⁶ Gómez-Torres, E.; Alonso, D. A.; Gómez-Bengoa, E.; Nájera, C. *Eur. J. Org. Chem.* **2013**, 1434-1440.

imidazole, we thought receptor **182** could catalyse this reaction, however we did not observe improvement in the reaction rate. What it was detected by mass spectrometry was that, under the reaction conditions, catalyst **182** was alkylated with methyl vinyl ketone.

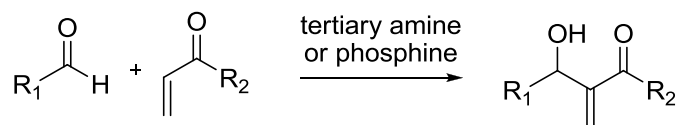


Figure 7.30. Morita-Baylis-Hillman reaction.

7.2.5.2.5. Addition of alcohols to epoxides and tetrahydropyrans

We did not observe catalysis in the two reactions shown in figure 7.31, in which Schreiner thiourea has been very effective.²⁵⁷

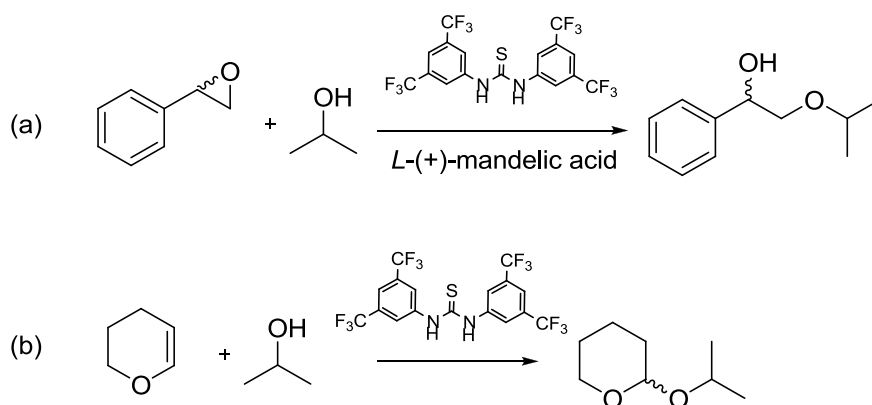


Figure 7.31. (a) Epoxides opening catalysed by L-(+)-mandelic acid and Schreiner thiourea and (b) reaction of an alcohol with THP catalysed by Schreiner thiourea.

7.2.5.2.6. Transesterification

Another reaction studied with catalyst **182** was the transesterification of an ester with an alcohol. We expected that the ester carbonyl formed a hydrogen bond with the enol of the catalyst, while benzimidazole could activate the methanol molecule, making it more nucleophilic. The molecular modelling studies supported this hypothesis.

²⁵⁷ (a) Weil, T.; Kotke, M.; Kleiner, C. M.; Schreiner, P. R. *Org. Lett.* **2008**, *10*, 1513-1516; (b) Kotke, M.; Schreiner, P. R. *Synthesis* **2007**, 779-790.

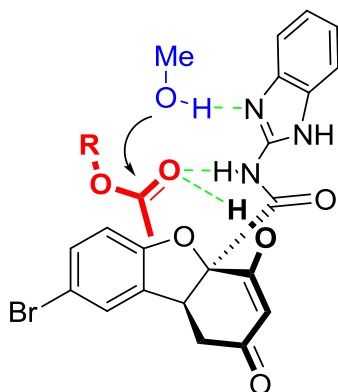


Figure 7.32. Proposed associate between catalyst **182**, an ester and methanol.

The first experiments were carried out with ethyl acetate and methanol using deuteriochloroform as solvent, in order to analyze the reaction by ^1H NMR. No methanolysis of ethyl acetate was observed, however, the hydrolytic activity of the catalyst itself was clear, because it could be observed the substitution of the aminobenzimidazole group of the receptor with a methanol molecule. Since amides are functional groups difficult to hydrolyze, this reaction was a surprise, and we think that occurs because the active groups of the catalyst facilitate this transformation. Moreover, it is remarkable the aminobenzimidazole loss in the presence of methanol, since during the catalyst synthesis the replacement is obtained in the reverse sense.

Since we believed that this catalyst possessed hydrolytic activity, we looked for another more reactive substrate, which could react before the benzimidazole group in the catalyst.

The reaction between phenyl acetate (1 M) and MeOH (3 M) was studied, observing no reaction after 20 hours. However, it was found catalytic activity in the transesterification of *p*-nitrophenyl acetate with methanol. The speed increase observed was $\times 2$.

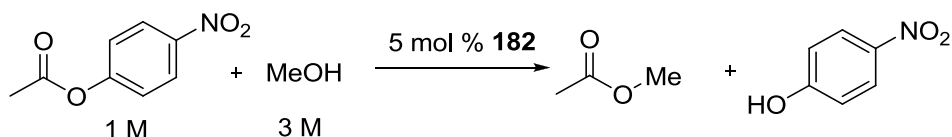


Figure 7.30. Transesterification of *p*-nitrophenyl acetate with methanol catalysed by compound **182**.

7.2.5.2.7. Anhydrides alcoholysis

Since receptor **182** showed catalytic activity in transesterification reactions we looked for a substrate on which it could show asymmetric induction. We thought in the methanolysis of cyclic anhydrides as a possible choice. In a cyclic anhydride with the appropriate substitution, the preferential attack of methanol to one carbonyl will generate an ester and an acid leading to a chiral molecule.

To study this hypothesis, we chose the Diels-Alder adduct obtained in the reaction between cyclopentadiene and maleic anhydride²⁵⁸ (figure 7.34).

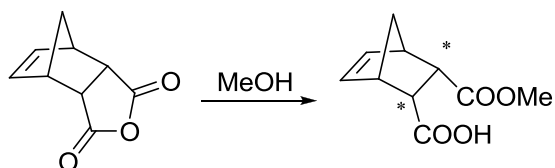


Figure 7.34. Methanolysis of a mixed anhydride which generates a chiral molecule.

The reaction was carried out again in an NMR tube, showing catalytic activity, since in the absence of the catalyst the reaction was slower. Although the molecular models seemed to predict that one carbonyl should react more rapidly with methanol than the other, the analysis of the reaction mixture by chiral HPLC showed that the enantiomeric excess was almost 0 %. Neither was enantioselectivity observed using isopropanol as a hindered alcohol.

A drawback of the methanolysis of cyclic anhydrides is that a carboxylic acid is produced in the reaction medium, and we know that carboxylic acids are good guests of the catalyst. Under these conditions, it prevents association of the anhydride, because carboxylic acids show higher association constants. Since the association between the anhydride and the receptor is prevented, the catalytic activity is lost. Looking for a substrate in which the alcoholysis does not generate an acid in the reaction medium we came across azlactones. Azlactones are cyclic compounds generated from amino acids in which the alcoholysis generates an ester of an acylamino acid, which is a neutral compound, as shown in figure 7.35.

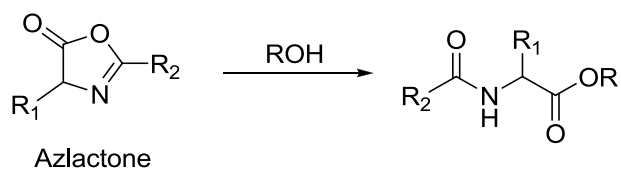


Figure 7.35. Azlactone and reaction with an alcohol.

7.2.5.2.8. Dynamic kinetic resolution of azlactones

Currently, there is great interest in obtaining enantiomerically pure α -amino acids, which are essential in the synthesis of peptides or peptoids and as starting materials in the preparation of pharmaceutical compounds, antibiotics, hormones, pesticides, sweeteners, organocatalysts, ligands for transition metal based catalysts, etc.²⁵⁹

²⁵⁸ Brown, A. H.; Sheares, V. V. *Macromolecules* **2007**, *40*, 4848-4853.

²⁵⁹ (a) Breuer, M.; Ditrich, K.; Habicher, T.; Hauer, B.; Keßeler, M.; Strmer, R.; Zelinski, T. *Angew. Chem., Int. Ed.* **2004**, *43*, 788-824; (b) Patel, R. N. En *Stereoselective Biocatalysis*; Patel, R. N., Ed.; Marcel Dekker: New York, 2000; pp. 877-902; (c) Jarvo, E. R.; Miller, S. J. *Tetrahedron* **2002**, *58*, 2481-2495; (d) Grger, H.; Drauz, K. En *Asymmetric Catalysis on Industrial Scale*; Blaser, H. U.; Schmidt, E., Eds.; Wiley-VCH: Weinheim, 2004; pp 131-147.

There are several ways to prepare enantiomerically pure α -amino acids: fermentation,²⁶⁰ asymmetric synthesis²⁶¹ or by dynamic kinetic resolution of azlactones. Azlactones are cyclic amino acid derivatives which readily racemize (the pK_a of the alpha proton is about 8.9 to 9.5 depending on the amino acid).²⁶² Indeed, this capability of racemization allows that the kinetic resolution is dynamic, ie, produces a total yield of 100 % for one enantiomer since one of the azlactone enantiomers can be transformed into the other. In a traditional kinetic resolution, each enantiomer will be separated reaching a maximum 50 % yield.

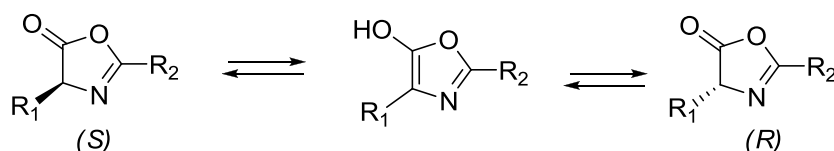


Figure 7.36. Equilibrium between the two enantiomers of the azlactone through the enol form.

When an azlactone reacts with an alcohol, the opening of the azlactone ring takes place to generate the corresponding acylamino acid ester. In the absence of a chiral auxiliary, the reaction will occur with both azlactones, producing the racemic mixture of both esters. However, some chiral organocatalysts are able to make react the nucleophilic alcohol with only one enantiomer of the azlactone, to generate a single amino acid derivative. If racemization speed is greater than the rate of alcohol addition to azlactone, as more of one enantiomer is consumed, the equilibrium shifts in the sense of generating more of the enantiomer of the azlactone that is being consumed, and at the end only one enantiomer of the acylaminoester is produced.

For asymmetric induction to occur it is necessary that the rate of racemization of the two azlactones (k_{rac}) is greater than the azlactone ring opening (k_{cat}) that, in turn, should be faster than the uncatalysed opening of the azlactone (k_{nocat}).

²⁶⁰ Schmidt-Kastner, G.; Egerer, P. En *Biotechnology*; Relm, H. J., Reed, G., Eds.; Verlag Chemie: Weinheimer, Deerfield Beach, FL, Basel, 1984; Vol. 6A, pp 387-421.

²⁶¹ (a) He, W.; Wang, Q.; Wang, Q.; Zhang, B.; Sun, X.; Zhang, S. *Synlett* **2009**, 1311-1314; (b) Ooi, T.; Kato, D.; Inamura, K.; Ohmatsu, K.; Maruoka, K. *Org. Lett.* **2007**, *9*, 3945-3948; (c) Chen, J.; Lu, X.; Lou, W.; Ye, Y.; Jiang, H.; Zeng, W. *J. Org. Chem.* **2012**, *77*, 8541-8548; (d) Beenen, M. A.; Weix, D. J.; Ellman, J. A. *J. Am. Chem. Soc.* **2006**, *128*, 6304-6305; (e) Dai, H.; Lu, X. *Org. Lett.* **2007**, *9*, 3077-3080; (f) Kobayashi, J.; Nakamura, M.; Mori, Y.; Yamashita, Y.; Kobayashi, S. *J. Am. Chem. Soc.* **2004**, *126*, 9192-9193; (g) Ooi, T.; Kameda, M.; Taniguchi, M.; Maruoka, K. *J. Am. Chem. Soc.* **2004**, *126*, 9685-9694; (h) Kobayashi, S.; Matsubara, R.; Nakamura, Y.; Kitagawa, H.; Sugiura, M. *J. Am. Chem. Soc.* **2003**, *125*, 2507-2515; (i) Zhang, H.; Mitsumori, S.; Utsumi, N.; Imia, M.; Garcia-Delgado, N.; Mifsud, M.; Albertshofer, K.; Cheong, P. H.-Y.; Houk, K. N.; Tanaka, F.; Barbas III, C. F. *J. Am. Chem. Soc.* **2008**, *130*, 875-886; (j) Zhang, H.; Mifsud, M.; Tanaka, F.; Barbas III, C. F. *J. Am. Chem. Soc.* **2006**, *128*, 9630-9631; (k) Kano, T.; Yamaguchi, Y.; Tokuda, O.; Maruoka, K. *J. Am. Chem. Soc.* **2005**, *127*, 16408-16409; (l) Saito, S.; Tsubogo, T.; Kobayashi, S. *J. Am. Chem. Soc.* **2007**, *129*, 5364-5365; (m) Uruguchi, D.; Kinoshita, N.; Ooi, T. *J. Am. Chem. Soc.* **2010**, *132*, 12240-12242; (n) Davis, F. A.; Reddy, R. E.; Portonovo, P. S. *Tetrahedron Lett.* **1994**, *35*, 9351-9354; (o) Ishitani, H.; Komiyama, S.; Hasegawa, Y.; Kobayashi, S. *J. Am. Chem. Soc.* **2000**, *122*, 762-766; (p) Huang, J.; Corey, E. J. *Org. Lett.* **2004**, *62*, 5027-5029; (q) Duthaler, R. O. *Tetrahedron* **1994**, *50*, 1539-1650.

²⁶² de Jersey, J.; Zerner, B. *Biochemistry* **1969**, *8*, 1967-1974.

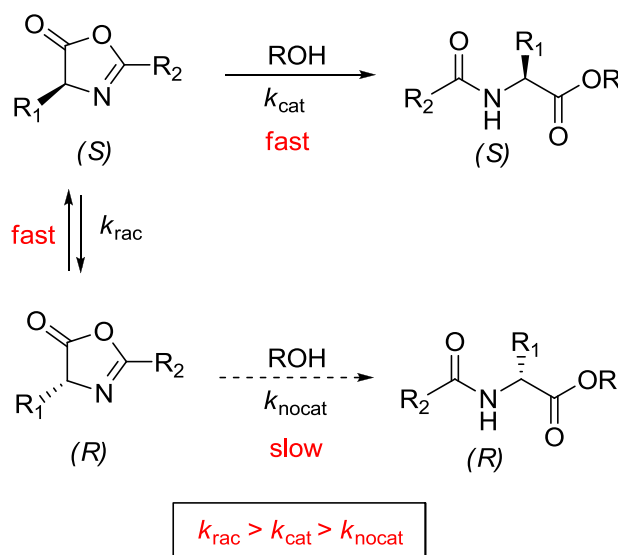


Figure 7.37. Dynamic kinetic resolution of azlactones.

Several strategies are described in the literature to perform the dynamic kinetic resolution of azlactones. Although no specific enzymes exist in nature for azlactone opening, several lipases²⁶³ have provided good results with high yields and enantiomeric excesses over 99 %, although with overall reaction times of days or weeks. Furthermore, enzymes have several disadvantages as their specificity and instability, low tolerance to the substrate, etc.

Consequently, several authors²⁶⁴ have developed catalysts based on transition metals and organocatalysts for dynamic kinetic resolution of azlactones, as summarized in figure 7.38. Lewis acids, Lewis bases, Brønsted acids and bifunctional catalysts have been used.

²⁶³ (a) Brown, S. A.; Parker, M.-C.; Turner, N. J. *Tetrahedron: Asymmetry* **2000**, *11*, 1687-1690; (b) Turner, N. J.; Winterman, J. R.; McCague, R.; Parratt, J. S.; Taylor, S. J. C. *Tetrahedron Lett.* **1995**, *36*, 1113-1116; (c) Crich, J. Z.; Brieva, R.; Marquart, P.; Gu, R. L.; Flemming, S.; Sih, C. J. *J. Org. Chem.* **1993**, *58*, 3252-3258; (d) Gu, R. L.; Lee, I.-S.; Sih, C. J. *Tetrahedron Lett.* **1992**, *33*, 1953-1956.

²⁶⁴ (a) Seebach, D.; Jaeschke, G.; Gottwald, K.; Matsuda, K.; Formisano, R.; Chaplin, D. A.; Breuning, M.; Bringmann, G. *Tetrahedron* **1997**, *53*, 7539-7556; (b) Gottwald, K.; Seebach, D. *Tetrahedron* **1999**, *55*, 723-738; (c) Xie, L.; Hua, W.; Chan, A. S. C.; Leung, Y.-C. *Tetrahedron: Asymmetry* **1999**, *10*, 4715-4728; (d) Liang, J.; Ruble, J. C.; Fu, G. C. *J. Org. Chem.* **1998**, *63*, 3154-3155; (e) Belokon, Y. N.; Bachurina, I. B.; Tararov, V. I.; Saporovskaya, M. B. *Bull. Acad. Sci. USSR, Div. Chem. Sci.* **1992**, *41*, 422-429; (f) Berkessel, A.; Cleeman, F.; Mukherjee, S.; Müller, T. N.; Lex, J. *Angew. Chem., Int. Ed.* **2005**, *44*, 807-811; (g) Berkessel, A.; Mukherjee, S.; Cleeman, F.; Müller, T. N.; Lex, J. *Chem. Commun.* **2005**, 1898-1820; (h) Berkessel, A.; Mukherjee, S.; Müller, T. N.; Cleeman, F.; Roland, K.; Brandenburg, M.; Neudörfl, J.-M.; Lex, J. *Org. Biomol. Chem.* **2006**, *4*, 4319-4330; (i) Peschiulli, A.; Quigley, C.; Tallon, S.; Gun'ko, Yu. K.; Cannon, S. J. *J. Org. Chem.* **2008**, *73*, 6409-6412; (j) Lee, J. W.; Ryu, T. H.; Oh, J. S.; Bae, H. Y.; Jang, H. B.; Song, C. E. *Chem. Commun.* **2009**, 7224-7226; (k) Yang, X.; Lu, G.; Birman, V. B. *Org. Lett.* **2010**, *12*, 892-895; (l) Lu, G.; Birman, V. B. *Org. Lett.* **2011**, *13*, 356-358.

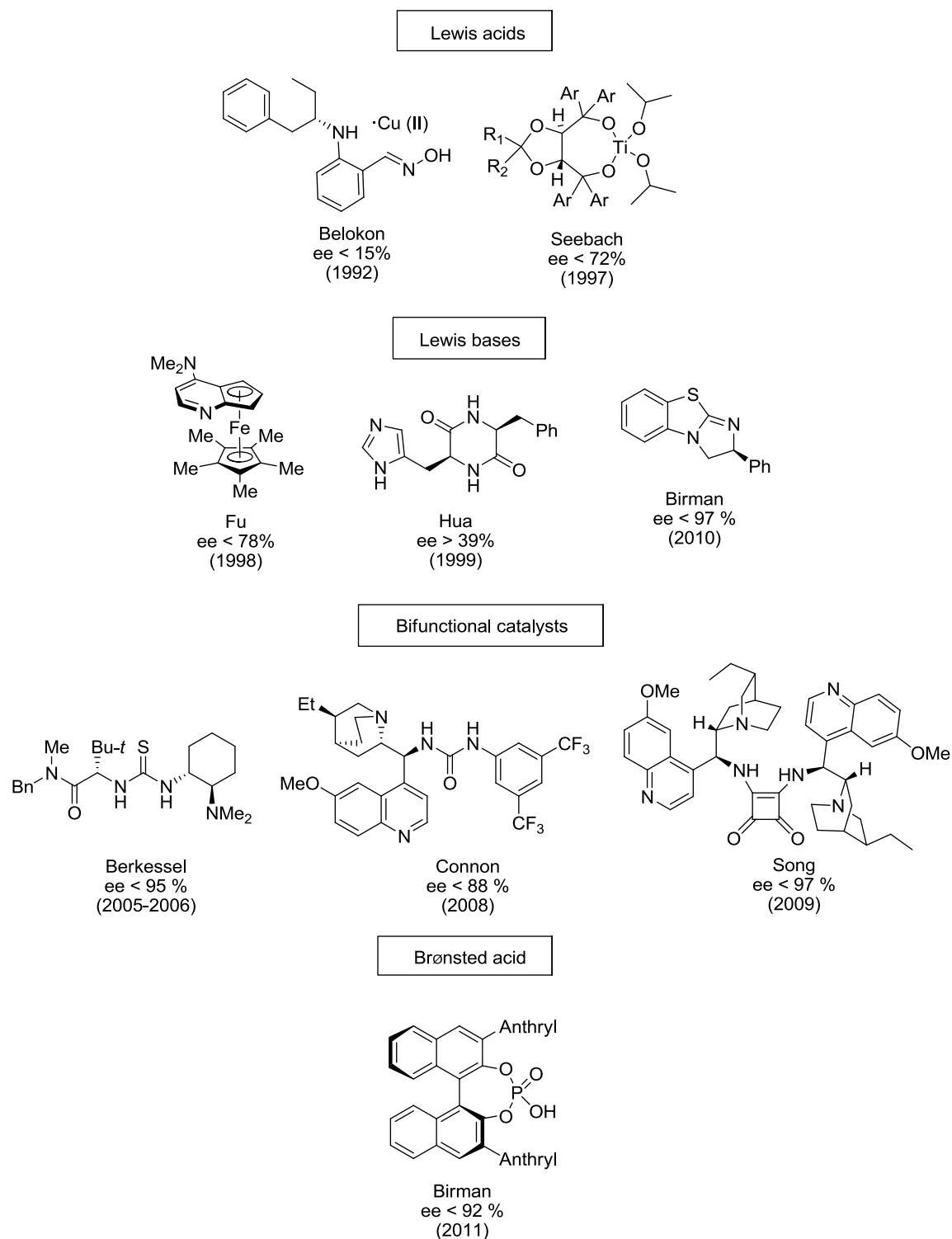


Figure 7.38. Catalysts described in the literature for the dynamic kinetic resolution of azlactones.

However, reaction rates remain relatively slow and the substrates which are reacted are limited. It is noteworthy the study conducted by Song^{264j} who, using a squaramide functionalized with two cinchona derivatives, is able to achieve enantioselectivities up to 97 % and reaction times of hours. He also justifies the use of two cinchona groups to prevent the

formation of dimers, which decrease the rate and enantioselectivity of the reaction, as has been demonstrated.

Catalyst **182** could work in a similar way as the bifunctional catalysts shown in figure 7.38. On one hand it has an acid, capable of associating the carbonyl group of azlactones, and it has a basic group that is responsible for increasing the nucleophilicity of the alcohol by hydrogen bonding with the Brønsted base of the catalyst.

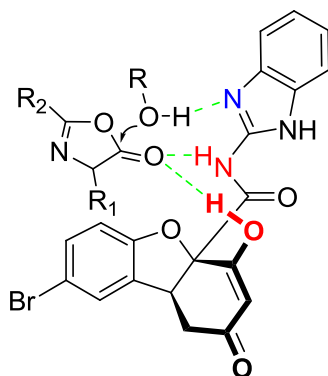


Figure 7.39. Associate proposed for catalyst **182**, azlactone and methanol.

A molecular modelling study was carried out to know if catalyst **182** was suitable to obtain azlactones opening with enantiomeric induction. In figure 7.40 the two transition states obtained for the opening reaction of an alanine azlactone with methanol as nucleophile is shown.

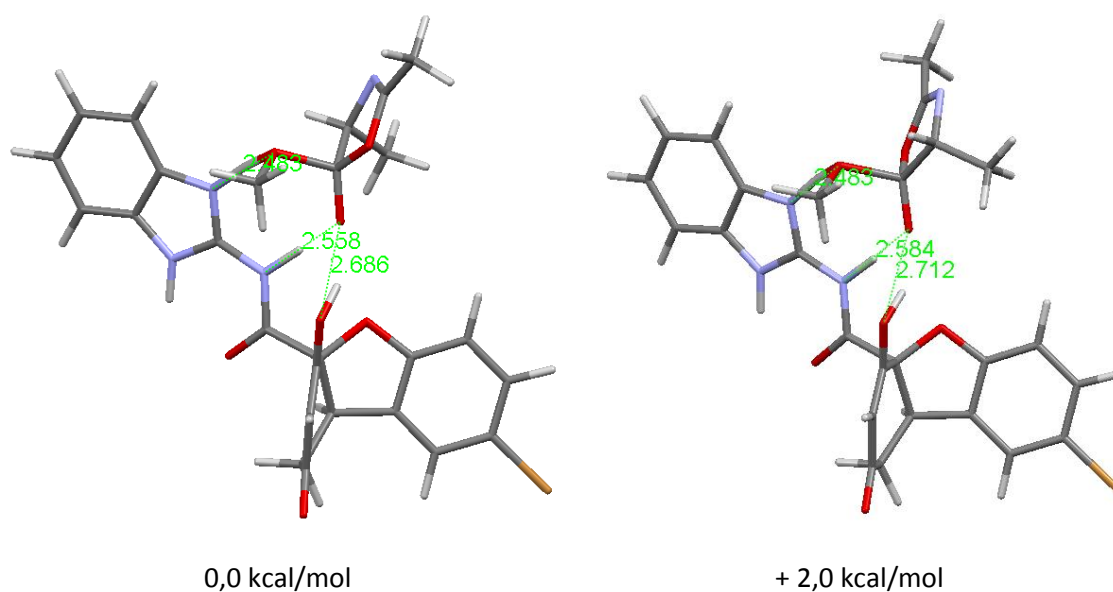


Figure 7.40. Transition states obtained by molecular modelling for the opening reaction of alanine methylazlactone with methanol catalysed by receptor **182**. Hydrogen bonds between reactants and catalyst (in Å) are also shown.

In both transition states it is observed the formation on an oxyanion hole between the amide NH and the enol OH (heteroatom-heteroatom distance 3.07 Å, figure 7.41); distance which may be slightly small in accordance with the observed values found in enzymes. However, this oxyanion hole is effective in forming two hydrogen bonds with the carbonyl group of azlactone, while methanol is forming a strong hydrogen bond with the basic N of benzimidazole (2.48 Å), as it attacks the carbonyl group of azlactone. The energy difference between the two transition states is 2.0 kcal/mol, and would be determined by the different orientation of the OMe group when it attacks the azlactone. In the less energetic transition state, the OMe group is *anti* to the C(ester)-CHR bond; however, in the transition state of higher energy is *anti* to the C(ester)-O alkyl bond, existing a *gauche* interaction with the azlactone CH, which is what is likely to produce the energy difference.

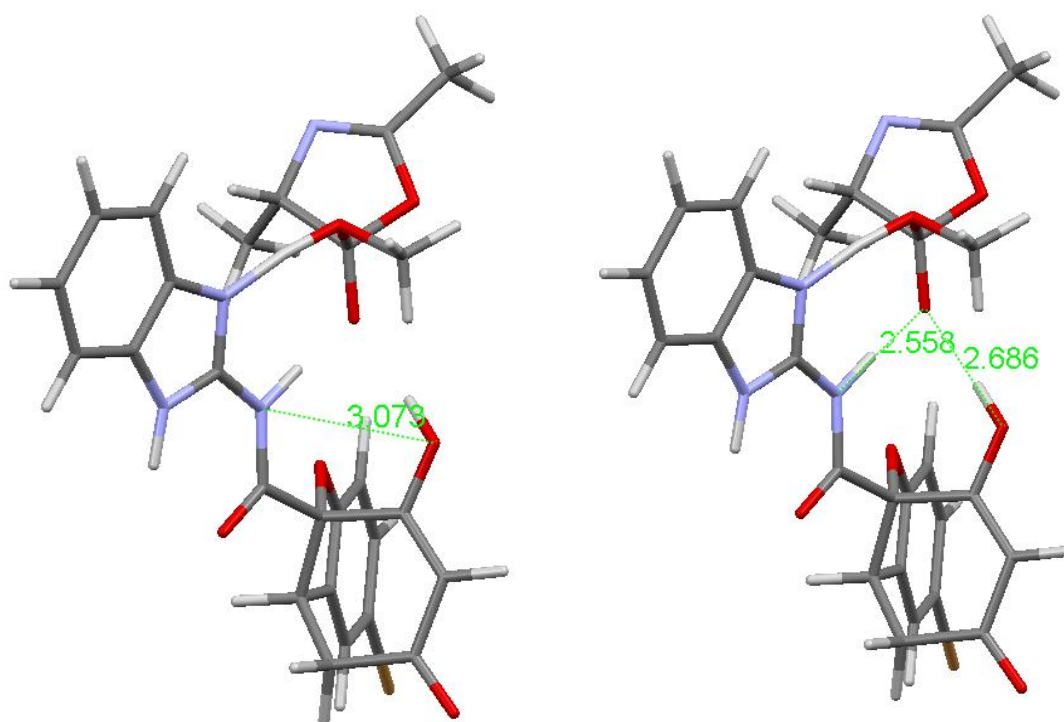


Figure 7.41. More stable transition state in which the oxyanion hole (left) and interactions with the azlactone carbonyl (right) are shown.

Encouraged by the results of the modelling transition states, we conducted a study on the alcoholysis of azlactones.

Firstly, we chose as substrate the phenylalanine methylazlactone because it is very easily obtained from phenylalanine and acetic anhydride.²⁶⁵

²⁶⁵ (a) Müller, E. D. *Houben-Weyl, Methoden der Organischen*; George Thieme Verlag: Stuttgart, 1958; (b) Bergmann, M.; Stern, F.; Witte, A. *Liebigs Ann.* **1926**, 449, 227.

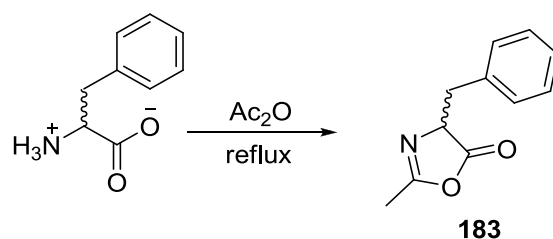


Figure 7.42. Synthesis of phenylalanine methylazlactone.

7.2.5.2.8.1. Kinetic study

a) Reaction Order

Our literature research has shown that there is an extensive work on alcoholysis of azlactones, however, we found for this process, no kinetic work in which the reaction order is displayed for each of the two reagents. We believe that these data are important to understand the mechanism of the reaction, as the attack of the alcohol to the azlactone carbonyl requires the transport of a proton to the carbonyl group, in order to avoid the formation of an oxonium salt in the alcohol oxygen, which would render a high activation energy barrier for the process. This transport of the proton can be carried out either by a "proton switch" mechanism, in which the hydroxyl group performs the transport (figure 7.43) or by "proton slide" mechanism, in which the pair of electrons from the azlactone nitrogen performs this function, as shown in figure 7.43.

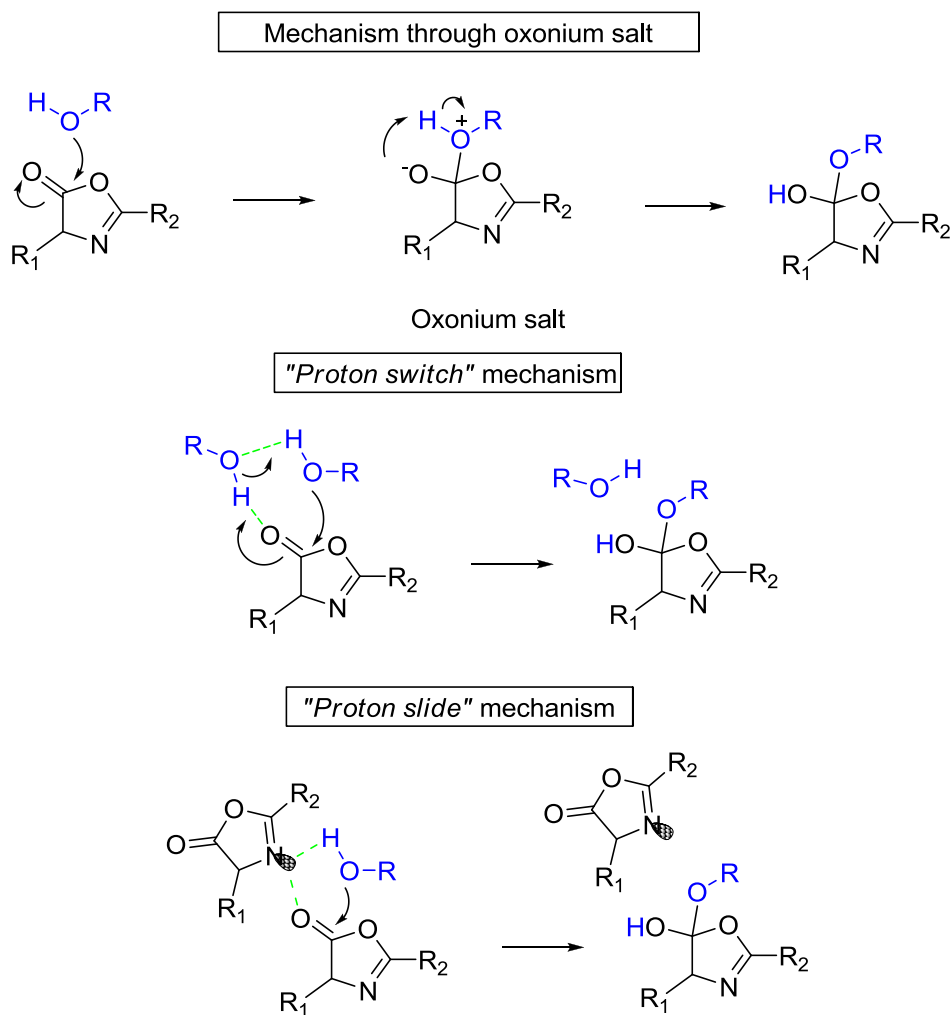
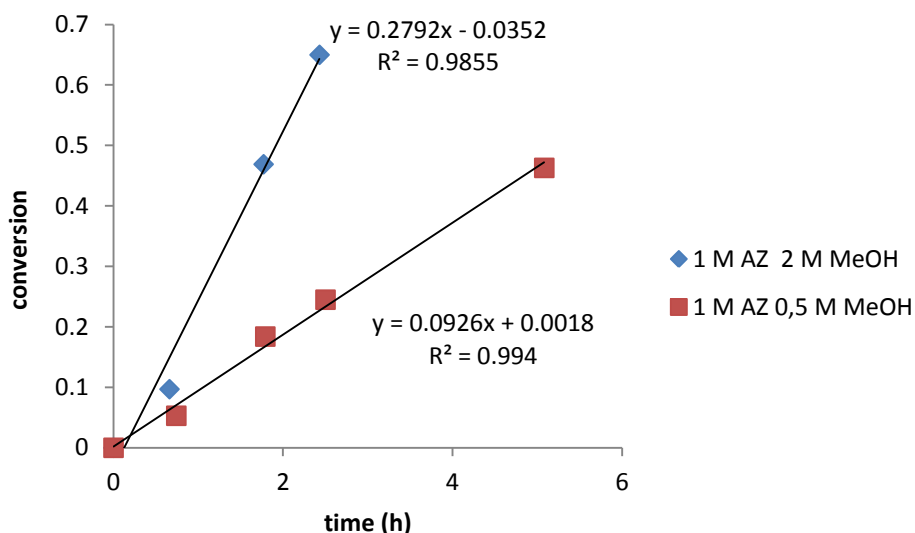


Figure 7.43. "Proton switch" and "proton slide" mechanisms for proton transport during the alcoholysis of azlactone.

Both mechanisms can be differentiated kinetically, because if the alcohol transports the proton, it would appear in the kinetic study with second order, whereas if the nitrogen is providing the transport, it will be the azlactone the compound with second order in the reaction kinetics.

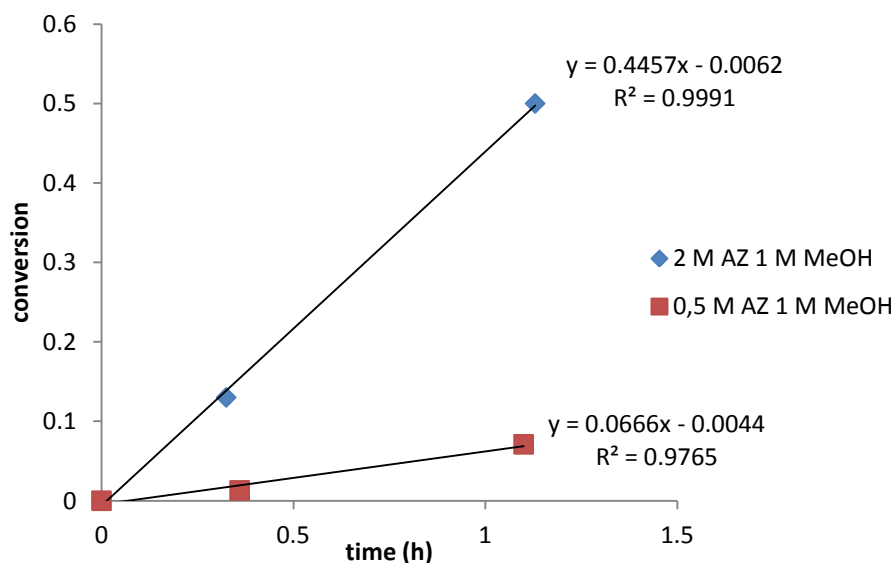
Thus, the study of the initial rates will provide the mechanism, once known the reaction order of the reagents.

The study was carried out in a chloroform solution in order to monitor the progress of the reaction by NMR. 0.5 M and 2.0 M MeOH solutions were prepared keeping constant the concentration of azlactone (1.0 M) to determine the reaction order in methanol.



Graph 7.1. Graphical representation to determine the reaction order in methanol.

Similarly, azlactone concentrations were varied, and 0.5 M and 2.0 M solutions were prepared keeping constant the concentration of MeOH (1.0 M) to determine the reaction order in azlactone.



Graph 7.2. Graphical representation to determine the reaction order in azlactone.

From data obtained, we conclude that the reaction is bimolecular in azlactone, and should be the nitrogen of a second azlactone molecule which facilitates the reaction.

This is interesting due to the fact that it supports our proposed mechanism for the receptor, in which the methanol attack is preceded by formation of a hydrogen bond with the nitrogen of the benzimidazole. This hydrogen subsequently ends in the carbonyl oxygen when the tetrahedral intermediate is reached.

b) Racemization study

A key piece to have asymmetric induction is that azlactone racemization should be faster than the opening of the heterocycle by the alcohol, otherwise, both enantiomers of the azlactone will react generating the racemic acylamino acids mixture.

To examine the relative racemization rate of azlactone versus azlactone opening in the presence of an alcohol, we prepared a solution of azlactone **183** in deuteriochloroform and added deuterated methanol. Due to the relatively large concentration of deuterated methanol, we expected that the racemization of the azlactone lead to the deuteration of the alpha position, while after the opening of the amino acid, as the alpha proton is less acidic, labelling is not expected with deuterium.

The result was that heterocycle opening was at least ten times faster than racemization, since no labelling with deuterium was observed on the acylamino acid alpha carbon.

Since literature emphasizes the high speed at which azlactones racemize, we found this result surprising; however, it has to be considered that in the vast majority of articles in which the dynamic kinetic resolution is studied, they work with azlactones derived from benzoyl amino acids. For this reason, we conducted a similar experiment in which the substrate was the phenylazlactone of phenylalanine **184**. In this case the result was the opposite, the addition of deuterated methanol led to immediate deuteration in the alpha position of the azlactone, which only experienced the opening of the cycle at a much slower rate, after several hours.

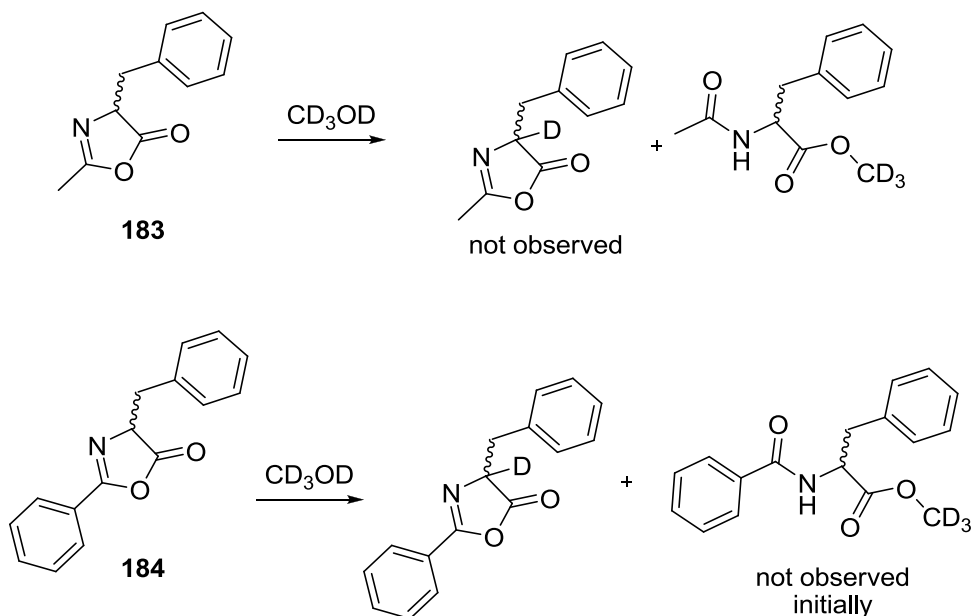


Figure 7.44. Racemization studies of methylazlactone of phenylalanine **183** and phenylazlactone of phenylalanine **184**.

7.2.5.2.8.2. Catalysis study

Although from a technical point of view acetyl derivatives of amino acids are more interesting than benzoyl derivatives, because the latter are more difficult to hydrolyze, the slow racemization advised us to begin the study with phenylazlactones.

These azlactones were prepared by benzylation of the corresponding amino acid and subsequent cyclization with DCC. The filtration of the dicyclohexylurea which is formed as a by-product leaves a crude azlactone, which still has small amounts of the urea. However, we have not further purify it because of the high sensitivity to moisture which these azlactones exhibit.

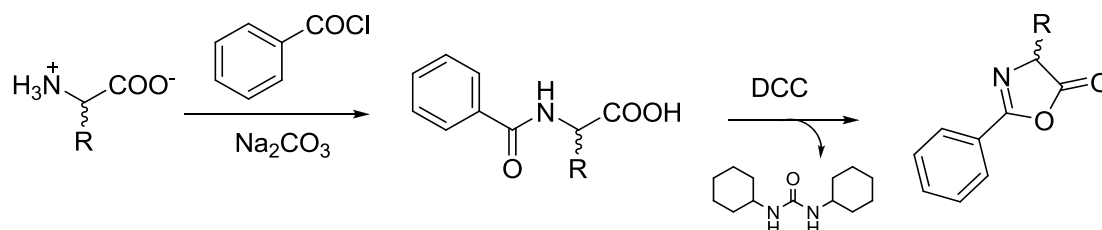
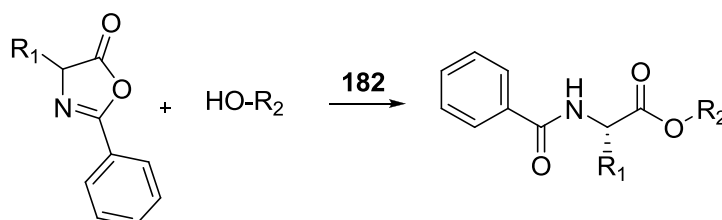


Figure 7.45. Preparation of phenylazlactones.

The experiments were carried out using an excess of alcohol and 7-20 mol % catalyst **182**. The enantiomeric excesses were determined by chiral HPLC.

Table 7.2. Results obtained in the phenylazlactone opening with several alcohols in the presence of catalyst **182**, at 20 °C.



entry	R ₁	R ₂	mol % 182	conversion (%)	time (h)	ee (%)
1 ^a	-CH ₂ C ₆ H ₅	-CH ₃	10	99	0.25	9
2	-CH(CH ₃) ₂	-CH ₃	19	61	7	2
3	-CH(CH ₃)(CH ₂ CH ₃)	-C ₅ H ₁₁	9	68	65	8
4	-CH(CH ₃)(CH ₂ CH ₃)	-CH ₂ CH(CH ₃) ₂	8	51	53	9
5 ^b	-CH ₃	-CH(CH ₃) ₂	12	63	19	14
6 ^a	-CH ₂ C ₆ H ₅	-CH(CH ₃) ₂	13	58	14.5	1
7 ^b	-CH(CH ₃) ₂	-CH(CH ₃) ₂	17	40	98	3
8 ^a	-CH(CH ₃)(CH ₂ CH ₃)	-CH(CH ₃) ₂	8	49	13	0
9	-C ₆ H ₅	-CH(CH ₃) ₂	14	79	83	13
10 ^b	-CH ₃	-CH(C ₆ H ₅) ₂	14	61	39	3
11 ^a	-CH(CH ₃)(CH ₂ CH ₃)	-CH(C ₆ H ₅) ₂	7	57	13	13
12 ^b	-CH ₂ C ₆ H ₅	-C ₆ H ₅	10	71	13	15
13	-CH(CH ₃)(CH ₂ CH ₃)	terpineol	11	-	-	-

^a t = 50-60 °C.

^b With chlorobenzene as solvent.

As can be observed, the enantiomeric excesses are small, and since the theoretical predictions indicated that they should be higher, we thought in a possible decomposition of the catalyst **182**. To check this, we conducted an experiment in which the stability of the catalyst was studied during the reaction by HPLC. It was observed that when MeOH was used as alcohol, the benzimidazole methanolysis occurs overnight; however, the use of more hindered alcohols slowed down this process, nevertheless, alcoholysis of the catalyst is a potential handicap with phenylazlactones.

Since in the deuteration experiments we have observed that methylazlactones were much more reactive than phenylazlactones, we considered to include methylazlactones in the study. The problem already mentioned is that methylazlactones racemize slower than the opening of the heterocycle with methanol, so that this alcohol is not appropriate for obtaining enantiomeric excesses. The use of a hindered alcohol seems an ideal solution, since while the racemization rate is independent of the nucleophilicity of the alcohol, the opening of the heterocycle is delayed considerably, so that we proposed the use of isopropanol.

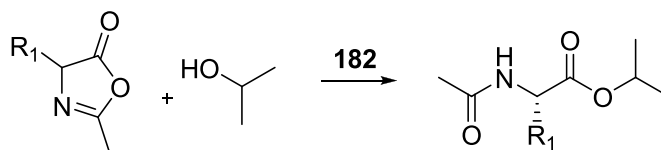
The reaction was carried out in the absence of solvent with phenylalanine methylazlactone **183**, catalyst **182** and isopropyl alcohol. At 70 °C (1.4 equivalents of isopropyl alcohol, 7.1 mol % catalyst), the reaction goes to completion in only 30 minutes and the enantiomeric excess is 38 %.

The reaction also proceeds at room temperature, although more slowly. Under these conditions, after 6 hours, the catalysed reaction had progressed 85 % while the uncatalysed reaction 39 %. Enantiomeric excess rose up to 45 %.

It is still possible to further diminish temperature, yielding at 0 °C 47 % ee.

This promising result led us to use other amino acid methylazlactones. The enantiomeric excesses determined by chiral HPLC are shown in table 7.3.

Table 7.3. Results obtained in the opening of methylazlactones with isopropyl alcohol and catalyst **182**, at 20 °C.



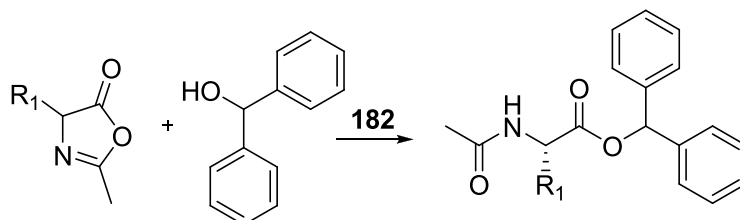
entry	R ₁	mol % 182	conversion (%)	time (h)	ee (%)
1 ^a	-CH ₃	5	99	15	25
2	-CH ₂ C ₆ H ₅	8	85	6,5	45
3 ^a	-CH(CH ₃) ₂	10	99	18,5	31
4	-CH(CH ₃)(CH ₂ CH ₃)	13	75	19	13
5	-C ₆ H ₅	27	99	4	23

^a With chlorobenzene as solvent.

The stability of the catalyst in the reaction medium was studied again by HPLC taking aliquots of the reaction between phenylalanine methylazlactone **183** and isopropyl alcohol, showing that the catalyst remained stable over time, something that we have observed that did not occur with methanol.

Since the catalyst is relatively stable in the reaction medium, we considered the possibility that the enantiomeric excesses were small because azlactone racemization speed was still relatively small compared to the heterocycle opening. Therefore, we looked for a more hindered alcohol, and since modelling studies showed that diphenylmethanol could generate a large enantiomeric excess, we used this nucleophile. The reaction of phenylalanine methylazlactone **183** with diphenylmethanol is much slower than with isopropyl alcohol, which in our opinion warrants racemization speed should be enough under these conditions. However, enantiomeric excess was not superior to that obtained with isopropyl alcohol, so we discarded a slow racemization rate as responsible of the small enantiomeric excesses.

Table 7.4. Results obtained in the opening of methylazlactones with diphenylmethanol and catalyst **182**, at 20 ° C.



entry	R ₁	mol % 182	conversion (%)	time (h)	ee (%)
1 ^a	-CH ₂ C ₆ H ₅	17	77	13,5	22
2 ^b	-CH ₂ C ₆ H ₅	23	42	167	4
3	-CH(CH ₃) ₂	10	50	18,5	0
4	-CH(CH ₃)(CH ₂ CH ₃)	16	51	11	0

^a With chlorobenzene as solvent.

^b With toluene as solvent and after an azeotropic distillation of reactants and catalyst. In this case receptor **149** was used as catalyst.

Although esters of tertiary alcohols are difficult to obtain, we have been able to carry out the reaction of azlactones with *t*-butanol in the presence of catalyst **182**. These *t*-butyl esters are very useful in synthesis because they are readily hydrolyzed in acidic medium. The asymmetric induction we have achieved in this process has only been modest, 41 % for phenylalanine methylazlactone **183**. Since the reaction with *t*-butanol is even slower than with diphenylmethanol, we discarded again a slow racemization to be responsible for the small enantiomeric excess.

Moreover, poorer nucleophiles like thiols should have a similar effect on the relationship between racemization and heterocycle opening. The use of thiols involves small speeds in regards to heterocycle opening, but in any case, enantiomeric excesses did not improved, so we confirmed again that it is not a small racemization rate which prevents the generation of larger enantiomeric excesses.

A final argument that may explain why results are not better is the attack of the alcohol to the imine nitrogen. Although it may not seem very probable that the alcohol attacks the imine carbon, it should be noted that the catalyst used in these reactions is acid, and the iminium salt is more reactive than the neutral carbonyl. The attack on the imine would have very negative consequences for the asymmetric induction of the reaction, since a carboxylic acid is generated and we know that it is a good guest for catalyst **182**, leading to competitive inhibition by the product, and moreover, as it is acidic, it is a potentially catalyst for the reaction.

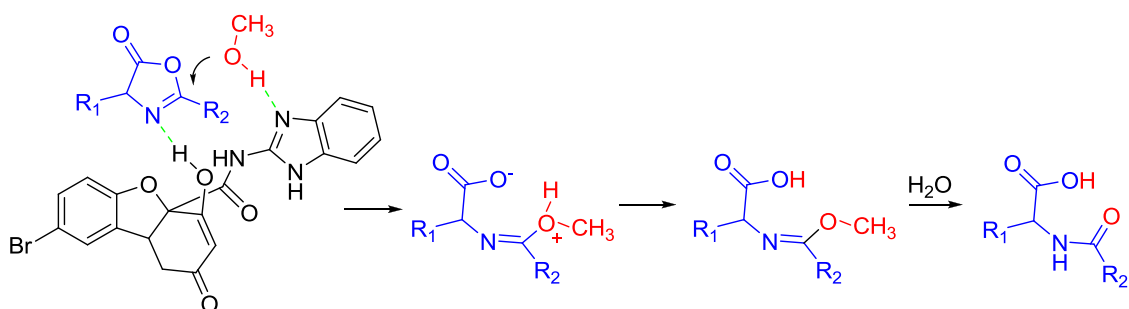


Figure 7.46. Azlactone hydrolysis product if alcohol is added to the imine carbon.

To study the effect that the carboxylic acid of the amino acid has on the reaction, we prepared acetyl-*L*-phenylalanine. The use of the optically pure amino acid should allow us to further explore whether this compound has asymmetric induction in the reaction. Acetyl *L*-phenylalanine was able to accelerate the reaction as much as catalyst **182**, but it showed no enantioselectivity.

So far we have not been able to show that the alcohol really attacks the imine carbon, because the work up of the reaction would hydrolyze this compound rapidly to the acetyl amino acid, just the same structure that would have been produced if there had been small amounts of water in the reaction medium.

However, the important role played by the enol group of the catalyst is evident because when methyl ether **185** is used as catalyst, the reaction is four times slower than with receptor **182**. It also generates other by-products in the reaction medium. Regarding the enantiomeric excess it falls from 45 to only 8%.

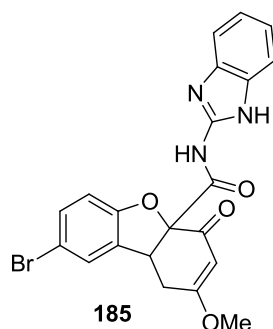


Figure 7.47. Methyl ether **185** generated from enol **182**.

We expect that small changes in the catalyst structure will allow higher enantiomeric excesses in the future.

7.2.6. Preparation of a catalyst soluble in non-polar solvents

Until now we have found that many of the reactions in which compound **182** is used as catalyst are limited by its low solubility in organic solvents. Although this problem could be solved using polar solvents, in these conditions, it is likely that the hydrogen bonds necessary for the catalyst to form the associate and catalyze the reaction are not formed.

One possible solution is to introduce a structural change in the receptor to make it more soluble in nonpolar solvents. The place to introduce these changes is not trivial, since above all it is necessary to preserve the acidic and basic functional groups capable of generating catalysis. We thought that the enol group of the catalyst could be used to introduce long alkyl chains. In fact, we had already observed alkylation with methyl vinyl ketone when trying to use compound **182** as a catalyst for the Morita-Baylis-Hillman reaction.

Taking advantage of the enol reactivity, the Mannich reaction gave us a good chance to introduce alkyl chains. Thus, we studied the incorporation of different groups.

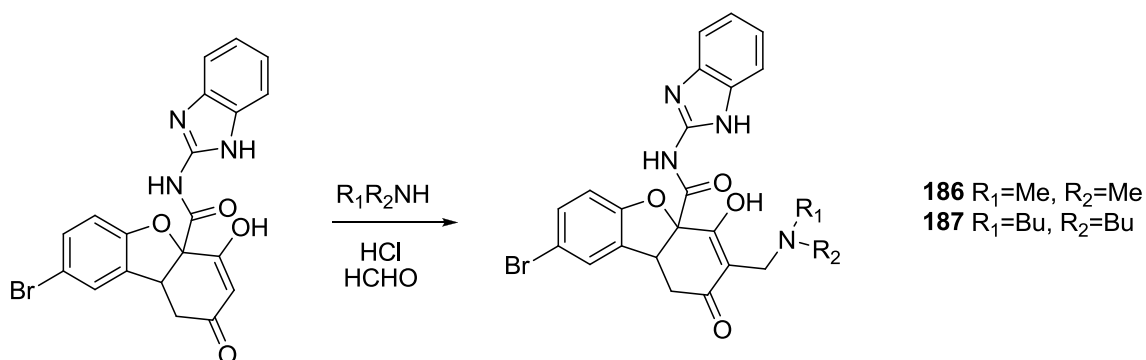


Figure 7.48. Mannich reaction with receptor **182**.

However, while carrying out the reaction we found that the Mannich product decomposed on heating. We believe it is the removal of the ammonium group which leads to decomposition, generating a strongly activated double bond which is conjugated with two carbonyls. These types of double bonds are easily polymerized, giving complex oligomer mixtures.

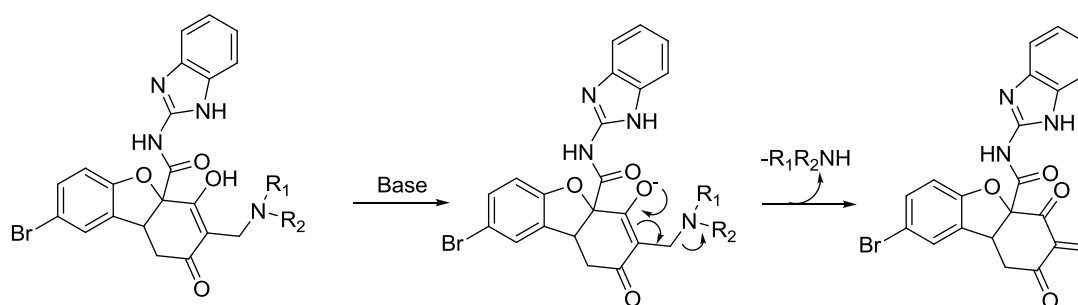


Figure 7.49. Proposed mechanism for elimination reaction in compounds **186** and **187**.

The formation of this compound led us to think that it would be possible to replace the amino group generated in the Mannich reaction with another lipophilic nucleophile. Thus, by heating the Mannich product slightly (50 °C) for 50 min in the presence of dodecanethiol, the addition compound in which the double bond is captured by the thiol is obtained. This new compound, with its long alkyl chain, is very soluble in chloroform.

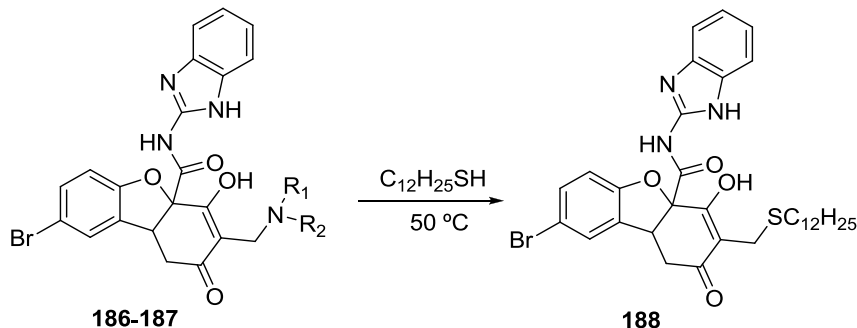


Figure 7.50. Replacement of the amino group by dodecanethiol.

Although the spectroscopic data seem to corroborate the proposed structure, the ^1H NMR spectrum in CDCl_3 shows some signs that are, at least, unusual for this type of compound. Thus, there is not observed a single broad singlet for the thiol CH_2 chain, but it can be seen at least three broad singlets. We believe this is because the receptor dimerizes, so that the thiol CH_2 chain crosses the aminobenzimidazole aromatic ring, thereby shielding multiple methylene groups. A proposal for the dimer structure is shown in figure 7.51.

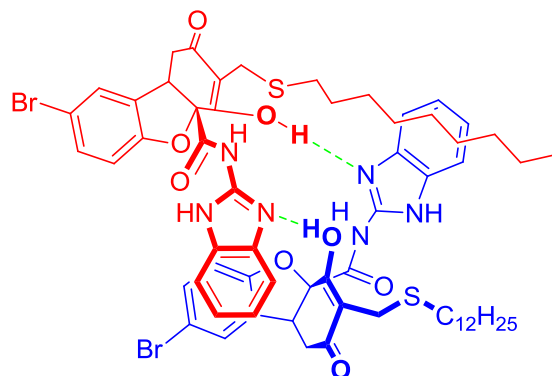


Figure 7.51. Receptor **188** dimer.

However, we believe that in the presence of a guest which forms a strong complex with the receptor, the dimer will break down.

Thus, with the help of the CPK models, we designed a new guest **189** in which, on one hand, a carboxyl group would interact with the benzimidazole and, on the other hand, a hydroxyl forms a hydrogen bond with the receptor enol. This time, both groups are further than the distance between the carboxyl and NH of triflates and dinitrobenzoyl amino acid derivatives, with which constants had been small. In addition, the guest has an aromatic ring with could cause some kind of steric hindrance with the receptor.

The guest **189** is shown in figure 7.52 and is easily synthesized from maleic anhydride, by melting with norephedrine.

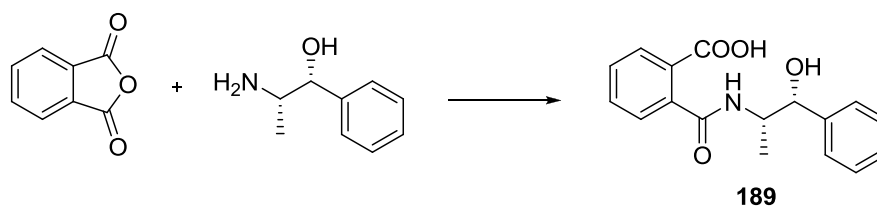


Figure 7.52. Synthesis of guest **189** from maleic anhydride and norephedrine.

Fortunately we noted the existence of enantioselectivity, since the addition of the guest to a solution of the racemic receptor in chloroform resulted in the splitting of its signals in the ^1H NMR spectrum, obtaining a constant ratio of 8. A proposed geometry between receptor **188** and guest **189** is shown in figure 7.53.

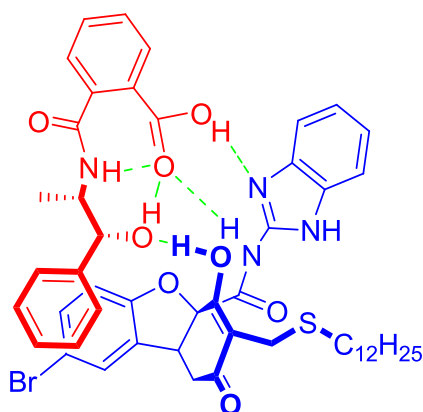


Figure 7.53. Proposed complex between receptor **188** and guest **189**.

We are currently trying to resolve the racemic mixture of receptor **189** to perform catalysis tests.

7.3. CONCLUSIONS

Thanks to the knowledge acquired in chapters 5 and 6 about benzofuran derived receptors, in this seventh and final chapter we have synthesized new derivatives of the above compounds, which have been used as organocatalysts in several reactions.

The synthesis of these receptors was carried out using the methodology described in the previous chapters. Furthermore, the existence of the enol group in the molecules allowed us to perform the resolution of the racemic mixtures of receptors by crystallization with cinchonidine. Fortunately, we have obtained crystals of enough quality for analysis by X-ray diffraction which has allowed us to know the exact structure of the catalysts and their absolute configuration.

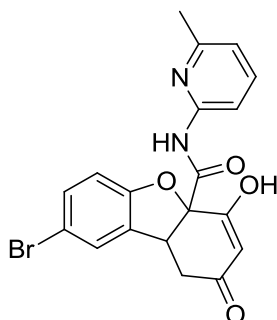
The geometry obtained by X-ray diffraction of receptor **182** was surprising, since it is a benzimidazole derivative in which the tautomer which crystallizes possesses a fulvene-type structure.

This receptor has been used in the extraction of amino acids and their derivatives. However, it has presented better properties in the catalysis of several reactions, among which the dynamic kinetic resolution of azlactones deserves a special mention. However, although it has shown good catalytic properties, the enantiomeric excesses generated have been lower than expected. Probably the receptor is too simple and requires the addition of a group that establishes more additional hydrogen bonds with the substrate or at least greater steric hindrance.

In our research group, experiments to improve the results are currently underway, increasing the solubility of the catalyst with long alkyl chains.

7.4. EXPERIMENTAL

- 8-Bromo-4-hydroxy-*N*-(6-methylpyridine-2-yl)-2-oxo-1,2,4a,9b-tetrahydrodibenzo[*b,d*]furan-4a-carboxamide (149)

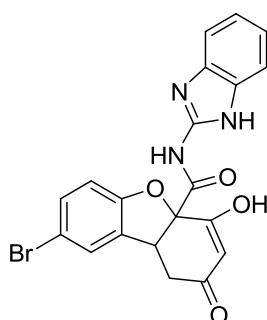


This compound was synthesized as in chapter 6, and its physical and spectroscopic properties were described.

Its resolution was carried out following the same experimental procedure described for receptor **147** in chapter 6, obtaining the more insoluble enantiomer with 65 % yield.

$[\alpha]_D^{20} = +142.4$ ($c = 1.22$, CHCl_3).

- *N*-(1*H*-benzo[*d*]imidazol-2-yl)-8-bromo-4-hydroxy-2-oxo-1,2,4a,9b-tetrahydrodibenzo[*b,d*]furan-4a-carboxamide (182)



In a round bottom flask sodium (5.0 g, 0.22 mol) was added to 60 mL of anhydrous methanol (dried with 4.5 mL of methyl orthoformate and two drops of acetyl chloride) and heated to reflux until it was dissolved. Then it was cooled with a water bath and compound **88** (25.0 g, 0.07 mol)²⁶⁶ was added with stirring for 5 minutes at 50-60 °C. Next, 2-aminobenzimidazole (16.0 g, 0.12 mol) was added and the solution was refluxed for 10 minutes. The reaction mixture was cooled and added to a solution of formic acid (25 mL) in water (500 mL) with ice.

²⁶⁶ It was prepared in the experimental section of chapter 5, page 279.

The reaction product precipitated as a white solid which was washed with water until the filtrate showed no acidic pH and then with hexane. 33.7 g were obtained and were purified by recrystallization from THF, obtaining compound **182** as a white solid in 68 % yield (20.0 g, 0.05 mol).

mp: 210-212 °C.

¹H RMN (DMSO-*d*₆) δ (ppm): 2.81 (dd, *J* = 2.1, 17.0 Hz, 1H), 2.97 (dd, *J* = 6.7, 17.0 Hz, 1H), 4.17 (d, *J* = 2.7 Hz, 1H), 5.33 (s, 1H), 6.84 (d, *J* = 8.5 Hz, 1H), 7.14 (dd, *J* = 3.2, 5.6 Hz, 2H), 7.30 (d, *J* = 8.8 Hz, 1H), 7.39 (dd, *J* = 3.2, 5.6 Hz, 2H), 7.45 (s, 1H).

RMN ¹³C (DMSO-*d*₆) δ (ppm): (tautomers mixture) 25.8 (CH₂), 34.7 (CH₂), 44.0 (CH), 67.7 (CH₂), 85.4 (C), 86.4 (C), 87.3 (C), 90.5 (C), 106.3 (CH), 112.0 (CH), 112.3 (CH), 112.4 (C), 112.6 (CH), 112.9 (CH), 113.0 (C), 113.2 (CH), 113.7 (C), 114.3 (C), 117.9 (CH), 118.6 (CH), 121.8 (CH), 122.3 (CH), 122.5 (CH), 122.9 (CH x 2), 123.1 (CH), 127.1 (CH), 128.1 (CH), 128.7 (CH), 131.7 (C), 131.9 (CH), 132.5 (CH), 132.7 (C), 133.1 (C), 133.3 (C), 133.7 (C), 133.8 (C), 141.6 (C), 142.3 (C), 146.1 (C), 147.1 (C), 147.5 (C), 147.8 (C), 150.7 (C), 152.1 (C), 155.9 (C), 157.0 (C), 157.6 (C), 157.8 (C), 158.9 (C), 163.9 (C), 165.6 (C), 166.6 (C), 171.1 (C), 174.1 (C), 178.8 (C), 188.7 (C), 204.8 (C), 205.9 (C).

IR (nujol, cm⁻¹): 3156, 2916, 2852, 2728, 1710, 1632, 1580, 1463, 1379, 1229, 1171.

HRMS (ESI): 440.0264 (M + H)⁺, calcd for C₂₀H₁₅BrN₃O₄ 440.0240.

Chiral resolution by crystallization

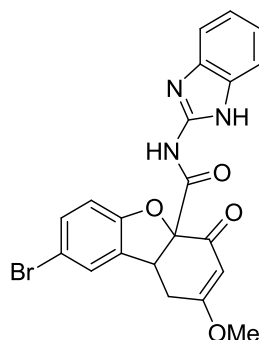
It was carried out similarly to the above receptor but with a CHCl₃-MeOH 4:1 ratio. The more insoluble enantiomer was obtained with a 59 % yield.

[α]_D²⁰ = +205.6 (*c* = 0.98, MeOH).

And the enantiomer which crystallizes in the second place with a 55 % yield.

[α]_D²⁰ = -191.5 (*c* = 1.05, MeOH).

- *N*-(1*H*-benzo[*d*]imidazol-2-yl)-8-bromo-2-methoxy-4-oxo-1,4,4a,9b-tetrahydrodibenzo[*b,d*]furan-4a-carboxamide (185)



To a solution of methyl orthoformate (0.5 mL, 4.57 mmol) and acetyl chloride (0.13 mL, 1.80 mmol) in 3.4 mL of anhydrous methanol cooled in an ice bath, compound **182** (0.20 g, 0.44 mmol) was added. The progress of the reaction was followed by TLC with EtOAc-MeOH. Then the reaction mixture was added over 20 mL of an aqueous solution with ice and 1 mL of aqueous NH₃ (28 %) precipitating the desired compound, which was filtered to yield 120 mg with a 60 % yield.

$[\alpha]_D^{20} = +197.0$ ($c = 1.04$, DMSO).

mp: 160-162 °C.

¹H RMN (DMSO-*d*₆) δ (ppm): 3.01 (dd, $J = 2.4, 17.7$ Hz, 1H), 3.24 (dd, $J = 7.3, 18.3$ Hz, 1H), 3.72 (s, 3H), 4.20 (d, $J = 5.5$ Hz, 1H), 5.58 (s, 1H), 6.85 (d, $J = 8.5$ Hz, 1H), 7.15 (dd, $J = 3.2, 5.9$ Hz, 2H), 7.31 (d, $J = 8.4$ Hz, 1H), 7.37 (dd, $J = 3.2, 5.9$ Hz, 2H), 7.53 (s, 1H).

¹³C RMN (DMSO-*d*₆) δ (ppm): 28.8 (CH₂), 43.1 (CH), 56.3 (CH₃), 90.7 (C), 103.0 (CH), 111.5 (CH), 112.1 (CH x 2), 112.4 (C), 122.2 (CH), 122.4 (CH), 126.5 (CH), 130.7 (C), 131.4 (CH), 131.6 (C x 2), 150.8 (C), 157.5 (C), 174.0 (C), 175.8 (C), 191.0 (C).

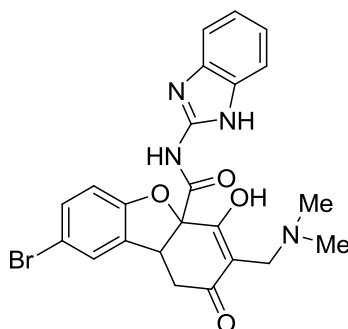
IR (film, cm⁻¹): 3397, 2923, 1664, 1619, 1567, 1469, 1398, 1236, 1203, 1171, 1048, 840, 808.

HRMS (ESI): 454.0405 (M + H)⁺, calcd for C₂₁H₁₇BrN₃O₄ 454.0397.

-Preparation of azlactones

All azlactones have been prepared according to the experimental procedure described in the literature, showing the same physical and spectroscopic properties.¹⁶⁴

- *N*-(1*H*-benzo[*d*]imidazol-2-yl)-8-bromo-3-((dimethylamino)methyl)-4-hydroxy-2-oxo-1,2,4a,9b-tetrahydrodibenzo[*b,d*]furan-4a-carboxamide (186)



Compound **182** (300 mg, 0.68 mmol) was suspended in 1 mL of THF and 3 drops of HCl 35 % v/v was added. Then formaldehyde 37 wt. % in H₂O (285 μ L, 3.83 mmol) was added and finally dimethylamine (71 μ L, 1.07 mmol). After two hours, the reaction mixture was added dropwise over water with ice crystallizing 163 mg of the desired compound with 48 % yield.

mp: > 230 °C.

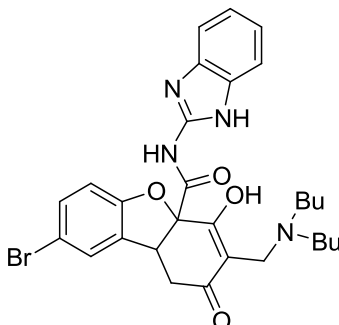
¹H RMN (DMSO-*d*₆) δ (ppm): 2.52 (s, 3H), 2.54 (s, 3H), 2.66 (dd, *J* = 8.6, 16.8 Hz, 1H), 2.85 (dd, *J* = 7.0, 16.8 Hz, 1H), 3.73 (s, 2H), 4.13-4.26 (m, 1H), 6.81 (d, *J* = 8.2 Hz, 1H), 7.10 (dd, *J* = 3.1, 5.9 Hz, 2H), 7.28 (dd, *J* = 1.6, 8.6 Hz, 1H), 7.36-7.52 (m, 3H).

¹³C RMN (DMSO-*d*₆) δ (ppm): 35.1 (CH₃ x 2), 36.1 (CH₂), 42.3 (CH), 52.6 (CH₂), 90.6 (C), 103.7 (C), 112.5 (C), 112.5 (CH x 2), 113.0 (CH), 122.1 (CH x 2), 127.1 (CH), 128.3 (C), 131.6 (CH), 134.2 (C), 134.4 (C x 2), 147.4 (C), 157.3 (C), 180.8 (C), 188.9 (C).

IR (nujol, cm⁻¹): 3390, 2923, 2865, 1690, 1632, 1573, 1528, 1450, 1379, 1242, 1165, 1035.

HRMS (ESI): 497.0831 (M + H)⁺, calcd for C₂₃H₂₂BrN₄O₄ 497.0819.

- *N*-(1*H*-benzo[*d*]imidazol-2-yl)-8-bromo-3-((dibutylamino)methyl)-4-hydroxy-2-oxo-1,2,4a,9b-tetrahydrodibenzo[*b,d*]furan-4a-carboxamide (187)



The same experimental procedure was followed as in the previous compound. The only difference was using dibutylamine instead of dimethylamine.

The experimental procedure followed was the same as for the above compound, substituting dibutylamine with dimethylamine (85 % yield). In this case, a further purification of the solid obtained was needed. For this purpose it was added over an aqueous solution of formic acid 10% v/v.

mp: 183-185 °C.

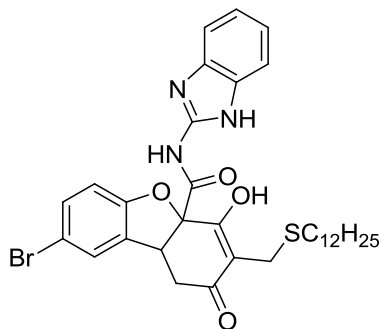
¹H RMN (CDCl₃) δ (ppm): 0.87 (t, *J* = 7.2 Hz, 3H), 0.89 (t, *J* = 7.2 Hz, 3H), 1.11-1.37 (m, 4H), 1.45-1.75 (m, 4H), 2.72-2.95 (m, 5H), 3.15 (dd, *J* = 6.8, 17.0 Hz, 1H), 4.00 (s, 2H), 4.28 (dd, *J* = 2.7, 6.6 Hz, 1H), 6.75 (d, *J* = 8.6 Hz, 1H), 7.21 (dd, *J* = 3.1, 5.9 Hz, 2H), 7.25-7.30 (m, 3H), 7.48 (dd, *J* = 3.3, 5.7 Hz, 2H).

¹³C RMN (CDCl₃) δ (ppm): 13.7 (CH₃ x 2), 20.0 (CH₂), 20.2 (CH₂), 25.8 (CH₂), 26.4 (CH₂), 27.9 (CH₂), 42.6 (CH), 47.6 (CH₂), 52.4 (CH₂), 52.7 (CH₂), 91.5 (C), 103.6 (C), 112.0 (CH x 3), 114.4 (C), 122.7 (CH x 2), 126.7 (CH), 131.7 (C), 131.9 (C), 132.0 (CH), 132.4 (C), 146.3 (C), 156.2 (C), 168.0 (C), 190.7 (C), 194.0 (C).

IR (film, cm⁻¹): 3280, 3059, 2968, 2942, 2865, 2735, 2235, 1703, 1619, 1521, 1463, 1411, 1229, 1054, 1015, 911, 814, 743.

HRMS (ESI): 581.1762 (M + H)⁺, calcd for C₂₉H₃₄BrN₄O₄ 581.1758.

- ***N*-(1*H*-benzo[*d*]imidazol-2-yl)-8-bromo-3-(dodecylthiomethyl)-4-hydroxy-2-oxo-1,2,4a,9b-tetrahydrodibenzo[*b,d*]furan-4a-carboxamide (188)**



Compound **186** (347 mg, 0.70 mmol) and dodecanethiol (195 mg, 0.96 mmol) were dissolved in 1.5 mL of chlorobenzene. The mixture was heated at 55 °C for 2 minutes and then added to an aqueous solution of formic acid (0.5 % v/v approx) precipitating 100 mg of the desired compound **188** (22 % yield). It is possible to obtain more product from the filtrate by extraction with EtOAc.

mp: 124-126 °C.

¹H RMN (DMSO-*d*₆) δ (ppm): 0.83 (t, *J* = 6.6 Hz, 3H), 1.00-1.38 (m, 19H), 1.43-1.62 (m, 1H), 2.15 (t, *J* = 7.2 Hz, 2H), 2.70-3.04 (m, 2H), 3.23 (d, *J* = 12.1 Hz, 1H), 3.33 (d, *J* = 12.5 Hz, 1H), 4.13-4.24 (m, 1H), 6.73 (d, *J* = 8.6 Hz, 1H), 7.03-7.24 (m, 4H), 7.36-7.52 (m, 2H).

¹³C RMN (DMSO-*d*₆) δ (ppm): 14.6 (CH₃), 19.9 (CH₂), 22.8 (CH₂), 23.4 (CH₂), 28.2 (CH₂), 29.2 (CH₂), 29.3 (CH₂), 29.4 (CH₂), 29.7 (CH₂ x 2), 30.1 (CH₂), 31.2 (CH₂), 32.0 (CH₂), 43.2 (CH), 47.2 (CH₂), 90.9 (C), 112.2 (CH), 113.1 (CH x 2), 113.2 (C), 115.4 (C), 122.9 (CH x 2), 126.9 (CH), 131.8 (CH), 132.4 (C), 133.0 (C), 147.1 (C), 147.9 (C), 150.6 (C), 157.5 (C), 173.9 (C), 193.9 (C).

IR (film, cm⁻¹): 3260, 2929, 2858, 1684, 1632, 1580, 1534, 1469, 1418, 1359, 1229, 1184, 1035.

HRMS (ESI): 654.2017 (M + H)⁺, calcd for C₃₃H₄₁BrN₃O₄S 654.1996.

- Guest **189**²⁶⁷ has already been described in the literature.

²⁶⁷ (a) Fischer, F.; Preisser, G.; Strauss, D. *Liebigs Ann.* **1961**, *643*, 110-116; (b) Drefahl, G.; Fischer, F.; Fischer, W. *Liebigs Ann.* **1957**, *610*, 166-172.



**UNIVERSIDAD
DE SALAMANCA**

CAMPUS DE EXCELENCIA INTERNACIONAL

APPENDIX A.1.

A.1.1. Instrumental and chromatographic techniques

Nuclear magnetic resonance (NMR) spectra were recorded on a *Bruker WP-200-SY* (200 MHz for ^1H and 50 MHz for ^{13}C), *Varian 200 Mercury VS 2000* (200 MHz for ^1H and 50 MHz for ^{13}C) and *Bruker Advance DRX* spectrometers (400 MHz for ^1H and 100 MHz for ^{13}C). Chemical shifts (δ) are expressed in parts per million (ppm) using the solvent signal as internal standard. Coupling constants (J) are expressed in hertz (Hz), using the following abbreviations for the multiplicities: s, singlet; d, doublet; t, triplet; m, multiplet; q, quartet; quint, quintet; h: hexaplet; dd, doublet of doublets; dt, double triplet; br, broad signal.

Infrared spectra (IR) were made in nujol or as films, with a window of NaCl and were recorded on a *Nicolet IR100* spectrophotometer. The bands are expressed in cm^{-1} .

Optical rotations (α) were measured on a *Perkin Elmer 341* polarimeter using a 10 cm path length cell and the D line of Na at 589 nm.

Melting points (mp) were determined with a *Stuart Scientific SM3P* capillary apparatus and a *Leica Galen III* microscope.

Mass spectra were recorded on a quadrupole *Waters ZQ4000*, the ionization technique was electrospray. For the high resolution mass spectrometry, an *Applied Biosystems QSTAR XL* was used.

The enantiomeric excesses (ee) of the products were determined by chiral HPLC using an *Agilent 1100 HPLC* chromatograph. Detection was performed by UV using conditions described in literature (Mass Spectrometry Service of the University of Salamanca).

Analytical thin layer chromatography was performed using pre-coated aluminium-backed plates (Merck Kieselgel 60 F₂₅₄) and visualized by UV ($\lambda = 250$ nm). For column chromatography silica gel (SDS 60, 70-200 μm) was used.

The determination of the crystal structures was carried out at the X-ray Diffraction Service of the University of Salamanca. To do this, single crystals of suitable size and quality were mounted on a glass capillary with random orientation. Data collection was performed with an automatic four-circle diffractometer *Bruker Kappa Apex II* equipped with a CCD (*charge-coupled device*) area detector with a high sensitivity. All crystals were measured at room temperature, using the $\text{CuK}\alpha$ ($\lambda = 1.54178$ Å) radiation, with the X-ray generator operating at 40 kV and 30 mA.

The reciprocal space was explored in three different orientations collecting a total of 36 pictures, from which a determined number of reflections were obtained and were adjusted by a least squares method to determine the unit cell dimensions. Then we proceeded to collect data over a full sphere of reciprocal space; 1638 images were collected with a scan width of 0.5° and an exposure time of 10 s/image. The images were integrated with the SAINT

program²⁶⁸ using an integration algorithm narrow-image. Empirical absorption corrections were applied to the intensities of the measured reflections using the SADABS program.²⁶⁹

The structures were resolved by direct methods and were refined by the least squares method based on F^2 using the program package SHELXTLTM.²⁷⁰ The positions of the hydrogen atoms were fixed geometrically, but some of them were obtained by synthesis of Fourier differences. The representations of the molecules were made with SHELXTLTM ²⁷⁰ and MERCURY programs.²⁷¹

In scheme 1 the process of crystal structures resolution which has been carried out is shown, and consists of several stages:

- Obtaining the dimensions of the unit cell and data collection of diffraction intensities.
- Data reduction consists on performing a series of corrections of the measured intensities, to turn these intensities into useful values for application to the resolution of structures. This process provides positive amounts $|F_{hkl}|$ called "Structure Factor Module ". These amounts can be theoretically calculated from a model.

The measured intensities are related to the moduli of the structure factors $|F_{hkl}|$ by the following relationship:

$$|F_{hkl}| = (K I_{hkl} / L \cdot p)^{1/2} A$$

where:

L: Lorenz factor

p: polarization factor

K: Scale Factor

A: Absorption Factor

- The structural resolution consists on obtaining atomic coordinates from structure factors experimentally measured, applying direct methods or Patterson method. Once a model is obtained, successive Fourier synthesis and structure factors calculations allow to locate the rest of the atoms in order to obtain a complete model.
- The refinement of the model is done by adjusting, in a first step, the three positional coordinates (x, y, z) of each atom and a thermal parameter which realizes his state of

²⁶⁸ Bruker, *SAINTE*. Data Reduction Program. Version 7.68A, Bruker AXS Inc., Madison. Wisconsin, USA, 2006.

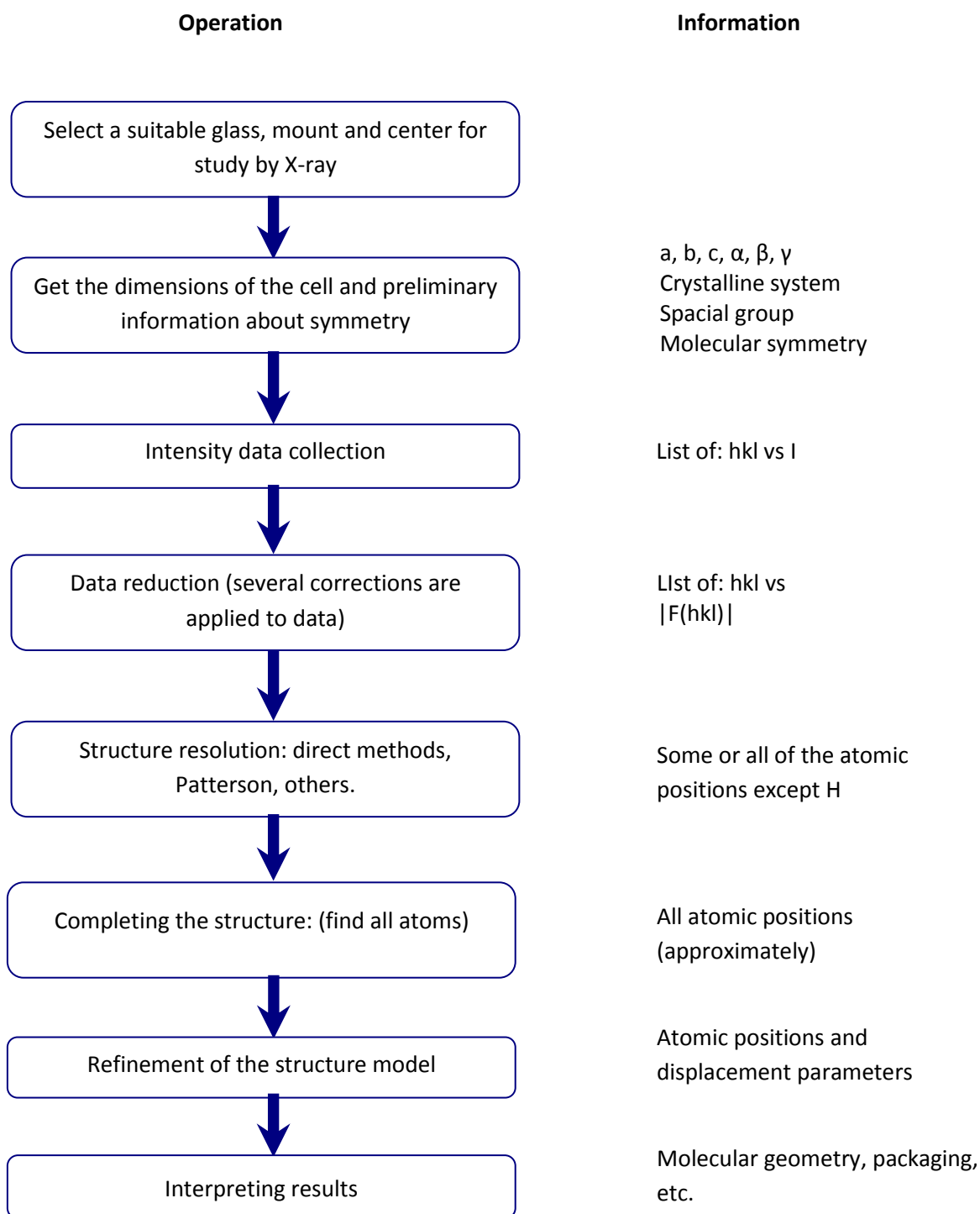
²⁶⁹ Bruker, *SADABS*. Empirical Absorption Program. Version 2.03, Bruker AXS Inc., Madison. Wisconsin, USA, 2006.

²⁷⁰ Sheldrick G.M., *SHELXTLTM*. Structure Determination Software Suit. Version 6.14, Bruker AXS, Inc., Madison, Wisconsin, USA 2003.

²⁷¹ Macrae, C.F.; Edgington, P.R.; McCabe, P.; Pidcock, E.; Shields, G.P.; Taylor, R.; Towler, M.; van de Streek, J. *MERCURY*. Molecular graphics. Version 3.0. *J. Appl. Cryst.* **2006**, *39*, 453-457.

isotropic thermal vibration (spherical) around its balance position. In the second stage, it is possible to carry out a refinement assigning a tensor (6 variables) at each atomic position that expresses the state of vibration in an anisotropic way, ie, distinguishing between different vibration directions with ellipsoid shape. The refining process ends when the best agreement between the values of the calculated spectrum (F_c) with the model (coordinates + vibration factors) and the observed spectrum (F_o) is reached. The agreement factor is defined as:

$$R = \frac{\sum [| | F_o | - | F_c | |]}{| F_c |}$$



Scheme 1. Resolution process of crystal structures by monocrystal X-ray diffraction.

Data collection and the resolution of the crystal structures appearing herein have been carried out by the general procedure outlined in the previous scheme.

A.1.2. PUBLICATIONS

The following publications arise as a result of research conducted in this thesis to date:

- Proline imidazolidinones and enamines in Hajos-Wiechert and Wieland-Miescher ketone synthesis, *Tetrahedron* **2009**, *65*, 4841-4845.

- Imidazolidinone intermediates in prolinamide-catalyzed aldol Reactions, *Org. Biomol. Chem.* **2010**, *8*, 2979-2985.

- Synthesis of Monoacylated Derivatives of 1,2-Cyclohexanediamine. Evaluation of their Catalytic Activity in the Preparation of Wieland-Miescher ketone, *J. Org. Chem.* **2010**, *75*, 8303-8306.

- A Twitchell Reagent Revival: Biodiesel Generation from Low Cost Oils, *Adv. Synth. Catal.* **2011**, *353*, 2681-2690.

- 4,5-Dibromo-2,7-di-*tert*-butyl-9,9-dimethyl-9*H*-thioxanthene, *Acta Cryst.* **2012**, *E68*, o1814.

- Chiral recognition with a benzofuran receptor which mimics an oxyanion hole, *Org. Biomol. Chem.* **2014**, *in press*.

A patent was also registered:

- Sulfonic acid derivatives for biodiesel synthesis, 2 393 352, 2013.



Proline imidazolidinones and enamines in Hajos–Wiechert and Wieland–Miescher ketone synthesis

Ángel L. Fuentes de Arriba^a, Luis Simón^a, César Raposo^b, Victoria Alcázar^c, Joaquín R. Morán^{a,*}

^aOrganic Chemistry Department, Plaza de los Caídos 1-5, Universidad de Salamanca, 37008 Salamanca, Spain

^bMass Spectrometry Service, Plaza de los Caídos, 1-5, Universidad de Salamanca, 37008 Salamanca, Spain

^cIndustrial Chemistry and Environmental Engineering Department, José Gutiérrez Abascal 2, Universidad Politécnica de Madrid, 28006 Madrid, Spain

ARTICLE INFO

Article history:

Received 11 March 2009

Accepted 9 April 2009

Available online 18 April 2009

Keywords:

Hajos–Wiechert ketone

Wieland–Miescher ketone

L-Prolinamide catalysis

Imidazolidinones and enamine intermediates

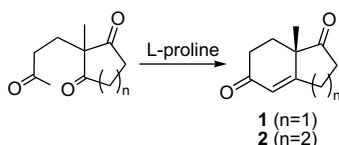
ABSTRACT

Readily available aromatic prolinamides obtained from the acid chloride of proline hydrochloride and anilines induce large enantiomeric excesses in intramolecular aldol condensations. Imidazolidinones derived from the reaction of the catalyst and enamines have been found as intermediates in these reactions.

© 2009 Elsevier Ltd. All rights reserved.

1. Introduction

Since its discovery nearly 40 years ago,¹ the proline-catalyzed intramolecular aldol reaction has been applied to several substrates and building blocks such as the Hajos–Wiechert (Parrish) ketone (1) and the Wieland–Miescher ketone (2) (Scheme 1). These compounds present interesting industrial applications.²



Scheme 1. Proline-catalyzed intramolecular aldol cyclization.

While proline is a good catalyst for the enantioselective synthesis of the Hajos–Wiechert ketone 1, the results are poor in the six-membered ring closure of the Wieland–Miescher compound.³

The mechanisms of proline catalysis are still a matter of discussion⁴ and four different ones have been proposed. A reasonable mechanism that accounts for the observed enantioselectivity is the one proposed by Houk and List,⁵ in which an intermediate enamine attacks the carbonyl group assisted by the proline carboxylic acid. If

this is the case, proline might not be an ideal catalyst for the following reasons:

- Protonation of the reactive intermediate always takes place from the *syn* carboxylic acid, while *anti* carboxylic acids are more stable.⁶
- Proline shows a zwitterionic structure and is sparingly soluble in apolar organic solvents. A higher solubility would be desirable.
- Nucleophilic attack from the proline nitrogen is necessary to generate the enamine intermediate, but the concentration of the basic amine is very low due to the high acidity of the proline carboxylic acid.

An alternative strategy to overcome these drawbacks is to use proline derivatives that exhibit better solubility and the appropriate acidity. In fact, proline amides have already shown promising results in these cyclizations and intermolecular aldol condensations.⁷

To study the effect of the NH acidity several proline amides were prepared starting from the acid chloride of L-proline hydrochloride and substituted anilines as shown in Table 1.

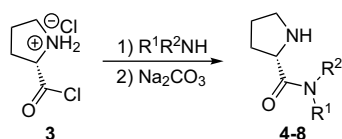
2. Results and discussion

We evaluated the catalytic properties of these prolinamides (4–8) in the Hajos–Parrish reaction and compared them with the

* Corresponding author. Tel.: +34 923294481; fax: +34 923294574.

E-mail address: romoran@usal.es (J.R. Morán).

Table 1
Structure of L-prolinamides **4–8**



Prolinamide	R ¹	R ²
4	4-Methylphenyl	H
5	4-Nitrophenyl	H
6	3,5-Bis(trifluoromethyl)phenyl	H
7	3,5-Bis(methoxycarbonyl)phenyl	H
8	Phenyl	Me

catalytic activity of L-proline butyl ester (**9**) and that of L-proline itself (**10**). The results are summarized in Table 2.

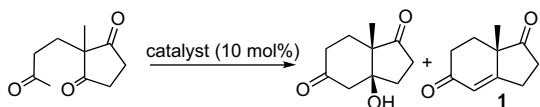
As shown in Table 2, rate acceleration and improvement in enantioselectivity were observed when using more acidic prolinamides. Thus, a comparison between catalyst **7** with the 3,5-bis(methoxycarbonyl)phenyl group and catalyst **4** with a 4-methylphenyl unit revealed the more acidic prolinamide **7** as a more active (rate acceleration of more than twofold) and more selective (98 vs 91% ee) catalyst (entries 1 and 4). These results were consistent with the Houk and List⁵ enamine mechanism for the intramolecular aldol reaction (Scheme 2).

Additionally, the dehydration step seemed to be related to the NH acidity of prolinamides (Scheme 3). While the previously mentioned toluidine catalyst **4** yielded mainly the aldol-type product (58%, entry 1) the isophthalic acid derivative **7** afforded the highest amount of the α,β -unsaturated ketone (40%, entry 4) among all the prolinamides studied.

To gain further insight into the reaction mechanism, we explored alternative catalyst modifications, preparing the tertiary prolinamide **8** and the proline butyl ester **9**. These compounds lack the amide NH, involved in the intramolecular hydrogen bonds depicted in Schemes 2 and 3. This NH proved to be essential for high enantiomeric induction since catalysis with **8** or **9** (entries 5 and 6) afforded low enantioselectivities (ee <24%).

Catalysis by the 3,5-bis(trifluoromethyl)phenyl derivative **6** proved to be an unexpected challenge owing to the complexity of the ¹H NMR spectra. To clarify the structure of the chemical species involved in the catalytic process, we analyzed the reaction

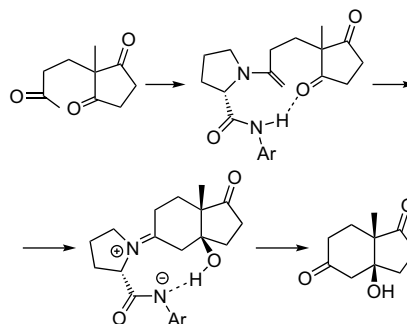
Table 2
Results obtained in the preparation of the Hajos–Wiechert (Parrish) ketone **1** in chloroform at 20 °C at 1.0 M concentration of triketone in the presence of 10 mol % catalyst



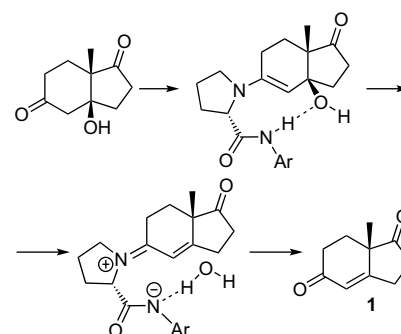
Entry	Catalyst	Conversion ^a (%)			Time (h)	ee ^b (%)
		Aldol	Ketone 1	Total		
1	4	58	14	72	330	91
2	5	57	35	92	95	92
3	6	72	20	92	101	95
4	7	44	40	84	167	98
5	8	72	23	95	24	–23
6	9	52	46	98	18	17
7	10	49	42	91	316	63

^a The yields of aldol-type and dehydrated products were determined through ¹H NMR integration.

^b Enantiomeric excess of the Hajos–Wiechert ketone **1** was determined by HPLC analysis.



Scheme 2. Proposed mechanism of the catalyzed intramolecular aldol reaction by prolinamides **4–7** to give the aldol product.



Scheme 3. Proposed mechanism for the dehydration of the aldol catalyzed by prolinamides **4–7** to yield the Hajos–Wiechert ketone **1**.

mixture using ¹H and ¹³C NMR working at 0 °C to prevent elimination.

After 2 h, the recorded ¹H NMR spectrum displayed three peaks for the quaternary methyl group protons at 1.10, 1.20, and 1.02 ppm, which were assigned to the starting material, the aldol-type product, and a new compound, respectively. The composition of the reaction mixture established by integration of the NMR signals was 12% of 2-methyl-2-(3-oxobutyl)-cyclopentane-1,3-dione, 12% of the aldol-type product, and 76% of a new compound, **11**.

The structure of intermediate **11** (Fig. 1) was elucidated on the basis of its spectroscopic properties (NMR and MS, see Experimental section). Key data to assess this structure were the quasi-molecular ion at *m/z* 491 and the presence of two quaternary carbons in the ¹³C NMR spectrum at 77.9 and 82.5 ppm, corresponding to the aminal carbon C-5 and the tertiary alcohol function C-3a, respectively.

The formation of the imidazolidinone **11** in the reaction medium was not completely unexpected. Oxazolidinones and imidazolidinones have already been found in the reaction of carbonyl compounds with proline and proline thioamides.^{4,8} Nevertheless, in the proline-catalyzed reactions these intermediates are difficult to detect, while in the catalysis with these prolinamides the imidazolidinone is an unstable compound but can be easily studied.

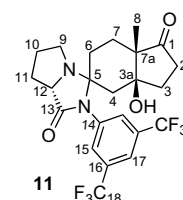
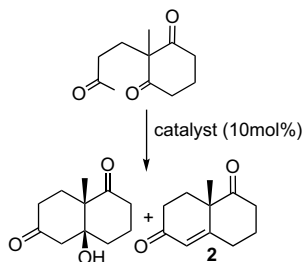


Figure 1. Proposed structure of the intermediate compound **11** in the synthesis of the Hajos–Wiechert ketone **1**, catalyzed by **6**.

Table 3

Enantiomeric excess obtained with prolinamide catalysts **4–8**, proline butyl ester **9**, and L-proline **10**, in the preparation of the Wieland–Miescher ketone **2** in chloroform at 20 °C at 1.0 M concentration of triketone in the presence of a 10 mol% catalyst



Entry	Catalyst	ee ^a (%)
1	4	94
2	5	87
3	6	96
4	7	92
5	8	–1
6	9	9
7	10	60

^a The enantiomeric excess of the Wieland–Miescher ketone **2** was determined by HPLC analysis.

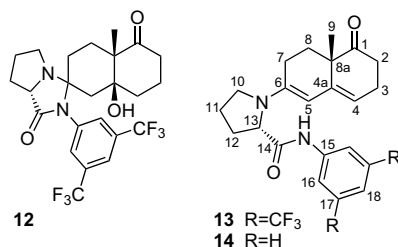


Figure 2. Intermediate compounds in the preparation of the Wieland–Miescher ketone **2** when catalyzed by aromatic prolinamides.

Cyclization of 2-methyl-2-(3-oxobutyl)-cyclohexane-1,3-dione to yield the Wieland–Miescher ketone (**2**) with prolinamides **4–8** afforded different results. While many other catalysts, as the ones shown by Barbas,⁹ yielded only the aldol-type product, these prolinamides rendered the unsaturated ketone **2**, and the aldol intermediate cannot be easily detected in the ¹H NMR spectra. The reaction rate is still related to the acidity of the amide proton, but the enantiomeric excesses do not correlate clearly with this parameter (Table 3).

Reaction with the 3,5-bis(trifluoromethylphenyl) prolinamide **6**¹⁰ revealed an initial stage in its ¹H NMR spectrum in which the aldol imidazolidinone **12** was formed. Almost simultaneously, a compound **13** started to accumulate. HPLC–MS of an aliquot of this mixture afforded a peak with a quasi-molecular ion at *m/z* 487. The presence of olefinic signals (a singlet at 5.68 ppm and a triplet (*J*=4 Hz) at 5.17 ppm in ¹H NMR, and 99.5 ppm for the enamine CH in ¹³C NMR) suggested the structure shown in Figure 2 for compound **13**. While compound **12** disappeared from the reaction mixture after 6 h, the enamine **13** was still present 24 h later at 20% molar ratio.

Working under conditions similar to those described by Stork,¹¹ enamine **14** could be obtained in good yield.

3. Conclusion

Prolinamides are among the best catalysts for the Hajos–Parrish and Wieland–Miescher reactions. In these aldol cyclizations catalyzed by aromatic prolinamides, the phenyl ring should be activated

with electron withdrawing groups to improve the reaction rates and, in most cases, increase also the enantioselectivities. The behavior of triketones 2-methyl-2-(3-oxobutyl)-cyclopentane-1,3-dione and 2-methyl-2-(3-oxobutyl)-cyclohexane-1,3-dione is different: while cyclopentanedione forms preferentially the imidazolidinone, cyclohexanedione yields the enamine derivative. These enamine compounds can be useful building blocks in the synthesis of steroids and other natural products.

4. Experimental

4.1. General

IR spectra were recorded with a Nicolet IR100 spectrometer. ¹H and ¹³C NMR spectra were recorded at room temperature with Bruker WP-200-SY, Varian Mercury VS. 2000 or Bruker Advance DRX spectrometer in deuterated chloroform (unless otherwise stated). *J* values are reported in hertz and chemical shifts are reported in parts per million with the solvent signal as an internal standard. Mass spectra were recorded with an Applied Biosystems QSTAR XL or Waters ZQ 4000. Optical rotations were determined in a PERKIN ELMER digital polarimeter 341. Melting points were taken on a Stuart Scientific SM3P capillary apparatus. The enantiomeric ratio of products was determined by chiral HPLC analysis (Chiralpak[®] AD-H column, 150×4.6 mm, eluent *n*-hexane/ⁱPrOH, 80:20 v/v %).

4.2. L-Proline chlorhydrate acid chloride (**3**)

This compound was prepared according to the Fischer procedure.¹² Phosphorus pentachloride (38.0 g, 182 mmol) was suspended in chloroform (100 mL) under argon in an ice–salt bath. L-Proline (20.0 g, 173 mmol) was added to the reaction mixture in small portions, keeping the reaction temperature below 10 °C. After ca. 30 min, the crystalline solid was filtered under argon and dried under vacuum: 25.3 g (149 mmol), 86% yield. Compound **3** is stable under argon and at –20 °C for several months.

4.3. General procedure for the preparation of the prolinamide catalysts **4–8**

The appropriate amine (13 mmol) was dissolved in 30 mL of dry THF under argon atmosphere. L-Proline chlorhydrate acid chloride **3** (2.67 g, 15.7 mmol) was added and the mixture was stirred for a few minutes. The progress of the reaction was monitored by TLC and more proline chlorhydrate acid chloride could be added if necessary. When the reaction was finished, a small amount of H₂O (5 mL) was added to hydrolyze the excess of acid chloride **3**. THF was then removed under reduced pressure, the residue dissolved in ethyl acetate, and washed with saturated sodium carbonate solution. The combined organic layers were dried over anhydrous Na₂SO₄ and the solvent was evaporated to dryness. Column chromatography on silica gel (CH₂Cl₂/methanol) gave the desired prolinamides.

Prolinamides **4** and **5** are known and their physical and spectroscopic properties are consistent with literature.⁷¹

4.4. (S)-N-(3,5-Bis(trifluoromethyl)phenyl)pyrrolidine-2-carboxamide (**6**)

Pale yellow oil, yield 68%. [α]_D²⁵ –37.52 (c 1.33, CHCl₃); ¹H NMR: δ 1.74–1.81 (m, 2H), 2.01–2.14 (m, 1H), 2.15–2.30 (m, 1H), 2.95–3.2 (m, 2H), 3.90 (dd, *J*₁=9 Hz, *J*₂=3 Hz, 1H), 7.58 (s, 1H), 8.12 (s, 2H), 10.13 (s, 1H, NH) ppm; ¹³C NMR: δ 26.5, 30.9, 47.6, 61.2, 117.3, 119.1, 126.1, 132.1, 139.4, 174.3 ppm; IR (ν): 1625, 1696, 2922, 3247 cm^{–1}; ESIHRMS calcd for C₁₃H₁₃N₂O₆ [M+H]⁺: 327.0927, found: 327.0904.

4.5. (S)-N-(3,5-Bis(methoxycarbonyl)phenyl)pyrrolidine-2-carboxamide (7)

White solid, yield 76%; mp: 130–131 °C; $[\alpha]_D^{25}$ –30.18 (c 1.12, EtOH); $^1\text{H NMR}$: δ 1.73–1.80 (m, 2H), 1.90–2.30 (m, 2H), 2.90–3.10 (m, 2H), 3.85–3.96 (m, 1H), 3.94 (s, 6H), 8.40 (s, 1H), 8.46 (s, 2H) ppm; IR (ν): 1462, 1586, 1729, 2854, 2924 cm^{-1} ; ESIHRMS calcd for $\text{C}_{15}\text{H}_{19}\text{N}_2\text{O}_5$ $[\text{M}+\text{H}]^+$: 307.1288, found: 307.1284.

4.6. (S)-N-Methyl-N-phenyl-pyrrolidine-2-carboxamide (8)

White solid, yield 83%; mp: 96–98 °C; $[\alpha]_D^{25}$ –37.80 (c 1.29, CHCl_3); $^1\text{H NMR}$: δ 1.52–1.68 (m, 2H), 2.67 (m, 2H), 2.80–3.15 (m, 2H), 3.20 (s, 3H), 3.46–3.60 (m, 1H), 7.19 (dd, $J_1=6$ Hz, $J_2=1.4$ Hz, 2H), 7.35–7.43 (m, 3H) ppm; $^{13}\text{C NMR}$: δ 26.9, 31.8, 38.0, 48.0, 58.8, 127.9 ($\times 2$), 128.3, 129.9 ($\times 2$), 143.3, 174.6 ppm; ESIHRMS calcd for $\text{C}_{12}\text{H}_{17}\text{N}_2\text{O}$ $[\text{M}+\text{H}]^+$: 205.1335, found: 205.1323.

4.7. Preparation of L-proline-n-butyl ester (9)

L-Proline (5 g, 43.4 mmol), thionyl chloride (5 mL, 68 mmol), and n-butanol (50 mL) were refluxed together for 2 h. The solvent was removed under reduced pressure and the crude residue was extracted with ethyl acetate (50 mL) and added to aqueous sodium carbonate (10% w/v, 100 mL). The organic layer was dried over Na_2SO_4 , and the organic solvent was evaporated to dryness to afford butyl ester **9** as an oily compound (85% yield). $[\alpha]_D^{25}$ –37.86 (c 1.38, CHCl_3); $^1\text{H NMR}$: δ 0.90 (t, $J=7.2$ Hz, 3H), 1.29–1.40 (m, 2H), 1.56–1.89 (m, 5H), 2.03–2.20 (m, 1H), 2.81–2.92 (m, 1H), 3.02–3.11 (m, 1H), 3.71 (dd, $J_1=8.8$ Hz, $J_2=5.8$ Hz, 1H), 4.09 (t, $J=6.7$ Hz, 2H) ppm; $^{13}\text{C NMR}$: δ 13.9, 19.3, 25.7, 30.5, 30.9, 47.3, 60.0, 64.9, 175.8 ppm; IR (ν): 1469, 1677, 1742, 2858, 2917 cm^{-1} ; ESIHRMS calcd for $\text{C}_9\text{H}_{18}\text{NO}_2$ $[\text{M}+\text{H}]^+$: 172.1332, found: 172.1326.

4.8. Preparation of imidazolidinone 11

2-Methyl-2-(3-oxobutyl)-cyclopentane-1,3-dione (224 mg, 1.23 mmol) was dissolved in 0.4 mL of CDCl_3 and mixed with 393 mg (1.20 mmol) of the prolinamide catalyst **6**. The reaction mixture was transferred to an NMR tube and allowed to react at 0 °C. After 2 h, the $^1\text{H NMR}$ spectrum recorded displayed the presence of the imidazolidinone **11** in 76% yield, according to the integration of the NMR signals. $^1\text{H NMR}$: δ 0.95 (s, 3H, H-8), 1.50–2.50 (m, 14H), 3.10 (m, 2H, H-9), 4.10 (dd, 1H, H-12), 7.43 (s, 2H, H-15), 8.06 (s, 1H, H-17) ppm; $^{13}\text{C NMR}$: δ 19.0 (C-8), 24.9 (C-7), 25.4 (C-10), 28.9 (C-6), 29.2 (C-3), 30.6 (C-2), 33.4 (C-11), 42.8 (C-4), 47.1 (C-9), 52.3 (C-7a), 63.2 (C-12), 77.9 (C-3a), 82.5 (C-5), 122.0 (C-17), 122.7 (C-18, q, $J=275$ Hz), 129.8 (C-15), 132.8 (C-16, q, $J=35$ Hz), 137.2 (C-14), 176.3 (C-13), 217.8 (C-1); ESI-MS m/z 491.3 $[\text{M}+\text{H}]^+$.

4.9. (S)-N-Phenyl-pyrrolidine-2-carboxamide (15)

Freshly distilled aniline (11.8 mL, 129.4 mmol) was dissolved in dry THF (50 mL) under argon atmosphere and in an ice–salt bath. Compound **3** (11 g, 64.7 mmol) was added in small portions and the progress of the reaction was monitored by TLC. Once the reaction was finished, it was poured into 100 mL of water, Na_2CO_3 (20 g, 188 mmol) was added, and stirred. Steam distillation and cooling afforded, after filtration, the pure compound **15** in 81% yield as a white solid. Prolinamide **15** is a known compound and its physical and spectroscopic properties are consistent with literature.^{7j}

4.10. Preparation of enamine 14

2-Methyl-2-(3-oxobutyl)-cyclohexane-1,3-dione (530 mg, 2.7 mmol) and aniline prolinamide **15** (513 mg, 2.7 mmol) were

dissolved in toluene (5 mL) and allowed to react at 40 °C and 20 mmHg for 2 h. Additional toluene portions were added under argon atmosphere when the reaction mixture turned viscous. Diethyl ether (20 mL) was then added and the mixture was cooled to –80 °C. The precipitate of the product was filtered under argon (crystals melted before reaching room temperature and decomposed in the presence of oxygen) and dried under vacuum (0.1 mmHg, 100 °C, 3 h) to obtain the enamine **14** (600 mg, 65% yield). $[\alpha]_D^{25}$ –124 (c 0.62, CHCl_3); $^1\text{H NMR}$: δ 1.20 (s, 3H, H-9), 2.74–1.58 (m, 12H), 3.20 (q, $J=9.6$ Hz, 1H, H-10), 3.58 (t, $J=9$ Hz, 1H, H-10), 4.07 (dd, $J_1=9$ Hz, $J_2=3$ Hz, 1H, H-13), 5.05 (s, 1H, H-5), 5.34 (t, $J=4.8$ Hz, 1H, H-4), 7.10 (t, $J=8$ Hz, 1H, H-18), 7.29 (t, $J=8$ Hz, 2H, H-17), 7.48 (d, $J=8$ Hz, 2H, H-16), 8.16 (s, 1H, NH) ppm; $^{13}\text{C NMR}$: δ 22.2 (C-9), 23.9 (C-3, C-11), 28.9 (C-12), 31.3 (C-8), 35.7 (C-2), 44.8 (C-8a), 49.1 (C-10), 63.6 (C-13), 99.9 (C-5), 115.6 (C-4), 119.8 (C-18), 124.4 (C-17), 128.9 (C-16), 137.3 (C-4a), 139.5 (C-15), 142.3 (C-6), 172.1 (C-14), 215.4 (C-1); IR (ν): 694, 1716, 2923, 3285 cm^{-1} ; ESIHRMS calcd for $\text{C}_{22}\text{H}_{27}\text{N}_2\text{O}_2$ $[\text{M}+\text{H}]^+$: 351.2067, found: 351.2054.

Acknowledgements

We wish to thank Prof. Francisco Bermejo for fruitful discussions, Anna Lithgow for the 400 MHz spectra, and the Spanish Dirección General de Investigación, Ciencia y Tecnología (DGICYT) (CTQ-2005-074007BQU).

Supplementary data

$^1\text{H NMR}$, $^{13}\text{C NMR}$, 2D NMR (COSY, HMQC, HMBC), and HRMS spectra of enamine **14** are provided. HRMS of prolinamides **6–8** and butyl ester **9** are also included. Supplementary data associated with this article can be found in the online version, at doi:10.1016/j.tet.2009.04.050.

References and notes

- (a) Hajos, Z. G.; Parrish, D. R. German Patent DE 2102623, 1971; (b) Eder, U.; Sauer, G.; Wiechert, R. German Patent DE 2014757, 1971; (c) Eder, U.; Sauer, G.; Wiechert, R. *Angew. Chem., Int. Ed. Engl.* **1971**, *10*, 496.
- (a) Nising, C. F.; Braese, S. *Angew. Chem., Int. Ed.* **2008**, *47*, 9389; (b) Kennedy, J. W. J.; Vietrich, S.; Weinmann, H.; Brittain, D. E. A. *J. Org. Chem.* **2008**, *73*, 5151; (c) Katona, B. W.; Rath, N. P.; Anant, S.; Stenson, W. F.; Covey, D. F. *J. Org. Chem.* **2007**, *73*, 9298; (d) Jastrzebska, I.; Scaglione, J. B.; Dekoster, N. P.; Rath, N. P.; Covey, D. F. *J. Org. Chem.* **2007**, *73*, 4837; (e) Chochrek, P.; Wicha, J. *Org. Lett.* **2006**, *8*, 2551; (f) Buchschacher, P.; Furst, A.; Gutzwiller, J. *Organic Syntheses*; Wiley & Sons: New York, NY, 1990; Vol. VII, p 368.
- (a) Ramachary, D. B.; Kishor, M. *J. Org. Chem.* **2007**, *72*, 5056; (b) Davies, S. G.; Russell, A. J.; Sheppard, R. L.; Smith, A. D.; Thomson, J. E. *Org. Biomol. Chem.* **2007**, *5*, 3190; (c) Kanger, T.; Kriis, K.; Laars, M.; Kailas, T.; Muurisepp, A. M.; Pehk, T.; Lopp, M. *J. Org. Chem.* **2007**, *72*, 5168.
- Seebach, D.; Beck, A. K.; Badine, D. M.; Limbach, M.; Eschenmoser, A.; Treasurywala, A. M.; Hobi, R. *Helv. Chim. Acta* **2007**, *90*, 425.
- (a) Clemente, F. R.; Houk, K. N. *J. Am. Chem. Soc.* **2005**, *127*, 11294; (b) Clemente, F. R.; Houk, K. N. *Angew. Chem., Int. Ed.* **2004**, *43*, 5766; (c) Bahmanyar, S.; Houk, K. N.; Martin, H. J.; List, B. *J. Am. Chem. Soc.* **2003**, *125*, 2475.
- (a) Dale, J. *Stereochemistry and Conformational Analysis*; Chemie: Weinheim, 1978; (b) Fausto, R.; Batista de Carvalho, A. E.; Teixeira-Dias, J. J. C.; Ramos, M. N. *J. Chem. Soc., Faraday Trans. 2* **1989**, *85*, 1945.
- (a) Almasi, D.; Alonso, D. A.; Najera, C. *Adv. Synth. Catal.* **2008**, *350*, 2467; (b) Sato, K.; Kuriyama, M.; Shimazawa, R.; Morimoto, T.; Kakiuchi, K.; Shirai, R. *Tetrahedron Lett.* **2008**, *49*, 2402; (c) Li, X.-J.; Zhang, G.-W.; Wang, L.; Hua, M.-Q.; Ma, J.-A. *Synlett* **2008**, 1255; (d) Guillena, G.; Najera, C.; Vióquez, S. F. *Synlett* **2008**, 3031; (e) Gryko, D.; Saletta, W. *J. Org. Biomol. Chem.* **2007**, *5*, 2148; (f) Ma, G.-N.; Zhang, Y.-P.; Shi, M. *Synthesis* **2007**, *2*, 197; (g) Sathapornvavajana, S.; Villaivan, T. *Tetrahedron* **2007**, *63*, 10253; (h) Chen, J.-R.; Lu, H.-H.; Cheng, L.; Wan, J.; Xiao, W.-J. *Org. Lett.* **2005**, *7*, 4543; (i) Tang, Z.; Jiang, F.; Cui, X.; Gong, L.-Z.; Mi, A.-Q.; Jiang, Y.-Z.; Wu, Y.-D. *PNAS* **2004**, *101*, 5755; (j) Moorthy, J. N.; Saha, S. *Eur. J. Org. Chem.* **2009**, *6*, 739.
- (a) List, B.; Hoang, L.; Martin, H. J. *PNAS* **2004**, *101*, 5839; (b) Zotova, N.; Franzke, A.; Armstrong, A.; Blackmond, D. G. *J. Am. Chem. Soc.* **2007**, *129*, 15100; (c) Gryko, D.; Lipinski, R. *Eur. J. Org. Chem.* **2006**, 3864; (d) Isart, C.; Burés, J.; Villarrasa, J. *Tetrahedron Lett.* **2008**, *49*, 5414.

9. Bui, T.; Barbas, C. F. *Tetrahedron Lett.* **2000**, *41*, 6951.
10. Catalyst **6** (209 mg, 0.64 mmol) was added to 0.64 mL of a 1 M solution of 2-methyl-2-(3-oxobutyl)-cyclohexane-1,3-dione in CDCl₃ in an NMR tube and allowed to react at 20 °C.
11. Stork, G.; Brizzolara, A.; Landesman, H.; Szmuszkovicz, J.; Terrell, R. J. *Am. Chem. Soc.* **1963**, *85*, 207.
12. (a) Fischer, E. *Chem. Ber.* **1905**, *38*, 2914; (b) *Methoden der Organische Chemie*; Houben-Weyl, Ed.; George Thieme: Stuttgart, 1958; Band XI/2, p 358.

Imidazolidinone intermediates in prolinamide-catalyzed aldol reactions†

Ángel L. Fuentes de Arriba,^a Luis Simón,^b César Raposo,^c Victoria Alcázar,^d Francisca Sanz,^e Francisco M. Muñiz^a and Joaquín R. Morán^{*a}

Received 14th December 2009, Accepted 23rd April 2010

First published as an Advance Article on the web 12th May 2010

DOI: 10.1039/b926284a

The reaction between acetone and 4-nitrobenzaldehyde catalyzed by aniline prolinamide **1** was studied in depth. Working in different solvents with equimolar amounts of reagents and monitoring the reaction by ¹H NMR, we detected and identified several imidazolidinones, such as those of the acetone **4**, the aldol products **5a** and **5b**, and aldehydes **10a** and **10b**. According to our results, these compounds could influence the reaction rate and diminish product enantioselectivity. Furthermore, acetone imidazolidinone **4** was seen to react with 4-nitrobenzaldehyde to furnish the aldol product **3**. This reaction can be catalyzed by different nucleophiles and acids. In fact, strong acids such as camphorsulfonic or trifluoroacetic acid, convert imidazolidinones into iminium salts and afford more enantioselective aldol reactions when different aromatic prolinamides are used. Enantiomeric excesses of ca. 82% are reached.

Introduction

In recent years aldol reactions catalyzed by prolinamides have attracted a great deal of interest owing to the possibility of achieving high enantiomeric ratio inductions.¹ Moreover, prolinamides are assumed to overcome some of the drawbacks of proline, such as:

1. limited solubility in apolar organic solvents;
2. the low concentration of the basic amine necessary to generate the enamine intermediate (in solution, most of the proline is present in the zwitterionic form);
3. the geometric requirements for the protonation of the reactive intermediate from the *syn* carboxylic acid, while *anti* carboxylic acids are more stable.

Custom-made catalysts, based on prolinamides, can be readily synthesized using different amines. This explains the interest in the use of prolinamides as organocatalysts.² Although in many cases the yields and enantiomeric excesses obtained are impressive,³ different results have been reported for the same aldol reaction catalyzed by the same prolinamide. As an illustrative example, the aldol reaction between acetone and 4-nitrobenzaldehyde catalyzed by the prolinamides **1**⁴ and **2**,^{5a} yielded disparate results as shown in Table 1.

^aDepartamento de Química Orgánica, Universidad de Salamanca, Plaza de los Caídos 1-5, E-37008, Salamanca, Spain. E-mail: romoran@usal.es; Fax: +34 923294574; Tel: +34 923294481

^bDepartamento de Ingeniería Química, Universidad de Salamanca, Plaza de los Caídos 1-5, E-37008, Salamanca, Spain

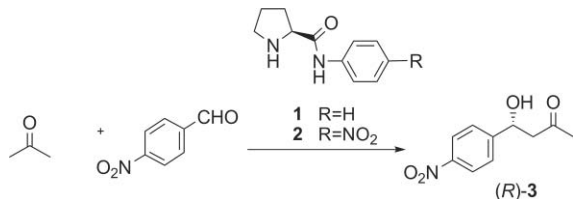
^cServicio de Espectrometría de Masas, Universidad de Salamanca, Plaza de los Caídos 1-5, E-37008, Salamanca, Spain

^dDepartamento de Ingeniería Química Industrial y Medio Ambiente, Universidad Politécnica de Madrid, José Gutiérrez Abascal 2, E-28006, Madrid, Spain

^eServicio de Rayos X, Universidad de Salamanca, Plaza de los Caídos 1-5, E-37008, Salamanca, Spain

† Electronic supplementary information (ESI) available: Experimental procedures, ¹H and ¹³C NMR spectra of the catalyzed reaction mixtures at different times, spectroscopic NMR data for the new compounds, graphic for competitive titration and CIF files of imidazolidinones **4**, **10a** and **10b**. CCDC reference numbers 741181–741183. For ESI and crystallographic data in CIF or other electronic format see DOI: 10.1039/b926284a

Table 1 Reported results for the aldol reaction of 4-nitrobenzaldehyde with acetone catalyzed by prolinamides **1** and **2** (20 mol% of the catalyst)



Entry	Catalyst	Yield (%)	ee (%)
1 ^a	1	88	8
2 ^b	1	87	15
3 ^c	1	88	37
4 ^d	1	68	71
5 ^e	2	80	39
6 ^a	2	80	54
7 ^d	2	76	72

^a The reaction of aldehyde (0.3 mmol, 1 equiv) with acetone (6.0 mmol, 20 equiv) was run in HMPA/H₂O in the presence of catalyst (0.06 mmol, 0.2 equiv).^{5 b} 4-Nitrobenzaldehyde (2 mmol, 1 equiv), acetone (40 mmol, 20 equiv) in H₂O using 1-HBr (0.4 mmol, 0.2 equiv).⁶ ^c 4-Nitrobenzaldehyde (0.5 mmol, 0.5 M) in neat acetone and catalyst (0.1 mmol, 0.1 M).^{3a} ^d The reaction was run in DMF with 4-nitrobenzaldehyde (0.66 mmol, 1 equiv), catalyst (0.13 mmol, 0.2 equiv), acetone (13.2 mmol, 20 equiv) and TFA (0.066 mmol, 0.1 equiv).⁷

The mechanism of these reactions is assumed to be similar to that proposed by Houk for proline catalysis,⁸ in which a Zimmerman–Traxler intermediate generates the enantioselectivity. Nevertheless, the details of the process are not fully known.⁹ One of the main points of discussion is the role of oxazolidinones (in proline catalysis)¹⁰ or imidazolidinones (when prolinamides are used)^{2k–m} in these reactions.

Prolinamides have proven to be satisfactory catalysts in intramolecular aldol additions,¹¹ and recently we have found imidazolidinones as intermediates in these processes.¹² In this paper, we study the possible relevance of imidazolidinones in intermolecular aldol reactions. We start with the model aldol reaction¹³ between

acetone and 4-nitrobenzaldehyde catalyzed by the readily available aniline prolinamide **1** in neat acetone where the large excess of acetone favored the aldol addition product. As has been shown in the literature, this reaction is very sensitive to solvent changes; so we turn our attention to other solvents as chloroform and methanol and finally we evaluate the role of imidazolidinones in enantioselectivity.

Results and discussion

Deuteroacetone as solvent

As a starting point for this study, the concentrations of aldehyde and prolinamide were set to the same value, 1.0 M.

Five minutes after dissolving 4-nitrobenzaldehyde and prolinamide **1** in neat deuteroacetone, a new compound was detected in the ^1H NMR spectrum. Its signals (methyl groups at 1.31 and 1.45 ppm) could be assigned to the acetone imidazolidinone **4** (yield > 95%) similar to the thioimidazolidinones previously reported.^{2k-m}

The structure of this compound was confirmed by an X-ray diffraction study (Fig. 1).¹⁴ As prolinamide **1** has been synthesized starting from enantiopure L-proline (*S* en C2), the absolute stereochemistry of imidazolidinone **4** could be established. The most interesting feature is the almost 90° dihedral angle which the phenyl aniline ring forms with the proline carbonyl group, showing that this is a strained compound with a large loss of conjugation energy. The same characteristic can be observed in solution, as revealed by the ^1H NMR chemical shifts, since the aniline *ortho* protons are strongly shielded with respect to the same protons in the prolinamide (from 7.69 ppm in prolinamide **1** to 7.12 ppm in the imidazolidinone **4**, ESI†).

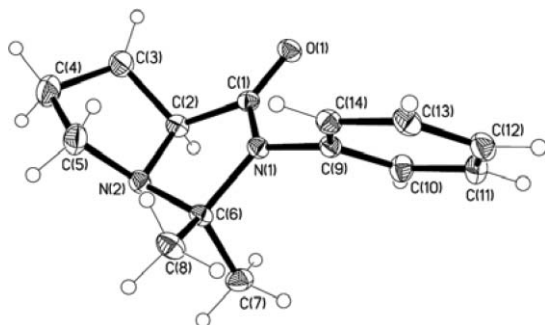
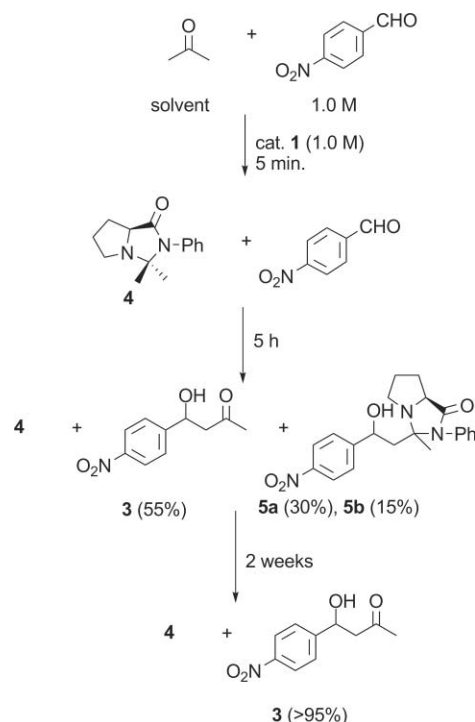


Fig. 1 ORTEP diagram of the acetone imidazolidinone **4**. Thermal ellipsoids are drawn at the 50% probability level.

After 5 h, the reaction in acetone was almost complete, since only a very small amount of the aldehyde was detected in the ^1H NMR spectrum (see the ESI†). The other reaction products were the expected aldol **3** (55% yield respect to the initial aldehyde), the acetone imidazolidinone **4**, and two new imidazolidinones, **5a** and **5b** (at a proportion of 2 : 1, 30% and 15% yield respectively, according to ^1H NMR integration), which corresponded to two different stereoisomers of the aldol imidazolidinones (Scheme 1).

A study of the evolution of the reaction over time revealed that the minor aldol imidazolidinone **5b** was transcarbonylated faster than the major **5a** (see the ESI†). After two weeks, these two imidazolidinones **5a** and **5b** had disappeared from the solution,



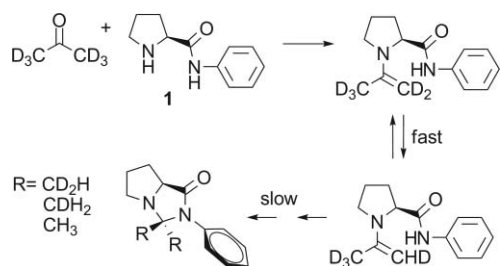
Scheme 1 Evolution of the reaction between acetone (solvent) and 4-nitrobenzaldehyde catalyzed by prolinamide **1**.

and only the mixture of aldol **3** (yield > 95%) and acetone imidazolidinone **4** was detected in the spectrum.

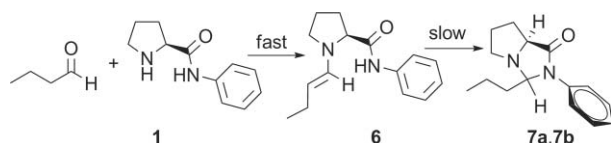
The structure of imidazolidinones **5a** and **5b** was established from their NMR spectra and a tentative assignment of all their signals was accomplished (see the ESI†). Both compounds showed the aminal carbons at 82.1 and 82.8 ppm. Comparison of the ^{13}C chemical shifts of the methyl groups of **5a** (19.7 ppm) and **5b** (22.1 ppm) with those of imidazolidinone **4** (*endo* methyl group at 23.7 ppm; *exo* methyl group at 28.4 ppm) unambiguously assigned through bidimensional correlations, showed that only the *exo* methyl group supported aldol addition.

Since the acetone imidazolidinone was the first reaction product in neat acetone, it was thought to be of interest to study this compound. The generation of imidazolidinone **4** in deuteroacetone (deuteration degree 99.8%) should yield a compound with a high degree of deuteration in the methyl groups; however, at the beginning of the reaction the deuteriums of the imidazolidinone methyl groups were replaced by the protons originally standing in the prolinamide NH groups. After 45 min, it was possible to estimate a 1.3–1.4 average degree of exchange (almost the statistical amount between 2 CH_3 groups and H_2O). This was reduced to 0.2 after two weeks. From the shape of the methyl signals in the ^1H NMR spectrum (see the ESI†) it was possible to deduce a total proton scramble in both methyl groups. This is consistent with a mechanism in which enamines would be generated, as shown in Scheme 2.

The above-formulated hypothesis was also supported by the results concerning the reaction of butyraldehyde and prolinamide **1** in CDCl_3 . The initial product observed in the ^1H NMR was the enamine **6** (Scheme 3). Cyclization to the imidazolidinones **7a** and **7b** was the slowest process (see the ESI†). Nevertheless, these were the most stable compounds and they accumulated in the reaction



Scheme 2 Formation of imidazolidinones **4** (with different degrees of deuteration) in deuterioacetone.



Scheme 3 Reaction of the prolinamide **1** (0.1 M) with n-butyraldehyde (0.1 M) in deuteriochloroform.

mixture. Only the most stable imidazolidinone **7b**, with the propyl group in the *exo* position, was isolated after equilibration in hot acetic acid.

Gryko and Lipinski^{21,m} reported that the use of thioimidazolidinone as catalyst instead of prolinthioamide affords slower reactions and lower enantioselectivities. In our hands, this was also the case. The purified imidazolidinone **4** reacted very slowly with 4-nitrobenzaldehyde, as shown in Fig. 2.

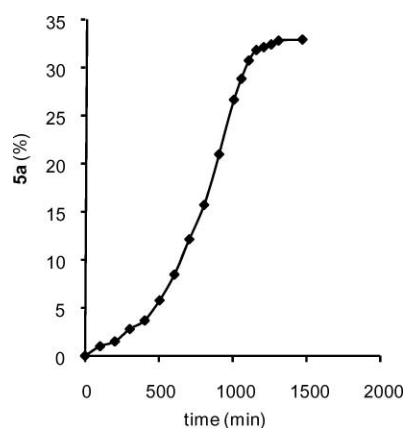


Fig. 2 Generation of aldol **5a** in the reaction of the imidazolidinone **4** (1.0 M) with 4-nitrobenzaldehyde (1.0 M) in CD_3COCD_3 at 20 °C.

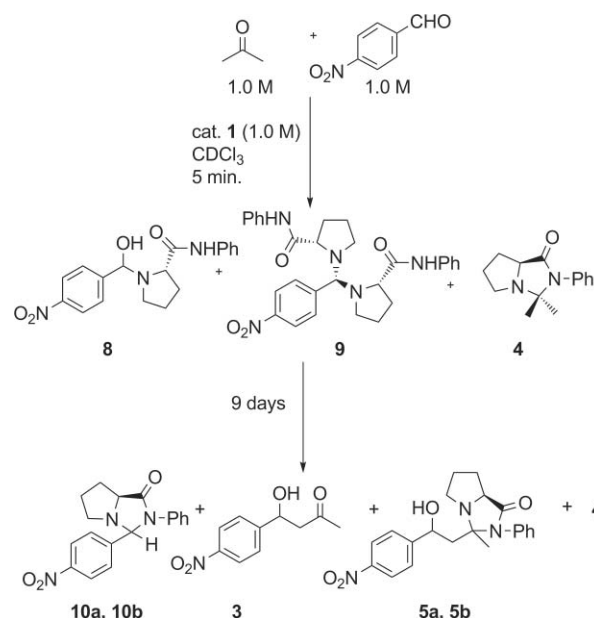
Scrutiny of the kinetics suggested that, as in other similar processes,^{10e,15} the reaction is autocatalytic, and a good reason for this could be the presence of a hydroxyl group in the aldol. Indeed, water was also able to catalyze the aldol reaction of the imidazolidinone **4** with 4-nitrobenzaldehyde, and this might explain the previous observations of Gryko and Saletra.²ⁿ Other nucleophiles such as dodecanethiol, imidazole or methanol also showed catalytic activity (Table 2).¹⁶ Acids such as phenol (entry 6) or 4-nitrophenol (entry 2) catalyzed the aldol reaction in deuterioacetone too.

Table 2 Exploration of several catalysts (0.5 M) for the aldol reaction between acetone imidazolidinone **4** (1.0 M) and 4-nitrobenzaldehyde (1.0 M) in deuterioacetone

Entry	Catalyst	$t_{1/2}/\text{min}$
1	None	700
2	4-Nitrophenol	2
3	Decanoic acid	8
4	Imidazole	28
5	Dodecanethiol	31
6	Phenol	46
7	H_2O	260

Deuteriochloroform as solvent

When the aldol reaction was run in deuteriochloroform with equimolar concentrations of 4-nitrobenzaldehyde, acetone and prolinamide (1.0 M), ¹H NMR analysis revealed the presence of several compounds, some of them different from the intermediates previously detected for the reaction in neat acetone. (Scheme 4).



Scheme 4 Evolution of the reaction between acetone and 4-nitrobenzaldehyde in CDCl_3 catalyzed by aniline prolinamide **1**.

After five minutes, together with the absorptions from the aldehyde, acetone and prolinamide, the ¹H NMR spectrum (see the ESI⁺) displayed signals that suggested the presence of the following compounds: the addition product **8** of the prolinamide to the aldehyde (singlets at 5.42 and 5.44 ppm, corresponding to both stereoisomers), the 4-nitrobenzaldehyde aminal **9** (singlet at 4.52 ppm) and the acetone imidazolidinone **4** (methyl groups at 1.23 and 1.40 ppm). After nine days, the recorded spectrum no longer showed the initial aldehyde adducts (**8** and **9**); instead, the aldehyde imidazolidinones (56%) **10a** and **10b** (6.34 ppm and 5.72 ppm, respectively) and the acetone imidazolidinone **4** (4.05 ppm, 30%) were the main products as established by integration of the NMR signals.

Other signals in the ¹H NMR spectrum (14%) could be assigned to the expected aldol products (**3**, 5.1 ppm) and to a structure that might correspond to the imidazolidinones of these

aldols (**5a**, 4.87 ppm; **5b**, 5.13 ppm). Acetone and traces of 4-nitrobenzaldehyde were also present (Scheme 4).

While aldehyde adducts **8** and **9** were difficult to isolate owing to their instability, it was possible to obtain the aldehyde imidazolidinones **10a** and **10b**. These compounds could be prepared from 4-nitrobenzaldehyde and prolinamide **1** in deuteriochloroform as solvent. However, this reaction was sluggish (as already shown). Finally, after nine days a mixture of imidazolidinones (5 : 1 according to the ^1H NMR integration signals of singlets at 6.34 ppm and 5.72 ppm respectively) was obtained. It was possible to purify the major compound **10a** by crystallization (CH_2Cl_2 –hexane). X-Ray diffraction¹⁷ revealed a structure with the nitrophenyl group in the *endo* position. The absolute stereochemistry at C2 (*S*) and C6 (*S*) could be unambiguously assigned as configuration at C2 is already known from the synthesis. Its ^1H NMR spectrum (see the ESI†) showed a strong shielding in the proline 5-H protons (0.6 ppm upfield), consistent with a structure in which the nitrophenyl ring occupies an *endo* position, as shown in Fig. 3.

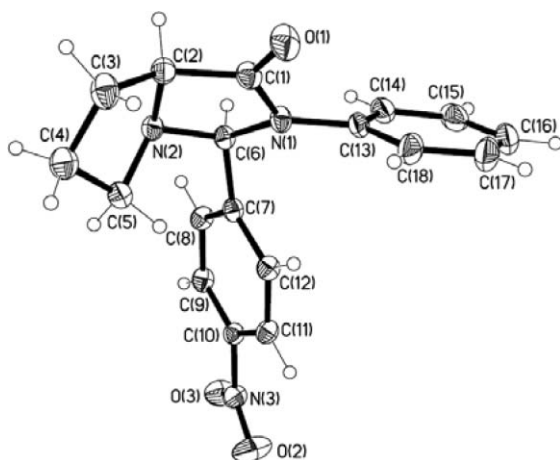


Fig. 3 ORTEP diagram of the imidazolidinone **10a**. Thermal ellipsoids are drawn at the 50% probability level.

Since the isomer with the nitrophenyl ring in the *exo* position should be more stable, equilibration of the isomers was carried out in hot acetic acid, to yield essentially compound **10b**. X-Ray diffraction indeed revealed an *exo* nitrophenyl group in this structure (Fig. 4).¹⁸ As in the case of compound **10a**, absolute configurations at C2 (*S*) and C6 (*R*) could be unequivocally established.

An explanation of the formation of the initial kinetic aldehyde imidazolidinone is shown in Scheme 5; cyclization from the most stable iminium salt yielded the most hindered imidazolidinone **10a**. Harsher conditions were needed to obtain imidazolidinone **10b** since it is produced from a less stable iminium salt.

Deuteromethanol as solvent

Since alcohols are good catalysts for imidazolidinone aldol additions, the reaction was also tested in deuteromethanol. Two observations regarding this process were of interest. The first was that the reaction with the aldehyde led to an equilibrium, as shown in Scheme 6.

Indeed, when the aldol **3** (1.0 M) was reacted with prolinamide **1** (1.0 M) in deuteriochloroform a similar mixture of products was

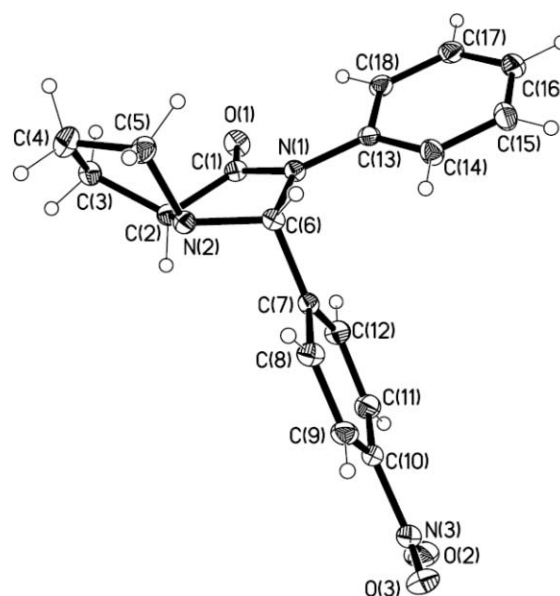
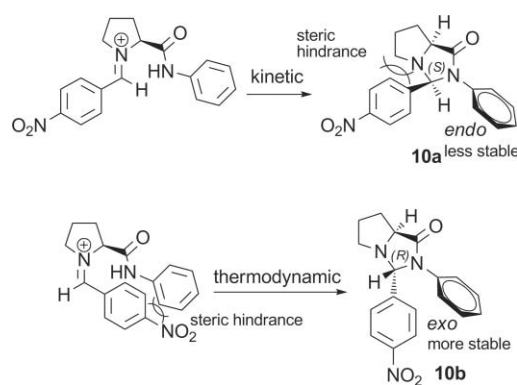
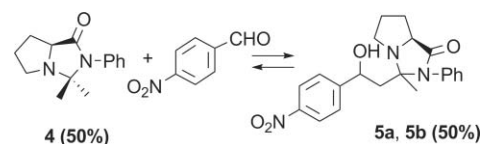


Fig. 4 ORTEP diagram of the imidazolidinone **10b**. Thermal ellipsoids are drawn at the 50% probability level.



Scheme 5 Possible explanation for the formation of aldehyde imidazolidinones **10a** and **10b**.

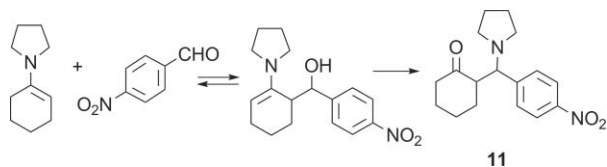


Scheme 6 Reaction between acetone imidazolidinone **4** (0.5 M) and 4-nitrobenzaldehyde (0.5 M) in deuteromethanol after 14 h.

obtained, because of the occurrence of a retroaldol reaction. The acetone imidazolidinone **4**, aldehyde imidazolidinones **10a** and **10b**, the aldol imidazolidinone **5a** and even 4-nitrobenzaldehyde and acetone were detected (see the ESI†).

Taking into account the small driving force of aldol reactions, this result is not surprising. In fact, when cyclohexanone enamine was reacted with 4-nitrobenzaldehyde after initial addition the reaction stopped. Other processes took over; in our hands, the final product was the Mannich compound **11** (see Scheme 7 and the ESI†).

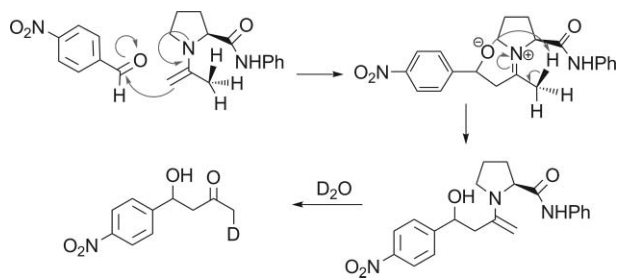
This lack of driving force, even with a very reactive compound such as 4-nitrobenzaldehyde, explains the limited use of these reactions until recently; for example, in the enamine reviews



Scheme 7 Reaction of the pyrrolidine cyclohexanone enamine (0.16 M) and 4-nitrobenzaldehyde (0.16 M) in deuteriochloroform.

from Hickmott¹⁹ there are no references to reactions of enamines with aldehydes. The current successful results reported in the literature^{2,3} correspond to catalytic amounts of prolinamides in which the enamines are always hydrolyzed or undergo transcarbonylation after the aldol addition to the corresponding carbonyl compounds.

The other interesting feature of the reaction of the imidazolidinone **4** (0.5 M) and 4-nitrobenzaldehyde (0.5 M) in deuteromethanol was the deuteration exchange. A large amount of deuteration exchange arose in the imidazolidinone methyl group after the aldol addition, as judged from the shape and integral of its NMR signal, while a small degree of deuteration was observed in the methylene group. This suggests that the reaction yields the enamine in the α' -carbon, as shown in Scheme 8, which might indicate a concerted ene-like mechanism. In this mechanism, the role of the prolinamide NH is limited to setting a strong H-bond with the aldehyde carbonyl group, which stabilizes the transition state.



Scheme 8 A possible ene-like mechanism for aldol reaction catalyzed by prolinamides.

Influence of imidazolidinones in enantioselectivity

As shown in the introduction, the reaction of acetone with 4-nitrobenzaldehyde catalyzed by aniline prolinamide **1** has been reported to yield very different enantiomeric excesses. (Table 1, entries 1–4).

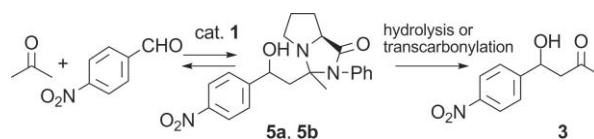
In our hands, the enantioselectivity could be even lower (Table 3, entry 1). When the aldol reaction was conducted in neat deuterioacetone with aldehyde (0.68 M) and 10 mol% of catalyst **1**, an enantiomeric excess as low as 10% was obtained. The formation of the aldol imidazolidinones **5a** and **5b** as reaction intermediates could explain these poor results. Their presence in the solution, as revealed in the ¹H NMR spectra, shows a rate-limiting transcarbonylation of the compounds. Hence the initial aldol addition products, which should be generated with good chiral assistance, can revert back to reagents. Therefore, part of the enantioselectivity of the products being lost (Scheme 9).

We have observed that the addition of trifluoroacetic acid (TFA) can overcome this drawback, since with TFA as an additive

Table 3 Enantiomeric excesses for the aldol reaction catalyzed by prolinamides either in neutral form or as their trifluoroacetate salts

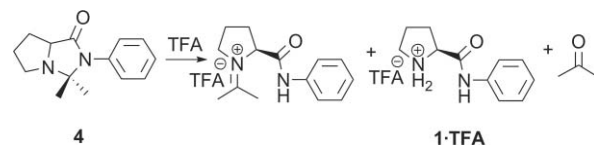
Entry	Catalyst	Time/h	Yield (%)	ee (%) ^a
1	1 ^b	70	21	10
2	1 ·TFA	5	21	61
3	12 ^c	12	31	2
4	12 ·TFA	11	35	65
5	13 ^d	2	>99	60
6	13 ·TFA	7	72	82
7	14 ^e	67	95	13
8	14 ·TFA	43	66	80
9	15 ^f	5	93	32
10	15 ·TFA	126	24	16
11	16 ^g	3	86	28
12	16 ·TFA	47	18	2

^a Enantiomeric excesses were determined by chiral HPLC. ^b For reported results for the same catalyst see ref. 3a and 6. ^c For reported results for the same catalyst see ref. 12^d. For reported results for the same catalyst see ref. 5. ^e For reported results for the same catalyst see ref. 7. ^f For reported results for the same catalyst see ref. 13^f. ^g For reported results for the same catalyst see ref. 3a.



Scheme 9 Aldol imidazolidinones as intermediates in the reaction between acetone and 4-nitrobenzaldehyde catalyzed by prolinamide **1**.

imidazolidinones were not accumulated. Instead, the protonated prolinamides and iminium salts are identified in the NMR spectra, as shown by Gryko *et al.*^{2k} (Scheme 10).



Scheme 10 Iminium salt and protonated prolinamide generated from imidazolidinone **4** in the presence of TFA.

We suggest that the explanation for the lack of imidazolidinones under acidic conditions is their surprisingly low pK_a . After the addition of camphorsulfonic acid to a mixture of prolinamide **1** and its acetone imidazolidinone **4** in deuteriochloroform we observed protonation only in the prolinamide **1** nitrogen. After

this compound had been completely protonated, the subsequent protonation of the imidazolidinone **4** took place (see the ESI[†]).

Other ¹H NMR competitive titrations between the imidazolidinone and pyridine afforded similar p*K*_a values (p*K*_apyridine/p*K*_aimidazolidinone **4** = 1.34), while in chloroform the prolinamide had almost the same p*K*_a as imidazole.

When the prolinamide was used as its trifluoroacetate salt (**1**·TFA), the enantiomeric excess was increased up to ee = 61% (Table 3, entry 2), in agreement with the absence of imidazolidinones as the rate-limiting step. Other aromatic prolinamides (**12**, **13** and **14**) showed a similar behaviour (Table 3, entries 3–8).

Bis(trifluoromethylaniline)prolinamide **12** behaved like prolinamide **1**, while trinitroanilineprolinamide **13** afforded up to 82% enantiomeric excess (Table 3, entry 6). Pentafluoroanilineprolinamide **14** yielded the most remarkable effect, changing from only 13% ee for the neutral prolinamide to 80% ee in the presence of TFA (Table 3, entries 7 and 8). However, when non-aromatic prolinamides were used the situation was more complex. The presence of TFA was detrimental to both the enantioselectivity and conversion (Table 3, entries 9–12) affording nearly racemic aldol **3** when the reaction was catalyzed for prolinamide **16** as its trifluoroacetate salt. (Table 3, entry 12).

Conclusions

In summary, we have shown that imidazolidinones can be formed from aniline prolinamide **1** and all the carbonyl compounds present in the reaction medium during the aldol addition. Aldol imidazolidinones influence the reaction enantioselectivity explaining the different results reported in the literature. Under neutral conditions, imidazolidinone hydrolysis is at least partially rate-limiting, and the enantiomeric excesses are reduced. In contrast, under acidic conditions the low basicity of imidazolidinones prevents their formation and enantioselectivity is enhanced.

Acetone imidazolidinone and both aldehyde imidazolidinones have been isolated and their X-ray structures have been obtained.

Experimental

(*S*)-3,3-Dimethyl-2-phenyl-hexahydropyrrolo[1,2-*e*]imidazol-1-one (**4**)

Prolinamide **1** (1.27 g, 6.68 mmol) was dissolved in acetone (10 cm³) and either anhydrous Na₂SO₄ or K₂CO₃ (1 g) was added. The mixture was stirred for 12 h at room temperature and then filtered to remove the salts. Then, the acetone was evaporated to afford the crude product which was purified by recrystallization from acetone (1.13 g, 73.5%), mp 89–92 °C; [α]_D²⁵ +46 (*c* 0.98 in CHCl₃). (Found: C, 73.10; H, 7.75; N, 11.98. C₁₄H₁₈N₂O requires C, 73.01; H, 7.88; N, 12.16); *v*_{max}(film cm⁻¹) 3059, 1690, 1378 and 717; δ_H(400 MHz, CD₃COCD₃) 1.72 (3H, s), 1.86 (3H, s), 2.13 (1H, m), 2.24 (1H, m), 2.33 (1H, m), 2.48 (1H, m), 3.05 (1H, m), 3.35 (1H, t, *J* 7.6), 4.36 (1H, dd, *J* 4.6 and 9.6), 7.60 (2H, d, *J* 8), 7.72 (1H, t, *J* 8), 7.82 (2H, t, *J* 8); δ_C(100 MHz, CD₃COCD₃) 23.7, 25.9, 26.5, 28.4, 49.1, 63.9, 81.1, 127.9, 138.2 and 176.1; HRMS calcd for C₁₄H₁₈N₂O + Na requires 253.1311, found 253.1316.

(3*S*,7*aS*)-3-(4-Nitrophenyl)-2-phenylhexahydropyrrolo[1,2-*e*]imidazol-1-one (**10a**)

4-Nitrobenzaldehyde (72 mg, 0.48 mmol) and aniline prolinamide **1** (94.7 mg, 0.50 mmol) were dissolved in CDCl₃ (0.5 cm³). The reaction was monitored by ¹H NMR. After nine days, the solvent was evaporated off under reduced pressure and the crude product was recrystallized from CH₂Cl₂/undecane, mp 71–72 °C; [α]_D²⁵ +16.9 (*c* 0.95 in CHCl₃); (Found: C, 55.64; H, 4.68; N, 10.30. C₁₈H₁₇N₃O₃·CH₂Cl₂ requires C, 55.89; H, 4.69; N, 10.29); *v*_{max}(film cm⁻¹) 1703, 1599, 1346 and 729; δ_H(200 MHz, CDCl₃) 1.79 (2H, m), 2.29 (3H, m), 2.40 (1H, m), 4.03 (1H, dd, *J* 3.4 and 8.4), 6.45 (1H, s), 7.09 (1H, m), 7.28 (4H, m), 7.45 (2H, d, *J* 8.8), 8.14 (2H, d, *J* 8.8); δ_C(50 MHz, CDCl₃) 25.1, 27.2, 49.2, 65.9, 78.2, 122.2, 124.0, 125.7, 129.2, 129.6, 137.2, 141.9, 148.3 and 176.7; HRMS calcd for C₁₈H₁₇N₃O₃ + Na requires 346.1168, found 346.1146.

(3*R*,7*aS*)-3-(4-Nitrophenyl)-2-phenylhexahydropyrrolo[1,2-*e*]imidazol-1-one (**10b**)

4-Nitrobenzaldehyde (0.42 g, 2.78 mmol) and aniline prolinamide **1** (0.52 g, 2.74 mmol) were dissolved in glacial acetic acid (1 cm³) and heated at 75–80 °C for three hours. The reaction mixture was then treated with an aqueous solution of sodium carbonate (4%) and extracted with ethyl acetate. The combined organic layers were dried over Na₂SO₄ and the solvent was evaporated off to yield a crude compound that was purified by recrystallization (CH₂Cl₂/undecane) to afford compound **10b** as a white solid (0.84 g, 95%), mp 159–161 °C; [α]_D²⁵ –19.2 (*c* 1.2 in CHCl₃); (Found: C, 66.57; H, 5.33; N, 12.96. C₁₈H₁₇N₃O₃ requires C, 66.86; H, 5.30; N, 13.00); *v*_{max}(film cm⁻¹) 3072, 1696, 1339, 827 and 762; δ_H(200 MHz, CDCl₃) 1.92 (2H, m), 2.22 (2H, m), 2.92 (1H, m), 3.44 (1H, m), 3.99 (1H, t, *J* 6.8), 5.77 (1H, s), 7.13 (1H, t, *J* 6.6), 7.29 (2H, t, *J* 6.6), 7.44 (2H, t, *J* 6.6), 7.47 (2H, d, *J* 14.6), 8.18 (2H, d, *J* 14.6); δ_C(50 MHz, CDCl₃) 25.1, 27.9, 56.5, 64.7, 82.9, 121.5, 124.5, 125.9, 127.5, 129.5, 137.3, 146.8, 148.1 and 174.8; HRMS calcd for C₁₈H₁₇N₃O₃ + Na requires 346.1168, found 346.1146.

(7*aS*)-2-Phenyl-3-propyl-hexahydropyrrolo[1,2-*e*]imidazol-1-one (**7b**)

Aniline prolinamide **1** (0.14 g, 0.74 mmol) and butyraldehyde (0.28 cm³, 3.10 mmol) were dissolved in glacial acetic acid (0.14 cm³) and heated at 70–80 °C for ten minutes. Then, the solution was quenched with a saturated solution of sodium carbonate and extracted with ethyl acetate. The combined organic layers were dried (Na₂SO₄) and the solvent was evaporated off under reduced pressure. Purification by column chromatography on silica gel (eluent, CH₂Cl₂–ethyl acetate) afforded the imidazolidinone **7b** as a pale yellow oil (0.14 g, 80%); [α]_D²⁵ –31.4 (*c* 2.5 in CHCl₃); (Found: C, 73.54; H, 8.39; N, 11.33. C₁₅H₂₀N₂O requires C, 73.74; H, 8.25; N, 11.47); *v*_{max}(film cm⁻¹) 3059, 1696, 1488 and 786; δ_H(200 MHz, CDCl₃) 0.87 (3H, t, *J* 7.4), 1.51 (3H, m), 1.83 (2H, m), 2.10 (3H, m), 2.70 (1H, m), 3.25 (1H, m), 3.98 (1H, dd, *J* 4.7 and 8.8), 4.71 (1H, dd, *J* 3.4 and 7.3), 7.17 (1H, t, *J* 8), 7.37 (2H, t, *J* 8), 7.48 (2H, d, *J* 8); δ_C(50 MHz, CDCl₃) 14.0, 18.4, 25.2, 27.9, 36.8, 56.7, 65.3, 82.7, 122.7, 125.8, 129.4, 137.3 and 174.3; MS (ESI) (*m/z*) 267.1 (M + Na)⁺, 245.1 (M + H)⁺.

Acknowledgements

Authors thank the Spanish Dirección General de Investigación, Ciencia y Tecnología (DGI-CYT) (CTQ-2008-01771/BQU) and a European Re-integration Grant (PERG04-GA-2008-239244) for their support in this work. The Spanish Ministerio de Educación y Ciencia (MEC) is acknowledged for the fellowships (F. M. M. and A.L.F.A.).

Notes and references

- For recent reviews, see: (a) S. Adachi and T. Harada, *Eur. J. Org. Chem.*, 2009, 3661; (b) J. Seayad and B. List, *Org. Biomol. Chem.*, 2005, 3, 719; (c) M. J. Gaunt, C. C. Johansson, A. McNally and N. T. Vo, *Drug Discovery Today*, 2007, 12, 8; (d) P. Melchiorre, M. Marigo, A. Carlone and G. Bartoli, *Angew. Chem., Int. Ed.*, 2008, 47, 6138; (e) B. List, *Synlett*, 2001, 1675; (f) L. M. Geary and P. G. Hultin, *Tetrahedron: Asymmetry*, 2009, 20, 131; (g) *Enantioselective Organocatalysis*, ed. P. I. Dalko, Wiley-VCH, Weinheim, 2007; (h) H. Pellissier, *Tetrahedron*, 2007, 63, 9267; (i) P. I. Dalko and L. Moisan, *Angew. Chem., Int. Ed.*, 2004, 43, 5138; (j) A. Dondoni and A. Massi, *Angew. Chem., Int. Ed.*, 2008, 47, 4638; (k) P. I. Dalko and L. Moisan, *Angew. Chem., Int. Ed.*, 2001, 40, 3726; (l) G. Guillena, C. Nájera and D. J. Ramón, *Tetrahedron: Asymmetry*, 2007, 18, 2249; (m) F. Peng and Z. Shao, *J. Mol. Catal. A: Chem.*, 2008, 285, 1; (n) S. Mukherjee, J. W. Yang, S. Hoffmann and B. List, *Chem. Rev.*, 2007, 107, 5471; (o) B. List, *Acc. Chem. Res.*, 2004, 37, 548; (p) E. R. Jarvo and S. J. Miller, *Tetrahedron*, 2002, 58, 2481.
- (a) Z. -H. Tzeng, H. -Y. Chen, R. J. Reddy, C. -T. Huang and K. Chen, *Tetrahedron*, 2009, 65, 2879; (b) D. Almasi, D. A. Alonso, A. -N. Balaguer and C. Nájera, *Adv. Synth. Catal.*, 2009, 351, 1123; (c) K. R. Reddy, G. G. Krishna and C. V. Rajasekhar, *Synth. Commun.*, 2007, 37, 4289; (d) Y. Okuyama, H. Nakano, Y. Watanabe, M. Makabe, M. Takeshita, K. Uwai, C. Kabuto and E. Kwon, *Tetrahedron Lett.*, 2009, 50, 193; (e) J. -R. Chen, H. -H. Lu, X. -Y. Li, L. Cheng, J. Wan and W. -J. Xiao, *Org. Lett.*, 2005, 7, 4543; (f) H. Torii, M. Nakada, K. Ishihara, S. Saito and H. Yamamoto, *Angew. Chem., Int. Ed.*, 2004, 43, 1983; (g) S. Sathapornvijana and T. Vilaivan, *Tetrahedron*, 2007, 63, 10253; (h) H. Yang and R. G. Carter, *Org. Lett.*, 2008, 10, 4649; (i) S. Chandrasekhar, K. Johnny and C. R. Reddy, *Tetrahedron: Asymmetry*, 2009, 20, 1742; (j) T. J. Dickerson, T. Lovell, M. M. Meijler, L. Noodleman and K. D. Janda, *J. Org. Chem.*, 2004, 69, 6603; (k) D. Gryko, M. Zimnicka and R. Lipinski, *J. Org. Chem.*, 2007, 72, 964; (l) D. Gryko and R. Lipinski, *Adv. Synth. Catal.*, 2005, 347, 1948; (m) D. Gryko and R. Lipinski, *Eur. J. Org. Chem.*, 2006, 3864; (n) D. Gryko and W. J. Saletta, *Org. Biomol. Chem.*, 2007, 5, 2148.
- (a) Z. Tang, F. Jiang, X. Cui, L. -Z. Gong, A. -Q. Mi, Y. -Z. Jiang and Y. -D. Wu, *Proc. Natl. Acad. Sci. U. S. A.*, 2004, 101, 5755; (b) D. Almasi, D. A. Alonso and C. Nájera, *Adv. Synth. Catal.*, 2008, 350, 2467; (c) X. -J. Li, G. -W. Zhang, L. Wang, M. -Q. Hua and J. -A. Ma, *Synlett*, 2008, 8, 1255; (d) G. Guillena, M. C. Hita, C. Nájera and S. F. Vióquez, *J. Org. Chem.*, 2008, 73, 5933; (e) S. Saha and J. N. Moorthy, *Tetrahedron Lett.*, 2010, 51, 912; (f) M. Lombardo, S. Easwar, F. Pasi and C. Trombini, *Adv. Synth. Catal.*, 2009, 351, 276.
- H. Y. Rhyoo, Y. -A. Yoon, H. -J. Park and Y. K. Chung, *Tetrahedron Lett.*, 2001, 42, 5045.
- K. Sato, M. Kuriyama, R. Shimazawa, T. Morimoto, K. Kakiuchi and R. Shirai, *Tetrahedron Lett.*, 2008, 49, 2402.
- S. S. Chimni, S. Singh and A. Kumar, *Tetrahedron: Asymmetry*, 2009, 20, 1722.
- J. N. Moorthy and S. Saha, *Eur. J. Org. Chem.*, 2009, 739.
- (a) S. Bahmanyar and K. N. Houk, *J. Am. Chem. Soc.*, 2001, 123, 11273; (b) S. Bahmanyar and K. N. Houk, *J. Am. Chem. Soc.*, 2001, 123, 12911; (c) H. Zhu, F. R. Clemente, K. N. Houk and M. P. Meyer, *J. Am. Chem. Soc.*, 2009, 131, 1632; (d) S. Bahmanyar, K. N. Houk, H. J. Martin and B. List, *J. Am. Chem. Soc.*, 2003, 125, 2475; (e) F. R. Clemente and K. N. Houk, *Angew. Chem., Int. Ed.*, 2004, 43, 5766; (f) F. R. Clemente and K. N. Houk, *J. Am. Chem. Soc.*, 2005, 127, 11294; (g) A. J. T. Smith, R. Müller, M. D. Toscano, P. Kast, H. W. Hellinga, D. Hilvert and K. N. Houk, *J. Am. Chem. Soc.*, 2008, 130, 15361; (h) X. Zhang and K. N. Houk, *J. Org. Chem.*, 2005, 70, 9712.
- (a) B. List, L. Hoang and H. J. Martin, *Proc. Natl. Acad. Sci. U. S. A.*, 2004, 101, 5839; (b) W. Parasuk and V. Parasuk, *J. Org. Chem.*, 2008, 73, 9388; (c) S. P. Mathew, H. Iwamura and D. G. Blackmond, *Angew. Chem., Int. Ed.*, 2004, 43, 3317; (d) F. J. S. Duarte, E. J. Cabrita, G. Frenking and A. G. Santos, *Eur. J. Org. Chem.*, 2008, 3397; (e) P. Hammar, A. Córdova and F. Himo, *Tetrahedron: Asymmetry*, 2008, 19, 1617.
- (a) C. Isart, J. Burés and J. Vilarrasa, *Tetrahedron Lett.*, 2008, 49, 5414; (b) F. Orsini, F. Pelizzoni, M. Forte, M. Sisti, G. Bombieri and F. Benetollo, *J. Heterocycl. Chem.*, 1989, 26, 837; (c) D. Seebach, A. K. Beck, D. M. Badine, M. Limbach, A. Eschenmoser, A. M. Treasurywala, R. Hobi, S. Prikoszovich and B. Linder, *Helv. Chim. Acta*, 2007, 90, 425; (d) N. Zotova, A. Franzke, A. Armstrong and D. G. Blackmond, *J. Am. Chem. Soc.*, 2007, 129, 15100; (e) H. Iwamura, D. H. Wells, S. P. Mathew, M. Klussmann, A. Armstrong and D. G. Blackmond, *J. Am. Chem. Soc.*, 2004, 126, 16312; (f) H. Iwamura, S. P. Mathew and D. G. Blackmond, *J. Am. Chem. Soc.*, 2004, 126, 11770; (g) N. El-Hamdouni, X. Companyó, R. Ríos and A. Moyano, *Chem.-Eur. J.*, 2010, 16, 1142.
- (a) D. B. Ramachary and M. Kishor, *J. Org. Chem.*, 2007, 72, 5056; (b) S. G. Davies, A. J. Russell, R. L. Sheppard, A. D. Smith and J. E. Thomson, *Org. Biomol. Chem.*, 2007, 5, 3190; (c) T. Kanger, K. Kriis, M. Laars, T. Kailas, A. M. Muurisepp, T. Pehk and M. Lopp, *J. Org. Chem.*, 2007, 72, 5168; (d) G. Guillena, C. Nájera and S. F. Vióquez, *Synlett*, 2008, 3031.
- Á. L. Fuentes de Arriba, L. Simón, C. Raposo, V. Alcázar and J. R. Morán, *Tetrahedron*, 2009, 65, 4841.
- For other references of this aldol reaction, apart from those cited in ref. 3, 5–7, see (a) E. Lacoste, Y. Landais, K. Schenk, J. -B. Verlhac and J. -M. Vincent, *Tetrahedron Lett.*, 2004, 45, 8035; (b) E. Lacoste, E. Vaique, M. Berlande, I. Pianet, J. -M. Vincent and Y. Landais, *Eur. J. Org. Chem.*, 2007, 167; (c) P. M. Pihko, K. M. Laurikainen, A. Usano, A. I. Nyberg and J. A. Kaavi, *Tetrahedron*, 2006, 62, 317; (d) G. -N. Ma, Y. -P. Zhang and M. Shi, *Synthesis*, 2007, 2, 197; (e) J. -R. Chen, X. -L. An, X. -Y. Zhu, X. -F. Wang and W. -J. Xiao, *J. Org. Chem.*, 2008, 73, 6006; (f) S. S. Chimni and D. Mahajan, *Tetrahedron: Asymmetry*, 2006, 17, 2108; (g) S. Luo, H. Xu, J. Li, L. Zhang and J. -P. Cheng, *J. Am. Chem. Soc.*, 2007, 129, 3074.
- Crystal data for **4**: C₁₄H₁₈N₂O, FW 230.30, orthorhombic, space group P2₁2₁1 (n° 19), a = 8.7304(3) Å, b = 8.9046(2) Å, c = 16.6172(5) Å, α = β = γ = 90°, V = 1291.83(7) Å³, Z = 4, D_c = 1.184 Mg m⁻³, m = (Cu-Kα) = 0.595 mm⁻¹, F(000) = 496. 7935 reflections were collected at 5.32 ≤ 2θ ≤ 65.57 and merged to give 2084 unique reflections (R_{int} = 0.0258), of which 2049 with I > 2σ(I) were considered to be observed. Final values are R = 0.0259, wR = 0.0687, GOF = 1.053, max/min residual electron density 0.099 and -0.089 e-Å⁻³. Flack value [0.1(2)].
- (a) Y. Takemoto, *Org. Biomol. Chem.*, 2005, 3, 4299; (b) J. S. Hill and N. S. Isaacs, *J. Chem. Res.*, 1988, 330; (c) M. Mauksch, S. B. Tsogoeva, S. Wei and I. M. Martynova, *Chirality*, 2007, 19, 816.
- Á. L. Fuentes de Arriba, L. Simón, J. R. Morán, presented in poster format at the 10th Tetrahedron Symposium, Paris, 2009.
- Crystal data for **10a**: C₁₈H₁₇N₃O₃ · CH₂Cl₂, FW 408.27, monoclinic, space group P2₁ (n° 4), a = 9.8341(4) Å, b = 8.8407(4) Å, c = 11.5844(6) Å, α = γ = 90°, β = 98.936(3)°, V = 994.93(8) Å³, Z = 2, D_c = 1.363 Mg m⁻³, m = (Cu-Kα) = 3.142 mm⁻¹, F(000) = 424. 5546 reflections were collected at 3.86 ≤ 2θ ≤ 64.58 and merged to give 2820 unique reflections (R_{int} = 0.0303), of which 2368 with I > 2σ(I) were considered to be observed. Final values are R = 0.0614, wR = 0.1745, GOF = 1.051, max/min residual electron density 0.465 and -0.267 e-Å⁻³. Flack value [0.04(4)].
- Crystal data for **10b**: C₁₈H₁₇N₃O₃, FW 323.35, orthorhombic, space group P2₁2₁1 (n° 19), a = 6.6712(2) Å, b = 14.9403(4) Å, c = 15.7482(4) Å, α = β = γ = 90°, V = 1569.62(7) Å³, Z = 4, D_c = 1.368 Mg m⁻³, m = (Cu-Kα) = 0.780 mm⁻¹, F(000) = 680. 9894 reflections were collected at 5.62 ≤ 2θ ≤ 64.85 and merged to give 2441 unique reflections (R_{int} = 0.0178), of which 2337 with I > 2σ(I) were considered to be observed. Final values are R = 0.0262, wR = 0.0695, GOF = 1.043, max/min residual electron density 0.100 and -0.089 e-Å⁻³. Flack value [0.0(2)].
- (a) P. W. Hickmott, *Tetrahedron*, 1982, 38, 1975; (b) P. W. Hickmott, *Tetrahedron*, 1982, 38, 3363.

Synthesis of Monoacylated Derivatives of 1,2-Cyclohexanediamine. Evaluation of their Catalytic Activity in the Preparation of Wieland–Miescher Ketone[†]

Ángel L. Fuentes de Arriba,[‡] David G. Seisededós,[‡] Luis Simón,[‡] Victoria Alcázar,[§] César Raposo,^{||} and Joaquín R. Morán^{*‡}

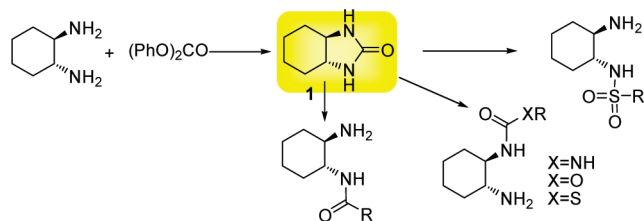
[‡]Organic Chemistry Department, Plaza de los Caídos 1-5, Universidad de Salamanca, Salamanca 37008, Spain,

[§]Industrial Chemistry and Environmental Engineering Department, José Gutiérrez Abascal 2, Universidad Politécnica de Madrid, Madrid 28006, Spain, and

^{||}Mass Spectrometry Service, Plaza de los Caídos, 1-5, Universidad de Salamanca, Salamanca 37008, Spain

romoran@usal.es

Received September 1, 2010



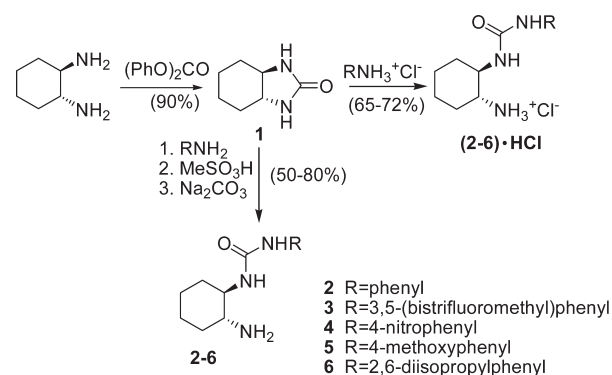
Ureas, carbamoyl derivatives, amides, and sulfonamides can be easily prepared from the strained (*R,R*)-cyclohexanediamine urea (**1**) in high yield, leaving a free amino group that shows good catalytic activity in intramolecular aldol condensations. The preparation of Wieland–Miescher ketone has been studied with these catalysts.

Although the formation of amide bonds by reaction of amines with acid chlorides is a common procedure in organic synthesis, high-yield monoacylation of symmetrical diamines may be, in some cases, a difficult process. Several hypotheses have been proposed to explain these findings, such as an inefficient mixture of reagents or intramolecular catalysis by the first-formed amide group.¹ However, monoacylation has been shown to be possible by working with low reactivity compounds like esters,² by employing aggregation effects,³ or by making use of steric hindrance.⁴

trans-Cyclohexanediamine is widely exploited as a source of chirality in many organic chemistry processes,⁵ and numerous derived bifunctional catalysts have been prepared. Many of these organocatalysts combine the presence of the chiral primary amine group with another functionality (thiourea, urea, sulfonamide, etc.), so selective monoacylation is desired.⁶

Monoacylation of cyclohexanediamine can be achieved following the procedure of Kim et al.,⁴ protecting both amines as their benzyloxycarbonyl derivatives, followed by reaction with Boc_2O and hydrogenolysis. Here, we develop an alternative procedure for monoacylation based on the reactivity of urea **1** (Scheme 1).

SCHEME 1. Preparation of Ureas Starting from (*R,R*)-Cyclohexanediamine



Cyclic urea **1** can be obtained when cyclohexanediamine is reacted with the gaseous and toxic carbonyl sulfide.⁷ A simple and high-yield alternative synthesis is based on the use of diphenylcarbonate, which can also be employed when the starting material is the straightforwardly obtained enantiopure (*R,R*)-cyclohexanediamine tartrate salt.⁸

Owing to the *trans*-fused rings, under acidic conditions urea **1** shows suitable reactivity with nucleophiles.⁹ Thus, aromatic amines can open the urea **1** ring in the presence of methanesulfonic acid to afford the corresponding aminoureas **2–6** after basic workup (Scheme 1). The reaction seems to be general for all anilines, including electron-poor (**3** and **4**)

(5) (a) Xue, F.; Zhang, S.; Duan, W.; Wang, W. *Adv. Synth. Catal.* **2008**, *350*, 2194. (b) Lalonde, M. P.; Chen, Y.; Jacobsen, E. N. *Angew. Chem., Int. Ed.* **2006**, *45*, 6366. (c) Uehara, H.; Barbas, C. F., III. *Angew. Chem., Int. Ed.* **2009**, *48*, 9848. (d) Tsogoeva, S. B.; Wei, S. *Chem. Commun.* **2006**, 1451. (e) Sohtome, Y.; Tanatani, A.; Hashimoto, Y.; Nagasawa, K. *Chem. Pharm. Bull.* **2004**, *52*, 477. (f) Rasappan, R.; Reiser, O. *Eur. J. Org. Chem.* **2009**, 1305. (g) Peng, F.; Shao, Z. *J. Mol. Catal. A: Chem.* **2008**, *285*, 1. (h) Luo, S.; Xu, H.; Li, J.; Zhang, L.; Cheng, J.-P. *J. Am. Chem. Soc.* **2007**, *129*, 3074. (i) Mei, K.; Jin, M.; Zhang, S.; Li, P.; Liu, W.; Chen, X.; Xue, F.; Duan, W.; Wang, W. *Org. Lett.* **2009**, *11*, 2864. (j) Wang, J.; Wang, X.; Ge, Z.; Cheng, T.; Li, R. *Chem. Commun.* **2010**, 1751. (k) Ma, H.; Liu, K.; Zhang, F.-G.; Zhu, C.-L.; Nie, J.; Ma, J.-A. *J. Org. Chem.* **2010**, *75*, 1402. (l) Huang, H.; Jacobsen, E. N. *J. Am. Chem. Soc.* **2006**, *128*, 7170. (m) Liu, K.; Cui, H.-F.; Nie, J.; Dong, K.-Y.; Li, X.-J.; Ma, J.-A. *Org. Lett.* **2007**, *9*, 923. (n) He, T.; Gu, Q.; Wu, X.-Y. *Tetrahedron* **2010**, *66*, 3195.

(6) Mitchell, J. M.; Finney, N. S. *Tetrahedron Lett.* **2000**, *41*, 8431.

(7) Davies, S. G.; Mortlock, A. A. *Tetrahedron* **1993**, *49*, 4419.

(8) Schanz, H.-J.; Linseis, M. A.; Gilheany, D. G. *Tetrahedron: Asymmetry* **2003**, *14*, 2763.

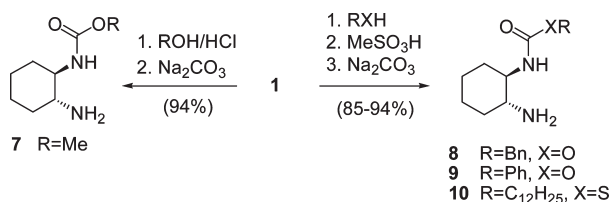
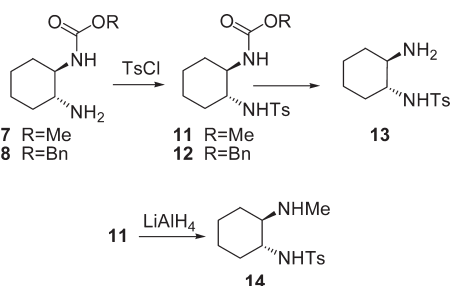
(9) Hutchby, M.; Houlden, C. E.; Ford, J. G.; Tyler, S. N. G.; Gagné, M. R.; Lloyd-Jones, G. C.; Booker-Milburn, K. I. *Angew. Chem., Int. Ed.* **2009**, *48*, 8721.

[†] Dedicated to Professor Carmen Nájera on the occasion of her 60th birthday. (1) Jacobson, A. R.; Makris, A. N.; Sayre, L. M. *J. Org. Chem.* **1987**, *52*, 2592.

(2) Tang, W.; Fang, S. *Tetrahedron Lett.* **2008**, *49*, 6003.

(3) Muñoz, F. M.; Simón, L.; Sáez, S.; Raposo, C.; Morán, J. R. *Tetrahedron Lett.* **2008**, *49*, 790.

(4) Kim, Y. K.; Lee, S. J.; Ahn, K. H. *J. Org. Chem.* **2000**, *65*, 7807.

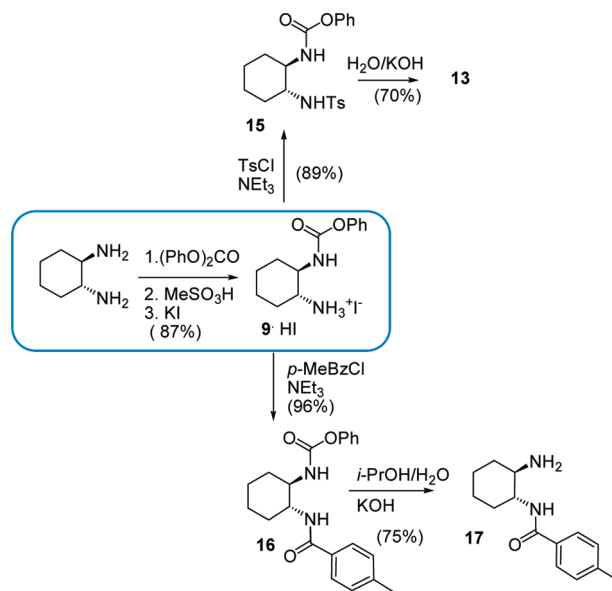
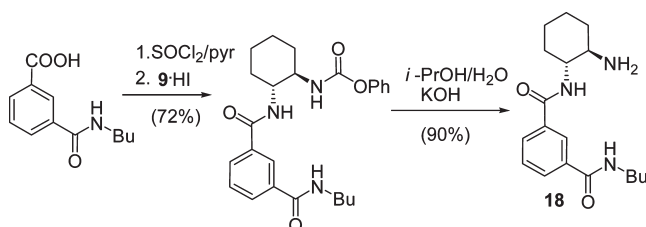
SCHEME 2. Monoprotection of Cyclohexanediamine as Carbamoyl (Carbamothioyl) Derivatives

SCHEME 3. Transformation of the Carbamoyl Derivatives into Sulfonamides


and electron-rich systems (**5**) and hindered amines (**6**). Ring opening can also be carried out without methanesulfonic acid when the hydrochloride salt of the aromatic amine is employed. In this case, the reaction also works well and the isolation of the corresponding ureas may be easily accomplished by precipitation upon addition of a proper solvent to the reaction medium (see the Supporting Information). By contrast, aliphatic amines failed to produce the desired ring opening under the above conditions.

Monoamides and sulfonamides are other target compounds whose synthesis is achieved through the monocarbamoyl derivatives (see Schemes 3 and 4). Hence, the first step in the synthesis comprises the reaction of urea **1** with alcohols yielding the monocarbamates (Scheme 2). Compound **7** was obtained by reacting the cyclic urea **1** with MeOH/HCl, and the carbamoyl derivatives **8** and **9** were prepared by treatment with the corresponding alcohols and MeSO₃H. Under the same conditions, dodecanethiol afforded the monocarbamothioyl derivative **10**.

Preparation of sulfonamides **11** and **12** was carried out in two steps, starting from the related carbamoyl derivatives. For the obtention of sulfonamides, compounds **7** and **8**, respectively, were reacted with tosyl chloride. These sulfonamides may be deprotected yielding the primary amine **13** (Scheme 3). Deprotection can be carried out under basic conditions, nucleophilic displacement in the case of the methyl group,¹⁰ or hydrogenolysis for the benzyl group. Additionally, the tosyl derivative **11** was converted to the corresponding methylamine **14** through reduction of the carbamoyl group with LiAlH₄.

The one-pot synthesis of the monocarbamate **9** starting from the cyclohexanediamine tartrate salt offers an attractive possibility to achieve the monoprotected compounds (Scheme 4). Since urea **1** can be obtained from diphenyl carbonate, generating two phenol equivalents in situ, the addition of methanesulfonic acid led to ring opening, directly affording the

SCHEME 4. One-Pot Synthesis of Carbamate 9 and Preparation of Amides and Sulfonamides

SCHEME 5. Preparation of Catalyst 18


monocarbamoylated compound **9**. This compound is highly water-soluble as its methanesulfonate salt but readily crystallizes as the hydroiodide. Tosylation or benzylation, for example, can be carried out in chloroform in the presence of triethylamine to yield compounds **15** and **16**. Hydrolysis of the phenylcarbamoyl group can be readily achieved under mild basic conditions to yield the sulfonamide **13** and the amide **17** (Scheme 4).

The “oxyanion hole” properties of isophthalic derivatives¹¹ inspired us to prepare compound **18**, which incorporates an extra amide functionality. This cyclohexanediamine derivative is obtained starting from the isophthalic acid monobutyl amide,¹² according to the synthetic procedure depicted in Scheme 5 (see the Supporting Information).

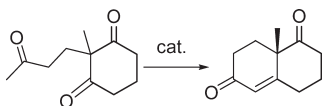
Chiral amines derived from daminocyclohexane have proved to be efficient organocatalysts for the aldol reaction.¹³ Due to

(10) Elsinger, F.; Schreiber, J.; Eschenmoser, A. *Helv. Chim. Acta* **1960**, *43*, 113.

(11) (a) Dixon, R. P.; Geib, S. J.; Hamilton, A. D. *J. Am. Chem. Soc.* **1992**, *114*, 365. (b) Gale, P. A. *Coord. Chem. Rev.* **2003**, *240*, 191. (c) Muñiz, F. M.; Montero, V. A.; Fuentes de Arriba, A. L.; Simón, L.; Raposo, C.; Morán, J. R. *Tetrahedron Lett.* **2008**, *49*, 5050.

(12) Oliva, A. I.; Simón, L.; Muñiz, F. M.; Sanz, F.; Morán, J. R. *Tetrahedron* **2004**, *60*, 3755.

(13) (a) Raj, M.; Parashari, G. S.; Singh, V. K. *Adv. Synth. Catal.* **2009**, *351*, 1284. (b) Nakayama, K.; Maruoka, K. *J. Am. Chem. Soc.* **2008**, *130*, 17666. (c) Luo, S.; Xu, H.; Chen, L.; Cheng, J.-P. *Org. Lett.* **2008**, *10*, 1775. (d) Luo, S. Z.; Xu, H.; Li, J. Y.; Zhang, L.; Cheng, J. P. *J. Am. Chem. Soc.* **2007**, *129*, 3074. (e) Mei, K.; Zhang, S.; He, S.; Li, P.; Jin, M.; Xue, F.; Luo, G.; Zhang, H.; Song, L.; Duan, W.; Wang, W. *Tetrahedron Lett.* **2008**, *49*, 2681. (f) Liu, J.; Yang, Z.; Wang, Z.; Wang, F.; Chen, X.; Liu, X.; Feng, X.; Su, Z.; Hu, C. *J. Am. Chem. Soc.* **2008**, *130*, 5654.

TABLE 1. Preparation of the Wieland–Miescher Ketone in CDCl_3 (1.0 M) with 10 mol % of Catalyst at 20 °C

entry	catalyst	conversion ^a (%)	yield ^b (%)	time (h)	ee ^c (%)
1	2^d	95	76	22	85
2	3	94	82	30	89
3	4	81	63	117	75
4	8	76	59	117	65
5	13	3	n.d.	161	61
6	14	24	n.d.	161	–11
7	17	94	77	44	91
8	18^d	100	85	16	95

^aDetermined by integration of the corresponding signals in the ¹H NMR spectra. ^bIsolated yield after silica gel chromatography. ^cDetermined by chiral HPLC (Daicel Chiralpak IC column). ^d2.0 M concentration of the ketone, 10 mol % catalyst. Higher concentrations of the ketone yielded reduced enantioselectivities.

our interest in this reaction,¹⁴ we decided to explore the ability of these compounds in the preparation of the Wieland–Miescher ketone.¹⁵ Ureas **2–4** are good organocatalysts for this reaction, showing high enantioselectivities (Table 1, entries 1–3). The catalytic activity of the carbamoyl derivative **8** was also evaluated (entry 4, Table 1), but enantioselectivity was reduced in comparison with that obtained with the urea compounds.

Considering enantioselectivity, sulfonamide **13** proved to be a similar catalyst to the carbamoyl derivative **8** (entries 4 and 5, Table 1), although the conversion rate was considerably reduced. To test the influence of a secondary amine in the conversion and enantioselectivity, we prepared the sulfonamide **14** with a methylamino group (entry 6, Table 1). This catalyst showed the lowest enantioselectivity with the opposite enantiomer as the major product.

When amide **17** was used, enantioselectivity was increased up to 91% ee (entry 7, Table 1). The isophthalic derivative **18**, which resembles the oxyanion hole geometry, gave the best enantioselectivity (95% ee) with a complete conversion within 16 h (entry 8, Table 1). This catalyst has also been tested in

the preparation of the Hajos–Wiechert ketone; however, in this case, the reaction was much slower (only 20% conversion to the ketone after 94 h and 81% ee), which limits its use for preparative purposes.

In summary, an alternative approach to the synthesis of monofunctionalized 1,2-cyclohexanediamines has been described, starting from the readily available (*R,R*)-cyclohexanediamine urea and taking advantage of the reactivity provided by the *trans* ring junction. In addition, we have explored the possibilities of these compounds as catalysts in the intramolecular aldol condensation yielding the Wieland–Miescher ketone, with the best results being obtained for ureas and amides, reaching up to 95% ee.

Experimental Section

(3a*R*,7a*R*)-Hexahydro-1*H*-benzo[*d*]imidazol-2(3*H*)-one (1). Enantiopure (*R,R*)-cyclohexanediamine tartrate salt was readily obtained starting from the racemic *trans*-cyclohexane-1,2-diamine and L-tartaric acid.⁸ This tartrate salt (40.0 g, 150.8 mmol) and KOH (17.0 g, 303.6 mmol) were dissolved in H₂O (30 mL) to generate the free diamine. The reaction mixture was heated until all of the solid was dissolved. Then, 2-propanol (100 mL) was added, and the solution was stirred and cooled (ice bath) to yield a potassium tartrate precipitate. To complete the precipitation and remove the water, powdered sodium sulfate (40.0 g) was added and the precipitate was filtered off. The solid was washed with more 2-propanol (2 × 20 mL), diphenyl carbonate (35.0 g, 163 mmol) was added to the filtrate, and the mixture was refluxed for 30 min. Steam distillation and water evaporation allowed us to obtain a crude urea which could be further purified by recrystallization from EtOH/H₂O (1:1) to yield 18.8 g (90% yield) of a compound with the same physical properties as those described in the literature.¹⁶

General Procedure for the Preparation of Monoureas (2–6) with Methanesulfonic Acid (Procedure A). To a mixture of the urea **1** (2.2 mmol) and the aromatic amine (2.2 mmol) in diglyme (2 mL) was added methanesulfonic acid (0.15 mL) was added, and the reaction mixture was heated at 120 °C for ~1 h with stirring under argon atmosphere. After the mixture was cooled to room temperature, H₂O (10 mL) and Na₂CO₃ (2.0 g, 19 mmol) were added, and a crystalline solid precipitated that was filtered to afford the desired compound. If the urea did not crystallize spontaneously, diethyl ether (2 mL) was added to assist the precipitation. This procedure has been carried out on a 2–15 mmol scale.

(1*R*,2*R*)-1,2-Diaminocyclohexane 3,5-bis(trifluoromethyl) phenylurea (3). Urea **1** (2.0 g, 14.2 mmol), 3,5-bis(trifluoromethyl)aniline (3.4 g, 14.8 mmol), and methanesulfonic acid (1 mL) were dissolved in diglyme (2 mL), and the mixture was heated at 120 °C for 30 min. Then, H₂O (30 mL) and Na₂CO₃ (7 g, 66 mmol) were added. The product was extracted with ethyl acetate (2 × 20 mL), and the solvent was evaporated. The crude residue was purified by recrystallization from ether–hexane at 0 °C to afford 3.5 g (66% yield) of compound **3**, whose properties are in agreement with those published.^{5c}

General Procedure for the Preparation of Monoureas (2–6) Starting from the Hydrochloride Salts of the Amines (Procedure B). Urea **1** (3.5 mmol) and the amine hydrochloride (3.5 mmol) were heated in diglyme (2 mL) at 120 °C. After the mixture was heated for ~1 h, a solid precipitated from the reaction medium. NMR ¹H analysis of an aliquot confirmed that the reaction had finished. The mixture was cooled to room temperature, and diethyl ether (10 mL) was added. The solid was filtered and dried under vacuum (0.1 mmHg) heating at 90 °C to remove completely the traces of diglyme, affording the monoureas as their hydrochloride salts.

This procedure has been carried out on a 1–5 mmol scale.

(14) (a) Fuentes de Arriba, Á. L.; Simón, L.; Raposo, C.; Alcázar, V.; Morán, J. R. *Tetrahedron* **2009**, *65*, 4841. (b) Fuentes de Arriba, A. L.; Simón, L.; Raposo, C.; Alcázar, V.; Sanz, F.; Muñoz, F. M.; Morán, J. R. *Org. Biomol. Chem.* **2010**, *8*, 2979.

(15) (a) Almasi, D.; Alonso, D. A.; Balaguer, A.-N.; Nájera, C. *Adv. Synth. Catal.* **2009**, *351*, 1123. (b) Almasi, D.; Alonso, D. A.; Nájera, C. *Adv. Synth. Catal.* **2008**, *350*, 2467. (c) Bradshaw, B.; Etxebarria-Jardi, G.; Bonjoch, J.; Vióquez, S. F.; Guillena, G.; Nájera, C. *Adv. Synth. Catal.* **2009**, *351*, 2482. (d) Davies, S. G.; Sheppard, R. L.; Smith, A. D.; Thomson, J. E. *Chem. Commun.* **2005**, 3802. (e) Lacoste, E.; Vaïque, E.; Berlande, M.; Pianet, I.; Vincent, J.-M.; Landais, Y. *Eur. J. Org. Chem.* **2007**, 167. (f) He, L. *Hecheng Huaxue (Chin. J. Synth. Chem.)* **2007**, *15*, 231. (g) Akahane, Y.; Inage, N.; Nagamine, T.; Inomata, K.; Endo, Y. *Heterocycles* **2007**, *74*, 637. (h) Akahane, Y.; Inomata, K.; Endo, Y. *Heterocycles* **2009**, *77*, 1065. (i) D'Elia, V.; Zwignagel, H.; Reiser, O. *J. Org. Chem.* **2008**, *73*, 3262. (j) Guillena, G.; Hita, M. d. C.; Nájera, C.; Vióquez, S. F. *J. Org. Chem.* **2008**, *73*, 5933. (k) Kanger, T.; Kriis, K.; Laars, M.; Kailas, T.; Muurisepp, A.-M.; Pehk, T.; Lopp, M. *J. Org. Chem.* **2007**, *72*, 5168. (l) Davies, S. G.; Russell, A. J.; Sheppard, R. L.; Smith, A. D.; Thomson, J. E. *Org. Biomol. Chem.* **2007**, *5*, 3190. (m) Guillena, G.; Nájera, C.; Vióquez, S. F. *Synlett* **2008**, *19*, 3031. (n) Kriis, K.; Kanger, T.; Laars, M.; Kailas, T.; Muurisepp, A.-M.; Pehk, T.; Lopp, M. *Synlett* **2006**, *11*, 1699. (o) Nozawa, M.; Akita, T.; Hoshi, T.; Suzuki, T.; Hagiwara, H. *Synlett* **2007**, *4*, 661. (p) Zhang, X.-M.; Wang, M.; Tu, Y.-Q.; Fan, C.-A.; Jiang, Y.-J.; Zhang, S.-Y.; Zhang, F.-M. *Synlett* **2008**, *18*, 2831. (q) Agami, C.; Meynier, F.; Puchot, C.; Guilhem, J.; Pascard, C. *Tetrahedron* **1984**, *40*, 1031. (r) Bui, T.; Barbas, C. F. *Tetrahedron Lett.* **2000**, *41*, 6951.

(16) Davies, S. G.; Mortlock, A. A. *Tetrahedron* **1993**, *49*, 4419.

(1*R*,2*R*)-1,2-Diaminocyclohexane Phenylurea (2). Urea **1** (495 mg, 3.5 mmol) and aniline hydrochloride (460 mg, 3.5 mmol) were heated in diglyme (2 mL) at 120 °C. After the mixture was heated for ~1 h, a solid precipitated from the reaction medium. ¹H NMR analysis of an aliquot confirmed that the reaction had finished. The mixture was cooled to room temperature, and diethyl ether (10 mL) was added. The solid was filtered and dried under vacuum (0.1 mmHg) heating at 90 °C to remove completely the traces of diglyme. The urea **2** as its hydrochloride salt (621 mg, 66%) was obtained. Spectral and physical data of the free amine (liberated with aqueous KOH (3.3 mL, 6 mM) and extracted with diethyl ether) were in agreement with those published.¹⁷

Phenyl (1*R*,2*R*)-2-Aminocyclohexylcarbamate 9. Initially, (*R,R*)-cyclohexane-1,2-diamine tartrate salt (10.02 g, 37.9 mmol) was reacted under the same conditions described for the preparation of urea **1**. After the mixture was refluxed with diphenyl carbonate (8.11 g, 37.9 mmol) in 2-propanol, the solvent was evaporated under reduced pressure, and the crude residue was dried through azeotropic distillation with benzene (100 mL). To this mixture of phenol and the urea **1** was added 1 equiv of methanesulfonic acid (2.5 mL), and the reaction was heated at 110 °C with stirring for 1 h under Ar atmosphere. Then the solution was cooled, water (30 mL)

was added, and the phenol was extracted with ethyl acetate (2 × 30 mL). To the aqueous layer, cooled to 0 °C, was added KI (7.0 g, 42 mmol), and a precipitate of the hydroiodide salt of compound **9** (12 g, 87% yield) was obtained: mp 187–189 °C; $[\alpha]_D^{20}$ -6.33 (*c* 0.6, CH₃OH); ¹H NMR (200 MHz, CDCl₃/CD₃OD) δ 7.22–7.15 (2H, m), 7.06–6.97 (3H, m), 3.38 (1H, m), 3.03 (1H, m), 1.94–1.84 (2H, m), 1.65–1.55 (2H, m), 1.30–1.16 (4H, m); ¹³C NMR (50 MHz, CDCl₃/CD₃OD) δ 155.9 (C), 150.9 (C), 129.3 (CH), 125.6 (CH), 121.8 (CH), 54.6 (CH), 53.1 (CH), 31.7 (CH₂), 29.9 (CH₂), 24.4 (CH₂), 23.7 (CH₂); IR (film) 3565, 3318, 1729, 1599, 1462 cm⁻¹. Anal. Calcd for C₁₃H₁₉N₂O₂: C, 43.11; H, 5.29; N, 7.73. Found: C, 42.89; H, 5.38; N, 7.83.

Acknowledgment. This work was supported by the Spanish Dirección General de Investigación, Ciencia y Tecnología (DGICYT) (CTQ-2008-01771/BQU), and the UE (European Reintegration Grant PERG04-GA-2008-239244). A.L.F.A. thanks the Ministerio de Educación y Ciencia for a FPU Grant and Angélica del Castillo for working with us.

Supporting Information Available: Synthesis of catalysts, characterization data (including ¹H and ¹³C spectra of the new compounds), and HPLC chromatograms. This material is available free of charge via the Internet at <http://pubs.acs.org>.

(17) Bied, C.; Moreau, J. J. E.; Wong Chi Man, M. *Tetrahedron: Asymmetry* **2001**, *12*, 329.

A Twitchell Reagent Revival: Biodiesel Generation from Low Cost Oils


Ángel L. Fuentes de Arriba,^a Luis Simón,^a Victoria Alcázar,^b Jorge Cuellar,^c Patricia Lozano-Martínez,^c and Joaquín R. Morán^{a,*}

^a Organic Chemistry Department, University of Salamanca, Plaza de los Caídos 1–5, E-37008 Salamanca, Spain
Fax: (+34)-923-294-574; phone: (+34)-923-294-481; e-mail: romoran@usal.es

^b Department of Industrial Chemical Engineering and the Environment, Technical University of Madrid, José Gutiérrez Abascal 2, E-28006 Madrid, Spain

^c Department of Chemical Engineering, University of Salamanca, Plaza de los Caídos 1–5, E-37008 Salamanca, Spain

Received: April 13, 2011; Revised: June 13, 2011; Published online: October 10, 2011

 Supporting information for this article is available on the WWW under <http://dx.doi.org/10.1002/adsc.201100278>.

Abstract: The transesterification of triglycerides with short-chain alcohols, such as methanol, is the most used process for the obtention of biodiesel. This is a biphasic reaction which can occur both in polar and apolar phases. Using lipophilic sulphonic acids as catalysts, the transesterification reaction takes place primarily in the oil phase. Under these conditions, the reaction rates are considerably improved, with conversions up to 98% in 90 min at 80°C and with 17.6% mol of catalyst. The most remarkable features of this process are that the catalytic efficiency is not affected by the presence in the oil of free fatty acids

or small amounts of water, the transesterification takes place at low temperature (below the boiling point of methanol) and high conversions are reached within a short time. Therefore, low-cost feedstocks containing high levels of FFA (free fatty acids) and water can be used as raw material for biodiesel production. Finally, catalyst recovery by adsorption on a silica gel column was also tested.

Keywords: biodiesel; homogeneous acid catalysis; lipophilic sulphonic acids; transesterification; Twitchell reagents

Introduction

Over the past years, biodiesel has gained importance as an alternative to fossil fuels due, among others, to environmental reasons.^[1] To date, the best procedure for the transformation of triglycerides in biodiesel is the transesterification with short-chain alcohols to yield the corresponding esters and glycerine.^[2]

The search for an ideal catalyst for this apparently simple transformation is, still, an ongoing work.^[3] The most popular catalysts in use are alkaline metal hydroxides;^[4] nevertheless, these reagents show the following disadvantages.^[5] (i) The presence of free fatty acids in oils leads to non-practical procedures. (ii) The phase separation is complicated by the generation of emulsions. (iii) The presence of water in the alcohol increases the soap formation, yielding non-efficient processes. (iv) Additionally, an acidic reagent is necessary to neutralize the base, this leads to an increase in the biodiesel price. (v) Glycerine is obtained in the presence of salts, increasing the cost of glycerine pu-

rification, which is an important by-product for a cost-efficient procedure.

On the other hand, acid catalysts such as sulphuric acid or sulphonic acids do not show these pitfalls, but reactions are slow and large amounts of alcohol are necessary.^[6] A comparison between transesterification and the traditional fat hydrolysis reactions can be useful to understand this low reactivity. The transformation of triglycerides into the corresponding fatty acids has been thoroughly studied until the 1950s; the preparation of soap and glycerine justified this work,^[7] but the commercialization of detergents and the development of new procedures to obtain glycerine,^[8] led to a fast decay in this research work. The conclusions reached in these studies can be summarized as follows.^[9] (i) Triglyceride hydrolysis is a biphasic procedure due to the low solubility of oil and water. (ii) Esters which exhibit partial solubility in water, hydrolyse in the aqueous phase following the classic Ingold mechanism.^[10] Kinetics show zero order in the esters, since ester concentration remains con-

stant during the process due to solubilization from the apolar phase. (iii) Esters that are sparingly water soluble, such as triglycerides, prefer to react fast in the apolar phase, with only a minor contribution from the aqueous phase. Complex kinetics are obtained revealing an induction period, followed by a fast reaction in the fat, and finally a slow reaction due to consumption of the reagents. (iv) Hydrophilic acids, like hydrochloric or sulphuric acids, choose the water phase, and therefore are poor catalysts for triglyceride hydrolysis. On the other hand, long-chain sulphonic acids (Twitchell reagents)^[11] are good catalysts for the reaction since they dissolve better in the triglyceride phase.

Triglyceride transesterification with methanol in the presence of an acid catalyst shows a remarkable resemblance to the previous hydrolysis. The water molecule is now substituted by the more lipophilic methanol, but the mutual solubility with the triglyceride is still small and the reaction is again a biphasic process. As in hydrolysis, the transformation of the triglyceride can take place in both polar and apolar phases. Hydrophilic catalysts, such as sulphuric acid, render reactions which are faster in the methanolic phase. This can be easily shown since the reaction rate is proportional to the methanol volume.^[12] However, the small triglyceride concentration in the methanolic phase (1/300 mol/mol measured for sunflower seed oil) yields small reaction rates. The fact that the lack of solubility of the triglyceride is a main problem can be readily demonstrated by comparing the rate of transesterification with the esterification of fatty acids. Since fatty acids are soluble in methanol, they undergo esterification at a reasonable rate, and this reaction can be used in industrial processes for biodiesel preparation. Nevertheless, the transesterification of triglycerides is slow, and the resultant generation of water further re-

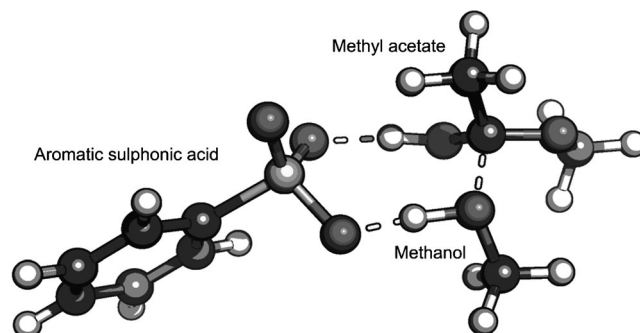


Figure 1. Transition state of the reaction of methanol with methyl acetate catalysed by phenylsulphonic acid (B3LYP/6-31G**).

duces the solubility of the triglyceride in methanol, making transesterification even more difficult.

As in fat hydrolysis, a good alternative may be to promote the reaction in the apolar triglyceride phase, since the methanol molar concentration in this phase is, by far, larger (1/0.4 mol/mol measured in refined sunflower seed oil) than the triglyceride concentration in the polar phase. Recent calculations related to lactone polymerizations suggest a possible mechanism for this transformation in the apolar phase (Scheme 1).^[13]

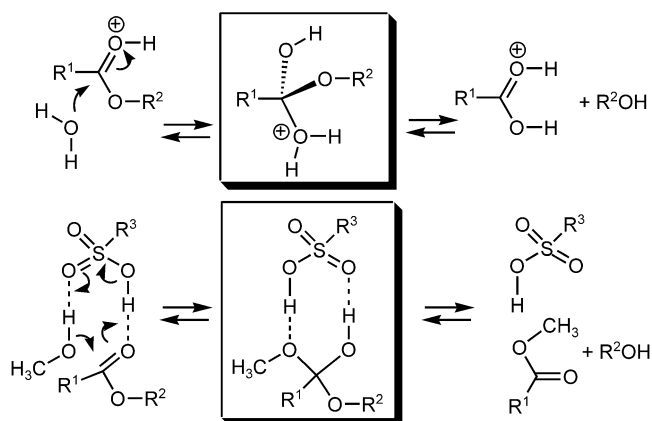
Our own calculations reveal that a similar mechanism is also operative in the transesterification of acyclic esters (Figure 1).

To make use of this alternative, the acid catalyst should preferentially dissolve in the triglyceride phase, therefore a Twitchell reagent could be a good choice.^[11] The use of such a lipophilic acid catalyst may offer some interesting advantages in the biodiesel preparation. (i) The presence of large amounts of free fatty acids may be of little effect in the transesterification reaction, because they do not interfere with the acid catalyst. (ii) The existence of small amounts of water (from fatty acid esterification or from a low quality methanol, or a wet fat), which will remain in the methanolic phase, should not strongly influence the reaction kinetics in the apolar phase. (iii) Since methanol will be saturating the triglyceride phase, its total amount will not affect the reaction rate, and therefore its amount can be kept at a minimum. (iv) Glycerine can thus be obtained in the absence of salts and its purification becomes an easy process.

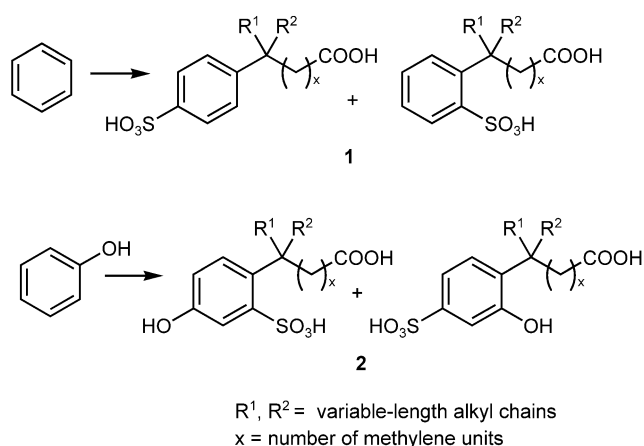
Results and Discussion

Twitchell Reagents

Twitchell reagents have been prepared from several different sources. Although the initial Twitchell re-



Scheme 1. Proposed mechanisms – showing tetrahedral intermediates– for the classic ester hydrolysis (*top*) and transesterification in an apolar phase (*bottom*).



Scheme 2. Proposed structures for the Twitchell reagents **1** and **2**, prepared from benzene or phenol, respectively.

ports^[11] utilized oleic acid, an aromatic hydrocarbon (benzene or naphthalene) and sulphuric acid, later procedures broadened the scope of the reaction making use of different aromatic rings (xylenes, phenol),^[14] or changing the oleic acid for triglycerides, petroleum derivatives or butanol.^[15] These reagents were commercialized under several different names such as Pfeilring, Neokontakt, Idrapid and Divuslon, but nowadays they cannot be purchased any more.

Therefore, to test the efficiency of these lipophilic aromatic compounds in the biodiesel preparation, we have synthesized two Twitchell reagents, **1** and **2**, starting from olive oil (due to its high content in oleic acid), benzene or phenol and sulphuric acid. An excess of the aromatic compounds was used to prevent dialkylation of these rings. But even in this case, Twitchell reagents turn out to be complex mixtures of compounds, due to rearrangement of the oleic acid alkyl chains and different substitution patterns in the aromatic rings. Nevertheless, the aromatic portions of both Twitchell reagents **1** and **2** can be easily recognized in the ¹H NMR spectra (see Supporting Information), and are in agreement with the structures shown in Scheme 2.

Catalytic Activity of Twitchell Reagents

The catalytic properties of reagents **1** and **2** were tested in the transesterification of commercial sunflower seed oil, and compared with those of sulphuric acid. In a typical reaction, methanol (6 mmol) and triglyceride (1 mmol) were reacted at 60 °C and in the presence of 1 wt% sulphuric acid or the same molar amounts of Twitchell reagents **1** and **2**. The conversion of the transesterification reaction was determined by ¹H NMR spectroscopy (see Supporting Information).

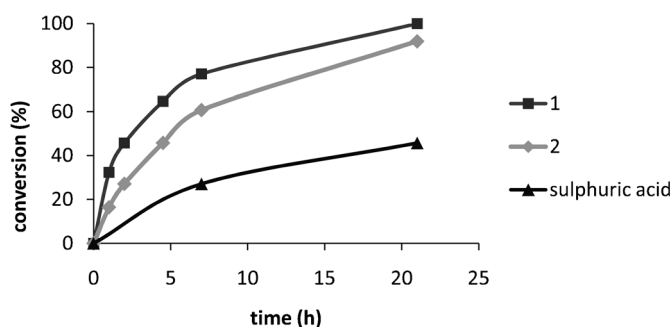


Figure 2. Sunflower seed oil transesterification with 1 wt% sulphuric acid and the same molar amounts of Twitchell reagents **1** and **2**. The molar ratio methanol to triglyceride was kept at 6/1 and the temperature at 60 °C.

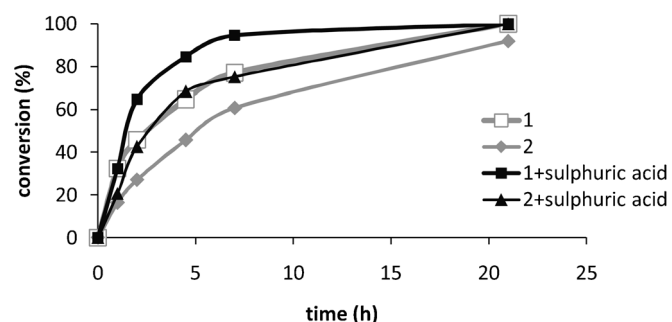


Figure 3. Sunflower seed oil transesterification with Twitchell reagents **1** and **2**, in the presence and absence of 1 wt% sulphuric acid. The molar ratio methanol to triglyceride was kept at 6/1 and the temperature at 60 °C.

Results are shown in Figure 2. The hydrophilic sulphuric acid showed a very small catalytic activity, while the catalyst **1** derived from benzene provided the best results. The phenolic group in catalyst **2**, which increases the hydrophilicity, yielded slower reaction rates.

It is well established that one of the reasons for a loss of catalytic activity of Twitchell reagents in fat hydrolysis reactions is their partition between water and the oil phase; as much as 45% of the catalyst can remain in the water phase.^[14] If an unfavourable partition constant reduces the reaction rate, a simple way to improve the catalytic properties of Twitchell reagents is to add a small amount of sulphuric acid to the water phase. The presence of this strong acid decreases the dissociation of sulphonic acid, raising the Twitchell reagent concentration in the apolar phase.^[14a,16]

Partition between methanol and the triglyceride can be even less favourable than with water, therefore we tested the effect of added sulphuric acid to the reaction. As shown in Figure 3, the catalytic properties of both Twitchell reagents **1** and **2** improved in the

presence of 1 wt% sulphuric acid, when tested under the previous conditions.

The use of sulphuric acid as a co-catalyst has, however, several drawbacks. (i) Sulphuric acid is a sulphonating and dehydrating compound which can transform glycerine into acrolein.^[17] (ii) Separation of the sulphuric acid from the polar phase will increase the cost of the transesterification process. (iii) Sulphuric acid is a corrosive reagent to the equipment.

Since the major role of sulphuric acid is only to improve the partition constant of the catalyst towards the apolar phase, it should not be necessary in the presence of a highly lipophilic catalyst with a more favourable partition coefficient to the triglyceride phase.

Lipophilic Sulphonic Acids

To test this hypothesis catalyst **3** was prepared using a known procedure (Figure 4).^[18] Since it lacks the hydrophilic carboxylic group, it should be more lipophilic than the previous Twitchell reagents **1** and **2** (Figure 5).

Catalyst **3** was tested under the same previous conditions, showing improved results with respect to the Twitchell reagents **1** and **2**, in both the presence and absence of sulphuric acid.

To confirm the relevance of the catalyst lipophilicity, the partition constant between sunflower seed oil and methanol was studied by ¹H NMR. Integration of the catalyst signals in deuterated methanol, before and after partition with the oily phase, allowed the

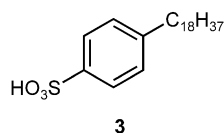


Figure 4. Structure of catalyst **3**.

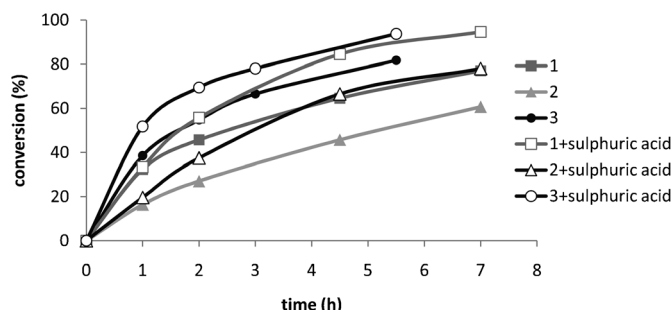


Figure 5. Sunflower seed oil transesterification with Twitchell reagents **1** and **2** and catalyst **3**, in the presence and absence of 1 wt% sulphuric acid. The molar ratio methanol to triglyceride was kept at 6/1 and the temperature at 60 °C.

determination of the constant. As shown in Table 1 (entry 1), catalyst **3** still prefers the methanolic phase, and therefore more lipophilic catalysts could improve the catalytic results.

Table 1. Partition constants between methanol and sunflower seed oil calculated by integration of ¹H NMR signals.

Entry	Catalyst	Partition constant
1	3	9/1
2	4	1/1
3	4	6/4 ^[a]
4	5	2/98 ^[b]

^[a] MeOD with 10% v/v D₂O.

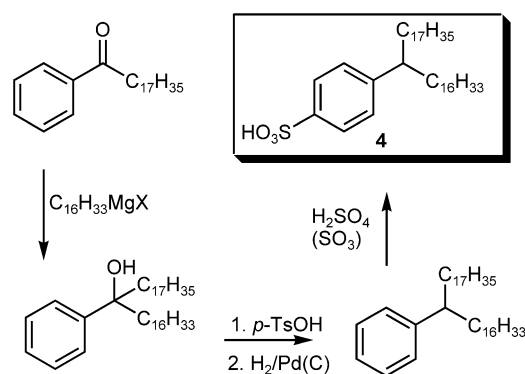
^[b] Estimated.

A new catalyst, **4**, comprising an aliphatic 34-carbon atom chain, was designed and synthesized (Scheme 3).

Catalyst **4** showed a suitable partition constant (Table 1, entry 2) with similar affinity for both phases methanol and oil. Taking into account the small methanol volume under the reaction conditions, most of the catalyst should stay in the oil. The catalytic properties of this lipophilic catalyst **4** are displayed in Figure 6. In agreement with its enhanced partition constant, compound **4** shows a higher catalytic activity and the effect of the addition of sulphuric acid is less pronounced than in the previous catalysts.

Finally, an even more lipophilic catalyst **5** was prepared starting from isophthalic acid dimethyl ester as shown in Scheme 4.

Catalyst **5** turned out to be a crystalline compound with a low solubility in methanol but with a favourable partition constant in the triglyceride (Table 1, entry 4). Accordingly, this new catalyst **5** further increased the reaction rate with respect to catalyst **4**, affording similar results to those obtained when catalyst **4** was combined with sulphuric acid. Moreover, the addition of sulphuric acid to catalyst **5** led to no im-



Scheme 3. Synthesis of catalyst **4**.

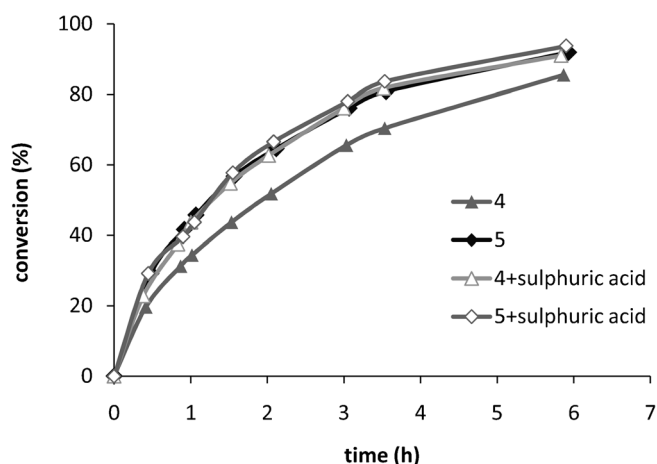
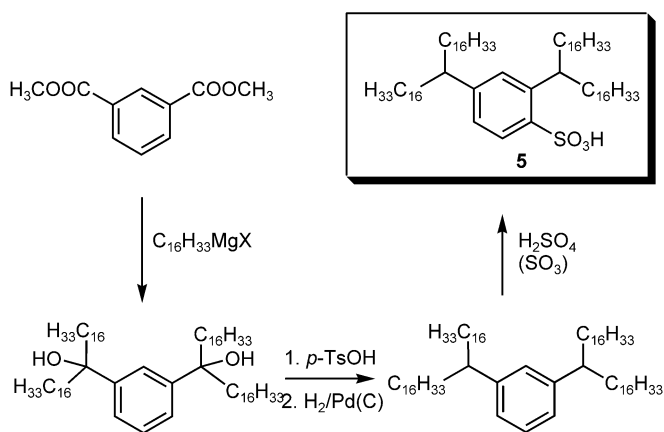


Figure 6. Sunflower seed oil transesterification with catalysts **4** and **5**, in the presence and absence of 1 wt% sulphuric acid. The molar ratio methanol to triglyceride was kept at 6/1 and the temperature at 60 °C.



Scheme 4. Synthesis of catalyst **5**.

provement, which may indicate that no further reaction rate increase will be achieved by increasing the lipophilicity of the catalyst.

Since catalysts **4** and **5** showed the best performance, both of them were selected to study the influence of different factors in the transesterification reaction.

Influence of the Free Fatty Acids Content of Oil

As already pointed out, the presence of free fatty acids (FFA) makes the conventional alkaline transesterification inappropriate.^[19] However, this inconvenience could be overcome by using acid catalysts like **4** and **5**. The effect of FFA content in the reaction rate was investigated.

Figure 7 shows the influence of 5, 10, 20%, w/w of stearic acid added to the sunflower seed oil. Even

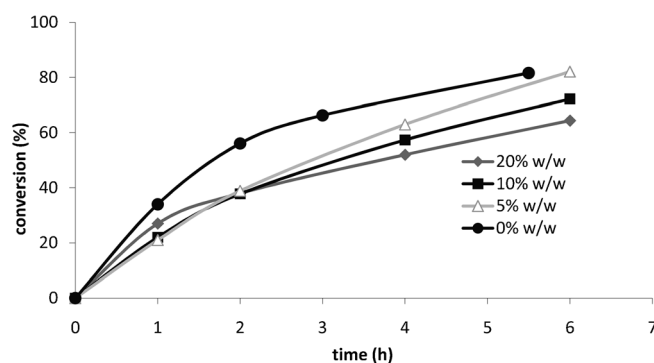


Figure 7. Sunflower seed oil transesterification with catalyst **4**, in the presence of oil containing 5, 10, 20% (w/w) of stearic acid. The molar ratio methanol to triglyceride was kept at 6/1 and the temperature at 60 °C (FAME integral was used to measure the conversion).

high free fatty acid contents have little influence on the reaction rate, despite the generation of a certain amount of water due to the esterification of the free carboxylic acids.

Influence of the Water Content

The presence of water in the reaction mixture slightly reduces the yield and the reaction rate. This effect has been studied for catalysts **4** and **5** with 5, 10, 20% (v/v) water in the methanol phase (see Supporting Information). These results can be explained due to a change in the partition constant between the methanol and triglyceride phases. In the presence of water, the partition constant for catalyst **4** increases from 1/1 to 6/4 (Table 1, entries 2 and 3) which now favours the methanolic phase. Since a smaller amount of the catalyst is now present in the oily phase, a lower reaction rate is expected. On the other hand, this effect is smaller in the case of the more lipophilic catalyst **5**, which prefers the oily phase, and therefore a smaller effect from water is expected (Figure 8). Since these catalysts are not water soluble, the effect of water in the partition constant is somehow surprising, but it can be explained due to the basicity of the water molecule which probably favours the ionization of the sulphonic acid in the methanolic phase, at least if a relatively small amount of water is used. In any case, the effect of water in this reaction is relatively small.

Influence of the Methanol/Triglyceride Molar Ratio

The effect of a very small excess of methanol was also analysed with catalyst **4**. Working with a molar ratio methanol to triglyceride of only 3.5/1, rendered reactions which are faster at the beginning. This fact is in agreement with a larger amount of the catalyst in the

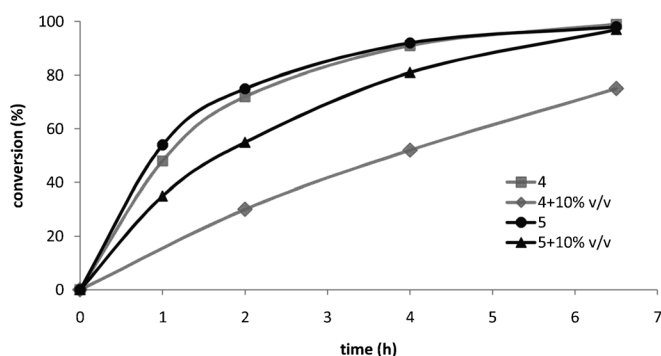


Figure 8. Sunflower seed oil transesterification with catalysts **4** and **5**, in the presence of methanol containing 0, 10% (v/v) of water. The molar ratio methanol to triglyceride was kept at 6/1 and the temperature at 60 °C.

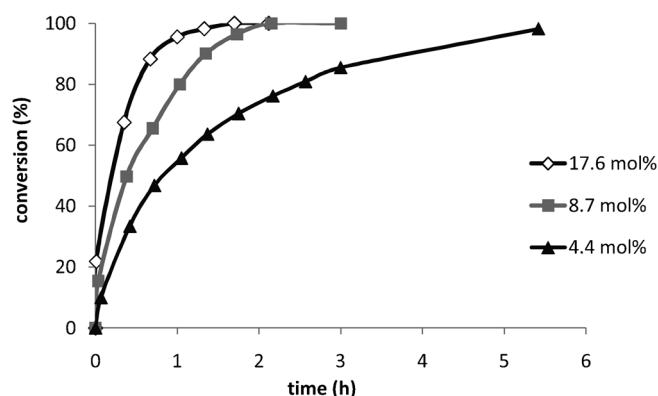


Figure 10. Jatropha seed oil transesterification with 4.40, 8.70 and 17.60 mol% catalyst **5**. The molar ratio methanol to triglyceride was kept at 6/1 and the temperature at 80 °C.

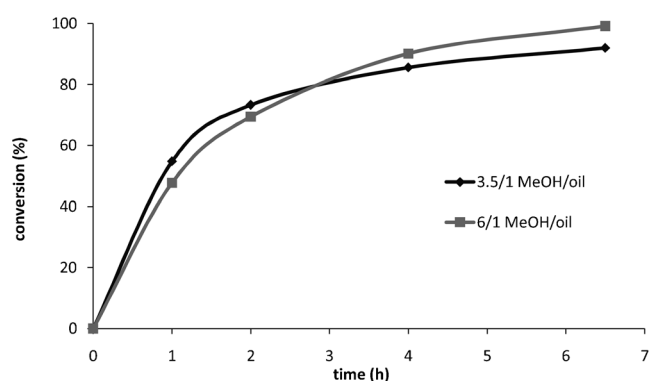


Figure 9. Sunflower seed oil transesterification with catalyst **4** and molar ratios methanol to triglyceride of 3.5/1 and 6/1. The temperature was kept at 60 °C.

apolar phase. Nevertheless, as the reaction proceeds and most of the methanol is consumed, the reaction rate is reduced (Figure 9).

Influence of the Catalyst Amount

The amount of catalyst was also tested as depicted in Figure 10. Within the range of concentrations studied, the reaction rate increased linearly with the catalyst concentration. This is interesting since it is well known that in hydrolysis reactions with Twitchell reagents, there is a saturation effect when the catalyst is around 1% w/w.^[16]

The molar ratio methanol to triglyceride was kept at 6/1 and the temperature at 80 °C.

Influence of the Temperature

Higher temperatures also provide better reaction rates, yielding short reaction times. Working at 80 °C

with catalyst **5**, the reaction is practically finished after only 90 min (Figure 10).

It is also possible to work at room temperature with longer reaction times. Catalyst **5**, due to its low solubility led to non-practical procedures, however, large conversions after 3 days were obtained with catalyst **3** (78%) and **4** (97%).

Jatropha Oil as Biofuel Source

To illustrate that indeed these catalysts are promising in the preparation of biodiesel from low cost raw materials, jatropha oil was used. As can be seen in Figure 11, the results found in this case are quite similar to those reported for the sunflower seed oil previously studied.

Catalyst Recovery

In biodiesel production technologies the recovery of the catalyst can be an important factor due to the fol-

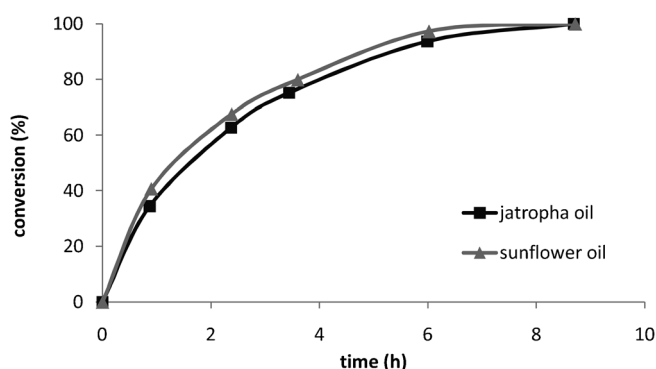


Figure 11. Jatropha oil and sunflower seed oil transesterification catalysed by compound **5**. The molar ratio methanol to triglyceride was kept at 6/1 and the temperature at 60 °C.

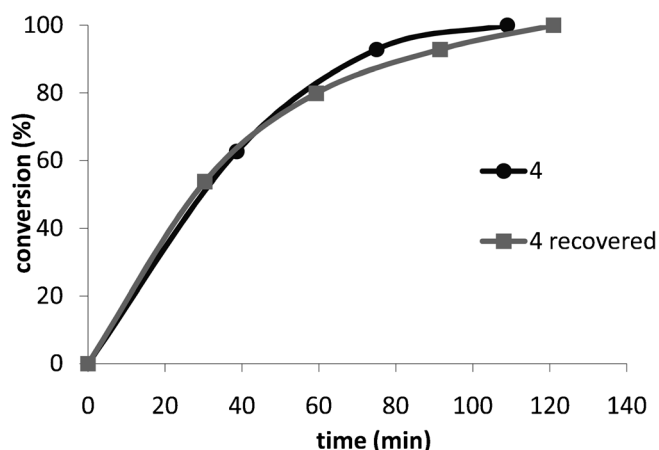


Figure 12. Sunflower seed oil transesterification catalysed by 18.5 wt% of compound **4** and catalyst **4** recovered. The molar ratio methanol to triglyceride was kept at 6/1 and the temperature at 80 °C.

lowing reasons. (i) Sulphonic acid catalyst is corrosive and may damage the fuel deposit or the engine. (ii) A maximum amount of sulphur has been established in the diesel contents.^[20] (iii) The content of acid in biodiesel (acid number) has been stipulated to a maximum value of 0.50 mg KOH per g biodiesel.^[21] (iv) The cost of the catalyst makes its recovery important for a cost-efficient procedure.

Separation of catalyst **4** from the biodiesel was achieved by adsorption of the catalyst on a silica gel column. Once the reaction was finished, the glycerine was separated from the crude biodiesel through decantation. Methanol was distilled from the biodiesel phase and the remaining liquid was passed through a short silica gel column. The highly polar sulphonic acid protonated the basic stationary phase groups, and stayed in the adsorbent, while the fatty acid methyl esters were eluted from the column. Ten grams of silica per gram of catalyst were enough to provide a clean catalyst separation. FAMES can be eluted with petroleum ether from the column, but in this case, the solvent has to be distilled before biodiesel commercialization. Alternatively, since biodiesel is sold as a blend with diesel fuel, this last compound can be used to elute the biodiesel yielding directly the desired commercial fuel. Finally, elution with methanol allowed recovery of the catalyst, which showed the same activity as the initial catalyst **4** (Figure 12).

Acid Content in the Biodiesel

Although crude biodiesel phase reacted strongly with methyl orange, after adsorption on silica gel, this reaction completely disappeared, showing no mineral or sulphonic acids in the biodiesel.

Determination of the acid content in biodiesel was performed following the procedure described in UNE-EN 14104,^[22] affording an acid number of 0.16 mg KOH/g, a value that complies with the requirements of both ASTM D 6751 and EN 14214. On the other hand, the acid number for the triglyceride source, the jatropha oil, proved to be 5.33–5.86 mg KOH/g.

Conclusions

Lipophilic sulphonic acids such as **4** and **5**, have proven to be an alternative for biodiesel manufacture. Because triglyceride transesterification with methanol is a biphasic reaction which can take place in both phases, lipophilic sulphonic acids will strongly catalyse this reaction in the oil phase since their partition constant favours the triglyceride phase. This allows one to work at temperatures below the boiling point of methanol and in reasonable reaction times.

A correlation between the partition constant and the catalytic efficiency is also observed.

When sulphuric acid is used as co-catalyst, only those sulphonic acids with more favourable partition into the polar phase improve their catalytic properties; on the other hand, addition of sulphuric acid has no influence on reaction rates when more lipophilic sulphonic acids are used.

Under these reaction conditions, neither free fatty acids nor small amounts of water change significantly the reaction rates; nevertheless, large amounts of water reduce the reaction rate in the case of the less lipophilic catalysts.

Although most of the experiments have been carried out with refined sunflower seed oil, low cost raw materials as jatropha oil show under these conditions the same behaviour.

Increasing the temperature (from 60 °C to 80 °C) and the amount of the catalyst speed up the reaction rates.

Catalyst recovery can be accomplished by adsorption of the crude FAMES on silica; elution with methanol allows one to get a mixture of the catalysts, monoglycerides, diglycerides and the fatty acid methyl esters, which can be used as catalyst for the next batch.

Finally, the acid content in the obtained biodiesel is further below the limit of 0.5 mg g⁻¹ stipulated by the ASTM D 6751 and EN 14214 although the triglyceride source presents a high FFA content.

Experimental Section

Materials and Instrumentation

IR spectra were recorded with a Nicolet IR100. ^1H and ^{13}C NMR spectra were recorded at room temperature with Bruker model WP-200-SY, Varian model Mercury VS 2000, or Bruker Advance DRX spectrometers in deuterated chloroform (unless otherwise stated). J values are reported in Hertz and chemical shifts in ppm with the solvent signal as internal standard. Mass spectra were recorded on a Bruker ultraflex III spectrometer. Melting points were determined using a Leica Galen III microscope. Analytical thin layer chromatography was performed using pre-coated aluminium-backed plates and visualized by UV. For column chromatography silica gel (70–200 μm) was used.

Reagents were purchased and used without further purification unless otherwise noted. Refined sunflower seed oil was purchased from Aceites Coosur, S. A., Vilches (Jaén, Spain). Jatropha oil was gently provided by Miguel Cobo (Biotel).

General Procedure for the Transesterification Reaction

Methanol (0.67 mL, 16.68 mmol) and triglyceride (2.5 g, 2.78 mmol) were reacted in the presence of catalyst in a glass tube equipped with a screw cap with septum and magnetic stirring. The temperature of the sample was kept constant with a thermostat bath. The progress of the reaction was monitored by ^1H NMR analysis of aliquots. The initial biphasic reaction may turn homogeneous (15 min at 80 °C). Close to the end of the reaction, glycerine decantation provides a biphasic reaction mixture again (45 min at 80 °C). The conversion was measured by integration of the glycerine triglyceride signals or from the methyl ester signal of the fatty acids (see Supporting Information).

Determination of Partition Constant

A reference ^1H NMR spectrum of the catalyst **3** (20 mg, 48.7 μmol) in deuteromethanol (0.5 mL) was taken, and the signals of the catalyst were integrated against the solvent methyl protons. After extraction with the triglyceride (1.0 mL), a new ^1H NMR spectrum was run and integrated yielding the new catalyst concentration in the methanolic phase, from which the partition constant was calculated.

For catalysts **4** and **5** the procedure was similar, only changing the volume of triglyceride from 1.0 mL to 0.5 mL.

Recovery of the Catalyst

In a typical transesterification experiment [triglyceride (16.0 g) and catalyst **4** (1.0 g)], glycerine and methanol were removed by decantation and distillation, respectively. Crude biodiesel (17.0 g) was dissolved in petroleum ether or diesel fuel (32 mL). This solution was allowed to pass through a silica gel column (10.0 g) and eluted with petroleum ether or diesel fuel (32 mL) to yield FAME (14 g). Finally, methanol (32 mL) was added to the column affording a mixture of catalyst (0.9 g), FAME (1.4 g), diglycerides and monoglycerides (0.7 g), which were used in the next batch after methanol distillation.

Materials

4-(Tetratriacontan-17-yl)benzenesulphonic acid (4): A solution of 1-phenyloctadecan-1-one^[18] (26.5 g, 77 mmol) in diethyl ether (100 mL) was added dropwise to a Grignard reagent prepared from a mixture of 1-iodohexadecane (2.0 g, 5.7 mmol) and 1-chlorohexadecane (27.6 g, 106 mmol) with magnesium turnings (7.5 g) and a small crystal of iodine in ether (80 mL). After the addition, the reaction was stirred at room temperature for 12 h. Then the mixture was poured onto ice and acidified with 2M hydrochloric acid. The aqueous phase was discarded, the organic layer dried over Na_2SO_4 and the solvent evaporated to dryness. The residue was purified by column chromatography on silica gel with dichloromethane as the eluent, yielding the corresponding alcohol, 17-phenyltetratriacontan-17-ol, as a white solid; yield: 37.4 g (85%).

The above alcohol (13.7 g, 24 mmol) and a catalytic amount of *p*-toluenesulphonic acid (162 mg, 0.94 mmol) were refluxed in toluene (280 mL) until no further water appeared. The mixture was washed with aqueous NaHCO_3 and the toluene was evaporated under reduced pressure. The crude residue was purified by column chromatography with hexane as eluent to afford the dehydrated compound; yield: 11.0 g (83%).

This unsaturated compound (11.0 g, 19.9 mmol) was dissolved in ethanol (40 mL) and hydrogenated (4 bar) in the presence of Pd/C (5%) (450 mg) at room temperature. After 12 h the catalyst was filtered and the solvent was removed. Silica gel percolation with hexane furnished the expected saturated hydrocarbon, tetratriacontan-17-ylbenzene; yield: 9.40 g (85%).

Finally, fuming sulphuric acid (20% SO_3 , 6.8 g) was added to a solution of tetratriacontan-17-ylbenzene (9.40 g, 17 mmol) in dry CH_2Cl_2 (100 mL). After stirring for 5 min, ^1H NMR analysis of an aliquota revealed that the reaction had finished. Ice was then added to the reaction mixture and the layers were separated. The organic layer was dried over cellulose and the solvent removed under reduced pressure to afford the desired compound **4**, as a white solid; yield: 10.5 g (98%); mp 33–35 °C. ^1H NMR (200 MHz, CDCl_3): δ = 7.74 (d, J = 8.0 Hz, 2H), 7.16 (d, J = 8.0 Hz, 2H), 2.50 (m, 1H), 1.50 (m, 4H), 1.25 (br s, 58H), 0.88 (t, J = 6.6 Hz, 6H); ^{13}C NMR (50 MHz, CDCl_3): δ = 151.1, 138.7, 128.2, 126.3, 46.3, 36.9, 32.2, 30.0, 29.8, 29.6, 27.8, 22.9, 14.3; IR (film): ν = 3409, 2916, 2851, 1735, 1469, 1378, 1150, 1041, 1002 cm^{-1} ; HR-MS: m/z = 679.5065, calcd. for $\text{C}_{40}\text{H}_{73}\text{Na}_2\text{O}_3\text{S}$ [$\text{M}-\text{H}+\text{Na}$] + Na^+ : 679.5070.

2,4-Di(tritriacontan-17-yl)benzenesulphonic acid (5): A solution of dimethyl isophthalate (3.9 g, 20.2 mmol) in diethyl ether (30 mL) was added dropwise to a Grignard reagent prepared from a mixture of 1-iodohexadecane (2.1 g, 6 mmol) and 1-chlorohexadecane (28.4 g, 109 mmol) with magnesium turnings (8.0 g) and a small crystal of iodine in ether (80 mL). After the addition, the resulting mixture was allowed to react at room temperature for 12 h. The reaction mixture was worked up in the same way as for the preparation of catalyst **4**, yielding the corresponding diol, 17,17-(1,3-phenylene)dinitritriacontan-17-ol, yield: 19.0 g (89%). The diol (17.0 g, 16.5 mmol) was dehydrated with *p*-toluenesulphonic acid in refluxing toluene following the same procedure as described previously, affording the unsaturated hydrocarbon; yield: 16.0 g (96%). Hydrogenation of this

compound (7.0 g, 7.0 mmol) was carried out in THF (40 mL) under 4 bar of hydrogen pressure at 40 °C with Pd/C (5%) (500 mg) in 12 h. The catalyst was removed by filtration, the solvent evaporated and the residue purified by percolation through silica gel (hexane as eluent) to yield the saturated hydrocarbon, 1,3-di(tritriacontan-17-yl)benzene; yield: 6.1 g (86%). The sulphonation of this compound (6.1 g, 6 mmol) was carried out under the same conditions previously described for catalyst **4**, to afford the expected compound as a white solid; yield: 6.2 g (96%); mp 79–80 °C. ¹H NMR (200 MHz, CDCl₃): δ = 7.85 (d, *J* = 8.4 Hz, 2H), 7.14 (s, 1H), 7.00 (d, *J* = 8.4 Hz, 2H), 2.51 (m, 2H), 1.60 (m, 8H), 1.25 (br s, 112H), 0.88 (t, *J* = 6.4 Hz, 12H); ¹³C NMR (50 MHz, CDCl₃): δ = 151.8, 146.5, 135.7, 128.2, 127.7, 124.9, 50.9, 46.2, 40.6, 37.1, 36.9, 32.2, 30.4, 30.0, 29.9, 29.6, 27.8, 27.6, 22.9, 14.3; IR (film): ν = 3403, 2916, 2365, 1599, 1456, 1378, 1314, 1164, 1074, 1002, 892, 710 cm⁻¹; HR-MS: *m/z* = 1128.0108, calcd. for C₇₂H₁₃₈O₃S [M–H+Na]⁺+Na⁺: 1128.0078.

Acknowledgements

The authors thank the Spanish Dirección General de Investigación, Ciencia y Tecnología (DGI-CYT) (CTQ2010-19906/BQU) and the EU (European Re-integration Grant PERG04-GA-2008-239244) for their support in this work. The Spanish Ministerio de Educación y Ciencia (MEC) is acknowledged for the fellowship (A. L. F. A.). The authors are also grateful to Miguel Cobo for jatropha oil supply and for his fruitful advice. Thanks to Repsol, Biotel, Bio-Oils, Biocarburantes de Castilla SA and Andalusí Corporation for supporting this project and Diego García-Gómez for providing the pH indicators.

References

- [1] a) European Parliament and the Council. Directive 2003/30/EC of the European Parliament and of the Council of 8 May 2003 on the promotion of the use of biofuels or other renewable fuels for transport. *Official Journal of the European Union* 17.5.2003; b) M. F. Demirbas, M. Balat, H. Balat, *Energy Convers. Manage.* **2011**, 52, 1815; c) L. Lin, Z. Cunshan, S. Vitayapadung, S. Xiangqian, D. Mingdong, *Appl. Energy* **2011**, 88, 1020; d) J. Janaun, N. Ellis, *Renewable Sustainable Energy Rev.* **2010**, 14, 1312.
- [2] a) F. Ma, M. A. Hanna, *Bioresour. Technol.* **1999**, 70, 1; b) D. Y. C. Leung, X. Wu, M. K. H. Leung, *Applied Energy*, **2010**, 87, 1083.
- [3] a) M. G. Kulkarni, R. Gopinath, L. C. Meher, A. K. Dalai, *Green Chem.* **2006**, 8, 1056; b) J. M. Marchetti, V. U. Miguel, A. F. Errazu, *Renewable Sustainable Energy Rev.* **2007**, 11, 1300; c) D. Ganesan, A. Rajendran, V. Thangavelu, *Rev. Environ. Sci. Biotechnol.* **2009**, 8, 367; d) M. Di Serio, M. Cozzolino, M. Giordano, R. Tesser, P. Patrono, E. Santacesaria, *Ind. Eng. Chem. Res.* **2007**, 46, 6379; e) M. K. Lam, K. T. Lee, A. R. Mohamed, *Biotechnol. Adv.* **2010**, 28, 500; f) E. Minami, S. Saka, *Fuel* **2006**, 85, 2479; g) M. Cerro-Alarcón, A. Corma, S. Iborra, C. Martínez, M. J. Sabater, *Appl. Catal. A: Gen.* **2010**, 382, 36; h) D. Fang, J. Yang, C. Jiao, *ACS Catal.* **2011**, 1, 42; i) R. Jothiramingalingam, M. K. Wang, *Ind. Eng. Chem. Res.* **2009**, 48, 6162; j) C.-W. Wang, J.-F. Zhou, W. Chen, W.-G. Wang, Y.-X. Wu, J.-F. Zhang, R.-A. Chi, W.-Y. Ying, *Energy Fuels* **2008**, 22, 3479; k) M. Gamba, A. A. M. Lapis, J. Dupont, *Adv. Synth. Catal.* **2008**, 350, 160; l) F. Chai, F. Cao, F. Zhai, Y. Chen, X. Wang, Z. Sua, *Adv. Synth. Catal.* **2007**, 349, 1057; m) B. A. D. Neto, M. B. Alves, A. A. M. Lapis, F. M. Nachtigall, M. N. Eberlin, J. Dupont, P. A. Z. Suarez, *J. Catal.* **2007**, 249, 154; n) A. A. M. Lapis, L. F. de Oliveira, B. A. D. Neto, J. Dupont, *ChemSusChem* **2008**, 1, 759; o) J. Dupont, P. A. Z. Suarez, M. R. Meneghetti, S. M. P. Meneghetti, *Energy Environ. Sci.* **2009**, 2, 1258.
- [4] L. Bournay, D. Casanave, B. Delfort, G. Hillion, J. A. Chodorge, *Catal. Today* **2005**, 106, 190.
- [5] G. Vicente, M. Martínez, J. Aracil, *Bioresour. Technol.* **2004**, 92, 297.
- [6] a) E. Lotero, Y. Liu, D. E. Lopez, K. Suwannakarn, D. A. Bruce, J. G. Goodwin Jr, *Ind. Eng. Chem. Res.* **2005**, 44, 5353; b) U. Boesel, U. Becher, A. Ingendoh, *PCT Int. Appl.* WO 2011018228 A1 20110217, **2011**; c) U. Boeger, U. Becher, A. Ingendoh, *Ger. Offen.* DE 102009037579 A1 20110217, **2011**; d) M. Zhu, B. He, W. Shi, Y. Feng, J. Ding, J. Li, F. Zeng, *Fuel* **2010**, 89, 2299; e) M. Hara, *Top. Catal.* **2010**, 53, 805; f) J. Dhainaut, J.-P. Dacquin, A. F. Lee, K. Wilson, *Green Chem.* **2010**, 12, 296; g) A. A. Kiss, A. C. Dimian, G. Rothenberg, *Adv. Synth. Catal.* **2006**, 348, 75; h) W.-Y. Lou, M.-H. Zong, Z.-Q. Duan, *Bioresour. Technol.* **2008**, 99, 8752; i) G. Chen, B. Fang, *Bioresour. Technol.* **2011**, 102, 2635; j) J. A. Melero, L. F. Bautista, G. Morales, J. Iglesias, D. Briones, *Energy Fuels* **2009**, 23, 539; k) J. A. Melero, L. F. Bautista, G. Morales, J. Iglesias, R. Sánchez-Vázquez, *Chem. Eng. J.* **2010**, 161, 323; l) Y.-S. Lien, L.-S. Hsieh, J. C. S. Wu, *Ind. Eng. Chem. Res.* **2010**, 49, 2118.
- [7] a) G. B. Bradshaw, *Soap* **1942**, 18, 23, 69; b) G. B. Bradshaw, W. C. Meuly, U.S. Patent 2,271,619, **1942**; c) G. B. Bradshaw, W. C. Meuly, U.S. Patent 2,360,844, **1944**; d) C. J. Arrowsmith, J. Ross, U.S. Patent 2,383,580, **1945**; e) H. D. Allen, W. A. Kline, U.S. Patent 2,383,579, **1945**; f) J. H. Percy, U.S. Patent 2,383,614, **1945**; g) G. I. Keim, U.S. Patent 2,383,601, **1945**; h) W. R. Trent, U.S. Patent 2,383,632, **1945**.
- [8] K. Weissmehl, H.-J. Arpe, *Industrial Organic Chemistry*, Wiley-VCH, Weinheim, **2003**, pp 301–304.
- [9] a) T. J. Suen, T. P. Chien, *Ind. Eng. Chem.* **1941**, 33, 1043; b) L. Lascaray, *Ind. Eng. Chem.* **1949**, 41, 786.
- [10] C. K. Ingold, *J. Chem. Soc.* **1930**, 1032.
- [11] a) E. Twitchell, *J. Am. Chem. Soc.* **1900**, 22, 22; b) E. Twitchell, *J. Am. Chem. Soc.* **1906**, 28, 196; c) E. Twitchell, *J. Am. Chem. Soc.* **1907**, 29, 556.
- [12] S. Zheng, M. Kates, M. A. Dubé, D. D. McLean, *Biomass Bioenergy* **2006**, 30, 267.
- [13] a) N. Susperregui, D. Delcroix, B. Martin-Vaca, D. Bourissou, L. Maron, *J. Org. Chem.* **2010**, 75, 6581; b) L. Simón, J. M. Goodman, *J. Org. Chem.* **2007**, 72, 9656; c) A. Chuma, H. W. Horn, W. C. Swope, R. C. Pratt, L. Zhang, B. G. G. Lohmeijer, C. G. Wade, R. M.

- Waymouth, J. L. Hedrick, J. E. Rice, *J. Am. Chem. Soc.* **2008**, *130*, 6749.
- [14] N. O. V. Sonntag, *J. Am. Oil Chem. Soc.* **1979**, *56*, 729 A.
- [15] K. Fukuzumi, S. J. Ozaki, *Chem. Soc. Jpn. Ind. Chem. Sect.* **1951**, *54*, 727.
- [16] L. Lascaray, *J. Am. Oil Chem. Soc.* **1952**, *29*, 362.
- [17] H. Adkins, W. H. Hartung, *Org. Syn. Coll. Vol. 1*, p. 15, **1941**; H. Adkins, W. H. Hartung, *Org. Syn. Coll. Vol. 6*, p 1, **1926**.
- [18] C. Hu, J. Wang, J. Zhou, H. Chen, X. Shi, H. Yang, X. Xu, Y. Wang, J. Zhang, W. Xiang, *Faming Zhuanli Shenqing Gongkai Shuomingshu* CN 101716475 A20100602, **2010**.
- [19] a) K. S. Markley in; *Fatty acids*, 1st edn., Interscience, New York, **1960**; b) M. Canakci, J. V. Gerpan, *Trans. Am. Soc. Agric. Eng.* **2001**, *44*, 1429.
- [20] EN 590:2009.
- [21] ASTM D 6751 and EN 14214.
- [22] UNE-EN 14104.
-

Acta Crystallographica Section E

Structure Reports

Online

ISSN 1600-5368

4,5-Dibromo-2,7-di-*tert*-butyl-9,9-dimethyl-9*H*-thioxantheneOmayra H. Rubio,^a Angel L. Fuentes de Arriba,^a Francisca Sanz,^b Francisco M. Muniz^c and Joaquín R. Morán^{a*}

^aDepartamento de Química Orgánica, Universidad de Salamanca, Plaza de los Caídos, 37008 Salamanca, Spain, ^bServicio Difracción de Rayos X, Universidad de Salamanca, Plaza de los Caídos, 37008 Salamanca, Spain, and ^cInstituto de Cerámica y Vidrio, CSIC, Kelsen 5, 28049 Madrid, Spain

Correspondence e-mail: romoran@usal.es

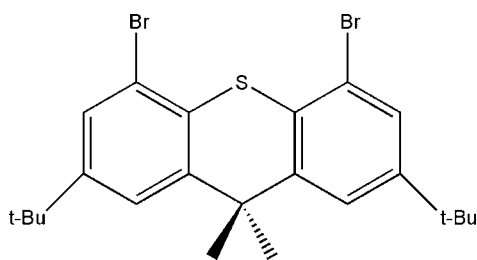
Received 3 April 2012; accepted 7 May 2012

Key indicators: single-crystal X-ray study; $T = 298$ K; mean $\sigma(\text{C}-\text{C}) = 0.007$ Å; R factor = 0.040; wR factor = 0.114; data-to-parameter ratio = 13.5.

In the title compound, $\text{C}_{23}\text{H}_{28}\text{Br}_2\text{S}$, the thioxanthene unit is twisted, showing a dihedral angle of $29.3(5)^\circ$ between the benzene rings. When projected along [001], the packing shows two types of channels. The crystal studied was a racemic twin.

Related literature

For the preparation, see: Emslie *et al.* (2006). For the use of the title compound as a starting material in the preparation of rigid ligands for different transition metals, see: Emslie *et al.* (2008).



Experimental

Crystal data

 $\text{C}_{23}\text{H}_{28}\text{Br}_2\text{S}$ $M_r = 496.33$

Tetragonal, $I4_1cd$
 $a = 21.8234(2)$ Å
 $c = 18.8025(5)$ Å
 $V = 8954.9(3)$ Å³
 $Z = 16$

Cu $K\alpha$ radiation
 $\mu = 5.48$ mm⁻¹
 $T = 298$ K
 $0.12 \times 0.10 \times 0.08$ mm

Data collection

Bruker APEXII CCD area-detector diffractometer
 Absorption correction: multi-scan (SADABS; Bruker, 2006)
 $T_{\min} = 0.544$, $T_{\max} = 0.645$

26972 measured reflections
 3272 independent reflections
 3038 reflections with $I > 2\sigma(I)$
 $R_{\text{int}} = 0.045$

Refinement

$R[F^2 > 2\sigma(F^2)] = 0.040$
 $wR(F^2) = 0.114$
 $S = 1.08$
 3272 reflections
 243 parameters
 1 restraint

H-atom parameters constrained
 $\Delta\rho_{\text{max}} = 0.34$ e Å⁻³
 $\Delta\rho_{\text{min}} = -0.83$ e Å⁻³
 Absolute structure: Flack (1983),
 2739 Friedel pairs
 Flack parameter: 0.49 (3)

Data collection: APEX2 (Bruker 2006); cell refinement: SAINT (Bruker 2006); data reduction: SAINT; program(s) used to solve structure: SHELXS97 (Sheldrick, 2008); program(s) used to refine structure: SHELXL97 (Sheldrick, 2008); molecular graphics: Mercury (Macrae *et al.*, 2008); software used to prepare material for publication: SHELXL97.

The authors thank the Spanish Dirección General de Investigación, Ciencia y Tecnología (DGI-CYT; CTQ2010-19906/BQU) and the Junta de Castilla y León (SA223A11-2) for their support of this work. The Spanish Ministerio de Educación (MEC) is acknowledged for a fellowship to ALFA.

Supplementary data and figures for this paper are available from the IUCr electronic archives (Reference: NG5262).

References

- Bruker (2006). APEX2, SAINT and SADABS. Bruker AXS Inc., Madison, Wisconsin, USA.
 Emslie, D. J. H., Blackwell, J. M., Britten, J. F. & Harrington, L. E. (2006). *Organometallics*, **25**, 2412–2414.
 Emslie, D. J. H., Harrington, L. E., Jenkins, H. A., Robertson, C. M. & Britten, J. F. (2008). *Organometallics*, **27**, 5317–5325.
 Flack, H. D. (1983). *Acta Cryst.* **A39**, 876–881.
 Macrae, C. F., Bruno, I. J., Chisholm, J. A., Edgington, P. R., McCabe, P., Pidcock, E., Rodriguez-Monge, L., Taylor, R., van de Streek, J. & Wood, P. A. (2008). *J. Appl. Cryst.* **41**, 466–470.
 Sheldrick, G. M. (2008). *Acta Cryst.* **A64**, 112–122.

supplementary materials

Acta Cryst. (2012). E68, o1814 [doi:10.1107/S1600536812020624]

4,5-Dibromo-2,7-di-*tert*-butyl-9,9-dimethyl-9*H*-thioxanthene

Omayra H. Rubio, Angel L. Fuentes de Arriba, Francisca Sanz, Francisco M. Muniz and Joaquín R. Morán

Comment

Thioxanthenes are very valuable building blocks for several purposes. Specifically, the compound described in this paper has been used as a starting material in the preparation of rigid ligands for different transition metals as Ni, Pd, Fe, *etc* (Emslie *et al.*, 2008).

The crystal contains a unique molecule as the asymmetric unit. The molecule consists of a thioxanthene framework with a *tert*-butyl group at C2 and C8, two methyl groups at C5 and a bromine atom at C10 and C13 as substituents. The thioxanthene core is twisted with a torsion angle of 29.3 (5)° (C11—S1—C12—C4). All the bond lengths and angles are within the normal ranges. The S1—C11 and S1—C12 bond lengths are 1.751 (5) Å and 1.769 (5) Å, and the C11—S1—C12 angle is 99.5 (2)°. The bromine atoms are coplanar with the thioxanthene framework; the Br1—C13—C1—C2 and Br2—C10—C9—C8 torsion angles are 179.8 (2)° and -179.8 (9)°, respectively.

The molecules in the cell unit are orientated in opposite directions forming parallel sheets along the *a* and *b* axes, which intersect perpendicularly originating two types of channels A and B, as is shown in Fig. 2 and 3.

Experimental

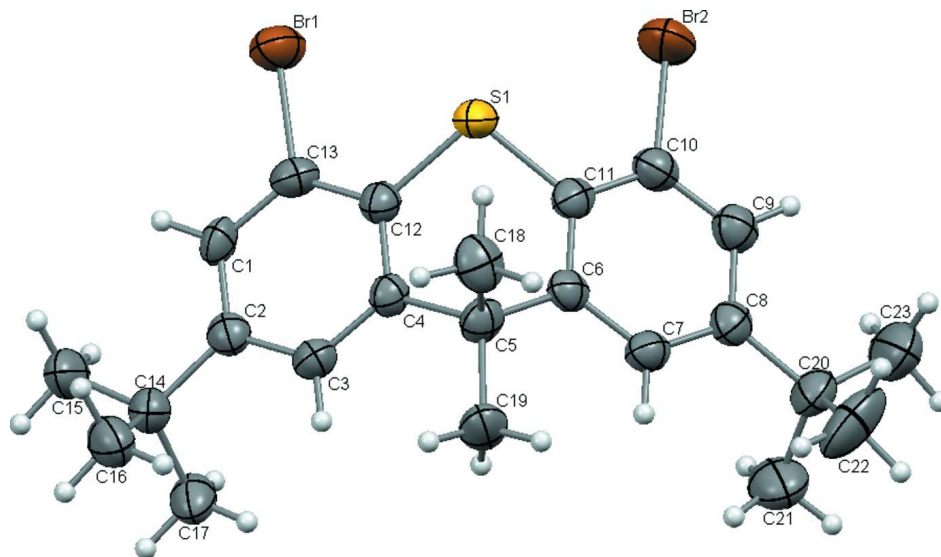
The title compound was obtained from thioxanthone according to a method described previously (Emslie *et al.*, 2006). Thioxanthone reacted with AlMe₃ to give 9,9-dimethylthioxanthene. This compound (0.75 g, 3.31 mmol) was mixed with 2-chloro-2-methylpropane (1.04 ml, 9.56 mmol) in chloroform (18 ml) at 273 K and aluminium trichloride (0.26 g, 1.95 mmol) was added in a Friedel-Crafts procedure. Reaction of this compound (0.57 g, 1.68 mmol) with bromine (0.34 ml, 6.64 mmol) in a mixture of glacial acetic acid (6.8 ml) and dichloromethane (3 ml) gave 2,7-di-*tert*-butyl-4,5-dibromo-9,9-dimethylthioxanthene. Crystals were obtained from a dichloromethane solution and their characterization was in agreement with the reported data.

Refinement

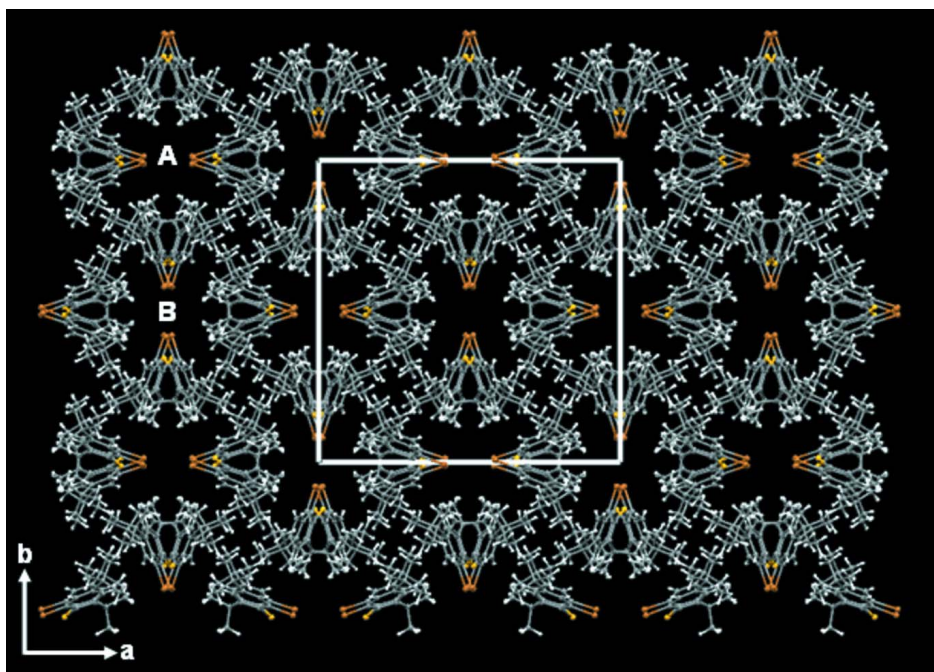
The hydrogen atoms were positioned geometrically, with C—H distances constrained to 0.93 Å (aromatic CH) and 0.96 Å (methyl CH₃) and refined in riding mode with $U_{\text{iso}}(\text{H}) = xU_{\text{eq}}(\text{C})$, where $x = 1.5$ for methyl H atoms and $x = 1.2$ for all other atoms.

Computing details

Data collection: *APEX2* (Bruker 2006); cell refinement: *SAINTE* (Bruker 2006); data reduction: *SAINTE* (Bruker 2006); program(s) used to solve structure: *SHELXS97* (Sheldrick, 2008); program(s) used to refine structure: *SHELXL97* (Sheldrick, 2008); molecular graphics: Mercury (Macrae *et al.*, 2008); software used to prepare material for publication: *SHELXL97* (Sheldrick, 2008).

**Figure 1**

Molecular structure of $C_{23}H_{28}Br_2S$. Displacement ellipsoids are drawn at the 50% probability level. Hydrogen atoms are shown as spheres of arbitrary radius.

**Figure 2**

Crystal packing of $C_{23}H_{28}Br_2S$ view along c -axis, showing two kind of channels.

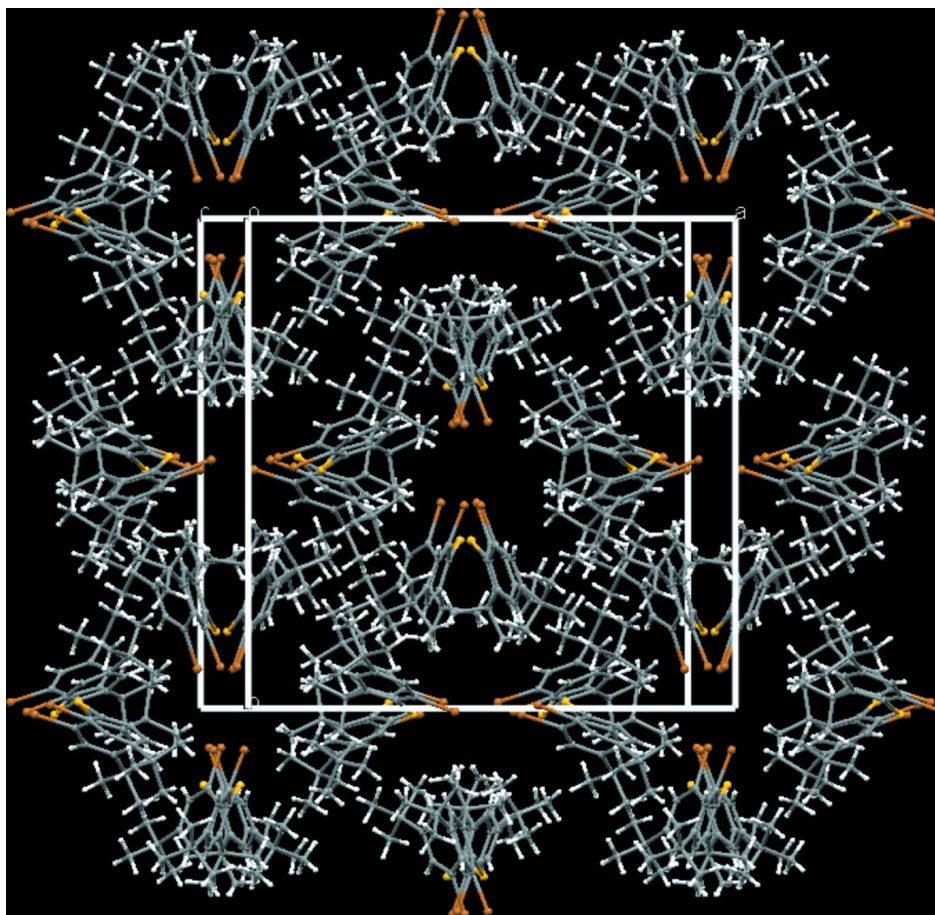


Figure 3

Crystal packing showed in Figure 2 moved along x axis.

4,5-Dibromo-2,7-di-*tert*-butyl-9,9-dimethyl-9*H*-thioxanthene

Crystal data

$C_{23}H_{28}Br_2S$

$M_r = 496.33$

Tetragonal, $I4_1cd$

Hall symbol: I 4bw -2c

$a = 21.8234$ (2) Å

$c = 18.8025$ (5) Å

$V = 8954.9$ (3) Å³

$Z = 16$

$F(000) = 4032$

$D_x = 1.473$ Mg m⁻³

Cu $K\alpha$ radiation, $\lambda = 1.54178$ Å

Cell parameters from 6340 reflections

$\theta = 4.1$ – 65.0°

$\mu = 5.48$ mm⁻¹

$T = 298$ K

Prism, brown

$0.12 \times 0.10 \times 0.08$ mm

Data collection

Bruker APEXII CCD area-detector
diffractometer

Radiation source: fine-focus sealed tube

Graphite monochromator

ϕ and ω scans

Absorption correction: multi-scan

(*SADABS*; Bruker, 2006)

$T_{\min} = 0.544$, $T_{\max} = 0.645$

26972 measured reflections

3272 independent reflections

3038 reflections with $I > 2\sigma(I)$

$R_{\text{int}} = 0.045$

$\theta_{\max} = 67.1^\circ$, $\theta_{\min} = 4.1^\circ$

$h = -24 \rightarrow 24$

$k = -25 \rightarrow 24$

$l = -21 \rightarrow 19$

Refinement

Refinement on F^2

Least-squares matrix: full

$R[F^2 > 2\sigma(F^2)] = 0.040$

$wR(F^2) = 0.114$

$S = 1.08$

3272 reflections

243 parameters

1 restraint

Primary atom site location: structure-invariant
direct methods

Secondary atom site location: difference Fourier
map

Hydrogen site location: inferred from
neighbouring sites

H-atom parameters constrained

$w = 1/[\sigma^2(F_o^2) + (0.069P)^2 + 8.551P]$

where $P = (F_o^2 + 2F_c^2)/3$

$(\Delta/\sigma)_{\max} < 0.001$

$\Delta\rho_{\max} = 0.34 \text{ e } \text{\AA}^{-3}$

$\Delta\rho_{\min} = -0.83 \text{ e } \text{\AA}^{-3}$

Absolute structure: Flack (1983), 2739 Friedel
pairs

Flack parameter: 0.49 (3)

Special details

Geometry. All e.s.d.'s (except the e.s.d. in the dihedral angle between two l.s. planes) are estimated using the full covariance matrix. The cell e.s.d.'s are taken into account individually in the estimation of e.s.d.'s in distances, angles and torsion angles; correlations between e.s.d.'s in cell parameters are only used when they are defined by crystal symmetry. An approximate (isotropic) treatment of cell e.s.d.'s is used for estimating e.s.d.'s involving l.s. planes.

Refinement. Refinement of F^2 against ALL reflections. The weighted R -factor wR and goodness of fit S are based on F^2 , conventional R -factors R are based on F , with F set to zero for negative F^2 . The threshold expression of $F^2 > \sigma(F^2)$ is used only for calculating R -factors(gt) *etc.* and is not relevant to the choice of reflections for refinement. R -factors based on F^2 are statistically about twice as large as those based on F , and R -factors based on ALL data will be even larger.

Fractional atomic coordinates and isotropic or equivalent isotropic displacement parameters (\AA^2)

	x	y	z	$U_{\text{iso}}^*/U_{\text{eq}}$
Br1	0.00721 (3)	0.08500 (2)	0.15791 (4)	0.0637 (2)
Br2	-0.01257 (4)	0.08030 (3)	0.44522 (4)	0.0759 (3)
S1	0.01309 (5)	0.15662 (5)	0.30465 (9)	0.0469 (3)
C1	-0.0512 (2)	0.1937 (2)	0.1083 (2)	0.0399 (10)
H1	-0.0539	0.1723	0.0657	0.048*
C2	-0.07413 (19)	0.2520 (2)	0.1132 (3)	0.0397 (10)
C3	-0.0652 (2)	0.2836 (2)	0.1773 (3)	0.0396 (10)
H3	-0.0796	0.3235	0.1808	0.048*
C4	-0.03594 (19)	0.25826 (19)	0.2354 (3)	0.0351 (9)
C5	-0.0220 (2)	0.29427 (18)	0.3048 (3)	0.0414 (9)
C6	-0.0430 (2)	0.2563 (2)	0.3677 (2)	0.0377 (10)
C7	-0.07826 (19)	0.2811 (2)	0.4233 (3)	0.0416 (10)
H7	-0.0916	0.3214	0.4192	0.050*
C8	-0.0943 (2)	0.2484 (2)	0.4845 (3)	0.0417 (10)
C9	-0.0731 (2)	0.1878 (2)	0.4897 (3)	0.0463 (11)
H9	-0.0815	0.1645	0.5299	0.056*
C10	-0.0395 (2)	0.1630 (2)	0.4339 (3)	0.0442 (11)
C11	-0.02527 (19)	0.1948 (2)	0.3734 (3)	0.0393 (10)
C12	-0.0171 (2)	0.1968 (2)	0.2308 (3)	0.0384 (10)
C13	-0.02398 (19)	0.1666 (2)	0.1671 (3)	0.0416 (10)
C14	-0.1076 (2)	0.2842 (2)	0.0513 (3)	0.0436 (9)
C15	-0.1193 (3)	0.2409 (3)	-0.0107 (3)	0.0638 (15)
H15A	-0.1418	0.2621	-0.0471	0.096*
H15B	-0.1427	0.2064	0.0055	0.096*

H15C	-0.0809	0.2270	-0.0296	0.096*
C16	-0.0707 (3)	0.3385 (3)	0.0251 (3)	0.0598 (15)
H16A	-0.0629	0.3659	0.0640	0.090*
H16B	-0.0933	0.3596	-0.0113	0.090*
H16C	-0.0324	0.3244	0.0059	0.090*
C17	-0.1701 (2)	0.3078 (3)	0.0782 (3)	0.0581 (14)
H17A	-0.1639	0.3342	0.1184	0.087*
H17B	-0.1951	0.2736	0.0921	0.087*
H17C	-0.1902	0.3302	0.0410	0.087*
C18	0.0481 (2)	0.3047 (2)	0.3083 (3)	0.0550 (12)
H18A	0.0577	0.3303	0.3483	0.083*
H18B	0.0616	0.3243	0.2654	0.083*
H18C	0.0686	0.2660	0.3134	0.083*
C19	-0.0520 (3)	0.35770 (19)	0.3027 (4)	0.0557 (12)
H19A	-0.0956	0.3532	0.2975	0.084*
H19B	-0.0361	0.3805	0.2632	0.084*
H19C	-0.0433	0.3791	0.3461	0.084*
C20	-0.1332 (2)	0.2772 (3)	0.5422 (3)	0.0521 (13)
C21	-0.1930 (3)	0.3015 (4)	0.5106 (4)	0.080 (2)
H21A	-0.2188	0.3164	0.5482	0.119*
H21B	-0.2136	0.2691	0.4857	0.119*
H21C	-0.1841	0.3343	0.4782	0.119*
C22	-0.0982 (3)	0.3323 (4)	0.5735 (5)	0.093 (3)
H22A	-0.0622	0.3180	0.5977	0.140*
H22B	-0.1241	0.3537	0.6065	0.140*
H22C	-0.0865	0.3596	0.5358	0.140*
C23	-0.1493 (4)	0.2334 (4)	0.6019 (4)	0.091 (2)
H23A	-0.1132	0.2244	0.6291	0.136*
H23B	-0.1655	0.1962	0.5823	0.136*
H23C	-0.1795	0.2520	0.6322	0.136*

Atomic displacement parameters (\AA^2)

	U^{11}	U^{22}	U^{33}	U^{12}	U^{13}	U^{23}
Br1	0.0755 (4)	0.0508 (3)	0.0647 (5)	0.0202 (2)	-0.0148 (4)	-0.0147 (3)
Br2	0.1107 (6)	0.0513 (3)	0.0655 (5)	0.0278 (3)	-0.0034 (5)	0.0074 (3)
S1	0.0510 (6)	0.0474 (5)	0.0423 (6)	0.0192 (4)	-0.0057 (7)	-0.0050 (6)
C1	0.045 (2)	0.046 (2)	0.029 (2)	-0.0015 (18)	-0.0009 (19)	-0.0120 (19)
C2	0.035 (2)	0.045 (2)	0.039 (3)	0.0011 (16)	0.0009 (19)	0.001 (2)
C3	0.044 (2)	0.036 (2)	0.039 (3)	0.0047 (17)	0.002 (2)	-0.0038 (18)
C4	0.036 (2)	0.036 (2)	0.033 (2)	-0.0014 (16)	-0.0028 (17)	-0.0045 (19)
C5	0.049 (2)	0.0350 (19)	0.040 (2)	-0.0015 (15)	0.000 (2)	-0.008 (2)
C6	0.040 (2)	0.038 (2)	0.035 (2)	0.0025 (16)	-0.0108 (19)	-0.0035 (18)
C7	0.044 (2)	0.038 (2)	0.043 (3)	0.0067 (16)	-0.005 (2)	-0.006 (2)
C8	0.039 (2)	0.049 (2)	0.037 (3)	0.0031 (18)	-0.0048 (18)	-0.003 (2)
C9	0.052 (3)	0.044 (2)	0.043 (3)	-0.0006 (19)	-0.007 (2)	-0.002 (2)
C10	0.050 (2)	0.038 (2)	0.045 (3)	0.0033 (18)	-0.009 (2)	0.002 (2)
C11	0.035 (2)	0.043 (2)	0.039 (3)	0.0047 (17)	-0.0084 (19)	-0.008 (2)
C12	0.037 (2)	0.043 (2)	0.035 (3)	0.0047 (17)	-0.0027 (19)	-0.005 (2)
C13	0.040 (2)	0.036 (2)	0.049 (3)	0.0064 (16)	0.002 (2)	-0.005 (2)

C14	0.048 (2)	0.048 (2)	0.035 (2)	0.0067 (18)	0.000 (3)	-0.001 (2)
C15	0.082 (4)	0.067 (3)	0.042 (3)	0.023 (3)	-0.015 (3)	-0.010 (3)
C16	0.063 (3)	0.069 (4)	0.048 (3)	0.010 (3)	0.005 (3)	0.013 (3)
C17	0.043 (3)	0.088 (4)	0.043 (3)	0.016 (3)	0.001 (2)	-0.001 (3)
C18	0.055 (3)	0.059 (3)	0.051 (3)	-0.012 (2)	-0.012 (3)	-0.004 (3)
C19	0.084 (3)	0.034 (2)	0.048 (3)	0.009 (2)	-0.001 (3)	-0.006 (3)
C20	0.049 (2)	0.063 (3)	0.044 (3)	0.011 (2)	0.009 (2)	-0.006 (2)
C21	0.061 (4)	0.099 (5)	0.078 (5)	0.027 (3)	0.011 (3)	0.007 (4)
C22	0.086 (5)	0.103 (5)	0.091 (6)	-0.004 (4)	0.021 (4)	-0.059 (5)
C23	0.103 (5)	0.102 (5)	0.066 (4)	0.035 (5)	0.030 (4)	0.010 (4)

Geometric parameters (Å, °)

Br1—C13	1.915 (4)	C14—C17	1.543 (6)
Br2—C10	1.909 (4)	C15—H15A	0.9600
S1—C11	1.751 (5)	C15—H15B	0.9600
S1—C12	1.769 (5)	C15—H15C	0.9600
C1—C2	1.371 (7)	C16—H16A	0.9600
C1—C13	1.386 (7)	C16—H16B	0.9600
C1—H1	0.9300	C16—H16C	0.9600
C2—C3	1.402 (7)	C17—H17A	0.9600
C2—C14	1.544 (7)	C17—H17B	0.9600
C3—C4	1.381 (7)	C17—H17C	0.9600
C3—H3	0.9300	C18—H18A	0.9600
C4—C12	1.406 (7)	C18—H18B	0.9600
C4—C5	1.553 (7)	C18—H18C	0.9600
C5—C6	1.515 (7)	C19—H19A	0.9600
C5—C19	1.532 (6)	C19—H19B	0.9600
C5—C18	1.549 (6)	C19—H19C	0.9600
C6—C11	1.400 (7)	C20—C23	1.515 (10)
C6—C7	1.406 (7)	C20—C21	1.529 (8)
C7—C8	1.397 (7)	C20—C22	1.542 (9)
C7—H7	0.9300	C21—H21A	0.9600
C8—C9	1.405 (7)	C21—H21B	0.9600
C8—C20	1.514 (7)	C21—H21C	0.9600
C9—C10	1.389 (7)	C22—H22A	0.9600
C9—H9	0.9300	C22—H22B	0.9600
C10—C11	1.369 (7)	C22—H22C	0.9600
C12—C13	1.376 (7)	C23—H23A	0.9600
C14—C16	1.516 (8)	C23—H23B	0.9600
C14—C15	1.522 (8)	C23—H23C	0.9600
C11—S1—C12	99.5 (2)	C14—C15—H15C	109.5
C2—C1—C13	119.9 (4)	H15A—C15—H15C	109.5
C2—C1—H1	120.0	H15B—C15—H15C	109.5
C13—C1—H1	120.0	C14—C16—H16A	109.5
C1—C2—C3	117.6 (4)	C14—C16—H16B	109.5
C1—C2—C14	123.0 (4)	H16A—C16—H16B	109.5
C3—C2—C14	119.4 (4)	C14—C16—H16C	109.5
C4—C3—C2	123.3 (4)	H16A—C16—H16C	109.5

C4—C3—H3	118.4	H16B—C16—H16C	109.5
C2—C3—H3	118.4	C14—C17—H17A	109.5
C3—C4—C12	117.9 (4)	C14—C17—H17B	109.5
C3—C4—C5	123.6 (4)	H17A—C17—H17B	109.5
C12—C4—C5	118.5 (4)	C14—C17—H17C	109.5
C6—C5—C19	112.7 (4)	H17A—C17—H17C	109.5
C6—C5—C18	110.3 (4)	H17B—C17—H17C	109.5
C19—C5—C18	106.9 (4)	C5—C18—H18A	109.5
C6—C5—C4	108.6 (3)	C5—C18—H18B	109.5
C19—C5—C4	110.6 (4)	H18A—C18—H18B	109.5
C18—C5—C4	107.7 (4)	C5—C18—H18C	109.5
C11—C6—C7	117.5 (4)	H18A—C18—H18C	109.5
C11—C6—C5	120.0 (4)	H18B—C18—H18C	109.5
C7—C6—C5	122.4 (4)	C5—C19—H19A	109.5
C8—C7—C6	123.6 (4)	C5—C19—H19B	109.5
C8—C7—H7	118.2	H19A—C19—H19B	109.5
C6—C7—H7	118.2	C5—C19—H19C	109.5
C7—C8—C9	117.0 (4)	H19A—C19—H19C	109.5
C7—C8—C20	121.3 (4)	H19B—C19—H19C	109.5
C9—C8—C20	121.7 (5)	C8—C20—C23	113.6 (5)
C10—C9—C8	119.3 (5)	C8—C20—C21	110.1 (5)
C10—C9—H9	120.4	C23—C20—C21	108.0 (5)
C8—C9—H9	120.4	C8—C20—C22	108.6 (5)
C11—C10—C9	123.3 (4)	C23—C20—C22	108.9 (6)
C11—C10—Br2	120.2 (4)	C21—C20—C22	107.5 (6)
C9—C10—Br2	116.5 (4)	C20—C21—H21A	109.5
C10—C11—C6	119.2 (4)	C20—C21—H21B	109.5
C10—C11—S1	118.7 (4)	H21A—C21—H21B	109.5
C6—C11—S1	122.1 (4)	C20—C21—H21C	109.5
C13—C12—C4	118.6 (4)	H21A—C21—H21C	109.5
C13—C12—S1	119.2 (3)	H21B—C21—H21C	109.5
C4—C12—S1	122.2 (4)	C20—C22—H22A	109.5
C12—C13—C1	122.5 (4)	C20—C22—H22B	109.5
C12—C13—Br1	119.0 (3)	H22A—C22—H22B	109.5
C1—C13—Br1	118.5 (4)	C20—C22—H22C	109.5
C16—C14—C15	109.0 (5)	H22A—C22—H22C	109.5
C16—C14—C17	108.4 (4)	H22B—C22—H22C	109.5
C15—C14—C17	108.1 (4)	C20—C23—H23A	109.5
C16—C14—C2	110.4 (4)	C20—C23—H23B	109.5
C15—C14—C2	112.0 (4)	H23A—C23—H23B	109.5
C17—C14—C2	108.8 (4)	C20—C23—H23C	109.5
C14—C15—H15A	109.5	H23A—C23—H23C	109.5
C14—C15—H15B	109.5	H23B—C23—H23C	109.5
H15A—C15—H15B	109.5		

Cite this: DOI: 10.1039/c0xx00000x

www.rsc.org/xxxxxx

Chiral recognition with a benzofuran receptor which mimics an oxyanion hole

Ángel L. Fuentes de Arriba,^a Ángel Gómez Herrero,^a Luis Simón Rubio,^{*a} Francisca Sanz^b and Joaquín R. Morán^{*a}

5 Received (in XXX, XXX) Xth XXXXXXXXXX 20XX, Accepted Xth XXXXXXXXXX 20XX

DOI: 10.1039/b000000x

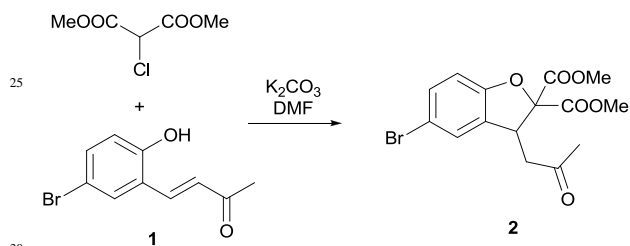
A new chiral benzofuran receptor has been synthesized and its properties in the association of amino acid derivatives have been studied. Several X-ray structures have been obtained and corroborate the presence of an oxyanion-hole motif in these structures.

10 Introduction

The oxyanion-hole is a common feature in many enzymes. In the active site, two NHs from the backbone establish strong linear H-bonds with a carbonyl oxygen.¹ In our group we have prepared molecular receptors that mimic oxyanion holes: chromenone,
15 xanthene and acridine derivatives have shown good results.² The previous scaffolds are however, planar heterocycles which do not help in chiral recognition.

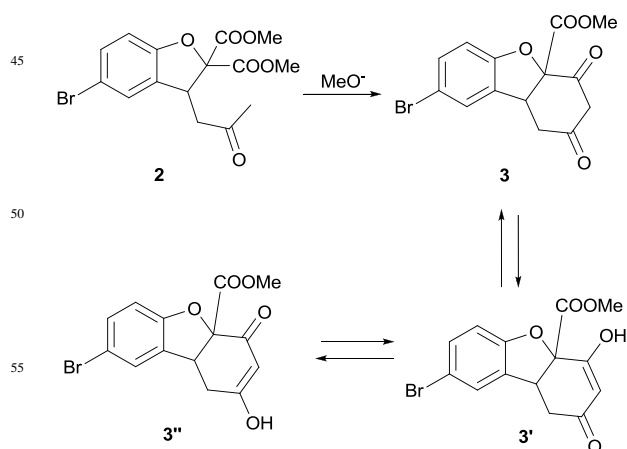
Results and discussion

Based on the easy and attractive preparation of benzofuran **2**
20 shown in figure 1,³ we have tried to transform this compound into a chiral receptor for carbonyl groups, which mimics an oxyanion hole.



Scheme 1. Benzofuran skeleton preparation from chalcone **1**.

Treatment of compound **2** with sodium methoxyde yields the expected intramolecular Claisen reaction (Scheme 2).



Scheme 2: Cyclization of compound **2**.

60 Compound **3** shows a complex NMR spectrum because it is a tautomeric mixture of two possible enols and the diketone, nevertheless it presents an attractive asymmetric skeleton, but still lacks the oxyanion-hole structure. Modelling studies show that direct amination of the aromatic ring provide a cleft which is
65 too wide for an oxyanion-hole mimic (Figure 1). Distances between the amine group and a hypothetical amide on the carboxyl group is around 5.1 Å, by far larger than the 4.4 Å of the natural oxyanion-holes.⁴

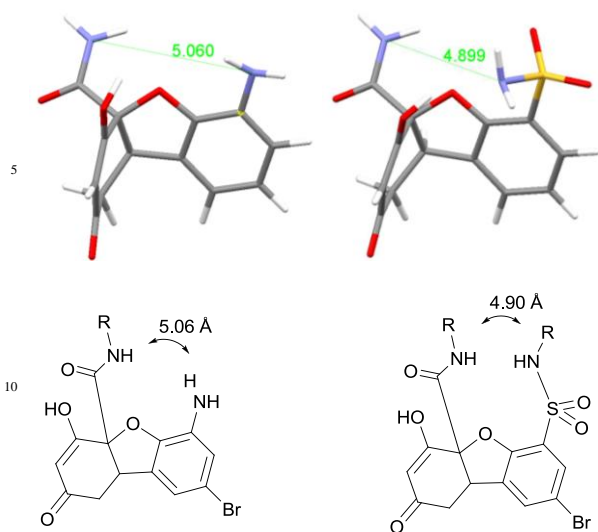
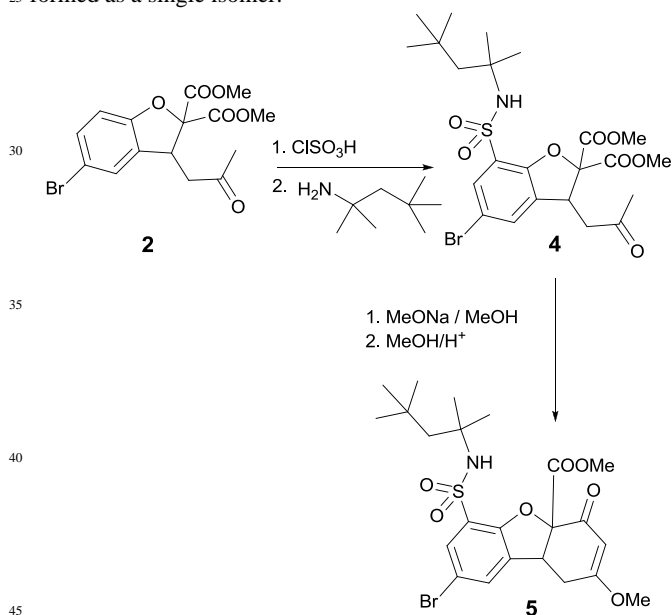


Figure 1. Distance between the H-bond donors in a possible oxyanion-hole mimic.

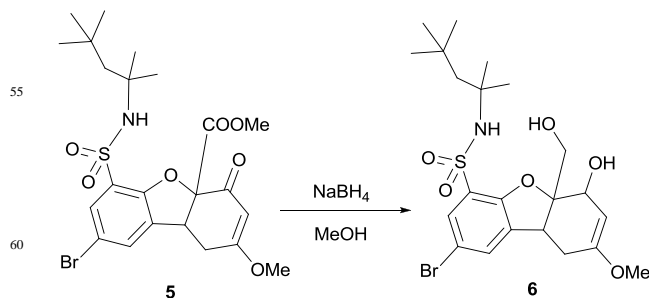
To reduce this distance, functionalization with a sulphonamide seems to be a reasonable strategy, since in this new molecule the cleft is reduced to 4.9 Å. (Figure 1).

Since modelling studies suggests the sulphonamide as a suitable group for an oxyanion-hole mimic, the synthesis of a first receptor was undertaken. The preparation of this compound is shown in Scheme 3 and, since the diketone shows up as a tautomer mixture, the enoether was prepared by treatment with methanol under acidic conditions. Luckily, the enoether is formed as a single isomer.



Scheme 3. Preparation of compound 5.

Since compound 5 lacks the necessary second H-bond to mimic an oxyanion hole, reduction with sodium borohydride was carried out. Surprisingly, both carbonyl and ester group undergo reaction at a similar rate, so, the diol 6 was obtained.



Scheme 4. Receptor 6 obtained from the sodium borohydride reduction.

An X-ray diffraction study of compound 6 has been possible. The crystals of this receptor shows a dimeric structure in which the oxyanion-hole structure is formed between the sulphonamide NH and the secondary hydroxyl group, with a cleft wide of 4.6 Å. The primary hydroxyl group of another molecule plays the role of the guest, forming two linear H-bond in the oxyanion-hole of 2.7 and 2.8 Å.

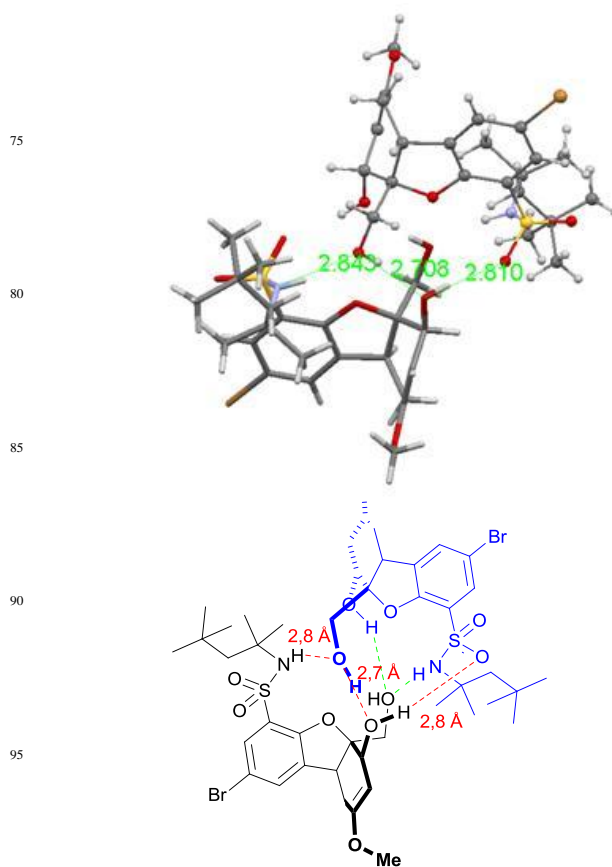
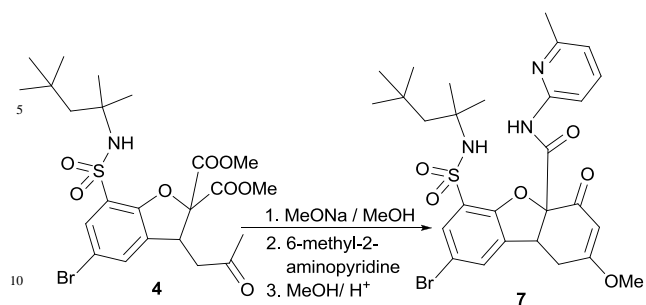


Figure 2. Solid structure of receptor 6.

To improve the association of carboxylic acid groups, a 6-methyl-2-aminopyridine unit was included in the basic structure of receptor 6, yielding receptor 7. The preparation is straightforward, since the aminopyridine reacts with the ester group under the basic conditions used for cyclization, as shown in scheme 5.



Scheme 5. Preparation of receptor 7.

It is also possible to know the detailed structure of the solid receptor 7. X-ray analysis shows again the presence of the 15 oxyanion hole (Figure 3).

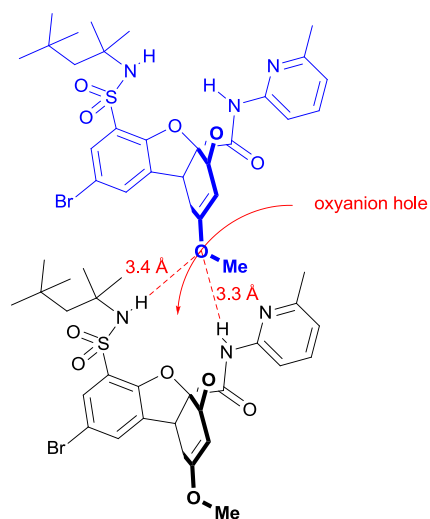
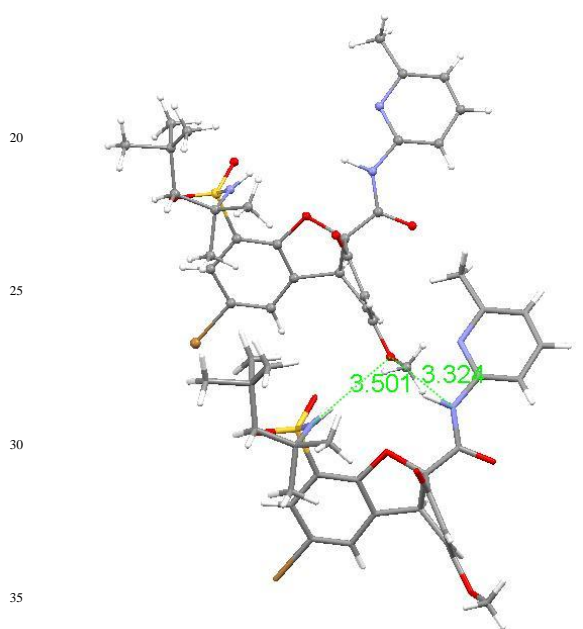


Figure 3. Solid structure of receptor 7.

In this case, the methoxy group is the oxyanion-hole guest, showing long H-bonds with the receptor donors, probably because this oxygen is a poor H-bond acceptor.

60 Receptor 7 was tested as an acid receptor with simple carboxylic acids. Association constants were measured in deuteriochloroform at 20 °C using standard procedures, and results show clearly an increase in the association constant with the guest acidity.

65 Table 1. Association constants between receptor 7 and carboxylic acids of increasing acidity.

entry	guest	p <i>K</i> _a (H ₂ O)	<i>K</i> _{ass} (M ⁻¹)
1	CH ₃ COOH	4.76	360
2	CCl ₃ COOH	0.65	500
3	CF ₃ COOH	-0.25	1700

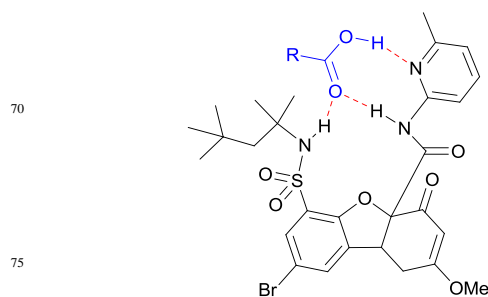


Figure 4. Geometry of receptor 7 associate with a carboxylic acid.

The cooperation of both receptor NHs in the carbonyl group association is clear from the NMR spectra since both one undergo large deshieldings, moving from 5.72 ppm to 6.49 ppm (for the sulfonamide NH; the carboxamide NH is difficult to follow because it becomes too broad).

Since the association constants have been below our 85 expectations, we tested the effect of the possible intramolecular H-bond between the carboxamide NH and the furan oxygen. The structure shown in figure 5 was allowed to compete for trichloroacetic acid with a simple aminopyridine benzoate. The benzoate forms a complex ten times stronger than the furan 90 derivative, proving that the intramolecular H-bond has a weakening effect on the carboxylic group association

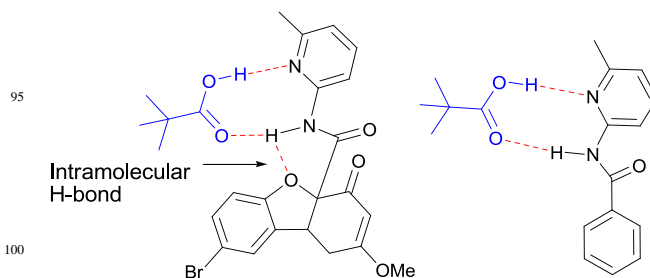


Figure 5. Associates studied to assess the intramolecular H-bond effect in the association stability. The furan associate is 10 times weaker than the benzoylaminopyridine.

Amino acid derivatives are expected to show larger association constants, since they may form a fourth H-bond, between the amino acid NH and one of the sulphuryl oxygens, as shown in figure 6.

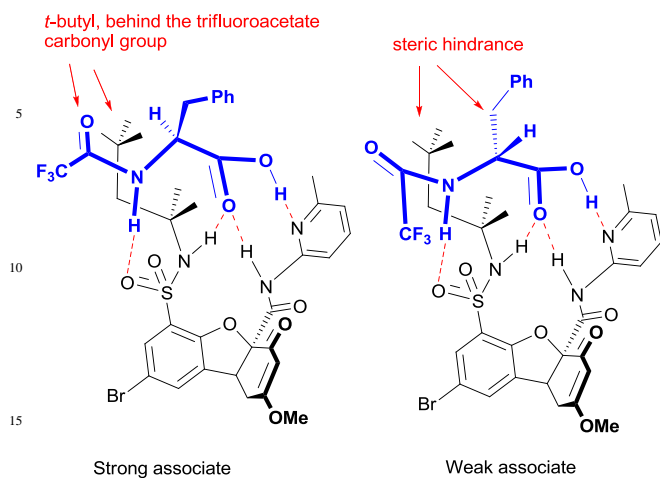


Figure 6. Strong and weak complexes of *L* and *D* trifluoroacetylphenylalanine and receptor **7**.

The effect of the additional H-bond in the amino acid derivative was tested with a competitive titration between phenylacetic acid and trifluoroacetylphenylglycine. The result shows a competitive constant of 14 in favour of the host with the additional NH, which is consistent with the four H-model proposed for the association of the amino acid.

The amino acid association model also predicts some degree of chiral discrimination, since the enantiomers of amino acids with side chains should point these groups in different space directions. In particular, one of the enantiomers should place the side chain close to the *t*-octyl group, leading to steric hindrance.

The chiral recognition of receptor **7** was tested in a competitive titration with trifluoroacetylphenylalanine. Adding the amino acid derivative to the receptor racemic mixture leads to a clear split of most of the receptor signals, proving the formation of two diastereomeric complexes

The large singlets of the *t*-butyl groups of the enantiomeric receptors offer an easy way to follow the competitive titration. From the movement of these signals it is possible to deduce a 2.2 ratio between the stability constants of the receptor enantiomers.

The relatively large shielding effect observed for the *t*-butyl group in the strong complex can be explained with the geometry shown in figure 6, since this group lies in the anisotropic shielding cone of the trifluoroacetate carbonyl group. The weak complex lacks this shielding effect, what explains the big split observed in the *t*-butyl group of both strong and weak complexes.

The geometry of these associates was confirmed with NOE effects. Steric hindrance is the main source for the chiral discrimination, since a proximity effect is found between the aromatic side chain and the *t*-butyl group in the weak complex, while the strong complex shows the correlation of the *t*-butyl group with the small amino acid alpha proton (see supporting information).

Other amino acid derivatives show similar results, from the corresponding competitive titrations it was possible to measure the values shown in figure 7.

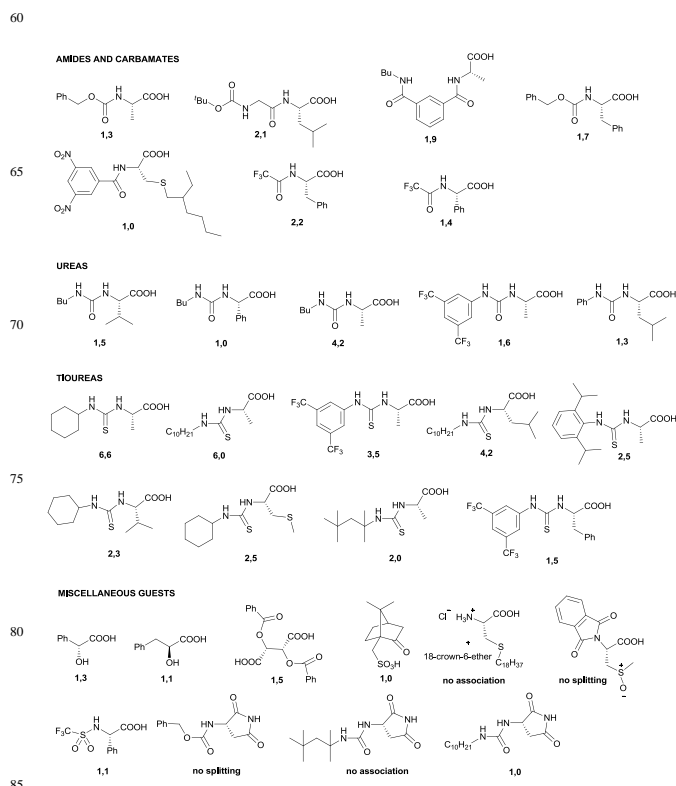


Figure 7. Relative association constants between amino acid derivatives and receptor **7**.

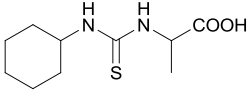
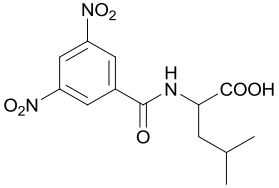
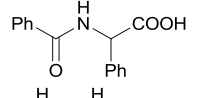
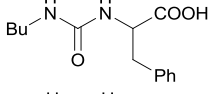
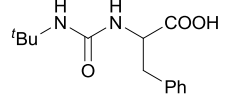
Since there is a clear discrimination between an optically pure amino acid derivative and the receptor enantiomers we tried to use this discrimination to achieve the receptor racemic mixture resolution. *L*-Phenylalanine trifluoroacetate was selected as the guest. Impregnation of TLC plates with a 2 % solution of the optically active guest in chloroform yields a stationary phase useful for the receptor enantiomer separation. Elution of the receptor mixture with methylene chloride several times yields two different spots with R_f 0.5 and R_f 0.4 for the receptor enantiomers. Scale up of this experiment impregnating 16 g SiO_2 preparative plates allows the separation of 20 mg mixture in each plate. Workup of the ethyl acetate solution with sodium carbonate allows the liberation of the free receptor **7**.

The racemic mixture resolution allows the measurement of the absolute association constant between each of receptor **7** enantiomers and the trifluoroacetate of *L*-phenylalanine. A standard titration using a constant receptor concentration in deuteriochloroform provides a large constant with a value of 6700 M^{-1} for the strong complex. The stability constant for the weak associate can be calculated in 3350 M^{-1} .

The free receptor can be used in enantioselective extractions of amino acid derivatives. To check the enantioselectivity of these extractions, a racemic guest (Table 2) added to an NMR tube with chloroform and then 1.1 eq of (-)-**7**. The spectrum shows the splitting of the guest signals, corresponding to the diastereomeric complexes guest-receptor. After treating this solution with aqueous guest as its lithium salt (10 eq), an equilibrium is reached in which most of the strong complex remains in the chloroform phase, while the guest enantiomer which forms the

more unstable complex moves to the aqueous phase. Integration of the signals corresponding to each complex should give a measure of the enantioselectivity of this process. Results are shown in Table 2.

Table 2. Enantiomeric extractions carried out with receptor **7**.

entry	guest	enantiomeric ratio
1		2,5:1
2		1:1
3		1:1
4		1,3:1
5		2:1

Conclusions

In summary, a new benzofuran-based receptor has been synthesized. It has been functionalized to create an oxyanion-hole motif in its structure with the aim to associate amino acid derivatives in a similar way as enzymes do in nature. The resolution of the receptor racemic mixture has been carried out making use of its supramolecular properties by preparative silica gel chromatography. The enantiomeric pure receptor has shown moderate enantiomeric ratio in chiral extractions of amino acid ureas and thioureas.

Experimental

General experimental procedures

Solvents were purified by standard procedures and distilled before use. Reagents and starting materials obtained from commercial suppliers were used without further purification IR spectra were recorded as neat film and frequencies are given in cm^{-1} . Melting points are given in $^{\circ}\text{C}$. NMR spectra were recorded on a 200 MHz and 400 MHz spectrometers. ^1H NMR chemical shifts were reported in ppm with tetramethylsilane (TMS) as the internal standard. Data for ^1H are reported as follows: chemical shift (in ppm), multiplicity (s = singlet, d = doublet, t = triplet, q = quartet, quint = quintet, h = hexplet, m = multiplet, br s = broad singlet), coupling constant (in Hz), number of hydrogen atoms. Splitting patterns that could not be clearly distinguished are designated as multiplets (m). Data for ^{13}C NMR are reported in ppm and hydrogen multiplicity is stated. High-resolution mass spectral analyses (HRMS) were measured using ESI ionization and a quadrupole TOF mass analyzer. Flash chromatography was

performed on 70-200 mesh silica gel.

(E)-4-(5-bromo-2-hydroxyphenyl) but-3-en-2-one (1). To a solution of 5-bromo-2-hydroxybenzaldehyde (290 g, 1.44 mol) in 1.4 L of acetone an aqueous solution of NaOH 1.2 M was added from a dropping funnel. After the addition, stirring was kept for 1 hour. Then the reaction mixture was added over ice and concentrated HCl, observing the appearance of a solid. The solid obtained was filtered and allowed to dry at room temperature, yielding 350 g of the desired product **1** with a yield of 84 %. Mp 148-149 $^{\circ}\text{C}$; ^1H NMR (400 MHz, DMSO- d_6) δ (ppm) 2.29 (3H, s), 6.88 (1H, d, $J = 8.7$ Hz), 6.90 (1H, d, $J = 16.4$ Hz), 7.37 (1H, dd, $J = 2.5, 8.7$ Hz), 7.68 (1H, d, $J = 16.4$ Hz), 7.77 (1H, d, $J = 2.5$ Hz); ^{13}C NMR (100 MHz, DMSO- d_6) δ (ppm) 27.6 (CH₃), 110.7 (C), 118.3 (CH), 123.3 (C), 127.8 (CH), 130.6 (CH), 133.8 (CH), 136.7 (CH), 156.1 (C), 198.0 (C); IR (KBr) ν 3054, 2373, 2347, 1628, 1593, 1259, 748 cm^{-1} ; HRMS Calcd for C₁₀H₁₀O₂Br 240.9859, found 240.9865.

5-bromo-3-(2-oxopropyl)-benzofuran-2, 2 (3H)-dicarboxylate (2). Chalcone **1** (160 g, 0.66 mol), dimethyl chloromalonate (200 mL, 1.16 mol), K₂CO₃ (170 g, 1.23 mol) and DMF (590 mL) were added into a round bottom flask. The reaction mixture was kept under stirring for 2 hours at room temperature, monitoring the reaction progress with ^1H NMR. After completion of the reaction, it was poured onto a mixture of water, ice, hexane, ether and concentrated HCl, stirred and a precipitate was obtained. The obtained solid was vacuum filtered, washed with water and dried. The product was purified by crystallization in MeOH at 0 $^{\circ}\text{C}$, obtaining 250 g of pure product **2** with 66 % yield. Mp 90-93 $^{\circ}\text{C}$; ^1H NMR (400 MHz, CDCl₃) δ (ppm) 2.16 (3H, s), 2.71 (1H, dd, $J = 8.9, 18.0$ Hz), 2.87 (1H, dd, $J = 4.9, 18.0$ Hz), 3.78 (3H, s), 3.80 (3H, s), 4.68 (1H, dd, $J = 4.9, 8.9$ Hz), 6.76 (1H, d, $J = 8.5$ Hz), 7.17 (1H, d, $J = 2.0$ Hz), 7.23 (1H, dd, $J = 2.0, 8.5$ Hz); ^{13}C NMR (100 MHz, CDCl₃) δ (ppm) 30.1 (CH₃), 43.0 (CH), 44.9 (CH₂), 53.2 (CH₃), 53.7 (CH₃), 91.9 (C), 111.6 (CH), 114.1 (C), 127.7 (CH), 130.5 (C), 131.8 (CH), 156.3 (C), 166.9 (C), 167.4 (C), 204.7 (C); IR (KBr) ν 3049, 1747, 1474, 1274, 1055, 743 cm^{-1} ; HRMS Calcd for C₁₅H₁₆O₆Br 371.0125, found 371.0131.

5-Bromo-7-(chlorosulfonyl)-3-(2-oxopropyl)-benzofuran-2, 2 (3H)-dicarboxylate. In a two-necked flask equipped with a magnetic stirrer, a low-temperature thermometer and an addition funnel under argon atmosphere, thionyl chloride (60 mL, 0.83 mol) was added and cooled in an ice-salt bath. Once the temperature was below 0 $^{\circ}\text{C}$, the intermediate **2** was added (30.3 g, 0.082 mol) and also chlorosulfonic acid (60 mL, 0.90 mol) from the addition funnel, leaving drip slowly and controlling the temperature did not exceed 5 $^{\circ}\text{C}$. Once the addition was completed, the mixture was maintained at a temperature of 5 $^{\circ}\text{C}$ for 62 hours, monitoring the reaction progress by ^1H NMR. Once the reaction had finished, it was diluted with CH₂Cl₂ (200 mL) and slowly poured over a mixture of CH₂Cl₂ and ice with stirring. Then the phases were separated, the organic phase was dried over anhydrous Na₂SO₄ and the solvent was removed by evaporation under vacuum to yield 37.0 g of the title product with 96% yield. Mp 124-126 $^{\circ}\text{C}$; ^1H NMR (400 MHz, CDCl₃) δ (ppm) 2.23 (3H, s), 2.78 (1H, dd, $J = 9.4, 18.3$ Hz), 3.04 (1H, dd, $J = 4.1, 18.3$ Hz), 3.84 (3H, s), 3.88 (3H, s), 4.75 (1H, dd, $J = 4.1, 9.4$ Hz),

7.54 (1H, d, $J = 1.9$ Hz), 7.85 (1H, d, $J = 1.9$ Hz); ^{13}C NMR (50 MHz, CDCl_3) δ (ppm) 30.1 (CH_3), 42.7 (CH), 44.2 (CH_2), 53.7 (CH_3), 54.1 (CH_3), 93.2 (C), 113.9 (C), 127.2 (C), 129.5 (CH), 134.5 (C), 135.2 (CH), 153.8 (C), 165.5 (C), 166.2 (C), 204.6 (C); IR (KBr) ν 2916, 2949, 2852, 1768, 1748, 1723, 1599, 1456, 1372, 1301, 1242, 1184, 1165, 1061 cm^{-1} ; HRMS Calcd for $\text{C}_{15}\text{H}_{18}\text{NO}_8\text{SClBr}$ 485.9620, found 485.9629.

Dimethyl-5-bromo-3-(2-oxopropyl)-7-(*N*-(2,4,4-trimethylpentan-2-yl)sulfamoyl)benzofuran-2,2(3*H*)dicarboxylate (4). To a solution of *t*-octylamine (6.13 g, 47.4 mmol) and triethylamine (5.5 mL, 39.7 mmol) in 27 mL of EtOAc, a solution of the previous chlorosulfonyl compound (11.8 g, 1 mmol) in 81 mL of EtOAc was added and stirred at room temperature for 5 hours. When the reaction was completed it was added over 2 M HCl (200 mL) with ice. The organic phase was separated, dried and evaporated. The solid obtained can be purified by crystallization from EtOAc yielding 5.3 g of the desired compound (38 % yield). Mp 138-140 °C; ^1H NMR (400 MHz, CDCl_3) δ (ppm) 1.01 (9H, s), 1.23 (3H, s), 1.25 (3H, s), 1.58 (1H, dd, $J = 14.9$ Hz), 1.63 (1H, d, $J = 14.9$ Hz), 2.19 (3H, s), 2.75 (1H, dd, $J = 8.7, 18.2$ Hz), 2.96 (1H, dd, $J = 4.4, 18.2$ Hz), 3.80 (3H, s), 3.83 (3H, s), 4.69 (1H, dd, $J = 4.4, 8.7$ Hz), 4.94 (NH, s), 7.33 (1H, s), 7.76 (1H, s); ^{13}C NMR (100 MHz, CDCl_3) δ (ppm) 29.1 (CH_3), 29.2 (CH_3), 30.0 (CH_3), 31.6 (CH_3), 32.9 (C), 42.8 (CH), 44.5 (CH_2), 53.4 (CH_3), 53.9 (CH_3), 54.7 (CH_2), 58.9 (C), 92.3 (C), 113.9 (C), 128.1 (C), 129.6 (CH), 131.4 (CH), 132.3 (C), 152.4 (C), 165.9 (C), 166.6 (C), 204.5 (C); IR (KBr) ν 3390, 3306, 2916, 2839, 1710, 1606, 1521, 1256, 1366, 1249, 1203, 1152 cm^{-1} ; HRMS Calcd for $\text{C}_{23}\text{H}_{36}\text{BrN}_2\text{O}_8\text{S}$ 579.1373, found 579.1365.

Methyl 8-bromo-2-methoxy-4-oxo-6-(*N*-(2,4,4-trimethylpentan-2-yl)sulfamoyl)-1,4,4a,9b-tetrahydrodibenzo[*b,d*]furan-4a-carboxylate (5). Under argon atmosphere, Na (1.0 g, 43.5 mmol) was added to 10 mL of MeOH (50 mL of MeOH were previously dried with 3.0 mL of methyl orthoformate and one drop of methanesulfonic acid). When sodium was completely dissolved it was cooled with an ice bath and compound 4 (3.8 g, 6.8 mmol) was added. The ice bath was removed and within minutes a solid begins to crystallize. After about 30 minutes, the reaction mixture was added over a solution of methyl orthoformate (4.9 mL, 44.8 mmol) and methanesulfonic acid (4.9 mL, 75.6 mmol) in dry MeOH (28 mL) at -10 °C. Then the temperature was allowed to rise to room temperature and Na_2CO_3 (8.4 g, 79.7 mmol) in water (70 mL) was added. Next, MeOH and THF were evaporated and the aqueous solution was extracted with EtOAc, yielding 3.1 g of the desired compound with a yield of 84 %. This compound was purified by silica gel column with CH_2Cl_2 -EtOAc as eluents, yielding 1.3 g with a final yield of 34%. Mp 175-177 °C; ^1H NMR (200 MHz, CDCl_3) δ (ppm) 0.99 (9H, s), 1.17 (3H, s), 1.19 (3H, s), 1.52 (1H, d, $J = 14.8$ Hz), 1.64 (1H, d, $J = 14.8$ Hz), 2.80 (1H, dd, $J = 3.2, 18.2$ Hz), 3.19 (1H, dd, $J = 7.4, 18.2$ Hz), 3.71 (3H, s), 3.80 (3H, s), 4.19 (1H, dd, $J = 3.2, 7.4$ Hz), 5.27 (1H, s), 5.52 (1H, s), 7.36 (1H, s), 7.73 (1H, s); ^{13}C NMR (50 MHz, CDCl_3) δ (ppm) 28.9 (CH_2), 29.1 (CH_3), 29.4 (CH_3), 31.6 ($\text{CH}_3 \times 3$), 31.6 (C), 42.1 (CH), 53.5 (CH_3), 54.4 (CH_2), 56.5 (CH_3), 59.1 (C), 89.6 (C), 102.3 (CH), 113.9 (C), 128.6 (C), 129.8 (CH), 129.9 (CH), 131.8 (C), 152.8 (C), 167.5 (C), 176.0 (C), 187.4

(C); IR (KBr) ν 3520, 3332, 3079, 2949, 2929, 2852, 1768, 1651, 1606, 1456, 1411, 1353, 1307, 1255, 1210, 1165, 1139, 1093, 1041, 983 cm^{-1} ; HRMS Calcd for $\text{C}_{23}\text{H}_{34}\text{BrN}_2\text{O}_7\text{S}$ 561.1265, found 561.1264.

2-Bromo-6-hidroxi-5a-(hidroximetil)-8-metoxi-*N*-(2,4,4-trimetilpentan-2-il)-5a,6,9,9a-tetrahidrodibenzo[*b,d*]furan-4-sulfonamida (6). Compound 5 (250 mg, 0.46 mmol) was dissolved in MeOH (6 mL) and NaBH_4 (34 mg, 0.90 mmol) was added. The reaction could be monitored by TLC, using CH_2Cl_2 -EtOAc as eluent. When it was finished it was diluted with EtOAc and 18 mL of 0.6 M aqueous NH_4Cl was added. Then, the organic phase was separated, dried and evaporated to give 210 mg of the compound 6 which was purified by crystallization from CH_2Cl_2 , obtaining 68 mg (29 % yield). Mp 128-130 °C; ^1H NMR (400 MHz, CD_3OD) δ (ppm) 1.05 (9H, s), 1.14 (3H, s), 1.18 (3H, s), 1.50 (1H, d, $J = 14.7$ Hz), 1.70 (1H, d, $J = 14.7$ Hz), 2.36 (1H, dd, $J = 2.5, 15.5$ Hz), 2.53 (1H, dd, $J = 6.8, 15.5$ Hz), 3.39 (3H, s), 3.78 (1H, dd, $J = 2.5, 6.8$ Hz), 3.85 (2H, s), 4.46 (1H, s), 4.58 (1H, s), 7.51 (1H, d, $J = 2.0$ Hz), 7.58 (1H, d, $J = 2.0$ Hz); ^{13}C NMR (100 MHz, CD_3OD) δ (ppm) 29.4 (CH_3), 30.8 (CH_3), 32.2 ($\text{CH}_3 \times 3$), 32.6 (C), 33.3 (CH_2), 42.7 (CH), 55.1 (CH_3), 55.6 (CH_2), 58.8 (C), 64.9 (CH_2), 68.5 (CH), 96.7 (C), 98.7 (CH), 112.4 (C), 127.9 (C), 130.1 (CH), 132.4 (CH), 138.3 (C), 156.6 (C), 156.9 (C); IR (KBr) ν 3455, 3221, 3105, 3179, 2923, 2832, 2728, 2670, 1677, 1586, 1463, 1379, 1314, 1262, 1236, 1216, 1139, 1041, 892, 814, 736; HRMS Calcd for $\text{C}_{22}\text{H}_{36}\text{BrN}_2\text{O}_6\text{S}$ 535.1472, found 535.1471.

8-Bromo-2-methoxy-*N*-(6-methylpyridin-2-yl)-4-oxo-6-(*N*-(2,4,4-trimethylpentan-2-yl)sulfamoyl)-1,4,4a,9b-tetrahydrodibenzo[*b,d*]furan-4a-carboxamide (7). In 75 mL of MeOH (previously dried using 3.0 mL of methyl orthoformate and two drops of methanesulfonic acid), a solution of Na (6.0 g, 0.26 mol) was prepared. When sodium was completely dissolved it was cooled with an ice-salt bath and compound 4 (25.0 g, 0.044 mol) was added. The temperature was raised to 10 °C. Initially compound 4 dissolved slowly in the reaction medium but then, it was observed the appearance of a precipitate. To follow the progress of the reaction an aliquot was added over water acidulated with MeSO_3H , precipitating a white solid whose ^1H NMR analysis indicated that its structure corresponded to the cyclization product. At this time, 2-amino-6-methylpyridine (15.8 g, 0.15 mol) and 20 mL of dry THF were added to the reaction medium. It was refluxed for two hours, until all the solid had dissolved. Then the reaction mixture was cooled and added over methanesulfonic acid (50 mL) in water and ice, and the obtained solid was filtered. The mother liquors were extracted with EtOAc, the layers were separated, and after evaporation of the organic solvent, the product obtained could be coupled with the above solid to afford 25.0 g of the enol (94 % yield).

Then, to a solution of methyl orthoformate (3.0 mL, 27 mmol) and acetyl chloride (350 μL , 4.92 mmol) in 18 mL of MeOH and cooled in an ice bath the enol prepared in the previous step was added (2.38 g, 3.92 mmol) and the solution was stirred. The reaction was monitored by TLC (DCM-EtOAc 1:1). The ice bath was removed and within minutes a precipitate corresponding to the hydrochloride of compound 7 showed up. The solid thus obtained was filtered, obtaining 1.0 g of compound 7 as the hydrochloride. To the filtrate solid Na_2CO_3 was added, the

carbonate was filtered and washed with more EtOAc. This solution was left to stand for 12 h and a precipitate, which corresponds to the neutral compound **7** (700 mg) appeared. Both fractions were joined, suspended in CHCl₃ and washed with aqueous saturated Na₂CO₃, yielding 1.2 g of compound **7** in a 49 % yield. Mp > 230 °C; ¹H NMR (400 MHz, CDCl₃) δ (ppm) 1.03 (9H, s), 1.23 (6H, s), 1.48 (1H, d, *J* = 14.9 Hz), 1.74 (1H, d, *J* = 14.9 Hz), 2.46 (3H, s), 2.89 (1H, d, *J* = 18.1 Hz), 3.40 (1H, dd, *J* = 7.2, 18.1 Hz), 3.76 (3H, s), 4.39 (1H, d, *J* = 7.2 Hz), 5.45 (NH, s), 5.60 (1H, s), 6.93 (1H, d, *J* = 7.6 Hz), 7.42 (1H, s), 7.57 (1H, t, *J* = 7.9 Hz), 7.84 (1H, s), 7.89 (1H, d, *J* = 8.2 Hz), 9.23 (NH, s). ¹³C NMR (100 MHz, CDCl₃) δ (ppm) 23.9 (CH₃), 29.0 (CH₂), 29.2 (CH₃), 29.5 (CH₃), 31.6 (CH₃ x 3), 31.6 (C), 41.9 (CH), 54.5 (CH₂), 56.4 (CH₃), 59.1 (C), 90.2 (C), 102.6 (CH), 111.0 (CH), 114.4 (C), 120.2 (CH), 129.0 (C), 129.7 (CH), 130.3 (CH), 132.2 (C), 138.4 (CH), 149.2 (C), 152.2 (C), 157.4 (C), 165.6 (C), 176.2 (C), 188.7 (C); IR (KBr) ν 3377, 3338, 2929, 2955, 2852, 1697, 1664, 1612, 1463, 1379, 1346, 1203, 1145, 1048, 976, 918 cm⁻¹; HRMS Calcd for C₂₈H₃₅BrN₃O₆S 620.1424, found 620.1432.

Acknowledgements

Authors would like to thank the Junta de Castilla y León (SA223A11-2) and the University of Salamanca for financial support. The Spanish “Ministerio de Educación” is acknowledged for the fellowship (A. L. F. A.). The authors are also grateful to Dr. César Raposo and Juan F. Boyero for mass spectra.

Notes and references

^a Organic Chemistry Department, Plaza de los Caídos 1-5, University of Salamanca, 37008 Salamanca, Spain. Fax: +34 923294574; Tel: +34 294481; E-mail: romoran@usal.es

^b X-Ray Diffraction Service, Plaza de los Caídos 1-5, University of Salamanca, 37008 Salamanca, Spain.

† Electronic Supplementary Information (ESI) available: [¹H and ¹³C NMR, IR and HRMS spectra of compounds **1-7** and hosts of figure 12, modeling studies of the complex of the associates between receptor **7** and *L*-trifluoroacetylphenylalanine and X-ray diffraction data of compounds **6** and **7** are included]. See DOI: 10.1039/b000000x/

‡ Footnotes should appear here. These might include comments relevant to but not central to the matter under discussion, limited experimental and spectral data, and crystallographic data.

- 1 D. M. Blow, *Acc. Chem. Res.*, 1976, **9**, 145. D. M. Blow, J. J. Birktoft and B. S. Hartley, *Nature*, 1969, **221**, 337. P. B. Sigler, D. M. Blow, B. W. Matthews and R. Henderson, *J. Mol. Biol.*, 1968, **35**, 143.
- 2 (a) L. Simón, F. M. Muñoz, S. Sáez, C. Raposo and J. R. Morán, *ARKIVOC*, 2007, 47. (b) L. Simón, F. M. Muñoz, S. Sáez, C. Raposo and J. R. Morán, *Eur. J. Org. Chem.*, 2008, 2397. (c) L. Simón, F. M. Muñoz, S. Sáez, C. Raposo, F. Sanz and J. R. Morán, *Helv. Chim. Acta*, 2005, **88**, 1682. (d) M. Crego, C. Raposo, M^a L. Mussons, A. Berrocal, M^a C. Caballero and J. R. Morán, *Heterocycles*, 1995, **40**, 139. (e) L. Simón, F. M. Muñoz, Á. Fuentes de Arriba, V. Alcázar, C. Raposo and J. R. Morán, *Org. Biomol. Chem.* 2010, **8**, 1763. (f) C. Raposo, M. Almaraz, M. Martín, M^a C. Caballero and J. R. Morán, *Tetrahedron Lett.*, 1996, **37**, 6947. (g) C. Raposo, M. Crego, A. Partearroyo, M^a L. Mussons, M^a C. Caballero and J. R. Morán, *Tetrahedron Lett.*, 1993, **34**, 1995. (h) C. Raposo, A. Luengo, M. Almaraz, M. Martín, M^a L. Mussons, M^a C. Caballero and J. R. Morán, *Tetrahedron*, 1996, **52**, 12323. (i) C. Raposo, M. Almaraz,

M. Crego, M^a L. Mussons, N. Pérez, M^a C. Caballero, J. R. Morán, *Tetrahedron Lett.*, 1994, **35**, 7065. (j) M. Crego, C. Raposo, M^a L. Mussons, M^a C. Caballero, J. R. Morán, *Tetrahedron Lett.*, 1994, **35**, 1929.

- 3 Q.-B. Li, F.-T. Zhou, Z.-G. Liu, X.-F. Li, W.-D. Zhu, J.-W. Xie, *J. Org. Chem.*, 2011, **76**, 7222.
- 4 L. Simón, J. M. Goodman, *J. Org. Chem.*, 2010, **75**, 1831.

19



OFICINA ESPAÑOLA DE
PATENTES Y MARCAS

ESPAÑA



11 Número de publicación: **2 393 352**

21 Número de solicitud: 201130945

51 Int. Cl.:

C07C 309/28 (2006.01)

B01J 31/02 (2006.01)

C11C 3/00 (2006.01)

12

PATENTE DE INVENCION

B1

22 Fecha de presentación:

07.06.2011

43 Fecha de publicación de la solicitud:

20.12.2012

Fecha de la concesión:

22.10.2013

45 Fecha de publicación de la concesión:

04.11.2013

73 Titular/es:

**UNIVERSIDAD DE SALAMANCA (100.0%)
Patio de Escuelas, 1
37008 Salamanca (Salamanca) ES**

72 Inventor/es:

**RODRÍGUEZ MORÁN, Joaquín;
FUENTES DE ARRIBA, Ángel Luis y
CUÉLLAR ANTEQUERA, Jorge**

74 Agente/Representante:

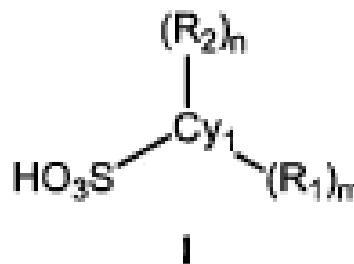
PONS ARIÑO, Ángel

54 Título: **DERIVADOS DE ÁCIDO SULFÓNICO PARA SÍNTESIS DE BIODIÉSEL.**

57 Resumen:

Derivados de ácido sulfónico para síntesis de biodiésel.

Derivados de ácido sulfónico de fórmula I, donde Cy_1 es un grupo aromático. Estos compuestos son útiles como catalizadores en reacciones orgánicas, particularmente en reacciones de síntesis de biodiésel.



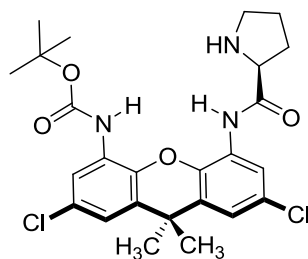
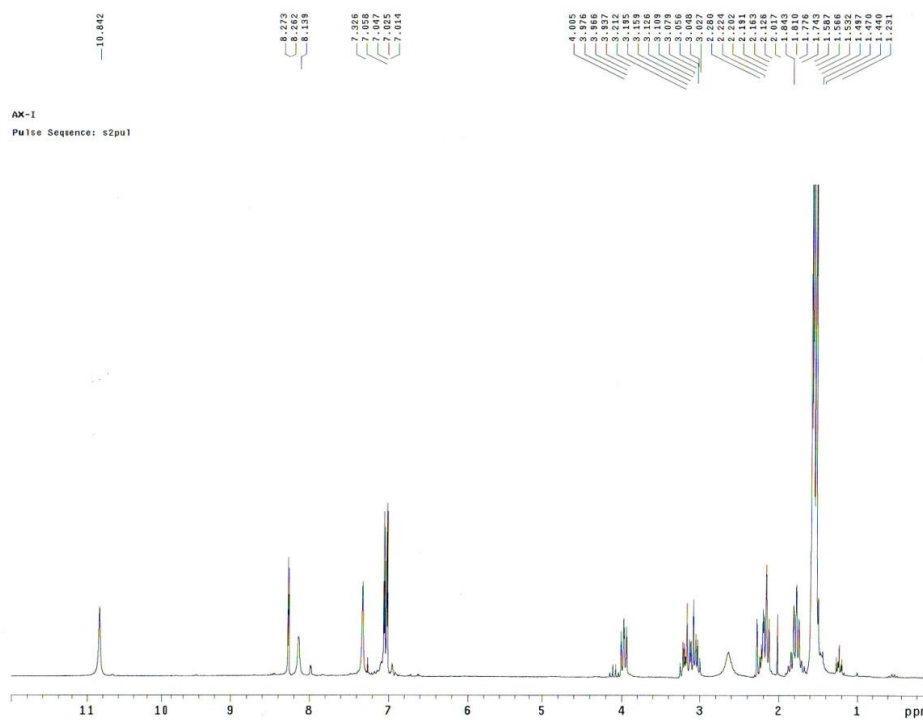
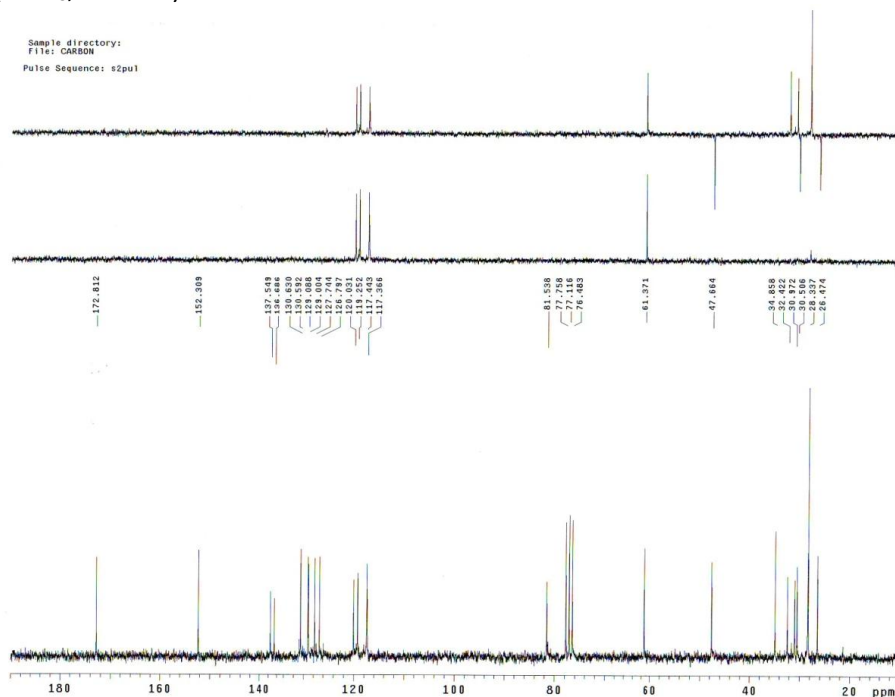
ES 2 393 352 B1



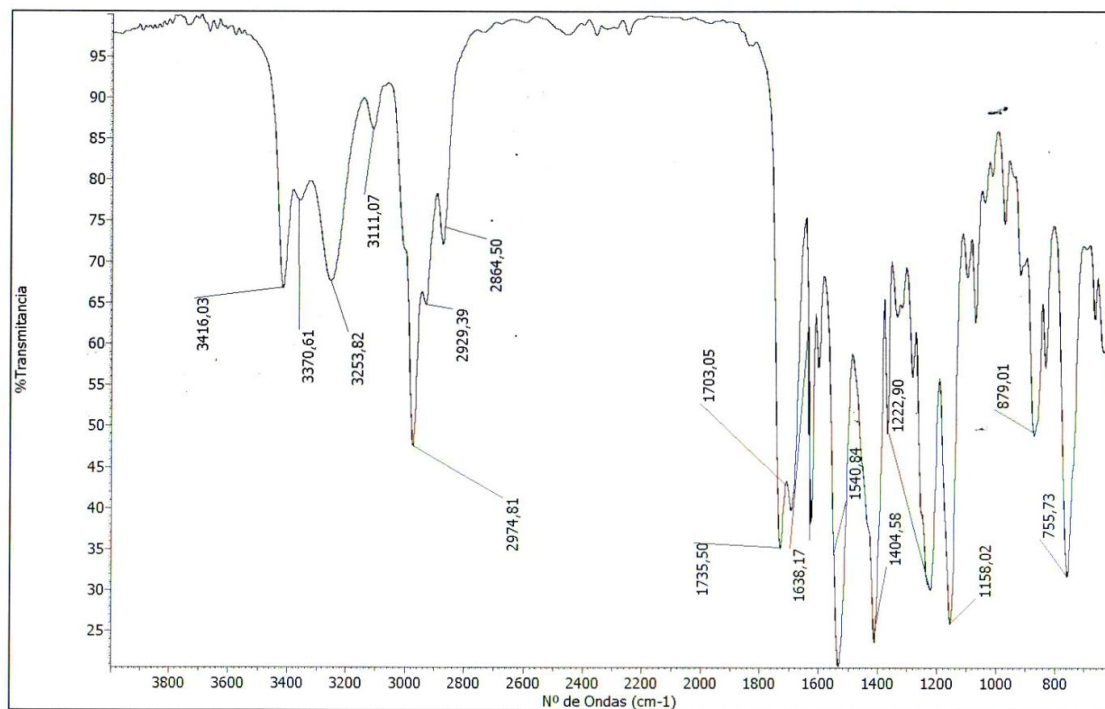
**VNiVERSiDAD
D SALAMANCA**

CAMPUS DE EXCELENCIA INTERNACIONAL

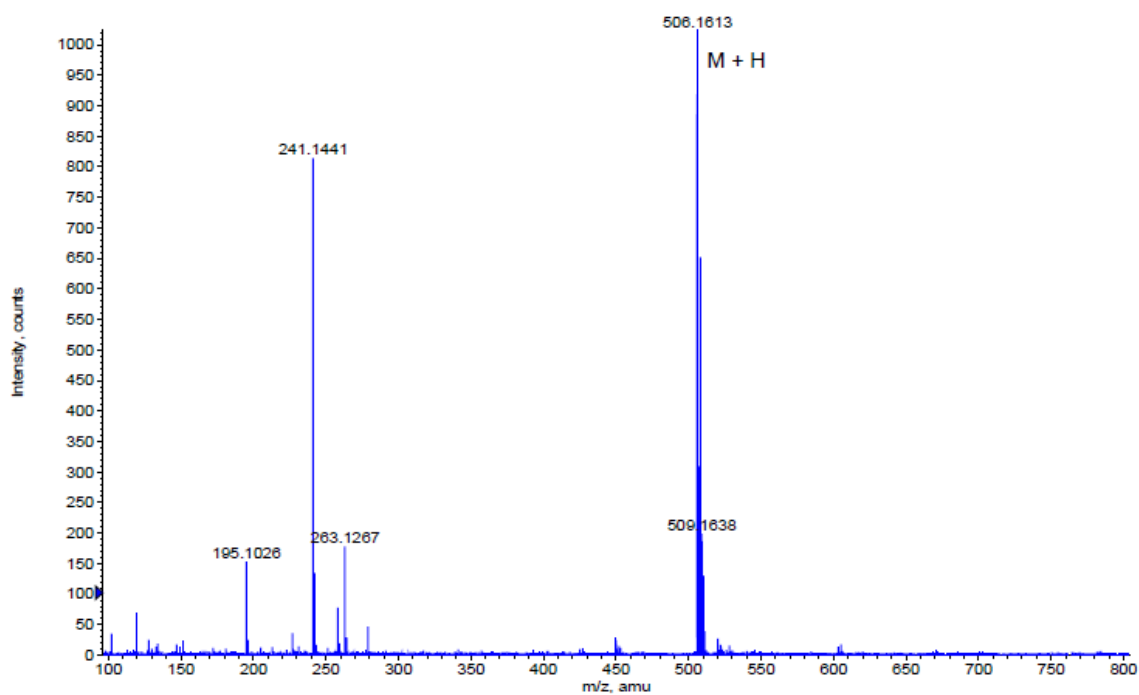
APPENDIX A.2. SPECTROSCOPY AND SPECTROMETRY

-Tert-butyl-2,7-dichloro-9,9-dimethyl-5-(pyrrolidin-2-carboxamido)-9H-xanthene-4-ylcarbamate (7)¹H NMR (CDCl₃, 200 MHz)¹³C NMR (CDCl₃, 50 MHz)

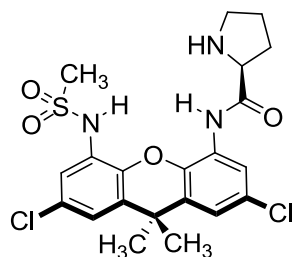
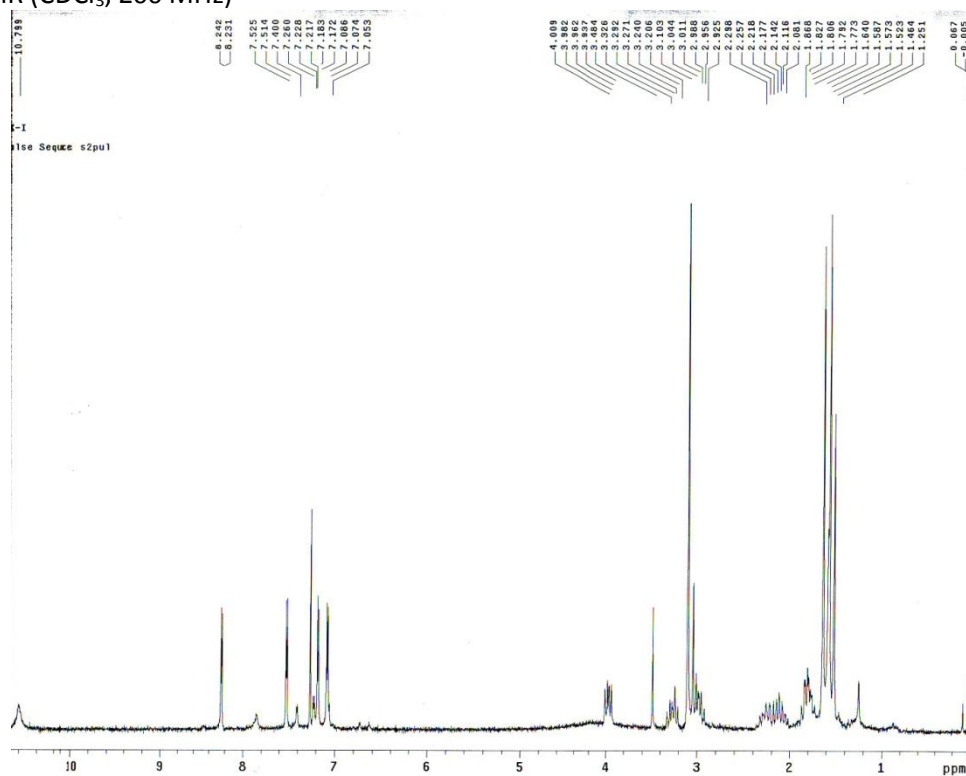
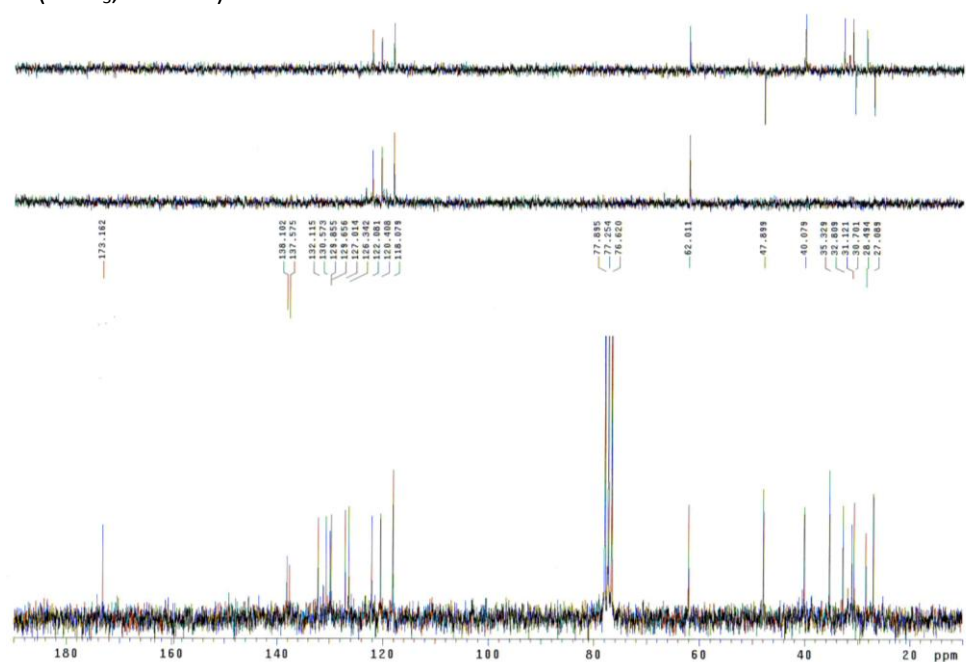
IR



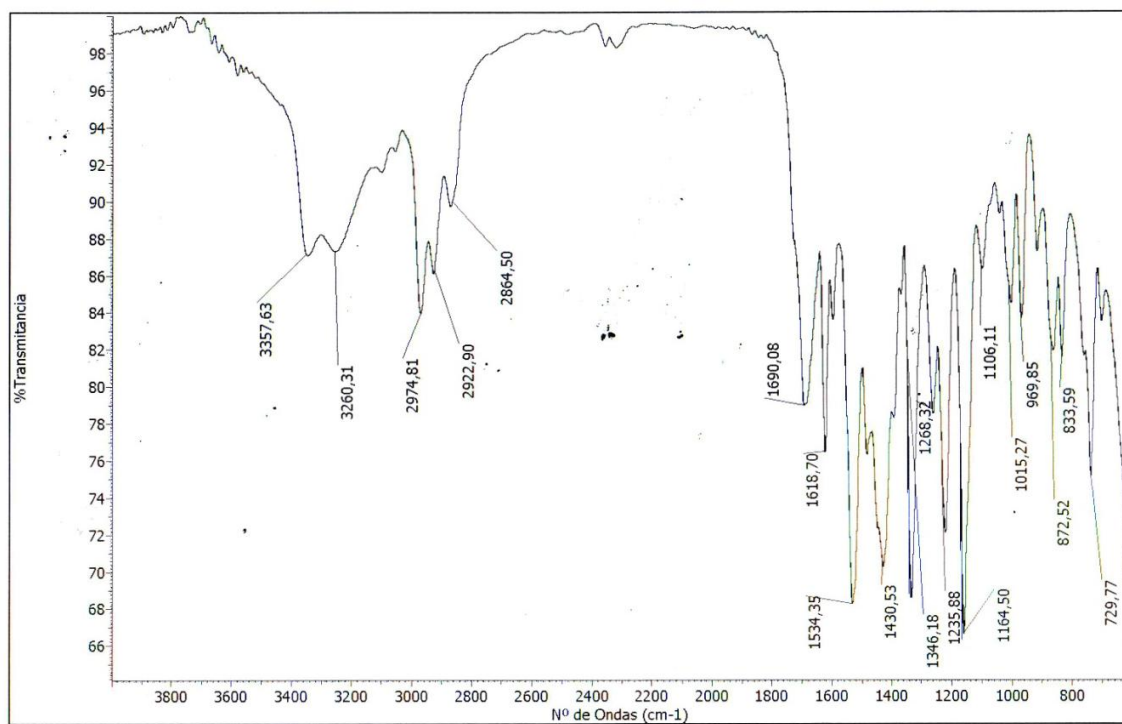
HRMS



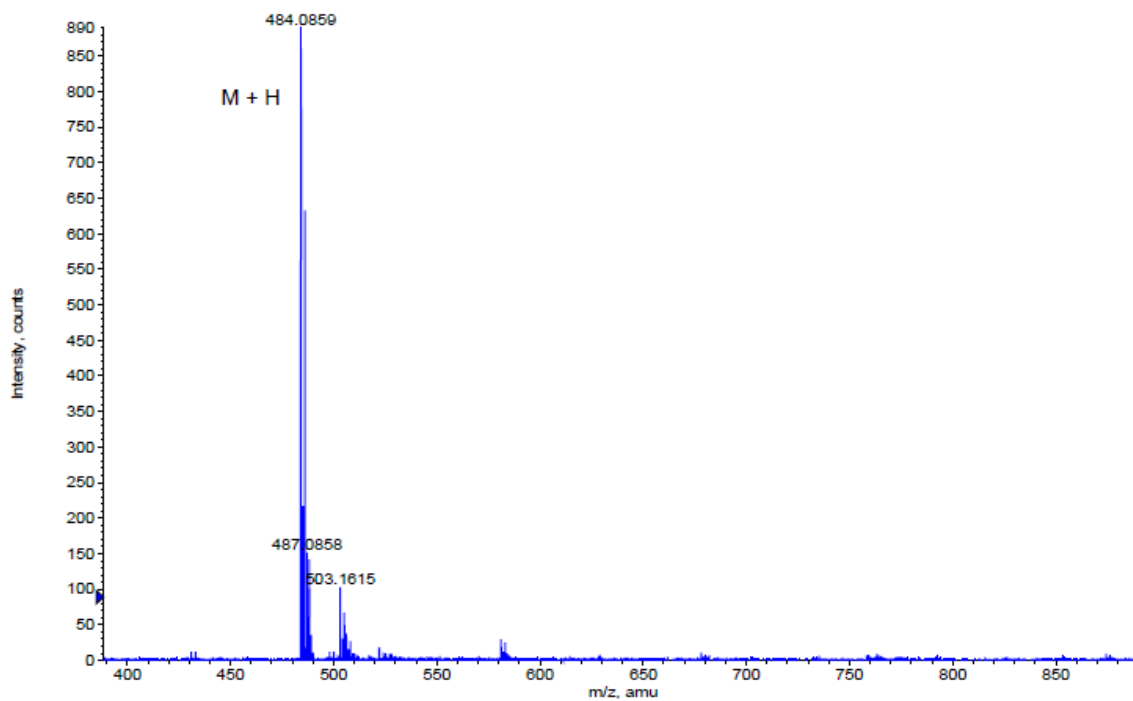
Formula	CalculatedMass	mDaError	ppmError	RDB
C ₂₅ H ₃₀ N ₃ O ₄ Cl ₂	506.160789	0.511338	1.010226	11.5
C ₃₀ H ₃₀ N O ₂ Cl ₂	506.164811	-3.511366	-6.93724	15.5
C ₂₀ H ₃₀ N ₅ O ₆ Cl ₂	506.156766	4.534042	8.957692	7.5

-N-(2,7-dichloro-9,9-dimethyl-5-(methylsulfonamido)-9H-xanthen-4-yl)pyrrolidine-2-carboxamide (8)¹H NMR (CDCl₃, 200 MHz)¹³C NMR (CDCl₃, 50 MHz)

IR

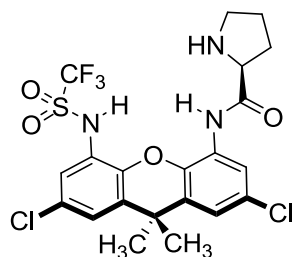


HRMS

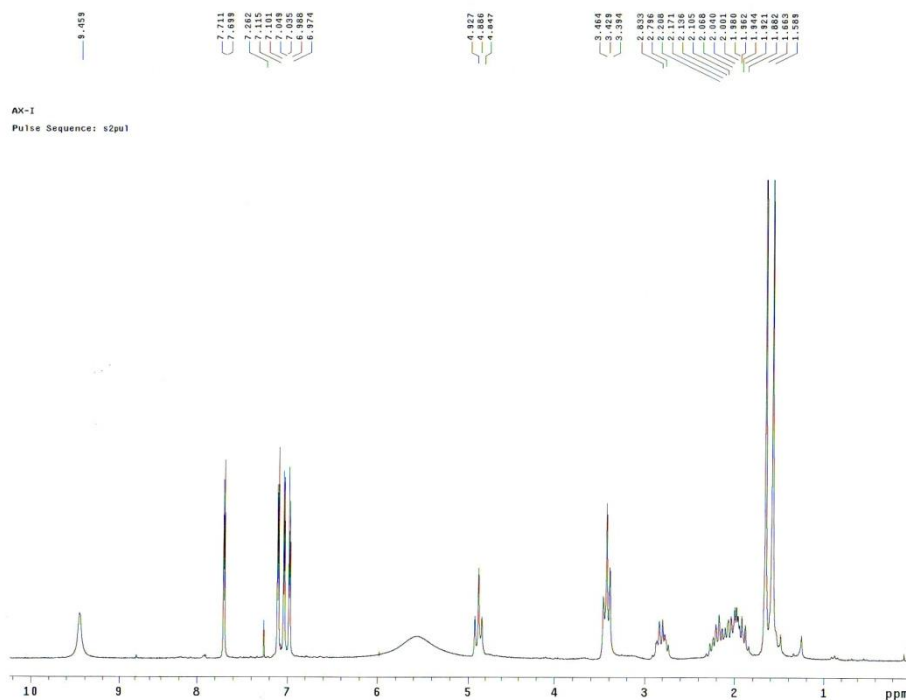


Formula	CalculatedMass	mDaError	ppmError	RDB
C ₂₁ H ₂₄ N ₃ O ₄ S Cl ₂	484.08591	-0.010222	-0.021116	10.5
C ₂₄ H ₂₅ N ₂ O ₂ Na S Cl ₂	484.087528	-1.627666	-3.362346	11.5
C ₁₉ H ₂₅ N ₃ O ₄ Na S Cl ₂	484.083505	2.395038	4.947542	7.5
C ₁₆ H ₂₄ N ₅ O ₆ S Cl ₂	484.081888	4.012482	8.288772	6.5
C ₂₆ H ₂₄ N ₂ O ₂ S Cl ₂	484.089933	-4.032926	-8.331004	14.5

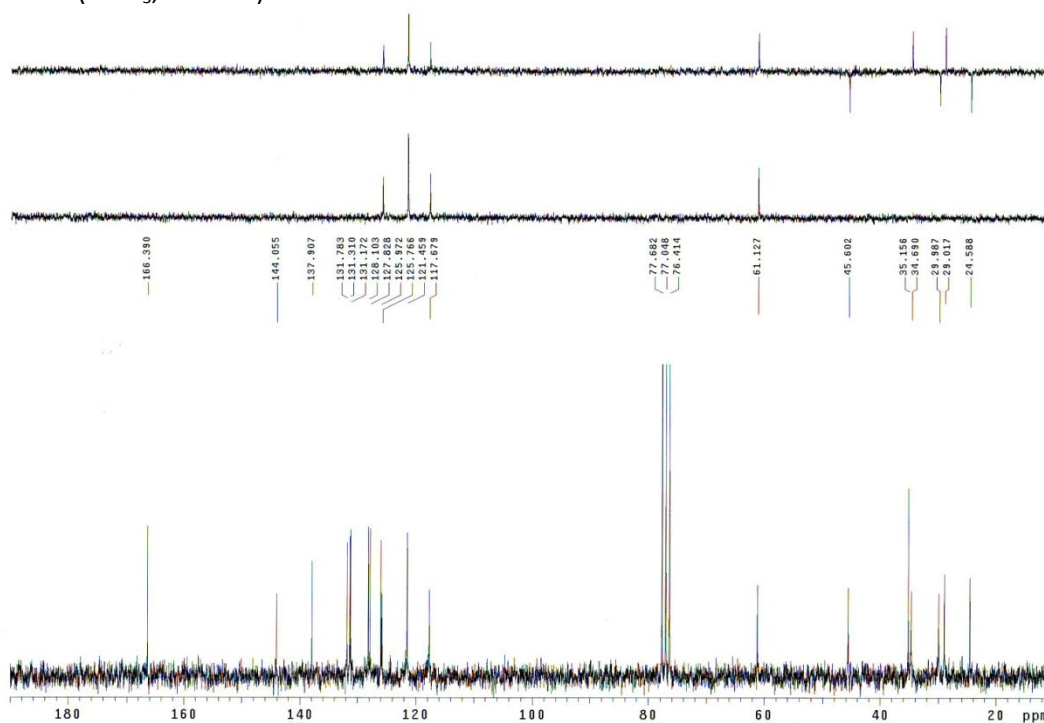
- *N*-(2,7-dichloro-9,9-dimethyl-5-(trifluoromethylsulfonamido)-9*H*-xanthen-4-yl) pyrrolidine-2-carboxamide (9)



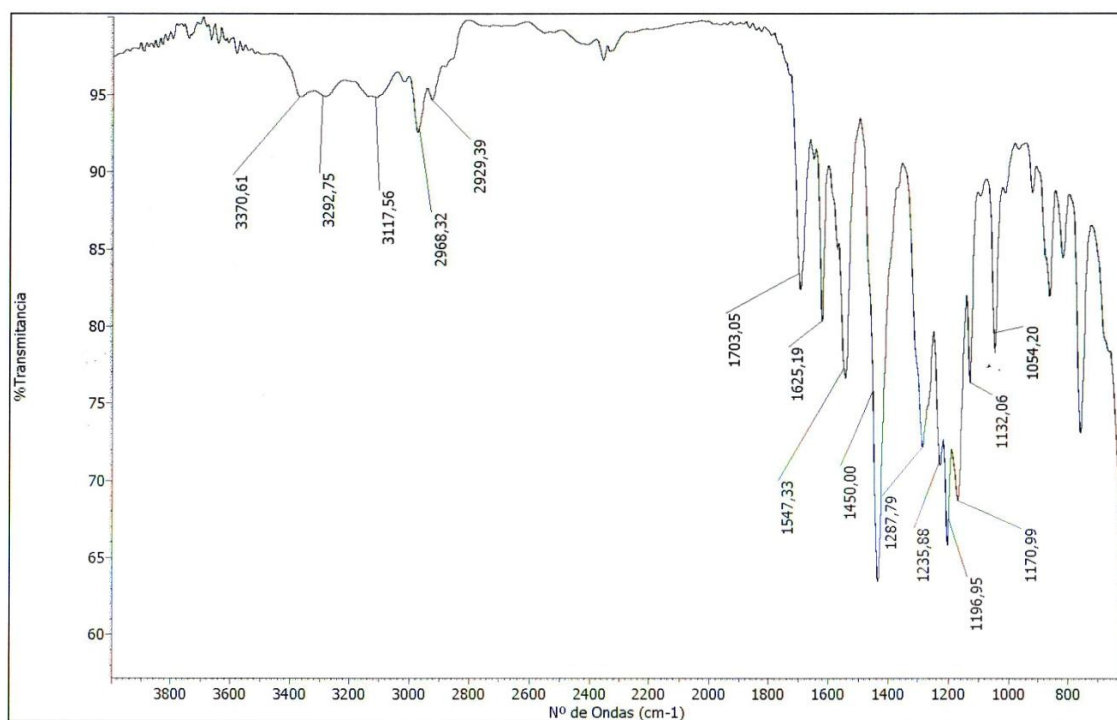
^1H NMR (CDCl_3 , 200 MHz)



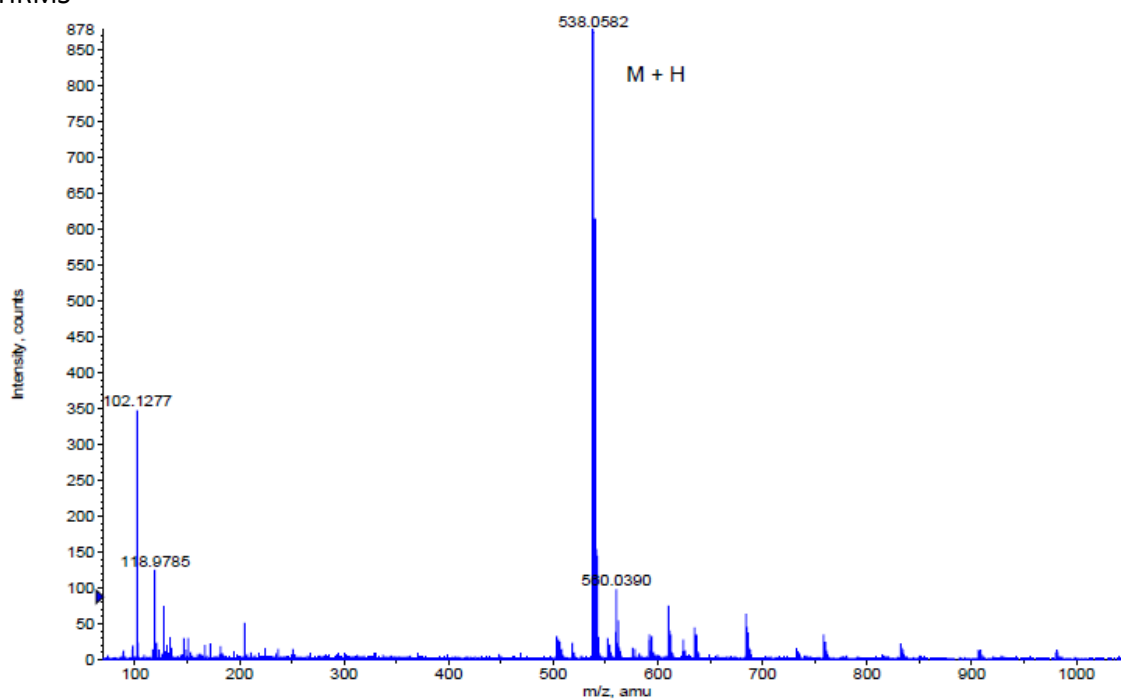
^{13}C NMR (CDCl_3 , 50 MHz)



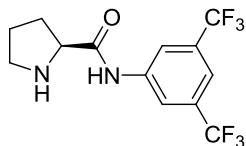
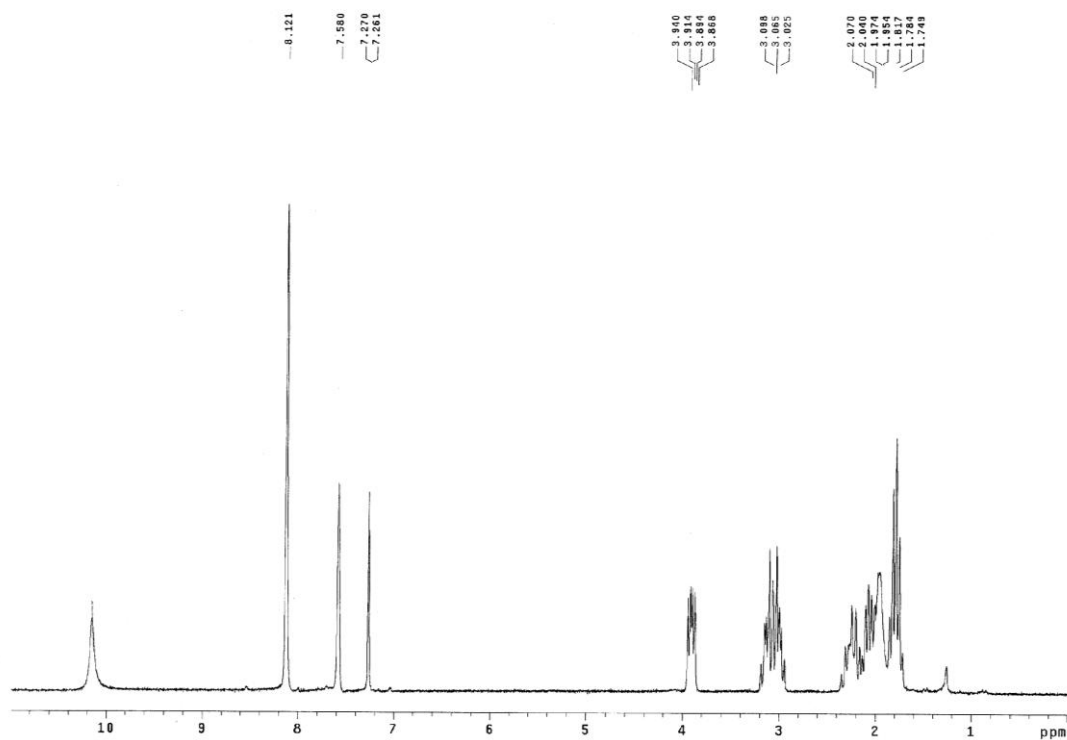
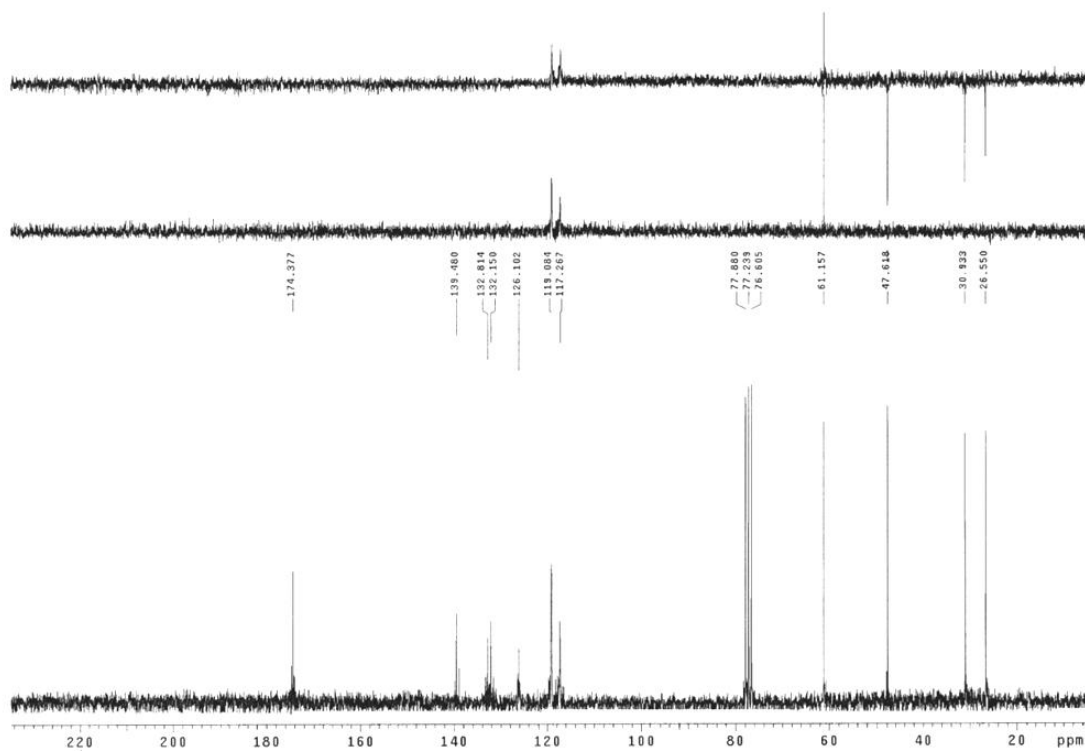
IR



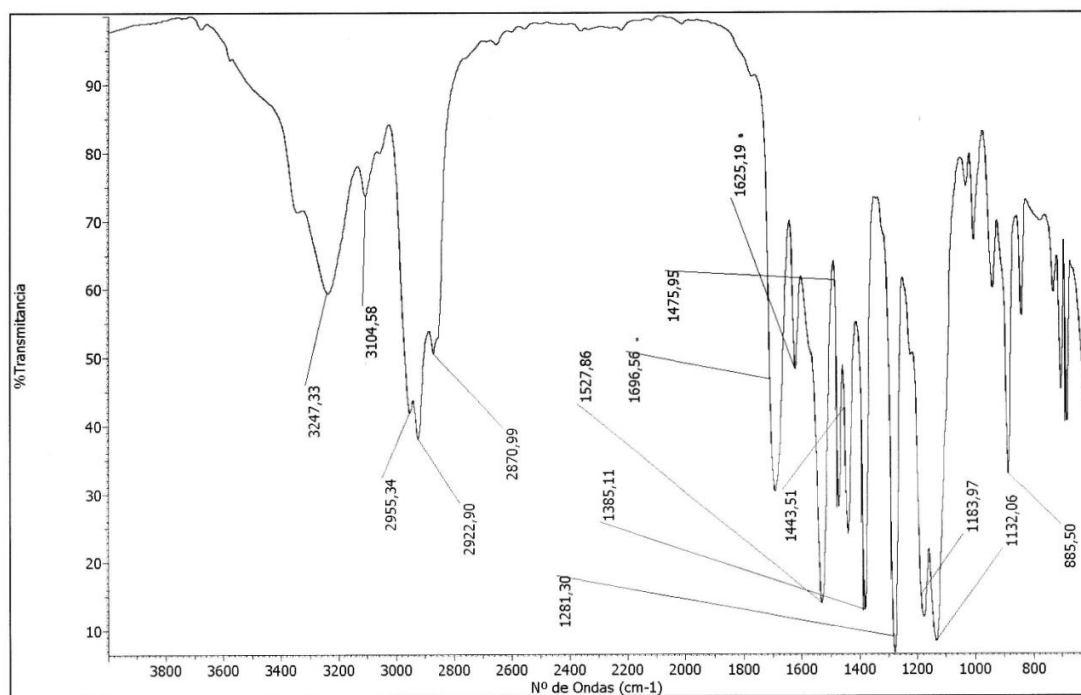
HRMS



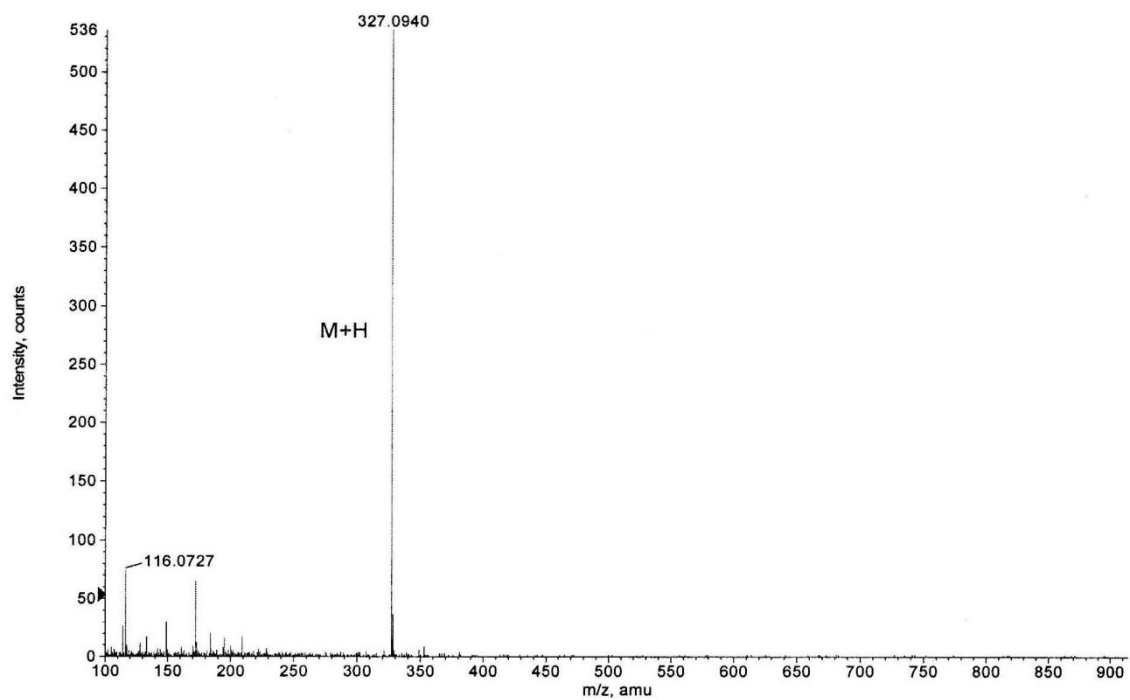
Formula	CalculatedMass	mDaError	ppmError	RDB
C ₂₁ H ₂₁ N ₃ O ₄ F ₃ S Cl ₂	538.057645	0.555148	1.031761	10.5
C ₂₆ H ₂₁ N O ₂ F ₃ S Cl ₂	538.061668	-3.467556	-6.444568	14.5
C ₁₆ H ₂₁ N ₅ O ₆ F ₃ S Cl ₂	538.053622	4.577852	8.50809	6.5
C ₁₄ H ₂₅ N ₃ O ₉ F ₃ S Cl ₂	538.063518	-5.318212	-9.884073	1.5

- (S)-N-(3,5-bis(trifluoromethyl)phenyl)pyrrolidin-2-carboxamide (12)¹H NMR (CDCl₃, 200 MHz)¹³C NMR (CDCl₃, 50 MHz)

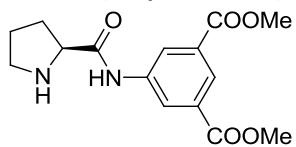
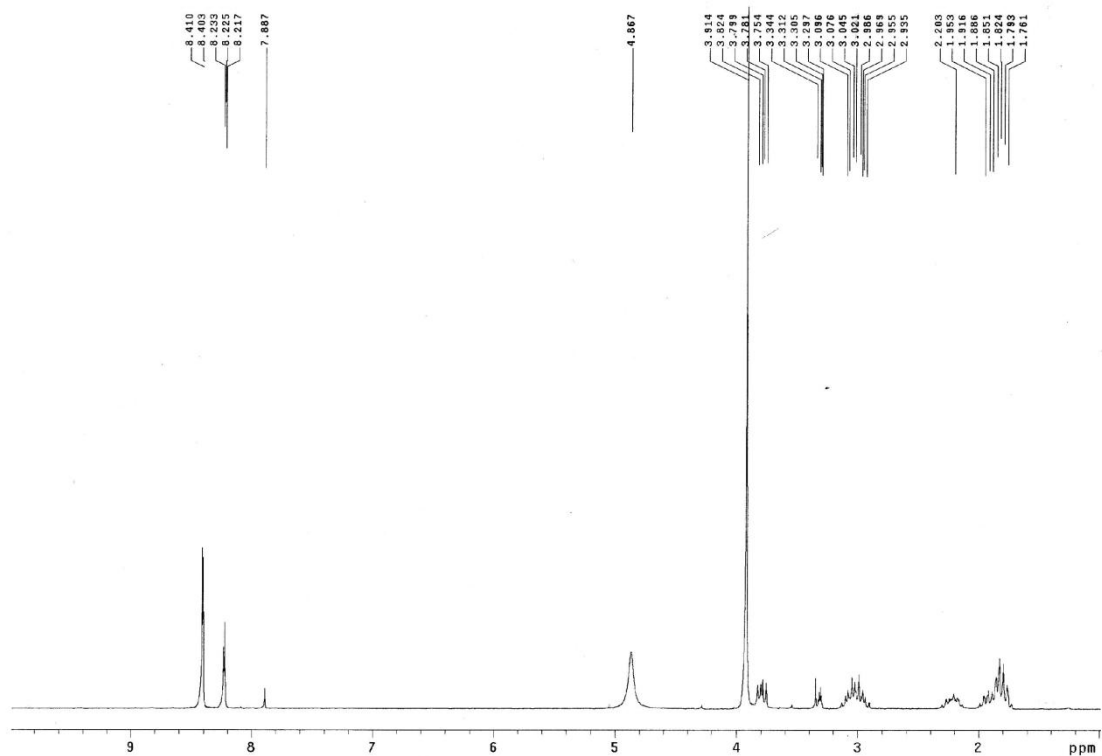
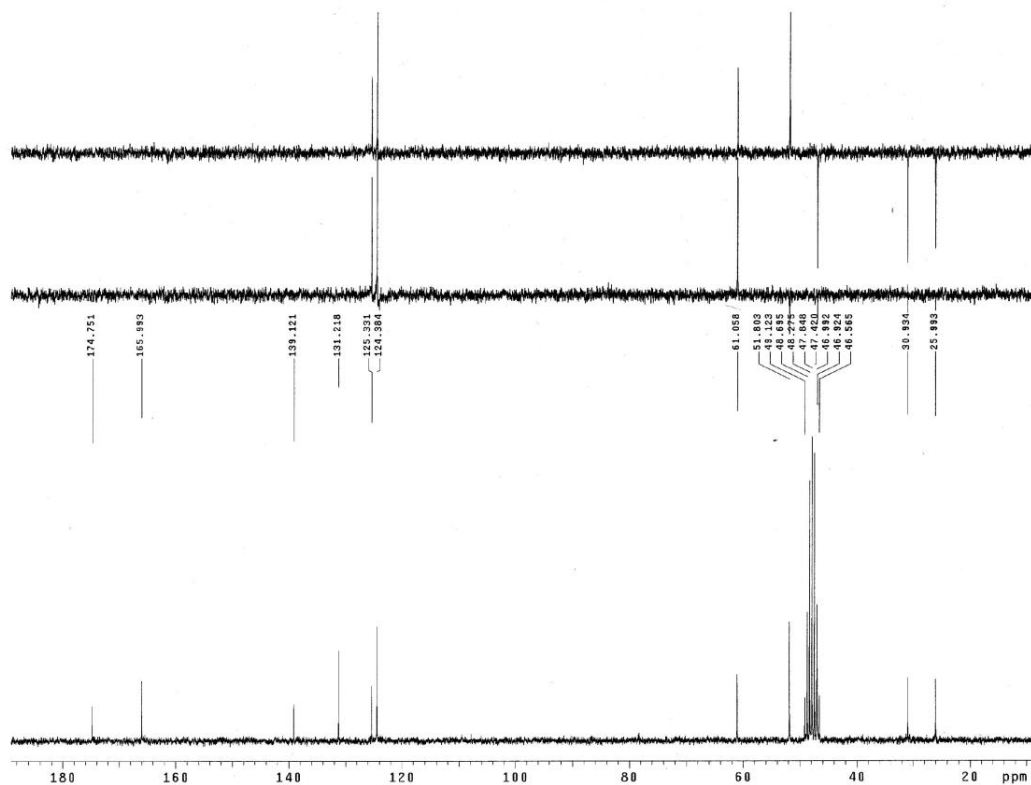
IR



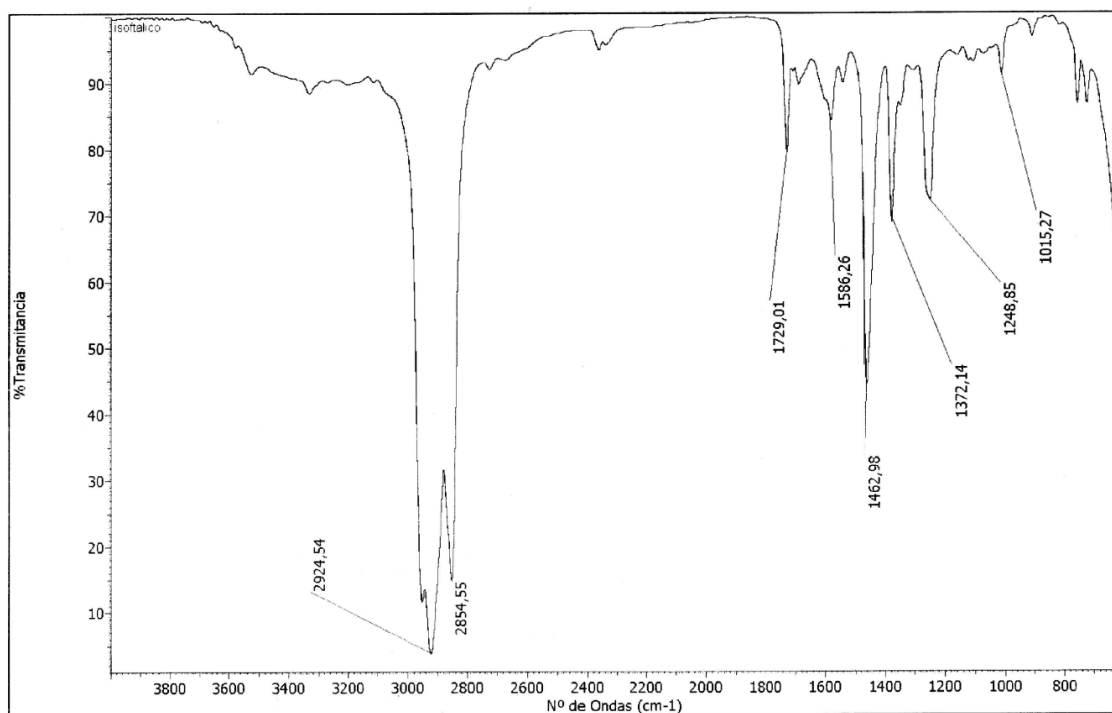
HRMS



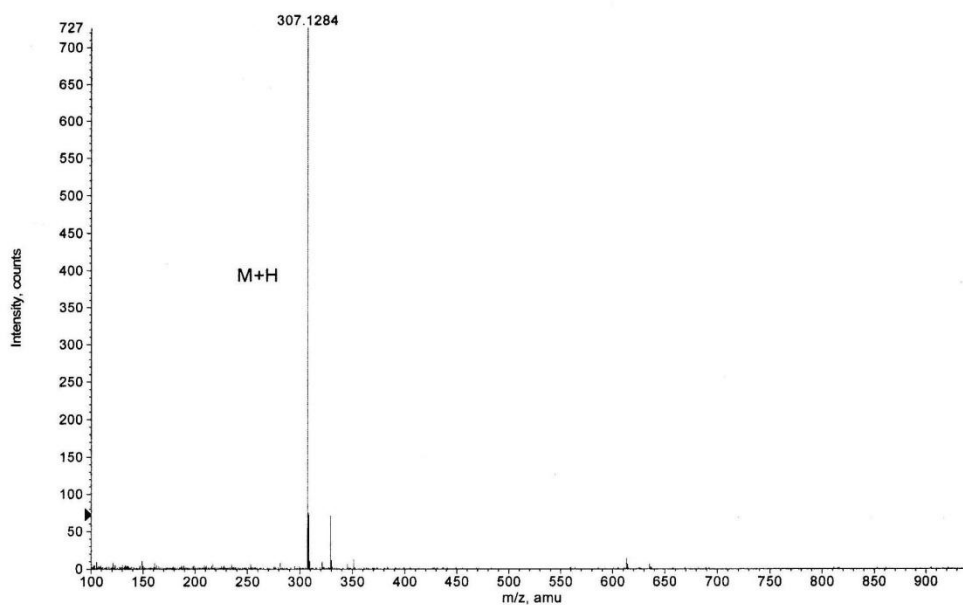
Formula	CalculatedMass	mDaError	ppmError	RDB
C H10 N12 F6 Na	327.094779	-0.779116	-2.381929	-0.5
C13 H13 N2 O F6	327.092659	1.340904	4.099439	5.5
C3 H9 N12 F6	327.097184	-3.184376	-9.735338	2.5

- (S)-dimethyl-5-(pyrrolidin-2-carboxamido)isophthalate (13) ^1H NMR (CD_3OD , 200 MHz) ^{13}C NMR (CD_3OD , 50 MHz)

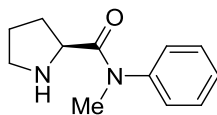
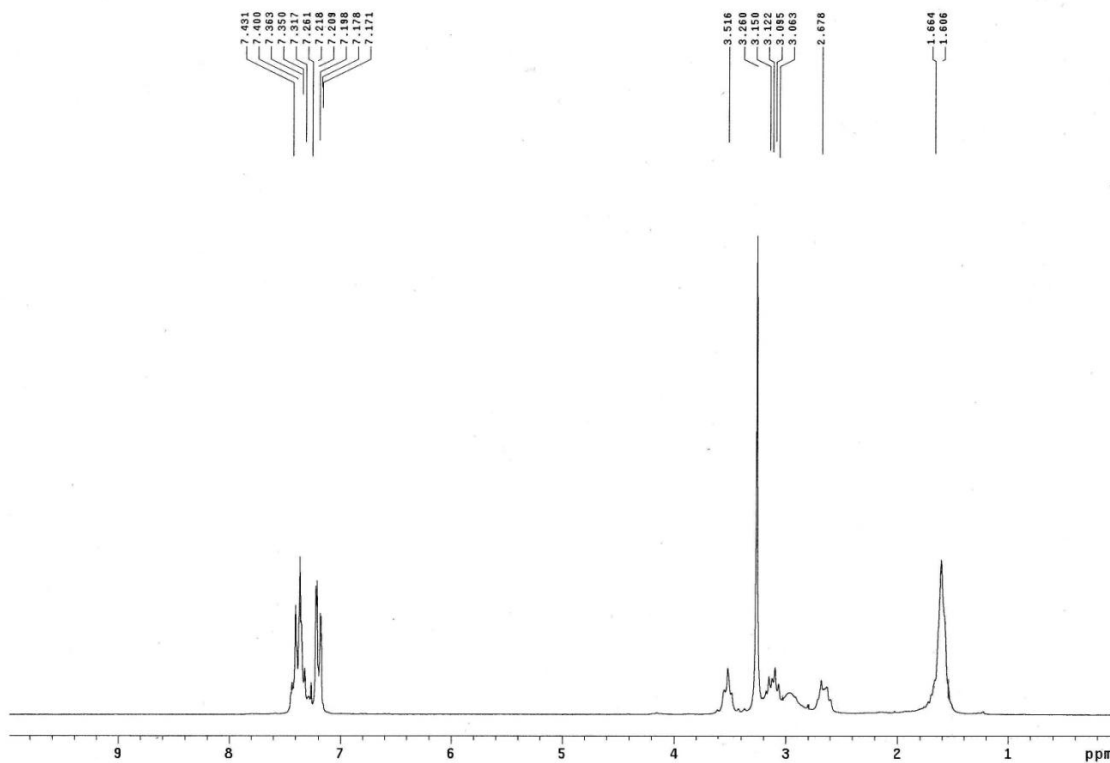
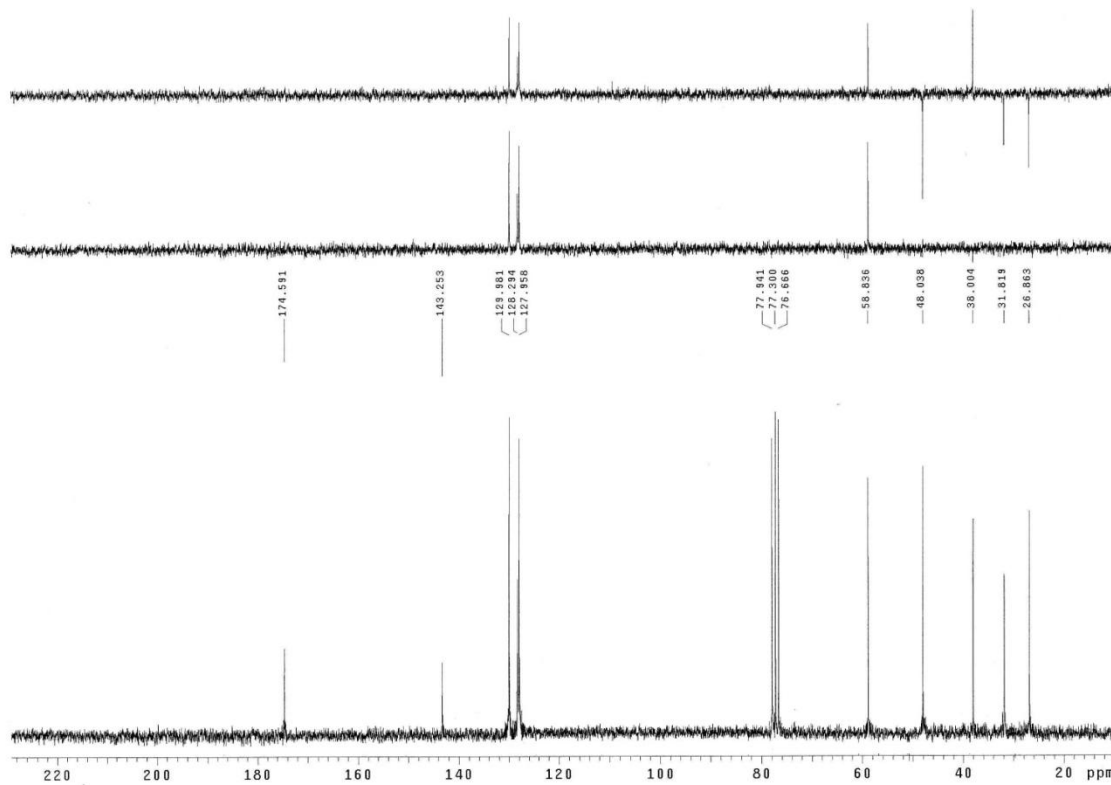
IR



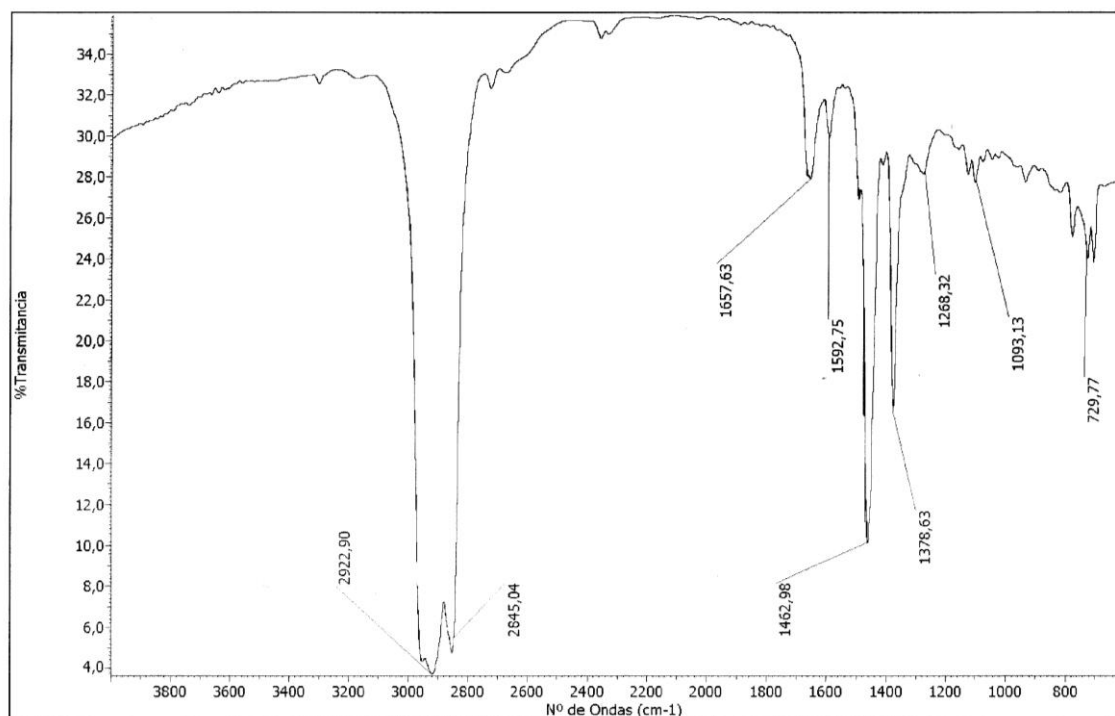
HRMS



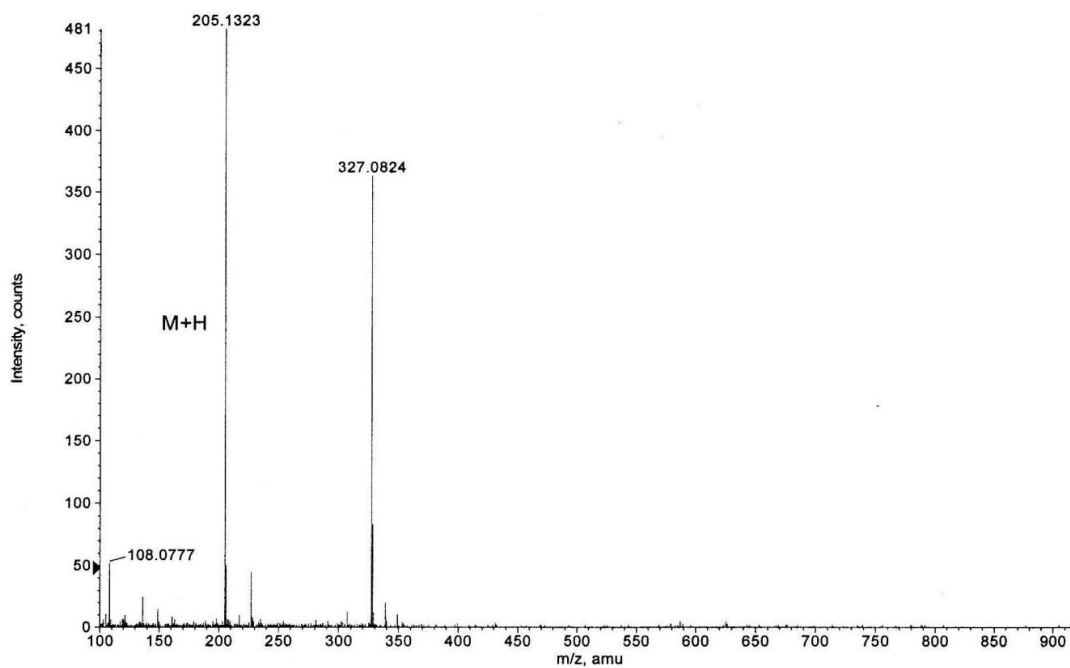
Formula	CalculatedMass	mDaError	ppmError	RDB
C15 H19 N2 O5	307.128848	-0.448396	-1.45996	7.5
C14 H16 N6 O Na	307.12778	0.619552	2.017237	9.5
H15 N14 O6	307.129351	-0.950972	-3.096328	0.5
C16 H15 N6 O	307.130186	-1.785708	-5.814196	12.5
C13 H20 N2 O5 Na	307.126443	1.956864	6.371474	4.5
C18 H20 O3 Na	307.130466	-2.06584	-6.726295	8.5
C11 H15 N8 O3	307.126163	2.236996	7.283573	8.5
C3 H16 N12 O4 Na	307.130968	-2.568416	-8.362663	1.5

- (S)-N-methyl-N-phenylpyrrolidine-2-carboxamide (14)¹H NMR (CDCl₃, 200 MHz)¹³C NMR (CDCl₃, 50 MHz)

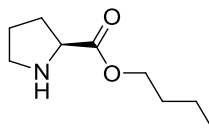
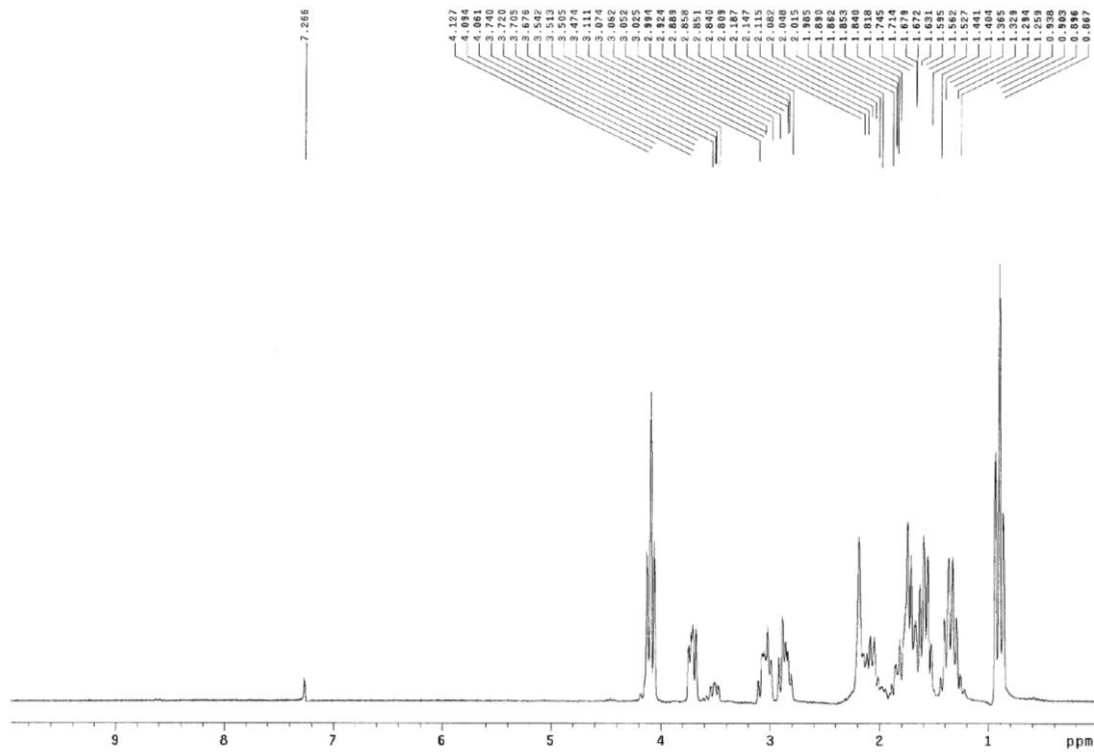
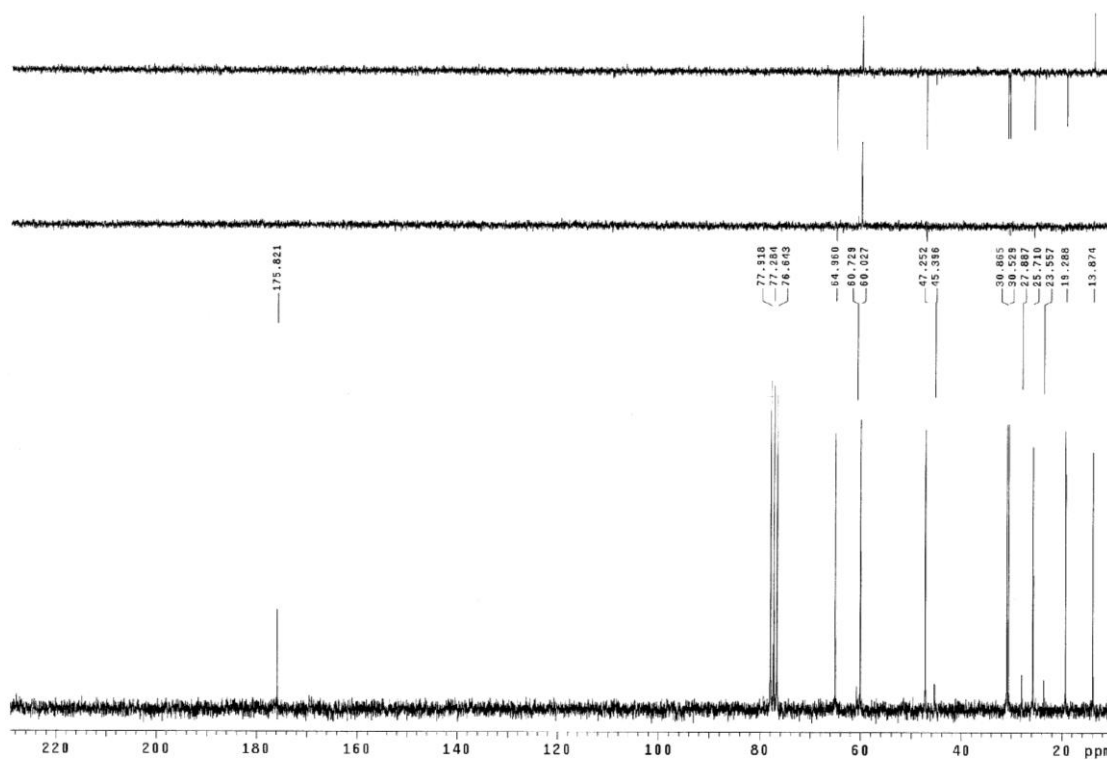
IR



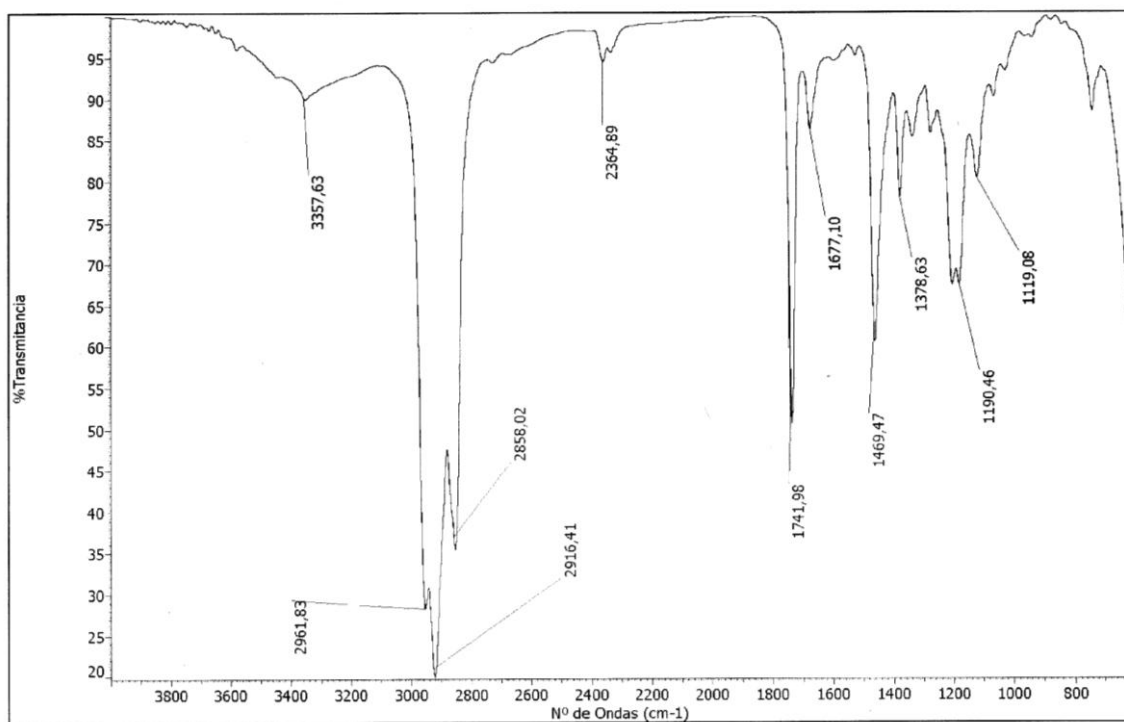
HRMS



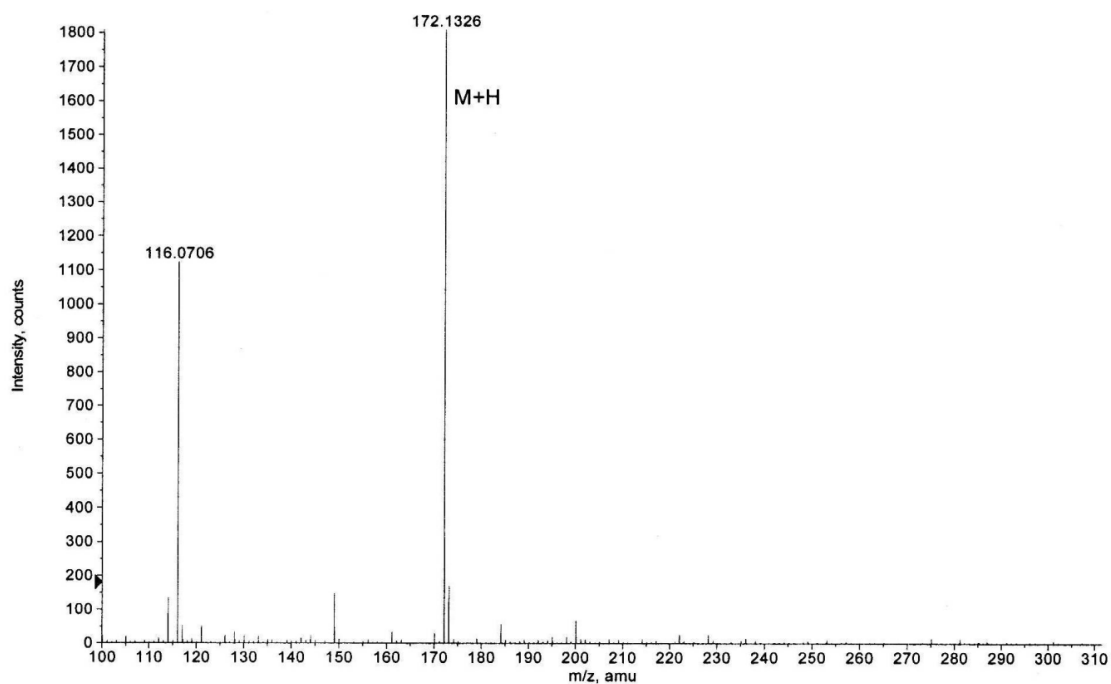
Formula	CalculatedMass	mDaError	ppmError	RDB
C10 H18 N2 O Na	205.131134	1.165504	5.681703	2.5
C12 H17 N2 O	205.13354	-1.239756	-6.043674	5.5

- (S)-butyl-pyrrolidin-2-carboxylate (15)¹H NMR (CDCl₃, 200 MHz)¹³C NMR (CDCl₃, 50 MHz)

IR

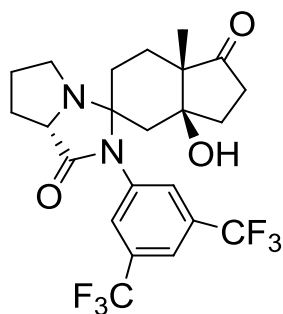


HRMS

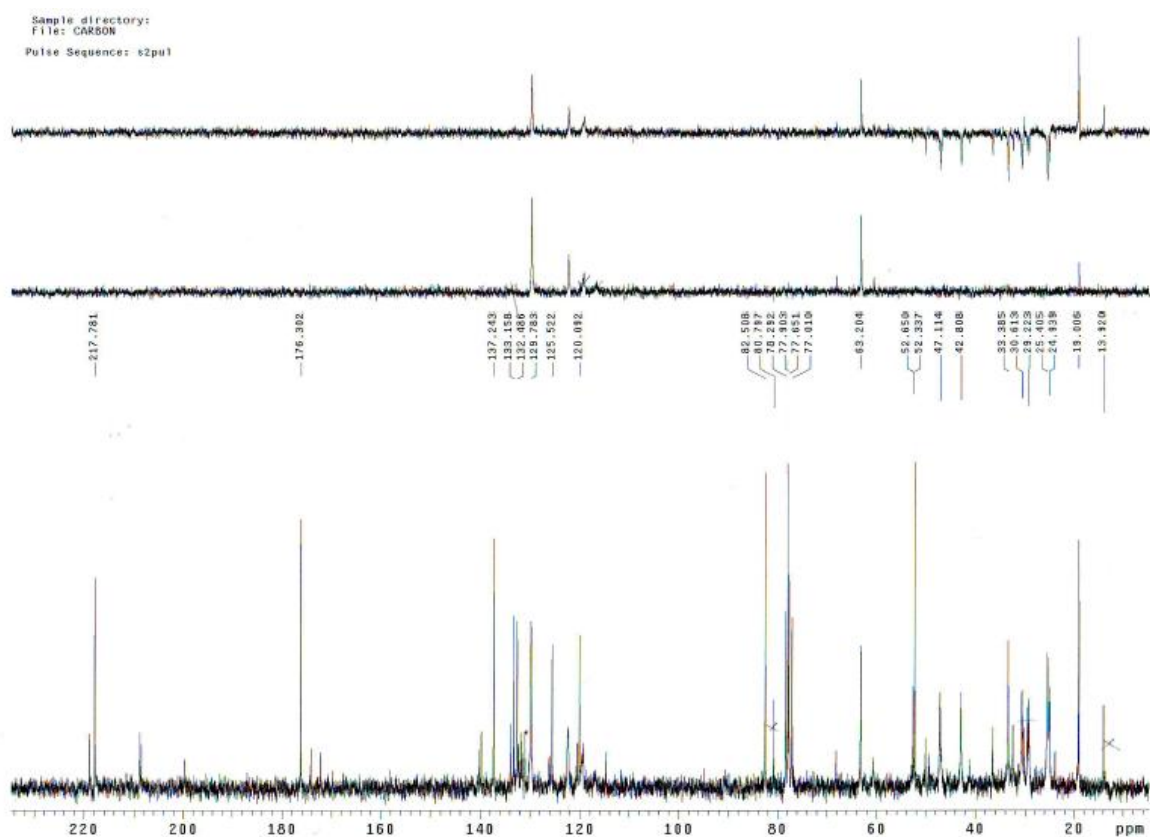


Formula	CalculatedMass	mDaError	ppmError	RDB
C ₉ H ₁₈ N ₂ O ₂	172.133205	-0.605428	-3.517207	1.5

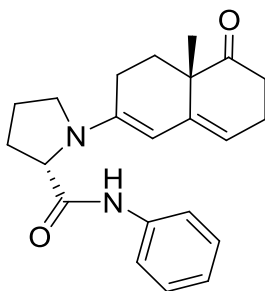
-(3*a*S,7*a*S,7*a'*S)-2'--(3,5-bis(trifluoromethyl)phenyl)-3*a*-hydroxy-7*a*-methyldecahydrospiro[indene-5,3'-pyrrolo[1,2-*c*]imidazole]-1,1'(2'*H*,6*H*)-dione (16)



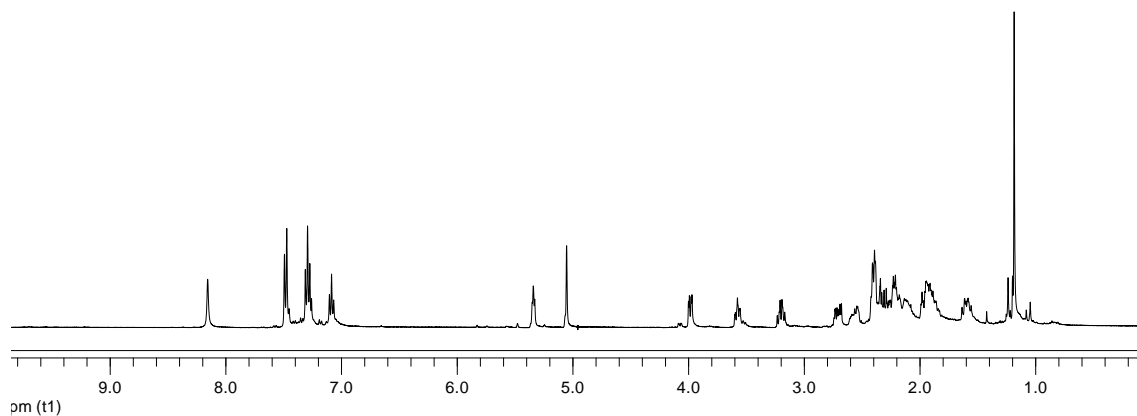
^{13}C NMR (CDCl_3 , 50 MHz)



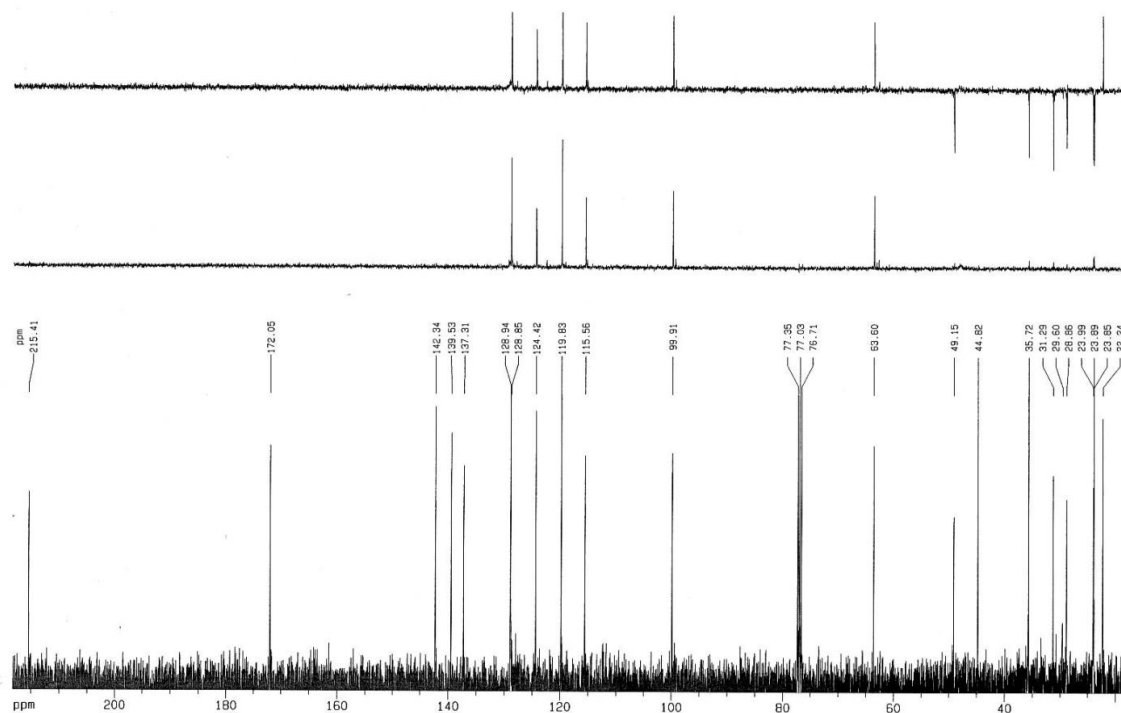
- (S)-1-((S)-4a-methyl-5-oxo-3,4,4a,5,6,7-hexahydronaphthalen-2-yl)-N-phenylpyrrolidine-2-carboxamide (19)



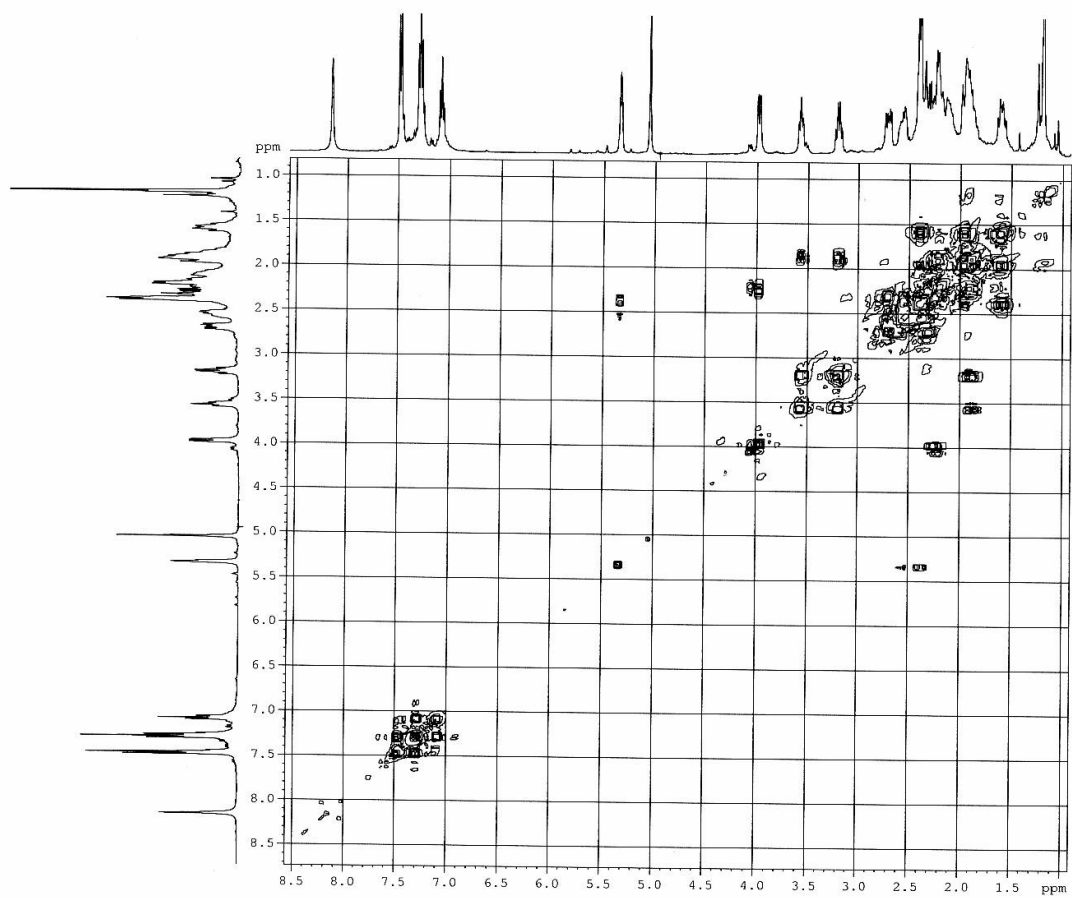
^1H NMR (CDCl_3 , 400 MHz)



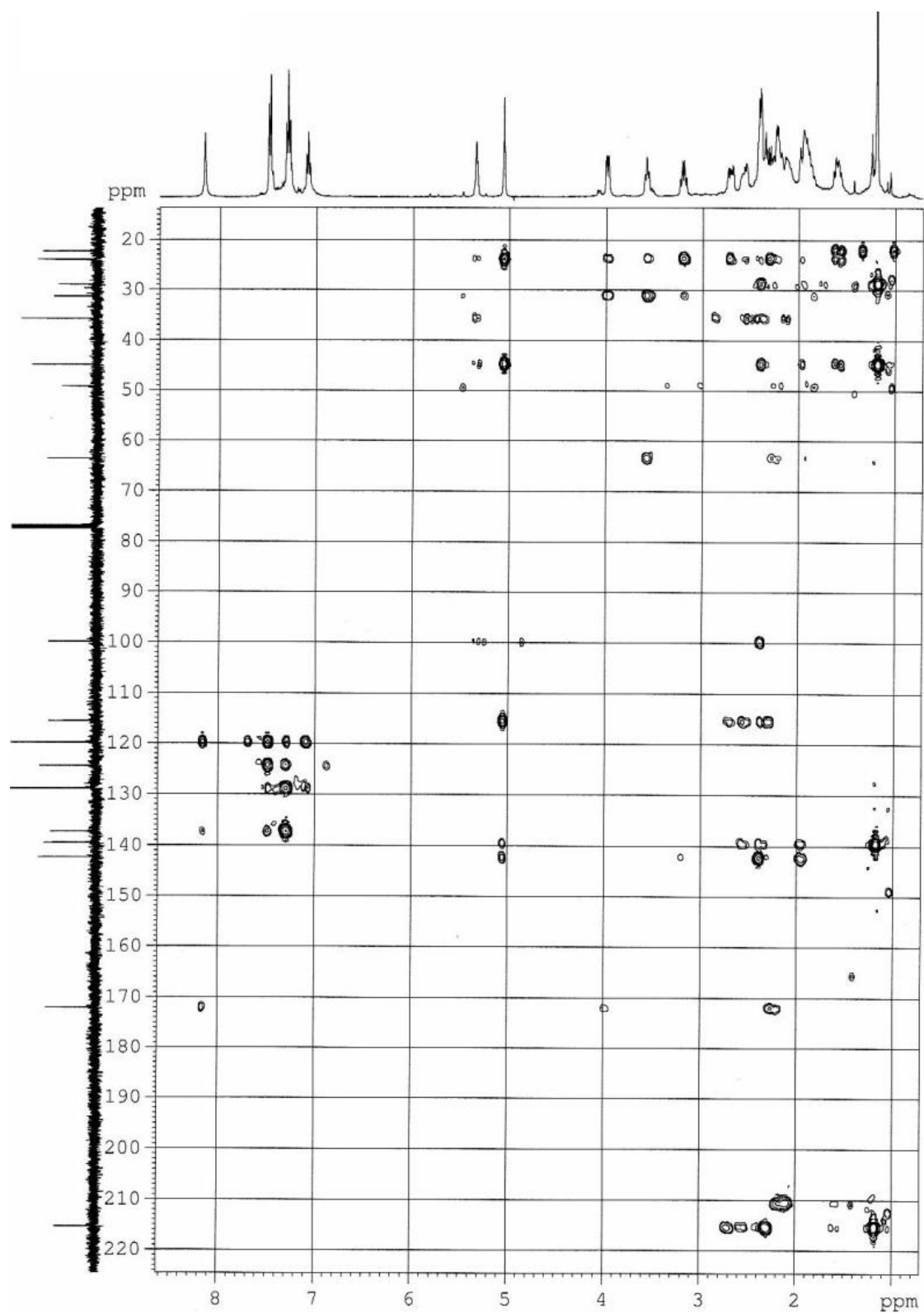
^{13}C NMR (CDCl_3 , 100 MHz)



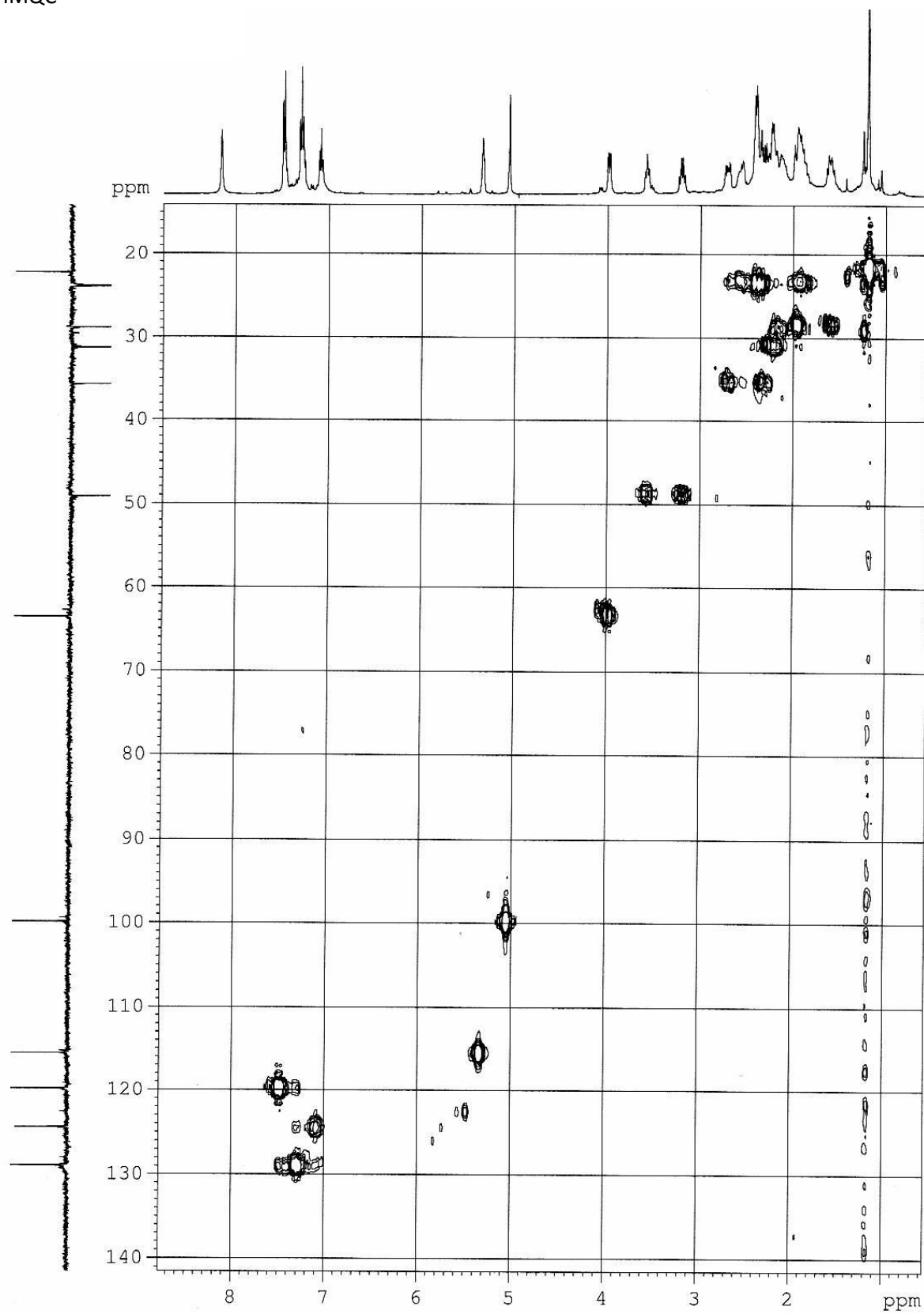
COSY



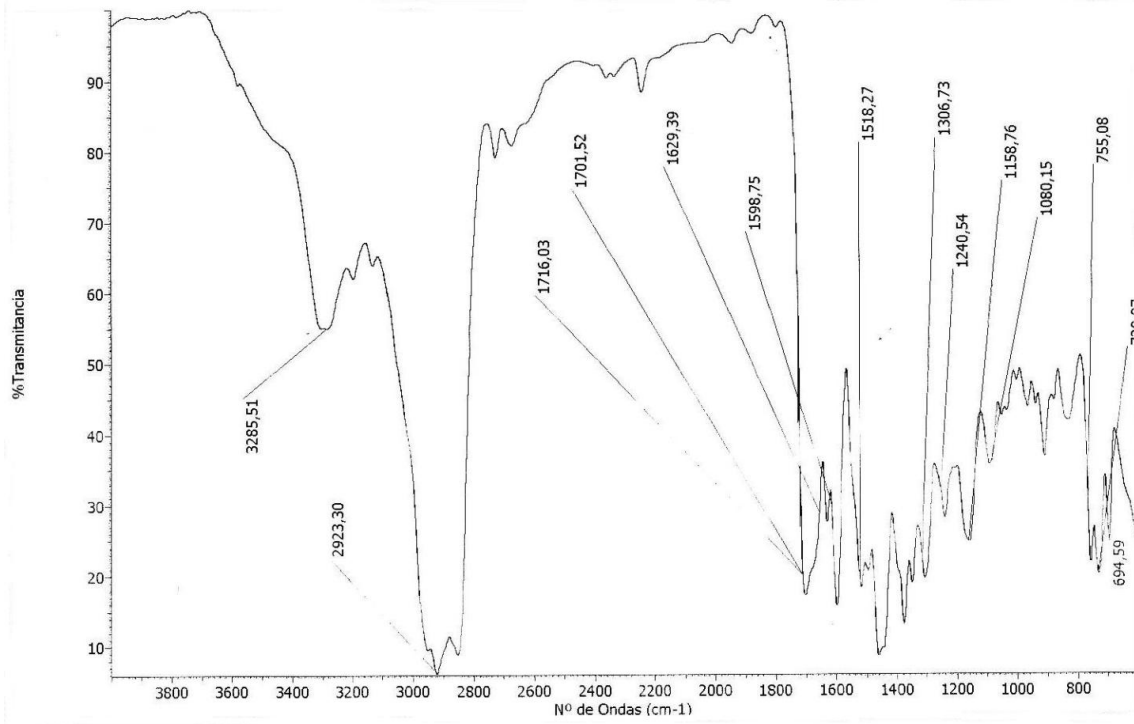
HMBC



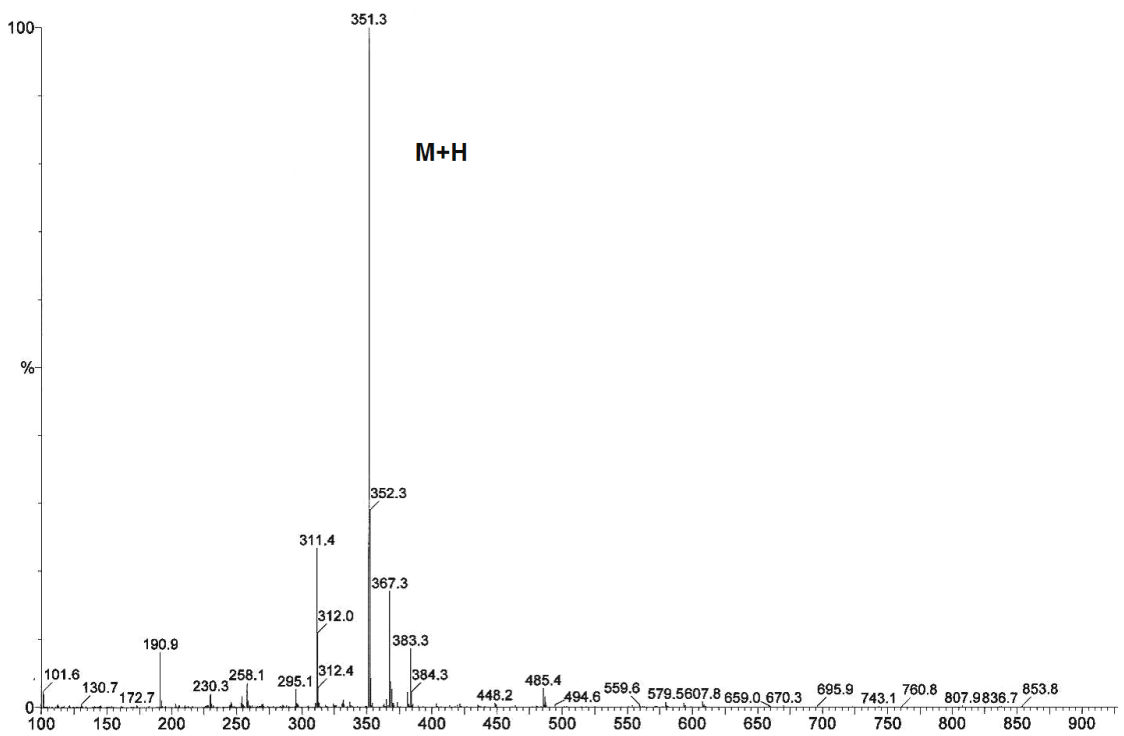
HMQC



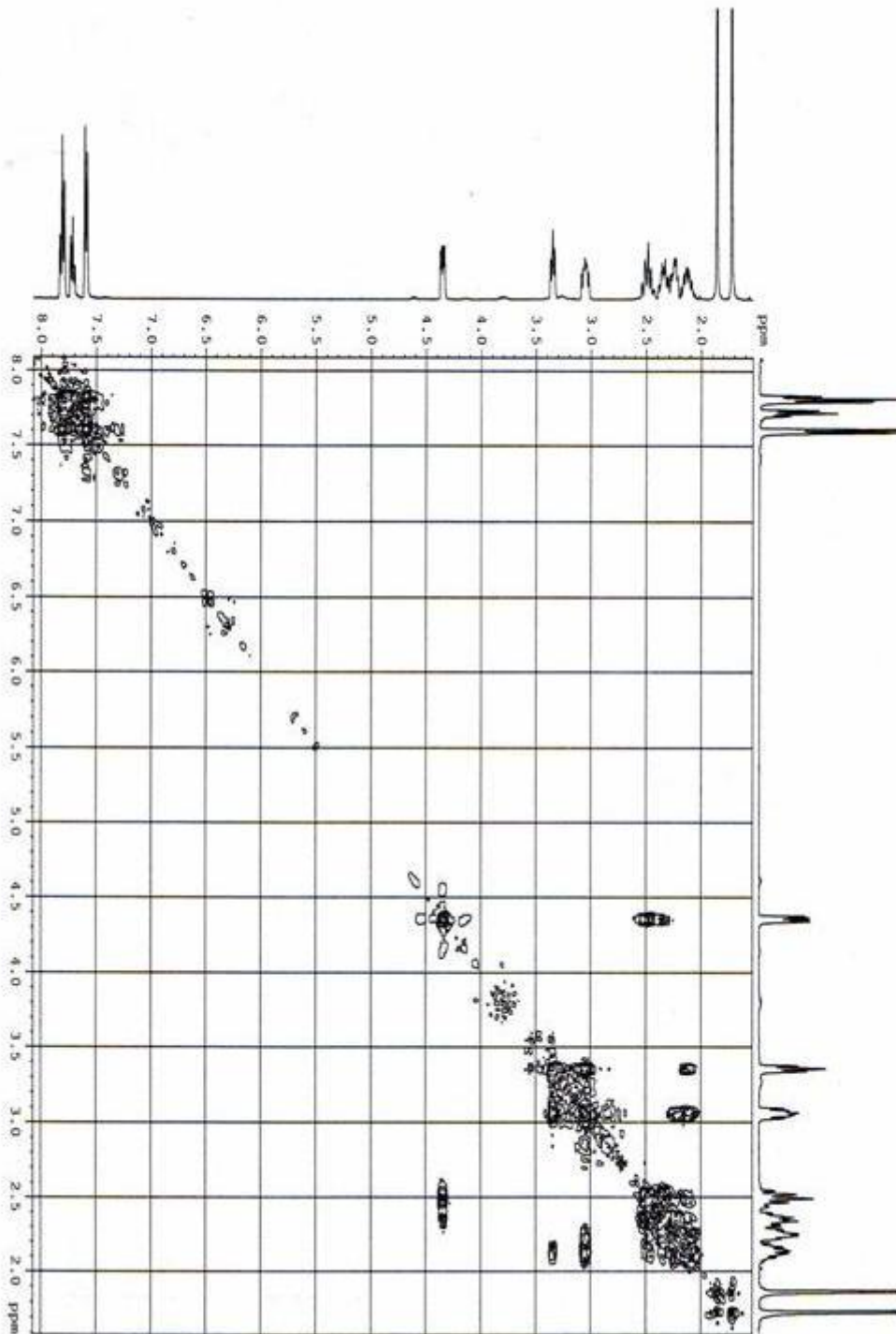
IR



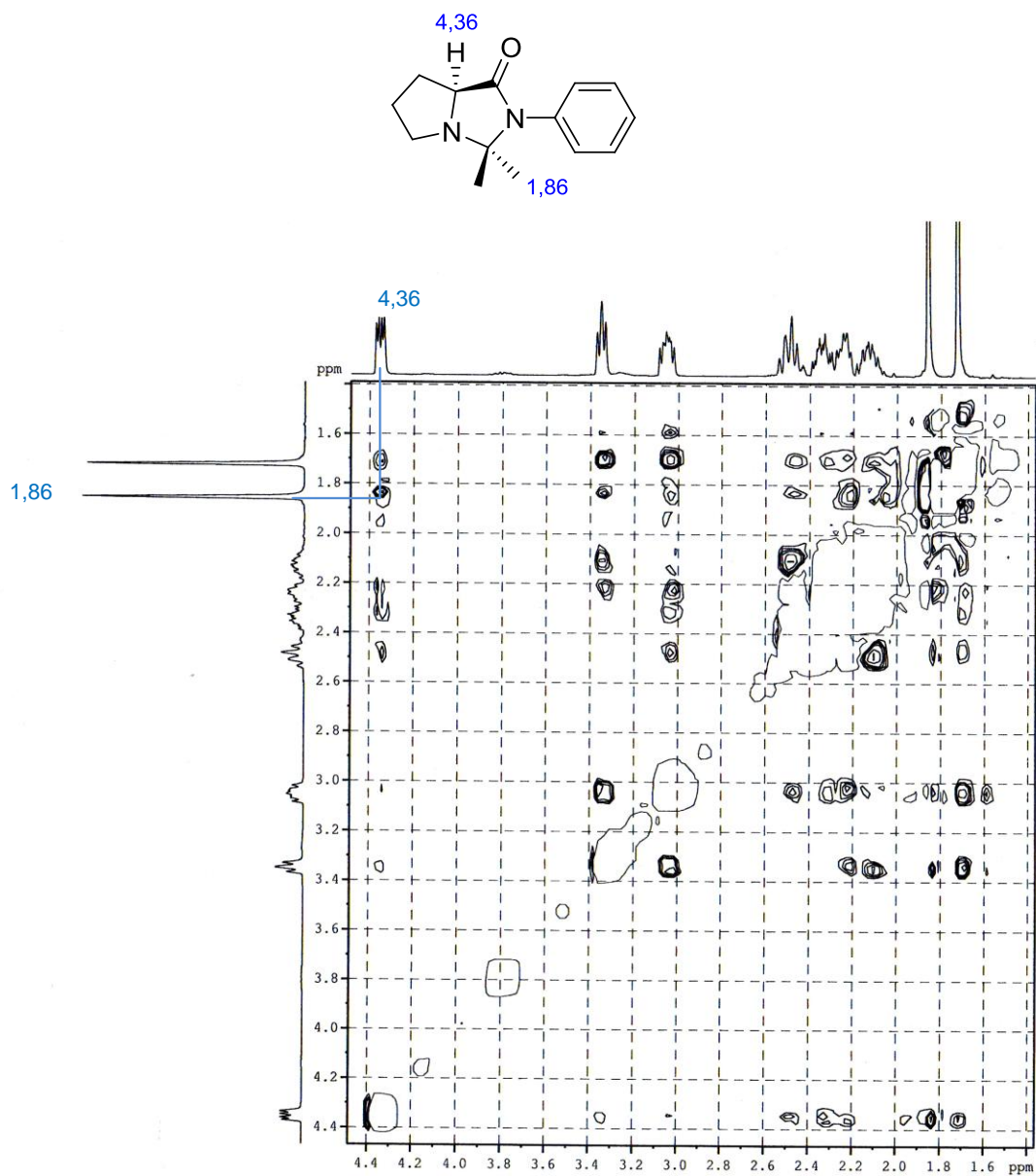
MS



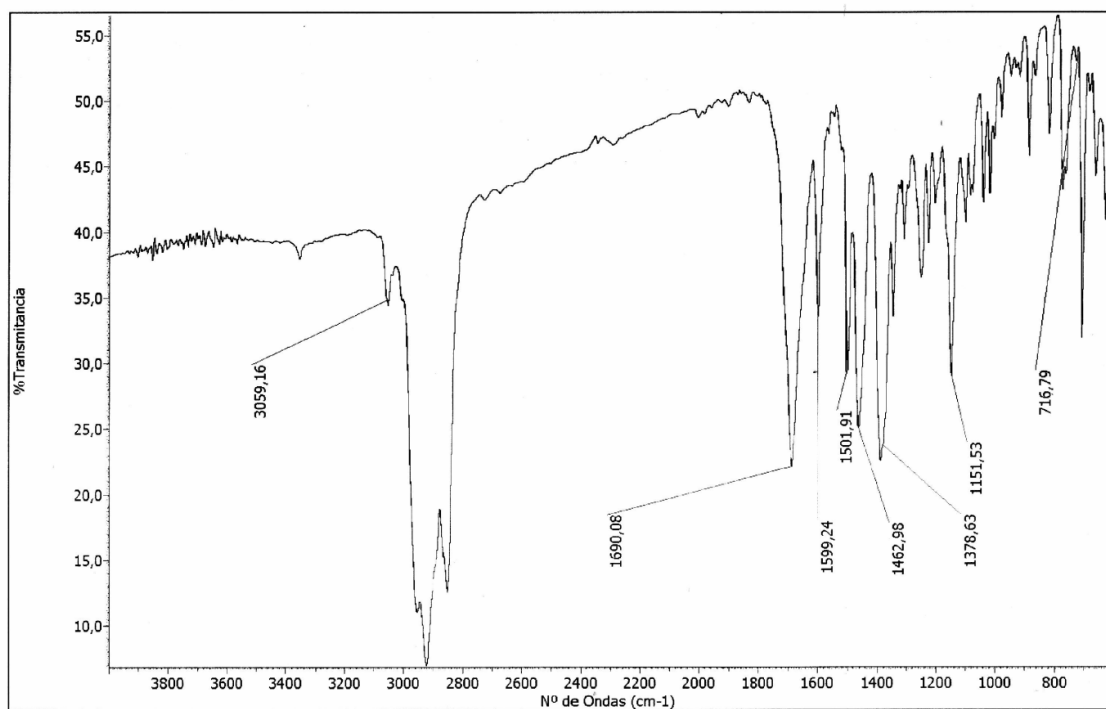
COSY



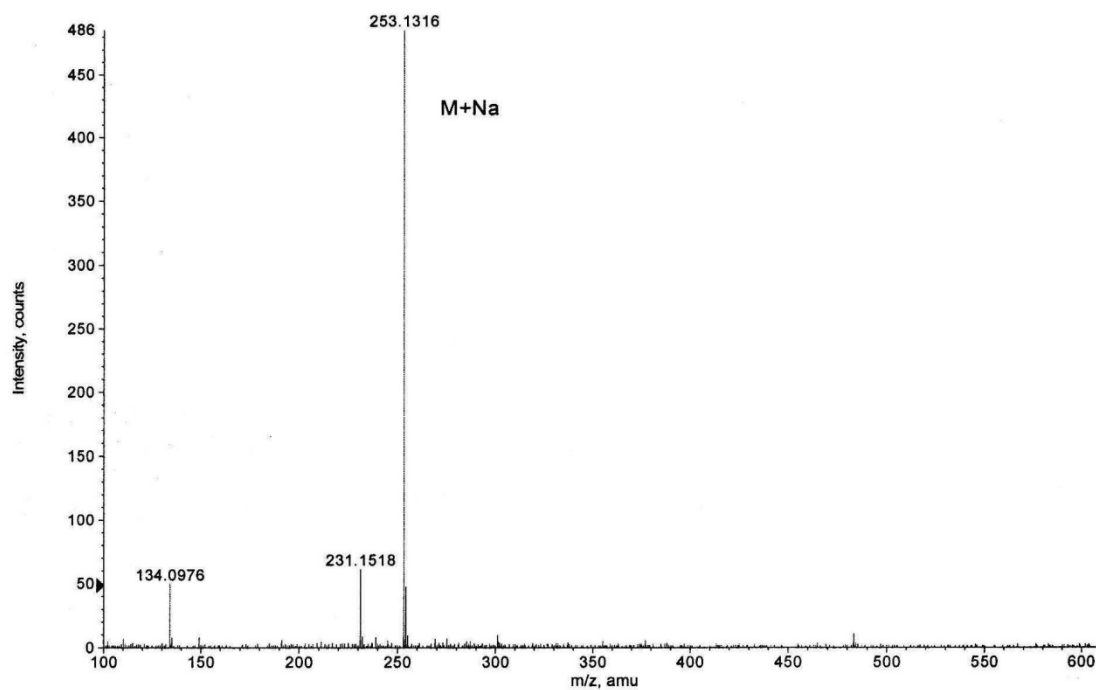
ROESY



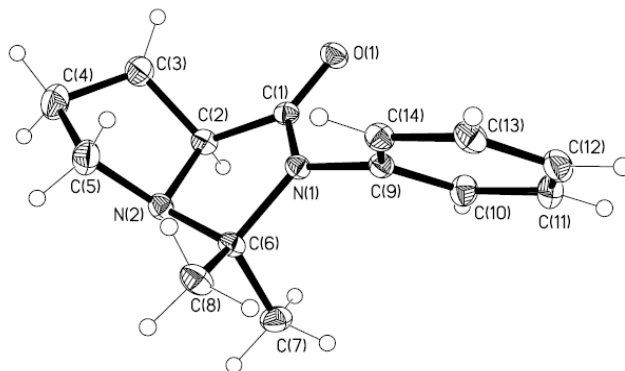
IR



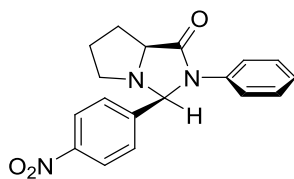
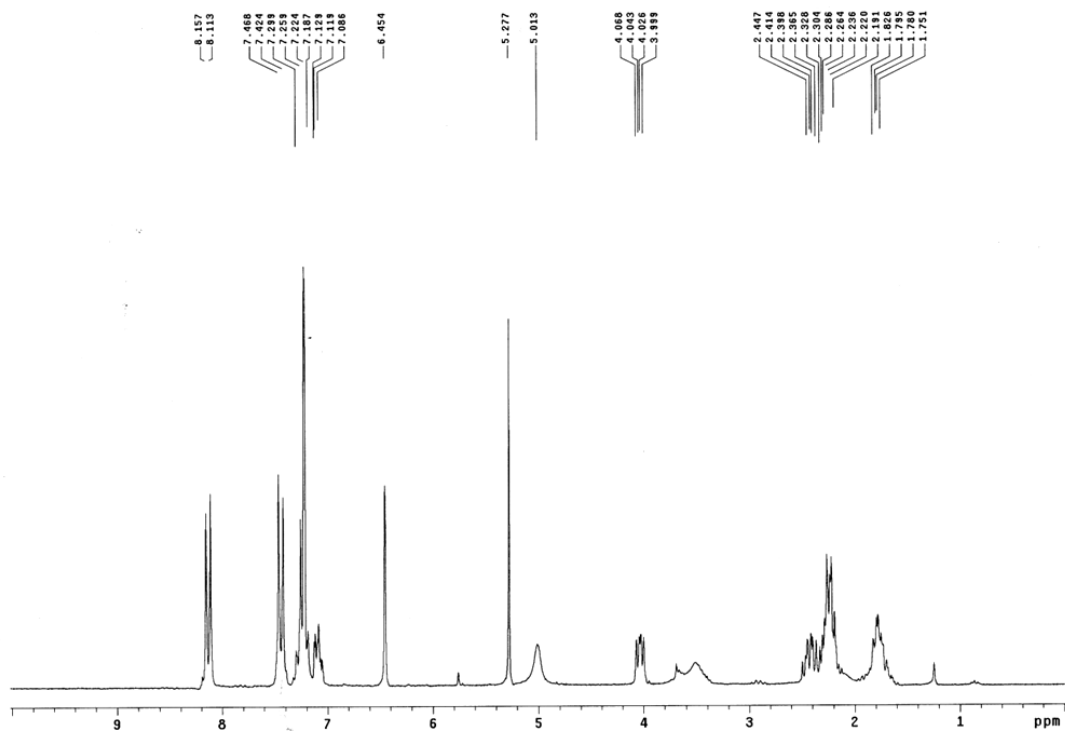
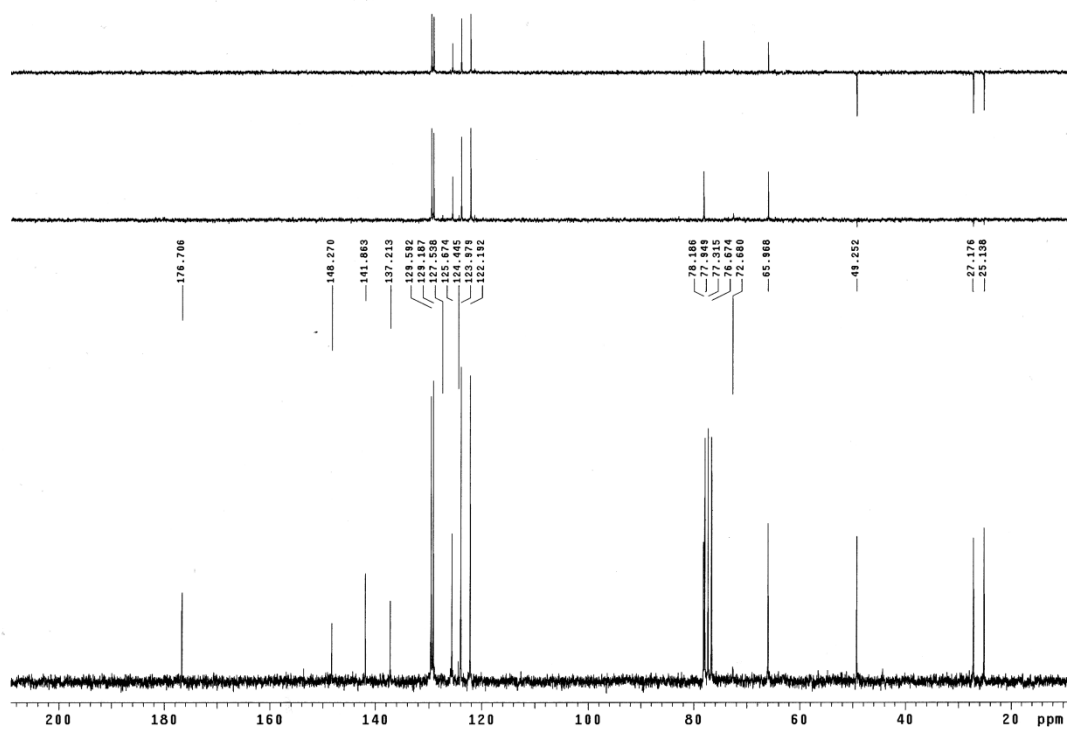
HRMS



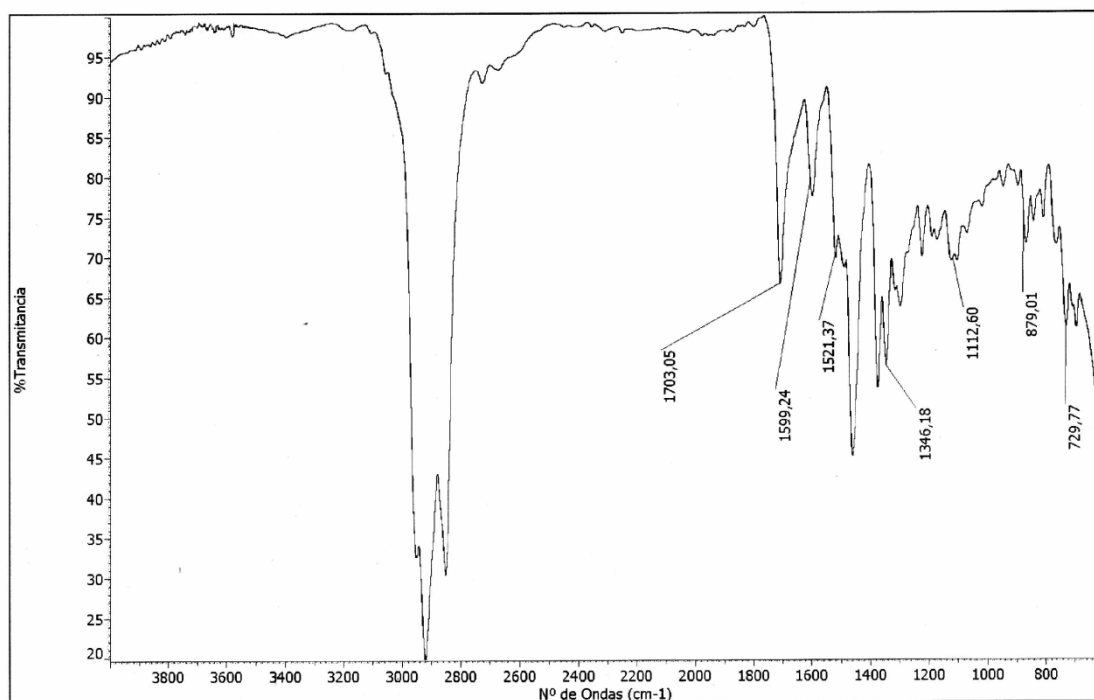
Formula	CalculatedMass	mDaError	ppmError	RDB
C ₁₄ H ₁₈ N ₂ O Na	253.131134	0.465504	1.838976	6.5
C ₁₆ H ₁₇ N ₂ O	253.13354	-1.939756	-7.663017	9.5
C ₁₁ H ₁₇ N ₄ O ₃	253.129517	2.082948	8.228698	5.5
C H ₁₃ N ₁₄ O ₂	253.134042	-2.442332	-9.648447	2.5

X-ray structure, cristal and refinement data of compound **23**

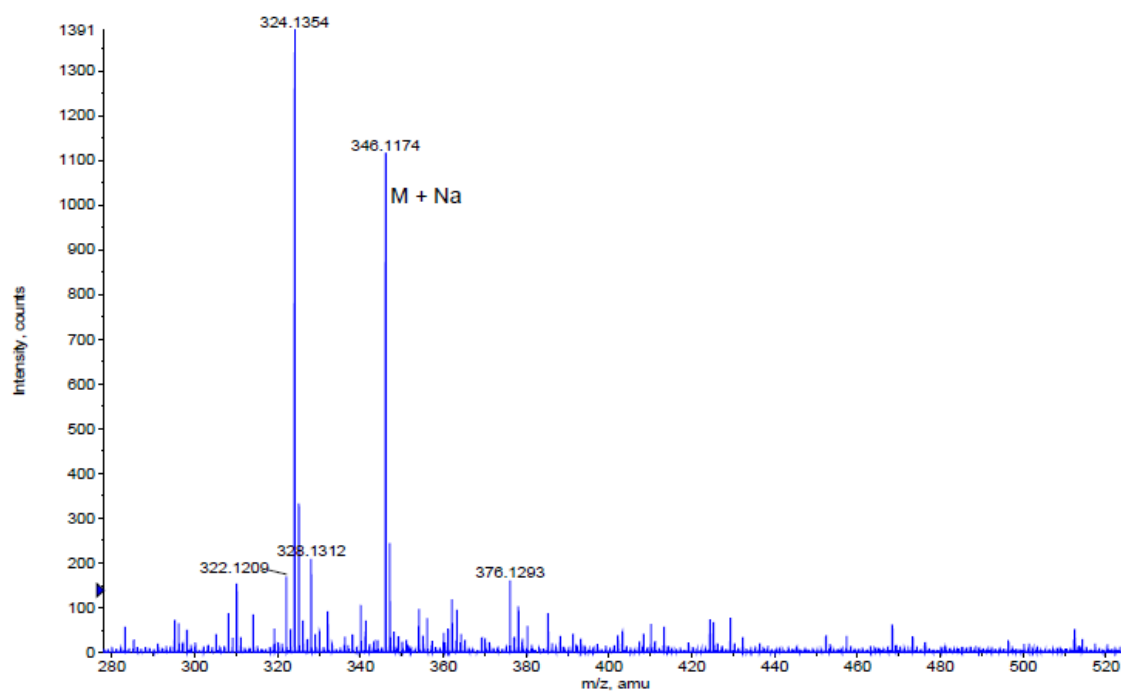
Empirical formula	$C_{14}H_{18}N_2O$
Molecular weight	230.30
Temperature	293 (2) K
Wavelength	1.54178 Å
Crystal system, Space group	Orthorhombic, P2(1)2(1)2(1)
Unit cell dimensions	a = 8.7304 (3) Å $\alpha = 90.00^\circ$ b = 8.9046 (2) Å $\beta = 90.00^\circ$ c = 16.6172 (5) Å $\gamma = 90.00^\circ$
Volume	1291.83 (7) Å ³
Z; Density (calculated)	4; 1.184 mg/m ³
Absorption coefficient	0.595 mm ⁻¹
F(000)	496
Crystal size	0.10 x 0.08 x 0.06 mm
θ range	5.32 – 65.57 °
Limiting indices h, k, l	-10 ≤ h ≤ 10, -8 ≤ k ≤ 10, -18 ≤ l ≤ 18
Reflections collected/independent	7935/2084 $R_{int} = 0.0258$
Refinement method	Least squares method with full matrix in F^2
Data/restraints/parameters	2084/0/161
Goodness-of-fit on F^2	1.053
Final R indices [$I > 2\sigma(I)$]	$R_1 = 0.0259$, $\omega R_2 = 0.0687$
R indices (all data)	$R_1 = 0.0263$, $\omega R_2 = 0.0692$
Extinction coefficient	0.0210 (11)

- (3*S*,7*aS*)-3-(4-Nitrophenyl)-2-phenylhexahydropyrrolo[1,2-*e*]imidazol-1-one (24a)¹H NMR (CDCl₃, 200 MHz)¹³C NMR (CDCl₃, 50 MHz)

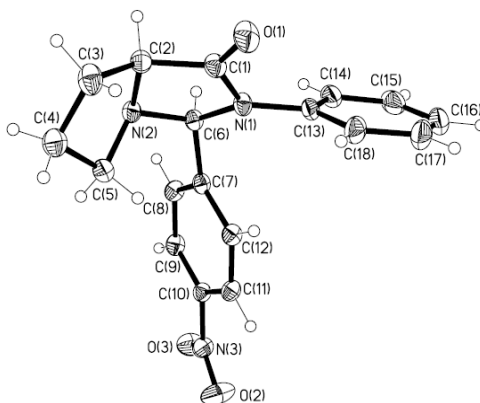
IR



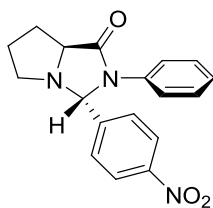
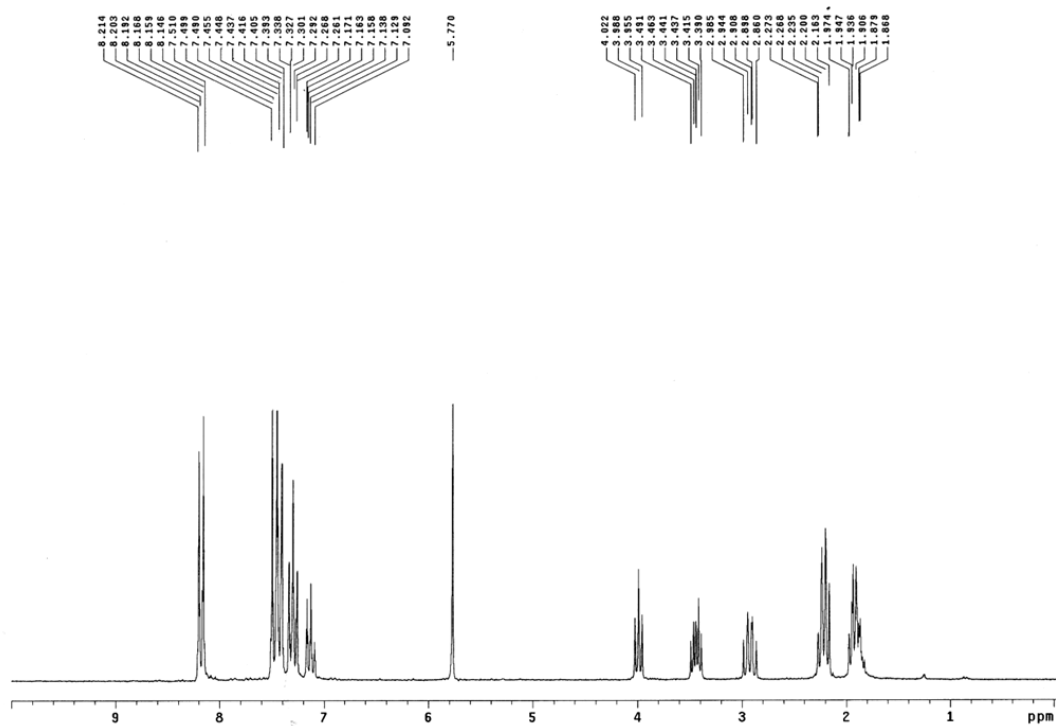
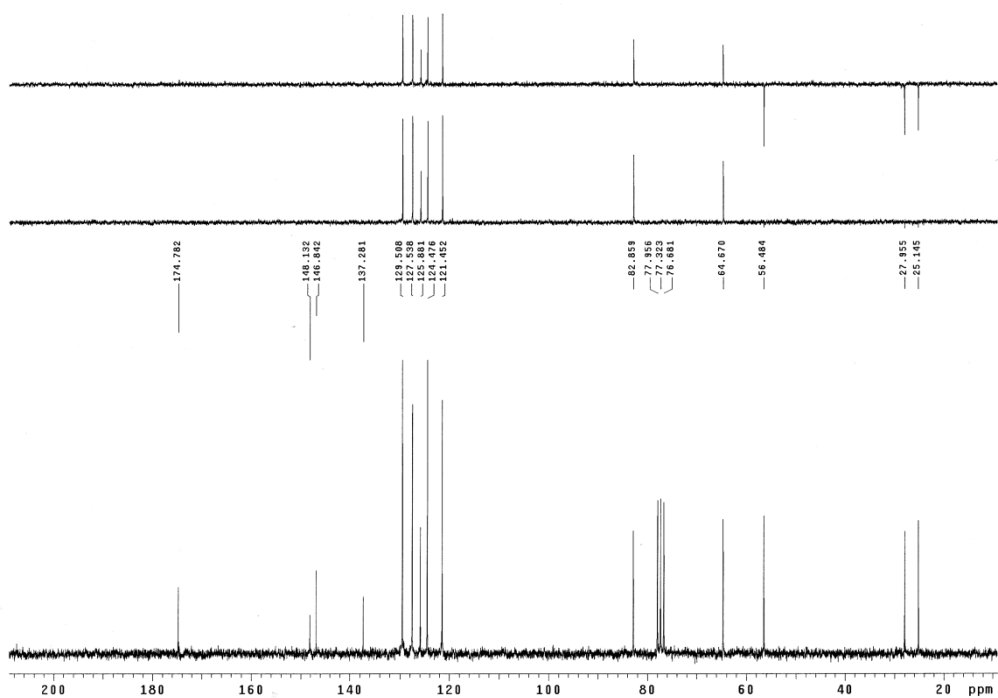
HRMS



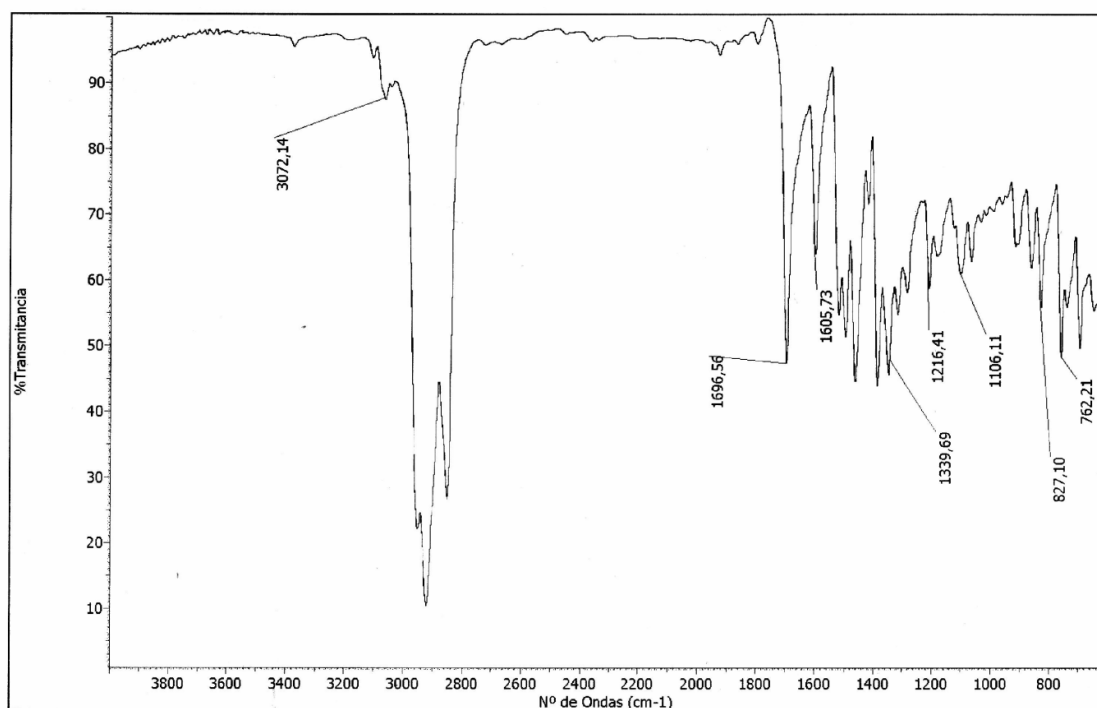
Formula	CalculatedMass	mDaError	ppmError	RDB
C18 H17 N3 O3 Na	346.116213	1.187256	3.430206	11.5
C20 H16 N3 O3	346.118618	-1.218004	-3.519043	14.5
C15 H16 N5 O5	346.114595	2.8047	8.103307	10.5
C23 H17 N O Na	346.120235	-2.835448	-8.192144	15.5
C8 H20 N5 O10	346.120469	-3.06866	-8.865937	1.5

X-ray structure, cristal and refinement data of compound **24a**

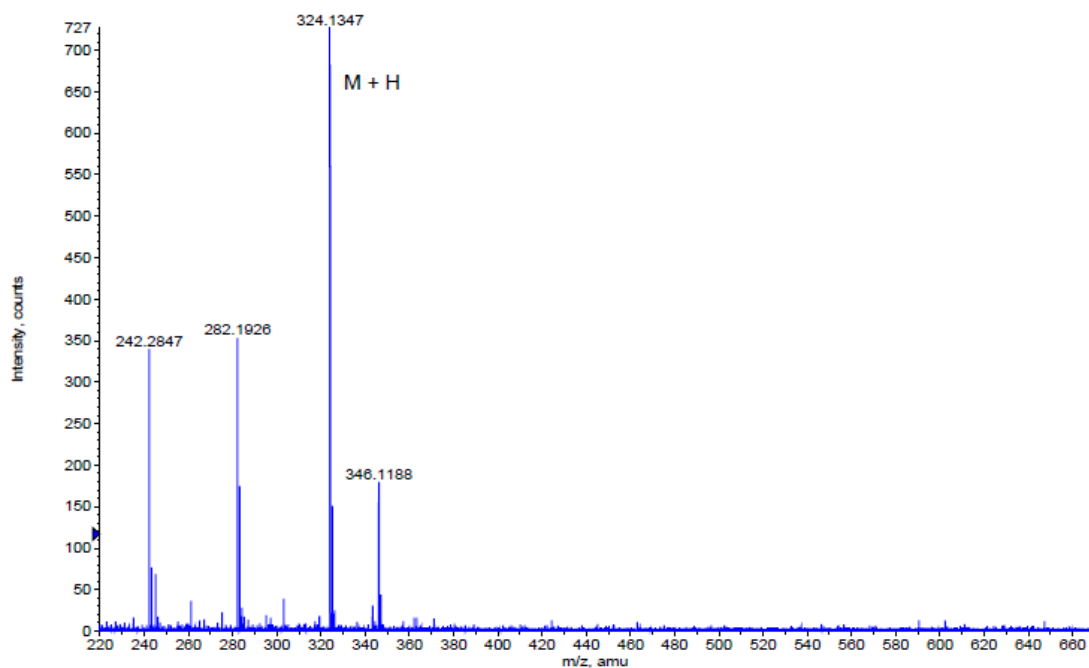
Empirical formula	$C_{18}H_{17}N_3O_3 \cdot CH_2Cl_2$
Molecular weight	408.27
Temperature	293 (2) K
Wavelength	1.54178 Å
Crystal system, Space group	Monoclinic, P2(1)
Unit cell dimensions	$a = 9.8341 (4) \text{ \AA}$ $\alpha = 90.00^\circ$ $b = 8.8407 (4) \text{ \AA}$ $\beta = 98.936 (3)^\circ$ $c = 11.5844 (6) \text{ \AA}$ $\gamma = 90.00^\circ$
Volume	$994.93 (8) \text{ \AA}^3$
Z; Density (calculated)	2; 1.363 mg/m^3
Absorption coefficient	3.142 mm^{-1}
F(000)	424
Crystal size	0.15 x 0.10 x 0.08 mm
θ range	$3.86 - 64.58^\circ$
Limiting indices h, k, l	$-11 \leq h \leq 11, -10 \leq k \leq 10, -13 \leq l \leq 7$
Reflections collected/independent	5546/1820 $R_{\text{int}} = 0.0303$
Refinement method	Least squares method with full matrix in F^2
Data/restraints/parameters	2820/1/252
Goodness-of-fit on F^2	1.051
Final R indices [$I > 2\sigma(I)$]	$R_1 = 0.0614, \omega R_2 = 0.1745$
R indices (all data)	$R_1 = 0.0715, \omega R_2 = 0.1867$
Extinction coefficient	0.0108(5)

- (3*R*,7*aS*)-3-(4-Nitrophenyl)-2-phenylhexahydropyrrolo[1,2-*e*]imidazol-1-one (24b)¹H NMR (CDCl₃, 200 MHz)¹³C NMR (CDCl₃, 50 MHz)

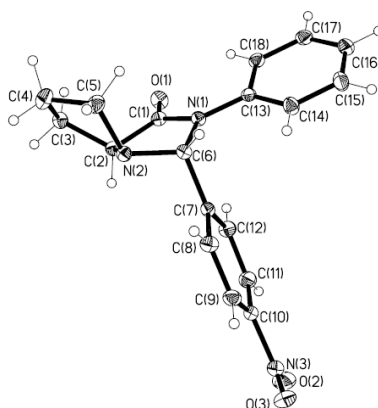
IR



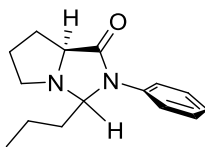
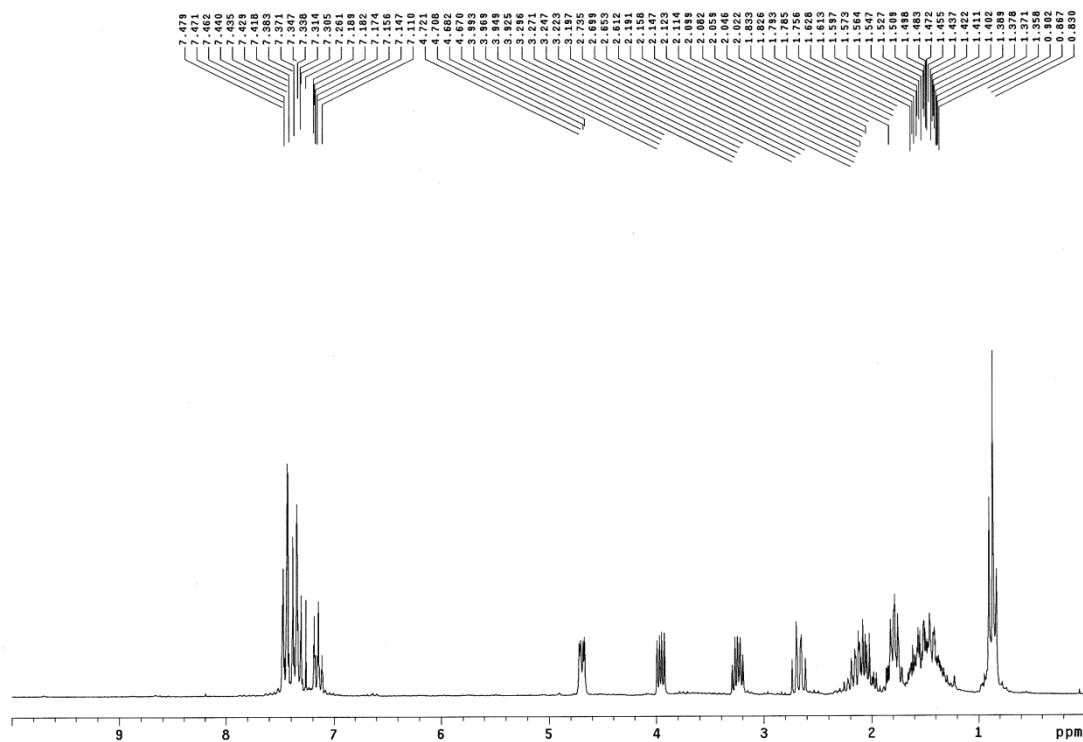
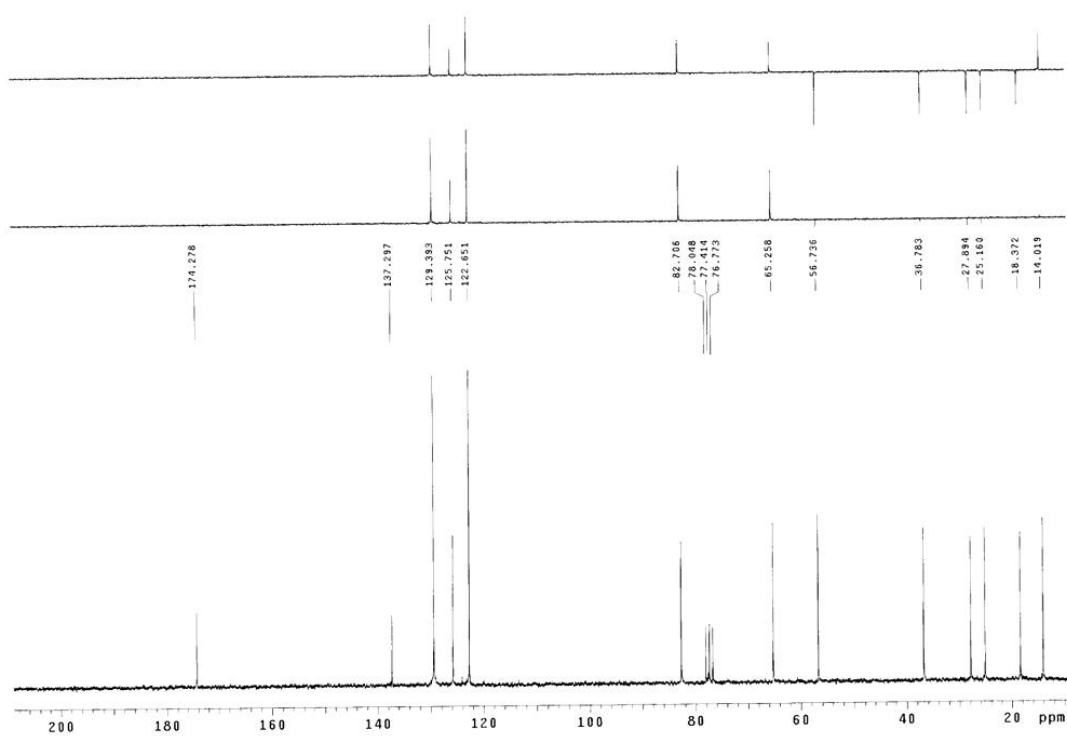
HRMS



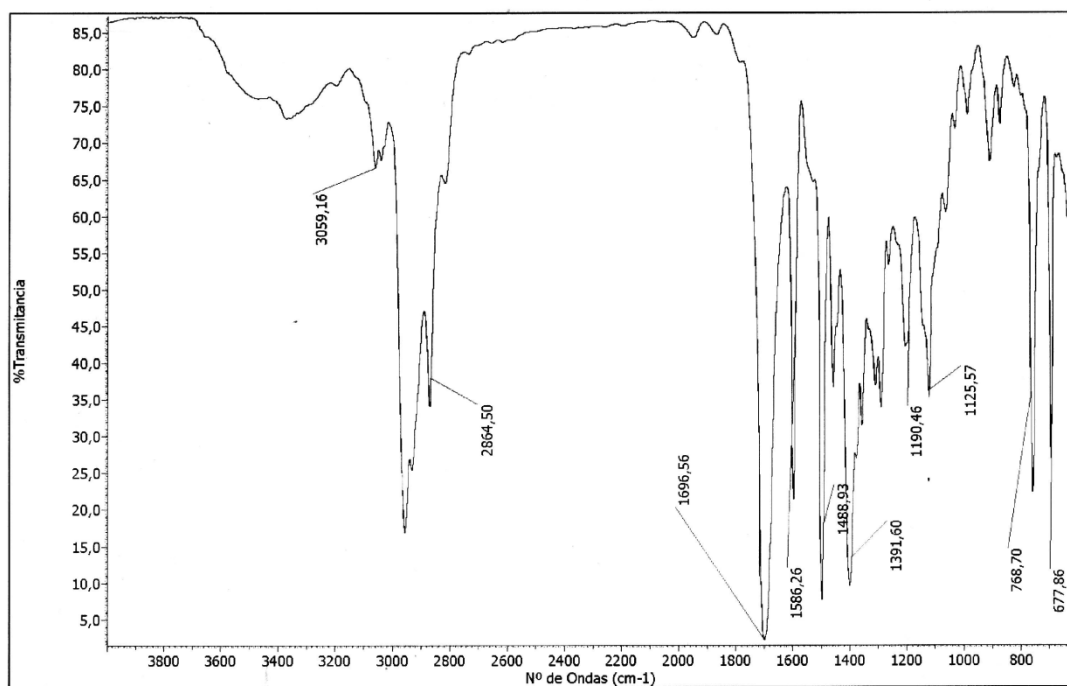
Formula	CalculatedMass	mDaError	ppmError	RDB
C18 H18 N3 O3	324.134268	0.431916	1.332518	11.5
C21 H19 N O Na	324.135886	-1.185528	-3.65751	12.5
C16 H19 N3 O3 Na	324.131863	2.837176	8.753062	8.5
C9 H23 N3 O8 Na	324.137736	-3.036184	-9.367028	-0.5

X-ray structure, cristal and refinement data of compound **24b**

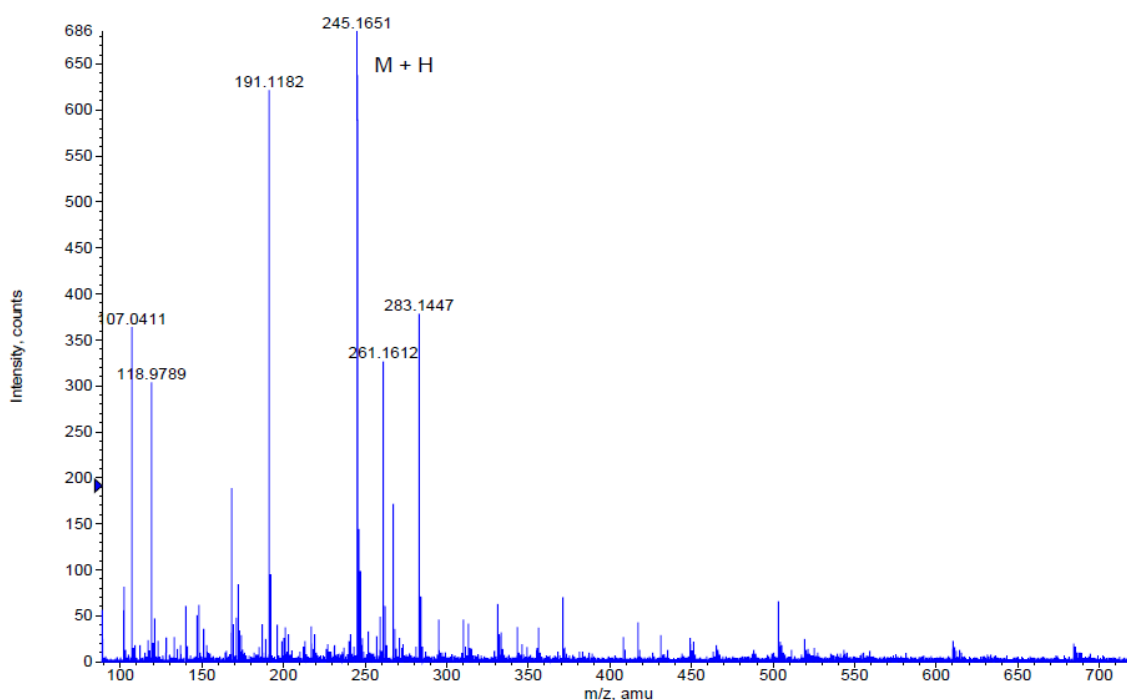
Empirical formula	$C_{18}H_{17}N_3O_3$
Molecular weight	323.35
Temperature	293 (2) K
Wavelength	1.54178 Å
Crystal system, Space group	Orthorhombic, P2(1)2(1)2(1)
Unit cell dimensions	a = 6.6712 (2) Å $\alpha = 90.00^\circ$ b = 14.9403 (4) Å $\beta = 90.00^\circ$ c = 15.7482 (4) Å $\gamma = 90.00^\circ$
Volume	1569.62 (7) Å ³
Z; Density (calculated)	4; 1.368 mg/m ³
Absorption coefficient	0.780 mm ⁻¹
F(000)	680
Crystal size	0.20 x 0.15 x 0.10 mm
θ range	5.62 – 64.85 °
Limiting indices h, k, l	-6 ≤ h ≤ 7, -14 ≤ k ≤ 16, -18 ≤ l ≤ 17
Reflections collected/independent	5546/2820 $R_{int} = 0.0178$
Refinement method	Least squares method with full matrix in F^2
Data/restraints/parameters	2820/1/252
Goodness-of-fit on F^2	1.043
Final R indices [$I > 2\sigma(I)$]	$R_1 = 0.0262$, $\omega R_2 = 0.0695$
R indices (all data)	$R_1 = 0.0277$, $\omega R_2 = 0.0708$
Extinction coefficient	0.0108 (3)

- (7aS)-2-Phenyl-3-propyl-hexahydropyrrolo[1,2-e]imidazol-1-one (29b)¹H NMR (CDCl₃, 200 MHz)¹³C NMR (CDCl₃, 50 MHz)

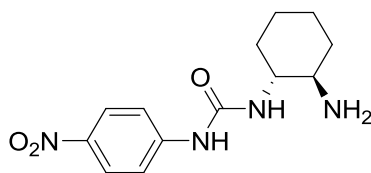
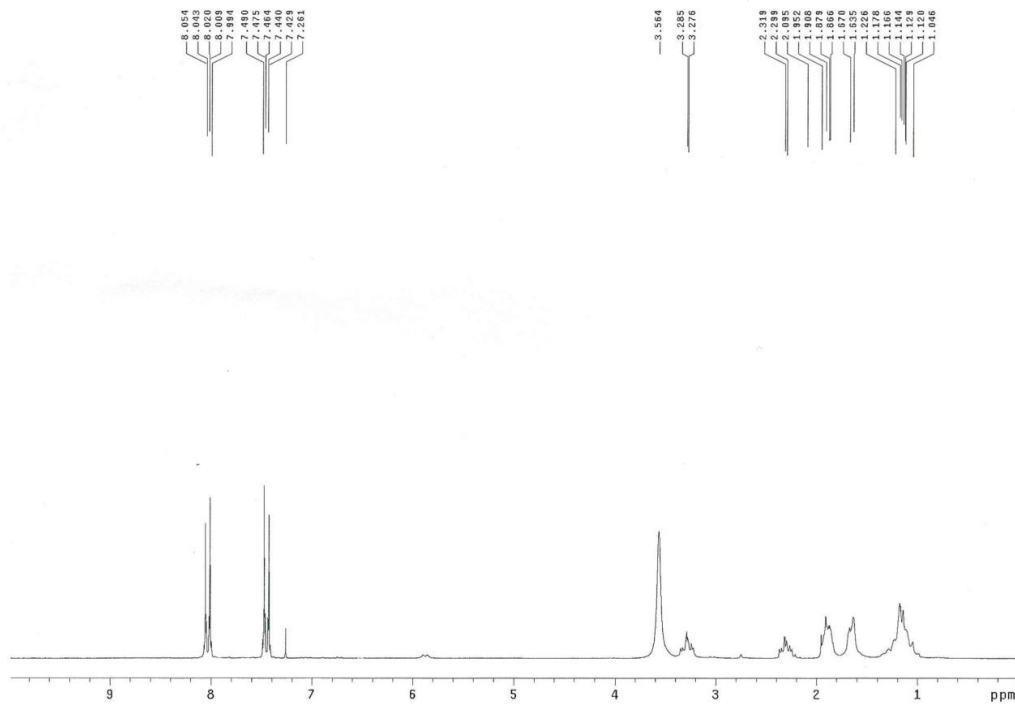
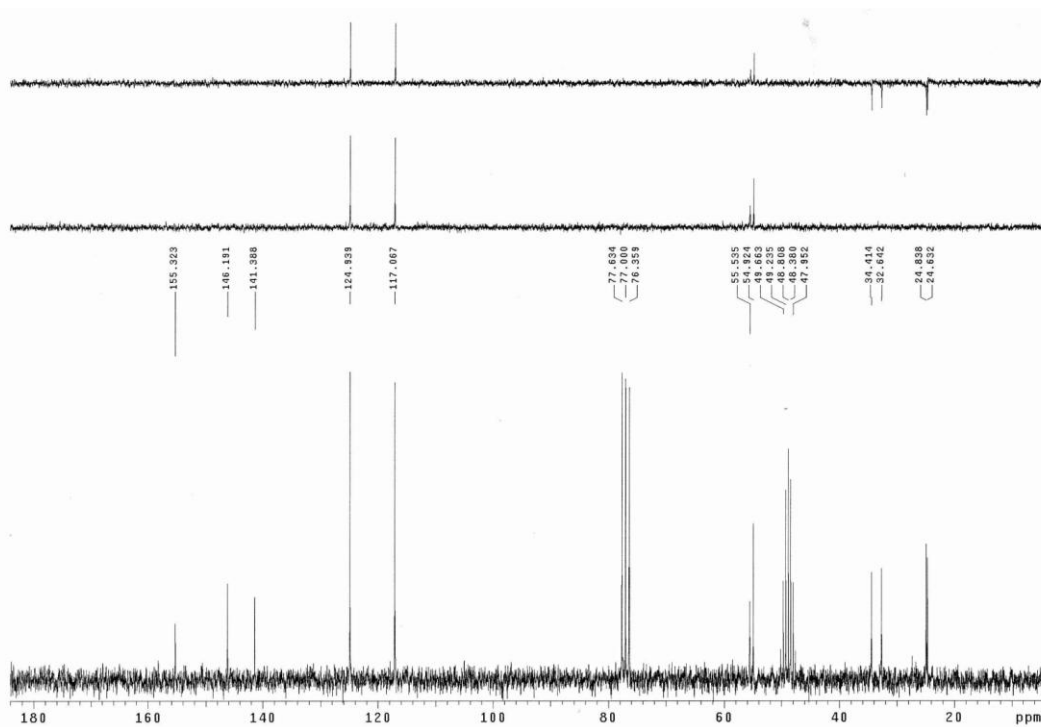
IR



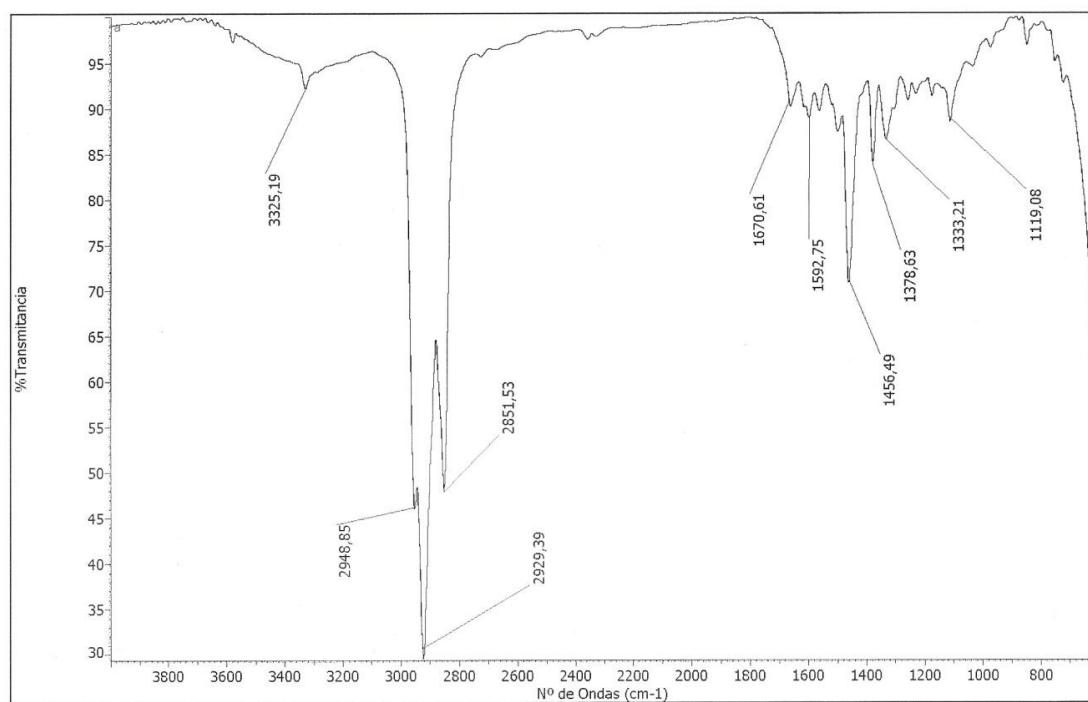
HRMS



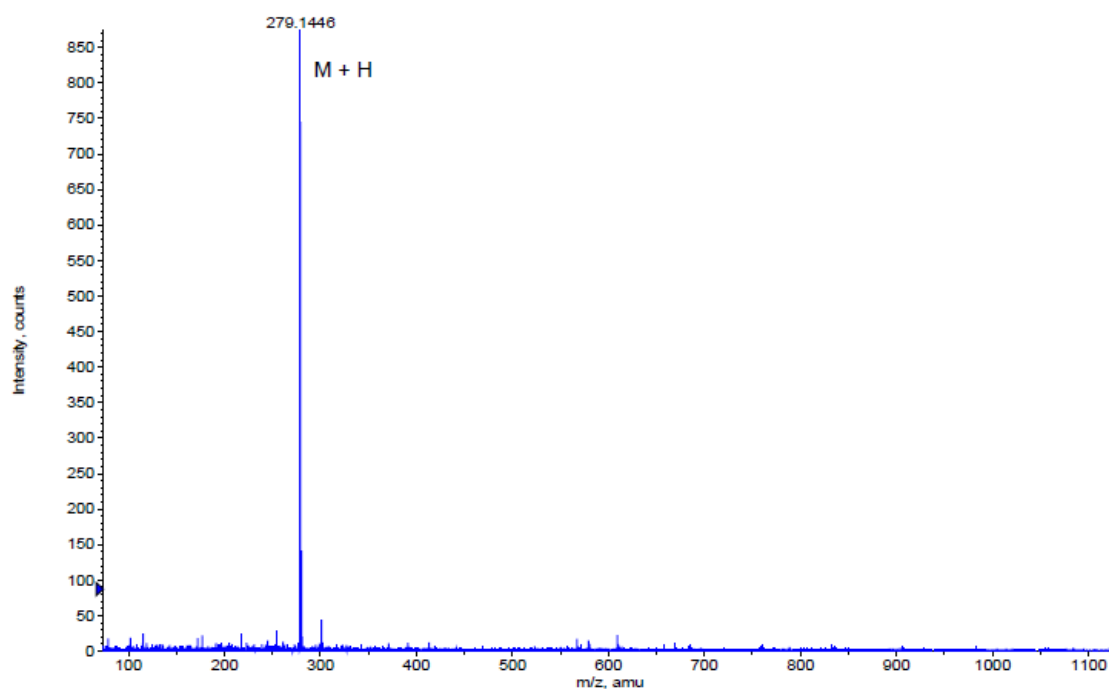
Formula	CalculatedMass	mDaError	ppmError	RDB
C ₁₅ H ₂₁ N ₂ O	245.16484	0.260084	1.06085	6.5

- (1*R*,2*R*)-1,2-diaminocyclohexane 4-nitrophenylurea (42)¹H RMN (CDCl₃-CD₃OD, 200 MHz)¹³C RMN (CDCl₃-CD₃OD, 50 MHz)

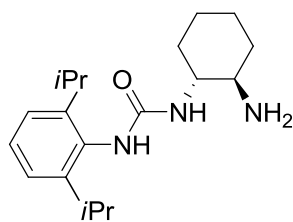
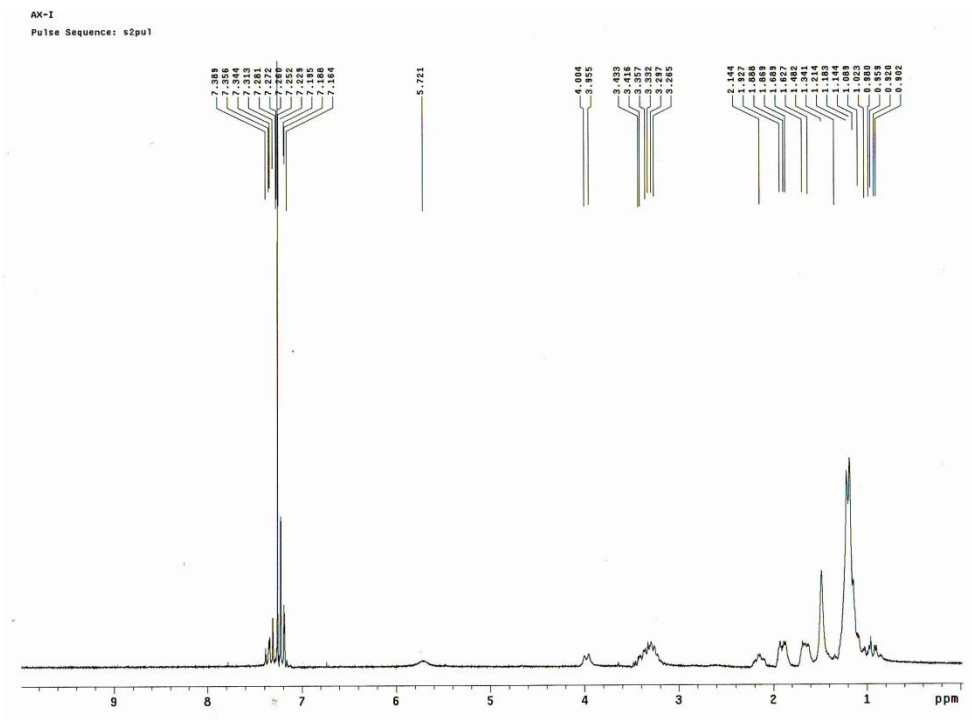
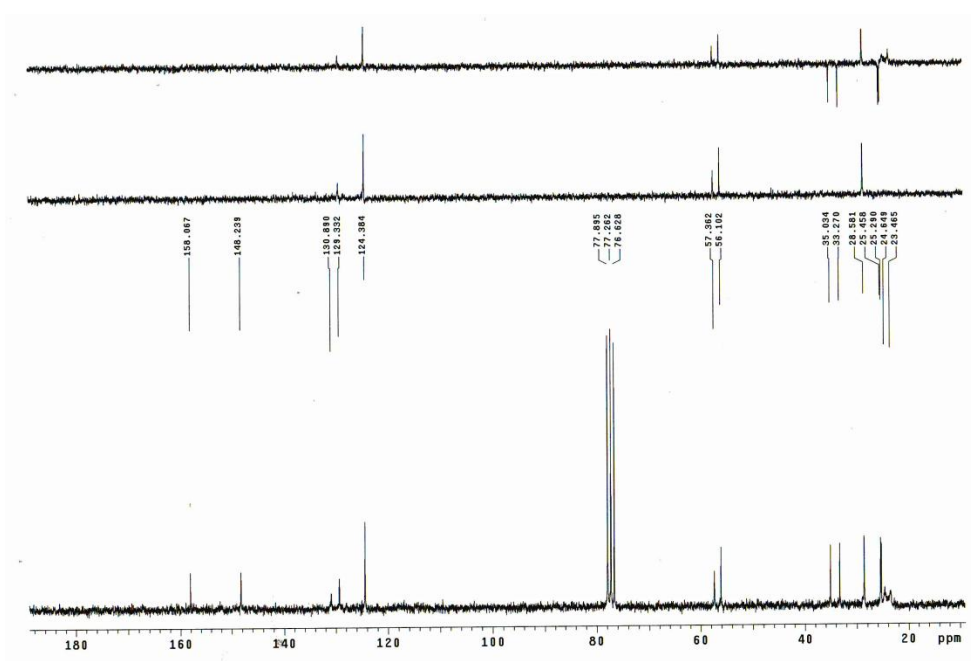
IR



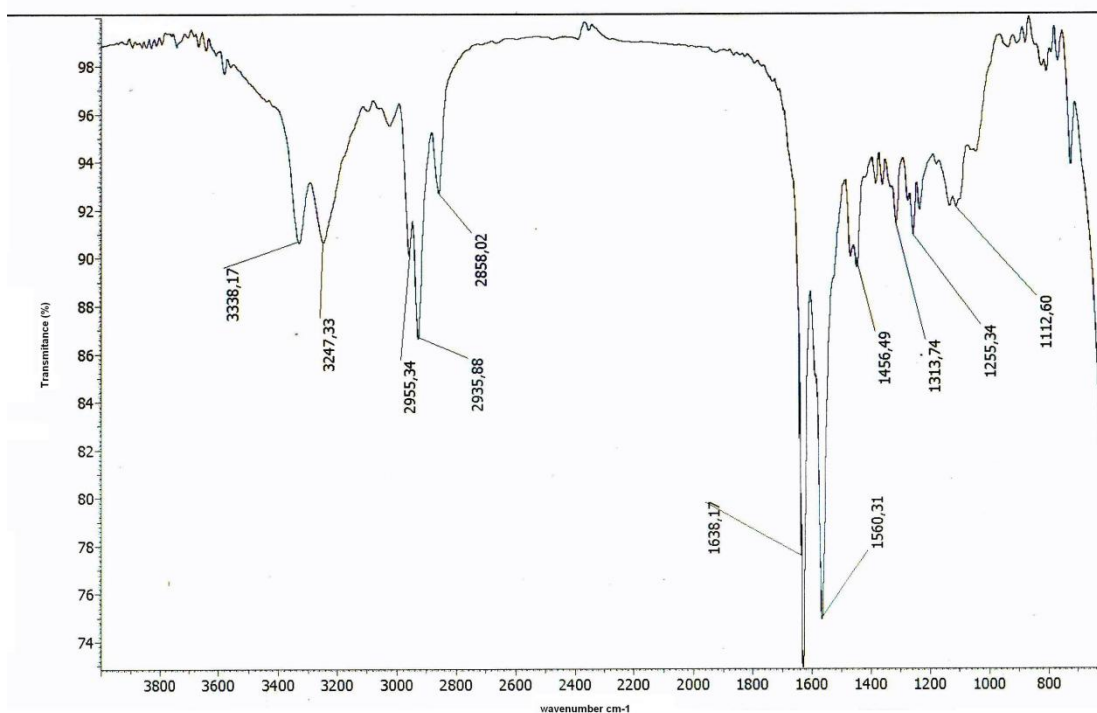
HRMS



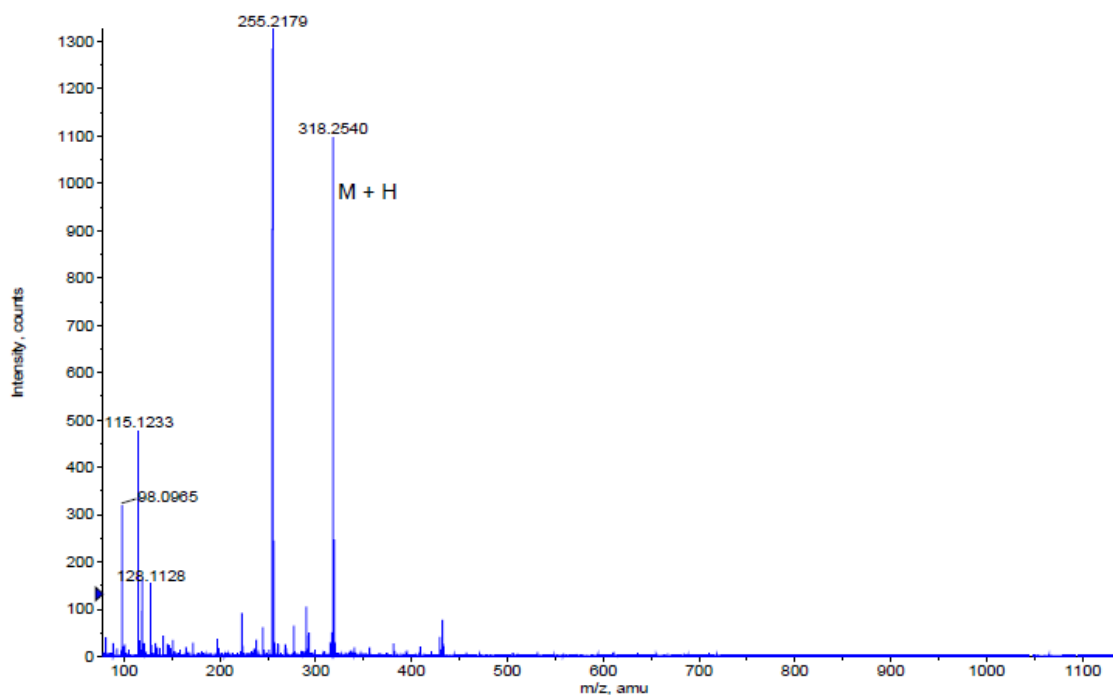
Formula	CalculatedMass	mDaError	ppmError	RDB
C13 H19 N4 O3	279.145167	-0.567132	-2.031674	6.5
C12 H23 O7	279.14383	0.77018	2.759066	1.5
C11 H20 N4 O3 Na	279.142762	1.838128	6.584847	3.5
C16 H20 N2 O Na	279.146785	-2.184576	-7.82595	7.5

- (1*R*,2*R*)-1,2-diaminocyclohexane 2,6-diisopropylphenylurea (44)¹H RMN (CDCl₃, 200 MHz)¹³C RMN (CDCl₃, 50 MHz)

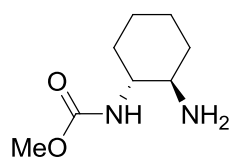
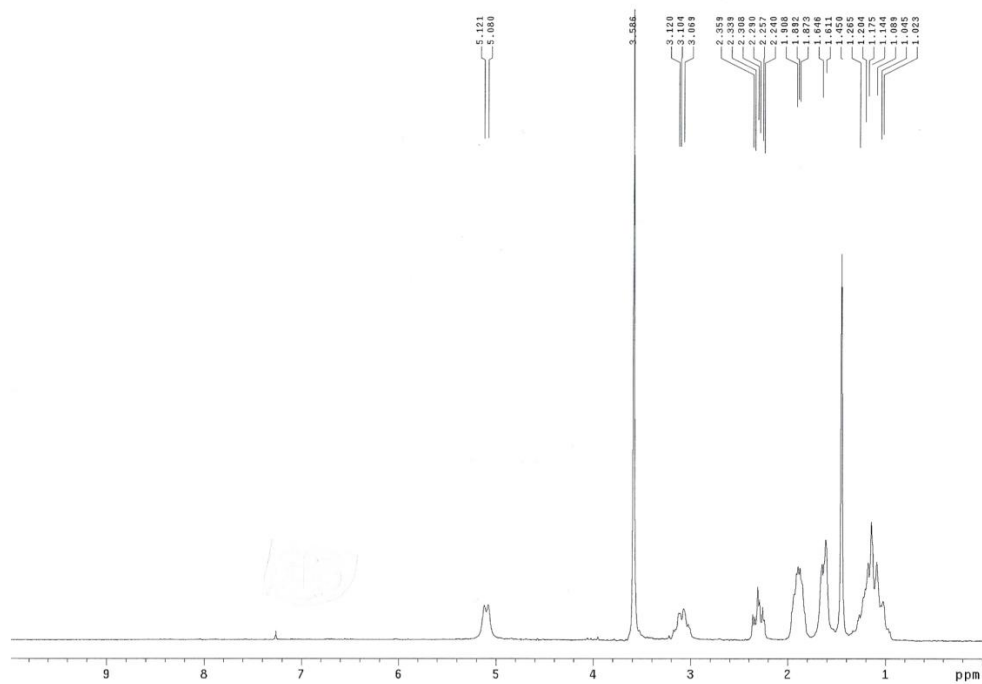
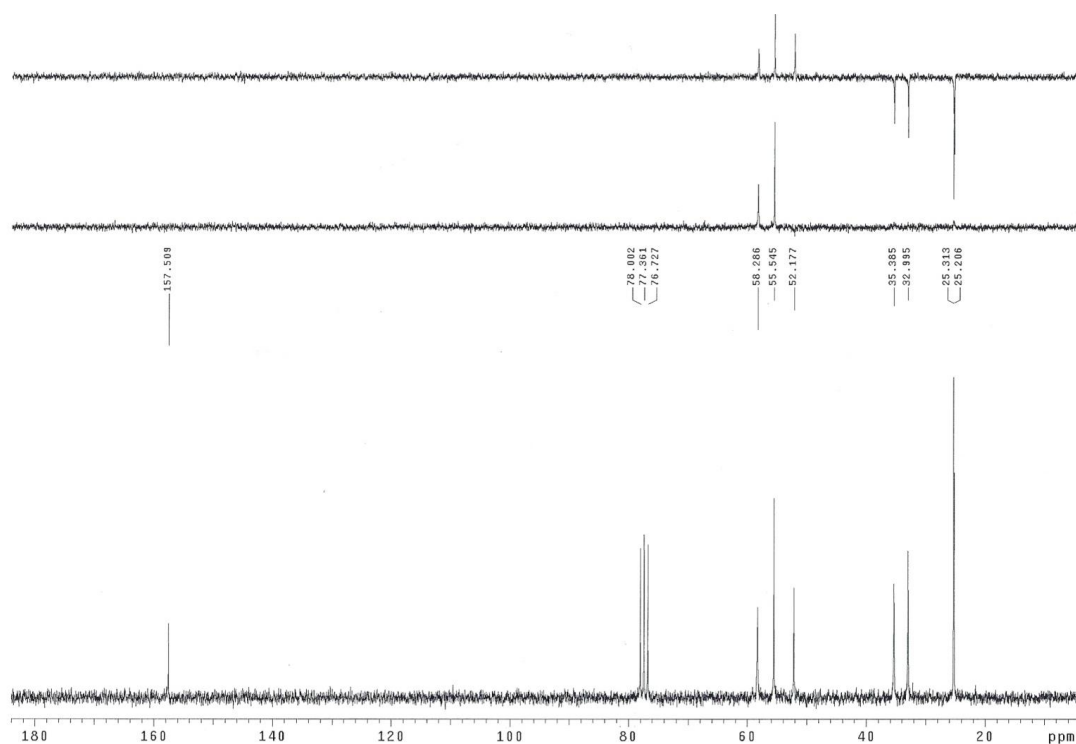
IR



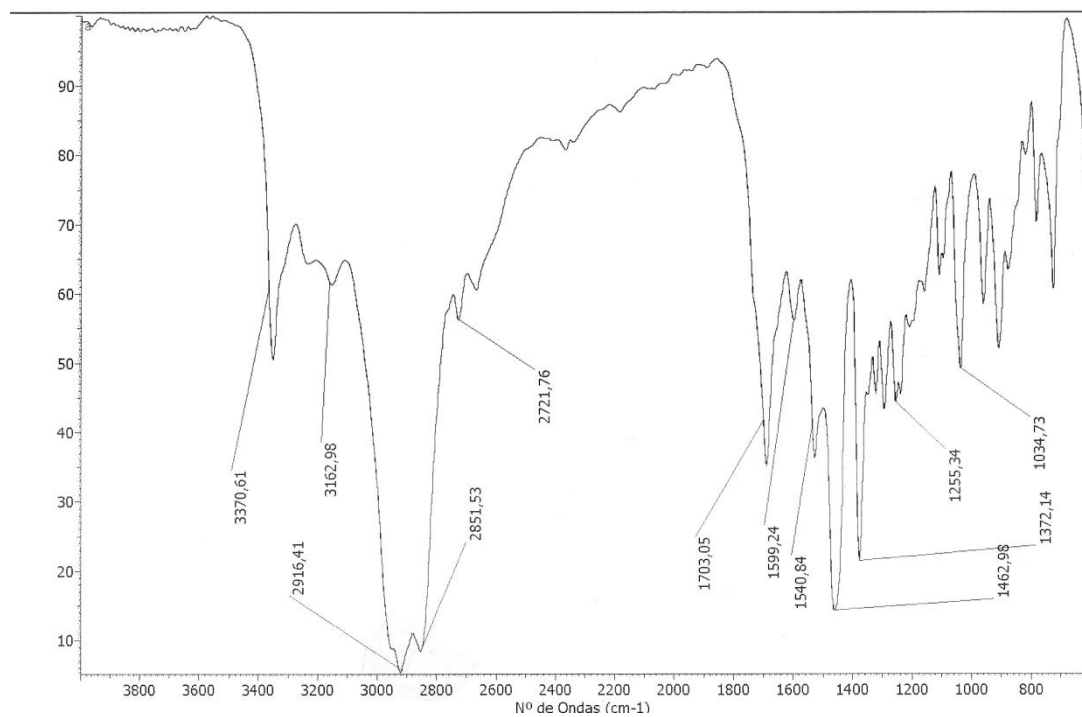
HRMS



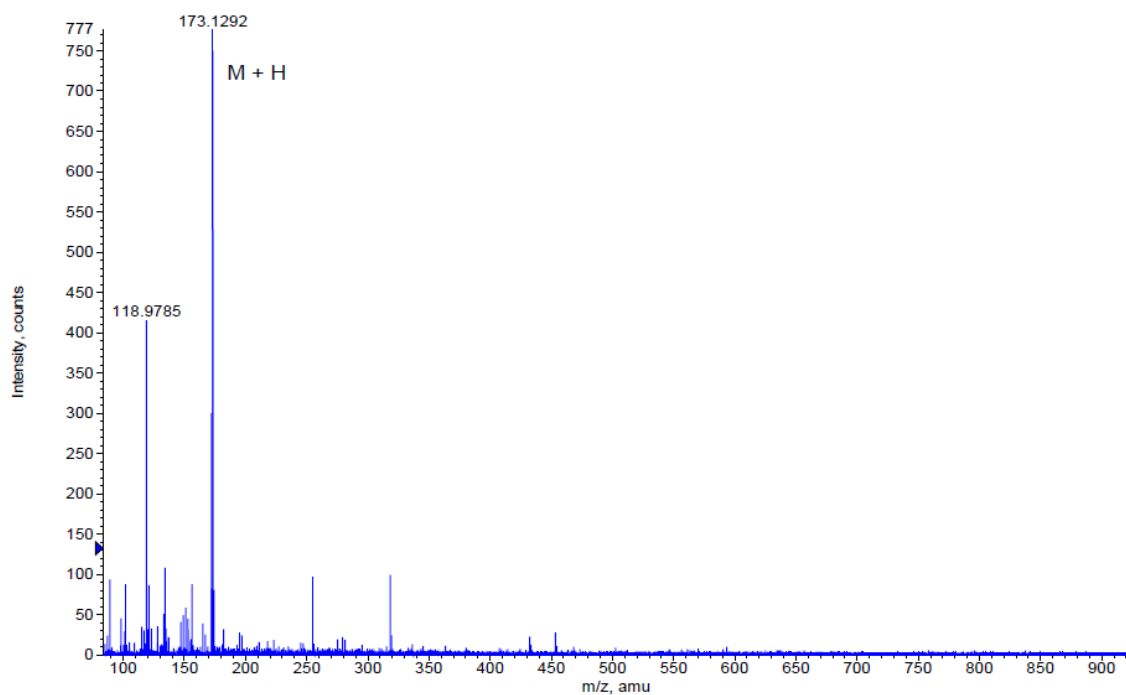
Formula	CalculatedMass	mDaError	ppmError	RDB
C ₁₉ H ₃₂ N ₃ O	318.253989	0.010636	0.03342	5.5
C ₁₇ H ₃₃ N ₃ O Na	318.251584	2.415896	7.591081	2.5

- Methyl (1*R*,2*R*)-2-aminocyclohexylcarbamate (45)¹H RMN (CDCl₃, 200 MHz)¹³C RMN (CDCl₃, 50 MHz)

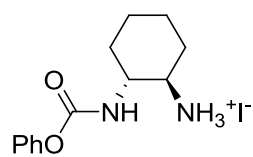
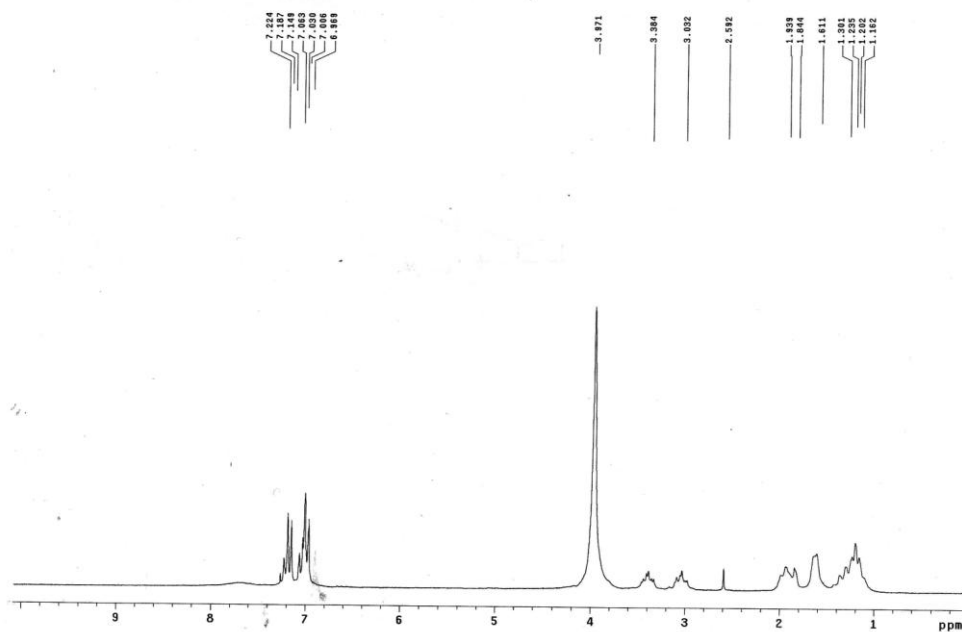
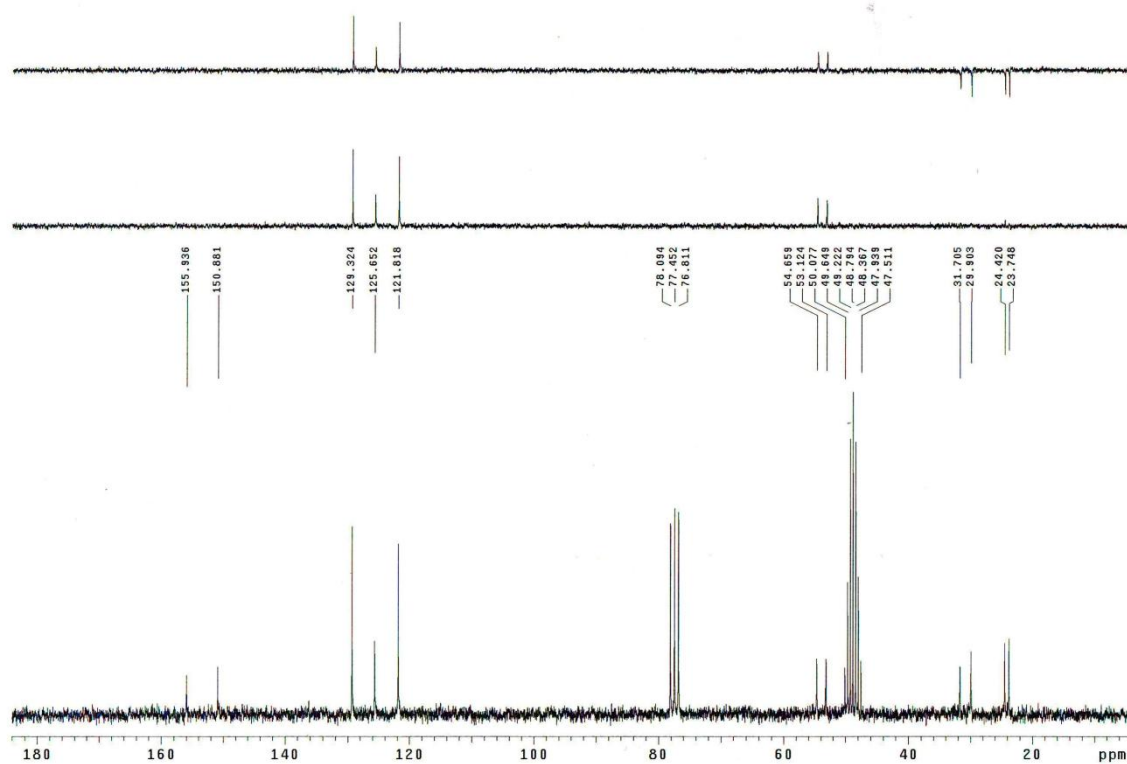
IR



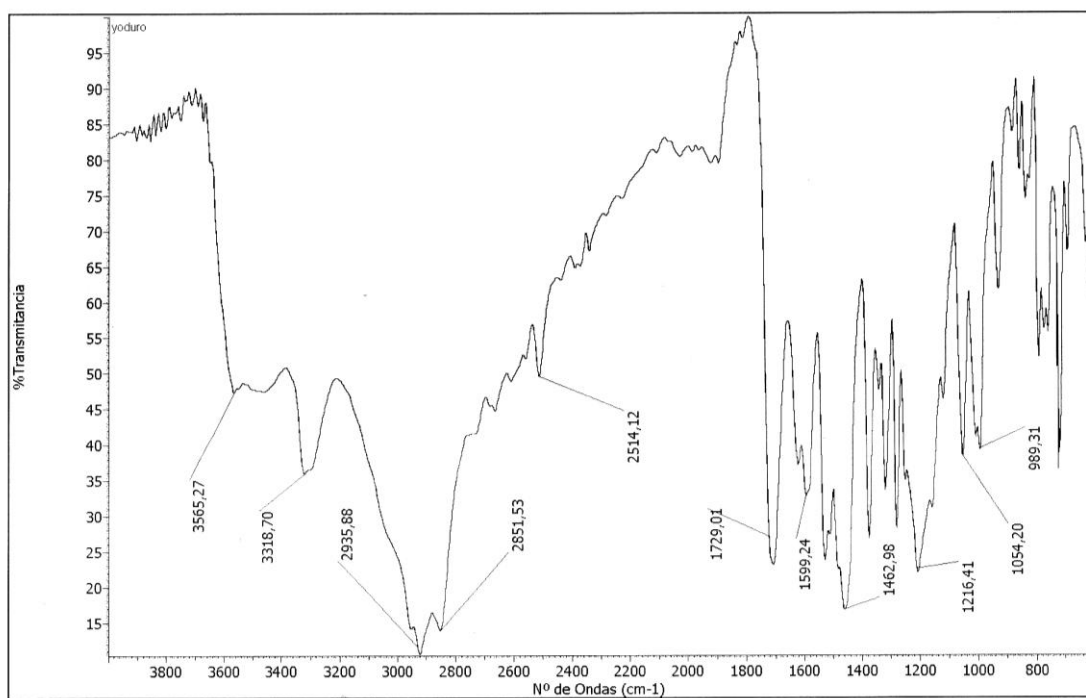
HRMS



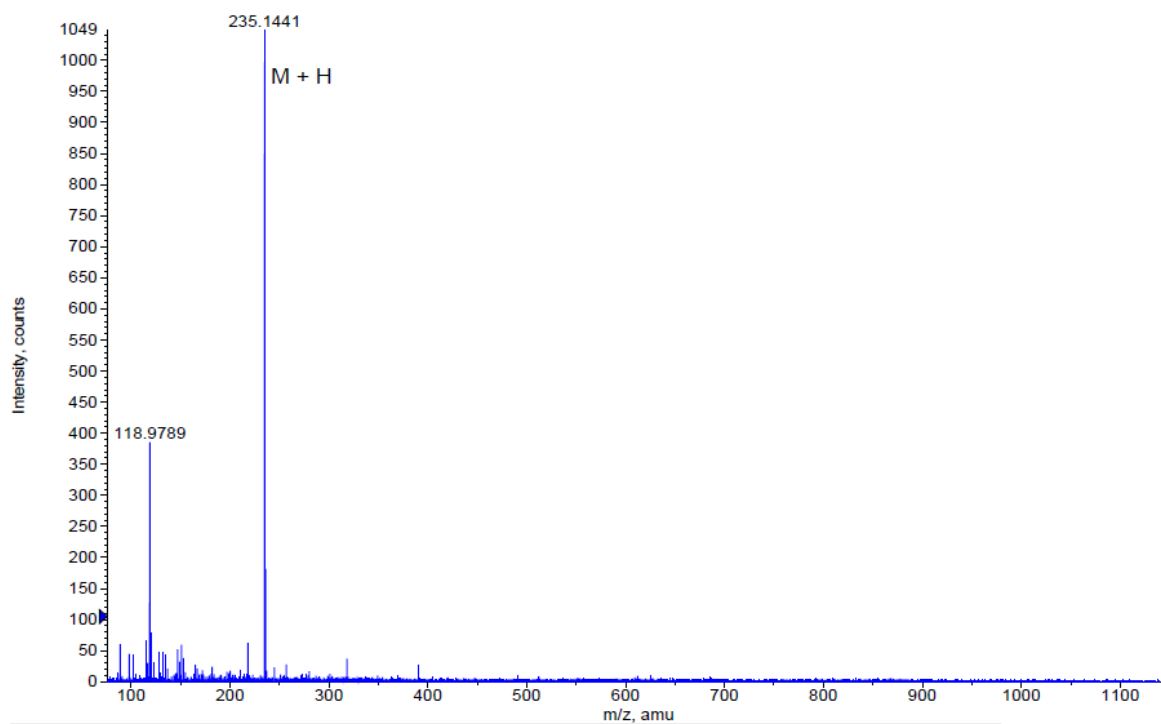
Formula	CalculatedMass	mDaError	ppmError	RDB
C8 H17 N2 O2	173.128454	0.745604	4.30662	1.5
C11 H18 Na	173.130072	-0.87184	-5.035761	2.5

- Phenyl (1*R*,2*R*)-2-aminocyclohexylcarbamate (47)¹H RMN (CDCl₃-CD₃OD, 200 MHz)¹³C RMN (CDCl₃-CD₃OD, 50 MHz)

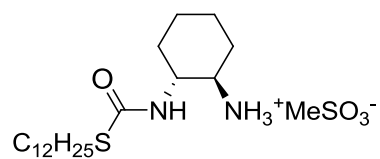
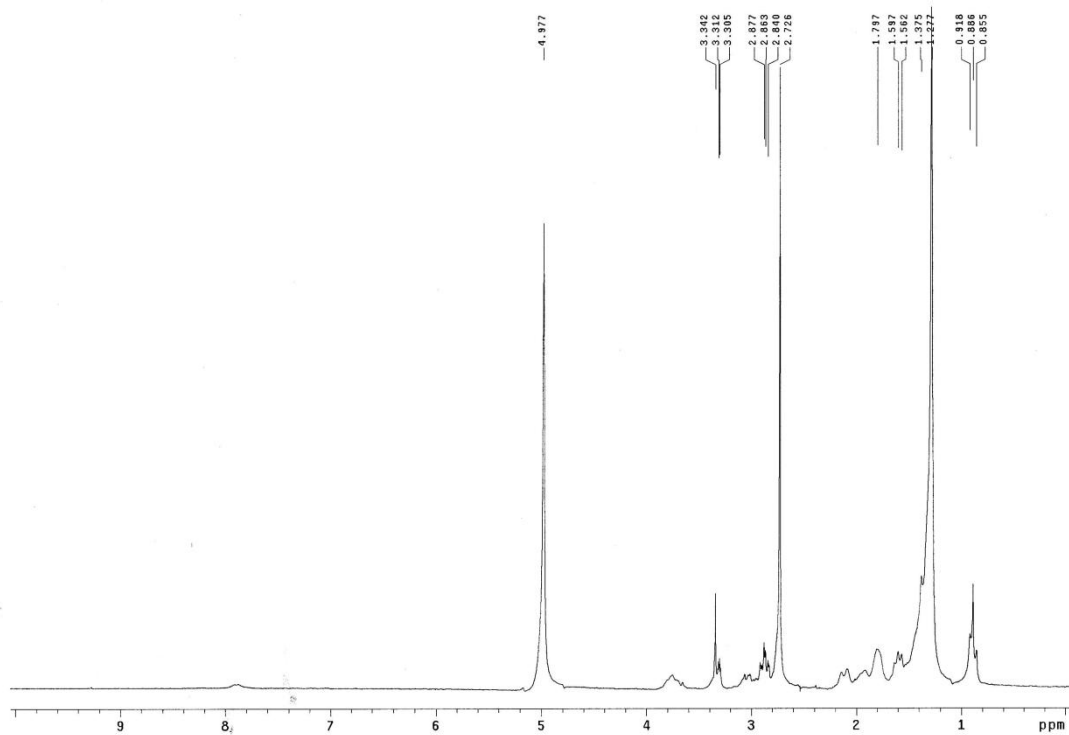
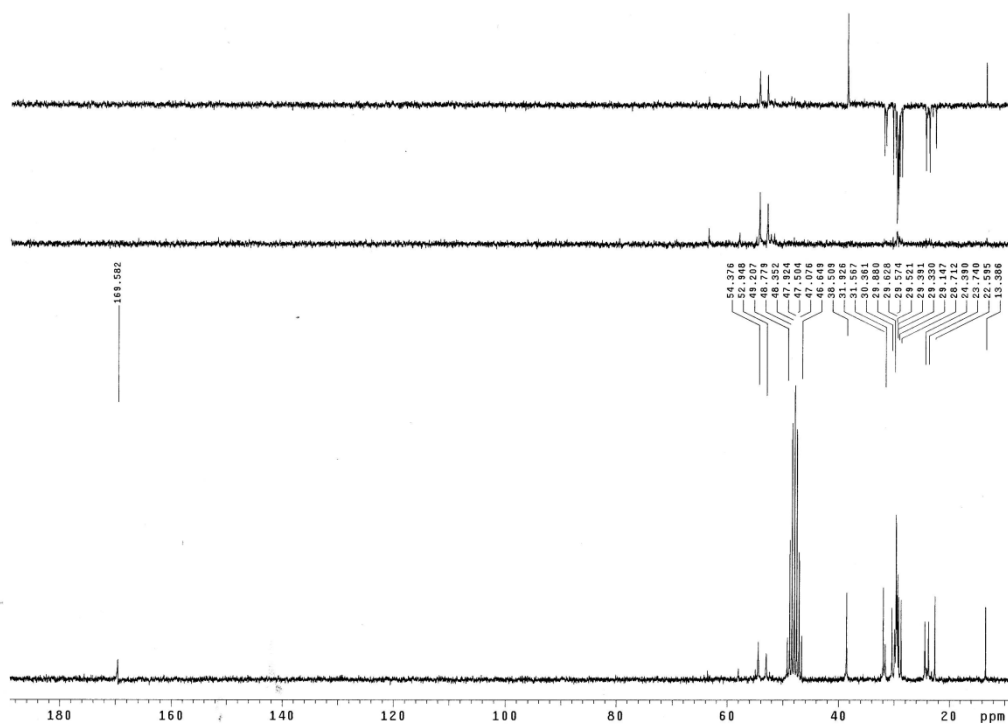
IR



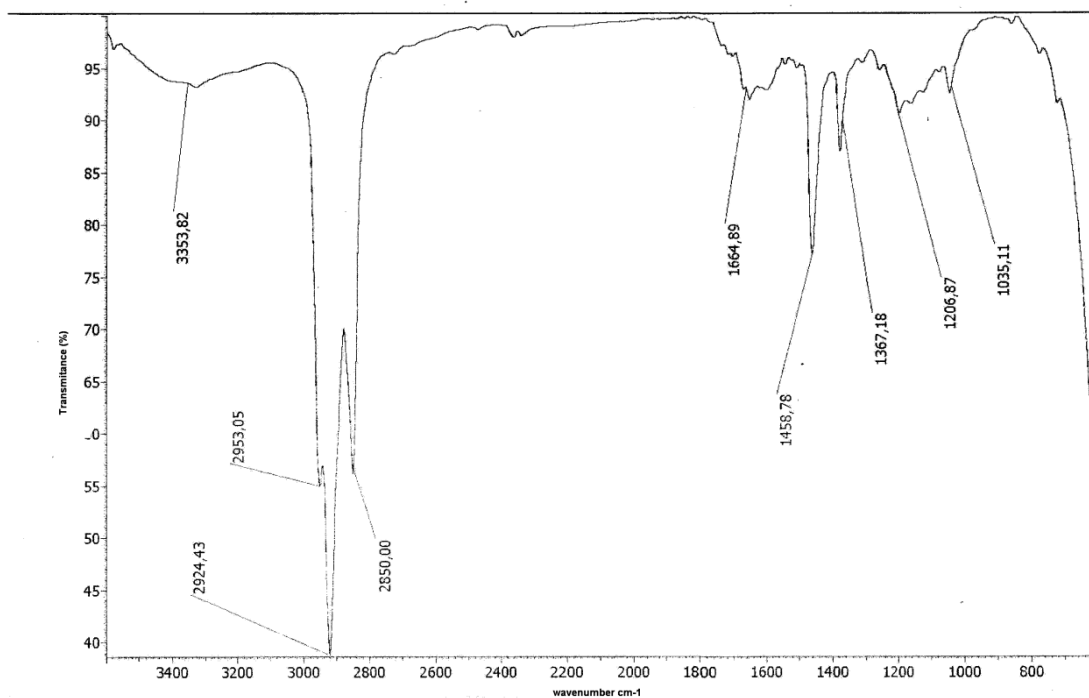
HRMS



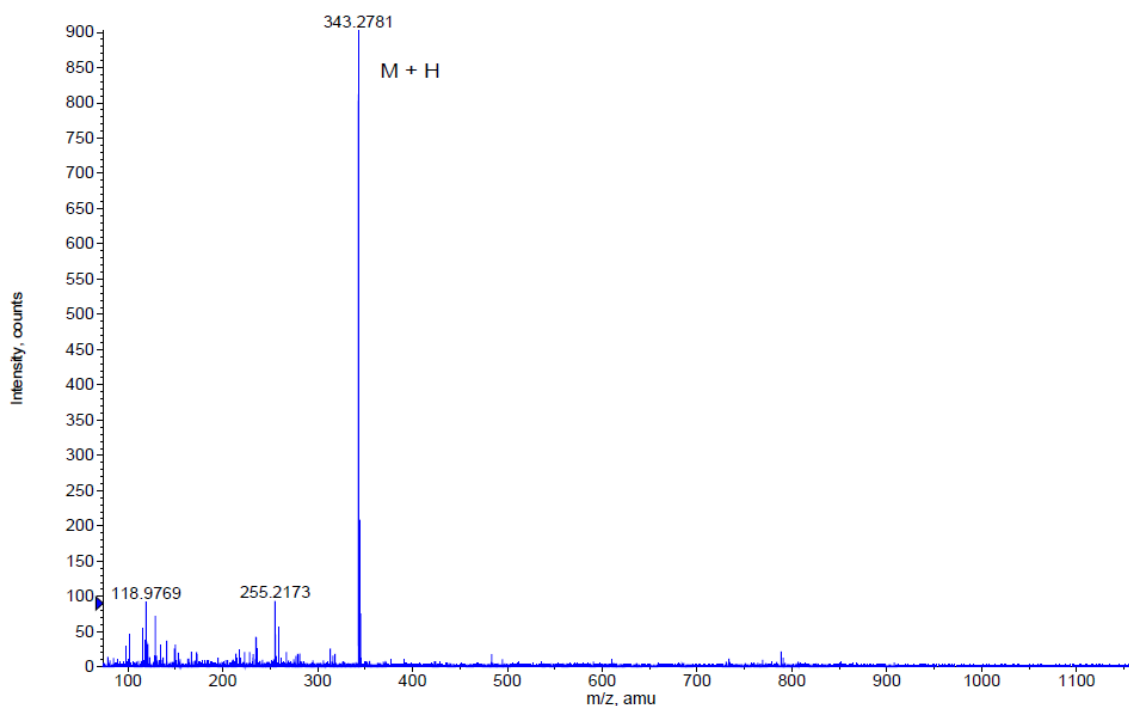
Formula	CalculatedMass	mDaError	ppmError	RDB
C13 H19 N2 O2	235.144104	-0.004476	-0.019035	5.5
C16 H20 Na	235.145722	-1.62192	-6.897542	6.5

- S-dodecyl (1R,2R)-2-aminocyclohexylcarbamothioate (48) 1H RMN (CD_3OD , 200 MHz) ^{13}C RMN (CD_3OD , 50 MHz)

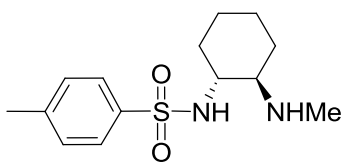
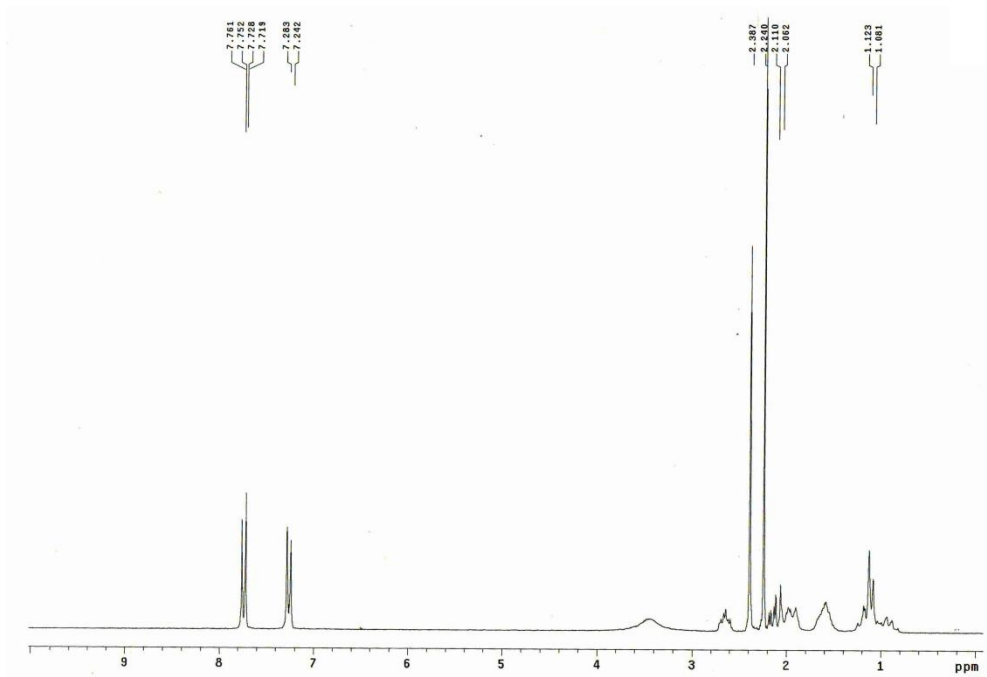
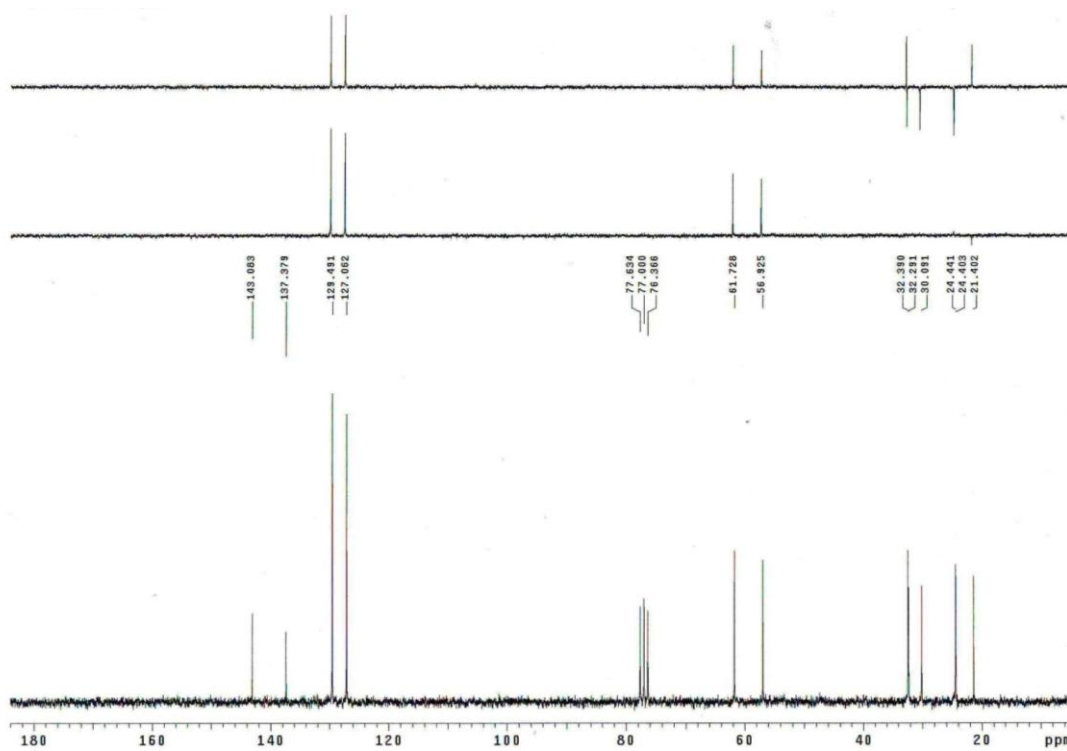
IR



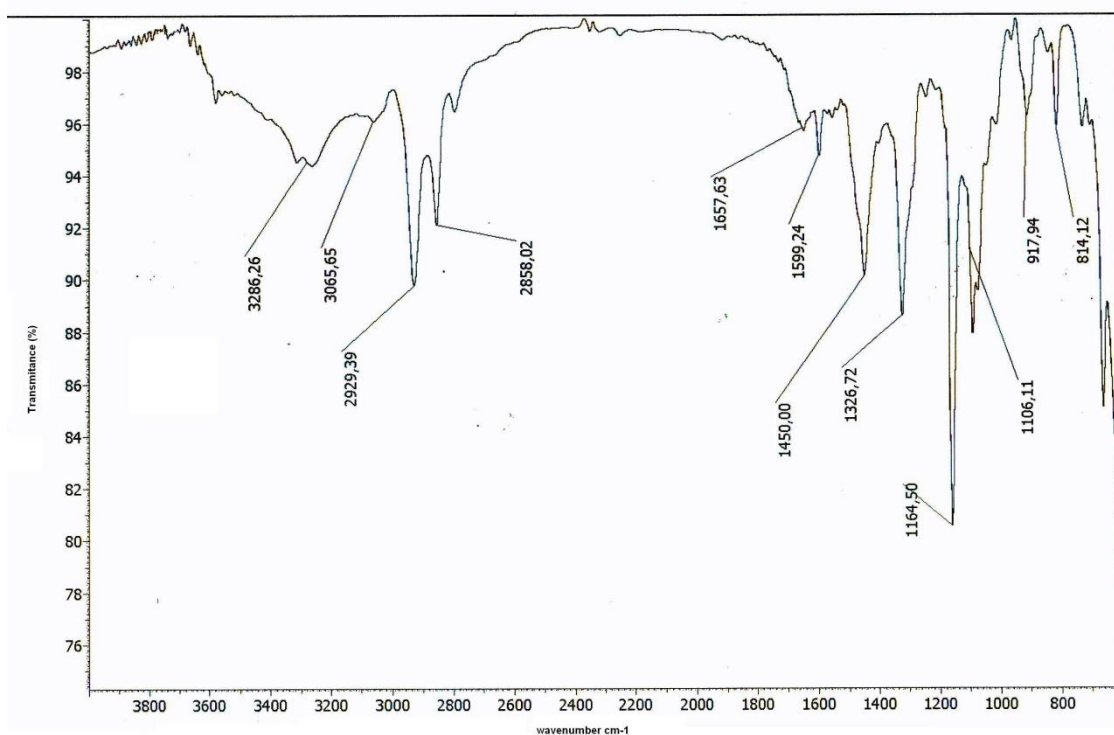
HRMS



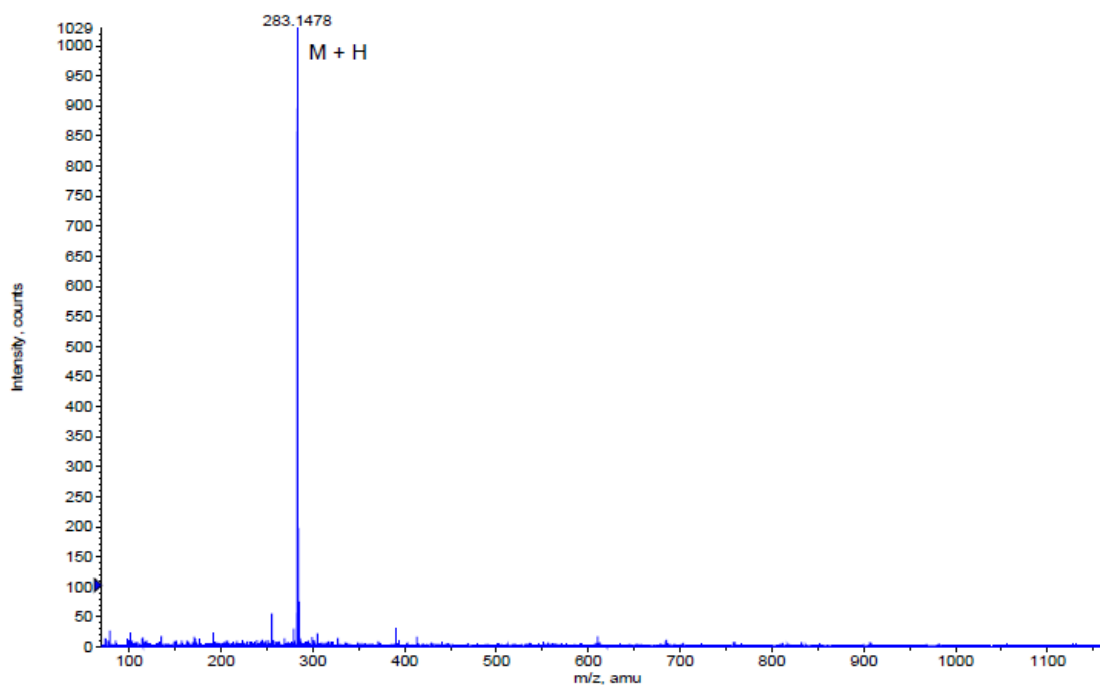
Formula	CalculatedMass	mDaError	ppmError	RDB
C ₁₉ H ₃₉ N ₂ O ₅	343.277762	0.337564	0.983353	1.5

- 4-Methyl-N-((1R,2R)-2-(methylamino)cyclohexyl)benzenesulfonamide (52)¹H RMN (CDCl₃, 200 MHz)¹³C RMN (CDCl₃, 50 MHz)

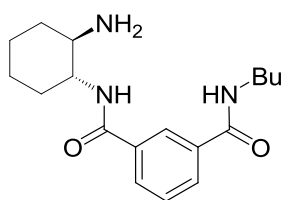
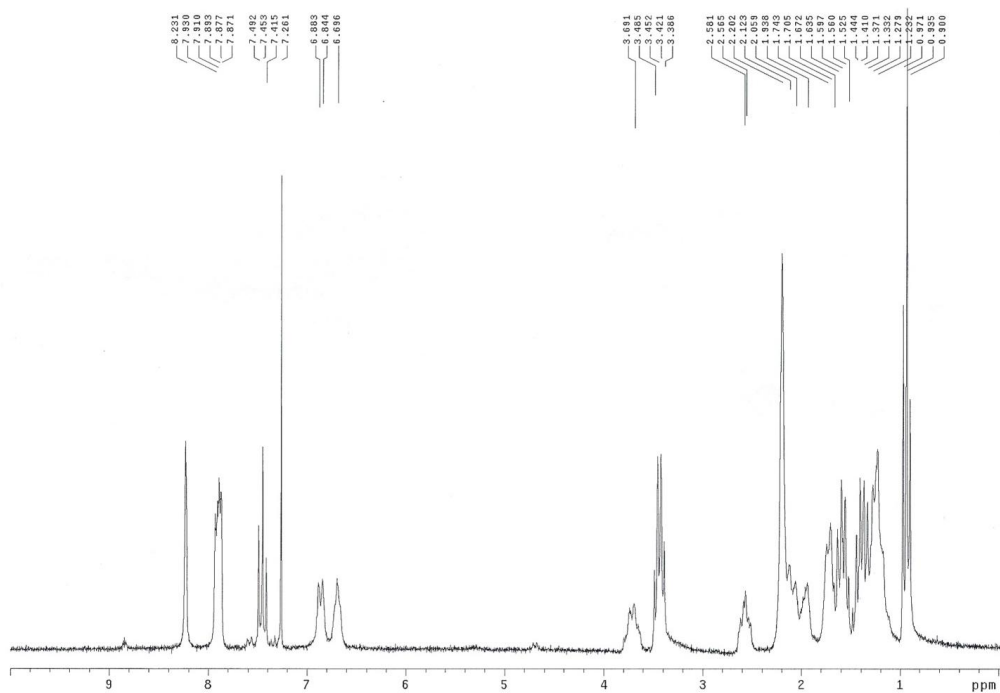
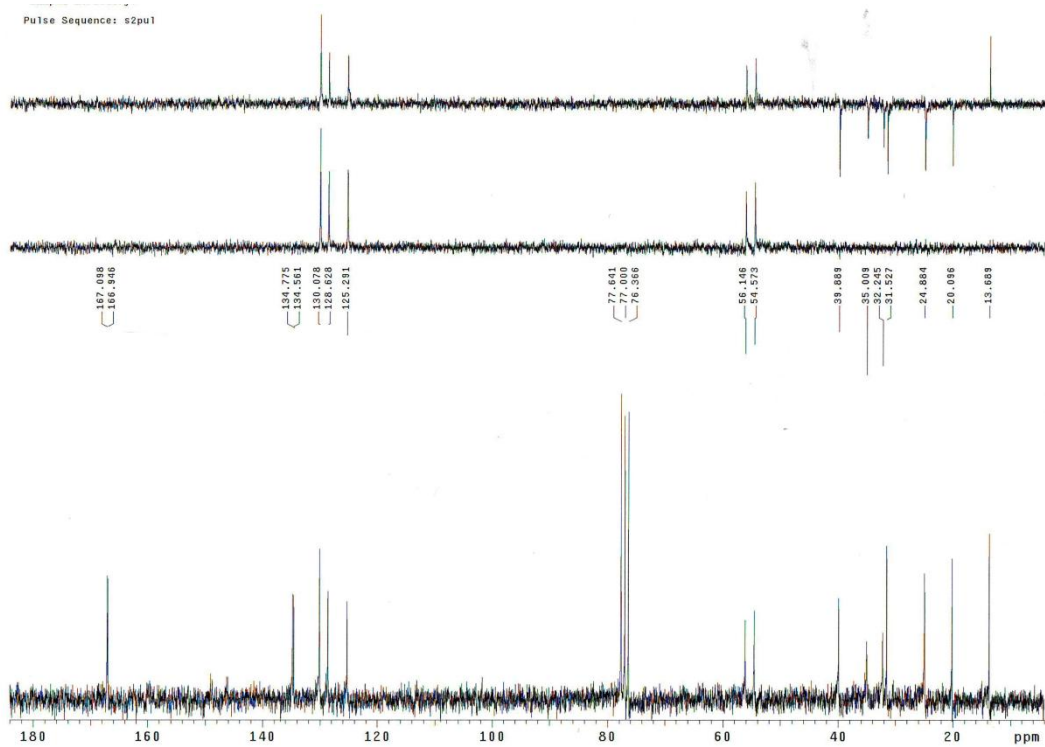
IR



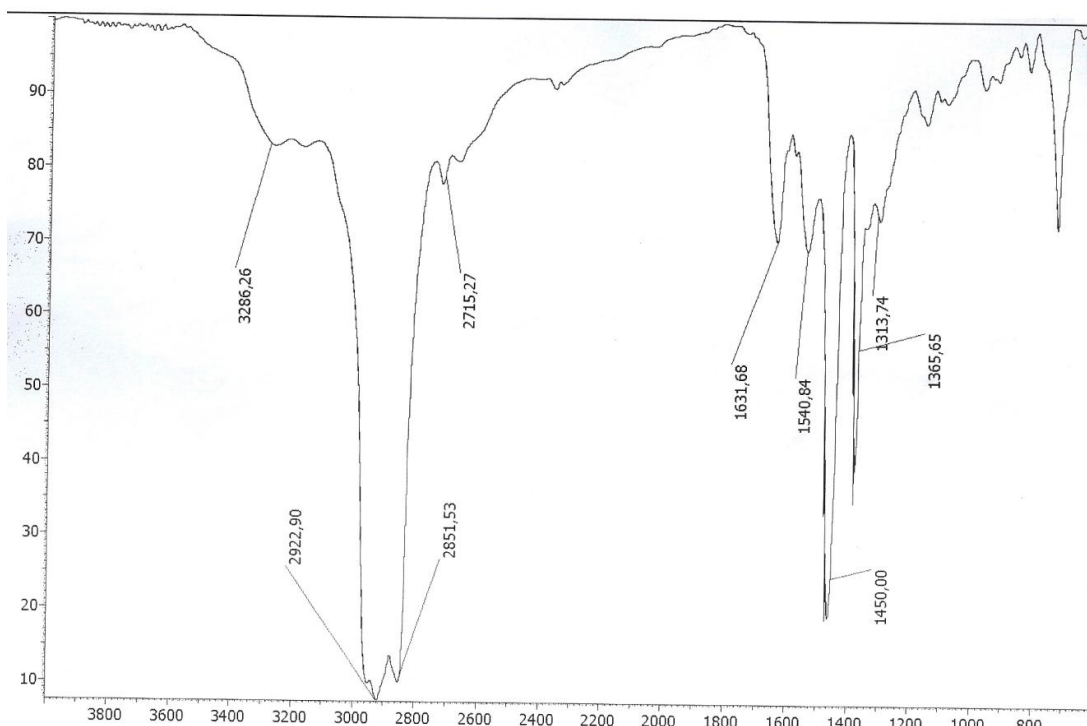
HRMS



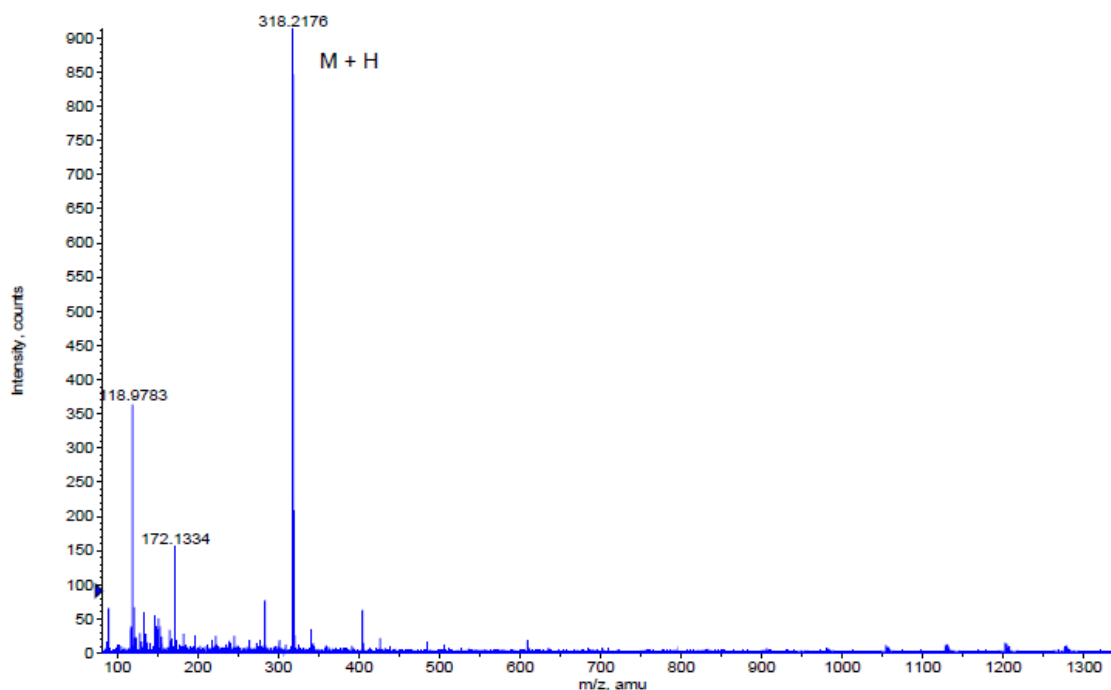
Formula	CalculatedMass	mDaError	ppmError	RDB
C ₁₄ H ₂₃ N ₂ O ₂ S	283.147476	0.323564	1.142737	4.5
C ₂₂ H ₁₉	283.148127	-0.32718	-1.155507	13.5
C ₁₇ H ₂₄ Na S	283.149094	-1.29388	-4.569619	5.5
C ₂₀ H ₂₀ Na	283.145722	2.07808	7.339192	10.5
C ₁₀ H ₂₃ N ₂ O ₇	283.149978	-2.177836	-7.691502	0.5
C ₁₂ H ₂₄ N ₂ O ₂ Na S	283.145071	2.728824	9.637436	1.5

- N^1 -((1*R*,2*R*)-2-aminocyclohexyl)- N^3 -butylisophthalamide (58) ^1H RMN (CDCl_3 , 200 MHz) ^{13}C RMN (CDCl_3 , 50 MHz)

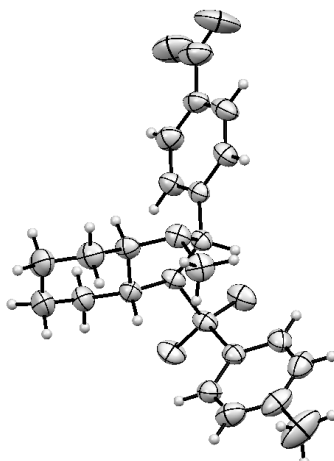
IR



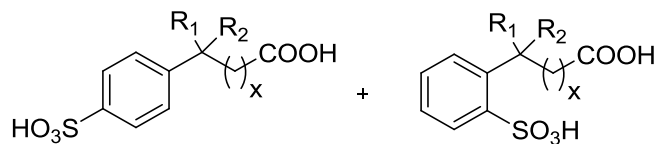
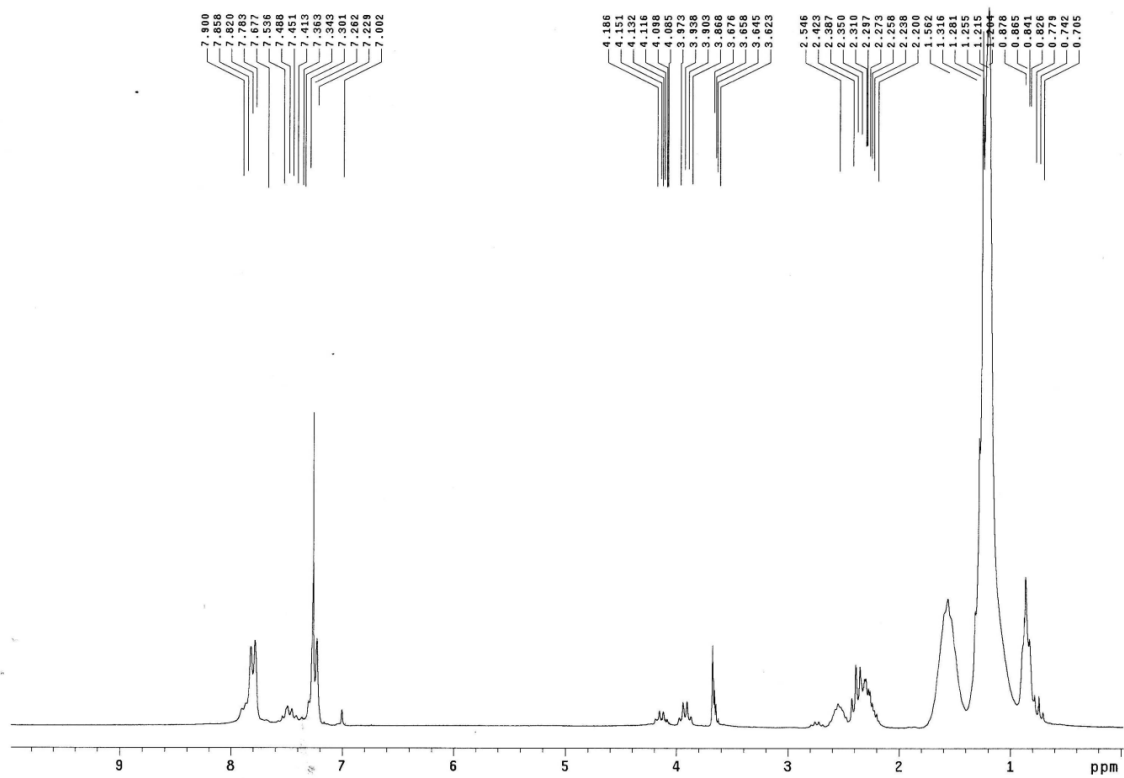
HRMS

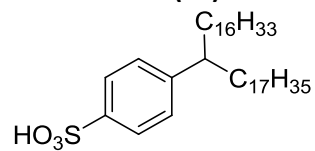
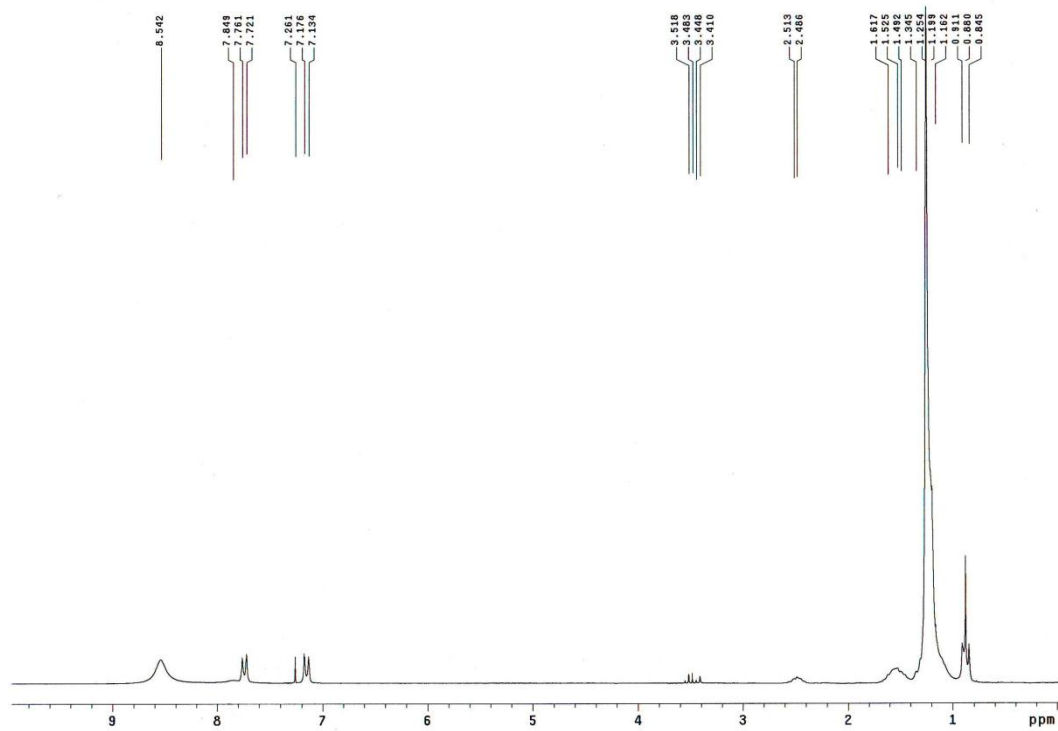
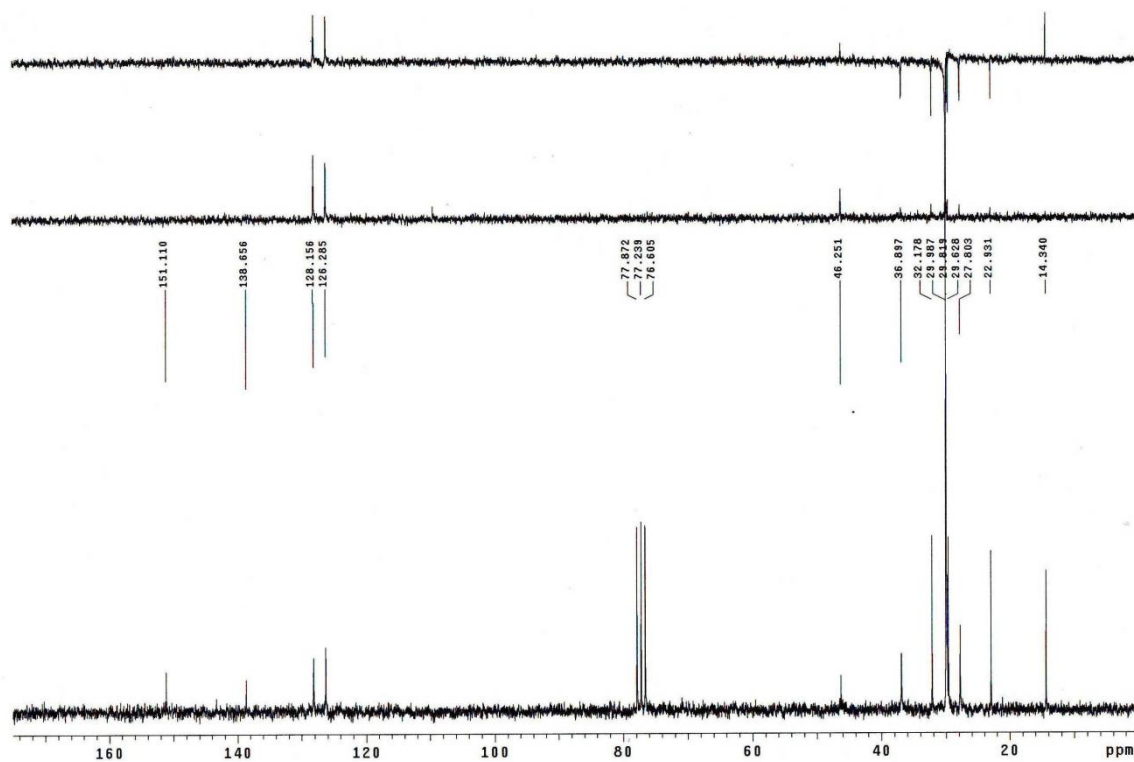


Formula	CalculatedMass	mDaError	ppmError	RDB
C ₁₈ H ₂₈ N ₃ O ₂	318.217604	-0.003844	-0.01208	6.5
C ₂₁ H ₂₉ N Na	318.219221	-1.621288	-5.094895	7.5
C ₁₆ H ₂₉ N ₃ O ₂ Na	318.215199	2.401416	7.546446	3.5

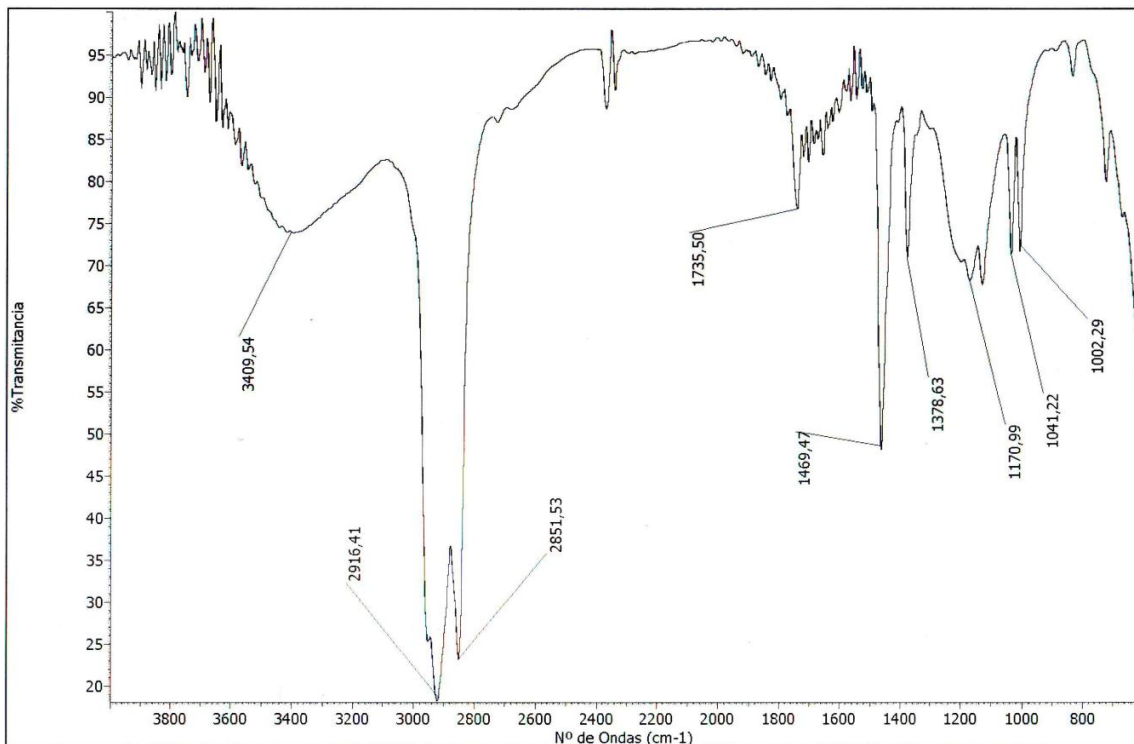
X-ray structure, cristal and refinement data of compound **60**

Empirical formula	$C_{21}H_{25}N_3O_4S$
Molecular weight	415.50
Temperature	293 (2) K
Wavelength	1.54178 Å
Crystal system, Space group	Monoclinic, P2(1)
Unit cell dimensions	$a = 8.2524(2)$ Å $\alpha = 90.00^\circ$ $b = 10.9519(2)$ Å $\beta = 94.7340(10)^\circ$ $c = 11.6248(3)$ Å $\gamma = 90.00^\circ$
Volume	1047.06(4) Å ³
Z; Density (calculated)	2; 1.368 mg/m ³
Absorption coefficient	1.644 mm ⁻¹
F(000)	440
Crystal size	- mm
θ range	3.82 – 66.85 °
Limiting indices h, k, l	$-9 \leq h \leq 9, -12 \leq k \leq 11, -13 \leq l \leq 11$
Reflections collected/independent	4869/2555 $R_{int} = 0.0215$
Refinement method	Least squares method with full matrix in F^2
Data/restraints/parameters	2555/1/266
Goodness-of-fit on F^2	1.065
Final R indices [$I > 2\sigma(I)$]	$R_1 = 0.0248, \omega R_2 = 0.0673$
R indices (all data)	$R_1 = 0.0253, \omega R_2 = 0.0676$
Extinction coefficient	0.0117 (7)

- Twitchell reagent ^1H NMR (CDCl_3 , 200 MHz)

- 4-(Tetatriacontan-17-yl)benzenesulfonic acid (64) ^1H NMR (CDCl_3 , 200 MHz) ^{13}C NMR (CDCl_3 , 50 MHz)

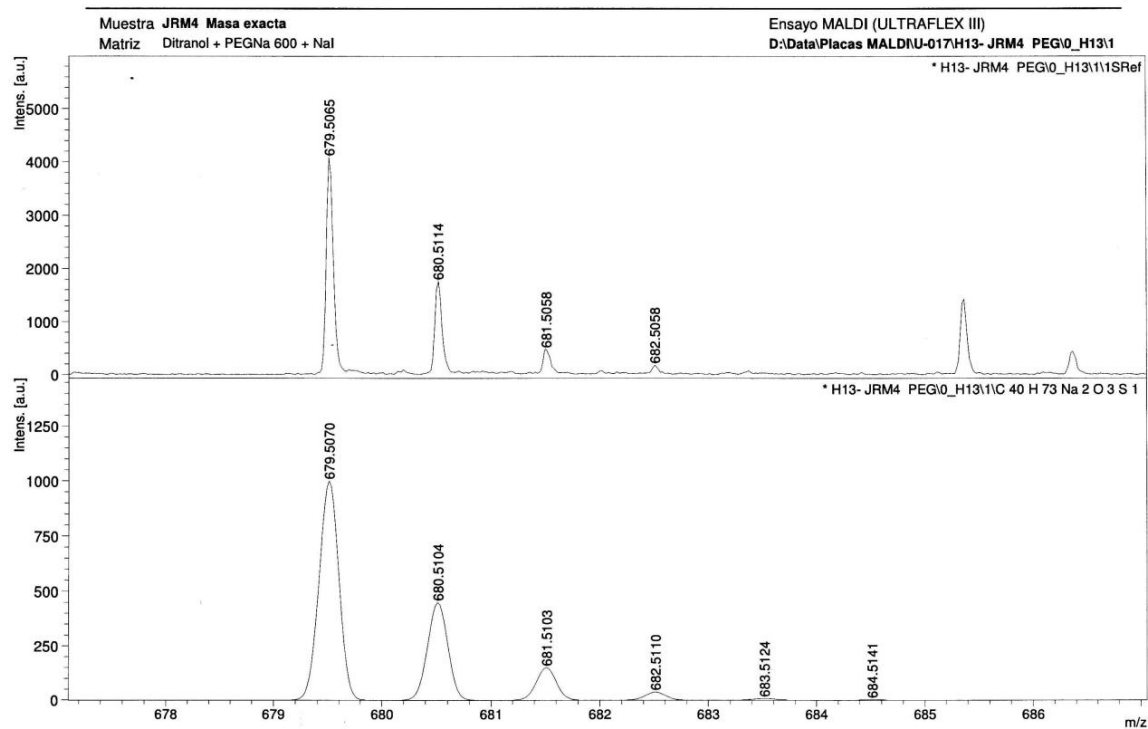
IR

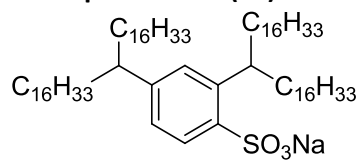
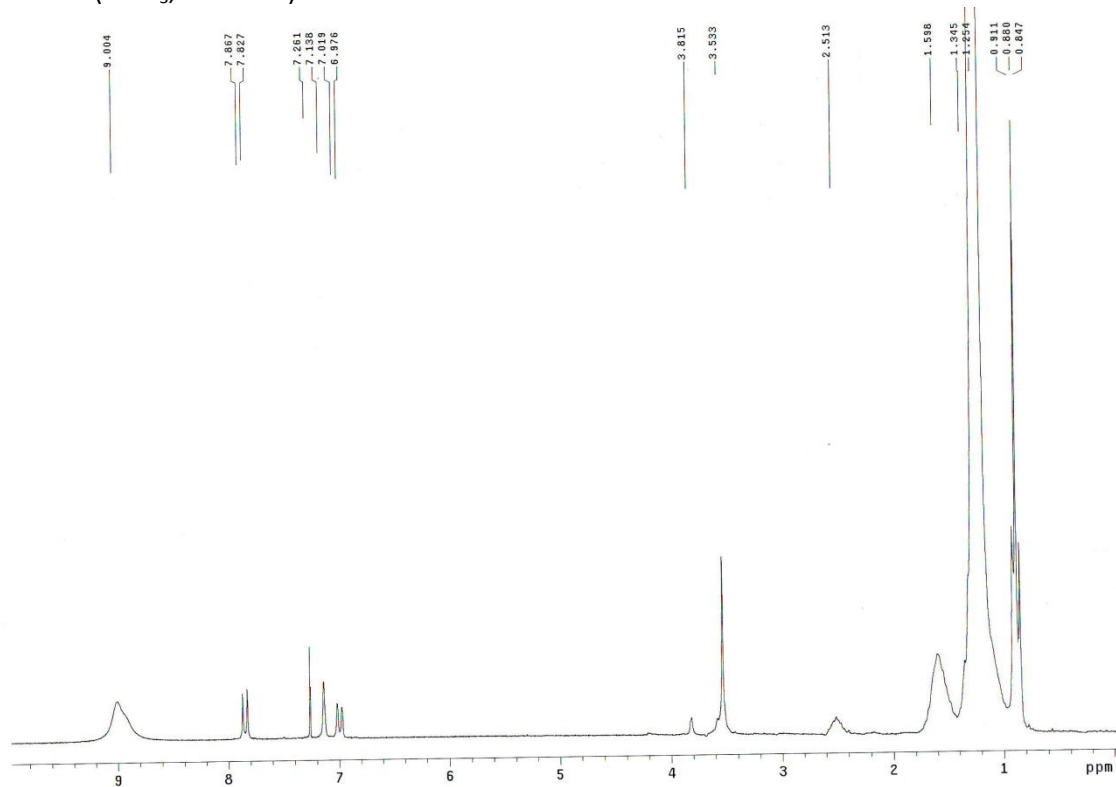
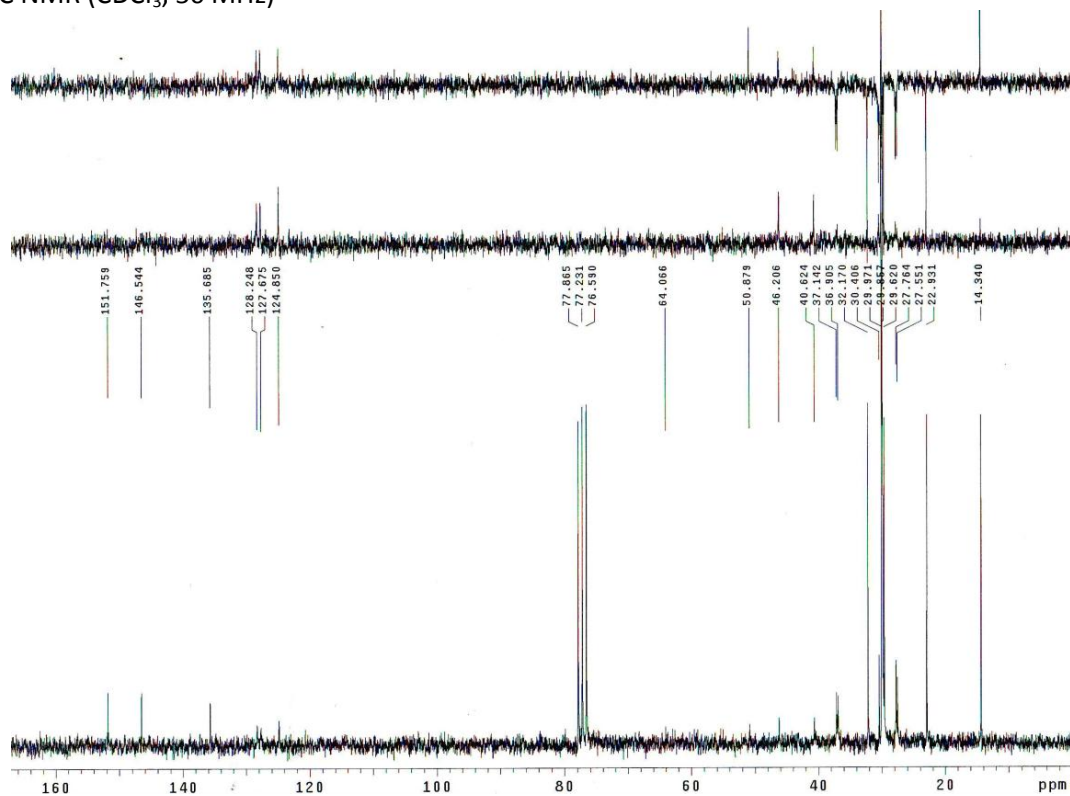


HRMS

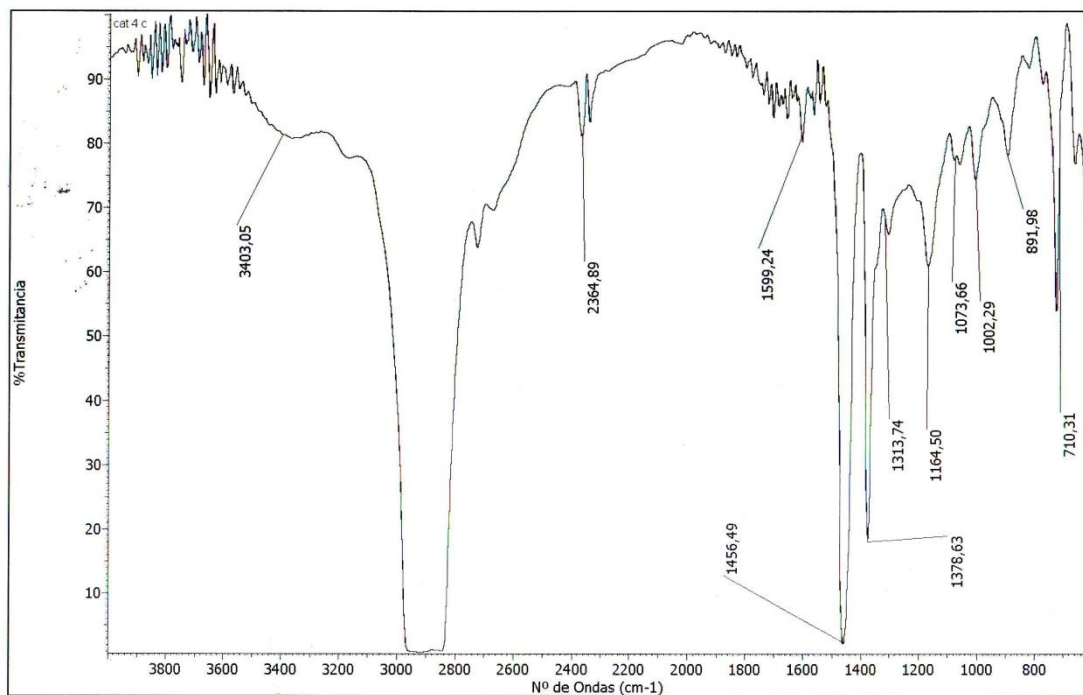
Generated Molecular Formulas

Formula	Mass	Error	DbIEq	N rule	Electron Configuration
C 40 H 73 Na 2 O 3 S 1	679.5070	0.7839	3.50	ok	even
C 35 H 78 Na 3 O 3 S 2	679.5080	2.2048	-4.50	ok	even
C 38 H 74 Na 3 O 3 S 1	679.5046	2.7559	0.50	ok	even
C 42 H 72 Na 1 O 3 S 1	679.5094	4.3237	6.50	ok	even
C 37 H 77 Na 2 O 3 S 2	679.5104	5.7446	-1.50	ok	even
C 39 H 76 Na 1 O 3 S 2	679.5128	9.2843	1.50	ok	even



- 2,4-Di(tritriacontan-17-yl)benzenesulphonic acid (65) ^1H NMR (CDCl_3 , 200 MHz) ^{13}C NMR (CDCl_3 , 50 MHz)

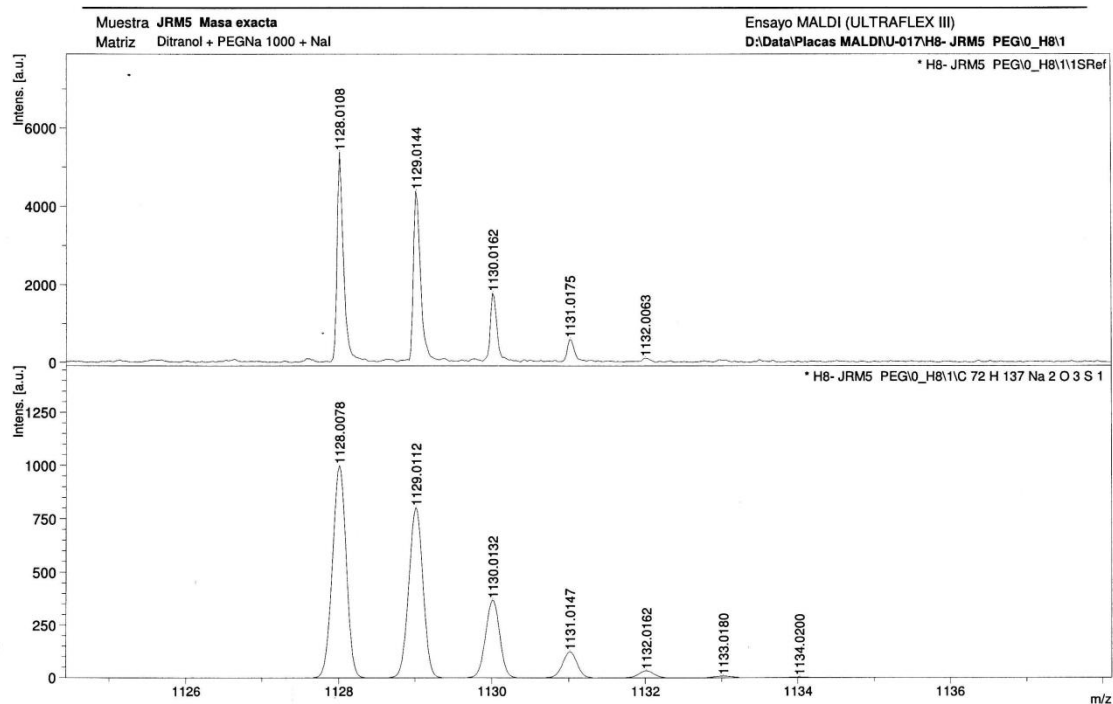
IR

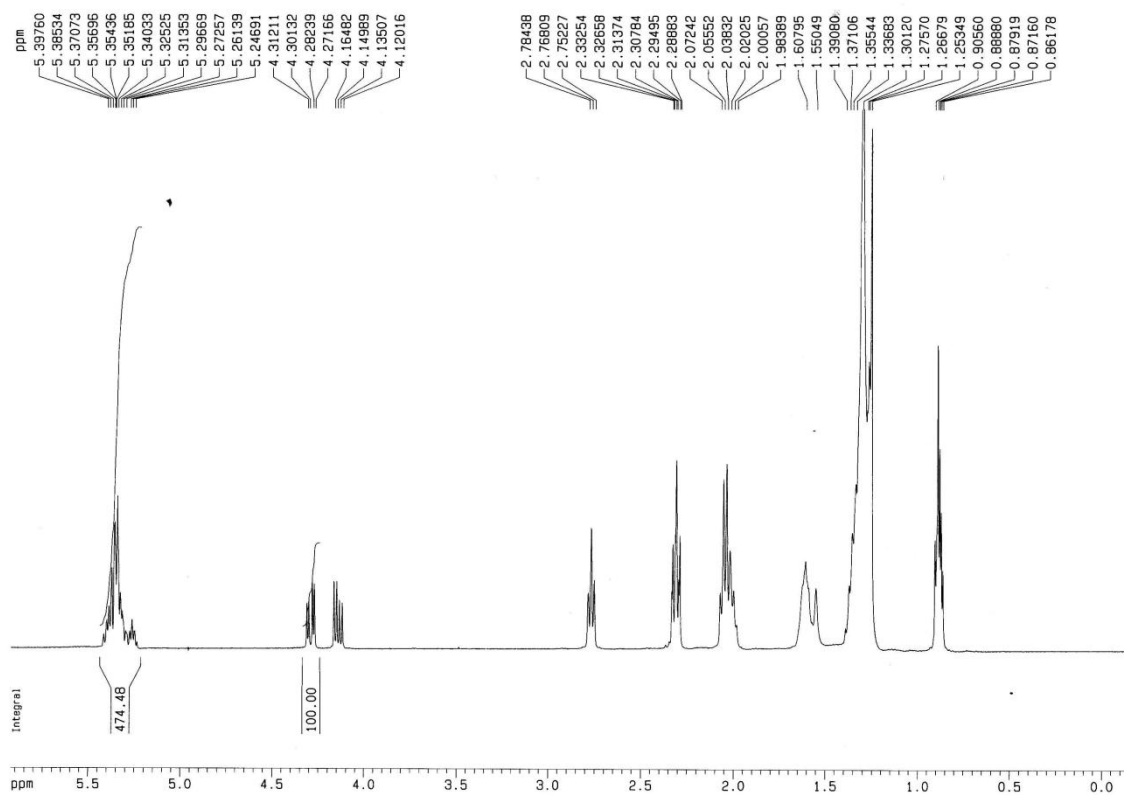


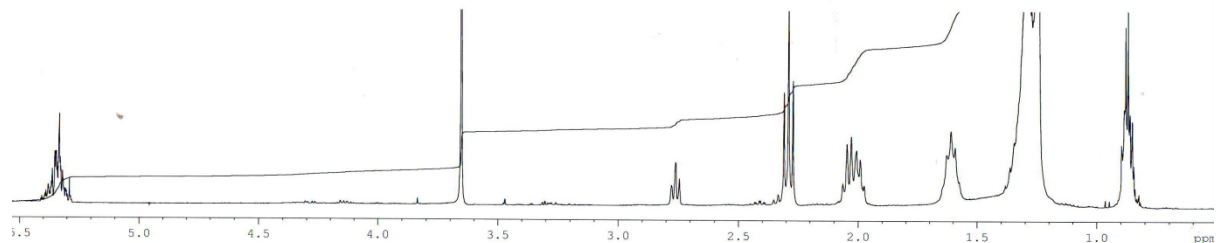
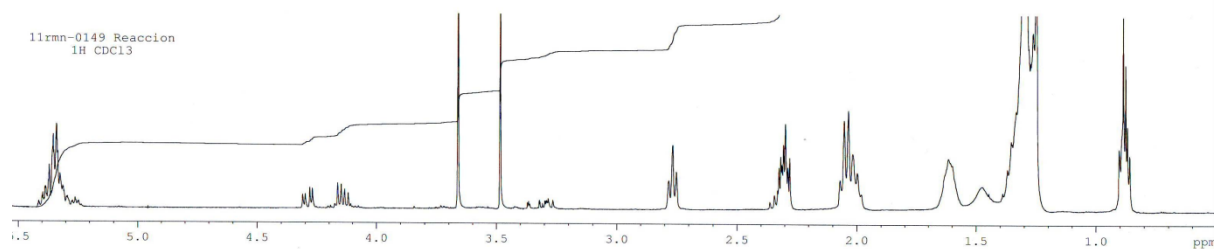
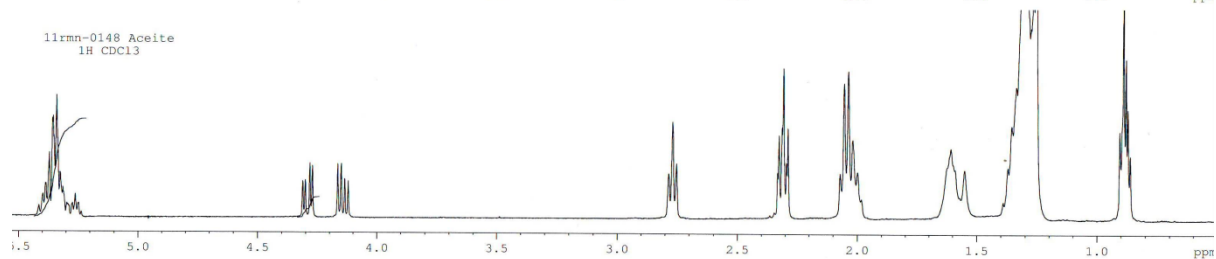
HRMS

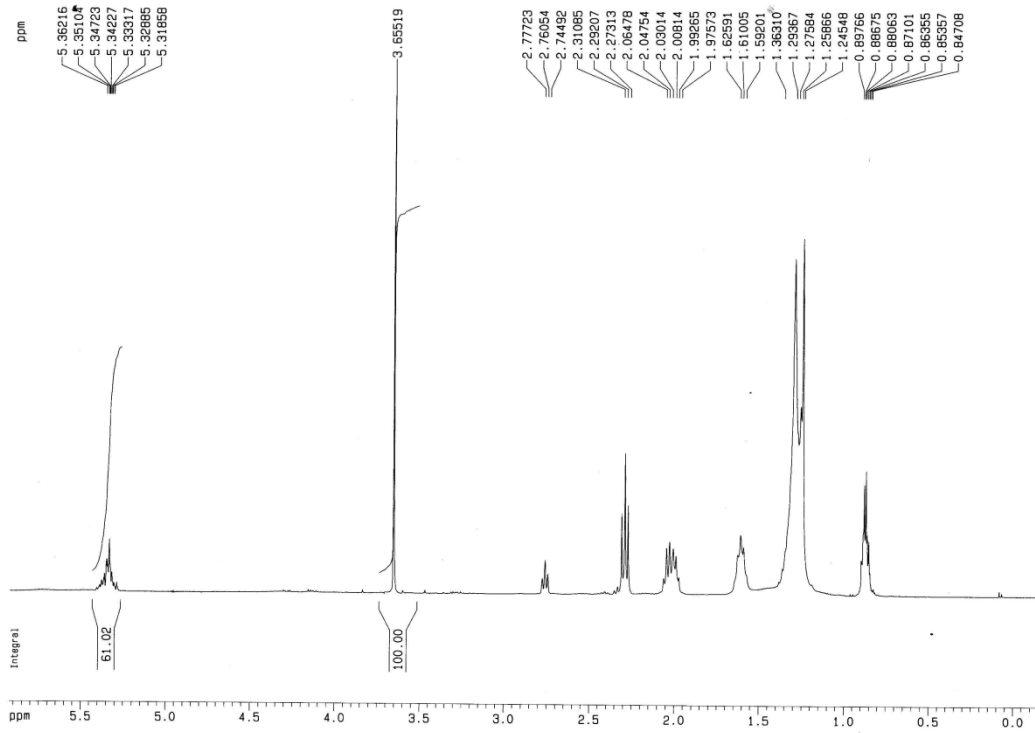
Generated Molecular Formulas

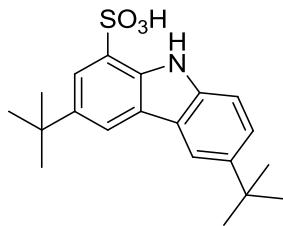
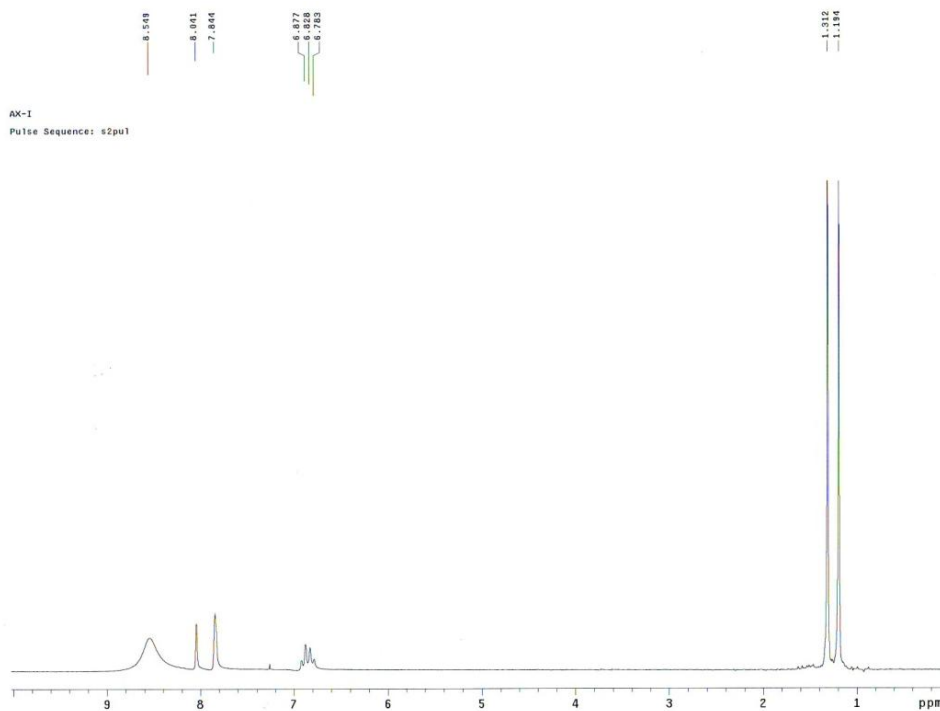
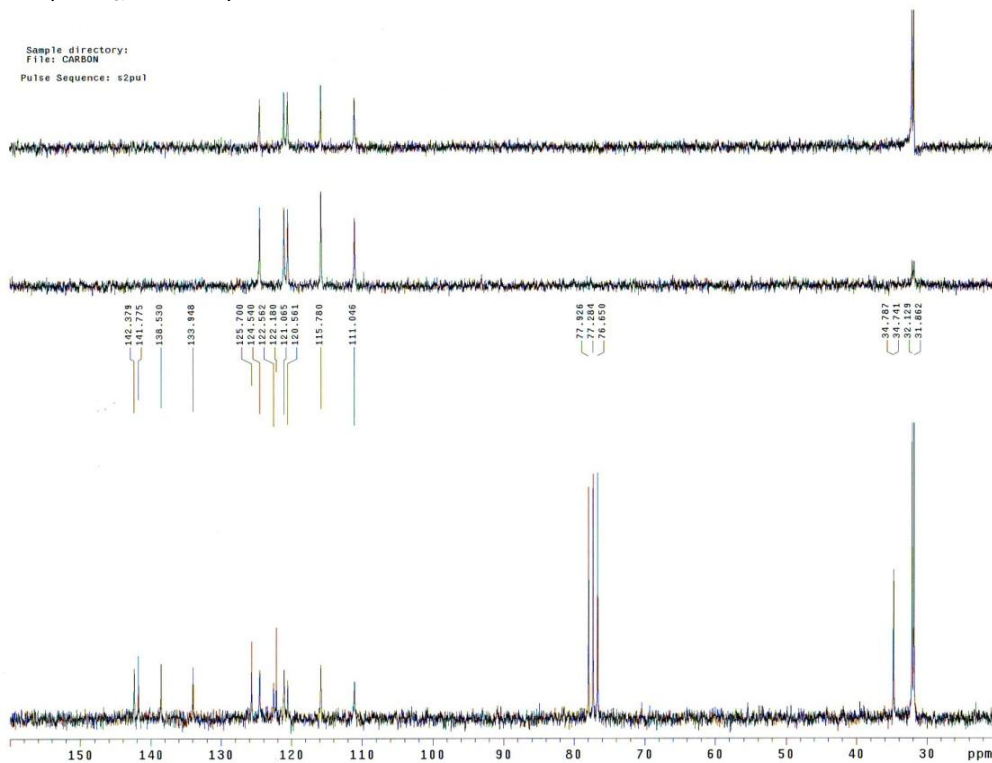
Formula	Mass	Error	DbtEq	N rule	Electron Configuration
C 69 H 141 Na 2 O 3 S 2	1,128.0112	0.3595	-1.50	ok	even
C 74 H 136 Na 1 O 3 S 1	1,128.0102	0.4964	6.50	ok	even
C 67 H 142 Na 3 O 3 S 2	1,128.0088	1.7728	-4.50	ok	even
C 71 H 140 Na 1 O 3 S 2	1,128.0136	2.4918	1.50	ok	even
C 72 H 137 Na 2 O 3 S 1	1,128.0078	2.6288	3.50	ok	even
C 70 H 138 Na 3 O 3 S 1	1,128.0054	4.7611	0.50	ok	even



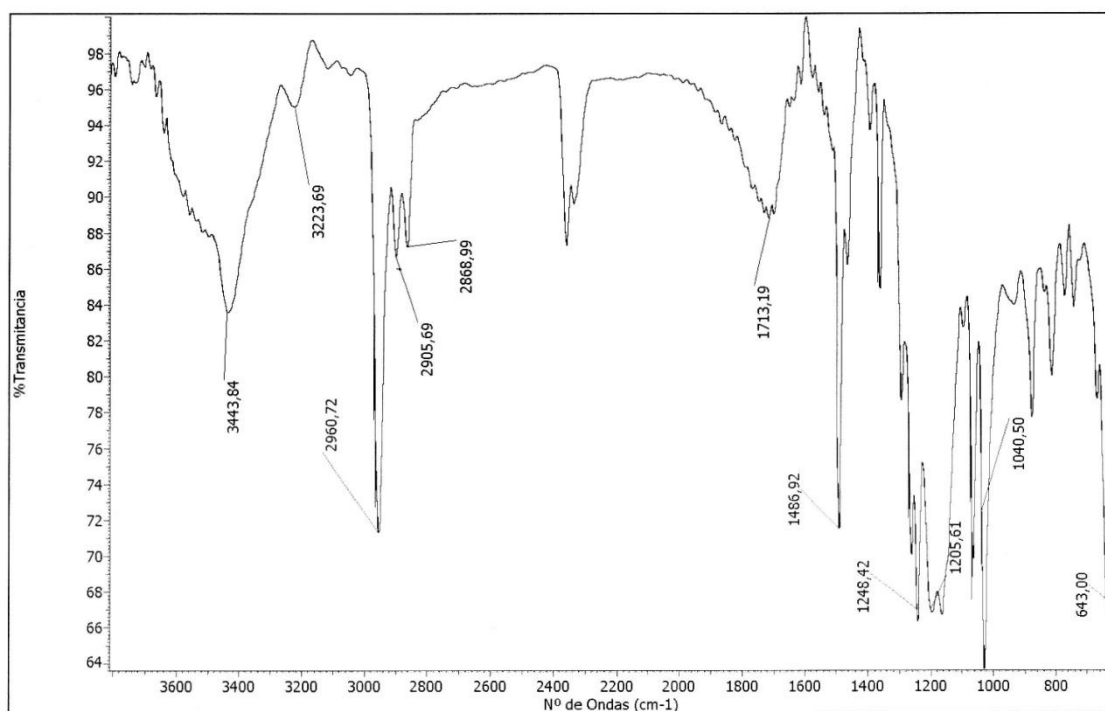
- ^1H NMR spectrum of triglyceride displaying the integral of the region of interest ^1H NMR (CDCl_3 , 400 MHz)

- ^1H NMR spectra of the progress of the transesterification reaction catalyzed by 64. ^1H NMR (CDCl_3 , 400 MHz)11rmn-0150 FAME
1H CDCl311rmn-0149 Reaccion
1H CDCl311rmn-0148 Aceite
1H CDCl3

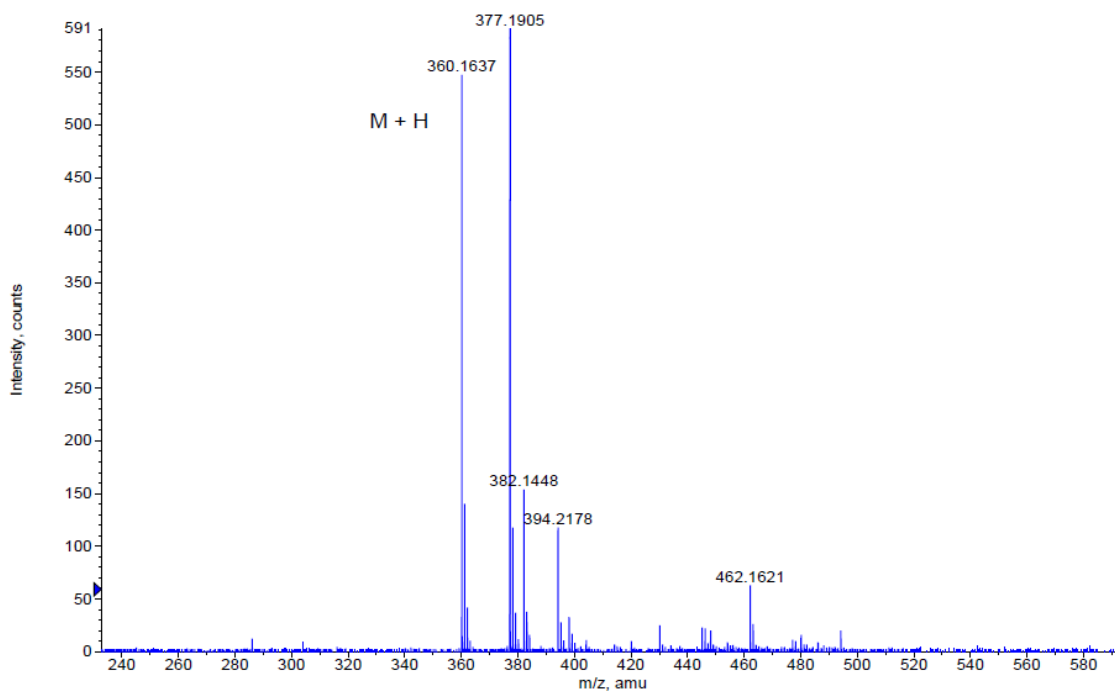
- ^1H NMR spectrum of fatty acids methyl esters (FAME) ^1H NMR (CDCl_3 , 400 MHz)

- 3,6-di-*tert*-butyl-9H-carbazole-1-sulfonic acid (71)¹H RMN (CDCl₃, 200 MHz)RMN ¹³C (CDCl₃, 50 MHz)

IR

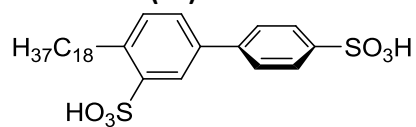
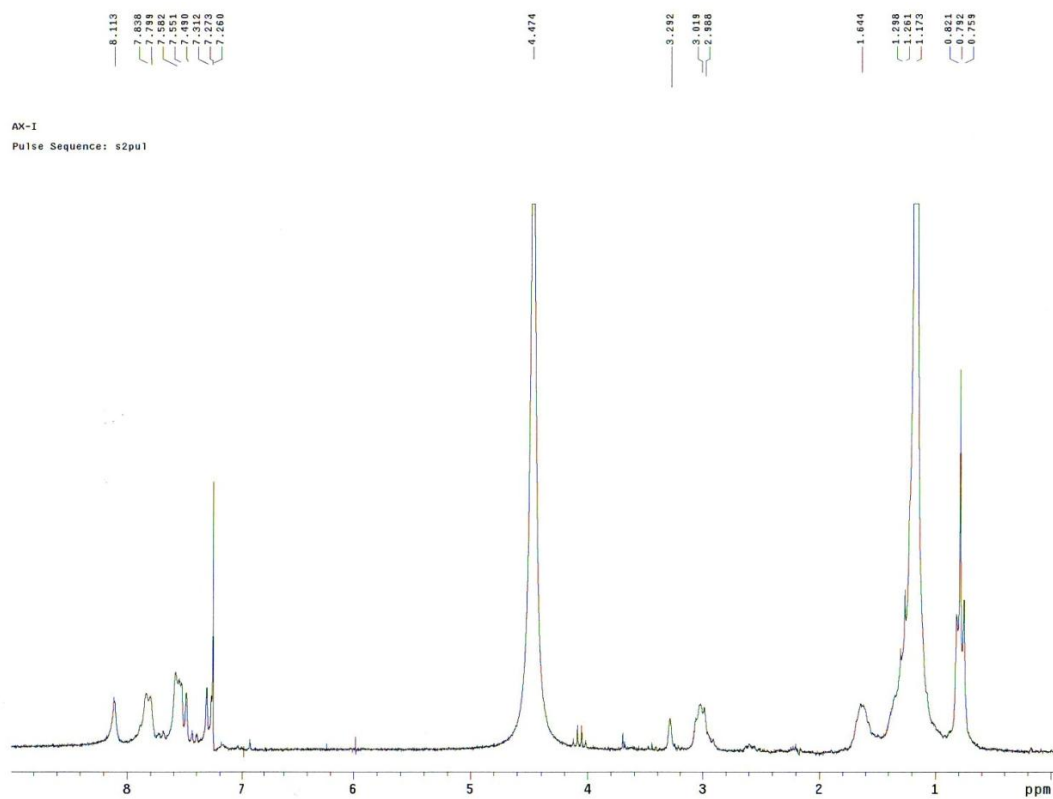
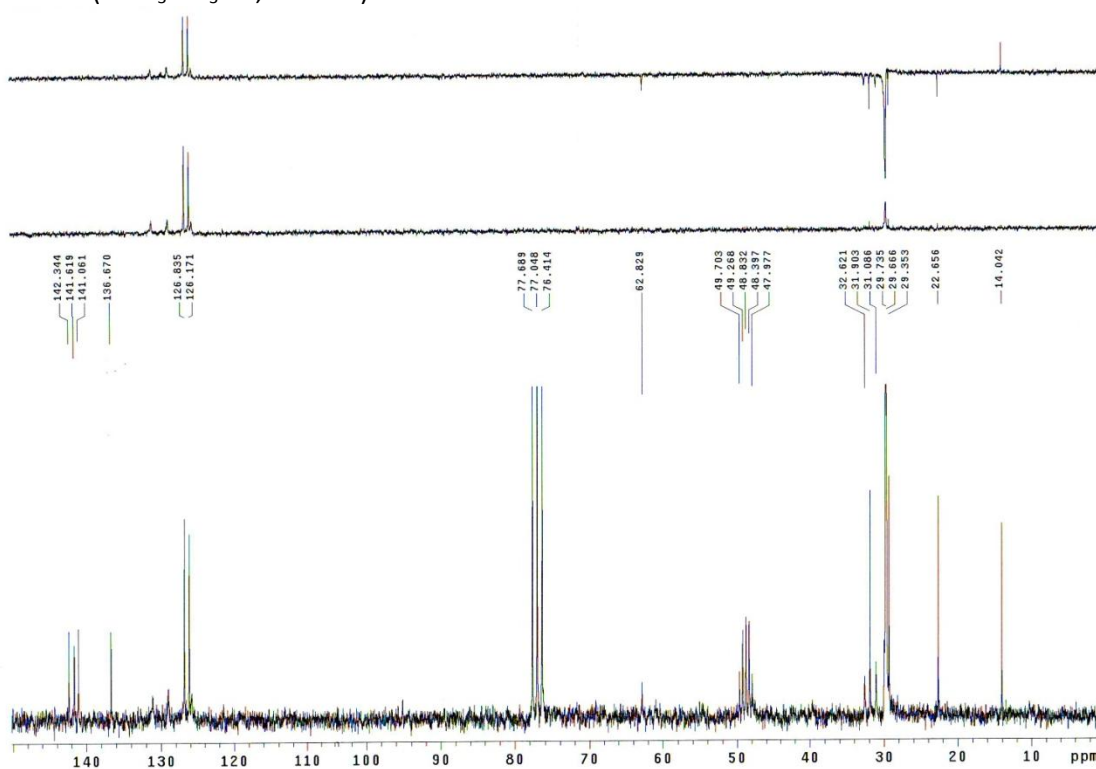


HRMS

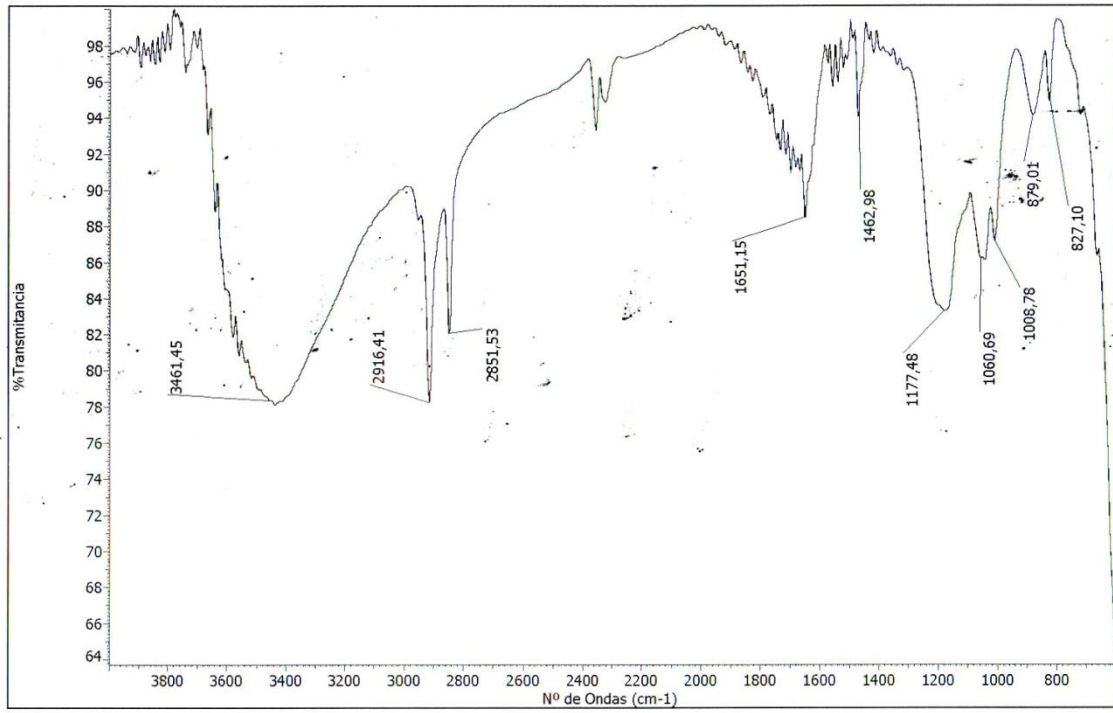


Formula	CalculatedMass	mDaError	ppmError	RDB
C ₂₀ H ₂₆ N O ₃ S	360.162792	0.907812	2.52055	8.5
C ₁₈ H ₂₇ N O ₃ Na S	360.160387	3.313072	9.198781	5.5

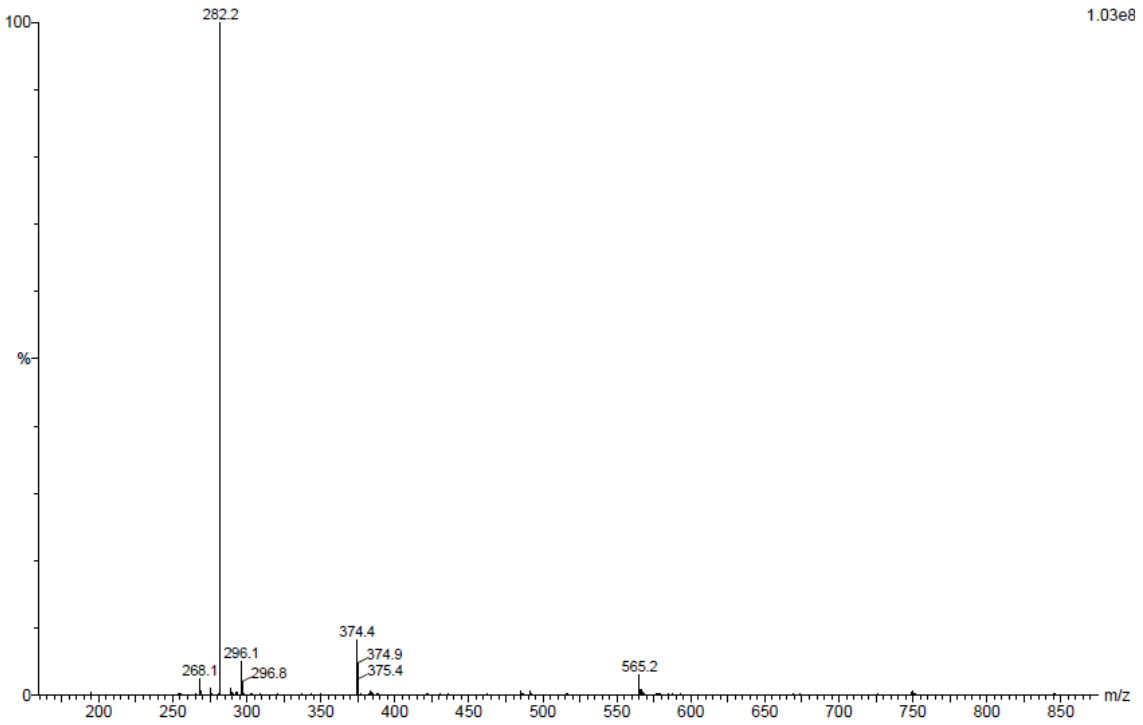
- 4-octadecylbiphenyl-3,4'-disulfonic acid (72)

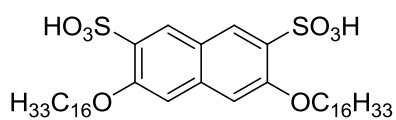
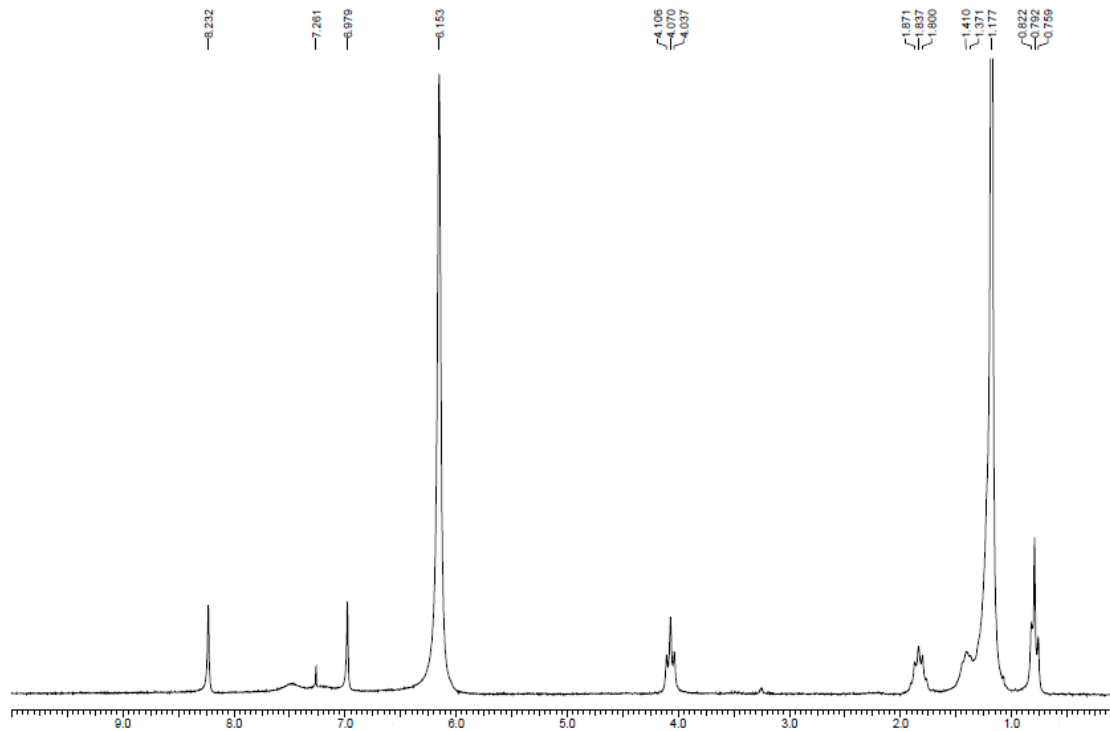
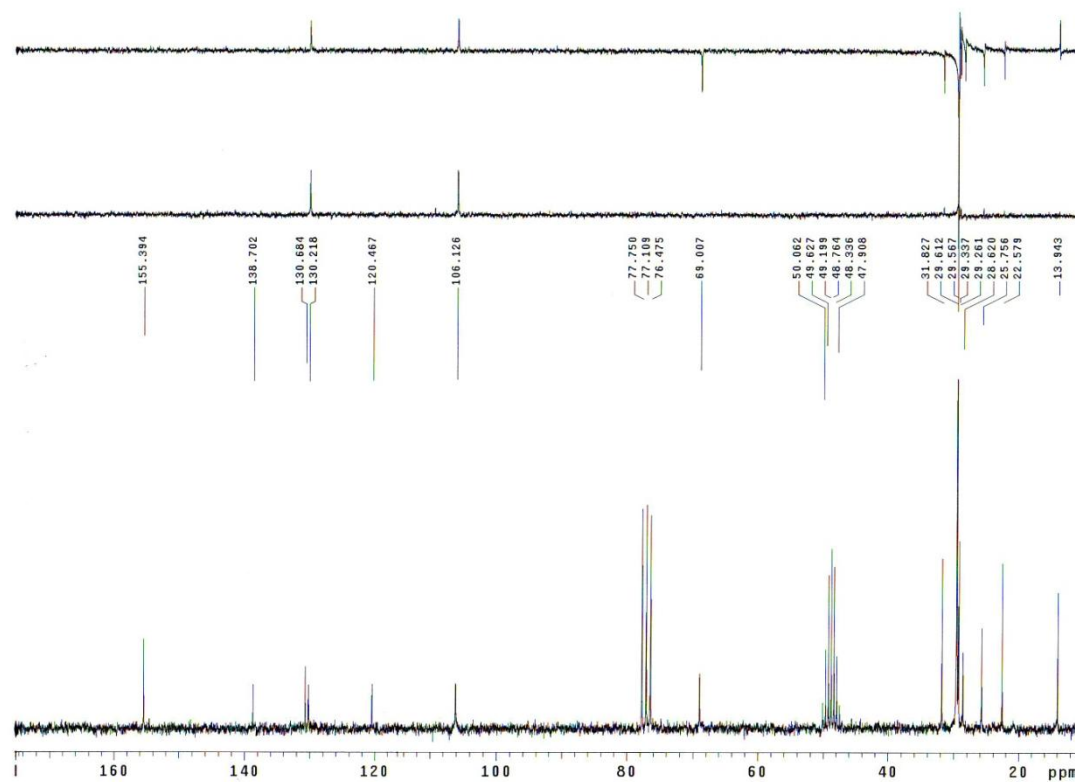
 ^1H RMN ($\text{CDCl}_3\text{-CD}_3\text{OD}$, 200 MHz)RMN ^{13}C ($\text{CDCl}_3\text{-CD}_3\text{OD}$, 50 MHz)

IR

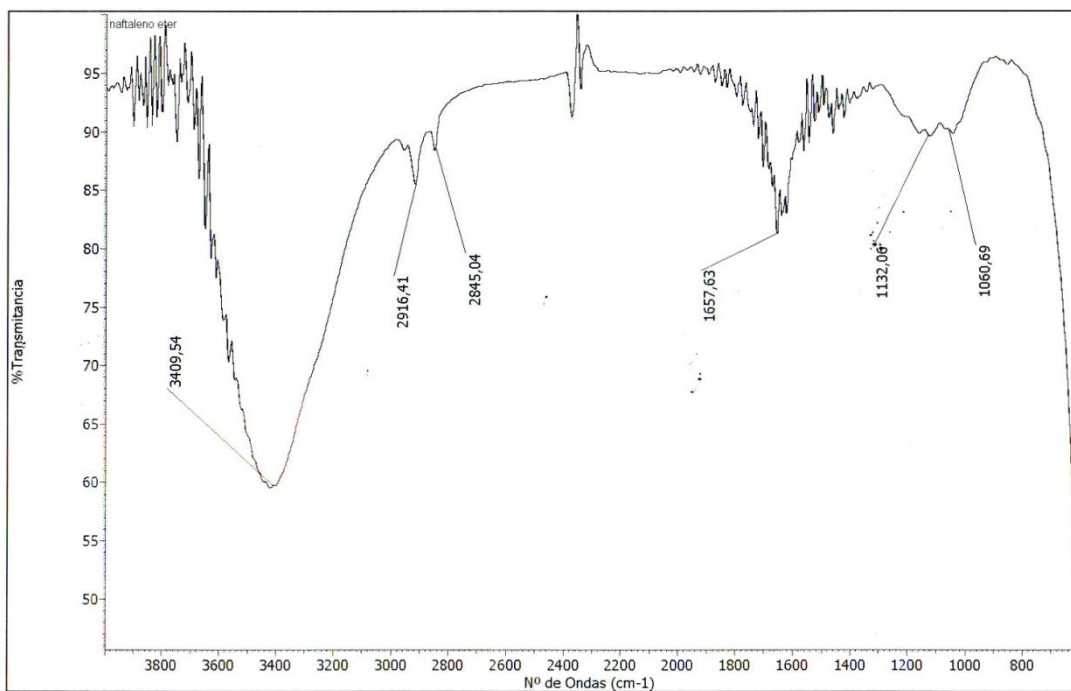


MS

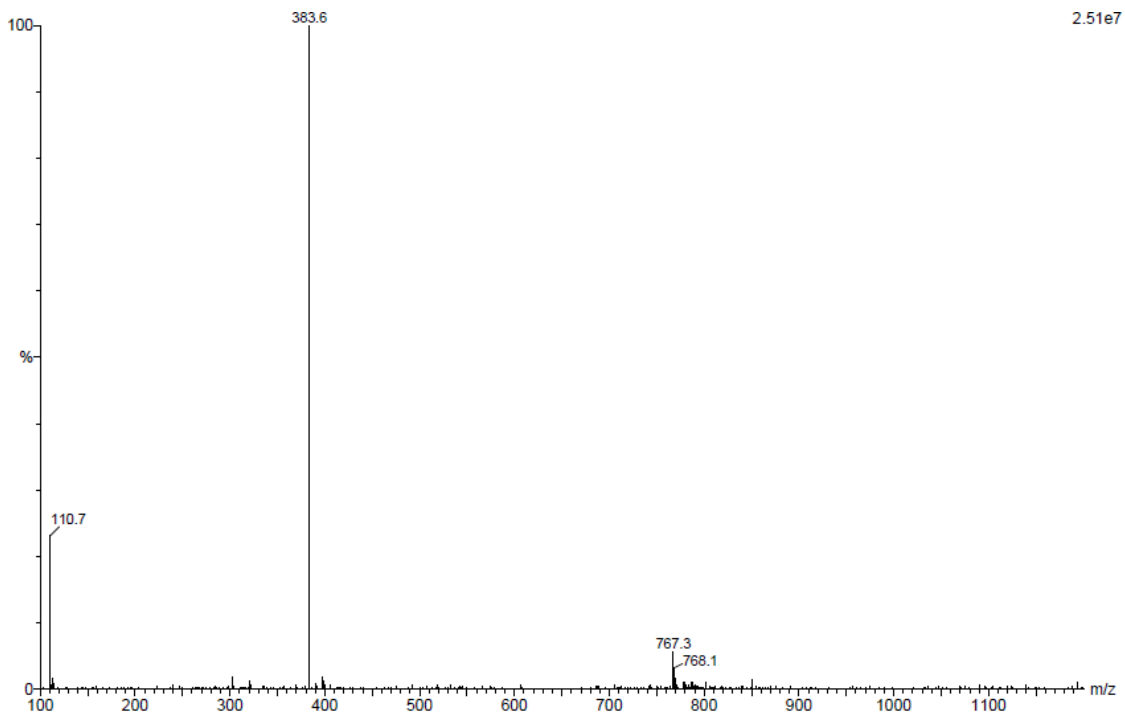


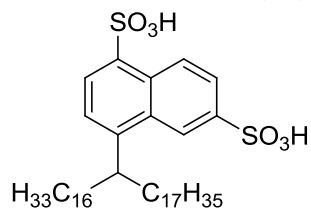
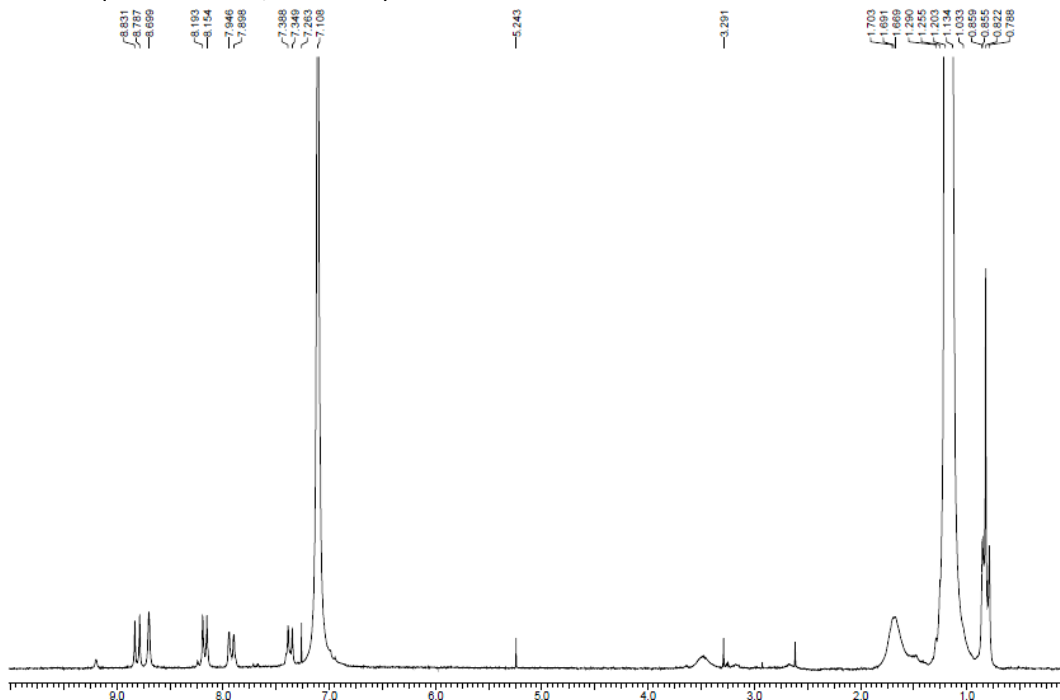
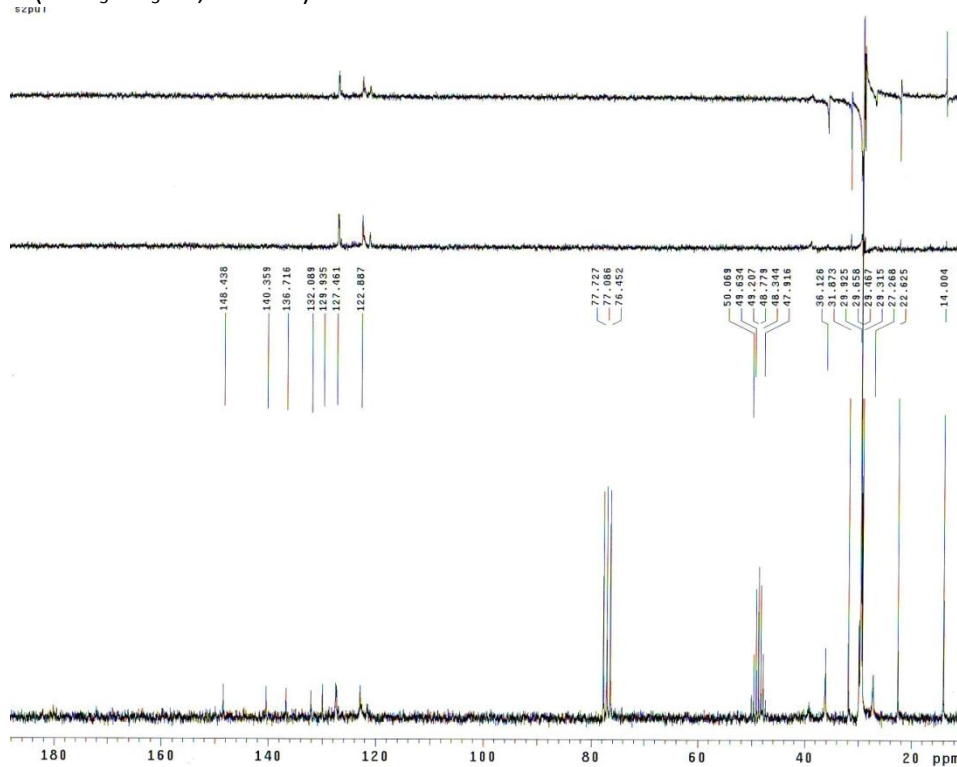
- 3,6-bis(hexadecyloxy)naphthalene-2,7-disulfonic acid (73) ^1H RMN ($\text{CDCl}_3\text{-CD}_3\text{OD}$, 200 MHz) ^{13}C RMN ($\text{CDCl}_3\text{-CD}_3\text{OD}$, 50 MHz)

IR

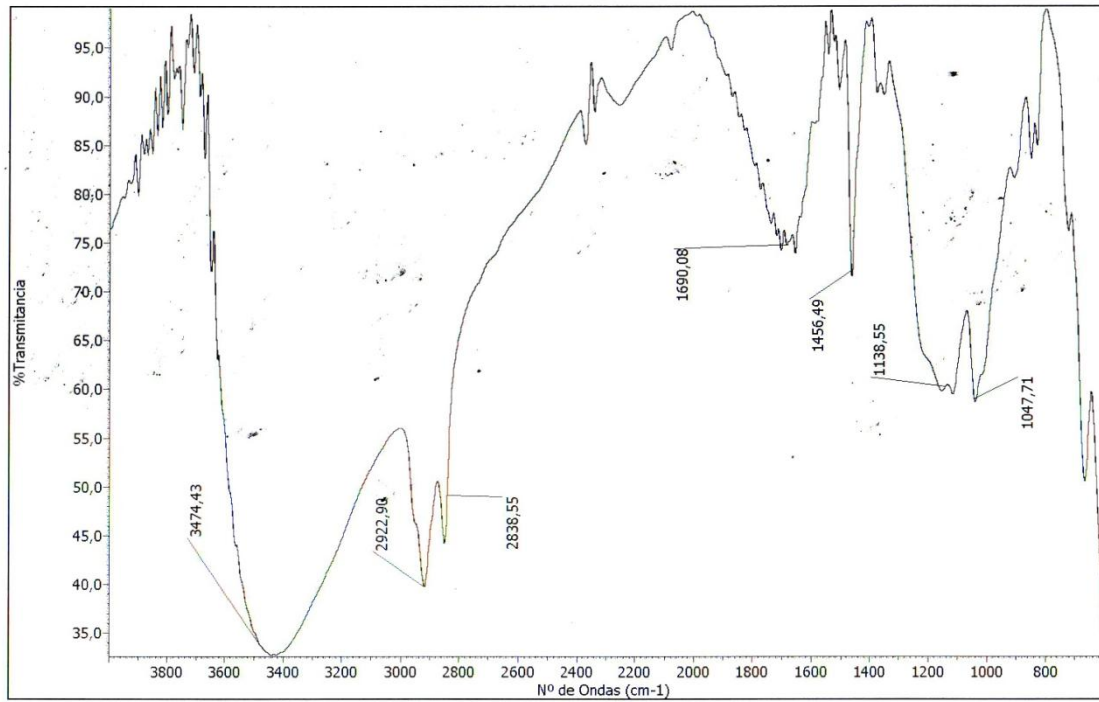


MS

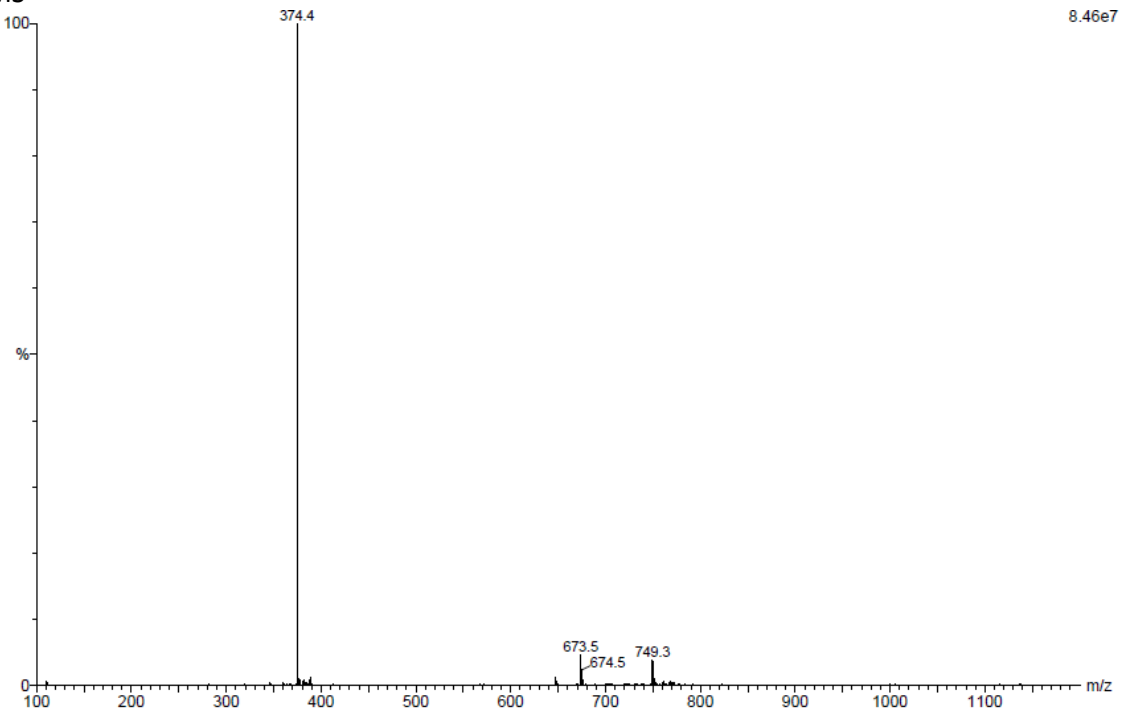


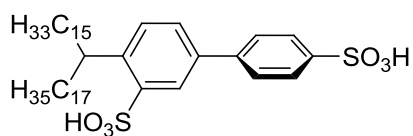
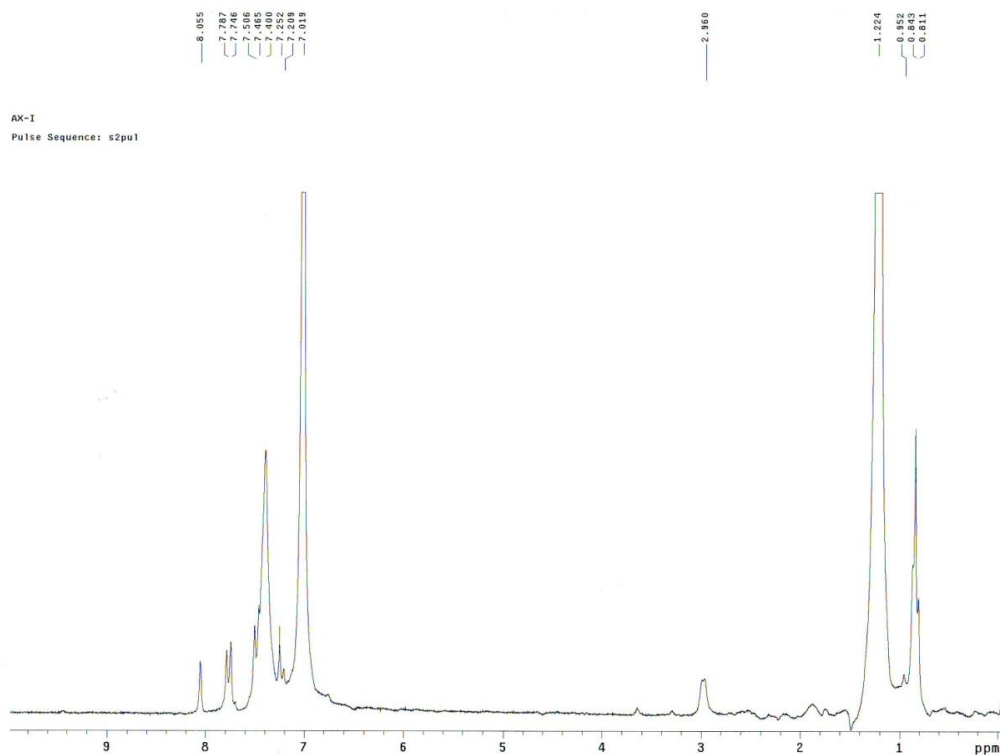
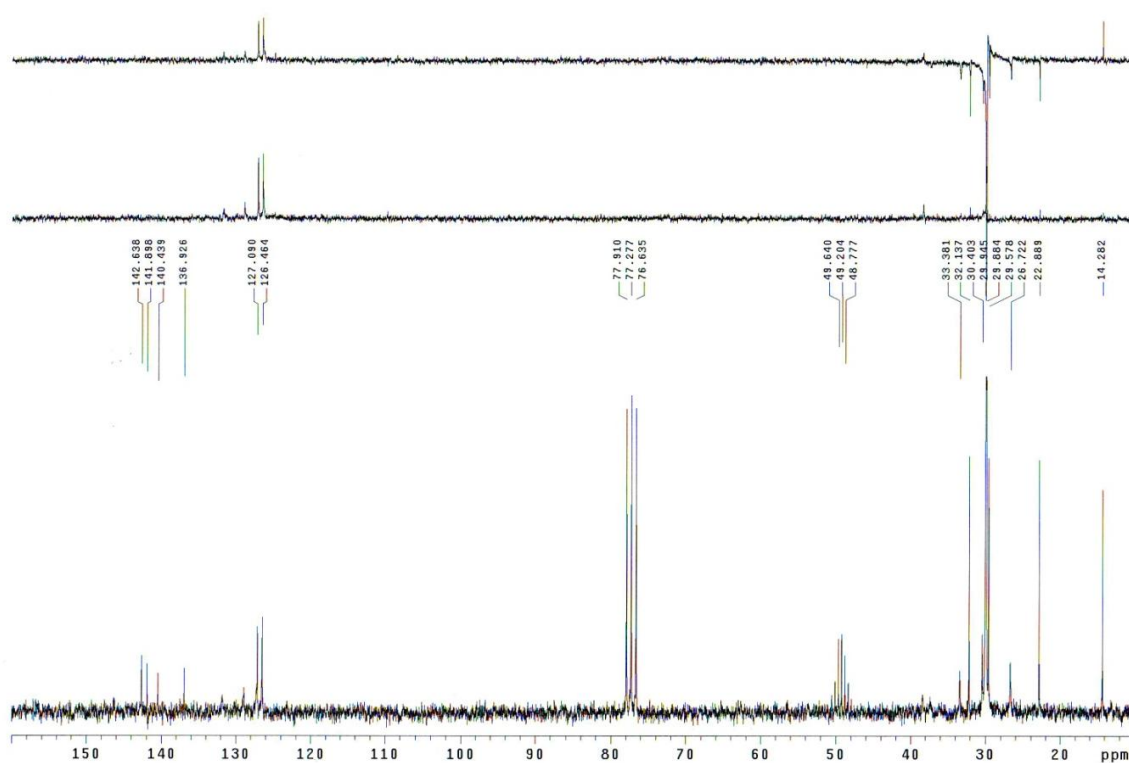
- 4-(tetraatriacontan-17-yl)naphthalene-1,6-disulfonic acid (74)¹H RMN (CDCl₃-CD₃OD, 200 MHz)¹³C RMN (CDCl₃-CD₃OD, 50 MHz)

IR

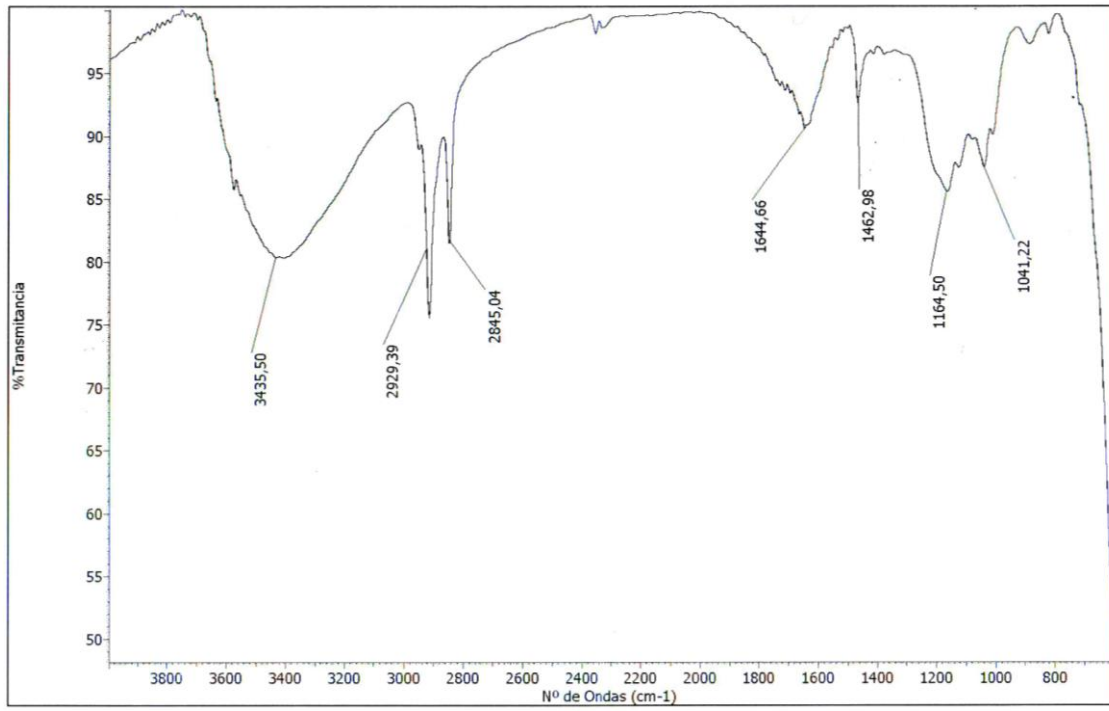


MS

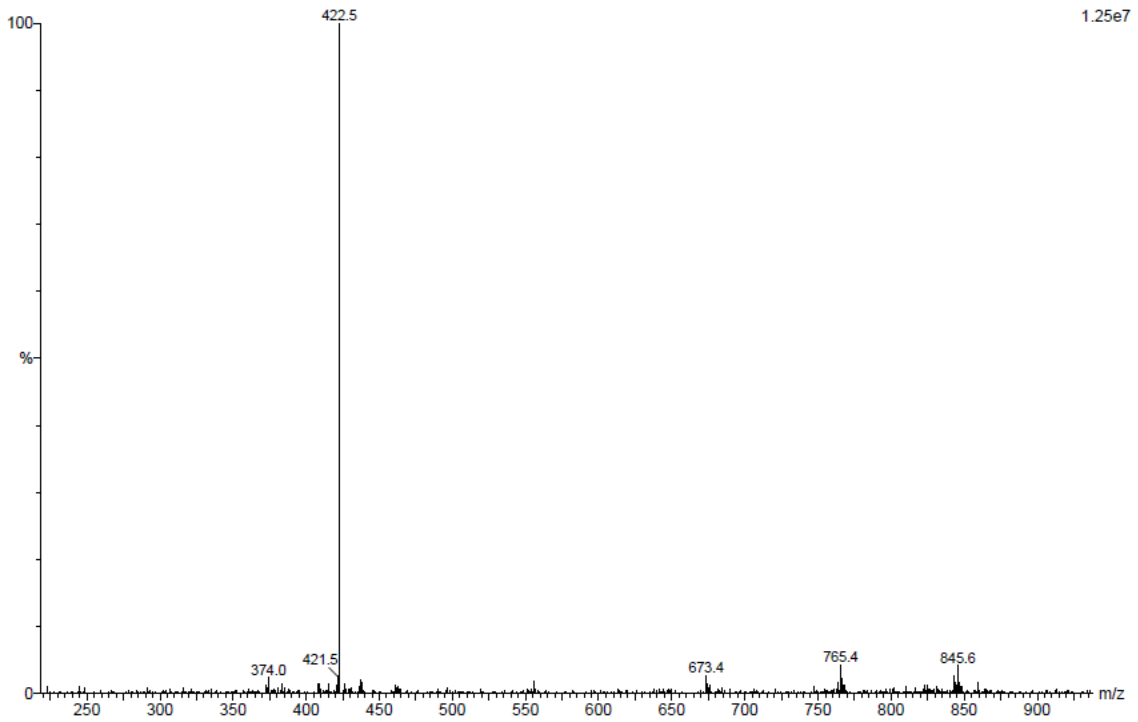


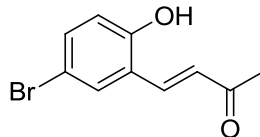
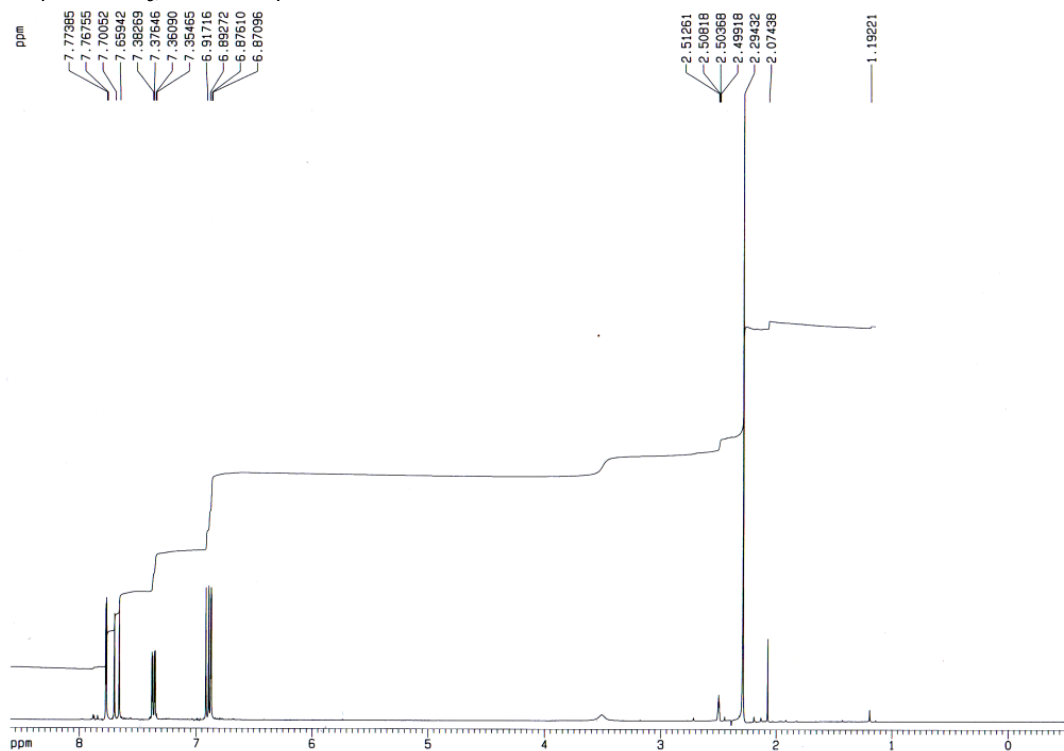
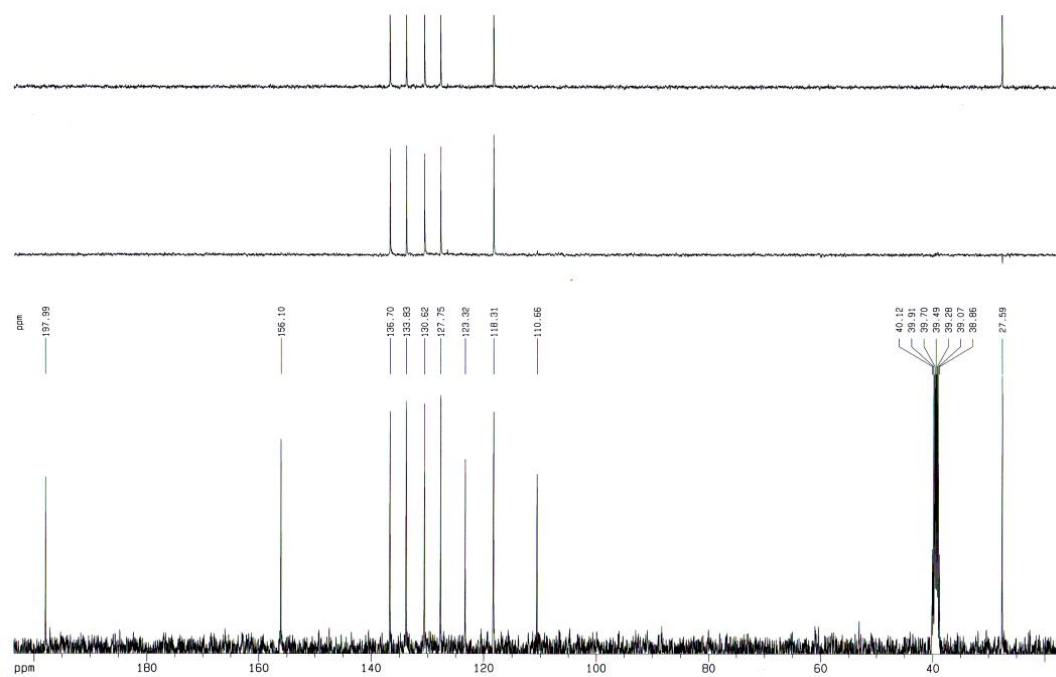
- 4-(tetraatriacontan-17-yl)biphenyl-3,4'-disulfonic acid (75) ^1H RMN ($\text{CDCl}_3\text{-CD}_3\text{OD}$, 200 MHz) ^{13}C RMN ($\text{CDCl}_3\text{-CD}_3\text{OD}$, 50 MHz)

IR

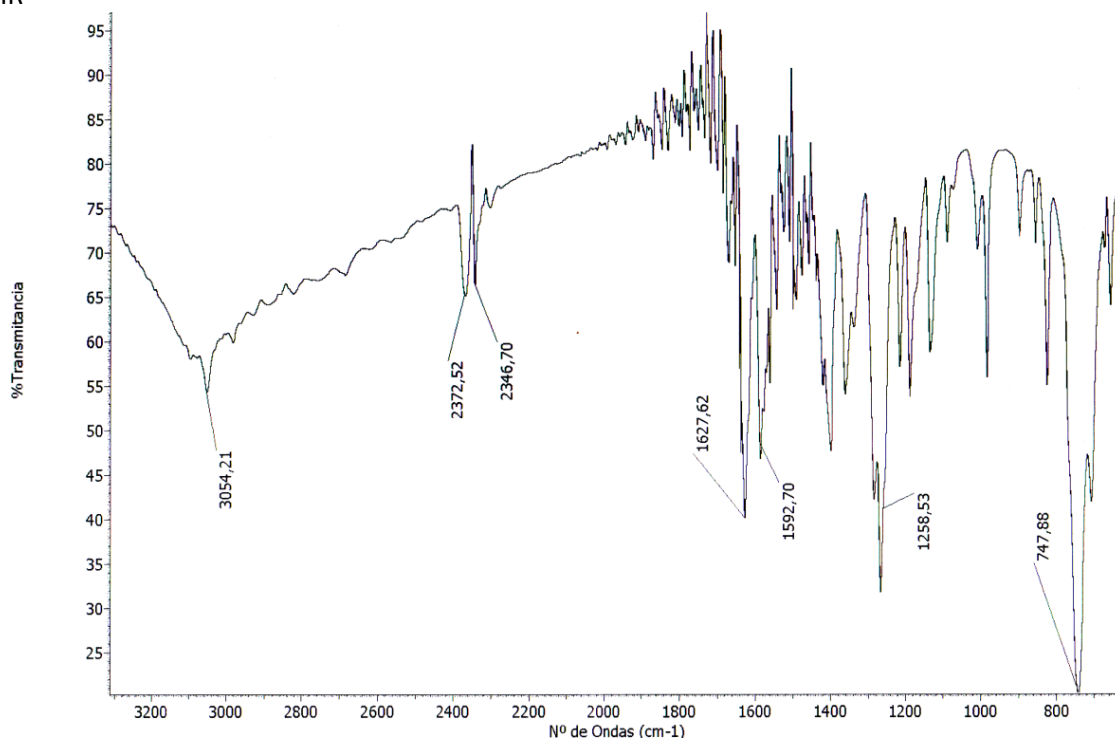


MS

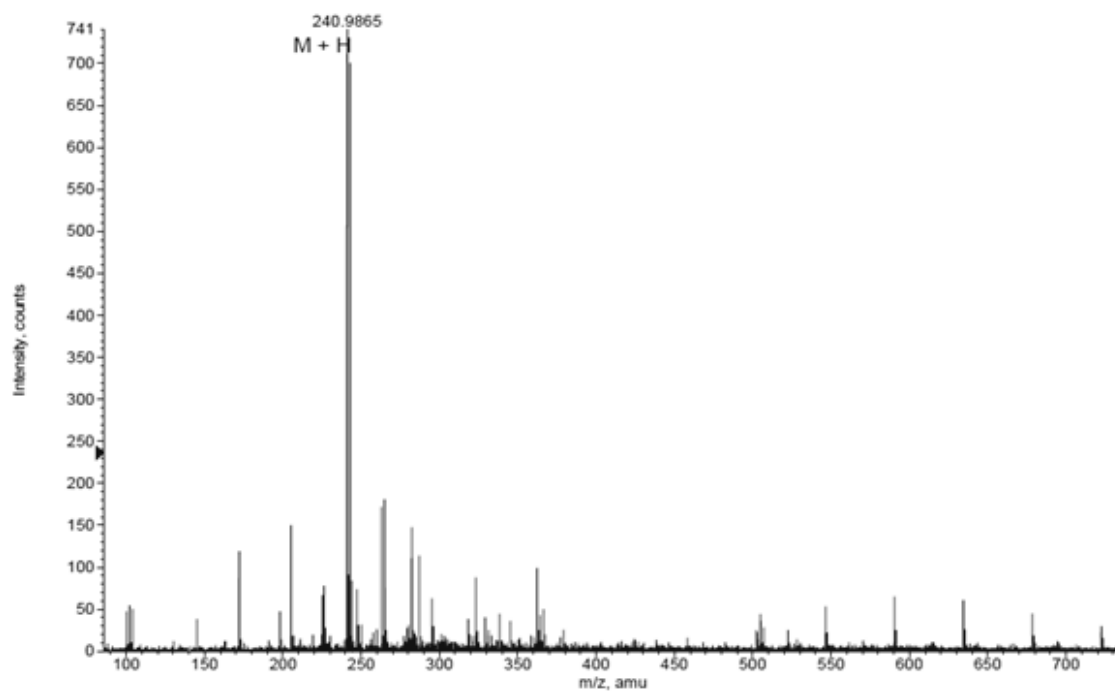


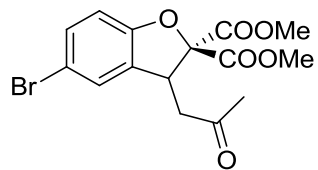
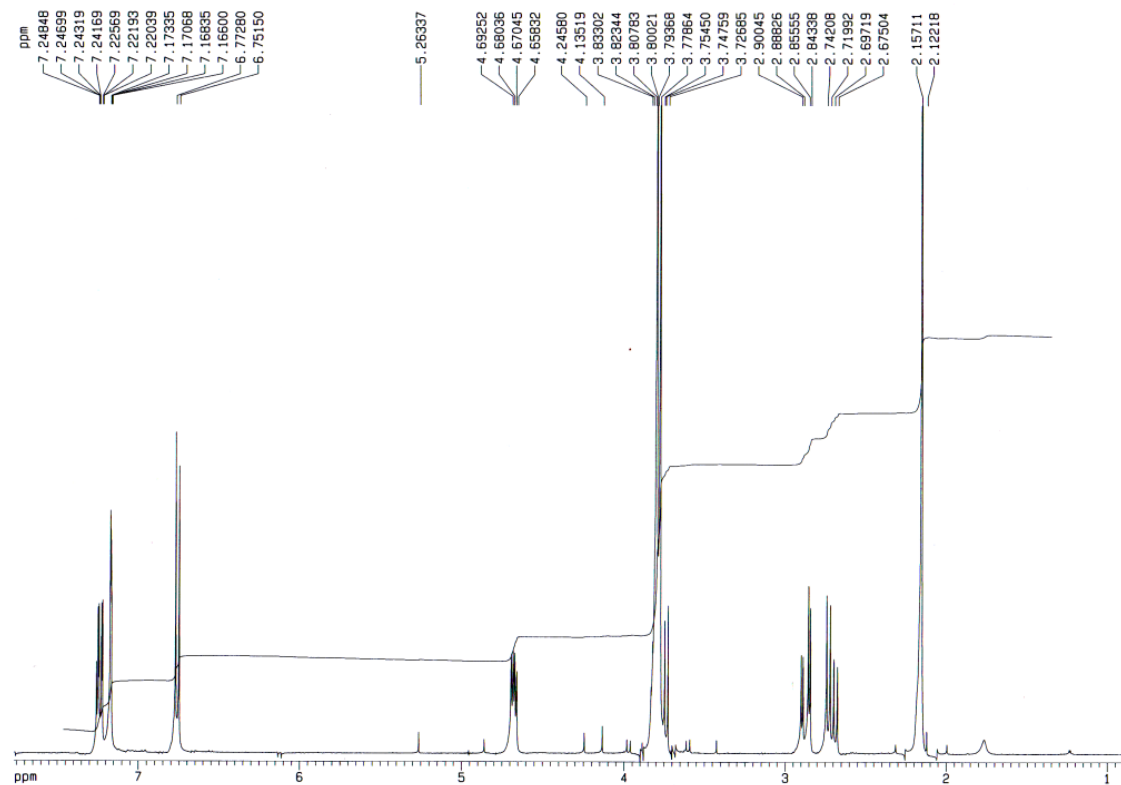
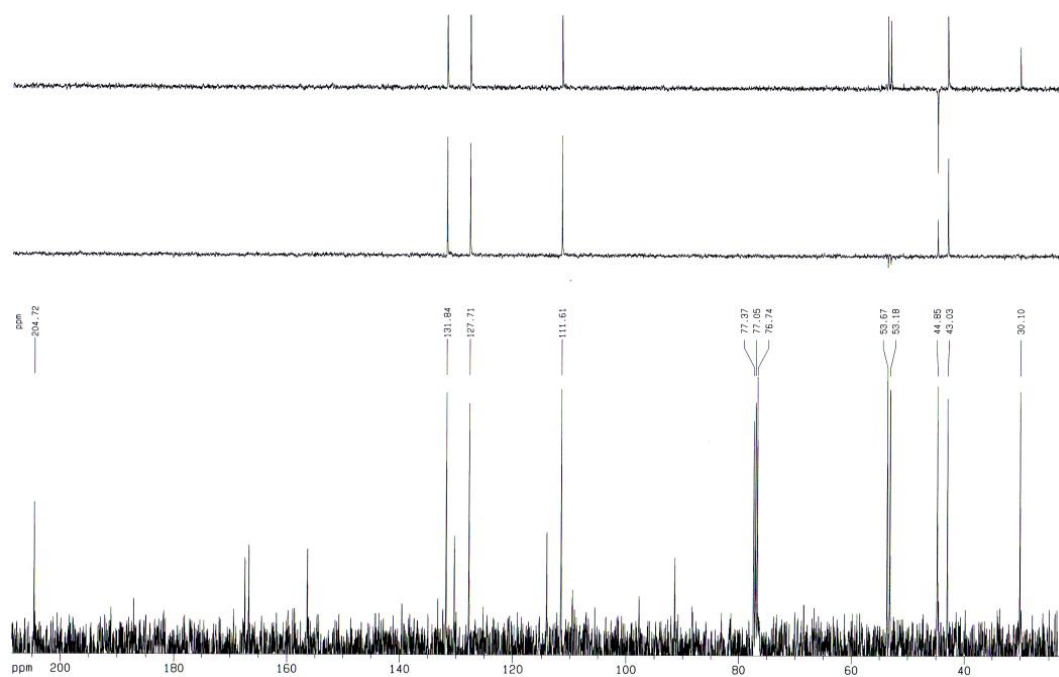
- (E)-4-(5-bromo-2-hydroxyphenyl) but-3-en-2-one (86)**¹H RMN (DMSO-*d*₆, 400 MHz)****¹³C RMN (DMSO-*d*₆, 100 MHz)**

IR

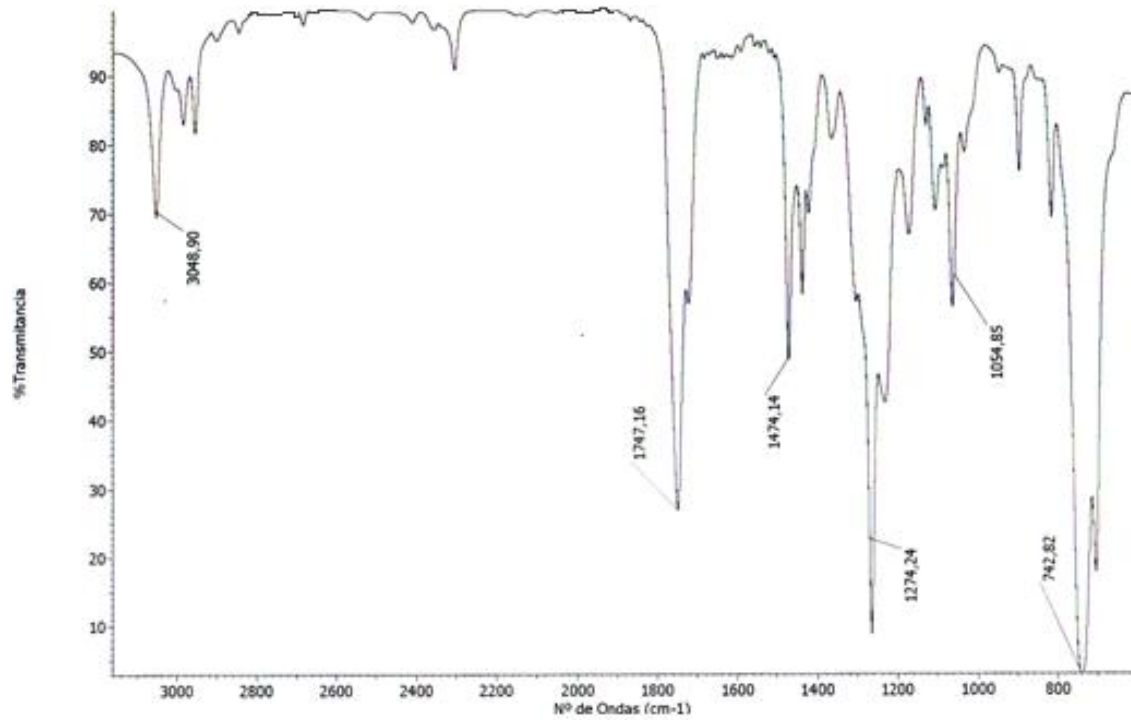


HRMS

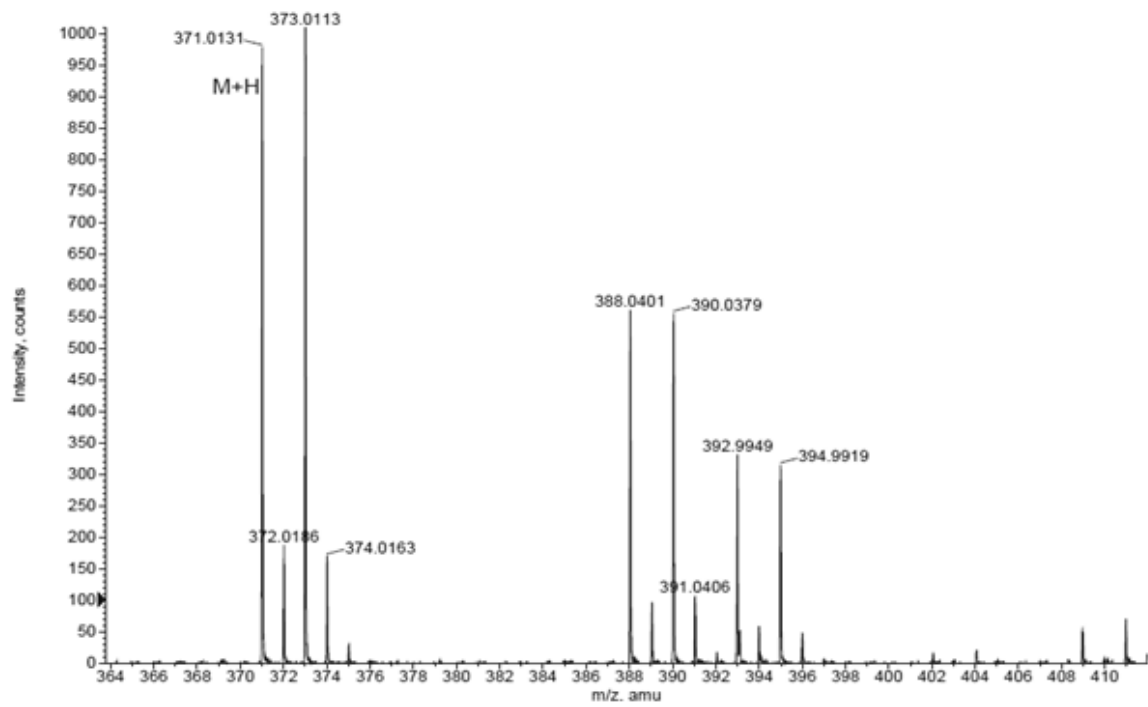


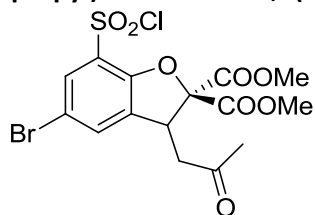
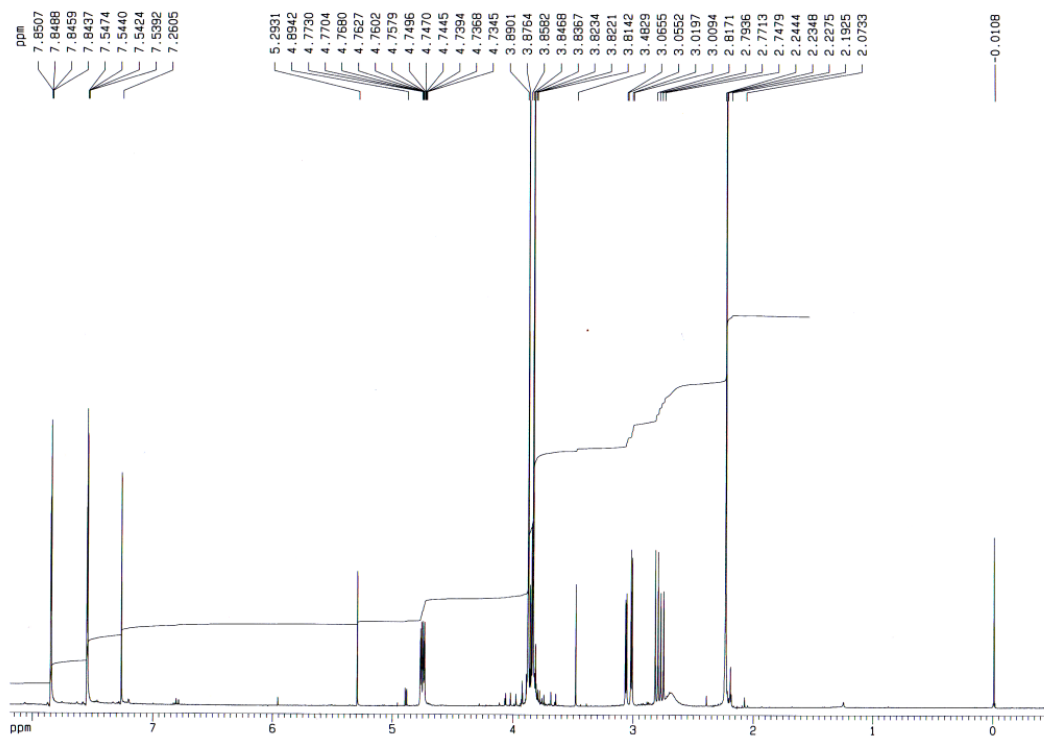
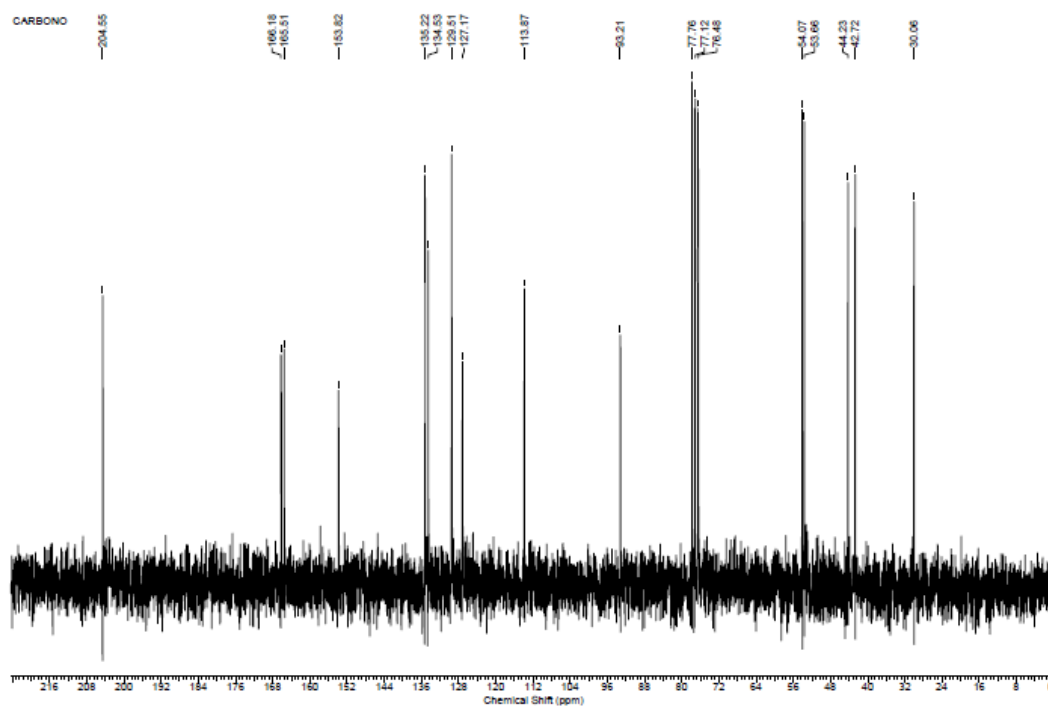
- 5-bromo-3-(2-oxopropyl)-benzofuran-2, 2(3H)-dicarboxylate (88)¹H RMN (CDCl₃, 400 MHz)¹³C RMN (CDCl₃, 400 MHz)

IR

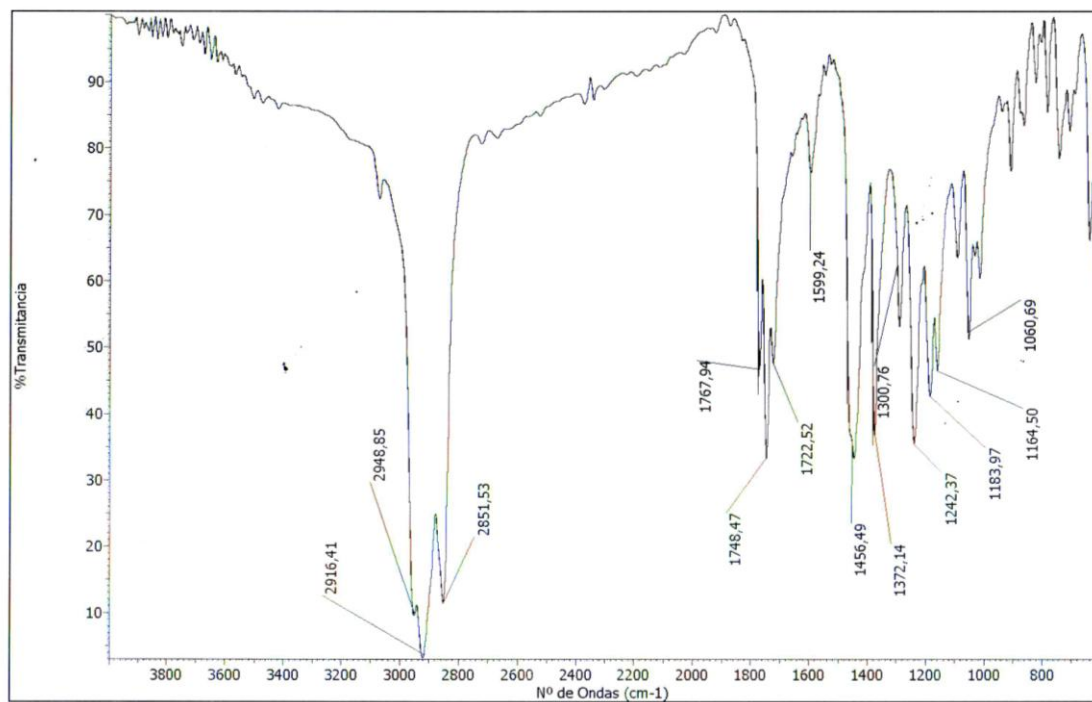


HRMS

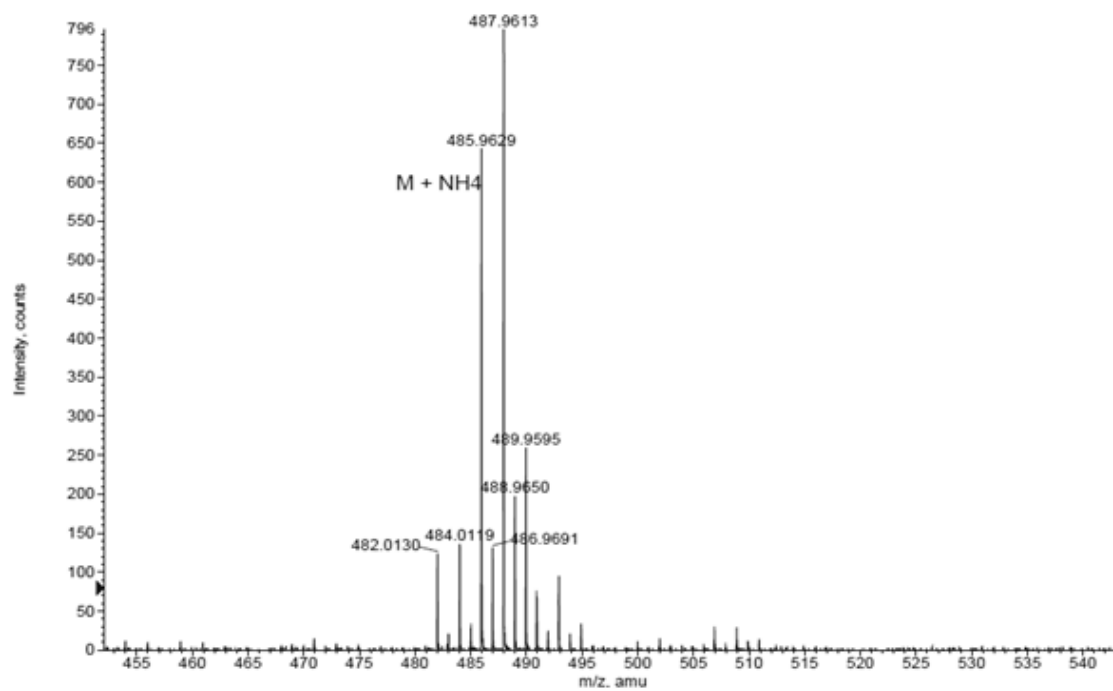


- 5-Bromo -7-(chlorosulfonyl)-3-(2-oxopropyl)-benzofuran-2,2(3H)-dicarboxylate (89)¹H RMN (CDCl₃, 400 MHz)¹³C RMN (CDCl₃, 100 MHz)

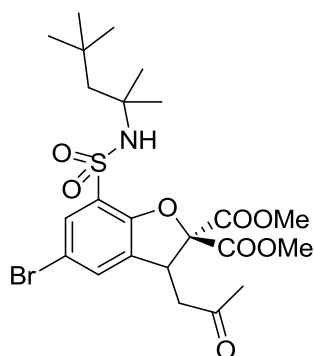
IR



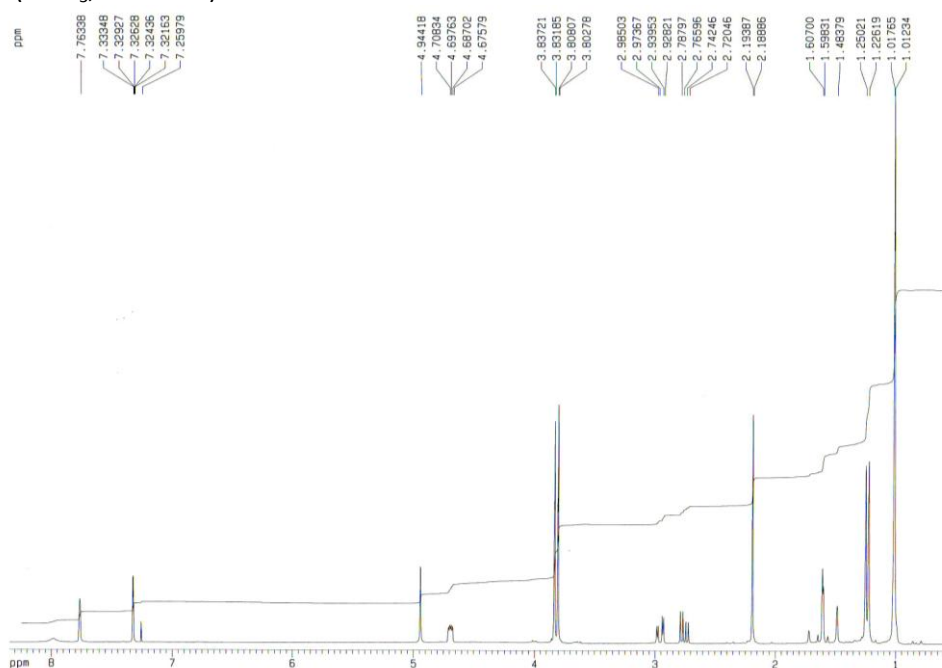
HRMS



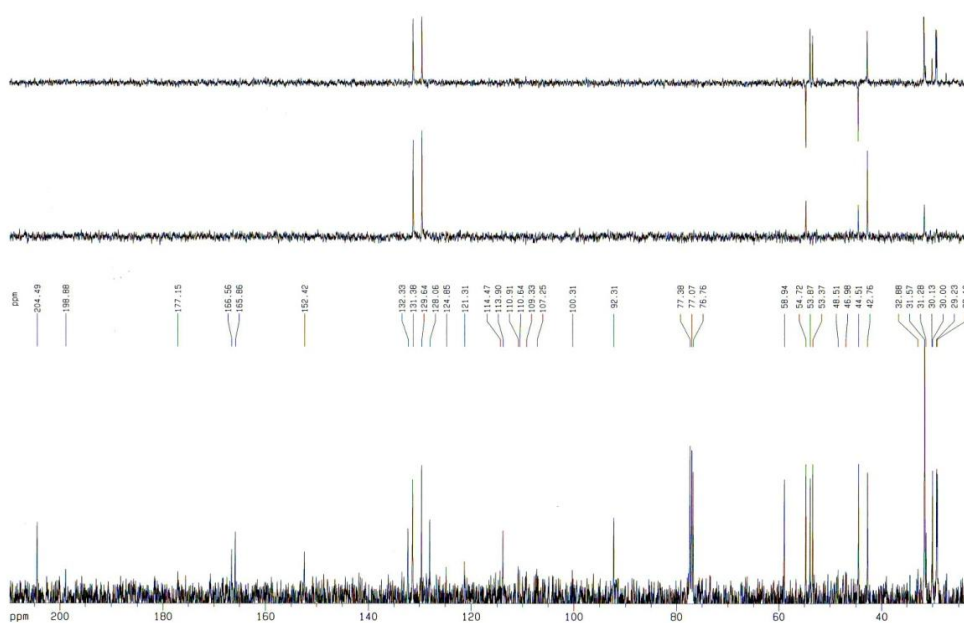
- 5-bromo-3-(2-oxopropyl)-7-(*N*-(2,4,4-trimethylpentan-2-yl)sulfamoyl)benzofuran-2,2(3*H*)dicarboxylate (90)



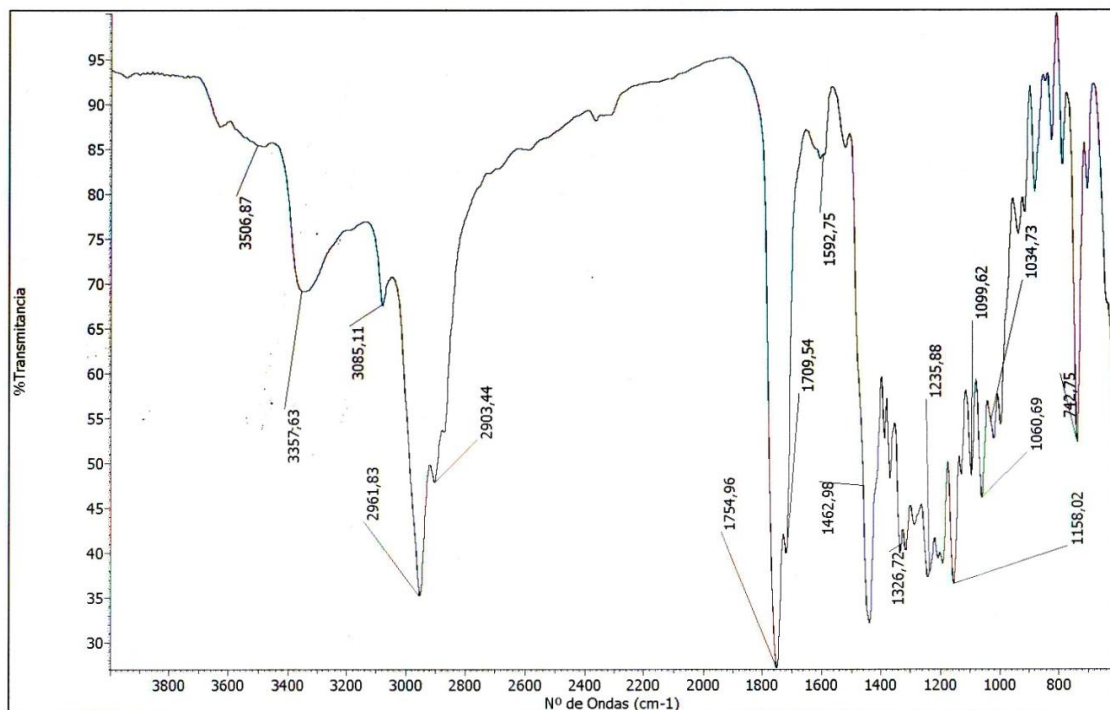
^1H RMN (CDCl_3 , 400 MHz)



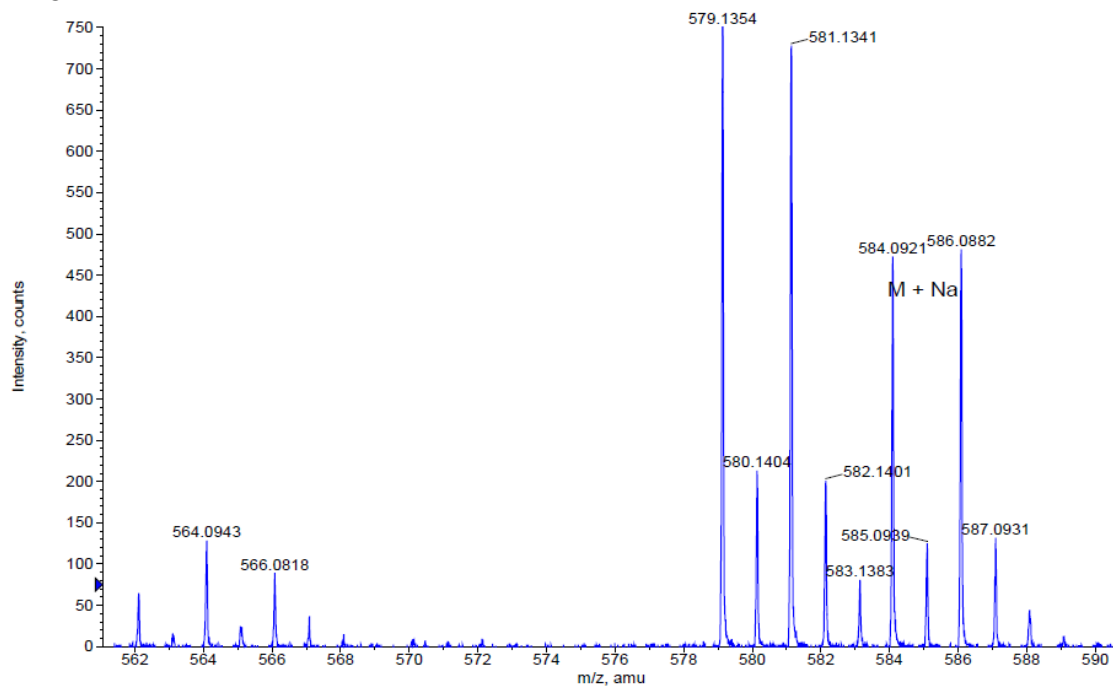
^{13}C RMN (CDCl_3 , 100 MHz)



IR

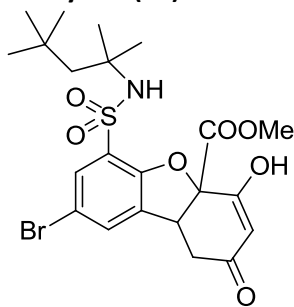


HRMS

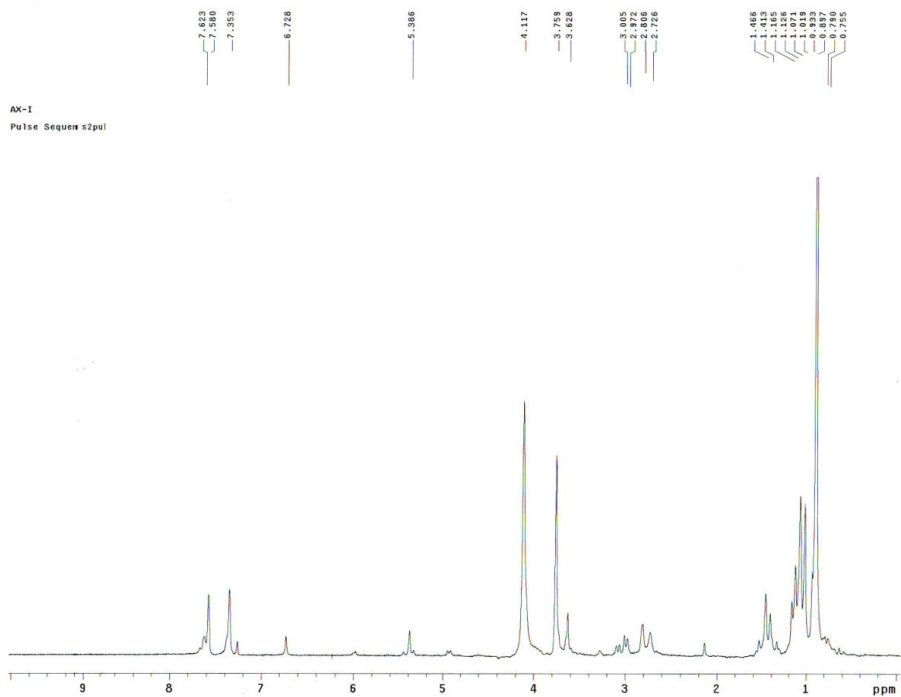


Formula	CalculatedMass	mDaError	ppmError	RDB
C23 H32 N O8 Na S Br	584.092421	-0.321428	-0.550303	7.5

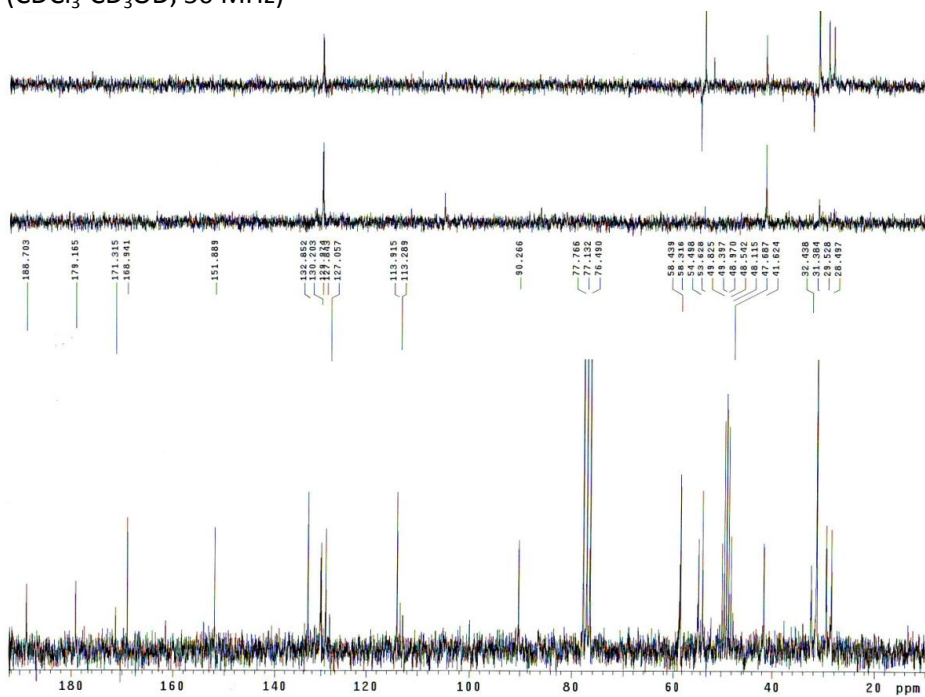
- Methyl 8-bromo-2-hydroxy-2-oxo-6-(*N*-(2,4,4-trimethylpentan-2-yl)sulfamoyl)-1,4,4a,9b-tetrahydrobenzo[*b,d*]furan-4a-carboxylate (93)



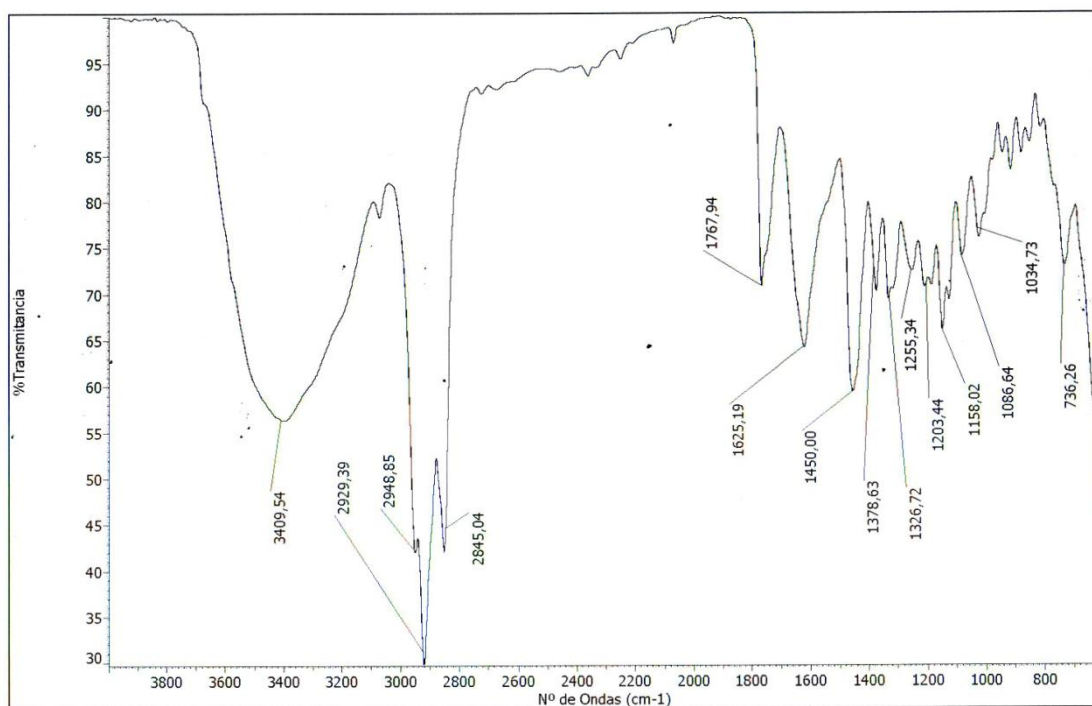
^1H RMN ($\text{CDCl}_3\text{-CD}_3\text{OD}$, 200 MHz)



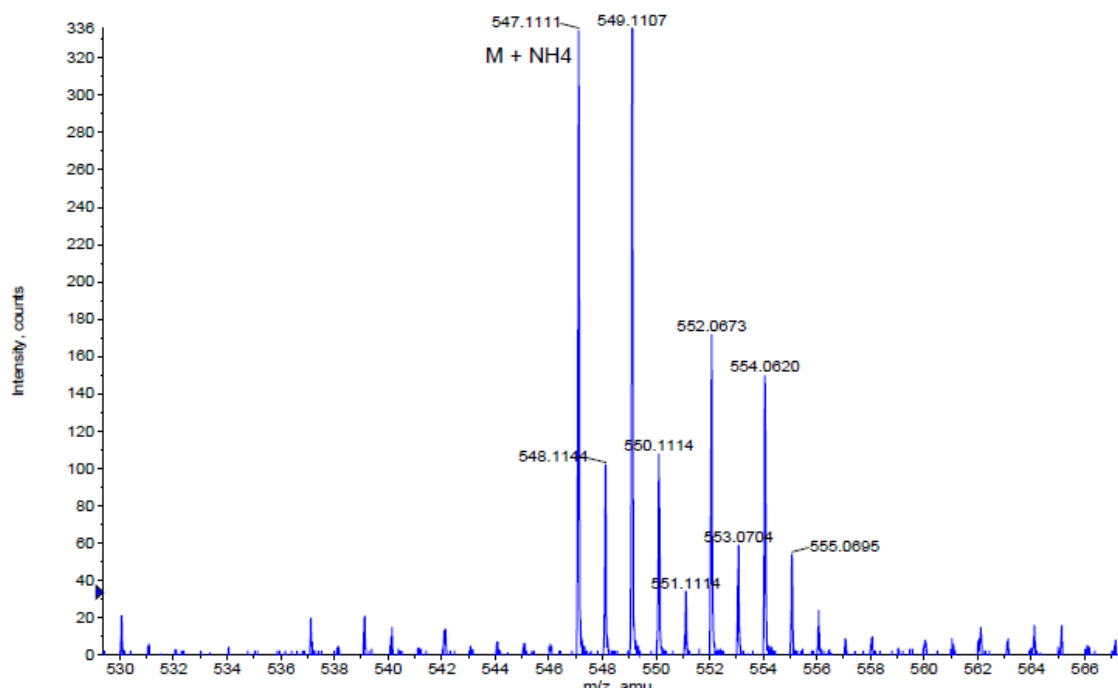
^{13}C RMN ($\text{CDCl}_3\text{-CD}_3\text{OD}$, 50 MHz)



IR

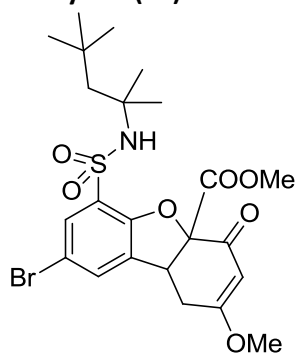


HRMS

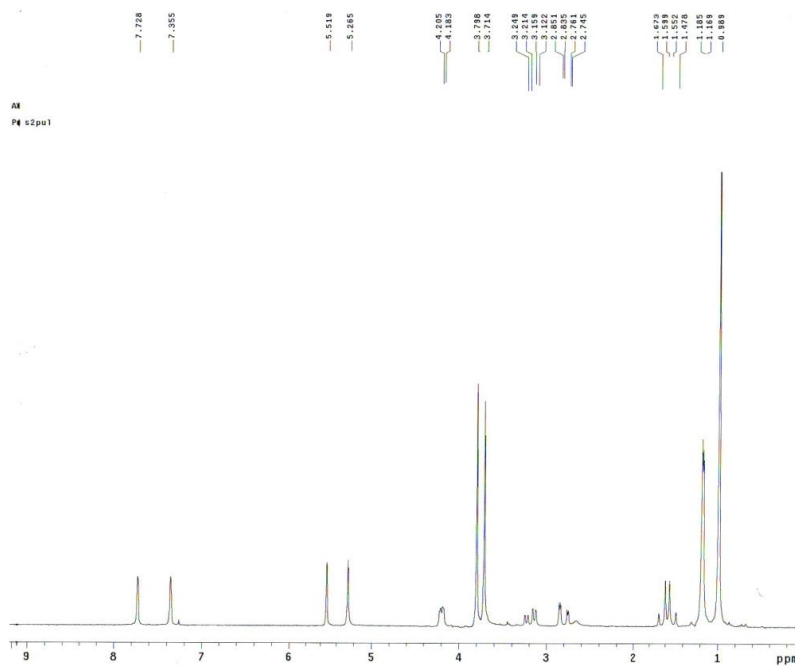


Formula	CalculatedMass	mDaError	ppmError	RDB
C27 H22 N4 O4 S Cl	533.104481	0.118579	0.222431	18.5
C14 H30 N2 O15 S Cl	533.104995	-0.394765	-0.740501	0.5
C26 H26 O8 S Cl	533.103144	1.455891	2.730964	13.5
C30 H23 N2 O2 Na S Cl	533.106099	-1.498865	-2.811575	19.5
C17 H31 O13 Na S Cl	533.106612	-2.012209	-3.774507	1.5
C25 H23 N4 O4 Na S Cl	533.102076	2.523839	4.734224	15.5
C18 H27 N4 O9 Na S Cl	533.10795	-3.349521	-6.28304	6.5
C24 H27 O8 Na S Cl	533.100739	3.861151	7.242757	10.5
C32 H22 N2 O2 S Cl	533.108504	-3.904125	-7.323368	22.5
C19 H30 O13 S Cl	533.109017	-4.417469	-8.2863	4.5

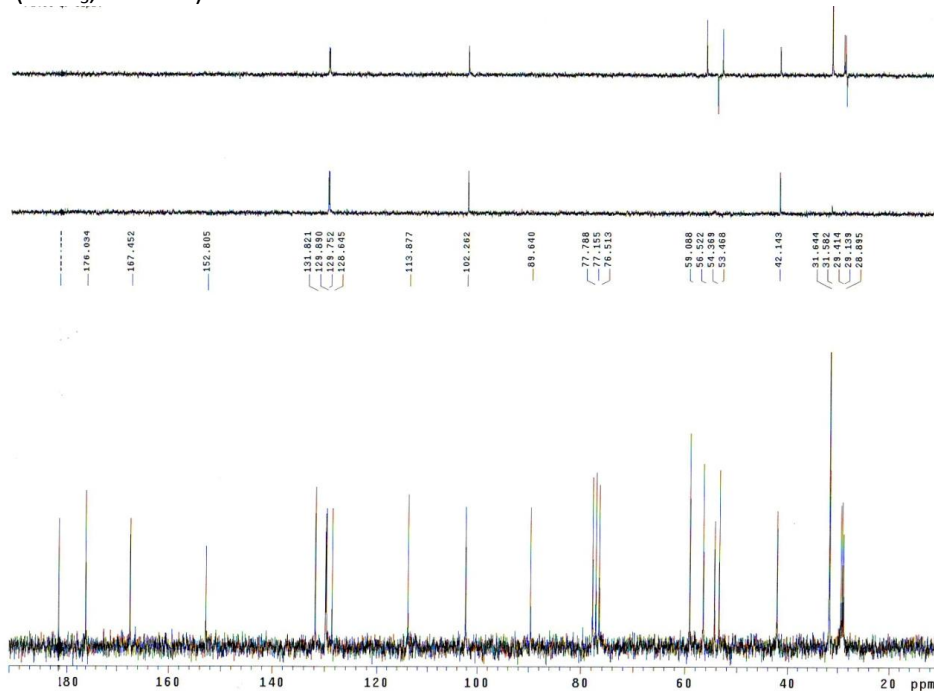
- Methyl 8-bromo-2-methoxy-4-oxo-6-(*N*-(2,4,4-trimethylpentan-2-yl)sulfamoyl)-1,4,4a,9b-tetrahydrobenzo[*b,d*]furan-4a-carboxylate (91)



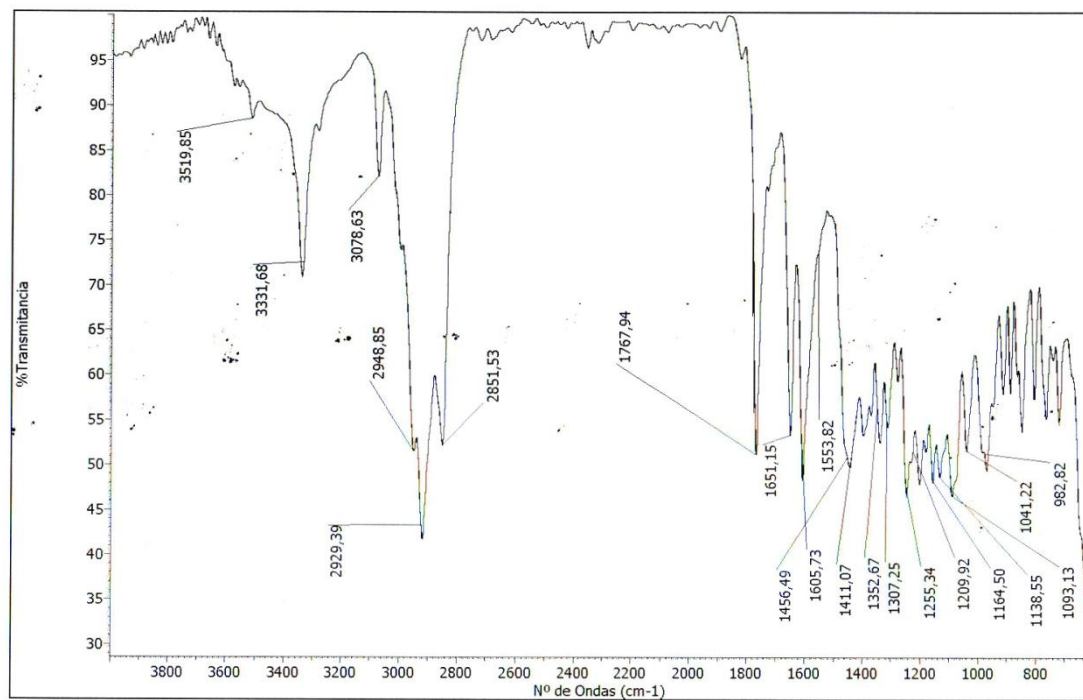
^1H RMN (CDCl_3 , 200 MHz)



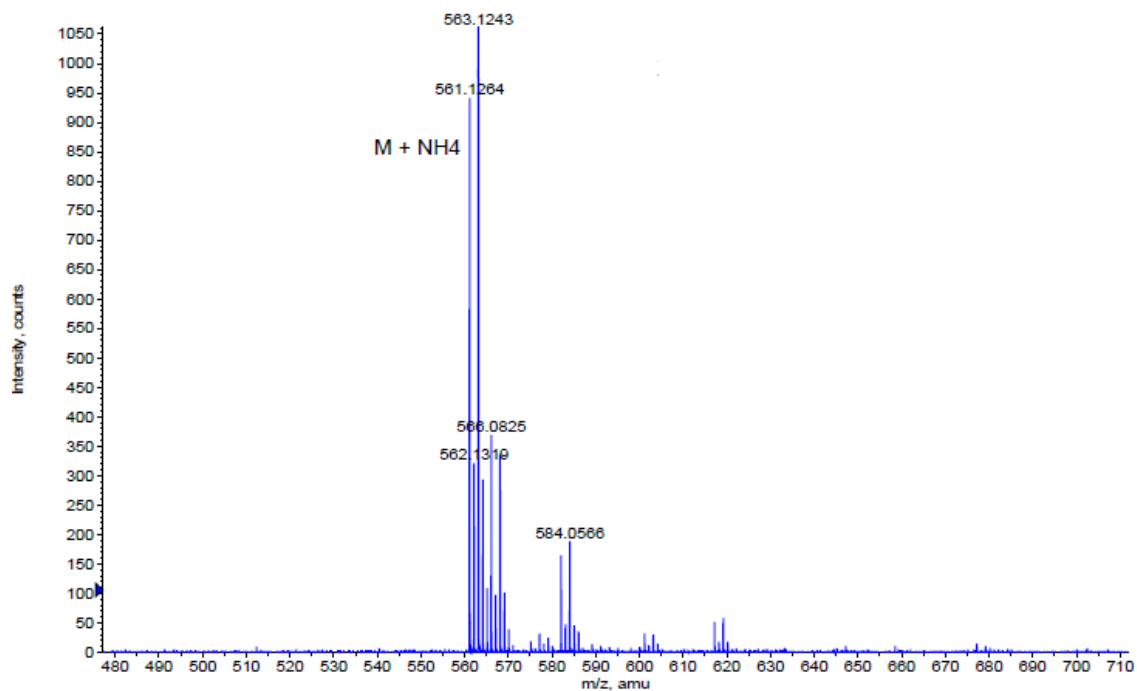
^{13}C RMN (CDCl_3 , 50 MHz)



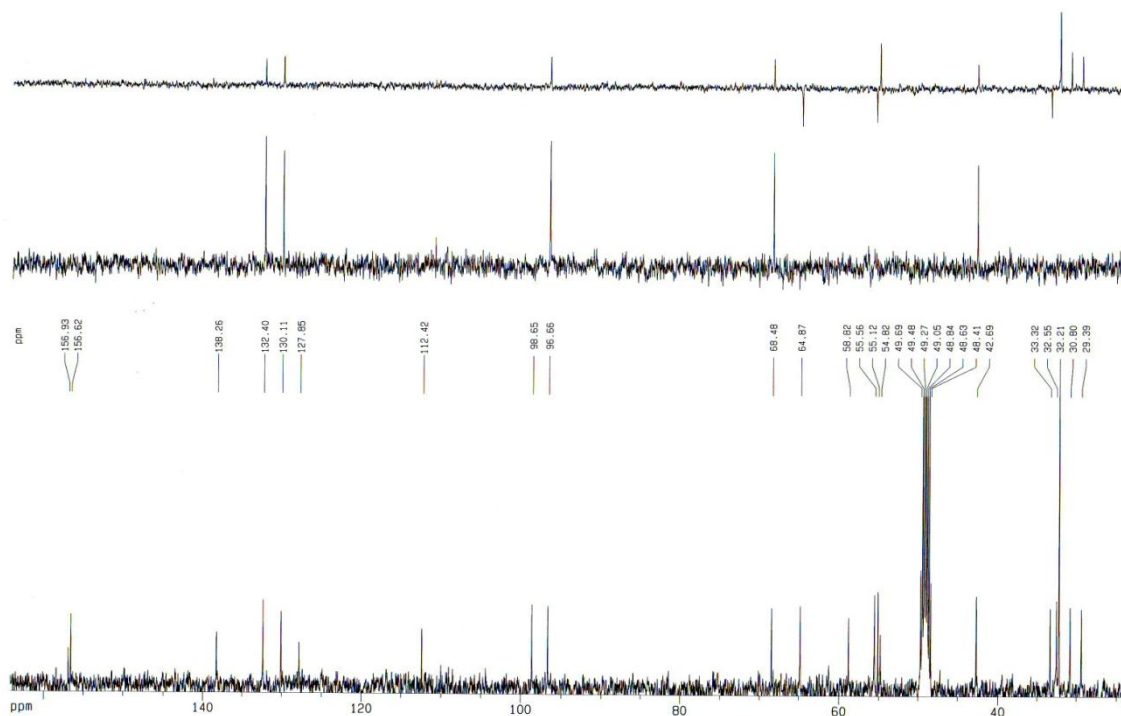
IR



HRMS

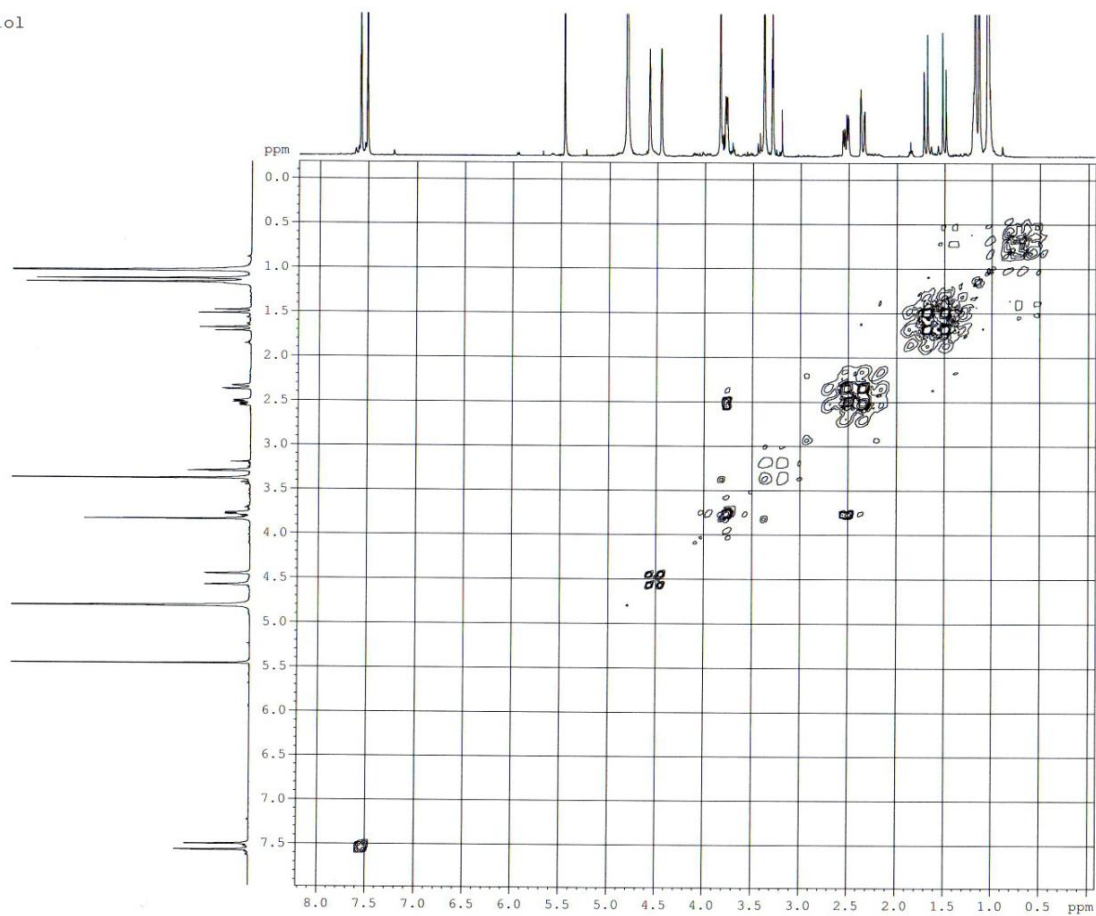


Formula	CalculatedMass	mDaError	ppmError	RDB
C23 H34 N2 O7 S Br	561.126461	-0.061176	-0.109023	7.5
C26 H35 O5 Na S Br	561.128079	-1.67862	-2.991516	8.5
C35 H30 S Br	561.124611	1.78948	3.189082	20.5
C21 H35 N2 O7 Na S Br	561.124056	2.344084	4.177458	4.5
C27 H31 N4 O Na S Br	561.129416	-3.015932	-5.374777	13.5
C18 H34 N4 O9 S Br	561.122438	3.961528	7.05995	3.5
C28 H34 O5 S Br	561.130484	-4.08388	-7.277997	11.5
C33 H31 Na S Br	561.122205	4.19474	7.475563	17.5
C29 H30 N4 O S Br	561.131821	-5.421192	-9.661258	16.5

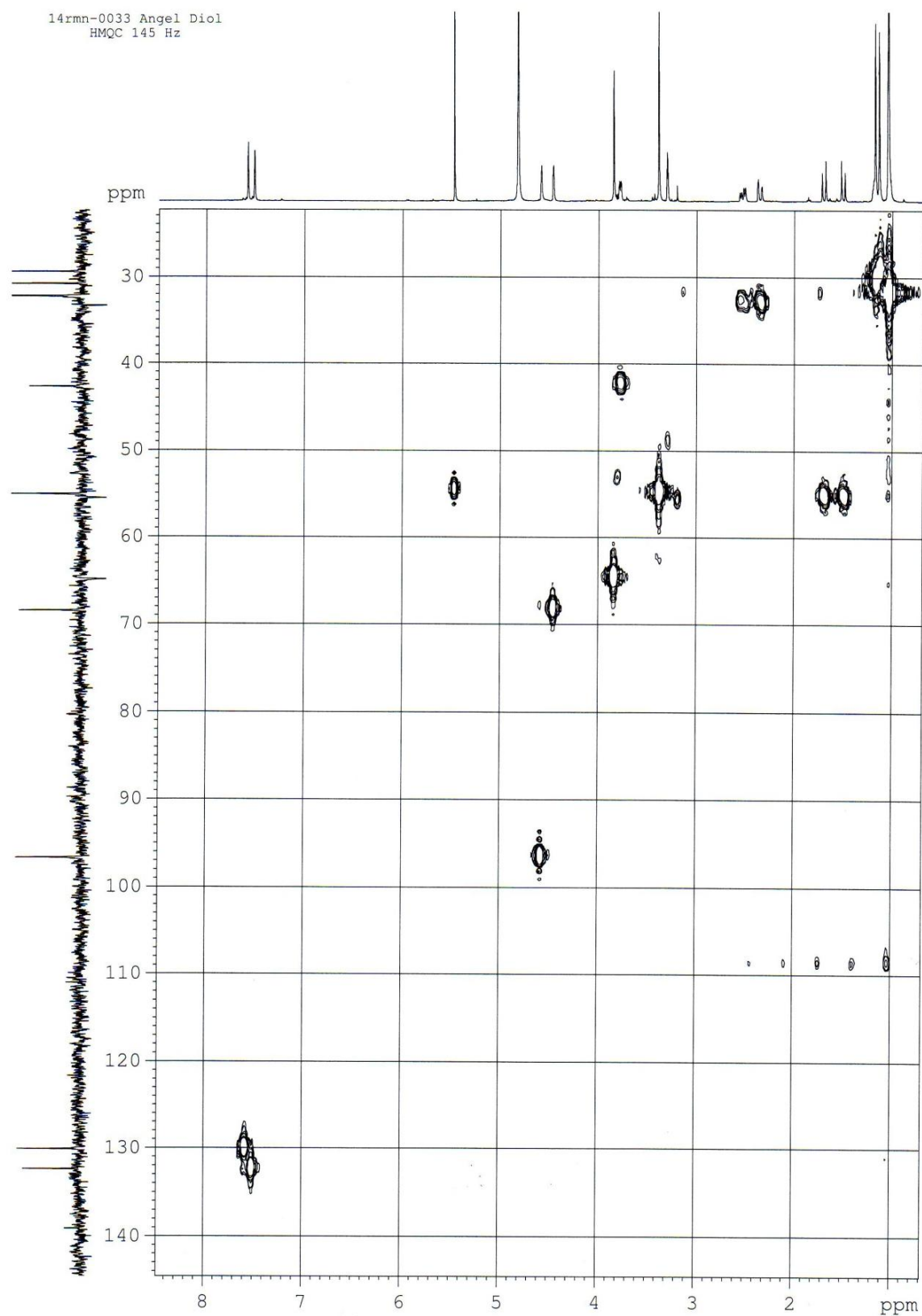
^{13}C RMN (CD_3OD , 100 MHz)

COSY

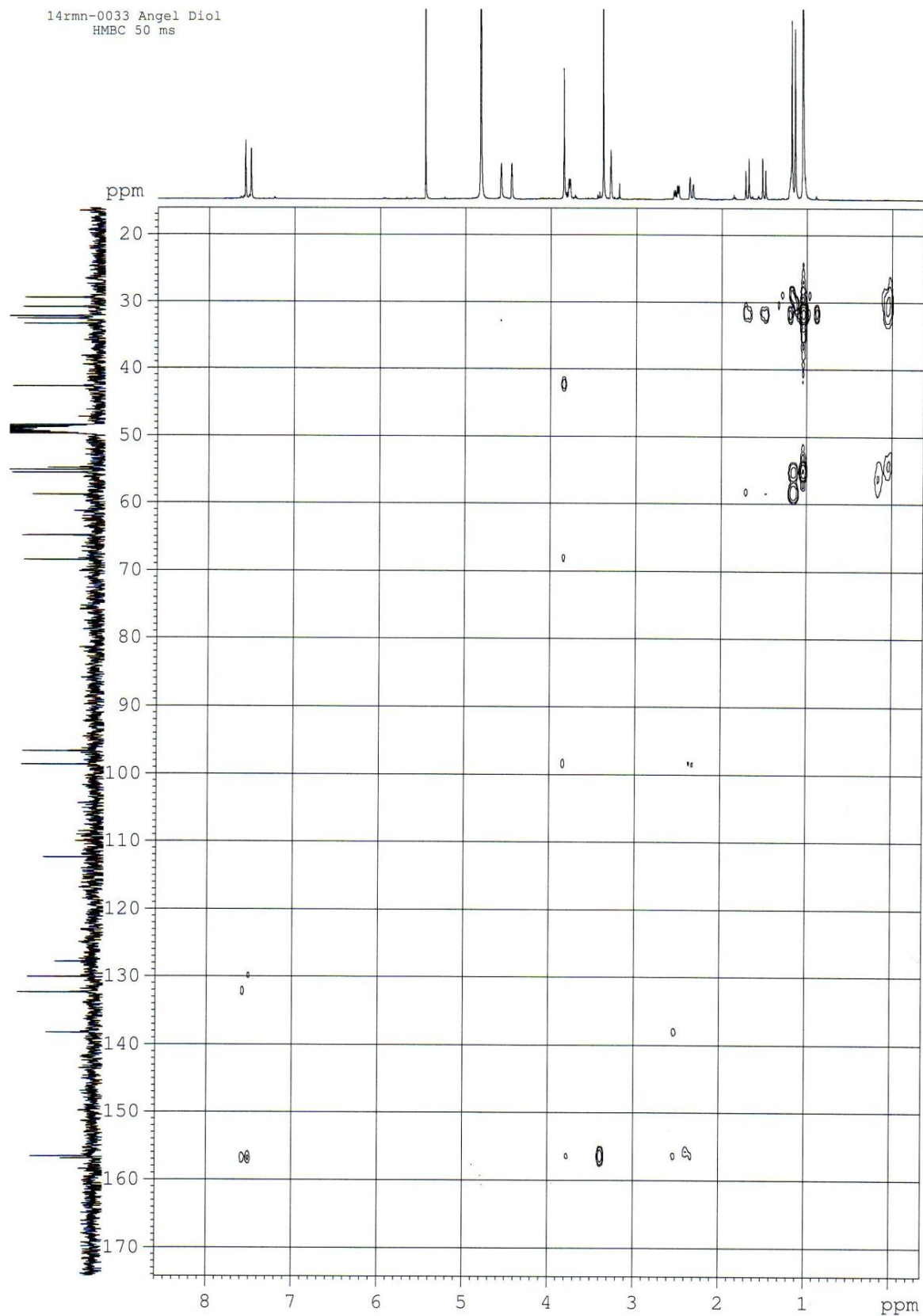
iol



HMQC

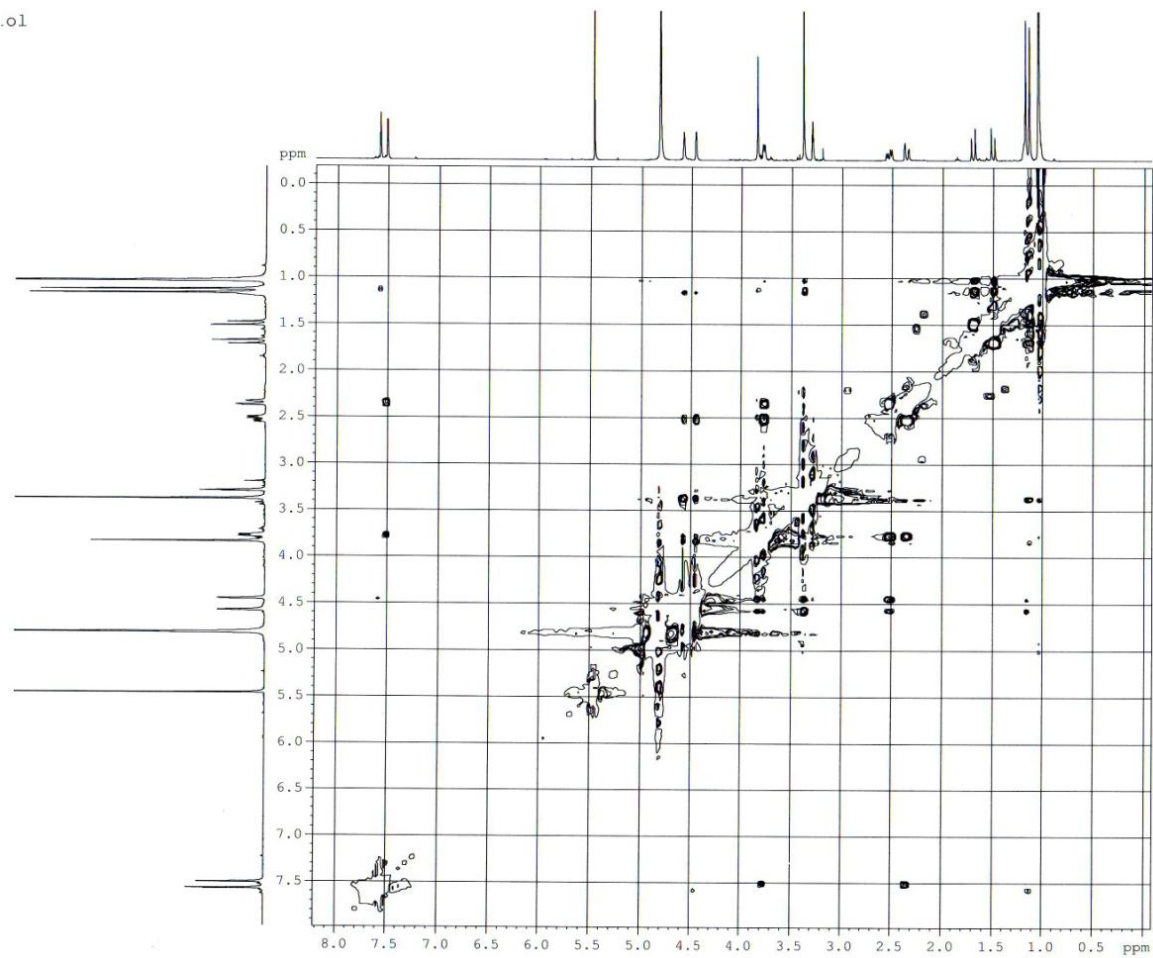


HMBC

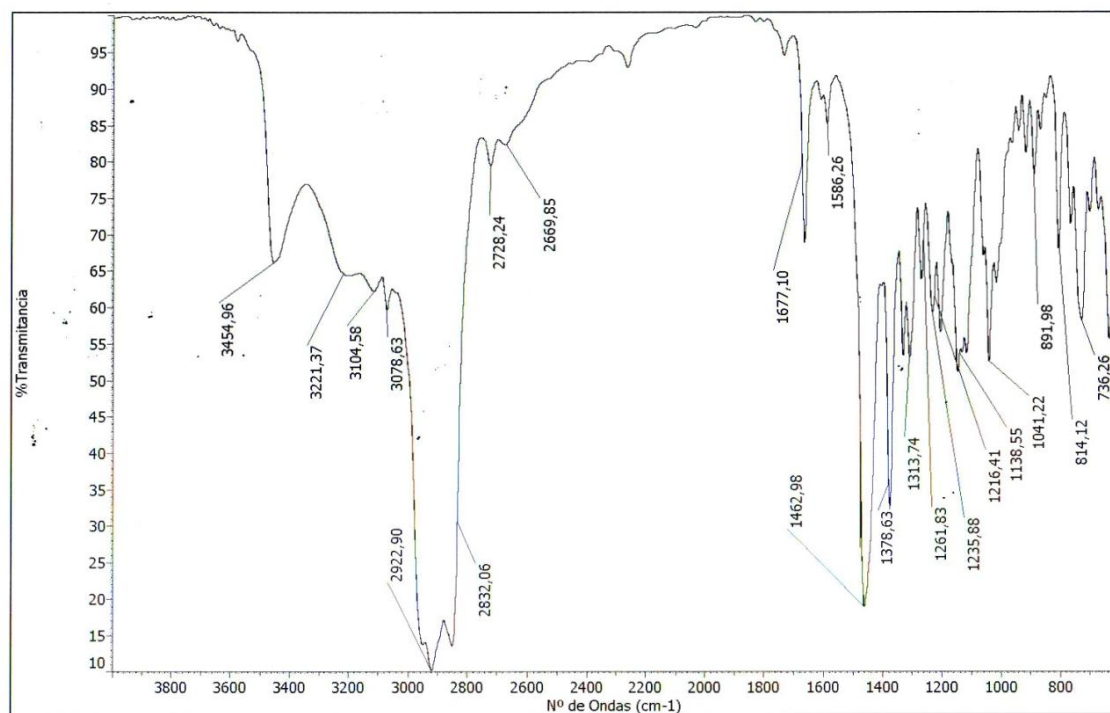


ROESY

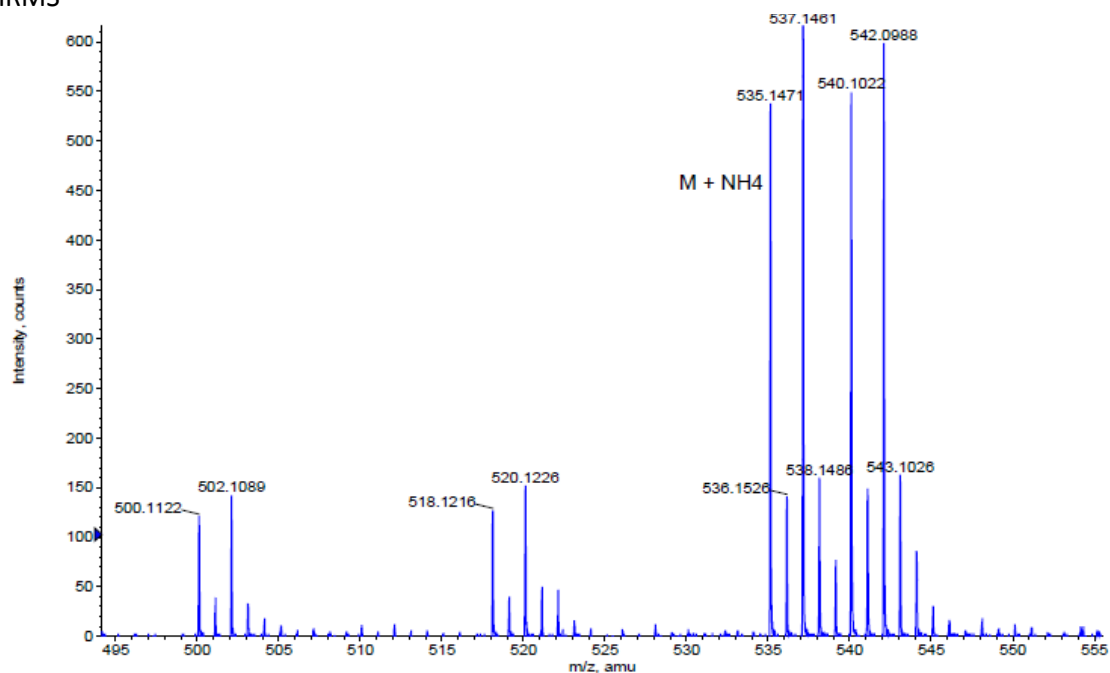
.o1



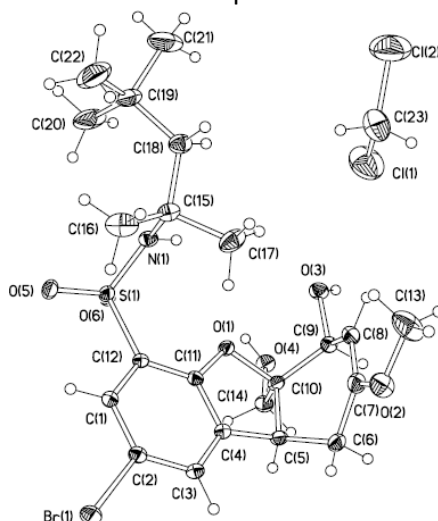
IR



HRMS

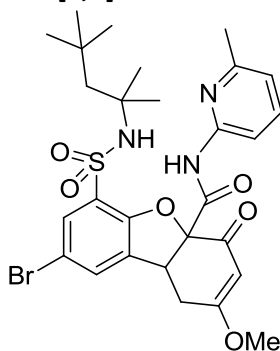


Formula	CalculatedMass	mDaError	ppmError	RDB
C22 H36 N2 O6 S Br	535.147197	-0.096616	-0.180541	5.5
C25 H37 O4 Na S Br	535.148814	-1.71406	-3.202967	6.5
C20 H37 N2 O6 Na S Br	535.144791	2.308644	4.314032	2.5
C26 H33 N4 Na S Br	535.150151	-3.051372	-5.701925	11.5
C17 H36 N4 O8 S Br	535.143174	3.926088	7.336458	1.5
C27 H36 O4 S Br	535.151219	-4.11932	-7.697539	9.5

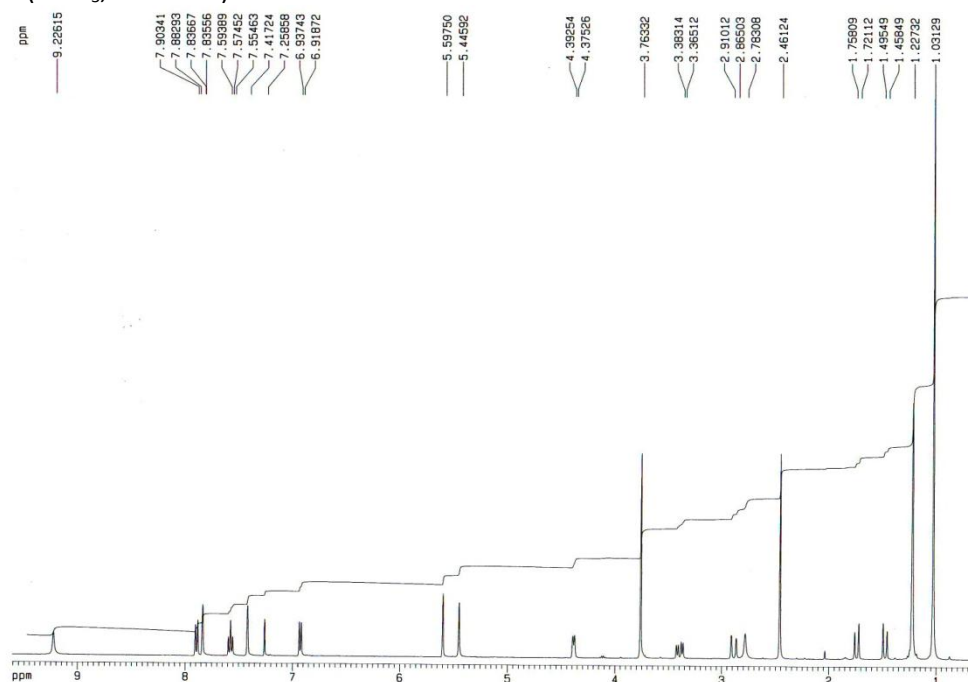
X-ray structure, crystal and refinement data of compound **92**

Empirical formula	$C_{22}H_{32}BrNO_6S, CH_2Cl_2$
Molecular weight	603.38
Temperature	298 (2) K
Wavelength	1.54178 Å
Crystal system, Space group	Triclinic, P-1
Unit cell dimensions	$a = 9.7902 (6) \text{ \AA}$ $\alpha = 77.203 (4)^\circ$ $b = 11.9074 (7) \text{ \AA}$ $\beta = 73.176 (4)^\circ$ $c = 13.2668 (7) \text{ \AA}$ $\gamma = 71.420 (4)^\circ$
Volume	1338.92 (14) Å ³
Z; Density (calculated)	2; 1.443 mg/m ³
Absorption coefficient	4.800 mm ⁻¹
F(000)	624
Crystal size	0.25 x 0.20 x 0.15 mm
θ range	3.96 – 66.78 °
Limiting indices h, k, l	-11 ≤ h ≤ 11, -14 ≤ k ≤ 13, -11 ≤ l ≤ 15
Reflections collected/independent	7816/4245 $R_{int} = 0.0433$
Refinement method	Least squares method with full matrix in F^2
Data/restraints/parameters	4245/0/331
Goodness-of-fit on F^2	1.056
Final R indices [$I > 2\sigma(I)$]	$R_1 = 0.0743$, $\omega R_2 = 0.2204$
R indices (all data)	$R_1 = 0.0852$, $\omega R_2 = 0.2331$
Largest difference peak and hole	1.019 and -0.737

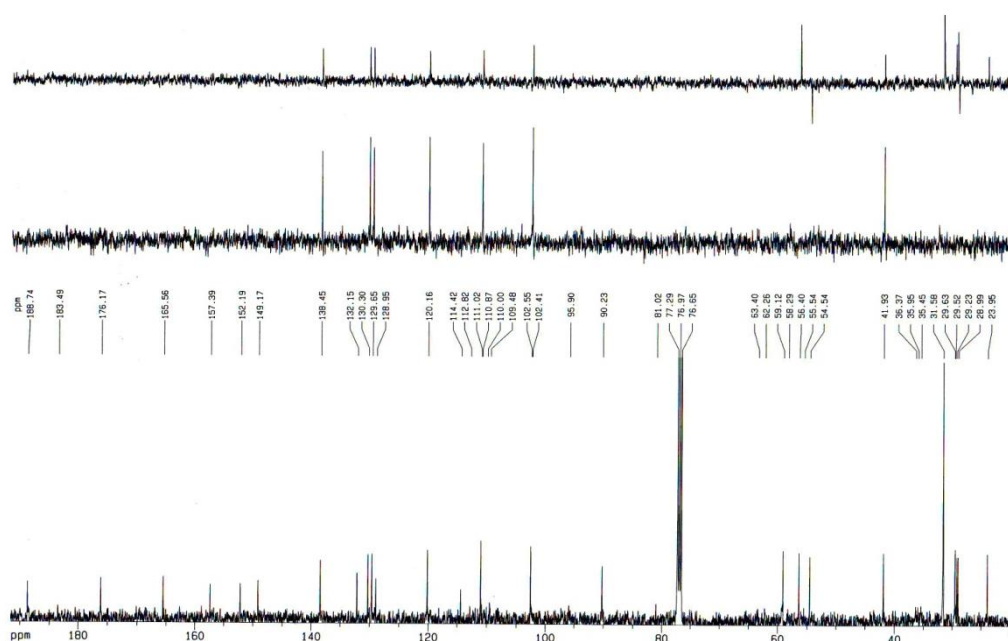
- 8-Bromo-2-methoxy-*N*-(6-methylpyridin-2-yl)-4-oxo-6-(*N*-(2,4,4-trimethylpentan-2-yl)sulfamoyl)-1,4,4a,9b-tetrahydrodibenzo[*b,d*]furan-4a-carboxamide (94)



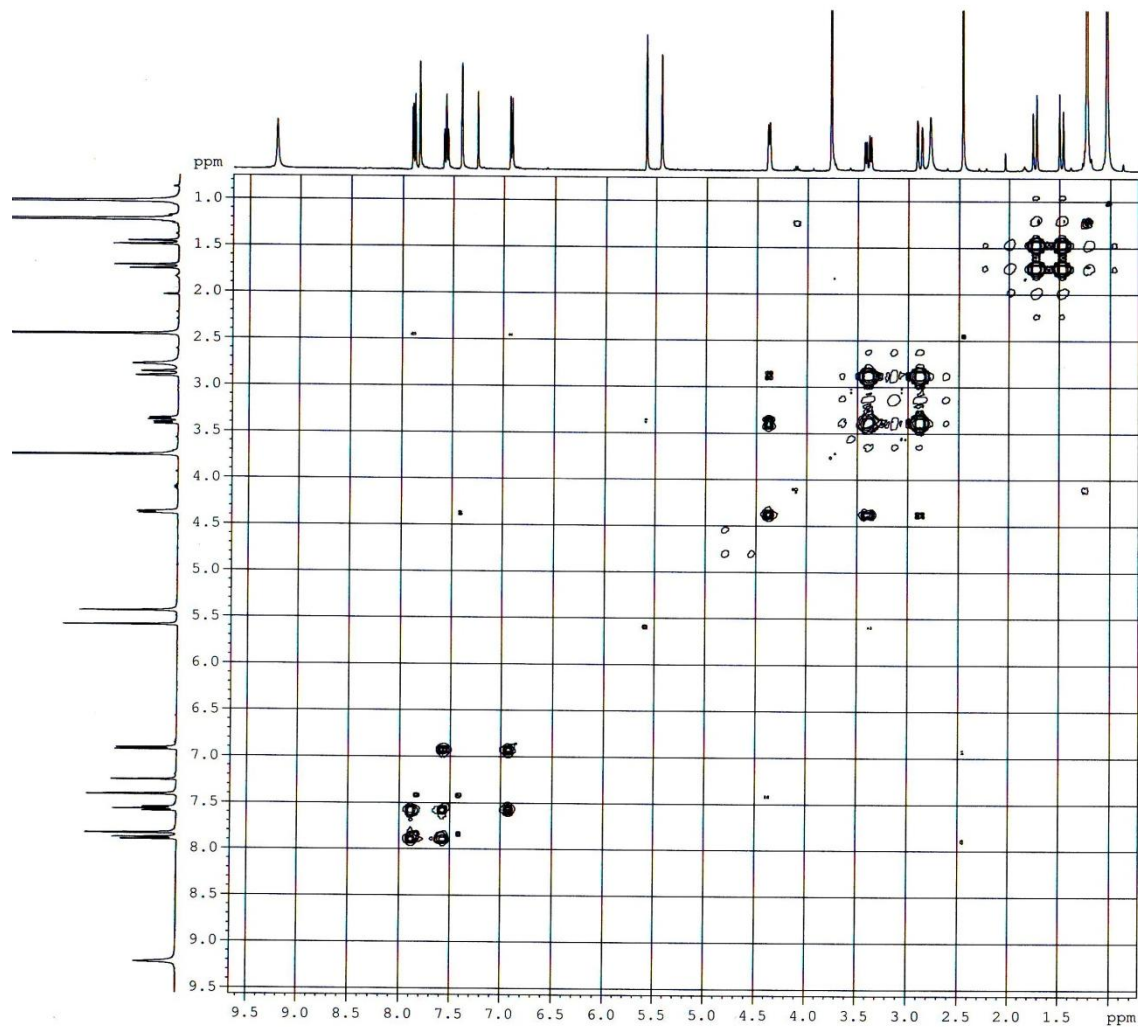
RMN ^1H (CDCl_3 , 400 MHz)



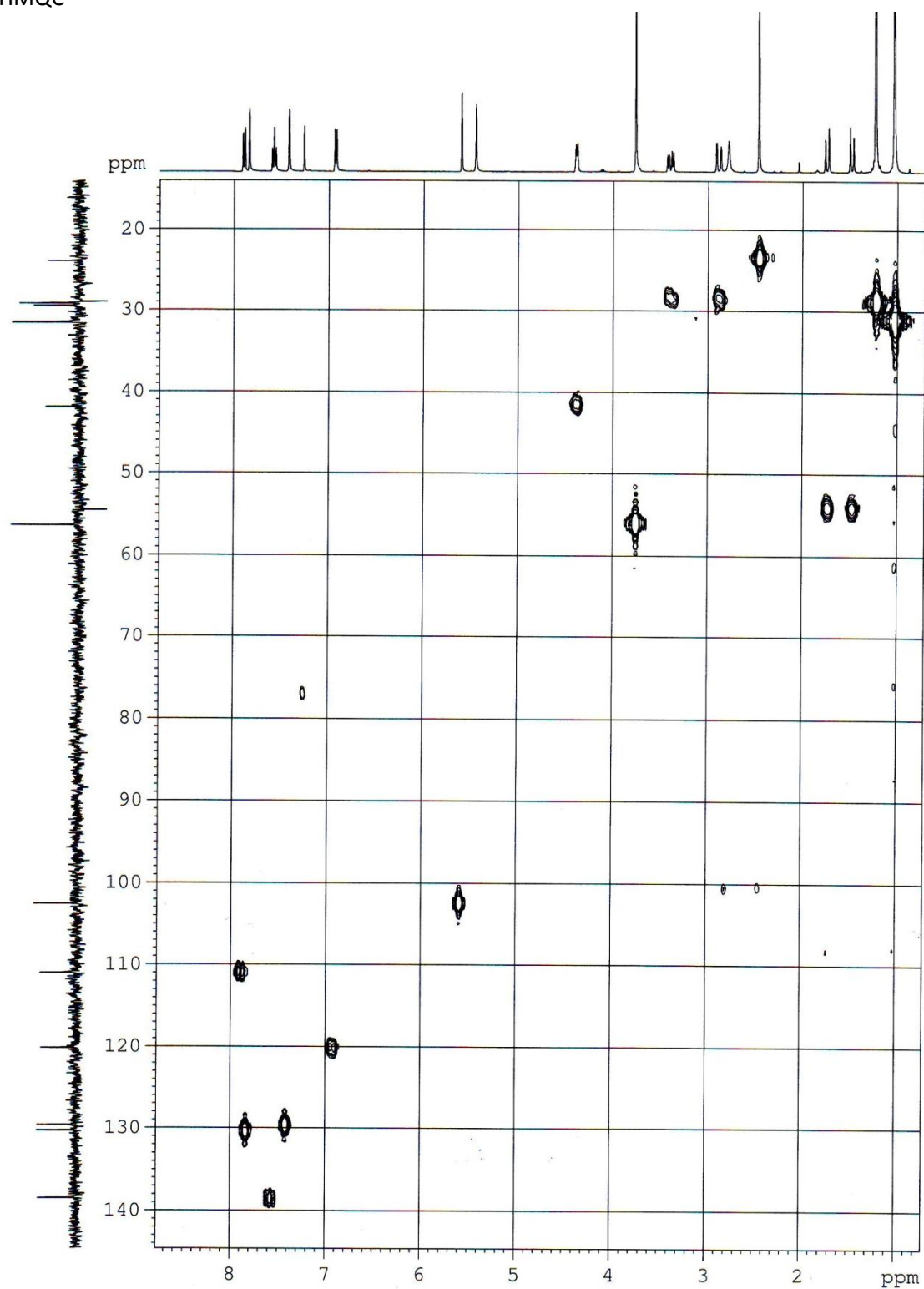
RMN ^{13}C (CDCl_3 , 200 MHz)



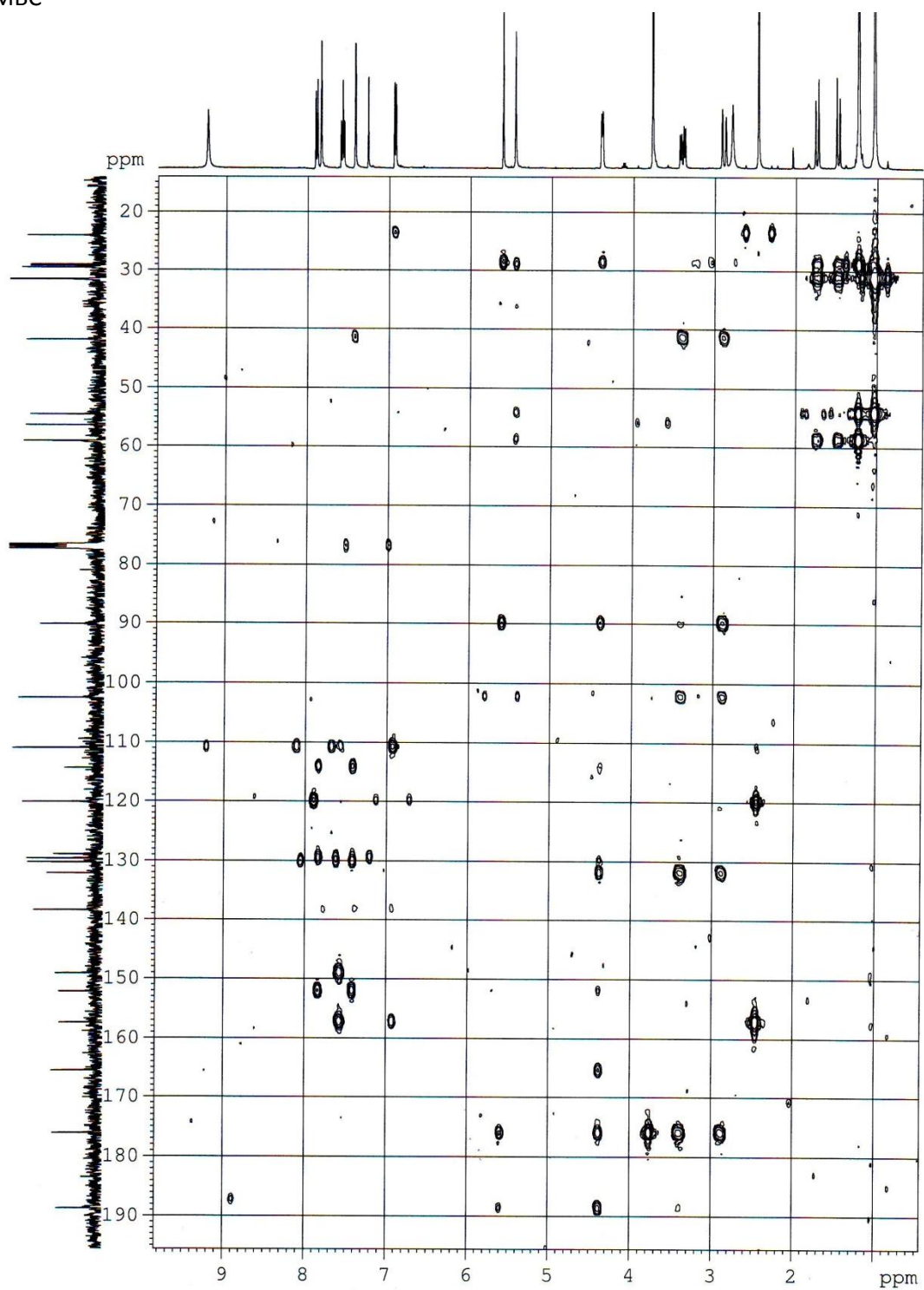
COSY



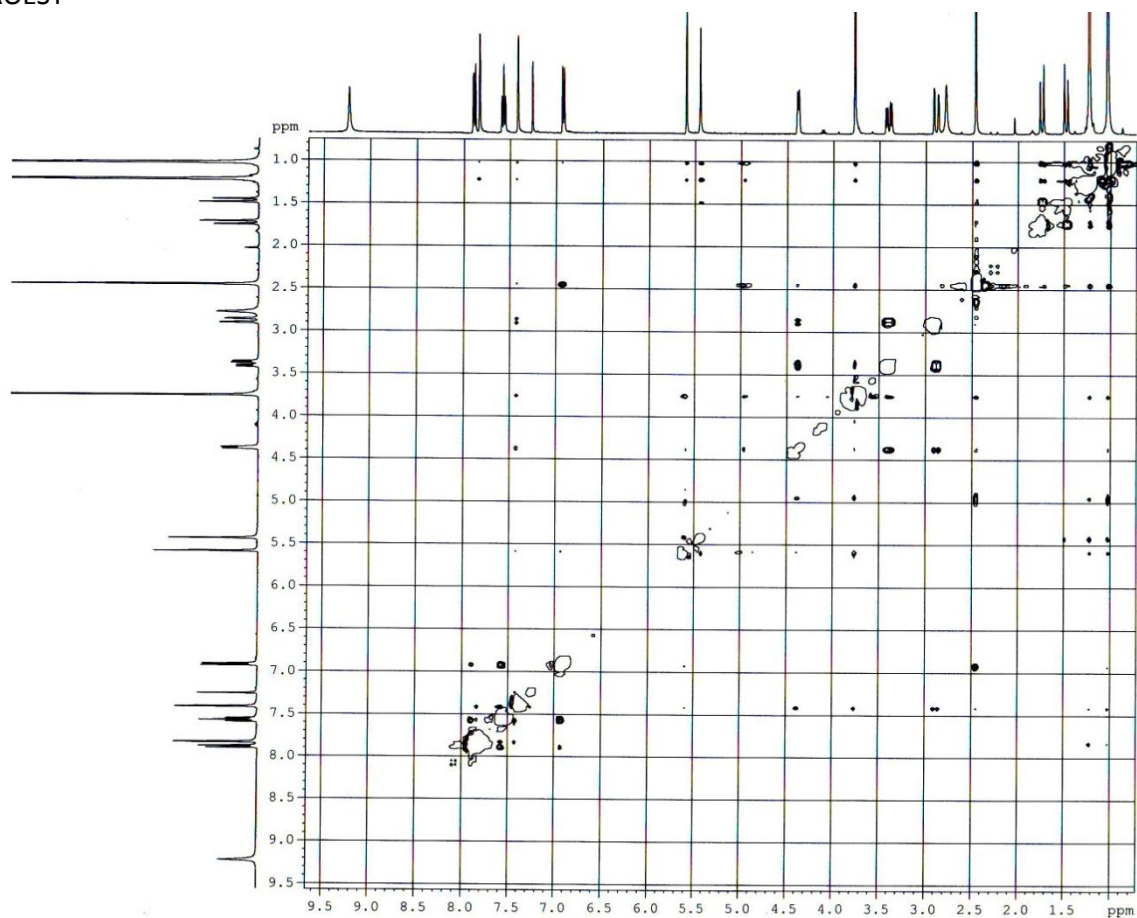
HMQC



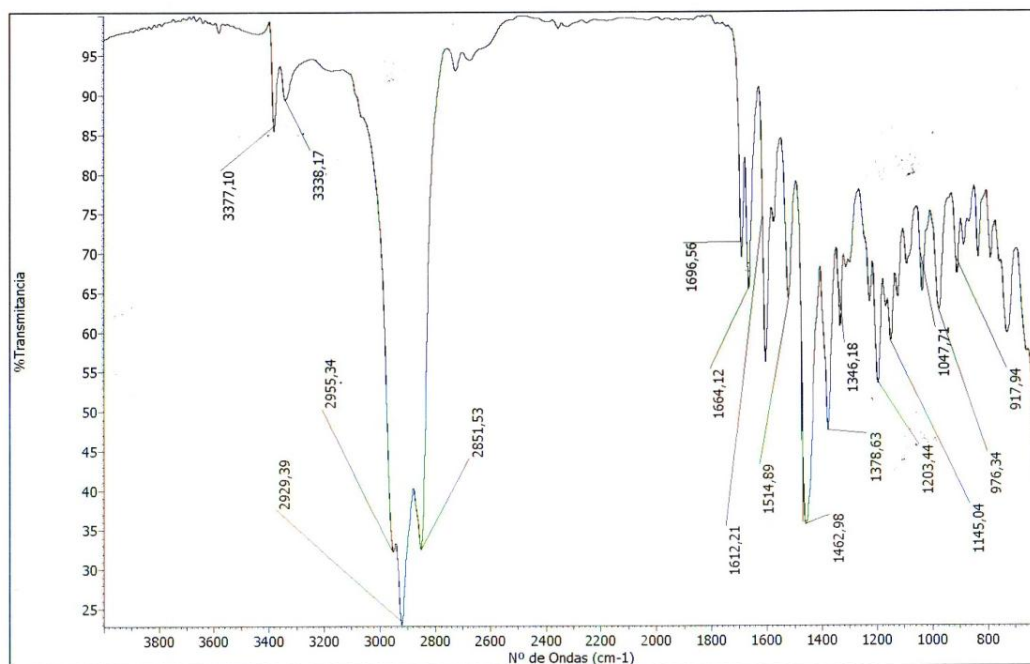
HMBC



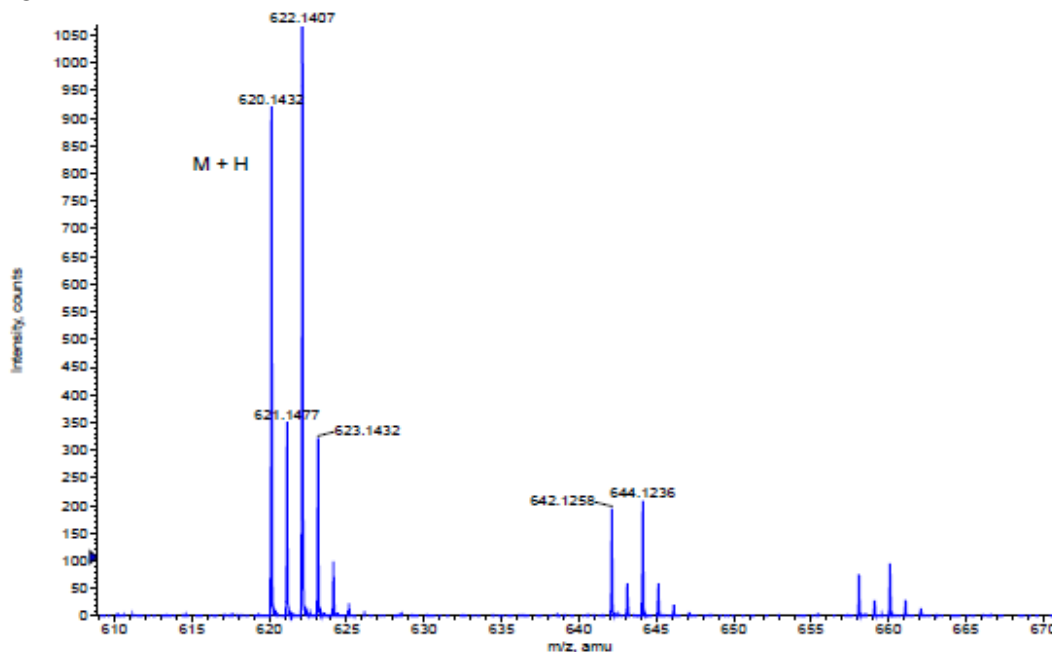
ROESY



IR

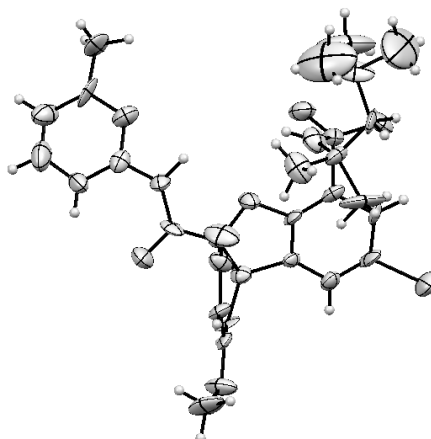


HRMS

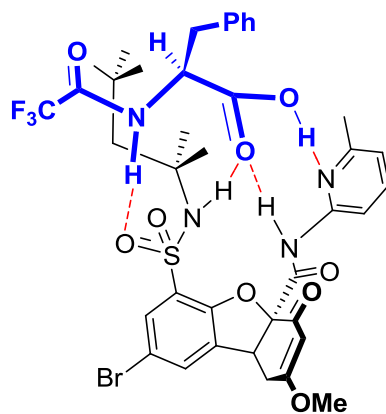
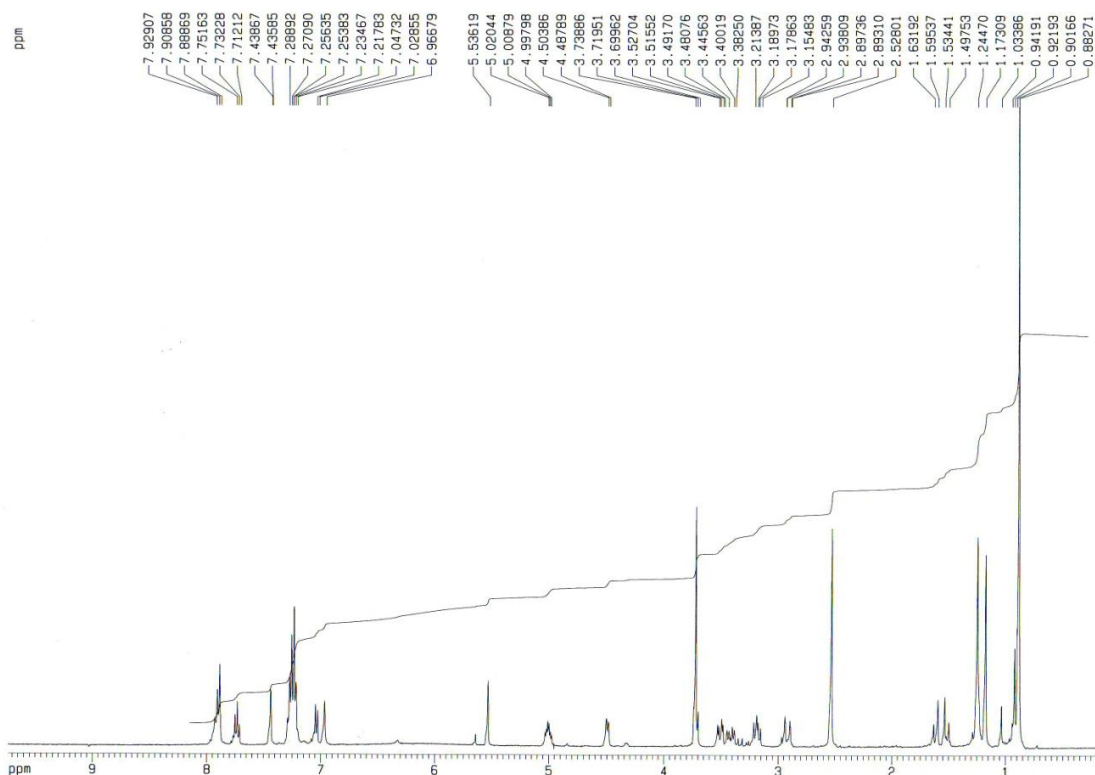


Fomula	CalculatedMass	mDaError	ppmError	RDB
C28 H35 N3 O6 S Br	620.142446	0.754416	1.216518	12.5
C31 H36 N O4 Na S Br	620.144063	-0.863028	-1.391658	13.5
C16 H39 N5 O13 S Br	620.144296	-1.09624	-1.767719	-0.5
C32 H32 N5 Na S Br	620.1454	-2.20034	-3.548113	18.5
C19 H40 N3 O11 Na S Br	620.145914	-2.713684	-4.375895	0.5
C26 H36 N3 O6 Na S Br	620.14004	3.159676	5.09507	9.5
C33 H35 N O4 S Br	620.146468	-3.268288	-5.27021	16.5
C34 H31 N5 S Br	620.147806	-4.6056	-7.426665	21.5
C23 H35 N5 O8 S Br	620.138423	4.77712	7.703246	8.5
C21 H39 N3 O11 S Br	620.148319	-5.118944	-8.254447	3.5
C22 H39 N O12 S Br	620.137086	6.114432	9.859701	3.5

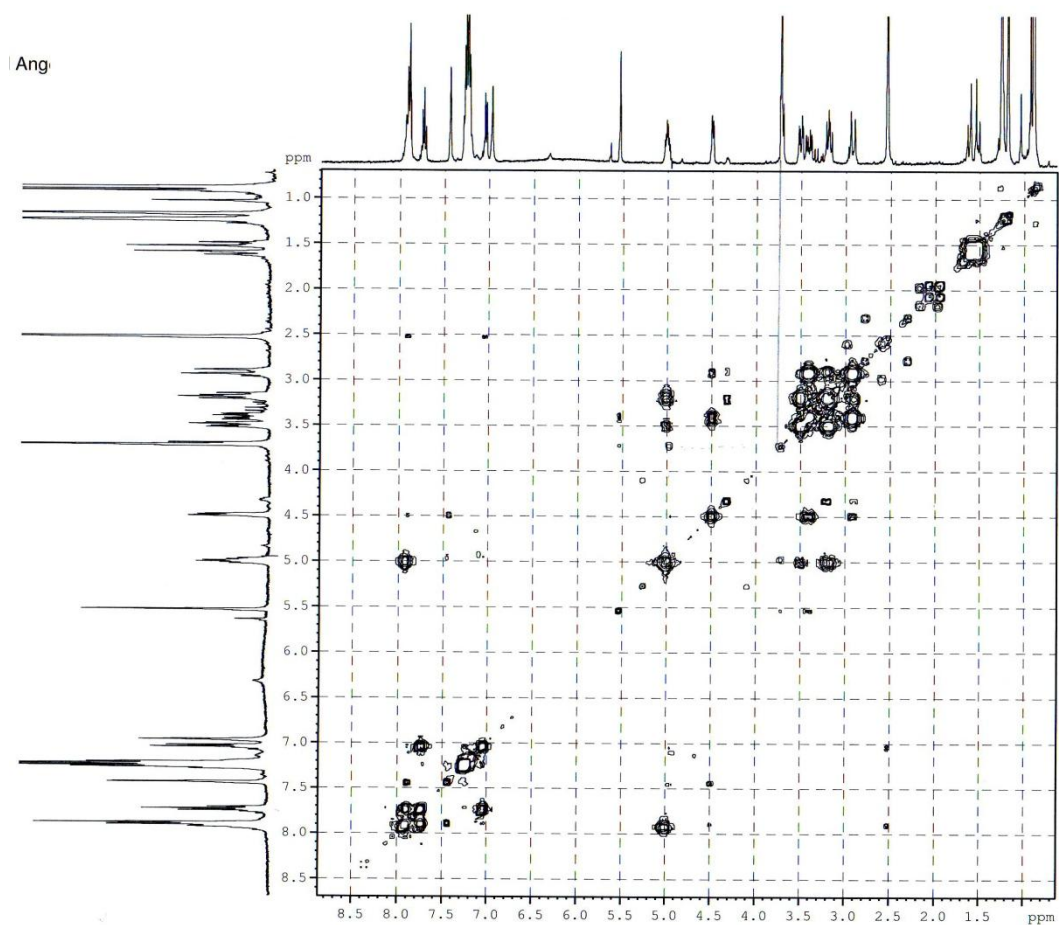
X-ray structure, crystal and refinement data of compound **94**



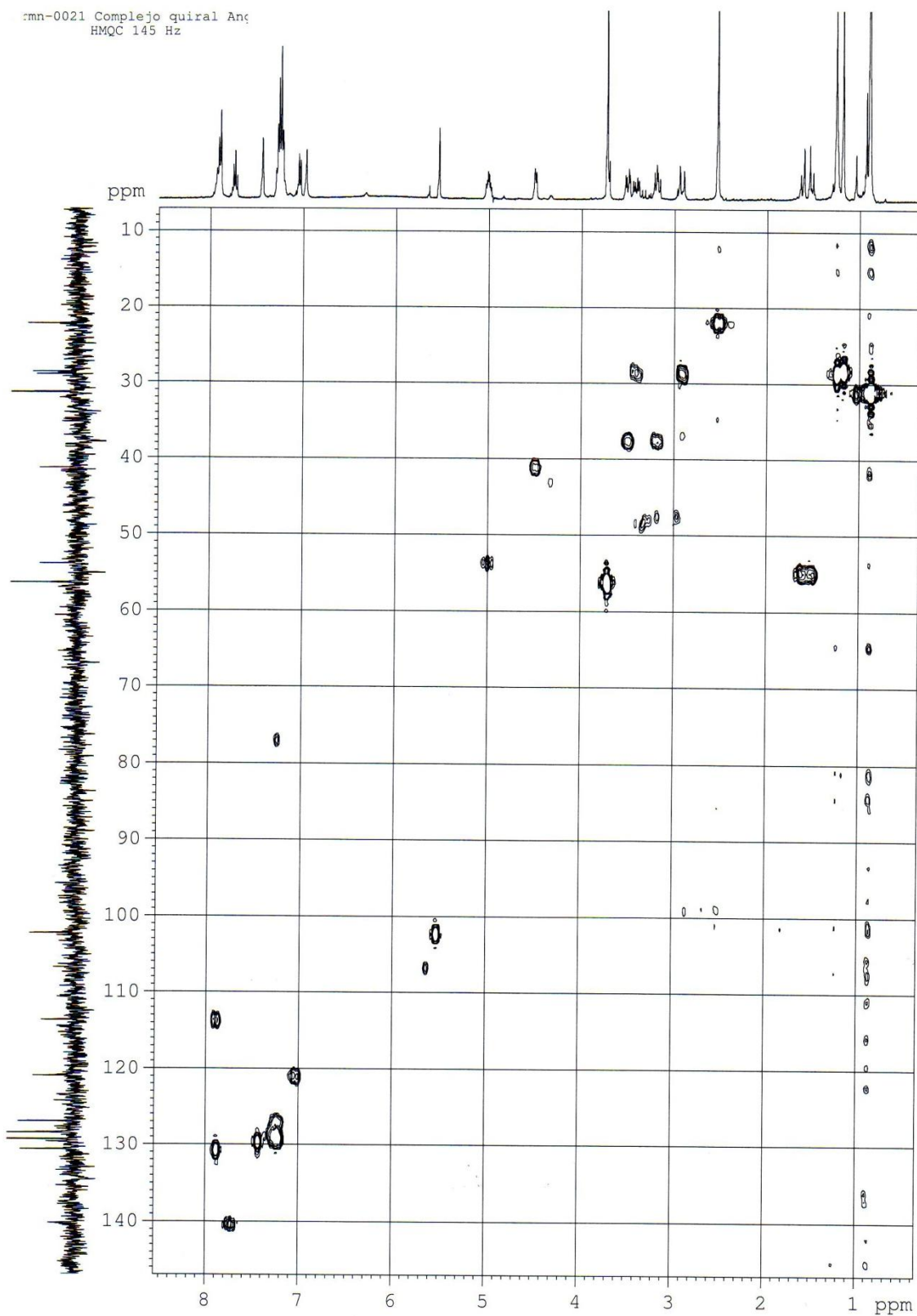
Empirical formula	$C_{28}H_{34}BrN_3O_6S$
Molecular weight	620.54
Temperature	298 (2) K
Wavelength	1.54178 Å
Crystal system, Space group	Monoclinic, Pc
Unit cell dimensions	$a = 8.3521(3)$ Å $\alpha = 90.0^\circ$ $b = 14.3086(6)$ Å $\beta = 97.573(2)^\circ$ $c = 23.7793(7)$ Å $\gamma = 90.0^\circ$
Volume	2817.00(18) Å ³
Z; Density (calculated)	3; 1.461 mg/m ³
Absorption coefficient	3.074 mm ⁻¹
F(000)	1284
Crystal size	-
θ range	3.09 – 67.28 °
Limiting indices h, k, l	$-8 \leq h \leq 9, -16 \leq k \leq 16, -28 \leq l \leq 25$
Reflections collected/independent	16276/6485 $R_{int} = 0.0380$
Refinement method	Least squares method with full matrix in F^2
Data/restraints/parameters	6485/3/711
Goodness-of-fit on F^2	1.176
Final R indices [$I > 2\sigma(I)$]	$R_1 = 0.0485, \omega R_2 = 0.1466$
R indices (all data)	$R_1 = 0.0623, \omega R_2 = 0.1526$
Largest difference peak and hole	0.470 and -0.439

- Strong chiral complex¹H RMN (CDCl₃, 400 MHz)

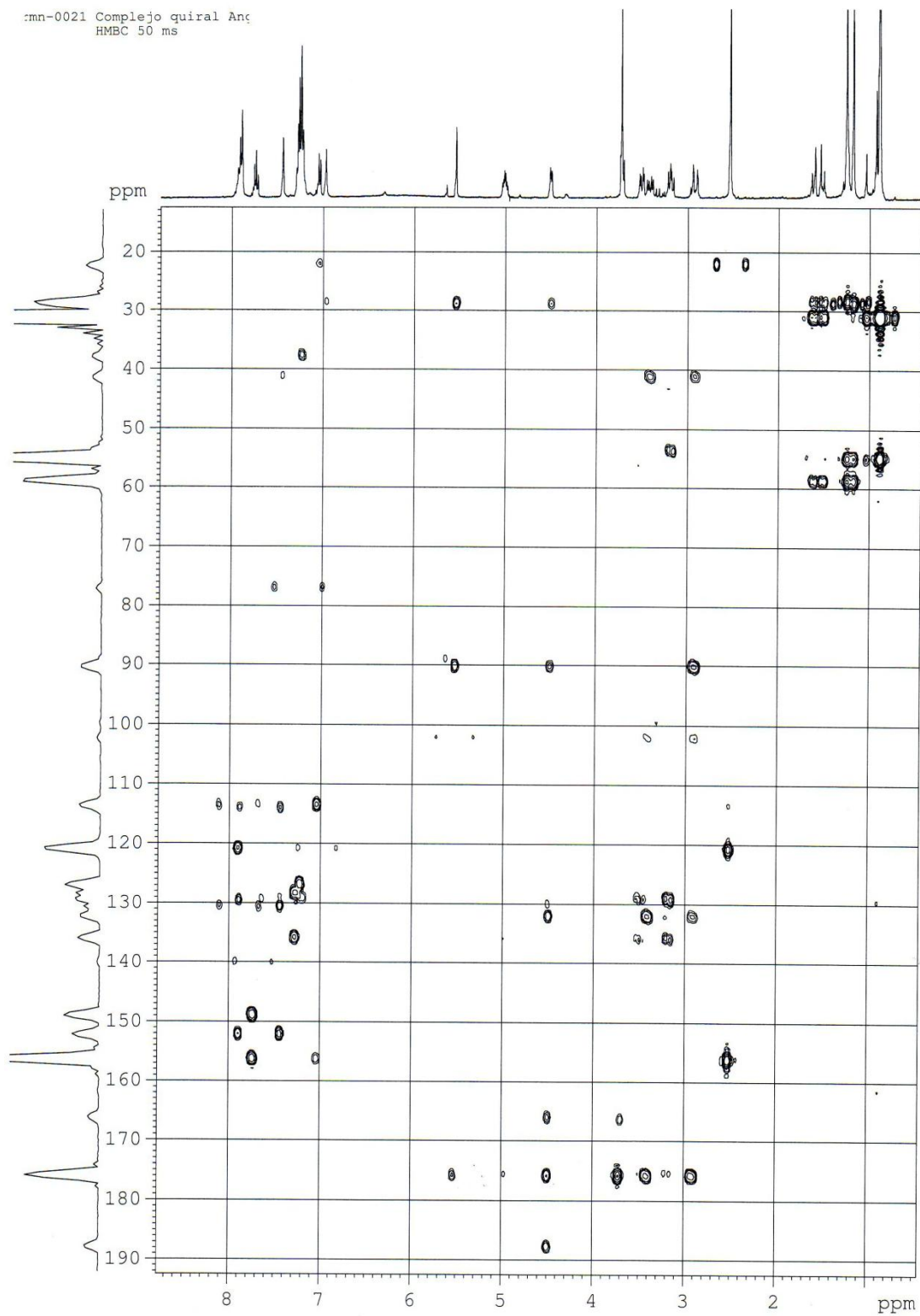
COSY



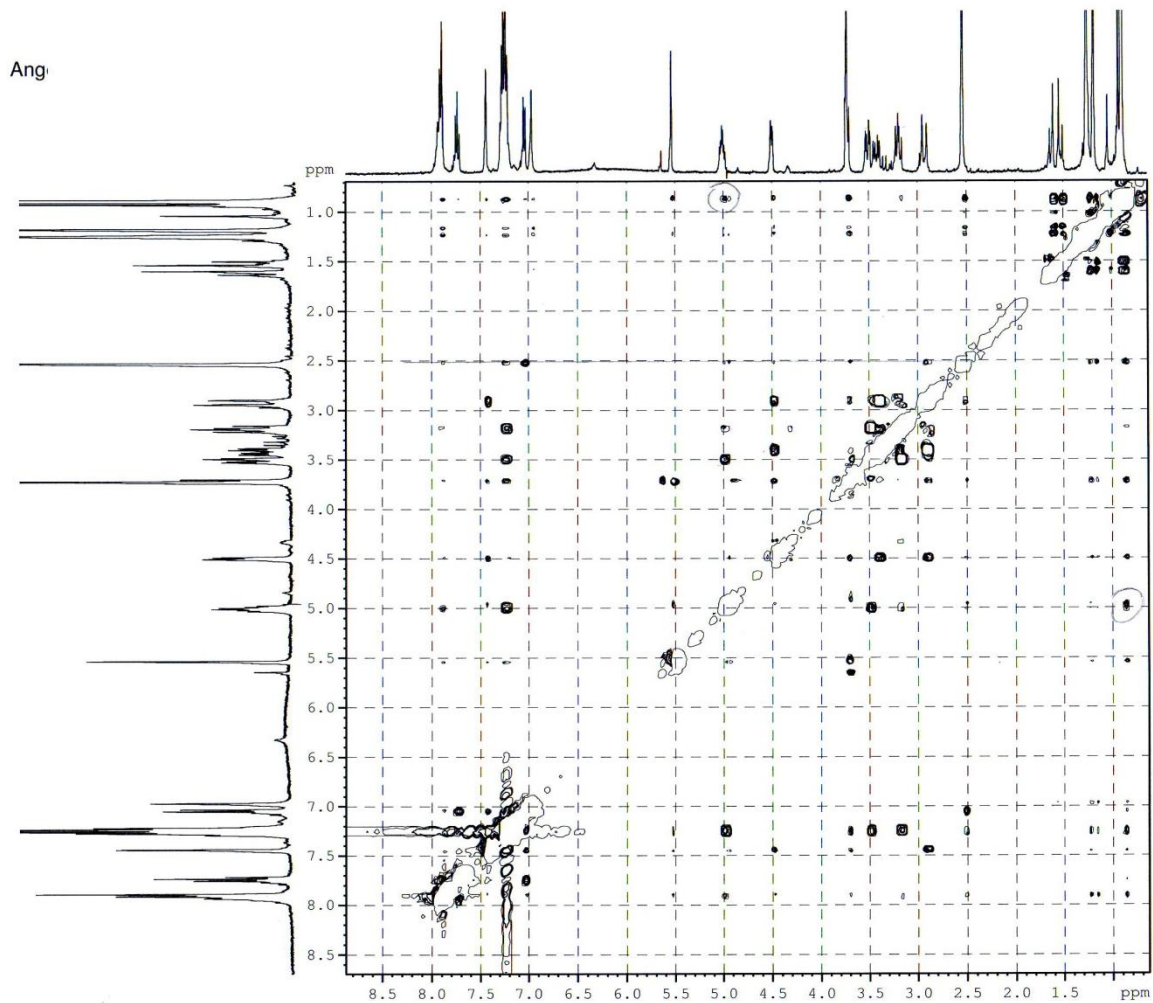
HMQC

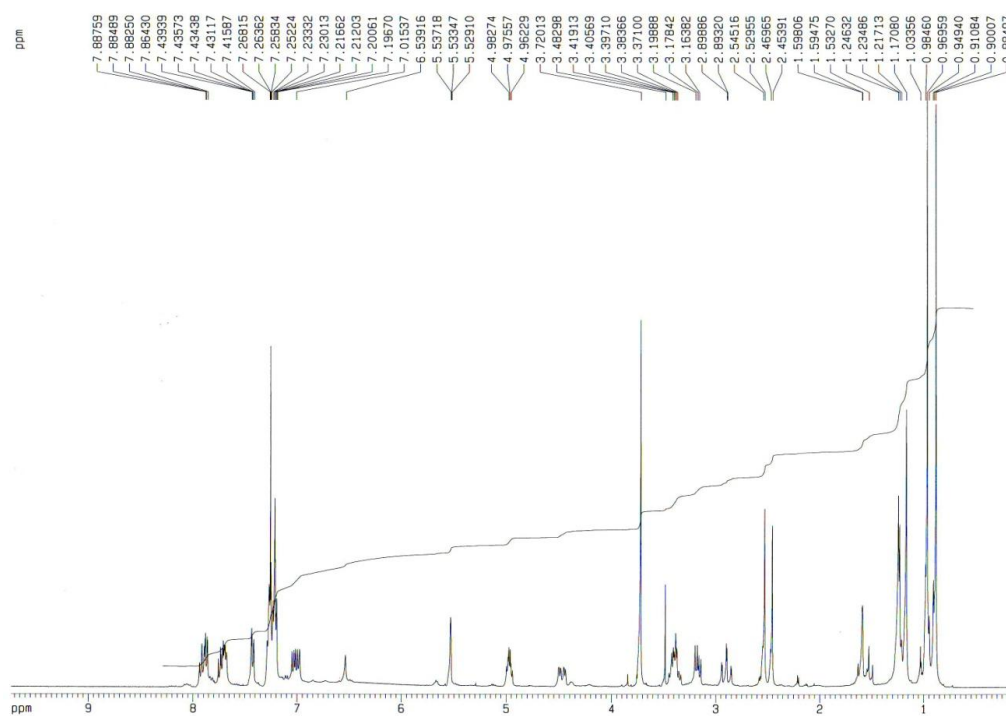


HMBC

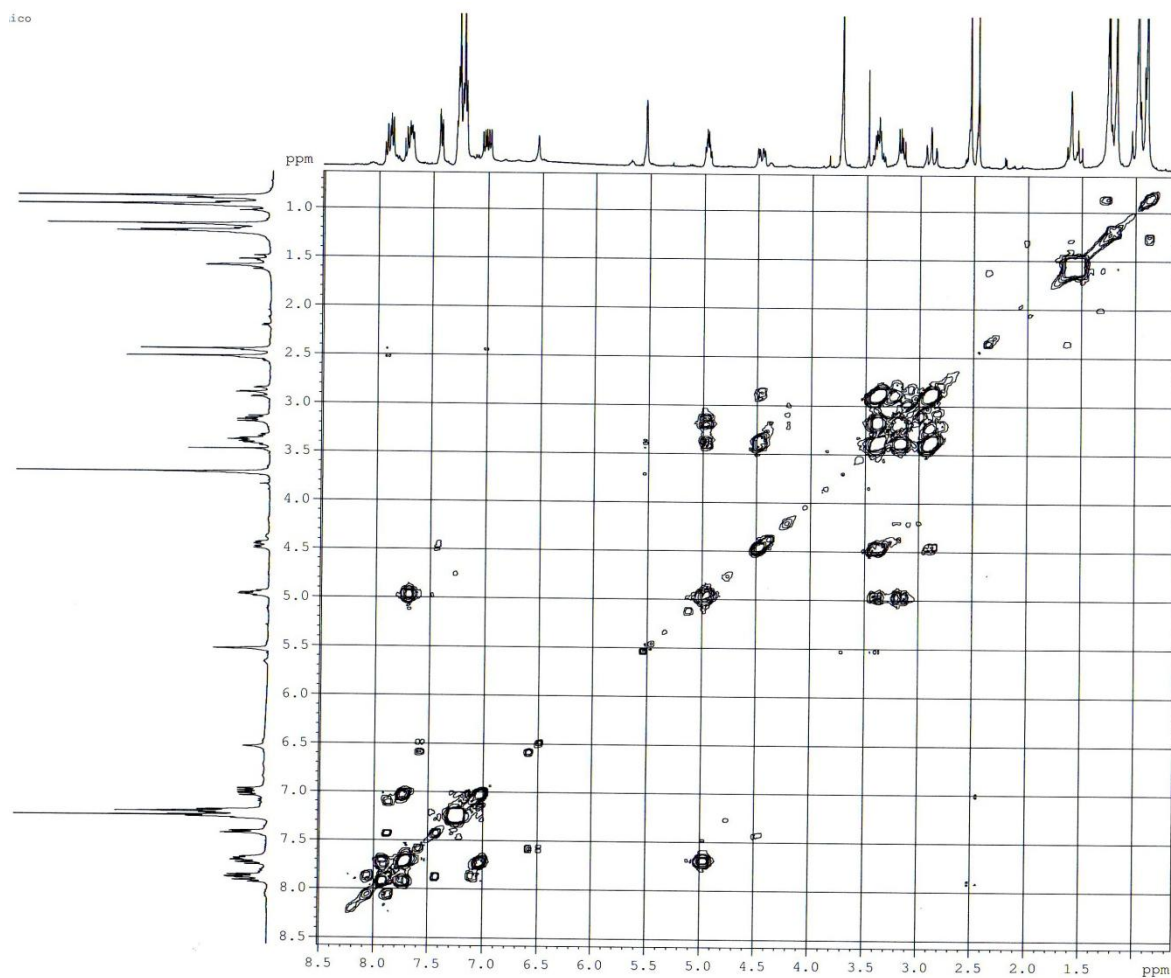


ROESY

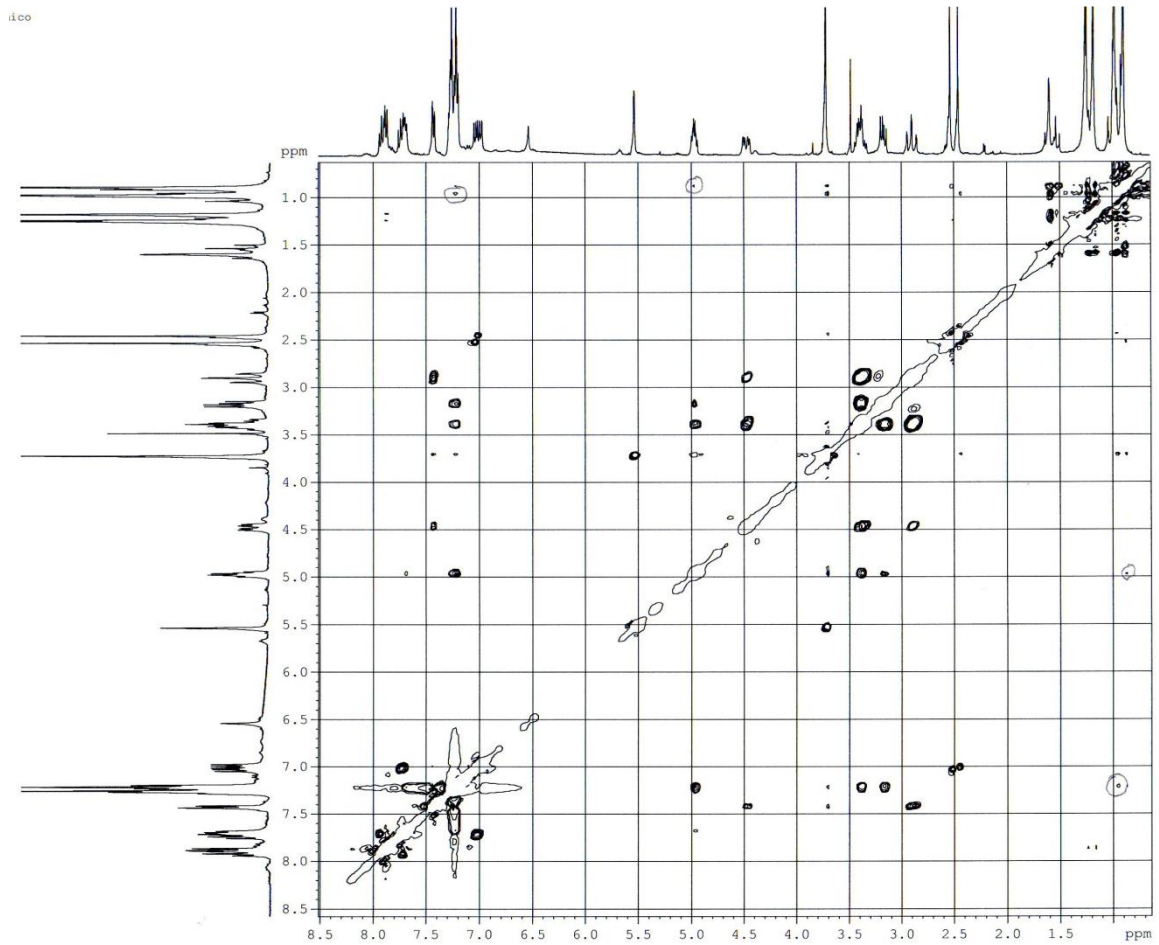


- Racemic complex ^1H RMN (CDCl_3 , 400 MHz)

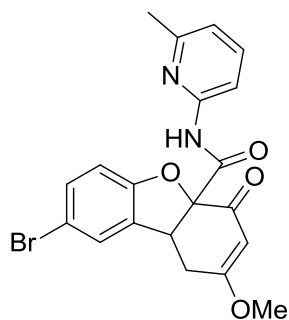
COSY



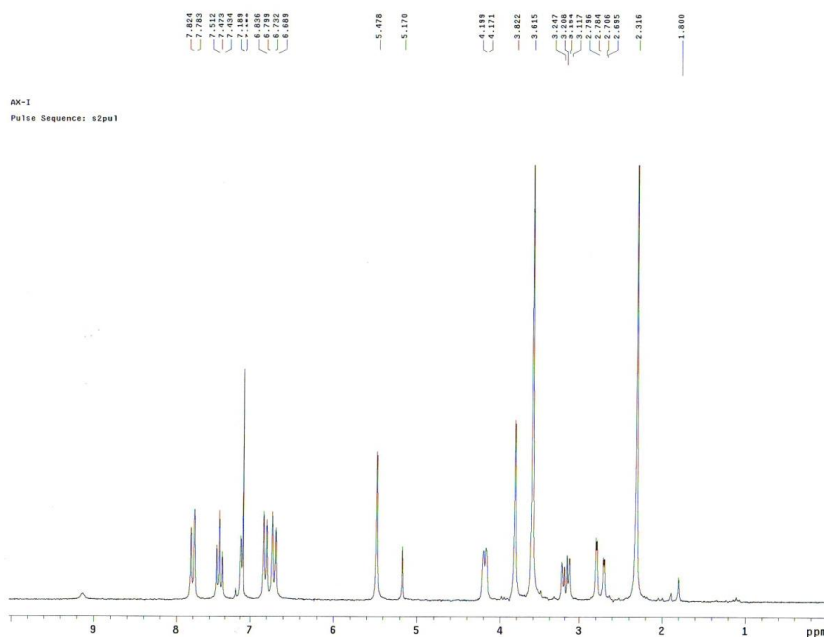
ROESY



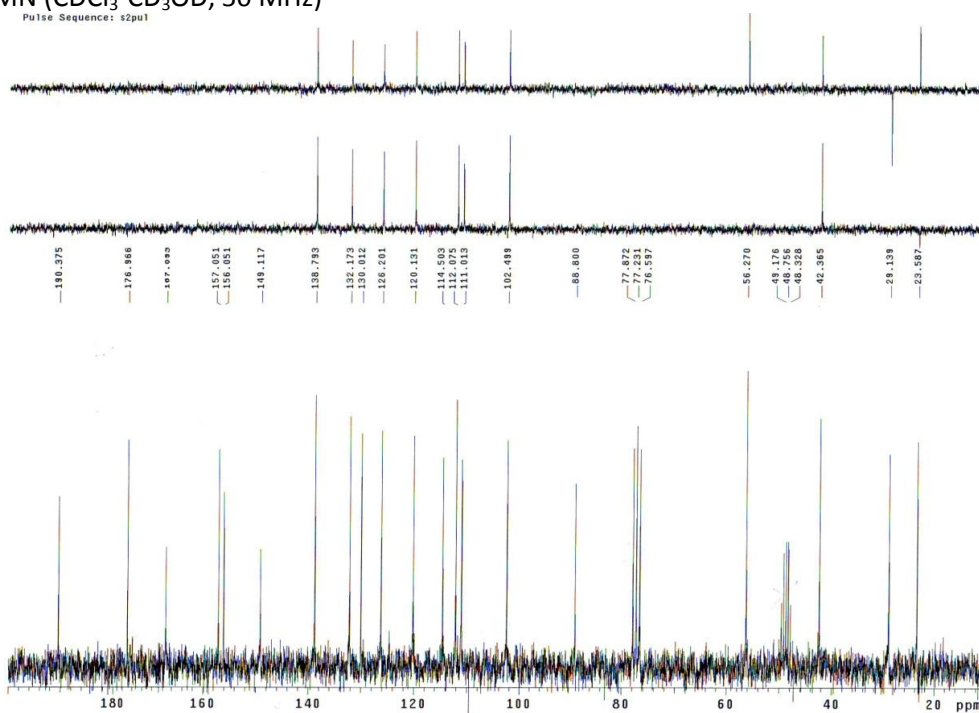
- 8-Bromo-2-methoxy-N-(6-methylpyridine-2-yl)-4-oxo -1, 4,4 a, 9b-tetrahydrobenzo [b, d]furan -4a-carboxamide (95)



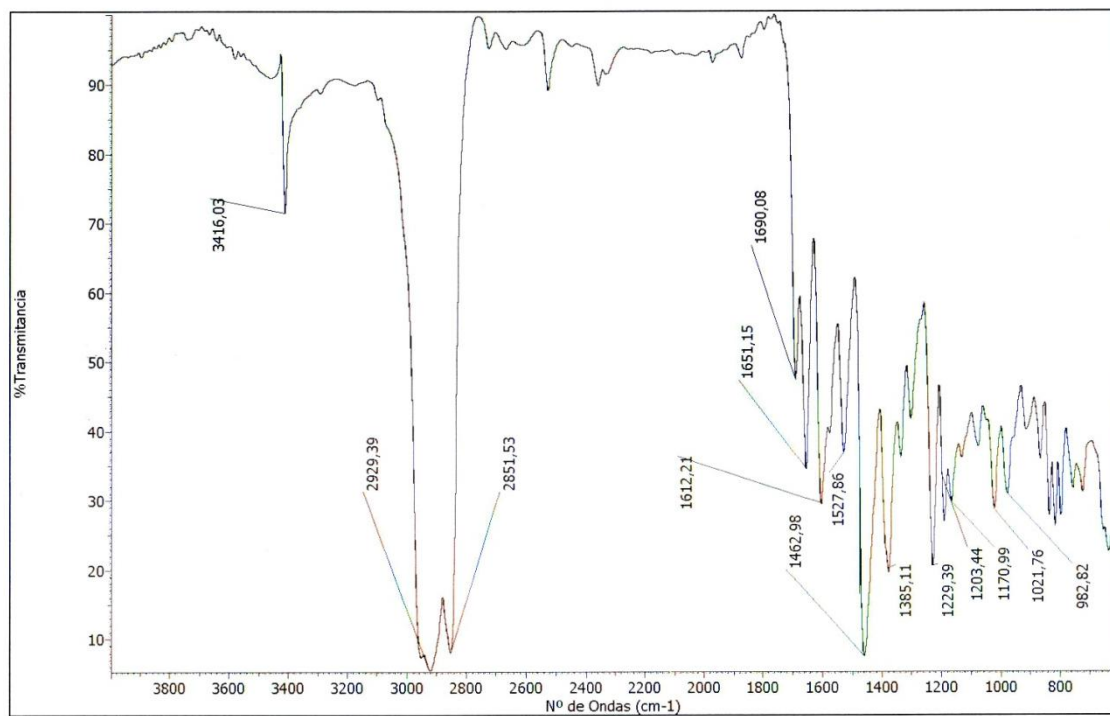
^1H RMN ($\text{CDCl}_3\text{-CD}_3\text{OD}$, 200 MHz)



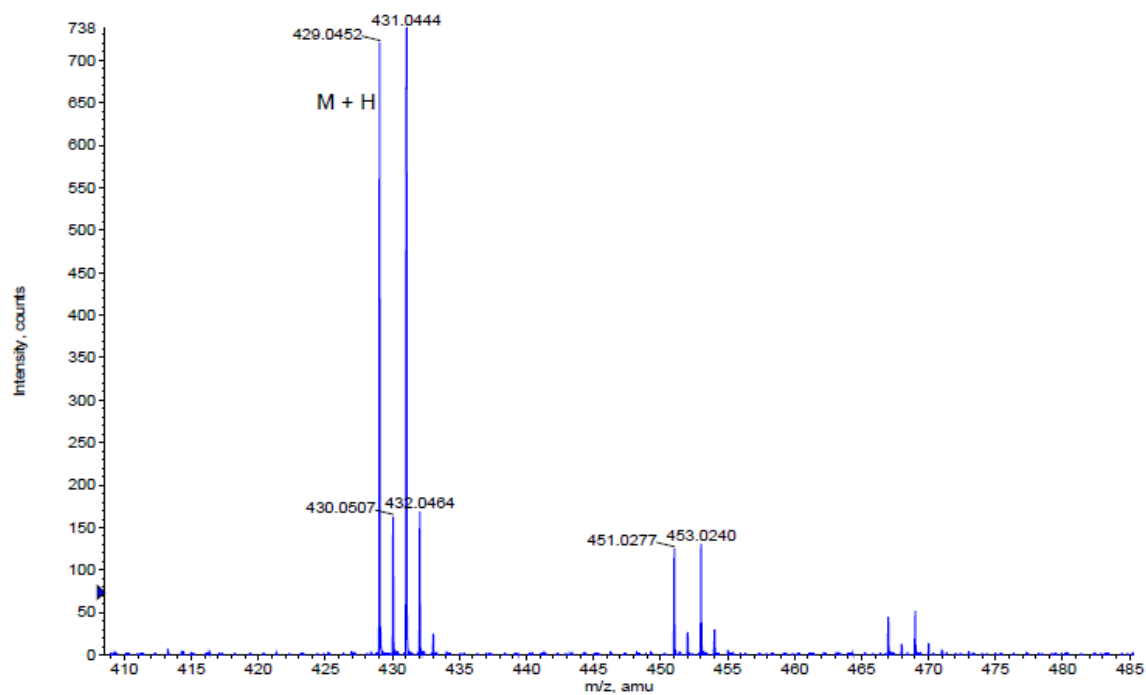
^{13}C RMN ($\text{CDCl}_3\text{-CD}_3\text{OD}$, 50 MHz)



IR

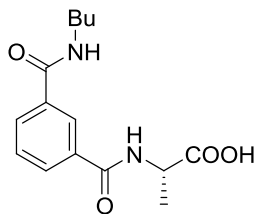
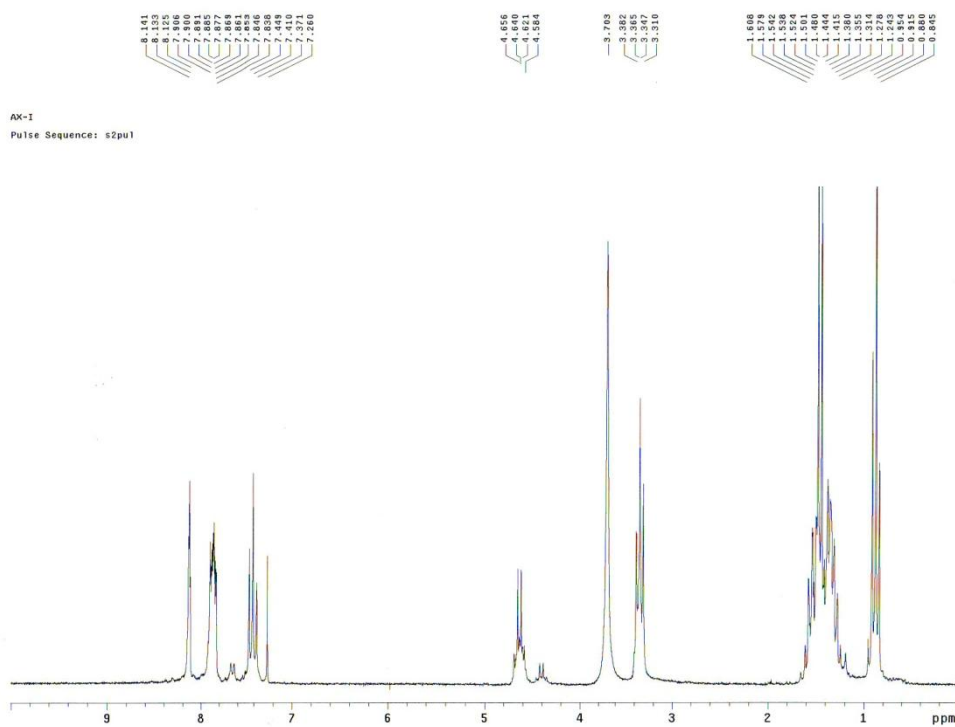
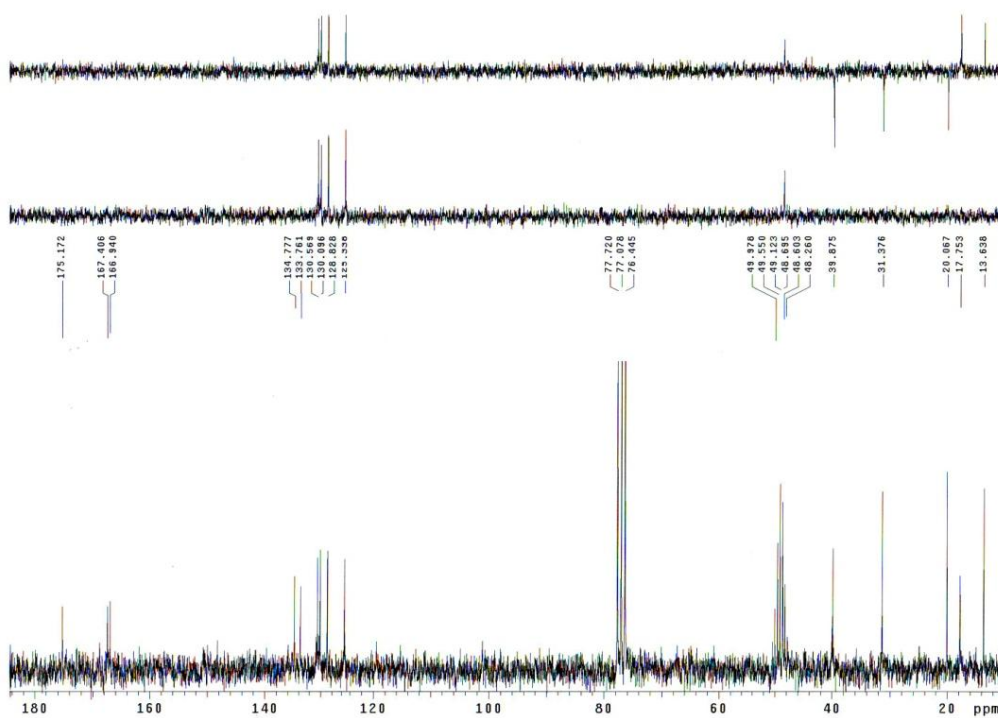


HRMS

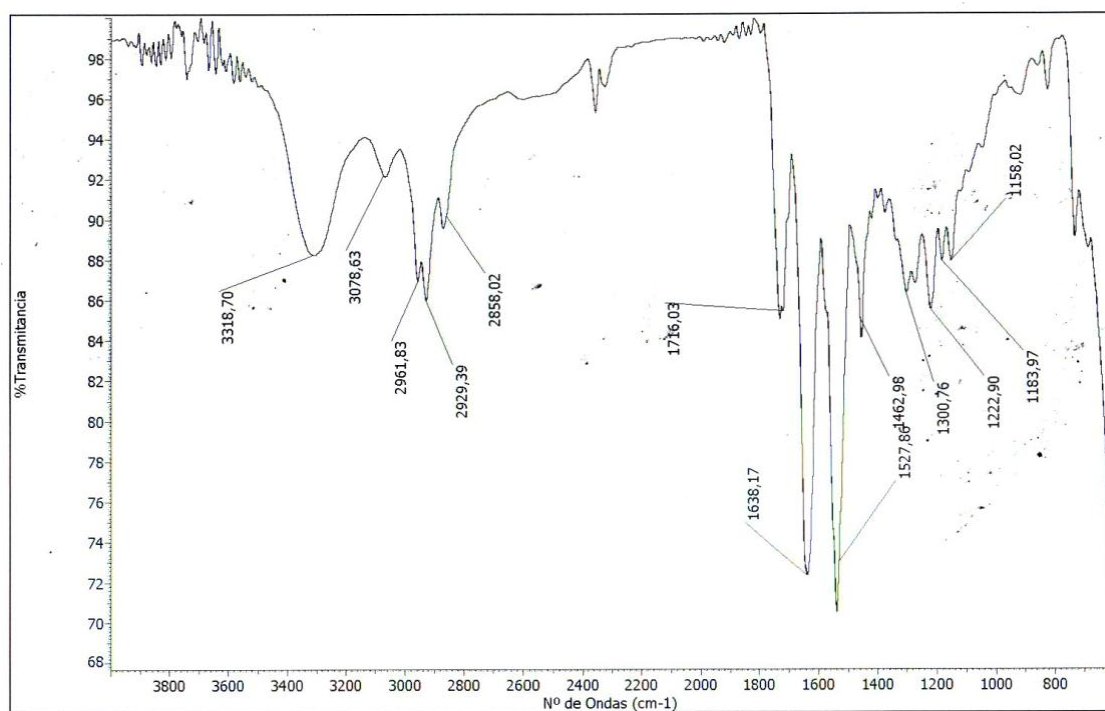


Formula	CalculatedMass	mDaError	ppmError	RDB
C20 H18 N2 O4 Br	429.044445	0.755184	1.760148	12.5
C23 H19 O2 Na Br	429.046062	-0.86226	-2.009716	13.5
C11 H23 N2 O9 Na Br	429.047913	-2.712916	-6.323139	0.5
C18 H19 N2 O4 Na Br	429.04204	3.160444	7.366217	9.5
C25 H18 O2 Br	429.048468	-3.26752	-7.615785	16.5

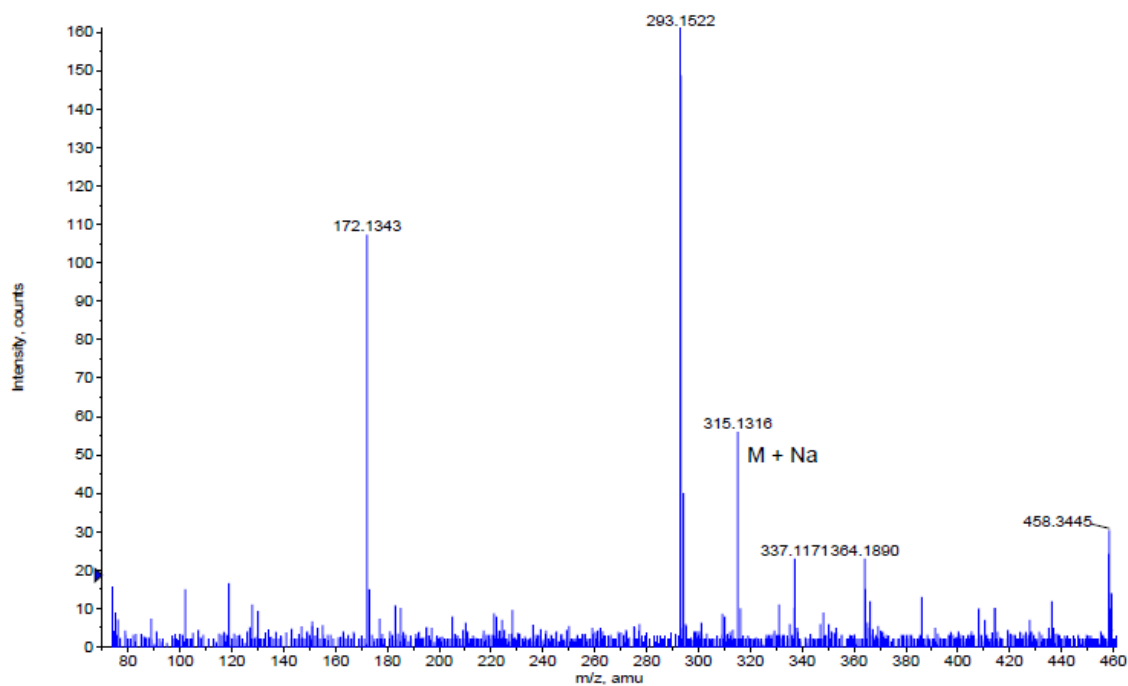
- (S)-2-(3-(butylcarbamoyl)benzamido)propanoic acid (101)

 ^1H RMN ($\text{CDCl}_3\text{-CD}_3\text{OD}$, 200 MHz) ^{13}C RMN ($\text{CDCl}_3\text{-CD}_3\text{OD}$, 50 MHz)

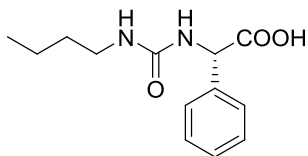
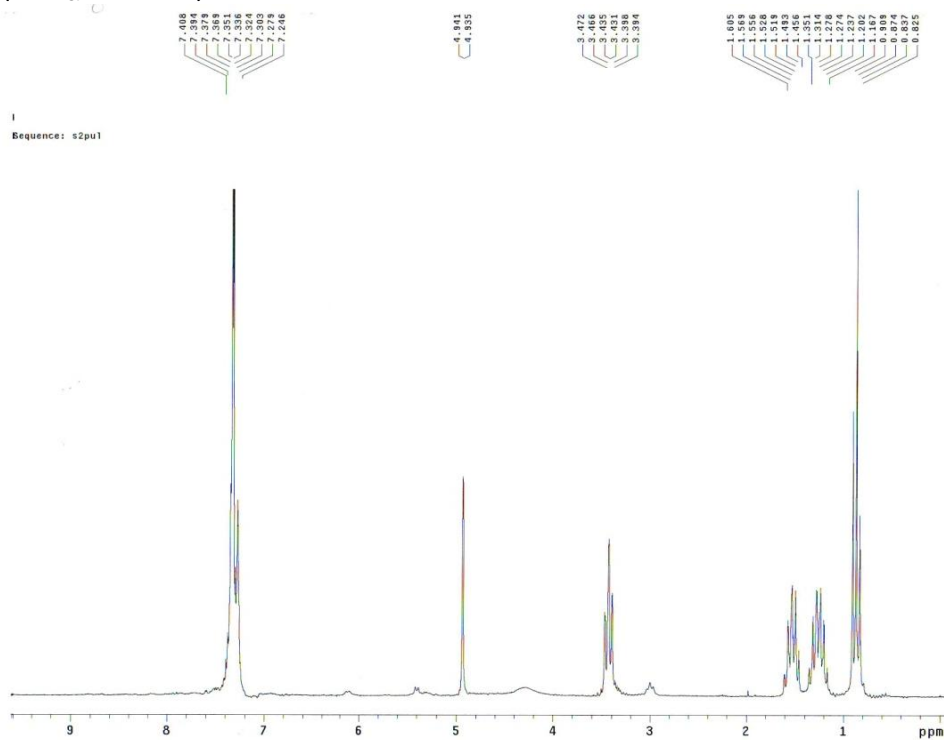
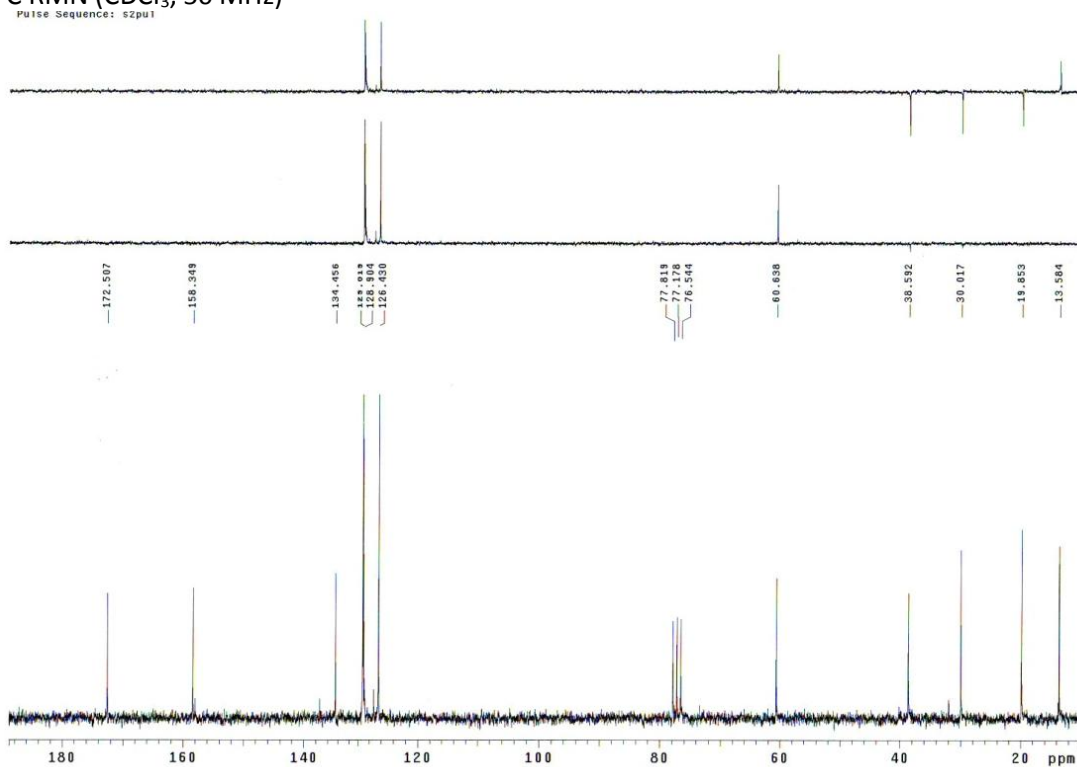
IR



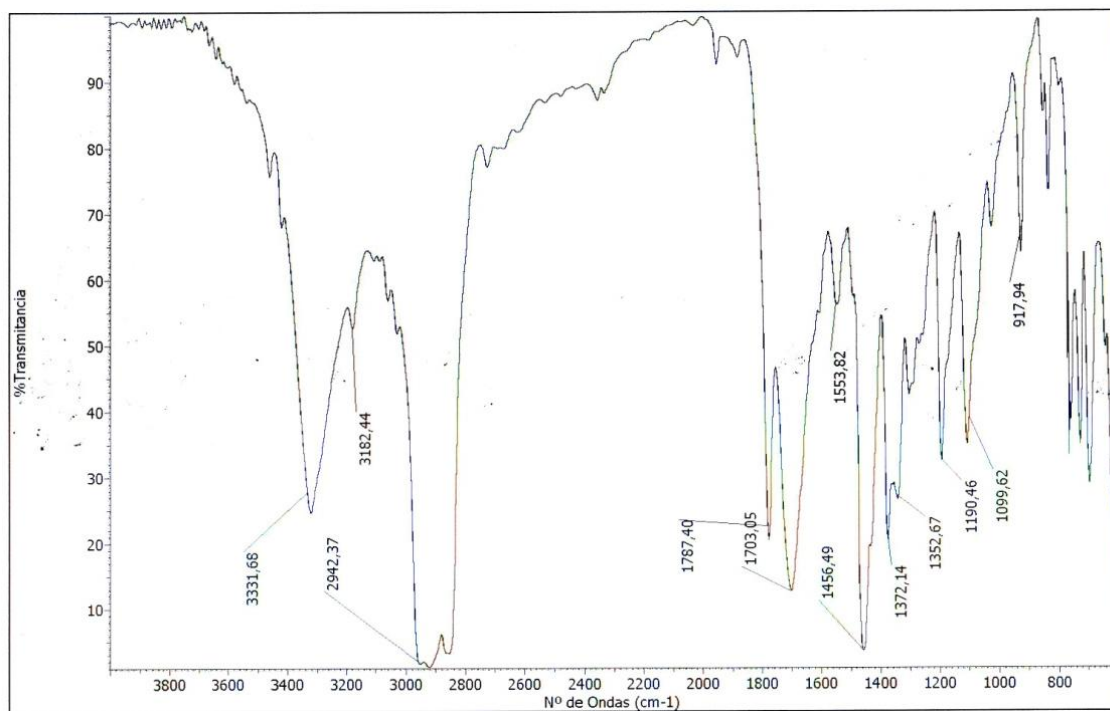
HRMS



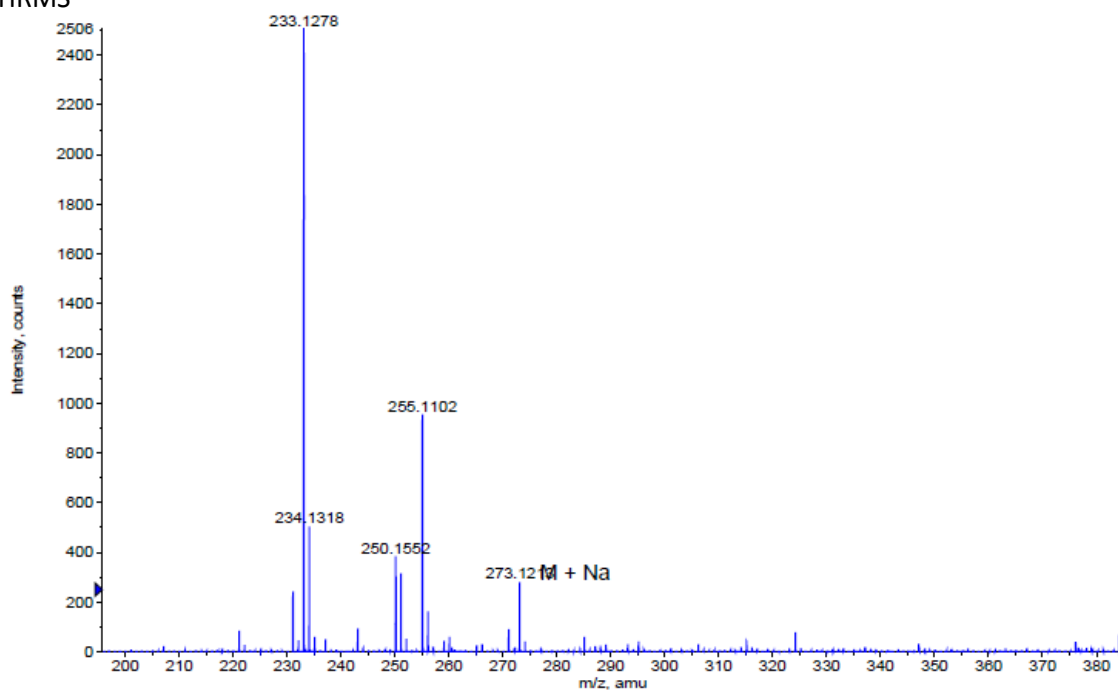
Formula	CalculatedMass	mDaError	ppmError	RDB
C ₁₅ H ₂₀ N ₂ O ₄ Na	315.131528	0.071504	0.226902	6.5
C ₁₂ H ₁₉ N ₄ O ₆	315.129911	1.688948	5.359491	5.5
C ₁₇ H ₁₉ N ₂ O ₄	315.133934	-2.333756	-7.405642	9.5
C ₁₁ H ₂₃ O ₁₀	315.128574	3.02626	9.603146	0.5

- (S)-2-(3-butylureido)-2-phenylacetic acid (109)¹H RMN (CDCl₃, 200 MHz)¹³C RMN (CDCl₃, 50 MHz)

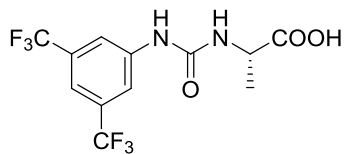
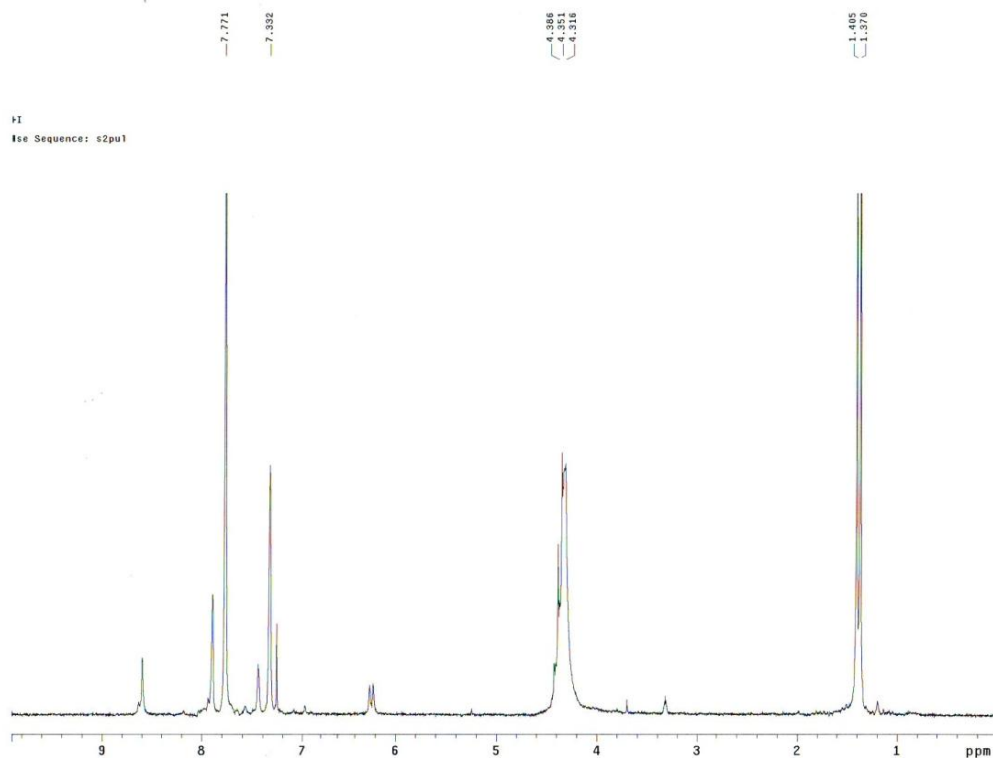
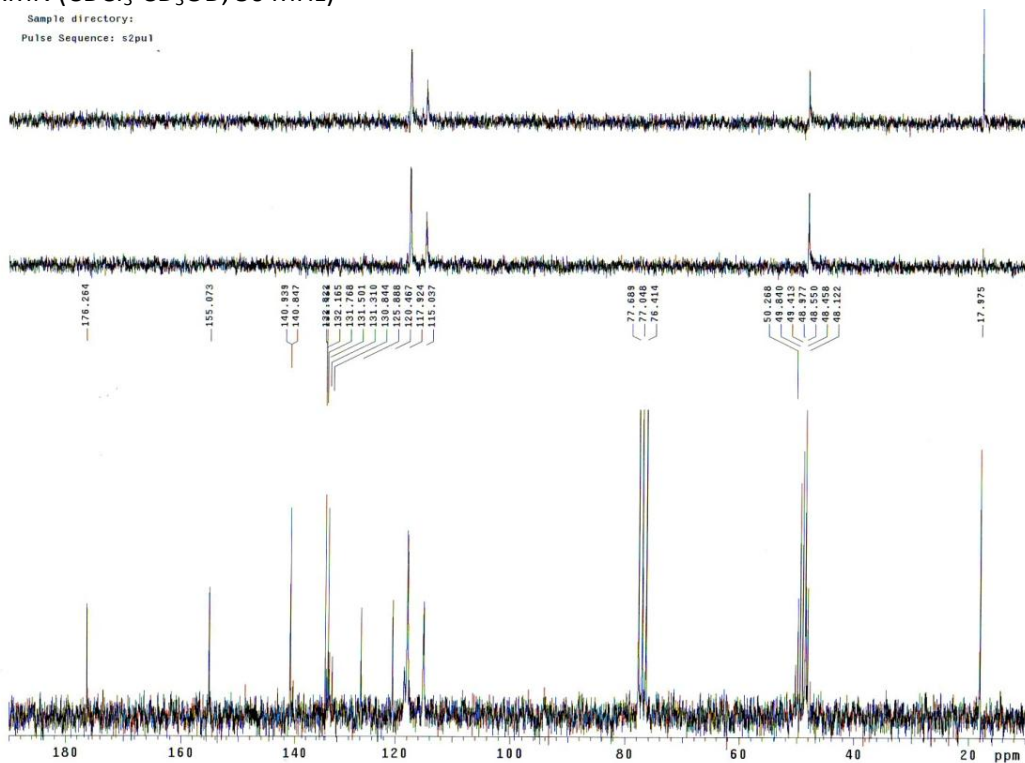
IR



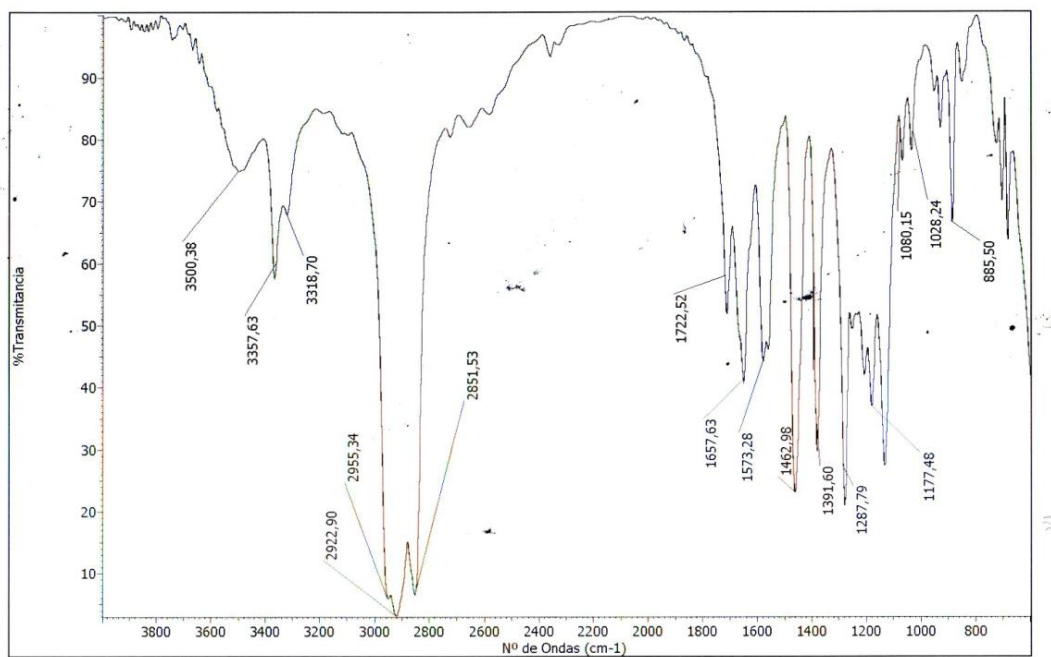
HRMS



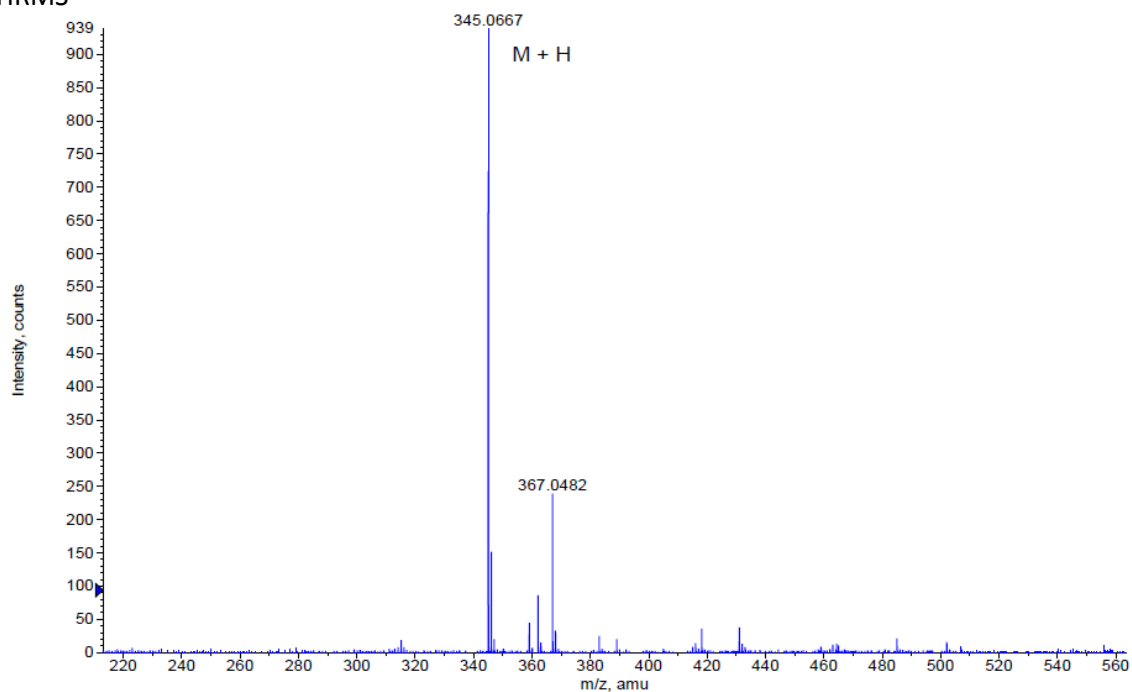
	CalculatedMass	mDaError	ppmError	RDB
C13 H18 N2 O3 Na	273.120964	0.336224	1.23104	5.5
C10 H17 N4 O5	273.119346	1.953668	7.1531	4.5
C15 H17 N2 O3	273.123369	-2.069036	-7.575505	8.5

- (S)-2-(3-(3,5-bis(trifluoromethyl)phenyl)ureido)propanoic acid (123)¹H RMN (CDCl₃-CD₃OD, 200 MHz)¹³C RMN (CDCl₃-CD₃OD, 50 MHz)

IR

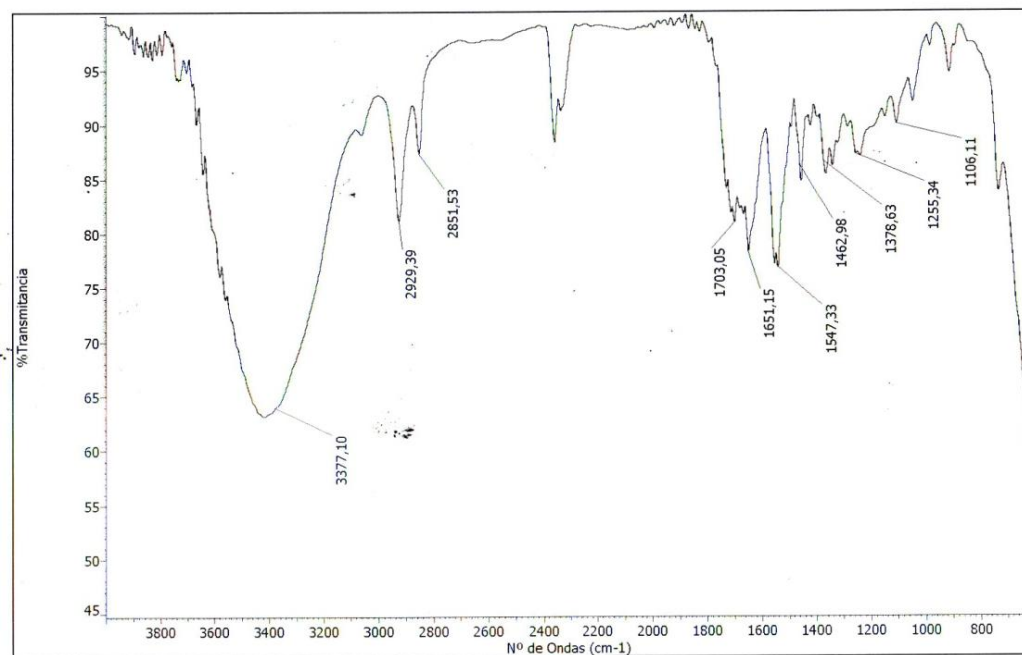


HRMS

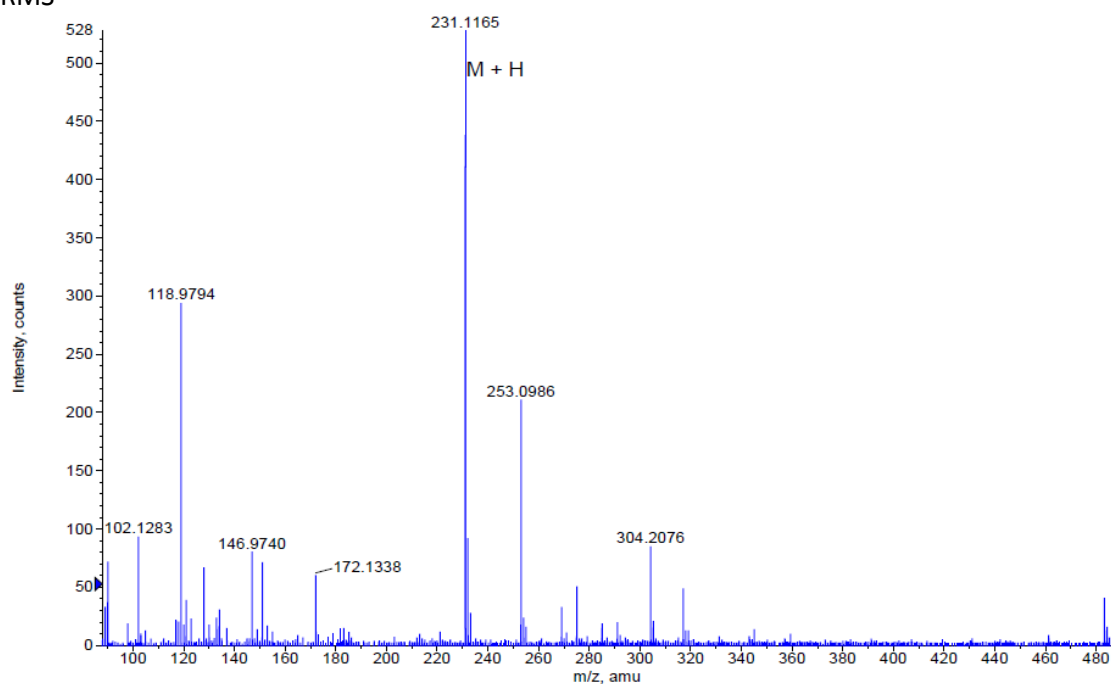


Formula	CalculatedMass	mDaError	ppmError	RDB
C ₁₂ H ₁₁ N ₂ O ₃ F ₆	345.066838	-0.138296	-0.40078	5.5
C ₁₅ H ₁₂ O F ₆ Na	345.068456	-1.75574	-5.08811	6.5
C ₁₀ H ₁₂ N ₂ O ₃ F ₆ Na	345.064433	2.266964	6.56963	2.5

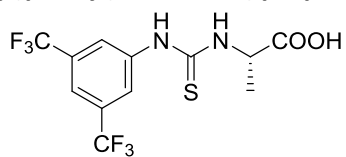
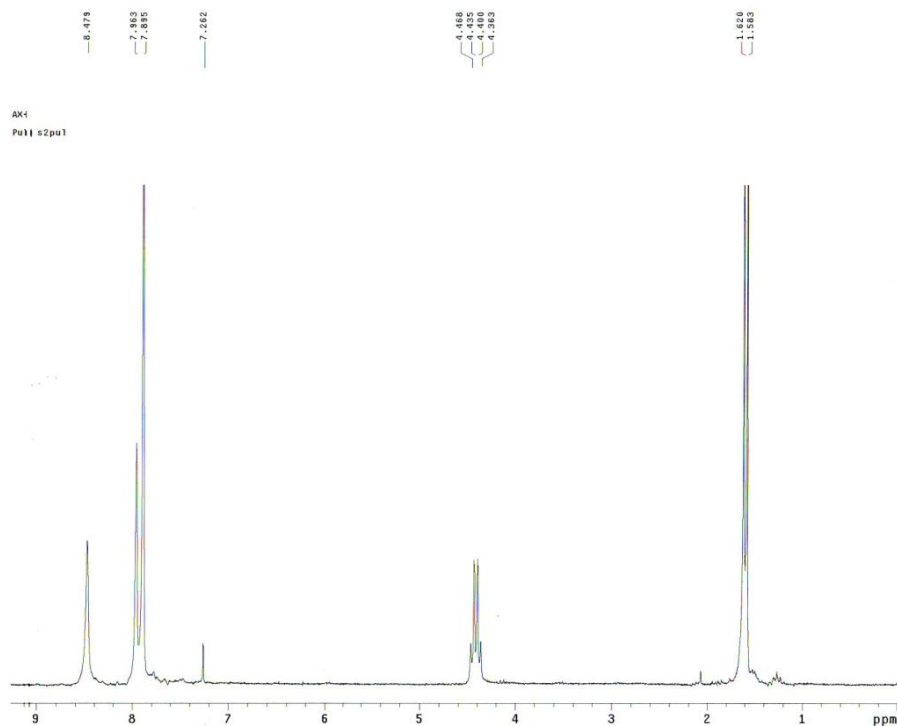
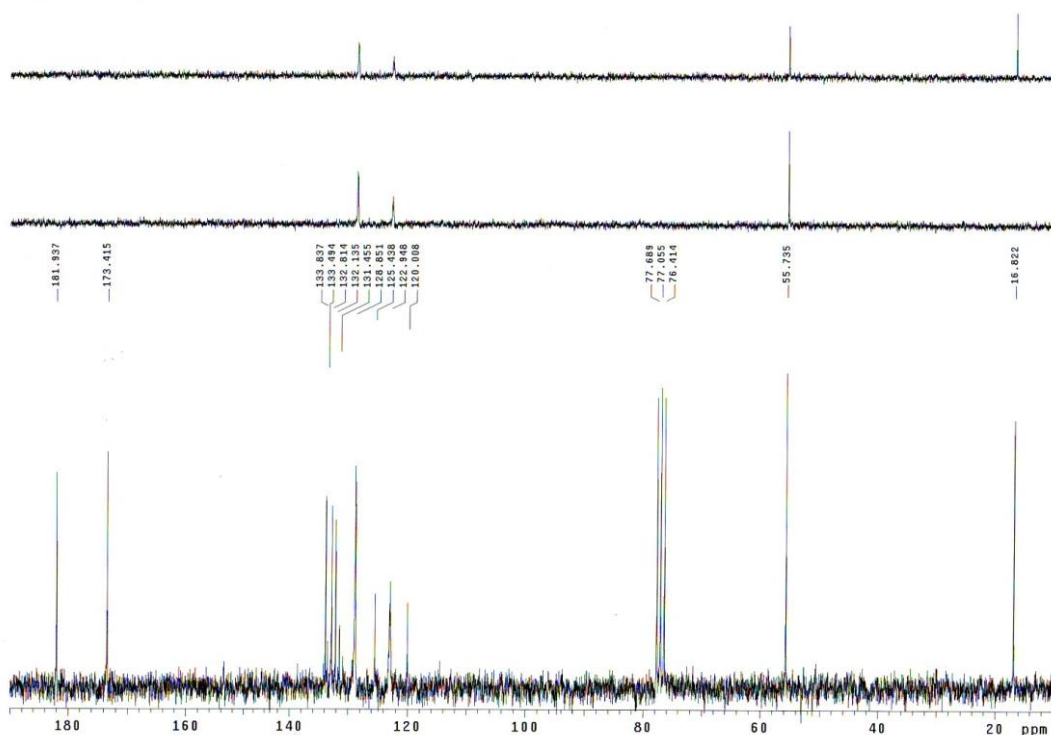
IR



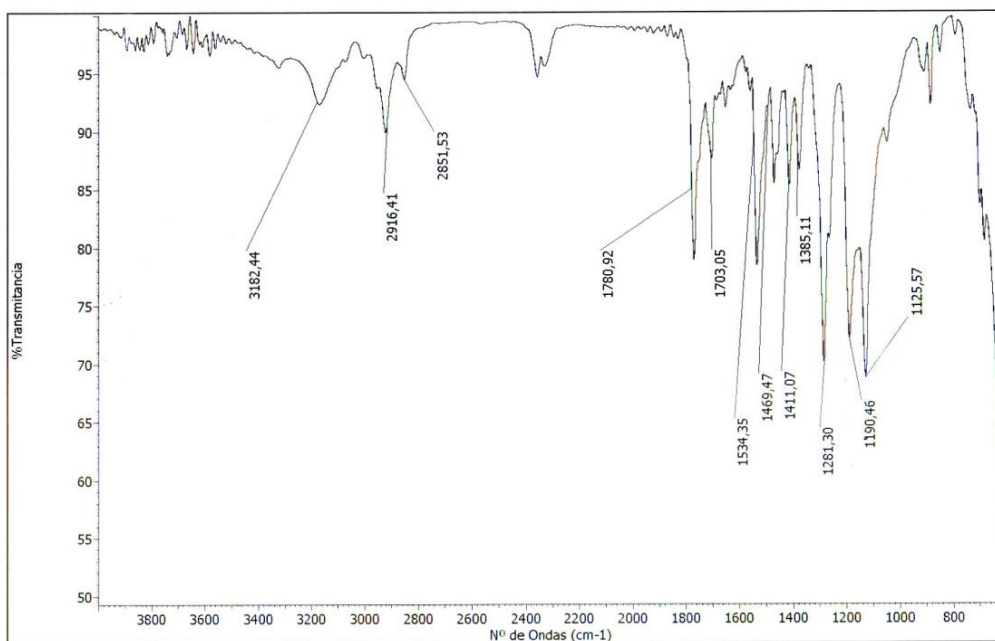
HRMS



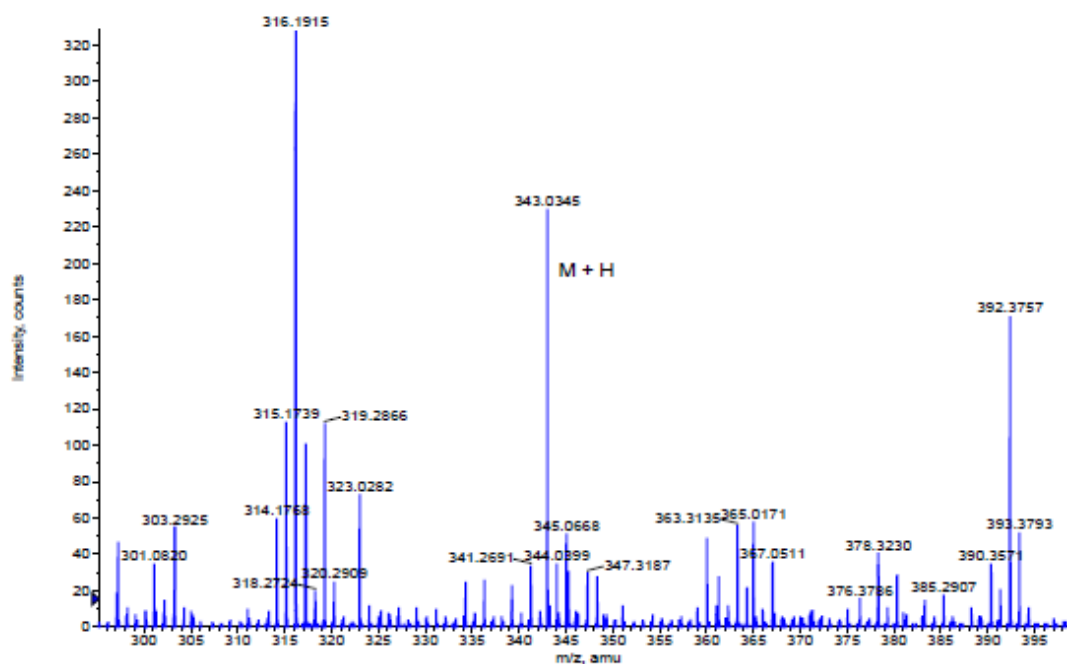
Formula	CalculatedMass	mDaError	ppmError	RDB
C10 H19 N2 O2 S	231.116176	0.323724	1.400693	2.5
C13 H20 Na S	231.117794	-1.29372	-5.597683	3.5

- (S) -2-(3-(3,5-bis(trifluoromethyl)phenyl)thioureido) propanoic acid (115)¹H RMN (CDCl₃, 200 MHz)¹³C RMN (CDCl₃, 50 MHz)

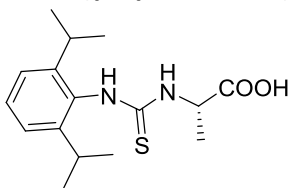
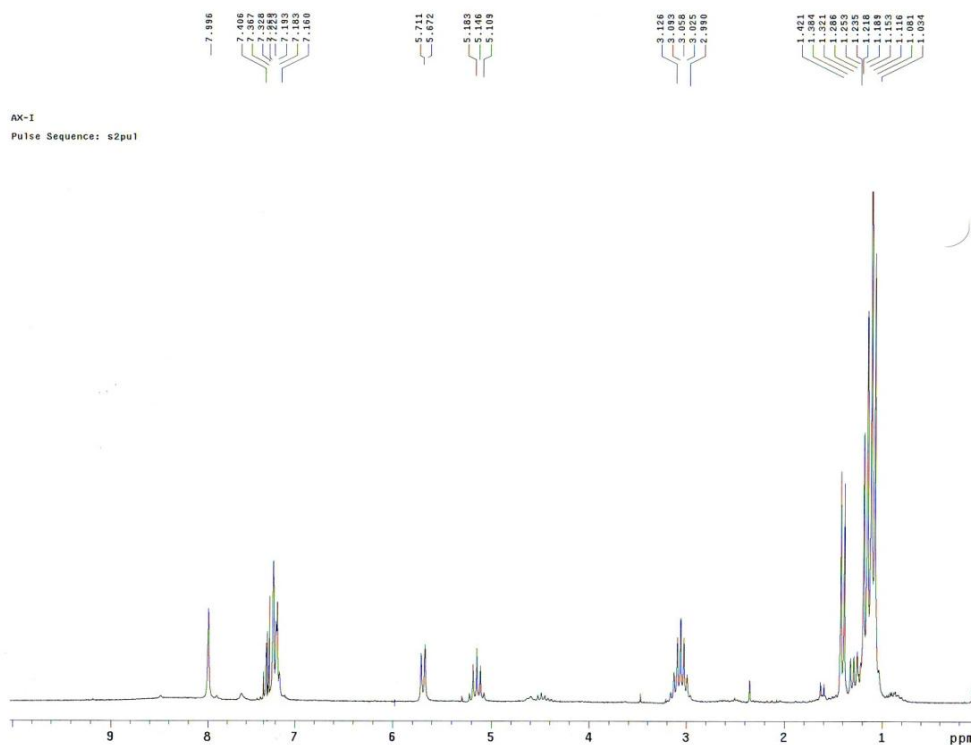
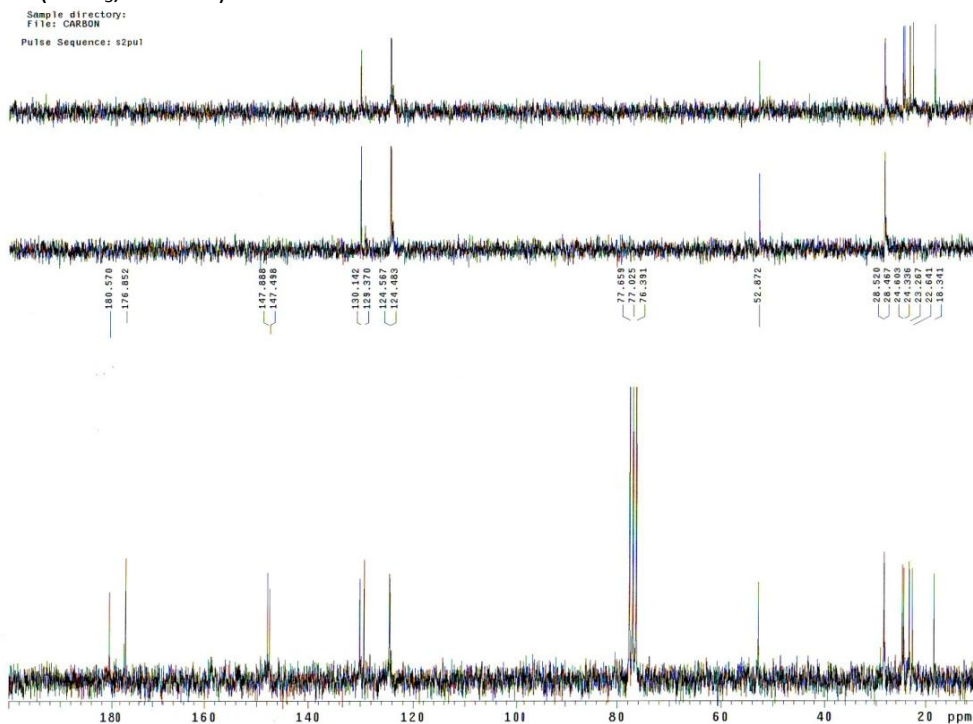
IR



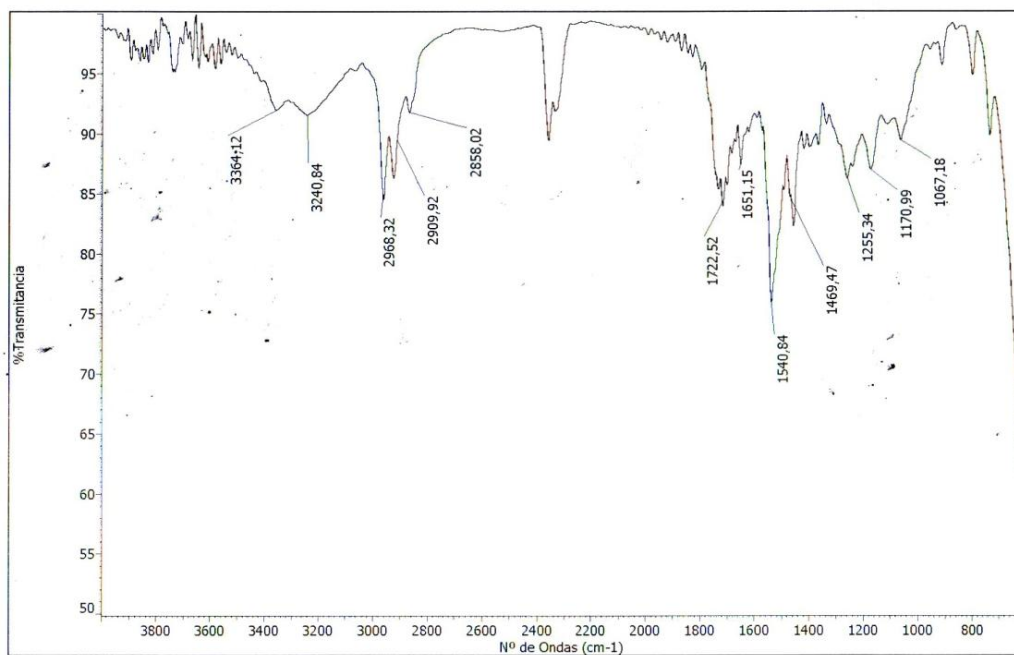
HRMS



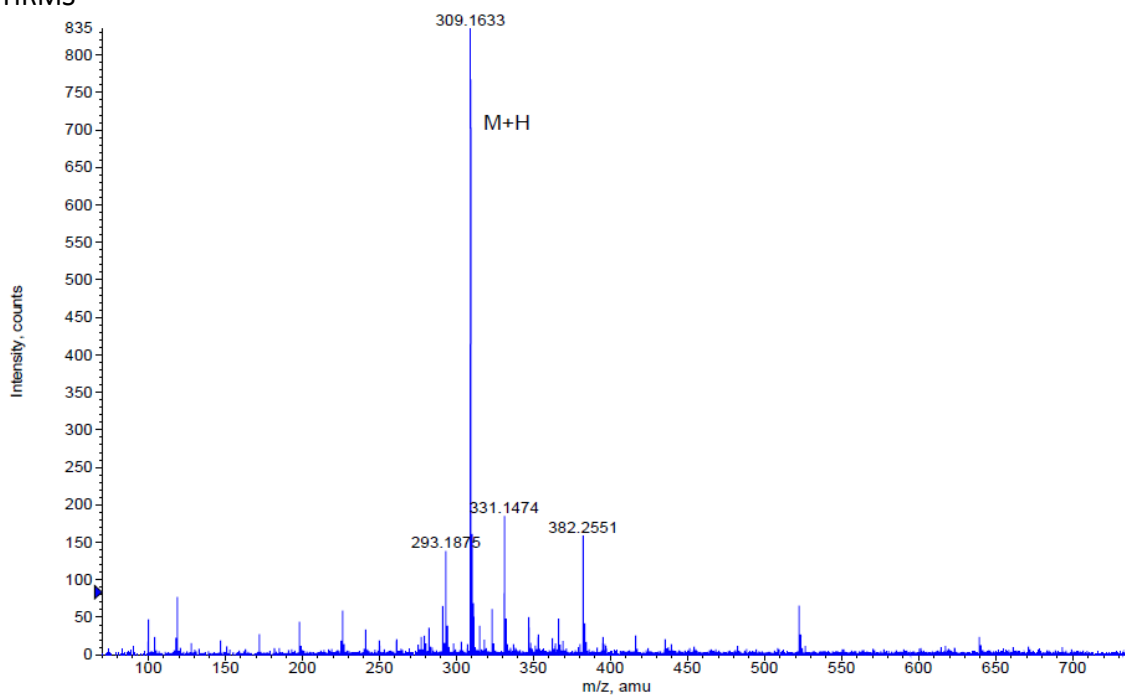
Formula	CalculatedMass	mDaError	ppmError	RDB
C9 H12 N2 O4 F4 Na S	343.034613	-0.112976	-0.329342	2.5
C12 H11 N2 O3 F3 Na S	343.03347	1.029954	3.002475	6.5
C12 H9 N2 O F6 S	343.033431	1.069264	3.117069	6.5
C14 H10 N2 O3 F3 S	343.035875	-1.375306	-4.009229	9.5
C6 H11 N4 O6 F4 S	343.032996	1.504468	4.385756	1.5
C15 H8 N2 F5 S	343.032288	2.212194	6.448886	10.5
C11 H11 N2 O4 F4 S	343.037018	-2.518236	-7.341046	5.5
C9 H10 N4 O5 F3 S	343.031853	2.647398	7.717573	5.5
C17 H11 O F3 Na S	343.037493	-2.99275	-8.724327	10.5

- (S) -2-(3-(2,6-diisopropylphenyl)thioureido)propanoic acid (116)¹H RMN (CDCl₃, 200 MHz)¹³C RMN (CDCl₃, 50 MHz)

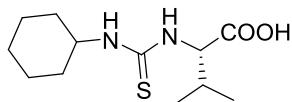
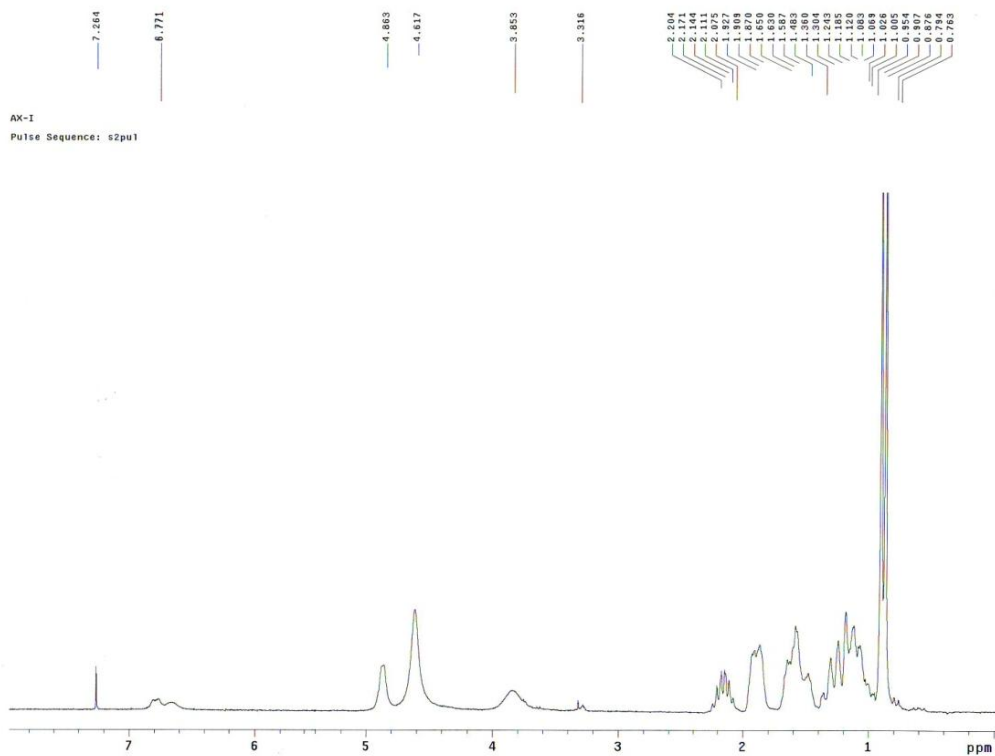
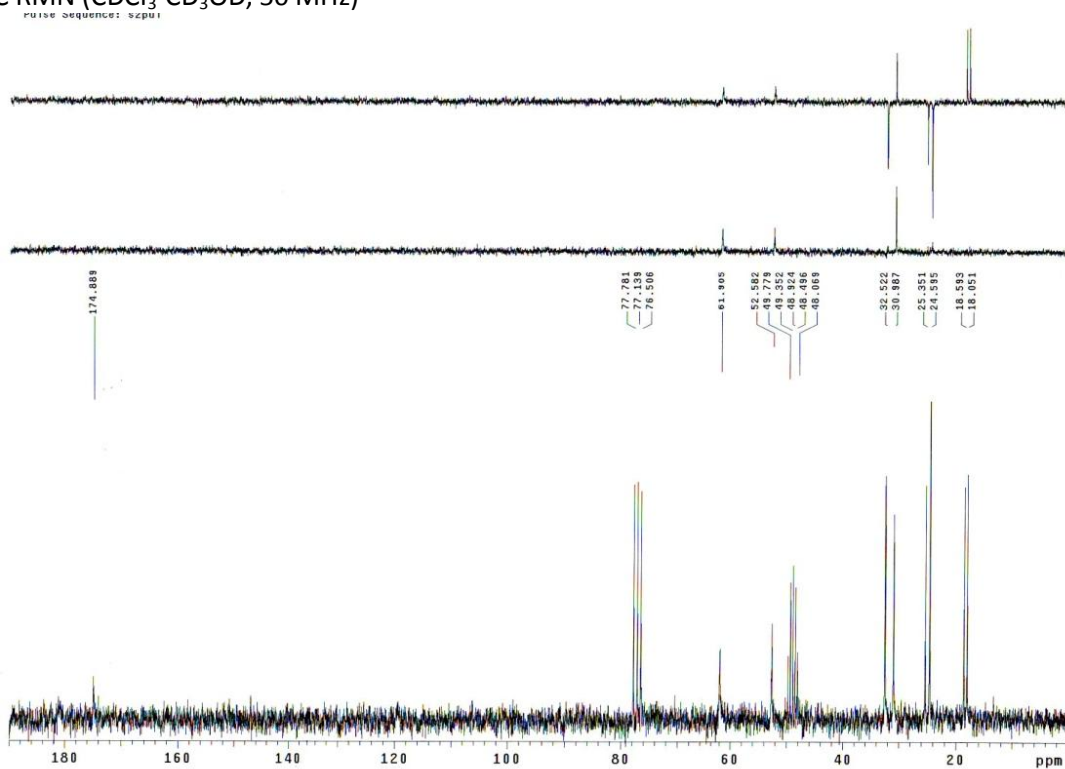
IR



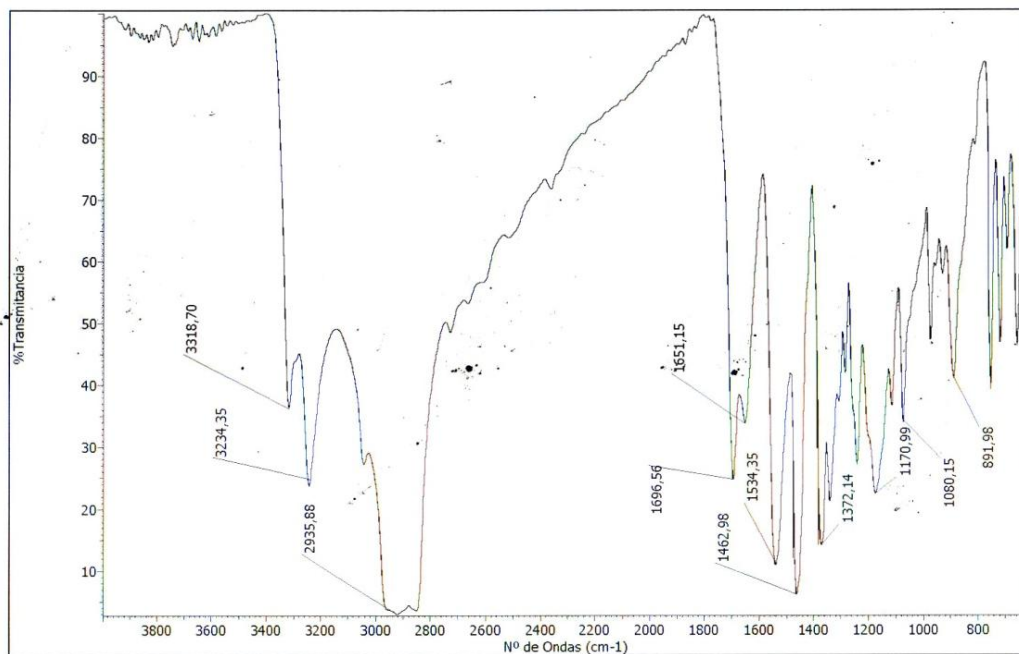
HRMS



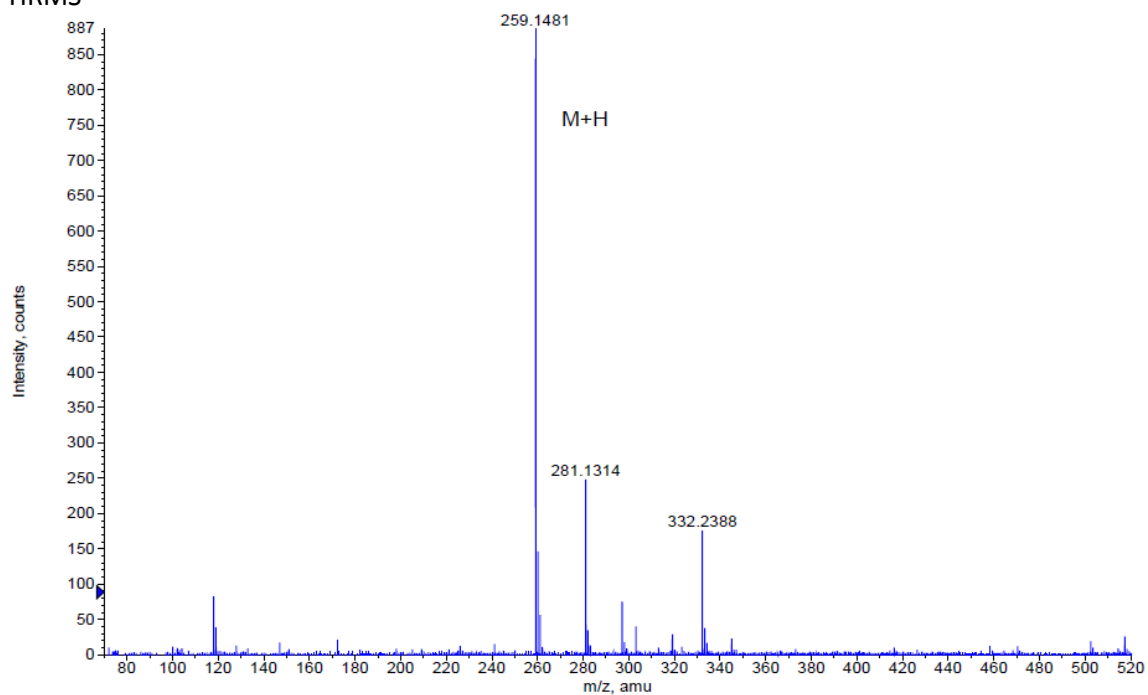
Formula	CalculatedMass	mDaError	ppmError	RDB
C ₁₆ H ₂₅ N ₂ O ₂ S	309.163127	0.173484	0.561139	5.5
C ₁₉ H ₂₆ Na S	309.164744	-1.44396	-4.670533	6.5
C ₁₄ H ₂₆ N ₂ O ₂ Na S	309.160721	2.578744	8.341027	2.5

- (S)-2-(3-ciclohexiltioureido)-3-methylbutanoic acid (117)¹H RMN (CDCl₃-CD₃OD, 200 MHz)¹³C RMN (CDCl₃-CD₃OD, 50 MHz)

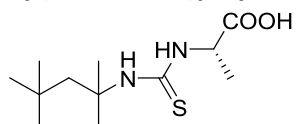
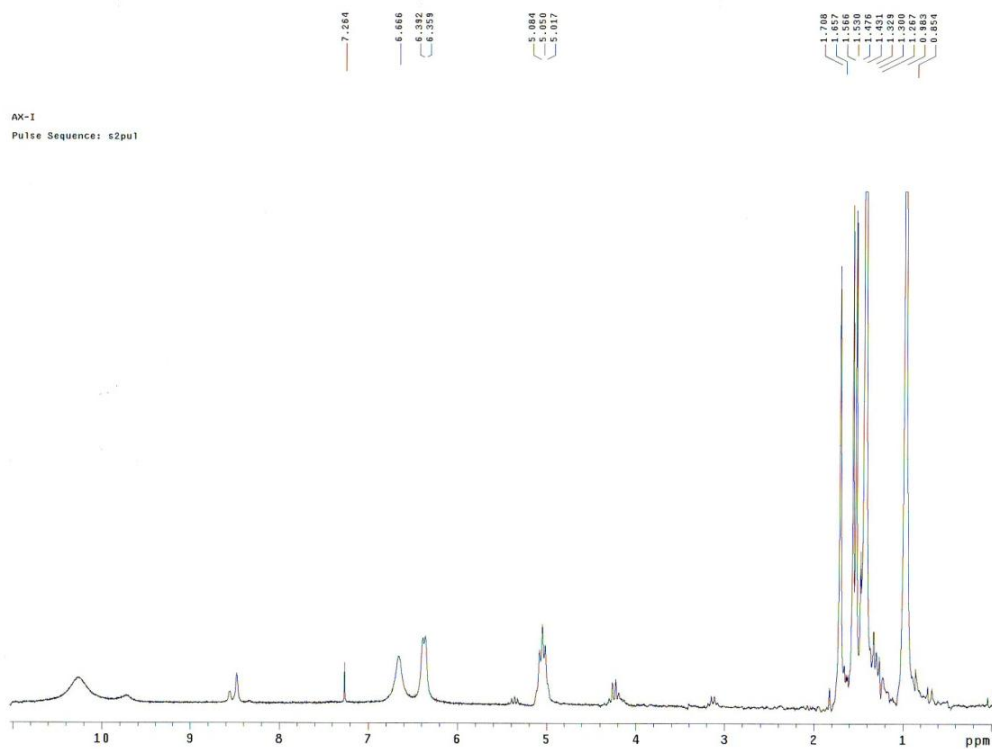
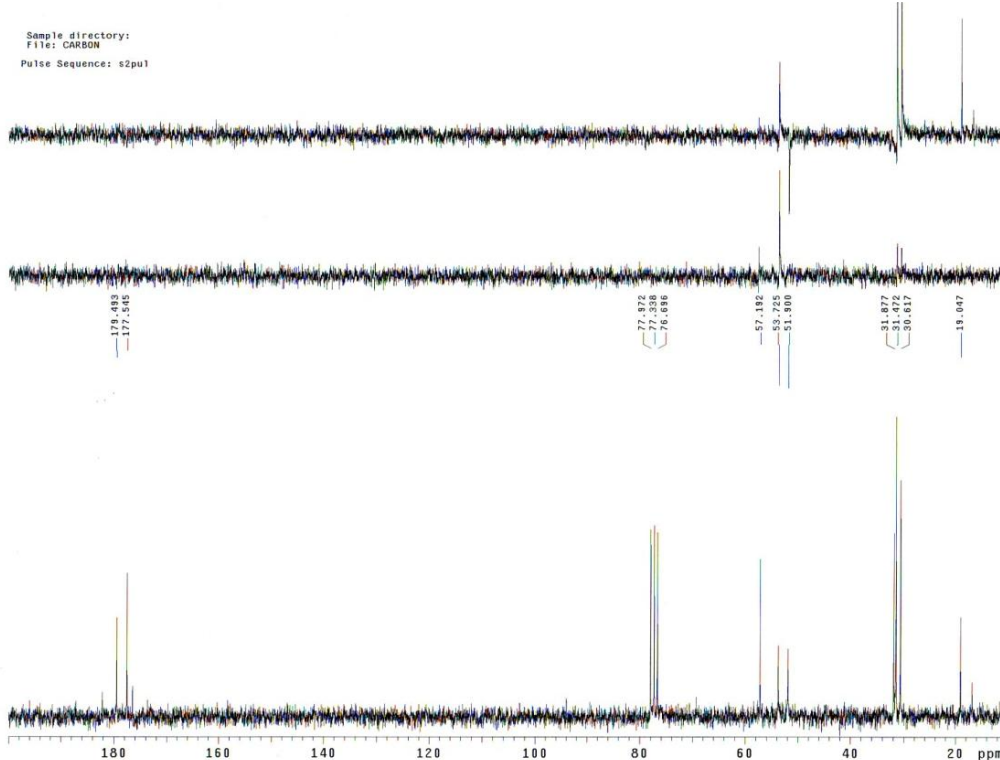
IR



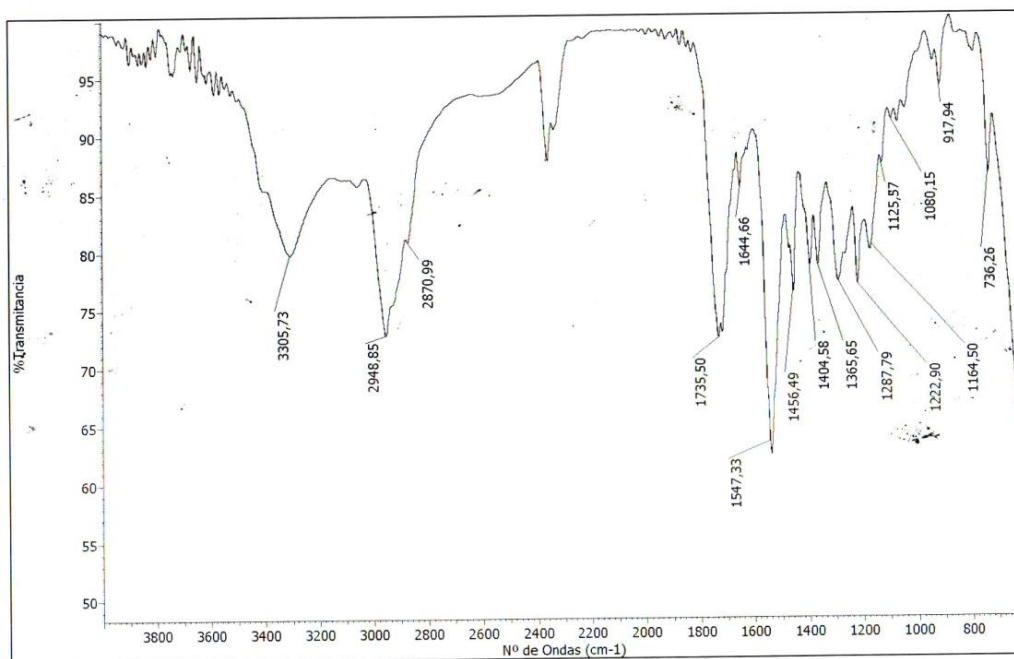
HRMS



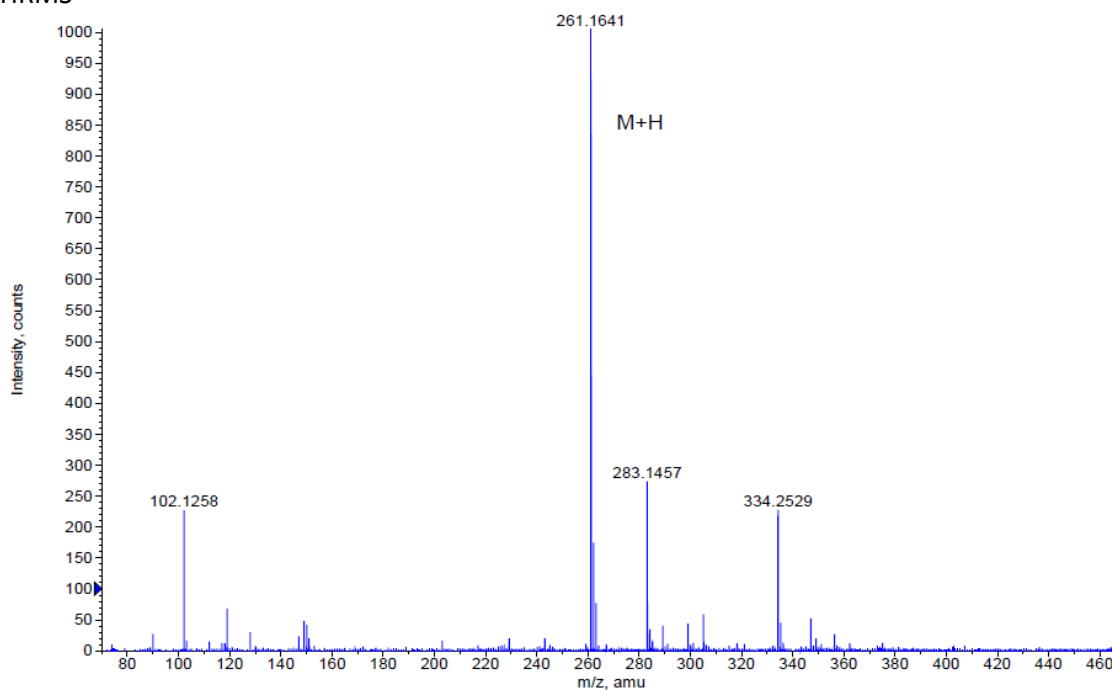
Formula	CalculatedMass	mDaError	ppmError	RDB
C ₁₂ H ₂₃ N ₂ O ₂ S	259.147476	0.623564	2.406202	2.5
C ₁₅ H ₂₄ Na S	259.149094	-0.99388	-3.835173	3.5

- (S) -2-(3-(2,4,4-trimethylpentan -2-yl) thiureido)propanoic acid (118)RMN ^1H (CDCl_3 , 200 MHz)RMN ^{13}C (CDCl_3 , 50 MHz)

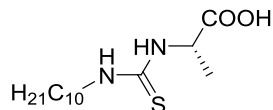
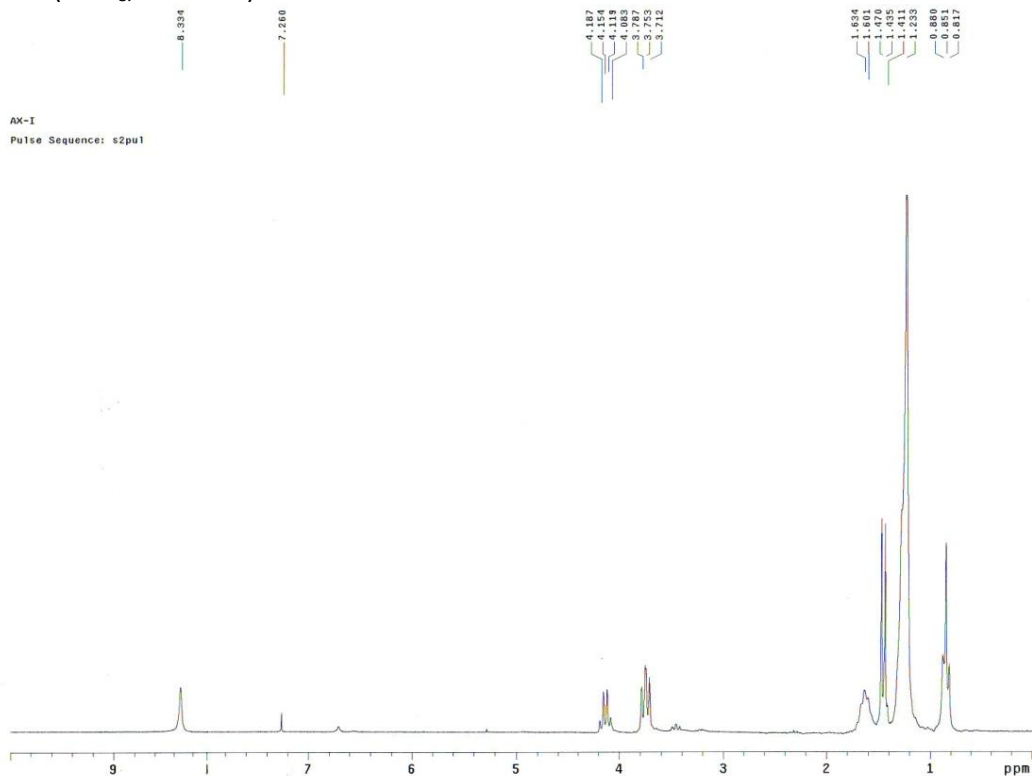
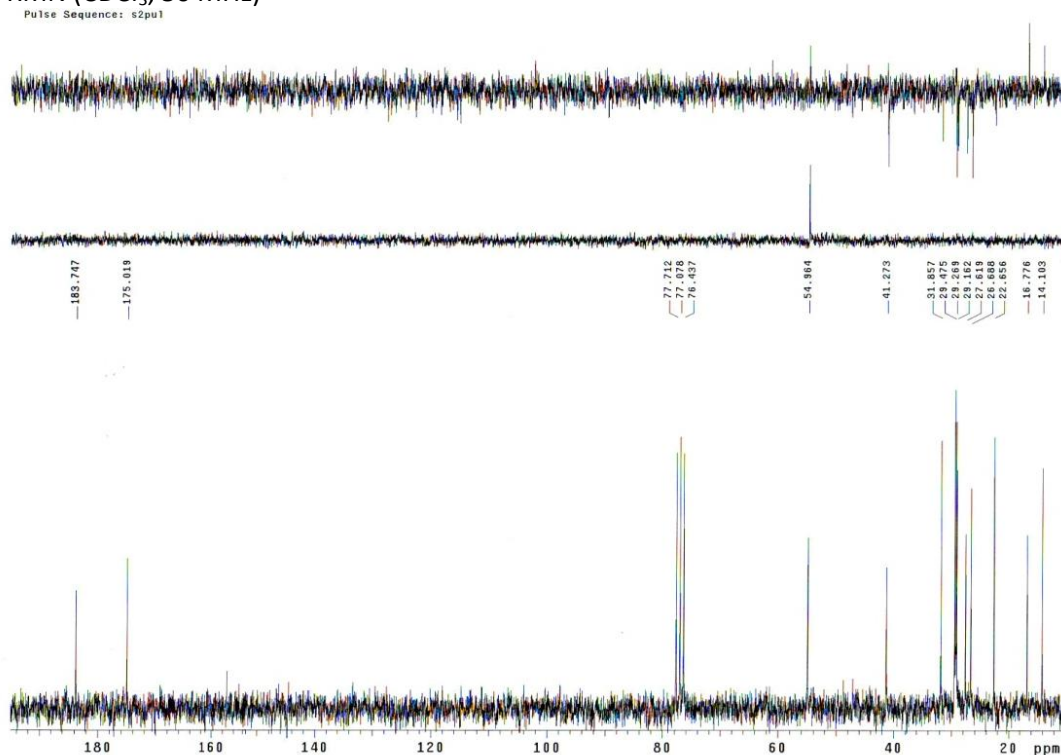
IR



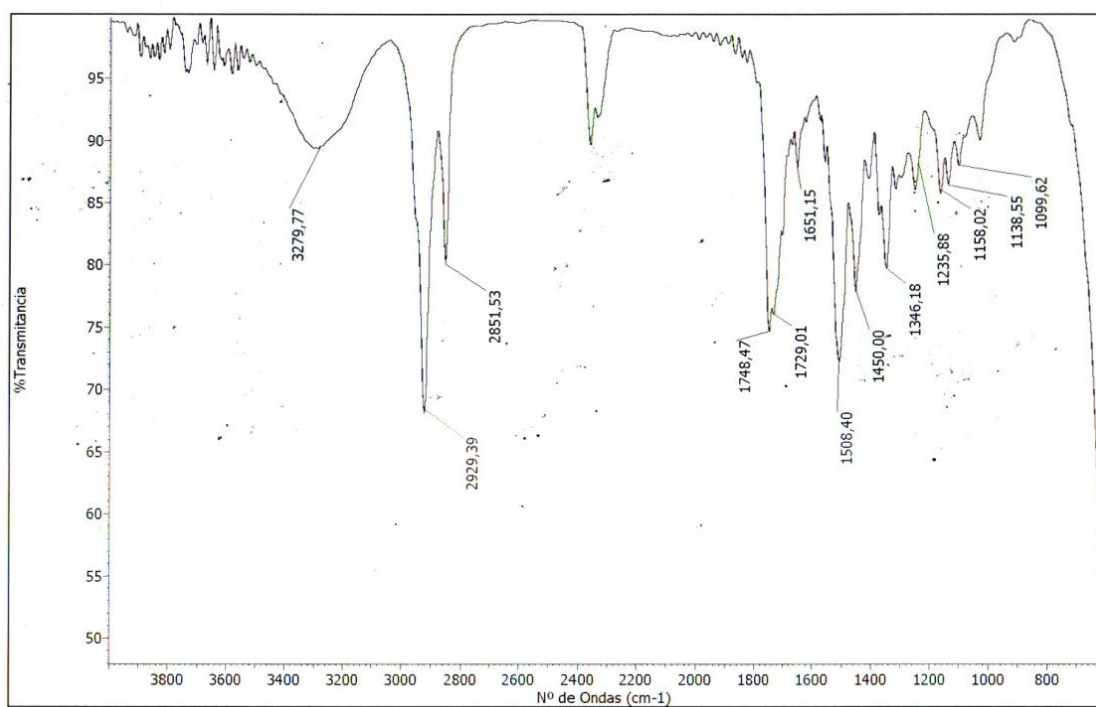
HRMS



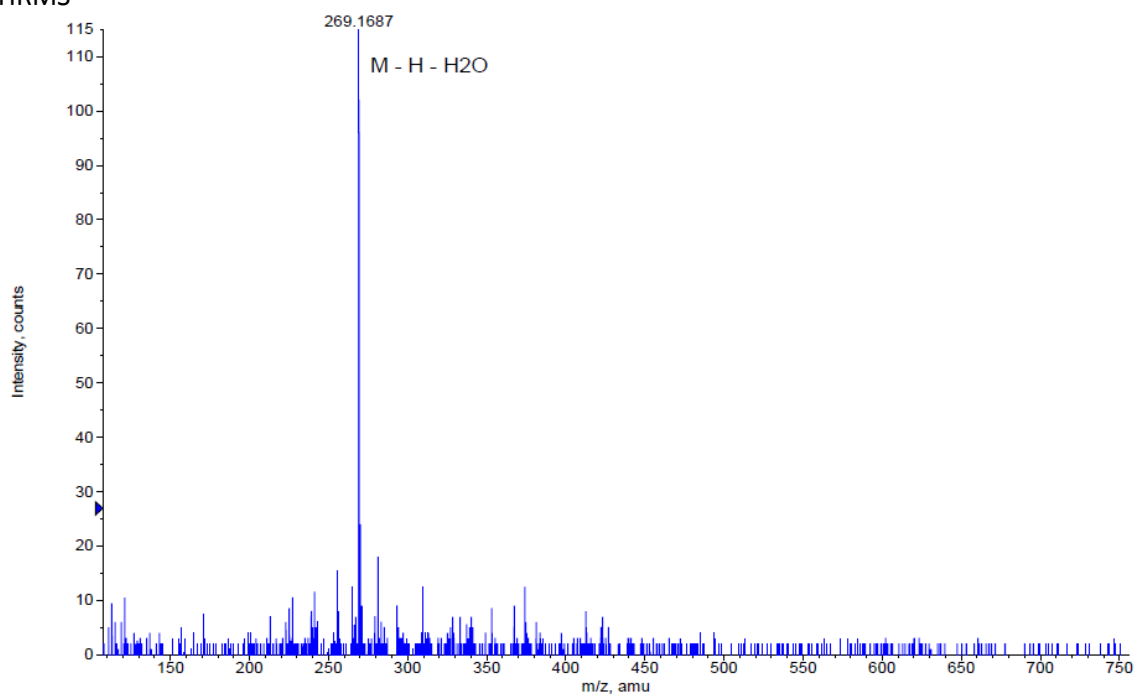
Formula	CalculatedMass	mDaError	ppmError	RDB
C ₁₅ H ₂₆ Na S	261.164744	-0.64396	-2.465724	2.5
C ₁₂ H ₂₅ N ₂ O ₂ S	261.163127	0.973484	3.727472	1.5

- (S) -2-(3-decylthioureido)propanoic acid (119)¹H RMN (CDCl₃, 200 MHz)¹³C RMN (CDCl₃, 50 MHz)

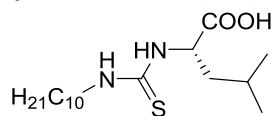
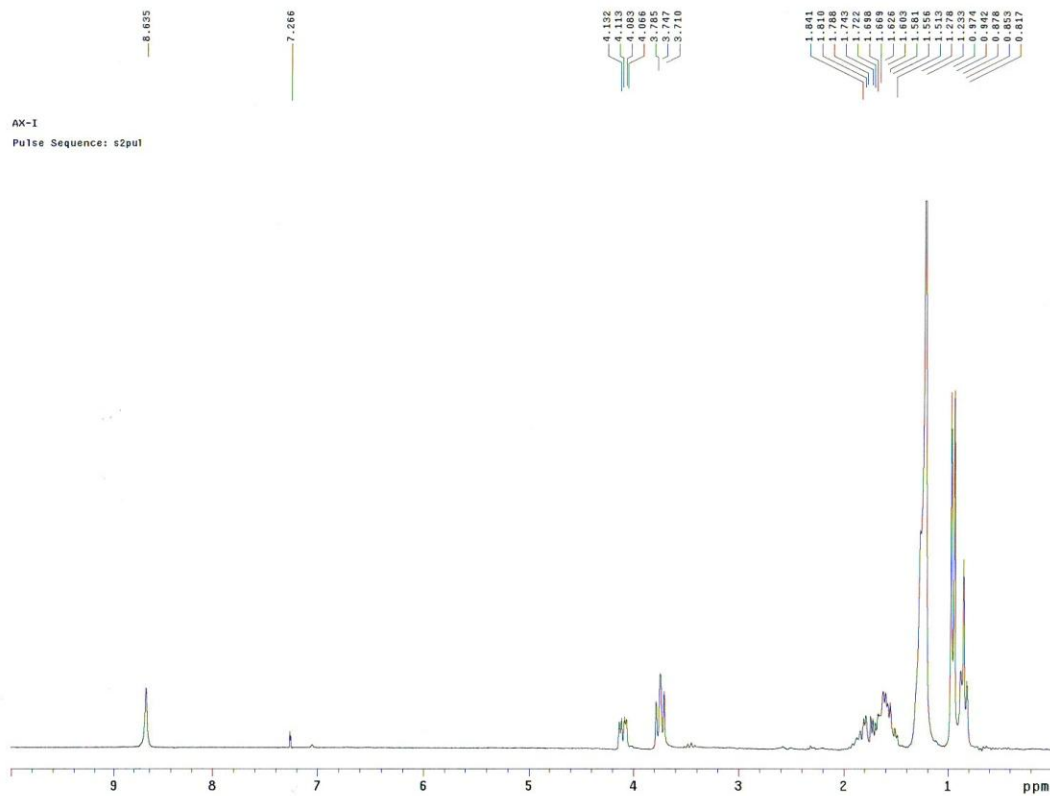
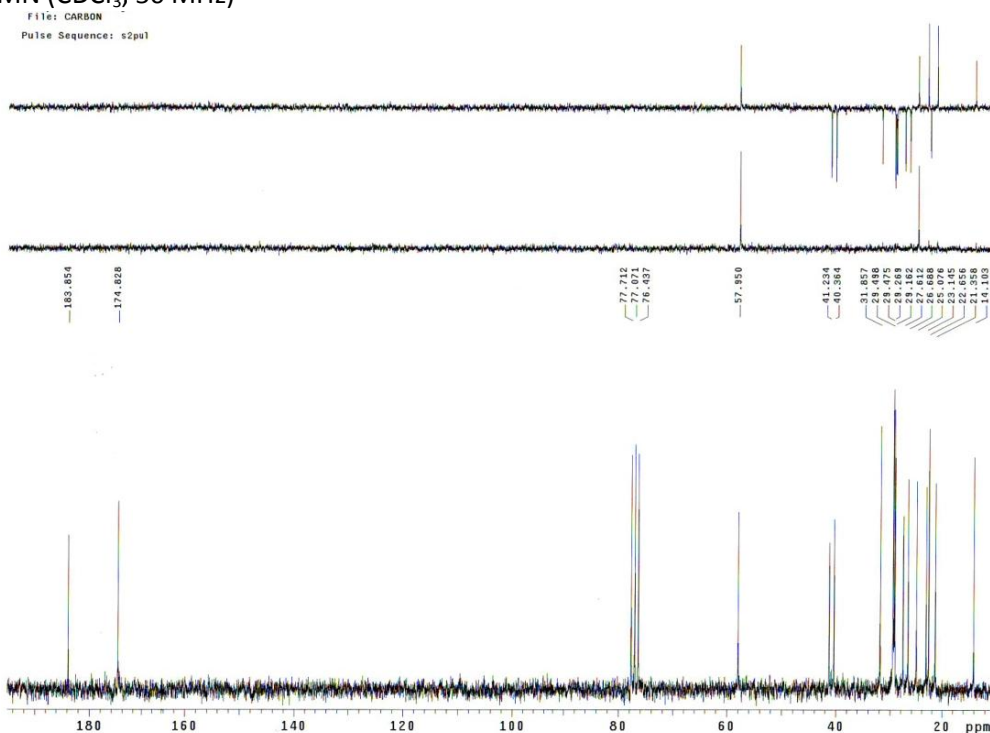
IR



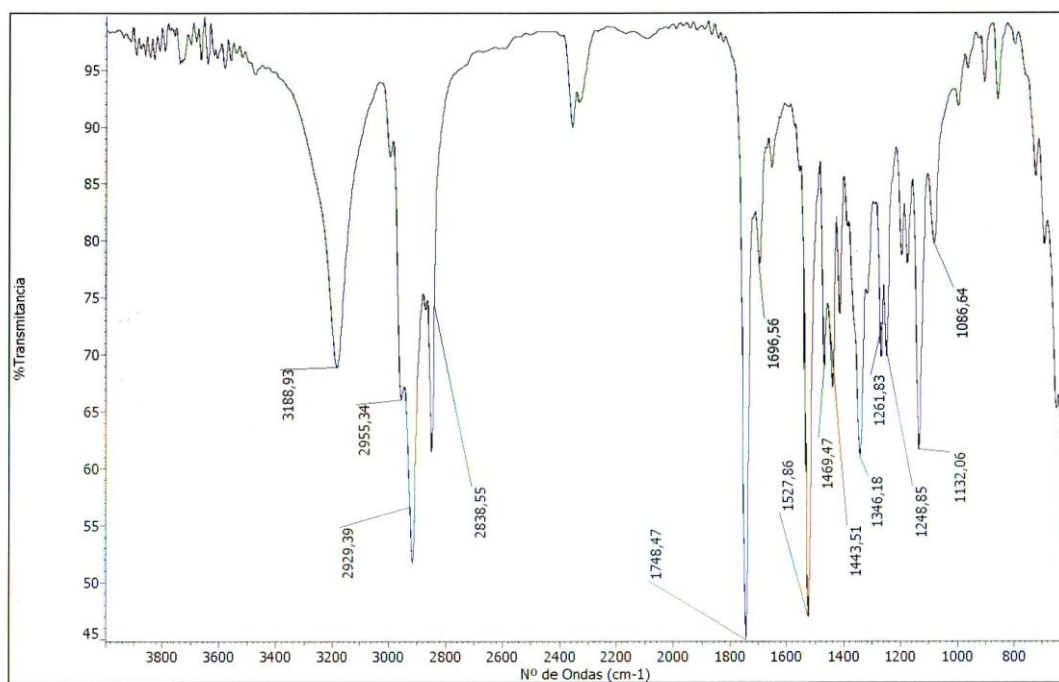
HRMS



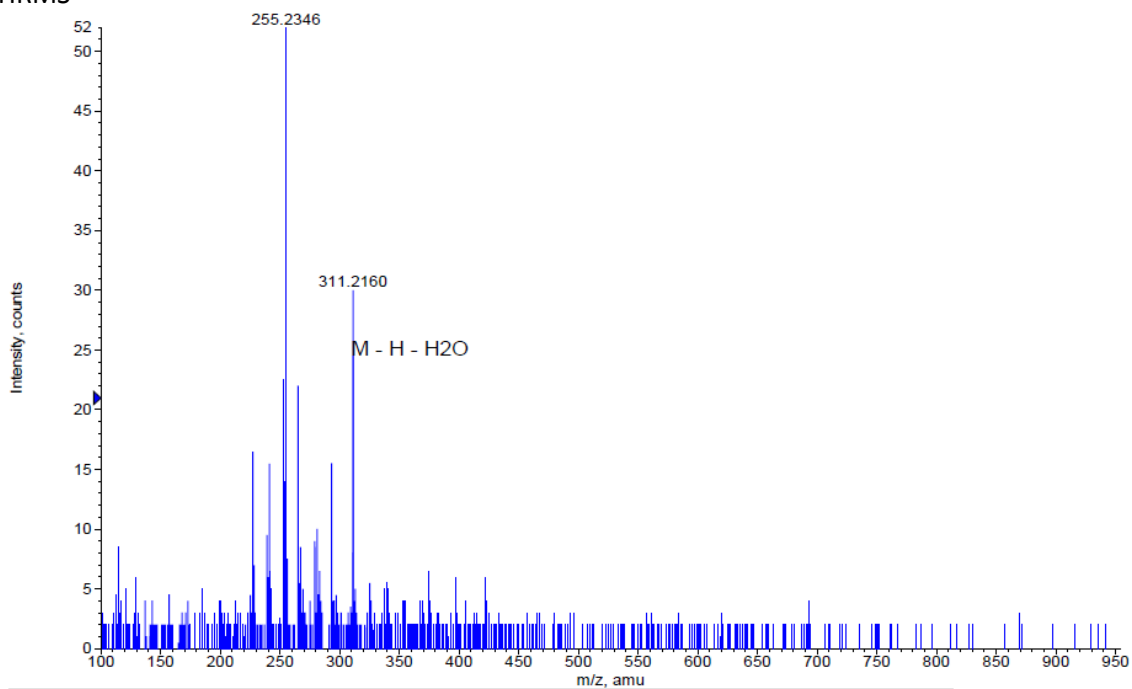
Formula	CalculatedMass	mDaError	ppmError	RDB
C ₁₄ H ₂₅ N ₂ O S	269.169309	-0.609036	-2.26266	3.5
C ₁₂ H ₂₆ N ₂ O Na S	269.166904	1.796224	6.673241	0.5

- (S)-2-(3-decylthioureido)-4-methylpentanoic acid (120)¹H RMN (CDCl₃, 200 MHz)¹³C RMN (CDCl₃, 50 MHz)

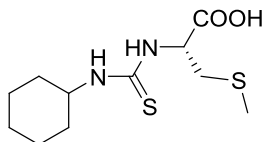
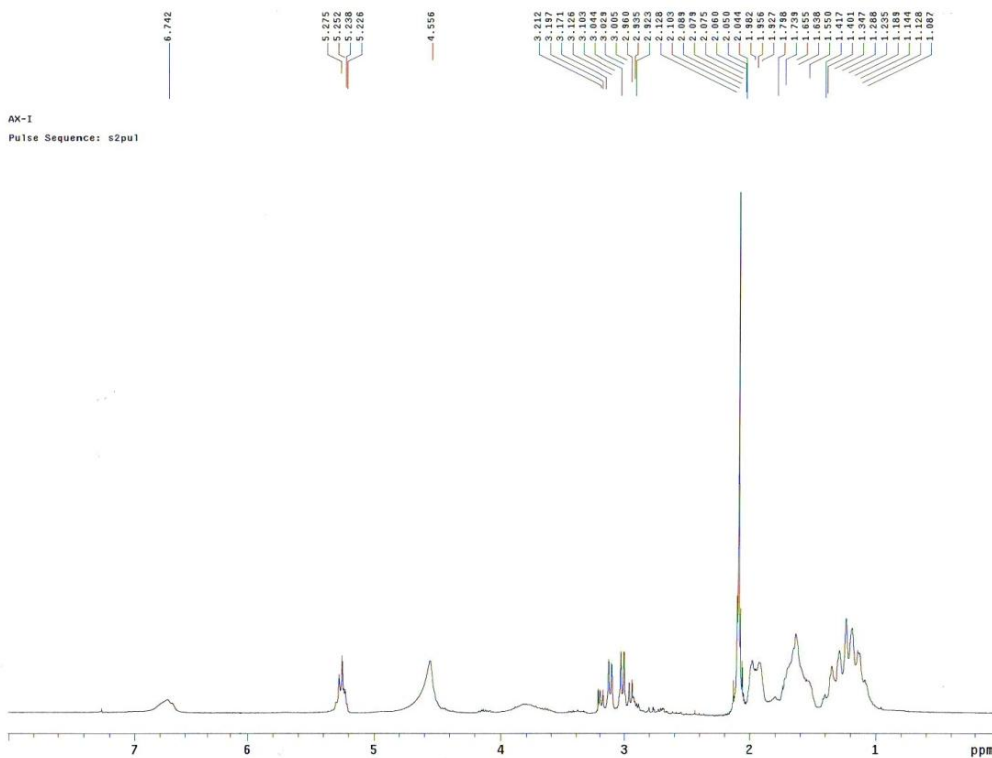
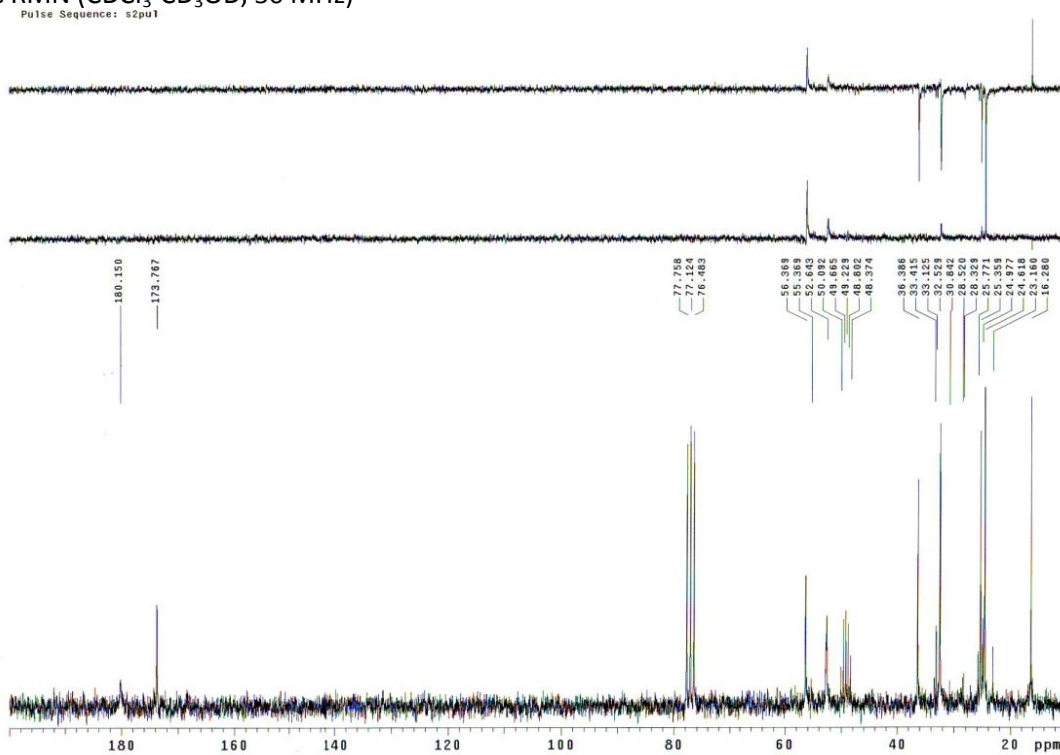
IR



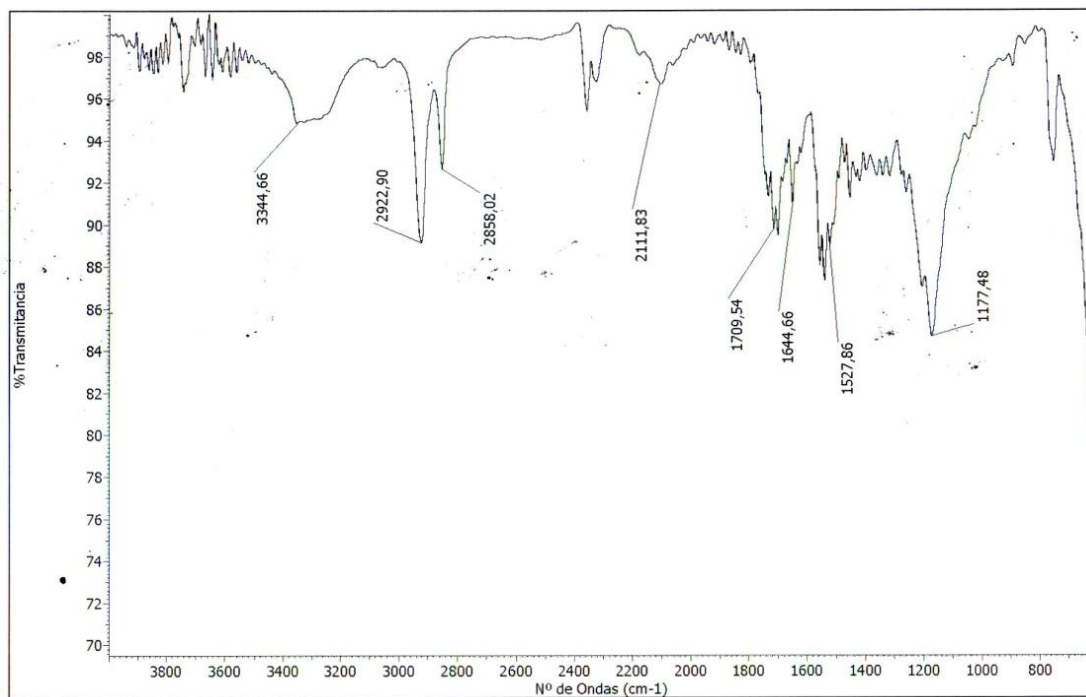
HRMS



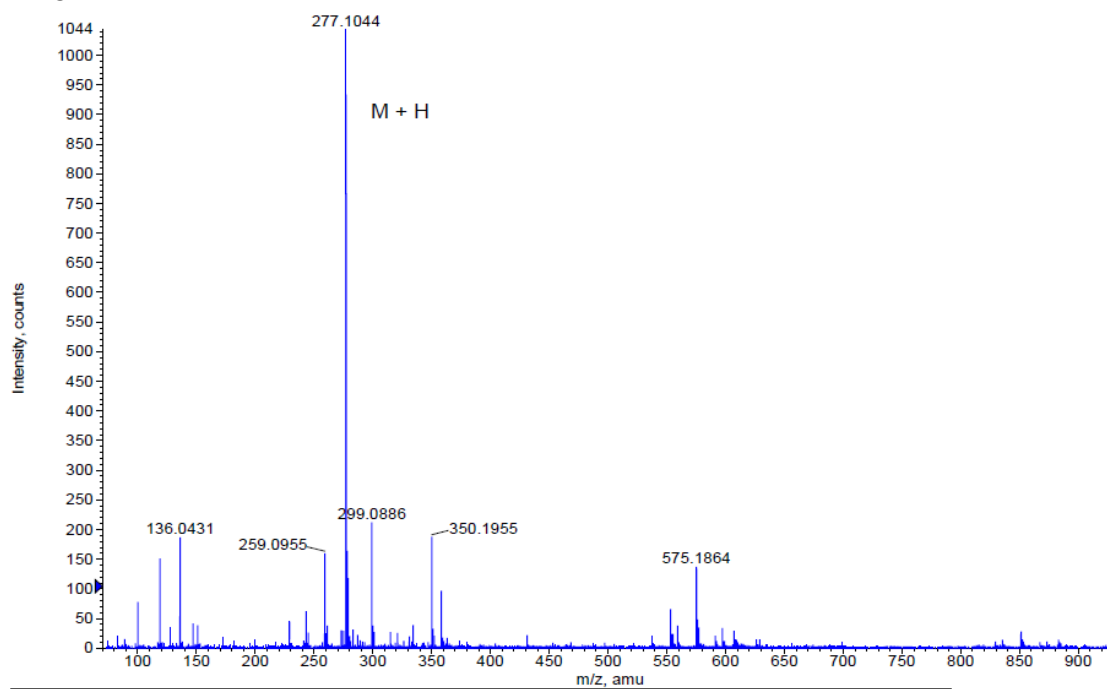
Formula	CalculatedMass	mDaError	ppmError	RDB
C17 H31 N2 O S	311.216259	-0.259276	-0.833108	3.5
C15 H32 N2 O Na S	311.213854	2.145984	6.895493	0.5

- (S) -2-(3-cyclohexylthioureido)-3-(methylthio)propanoic acid (121)¹H RMN (CDCl₃-CD₃OD, 200 MHz)¹³C RMN (CDCl₃-CD₃OD, 50 MHz)

IR

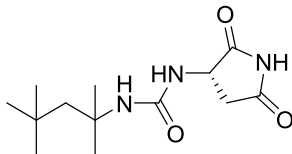
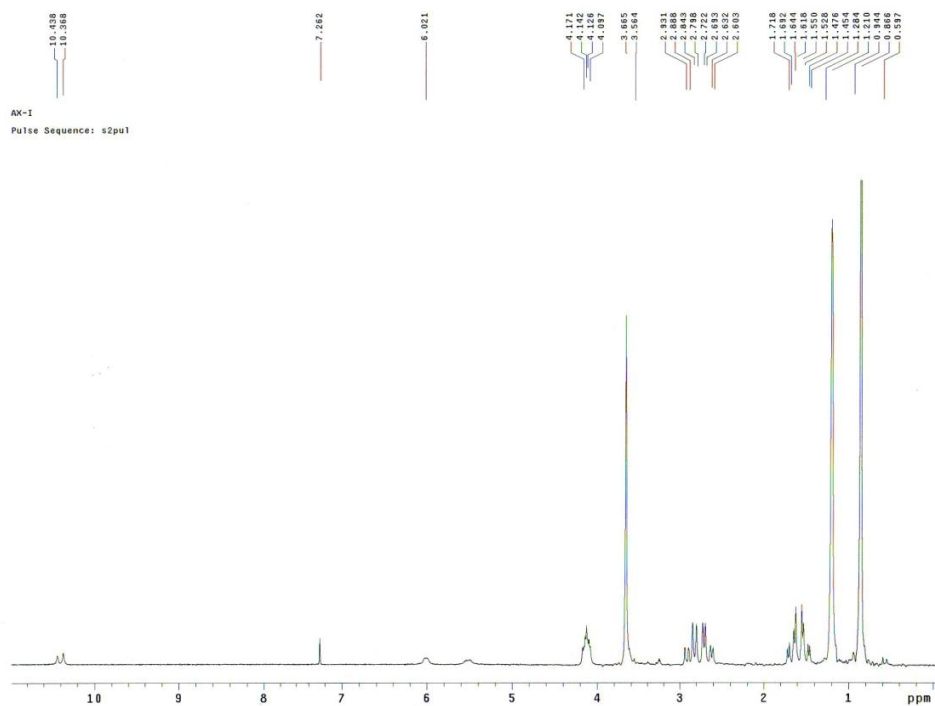
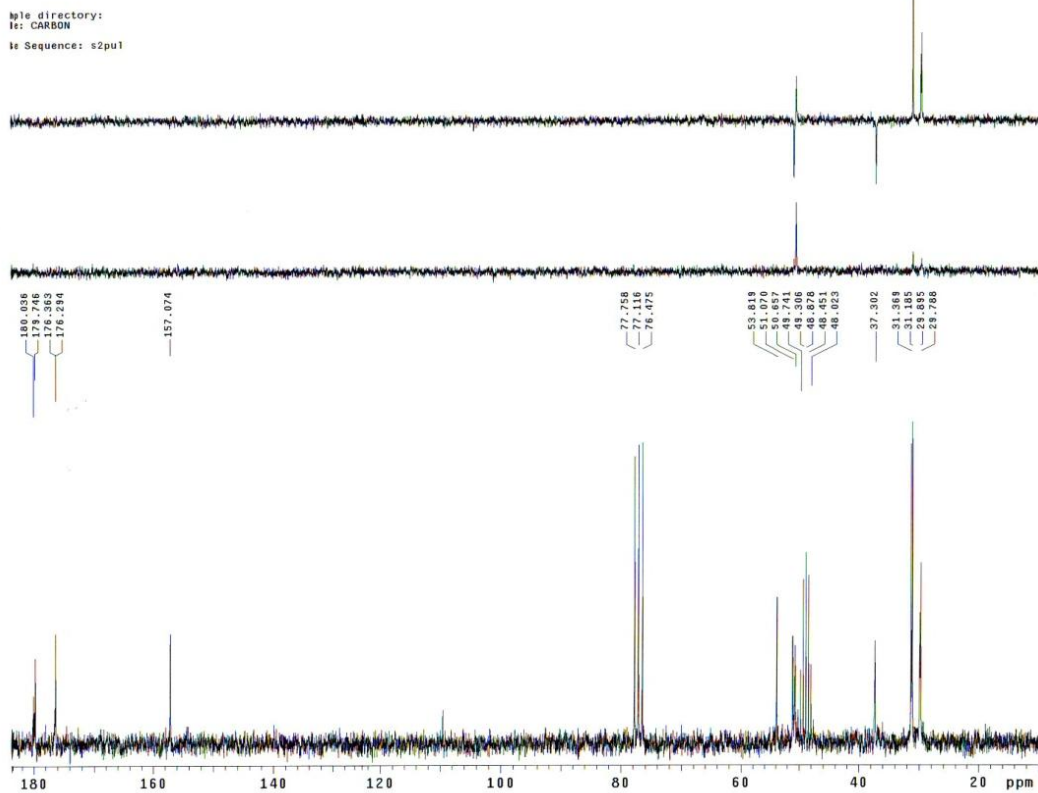


HRMS

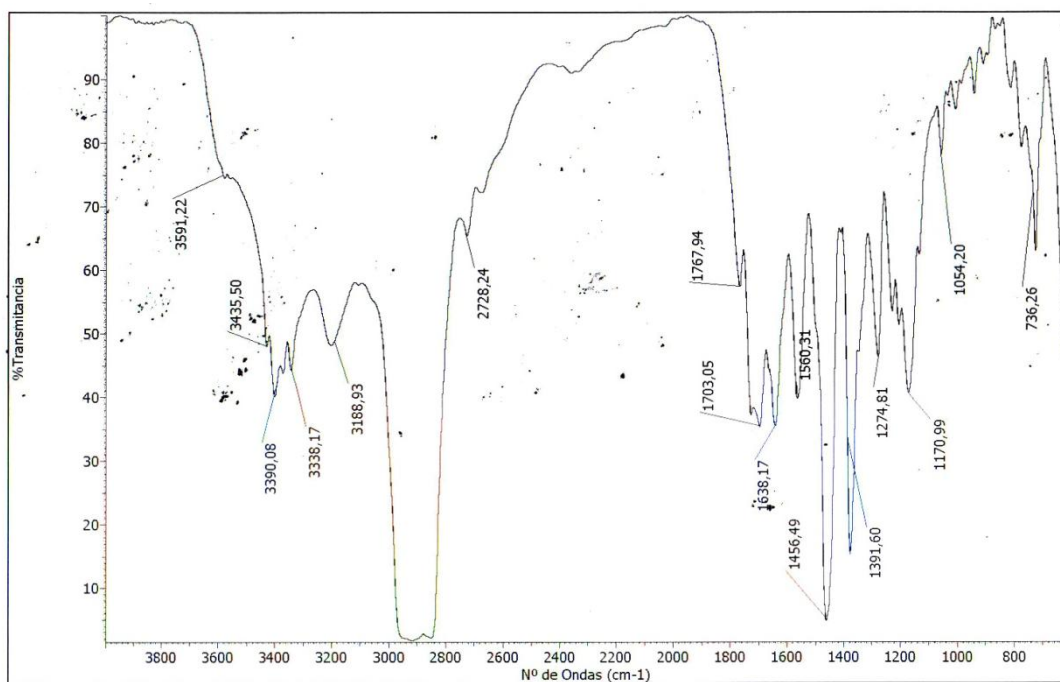


Formula	CalculatedMass	mDaError	ppmError	RDB
C11 H21 N2 O2 S2	277.103898	0.501844	1.811025	2.5
C14 H22 Na S2	277.105516	-1.1156	-4.025912	3.5

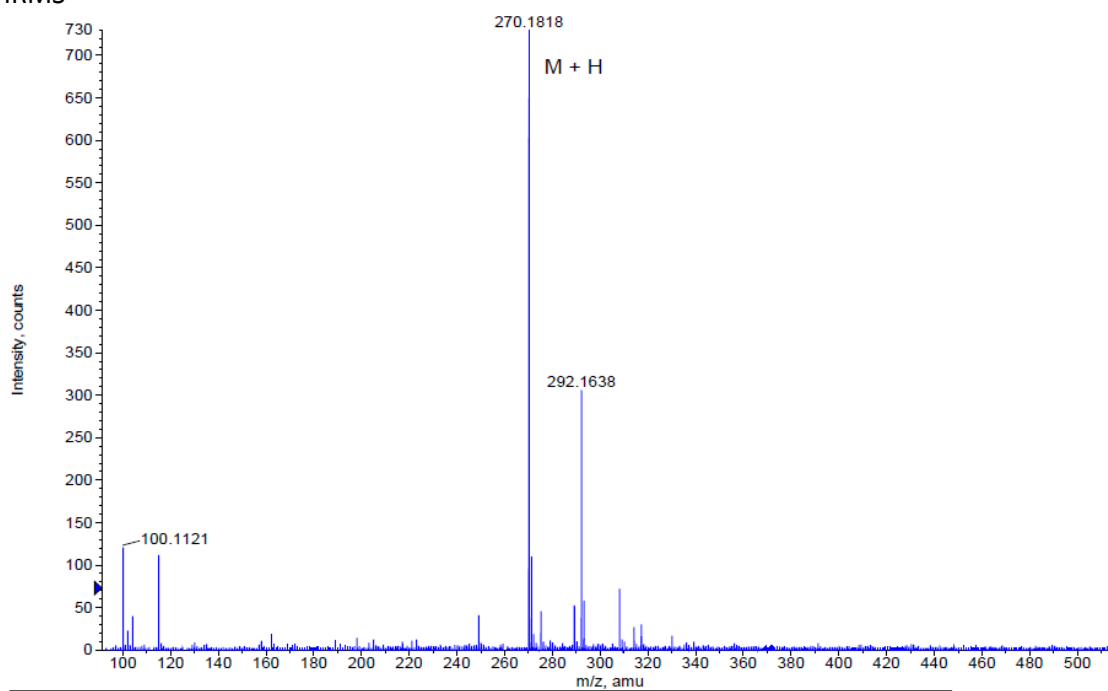
- (S)-1-(2,5-dioxopyrrolidin-3-yl)-3-(2,4,4-trimethylpentan-2-yl)urea (129)

 ^1H RMN ($\text{CDCl}_3\text{-CD}_3\text{OD}$, 200 MHz) ^{13}C RMN ($\text{CDCl}_3\text{-CD}_3\text{OD}$, 50 MHz)

IR

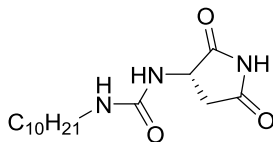
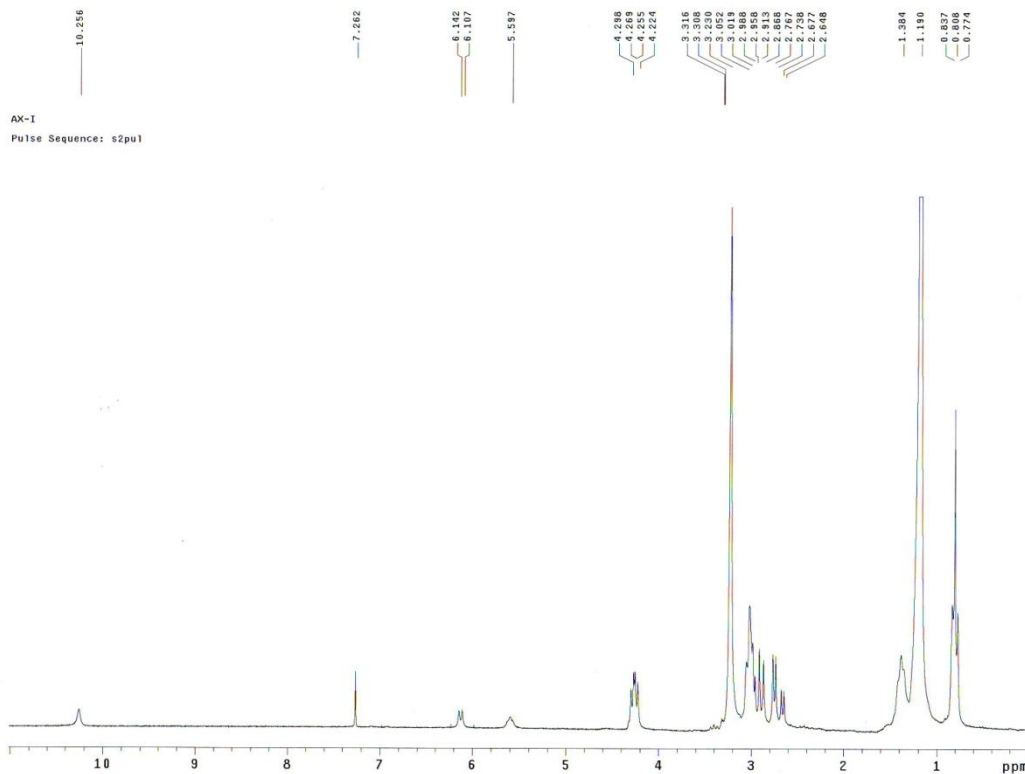
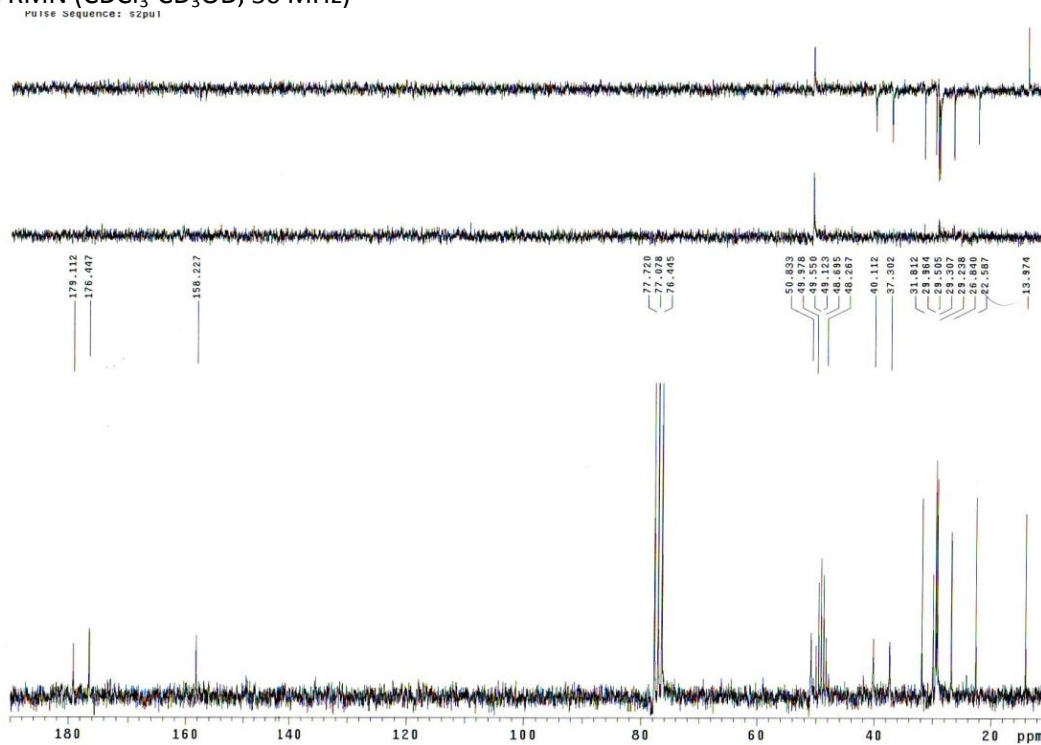


HRMS

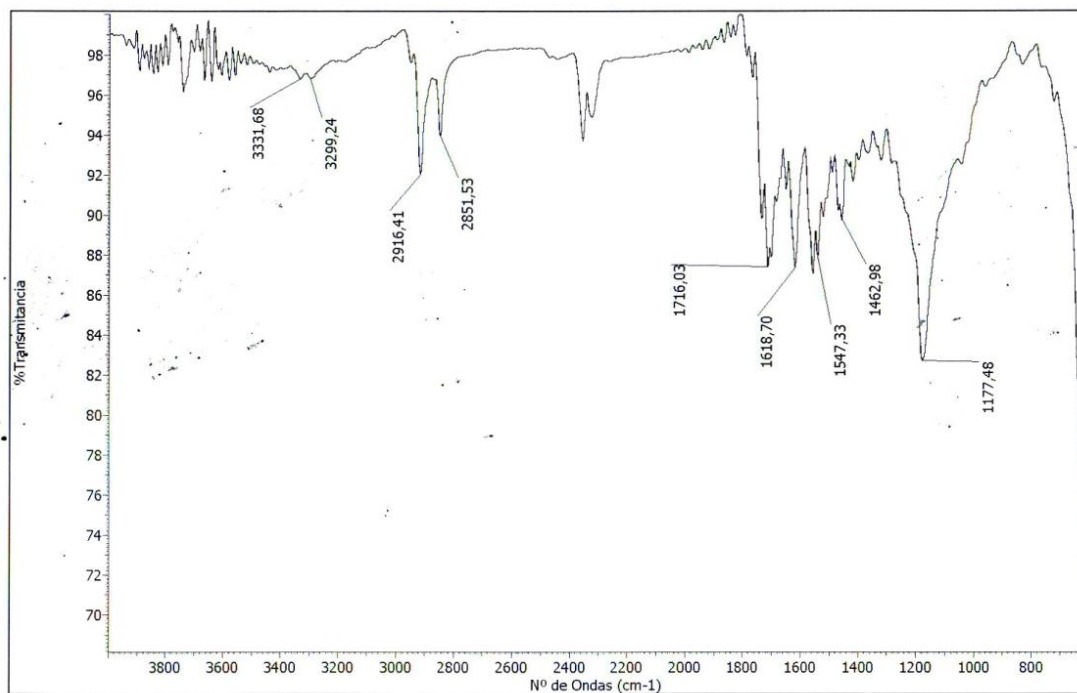


Formula	CalculatedMass	mDaError	ppmError	RDB
C ₁₃ H ₂₄ N ₃ O ₃	270.181218	0.581676	2.152902	3.5
C ₁₆ H ₂₅ N O Na	270.182836	-1.035768	-3.833589	4.5

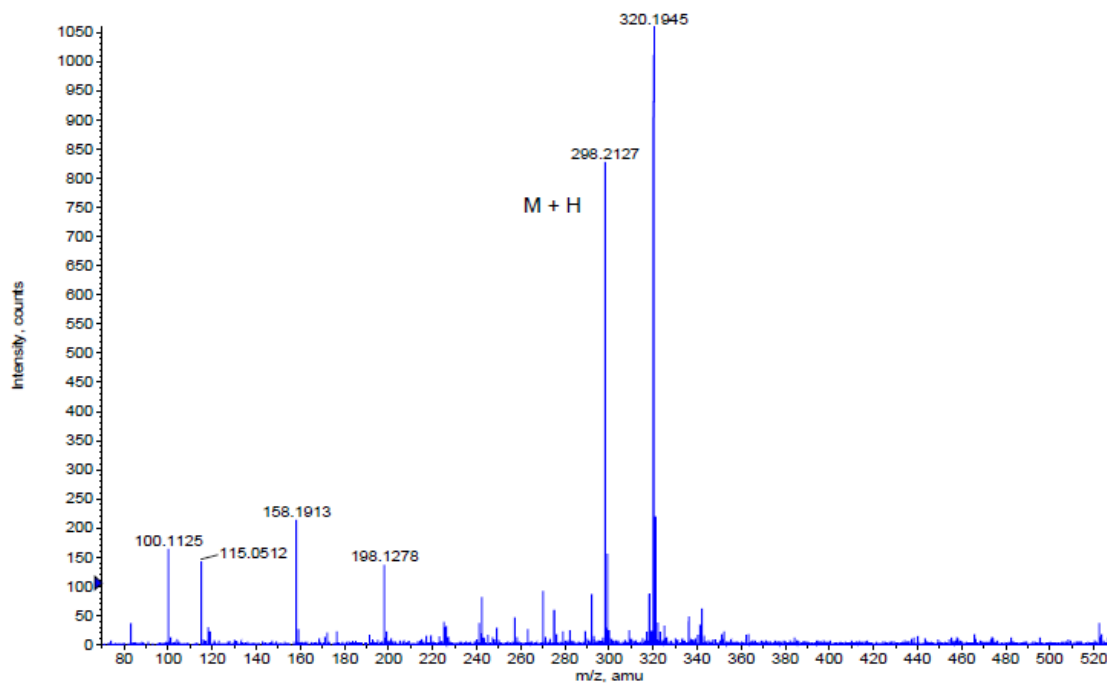
- (S)-1-decyl-3-(2,5-dioxopyrrolidin-3-yl)urea (130)

 ^1H RMN ($\text{CDCl}_3\text{-CD}_3\text{OD}$, 200 MHz) ^{13}C RMN ($\text{CDCl}_3\text{-CD}_3\text{OD}$, 50 MHz)

IR

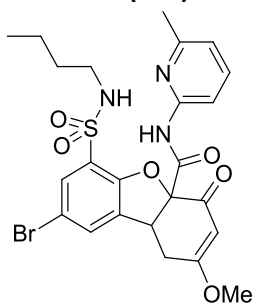


HRMS

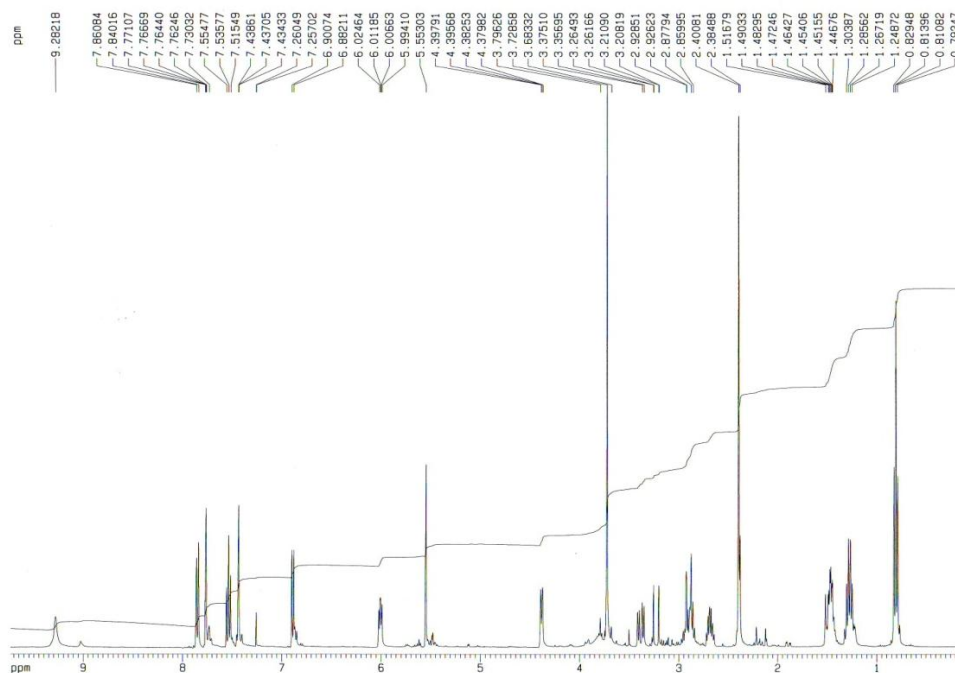


Formula	CalculatedMass	mDaError	ppmError	RDB
C ₁₅ H ₂₈ N ₃ O ₃	298.212518	0.181516	0.608679	3.5
C ₁₈ H ₂₉ N O Na	298.214136	-1.435928	-4.815105	4.5
C ₁₃ H ₂₉ N ₃ O ₃ Na	298.210113	2.586776	8.674249	0.5

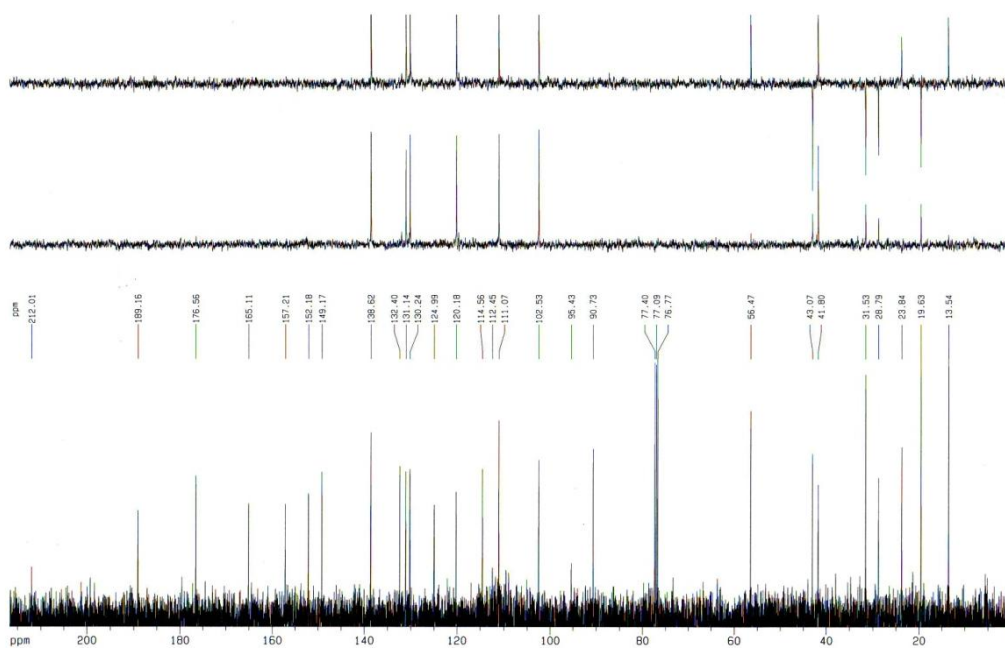
- 8-Bromo-6-(*N*-butylsulfamoyl)-2-methoxy-*N*-(6-methylpyridin-2-yl)-4-oxo-1,4,4a,9b-tetrahydrobenzo[*b,d*]furan-4a-carboxamide (131)



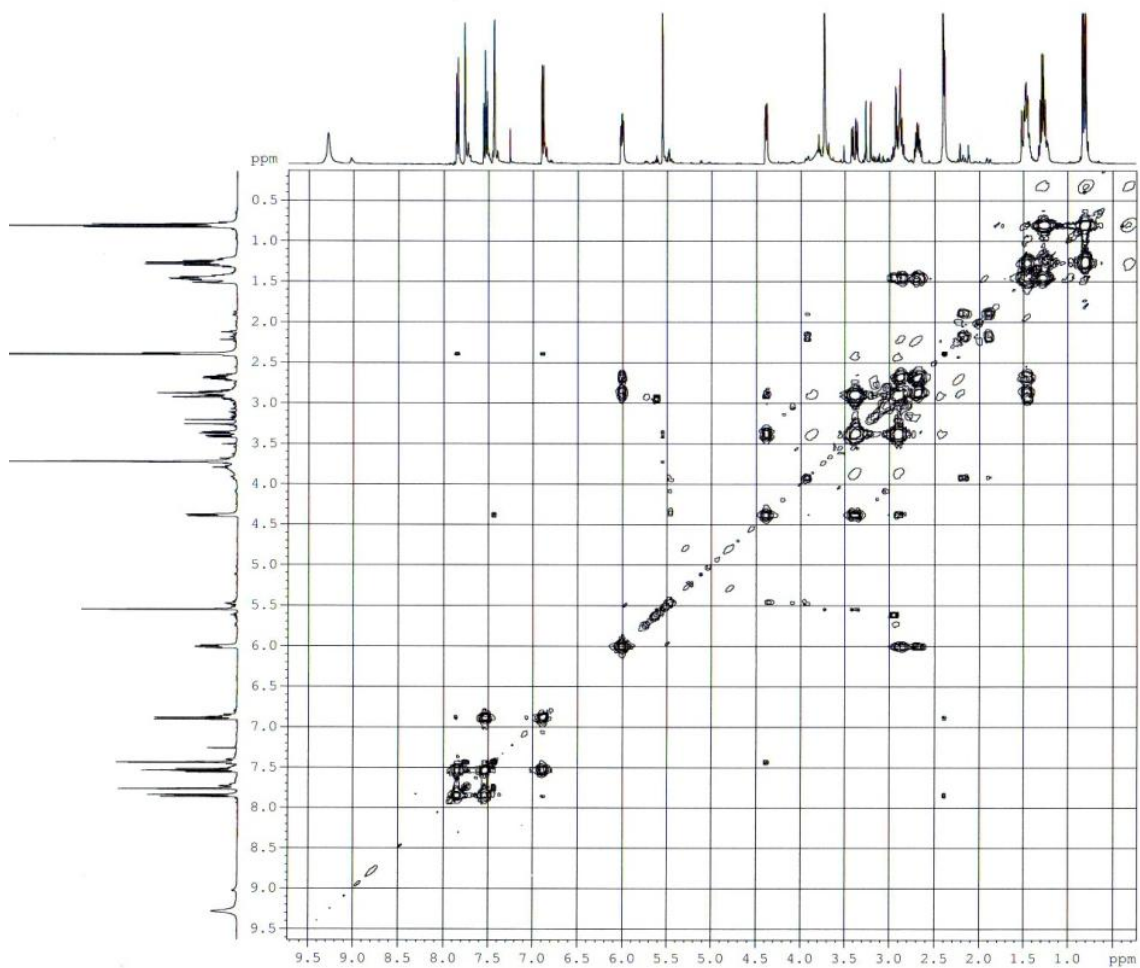
^1H NMR (CDCl₃, 400 MHz)



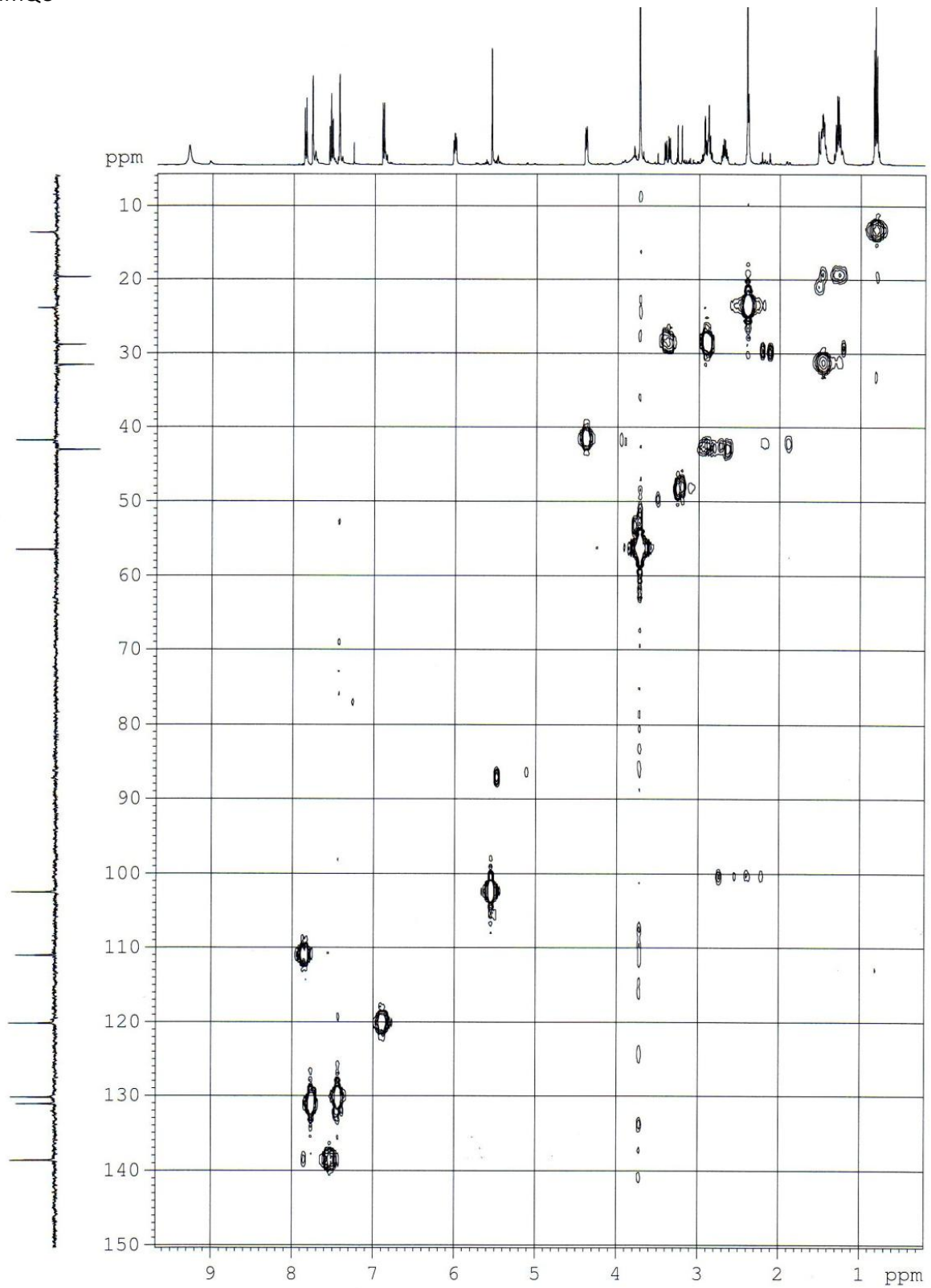
^{13}C NMR (CDCl₃, 100 MHz)



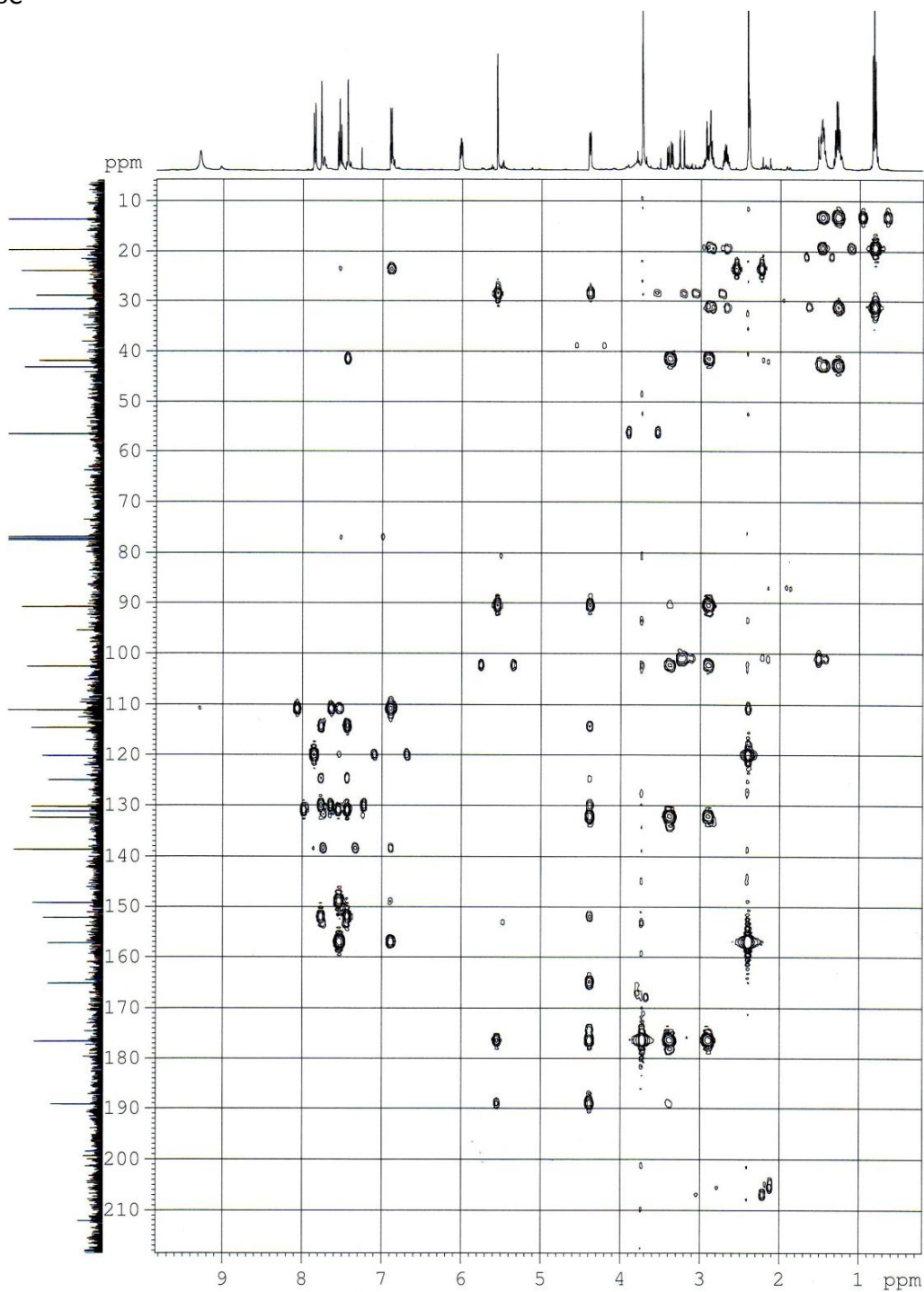
COSY



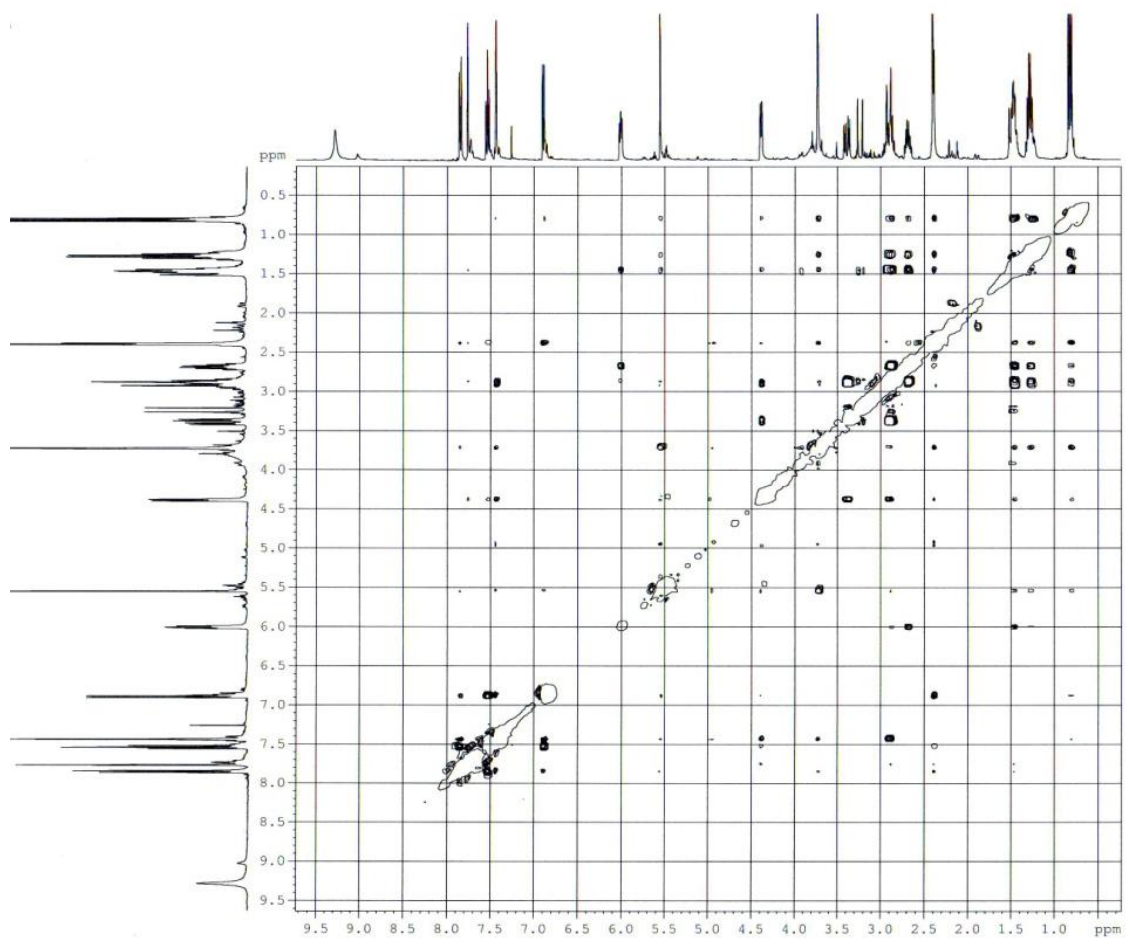
HMQC



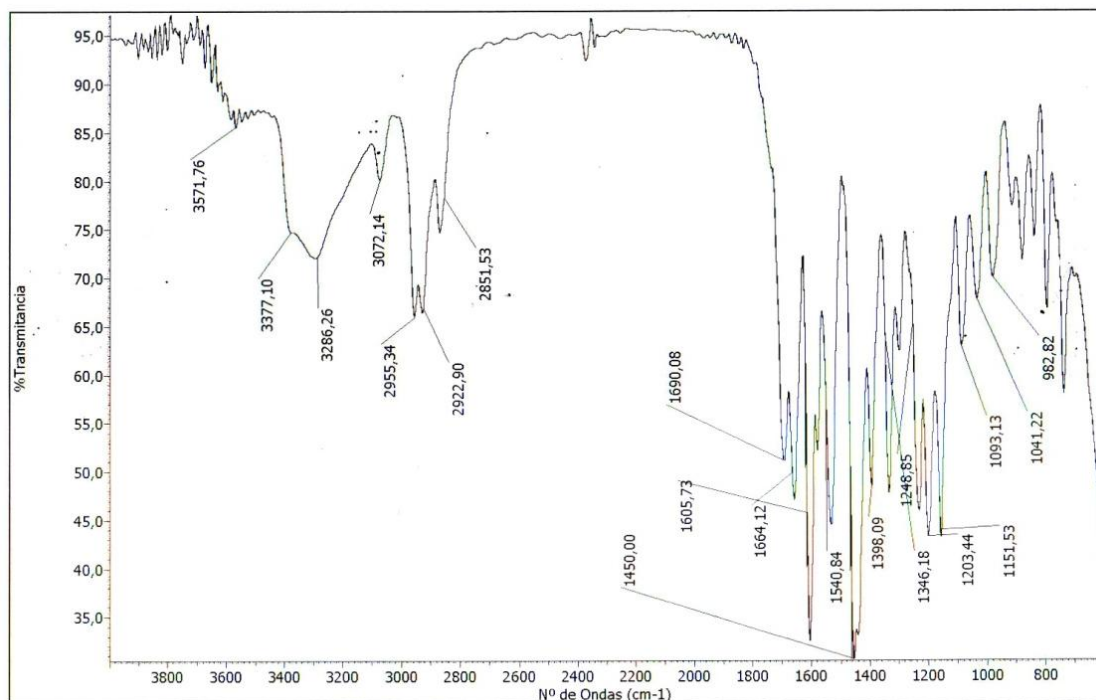
HMBC



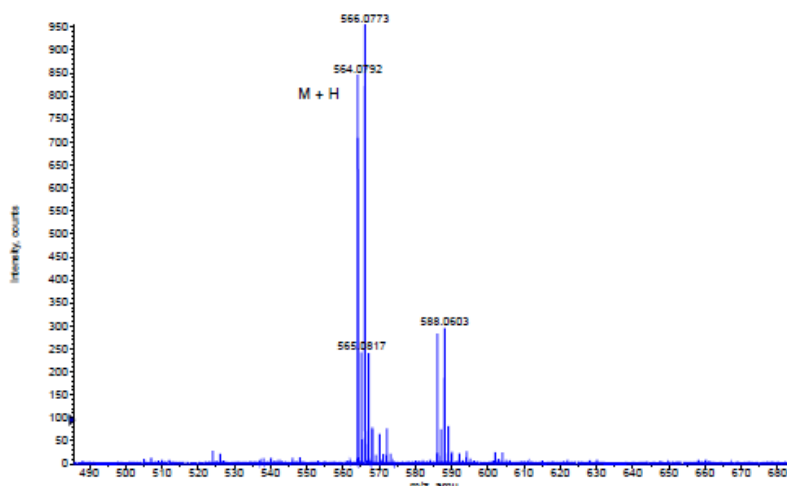
ROESY



IR

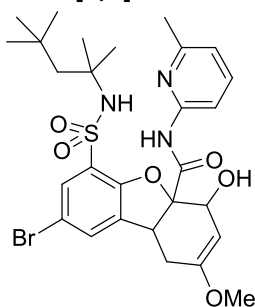


HRMS

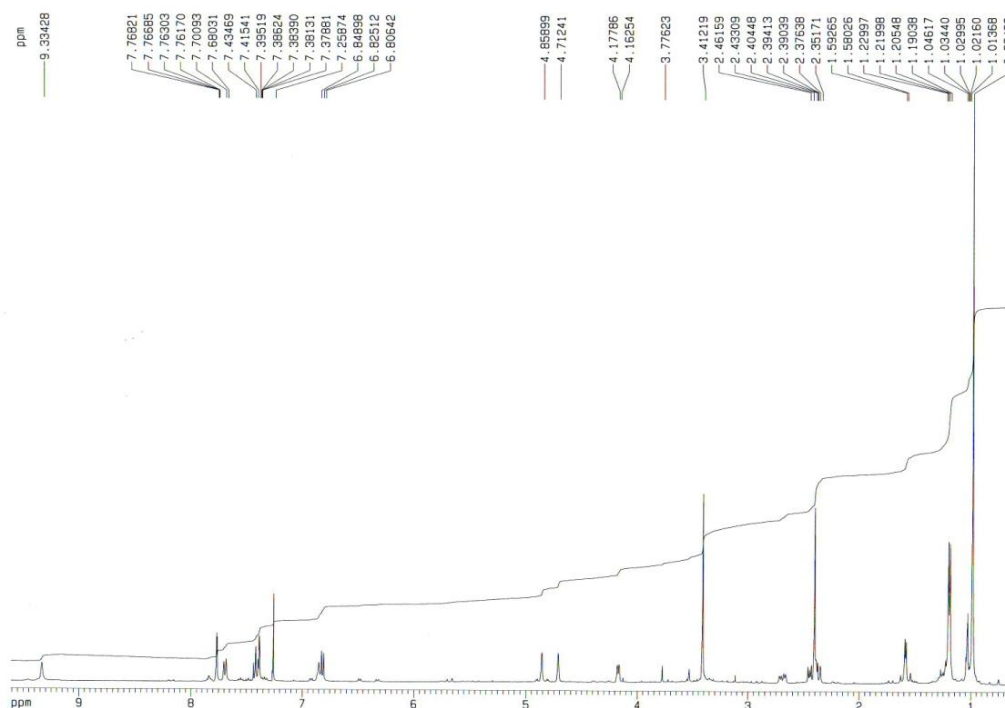


Formula	CalculatedMass	mDaError	ppmError	RDB
C24 H27 N3 O6 S Br	564.079845	-0.845264	-1.143923	12.5
C43 H11 N Na	564.078371	0.829432	1.470416	38.5
C37 H14 N3 O2 S	564.080125	-0.925084	-1.639988	32.5
C31 H15 N3 O7 Na	564.080221	-1.021224	-1.810425	25.5
C30 H24 N O4 Na Br	564.078091	1.109252	1.966481	18.5
C32 H23 N O4 Br	564.080496	-1.296008	-2.297562	21.5
C35 H15 N3 O2 Na S	564.07772	1.480176	2.624054	29.5
C45 H10 N	564.080776	-1.575828	-2.793626	41.5
C22 H28 N3 O6 Na S Br	564.07744	1.759996	3.120119	9.5
C27 H28 N O4 Na S Br	564.081463	-2.262708	-4.011326	13.5
C40 H10 N3 O2	564.076753	2.446876	4.337819	37.5
C40 H15 N Na S	564.081743	-2.542528	-4.507391	33.5
C27 H23 N3 O6 Br	564.076473	2.726696	4.833884	17.5
C33 H14 N3 O7	564.082626	-3.426484	-6.074467	28.5
C28 H19 N3 O7 Na S	564.083593	-4.393184	-7.788232	20.5
C31 H18 N O8 S	564.074765	4.434932	7.862243	23.5
C29 H27 N O4 S Br	564.083868	-4.667968	-8.275369	16.5
C23 H28 N O9 Na Br	564.083964	-4.764108	-8.445806	9.5
C38 H11 N3 O2 Na	564.074348	4.852136	8.601862	34.5
C42 H14 N S	564.084148	-4.947788	-8.771433	36.5
C36 H15 N O5 Na	564.084244	-5.043928	-8.94187	29.5
C25 H24 N3 O6 Na Br	564.074068	5.131956	9.097926	14.5
C31 H23 N3 O S Br	564.073972	5.228096	9.268363	21.5

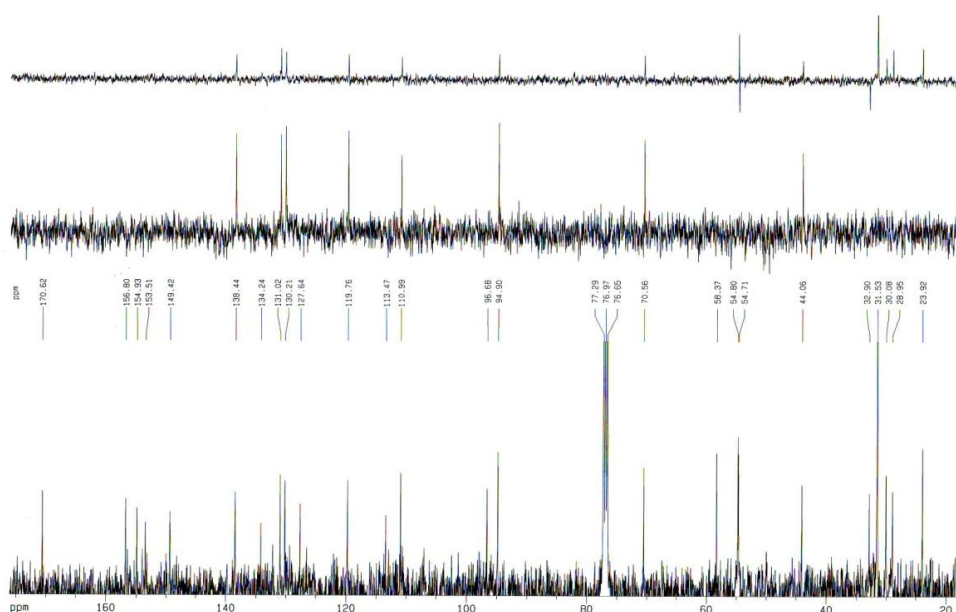
- **8-Bromo-4-hidroxy-2-methoxy-*N*-(6-methylpyridin-2-yl)-6-(*N*-(2,4,4-trimethylpentan-2-yl)sulfamoyl)-1,4,4a,9b-tetrahydrodibenzo[*b,d*]furan-4a-carboxamide (136)**



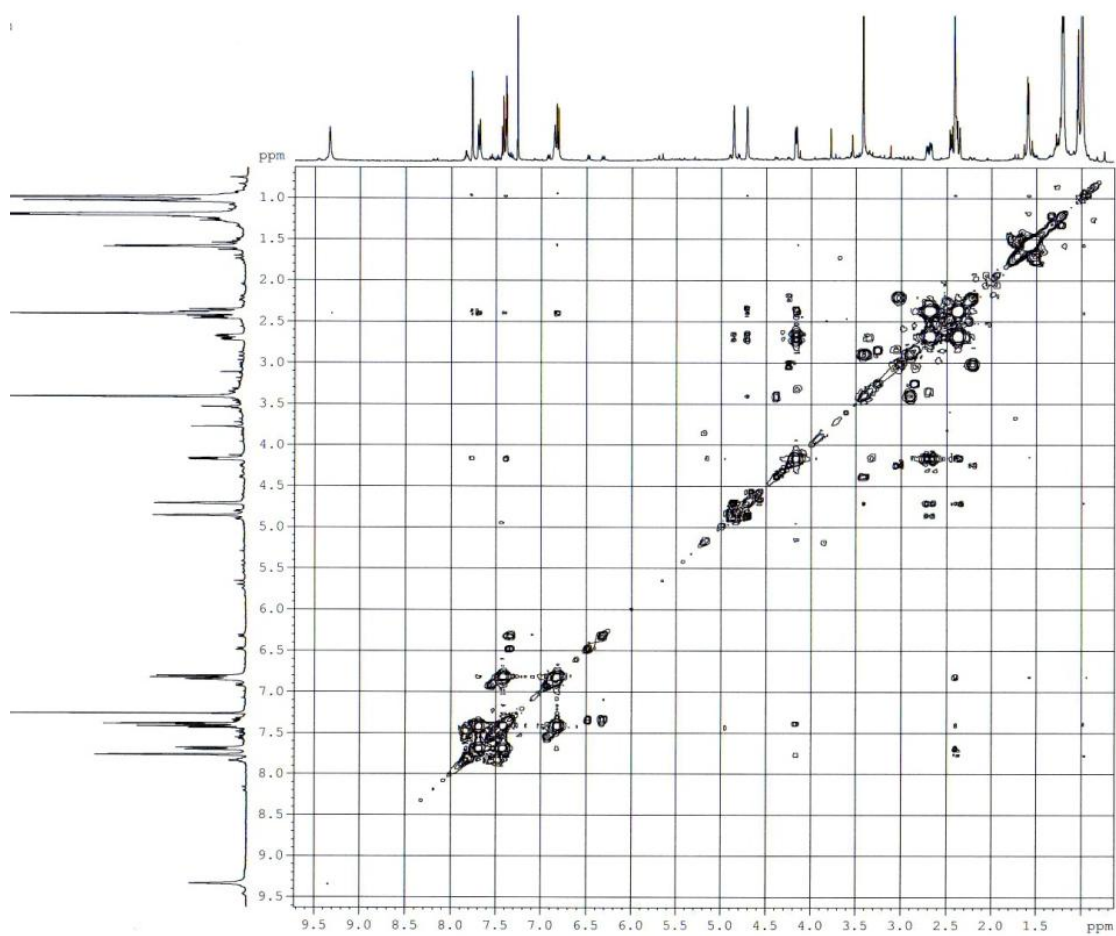
¹H NMR (CDCl₃, 400 MHz)



¹³C NMR (CDCl₃, 100 MHz)

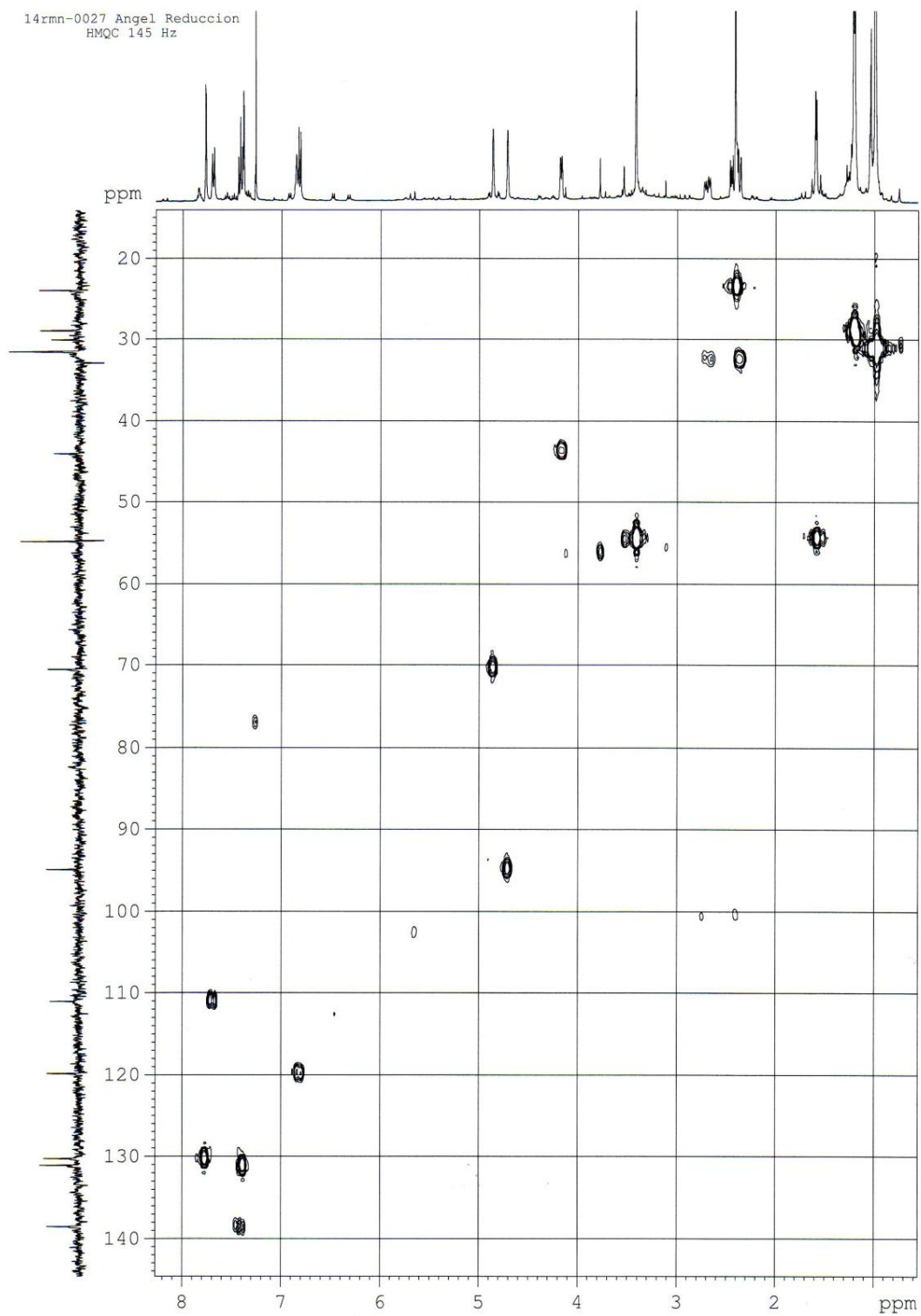


COSY

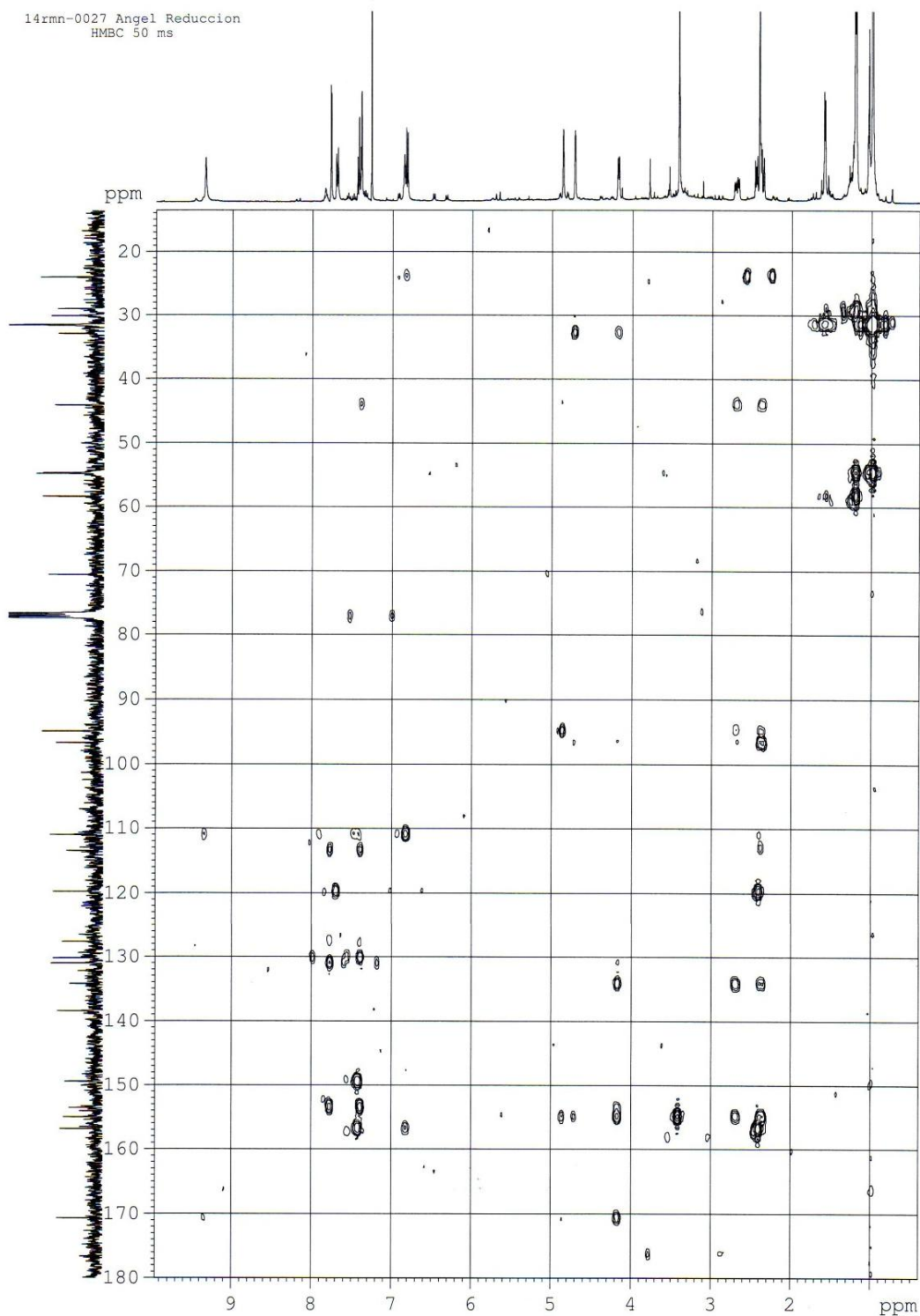


HMQC

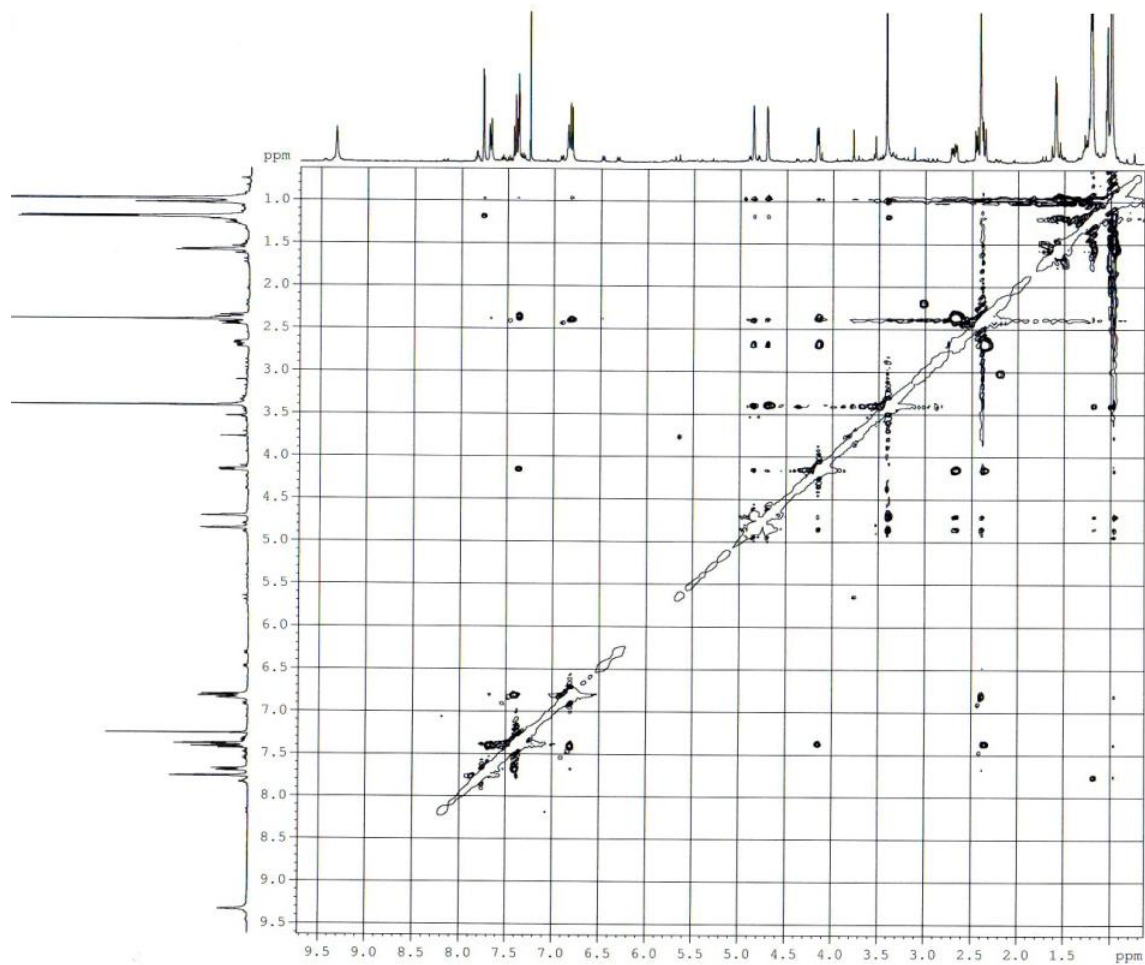
14rnm-0027 Angel Reduccion
HMQC 145 Hz



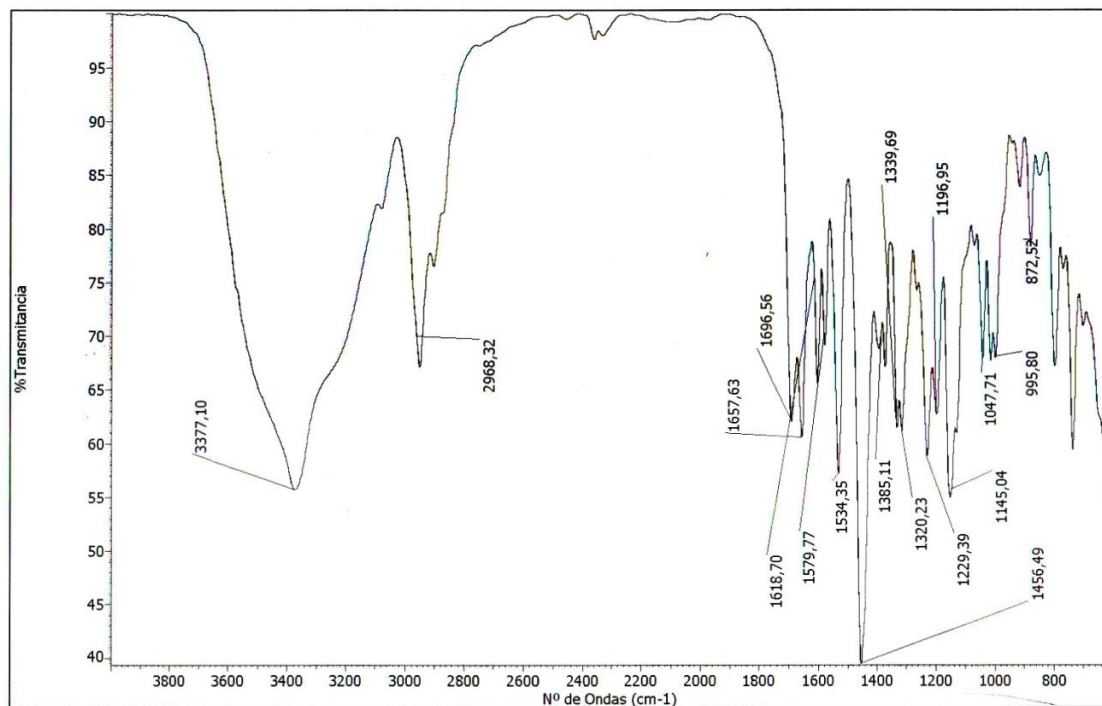
HMBC

14rnm-0027 Angel Reduccion
HMBC 50 ms

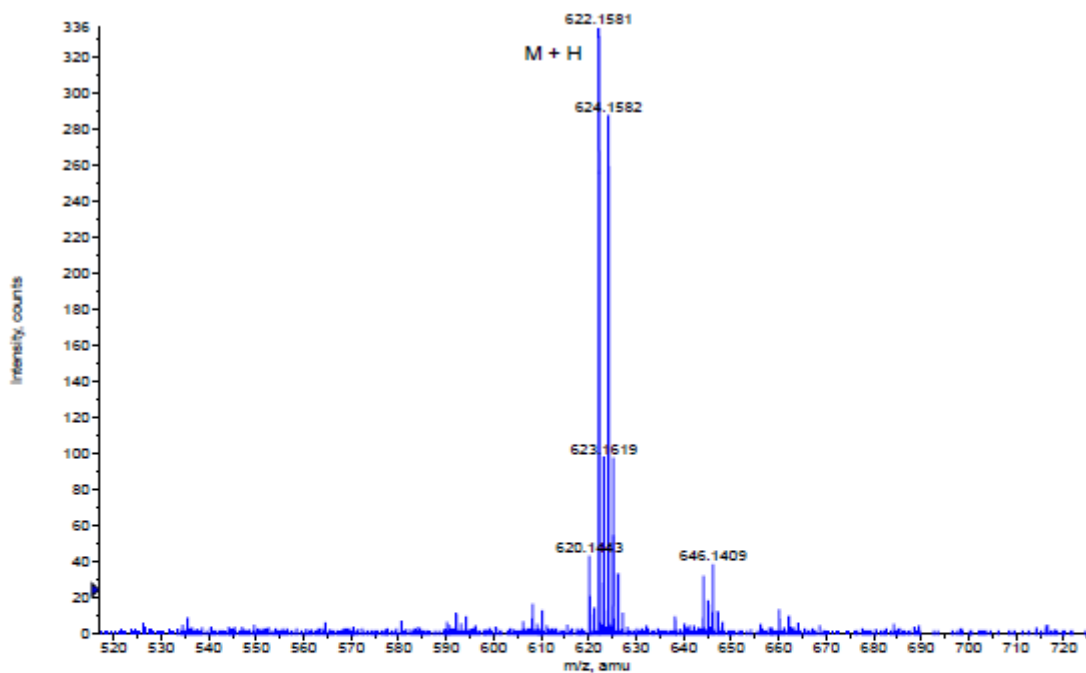
ROESY



IR

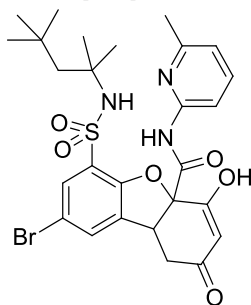


HRMS

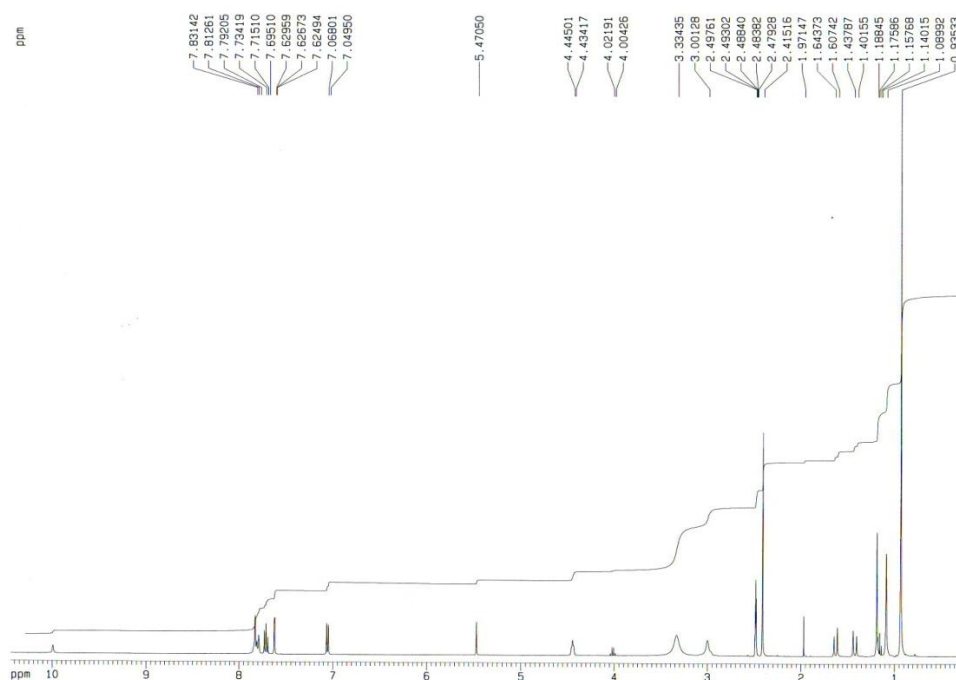


Formula	CalculatedMass	mDaError	ppmError	RDB
C28 H37 N3 O6 S Br	622.158096	0.004336	0.006969	11.5
C31 H38 N3 O4 Na S Br	622.159713	-1.613108	-2.59276	12.5
C26 H38 N3 O6 Na S Br	622.15569	2.409596	3.872961	8.5
C32 H34 N5 Na S Br	622.16105	-2.95042	-4.742231	17.5
C19 H42 N3 O11 Na S Br	622.161564	-3.463764	-5.567332	-0.5
C33 H37 N3 O4 S Br	622.162118	-4.018368	-6.458751	15.5
C23 H37 N5 O8 S Br	622.154073	4.02704	6.47269	7.5
C34 H33 N5 S Br	622.163456	-5.35568	-8.608222	20.5
C22 H41 N3 O12 S Br	622.152736	5.364352	8.622161	2.5
C21 H41 N3 O11 S Br	622.163969	-5.869024	-9.433324	2.5
C35 H33 N3 O S Br	622.152222	5.877696	9.447262	20.5

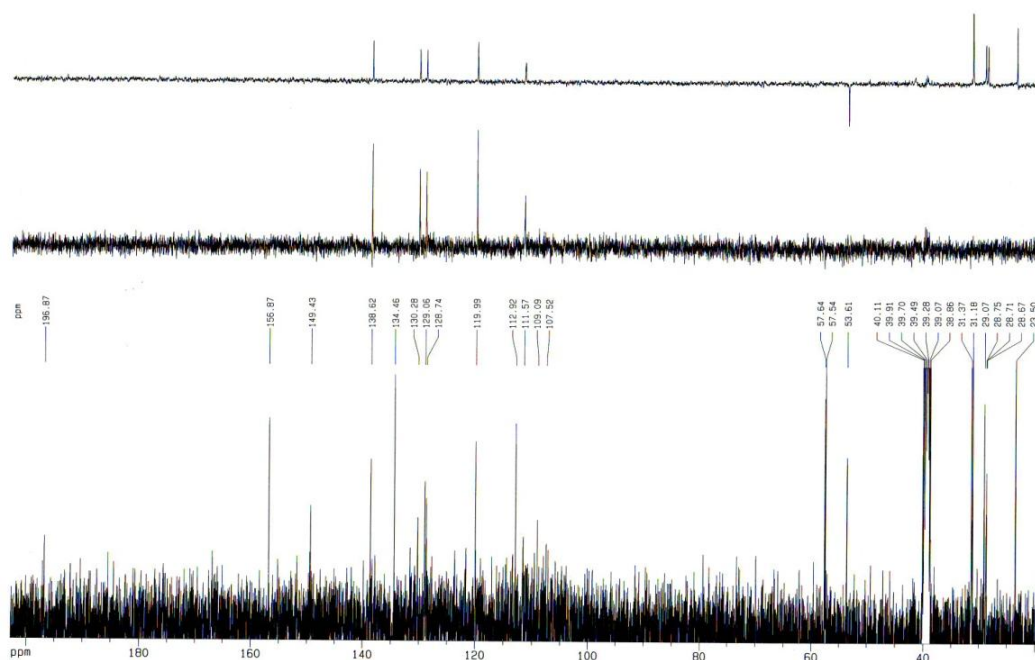
- 8-Bromo-4-hydroxy-*N*-(6-methylpyridin-2-yl)-2-oxo-6-(*N*-(2,4,4-trimethylpentan-2-yl)sulfamoyl)-1,2,4a,9b-tetrahydrodibenzo[*b,d*]furan-4a-carboxamide (147)



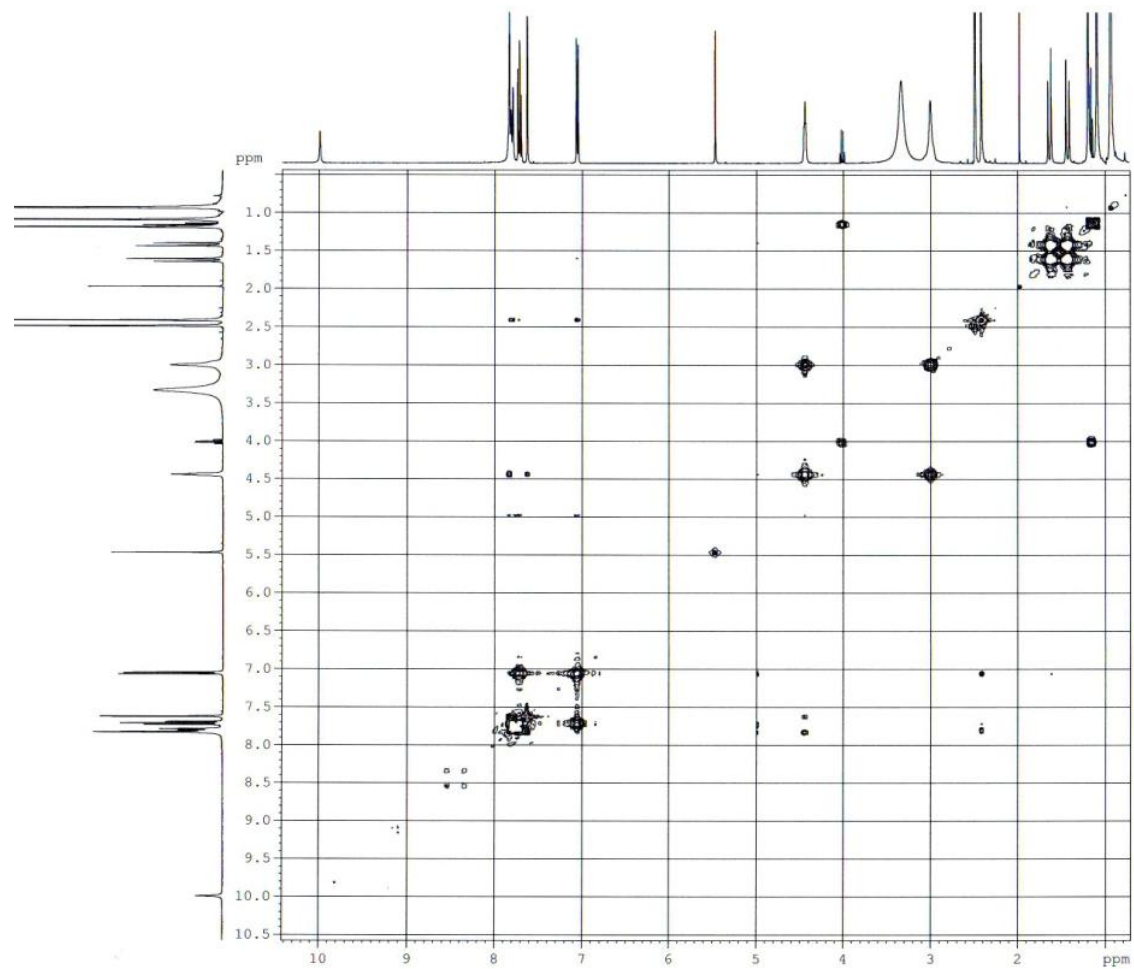
^1H NMR (DMSO- d_6 , 400 MHz)



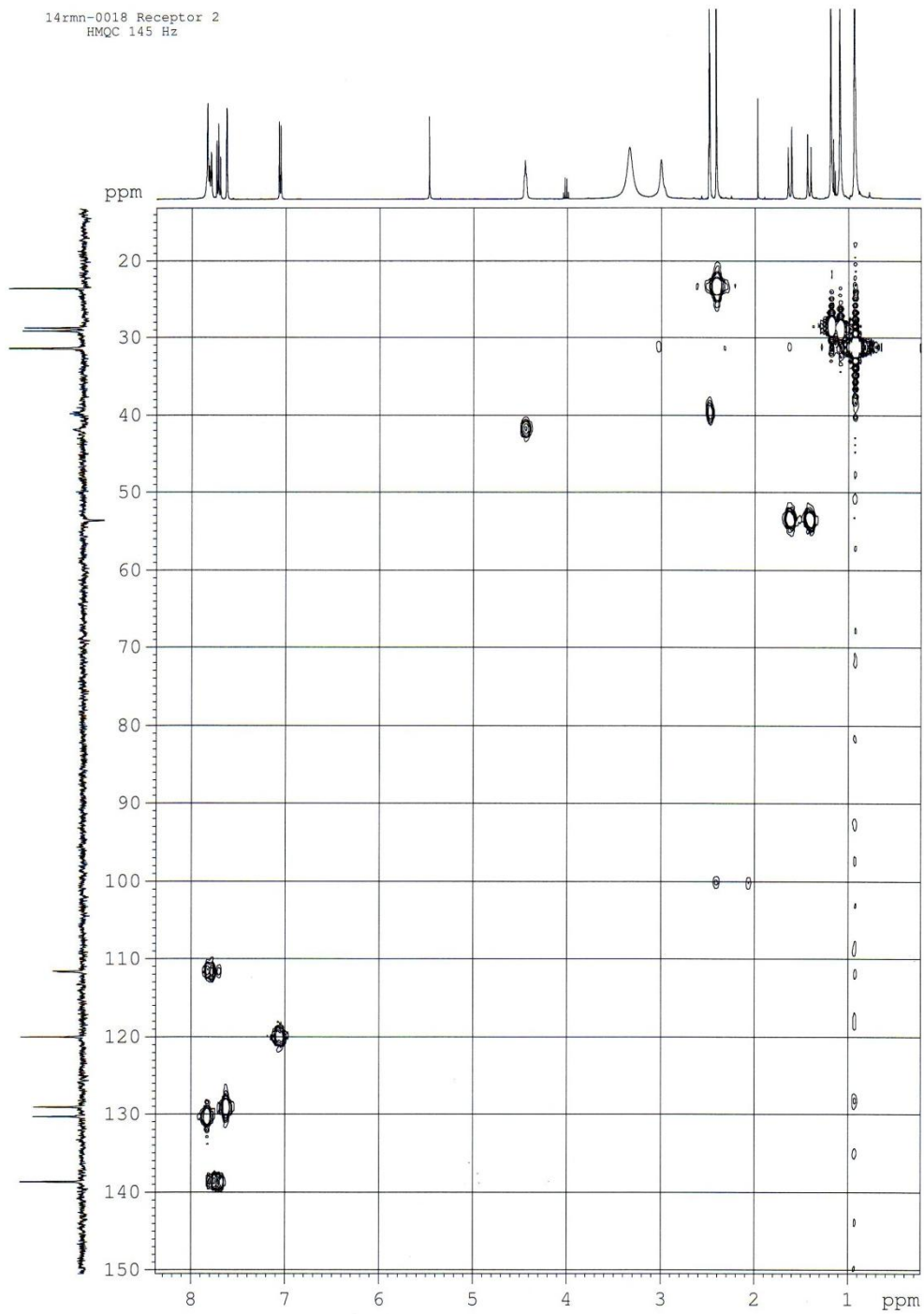
^{13}C NMR (DMSO- d_6 , 100 MHz)



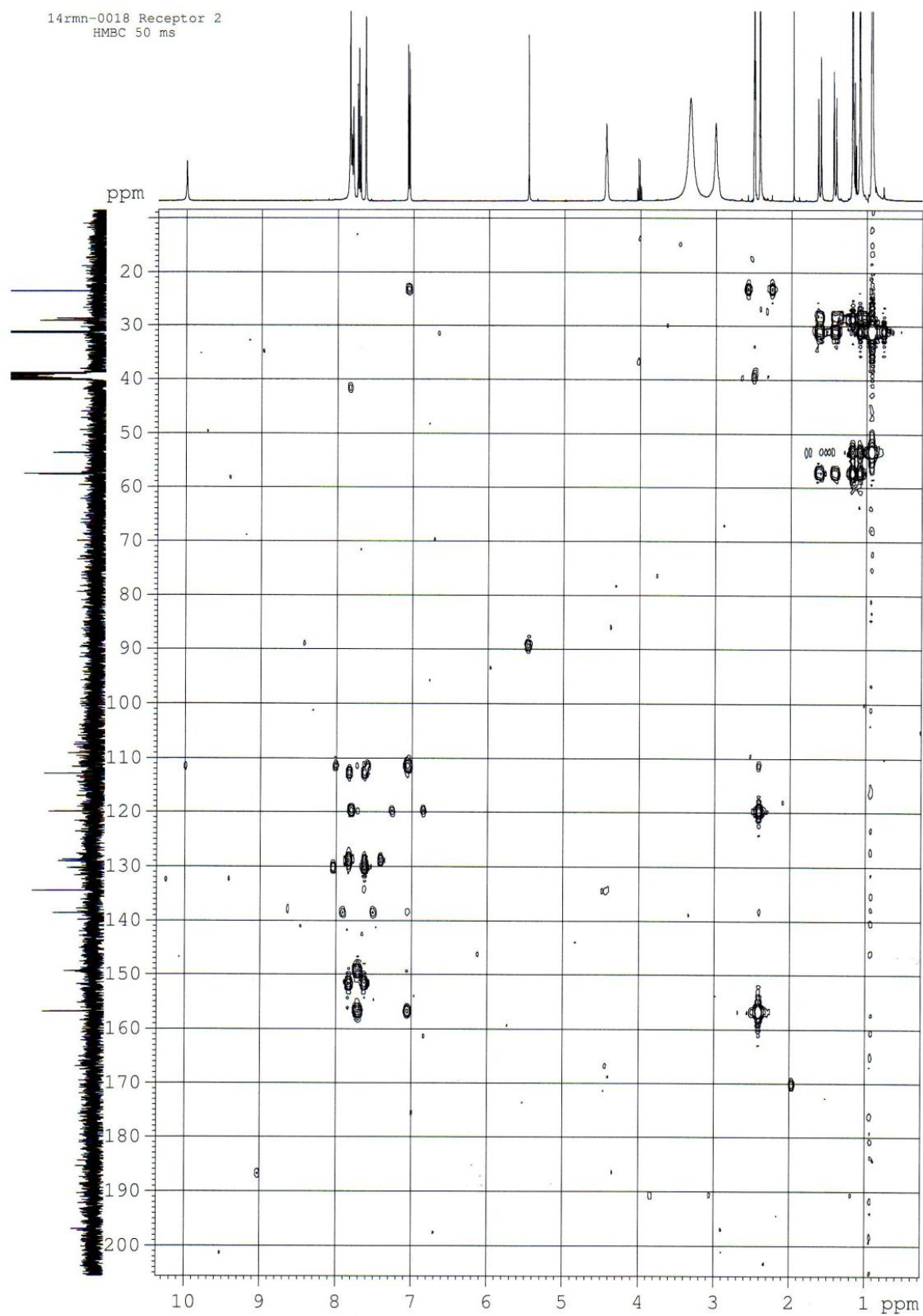
COSY



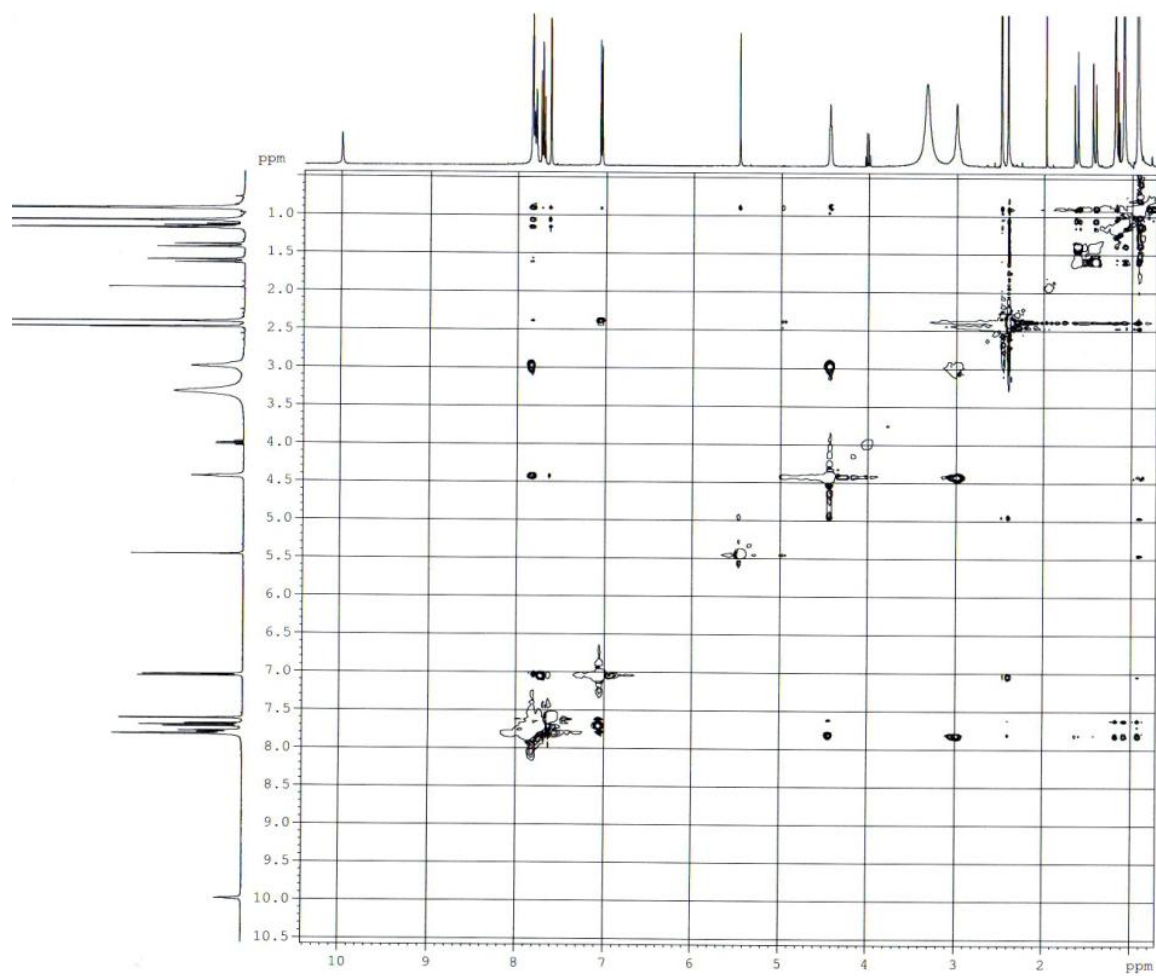
HMQC



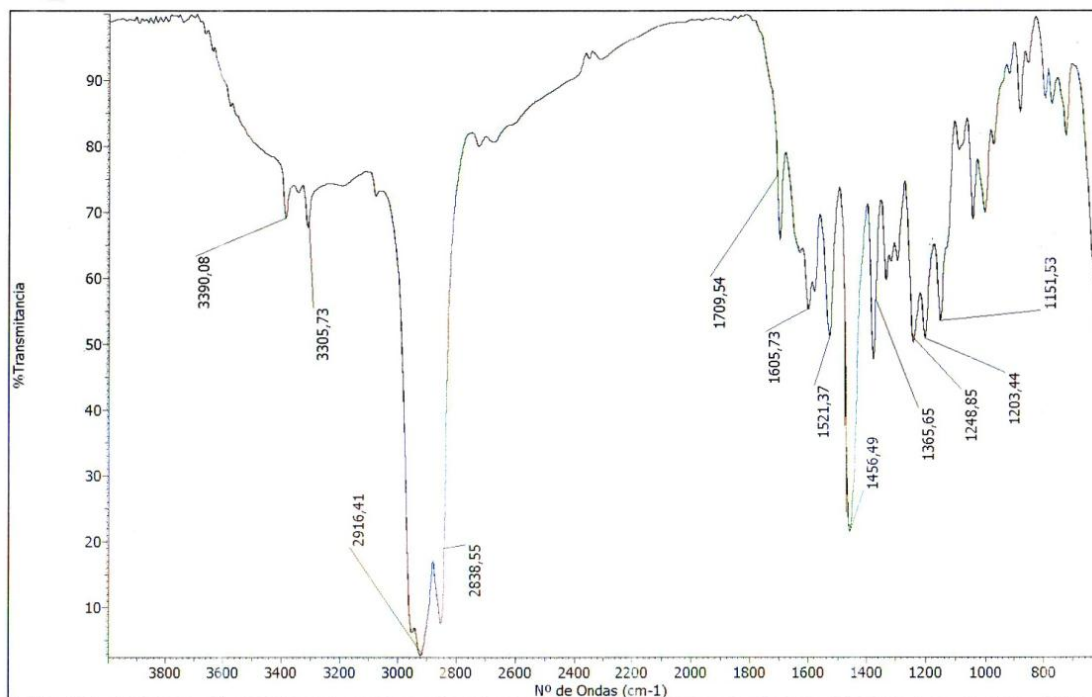
HMBC

14rnm-0018 Receptor 2
HMBC 50 ms

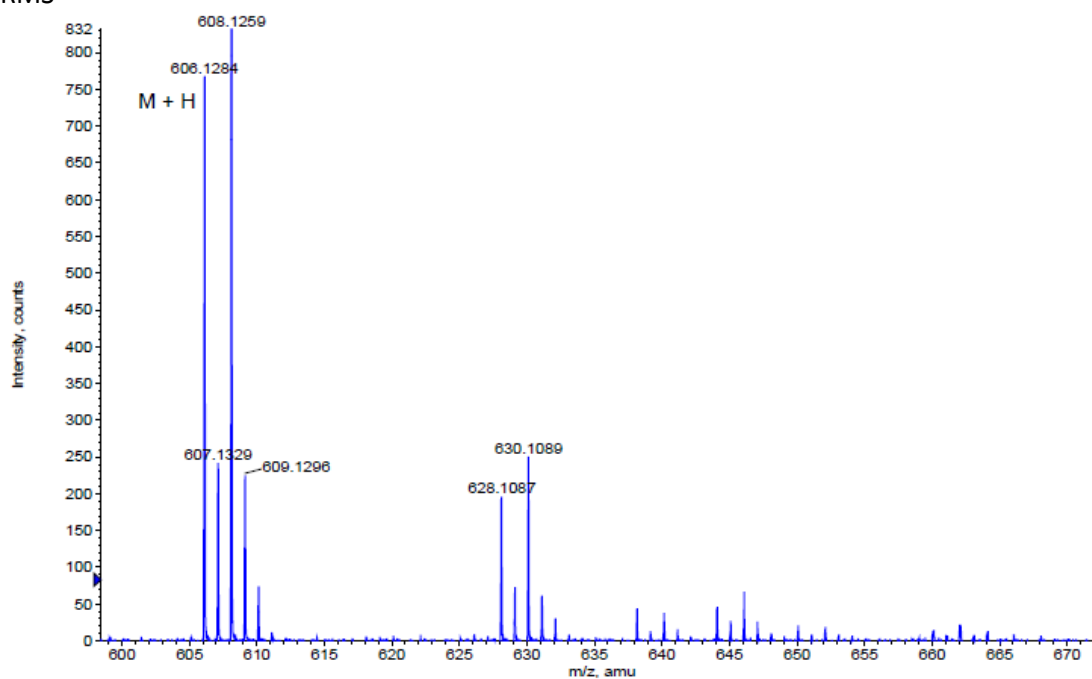
ROESY



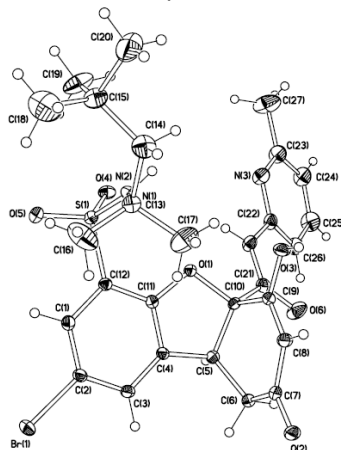
IR



HRMS

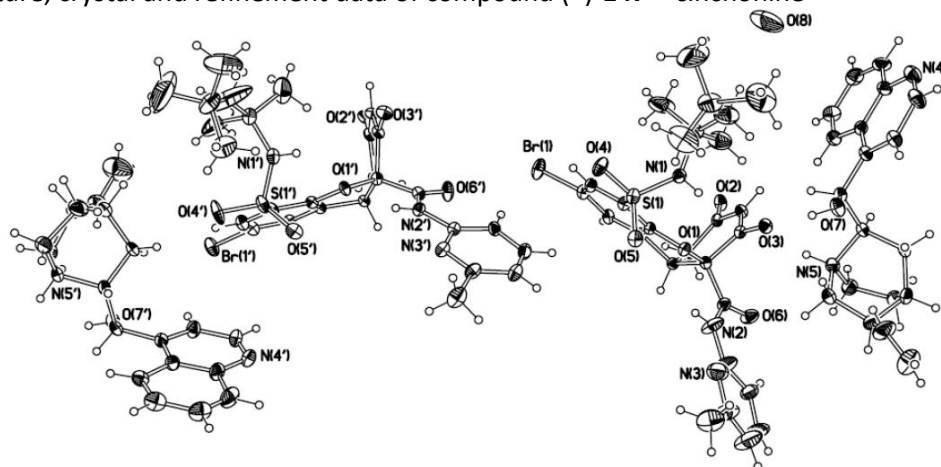


Formula	CalculatedMass	mDaError	ppmError	RDB
C30 H34 N O4 Na S Br	606.128413	-0.012948	-0.021362	13.5
C31 H30 N5 Na S Br	606.12975	-1.35026	-2.227678	18.5
C27 H33 N3 O6 S Br	606.126796	1.604496	2.64712	12.5
C32 H33 N O4 S Br	606.130818	-2.418208	-3.989593	16.5
C33 H29 N5 S Br	606.132156	-3.75552	-6.195909	21.5
C25 H34 N3 O6 Na S Br	606.12439	4.009756	6.615351	9.5
C22 H33 N5 O8 S Br	606.122773	5.6272	9.283833	8.5
C23 H38 N O9 Na S Br	606.134286	-5.886308	-9.711313	4.5

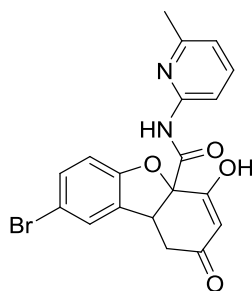
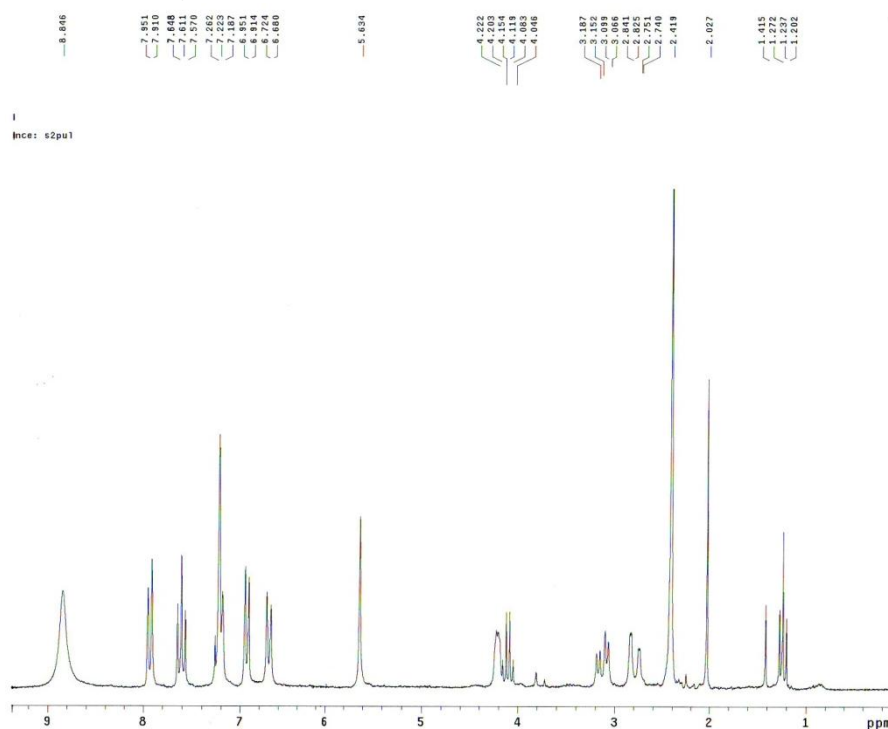
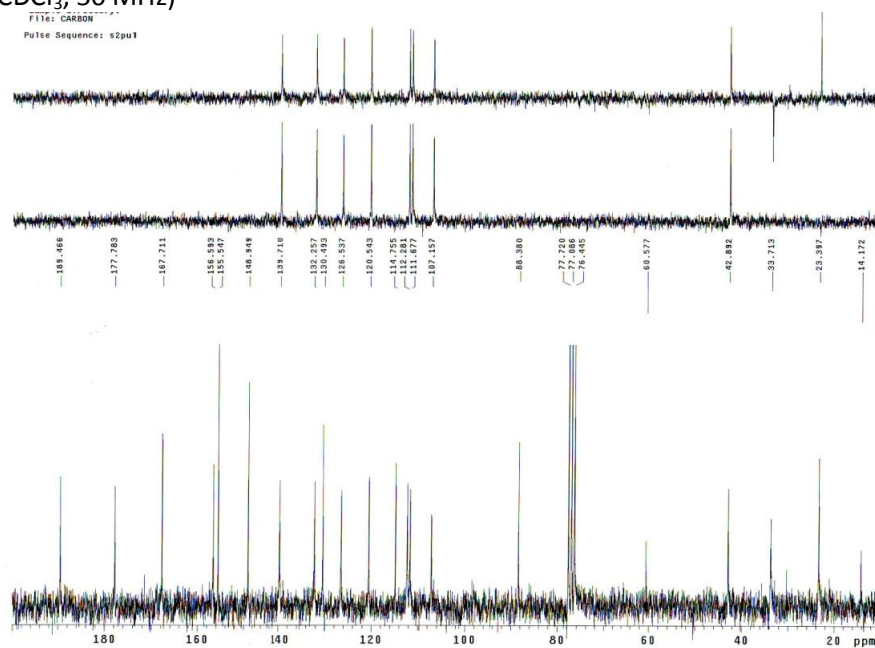
X-ray structure, crystal and refinement data of compound **147**

Empirical formula	$C_{27}H_{32}BrN_4O_5S$
Molecular weight	606.53
Temperature	298 (2) K
Wavelength	1.54178 Å
Crystal system, Space group	Monoclinic, $P2_1/n$
Unit cell dimensions	$a = 13.4851 (5) \text{ \AA}$ $\alpha = 90.00^\circ$ $b = 8.5343 (4) \text{ \AA}$ $\beta = 103.401(3)^\circ$ $c = 25.6709 (12) \text{ \AA}$ $\gamma = 90.00^\circ$
Volume	$2873.9(2) \text{ \AA}^3$
Z; Density (calculated)	4; 1.402 mg/m^3
Absorption coefficient	3.001 mm^{-1}
F(000)	1256
Crystal size	0.18 x 0.16 x 0.10 mm
θ range	$3.42 - 67.03^\circ$
Limiting indices h, k, l	$-15 \leq h \leq 15, -7 \leq k \leq 10, -29 \leq l \leq 29$
Reflections collected/independent	20440/4819 $R_{\text{int}} = 0.0491$
Refinement method	Least squares method with full matrix in F^2
Data/restraints/parameters	4819/0/350
Goodness-of-fit on F^2	1.034
Final R indices [$I > 2\sigma(I)$]	$R_1 = 0.0572, \omega R_2 = 0.1517$
R indices (all data)	$R_1 = 0.0718, \omega R_2 = 0.1635$
Largest difference peak and hole	1.063 and -0.837

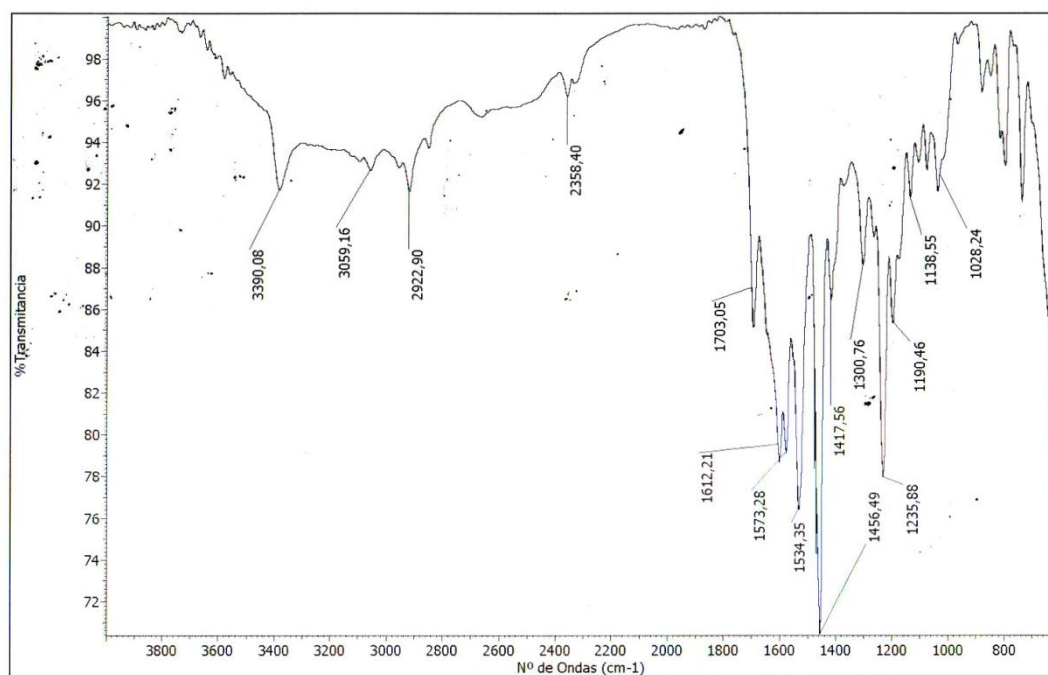
X-ray structure, crystal and refinement data of compound (+)-**147** + cinchonine



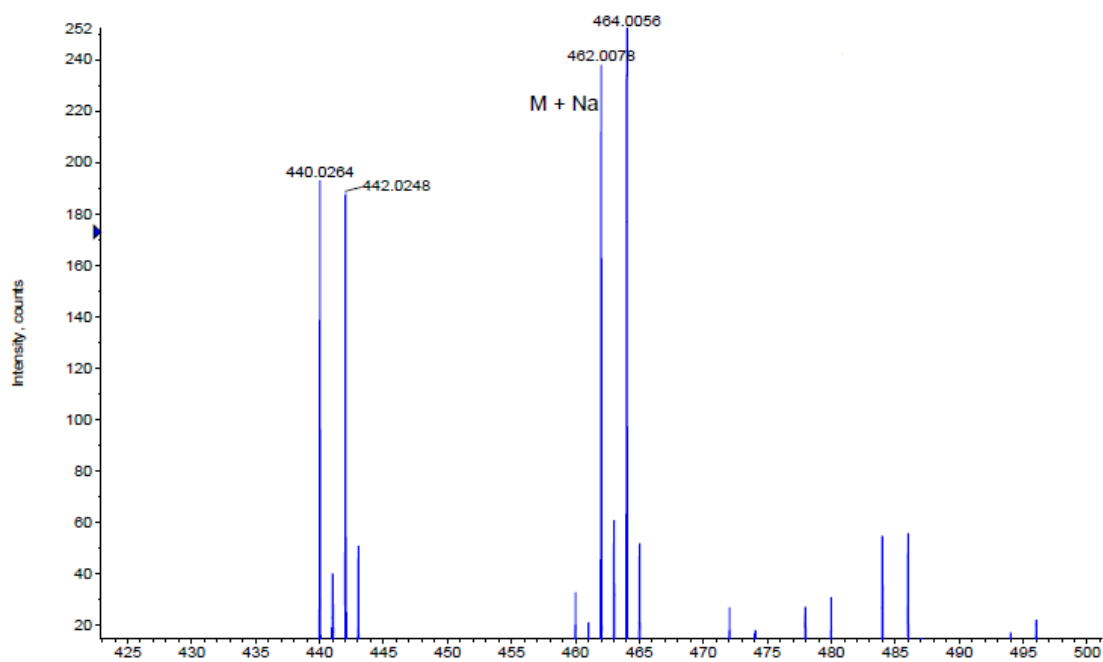
Empirical formula	$2(\text{C}_{27}\text{H}_{31}\text{BrN}_3\text{O}_6\text{S}), 2(\text{C}_{19}\text{H}_{23}\text{N}_2\text{O}), \text{O}$
Molecular weight	908.91
Temperature	298 (2) K
Wavelength	1.54178 Å
Crystal system, Space group	Monoclinic, $P2_1$
Unit cell dimensions	$a = 8.3467 (2) \text{ \AA}$ $\alpha = 90.00^\circ$ $b = 25.1787 (10) \text{ \AA}$ $\beta = 92.223 (3)^\circ$ $c = 22.2970 (8) \text{ \AA}$ $\gamma = 90.00^\circ$
Volume	$2226.0 (5) \text{ \AA}^3$
Z; Density (calculated)	4; 1.289 mg/m^3
Absorption coefficient	2.058 mm^{-1}
F(000)	1904
Crystal size	$0.12 \times 0.08 \times 0.06$
θ range	$1.98 - 67.48^\circ$
Limiting indices h, k, l	$-9 \leq h \leq 7, -27 \leq k \leq 29, -25 \leq l \leq 25$
Reflections collected/independent	38707/14076 $R_{\text{int}} = 0.0819$
Refinement method	Least squares method with full matrix in F^2
Data/restraints/parameters	14076/1/1105
Goodness-of-fit on F^2	1.029
Final R indices [$I > 2\sigma(I)$]	$R_1 = 0.0696, \omega R_2 = 0.1723$
R indices (all data)	$R_1 = 0.1013, \omega R_2 = 0.1966$
Largest difference peak and hole	0.936 and -0.493

- 8-Bromo-4-hydroxy-N-(6-methylpyridine-2-yl)-2-oxo-1,2,4a,9b-tetrahydrodibenzo[*b,d*]furan-4a-carboxamide (149)¹H NMR (CDCl₃, 200 MHz)¹³C NMR (CDCl₃, 50 MHz)

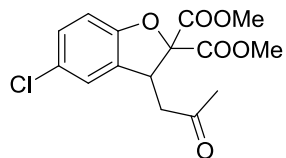
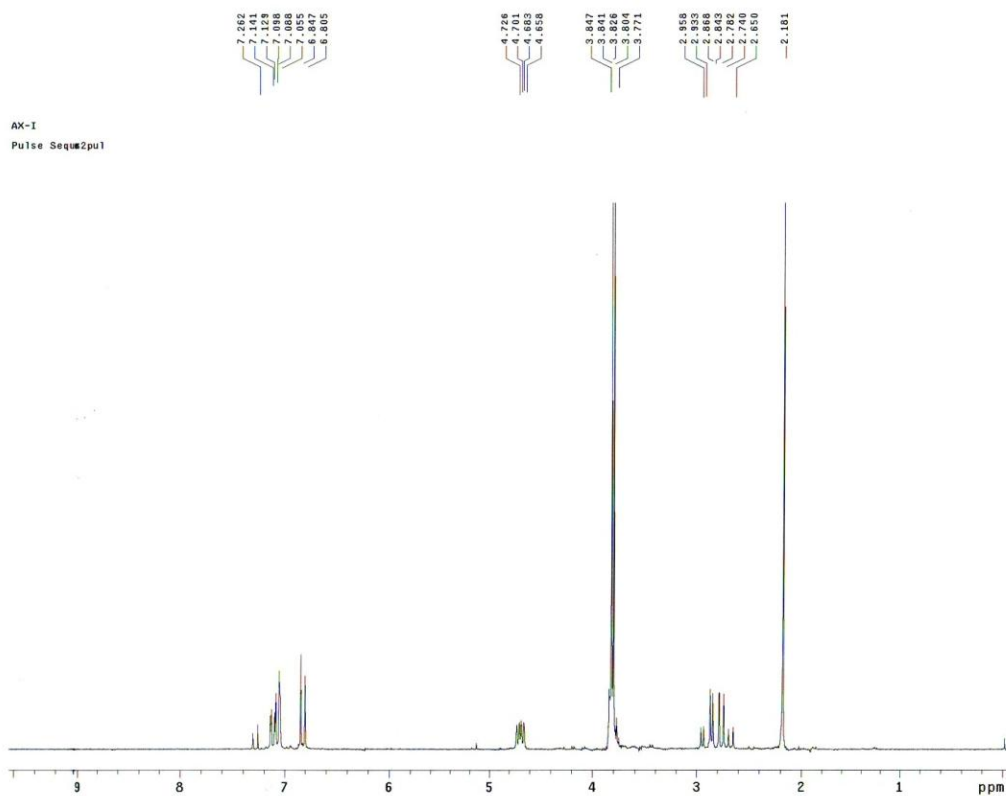
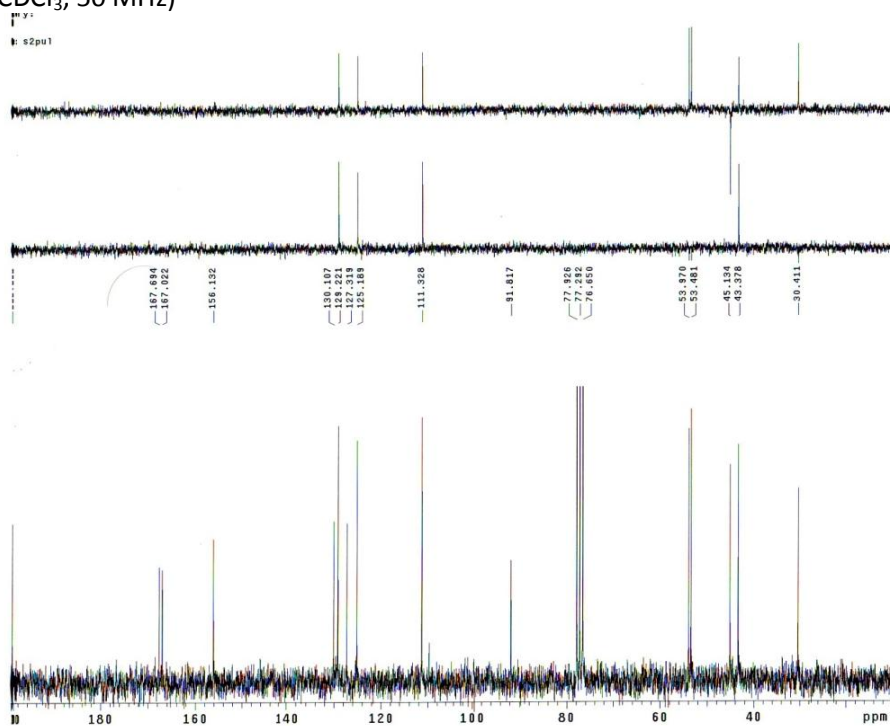
IR



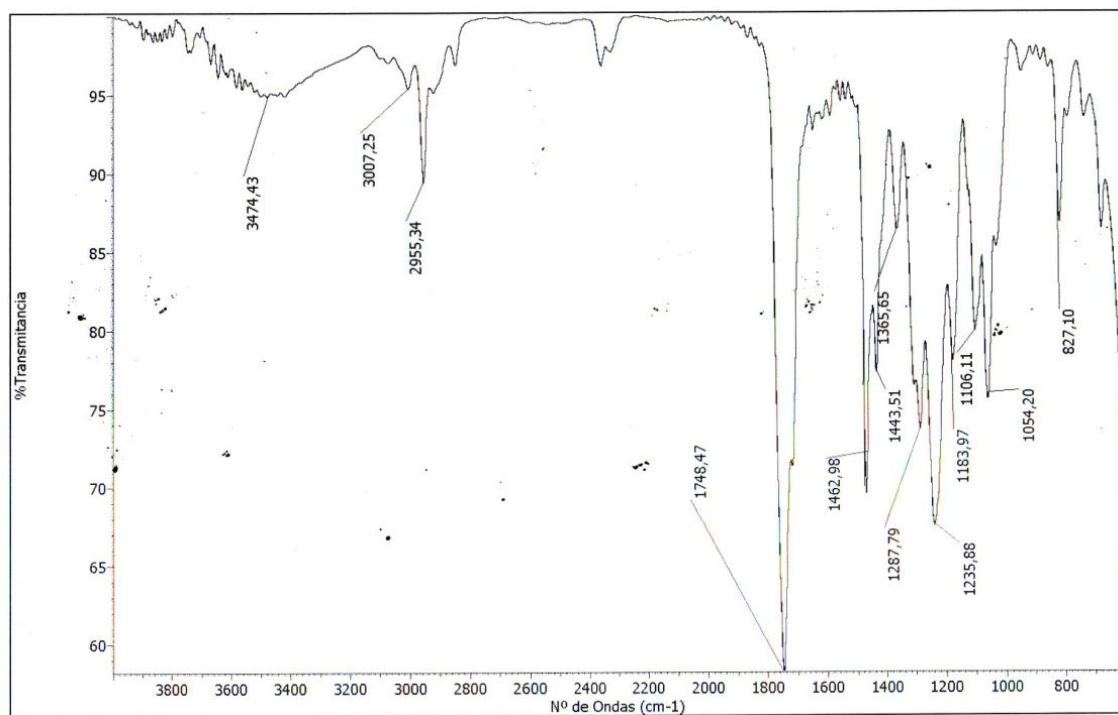
HRMS



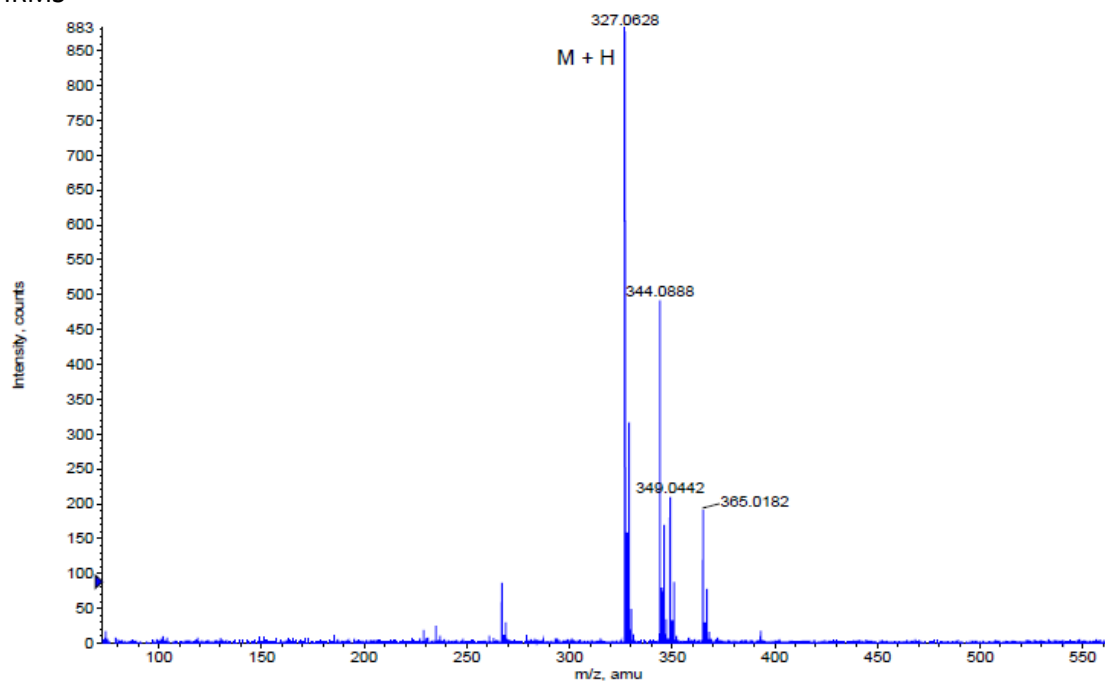
Formula	CalculatedMass	mDaError	ppmError	RDB
C22 H13 N3 O4 Br	462.008394	-0.593624	-1.284877	17.5
C20 H14 N3 O4 Na Br	462.005988	1.811636	3.921219	14.5
C25 H14 N O2 Na Br	462.010011	-2.211068	-4.785775	18.5
C17 H13 N5 O6 Br	462.004371	3.42908	7.422117	13.5
C13 H18 N3 O9 Na Br	462.011862	-4.061724	-8.791452	5.5
C27 H13 N O2 Br	462.012416	-4.616328	-9.991871	21.5

- 5-Chloro-3-(2-oxopropyl)-benzofuran-2,2(3H)-dicarboxylate (159)¹H NMR (CDCl₃, 200 MHz)¹³C NMR (CDCl₃, 50 MHz)

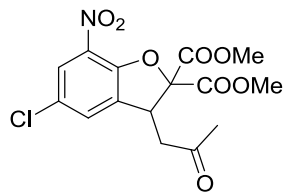
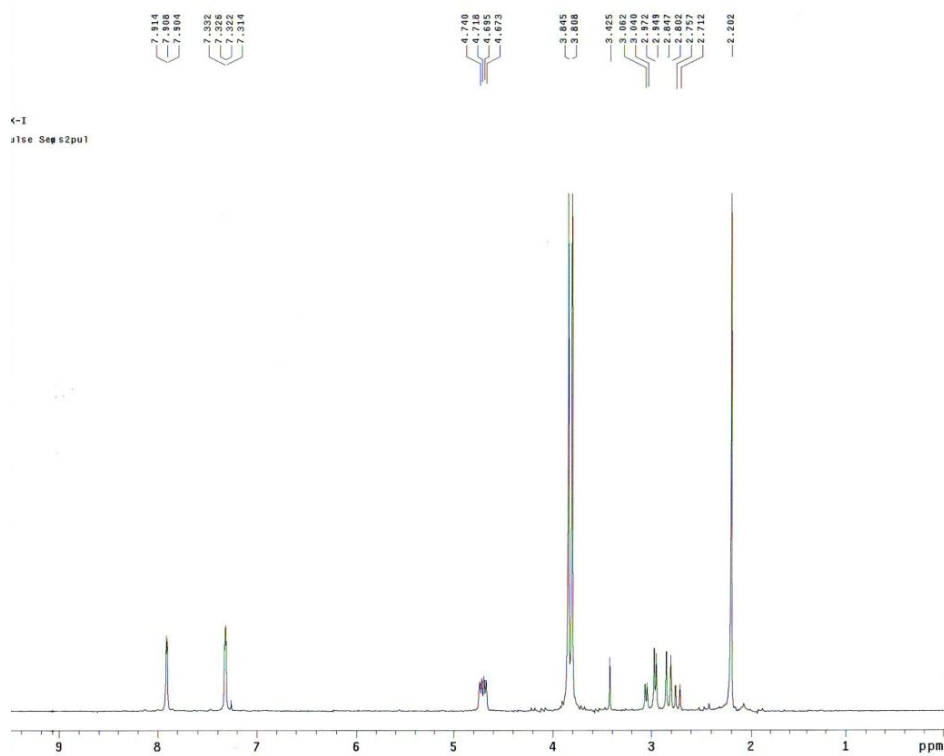
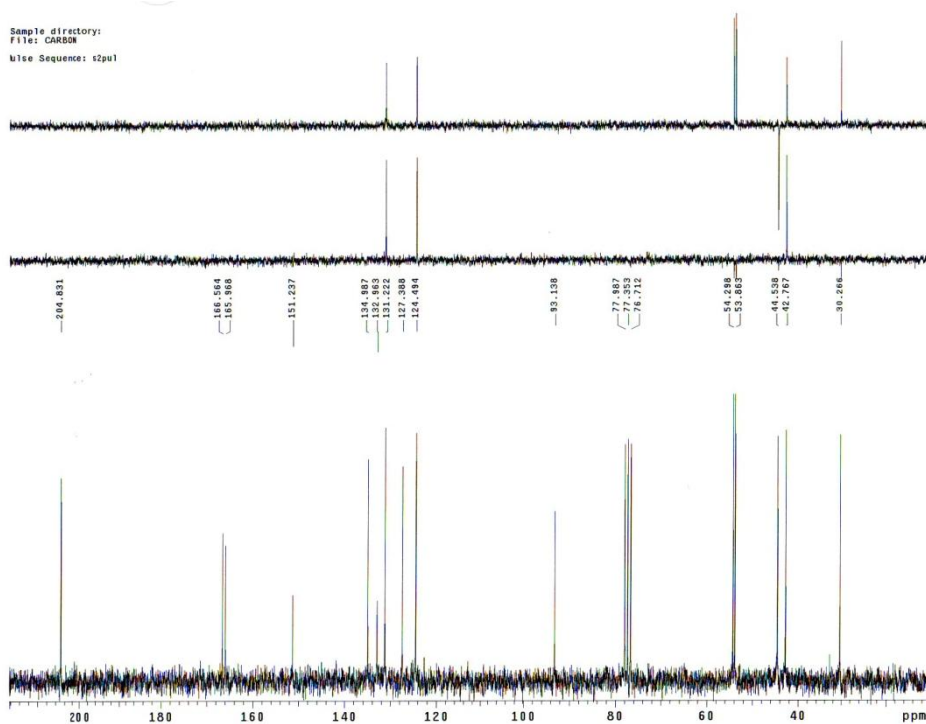
IR



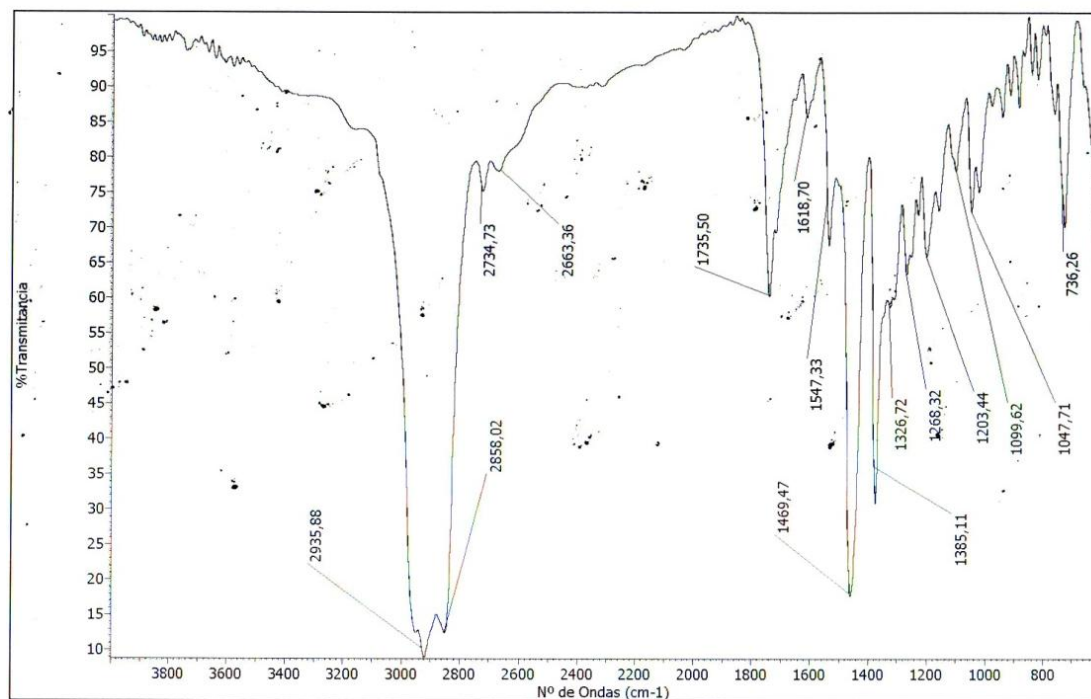
HRMS



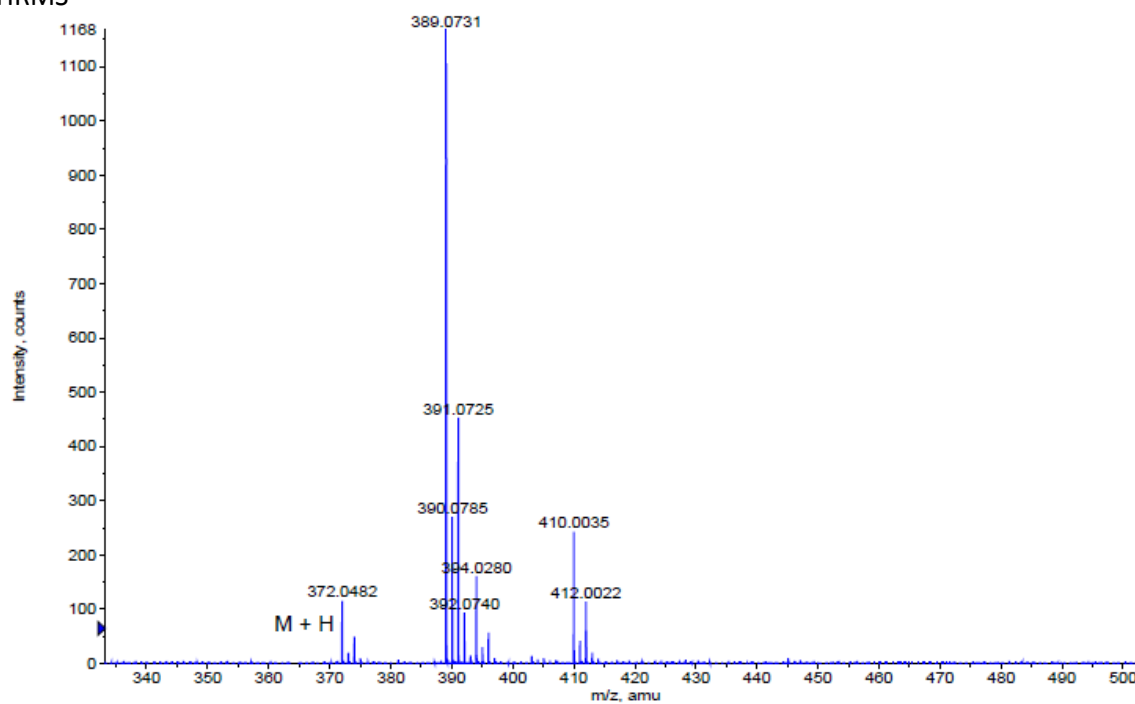
Formula	CalculatedMass	mDaError	ppmError	RDB
C ₁₅ H ₁₆ O ₆ Cl	327.062993	-0.192629	-0.588965	7.5
C ₁₄ H ₁₃ N ₄ O ₂ Na Cl	327.061925	0.875319	2.676298	9.5
C ₁₆ H ₁₂ N ₄ O ₂ Cl	327.06433	-1.529941	-4.677812	12.5
C ₁₃ H ₁₇ O ₆ Na Cl	327.060587	2.212631	6.765145	4.5
C ₁₉ H ₁₃ N ₂ Na Cl	327.065947	-3.147385	-9.623166	13.5

- 5-Chloro-7-nitro-3-(2-oxopropyl) benzofuran-2,2(3H)-dicarboxylate (160)¹H NMR (CDCl₃, 200 MHz)¹³C NMR (CDCl₃, 50 MHz)

IR

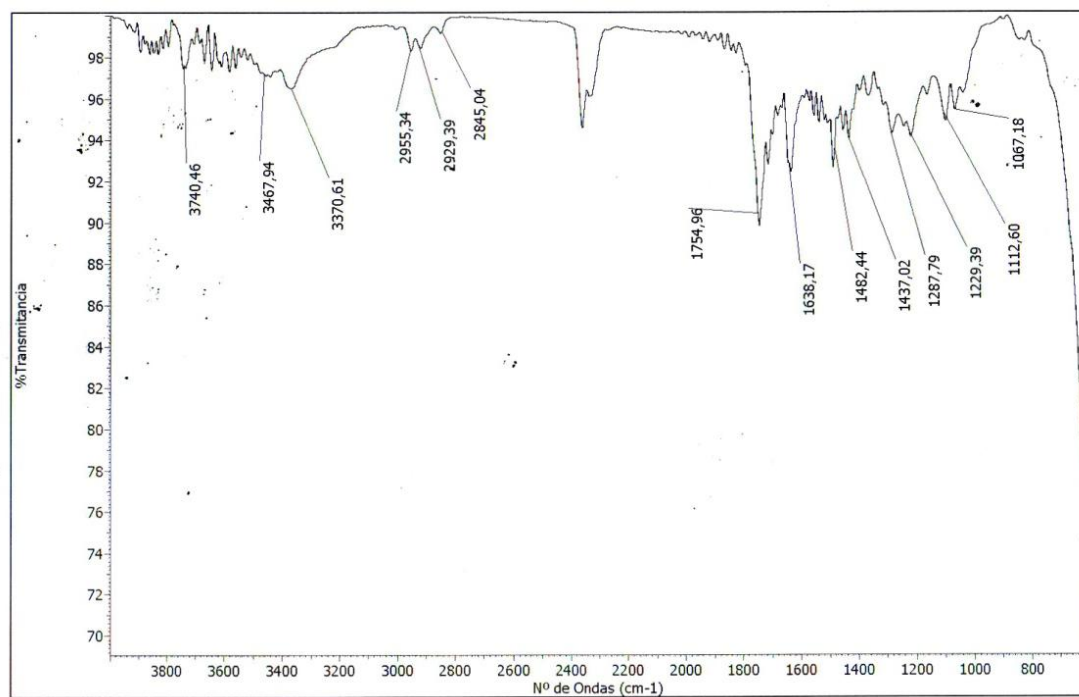


HRMS

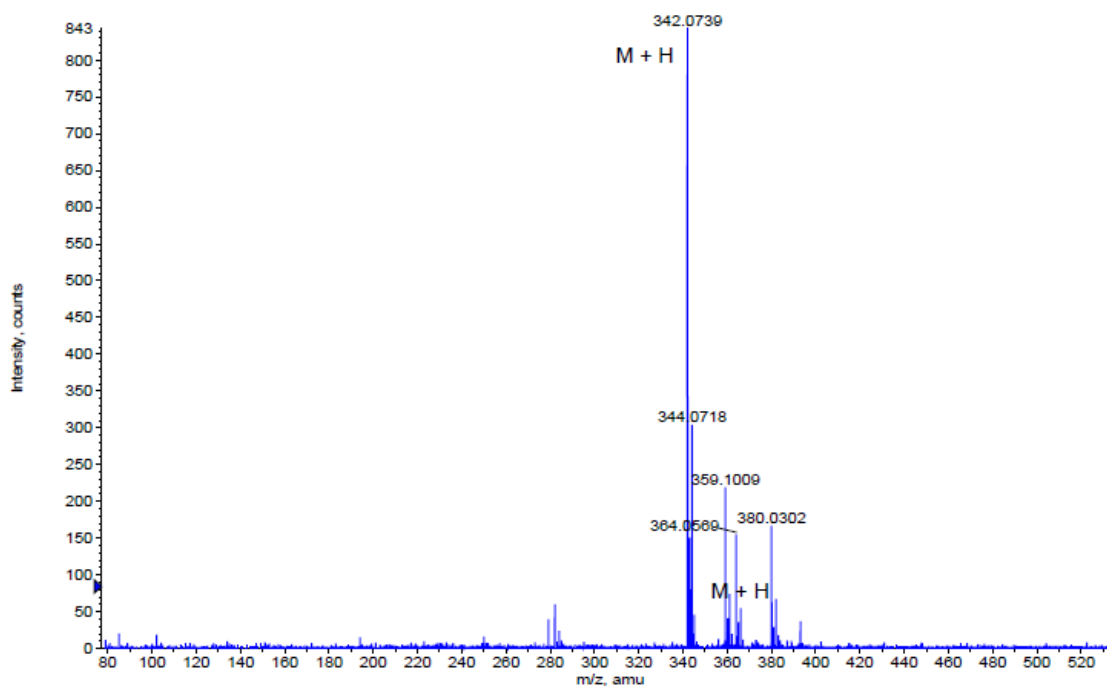


Formula	CalculatedMass	mDaError	ppmError	RDB
C ₁₅ H ₁₅ N ₀ O ₈ Cl	372.048071	0.129123	0.347059	8.5
C ₁₄ H ₁₂ N ₅ O ₄ NaCl	372.047003	1.197071	3.217511	10.5
C ₁₆ H ₁₁ N ₅ O ₄ Cl	372.049408	-1.208189	-3.247394	13.5
C ₁₃ H ₁₆ N ₀ O ₈ NaCl	372.045666	2.534383	6.811965	5.5
C ₁₉ H ₁₂ N ₃ O ₂ NaCl	372.051026	-2.825633	-7.594792	14.5

IR

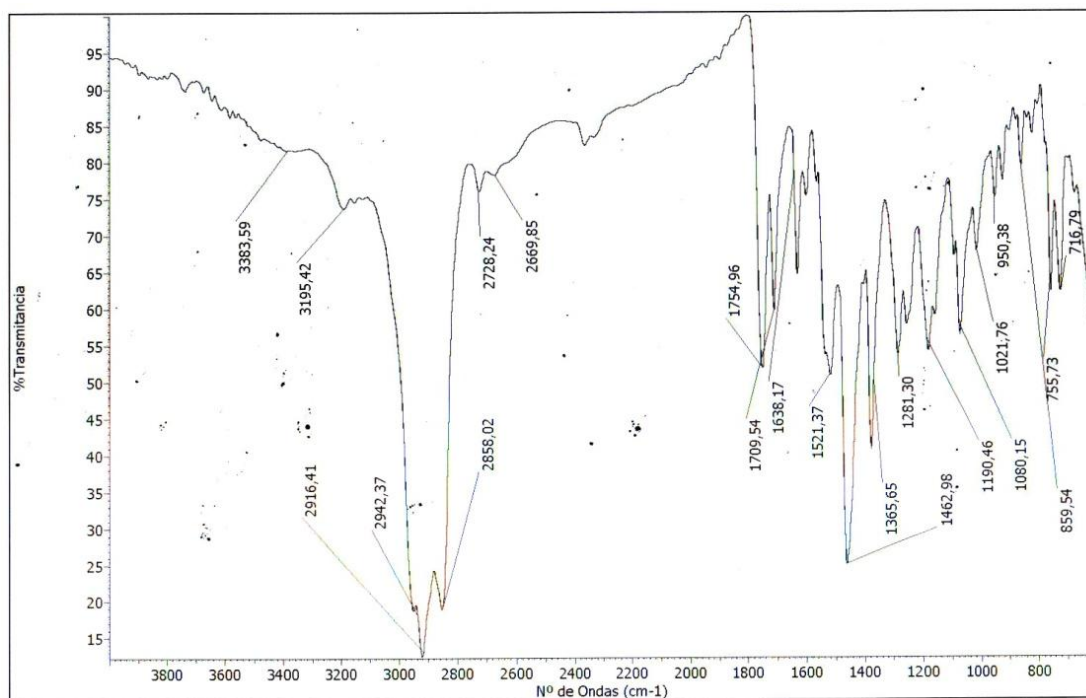


HRMS

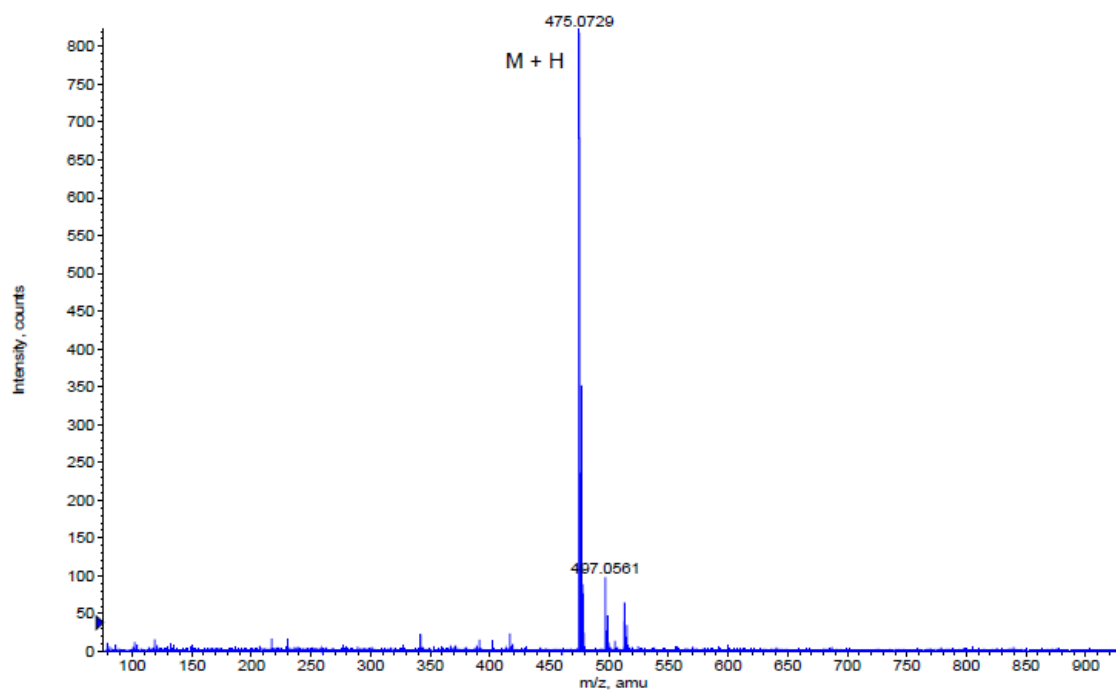


Formula	CalculatedMass	mDaError	ppmError	RDB
C ₁₅ H ₁₇ N ₁ O ₆ Cl	342.073892	0.008323	0.024331	7.5
C ₁₄ H ₁₄ N ₅ O ₂ NaCl	342.072824	1.076271	3.146306	9.5
C ₁₆ H ₁₃ N ₅ O ₂ Cl	342.075229	-1.328989	-3.885087	12.5
C ₁₃ H ₁₈ N ₁ O ₆ NaCl	342.071486	2.413583	7.055724	4.5
C ₁₉ H ₁₄ N ₃ NaCl	342.076846	-2.946433	-8.613426	13.5

IR

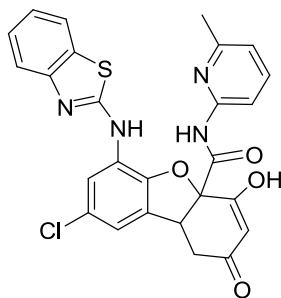


HRMS

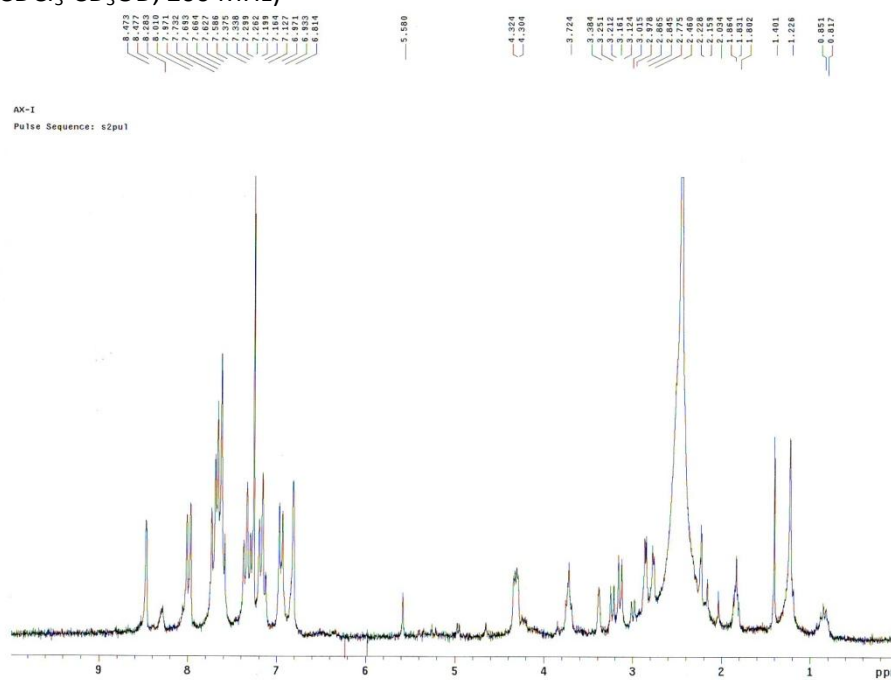


Formula	CalculatedMass	mDaError	ppmError	RDB
C22 H20 N2 O6 S Cl	475.072513	0.387395	0.815442	13.5
C25 H21 O4 Na S Cl	475.07413	-1.230049	-2.589176	14.5
C10 H24 N4 O13 S Cl	475.074363	-1.463261	-3.080073	0.5
C26 H17 N4 Na S Cl	475.075467	-2.567361	-5.404135	19.5
C20 H21 N2 O6 Na S Cl	475.070107	2.792655	5.878365	10.5
C13 H25 N2 O11 Na S Cl	475.075981	-3.080705	-6.484692	1.5
C27 H20 O4 S Cl	475.076535	-3.635309	-7.652099	17.5
C17 H20 N4 O8 S Cl	475.06849	4.410099	9.282984	9.5

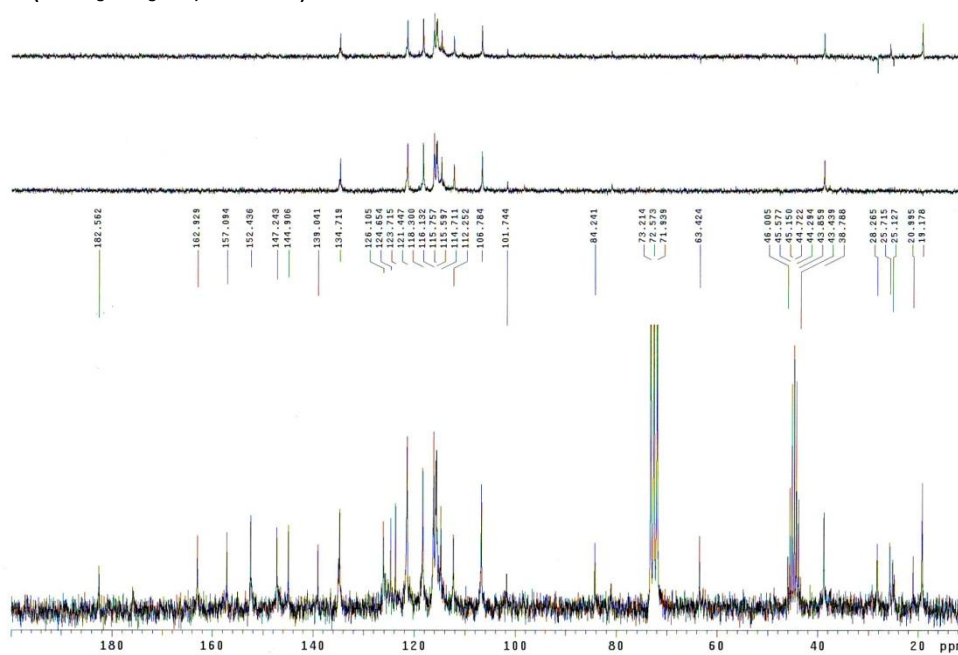
- 6-(Benzo[d]thiazol-2-ylamino)-8-chloro-4-hydroxy-N-(6-methylpyridin-2-yl)-2-oxo-1,2,4a,9b-tetrahydrobenzo[b,d]furan-4a-carboxamide (166)



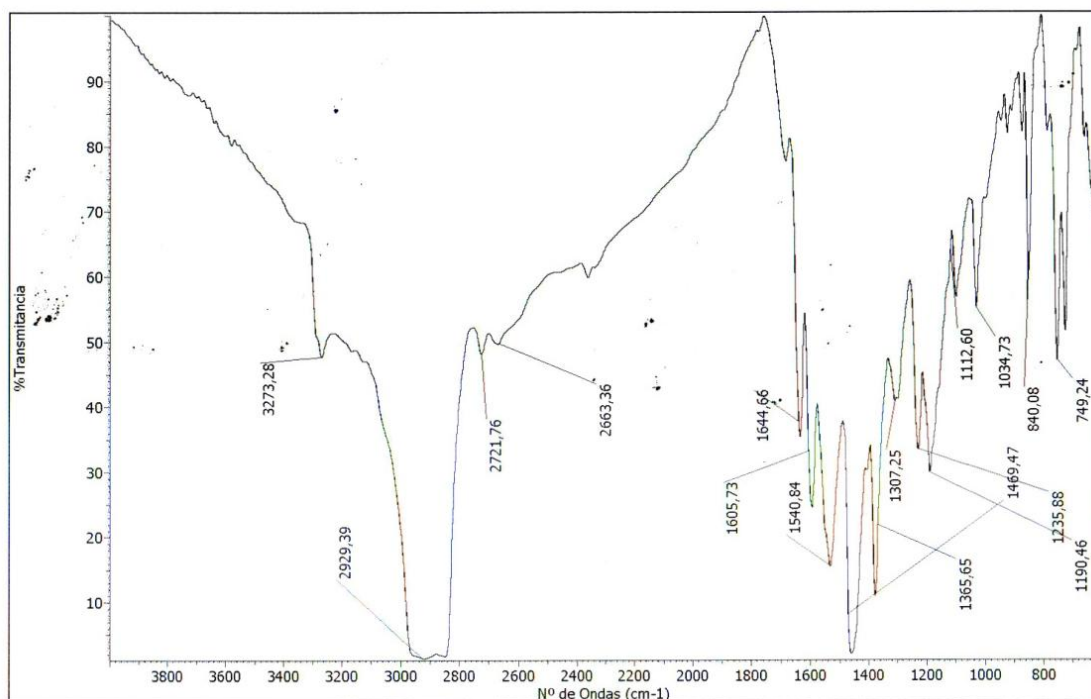
^1H NMR ($\text{CDCl}_3\text{-CD}_3\text{OD}$, 200 MHz)



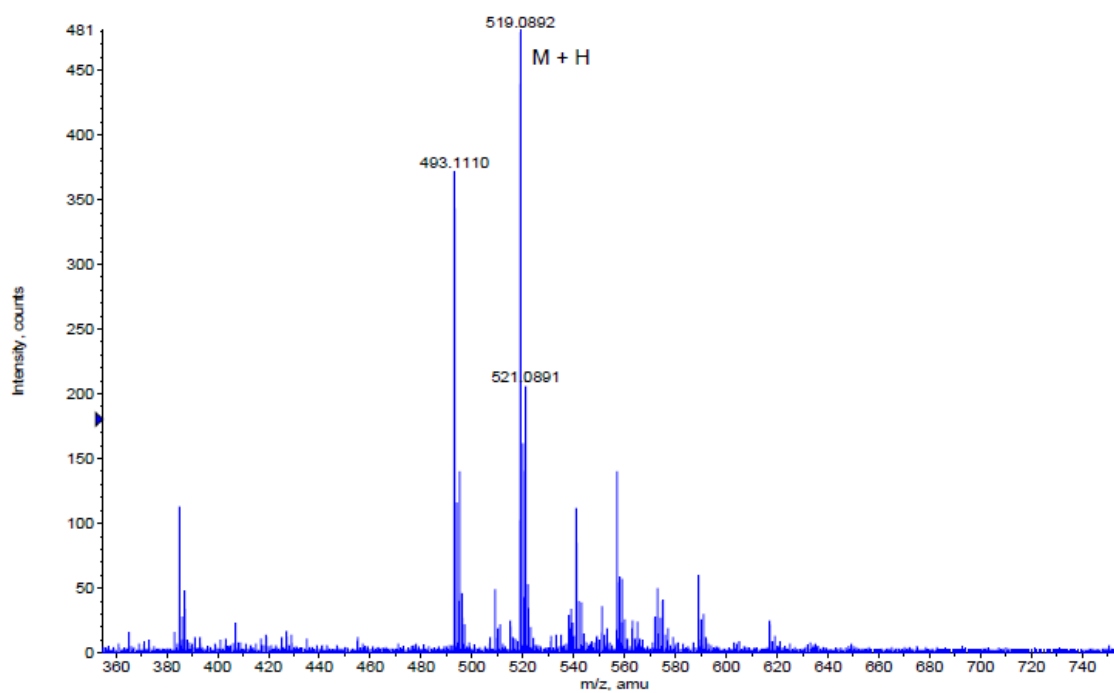
^{13}C NMR ($\text{CDCl}_3\text{-CD}_3\text{OD}$, 50 MHz)



IR

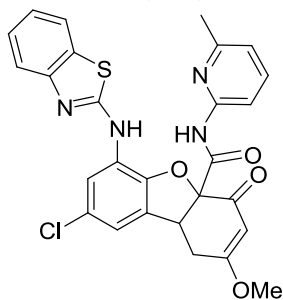


HRMS

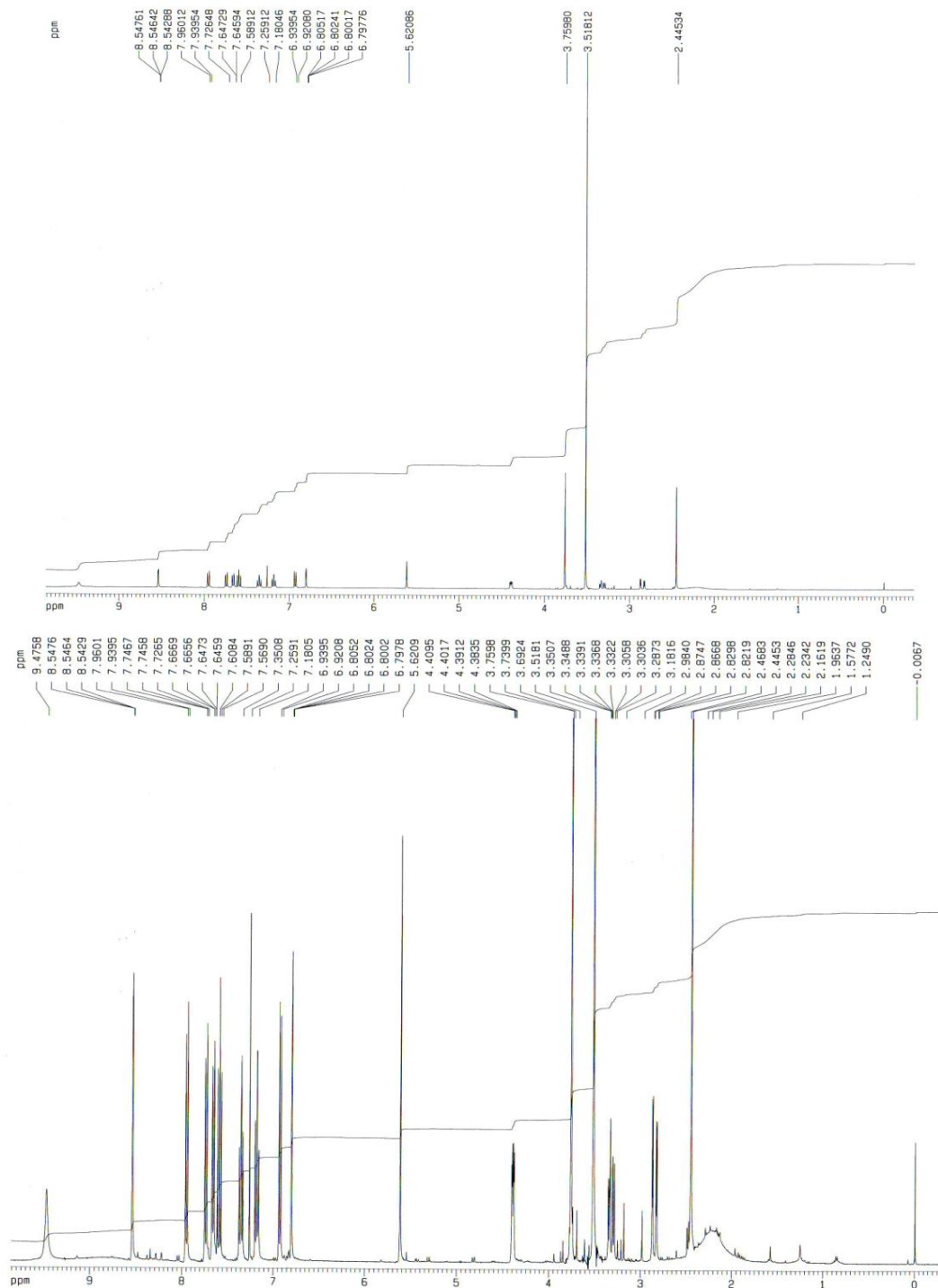


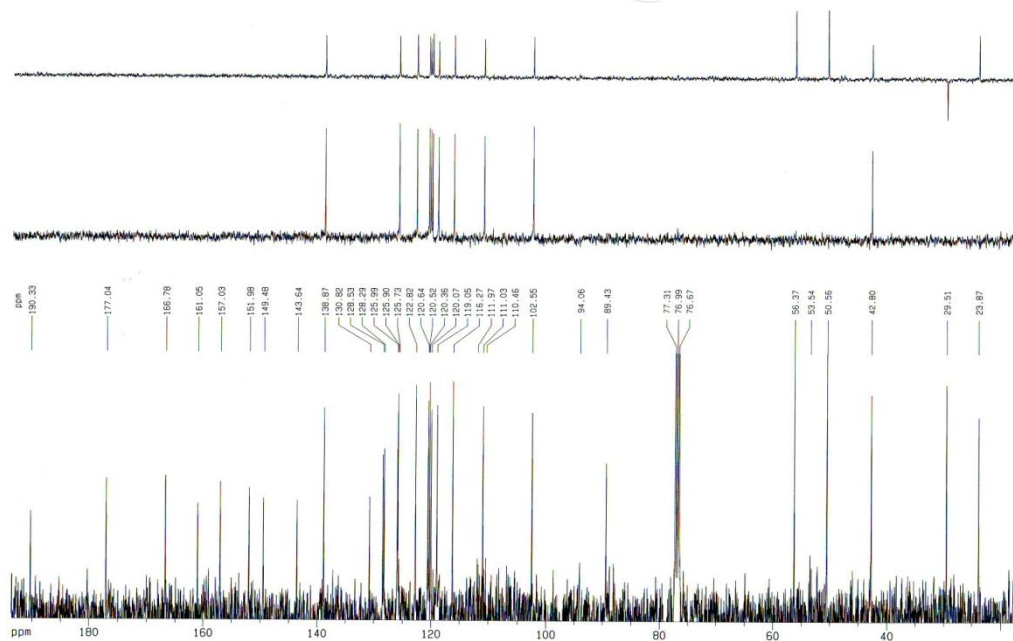
Formula	CalculatedMass	mDaError	ppmError	RDB
C ₂₆ H ₂₀ N ₄ O ₄ S Cl	519.088831	0.368659	0.710203	18.5
C ₂₉ H ₂₁ N ₂ O ₂ Na S Cl	519.090449	-1.248785	-2.405721	19.5
C ₂₅ H ₂₄ O ₈ S Cl	519.087494	1.705971	3.286466	13.5
C ₂₄ H ₂₁ N ₄ O ₄ Na S Cl	519.086426	2.773919	5.343814	15.5
C ₁₇ H ₂₅ N ₄ O ₉ Na S Cl	519.092299	-3.099441	-5.970915	6.5
C ₃₁ H ₂₀ N ₂ O ₂ S Cl	519.092854	-3.654045	-7.039332	22.5
C ₂₃ H ₂₅ O ₈ Na S Cl	519.085089	4.111231	7.920077	10.5

- 6-(Benzo[d]thiazol-2-ylamino)-8-chloro-2-methoxy-N-(6-methylpyridin-2-yl)-4-oxo-1,4,4a,9b-tetrahydrobenzo[b,d]furan-4a-carboxamide (169)

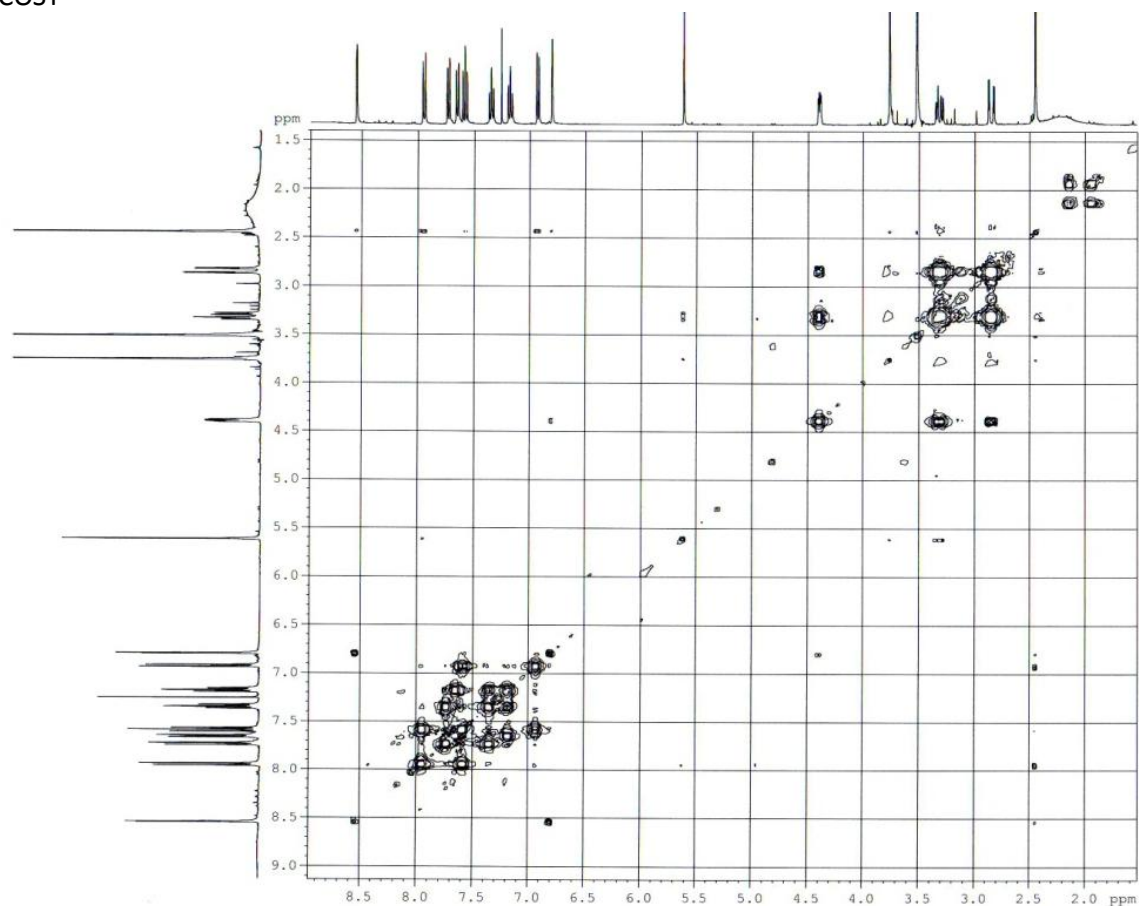


^1H NMR (CDCl_3 , 400 MHz)

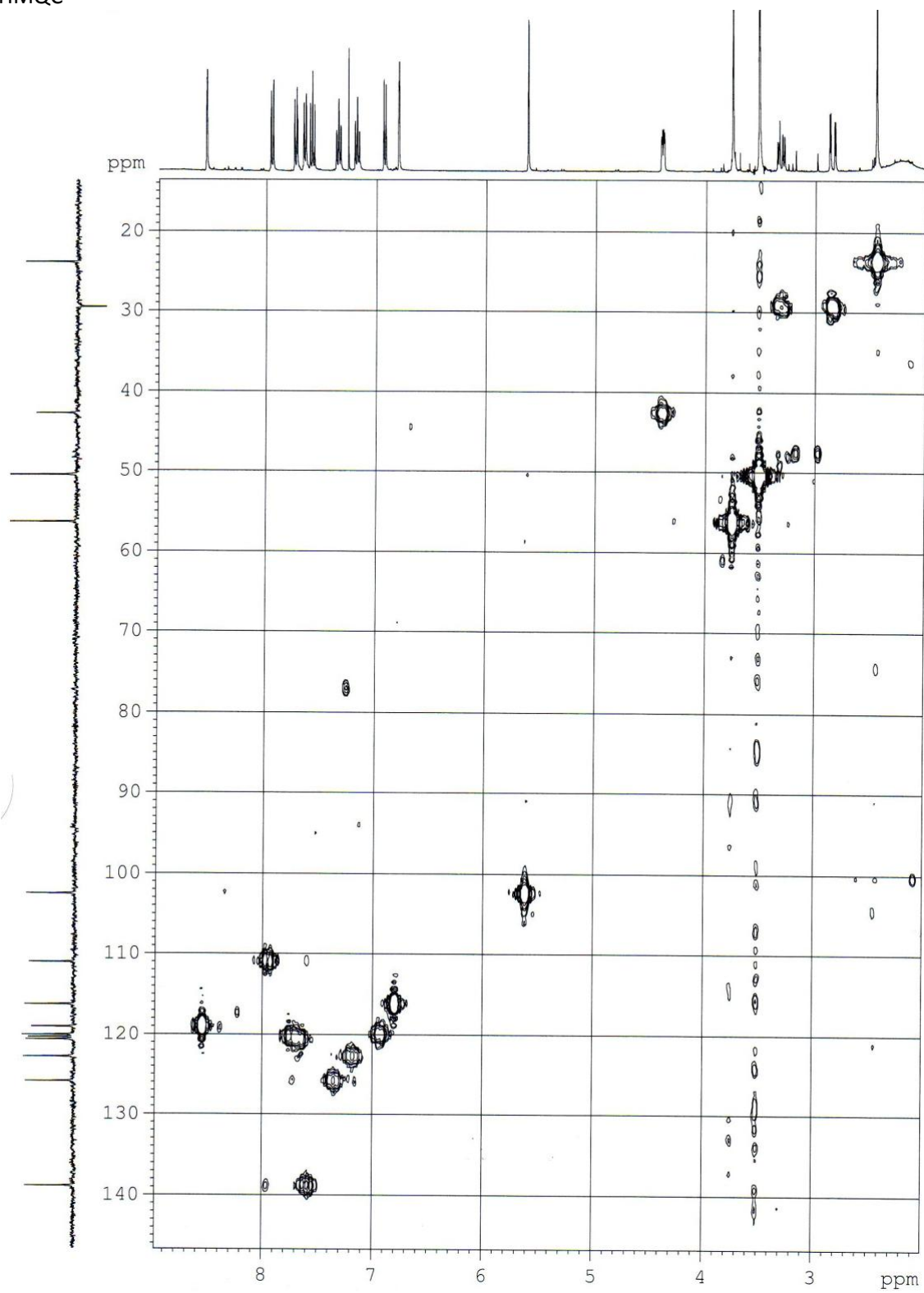


^{13}C NMR (CDCl_3 , 100 MHz)

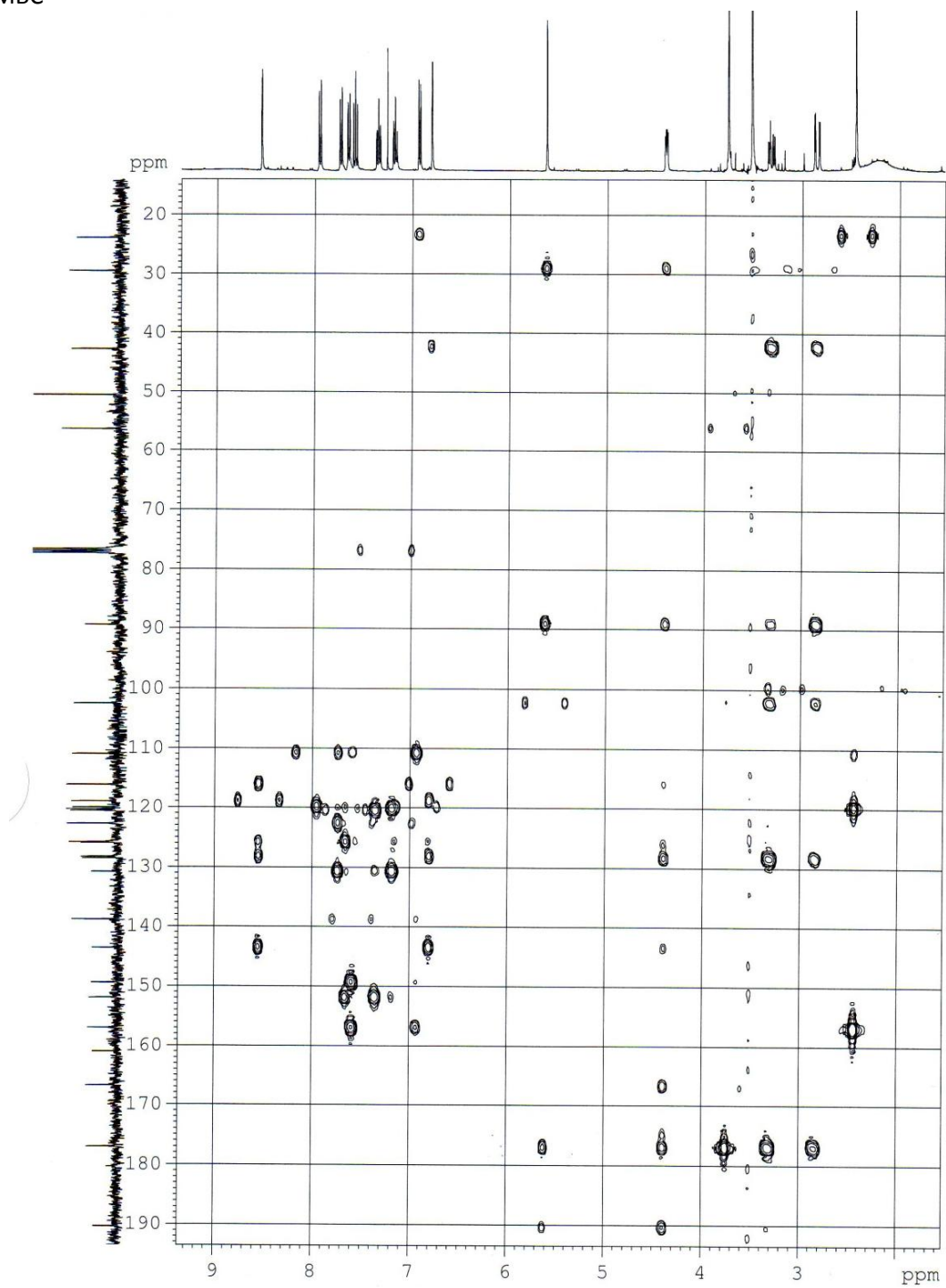
COSY



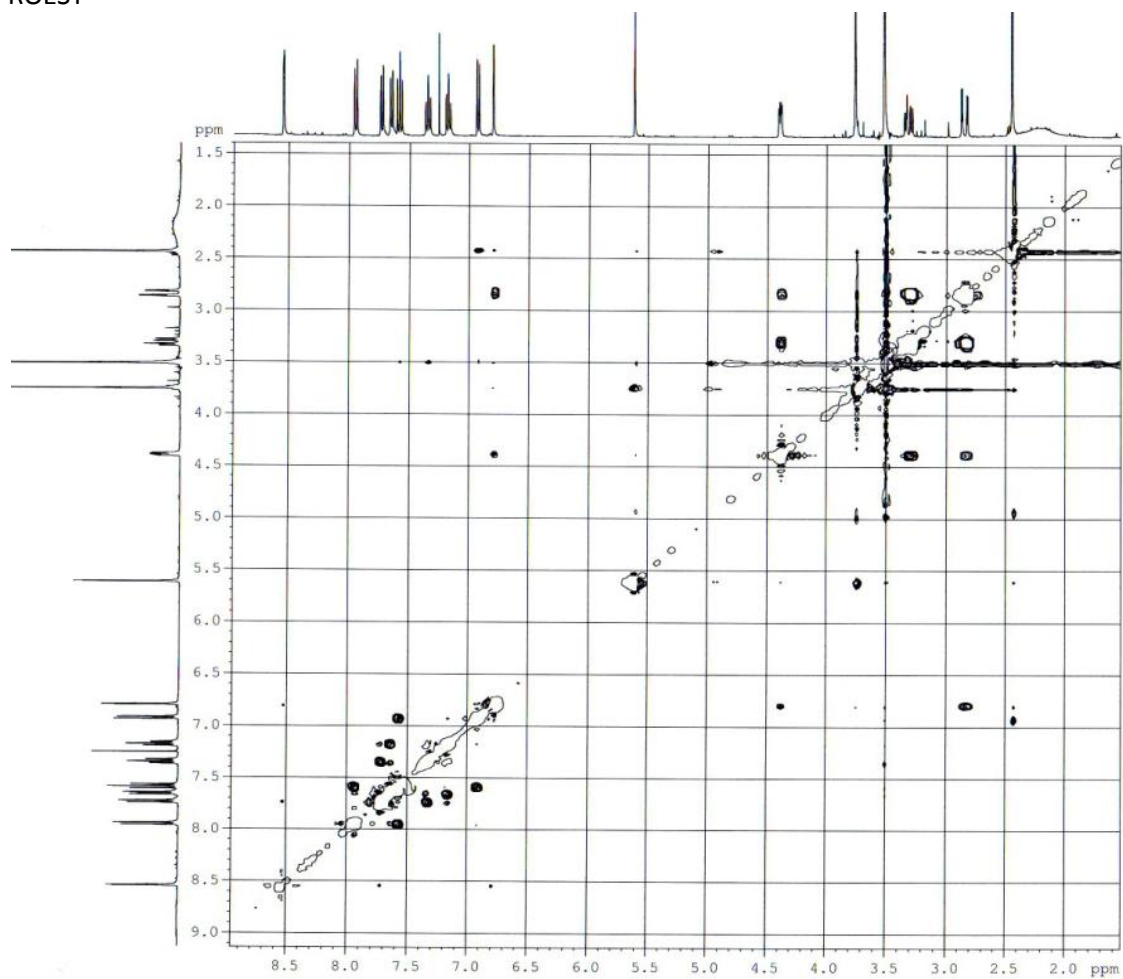
HMQC



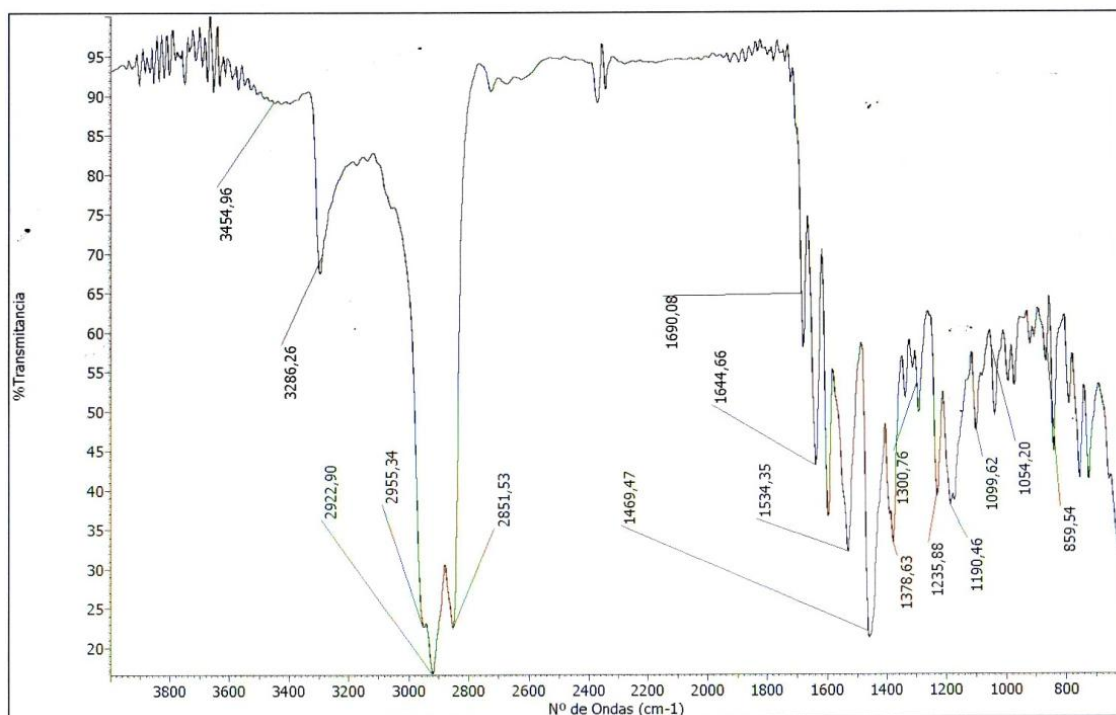
HMBC



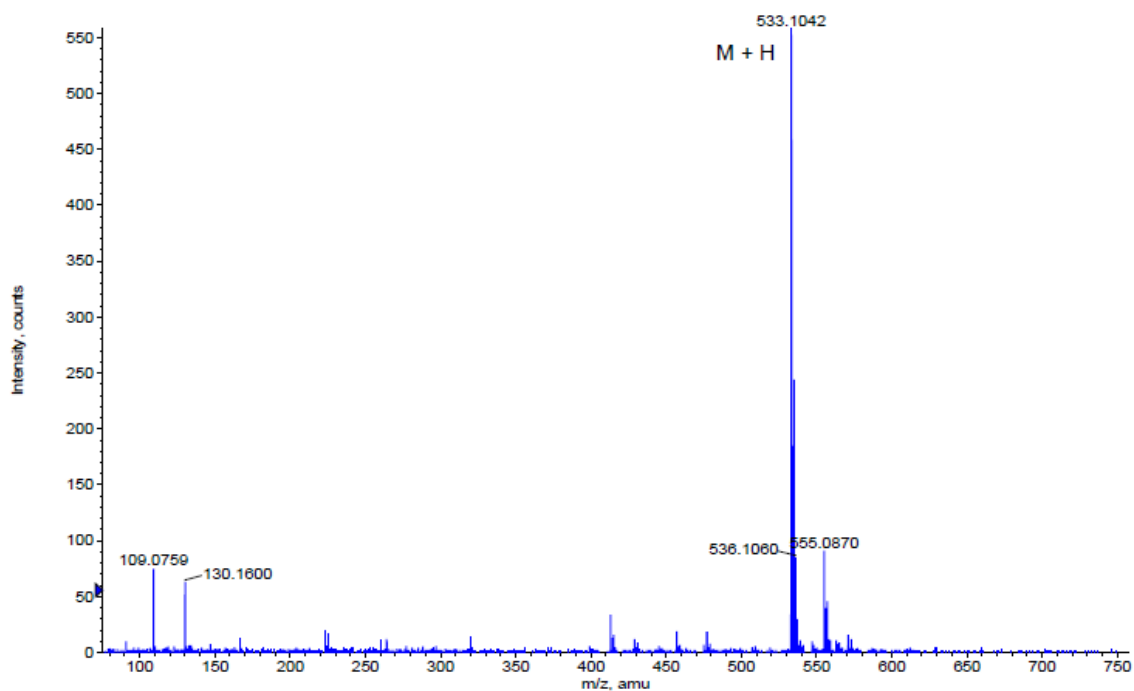
ROESY



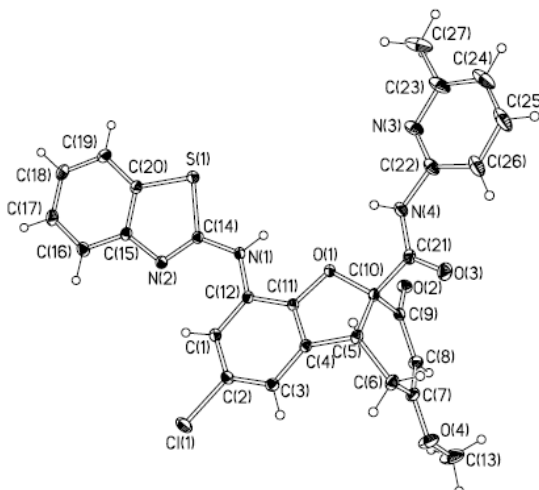
IR



HRMS

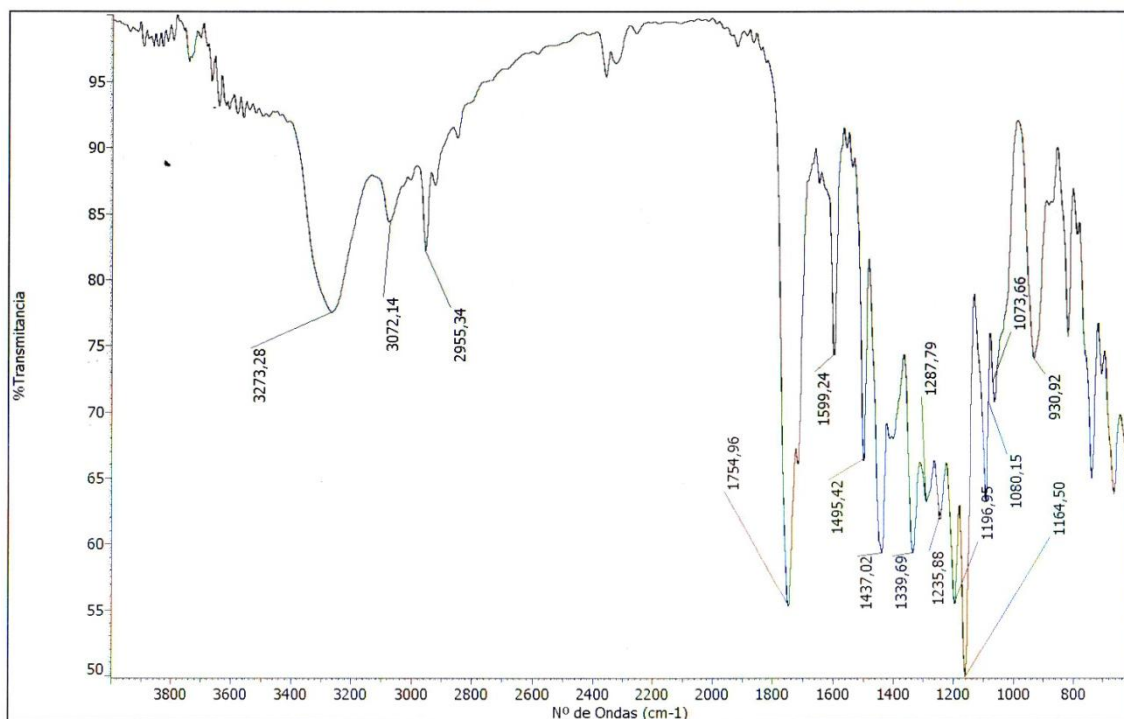


Formula	CalculatedMass	mDaError	ppmError	RDB
C27 H22 N4 O4 S Cl	533.104481	-0.281421	-0.527891	18.5
C26 H26 O8 S Cl	533.103144	1.055891	1.980645	13.5
C30 H23 N2 O2 Na S Cl	533.106099	-1.898865	-3.561898	19.5
C25 H23 N4 O4 Na S Cl	533.102076	2.123839	3.983906	15.5
C24 H27 O8 Na S Cl	533.100739	3.461151	6.492441	10.5
C18 H27 N4 O9 Na S Cl	533.10795	-3.749521	-7.033366	6.5
C32 H22 N2 O2 S Cl	533.108504	-4.304125	-8.073695	22.5
C21 H26 N2 O10 S Cl	533.099121	5.078595	9.526449	9.5

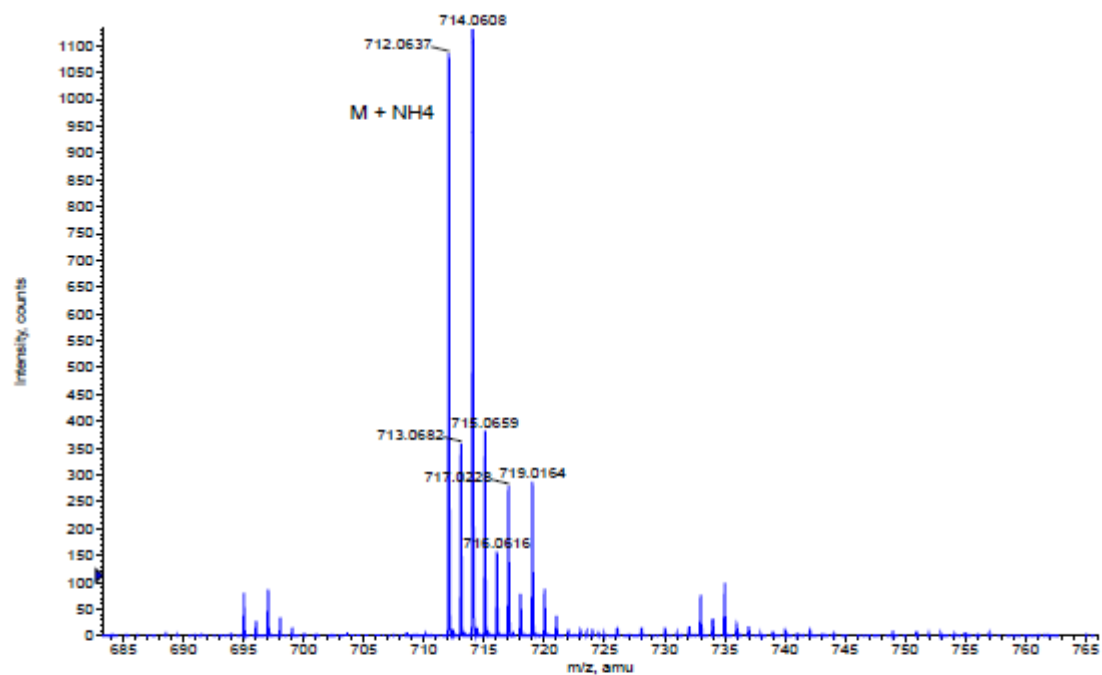
X-ray structure, crystal and refinement data of compound **169**

Empirical formula	$C_{27}H_{21}ClN_4O_4S$
Molecular weight	532.99
Temperature	298 (2) K
Wavelength	1.54178 Å
Crystal system, Space group	Monoclinic, $P2_1/c$
Unit cell dimensions	$a = 10.3542 (2) \text{ \AA}$ $\alpha = 90.0^\circ$ $b = 10.8396 (2) \text{ \AA}$ $\beta = 98.3550 (10)^\circ$ $c = 22.7202 (4) \text{ \AA}$ $\gamma = 90.0^\circ$
Volume	$2522.95 (8) \text{ \AA}^3$
Z; Density (calculated)	4; 1.409 mg/m^3
Absorption coefficient	2.467 mm^{-1}
F(000)	1104
Crystal size	0.18 x 0.15 x 0.10 mm
θ range	$3.93 - 66.83^\circ$
Limiting indices h, k, l	$-12 \leq h \leq 10, -12 \leq k \leq 12, -23 \leq l \leq 26$
Reflections collected/independent	19366/4256 $R_{\text{int}} = 0.0322$
Refinement method	Least squares method with full matrix in F^2
Data/restraints/parameters	4256/0/336
Goodness-of-fit on F^2	1.033
Final R indices [$I > 2\sigma(I)$]	$R_1 = 0.0397, \omega R_2 = 0.1018$
R indices (all data)	$R_1 = 0.0454, \omega R_2 = 0.1060$
Largest difference peak and hole	0.470 and -0.502

IR

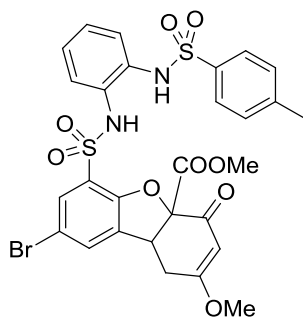


HRMS

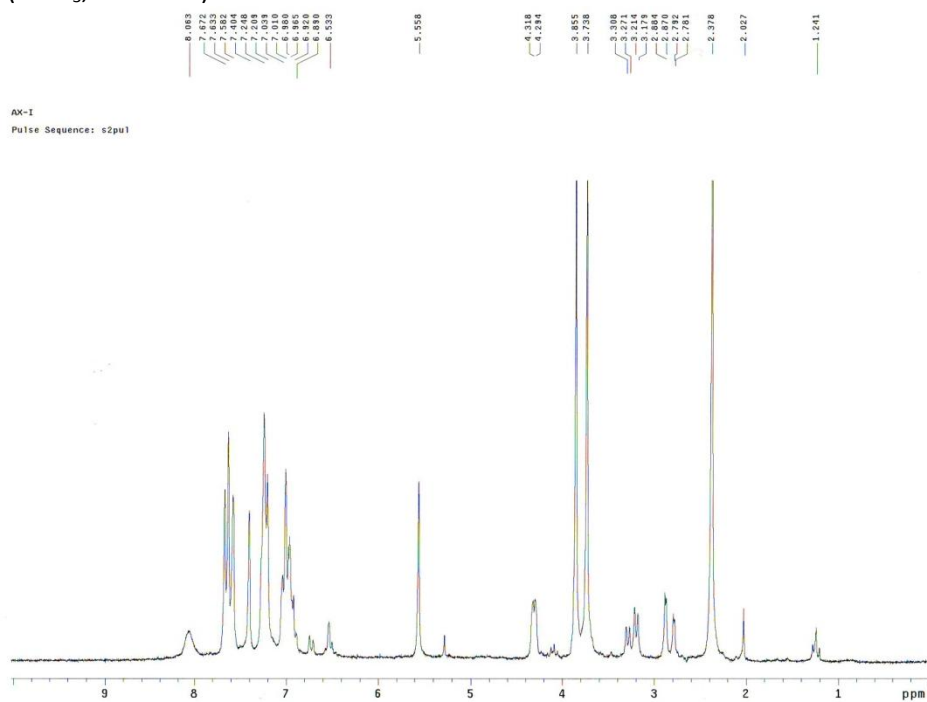


Formula	CalculatedMass	mDaError	ppmError	RDB
C31 H32 N O8 Na S2 Br	712.064493	-0.793228	-1.113984	15.5
C28 H31 N3 O10 S2 Br	712.062876	0.824216	1.157502	14.5
C32 H28 N5 O4 Na S2 Br	712.065831	-2.13054	-2.992061	20.5
C40 H27 N O3 S2 Br	712.061025	2.674872	3.756504	27.5
C33 H31 N O8 S2 Br	712.066898	-3.198488	-4.491853	18.5
C26 H32 N3 O10 Na S2 Br	712.060471	3.229476	4.535372	11.5
C34 H27 N5 O4 S2 Br	712.068236	-4.5358	-6.369931	23.5
C38 H28 N O3 Na S2 Br	712.05862	5.080132	7.134373	24.5
C37 H28 N3 O2 Na S2 Br	712.069853	-6.153244	-8.641417	24.5
C35 H27 N3 O5 S2 Br	712.057002	6.697576	9.405859	23.5

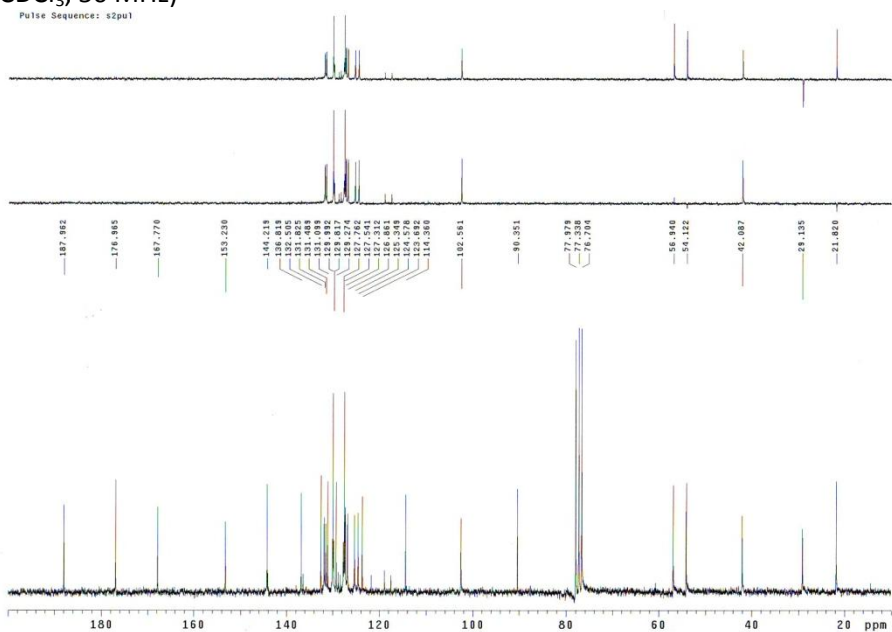
- Methyl 8-bromo-2-methoxy-6-(*N*-(2-(4-methylphenylsulfonamido)phenyl)sulfamoyl)-4-oxo-1,4,4a,9b-tetrahydrodibenzo[*b,d*]furan-4a-carboxylate (177)



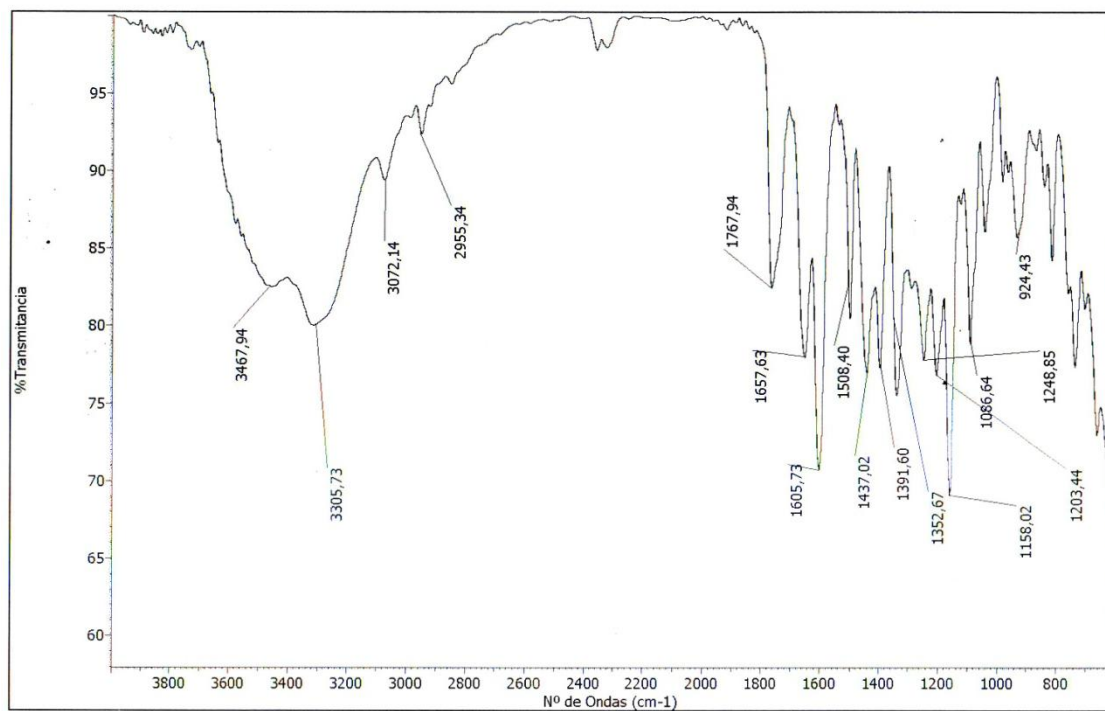
^1H NMR (CDCl_3 , 200 MHz)



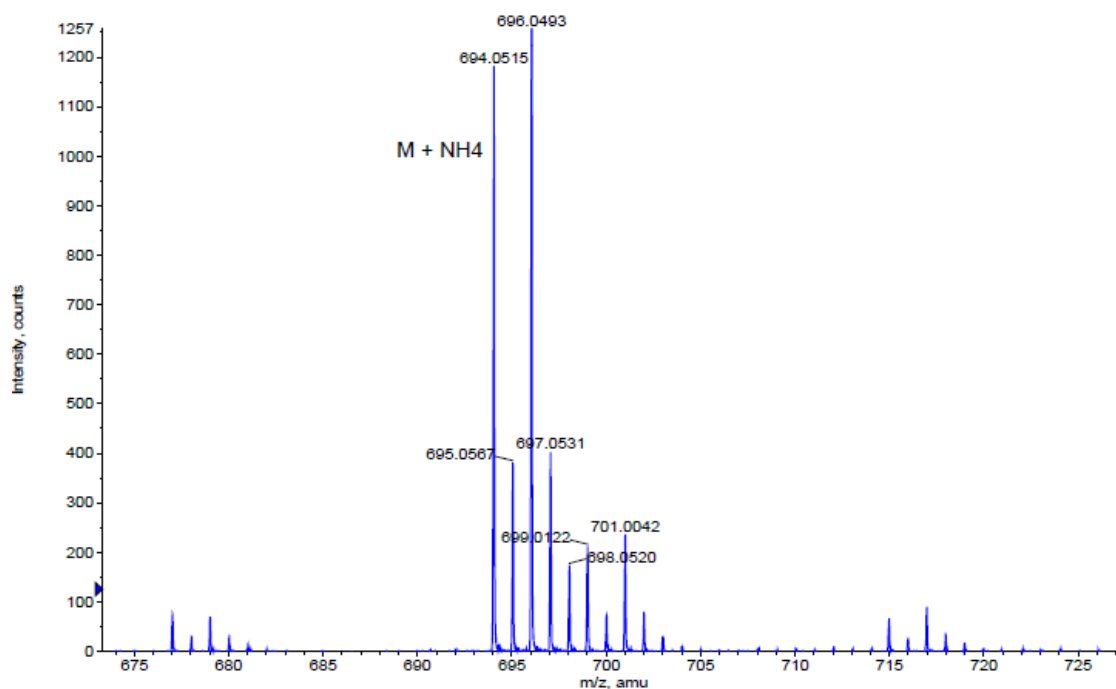
^{13}C NMR (CDCl_3 , 50 MHz)



IR

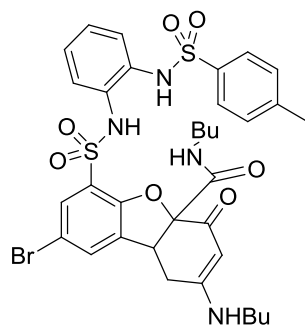


HRMS

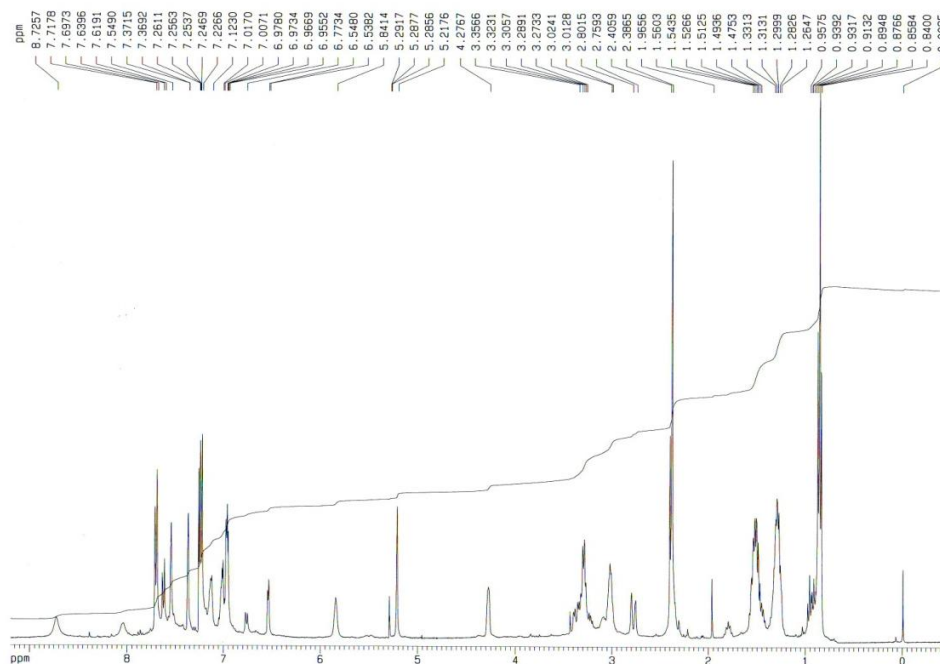


Formula	CalculatedMass	mDaError	ppmError	RDB
C28 H29 N3 O9 S2 Br	694.052311	-0.811064	-1.168592	15.5
C40 H25 N O2 S2 Br	694.05046	1.039592	1.497859	28.5
C26 H30 N3 O9 Na S2 Br	694.049906	1.594196	2.29694	12.5
C31 H30 N O7 Na S2 Br	694.053929	-2.428508	-3.499029	16.5
C38 H26 N O2 Na S2 Br	694.048055	3.444852	4.963391	25.5
C33 H29 N O7 S2 Br	694.056334	-4.833768	-6.964561	19.5
C35 H25 N3 O4 S2 Br	694.046438	5.062296	7.293828	24.5

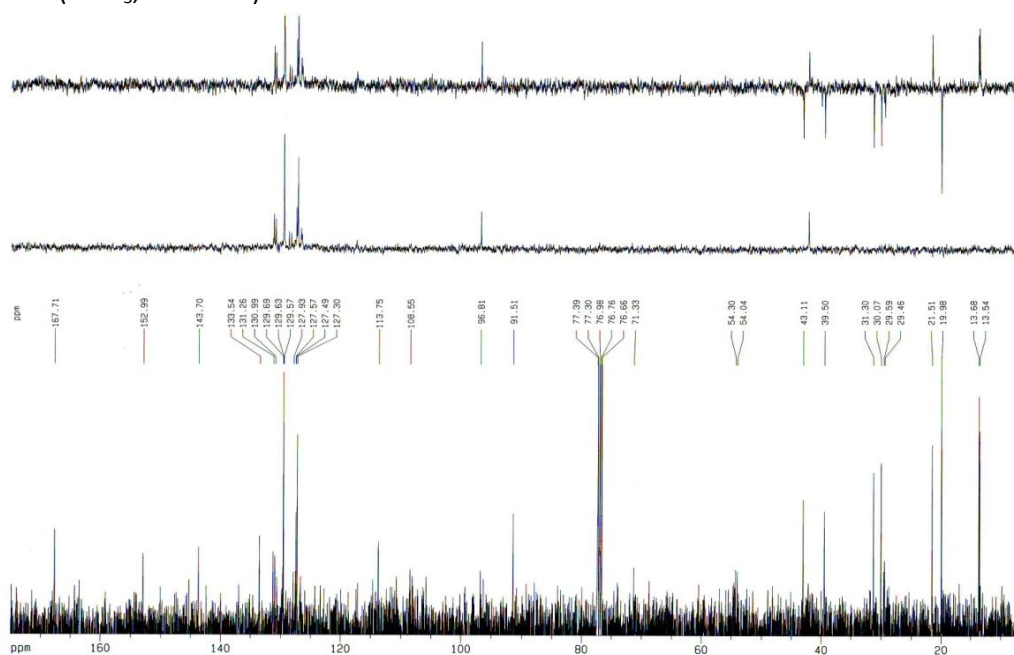
- 8-Bromo-*N*-butyl-2-(butylamino)-6-(*N*-(2-(4-methylphenylsulfonamido)phenyl)sulfamoyl)-4-oxo-1,4,4a,9b-tetrahydrodibenzo[*b,d*]furan-4a-carboxamide (178)



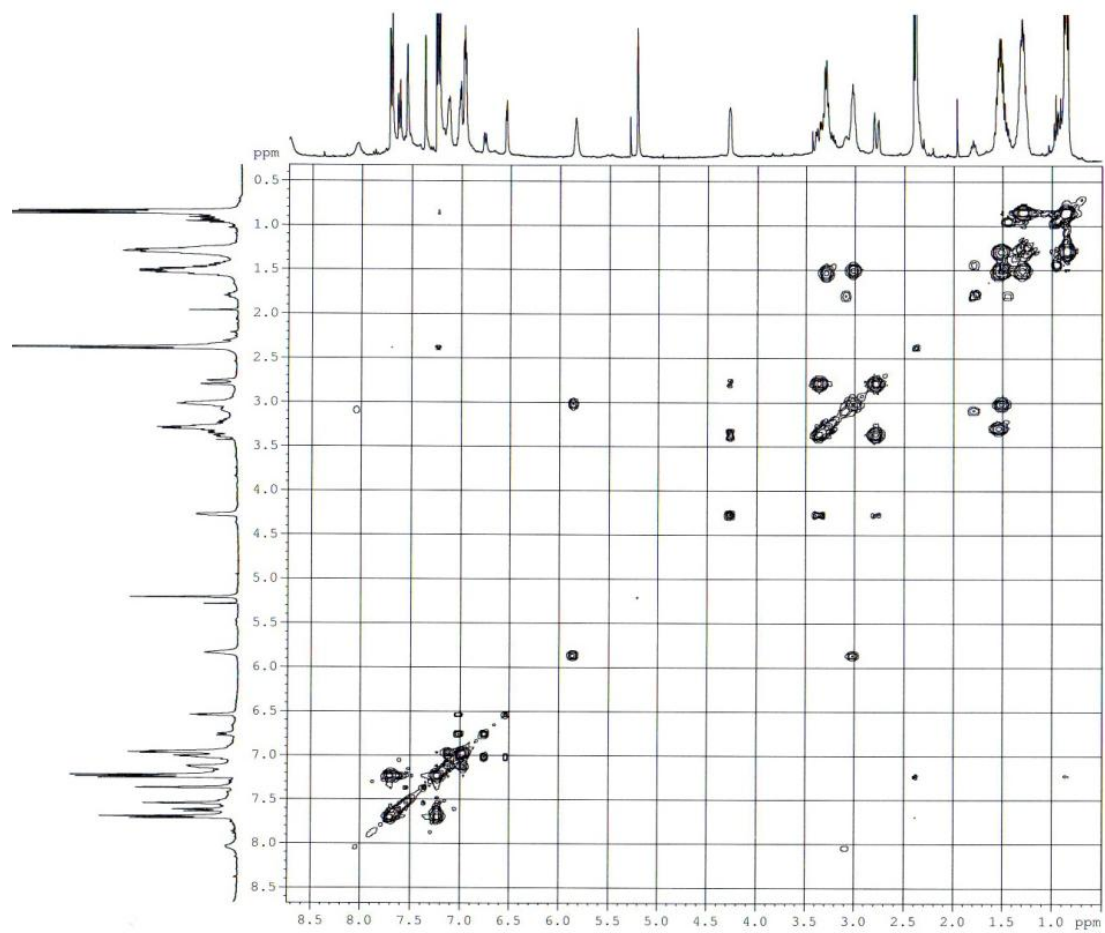
¹H NMR (CDCl₃, 400 MHz)



¹³C NMR (CDCl₃, 100 MHz)

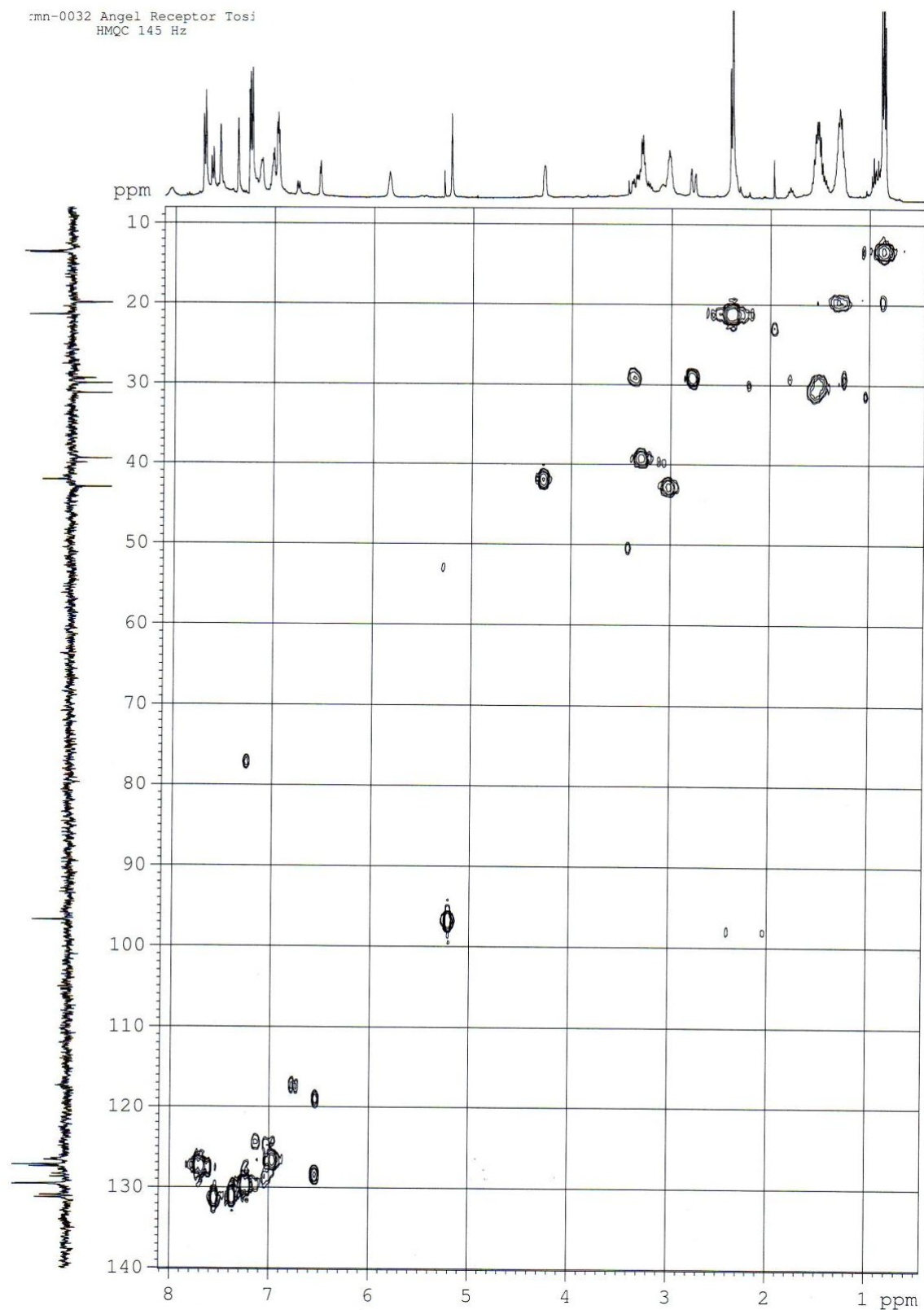


COSY



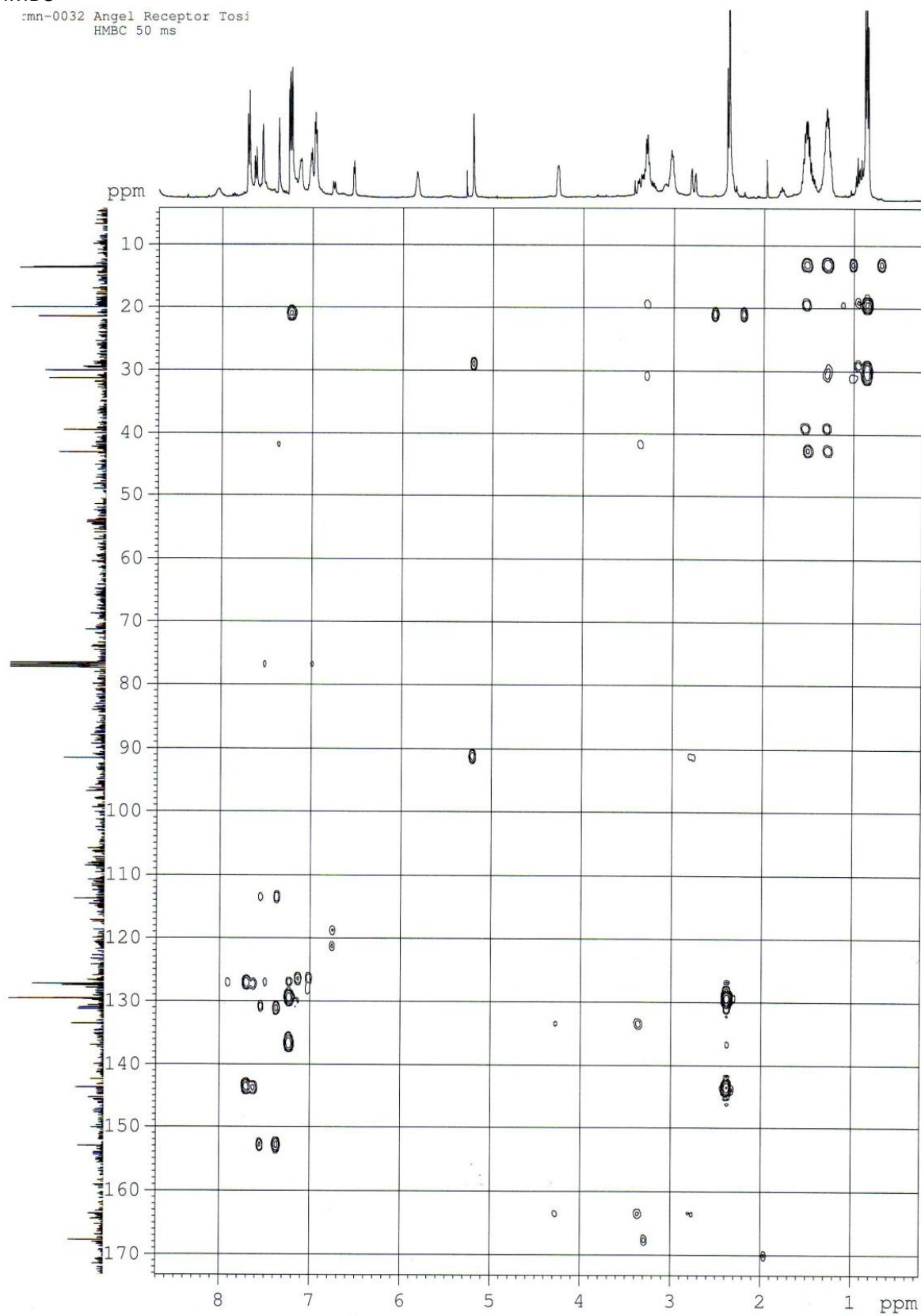
HMQC

:mn-0032 Angel Receptor Tosi
HMQC 145 Hz

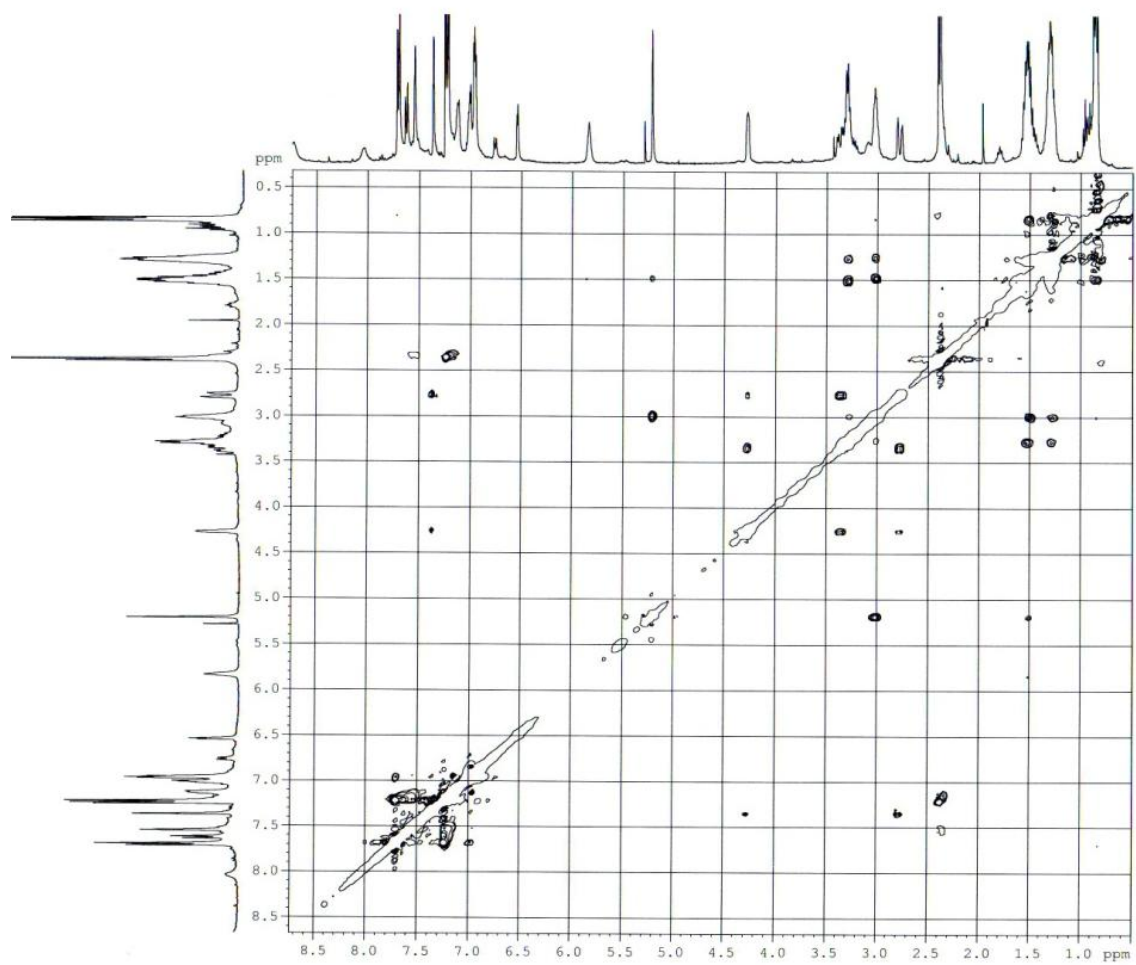


HMBC

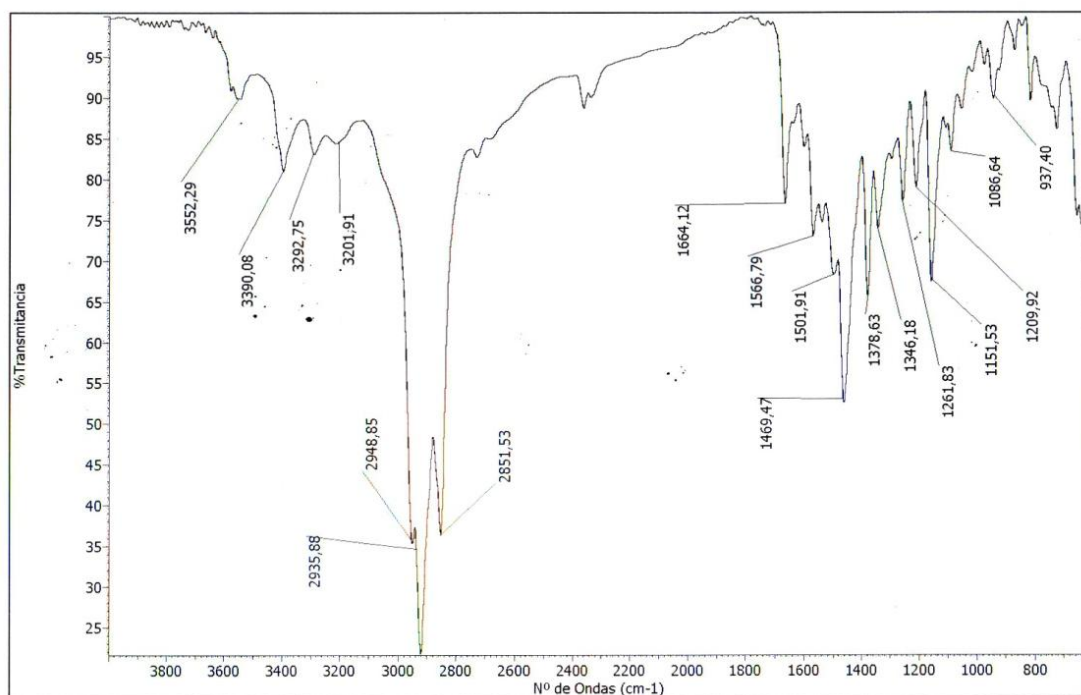
:mn-0032 Angel Receptor Tos;
HMBC 50 ms



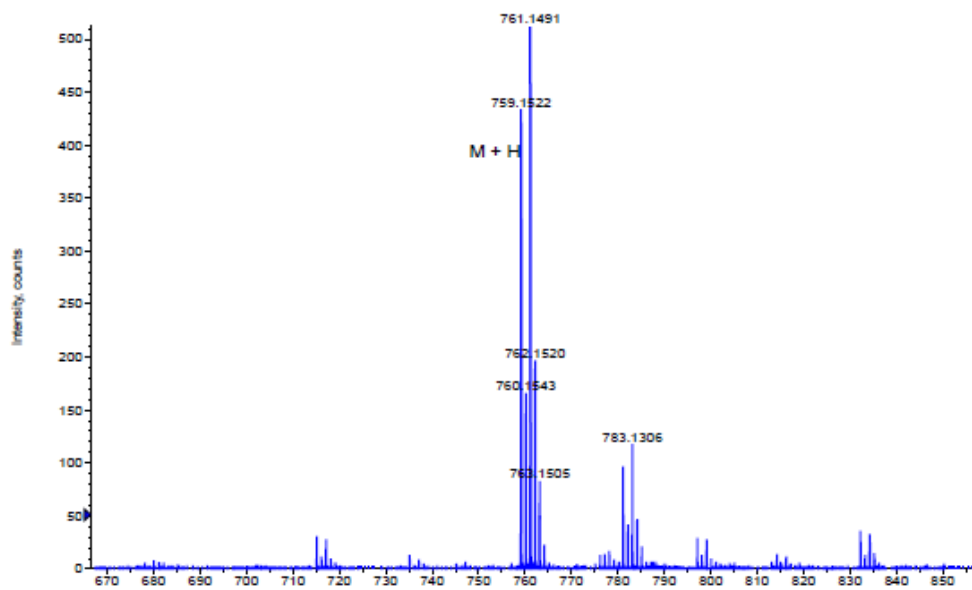
ROESY



IR

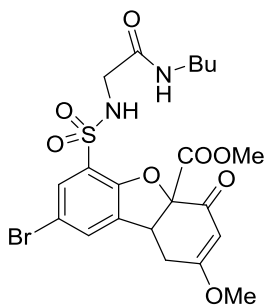


HRMS

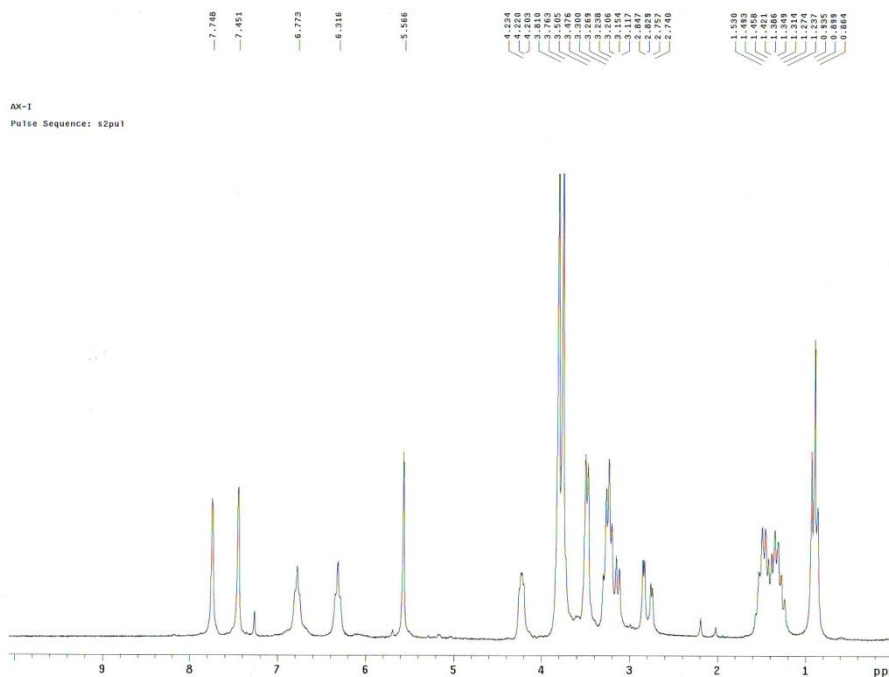


Formula	CalculatedMass	mDaError	ppmError	RDB
C34 H40 N4 O7 S2 Br	759.151631	0.568768	0.749214	16.5
C37 H41 N2 O5 Na S2 Br	759.153249	-1.048676	-1.381377	17.5
C24 H49 O16 Na S2 Br	759.153762	-1.56202	-2.057583	-0.5
C33 H44 O11 S2 Br	759.150294	1.90608	2.510799	11.5
C46 H36 N2 S2 Br	759.149781	2.419424	3.187006	29.5
C25 H45 N4 O12 Na S2 Br	759.155099	-2.899332	-3.819168	4.5
C32 H41 N4 O7 Na S2 Br	759.149226	2.974028	3.917562	13.5
C39 H40 N2 O5 S2 Br	759.155654	-3.453936	-4.549725	20.5
C26 H48 O16 S2 Br	759.156167	-3.96728	-5.225931	2.5
C31 H45 O11 Na S2 Br	759.147889	4.31134	5.679147	8.5
C44 H37 N2 Na S2 Br	759.147375	4.824684	6.355353	26.5
C42 H41 O3 Na S2 Br	759.157271	-5.07138	-6.680316	21.5
C27 H44 N4 O12 S2 Br	759.157505	-5.304592	-6.987516	7.5
C28 H44 N2 O13 S2 Br	759.146271	5.928784	7.809738	7.5
C41 H36 N4 O2 S2 Br	759.145758	6.442128	8.485944	25.5
C30 H45 N2 O10 Na S2 Br	759.159122	-6.922036	-9.118107	8.5
C44 H40 O3 S2 Br	759.159677	-7.47664	-9.848664	24.5

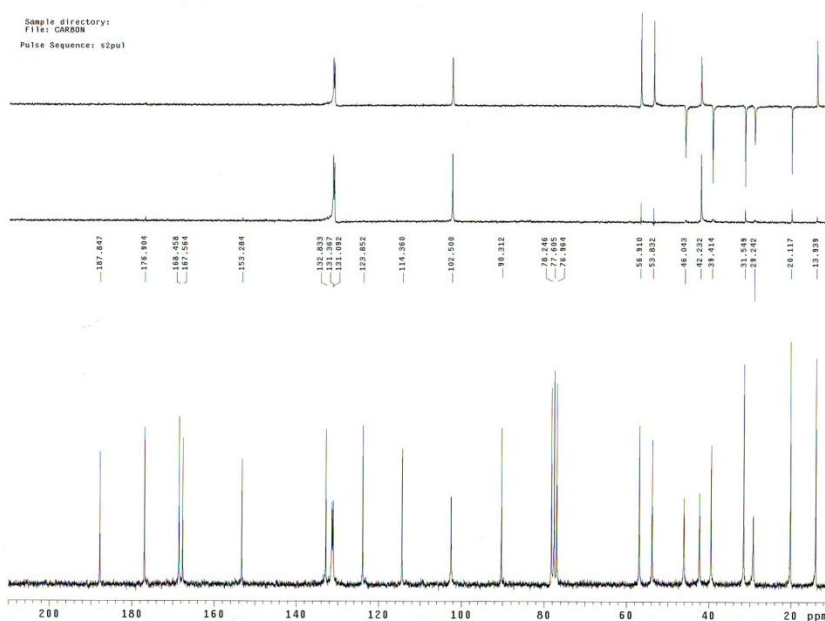
- Methyl-8-bromo-6-(*N*-(2-(butylamino)-2-oxoethyl)sulfamoyl)-2-methoxy-4-oxo-1,4,4a,9b-tetrahydrobenzo[*b,d*]furan-4a-carboxylate (180)



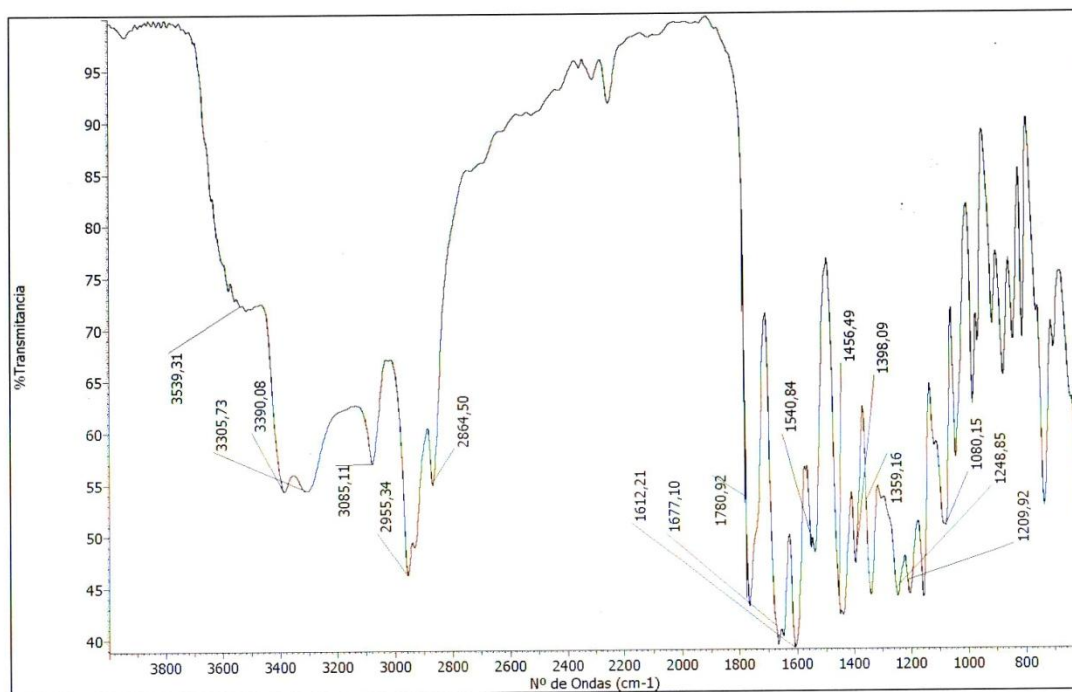
^1H NMR (CDCl_3 , 200 MHz)



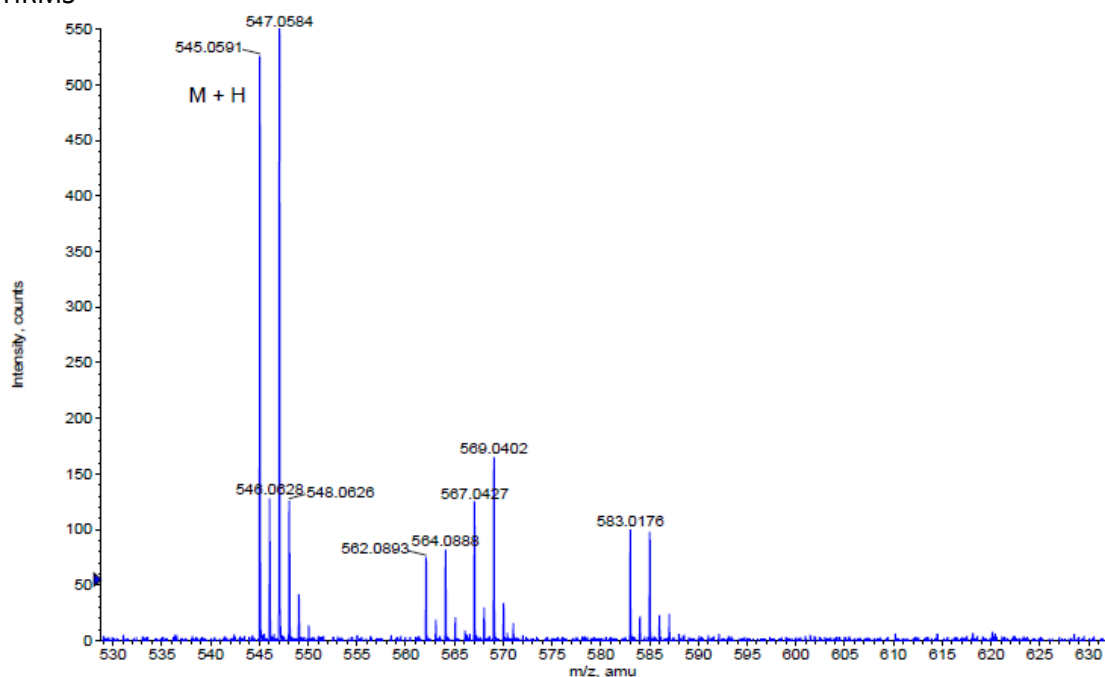
^{13}C NMR (CDCl_3 , 50 MHz)



IR

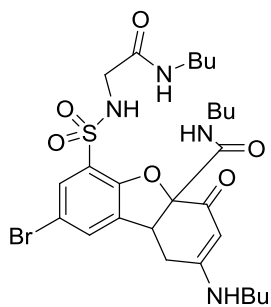


HRMS

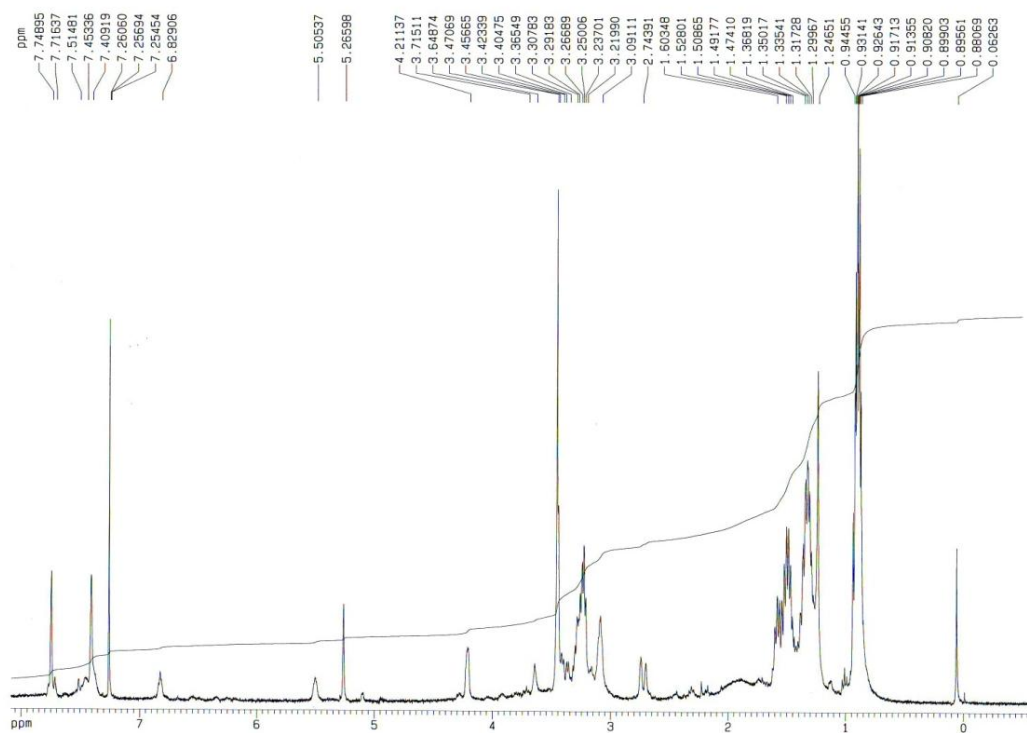


Formula	CalculatedMass	mDaError	ppmError	RDB
C21 H26 N2 O8 S Br	545.058775	0.324504	0.595355	9.5
C24 H27 O6 Na S Br	545.060393	-1.29294	-2.372107	10.5
C33 H22 O S Br	545.056925	2.17516	3.990682	22.5
C25 H23 N4 O2 Na S Br	545.06173	-2.630252	-4.825622	15.5
C19 H27 N2 O8 Na S Br	545.05637	2.729764	5.008193	6.5
C26 H26 O6 S Br	545.062798	-3.6982	-6.784945	13.5
C16 H26 N4 O10 S Br	545.054753	4.347208	7.975656	5.5
C31 H23 O Na S Br	545.05452	4.58042	8.403521	19.5
C27 H22 N4 O2 S Br	545.064136	-5.035512	-9.23846	18.5

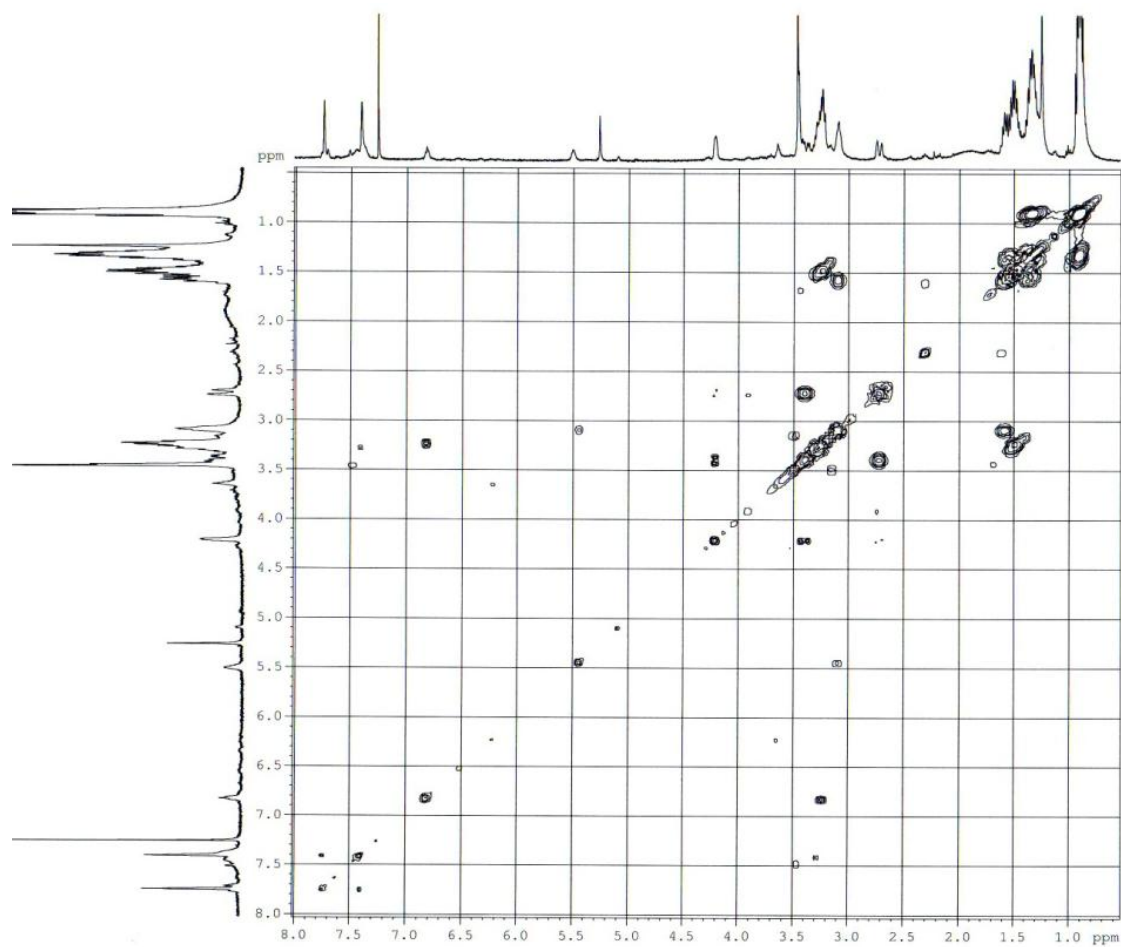
- **8-Bromo-*N*-butyl-2-(butylamino)-6-(*N*-(2-(butylamino)-2-oxoethyl)sulfamoyl)-4-oxo-1,4,4a,9b-tetrahydrodibenzo[*b,d*]furan-4a-carboxamide (181)**



^1H NMR (CDCl_3 , 400 MHz)

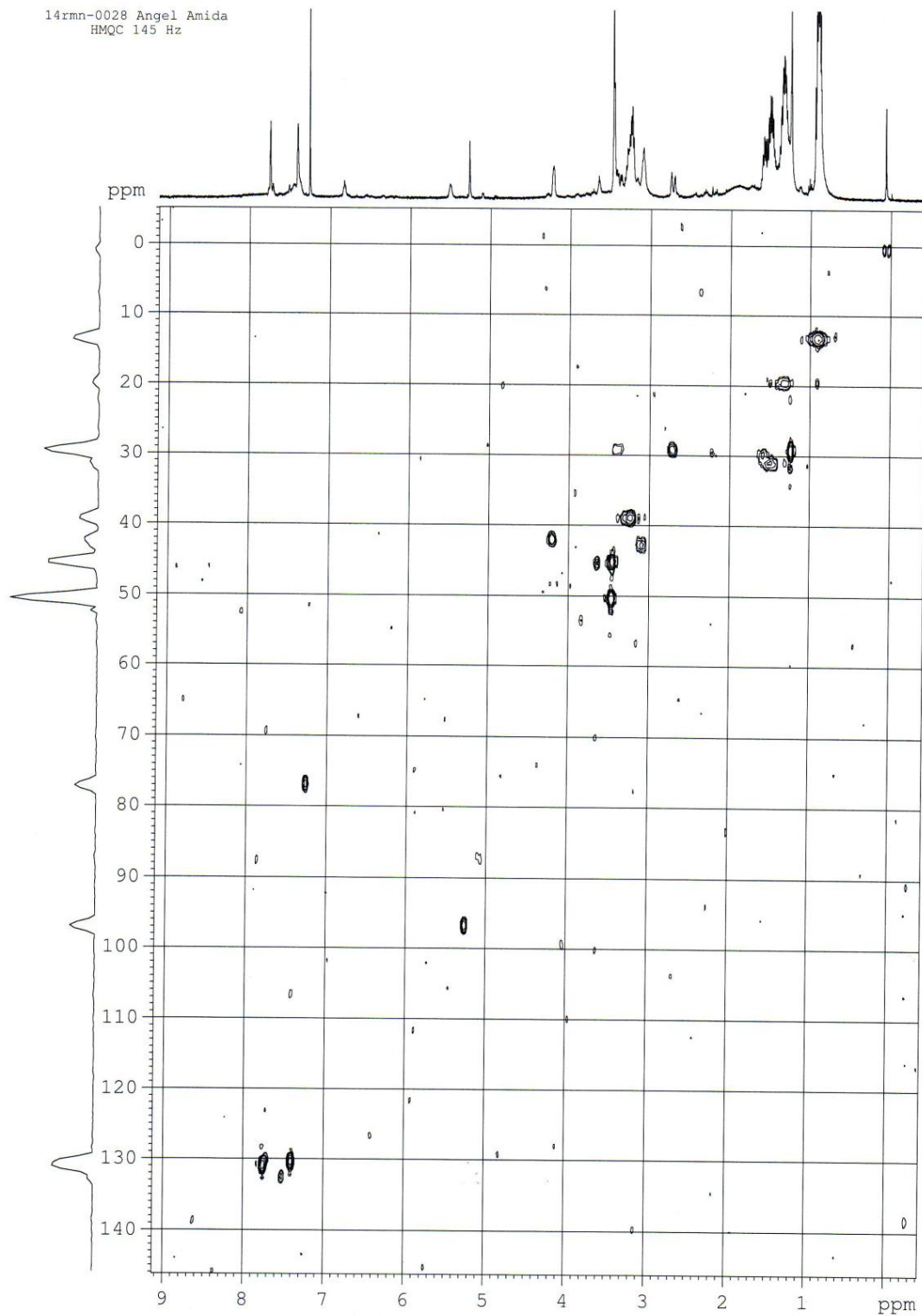


COSY

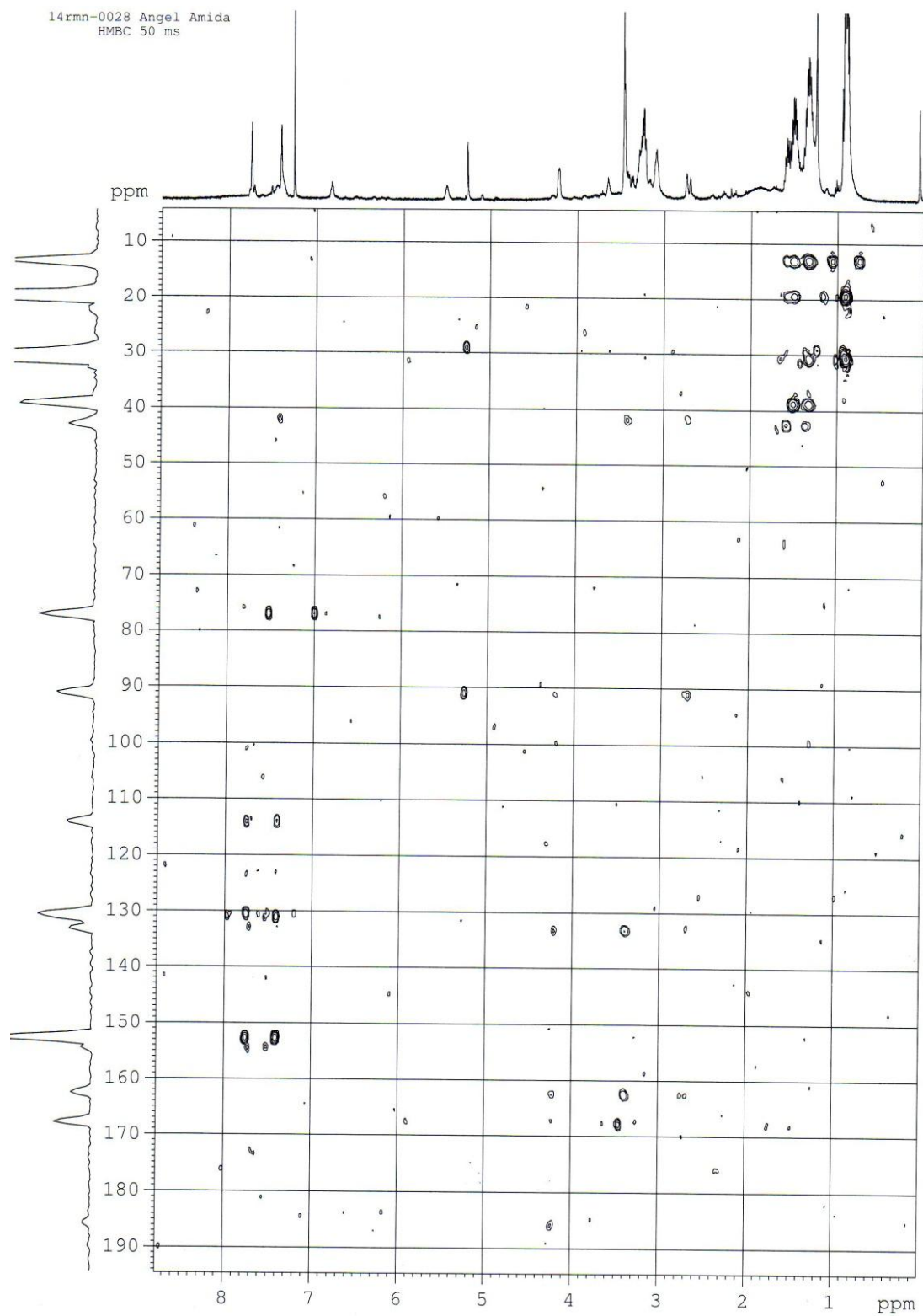


HMQC

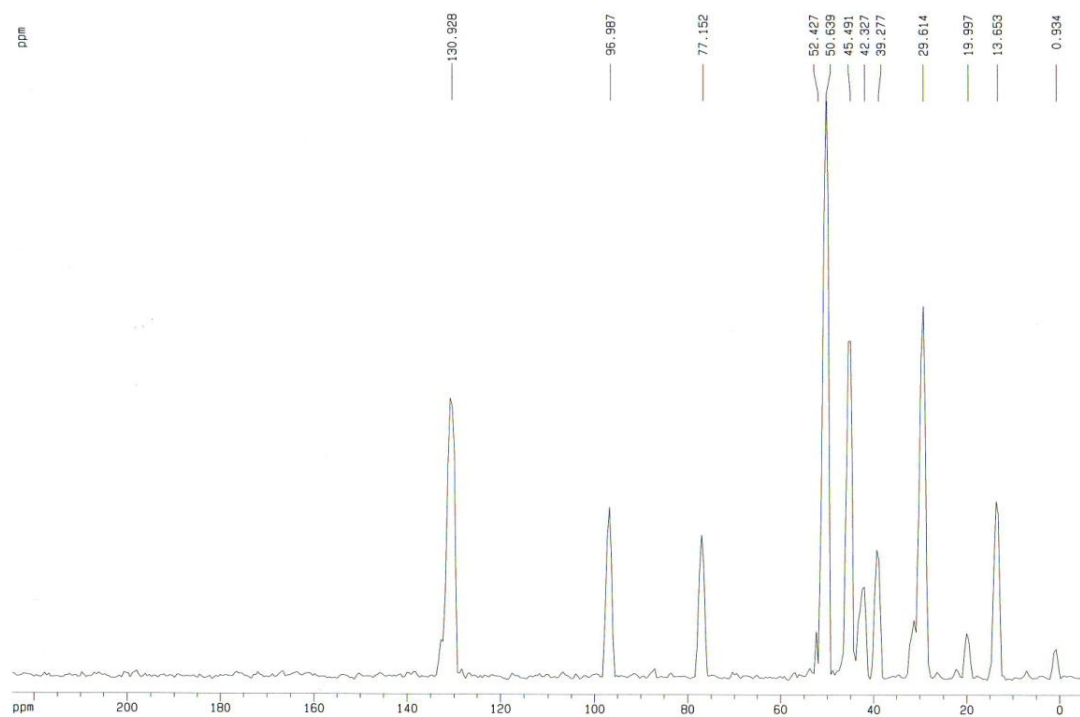
14rnm-0028 Angel Amida
HMQC 145 Hz



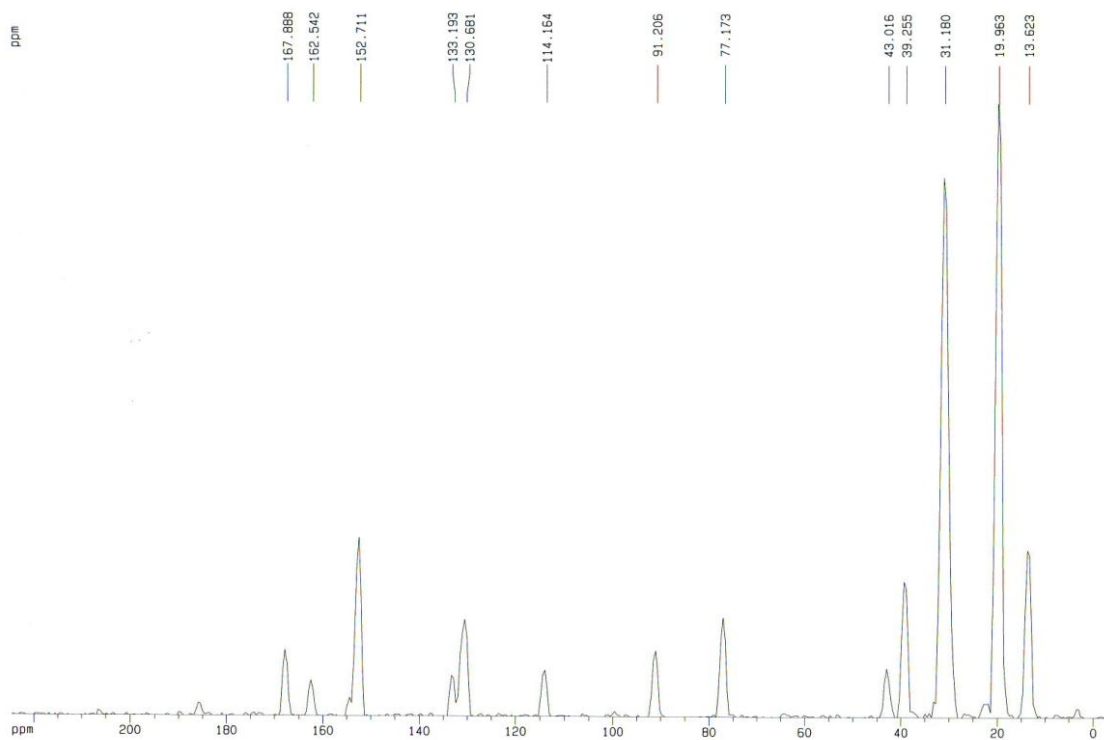
HMBC

14rmn-0028 Angel Amida
HMBC 50 ms

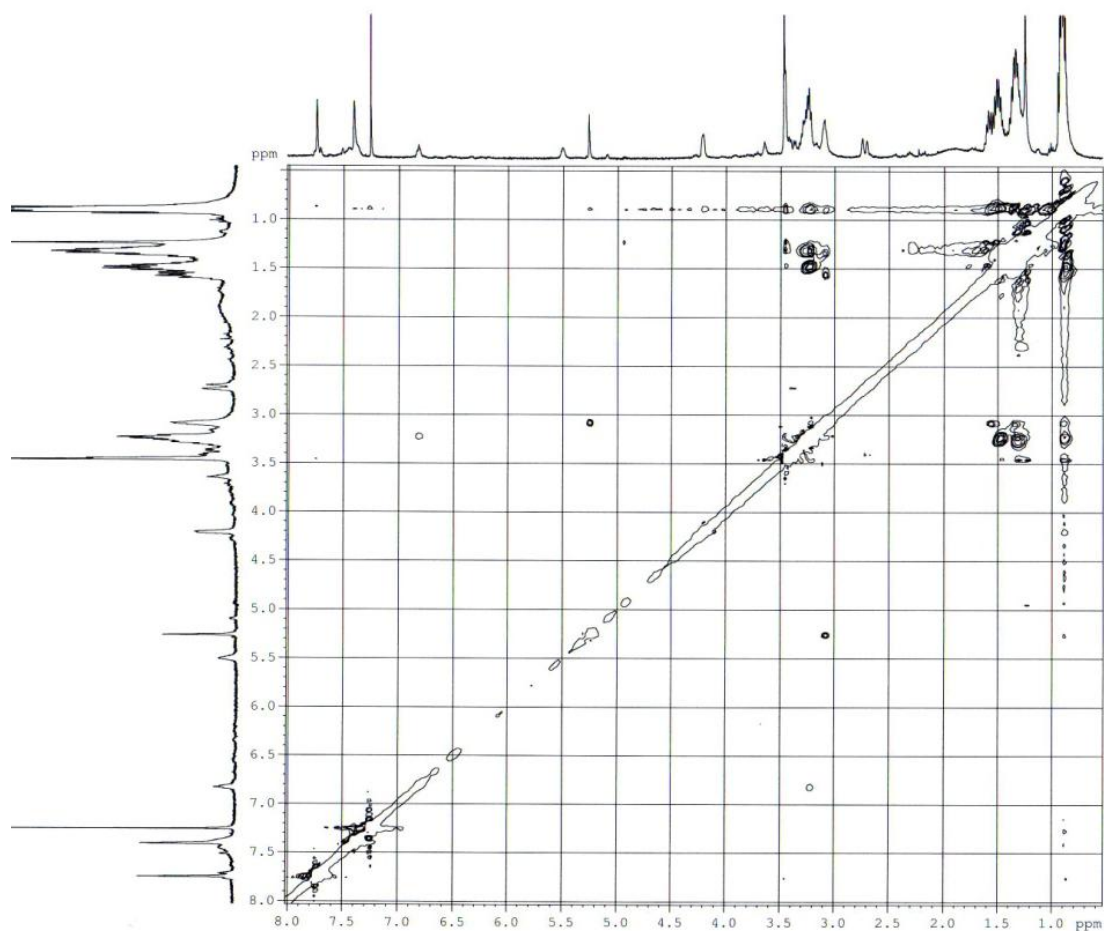
HMQC projection



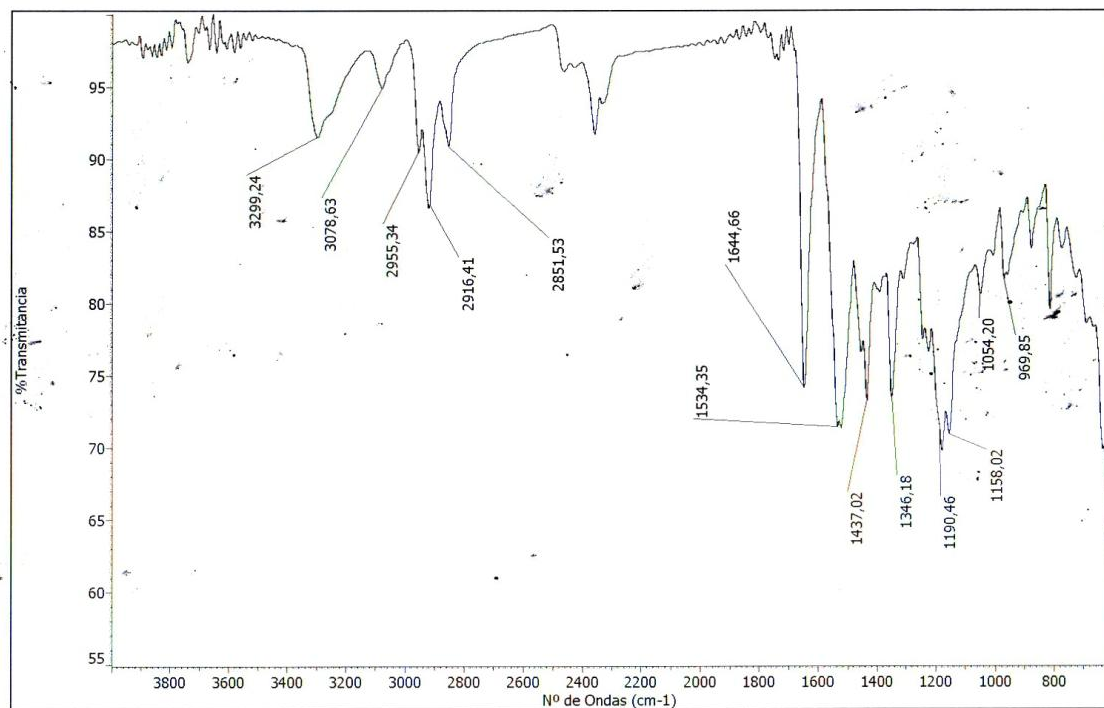
HMBC projection



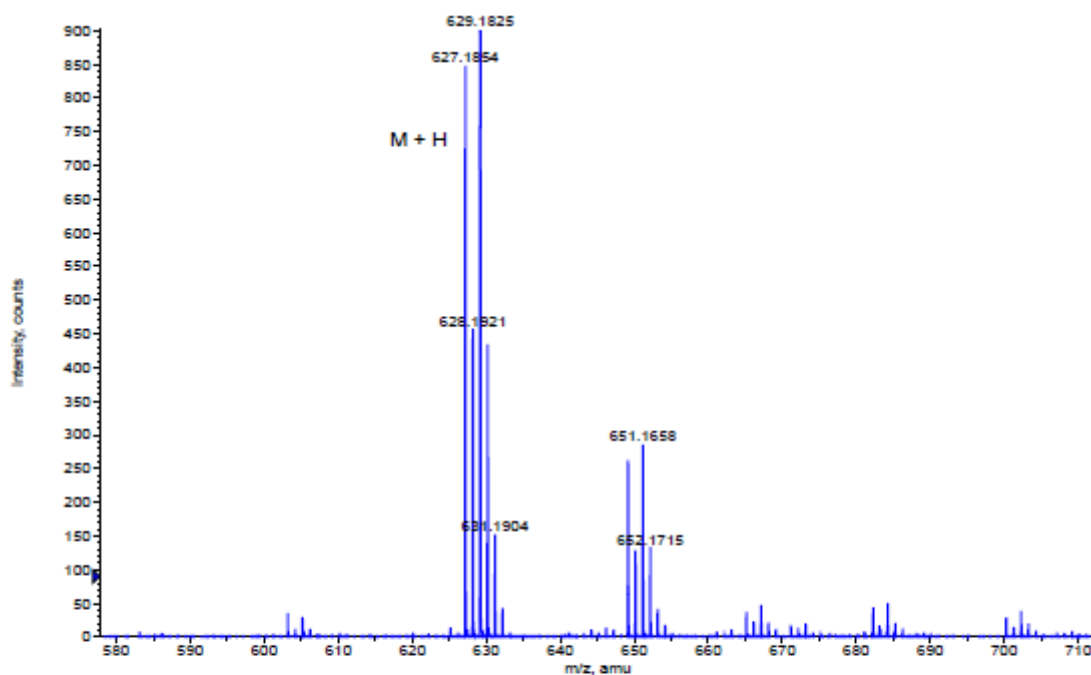
ROESY



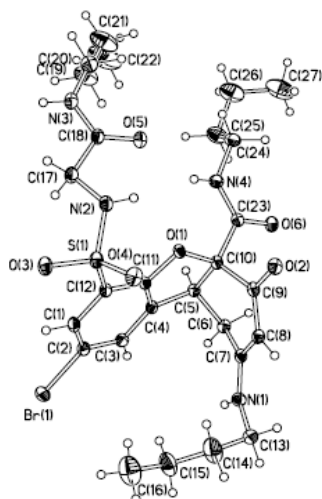
IR



HRMS

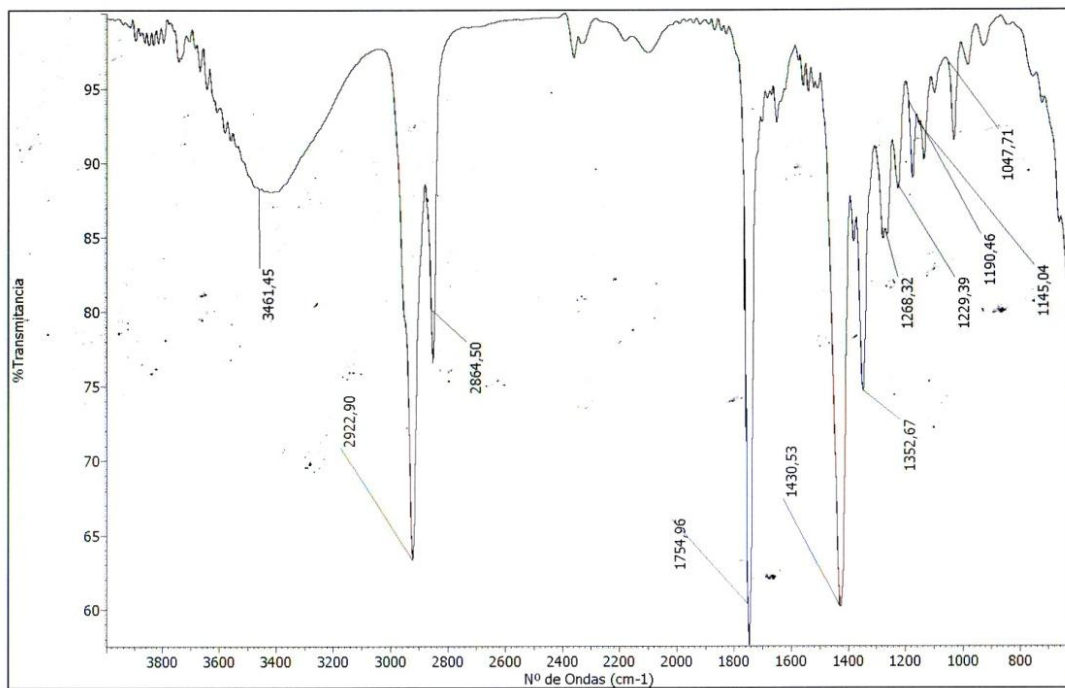


Formula	CalculatedMass	mDaError	ppmError	RDB
C27 H40 N4 O6 S Br	627.184645	0.755208	1.204121	9.5
C30 H41 N2 O4 Na S Br	627.186262	-0.862236	-1.374769	10.5
C26 H44 O10 S Br	627.183307	2.09252	3.336363	4.5
C25 H41 N4 O6 Na S Br	627.18224	3.160468	5.039124	6.5
C32 H40 N2 O4 S Br	627.188667	-3.267496	-5.209772	13.5
C24 H45 O10 Na S Br	627.180902	4.49778	7.171366	1.5
C35 H41 O2 Na S Br	627.190285	-4.88494	-7.788663	14.5
C20 H44 N4 O11 S Br	627.190518	-5.118152	-8.160502	0.5
C21 H44 N2 O12 S Br	627.179285	6.115224	9.750257	0.5

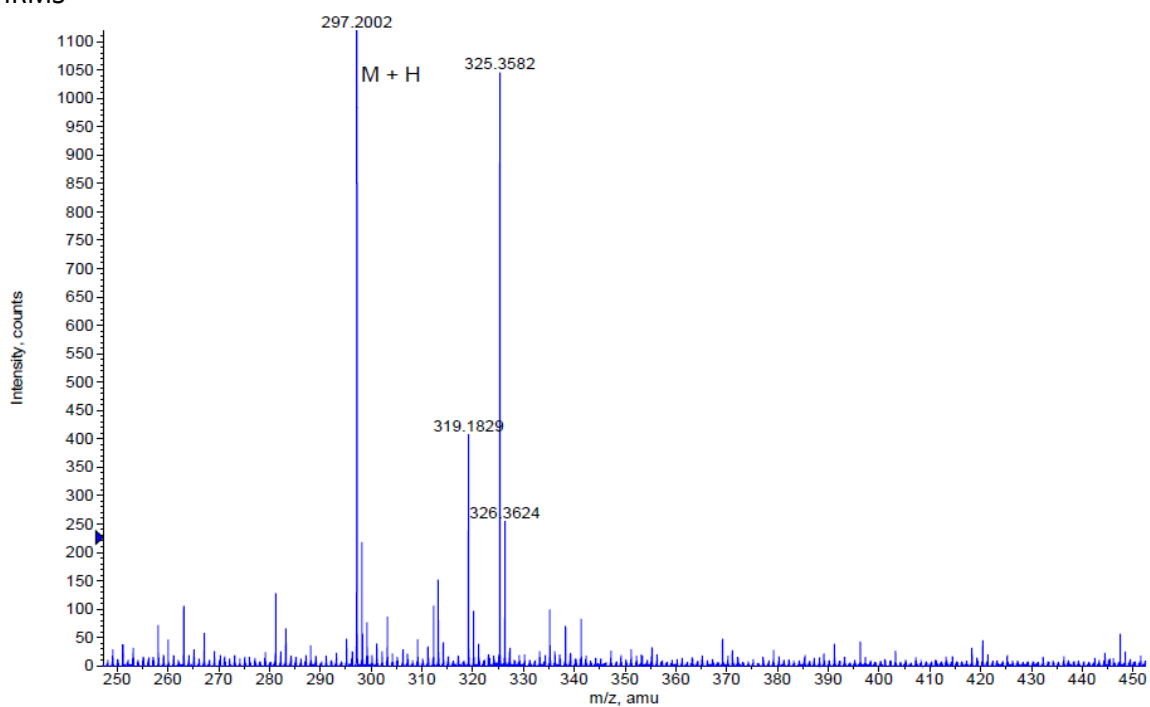
X-ray structure, crystal and refinement data of compound **181**

Empirical formula	$C_{27}H_{39}N_4O_6SBr$	
Molecular weight	627.59	
Temperature	298 (2) K	
Wavelength	1.54178 Å	
Crystal system, Space group	Monoclinic, $P2_1/n$	
Unit cell dimensions	$a = 14.6050 (6) \text{ \AA}$ $b = 12.9781 (5) \text{ \AA}$ $c = 16.5293 (7) \text{ \AA}$	$\alpha = 90.00^\circ$ $\beta = 106.059 (3)^\circ$ $\gamma = 90.00^\circ$
Volume	$3010.8 (2) \text{ \AA}^3$	
Z; Density (calculated)	4; 1.385 mg/m^3	
Absorption coefficient	2.888 mm^{-1}	
F(000)	1312	
Crystal size	0.20 x 0.18 x 0.12 mm	
θ range	3.58 – 67.02 °	
Limiting indices h, k, l	$-15 \leq h \leq 17, -15 \leq k \leq 13, -17 \leq l \leq 19$	
Reflections collected/independent	19475/4907 $R_{\text{int}} = 0.0512$	
Refinement method	Least squares method with full matrix in F^2	
Data/restraints/parameters	4907/0/371	
Goodness-of-fit on F^2	1.040	
Final R indices [$I > 2\sigma(I)$]	$R_1 = 0.0491, \omega R_2 = 0.1307$	
R indices (all data)	$R_1 = 0.0699, \omega R_2 = 0.1447$	
Largest difference peak and hole	0.861 and -0.561	

IR

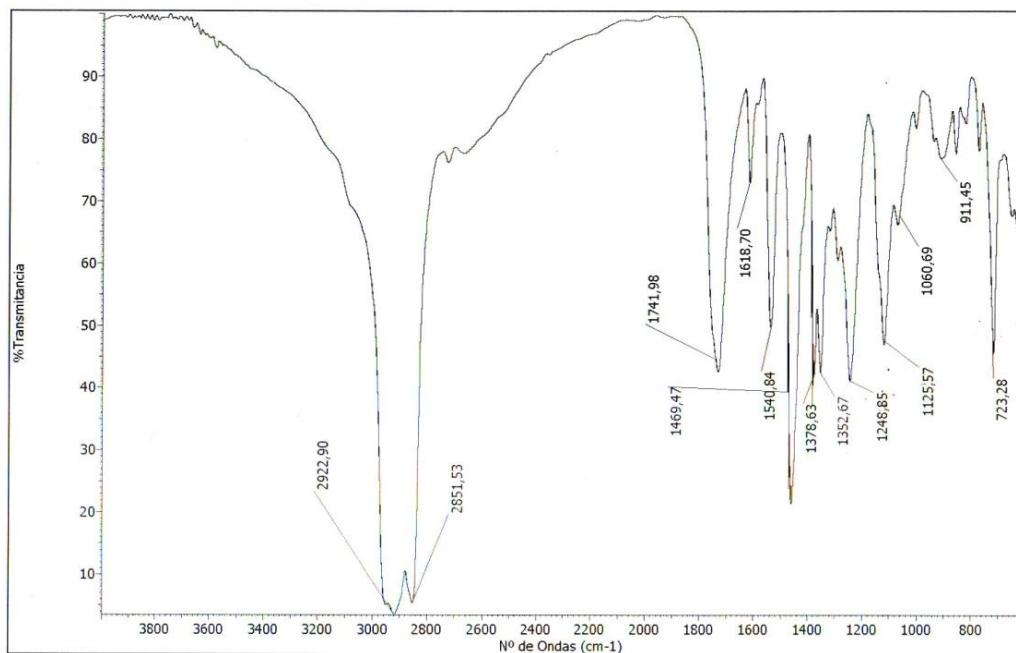


HRMS

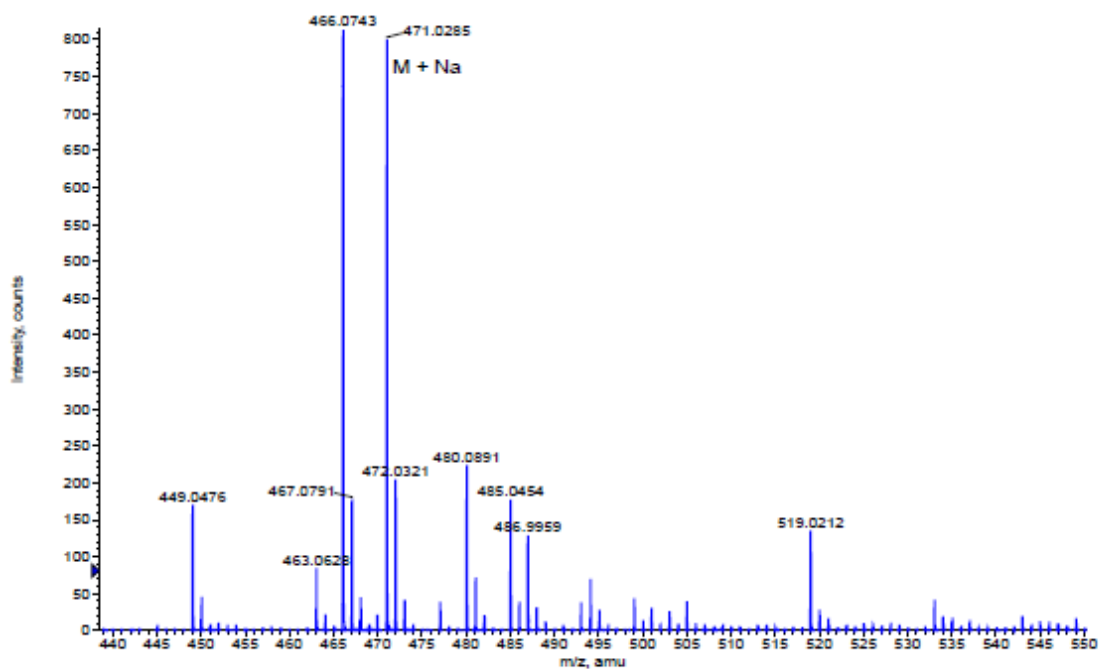


Formula	CalculatedMass	mDaError	ppmError	RDB
C16 H29 N2 O S	297.199512	0.687964	2.314812	3.5
C12 H29 N2 O6	297.202013	-1.813436	-6.101721	-0.5

IR

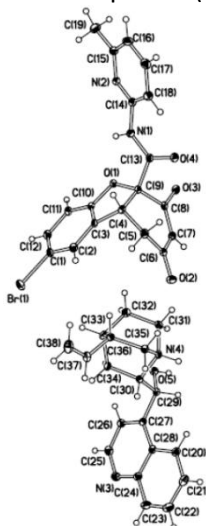


HRMS



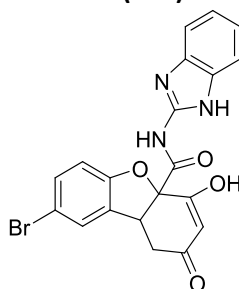
Formula	CalculatedMass	mDaError	ppmError	RDB
C ₁₈ H ₁₂ N ₂ O ₁₂ Na	471.028245	0.254704	0.540739	13.5
C ₃₂ H ₇ O ₅	471.0288	-0.2999	-0.636691	29.5
C ₃₁ H ₄ N ₄ O ₄ Na	471.027732	0.768048	1.630575	31.5
C ₃₃ H ₃ N ₄ O	471.030137	-1.637212	-3.47582	34.5
C ₁₅ H ₁₁ N ₄ O ₁₄	471.026628	1.872148	3.974591	12.5
C ₃₀ H ₈ O ₅ Na	471.026395	2.10536	4.469703	26.5
C ₂₀ H ₁₁ N ₂ O ₁₂	471.030651	-2.150556	-4.565655	16.5
C ₂₇ H ₇ N ₂ O ₇	471.024777	3.722804	7.903555	25.5
C ₂₃ H ₁₂ O ₁₀ Na	471.032268	-3.768	-7.999507	17.5
C ₁₃ H ₁₂ N ₄ O ₁₄ Na	471.024223	4.277408	9.080986	9.5

X-ray structure, crystal and refinement data of compound (+)- **149** + cinchonidine

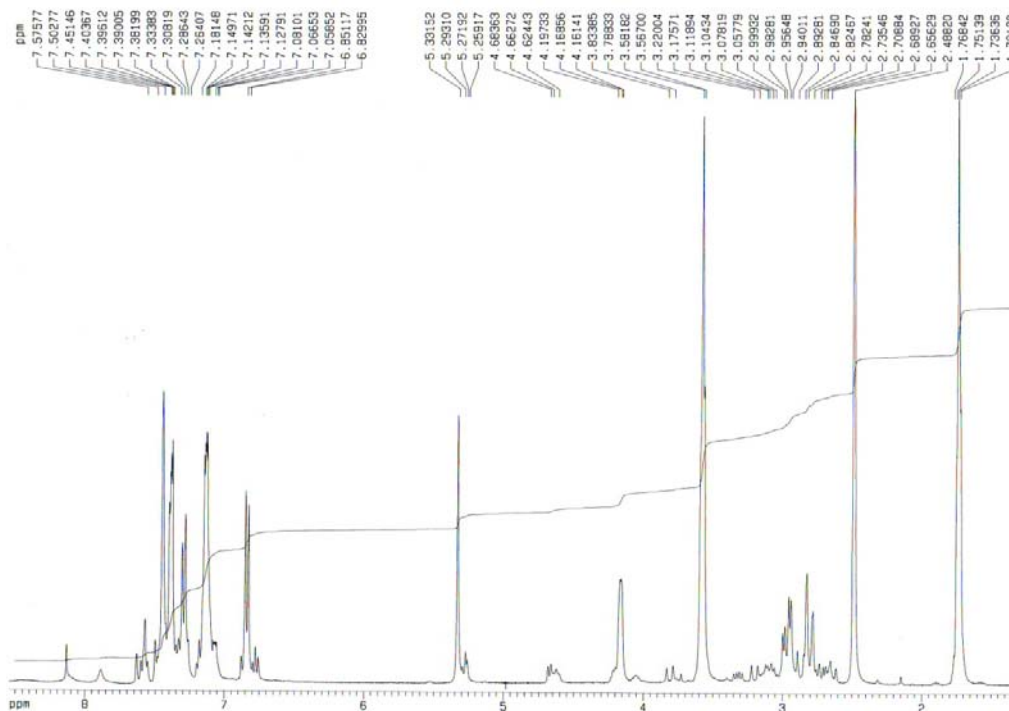


Empirical formula	C ₃₈ H ₃₇ N ₄ O ₅ Br	
Molecular weight	709.63	
Temperature	298 (2) K	
Wavelength	1.54178 Å	
Crystal system, Space group	Monoclinic, P2 ₁	
Unit cell dimensions	a = 14.8051 (8) Å	α = 90.00 °
	b = 6.2539 (3) Å	β = 90.868 (3) °
	c = 17.8406 (9) Å	γ = 90.00 °
Volume	1651.66 (15) Å ³	
Z; Density (calculated)	2; 1.427 mg/m ³	
Absorption coefficient	2.113 mm ⁻¹	
F(000)	736	
Crystal size	0.10 x 0.08 x 0.04 mm	
θ range	2.99 – 67.02 °	
Limiting indices h, k, l	-17 ≤ h ≤ 16, -6 ≤ k ≤ 7, -21 ≤ l ≤ 20	
Reflections collected/independent	11582/4119 R _{int} = 0.0669	
Refinement method	Least squares method with full matrix in F ²	
Data/restraints/parameters	4119/1/435	
Goodness-of-fit on F ²	1.093	
Final R indices [I > 2σ(I)]	R ₁ = 0.0442, ωR ₂ = 0.0993	
R indices (all data)	R ₁ = 0.0563, ωR ₂ = 0.1059	
Largest difference peak and hole	0.292 and -0.443	

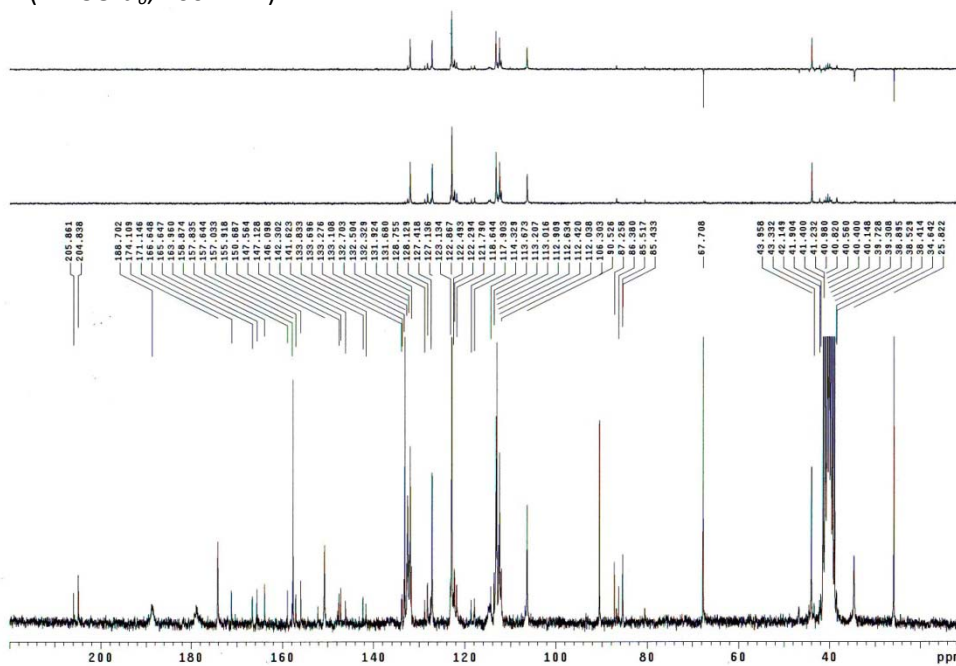
- *N*-(1*H*-benzo[*d*]imidazol-2-yl)-8-bromo-4-hydroxy-2-oxo-1,2,4a,9b-tetrahydrobenzo[*b,d*]furan-4a-carboxamide (182)



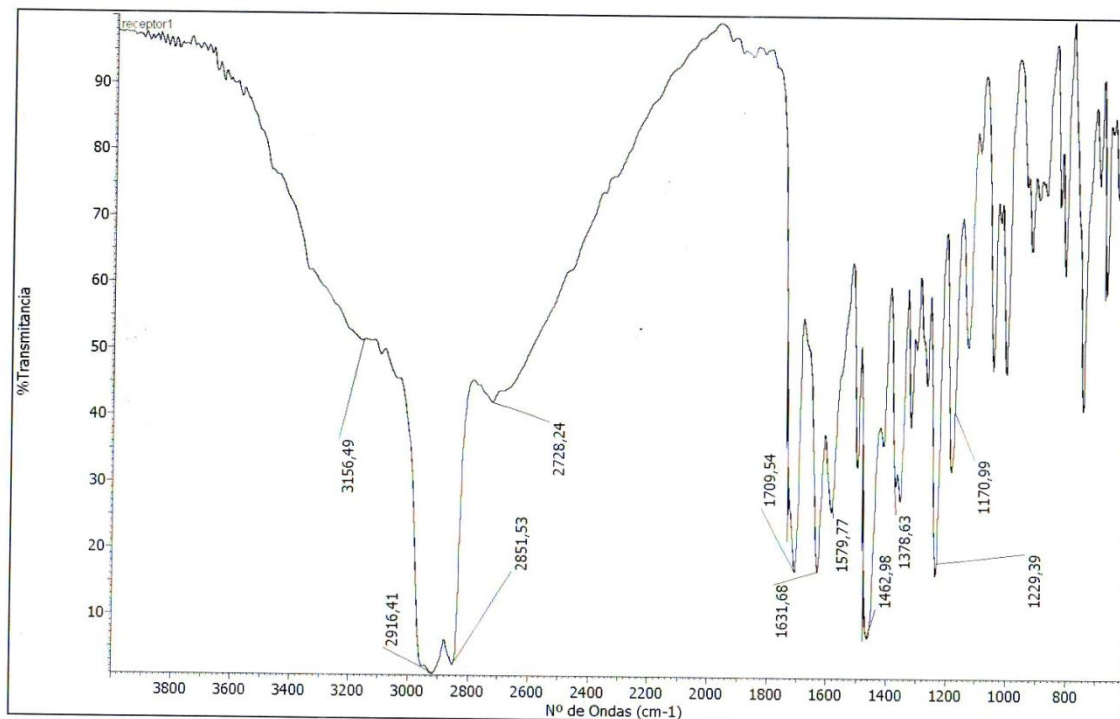
^1H RMN (DMSO- d_6 , 400 MHz)



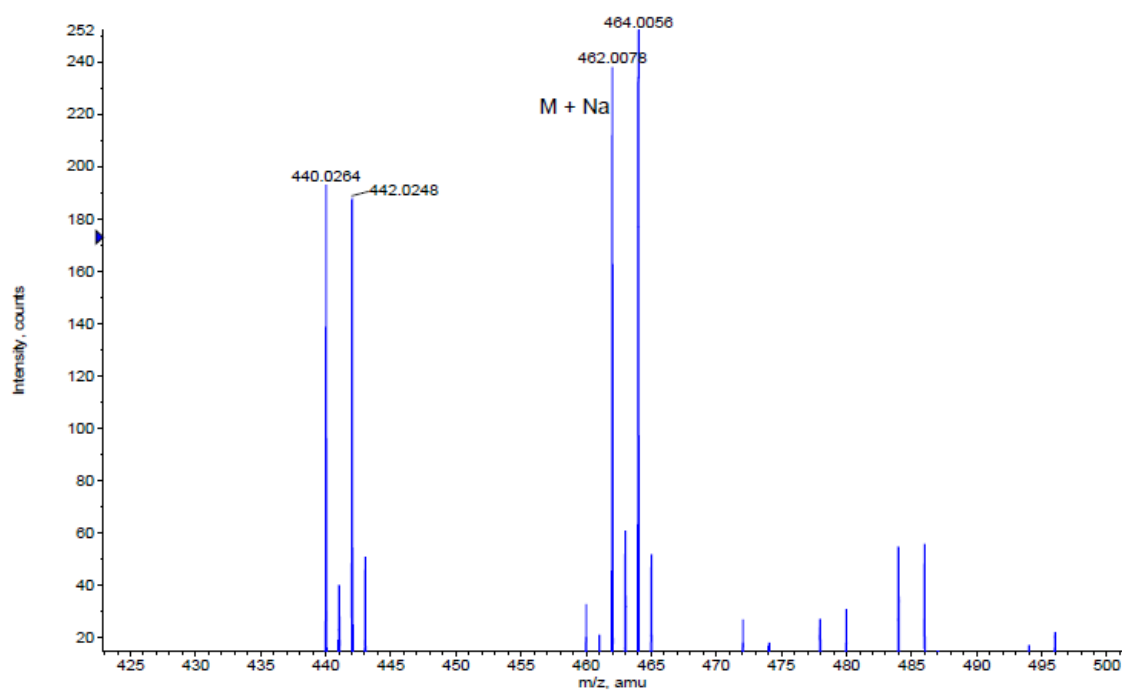
^{13}C RMN (DMSO- d_6 , 100 MHz)



IR

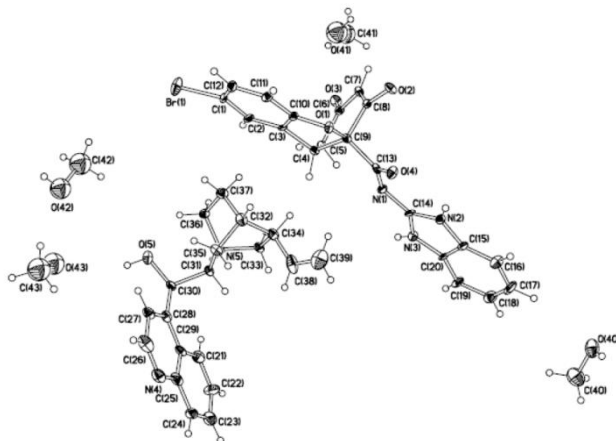


HRMS



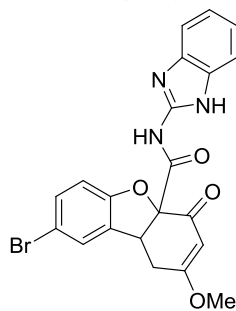
Formula	CalculatedMass	mDaError	ppmError	RDB
C22 H13 N3 O4 Br	462.008394	-0.593624	-1.284877	17.5
C20 H14 N3 O4 Na Br	462.005988	1.811636	3.921219	14.5
C25 H14 N O2 Na Br	462.010011	-2.211068	-4.785775	18.5
C17 H13 N5 O6 Br	462.004371	3.42908	7.422117	13.5
C13 H18 N3 O9 Na Br	462.011862	-4.061724	-8.791452	5.5
C27 H13 N O2 Br	462.012416	-4.616328	-9.991871	21.5

X-ray structure, crystal and refinement data of compound (+)-**182** + cinchonidine

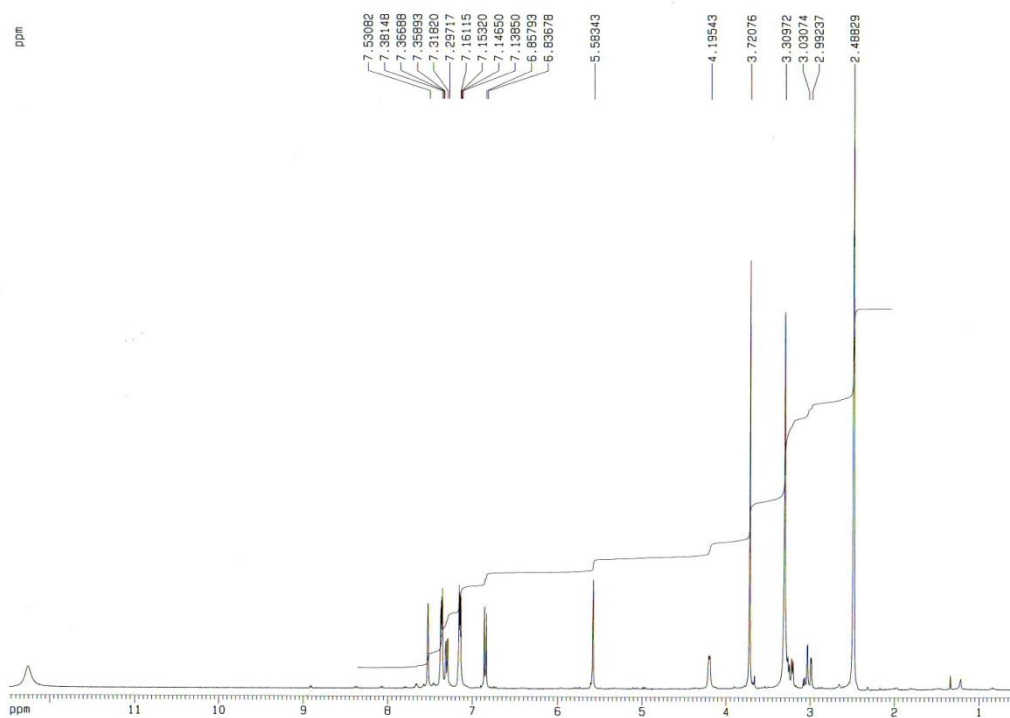


Empirical formula	$C_{20}H_{13}BrN_3O_4, C_{19}H_{22}N_2O, 4(CH_4O)$	
Molecular weight	861.80	
Temperature	298 (2) K	
Wavelength	1.54178 Å	
Crystal system, Space group	Monoclinic, $P2_1$	
Unit cell dimensions	$a = 14.7725 (17) \text{ \AA}$	$\alpha = 90.00^\circ$
	$b = 11.1943 (12) \text{ \AA}$	$\beta = 117.831 (8)^\circ$
	$c = 15.222 (2) \text{ \AA}$	$\gamma = 90.00^\circ$
Volume	2226.0 (5) Å ³	
Z; Density (calculated)	2; 1.286 mg/m ³	
Absorption coefficient	1.734 mm ⁻¹	
F(000)	902	
Crystal size	0.10 x 0.08 x 0.06	
θ range	3.28 – 66.83 °	
Limiting indices h, k, l	-15 ≤ h ≤ 17, -13 ≤ k ≤ 10, -16 ≤ l ≤ 18	
Reflections collected/independent	8628/4542 $R_{int} = 0,1011$	
Refinement method	Least squares method with full matrix in F^2	
Data/restraints/parameters	4542/3/498	
Goodness-of-fit on F^2	1.107	
Final R indices [$I > 2\sigma(I)$]	$R_1 = 0.0998, \omega R_2 = 0.2709$	
R indices (all data)	$R_1 = 0.1464, \omega R_2 = 0.2941$	
Largest difference peak and hole	0.418 and -0.486	

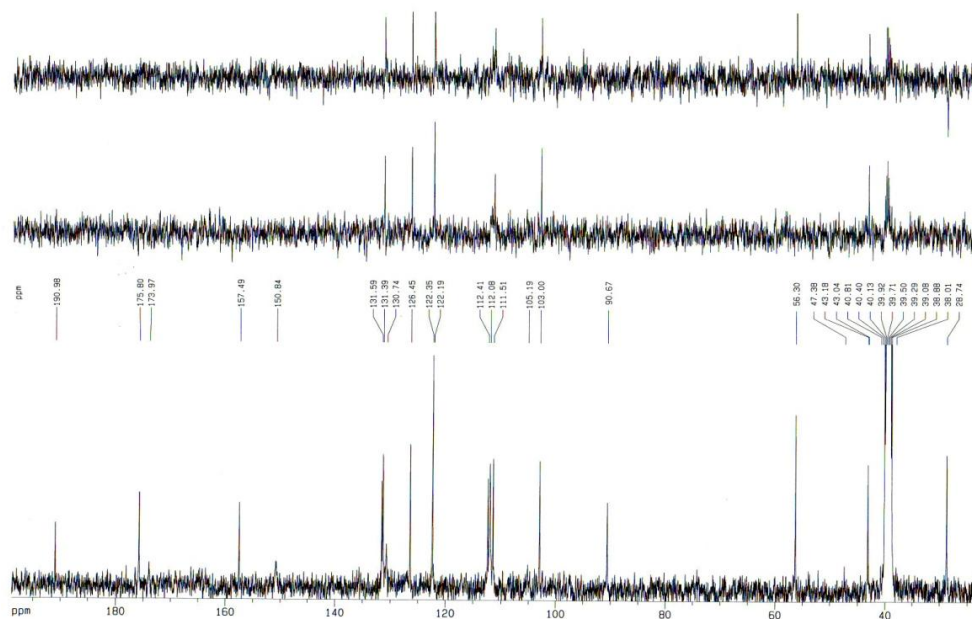
- *N*-(1*H*-benzo[*d*]imidazol-2-yl)-8-bromo-2-methoxy-4-oxo-1,4,4a,9b-tetrahydrobenzo[*b,d*]furan-4a-carboxamide (185)



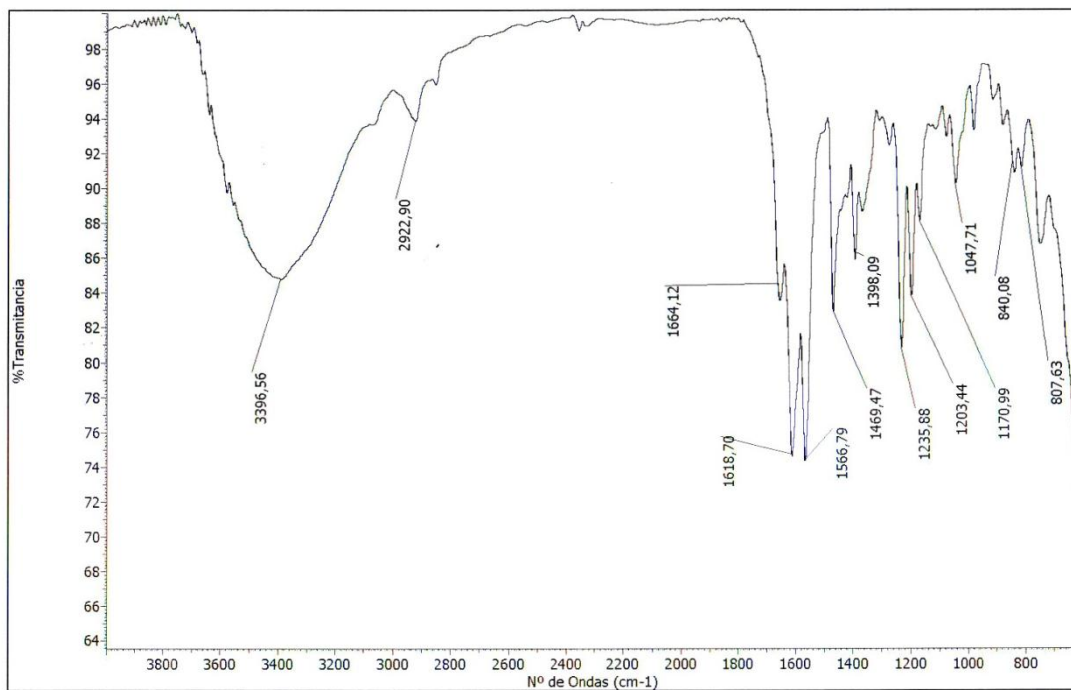
^1H RMN (DMSO-*d*₆, 400 MHz)



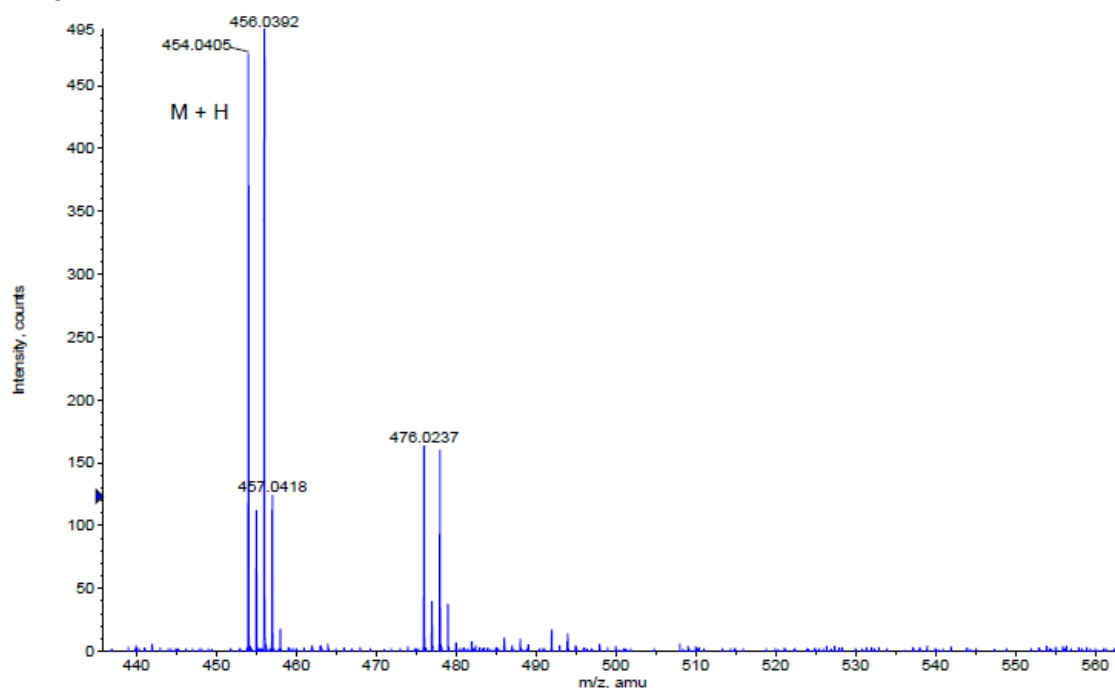
^{13}C RMN (DMSO-*d*₆, 100 MHz)



IR

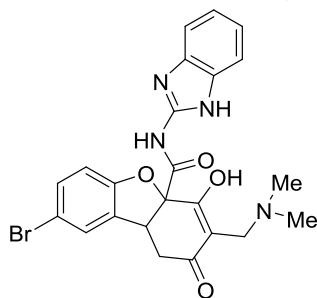


HRMS

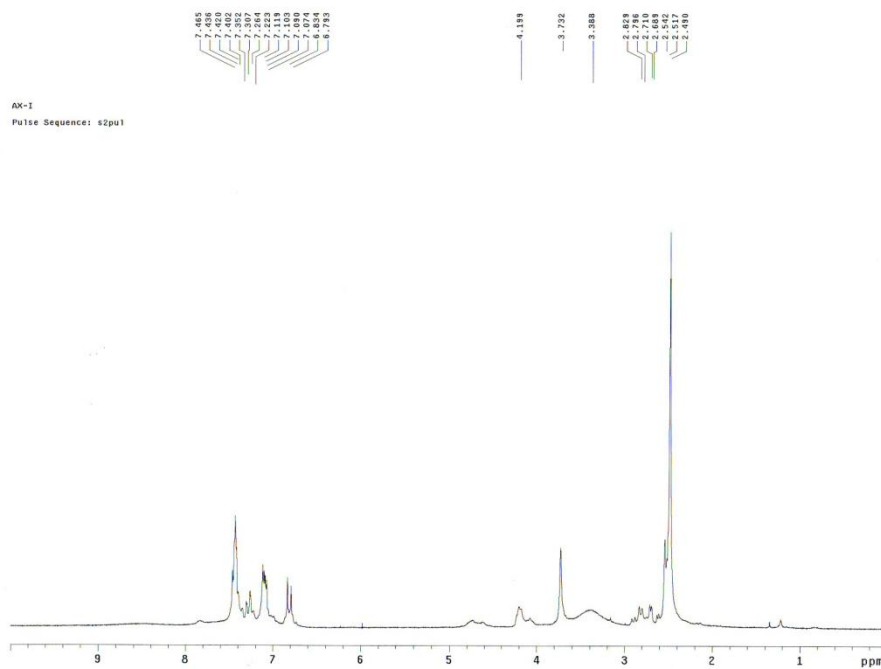


Formula	CalculatedMass	mDaError	ppmError	RDB
C ₂₁ H ₁₇ N ₃ O ₄ Br	454.039694	0.806216	1.775646	14.5
C ₂₄ H ₁₈ N O ₂ Na Br	454.041311	-0.811228	-1.786684	15.5
C ₁₂ H ₂₂ N ₃ O ₉ Na Br	454.043162	-2.661884	-5.862651	2.5
C ₁₉ H ₁₈ N ₃ O ₄ Na Br	454.037289	3.211476	7.073096	11.5
C ₂₆ H ₁₇ N O ₂ Br	454.043716	-3.216488	-7.084135	18.5

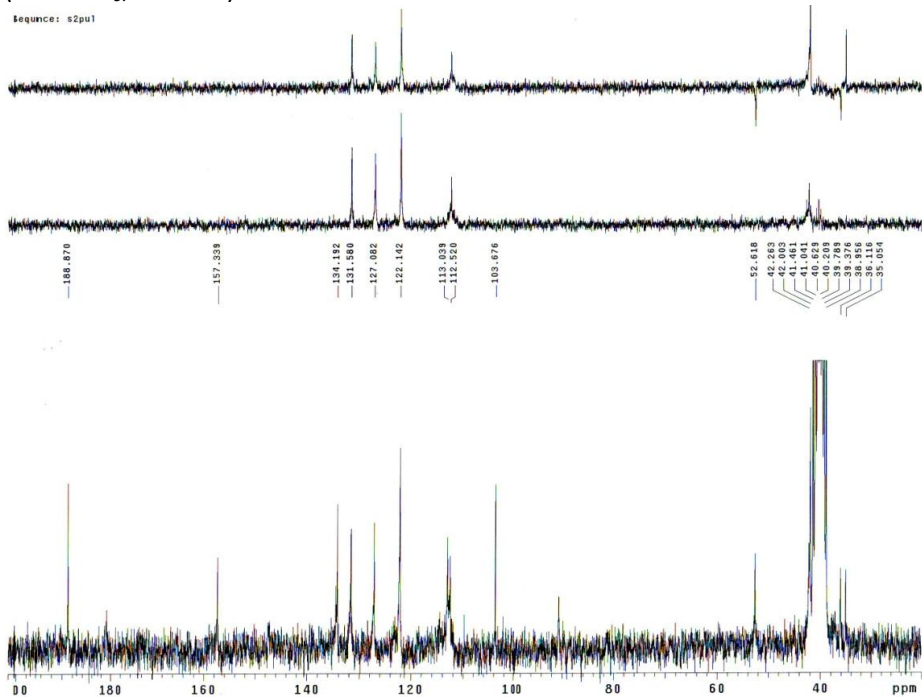
- ***N*-(1*H*-benzo[*d*]imidazol-2-yl)-8-bromo-3-((dimethylamino)methyl)-4-hydroxy-2-oxo-1,2,4a,9b-tetrahydrodibenzo[*b,d*]furan-4a-carboxamide (186)**



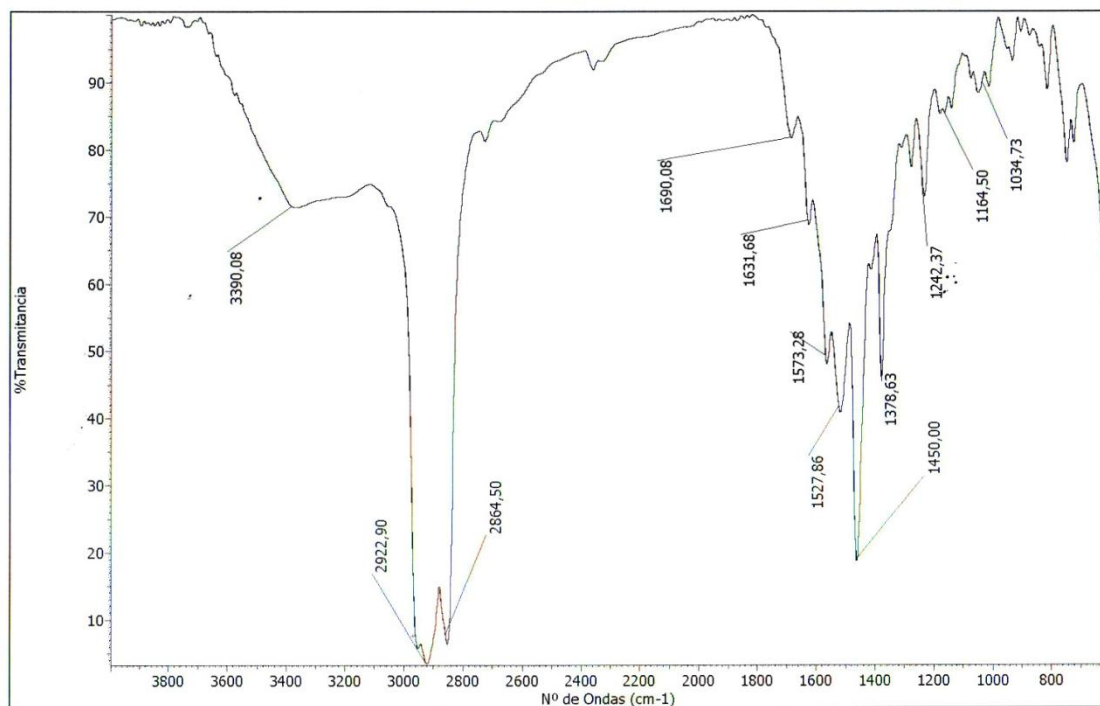
^1H RMN (DMSO- d_6 , 200 MHz)



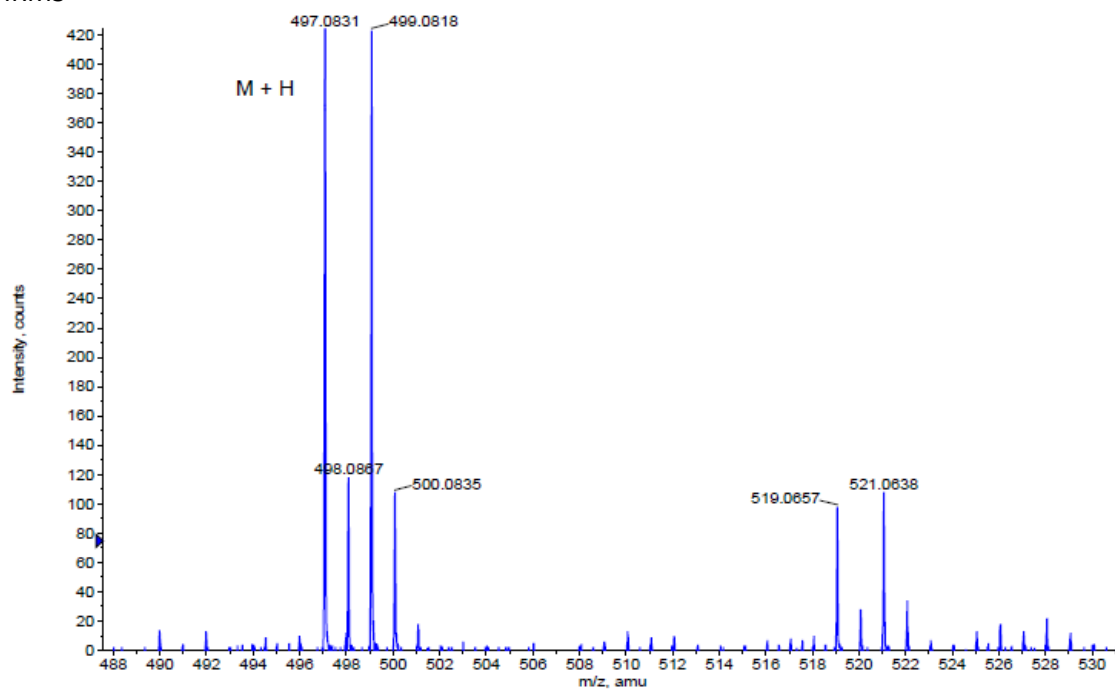
^{13}C RMN (DMSO- d_6 , 50 MHz)



IR

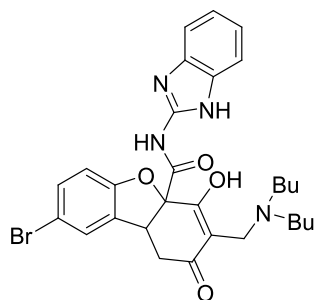


HRMS

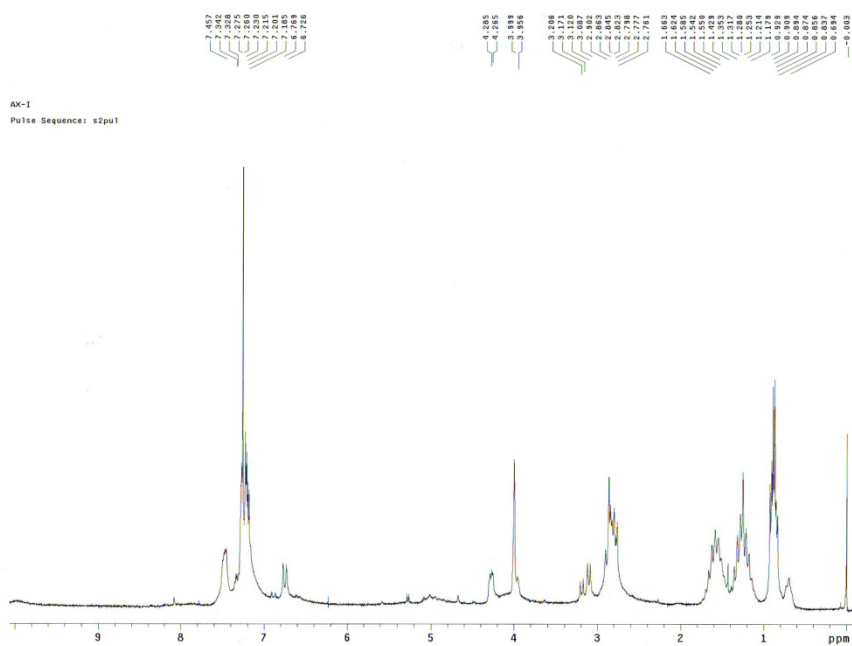


Formula	CalculatedMass	mDaError	ppmError	RDB
C ₂₆ H ₂₃ N ₂ O ₂ Na Br	497.08351	-0.410436	-0.825688	15.5
C ₂₃ H ₂₂ N ₄ O ₄ Br	497.081893	1.207008	2.428179	14.5
C ₁₄ H ₂₇ N ₄ O ₉ Na Br	497.085361	-2.261092	-4.548715	2.5
C ₂₂ H ₂₆ O ₈ Br	497.080556	2.54432	5.118495	9.5
C ₂₈ H ₂₂ N ₂ O ₂ Br	497.085916	-2.815696	-5.664431	18.5
C ₂₁ H ₂₃ N ₄ O ₄ Na Br	497.079488	3.612268	7.266922	11.5
C ₃₁ H ₂₃ Na Br	497.087533	-4.43314	-8.918298	19.5
C ₁₆ H ₂₆ N ₄ O ₉ Br	497.087766	-4.666352	-9.387458	5.5
C ₂₀ H ₂₇ O ₈ Na Br	497.07815	4.94958	9.957238	6.5

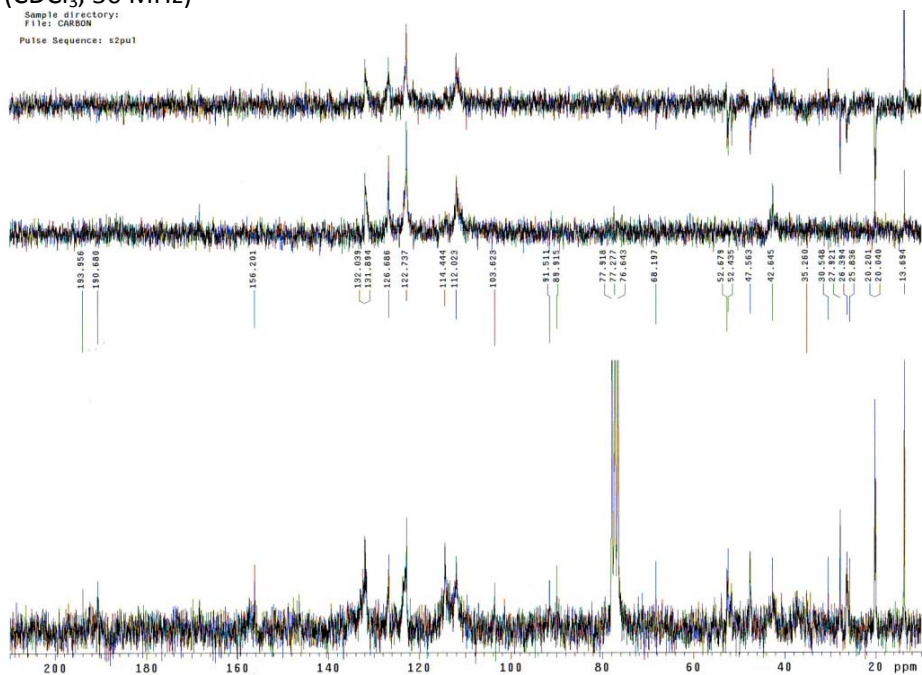
- *N*-(1*H*-benzo[*d*]imidazol-2-yl)-8-bromo-3-((dibutylamino)methyl)-4-hydroxy-2-oxo-1,2,4a,9b-tetrahydrodibenzo[*b,d*]furan-4a-carboxamide (187)



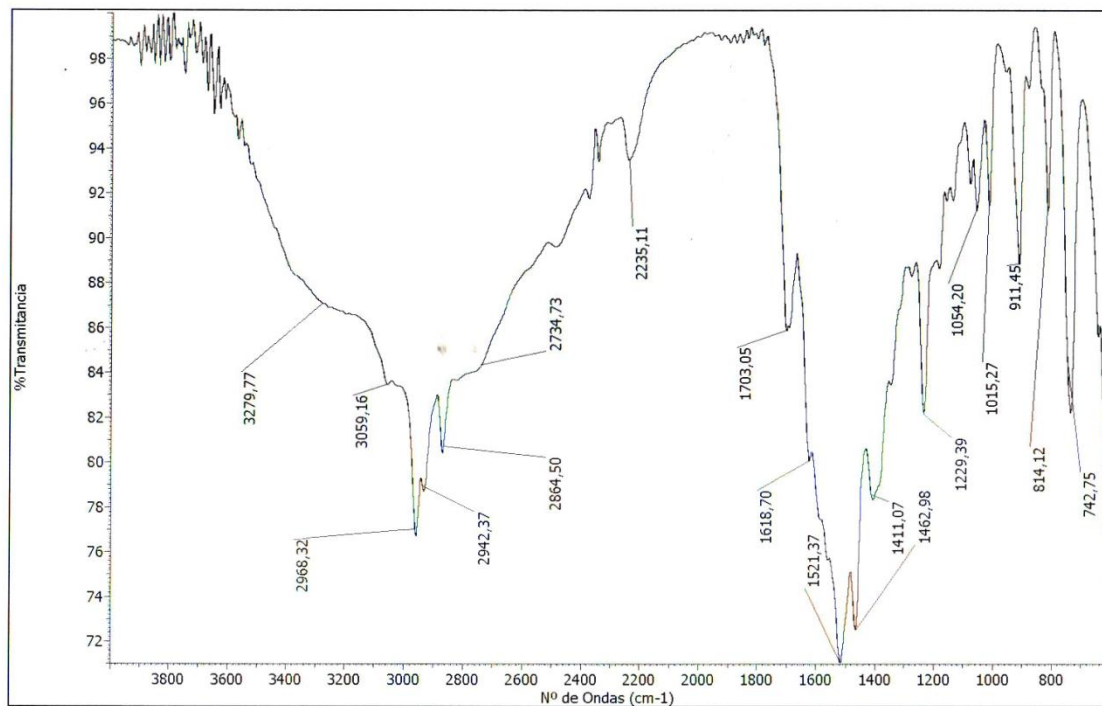
^1H RMN (CDCl_3 , 200 MHz)



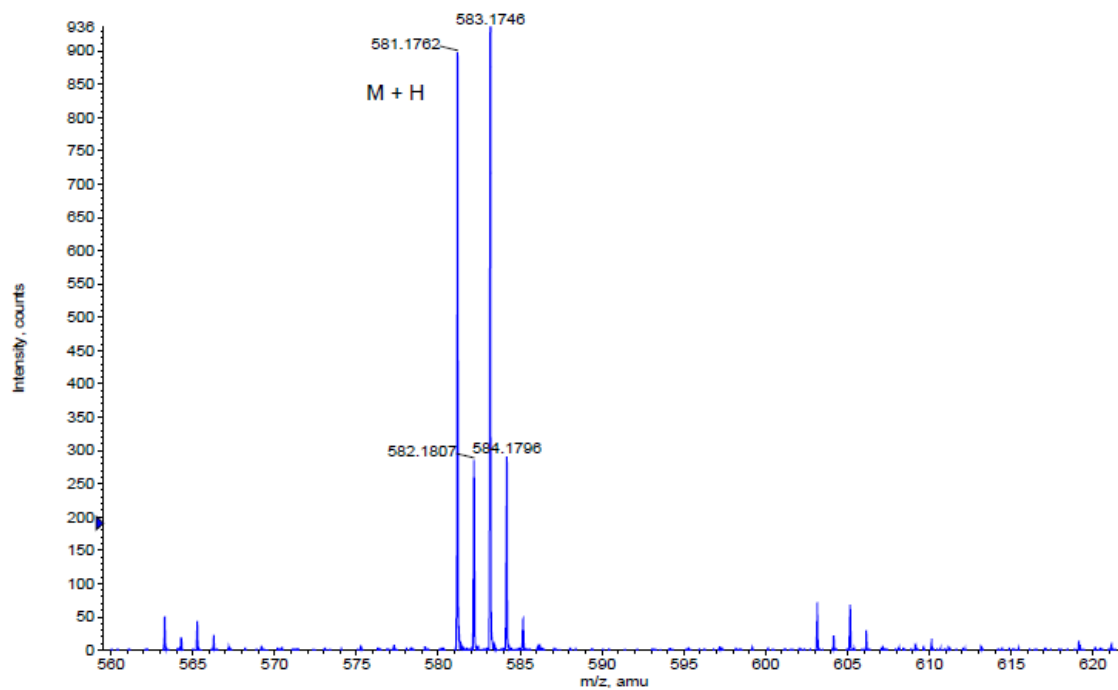
^{13}C RMN (CDCl_3 , 50 MHz)



IR

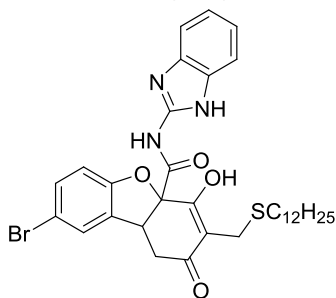


HRMS

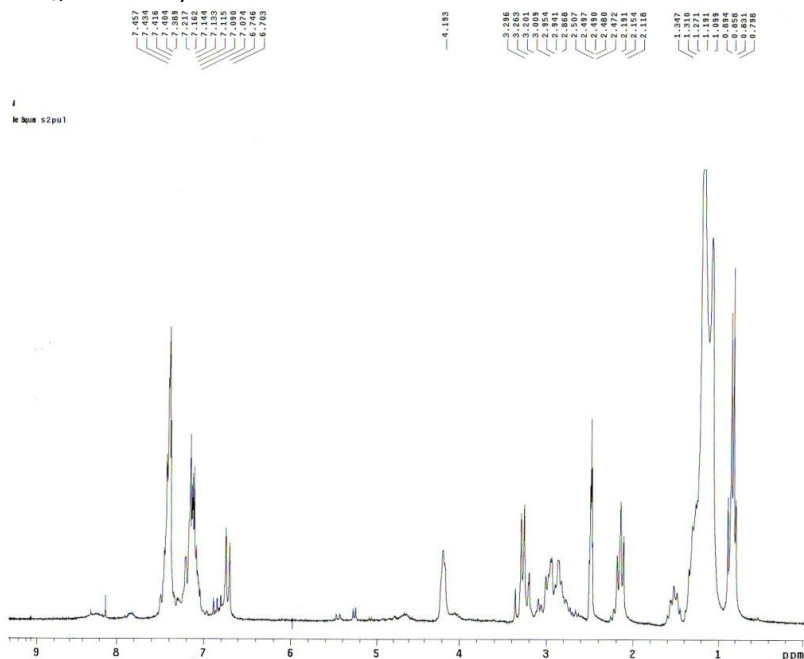


Formula	CalculatedMass	mDaError	ppmError	RDB
C ₂₉ H ₃₄ N ₄ O ₄ Br	581.175793	0.406528	0.699491	14.5
C ₃₂ H ₃₅ N ₂ O ₂ NaBr	581.177411	-1.210916	-2.083559	15.5
C ₂₈ H ₃₈ O ₈ Br	581.174456	1.74384	3.000533	9.5
C ₂₇ H ₃₅ N ₄ O ₄ NaBr	581.173388	2.811788	4.838094	11.5
C ₂₀ H ₃₉ N ₄ O ₉ NaBr	581.179262	-3.061572	-5.267885	2.5
C ₃₄ H ₃₄ N ₂ O ₂ Br	581.179816	-3.616176	-6.222162	18.5
C ₂₆ H ₃₉ O ₈ NaBr	581.172051	4.1491	7.139136	6.5
C ₃₇ H ₃₅ NaBr	581.181434	-5.23362	-9.005212	19.5
C ₂₂ H ₃₈ N ₄ O ₉ Br	581.181667	-5.466832	-9.406488	5.5
C ₂₃ H ₃₈ N ₂ O ₁₀ Br	581.170433	5.766544	9.922186	5.5

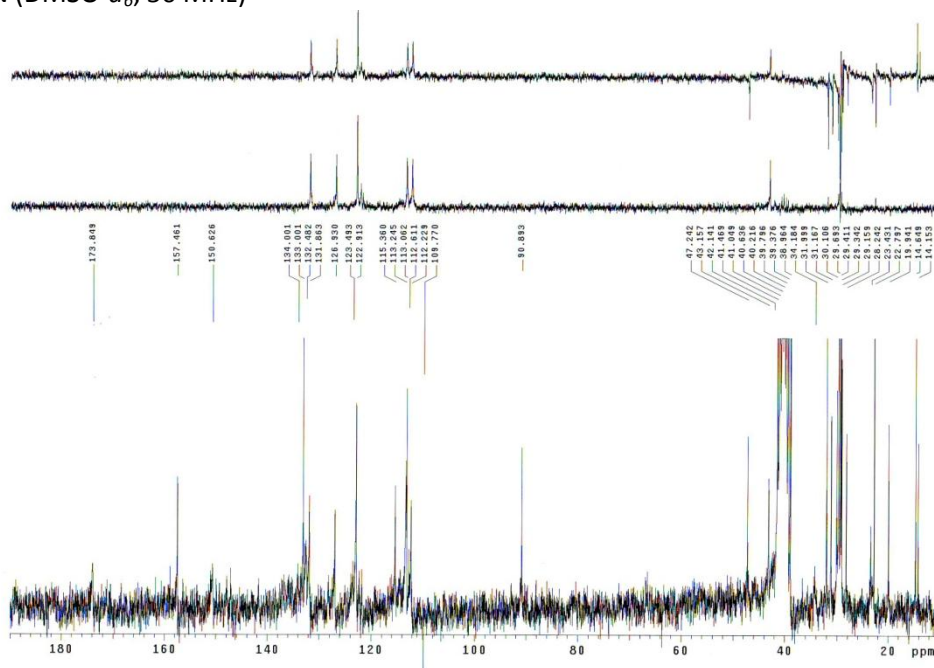
- ***N*-(1*H*-benzo[*d*]imidazol-2-yl)-8-bromo-3-(dodecylthiomethyl)-4-hydroxy-2-oxo-1,2,4a,9b-tetrahydrobenzo[*b*,*d*]furan-4a-carboxamide (188)**



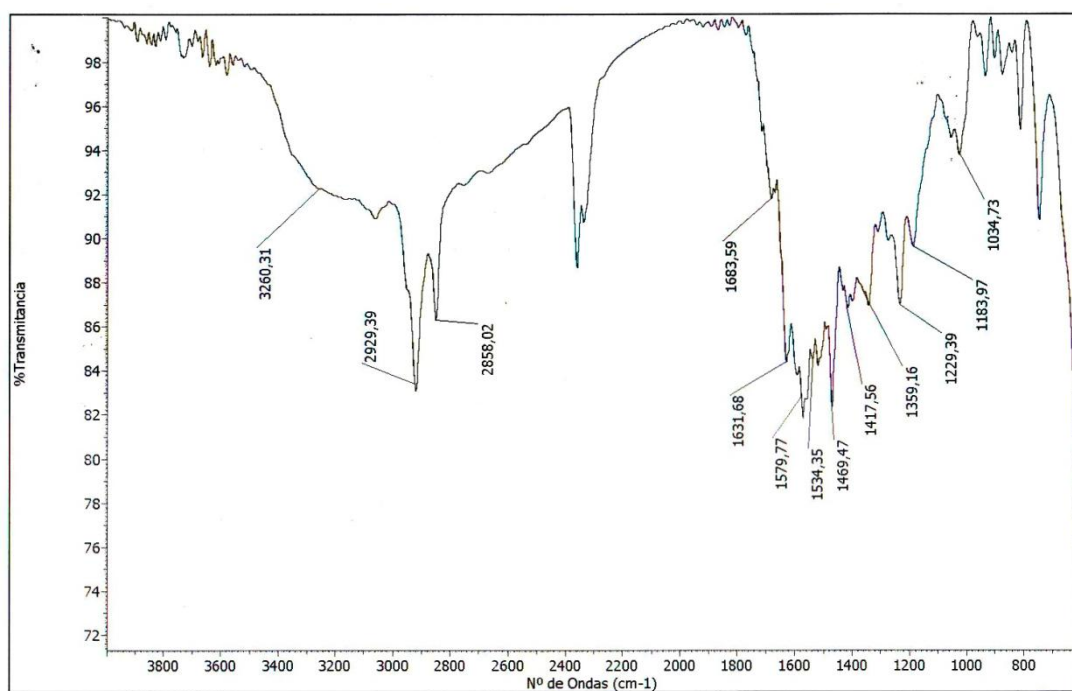
^1H RMN (DMSO- d_6 , 200 MHz)



^{13}C RMN (DMSO- d_6 , 50 MHz)



IR



MS

